MINERALS AND ENERGY RESEARCH INSTITUTE OF WESTERN AUSTRALIA

(MERIWA)

REPORT NO. 222

CHARACTERISATION AND METALLOGENIC SIGNIFICANCE OF ARCHAEAN GRANITOIDS OF THE YILGARN CRATON, WESTERN AUSTRALIA

Results of research carried out as MERIWA Project No. M281 at the Key Centre for Strategic Mineral Deposits, The University of Western Australia and Australian Geological Survey Organisation

by

K Cassidy, D Champion, N McNaughton, I Fletcher,
A Whitaker, I Bastrakova and A Budd

November, 2002

Distributed by: MERIWA
Mineral House
100 Plain Street
EAST PERTH WA 6004

To which all enquiries should be addressed

ISBN 0 7309 8532 6

AMIRA P482 Final Report

David C. Champion & Kevin F. Cassidy

Introduction

This, the final report for the AMIRA P482 project, presents the data, results and conclusions of that study. The report is accompanied by a second CD, containing the digital data from the project, presented as a granite GIS, comprising granite solid geology, geochemical data (including metallogenic parameters), geochronological data, outcrop geology, mineral deposits, and geophysical interpretation layers.

The final report is comprised of nine chapters, split into five themes as follows:

- Geophysical overview of the Yilgarn craton (Chapter 1)
- Description of the granite groups for each province (Chapters 2-5)
- SHRIMP geochronology, and Sm-Nd, Pb/Pb isotopic data and results (Chapters 6-7)
- Granite overview for the craton, including tectonothermal history (Chapter 8)
- Granite metallogenesis and links to mineralisation (Chapter 9)

The report also includes, as an appendix, a modified version of the 'Archean orogenic lode-gold deposits' paper by S.G. Hagemann & K.F. Cassidy (2000; in Reviews in Economic Geology, vol. 13, p.9-68).

Also included on this CD are the Minutes (WORD format) from the various AMIRA 6-monthly meetings, and the presentations from those meetings (POWERPOINT format).

Report Formats

This report is provided primarily in pdf format for which the ACROBAT Reader software is required. This can be downloaded free of charge from the ADOBE website. As some pdf files are large (up to 10 Megabytes), individual pdf files have been included for the text and each figure (in 'Individual_pdf' subdirectories). In addition to pdf format, the text for each chapter is supplied as a WORD 97 document, and the figures as various graphic formats (e.g., jpegs, coreldraw files). These files can be found in the relevant subdirectories within each chapter directory.

Reading this report

The easiest way to read this report is by going to the Table of Contents (below), from which each chapter can be accessed, by following the links.

Also included below is a location diagram illustrating the regions covered by the various chapters, again with links to the relevant chapters.

Chapter summaries

Summary sections for each chapter are bookmarked and so can be easily read by following the chapter links to the relevant chapter, and then using the bookmarks within each chapter to the relevant summary section.

AMIRA P482 FINAL REPORT

CONTENTS

Chapter 1. Alan Whitaker
Granite characteristics and structure of the Yilgarn Craton as inferred from the interpretation of geophysical data.

Chapter 2. David C. Champion & Kevin F. Cassidy
Granites of the northern Eastern Goldfields: their distribution, age, geochemistry, petrogenesis, relationship with mineralisation, and implications for tectonic environment (including a simplified key for discriminating granite groups in the northern Eastern Goldfields).

Chapter 3. Kevin F. Cassidy & David C. Champion
Granitoids of the southeastern Yilgarn Craton: Distribution, geochronology, geochemistry, petrogenesis and relationship to mineralisation

Chapter 4. Anthony R. Budd & David C. Champion
Granites of the northern Southern Cross Province: their distribution, age, geochemistry, petrogenesis, relationship with mineralisation, and implications for tectonic environment.

Chapter 5. David C. Champion & Kevin F. Cassidy
Granites of the northern Murchison Province: their distribution, age, geochemistry, petrogenesis, relationship with mineralisation, and implications for tectonic environment.

Chapter 6. Ian R. Fletcher and Neal J. McNaughton
Granitoid geochronology: SHRIMP zircon and titanite data

Chapter 7. Ian R. Fletcher and Neal J. McNaughton
Sm-Nd and Pb/Pb isotope geochemistry of Yilgarn granitoids

Chapter 8. David C. Champion, Kevin F. Cassidy & Anthony R. Budd
Overview of the Yilgarn Craton magmatism: Implications for crustal development

Chapter 9. Kevin F. Cassidy & David C. Champion
Granitoids of the Yilgarn Craton: Links to mineralisation

Appendix 1. Kevin F. Cassidy & Steffen G. Hagemann
Archean orogenic lode-gold mineralising systems: A synthesis of features.
(**Note**: This is a modified version of a paper by S.G. Hagemann & K.F. Cassidy, 2000, Archean orogenic lode-gold deposits, Reviews in Economic Geology, vol. 13, p.9-68.)

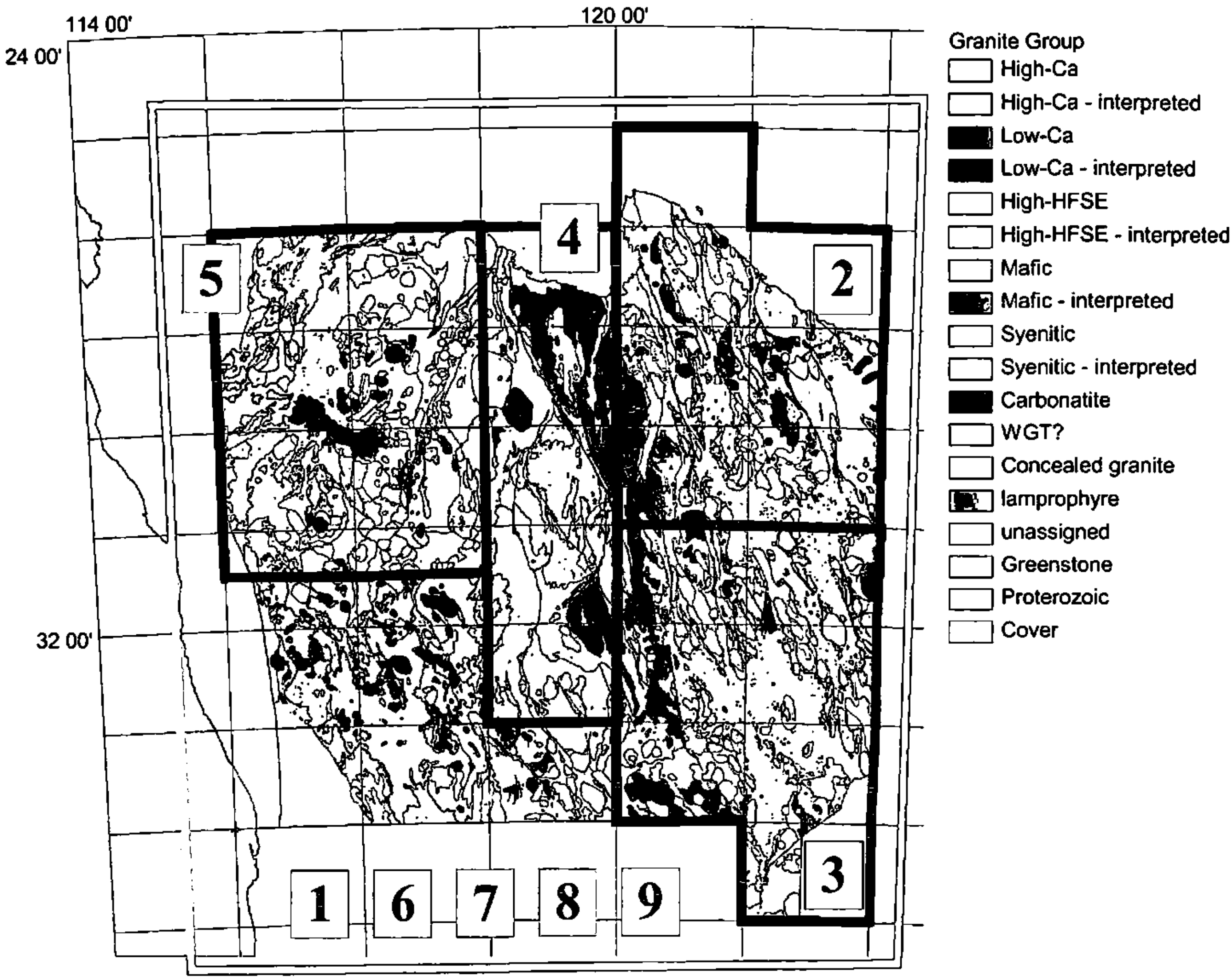

LOCATION DIAGRAM. Regions covered by Chapters 2, 3, 4, and 5, are shown in dark blue. Chapters 1, 6, 7, 8, and 9 cover all three provinces (Murchison, Southern Cross, and Eastern Goldfields). Chapter numbers are also links to each chapter.

Chapter 1.
Granite characteristics and structure of the Yilgarn Craton as inferred from the interpretation of geophysical data

Alan Whitaker

Summary
The Yilgarn Craton is very poorly exposed and geological models of its evolution and structure are poorly constrained. Aeromagnetic (and gravity) data are little influenced by thin regolith and provide a continuous model of the Craton. Approximately 75 percent of the Yilgarn Craton is composed of granite, or gneiss of granitic composition. Five main crustal elements (geophysical map units) are defined through interpretation of the aeromagnetic data: granite plutons; undivided gneiss-migmatite-granite (most abundant); parallel banded (granitic) gneiss; sinuous (variable composition) gneiss; and greenstone. Granitic and gneissic domes are identified in several areas. Eight large domains, equivalent to geological provinces, are defined and are composed of various mixes of the crustal elements. Granitic crust adjacent to or surrounding greenstone belts is also inferred to underlie them. The characteristics of faults and shears in this granitic crust provide a model for the nature of faults and shears in the greenstone belts. The Norseman–Wiluna belt is considered to be a 200 km wide, craton scale, shear zone with distinctive structure relative to crust on either side. Banded gneiss and greenstone are spatially correlated with shear zones. Magnetisation is not an effective discriminator of the geochemically defined granite suites. Further more, mineralised granite is not uniquely magnetised. The geophysical data do however provide useful detail of major changes in the crust, structural and compositional trends, and the boundaries of many intrusives.

1. Introduction
About 75 percent of the near surface crust of the Yilgarn Craton is composed of moderate to highly magnetised granite or gneiss of granitic composition. Poorly magnetised greenstones belts, which comprise the remainder of the crust, host most of the known gold mineralisation. While the majority of production has come from mafic rocks in the greenstone belts, alteration is commonly potassic, and mineralising fluids are thought to have at least interacted with granite. In general, granitic rocks of the Craton have been considered poorly mineralised. However, significant resources of gold have been outlined in granite in recent years (e.g., Tarmoola, Fairclough & Brown, 1998; Golden Cities, Kehal et al., 1999). Outcrop of the craton is poor (less than 15%), and geological understanding is consequently limited; particularly of the location and nature of boundaries between rock types and larger provinces. Interpretation of the aeromagnetic data provides considerable detail on the nature and distribution of discrete granite plutons, and also on the more problematic and extensive terranes of gneiss and granite.

The Yilgarn Craton has been previously subdivided into a Western Gneiss Terrane with abundant gneiss, and terranes to the east composed dominantly of granite and greenstone (Myers, 1990; Gee et al., 1981; Trendall, 1990). The position of boundaries between the terranes is poorly constrained and, in terms of the geophysical interpretation, some boundaries have been placed in regions where there is no apparent change in crustal material (e.g., parts of the Narryer-Murchison, Murchison- Southern Cross, Western Gneiss-Murchison Province boundaries). The aeromagnetic interpretation also indicates that gneiss is more abundant in the granite–greenstone provinces than indicated in the literature. To a large extent the granite-greenstone provinces of the Yilgarn Craton have been defined on the basis of greenstone characteristics including abundance of key lithologies and deformational trends. The interpretation presented below defines province-sized domains drawing extensively on the nature and contrasts in granitic crust as well as that of greenstone. Craton crossing faults (e.g., Youanmi, Ida) have been defined as structural, terrane or accretionary boundaries (e.g., Myers, 1995; 1997; Wilde et al., 1996). There is no geological or geophysical evidence to support the continuity or extent proposed for these faults.

This report provides information progress of the geophysical interpretation for the Yilgarn Craton, details of the mappable crustal elements, characteristics of the major domains or subdivisions of the Craton, and the geophysical characteristics of the geochemically defined granite groups.

2 Geophysical data sets & interpretation progress

2.1 Aeromagnetic data

Survey specifications for aeromagnetic data coverage of the Yilgarn Craton held by the Australian Geological Survey Organisation (AGSO) include a variety of flightline line spacings: 1500 m data over the sub-cropping area of the Craton (56 x 1:250 000 Sheets); 400 m data over the central and northeast areas of the Craton (17 x 1:250 000 Sheets); and 3-6 km data in areas of thick sedimentary cover in the north east and east of the Craton (4 x 1:250 000 Sheets). The only 200 m publicly available data accessible to the project is from the western parts of Rason and Throssell and parts of the recently acquired data for the Youanmi Sheet. Interpretation priorities were given to coverage of the sub-cropping areas of the Eastern Goldfields, Murchison, and Southern Cross and Provinces, in line with project objectives. Prior to the March 1999 Sponsors meeting, interpretation was completed on aeromagnetic data of the area from Leonora to Widgiemooltha in the Eastern Goldfields Province. During the past 18 months, interpretation and capture has been concluded for five 1:250 000 Sheets in the Wiluna 1:1M Sheet, all of the Perth and southern Meekatharra 1:1M Sheets, and the Rason Sheet on the Kalgoorlie 1:1M Sheet. Interpretation of the regional aeromagnetic data is ongoing and has been provided to this project prior to public release but remains in the public domain.

Several companies have generously provided access to detailed (100m and 200m line spacing) aeromagnetic data to complement the study. The data sets interpreted include coverage of greenstone in the north Murchison (Cue, Belele), the Yalgoo greenstone belt, Sandstone and Gum Creek greenstone belts, and parts of the Southern Cross and southern Eastern Goldfields Provinces (Southern Cross, Kellerberrin, Kalgoorlie, Kurnalpi, Widgiemooltha and Norseman Sheets). Most of the interpretations of these data sets have been captured but are yet to be integrated with the regional interpretation. However, Champion, Cassidy and Budd have incorporated relevant pluton outlines from the interpretations of company data in the granite solid geology compilation. The interpretations of sponsor company data will be subject to the confidentiality conditions of the project.

This study, by necessity, has had to draw extensively on contour plots and images of regional 1500 m data. These products were derived from grids of the data with a cell size of approximately 500 m which places significant constraints on the level of interpretation detail available relative to that provided by 400 m (100 m cell size) and 200 m (50 m cell size) data. In practice, the 1500 m data do not adequately resolve many small intrusives (some of these host mineralisation e.g., Tarmoola granite), much gneissic banding, and most of the intermediate or smaller sized faults and fractures. The regional data do however provide information on large scale features including the Craton and domain boundaries, regional trends and variability within domains, and the larger faults and shears.

To summarise progress, some twenty two (22) 1:250 000 Sheets of 1500 m data, fourteen (14) Sheets of 400 m data and approximately three (3) Sheets of 200 m data have been interpreted during the course of the project. The previously released interpretations of 1500 m data for the Albany, Esperance and eastern Kalgoorlie 1:1M sheets (24 1:250 000 sheets), have also been reviewed and are currently being edited and coded to complement the study.

Gamma-ray spectrometric data is available for most of the area for which AGSO has acquired 400 m aeromagnetic data. As effective ground penetration of gamma-rays is in the order of 0.5 m, and outcrop of the Yilgarn Craton is poor, these data mostly provide information about the regolith. No systematic analysis of these data has been undertaken for the project, however some observations will be included in the discussion of granite geochemical suites.

2.2 Gravity data

Gravity coverage of the Yilgarn Craton is based on the national 11 km grid. Additional data have been acquired in recent years for several areas. These surveys include: 2-4 km spaced data for twelve 1:250 000 Sheets for the Eastern Goldfields National Geoscience Mapping Accord area (AGSO/GSWA); detailed data in the region of the Collie coal field (GSWA); and road and seismic line traverses of <2-5 km station spacing (AGSO and company data). Some small area, very detailed surveys are also stored in the database, however, they are of limited value to this regional interpretation.

Because the station spacing of the gravity data is large (+1 km to ~11 km), resolution of geological features is considerably lower than that provided by the aeromagnetic data. For the Craton as a whole, large granite plutons correlate with the lowest gravity anomaly. Successively higher gravity anomaly is associated with gneiss-migmatite-granite and banded gneiss while layered intrusions and greenstone belts correlate with relative gravity highs. In the area of the more detailed Eastern Goldfields surveys, the gravity data yield complementary information to that provided by aeromagnetic data including evidence of dipping contacts between granite and greenstone, the extent of near surface granite underneath greenstone, and also some idea of relative granite thickness. The gravity data are also useful in defining the boundaries of the Craton particularly where inferred density contrasts are high or where there are significant changes in regional anomaly pattern. Elsewhere in the Craton, where granitic compositions dominate and station spacings are large, meaningful interpretation of the gravity data is more difficult. At this point in time, interpretation of the gravity coverage of the Craton has not been completed and results will not be discussed separately. Aspects of the gravity interpretation relevant to granite distribution will be covered in the section on crustal elements.

3. Aeromagnetic interpretation

Interpretation of the aeromagnetic data was undertaken at 1:250 000 scale as it is the most appropriate scale for analysis of 400 m and 1500 m line-spaced data and afforded progress at a rate suitable for the project timeframe. The rationale behind the interpretation has been to define a set of 'crustal elements' or geophysical map units that could be applied with some consistency across the Craton. The description of these elements is deliberately geological. In addition to the main crustal elements, faults, shears, dykes, sills, and other intrusives, complete the range of mapped features.

3.1 Crustal elements (geophysical map units)

The Yilgarn Craton is composed of five main crustal elements: granite plutons, undivided gneiss-migmatite-granite, parallel banded gneiss, sinuous gneiss and greenstone. The first three elements are largely composed of rocks of granitic composition. Greenstone and sinuous gneiss are composed of, or are inferred to be composed of, a wide variety of lithologies including mafic and felsic volcanic rocks, calc-silicates, and metasediments, but also enclose granite. The greater variation in lithologies relative to the granite-dominated elements is reflected in the aeromagnetic data by a greater abundance of inferred lithological banding. The symbology listed with each of the crustal elements below relates to that used to attribute the interpretation digital data. Many of the crustal elements include zones that have symbol suffixes of '_l', '_m, '_h' and '_r'. These suffixes refer to low, medium, high and remanent magnetisation respectively. Areas labelled with these modifiers were distinguished to emphasise regional compositional trends and zonation in granite.

Granite plutons (Ag, Ag_l, Ag_m, Ag_h, Ag_r)

Granite plutons comprise approximately 15% of the Yilgarn Craton. They show a wide range of magnetisations, from low to high levels, and, although most bodies are evenly magnetised, some are zoned. Granite plutons range in size from less than 1km to greater than 50 km in diameter. Joint-like fracture patterns are particularly evident as poorly magnetised lineaments in the larger, moderate to highly magnetised bodies. The range in shape of plutons is high and includes circular, ovoid, lensoidal, and dyke like forms. Where granite intrudes greenstone, three main shape and contact relationships are defined: ovoid to circular plutons which cross cut greenstone units; elongate lenses of granite which are drawn out in the direction of the regional trends with greenstone in parallel contact with the elongate margins; and bodies of granite about which the greenstones seem to have been deformed giving rise to asymmetric greenstone 'tails'. Simple timing of intrusion as inferred from these structural relationships has not been supported by zircon geochronology (Champion, pers. comm.); inconsistencies in timing are inferred to result from significant strain partitioning. Granite intrusion, as inferred from this interpretation, is distributed unevenly across the Yilgarn Craton with high abundances of plutons coincident with the area of the Norseman-Wiluna Belt of the Eastern Goldfields Province (Gee, 1979) and also in the southern Murchison Province. Within the Norseman-Wiluna Belt, plutons form spatial associations that are aligned with north-northwest regional structural trends. Most plutons are associated with local gravity lows, particularly where they intrude greenstone belts. Some of the larger plutons in the Norseman-Wiluna Belt are associated with the lowest gravity anomaly for the Yilgarn Craton (-850 to -700 $\mu m.sec^{-2}$).

Gneiss-migmatite-granite (Agmg, Agmg_l, Agmg_m, Agmg_h, Agmg_r)

Undivided gneiss-migmatite-granite is the most extensive crustal element comprising more than 45% of the Yilgarn Craton. Large regions of moderate magnetisation with low variability and few well defined internal boundaries or compositional banding is characteristic of the crustal element. Abundant remanent and normally magnetised dykes, and poorly magnetised fault and shears, are the most notable features in extensive areas of gneiss-migmatite-granite. Some zones of higher or lower average magnetisation have been distinguished and are inferred to show regional compositional trends. Sparse, irregular shaped areas of variable but higher average magnetisation are attributed to gneiss. Gneiss-migmatite-granite encloses examples of all other crustal elements. Greenstone is commonly in concordant contact with the margins of gneiss-migmatite-granite and metamorphosed to amphibolite grade. Lower grades of metamorphism are recorded farther from the contacts in the larger belts (Binns et al., 1975). Gneiss-migmatite-granite domains are associated with low to moderate gravity values (-700 to -600 μm.sec^{-2} in the Eastern Goldfields Province).

Banded geniss (Agn)
Banded gneiss comprises 5-10 percent of Yilgarn Craton and is more widespread than previously recognised. The gneiss occurs in elongate belts with variable but higher average magnetisation and higher average gravity anomaly (~100 μm.sec^{-2} higher) than adjacent gneiss-migmatite-granite. The belts are commonly 5 to 15 km in width and up to 150 km in length. Both the belts and their internal banding and are aligned with local north-northwest to north regional trends. Banded gneiss is particularly abundant in the Eastern Goldfields, Yeelirrie, and northern Southern Cross domains where they commonly abut or enclose amphibolite and greenstone. Enclaves of greenstone are aligned parallel to the local banding of the belts. Linear to curvilinear contacts of banded gneiss with greenstone are well defined, however, boundaries with adjacent gneiss-migmatite-granite are generally irregular and difficult to delineate. Banded gneiss is inferred to be composed dominantly of granitic composition, but is known to include paragneiss adjacent to the Ida lineament, west of Leonora (Thom & Barnes, 1977).

Sinuous gneiss (Anu)
Sinuous gneiss is confined to the central and western parts of the Yilgarn Craton. The gneiss occurs in elongate belts with quite variable magnetisation. Inferred compositional layering and large-scale folds are particularly abundant in the belts but are less coherent and less well aligned with local regional trends than for banded gneiss. A wide range of lithologies including mafic rocks, calc-silicates and other metasedimentary rocks are inferred to comprise the crustal element.

Greenstone (Aa)
Poorly magnetised greenstone occupies over 25 percent of Yilgarn Craton and occurs in elongate belts that are commonly aligned with regional shears and faults. The most extensive area of greenstone occurs within the Norseman-Wiluna Belt of the Eastern Goldfields Province. While most greenstone lithologies are poorly magnetised and not discriminated in aeromagnetic data, highly magnetised banded iron formation (BIF) and ultramafic rocks provide some information on the internal structure of the belts. The greenstone belts correlate with high gravity anomaly (-500 to –150 μm.sec^{-2} in the Eastern Goldfields Province).

Other mapped features - Granitic Domes, Shears and Faults
Circular to ovoid shaped domes composed of granite and gneiss are inferred in several areas of the Yilgarn Craton: at Yalgoo, to the north and east of the Windimurra layered intrusion; at Southern Cross; and in gneiss-migmatite-granite abutting the eastern margin of the Norseman-Wiluna Belt. Individual domes range in size from less than 10 km to greater than 50 km in diameter. They are characterised by either boundary parallel internal compositional banding, or by mantling of the inferred dome boundary by greenstone or gneiss in apparent concordant contact. The relationships of domes with surrounding rocks have been used to indicate reactivation of sialic basement (Archibald & Bettenay, 1976) and as evidence for extension tectonics early in the deformation history of the greenstones (Williams & Whitaker, 1993).

The extent and form of faults and shears within the greenstone belts is difficult to determine from aeromagnetic data as both the structures and most rock types are poorly magnetised. In areas of moderate to highly magnetised granitic crust however, the low magnetisation of faults and shears provides a suitable contrast to provide detail of their form. Granitic crust surrounding greenstone is inferred here to also underlie the greenstone. Thus the nature faults and shears in the adjacent granitic crust should provide a general model for dislocation structures, including those not readily mapped in greenstone domains.

Shear zones form large structures. They typically range from 50 to 200 km in length and from 5 to 10 km in width. In detail, shears consist of individual linear to elongate 'S' form curvilinear segments that step en echelon through granitic terrane. Apparent relative lateral movement of crust across shears, where measured, is in the order of 30 to 50 km. Associated deformation of the granitic crust is inferred to be partially ductile and partially brittle. These features are comparable with the characteristics of tectonic or shear zones geologically mapped in the greenstone belts. Numerous brittle fracture faults cut granitic terrane and also dislocate the shear zones. Most faults have lengths less than 50km and occur as discrete to anastomosing zones of 300 m width or less. Apparent movement on these structures is typically less than 5 km. Thus there would appear to have been an early period of more ductile deformation of granitic crust followed at some later time by brittle dislocation.

Shear zones are unevenly distributed in the Yilgarn Craton with the highest incidence in the Norseman-Wiluna Belt, followed by the Southern Cross Province, with much lower incidence to the east and west. Numerous shears in the Norseman-Wiluna Belt appear to inter-connect defining many rhomboid shaped areas 100-150 km in length by 50 km in width. Over all, the Norseman-Wiluna Belt has the appearance of a 200 km wide, craton scale shear zone where the rhombs of granite and greenstone comprise super-sized boudins. Accretionary models evoked in recent years to explain greenstone evolution and variation have included craton crossing faults which are also terrane boundaries (e.g., Myers, 1995). Parts of these faults are mapped in this study as shear zones across which crust may be correlated. In several areas, segments of the proposed faults pass through granitic or gneissic crust with no geophysical or geological evidence to support their continuity or in fact, their existence.

3.2 Subdivision and Structure of the Yilgarn Craton

The Yilgarn Craton can be subdivided into eight domains (Fig.1), each of which contains two or more of the crustal elements: undivided gneiss-migmatite-granite, banded gneiss, sinuous gneiss, greenstone, and granite plutons. For simplicity, and where appropriate, the domains have been assigned the name of the corresponding geological province. Boundaries between the domains are based on abrupt changes in average magnetisation, and anomaly abundance, variability, and orientation; in short, inferred changes in crustal composition.

Narryer domain

The Narryer domain is located in the northwest of the Yilgarn Craton and correlates approximately with the Narryer Gneiss Complex of Myers (1990). The domain is composed of poor to highly magnetised gneiss that is cut by numerous poorly magnetised faults. Metasedimentary belts are sparsely distributed throughout the domain. Some of these belts contain very highly magnetised BIF giving rise to similar appearance in aeromagnetic images to greenstone belts in the Murchison domain to the south and east. However, the metasedimentary belts are not associated with prominent gravity highs characteristic of basalt rich greenstones in other domains of the Craton. The domain is arcuate with the general strike of inferred lithological banding and major faults oriented northeast in the southwest of the domain and easterly in the northeast of the domain. Faults severely disrupt the structure of the domain. Geologically mapped Archaean granite within the domain ranges from low to high magnetisation and is on the whole poorly delimited in the regional 1500m data. Proterozoic granite, which intrudes the north east of the domain, is moderate to highly magnetised and occurs as oval shaped plutons. The Narryer domain is also intruded by numerous small intrusives of unknown affinity.

Murchison domain

The Murchison domain abuts the Narryer domain to the south and southeast. The domain can be subdivided into three sub-domains with differing characteristics; however, boundaries between the sub-domains are ill defined. In the northwestern sub-domain, approximately equal areas of low and moderate magnetisation correlate with regions of largely undifferentiated gneiss-migmatite-granite. A zone of low magnetisation with some coherent banding incorporates the area of the Murgoo Gneiss and parallels part of the boundary with the Narryer domain to the north west. Elsewhere in the sub-domain, gneissic banding is of relatively short strike length and shows little regional coherency. The northwestern sub-domain is elongate west-southwest – east-northeast and is inferred to have behaved semi-competently during interactions with the adjacent Narryer domain. Greenstone belts are few, appear to be distributed around a core of undivided granite and gneiss, and roughly align with adjacent margins of the sub-domain. Discrete, irregular shaped granite plutons of moderate to high magnetisation are evident.

Undivided gneiss-migmatite-granite of moderate magnetisation is the most abundant component of the central sub-domain. Coherent banding in gneiss is apparent locally, however, there is little overall regional directional control. The sub-domain hosts most of the greenstone belts of the Murchison domain. The greenstone belts are distributed in two main areas, centrally around the 'Yalgoo Dome', and in the north of the domain, along the eastern margin with the Southern Cross domain. There is no single overriding regional alignment of the central greenstone belts. Greenstone trends in areas abutting the 'Yalgoo Dome' parallel the adjacent margin of the dome. This area of the Murchison has some similarity of structural style to granite-greenstone terrane of the Pilbara Craton. Greenstone in the northeast of the sub-domain is grossly aligned north–south and parallel with the adjacent boundary with the Southern Cross domain. Granite plutons of low to moderate magnetisation are particularly abundant in and around the greenstone belts. These intrusives are commonly 5 - 20 km in diameter, ovoid to circular in plan and some exhibit complex zoning.

The southern Murchison sub-domain contains only minor greenstone and is dominantly composed of poor to moderately magnetised undivided gneiss-migmatite-granite. The sub-domain includes some elongate zones of inferred banded gneiss which are of higher average magnetisation than the surrounds. Trends of the banded gneiss zones are variable from north-northwest to north-northeast. The sub-domain also hosts a suite of moderate to highly magnetised granite plutons, commonly 10 to 25 km in diameter. The suite defines a northwest trending belt of approximately 80 km width and stretching from the eastern boundary with the Southern Cross domain to the western boundary of the sub-domain, which coincides with the Darling Fault. There is a weak coincidence between intrusion location and the intersection of the belt with the more northerly trending banded gneiss zones.

Interpretation of the 1500 m aeromagnetic data does not support the existence of a continuous Western Gneiss Terrane (Gee et al., 1981; Myers, 1990) which links the southwest of the Craton with the Narryer Gneiss Complex through the west of the Murchison domain. The eastern boundary of the Murchison domain is poorly defined in the north but is interpreted to bound greenstone to the east and pass between the Windimurra and Narndee intrusive complexes. Farther south the boundary is more evident. In this area, the margin of the domain contains moderately magnetised north to north-northeast trending sinuous gneiss that is truncated by the boundary. The Southern Cross domain to the east is composed of relatively poorly magnetised gneiss-migmatite-granite and northwest to north trending greenstone. This greenstone is also truncated at the boundary.

Toodyay-Lake Grace domain

The Toodyay-Lake Grace domain bounds the Murchison domain to the southwest and southeast. Overall the domain forms a relatively narrow (25 – 80 km) bifurcated belt with dominant north-northwest orientation and of approximately 400 km length. The domain is located to the east of, but grossly parallel to, the Southwest Seismic Zone. Abundant sinuous gneiss is oriented parallel to the local trends of the belt: north-northwest along the main elongation of the domain; north-northeast in the northeast segment. The domain is generally of higher magnetisation than surrounding domains however the area of the Jimperding Metamorphic Complex in the northwest is relatively poorly magnetised. The regional aeromagnetic data resolves only a few low to moderately magnetised granite plutons in the domain although geologically mapped granite is widespread.

South West domain

The South West domain occupies the southwest corner of the Yilgarn Craton and is bounded to the west by the Darling fault and Perth Basin, and to the South by the Proterozoic Albany-Fraser Province. The domain is largely composed of undivided gneiss-migmatite-granite of low to moderate magnetisation and with only minor compositional banding evident. A small region located in the south west of the domain with more common compositional banding, and of low average magnetisation, correlates with the area of the Balingup Metamorphic Complex. Boundaries of the Complex with the surrounding domain are poorly defined. Several large plutons of moderate to highly magnetised granite are located along the western margin of the domain. Elsewhere in the domain, plutons are rare or at least not well resolved in the regional 1500 m aeromagnetic data. The domain hosts relatively little greenstone and that present is also poorly resolved (e.g., Saddleback Greenstone Belt).

Southern Cross domain

The Southern Cross domain extends north–south across the Yilgarn Craton to the east of the Murchison and Toodyay-Lake Grace domains. Large regions of undivided gneiss-migmatite-granite are of lower average magnetisation than similar rocks in adjacent domains. The domain includes localised areas of more highly magnetised gneissic banding. Greenstone belts are relatively common throughout the domain and exhibit differences in magnetisation attributed to variations in lithology. Greenstone in the north of the domain contains abundant, very highly magnetised, banded iron formation. The gross appearance of the area of the belts in images of the aeromagnetic data is very similar to that associated with greenstone of the Murchison domain. Greenstone in the southern half of the domain contains fewer highly magnetised units. The greenstones are distributed as long sinuous belts oriented northwest to northeast. Granite plutons and granite-gniess domes of low to moderate magnetisation are particularly common in and around the greenstone belts. Several plutons of moderate to high magnetisation are also mapped in the areas of undivided gneiss-migmatite-granite.

Yeelirrie domain

The Yeelirrie domain is located between the Southern Cross and Eastern Goldfields domains. Undivided gneiss-migmatite-granite is moderate to highly magnetised and forms lensoidal regions commonly bounded by banded gneiss and shear zones. Elongation of the banded gneiss, and the orientation of shear zones are commonly aligned to the north-northwest, north, or to the north-northeast. Greenstone is spatially associated with the shear zones is but is preferentially oriented only in the north-northwest and north orientations. Granite plutons are moderately common in and around the greenstone belts and far less evident in regions of undivided gneiss-migmatite-granite.

Lake Johnston domain
The Lake Johnston domain abuts the Yeelirrie domain to the southeast and is also largely composed of moderate to highly magnetised gneiss-migmatite-granite. Sparse and relatively small greenstone belts, elongate to the northwest, provide limited information on the structure of the domain. Gneissic banding is rare. Poorly magnetised lineaments are common and some of the more prominent sets are oriented east-northeast, north-northeast, and north-northwest. Few granite plutons are resolved in regional data, however, more are evident in proprietary 200 m data covering the eastern part of the Boorabbin Sheet.

Eastern Goldfields domain
The Eastern Goldfields domain occupies the eastern third of the Yilgarn Craton. The domain is readily subdivided into two main areas, the Norseman –Wiluna Belt (Gee, 1979) in the west with abundant greenstone, and felsic dominated crust of the eastern gneiss sub-domain to the east.

Greenstone accounts for nearly 50 percent of the Norseman-Wiluna Belt. Three sub-domains composed largely of gneiss-migmatite-granite and banded gneiss are defined within the Belt, the Yandal, Ballard and Laverton sub-domains (Williams & Whitaker, 1993). These sub-domains have grossly similar characteristics being of low to moderate magnetisation with few internal boundaries and rare granite plutons. The sub-domains are separated by greenstone, but may be related crust that is in sheared contact at depth. Most greenstones in the Norseman-Wiluna Belt are poorly magnetised however highly magnetised ultramafic units provide some detail of the internal structure of the belts. Highly magnetised banded iron formation is much less abundant than in greenstone belts of the Southern Cross and Murchison domains. Margins of the greenstones are largely in concordant contact with the boundaries of the gneiss-migmatite-granite rich sub-domains. Granite plutons are abundant within the greenstone belts. The magnetisation of the plutons ranges from low to high and several are zoned with higher magnetisation in the outer margins. Many plutons are spatially associated and form elongate intrusive corridors that are grossly aligned with the dominant north-northwest regional trends.

The eastern gneiss sub-domain is largely composed of moderately magnetised, undivided gneiss-migmatite-granite with some banded gneiss. Relatively small greenstone belts are spatially associated with widely spaced shears. Abundant granitic and gneissic domes are mapped in 200 and 400 m aeromagnetic data along the margin of, and immediately to east of the Norseman-Wiluna Belt. Many of these structures were not evident in 1500m data coverage of the region. An east–west elongate area of sinuously deformed granitic gneiss truncates a north-northwest trending greenstone belt at the boundary between the Rason and Minigwal Sheets. The relationships in this area are at the very least unusual and not readily reconciled with the structural history described for the southern part of the Norseman-Wiluna Belt (e.g., Swager, 1997). Farther east, the sub-domain is cut by a large shear system that extends from Minigwal in the south, north-northwest to the southeast corner of Kingston. The shear system exceeds 20 km in width on the Rason Sheet and approximates the eastern limit of sub-cropping Archaean rocks. Greenstone is spatially associated with the shear system. Banded gneissic rocks of moderate to high magnetisation lie to the east of the shear system on the Rason Sheet. The gneissic banding defines an 80 by 40 km east–west elongated dome like structure that is coincident with a low amplitude gravity high. To the south, numerous poor to moderately magnetised granite plutons intrude undivided gneiss-migmatite-granite. To the north, inferred banded iron rich greenstone and granitic rocks underlie thick Proterozoic and Phanerozoic sediments.

4. Geochemical classification of granitoids in the northern Eastern Goldfields and links with geophysical characteristics

Interpretation of the regional aeromagnetic data suggests that considerable strain partitioning occurred throughout the Eastern Goldfields Province. The structural classification of granites (e.g., Witt & Davy, 1997) is, therefore, considered to be of limited use in understanding relationships including relative timing of intrusion. Champion & Sheraton (1997) defined five geochemical groups for the northern Eastern Goldfields and these will be used to discuss granite distribution and geophysical characteristics. The geochemical groups comprise High-Ca, Low-Ca, High-High Field Strength Elements (HSFE; Ti, Fe, Zr, Y), Mafic, and Syenitic types. Of these groups, the High-Ca and Low-Ca granite types are the most widespread and abundant.

High-Ca group (Menangina Association)

High-Ca group granites occur throughout both gneiss-migmatite-granite and greenstone domains. On present evidence they constitute the main component of the banded gneiss domains. Average magnetisation of the group ranges from poor to moderately high with most bodies uniformly magnetised except for crosscutting poorly magnetised fault and shear zones. Large plutons with strongly zoned magnetisation located in greenstone belts belong to the group as do the northern members of a linear association of similarly magnetised and weakly zoned granites, the Boyce domain of Williams & Whitaker (1993). The zoned granites have undergone fractional crystallisation with more mafic, highly magnetised, and often porphyritic margins which grade to more felsic, poorly magnetised and equigranular cores. Susceptibilities of the High-Ca group commonly occur in the range 5 to 1100 x 10^{-5} SI and can show variations of 300 to 1500 x 10^{-5} SI within a zoned pluton. Outcrops of these granites correlate with relative K channel anomalies, which display red in composite normalised K-Th-U (Red-Green-Blue) gamma-ray spectrometric images.

Low-Ca group (Mt Boreas Association)

The Low-Ca group occurs most commonly in the gneiss-migmatite-granite domains with a lower incidence (inferred; outcrop dependant) in the banded gneiss domains and rare examples from within the greenstone domains. The magnetisation of individual bodies in the group is generally uniform and ranges from poor to moderately high. Susceptibilities of 40 to 1600 x10^{-5} SI are common. There is some evidence for thin sheets of poorly magnetised Low-Ca granite (e.g., in the Yeelirrie domain; Yeelirrie 1:100 000 sheet) overlying more highly magnetised High Ca granite in the gneiss-migmatite-granite domains. In these areas, the change from High- to Low-Ca granite corresponds with a small but general lowering of average magnetisation and anomaly contrasts, and lower average gravity values. Outcrops of Low-Ca granite correlate with relative K, Th and U anomalous areas which display white in composite, normalised K-Th-U (Red-Green-Blue) gamma-ray spectrometric images. Total Count spectrometer readings over 150 c.p.s. from within gneiss-migmatite-granite domains are inevitably associated with Low Ca granites

High-HFSE group (Kookynie Association)

The High-HSFE granite group has only been found in, or marginal to, the greenstone domains. At least two of the occurrences are interpreted as deformed thin sheets that partially overlie greenstone. The magnetisation of the HSFE suite is low to moderate and the susceptibilities measured fall in the range of 10 to 350 x10^{-5} SI. One of the High-HFSE sheet-like bodies (near Yundamindera on the Edjudina Sheet) shows variability in magnetisation, however, it is unclear whether this is due to variations in original composition or loss of magnetisation associated with structural deformation or alteration. A radiometric signature has not been determined for this suite but is expected, on geochemical grounds, to be similar to the High Ca suite (red in K-Th-U ternary images).

Mafic group (Granny Smith Association)
The Mafic granite group, commonly intruded as small plutons and dykes, is dominantly found within the greenstone domains. With the exception of the Granny Smith and Liberty Granodiorites, the bodies are too small or too poorly magnetised to be resolved in the regional aeromagnetic data. Mafic granite intrudes High Ca granite at a number of localities. There is a common spatial association of the group with mineralisation in the Eastern Goldfields. Measured susceptibilities are quite variable and range from 40 to 1500 $x10^{-5}$ SI. A characteristic radiometric signature has not been determined for the group.

Syenites (Gilgarna Association)
The syenite group has largely been sampled from within the greenstone domains or within granite adjacent to the greenstone domains. Many of these bodies are associated with small area, moderate to high amplitude, 'bulls eye' type anomalies. Numerous anomalies of similar style and of either normal or reverse polarity occur through out all geophysical domains but may be caused by intrusives other than the syenite group. The measured susceptibilities of syenites have the greatest range for the granitoids (30 to 3500 $x10^{-5}$ SI). Some outcrops of syenite correlate with areas of yellow on ternary K-Th-U gamma-ray spectrometric images which is indicative of anomalously high K and Th relative to U. Syenites east of Laverton correlate with regions of white in the same images and have high K, Th, and U, relative to surrounding rocks and surface materials.

From the above overview it is apparent that the aeromagnetic data do not effectively discriminate the main geochemical groups of the granite classification. This said, zoned plutons and banded gneiss generally belong to the High-Ca group. The gamma ray spectrometric data can discriminate between High-Ca and Low-Ca granite groups but not between Low-Ca and Syenitic groups. The general lack of outcrop of the Yilgarn Craton also seriously limits the potential value of the gamma-ray data.

As far as gold prospectivity is concerned, mineralised granite is not uniquely magnetised (Granny Smith granodiorite– remanent magnetisation, Tarmoola granite – poorly magnetised, Liberty Granodiorite – moderately magnetised, Jupiter syenite – highly magnetised. Furthermore, some of the mineralised intrusives are not resolved or evident in the regional geophysical data (e.g., Tarmoola granite, the mafic granite at Golden Cities, the mafic dyke at Kanowna Belle). The aeromagnetic data do at least provide the boundaries (limits) for many plutons for which geochemical and isotopic attributes can be assigned to aid regional analysis.

5. Synopsis

- Crust of the Yilgarn Craton is characterised by five main crustal elements (geophysical map units): granite plutons, gneiss-migmatite-granite, banded gneiss, sinuous gneiss, and greenstone.
- Granite plutons are particularly abundant in the area of the Norseman-Wiluna Belt and in a northwest trending belt in the Southern Murchison domain.
- The resolution of 1500 m aeromagnetic data is inadequate to reliably map granite plutons as many are relatively small and have low magnetisation contrast with surrounding rocks.
- Dislocation features include both shears and faults. Shears are associated with the greatest demonstrable movements (30-50 km) while faults are associated with relatively minor movements (<less than 5 km).

- Current geologically-defined province boundaries cut across crustal elements and, in many instances, across domains where there is no geophysical evidence for changes in crustal composition.
- Eight large domains equivalent to geological provinces are defined: Narryer, Murchison, Toodyay-Lake Grace, South West, Southern Cross, Yeelirrie, Lake Johnston, and Eastern Goldfields domains.
- Norseman-Wiluna belt is a craton scale, 200 km wide, shear zone.
- Aeromagnetic data does not effectively distinguish the granite geochemical groups.
- Granite plutons hosting gold mineralisation are not uniquely magnetised.

Acknowledgments

There are many people from the sponsor companies who I would like to thank for valued discussion, and access to detailed data during the course of the past three and a half years. In that some of these individuals would prefer to remain anonymous, I wish to at least acknowledge the support of their companies - in particular Delta, Goldfields, Great Central, Herald, MPI, Normandy, North and WMC. I also wish to acknowledge Stockdale and Pitt Research, non-sponsor companies, for recently providing access to all of Stockdale's digital aeromagnetic and radiometric data coverage of the Yilgarn Craton.

References

Archibald, N.J., & Bettenay L.F., 1976. Indirect evidence for tectonic reactivation of a pre-greenstone sialic basement in Western Australia, *Earth and Planetary Science Letters* 33, 370 – 378.

Binns, R.A., Gunthorpe, R.J., & Groves, D.I., 1976. Metamorphic patterns and development of greenstone belts in the eastern Yilgarn Block, Western Australia. In: Windley, B.F., (Ed.), *The early history of the earth.*. Wiley, London, 303-313.

Champion, D.C. & Sheraton, J.W., 1997. Geochemistry and Sm-Nd isotope systematics of Archaean granitoids of the Eastern Goldfields Province, Yilgarn Craton, Australia: constraints on crustal growth. *Precambrian Research*, **83**, 109-132.

Fairclough, M.C., & Brown, J.C., 1998. Tarmoola gold deposit, In: D A Berkman and D H MacKenzie (Eds.) *Geology of Australian and Papua New Guinean Mineral Deposits* 173 – 178. The Australasian institute of mining and metallurgy: Melbourne.

Gee, R.D., 1979. Structure and tectonic style of the Western Australian shield. *Tectonophysics*, **58**, 327-369.

Gee, R.D., Baxter, J.L., Wilde S.A., & Williams, I.R., 1981. Crustal development in the Archaean Yilgarn Block, Western Australia. *Special Publications, Geological Society of Australia* **7**, 43-56.

Kehal, H., Stephens, J., Anderson, A., Shrimpton, K., Harris, S., & Osborne, M., 1999. Golden cities – The discovery of gold deposits in Archaean Granite In: *New Generation Gold Mines* 61-74. Australian Mineral Foundation Glenside SA.

Myers, J.S., 1990. Western Gneiss Terrane. In: Geology and Mineral Resources of Western Australia. *Geological Survey of Western Australia, Memoir* 3, 13-31.

Myers, J., 1995. The generation and assembly of an Archaean supercontinent: evidence from the Yilgarn Craton, Western Australia, In *Early Precambrian Processes*, eds, Coward, M.P., & Ries, A.C., *Geological Society of London, Special Publication* **95**, 143-154.

Myers, J.S., 1997. Archaean geology of the Eastern Goldfields of Western Australia - regional overview. *Precambrian Research*, **83**, 1-10.

Swager, C.P., 1997. Tectono-stratigraphy of late Archaean greenstone terranes in the southern Eastern goldfields, Western Australia. . *Precambrian Research*, **83**, 11-42.

Thom, R., & Barnes, R.G., 1977. Leonora, W.A. West Australian Geological Survey, 1:250 000 Geological Series explanatory notes.

Trendall, A.F., 1990. Cratons. In: Geology and Mineral Resources of Western Australia. *Geological Survey of Western Australia, Memoir* 3, 11-13.

Whitaker, A.J., 1993. Regional geophysical constraints on tectonic models for the Eastern Goldfields province. *In*: Williams, P.R., & Haldane, J.K. (Compilers) :*An International Conference on Crustal Evolution, Metallogeny and Exploration of the Eastern Goldfields*. Australian Geological Survey Organisation, Record **1993/54**, 63-67.

Whitaker, A.J., 1997. Granite-greenstone structures from regional geophysics in the northern Eastern Goldfields. *In*: Cassidy, K.F., Whitaker, A.J. & Liu, S.F., (Compilers) *An International Conference on Crustal Evolution, Metallogeny and Exploration of the Yilgarn Craton - An Update*. Australian Geological Survey Organisation, Record **1997/41**, 21-26.

Wilde, S.A., Middleton, M.F., & Evans, B.J., 1996. Terrane accretion in the southwestern Yilgarn Craton: evidence from a deep seismic crustal profile. *Precambrian Research*, **78**, 179-196.

Williams, P.R., & Whitaker, A.J., 1993, Gneiss domes and extensional deformation in the Archaean Eastern Goldfields Province, Western Australia, *Ore Geology Reviews*, **8**, 141-162.

Witt, W.K. & Davy, R., 1997. Geology and geochemistry of granitoid rocks in the Southwest Eastern Goldfields Province. *Geological Survey of Western Australia*, Report 49.

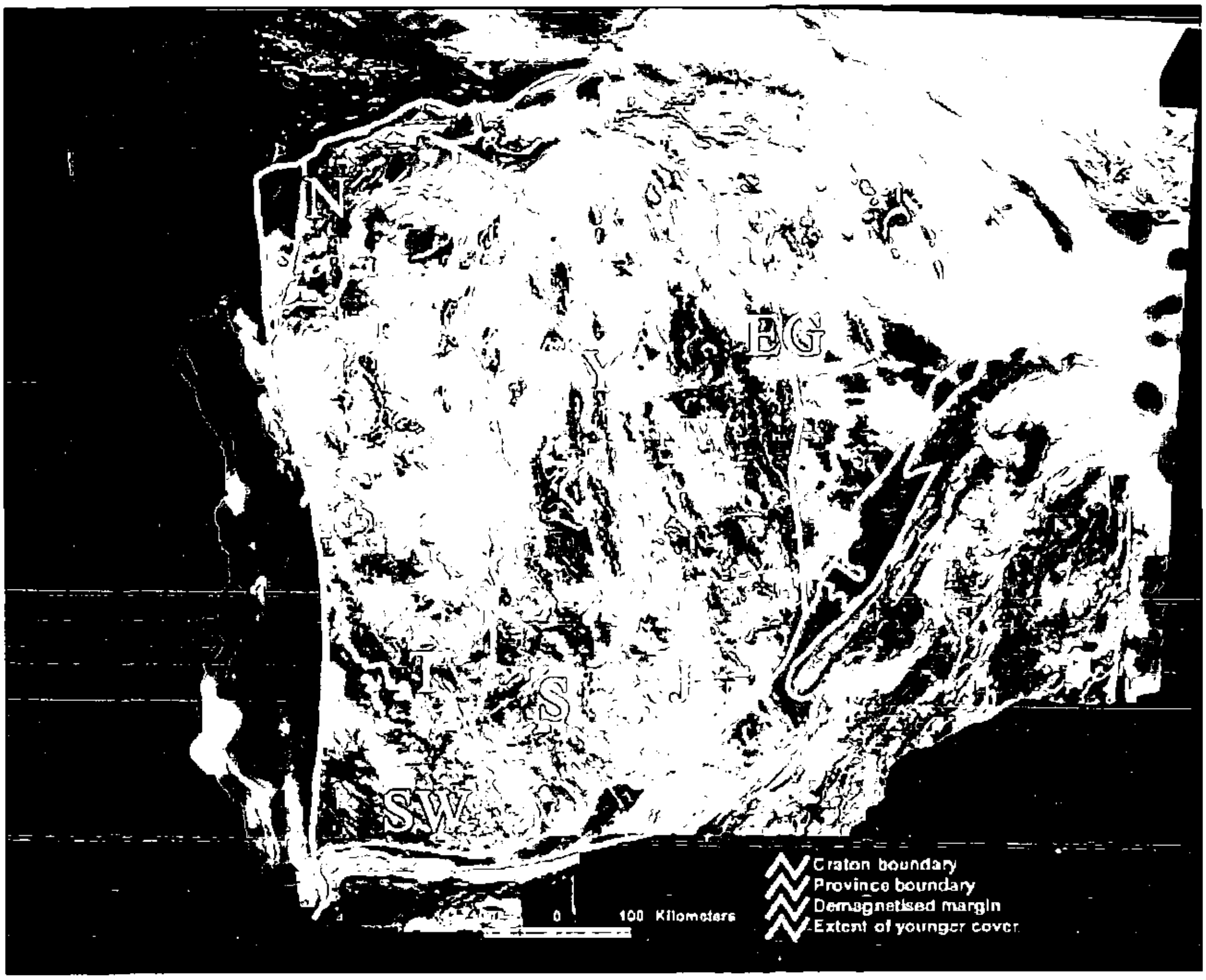

Figure 1. Total Magnetic Intensity image of the Yilgarn Craton, with domain boundaries superimposed. N - Narryer, M - Murchison, T - Toodyay/Lake Grace, SW - South West, S - Southern Cross, Y - Yeelirrie, J - Lake Johnston, EG - Eastern Goldfields, NW - Norseman-Wiluna belt.

Chapter 2.
Granites of the northern Eastern Goldfields: their distribution, age, geochemistry, petrogenesis, relationship with mineralisation, and implications for tectonic environment

(including a simplified key for discriminating granite groups in the northern Eastern Goldfields)

David C. Champion & Kevin F. Cassidy

Introduction

Champion & Sheraton (1993), studying the granites in the Leonora-Laverton region recognised 5 main granite groups (Table 7). More recent work (Champion & Sheraton, 1997; the current AMIRA P482 study), covering the whole of the northern Eastern Goldfields, comprising the northern Eastern Goldfields Province and the northwestern part of the Southern Cross Province, has confirmed and extended these granite groups (Fig. 1), with the identification of 24 clans within the five groups (Tables 1 to 6; Fig. 12). This latter work has proceeded simultaneously with the gathering of SHRIMP U-Pb geochronology, e.g., Nelson (1995, 1996, 1997, 1998, 1999); L. Black (written communication, 2000), AMIRA P482, such that over 60 ages are now available for granites of the northern Eastern Goldfields, for all granite groups (see Table 2). The combination of granite geochemistry and petrogenesis, with the geochronological data, is not only providing an overall framework for the region, but also insights of the finer detail, now emerging from the larger data sets.

This chapter systematically lists and details all groups, associations and clans of the northern Eastern Goldfields Province, and the easternmost part of the Southern Cross Province, i.e., Leonora, Laverton, Sir Samuel, Duketon, Wiluna, Kingston and Nabberu 1:250 000 sheets (collectively referred to as the northern Eastern Goldfields). A standard format is used for all entries. This covers distribution, geochronology, chemical characteristics, related mineralisation (if any), and includes a brief summary on petrogenesis and tectonic implications. The latter should be considered speculative, given the difficulties of assigning tectonic environment from granites alone, and the uncertain nature of plate tectonics in the Archaean. Similarly, petrogenesis and granite source rocks are treated in a simplified manner, mostly assuming a one- or two-component source, thereby facilitating a more coherent and more easily understood comparison between clans and groups etc. Also to assist in descriptions of distribution etc., the granites of the northern Eastern Goldfields have been subdivided into informal granite masses, bound by large-scale faults or greenstones (Fig. 1). These include the Yeelirrie, Raeside, Koonoonooka, Teutonic, Banjiwarn and the Cosmo masses. As expected given the structural grain of the region, the majority of these masses are elongate to the NNW. The boundary between the Eastern Goldfields Province and the Southern Cross Province, separating the Yeelirrie and Raeside masses (Fig. 1), is taken as the position of the Ida lineament. For the detailed distribution of associations and clans, the reader is referred to the accompanying 1:500 000 and smaller scale maps (on CD); the distribution of the granite groups is shown on Fig. 1.

The following section describes clans under the respective granite group, with individual clan descriptions following a more detailed description of the whole group. All five groups are discussed first as a whole – this effectively providing an overall summary of the granites of the northern Eastern Goldfields.

Also provided, in the last section, are simplified keys to aid recognition of granite groups from field and mineralogical data, and from geochemical data; these are accompanied by descriptions of the general methodologies involved.

Granite groups of the northern Eastern Goldfields

Member groups: High-Ca (Menangina & Diemals associations), Low-Ca (Mt Boreas & Beetle associations), Mafic (Granny Smith association), High-HFSE (Kookynie association), Syenitic group (Gilgarna association)

Distribution: The distribution of granites groups within the northern Eastern Goldfields is shown in Figure 1, from which a number of features are evident:

- both the High-Ca and Low-Ca groups make up the bulk of the granites in the region, occurring in all granite masses. This includes representatives in the Southern Cross Province (in the Yeelirrie mass, Fig. 1). Although members of both groups are commonly spatially associated, there are obvious zones where only one group dominates, e.g., Low Ca group in Yeelirrie mass.
- the High-HFSE group is strongly localised along a NNW zone encompassing the Teutonic mass, the margins of the Koonoonooka mass, and the greenstones around these two masses (Fig. 1)
- the Mafic group is largely confined to within or marginal to the greenstones, and comprises a widespread but small component of the granites as a whole.
- the Syenitic group occurs both within the greenstones and within the granite masses (e.g., Banjiwarn). The larger Syenitic group units appear to be concentrated broadly along the Celia lineament (roughly the western boundary of the Banjiwarn mass), and in a NNW zone within the greenstones between the Cosmo and Banjiwarn masses (in the Laverton region; Fig. 1).

Geochronology: Over 60 ages are now available for the granites of the northern Eastern Goldfields (Table 2), with the following observations:

- The majority of ages lie between 2700 and 2630 Ma, i.e., younger than the oldest greenstones in the region, though there are several older units around 2735 Ma and at 2760 Ma
- there is a pronounced peak, in granite ages, for the Eastern Goldfields Province, around 2670 to 2660 Ma, tailing off to 2630 Ma. This contrasts with the Southern Cross Province which appears to have a dearth of granitoids in the range 2670 to 2660 Ma
- the majority of High-Ca granites, in the Eastern Goldfields Province, give ages between 2680 and 2660 Ma; High-Ca granites in the Southern Cross Province appear to be slightly older (2680 to 2700+ Ma)
- the Low-Ca granites, in the Eastern Goldfields Province, lie between 2655 and 2637 Ma; a slightly more expanded range is evident in Low-Ca granites within the Southern Cross Province (2660 to 2630 Ma). Therefore, unlike the High-Ca magmatism, there is good evidence that Low-Ca magmatism was largely synchronous across both provinces (and the Murchison Province)
- the majority of Mafic granites in the northern Eastern Goldfields, especially those in the Granny Smith Clan, have ages within error of 2665 Ma
- the High-HFSE group granitoids span a large range from 2700 to 2658 Ma, and may include an age of 2738 Ma
- the Syenitic group appears to form a bimodal age distribution,, i.e., ca. 2665 Ma, and 2650 to 2640 Ma
- there is a change, around 2655 Ma from largely High-Ca magmatism to dominantly

Low-Ca and Syenitic magmatism.

The general sequence with relationship to greenstones and granite groups can be summarised as follows:

Ca. 2760 Ma Trump granodiorite, Raeside mass; High Ca group

2730-40 Ma Kathleen Valley gabbro (Mafic group), and Satisfaction Complex (High-HFSE group), both probably dating greenstone formation ages

2720-2670 Ma Greenstone, basaltic and felsic volcanism

2705 Ma Komatiitic magmatism

2700-2670 Ma Increasing High-Ca magmatism with decreasing age; also High-HFSE magmatism (& felsic volcanism) throughout this range, though mostly at 2690 to 2680 Ma

2670-2660 Ma Voluminous High-Ca magmatism, also Mafic, Syenitic, and minor High-HFSE group magmatism. Peak of magmatism in the Eastern Goldfields Province. Apparently only minor magmatism at this time in the Southern Cross Province.

2660-2630 Ma Long period of magmatism in the Eastern Goldfields Province. High-Ca, Mafic? and minor HFSE magmatism? to 2650 Ma and slightly younger. Voluminous and very widespread Low- Ca magmatism, across the Eastern Goldfields Province, and the Yilgarn. In the Eastern Goldfields Province accompanied by syenitic (and carbonatitic) magmatism.

Chemical characteristics: The geochemistry of the granite groups is discussed in detail under the relevant groups in the following section, and in the granite keys section. A number of broad generalisations can be made concerning possible trends:

- both the High-Ca and Mafic groups exhibit a marked range in the LILE and some of the HFSE. Similar, but smaller ranges in the LILE are evident in the Low-Ca and High-HFSE groups. The available geochronological data, although limited, appears to indicate a general trend of increasing LILE contents with decreasing ages, i.e., high-LILE clans are generally younger than, or of similar age to, low LILE clans. This trend mirrors that seen in the change from High-Ca to Low-Ca magmatism.
- the younger magmatism, post 2.655 Ma is markedly more potassic and LILE enriched, reflecting the change to Low-Ca and Syenitic group magmatism
- there are no significant differences between clans of the High-Ca and Low-Ca groups in the Southern Cross Province and Eastern Goldfields Province, i.e., chemically very similar clans can be found in both provinces. In addition, all groups, with the exception of the Syenitic group, occur within both provinces.

Mineralised members: Examples of granitoids hosting gold mineralisation or closely spatially associated, can be found in all granite groups, with the exception of the Low-Ca group. Examples of granitoids directly hosting significant gold mineralisation occur most commonly within the Mafic group, especially the members of the high LILE Granny Smith clan, e.g., Granny Smith, Lawlers, Porphyry, Liberty, Golden Cities. Members of the Mafic group, therefore, appear to be favoured hosts, although examples can be found within the High-Ca (Tarmoola) and Syenitic (Jupiter, Wallaby) groups as well. There appears to be no obvious features common to all granitoids hosting gold mineralisation (Champion & Cassidy, 1998), although nearly all of them fall within the lower silica compositional range (mostly <70% SiO_2, with higher Fe etc); the one major exception being the Tarmoola granite.

Petrogenesis: Petrogenetic models are discussed in detail for each group in the following section; results can be summarised as follows:

- the general characteristics of the High-Ca granites (low LILEs, sodic, Sr-undepleted) indicate derivation, at high pressures (>10 kbar), from a mostly mafic (broadly basaltic/amphibolitic), LILE-poor source. The range in the LILE and HFSE (between clans), however, indicates a more complex model, i.e., the involvement of at least two-components, either as a heterogeneous source (basaltic to quartz dioritic), or by some other process (assimilation of pre-existing crust, magma-mixing etc).
- the potassic, high LILE, high HFSE, Sr-undepleted nature of the Low-Ca group is most consistent with derivation, at moderate pressures (<10 kbars) from a relatively potassic and LILE-rich crustal source, i.e., reworked continental crust with compositions not unlike typical Archaean tonalites. A number of features, though, e.g., low CaO, very minor occurrence of amphibole, indicate partial melting was either via small volume melts or from a source with only minor amphibole. Additionally, the high levels of the HFSEs, in particular Zr, indicate high melting temperatures, suggesting elevated thermal gradients.
- the combination of high HFSE and low to moderate LILE, suggests the High-HFSE group granites were derived from LILE-poor, mafic to intermediate compositions. The more felsic clans within the group (Satisfaction, Kookynie) possibly represent fractionates of rocks similar in composition to the more mafic Bullshead clan of the group. The chemistry of the group (elevated Fe, Zr, Y), is also consistent with A-type granitoids in general, indicating high-temperature melts. The Sr-depleted, Y-undepleted nature of all members of the group, strongly imply generation at only moderate pressures, i.e., <10 kbars (<35 km thick), while the Sm-Nd isotope data indicate significant involvement of pre-existing crustal rocks in the generation of the High-HFSE granites. It is also evident that members of the High-HFSE group, especially the less siliceous ones, have some similarities to the members of the Kathleen Valley and Sweet Nell clans (Mafic group), possibly implying some minor involvement of such rocks in the history of the High-HFSE granites
- petrogenetic models for the Mafic group granites are largely equivocal, with evidence for both crustal and mantle-derived contributions. Notably, the variation in the LILE and LREE (between and within clans), requires at least two separate components, e.g., a mafic 'basaltic' source, (like the High-Ca source), and a more mafic, perhaps mantle-derived, LILE-rich source component. The origin of the LILE-rich component is equivocal, although the overlap of ages (ca. 2665 Ma), between the high LILE Mafic and some Syenitic group magmatism, indicates a possible source of, at least part of, the LILE and LREE enrichment. The minor Kathleen Valley and Sweet Nell clans of the Mafic group largely represent fractionates from a basaltic, tholeiitic parent.
- like the Mafic group, the petrogenesis of the Syenitic group is also equivocal with regards to the relative contributions of mantle versus crustal components, though, at least a significant crustal contribution, is implied by features such as lack of associated mafic rocks, the presence of quartz, the mostly high LILE contents, inherited? zircons, and strong negative Nb and Ti anomalies. Additionally, it is evident, that at least locally, some form of lower crustal/mantle lithosphere metasomatism has also contributed to the generation of the Syenitic group, evidenced by strong Ba and Sr enrichment in syenites around the Kambalda region, and in the Wallaby and Jupiter deposits. In these regions, the syenites are spatially associated with lamprophyric and carbonatitic magmatism, respectively.

Tectonic and other implications: The following discussion is a summary of the tectonic implications as indicated by the granite petrogenesis and geochronology. More detailed discussions of tectonics are given for each granite group in the next section.

The high pressure origins for the majority of the High-Ca granites (10-15 kbars), indicate derivation either deep within a thickened crust (>35-50 km) or, perhaps, from melting of a subducting slab. Available evidence, e.g., inherited zircons, Sm-Nd isotopic data, favour a thickened crust as the source. Regardless, both hypothesis appear to require the operation of some form of convergent tectonics in the Eastern Goldfields Province. Given the range in ages of the High-Ca group, such an environment would appear to have been operative, at least intermittently, from 2.7 Ga and earlier (including perhaps at 2760 Ma), but especially in the period 2.68-2.66 Ga, consistent with the D_2 compression event.

Further it is apparent, that whatever the tectonic environment was at 2680-2660 Ma, it didn't appear to produce significant magmatism at this time in the Southern Cross Province. The majority of High-Ca magmatism in the latter appears to have been earlier (>2700 to 2680 Ma). These differences may reflect a number of possible scenarios: 1) the Southern Cross Province was separate from the Eastern Goldfields Province before and/or during this period; 2) the thermal regime at this time was such that granite production was largely confined to the Eastern Goldfields Province, such as in a typical modern-day convergent environment; or, 3) the change across the two provinces is actually diachronous, as in a migrating arc-environment. Clearly further geochronology is needed, particularly along the eastern margin of the Southern Cross Province.

Finally, the large volume of High-Ca granites in the region require a correspondingly larger source (3 or more times volumetrically larger), implying, if indeed the High-Ca granites were largely crustal in origin, a very significant volume of pre-existing crust of basaltic to andesitic composition. Notably the Sm-Nd isotopic data suggests this crust is younger than the sources of the Low-Ca magmatism.

The simplest model for the Low-Ca granites is that they were generated from moderately dry tonalitic (or more felsic) pre-existing crust, in an extensional environment with an elevated geothermal gradient. This is clearly contrary to the High-Ca granites, indicating not only distinct source rocks, but distinct sites of granite generation for the two granite types, consistent with available Sm-Nd isotopic data. These differences are even more significant given the temporal change around 2660 to 2650 Ma, from voluminous dominantly High-Ca magmatism to less voluminous, but very widespread, dominantly Low-Ca (and Syenitic) magmatism. This changeover in magmatism most probably indicates a corresponding change in tectonic environment, presumably from a compressional or arc-related environment to one dominated by extension (and higher geothermal gradients), i.e., some mechanism produced a change in the thermal regime, that not only increased the thermal gradient (to allow generation of Low-Ca granites) but effectively turned off production of High-Ca granites.

The exact nature of this tectonic transition is largely dependent on the origin of the High-Ca granites. If the High-Ca granites were generated in thickened crust, then melting shifted to higher crustal-levels (the site of Low-Ca generation), with the thickened lower crust (High-Ca source) either somehow insulated from further melting or removed. The latter is favoured given the apparently higher geotherm required for the Low-Ca granites. In this regard, Smithies & Champion (1999) suggested that this post 2655 Ma thermal event may have resulted from lower-crustal delamination following the D_2 shortening deformation, perhaps heralding an additional tectonothermal event in the eastern Yilgarn

Craton, contemporaneous with lower-middle crustal high-grade metamorphism and regional Au mineralisation (e.g., Kent et al. 1996). If, however, the High-Ca granites were largely generated by slab-melting, then the change over to Low-Ca (and syenitic) magmatism may simply reflect some form of wide-scale extension, perhaps not unlike that presently operating in the Basin and Range province in the western United States, although with some differences.

The close spatial, temporal, and, at least locally, genetic, relationship between the High-HFSE granites and volcanics (pre 2700 to 2680 Ma), indicates that these granites were intimately related to greenstone formation, consistent with the A-type geochemistry of the High-HFSE granites which suggest emplacement in an extensional environment (Champion & Sheraton, 1997). The ages of these granites, mostly 2700 to 2680 Ma, can be used, therefore, to indicate periods of extension, most likely localised extension, given the overlap with High-Ca magmatism (especially if the latter were generated in thickened crust). The possible 2738 Ma age on part of the Satisfaction Complex (Nelson, 1998) may also signify an, earlier period of greenstone development in the northern Eastern Goldfields, consistent with the age of the Kathleen Valley clan (Mafic group). In a similar manner, the 2658 Ma age of the Weebo granodiorite (Nelson, 1997), may well have been related to the same locally-extensional environment that was responsible for the 2665 Ma syenites.

In this regard, it was originally envisaged, that many of the Mafic group granites, especially those generated around 2665 Ma were produced in some form of arc-environment, co-incident with the proposed main period of crustal shortening (D_2) in the Eastern Goldfields Province. The evidence for, at least locally, spatially associated Syenitic and, perhaps High-HFSE group magmatism, of similar age, however, raises the possibility, that all granitoids of this age were produced in a similar (locally?) extensional environment. Note that this could still be in an overall arc-environment.

The granitoids of the Kathleen Valley and Sweet Nell clans, were undoubtedly generated in periods of greenstone deposition and development, indicating, for the Kathleen Valley clan at least, greenstone formation around 2737 Ma.

As indicated by Smithies and Champion (1999), alkaline and sub-alkaline rocks such as those in the Syenitic group are good indicators of regions undergoing, at least local, extension, or an anorogenic (post-tectonic) environment. The timing and locations, therefore, of members of the Syenitic group provide some constraints on the tectonic evolution of the Eastern Goldfields Province. In this sense, the 2650 to 2640 Ma syenites, like the Low-Ca group, indicate a significant change in tectonic environment in the period 2660 to 2655 Ma, from voluminous, possibly arc-related, High-Ca magmatism, to 'post-tectonic', or extensional, Low-Ca and Syenitic magmatism.

Also of importance, is the recognition of syenitic magmatism around 2665 Ma that must reflect some form of rifting and/or local extension, as discussed earlier.

Finally, the presence of Archaean carbonatitic magmatism, closely spatially associated with the younger Mt Weld carbonatite, strongly suggests the existence of a major deep-crustal fault zone within the Laverton region. The possible presence of such a structure has obvious implications for tectonic models for development of the Norseman-Wiluna belt, e.g., perhaps such a fault forms part of a rift-related pair with the Ida Lineament to the west, and for models of fluid flow and mineralisation. Such a fault zone should be clearly visible on the planned seismic traverse for this region.

High-Ca group, northern Eastern Goldfields

Member Associations: Menangina Association (Eastern Goldfields Province)
Diemals Association (Southern Cross Province)

Distribution: The largest granite group within the northern Eastern Goldfields, representing up to and greater than 60% of the total granites (Fig. 1), within both the internal and external granites. Well represented in the Yeelirrie, Raeside, Koonoonooka, Teutonic and Banjiwarn masses. Seven clans have been recognised in the northern Eastern Goldfields Province, and 5 clans in the north-eastern Southern Cross Province (Table 1).

Geochronology: A large number of dated samples, mostly from the Eastern Goldfields Province part of the northern Eastern Goldfields indicate an age range from 2.72 to 2.65 Ga, with the majority falling between 2.685 to 2.66 Ga (Table 2a). Additionally, the geochronology indicates the common presence of inherited zircons, either from the source region or via assimilation of older crustal rocks. Good ages have been recorded from a number of inherited zircon populations, e.g., 2.7 and 2.85 Ga (Table 2a), ages consistent with Nd model ages (Champion & Sheraton, 1997). The available data also indicate strong temporal overlap between the various clans within the group.

Only one age has been determined on the High-Ca granites in the Southern Cross Province region of the northern Eastern Goldfields, with an age of 2679 Ma (Nelson, 1997). A similar age (within error) of 2689 Ma has been recorded for a High-Ca granite just to the south, on the Menzies sheet (Table 2a). Available geochronology for the Southern Cross Province further to the west and south suggests a marked difference between the age distributions of the High-Ca granites for both provinces. In particular, there appears to be a marked dearth of Southern Cross Province granites falling in the 2.67 to 2.66 Ga age range, contrary to the situation in the Eastern Goldfields Province.

Chemical characteristics. Characteristics for this group have been summarised by Champion & Sheraton (1997), and Champion (1997). Basically the High-Ca granites comprise sodic trondhjemite, granodiorite and granite characterised by low to moderate LILE (K_2O, Rb, Pb) and HFSE (LREE, HREE, Y, Zr) contents. In detail individual clans (Table 1), define a quasi-continuous range in LILE and HFSE contents, from low (Beasley clan) to moderate (Union Jack clan, see Figure 2), approaching values seen in the Low-Ca granites (Fig. 6). Given the range in the LILE and HFSE, an arbitrary divide splitting the High-Ca group into low-LILE and high-LILE members has been produced, largely for the basis of classification and descriptive purposes (Fig. 5). It is notable, that this divide can also be used to discriminate between the high-LILE (Granny Smith clan) and low-LILE (Kanowna Belle clan) clans of the Mafic group (Fig. 5).

The majority of granitoids from the High-Ca group are further characterised by moderate to high Sr contents (Sr-undepleted) coupled with low to moderate Y (and HREE) contents (Y-depleted; Fig. 3). However, like the LILE, there is a range in concentration of these elements, albeit it less pronounced, to Sr-depleted and Y-undepleted compositions.

Geochemical discrimination between the High-Ca and other groups is mostly relatively straightforward (Figs 12, 13, 14; see last section). Most difficulty occurs with the more siliceous members of the Kanowna Belle clan of the Mafic group whose compositions strongly converge with that of the low-LILE clans of the High-Ca group (Figs 12, 13). Although differences between the two are apparent, e.g., Ni, Cr, MgO, Mg# (Fig. 13), it is possible that the High-Ca group includes some members which more correctly belong to the Mafic group, and vice versa.

Mineralised members? Mineralised members include the Tarmoola and Tower Hill mines, both occurring within or close to the Raeside mass. Porphyries, spatially associated with gold mineralisation, but always mineralised also occur at the Mt Morgans, Jundee and Keringal deposits.

Petrogenesis: The general characteristics (low LILEs, sodic) indicate derivation from a mostly mafic LILE-poor source, probably broadly basaltic in composition. The range in the LILE and HFSE (between clans), however, points to a compositional range in the source also, i.e., the differences can not be solely due to varying degrees of partial melting. Such a compositional variety strongly indicates the involvement of at least two-components, either as a heterogeneous source (basaltic to quartz dioritic), or by some other process (assimilation of pre-existing crust, magma-mixing etc). Notably in this regard, the very similar epsilon Nd signature of all the High-Ca group granites in the northern Eastern Goldfields (Champion & Sheraton, 1997), coupled with the contrasting epsilon Nd signatures of the Low-Ca and High-Ca groups, indicate that no significant component of the Low-Ca source was involved in the generation of the High-Ca granites, i.e., the higher LILE and HFSE contents in some members of the High-Ca group (e.g., Union Jack) can not have resulted from the involvement of Low-Ca granites or their sources.

The Sr-undepleted, Y-depleted nature of the majority of the High-Ca granites indicate derivation at pressures great enough to stabilise garnet and destabilise plagioclase (10-15 kbars) either deep within a thickened crust (>35-50 km) or, perhaps, from melting of a subducting slab (e.g., Martin, 1986). Either process is feasible, though the presence of inherited zircons, the range in Sr and Y to Sr-depleted and Y-undepleted compositions, and the Sm-Nd isotopic data favour a thickened crust source.

Tectonic & other implications: Both the thickened crust or melting of a subducting slab hypotheses for petrogenesis of the High-Ca granites, require the operation of some form of convergent tectonics in the Eastern Goldfields Province, from 2.7 Ga and earlier, but especially in the period 2.68-2.66 Ga, consistent with the structural history of the region, in particular the D_2 compression event. The timing of this tectonic setting for the Eastern Goldfields Province (post 2.68 Ga) appears to contrast with available geochronology for the Southern Cross Province (see above). Clearly there are a number of possible scenarios, not mutually exclusive, that may explain these apparent differences, e.g., the Southern Cross Province was separate from the Eastern Goldfields Province before and/or during this period, or perhaps the thermal regime at this period was such that granite production was largely confined to the Eastern Goldfields Province, such as in a typical modern-day convergent environment. Clearly further geochronology is needed, particularly along the eastern margin of the Southern Cross Province, to confirm or refute these hypotheses.

In addition, the large volume of High-Ca granites in the northern Eastern Goldfields clearly requires a correspondingly larger source (3 or more times volumetrically larger). This has important implications if the High-Ca granites were crustal-derived, requiring a significant volume of pre-existing crust of mostly homogenous 'basaltic to andesitic' composition.

High-Ca Clan	**Diemals Association Supersuite**	**Southern Cross Province Suite**
Barr Smith	Barr Smith	Barr Smith, Blow well, Palm Well, unnamed,
	Bridal Well	Bridal Well, Critch Bore, Bridal Well?
	Never Despair	Nuendah, Never Despair, Twin Bores, Scottie Well, unnamed, Altona
	Perrinvale	Perrinvale
Calamity	Calamity	Bore Well, Calamity
	Chinaman	Chinaman
Cavity	Cavity	Cavity
	Reid Well	Reid Well
Hong Kong	Hong Kong	Hong Kong, unnamed
Kaluweerie Hill	Kaluweerie Hill	Kaluweerie Hill, unnamed
unnamed	unnamed	unnamed
High-Ca interpreted (SCP)		Diemals Association
unassigned	unassigned	various unassigned units
High-Ca Clan	**Menangina Assoc. Supersuite**	**Eastern Goldfields Province Suite**
Beasley	Beasley Well	Beasley Well, Hawks Nest, Pool Well, Transvaal, Honey Queen, Ranch Well, Mulloch, Durang, Carroll Well, Mt Dennis
	Jundee-1	Destiny Well, Gourdis, Keil, Jundee-1, Karrah Bore, Amees Bore, Mundy Bore
	Tarmoola	Tarmoola
	Waltha	Waltha
	Wingora	Wingora, Point Sheila
Hannans Bore	Hannans Bore	Hannans Bore , Koonoonooka
Kingsley	Cody Well	Cody Well, Pink Well, Hegarty
	Kingsley	Bullock, Kingsley, Kerry Lyn, Cork Bore
Nambi	Auckland	Auckland, White City Well
	Nambi	Bob Well, Kauri, Keep It Dark, Roman Well, Lent Well, Lignum, Paul Well
Netting Bore	Netting Bore	Mt Pasco, Netting Bore, Charlies Well, Morning Light, Melba Bore, unnamed
No. 2 Well	McKenzie Bore	McKenzie Bore, Bernie Bore
	No. 2 Well	Mopoke Well?, Jims Well, Peperill Hill, Snowys Well, Schmitz Well, unnamed, Bounty, Camel Well, Good Friday, Marshall, No. 2 Well, Robbies Well
	The Boats	The Boats, Cement Hole, Murphy
	Urarey	Urarey
Union Jack	Blue Well	Blue Well, unnamed
	Ivor Rocks	Ivor Rocks
	Junction Well	Junction Well
	Mt Gerard	Mt Gerard
	Octopus	Octopus, Fyfe Bore
	Quongdong	Quongdong, Yilly Yilly
	Union Jack	Sergies well, Union Jack, Table Well, Fourteen Mile, unnamed, Turkey Well, Lawlers dykes, Ivor Rocks
	Wanggannoo	Two Jacks, Kujelan Creek, Wanggannoo
	White Cliffs	White Cliffs
	Wiro	Wiro, Mt Martin
	Mulega	Mulega, Biddy
unassigned	unassigned	unassigned
High-Ca interpreted (EGP)		Menangina Association
unassigned	unassigned	various unassigned units

Table 1. Suites, supersuites, clans and associations of the High-Ca group, northern Eastern Goldfields.

Sampno	1:250 000	Unit	Supersuite	Clan	Age	inherited	Ref	Com
High-Ca								
118936	Sir Samuel	Barr Smith	Barr Smith	Barr Smith	2679 ±9	2798	5	OK
96969080	Laverton	Durang	Beasley Well	Beasley	2672 ±2		2	OK
118945	Duketon	Point Sheila	Wingora	Beasley	2697 ±6	?2771	5	OK
96969038	Wiluna	Amees Bore	Jundee-1?	Beasley?	2673 ±3	2739	2	OK
96969039	Wiluna	Cork Bore dyke	Kingsley	Kingsley	2658 ±2	2684	2	OK
89963380	Leonora	Auckland	Auckland	Nambi	2669 ±7		2	OK?
Liu1	Leonora	Trump	Auckland	Nambi	2760		2	OK?
118950	Sir Samuel	Morning Light	Netting Bore	Netting Bore	2666 ±6	2689	5	OK
92963248	Leonora	No. 2 Well	No. 2 Well	No. 2 Well	~2650 ±	2797 ±8	2	OK
92969067	Leonora	Peperill Hill	No. 2 Well	No. 2 Well	2678 ±7		2	OK
92969080A	Leonora	Wildara	No. 2 Well	No. 2 Well	2648 ±5		2	OK?
92969113	Laverton	Murphy	The Boats	No. 2 Well	2670		2	OK?
Fletcher-2	Leonora	Lawlers dykes	Union Jack	Union Jack	2666 ±7		12	OK?
92969038	Leonora	Turkey Well	Union Jack	Union Jack	2676 ±7		2	OK
92969082	Leonora	Table Well	Union Jack	Union Jack	2665 ±4		2	OK
88-469	Leonora	Union Jack	Union Jack	Union Jack	2664 ±8		1	OK
96969044	Sir Samuel	Kujelan Creek	Wanggannoo?	Union Jack	2665 ±3		2	OK
96969016	Menzies	SCP-Menzies			2689 ±4		2	OK
High-Ca?								
88-450	Leonora	Mt Ross sheared				2971, 2776, 2722	1	?
89-634	Sir Samuel	Perseverance gneiss			?2684 ±9	2856 to 2726	11	?
Low-Ca								
112117	Menzies	Clark Well		Beetle	2640 ±8		4	OK
118947	Duketon	Barney	Grant Duff	Grant Duff	2637 ±8		5	OK
96969025	Sir Samuel	Ryans Well	Mt Blackburn	Hard Times?	2641 ±5	2747; 2702	2	OK?
142815	Kingston	Yelma	Coolibah	Mt Boreas	2651 ±10		6	OK
142816	Wiluna	2A Tank	Mt Cleaver	Nulerie	2648 ±19	2872	6	OK
118946	Duketon	unnamed pod	Mt Waite	Nulerie	2654 ±9		5	OK
96969046	Duketon	Red Bore	Mt Waite	Nulerie	2647 ±3		2	OK
96969034	Sir Samuel	Wanjarri	Wobbly	Nulerie?	2652 ±4		2	OK
92964658	Leonora	Wallaby Nob	Rowe Range	Yeelirrie	2653 ±3		2	OK
96969002	Menzies	SCP-Menzies			2631 ±3		2	OK
96969006	Menzies	SCP-Menzies			2636 ±2		2	OK
96969007	Menzies	SCP-Menzies			2660 ±3		2	OK
96969010	Menzies	SCP-Menzies			2660 ±5		2	OK
96969012	Menzies	SCP-Menzies			2633 ±2		2	OK

Table 2a. Geochronological data for the High-Ca and Low-Ca groups of the northern Eastern Goldfields region; all ages (in Ma) are SHRIMP zircon ages unless indicated otherwise. Data sources: 1 – Hill et al. (1992); 2 – L. Black, AGSO (unpublished); 3 – Nelson (1995); 4 - Nelson (1996); 5 – Nelson (1997); 6 – Nelson (1998); 7 – Nelson (1999); 8 - Ojala et al. (1997); 9 – Yeats et al. (in press); 10 - Pidgeon & Wilde (1990) conventional zircon analysis; 11 - Hill & Campbell (unpublished); 12 - Fletcher et al. (submitted); 13 – AMIRA P482; 14 – AMIRA P482 Pb whole-rock feldspar; 15 – AMIRA P482 SHRIMP titanite. Com = comments and refers to the interpreted reliability of the age.

Sampno	1:250 000	Unit	Supersuite	Clan	Age	inherited	Ref	Com
Mafic								
96969032	Sir Samuel	Anomaly 45	Anomaly 45	Granny Smith	2667 ±3		2	OK
88-597	Laverton	Granny Smith	Granny Smith	Granny Smith	2665 ±4		1	OK?
Fletcher-1	Leonora	Lawlers	Lawlers	Granny Smith	2666 ±3		12	OK
88-600	Edjudina	Porphyry	Porphyry	Granny Smith	2667 ±4		1	OK?
P1	Edjudina	Porphyry	Porphyry	Granny Smith	2657 ±8	2691	9	OK
P2	Edjudina	Porphyry	Porphyry	Granny Smith	2660 ±11	2710	9	OK
P3	Edjudina	Porphyry	Porphyry	Granny Smith	2662 ±23	2815	9	OK
96969042	Sir Sanuel	Hurleys Reward	Hurleys Reward	Kanowna Belle		2956 ±5	2	OK
118940	Sir Samuel	Kens Bore	Kens Bore	Kanowna Belle	2669 ±6	2720	5	OK
142811	Sir Samuel	Bronzewing diorite	Sundowner	Kanowna Belle	~2655 ±4		6	?
Liu2	Sir Samuel	Kathleen Valley	Kathleen Valley	Kathleen Valley	2736 ±3		2	OK
Mafic?								
DAT4	Sir Samuel	Mt McClure dyke			2656 ±4	2852	9	OK?
DAT6	Sir Samuel	Mt McClure dyke			2663 ±4		9	OK?
DAT7	Sir Samuel	Mt McClure dyke			2668 ±10	2867, 2779, 2706	9	OK?
J1	Wiluna	Jundee dyke			2656 ±7	2866; 2765-2700	9	OK?
Syenitic								
142810	Sir Samuel	Woorana Soak	Ninnis	Gilgarna	2644 ±13		6	OK
93964145	Laverton	Hanns Camp	Ninnis	Gilgarna	2664 ±2		2	OK
118948	Sir Samuel	Wadarrah	Panakin	Panakin	2643 ±6	?2674	5	OK
148397	Nabberu	Panakin	Panakin	Panakin	2664 ±4		7	OK
132918	Edjudina	McAuliffe Well			2651 ±5	2676	5	OK
98967008	Widgiem.	Erayinia			2660 ±5		13	OK
99967174A	Laverton	Wallaby	Wallaby	Wallaby	2658 ±16		14	OK?
Syenitic?								
118996	Nabberu	Teague Ring	unassigned	unassigned	2648 ±8	~2740	5	OK
Carbonatite (syenitic)								
99967177B	Laverton	Wallaby carbonatite		carbonatite	2657 ±15		15	OK?
High-HFSE								
96969024	Menzies	Kookynie	Kookynie	Kookynie	2680 ±2		2	OK
96969076	Leonora	Kent complex	Penzance	Kookynie	2679 ±8	2713+/-8	2	OK
118951	Sir Samuel	Weebo	Weebo	Kookynie	2658 ±7	2704+/-28	5	OK
142813	Sir Samuel	Satisfaction	Satisfaction	Satisfaction	2738 ±6		6	OK
96969031	Sir Samuel	Mandilla Well	Satisfaction	Satisfaction	2699 ±2		2	OK
Felsic volcanics								
86-425	Leonora	Teutonic Bore			2689 ±5		1	OK?
110225	Menzies	Carpet Snake Soak			2681 ±4		4	OK
112159	Leonora	Royal Arthur			2692 ±4	2746 ±9	3	OK
118953	Sir Samuel	Spring Well South			2690 ±5		5	OK
118954	Sir Samuel	Rockys Reward			2720 ±14		5	OK
137251	Edjudina	Yerilla			2696 ±6		6	OK
142817	Wiluna	Camel Bore			2669 ±10		6	OK
142821	Sir Samuel	Darlot Mine			2702 ±5		5	OK
89-636	Sir Samuel	Perseverance			?2706±6	2734 ±5	11	?
SDD243225	Edjudina	Sunrise			2677 ±6		8	OK
W83	Leonora	Pig Well			2697 ±3		10	OK
W98	Leonora	Teutonic Bore			2688 ±4		10	OK
Dolerite dyke								
142859	Sir Samuel	Kaluweerie			2627 ±6	2662, 2980, >3000	6	?

Table 2b. Geochronological data for the High-HFSE, Mafic, and Syenitic groups of the northern Eastern Goldfields region, and miscellaneous other rocks. Details and data sources as for Table 2a.

Clans of the Menangina Association, High-Ca Group, Eastern Goldfields Province.

Union Jack Clan

Member Supersuites: Blue Well, Ivor Rocks, Junction Well, Mt Gerard, Octopus, Quongdong, Union Jack, Wanggannoo, White Cliffs, Wiro, Mulega

Distribution: One of the dominant clans of the Menangina Association, the Union Jack clan occurs across the whole northern Eastern Goldfields, in four main zones:

- north-south zone in Cosmo mass (White Cliffs, Ivor Rocks, Quongdong supersuites)
- north-south zone in western part of Banjiwarn mass (Wanggannoo, Wiro, Mt Gerard, Mulega supersuites)
- very minor in Koonoonooka mass (Junction Well, Octopus supersuites)
- north-south zone in Raeside mass (Union Jack, Blue Well supersuites)

Geochronology: 5 reported ages (Table 2a) from the clan that include 2676 Ma (Union Jack supersuite) and 4 which cluster within 2 Ma of 2665 Ma (3 Union Jack, 1 Wanggannoo supersuite). The younger ages include both strongly deformed and undeformed units. The 2676 Ma unit is also strongly deformed. The Union Jack clan also includes lithologies from banded gneiss which may be older.

Chemical characteristics: This clan represents the high LILE and higher HFSE end-member of the Menangina Association, and as such is distinguished by its elevated to higher K_2O, Rb, Pb, Th, Zr, Ce (Figs 2, 3, 5), particularly with regard to Beasley, Nambi, No. 2 Well and Netting Bore clans. Notably, elements such as Sr and Y show strong overlap with other clans of the association. The Union Jack clan shares many similarities with both the Hannans Bore and Kingsley clans, with some notable differences (lower Ba, Sr, higher Rb, Y and Nb in Hannans Bore, and lower Pb, Ba, Th and Ce in Kingsley clan: Fig. 3)

Mineralised members? None recorded.

Petrogenesis: As for the High-Ca group in general, though the higher LILE and HFSE require a more LILE-enriched component in their source. Geochemically, many of the features evident in the Union Jack clan trend towards the less-evolved members of the Low-Ca group. Notably, however, the Sm-Nd isotopic data (Champion & Sheraton, 1997), clearly indicate the two groups aren't related, i.e., distinct and separate sources for the Low-Ca and High-Ca groups.

Tectonic & other implications: As for the High-Ca group in general.

Nambi Clan

Member Supersuites: Auckland, Nambi

Distribution: A moderate sized clan that occurs in two main zones in the western half of the northern Eastern Goldfields:

- clustering along the eastern half of the Teutonic mass (Nambi supersuite), and
- along the eastern part of the Raeside mass, extending to the north into the Koonoonooka mass (Auckland supersuite).

Geochronology: Two, possibly-conflicting, age determinations are available, both on Auckland supersuite units around the Leonora area (both from L. Black, written communication, 2000), an age of 2669 Ma from the Auckland granitoid NW of Leonora, and a 2760 Ma age from the Trump granodiorite unit just west of Leonora (Table 2a). The latter age, if indeed correct (i.e., not inherited) would make this the oldest recorded granite within the Eastern Goldfields Province, with an age more akin to that found within the Southern Cross Province. However, both the Auckland and Trump units are chemically very similarly (grouped within the same Auckland suite) raising the possibility that they may be of similar age. Additional geochronology is undoubtedly required.

Chemical characteristics: The Nambi clan is geochemically intermediate between the low LILE Beasley and high LILE Union Jack clans, as evidenced by the lower MgO, CaO and higher K_2O, Ba, Rb, Pb, Ce etc, of the Nambi clan relative to the primitive Beasley clan (Figs 3, 5). Although presently separated, the Nambi clan is chemically very similar to the No. 2 Well Clan, with only a few minor differences (the former having lower K_2O, Pb, and higher MgO); further work may see both clans amalgamated. The Nambi Clan also has many similarities to the Netting Bore clan, with some significant differences, e.g., higher MgO and lower Na_2O, Sr, Pb, Ba and Ce in the latter (Fig. 3).

Mineralised members? Tower Hill

Petrogenesis: If the Union Jack and Beasley clans define the two end-members in LILE and HFSE contents in the Menangina Association of the High-Ca group (Fig. 2), than the Nambi (and No. 2 Well) clan can be thought of as best defining the characteristics of the average High-Ca granites (Fig. 3). As such this and the No. 2 Well clan can be used to approximate the source for the High-Ca granites, with the chemistry most consistent with a 'average' source composition somewhere between basaltic and andesitic, i.e., the LILE contents are too high for a purely basaltic/gabbroic precursor.

Tectonic & other implications: Mostly as for the High-Ca group in general. The 2760 Ma age, however, raises a number of possible implications, particularly given that it is from a unit that would expected to be older if regional extensional deformation and core-complex formation had occurred as envisaged by Williams and co-workers, e.g., Williams & Whitaker, (1993), Williams (1993). In such a model, the Trump granodiorite represents the basement to the Eastern Goldfields Province greenstones, with the much younger Auckland granite either having being emplaced at the time of core-complex formation or, more likely given its age, during some unrelated tectonic event, e.g., D_2 compression.

No. 2 Well Clan

Member Supersuites: McKenzie Bore, No. 2 Well, The Boats, Urarey

Distribution: Moderate sized clan that encompasses gneissic granites to undeformed porphyries. Three main regions of occurrence:

- within the Raeside mass (No. 2 Well supersuite)
- southern half of the Banjiwarn mass (The Boats & Urarey supersuites)
- southern part of the Teutonic mass (McKenzie Bore supersuite).

Geochronology: Four age determinations available, all from L. Black (written communication, 2000), with ages of 2678 (Peperill Hill), ca. 2650 (No. 2 Well) and 2648

Ma (Wildara), all from the No. 2 Well supersuite in Raeside mass, and 2670 Ma (Murphy granite, The Boats supersuite), from the Banjiwarn mass (Table 2a). These ages suggest a bimodal distribution. Although, the two older samples are from gneissic to strongly deformed units, the two younger units are also moderately deformed. The 2650 Ma ages are the youngest yet recorded for High-Ca granites in the Eastern Goldfields Province. Black (written communication, 2000) also reports an inherited age of 2797 Ma for a granite of the No. 2 Well supersuite, consistent with Nd model ages for the age of the source rocks (Champion & Sheraton, 1997).

Chemical characteristics: The No 2 Well clan, like the Nambi Clan, is geochemically intermediate between the low LILE Beasley and high LILE Union Jack clans (Figs 3, 5). Although presently separated, the No 2 Well clan is chemically very similar to the Nambi Clan, with only a few minor differences (the latter having lower K_2O, Pb, and higher MgO; Fig. 3); further work may see both clans amalgamated. The No 2 Well Clan also has many similarities to the Netting Bore clan, with some significant differences, e.g., higher MgO and lower Na_2O, Sr, Pb, Ba in the latter (Fig. 3).

Mineralised members? None known

Petrogenesis: Very similar chemically to Nambi Clan, with similar petrogenesis.

Tectonic & other implications: In general, as for the High-Ca group. The 2650 Ma ages for members of this clan extend the age limits of the High-Ca group and indicate greater overlap with the Low-Ca group granites than previously thought. Additionally, as is also found for members of the Low-Ca group, the overprinting structural fabric within these younger granites indicate deformation post-dating 2650 Ma, in various localities across the northern Eastern Goldfields. The results for the Nambi and No. 2 Well clans, indicate that very similar magmatism occurred at 2760, 2670-2660 and 2650 Ma, within the Raeside mass (and elsewhere?).

Beasley Clan

Member Supersuites: Beasley Well, Jundee-1, Tarmoola, Waltha, Wingora

Distribution: Widespread clan including gneiss and gneissic granite to variably deformed granites and porphyries. Occurrences include:

- lower half of Cosmo mass (Beasley Well supersuite)
- all through Banjiwarn mass, including porphyries to south (Waltha, Wingora, Beasley Well supersuites)
- north-eastern part of Koonoonooka mass, on the continuation of Banjiwarn trend, and including porphyries in the greenstones to the east (Jundee-1 supersuite)
- the main internal granite at the Tarmoola deposit (Tarmoola supersuite)

All except Tarmoola lie on the one broad NNW trend.

Geochronology: Three ages available, 2697 Ma (Point Sheila complex, Wingora supersuite; Nelson, 1997), 2672 Ma (Durang, Beasley Well supersuite; Black, written communication, 2000), and 2673 Ma (Amees Bore complex, Jundee-1 supersuite; Black, written communication, 2000), all from gneisses or gneissic granites. Further geochronology is required to ascertain if members of the clan extend to 2660 Ma and younger.

Chemical characteristics: As discussed or the High-Ca group, the Beasley Clan forms the most primitive end-member of the Menangina Association, characterised by low LILE and HFSE contents, e.g., sodic with low K_2O, Rb, Th, Ce, Zr (Figs 2, 3, 5); features that distinguish it from other clans. One notable difference is the higher MgO and mg# in the Beasley Clan.

Mineralised members? Tarmoola, porphyries spatially associated with mineralisation around Jundee, Keringal, Mt Morgans

Petrogenesis: Generally as discussed for the High-Ca group. The primitive (low-LILE) chemistry is most consistent with partial melting of a basaltic/amphibolitic pre-cursor, at moderate-high pressures. The higher MgO and mg# evident in most of the Beasley Clan may be the first good evidence for a subducted slab source for some of the High-Ca rocks, i.e., indicative of reaction with mantle-wedge peridotite (see Smithies & Champion, 2000).

Tectonic & other implications: As for High-Ca group in general.

Hannans Bore Clan

Member Supersuites: Hannans Bore

Distribution: A small clan and supersuite, comprising several units, confined to the central Koonoonooka mass.

Geochronology: None available.

Chemical characteristics: Most similarities with the Union Jack and Kingsley clans, with some notable distinctions, including lower Ba, Sr and higher Rb, Y and Nb in the Hannans Bore clan (Fig. 3). Has some affinities with the Low-Ca group, and could represent a mixed source.

Mineralised members? None

Petrogenesis: The lower Sr and higher Y within the Hannans Bore Clan suggest partial melting at lower pressures/higher crustal levels from a source similar to that for the Union Jack clan.

Tectonic & other implications: The postulated lower pressure origins of this clan, are consistent with the favoured model for the origin of the High-Ca in group, i.e., partial melting of thickened crust.

Kingsley Clan

Member Supersuites: Cody Well, Kingsley

Distribution: Small to moderate-sized clan, with granitoids confined to two regions:
- north-eastern part of the Raeside mass (Cody Well supersuite)
- north-eastern part of the Koonoonooka mass (Kingsley supersuite).

Geochronology: One age available on a dyke from the Kingsley supersuite (2658 Ma, L.Black, written communication, 2000), intruding gneisses of the Beasley Clan. Upper age limits not known, but inferred to be <2700 Ma.

Chemical characteristics: Belongs to the high LILE members of the High-Ca group (Fig. 5). As such, is chemically similar to the Union Jack clan, with minor differences, e.g., lower Ba, Th, Ce (Fig. 3). Also many similarities with the Hannans Bore clan (lower Ba, Sr and higher Rb, Y and Nb in the latter; Fig. 3).

Mineralised members? None known.

Petrogenesis: Similar to that for the Union Jack clan. The minor differences between the Kingsley and Union Jack clans, most probably reflecting minor differences in the source rocks.

Tectonic & other implications: As for the Union Jack clan and the High-Ca group in general.

Netting Bore Clan

Member Supersuites: Netting Bore

Distribution: A small clan and supersuite comprising 7 granite and granodiorite units occurring in two main regions:
- north-east Teutonic mass and its extension into the greenstones to the NNW
- western part of Koonoonooka mass.

Geochronology: One age recorded (Nelson, 1997), of 2666 Ma for the Morning Light granodiorite, from the Teutonic mass.

Chemical characteristics: The Netting Bore clan falls within the central area of the chemical range shown by the High-Ca group (Figs 3, 5), with most similarities to the Nambi and No. 2 Well clans. Differences with the latter 2 clans include higher MgO and lower Na_2O, Sr, Pb, Ba in the Netting Bore clan.

Mineralised members? None

Petrogenesis: Largely as for the Nambi and No. 2 Well clans.

Tectonic & other implications: As for the Nambi and No. 2 Well clans, and the High-Ca group in general.

Clans of the Diemals Association, High-Ca Group, Southern Cross Province

Barr Smith Clan

Member Supersuites: Barr Smith, Bridal Well, Never Despair, Perrinvale

Distribution: One of the major clans in the Southern Cross Province in the NEG area. Its distribution is localised to the north-eastern half of the Yeelirrie mass.

Geochronology: One age recorded, by Nelson (1997), of 2679 Ma, for the Barr Smith granite, belonging to the Barr Smith supersuite.

Chemical characteristics: Chemically, falls into the high LILE and HFSE end-members of the High-Ca group (Fig. 4, 5). Geochemical characteristics largely similar to those shown by the Union Jack clan of the Eastern Goldfields Province, i.e., elevated K_2O, Rb, Th, U, Pb, Zr, LREE. Differences include slightly higher CaO, Na_2O, and lower K_2O, Rb, in the Barr Smith clan, relative to the Union Jack Clan. Both clans show similar elevated levels of Th, U, LREE, and Zr (Figs 3, 4, 5).

Mineralised members? None.

Petrogenesis: Essentially similar to that for the Union Jack clan, Eastern Goldfields Province, i.e., from a 'source' more chemically evolved than basalt/amphibolite. Shares many similarities with the Calamity clan, Southern Cross Province, although the latter has lower Na_2O, and higher K_2O, Sr, Ba, Th, LREE.

Tectonic & other implications: Largely as for the Union Jack Clan, Eastern Goldfields Province, and the High-Ca group granites in general. One result of the present AMIRA project is the apparent lack of granites around 2.67 to 2.66 Ma in the Southern Cross Province, unlike the Eastern Goldfields Province, where the majority of High-Ca granites are of this age. Although the data is limited, this also appears to be consistent with the comparisons between the Barr Smith clan and many of the granites in the Union Jack clan, the latter which cluster strongly around 2665 Ma.

Calamity Clan

Member Supersuites: Calamity, Chinaman

Distribution: Small clan of 5 variably deformed units, with both supersuites occurring in a north-south zone, in the northern half of the Yeelirrie mass.

Geochronology: None available. Locally intruded by members of the Barr Smith Clan.

Chemical characteristics: Belongs to the high LILE part of the High-Ca group range (Figs 4, 5). Many similarities to the Barr Smith Clan but with higher LILE and HFSE, e.g., higher K_2O, Pb, Ba, Th, LREE, Zr (Fig. 4). Very similar chemically to the Union Jack clan of the Eastern Goldfields Province.

Mineralised members? None.

Petrogenesis: As for the Union Jack clan of the Eastern Goldfields Province, and the High-Ca granites in general. Relative to the Barr Smith clan, requires a source with higher LILE and HFSE, or, perhaps, represents slightly lower degrees of partial melting.

Tectonic & other implications: As for the Barr Smith clan and High-Ca group in general.

Cavity Clan

Member Supersuites: Cavity, Reid Well

Distribution: Small clan of two supersuites, each comprising only one unit, both occurring within the central zone of the Yeelirrie mass.

Geochronology: None. One unit (Cavity) intruded by members of the Barr Smith clan.

Chemical characteristics: Chemically not as LILE- or HFSE-rich as the Barr Smith clan, with lower TiO_2, Rb, Th, LREE, Zr, Y and Nb (Fig. 4). Most akin to the Nambi/No. 2 Well clans of the Eastern Goldfields Province, i.e., falling within the central part of the High-Ca range.

Mineralised members? None.

Petrogenesis: As for Nambi/No. 2 Well clans, Eastern Goldfields Province, and High-Ca granites in general.

Tectonic & other implications: As for Nambi/No. 2 Well clans, Eastern Goldfields Province, and High-Ca granites in general.

Hong Kong Clan

Member Supersuites: Hong Kong

Distribution: Small clan of one supersuite comprising 2 units, one of which (Hong Kong complex) may be substantially larger (based on aeromagnetic data). Confined to the eastern and central parts of the Yeelirrie mass.

Geochronology: None.

Chemical characteristics: Small data set of only three analyses, characterised by low LILE and generally low HFSE, e.g., low K_2O, Rb, Th, Zr, Y, especially compared to the Barr Smith clan (Fig. 4). Chemically most similar to the Beasley clan, Eastern Goldfields Province.

Mineralised members? None.

Petrogenesis: The Low-LILE composition, is most consistent with a basaltic/amphibolitic source composition, as for the Beasley clan, Eastern Goldfields Province.

Tectonic & other implications: When combined with the other Southern Cross Province High-Ca clans, clearly demonstrates that there is little difference between these High-Ca granites and those of the Eastern Goldfields Province, particularly in regard to the range of LILEs and HFSEs (Fig. 5). This can be taken further to indicate that source rocks and processes, responsible for production of the High-Ca granites, were also probably similar in both provinces.

Kaluweerie Hill Clan

Member Supersuites: Kaluweerie Hill

Distribution: Small clan comprising one supersuite with three units, occurring within the central part of the Yeelirrie mass.

Geochronology: None.

Chemical characteristics: Although a small clan with only four analyses, all show similar distinctive geochemistry. Such features include elevated Pb, Ba, Th, U, LREE, Zr, coupled with high Na_2O, Sr and low to moderate K_2O, Rb (Fig. 4). Compared to the Barr Smith clan, members of the Kaluweerie clan have higher CaO, Na_2O, Sr, LREE and Zr and lower K_2O and Rb. Notably, K_2O and Rb levels are as low as those found in the low-LILE Hong Kong clan (Figs 4, 5); it is equivocal whether these compositions are primary or reflect some post crystallisation modification, e.g., alteration?

Mineralised members? None.

Petrogenesis: The unusual decoupling of the LILE and HFSE in the Kaluweerie clan, if not due to alteration etc, strongly suggest either a unique source composition or, possibly, a mixed source.

Tectonic & other implications: As for the High-Ca group in general.

Low-Ca Group, northern Eastern Goldfields

Member Associations: Mt Boreas Association (Eastern Goldfields Province)
Beetle Association (Southern Cross Province)

Distribution: The second most dominant granite group within the northern Eastern Goldfields, representing up to and greater than 20% of total granites (up to 40% in the portion of the Southern Cross Province in the northern Eastern Goldfields, Fig. 1). Most dominant in the external granites, where it is often associated with older gneisses. Well represented in all the granite masses with the apparent exception of the Teutonic mass (Fig. 1). Six clans have been recognised in the northern Eastern Goldfields Province, and 2 clans in the north-eastern Southern Cross Province (Table 3). Apart from the widespread Nulerie and Mt Boreas clans, the clans in the Eastern Goldfields Province are localised to particular zones.

Geochronology: A moderate number of dated samples, mostly from the Eastern Goldfields Province indicate an age range from 2655 to 2637 Ma (Table 2a). As would be expected given the chemistry of the Low-Ca granites (i.e., high Zr levels indicating that the initial melts weren't zircon saturated), there is only minor evidence for inherited zircon. Data, available for two granites (one of which intrudes greenstones, i.e., the zircons may be xenocrystic), indicates age ranges for inherited zircons of 2700 to 2870 Ma (Table 2a). These 'inherited' ages are much younger than would be expected given the Nd model ages (2800 to 3000+ Ma, Champion & Sheraton, 1997).

Only one age (2653 Ma, L.Black, written communication, 2000) has been determined on the Low-Ca granites in the Southern Cross Province region of the northern Eastern Goldfields. Low-Ca granites, just to the south on the Menzies 1:250 000 sheet, record ages in the range 2660 to 2630 Ma (Table 2a). Available geochronology for the Southern Cross Province further to the south and west (and the Murchison Province) suggests that the Low-Ca magmatism extended to 2.64-2.63 Ga and younger, becoming more voluminous around 2.65-2.63 Ga (this project, Qui et al., 1997). This appears to be slightly different to the Eastern Goldfields Province, particularly the northern half of the province, where the limited data suggests the majority of Low-Ca magmatism occurred at 2655-2640 Ma, with only one Low-Ca granite recording an age below 2.64 Ga (Table 2a). Further geochronology will help clarify whether these differences are indeed real or just artefacts of the limited data to date.

Chemical characteristics. Characteristics for this group have been summarised by Champion & Sheraton (1997), and Champion (1997). Basically, the Low-Ca granites comprise potassic granite and lesser granodiorite, characterised by high LILE (K_2O, Rb, Pb, Th, U) and HFSE (LREE, HREE, Y, Zr) contents (Figs 5, 6, 7, 8, 13, 14). Individual clans (Table 3), exhibit a range in LILE and HFSE contents, from moderate (Nulerie, Mugs Bore clan) to high (Grant Duff, Hard Times, Mars Bore, Yeelirrie clans; Figs 6, 7, 8), though the range isn't as large as for the High-Ca group (Figs 5, 14). The majority of granitoids from this group are further characterised by (low to) moderate Sr contents (Sr-depleted) coupled with moderate to high Y (and HREE) contents (Y-undepleted; Figs 7, 8), although, the group does range to Sr-undepleted and variably Y-depleted compositions.

Mineralised members? Notably, there are no recorded examples of Low-Ca granites hosting gold mineralisation, despite them being either older or contemporaneous with the postulated main period of gold mineralisation around 2640 to 2630 Ma. Given the high Th and U contents of the Low-Ca granites it is considered very likely that the weathering of these granites contributed significantly, via weathering, to the U in calcrete deposits, e.g., Yeelirrie. Elsewhere in the Yilgarn, Low-Ca granites are associated with Be and Sn deposits, as would be expected given their fractionated nature.

Petrogenesis: The general characteristics of the Low-Ca group granites (potassic, high LILEs, elevated HFSEs) indicate derivation from a, at least moderately, potassic and LILE-rich crustal source, i.e., they represent reworked continental crust. Champion & Sheraton (1997) suggested source rocks with compositions not unlike tonalites found in Archaean terranes throughout the world, though the low CaO in the Low-Ca granites and the very minor occurrence of amphibole in the granites themselves, indicate partial melting was largely via dehydration melting driven by biotite breakdown, i.e., either small volume melts or from a source with only minor amphibole. Additionally, the high levels of the HFSEs, in particular Zr, in the Low-Ca granites, strongly indicate high temperature melting (i.e., zircon saturation and, hence, levels of Zr in a granite melt are strongly temperature dependent), a fact which may also be consistent with a generally water-poor (limited amphibole) source. Finally, the mostly Y-undepleted and Sr-depleted nature suggests that the Low-Ca granites were generated at moderate crustal levels (mostly <35 km).

The variation in LILE, in particular, and the HFSE, between the Low-Ca clans, may reflect a variety of processes, including:

- changes in percentage of partial melt, i.e., the greater percentage of melt, the lower the concentration of LILEs in the melt,
- variations in source compositions,
- variable mixing of two or more source components, e.g., perhaps a component of a source similar to that envisaged for the High-Ca granites.

The available evidence favours a combination of the first two hypothesis, though the third can not be ruled out. Notably, the differences between the Mt Boreas and Meredith clans appear to mostly reflect a change in the degree of partial melting.

Tectonic & other implications: The simplest model for the Low-Ca granites, would appear to require their generation from moderately dry tonalitic (or more felsic) pre-existing crust, in an extensional environment with an elevated geothermal gradient. This is clearly contrary to the general scenario for the High-Ca granites, indicating not only distinct source rocks, but distinct sites of granite generation for the two granite types. This is also supported by the available Sm-Nd isotopic data which indicates isotopically distinct source reservoirs for the two granite groups (Champion & Sheraton, 1997). These differences are even more significant when the age distributions of the two granites groups are taken into consideration, i.e., there is a temporal change from voluminous dominantly High-Ca magmatism to less voluminous, but very widespread, dominantly Low-Ca magmatism, around 2660 to 2650 Ma. This changeover in magmatism most probably indicates a corresponding change in tectonic environment, presumably from a compressional or arc-related environment to one dominated by extension or post-tectonic relaxation, i.e., some mechanism produced a change in the thermal regime, that not only increased the thermal gradient (to allow generation of Low-Ca granites) but effectively turned off production of High-Ca granites.

The exact nature of this tectonic transition is largely dependent on the origin of the High-Ca granites, which as described earlier, is not straight-forward. If, as favoured here, the High-Ca granites were generated by partial melting in thickened crust, then melting shifted to higher crustal-levels (the site of Low-Ca generation), with the thickened lower crust (High-Ca source) either somehow insulated from further melting or removed. In this regard, Smithies & Champion (1999) suggested that this post 2660 Ma thermal event may have resulted from lower-crustal delamination following crustal thickening during the main D_2 shortening deformation. These authors further speculated that this event represented an additional tectonothermal event in the eastern Yilgarn Craton, contemporaneous with lower-middle crustal high-grade metamorphism and regional Au mineralisation (e.g., Kent et al. 1996).

If, however, the High-Ca granites were largely generated by slab-melting, a scenario considered less likely given the geochemical, Sm-Nd isotopic and inherited zircon evidence, but still with some merit, then the change over to Low-Ca (and syenitic) magmatism may simply reflect some form of wide-scale extension, perhaps not unlike that presently operating in the Basin and Range province in the western United States, although with some differences, e.g., lack of contemporaneous felsic volcanism.

Low-Ca (SCP)	**Beetle Association**	
Clan	**Supersuite**	**Suite**
Mugs Bore	Mugs Bore	Mugs Bore, Dalray Creek
Yeelirrie	Rowe Range	Brets Bore, Rowe Range, Tunney Well
	Yeelirrie	Mystery Bore, Two Inch, Yeelirrie, Deadwood
	Breakaway Well	Breakaway Well
	Wild Cat	Wild Cat, Ohara Well, unnamed
	unassigned	unassigned (Break of Day)
Low-Ca interpreted (SCP)		Beetle Association
unassigned	unassigned	various unassigned units

Low-Ca (EGP)	**Mt Boreas Association**	
Clan	**Supersuite**	**Suite**
Grant Duff	Deeba	Freshwater, Far Comet, Deeba, New Bore, Mitika
	Grant Duff	Barney, Grant Duff, Turnback, Duff Range
	Lake Wells	Lake Wells, Dumbung
Hard Times	Hard Times	Hard Times, Alf Well
	Short Cut	Short Cut
	Sunday Bore	Sunday Bore
	Mt Blackburn	Mt Blackburn, Ryans Well, Kurrajong Bore
	unnamed	Forrest Well
Mars Bore	Mars Bore	Top Well, Jacks Bore, Mars Bore
Meredith	Meredith	Meredith, Darby Well, Start Hill, Pine Tree
	Point Pater	Point Pater
Mt Boreas	Coolibah	Calcalong, Porcupine, Coolibah, Yelma, Kukkabubba
	Mt Boreas	Mt Boreas
	Vickers Creek	Vickers Creek
	Carlee	No 22 Bore, Carlee, Sholl Range, unnamed
Nulerie	Mt Waite	Phils Fossey, Mt Waite, Red Bore, unnamed, Neckersgat
	Nulerie	Charleston Well, Boundary Well, Extension Tank, Nulerie
	Moxon	Moxon, Mt Tate, Miljie, Gerry Well
	Mt Cleaver	Mt Cleaver, 2A Tank
	Wobbly	Wobbly, Wanjarri, Old Brilliant, Eifel Tower
	Yillaree	Yillaree, Anderson
unassigned	unassigned	unassigned (Conglomerate Bore)
Low-Ca interpreted (EGP)		Mt Boreas Association
unassigned	unassigned	various unassigned units

Table 3. Suites, supersuites, clans and associations of the Low-Ca group, northern Eastern Goldfields Province.

Clans of the Mt Boreas Association, Low-Ca Group, Eastern Goldfields Province

Grant Duff Clan

Member Supersuites: Deeba, Grant Duff, Lake Wells

Distribution: Widely distributed clan of three supersuites and 10 units, confined to the eastern half of the northern Eastern Goldfields Province, i.e., east of the Celia lineament, as follows:
- all through the Cosmo mass (Deeba, Lake Wells supersuites)
- eastern half of Banjiwarn mass (Grant Duff supersuite)

Geochronology: One date of 2637 Ma (Nelson, 1997; Table 2a) on the Barney granite, Grant Duff supersuite.

Chemical characteristics: Archetypal Low-Ca clan, exhibiting all the features of Low-Ca granites, namely, high K_2O, Rb, Pb, Th, LREE, Zr, Nb, moderate to high HREE and Y, and low Na_2O, (Figs 6, 7, 8, 14). The majority of other Low-Ca clans exhibit compositional trends that lie between those of the Grant Duff clan and those of the Union Jack clan (the most LILE- and HFSE-enriched High-Ca clan; Fig. 6). The Grant Duff clan shares many similarities with the Hard Times and Mars Bore clans, and with the Yeelirrie clan, Beetle Association, of the Southern Cross Province.

Mineralised members? None

Petrogenesis: As for the Low-Ca group in general, particularly given the high LILE, high HFSE nature of this clan.

Tectonic & other implications: As for the Low-Ca group in general. Further geochronology is required to ascertain whether this clan is indeed younger, as the one age date suggests, than other Low-Ca clans in the region.

Hard Times Clan

Member Supersuites: Hard Times, Short Cut, Sunday Bore, Mt Blackburn, unnamed

Distribution: The 9 units of the 5 supersuites (one unnamed) belonging to this clan are confined to a circular area occupying the central parts of the Banjiwarn (Mt Blackburn supersuite) and Koonoonooka (Hard Times, Short Cut, Sunday Bore supersuites) masses.

Geochronology: No definitive ages, though one poorly-defined possible intrusive age of 2641 Ma on the Ryans Well granite, Mt Blackburn supersuite (L. Black, written communication, 2000; Table 2a). This granite also records a much better, inherited? age of 2747 Ma (Table 2a). This strongly foliated granite occurs along the western edge of the Banjiwarn mass intrusive into greenstones, so the older zircon ages may represent xenocrysts.

Chemical characteristics: Geochemically, falls into the high LILE, high HFSE end of the range shown by the Low-Ca group, and as such is chemically similar to the Grant Duff

Clan (Figs 6, 7). Minor differences include, higher Th, U, higher Nb, Y in the high-silica end-members, and more variable alkalis (K_2O, Na_2O, and Rb).

Mineralised members? None.

Petrogenesis: As for the Grant Duff clan, and the Low-Ca group in general.

Tectonic & other implications: As for the Grant Duff clan, and the Low-Ca group in general. The minor differences between the Grant Duff and Hard Times clans most probably reflect minor compositional differences in the source.

Mars Bore Clan

Member Supersuites: Mars Bore

Distribution: One supersuite comprising 3 small to large units in the Raeside mass, extending south onto the Menzies 1:250 000 sheet area. Two of the units lie along the western edge of the Eastern Goldfields Province, i.e., near the Ida Lineament.

Geochronology: None.

Chemical characteristics: Members of the Mars Bore clan lie towards the high LILE, high HFSE end of the Low-Ca group range, and, accordingly, share many similarities with the Grant Duff, and Hard Times clans. Differences include variable to lower K_2O, Rb, Th, U and variable to higher Pb and Ba (Fig. 7). The greatest differences are in total Fe, which is significantly higher in the Mars Bore clan. Notably, the geographically close Yeelirrie clan in the Southern Cross Province, has compositions which strongly overlap with the Mars Bore clan, including elevated total Fe.

Mineralised members? None.

Petrogenesis: The differences in total Fe (and mg#), between the Grant Duff and Mars Bore clans may either reflect differences in source geochemistry or mineralogy, or perhaps degree of partial melting. Given the similarity in LILEs, the former is the preferred option.

Tectonic & other implications: Given the similarities between the Mars Bore clan, Eastern Goldfields Province, and the Yeelirrie clan of the Southern Cross Province, it is clearly evident that either the crust does not significantly change across the Ida Lineament, or the surface location of the lineament does not correspond to its position at depth, i.e., the fault must dip to the east; the latter is the preferred option.

Meredith Clan

Member Supersuites: Meredith, Point Pater

Distribution: The Meredith clan, comprising two supersuites with 8 units in total, is largely confined to the Cosmo mass (Meredith, Point Pater supersuites), but also includes internal granites (Meredith supersuite) in the Laverton greenstone belt.

Geochronology: None.

Chemical characteristics: The Meredith clan falls into the lower LILE, lower HFSE end of the Low-Ca compositional range (Fig. 7), with lower Rb, Pb, Th, U, Y, variable to lower K_2O, Pb and Nb, and variable to higher Na_2O, CaO and Ba, relative to the Grant Duff Clan (Fig. 7). The Meredith clan has many similarities to the Nulerie clan, with some differences, including lower total Fe, K_2O, Rb, and higher Ba and LREE in the former.

Mineralised members? None.

Petrogenesis: As for the Low-Ca group in general. As discussed earlier, the geochemistry of the Meredith clan, relative to the Grant Duff clan, probably results from a combination of a greater degree of partial melting, and a more LILE-poor source.

Tectonic & other implications: As for the Low-Ca group in general.

Mt Boreas Clan

Member Supersuites: Coolibah, Mt Boreas, Vickers Creek, Carlee

Distribution: One of the larger clans of the Mt Boreas Association, the Mt Boreas clan is confined to the central part of the northern Eastern Goldfields Province, occurring in two pronounced clusters:

- northern third of the Koonoonooka mass (Coolibah supersuite)
- NNW trending zone in the central Banjiwarn mass (Mt Boreas, Vickers Creek, Carlee supersuites).

Geochronology: One age of 2651 Ma (Nelson, 1998), on the Yelma granite (Coolibah supersuite).

Chemical characteristics: Like the mostly similar Meredith clan, the Mt Boreas clan falls within the lower LILE and lower HFSE end of the Low-Ca spectrum. Significant differences with the Grant Duff and Hard Times clans (both high LILE & HFSE), include similar to higher Sr, higher Na_2O, lower K_2O, Th, and distinctly different (lower) trends for the LREE and Zr (Fig. 7), features also shared by the Nulerie and Meredith clans (Figs 6, 7). Differences between the Nulerie and Mt Boreas clans include generally higher K_2O, LREE, Zr, Y, and lower Na_2O in the latter. The Mt Boreas and Meredith clans are more closely akin, minor differences including higher Rb (and U) at similar K_2O contents.

Mineralised members? None

Petrogenesis: As for the Meredith clan, and the Low-Ca group in general. Notably the differences between the generally similar Meredith and Mt Boreas clans, in particular the similar K_2O contents but different Rb, and hence, K/Rb ratios, is most indicative of smaller degrees of partial melting in the generation of the Mt Boreas clan.

Tectonic & other implications: As for the Low-Ca group in general.

Nulerie Clan

Member Supersuites: Mt Waite, Nulerie, Moxon, Mt Cleaver, Wobbly, Yillaree

Distribution: The most widespread clan of the Mt Boreas Association, occurring right across the Eastern Goldfields Province, in all but the Teutonic mass, as follows:

- northern part of the Raeside mass (Yillaree supersuite)
- whole length of the Koonoonooka mass (Yillaree, Mt Cleaver, Wobbly supersuites)
- southern half of the Banjiwarn mass (Mt Waite, Moxon, Nulerie, supersuites)
- northern part of the Cosmo mass (Moxon supersuite)
- internal bodies in greenstone between the Cosmo and Banjiwarn masses (Nulerie supersuite).

Geochronology: Four age determinations available (Nelson, 1997, 1998; L.Black, written communication, 2000), - 2654, 2652, 2648, 2647 Ma, all within error of each other (Table 2a). These include two samples from the Koonoonooka mass - 2A Tank (Mt Cleaver supersuite), and Wanjarri (Wobbly supersuite), and two from the Banjiwarn mass - Red Bore and an unnamed pod in High-Ca gneiss (both Mt Waite supersuite).

Chemical characteristics: The Nulerie clan is one of the more chemically primitive clans of the Low-Ca group, i.e., lower LILE and lower HFSE (see Figs 5, 6, 7). Differences between the Nulerie and the Grant Duff clans (one of the high LILE & high HFSE members of the Low-Ca group) are graphically illustrated in Figure 6, from which the variations in K_2O, Na_2O, Rb, Zr, Th, and the LREE are clearly visible. It is also evident from Figure 6, that the Nulerie clan contains higher LILE and HFSE contents (e.g., K_2O, Rb, Zr, Ce) than the most LILE- and HFSE-enriched clan of the High-Ca group - the Union Jack clan. The distinction between the Low-Ca and High-Ca groups is also shown by the different Sm-Nd signature of each group, particularly in the western half of the northern Eastern Goldfields (see Champion & Sheraton, 1997). The Nulerie clan has many similarities to both the Mt Boreas and Meredith clans, though with some differences, e.g., lower Ce, Y, Zr than the Mt Boreas clan, and higher Na_2O, Rb, and lower Ce than the Meredith clan.

Mineralised members? None.

Petrogenesis: As for the Low-Ca group in general. The convergence in compositions between the most LILE- and HFSE-poor Low-Ca clan, and the most LILE- and HFSE-rich member of the High-Ca group (Union Jack clan; Fig. 6), also strongly suggests a convergence in source compositions for the two clans. As discussed earlier, though, the differences in Sm-Nd isotopic signatures effectively rule out any commonality of sources.

Tectonic & other implications: As for the Low-Ca group in general.

Clans of the Beetle Association, Low-Ca Group, Southern Cross Province

<u>Mugs Bore Clan</u>

Member Supersuites: Mugs Bore

Distribution: One supersuite, comprising 6 units, all localised within the central part of the Yeelirrie mass.

Geochronology: None.

Chemical characteristics: This clan falls within the low LILE and HFSE end of the Low-Ca compositional range, and is clearly distinct from the Yeelirrie clan (Fig. 8). The Mugs Bore clan is compositionally very similar to the Nulerie Clan in the Eastern Goldfields Province, with only minor differences, e.g., higher Na_2O, lower Rb in the latter.

Mineralised members? None.

Petrogenesis: As for the Nulerie clan, Eastern Goldfields Province, and the Low-Ca granites in general.

Tectonic & other implications: As for the Nulerie clan, Eastern Goldfields Province, and the Low-Ca granites in general. The similarity between clans of both the Southern Cross Province and Eastern Goldfields Province, strongly implicates both similar compositional source rocks and similar processes within both provinces.

Yeelirrie Clan

Member Supersuites: Rowe Range, Yeelirrie, Breakaway Well, Breakaway Well, Wild Cat, unnamed

Distribution: Extensive clan spanning the entire north-south range of the Yeelirrie mass in the northern Eastern Goldfields, particularly along the western half.

Geochronology: One available age (L.Black, written communication, 2000) of 2653 Ma on the Wallaby Knob granite, Rowe Range supersuite (Table 2b).

Chemical characteristics: The Yeelirrie clan falls into the high LILE and high HFSE end of the Low-Ca compositional range (Fig. 8), though is clearly not as evolved as the Grant Duff clan of the Eastern Goldfields Province (see Fig. 8). The Yeelirrie clan is compositionally very similar to the spatially close Mars Bore clan of the Eastern Goldfields Province, including having the distinctive higher total Fe contents present in the latter.

Mineralised members? None, though probably indirectly related to the Yeelirrie U in calcrete deposit, being the most likely source of the U (via weathering of the granites).

Petrogenesis: As for the Mars Bore clan, Eastern Goldfields Province, and the Low-Ca group in general.

Tectonic & other implications: As for the Mars Bore clan, Eastern Goldfields Province, and the Low-Ca group in general.

Kookynie Association, High-HFSE group, Eastern Goldfields Province

Member clans: Kookynie, Satisfaction, Bullshead?

Distribution: A strongly localised association confined to a NNW trending zone, from Kookynie to the south (Menzies 1:250 000 sheet), to north of Wiluna and Bronzewing, and including the Teutonic mass, and marginal to both sides of the Koonoonooka mass (Fig. 1).

Geochronology: Five ages available, 4 from the northern Eastern Goldfields, with three between 2700 and 2680 Ma (Table 2b). These ages overlap with those found for spatially associated, and, at least locally, genetically-related felsic volcanics (Table 2b). Two other ages include a younger 2658 Ma, and an anomalous older 2738 Ma (Nelson, 1997, 1998).

Chemical characteristics: The members of the High-HFSE group have been described in detail by Champion & Sheraton (1997), and Champion (1997), though additional work, largely as part of this project, has resulted in some redefinition of the group. Originally only containing high silica (>74% SiO_2) members, the high-HFSE group now has a silica range greater than both the High-Ca and Low-Ca groups (Fig. 9). The group, however, is still characterised by its combination of high total Fe, MgO, TiO_2, HFSE, low to moderate LILE, and Sr-depleted, Y-undepleted character (Fig. 9), features that readily distinguish the group from other granite groups in the northern Eastern Goldfields (Figs 9, 13).

Differences between the two most felsic clans (Kookynie, Satisfaction) are minor (mostly evident in Pb, Th and U, Fig. 9). The third clan, Bullshead, is significantly more silica poor (63-68% SiO_2) and has many similarities with members of the Mafic group, with which it may actually belong. Features such as high total Fe, coupled with low Rb, Sr, Pb, Th, and elevated Y and Zr, however, suggest some kinship with the High-HFSE group, and the Bullshead clan is tentatively included within that group.

Petrogenesis: Champion & Sheraton (1997), and Champion (1997), suggested that the High-HFSE group granites were crustal-derived melts from an intermediate to more siliceous source, the latter hypothesis based on the combination of high HFSE and only low to moderate LILE. While such a scenario is consistent with both the Satisfaction and Kookynie clans, the presence of less siliceous granites, such as those in the Bullshead clan, raises the possibility that the more siliceous end-members are actually fractionates of rocks similar in composition to the Bullshead clan granitoids. If the latter scenario is correct, then the ultimate source rocks for the granitoids of this group must have been both more mafic and even more LILE-poor than originally envisaged. Such a hypothesis is also consistent with the, high-temperature A-type characteristics of the High-HFSE group (elevated Fe, Zr, Y; Fig. 9).

The Sr-depleted, Y-undepleted nature of the group, strongly infer generation at only moderate crustal pressures, i.e., <10 kbars (<35 km thick). Similarly, as discussed by Champion & Sheraton (1997), the Sm-Nd isotope data indicate significant involvement of pre-existing crustal rocks in the generation of the High-HFSE granites.

In many regards, it is evident that members of the High-HFSE group, especially the less siliceous ones, have a number of similarities (though not as extreme) to the tholeiitic fractionates in the Kathleen Valley and Sweet Nell clans of the Mafic group, e.g., elevated Fe, Zr, Y, low LILEs, especially K_2O, Rb, Sr (Fig. 10). It is tempting, therefore, to suggest some minor involvement of such rocks in the history of the High-HFSE granites.

Tectonics and other implications: The close spatial, temporal, and, at least locally, genetic, relationship between the High-HFSE granites and volcanics (e.g., at Kookynie), indicates that these granites were intimately related to greenstone formation. More importantly, the geochemistry of the High-HFSE granites and their A-type affinities indicates emplacement in an, at least locally, extensional environment (as pointed out by Champion & Sheraton, 1997). The ages of these granites, mostly 2700 to 2680 Ma, especially the latter, can be then be used to indicate periods of local extension. In this regard, the veracity of the 2738 Ma age on part of the Satisfaction Complex (Nelson, 1998) becomes important, in that it may signify earlier greenstone development in the northern Eastern Goldfields than currently envisaged. Similarly, the younger age of the Weebo granodiorite (2658 Ma, Nelson, 1997), though appearing somewhat anomalous, may be related to the same environment that was responsible for the syenites of similar age (ca. 2666, Table 2b).

High-HFSE Clan	**Kookynie Association Supersuite**	**Suite**
Kookynie	Boo Boo	Boo Boo, Caledonian
	Penzance	Penzance, Chandlers, Bundarra
	Weebo	Weebo
	unassigned	unassigned (Gearless, Bebbington, Weebo unnamed-1, Weebo unnamed-2, Madman Well, Skeleton Well, Okeef Well)
Satisfaction	Satisfaction	Satisfaction, Gemchapps, Boomer Bore, Ives Find, Mandilla Well, Cocks Well
Bullshead	Bullshead	Wilsons Patch, Bullshead, Teutonic
High-HFSE interpreted (EGP)		Kookynie Association
unassigned	unassigned	Various unassigned units (Lehmann)

Table 4. Suites, supersuites, clans and associations of the High-HFSE group, northern Eastern Goldfields Province.

Clans of the Kookynie Association, High-HFSE Group, Eastern Goldfields Province

Kookynie clan

Member Supersuites: Boo Boo, Penzance, Weebo

Distribution: The Kookynie clan, comprising three supersuites in the NEG, is strongly localised along a NNW-trend, extending from Kookynie (Menzies 1:250 000 sheet), up to north of Wiluna, as follows:

- the western half of the Teutonic mass (Penzance supersuite)
- in the greenstones west of the Koonoonooka mass (Boo Boo supersuite), and
- in the greenstones north of the Teutonic mass (Weebo supersuite).

Geochronology: Two reported ages, 2679 Ma for the Kent Complex, Penzance supersuite (Black, written communication, 2000), and 2658 Ma for the Weebo granodiorite, Weebo supersuite (Nelson, 1997; Table 2b). The latter age is atypically young, with most

Kookynie Association granites 2680 to 2700 Ma (Table 2b). Both dated granites indicate some inheritance, around 2710 Ma (Table 2b).

Chemical characteristics: The Kookynie clan is the archetypal High-HFSE clan, containing the rocks that earlier published descriptions of the group were based on (e.g., Champion & Sheraton, 1997). Geochemical characteristics include the variably elevated total Fe, MgO, Y, LREE, Zr coupled with low to moderate Al_2O_3, K_2O, Rb, Sr, and only moderate Na_2O (Fig. 9). Plots of various element combinations, e.g., K_2O-Sr, K_2O-Al_2O_3 are very distinctive (Fig. 13). The Kookynie clan has many similarities to the Satisfaction clan, with most significant differences evident in the abundances of some of the LILEs, e.g., Rb, Pb, Th and U (Fig. 9). The Kookynie and Bullshead clans are spatially associated and also share many similarities.

An extra feature of the Kookynie clan is the presence of an altered subgroup, identified by lower K_2O, Rb, Pb? and elevated CaO, Na_2O and Sr (Fig. 9). Notably, within this subgroup, the LREE, traditionally thought of as immobile during most alteration, can also be seen to be highly variable. Good examples of the LREE variation include 2 samples from within several meters of each other which show Ce varying from >160 ppm to <50 ppm in the fresher sample. Although these differences probably reflect alteration of LREE-bearing minerals, e.g., allanite, sphene, they could also reflect the very heterogeneous distribution of such minerals throughout the host.

Mineralised members? Porphyries on the Wiluna 1:250 000 sheet spatially associated with gold mineralisation. Similarly, granites and porphyries spatially associated with gold mineralisation on the Edjudina and Menzies 1:250 000 sheets.

Petrogenesis: As for the High-HFSE group in general.

Tectonic & other implications: As for the High-HFSE group in general.

Satisfaction clan

Member Supersuites: Satisfaction

Distribution: This clan of one supersuite and six units, is strongly localised to a NNW trending zone along the eastern edge of the Koonoonooka mass (Fig. 1), either marginal to greenstones, or, as strongly foliated to gneissic granitoids intimately interlayered with greenstone remnants and lenses, e.g., Satisfaction Complex.

Geochronology: Two reported ages, 2738 Ma from a gneissic layer within the Satisfaction Complex (Nelson, 1998), and a younger 2699 Ma age on the Mandilla Well porphyry (L. Black, written communication, 2000), a dyke intruding greenstone (Table 2b). Dating, as part of this project, also recorded a 2608 Ma titanite age on the Gemchapps granite.

Chemical characteristics: Geochemically very similar to the Kookynie clan, with significant differences only present within some of the LILEs, e.g., lower Pb, Th, U and Rb in the latter (Fig. 9).

Mineralised members? None.

Petrogenesis: As for the High-HFSE group in general.

Tectonic & other implications: As for the High-HFSE group in general. The older age of the Satisfaction Complex layer is one of the oldest recorded for the northern Eastern Goldfields (Table 2), and raises a number of interesting points. Given that granites of this group have a strong spatial relationship with contemporaneous (and in part co-genetic) felsic volcanics, suggests the strong possibility that there are/were co-existing volcanics (and, hence, greenstone) of similar age (2738 Ma) in the region. Notably, Nelson (1997a) reports an age of 2720 ± 14 Ma (Table 2b) from a deformed felsic volcanic rock from the Rockys Reward mine, which although younger, is within experimental error of the Satisfaction Complex age. Similarly, the tonalitic phase of the Kathleen Valley Gabbro records an age of 2736 ± 3 Ma (L.P. Black, written communication, 2000; Table 2b), also suggesting the presence of older greenstone (to 2750 Ma) within the region.

Bullshead clan

Member Supersuites: Bullshead

Distribution: This clan, comprising the one supersuite, is localised within and adjacent to the western Teutonic mass. Although comprising only three named units (Table 4), both the Wilsons Patch and Bullshead granitoids occur as widespread small intrusions, either as outcrop or intersected in drill hole. The third unit, the Teutonic granodiorite is only found on mine dumps, from small historic gold mines, within the surrounding Kookynie clan granites.

Geochronology: None.

Chemical characteristics: The Bullshead clan is clearly distinct from the other two High-HFSE clans, in particular being considerably more mafic (Fig. 9). The clan has been tentatively placed within the High-HFSE group, largely on the combination of such features as high total Fe, elevated Y and Zr, coupled with low Rb, Sr, Pb, Th (Figs 9, 13). The Bullshead clan members are clearly distinguished from the dominant clans of the Mafic group (Granny Smith and Kanowna Belle clans), by the lower MgO, Sr, Ba, Pb, Th, U, Cr, and higher total Fe, Y and Zr in the Bullshead clan (Figs 10, 13). As described earlier, members of the Bullshead clan do, however, have a number of similarities to the distinctive Kathleen Valley and Sweet Nell clans of the Mafic group.

Mineralised members? Small gold deposits associated with the Teutonic granodiorite.

Petrogenesis: As discussed for the High-HFSE group in general.

Tectonic & other implications: As discussed for the High-HFSE group in general.

Granny Smith Association, Mafic group, Eastern Goldfields Province

Member clans: Granny Smith, Kanowna Belle, Lawlers High-Ti, Kathleen Valley, Sweet Nell.

Distribution: This group comprises 2 widely distributed clans (Kanowna Belle, Granny Smith) and three very small clans (Table 5), with the large majority of units occurring as small to moderate plutons and porphyries within the greenstones (Fig. 1), in particular:

- in the greenstone belt stretching from around Leonora in the south to Jundee in the north,
- in the greenstones around Laverton,
- at Lawlers
- as small bodies within the Teutonic mass
- in the Dingo Range greenstone belt.

Geochronology: The great majority of recorded ages for the Mafic group cluster around 2665 Ma (especially within the Granny Smith clan, Table 2b). The overall range of the group appears to be from at least 2676 Ma (Kanowna Belle porphyry, Krapez et al., 2000), to 2648 Ma (Liberty granodiorite, Kent, 1994).

Chemical characteristics: Champion & Sheraton (1997) and Champion (1997), originally defined the Mafic group as a variety of granite suites and supersuites largely characterised by their lower silica contents (55-70%) and variable LILE and LREE content (Fig. 10). Champion & Cassidy (1998) further studied the spread in the LILE and LREE, and subdivided the Mafic group into two broad subtypes, namely High-LILE and Low-LILE, now called the Granny Smith and Kanowna Belle clans, respectively. Notably, the approximate dividing line for these two clans is very similar to the arbitrary divide used for the low and high LILE members of the High-Ca group (Fig. 5). Another important feature is that the high LILE and LREE character of the Granny Smith clan extends even to the most mafic end-members, clearly indicating the fundamental differences from the Kanowna Belle clan (Fig. 10). Despite the differences in LILE and LREE, members of both clans are all dominantly Sr-undepleted. Y typically decreases with increasing silica, from Y-undepleted levels becoming Y-depleted. Similarly, epsilon Nd values are similar for both clans (Champion & Sheraton, 1997).

The other three clans (Table 5), each contain only one unit with distinctive geochemistry, e.g., Lawlers high-Ti clan – very high TiO_2, Kathleen Valley & Sweet Nell clans – high total Fe, Zr, Y, low LILE.

Mineralised members? One important feature of the Mafic group, is the relatively common association of members of the group with gold mineralisation, including units that directly host gold, e.g., Granny Smith, Lawlers, Liberty, Kanowna Belle, Golden Cities, to small bodies and porphyries spatially associated with mineralisation, e.g., porphyries at Jundee, Bronzewing.

Petrogenesis: As indicated by Champion (1997), the source of the Mafic group granites is largely equivocal, with evidence for both crustal and mantle-derived contributions. Clearly the variation in the LILE and LREE, evident in even the most mafic end-members, requires at least two separate components, just to produce the Kanowna Belle and Granny Smith clans (see discussion for Granny Smith clan). Champion (1997) suggested two such sources, namely a mafic 'basaltic' source, similar to that proposed for the High-Ca granites, and a more mafic, perhaps mantle-derived, LILE-rich source component. The similarity, at least in part, of sources for the Mafic group (Kanowna Belle clan) and the High-Ca group, is supported by the very similar chemistry of the two groups in their small region of overlap (Fig. 10). The origin of the High-LILE component is more equivocal (see discussion for Granny Smith clan). Notably the overlap of ages for Granny Smith clan, around 2665 Ma, with some Syenitic group magmatism (Table 2b), indicates a possible source of, at least part of, the LILE and LREE enrichment in the Granny Smith clan.

Origins for the minor Kathleen Valley and Sweet Nell clans are more straight forward, either resulting from fractionation, or partial melting, of a tholeiitic parent. The former is preferred for the Sweet Nell clan, and is clearly the case for the Kathleen Valley clan.

Mafic group	**Granny Smith Association**	
Clan	**Supersuite**	**Suite**
Granny Smith	Anomaly 45	Anomaly 45
	Bronzewing2	Bronzewing porphyry-2
	Granny Smith	Granny Smith, Mount Crawford
	Jerusalem	Jerusalem, Golden Ring, Woolshed Well
	Jindardie	Jindardie, Little Bore
	Jundee-3	Jundee-3
	Lawlers	Lawlers
	Linger and Die	Linger and Die, Pumping Station, Victory Corner, King of the Hills, Winston
	Mabel Creek	Mabel Creek
	Mt Joel	Mt Joel, Bronzewing porphyry-3
	Russell Well	Russell Well
	Sims Find	Sims Find
	Waihi Hills	Waihi Hills
Kanowna Belle	Bills Find	Bills Find
	Bronzewing	Mandaline, Bronzewing porphyry-1, unnamed suite, Lowlands, Thompsons Well
	Collavilla	Collavilla
	Golden Ring-2	Golden Ring-2
	Hurleys Reward	Hurleys Reward
	Jundee-2	Jundee-2
	Kens Bore	Kens Bore
	Mount Lucky	Mount Lucky
	Mount Stirling	Mount Stirling, Federation
	Sundowner	Sundowner, Bronzewing diorite
	Tommy Bore	Tommy Bore
	unnamed	unnamed
Kathleen Valley	Kathleen Valley	Kathleen Valley
Lawlers High-Ti	Lawlers High-Ti	Lawlers High-Ti
Sweet Nell	Sweet Nell	Sweet Nell

Table 5. Suites, supersuites, clans and associations of the Mafic group, northern Eastern Goldfields Province.

Tectonic & other implications: It was originally envisaged, by the author, that many of the Mafic group granites, especially those generated around 2665 Ma were produced in some form of arc-environment, co-incident with proposed main period of crustal shortening (D_2) in the Eastern Goldfields Province; such an environment being capable of producing the compositional variation in the LILE. The increasing evidence for Syenitic and other sub-alkaline magmatism at this time (e.g., Gilgarna, Panakin, Erayinia clans, Table 2b), however, raises the possibility, that both granitoids from the Syenitic and Mafic groups were produced, at that time (ca. 2665 Ma) in a similar (locally?) extensional environment. Note that this could still be in an overall arc-environment.

The granitoids of the Kathleen Valley and Sweet Nell clans, were undoubtedly generated in periods of greenstone deposition and development.

Clans of the Granny Smith Association, Mafic Group, Eastern Goldfields Province

Granny Smith clan

Member Supersuites: Anomaly 45, Bronzewing2, Granny Smith, Jerusalem, Jindardie, Jundee-3, Lawlers, Linger and Die, Mabel Creek, Mt Joel, Russell Well, Sims Find, Waihi Hills

Distribution: A clan comprising widely distributed supersuites, with the great majority of units occurring as small to moderate plutons and porphyries within the greenstones, in particular:
- in the greenstone belts stretching from around Leonora in the south to Jundee in the north (Anomaly 45, Bronzewing2, Jundee-3, Linger and Die, Mabel Creek, Mt Joel, Sims Find supersuites),
- in the greenstones around Laverton (Russell Well, Granny Smith, Jerusalem, Waihi Hills supersuites),
- at Lawlers (Lawlers supersuite supersuite).

In addition, a number of small bodies occur within the Teutonic mass (Jindardie supersuite).

Geochronology: Given the strong association with gold mineralisation, granites of this clan (and the Mafic group in general) have been well studied, and hence, dated (Table 2a). Notably, nearly all dated granites from the Granny Smith clan give ages within error of 2665 Ma (Table 2b); the only major exception being the Liberty granodiorite (2648 ± 6 Ma, Kent, 1994) in the southern Eastern Goldfields Province. It is noted that such a time specific clan is unusual within the Eastern Goldfields Province.

Chemical characteristics: As discussed earlier, the members of the Granny Smith clan, dominate the high-LILE compositional range of the Mafic group (Fig. 10). Geochemical characteristics include higher K_2O, Rb, Sr, Pb, LREE relative to the Kanowna Belle clan (Fig. 10). Champion & Cassidy (1998) noted that a simple K_2O-Ce plot can be used to discriminate between the majority of Kanowna Belle and Granny Smith clan members (Fig. 5). An important feature to note, however, is that even within the Granny Smith clan there is a considerable variation between LILE and LREE contents between individual supersuites (Fig. 10).

Mineralised members? The Granny Smith clan, includes mineralised granites at Granny

Smith and Lawlers (Porphyry, Liberty to the south), as well as a number of porphyries and smaller bodies spatially associated with mineralisation, e.g., Jundee, Bronzewing. The clan also includes a number of units sampled because of their association with sub-economic mineralisation (e.g., Sims Find, Anomaly 45).

Petrogenesis: Largely as for the Mafic group in general. The differences between the Granny Smith clan and the Kanowna Belle clan, may have been produced in a variety of ways, all concerning the nature and timing of the LILE enrichment, namely:

- essentially two completely separate sources (not supported by the range in LILE observed within the Granny Smith clan itself),
- a similar overall source, variably LILE-enriched (metasomatised) before partial melting, with the non- or poorly-metasomatised regions producing the Kanowna Belle clan, and the more strongly-enriched regions producing the Granny Smith clan,
- a heterogeneous (mixed) source region, or
- post-melting modification by a LILE-enriched fluid or melt, e.g., magma mixing.

At present it is difficult to choose between one or more of these models. Notably the strong clustering of ages for Granny Smith clan, around 2665 Ma, overlapping with syenitic and sub-alkaline magmatism of a similar age not only suggests a possibly similar tectonic environment of formation, but also indicates a possible source of, at least part of, the LILE and LREE enrichment in the Granny Smith clan.

Tectonic & other implications: Largely as for the Mafic group in general.

<u>Kanowna Belle clan</u>

Member Supersuites: Bills Find, Bronzewing, Collavilla, Golden Ring-2, Hurleys Reward, Jundee-2, Kens Bore, Mount Lucky, Mount Stirling, Sundowner, Tommy Bore, unnamed

Distribution: The Kanowna Belle clan comprises numerous, dominantly small bodies and porphyries, mostly within or marginal to greenstones, as follows:

- within the greenstone belt running from around Leonora to Jundee in the north (Bills Find, Bronzewing, Collavilla, Jundee-2, Kens Bore, Mount Stirling, Sundowner, Tommy Bore supersuites),
- in the greenstones around Laverton (Golden Ring-2, Mount Lucky supersuites), and
- in the Dingo Range greenstone belt (Hurleys Reward supersuite).

The distribution of units of the Kanowna Belle clan strongly overlap with those of the Granny Smith clan.

Geochronology: Only one reliable age has been reported for the Kanowna Belle clan in the northern Eastern Goldfields, an age of 2669 Ma for the Kens Bore granodiorite (Nelson, 1997; Table 2b). Geochronology on the Bronzewing diorite showed a complex zircon distribution, with a possible intrusive age of around 2655 Ma (Nelson, 1998). L. Black (written communication, 2000) obtained what appears to be a 2956 Ma inheritance age for the Hurleys Reward granodiorite.

Chemical characteristics: The Kanowna Belle clan encompasses the low LILE and LREE part of the Mafic group compositional range, evident in the low to moderate levels of K_2O, Rb, Sr, Pb, Ce (Figs 5, 10), but also does not extend to the less siliceous compositions of the Granny Smith clan. Many of the chemical characteristics of the Kanowna Belle clan are similar to those observed in the low-LILE clans of the High-Ca group (Beasley, Nambi, No. 2 Well clans; Figs 10, 13), making it difficult to separate members of the two groups in the region of overlap (around 69-72% SiO_2).

Both the Sweet Nell and Kathleen Valley clans also contain low LILE contents (Figs 5, 10), but are easily distinguished from the Kanowna Belle clan by their high to very high total Fe, Zr, Y and low Al_2O_3 (Fig. 10).

Mineralised members? In the northern Eastern Goldfields the Kanowna Belle clan includes a number of porphyries and small bodies spatially associated with gold mineralisation, e.g., at Bronzewing, Jundee.

Petrogenesis: Largely as for the Mafic group in general; also see discussion for the Granny Smith clan.

Tectonic & other implications: Largely as for the Mafic group in general.

Kathleen Valley clan

Member Supersuites: Kathleen Valley

Distribution: Confined to the felsic portions of the zoned Kathleen Valley Gabbro (see Liu, 2000) for descriptions.

Geochronology: One age (L.Black, written communication, 2000) of 2736 Ma (Table 2b).

Chemical characteristics: Strongly tholeiitic chemistry, marked by strong Fe-enrichment (very high-FeO*, low mg#), high levels of HFSE elements (e.g., Zr, Y, HREE) and very low LILE, in particular, K_2O, Rb (Figs 5, 10). Many similarities to the other tholeiitic clan - Sweet Nell (Fig. 10). Clearly distinct from the Kanowna Belle, Granny Smith and Lawlers High-Ti clans (e.g., total FeO, Al_2O_3, Zr, Y, Fig. 10).

Mineralised members? None.

Petrogenesis: The tholeiitic chemistry and other features (high-HFSE, low-LILE), are consistent with an origin through fractionation of the LILE-poor tholeiitic Kathleen Valley gabbro. The high levels of HFSE are a function of both the chemistry of the gabbro and the high temperatures of the magma.

Tectonic & other implications: The Kathleen Valley gabbro (and the more felsic parts), and surrounding rocks, are indicative of greenstone formation, The 2737 Ma age suggests the unit is possibly more akin to the Southern Cross Province, a view adopted by Liu (2000). It should be noted, however, that such ages are not unknown in the Eastern Goldfields Province.

Lawlers High-Ti clan

Member Supersuites: Lawlers High-Ti

Distribution: A small unit identified from drill core only in the Lawlers deposit (Cassidy, 1992). Relationships with the host Lawlers tonalite are uncertain, but probably represents a large pod within the Lawlers tonalite.

Geochronology: None, assumed to be of similar age to the Lawlers tonalite and porphyry dykes within the region, i.e. c. 2665 Ma (Table 2b).

Chemical characteristics: As the clan name suggests this unit is largely distinguished by significantly elevated TiO_2 contents (nearly twice the levels of the Kanowna Belle and Granny Smith clans). Other elements, e.g., LILE, HFSE, even P_2O_5 (which might be expected to mimic TiO_2), overlap with levels found in the Granny Smith and Kanowna Belle clans (Figs 5, 10).

Mineralised members? Spatially associated with mineralisation.

Petrogenesis: Largely as for the Kanowna Belle and Granny Smith clans. The elevated TiO_2 contents are difficult to explain, and may reflect a source rock feature, some unusual alteration effect, assimilation of greenstones, or perhaps a cumulate feature (not likely).

Tectonic & other implications: As for the Mafic group in general.

Sweet Nell clan

Member Supersuites: Sweet Nell

Distribution: One small unit within the greenstones of the northern Duketon area, hosted by a related? thick doleritic unit.

Geochronology: None (currently in progress).

Chemical characteristics: Like the very similar Kathleen Valley gabbro, the Sweet Nell granodiorite is characterised by high FeO*, low Al_2O_3, low LILE (especially K_2O, Rb, LREE) and elevated HFSE (Y, Zr; see Fig. 10).

Mineralised members? The unit is spatially associated with numerous small historic gold workings, largely concentrated along the contact with the surrounding dolerite.

Petrogenesis: Largely as for the Kathleen Valley gabbro which the Sweet Nell granodiorite largely resembles. Possibly related via fractionation, to the surrounding dolerite body.

Tectonic & other implications: The Sweet Nell granodiorite is very similar to the Kathleen Valley gabbro. Although both could be included in the one clan, they have been kept separate because the Kathleen Valley gabbro is most likely within the Southern Cross Province. Like the Kathleen Valley gabbro, the Sweet Nell granodiorite is almost certainly syn-greenstone formation. Currently being dated, the unit should give an approximate age to the greenstones within the region.

Gilgarna Association, Syenitic group, Eastern Goldfields Province

Member clans: Gilgarna, Panakin, Wallaby

Distribution: Conventionally thought of as being localised along linear NNW belts, mostly adjacent to the larger fault and shear zones (e.g., Smithies & Champion, 1999). This is, however, an oversimplification of the real situation, with their distribution best described as occurring within NNW-trending broad zones (Fig. 1). In this regard, Smithies and Champion (1999) identified four supersuites, namely Mount Monger, Emu, Claypan and Ninnis (all Gilgarna clan), in the Eastern Goldfields Province, each broadly confined to geographically distinct belts, with each belt corresponding to one of the major NNW to N fault systems, e.g., Emu Fault, Perseverance Fault.

Although, mostly occurring as small to moderate sized intrusives and porphyries, the group does include some larger units, dominantly belonging to the quartz monzonitic members (e.g., Panakin supersuite), in the very north of the northern Eastern Goldfields (and, notably, also in the southern part of the southern Eastern Goldfields).

The Wallaby Syenite, from the Wallaby deposit, appears to be spatially associated with carbonatite at that deposit. Relationships, from drill core, suggest that either some mixing has occurred or, possibly that there is some genetic relationship between the carbonatite and syenite.

Geochronology: The majority of available geochronology has indicated that members of the Syenitic group are in the range 2650 to 2640 Ma (Table 2b). More recent dating by Nelson (1999), L. Black (written communication, 2000) and the present AMIRA study (Table 2b) now suggests the presence of an additional? syenitic event around 2665 to 2660 Ma, i.e., there are now two distinct age groups for the Syenitic group. Note that the ages for the Wallaby syenite (and related? carbonatite) are within error of both time periods, so can not be reliably assigned to either.

Geochemical characteristics: The geochemistry of the Syenitic group and its members has been described in detail by Champion & Sheraton (1997), Smithies & Witt (1997), and Smithies & Champion (1999). The members of this group are easily recognisable by their combination of high total alkalis ($Na_2O + K_2O$), high K_2O, variable to high Rb, Ba, Sr, Pb, Th, U, Zr, LREE, Y, coupled with mostly lower MgO, CaO, total Fe and mg#, relative to the High-Ca group granites (Figs 11, 12). Members from the Gilgarna and Panakin clans, although petrographically distinct, are very similar geochemically; differences include lower K_2O, Rb, Th, U, Nb and marginally higher Sr. The Wallaby clan, comprising the syenites from the Wallaby and Jupiter gold deposits, is the most distinctive, with low TiO_2, FeO*, MgO and Rb and elevated Sr, Pb, Ba, Th, U and Nb (Fig. 11, although some of these differences may reflect the effects of hydrothermal alteration). An additional complexity, for the Wallaby Syenite at least, concerns the interaction with the carbonatite at that deposit.

Mineralised members? Both units of the Wallaby clan host gold mineralisation, as do members of the Gilgarna clan (e.g., Tin Dog). There is no recorded mineralisation associated with the Panakin clan members.

Petrogenesis: The petrogenesis of the Syenitic group has been described in some detail by Johnson (1991) and Smithies & Champion (1999), in particular the relative contributions of mantle versus crustal components – a constant problem in all petrogenetic models for syenites, especially quartz-normative syenites. Smithies and Champion (1999), pointed out that features such as the lack of associated mafic rocks, the presence of quartz within all syenites, the variable but mostly high LILE contents, the presence of some inherited? zircons (Table 2b), the presence of strong negative Nb and Ti anomalies, when all combined indicated a dominantly crustal origin; a conclusion also reached by Johnson (1991). Another important piece of evidence supporting this is present around the Kambalda region, where various members of the High-Ca, Mafic and Syenitic group all show evidence for strong Ba and Sr enrichment, a feature attributed to some form of lower crustal/mantle lithosphere metasomatism (e.g., Perring & Rock, 1991; Smithies & Champion, 1999).

In this regard, it is notable that the Wallaby clan, the most distinctive of the Syenitic group, is also characterised by high to very high Sr and Ba contents. This, together, with the close spatial relationship between the Wallaby syenite and carbonatite (a unit highly enriched in Ba and Sr), suggests, like the Kambalda area, that the syenitic source region around Laverton, has also been metasomatised to some extent.

Tectonic and other implications: As indicated by Champion (1997), and Smithies and Champion (1999), alkaline and sub-alkaline rocks such as those in the Syenitic group are good indicators of regions undergoing, at least local, extension, or an anorogenic (post-tectonic) environment. The timing and locations, therefore, of members of the Syenitic group provide some constraints on the tectonic evolution of the Eastern Goldfields Province. In this sense, the 2650 to 2640 Ma syenites, reinforce the inferences deduced from the Low-Ca magmatism, i.e., there is a significant change in tectonic environment in the period 2660 to 2655 Ma, from voluminous, possibly arc-related, High-Ca magmatism, to 'post-tectonic', or extensional, Low-Ca and Syenitic magmatism. Smithies and Champion (1999) speculated that this change reflected lower crustal delamination, caused by an unstable thickened crust produced in the D_2 compressional event.

Also of importance, is the recognition of syenitic magmatism around 2665 Ma (Table 2b), that must reflect some form of rifting and/or local extension. This has possible important implications for the origin of the high LILE contents found in the contemporaneous Granny Smith clan granitoids (Mafic group), and also to the Eastern Goldfields Province in general, given that the time around 2665 Ma is commonly assumed to be part of the D_2 compressional event.

Finally, the presence of Archaean carbonatitic magmatism, closely spatially associated with the younger Mt Weld carbonatite, strongly suggests the existence of a major deep-crustal fault zone within the Laverton region. The possible presence of such a structure has obvious implications for tectonic models for development of the Norseman-Wiluna belt, e.g., perhaps such a fault forms part of a rift-related pair with the Ida Lineament to the west, and for models of fluid flow and mineralisation. Such a fault zone should be clearly visible on the planned seismic traverse for this region.

Syenitic Clan	Gilgarna Association Supersuite	Suite
Gilgarna	Emu	Emu, Pig Well, Bulldog, Lorna Glen
	Mount Monger	Boiler Well
	Ninnis	Double Hole, Woorana Soak, Red Hill, Admiral, Beasley South, McKenna, Hanns Camp
Panakin	Panakin	Panakin, Pizzetti, Wadarrah, Old Darda, Jink Bore
Wallaby	Wallaby	Jupiter, Wallaby
unassigned	unassigned	unassigned (Teague impact syenite)
Syenitic – interpreted		Gilgarna Association
unassigned	unassigned	unassigned (Gravel Bore, Old Peculiar)

Table 6. Suites, supersuites, clans and associations of the Syenitic group, northern Eastern Goldfields Province.

Clans of the Gilgarna Association, Syenitic Group, Eastern Goldfields Province

Gilgarna clan

Member Supersuites: Emu, Mount Monger, Ninnis

Distribution: Smithies and Champion (1999) identified four supersuites, within the Gilgarna clan, namely Mount Monger, Emu, Claypan and Ninnis, each broadly confined to geographically distinct belts corresponding to one of the major NNW to N fault systems in the Eastern Goldfields Province, e.g., Emu Fault. Of these four supersuites, three (Ninnis, Emu, and Mt Monger, Table 6) extend into the northern half of the Eastern Goldfields Province, as follows:

- Mt Monger supersuite - Raeside mass
- Ninnis supersuite – greenstones around Laverton, Koonoonooka & Banjiwarn masses
- Emu supersuite – greenstones around Leonora, Teutonic and Banjiwarn masses

Geochronology: Two ages have been reported for this clan in the northern Eastern Goldfields, both from the Ninnis supersuite; 2644 Ma for the Woorana Soak syenite (Nelson, 1998), and 2664 for the Hanns Camp syenite (L. Black, written communication, 2000; Table 2b). Gilgarna clan units to the south give ages between 2650 and 2640 Ma (Table 2b; Smithies & Champion, 1999).

Chemical characteristics: Members of this clan are the archetypal syenites within the Eastern Goldfields Province. Their geochemistry has been described in detail by Smithies & Champion (1999). Basically, they are alkaline (high total alkalis, Na_2O, K_2O), with moderate to high Rb, variable to low MgO, CaO, and variable to high Sr, Pb, Zr, LREE, Y (Figs 11, 12). The three supersuites (Ninnis, Emu and Mount Monger) in the Gilgarna clan, northern Eastern Goldfields, are chemically relatively similar, with differences best seen in levels of Ba, Sr, Y, La, and Nb (see Smithies & Champion, 1999).

Mineralised members? None recorded in the northern Eastern Goldfields. Mineralised units known to the south (e.g., Tin Dog).

Petrogenesis: As for the Syenitic group in general. Smithies & Champion (1999) suggested the differing geochemistry shown between the supersuites largely reflected mainly subtle variations in crustal composition across the Eastern Goldfields Province.

Tectonic & other implications: As for the Syenitic group in general. The apparent presence of syenites of two distinct ages, strongly suggests at least 2 periods of extension (at least locally). In particular, the presence of syenites at 2665 Ma, has important implications for the timing of the major compressional event (D_2).

Panakin clan

Member Supersuites: Panakin

Distribution: This clan, comprising one supersuite of seven quartz monzonite units, is confined to a NNW-trending zone, in two separate regions in the northern half of the northern Eastern Goldfields, both straddling the Celia Lineament (Ninnis Fault):
- two units in the northern part of the Teutonic mass and central Banjiwarn mass, (Wadarrah, Old Darda),
- five units in the north-eastern part of the Koonoonooka mass and the north-western part of the Banjiwarn mass.

Geochronology: Two ages have been recorded for this clan, 2643 Ma for the Wadarrah quartz monzonite (Nelson, 1997), and 2664 Ma for the Panakin quartz monzonite (Nelson, 1999). Notably, these differing ages correspond to the two geographically separate outcrop regions, i.e., Wadarrah in the south, and Panakin in the north.

Chemical characteristics: Although petrographically distinctive, being largely quartz monzonitic (versus quartz syenitic), the Panakin clan has many chemical similarities with the Gilgarna clan, e.g., similar levels of MgO, FeO*, TiO_2, CaO, Na_2O, Ba, Sr, Th, LREE (Fig. 11). The main differences concern K_2O and Rb which are marginally lower in the Panakin clan (Fig. 11).

Mineralised members? None.

Petrogenesis: Largely as for the Syenitic group in general.

Tectonic & other implications: Largely as for the Syenitic group in general. Like the Gilgarna clan, the bimodal age distribution indicates, at least local, extension, around 2665 Ma, and later at 2650 to 2640 Ma.

Wallaby clan

Member Supersuites: Wallaby

Distribution: A number of small bodies around the Jupiter and Wallaby gold deposits.

Geochronology: Two indistinguishable ages, one on titanite (2657 ± 15 Ma) on a mixed syenitic-carbonatitic rock, the other a Pb feldspar-wholerock isochron age (2658 ±16 Ma) on the Wallaby syenite, both from the Wallaby deposit (both AMIRA P482 ages; Table 2b). Unfortunately, as described earlier, both these ages are are within error of the two recognised time periods for the Syenitic group (ca. 2665 and 2650-2640 Ma).

Chemical characteristics: The Wallaby supersuite syenites are distinguished by their consistently low TiO_2, FeO*, MgO, low to moderate Rb and Y, high Th and U, and high to very high Ba, Sr, and Pb, relative to other clans in the Syenitic group (Fig. 11). Like other members of this group, however, alkalis are high, and the LREE, Zr, Th and U are highly variable (Fig. 11).

Mineralised members? Units at both Wallaby and Jupiter are mineralised.

Petrogenesis: Largely as for the Syenitic group in general. It is noted that similar elevated to extreme Sr and Ba are present in syenites and other granites in the general area around Kambalda (part of the Mount Monger supersuite of Smithies & Champion, 1999). These authors suggested such enrichments reflected the influence of some metasomatising agent (lamprophyric magmatism around Kambalda), either before, or during syenite generation. A similar situation is envisaged for the Wallaby clan granites, a suggestion supported by the close spatial association with carbonatite (at Wallaby).

Tectonic & other implications: The close relationship between the syenite and carbonatite at the Wallaby deposit is very significant, with obvious implications for the origin of the syenites, particularly given the fact that there appears to be hybrid? mixes between the two lithologies. Whether the mixed syenite-carbonatite represents mixing at or near the source or more locally is not known. Certainly, the geochemistry strongly suggests the carbonatite is a true carbonatite and not some unusual alteration effect. Given the common association of carbonatites with large-scale deep faults and the presence of both an Archaean and the nearby younger Mt Weld carbonatite in the Laverton region strongly suggests the presence of one (or more) such deep-seated large faults in this region. Such a structure should be clearly visible on the east-west seismic traverse planned for the region. The presence of such a system, in tandem with the deep penetrating nature of the fault as imaged along the Ida lineament (Goleby et al., 1993), on the western margin of the Norseman-Wiluna belt, Eastern Goldfields Province suggests an interesting paired association, with implications for both tectonic development of the region and for gold mineralisation.

Simplified key for discriminating granite groups in the northern Eastern Goldfields.

This section describes keys and techniques developed to successfully discriminate between the five granite groups within the northern Eastern Goldfields. This approach relies on both petrology/mineralogy and geochemistry with the observation that it is difficult if not impossible to successfully identify all granite groups from petrology/mineralogy alone, i.e., geochemistry is a necessary ingredient. The basic technique involves what is best described as an inverse approach, moving from most easily recognisable to the more cryptic groups. Finally, it should be noted that there will be some granites that can not be confidently assigned to any one group.

Key for identification of associations and clans.
Keys 1 and 2 list keys for identifying granite groups on basis of mineralogical and field data (Key 1), and using geochemical data (Key 2). Table 7 lists characteristic field, mineralogical and geochemical features for granite groups and associations in the northern Eastern Goldfields region, encompassing the northern EGP and the south-eastern Southern Cross Province. Although, strictly only valid for this region the keys are, in general, applicable for all granites in the Eastern Goldfields Province at the group level, and probably to the majority of granite groups in the Southern Cross Province (and Murchison Province). Although keys can be used individually, they are best used together. Once a tentative group assignment has been made, further details should be checked against the group characteristics listed in Table 7 (and described in detail in the preceding sections).

Field and mineralogical discrimination
Geological and mineralogical characteristics of each group are shown in Table 7, with the more diagnostic features highlighted. For a number of the groups field identification is quite straight forward (see Key 1). For example, a quartz-poor feldspar-rich rock with common green mafic minerals most probably belongs to the Syenitic group (Gilgarna association). Members of the Mafic group (Granny Smith association), which include common host rocks for gold mineralisation (e.g., Granny Smith, Liberty, Golden Cities), where not altered, can be readily recognised by their darker colour, and common ferromagnesian minerals, mostly amphibole, though a small percentage of the High-HFSE group (mafic end-members) also have this characteristic. More felsic members of the High-HFSE group (Kookynie association), on the other hand, can be very difficult to distinguish in the field although their common close spatial association with, often related, volcanics, and their geographically-restricted distribution do help (Key 1). The Low-Ca and High-Ca groups can also be difficult to distinguish in the field. Perhaps the best means of in-situ discrimination is by use of a gamma-ray spectrometer, e.g., total counts of ~100 counts per second (cps), on AGSO's spectrometers appears to be a good approximate separation; above 100 cps suggests Low-Ca, below suggests the High-Ca group. Note though, that values above 120 cps are used in the key to eliminate High-Ca group outliers. Other indicators for Low-Ca granites include the presence of fluorite (typically purple) and common allanite and sphene (Key 1), especially in the more biotite-rich members, although these minerals can be difficult to see in hand specimen. In thin section, the relative abundances of K-feldspar to plagioclase, and the presence or absence of zoning can be diagnostic (Table 7).

KEY

1.	Common to abundant amphibole	2
1a.	Minor or no amphibole (biotite only)	4
2.	Green amphibole and/or pyroxene, mostly minor quartz (<10%), K-feldspar dominant, minor or no plagioclase; often common titanite; rare garnet.	Syenitic
2a.	Amphibole and/or pyroxene in very felsic rock	High-HFSE
2b.	Moderate to common quartz, common plagioclase, amphibole mainly dark	3
3.	Mafic group mostly, though could possibly be Bullshead Clan of High-HFSE group, particularly if around Teutonic Mass. Confirm with chemistry.	
4.	Fluorite present	Low-Ca
4a.	No fluorite	5
5.	Relatively common titanite <u>and</u> allanite (to few percent)	Low-Ca
5a.	Titanite or allanite (not both), or neither present	6
6.	Spectrometer available	7
6a.	No spectrometer readings	9
7.	High total counts; >120 cps on AGSO readings	Low-Ca
7a.	Lower total counts; <120 cps	8
8.	High-Ca group mostly, though could also be High-HFSE group, or Low-Ca. Confirm with chemistry.	
9.	Either High-Ca, Low-Ca, or perhaps High-HFSE group. Confirm with chemistry.	

Key 1. Simplified key using mineralogical features to identify granite groups. Note, geochemical characteristics will often also be required for full identification. Once an identification has been made, all characteristics should be checked with Table 7, Key 2 if possible, and the relevant preceding sections. The key will not work for moderately to strongly altered samples.

KEY

1.	High LOI (>2-3%), or anomalous ASI, S, CO_2, Na_2O, K_2O	altered
1a.	LOI and ASI okay	2
2.	**high Na_2O+K_2O, high Na_2O versus K_2O, high Ce & K_2O,** low to moderate MgO; (refer to plots in Figs 11, 12). Also verify mineralogical features (Key 1)	Syenitic
2a.	Not as above	3
3.	**high to very high total Fe, Y, Zr, very low Al_2O_3, K_2O, Rb, Pb** (Fig. 10)	4
3a.	not as above	5
4.	Kathleen Valley and Sweet Nell clans, Mafic group. At present only two units in these clans, i.e., rare	
5.	**low to moderate SiO_2 (<72%), high Ni, mg#,** low to moderate K_2O, Zr, high MgO for given K_2O (Fig. 13).	6
5a.	not as above	7
6.	Mafic group. Kanowna Belle clan can be difficult to distinguish from some High-Ca clans. Granny Smith clan more easily discriminated.	
7.	**Low Al_2O_3 & Sr for given K_2O, only moderate K_2O,** elevated Zr, Y (Fig. 13)	High-HFSE
7a.	not as above	8
8.	**high K_2O, K_2O/Na_2O, Rb, Th, Zr, LREE, moderate Na_2O,** moderate-high Y; (see Figure 14)	Low-Ca
8a.	**low-moderate K_2O, Rb, Th, Zr, LREE, moderate-high Na_2O,** low-moderate Y; (see Figure 14).	High-Ca

Key 2. Simplified key using geochemical features to identify granite groups; to be used in conjunction with Figures 10, 11, 12, 13, 14. Once an identification has been made, all characteristics should be checked with Table 7 and the relevant preceding sections. Also refer to the latter for clan identification The key is not designed for moderately to strongly altered samples.

High-Ca group (Menangina & Diemals Associations)

Field characteristics	Feldspar-quartz mineralogy	Fe-Mg minerals and accessories	Geophysics	Geochemistry
Often strongly deformed to gneissic. In the EGP can be strongly feldspar porphyritic	**plagioclase dominant often with common zoning or patchy cores**	biotite-bearing, minor amphibole; some allanite or sphene, rarely both.	***total* counts, K, Th and U all low**	**high Na_2O, low Th, LREE, Zr**

Low-Ca group (Mt Boreas & Beetle associations)

Field characteristics	Feldspar-quartz mineralogy	Fe-Mg minerals and accessories	Geophysics	Geochemistry
Commonly mildly deformed at best but can be locally strongly deformed. Also forms small pods to plutons in external gneisses; often have post-tectonic appearance	**common K-feldspar,** plagioclase typically unzoned	biotite-bearing, amphibole rare; **mafic compositions rich in both allanite and sphene (to 3%); fluorite commonly present**	**total counts, K, Th and U all generally high;** often high magnetic susceptibilty, to 10+ (10^{-3} SI units)	**high K_2O, low Na_2O, high Rb, Th, LREE, Zr**

High-HFSE group (Kookynie association)

Field characteristics	Feldspar-quartz mineralogy	Fe-Mg minerals and accessories	Geophysics	Geochemistry
variably deformed, commonly spatially associated with volcanic rocks and volcanic complexes; also **geographically restricted to north-south zone from S of Kookynie to N of Wiluna**	mostly very felsic, i.e., quartz and feldspar rich; does include plagioclase-rich granodiorites also	despite felsic nature can have either biotite and/or amphibole. The presence of amphibole in a very felsic rock is diagnostic of this group. More mafic variants contain amphibole ± pyroxene	moderate cps for total counts, K, Th and U	**distinctive combination of high FeO*, MgO, TiO_2, Y, Zr, with low Rb, Pb, Sr, Al_2O_3**

(Mafic group (Granny Smith association)

Field characteristics	Feldspar-quartz mineralogy	Fe-Mg minerals and accessories	Geophysics	Geochemistry
variably deformed, **distinctive dark-looking granites**	mostly plagioclase dominant (over K-feldspar); plagioclase has common zoning, often oscillatory.	**common to abundant amphibole ± biotite ± pyroxene.** Biotite may be relatively common in clans with high-LILE contents, e.g. Granny Smith clan	low to moderate total counts, K, Th and U	**low SiO_2 contents (55-70+%),** moderate to high Ni, Cr, MgO, mg#

Syenitic group (Gilgarna association)

Field characteristics	Feldspar-quartz mineralogy	Fe-Mg minerals and accessories	Geophysics	Geochemistry
commonly undeformed; commonly very distinctive red granites with green pyroxene (or amphiboles); often have haematitic or altered look	K-feldspar-rich, with little or no quartz;	common green pyroxene (locally amphible) and adundant sphene; notably ferromags are only locally strongly abundant; i.e. mostly low pyroxene/feldspar ratio; local garnet	moderate to locally high total counts, K, Th and U	high total alkalis ($Na_2O + K_2O$) 10-12%; often low MgO, FeO*, TiO_2; high Na_2O versus K_2O

Table 7. Characteristics of the 5 granite groups in the northern Eastern Goldfields. Distinctive features are highlighted in bold. It should be noted, however, that no single feature is 100% diagnostic.

Geochemical discrimination

Geochemical data, where available, is perhaps the best way to discriminate the granite groups, although it too is not definitive in all cases. Once a group classification has been made the corresponding field and mineralogical characteristics should also be checked.

Altered samples

Although most strongly altered samples can usually be easily recognised in the field or in hand specimen, this is not always the case. Additionally, their are occasions when access to hand specimens is not feasible, e.g., using data not personally collected. In these situations, it is necessary to be able to recognise moderately to strongly altered samples from their geochemistry. There are a number of parameters which can be used to indicate alteration, typically by increased or decreased contents of elements, or changes in ratios, e.g., LOI (loss on ignition), CO_2, H_2O, S, K_2O, Na_2O, and ratios involving Na_2O and K_2O, e.g., ASI (aluminium saturation index – ratio of Al to Ca+Na+K). The latter and LOI are shown in Figure 12. LOI (or, if measured, H_2O and/or CO_2), is one of the more simple indicators of alteration (or weathering), with most samples plotting above 2% (Figure 12) suggesting some modification. It is evident, from Figure 12, that many of the Mafic group granites are altered, which is to be expected given that many were collected from gold deposits. It is also evident that a subset of both the High-Ca and High-HFSE groups (Fig. 12) are also altered; these correspond to samples from Tarmoola, and samples east of Teutonic Bore, respectively. The ASI plot (Figure 12), also clearly shows a number of anomalous samples, plotting above and below the main trend. Once altered samples have been recognised, the data can still be used but must be treated with caution with regard to group classification. The use of anhydrous SiO_2, (simply major elements renormalised to 100% once LOI or combined H_2O and CO_2 are omitted), is useful in that it counteracts dilution effects due to hydration and carbonation.

Gilgarna Association, Syenitic group

Members of this group are, perhaps, the most distinctive of all EGP granites. They are readily and easily identifiable in the field, mineralogically, and geochemically (see Keys 1, 2; Table 7). Their chief chemical characteristics are high contents of the alkalis (K_2O, Na_2O+K_2O), coupled with generally low FeO*, MgO, TiO_2, and commonly elevated but quite variable HFSE, e.g., Zr, Y, REE (Figs 11, 12). A combination of total alkalis, Na_2O versus K_2O, Ce versus K_2O, and MgO (Fig. 12) are usually sufficient to discriminate members of this group. Most difficulty occurs for the high SiO_2 end-members, where compositions converge with those of the Low-Ca group; Na_2O versus K_2O is usually sufficient, however (Fig 12).

Kookynie Association, High-HFSE group

This group has a number of distinctive geochemical characteristics that make recognition relatively easy, in particular the combination of high total Fe, MgO, TiO_2, HFSE, low to moderate Al_2O_3, LILE, and Sr-depleted, Y-undepleted character (Figs 9, 13). While plots of these elements/oxides versus SiO_2 are often sufficient, it is combinations of these elements/oxides that are very diagnostic, e.g. Rb versus Y, K_2O versus Al_2O_3, Sr, Y, MgO (Fig. 13). For example, Figure 13 clearly shows that K_2O versus Sr and Al_2O_3, and SiO_2 versus K_2O together clearly discriminate this group from all other groups. In this regard the High-HFSE group is one group that is considerably easier to identify with geochemistry; in fact most classifications for this group are largely based on geochemistry alone. This reliance on chemistry can lead to some classification errors, so consideration should also be given to other attributes such as the association's localised distribution and common occurrence with volcanic rocks (Table 7). Most confusion with the group concerns the Bullshead clan, largely because it possesses a number of features clearly distinct from the other High-HFSE clans, in particular being considerably more mafic (Fig. 9). The clan has been placed within the High-HFSE group, and not the Mafic group, largely on the basis of common High-HFSE group features such as high total Fe, elevated Y and Zr, coupled with low Rb, Sr, Pb, Th (Figs 9, 13). The Bullshead clan members are clearly distinguished from the dominant clans of the Mafic group (Granny Smith and Kanowna Belle clans), by their lower MgO, Sr, Ba, Pb, Th, U, Cr, and higher total Fe, Y and Zr (Figs 10, 13). The members of the Bullshead clan do have a number of similarities to the Kathleen Valley and Sweet Nell clans of the Mafic group, but the very high total Fe and very low Al_2O_3 of the latter clans are diagnostic (Fig. 10).

Granny Smith Association, Mafic group

As the group name suggests, members of this association are largely characterised by low silica contents (<55 to >70% SiO_2). Other characteristics include high MgO, Ni and Cr contents and high mg* (Fig. 13). Granite samples (not including xenoliths) with 65% or less SiO_2 typically only belong to either this group or the Syenitic group; the distinctive chemistry of the latter makes confusion between the 2 groups unlikely. Accordingly, SiO_2 <65% and high MgO, Ni and Cr immediately suggest this group (see Fig. 13). As silica increases, however, especially to 70% and above, there is a convergence with the chemistry of the Menangina association, especially between the low LILE members of both groups. Distinction between the two associations is not always straightforward, but fortunately, can be made >90% of the time.

Mt Boreas & Beetle Associations, Low-Ca group

As a group, the members of the Low-Ca group have many distinctive characteristics that make their recognition easy, including high K_2O, K_2O/Na2O, high LILE and high HFSE (Rb, La, Ce, Zr, Th, U, F). This is particularly true for the more mafic end-members (i.e., 68-73% SiO_2), which are strongly enriched in Zr, LREE (La, Ce) and Th (Fig. 14) and K_2O. Plots of K_2O versus Zr, La, Ce or Th are also very diagnostic (e.g., Figs 12, 13, 14). There is some minor overlap with the more felsic (and hence more fractionated and more potassic) members of the High-Ca group. However, use of elements such as Ba, Rb and Y (Fig. 14), can be used to discriminate Low-Ca granites from such members of the High-Ca group.

Menangina & Diemals Associations, High-Ca group

Members of this group are, in the keys provided, identified largely by default, i.e., if the sample doesn't fit with the other four groups then it probably belongs to the High-Ca group. Therefore, once this stage in identification is reached, sample characteristics should be checked against the general characteristics of the High-Ca group, to confirm the classification. Features of the High-Ca group include low to moderate K_2O, K_2O/Na_2O, Rb, Th, Zr, LREE, Y and moderate to high Na_2O and Sr (Fig. 14), low MgO and moderate to high Sr, both relative to K_2O (Fig. 13), moderate to low Ni, Cr and mg# (Fig. 13), and moderate $Na_2O + K_2O$ (Fig. 12).

References:

Cassidy, K.F., 1992. Archaean granitoid-hosted gold deposits in greenschist to amphibolite faciesterrains: a high P-T to low P-T depositional continuum equivalent to greenstone-hosted deposits. PhD thesis, University of Western Australia.

Champion, D.C., 1997. Granitoids in the Eastern Goldfields. Australian Geological Survey Organisation, Record 1997/41, 71-76.

Champion, D. & Cassidy, K., 1998. Metallogenic potential of granitoids: Kanowna Belle and Granny Smith regions. Final Report to Golden Valley Joint Venture and Placer Pacific Ltd. Unpublished AGSO report.

Champion, D.C. & Sheraton, J.W., 1997. Geochemistry and Sm-Nd isotopic systematics of Archaean granitoids of the Eastern Goldfields Province, Yilgarn Craton, Australia: constraints on crustal growth. Precambrian Research, 83, 109-132.

Goleby, B.R., Rattenbury, M.S., Swager, C.P., Drummond, B.J., Williams, P.R., Sheraton, J.W., & Heinrich, C.A., 1993. Archaean crustal structure from seismic reflection profiling, Eastern Goldfields, Western Australia. Australian Geological Survey Organisation, Record 15.

Hill, R.I., Chappell, B.W. & Campbell, I.H., 1992. Late Archaean granites of the southeastern Yilgarn Block, Western Australia: age, geochemistry and origin. Transactions Royal Society of Edinburgh, Earth Sciences, 83, 211-226.

Johnson, G.I., 1991. The petrology, geochemistry and geochronology of the felsic alkaline suite of the eastern Yilgarn Block, Western Australia. PhD thesis, University of Adelaide.

Kent, A.J.R., 1994. Chronological constraints on the timing of Archaean gold mineralisation in the Yilgarn Craton, Western Australia. PhD thesis, Australian National University,

Kent, A.J.R., Cassidy, K.F. & Fanning, C.M., 1996. Archaean gold mineralisation synchronous with the final stages of cratonisation, Yilgarn Craton, Western Australia. Geology, 24, 879-882.

Krapez, B., Brown, S.J.A., Hand, J., Barley, M.E. & Cas, R.A.F., 2000. Age constraints on recycled crustal and supracrustal sources of Archaean metasedimenatry sequences, Eastern Goldfields Province, Western Australia: evidence from SHRIMP zircon dating. Tectonophysics, 322, 89-133.

Martin, H., 1986. Effect of steeper Archaean geothermal gradient on geochemistry of subduction-zone magmas. Geology, 14, 753-756.

Nelson, D.R., 1995. Compilation of SHRIMP U-Pb zircon geochronology data, 1994. Geological Survey of Western Australia, Record 1995/3.

Nelson, D.R., 1996. Compilation of SHRIMP U-Pb zircon geochronology data, 1995. Geological Survey of Western Australia, Record 1996/5.

Nelson, D.R., 1997. Compilation of SHRIMP U-Pb zircon geochronology data, 1996. Geological Survey of Western Australia, Record 1997/2.

Nelson, D.R., 1998. Compilation of SHRIMP U-Pb zircon geochronology data, 1997. Geological Survey of Western Australia, Record 1998/2.

Nelson, D.R., 1999. Compilation of SHRIMP U-Pb zircon geochronology data, 1998. Geological Survey of Western Australia, Record 1999/3.

Ojala, V.J., McNaughton, N.J., Ridley, J.R., Groves, D.I. & Fanning, C.M., 1997. The Archaean Granny Smith gold deposit, Western Australia: Age and Pb-isotope tracer studies. Chronique de la Recherche Miniere.

Perring, C.S. & Rock, N.M.S., 1991. Relationships between calc-alkaline acidic and basic (mantle-derived) magmas in Late Archaean composite dykes, Kambalda Goldfields, Western Australia. Precambrian Research, 52, 245-273.

Pidgeon, R.T. & Wilde, S.A., 1990. The distribution of 3.0 and 2.7 Ga volcanic episodes in the Yilgarn Craton of Western Australia. Precambrian Research, 48, 309-325.

Qui, Y.M., Groves, D.I. & McNaughton, N.J., 1997. Deep-seated granitoids: Implications for Late Archaean subduction-collision-lithospheric delamination and gold mineralisation in the Yilgarn Craton. Australian Geological Survey Organisation, Record 1997/42, 65-70.

Smithies, R.H. & Champion, D.C., 1999. Late Archaean felsic alkaline igneous rocks in the Eastern Goldfields, Yilgarn Craton, Western Australia: a result of lower crustal delamination? Journal of the Geological Society of London, 156, 561-576.

Smithies, R.H. & Witt, W.K., 1997. Distinct basement terranes identified from granite geochemistry in late Archaean granite-greenstones, Yilgarn Craton, Western Australia. Precambrian Research, 83, 185-201.

Williams, P.R. & Whitaker, A.J., 1993. Gneiss domes and extensional deformation in the Archaean Eastern Goldfields Province, Western Australia. Ore Geology Reviews, 8, 141-162.

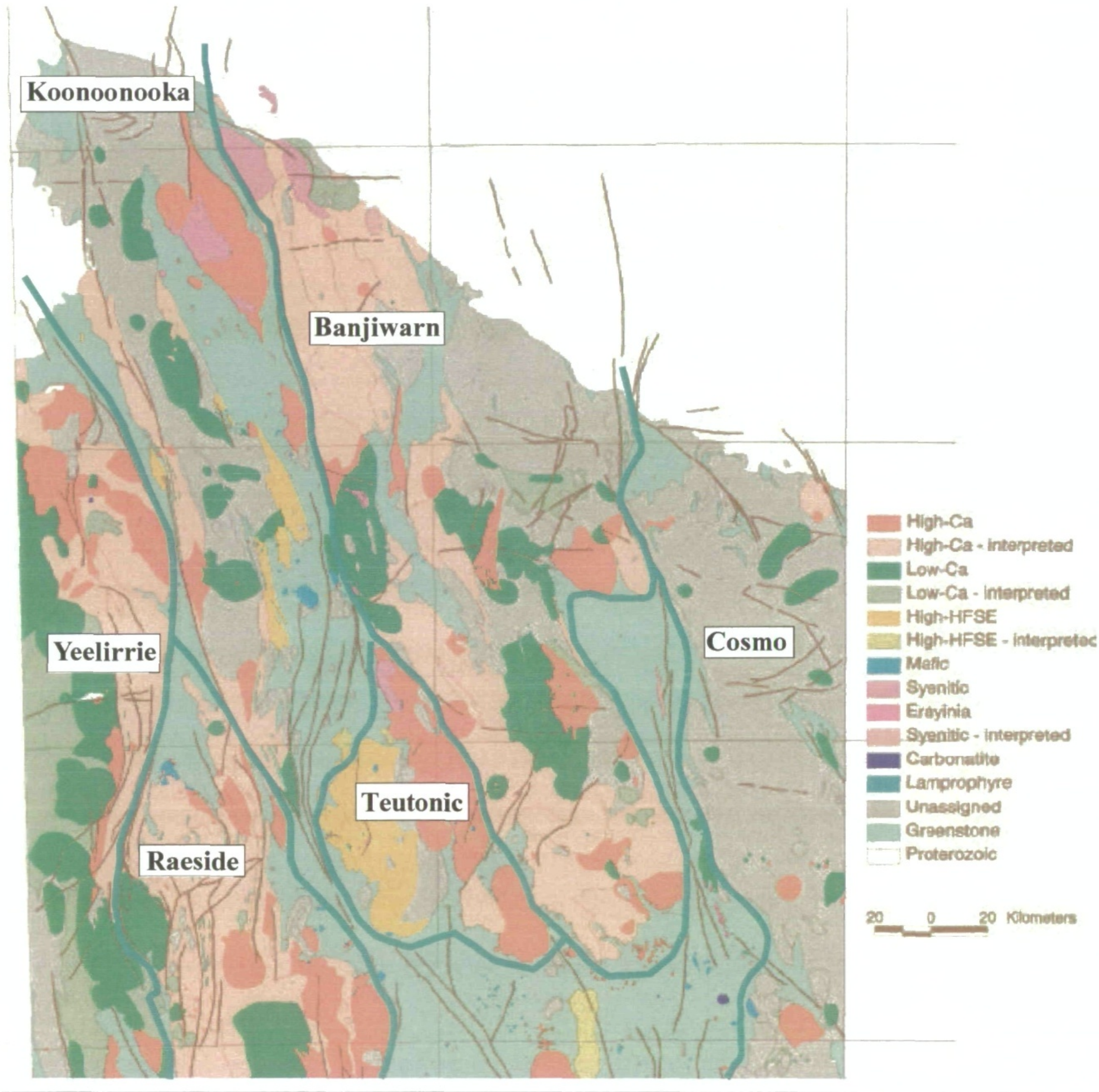

Figure 1. Granite masses in the northern Eastern Goldfields. Raeside, Koonoonooka, Teutonic, Banjiwarn, & Cosmo in the Eastern Goldfields Province, Yeelirrie in the Southern Cross Province.

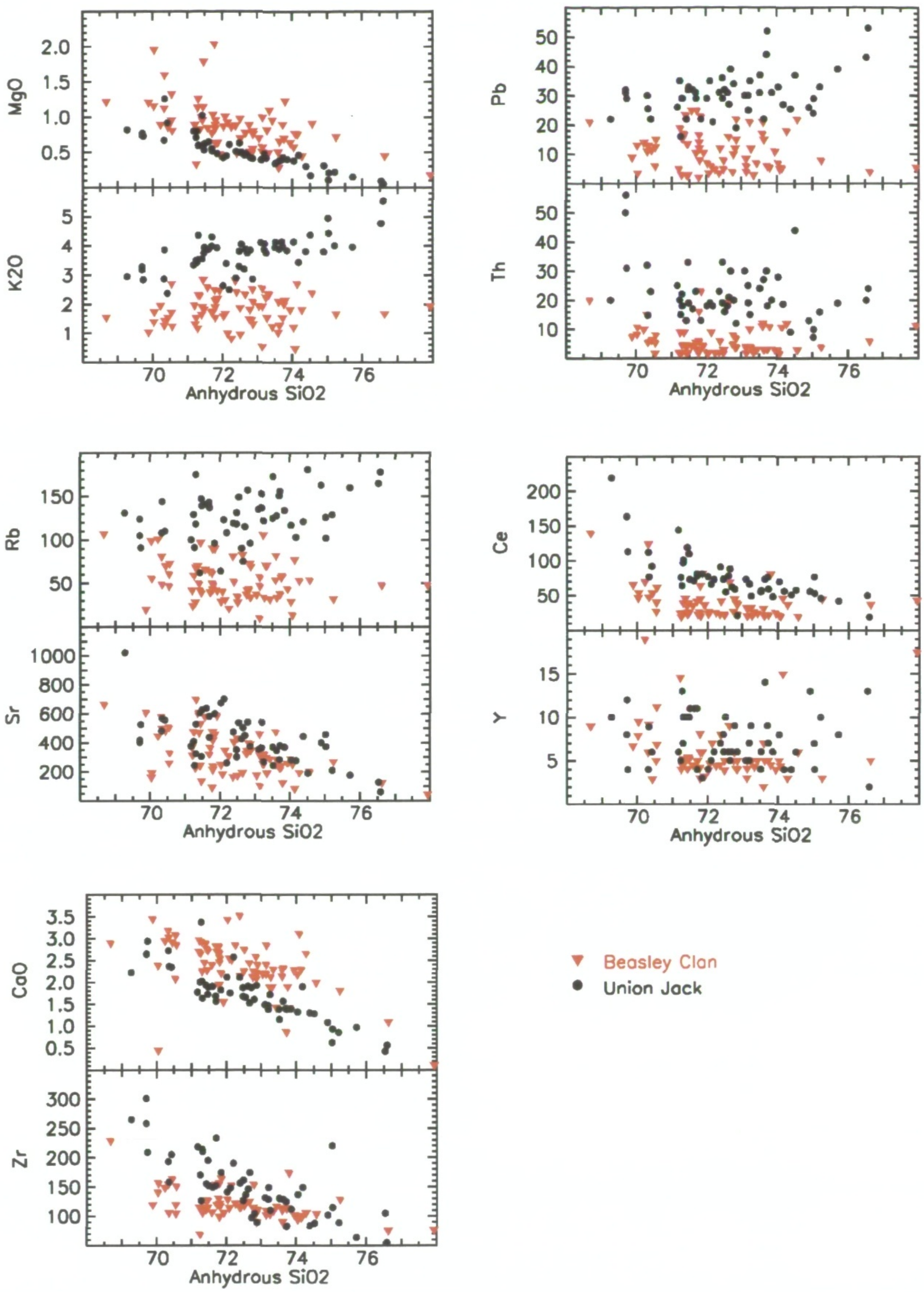

Figure 2. Comparison of the 'high-LILE' Union Jack clan, and the 'low-LILE' Beasley clan, both of the Menangina Association, High-Ca group, northern Eastern Goldfields Province. Nb. 'High-' and 'low-LILE' terms are relative, not absolute.

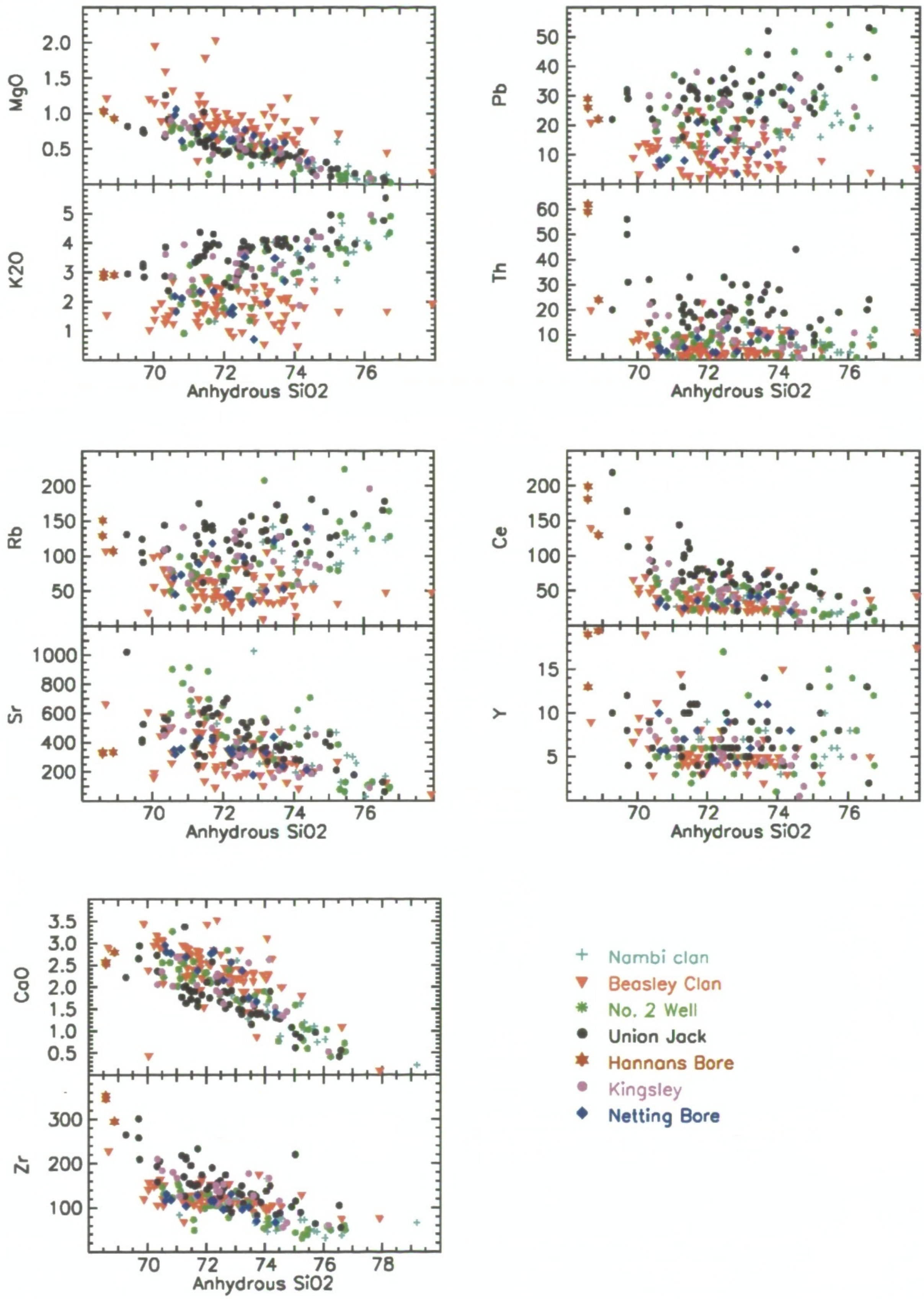

Figure 3. Clans of the Menangina Association, High-Ca Group, northern Eastern Goldfields Province.

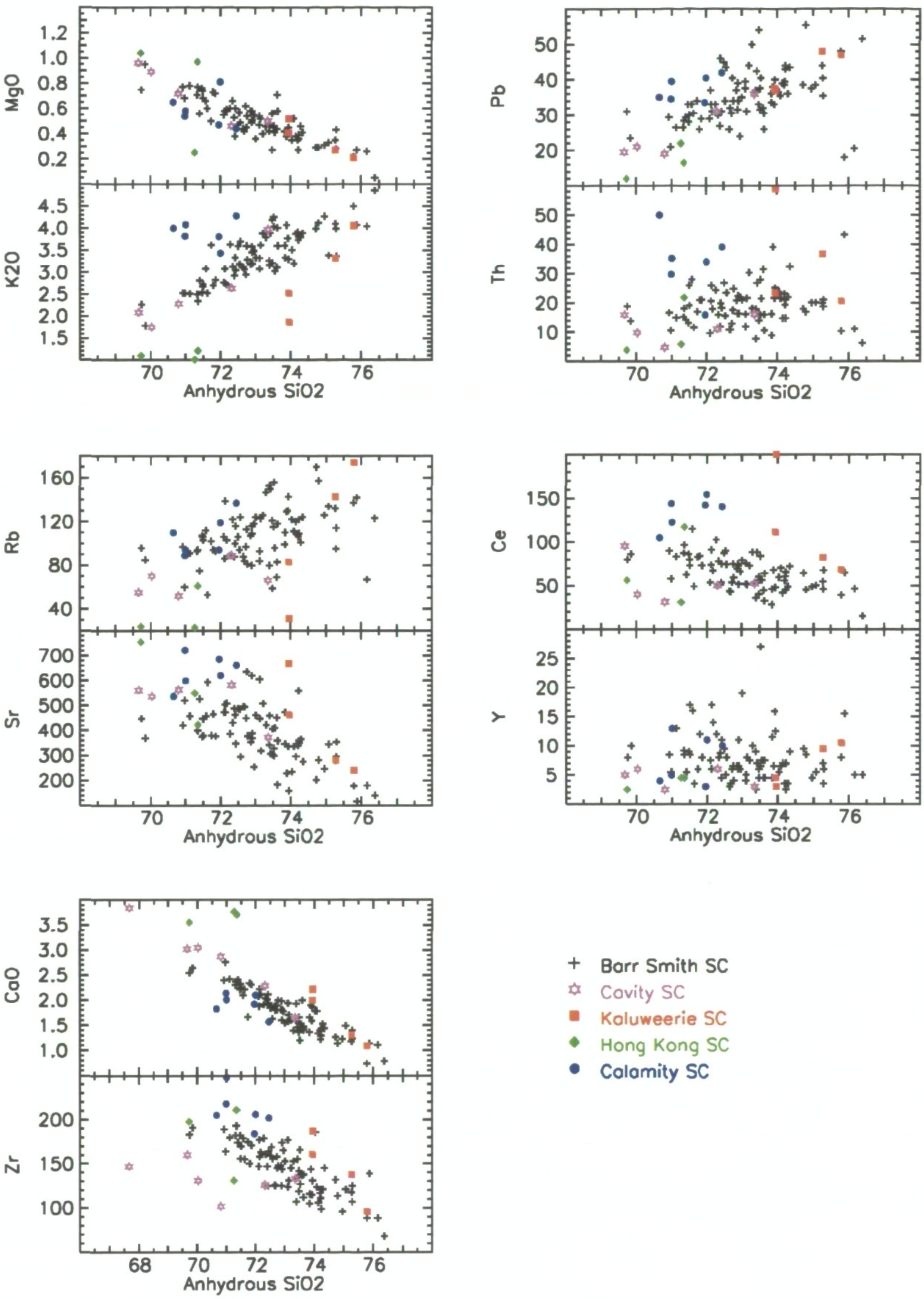

Figure 4. Clans of the Diemals Association, High-Ca Group, north-eastern Southern Cross Province.

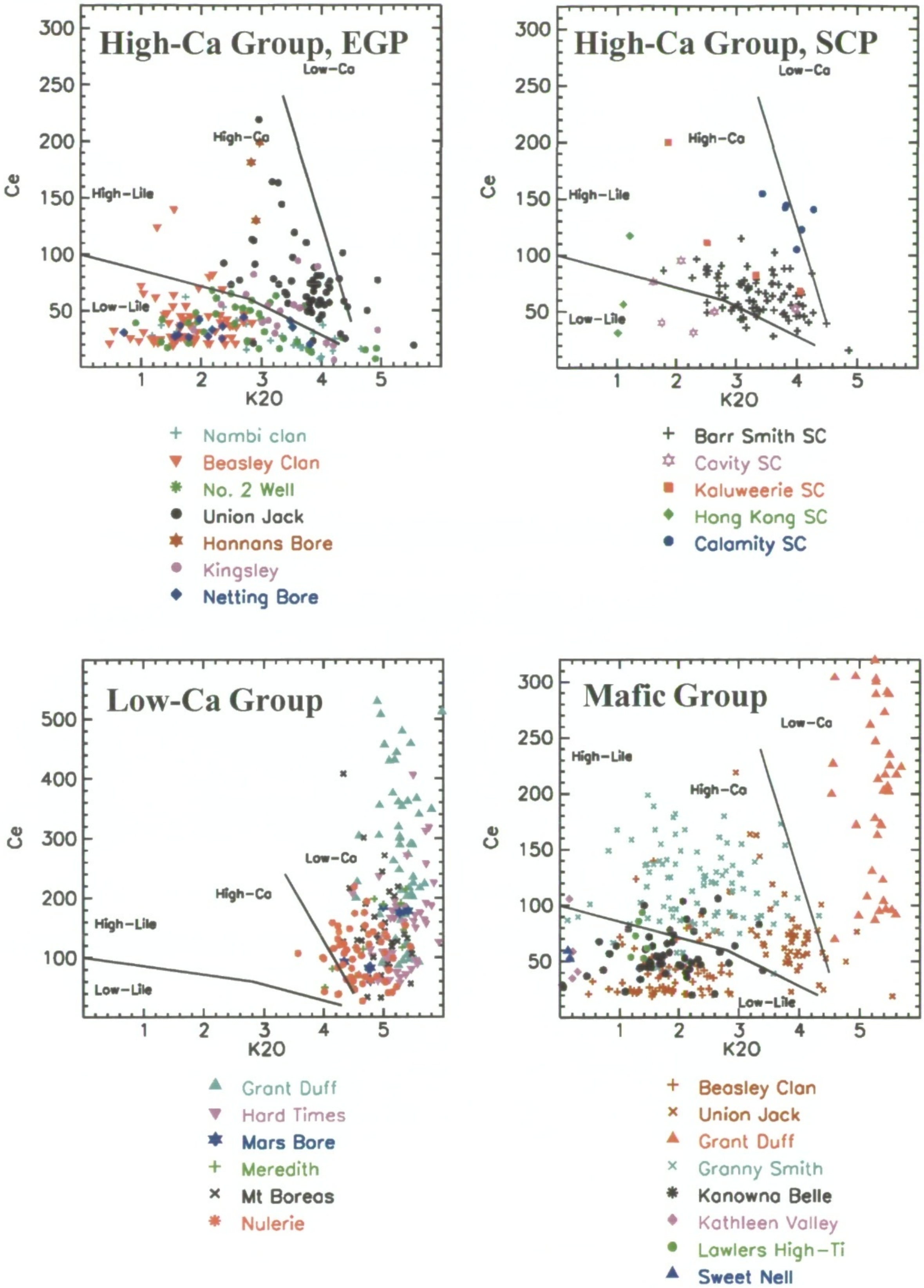

Figure 5. K2O-Ce plots illustrating the range in LILE and HFSE in the Menangina and Diemals Associations of the High-Ca group, in the Granny Smith Association, Mafic Group, and in theMt Boreas Association, Low-Ca group. The central line is an arbitrary divide between 'low-LILE' and 'high-LILE' end-members of the High-Ca and Mafic groups. Nb. The terms 'low-' and 'high-LILE' are used in a relative, not absolute, sense. Note expanded Ce axis for the Low-Ca group.

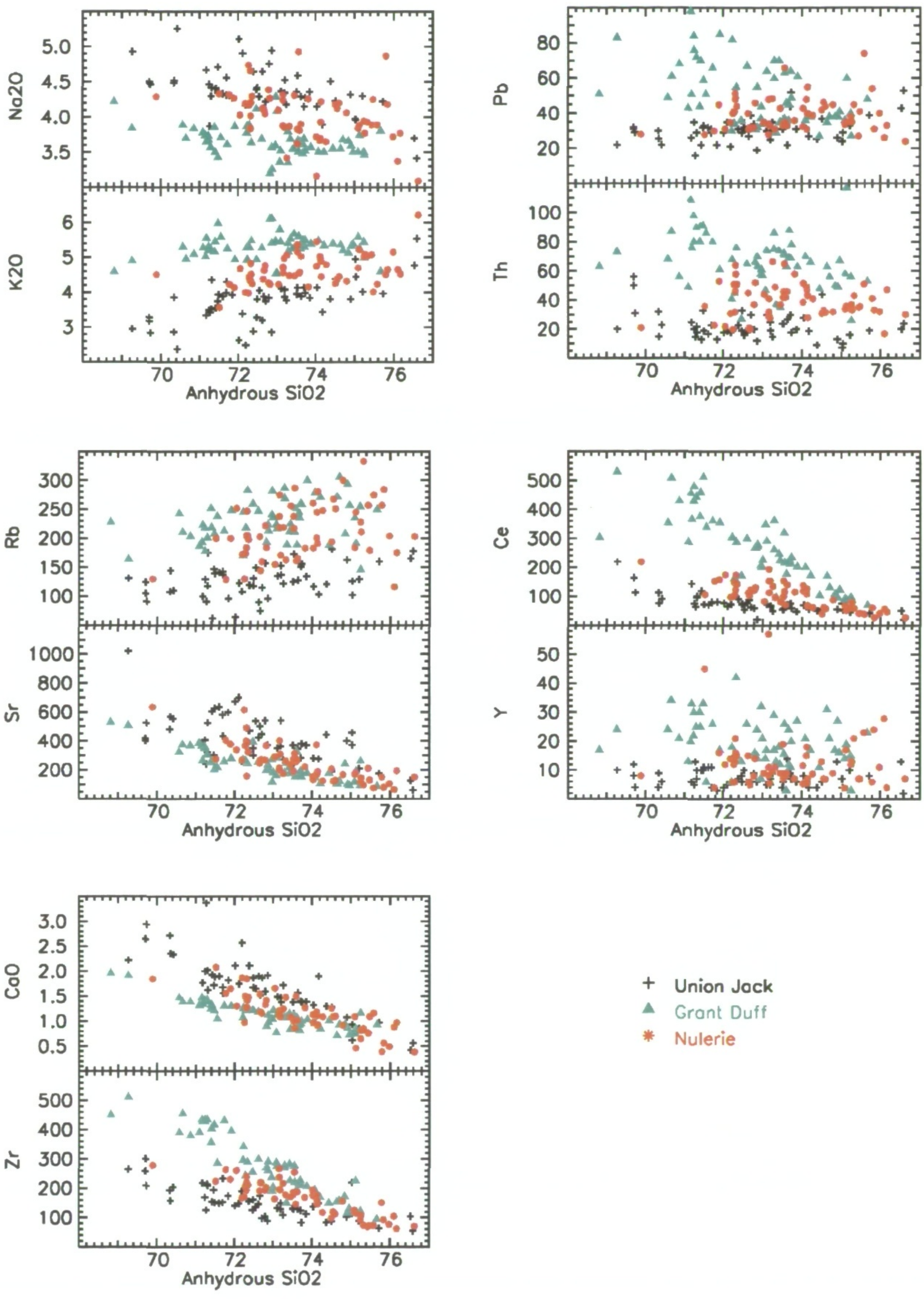

Figure 6. Comparison of the Grant Duff and Nulerie Clans (highest and lowest LILE- and HFSE-enriched Low-Ca clans, respectively), with the Union Jack Clan the most LILE- and HFSE-enriched clan of the High-Ca group.

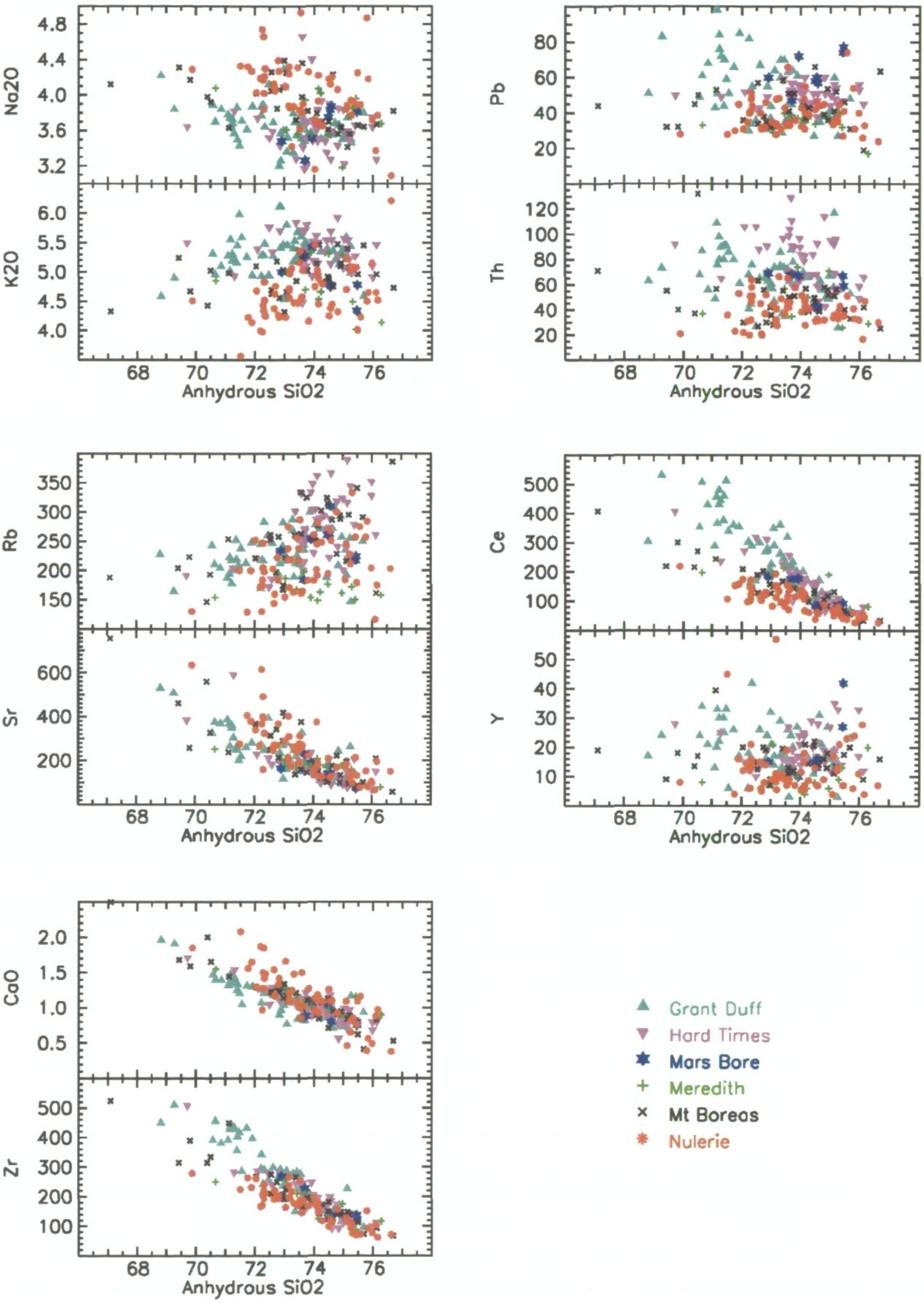

Figure 7. Clans of the Mt Boreas Association, Low-Ca group, northern Eastern Goldfields Province.

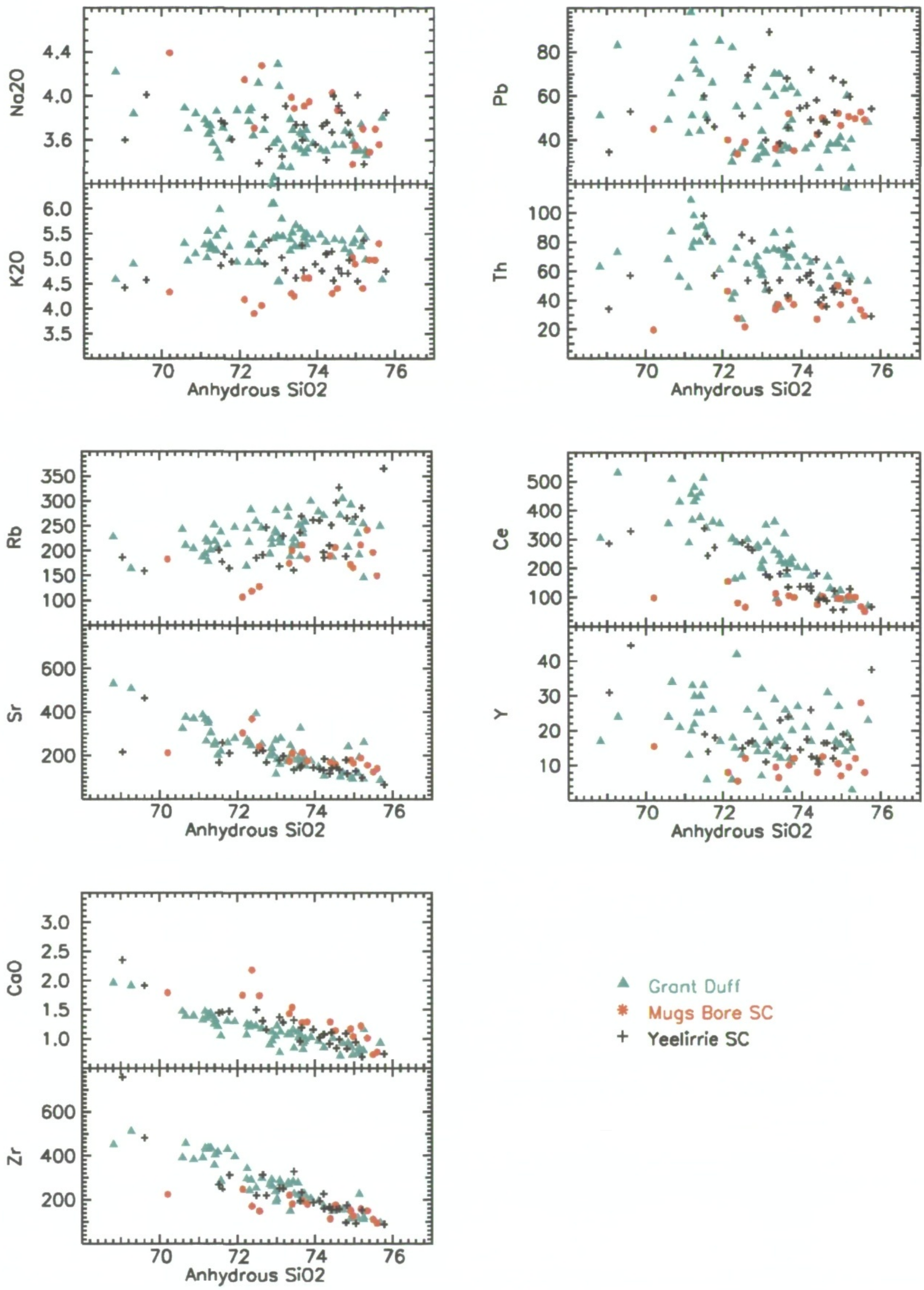

Figure 8. Clans of the Beetle Association, Low-Ca group, Southen Cross Province. The Grant Duff Clan, Mt Boreas Association, Eastern Goldfields Province, is shown for comparison.

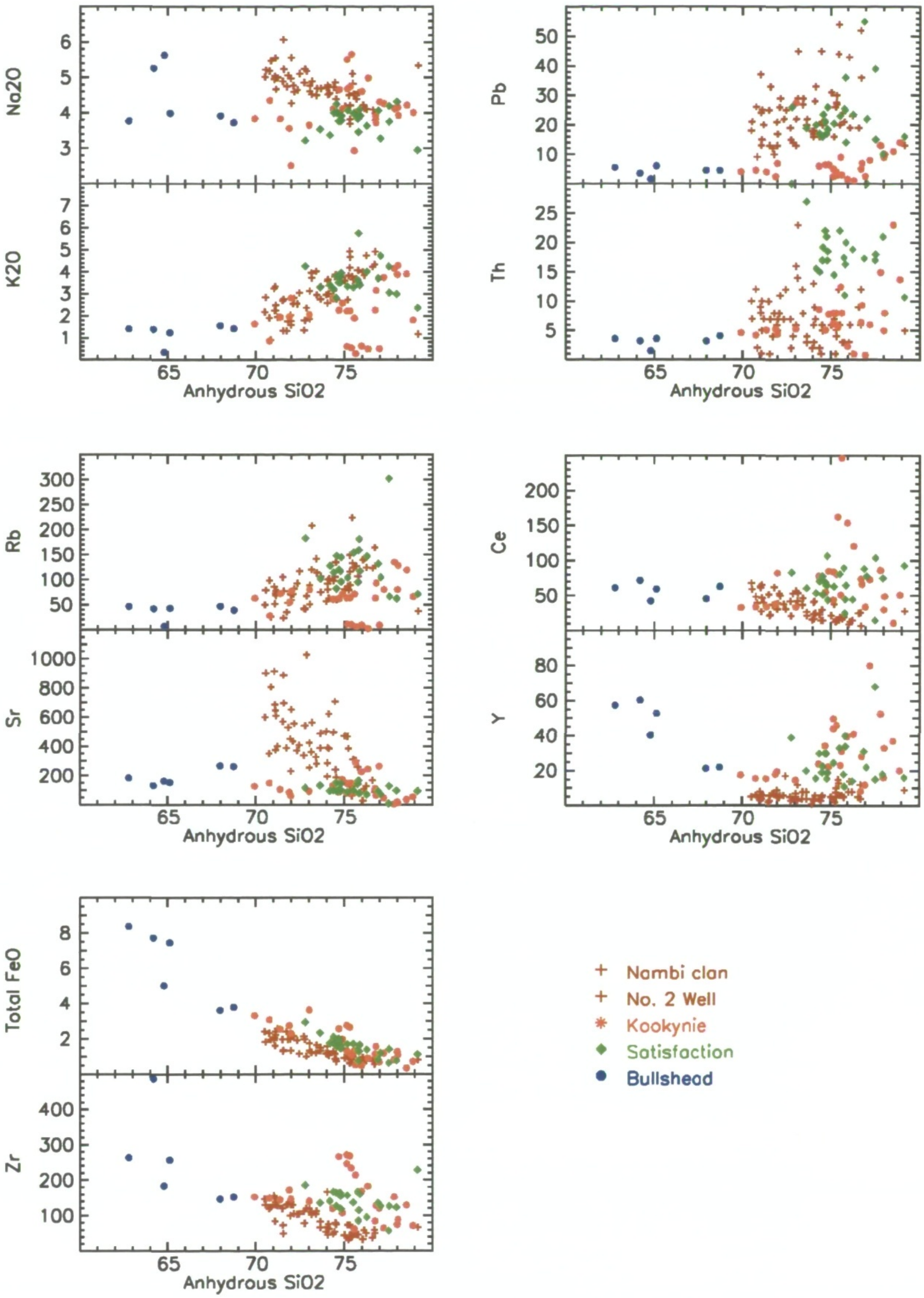

Figure 9. Clans of the Kookynie Association, High-HFSE group, northern Eastern Goldfields Province. The Nambi and No 2 Well clans of the Menangina Association, High-Ca group are shown for comparison.

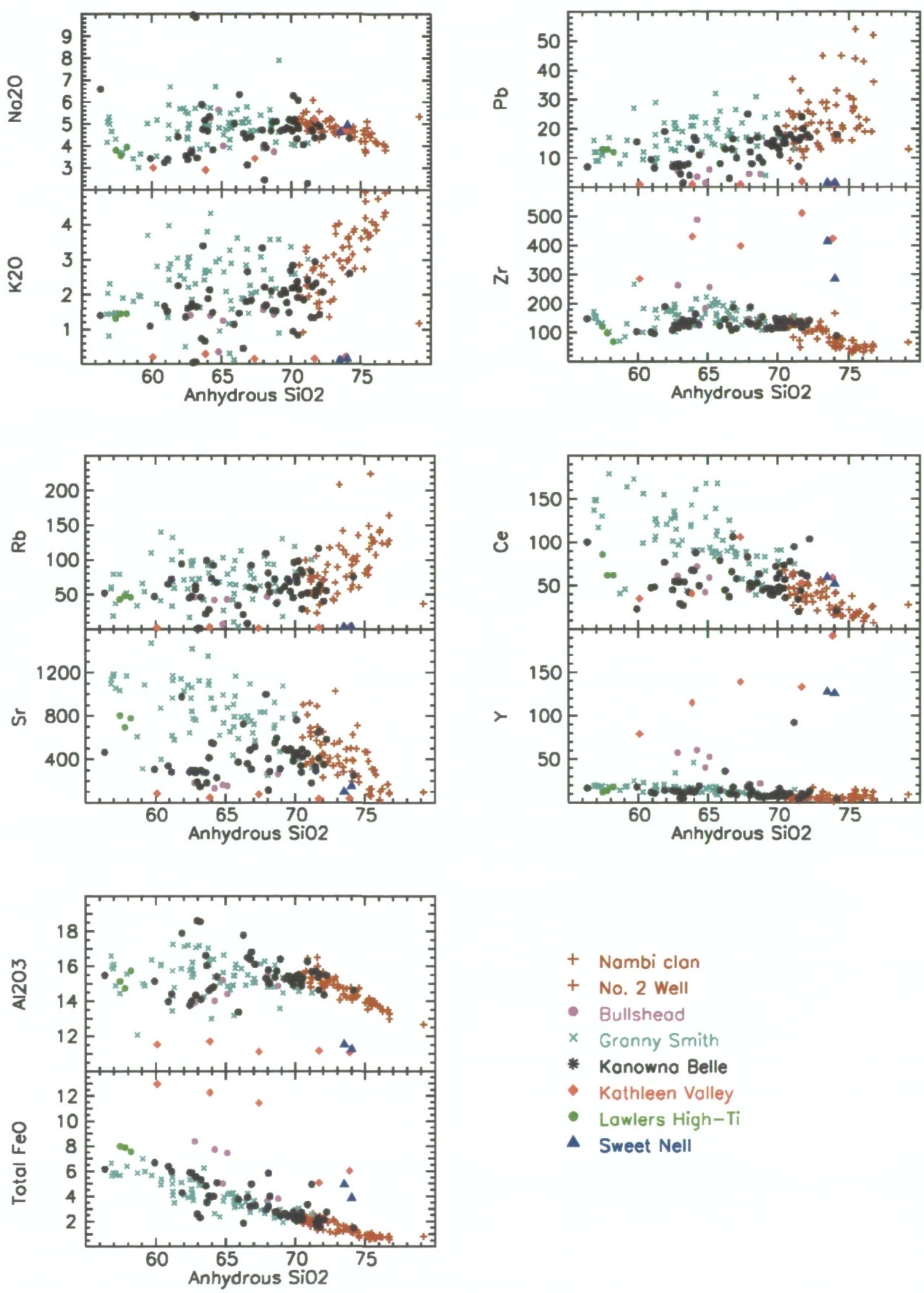

Figure 10. Clans of the Granny SmithAssociation, Mafic Group, northern Eastern Goldfields Province.The Nambi and No 2 Well clans of the Menangina Association, High-Ca group are shown for comparison, as is the mafic Bullshead clan of the Kookynie Association, High-HFSE group.

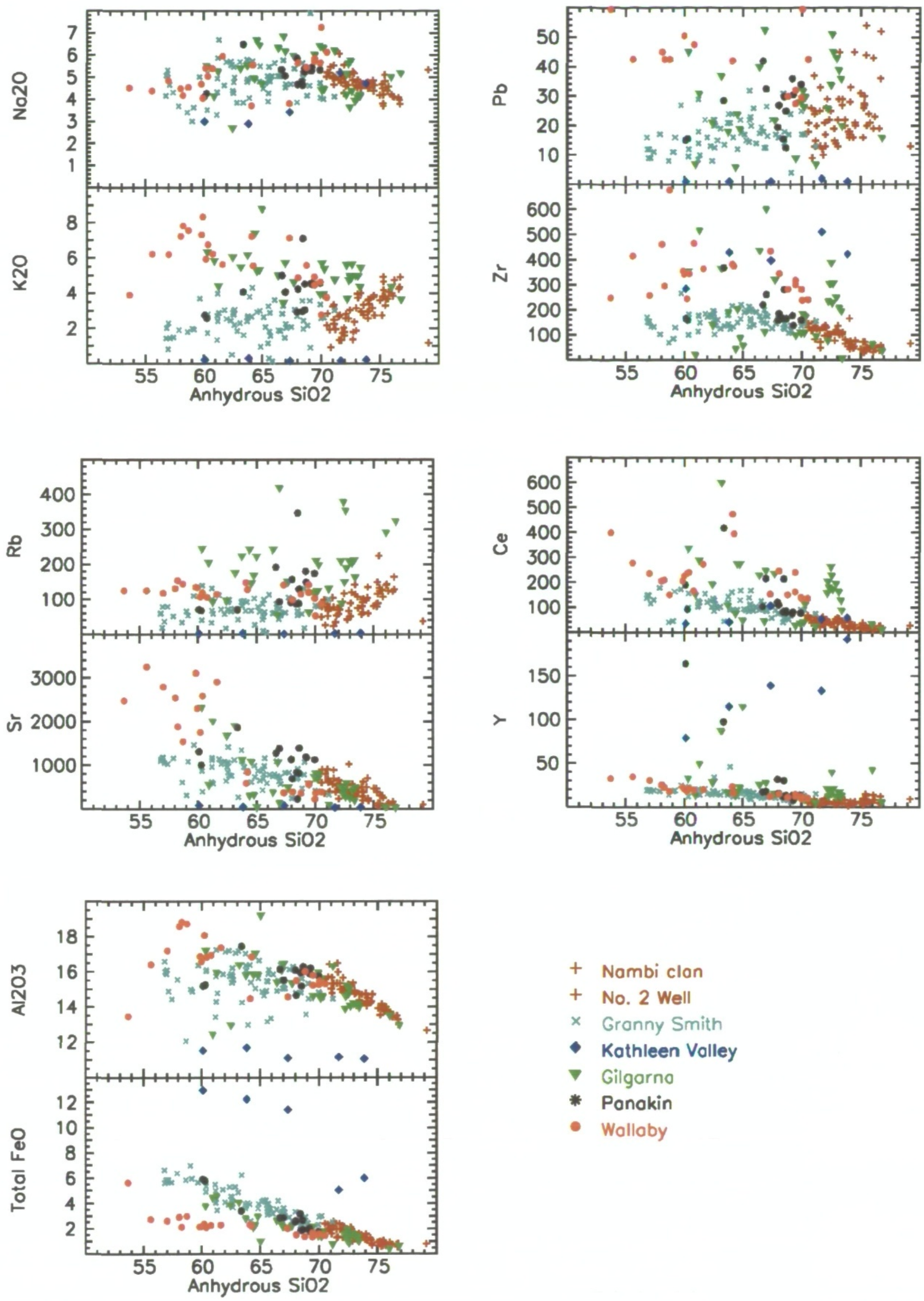

Figure 11. Clans of the Gilgarna Association, Syenitic group, northern Eastern Goldfields Province. Also shown are the Nambi and No 2 Well clans, both Menangina Association, High-Ca group, and the high-LILE Granny Smith clan, and tholeiitic Kathleen Valley clan, both Granny Smith Association, Mafic group.

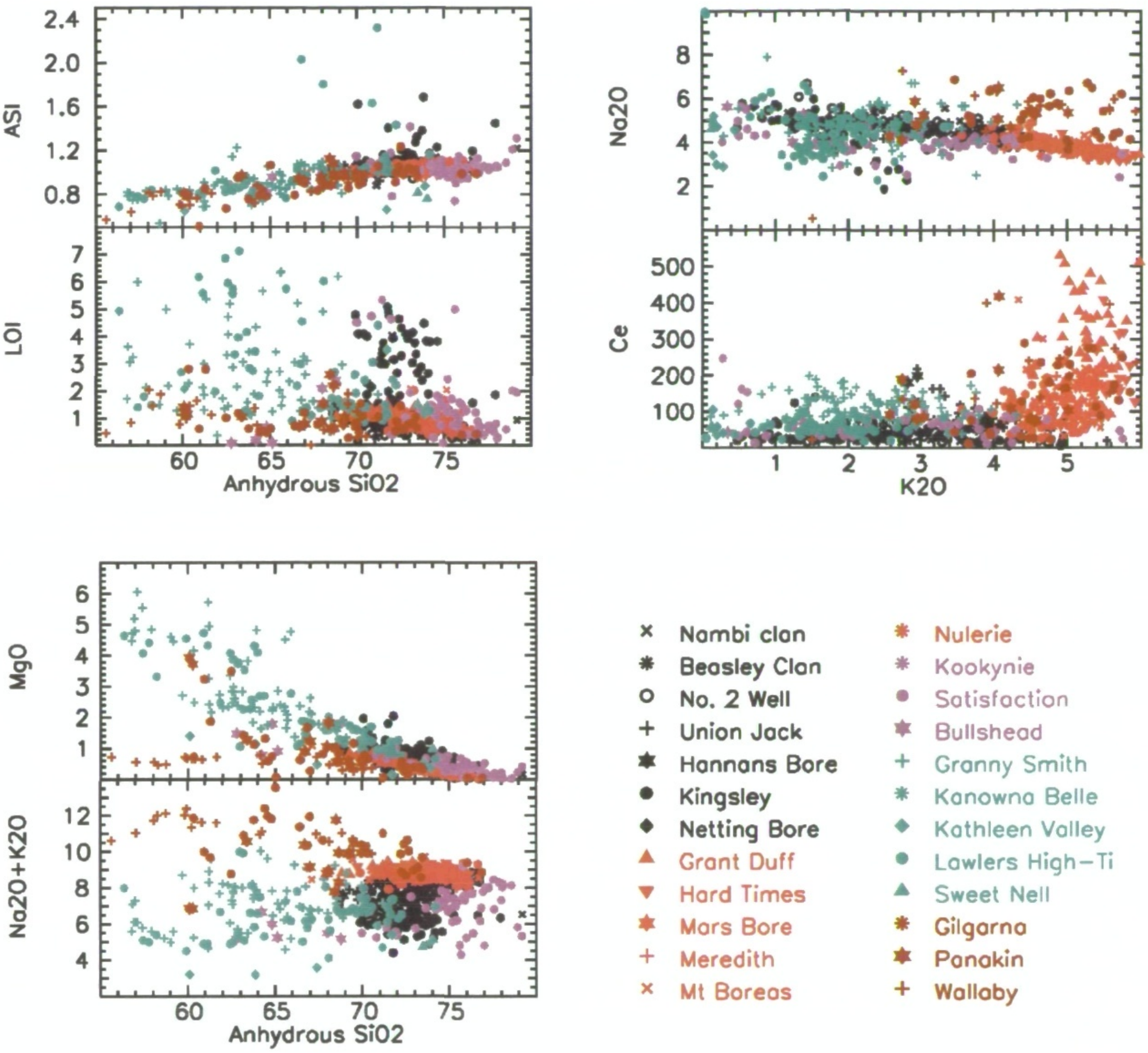

Figure 12. Discriminant plots for recognition of strongly altered analyses (using LOI - loss on ignition, & ASI - ratio of Al to Ca+Na+K), and discriminant plots for the Syenitic group (using Na2O+K2O, MgO, and Na2O/K2O and Ce/K2O ratios).

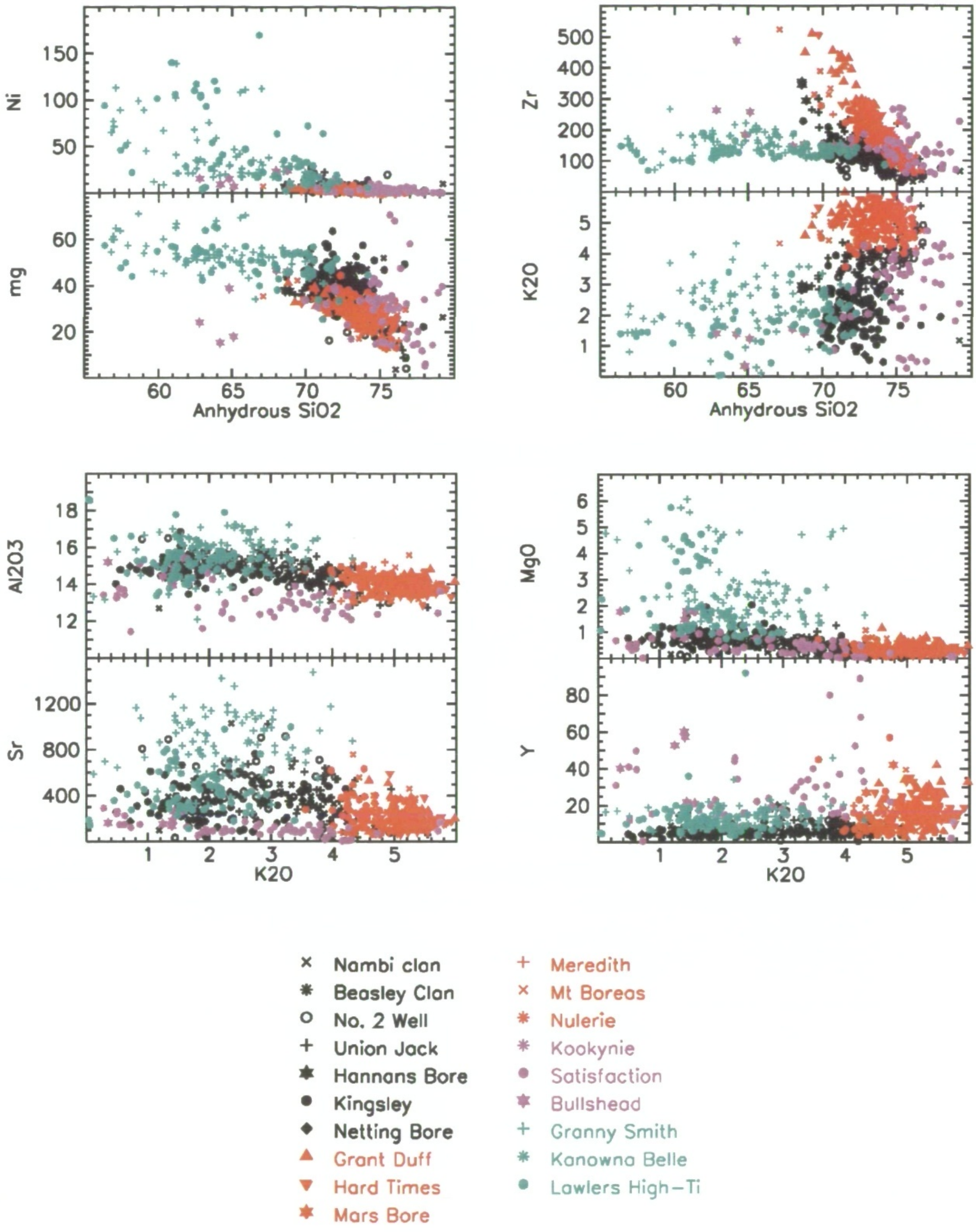

Figure 13. Discriminant plots for the Mafic (MgO, K2O, Zr, Ni, mg# - ratio of Mg to Mg+Fe), and High-HFSE (Al2O3, K2O, Sr, Zr, Y) groups.

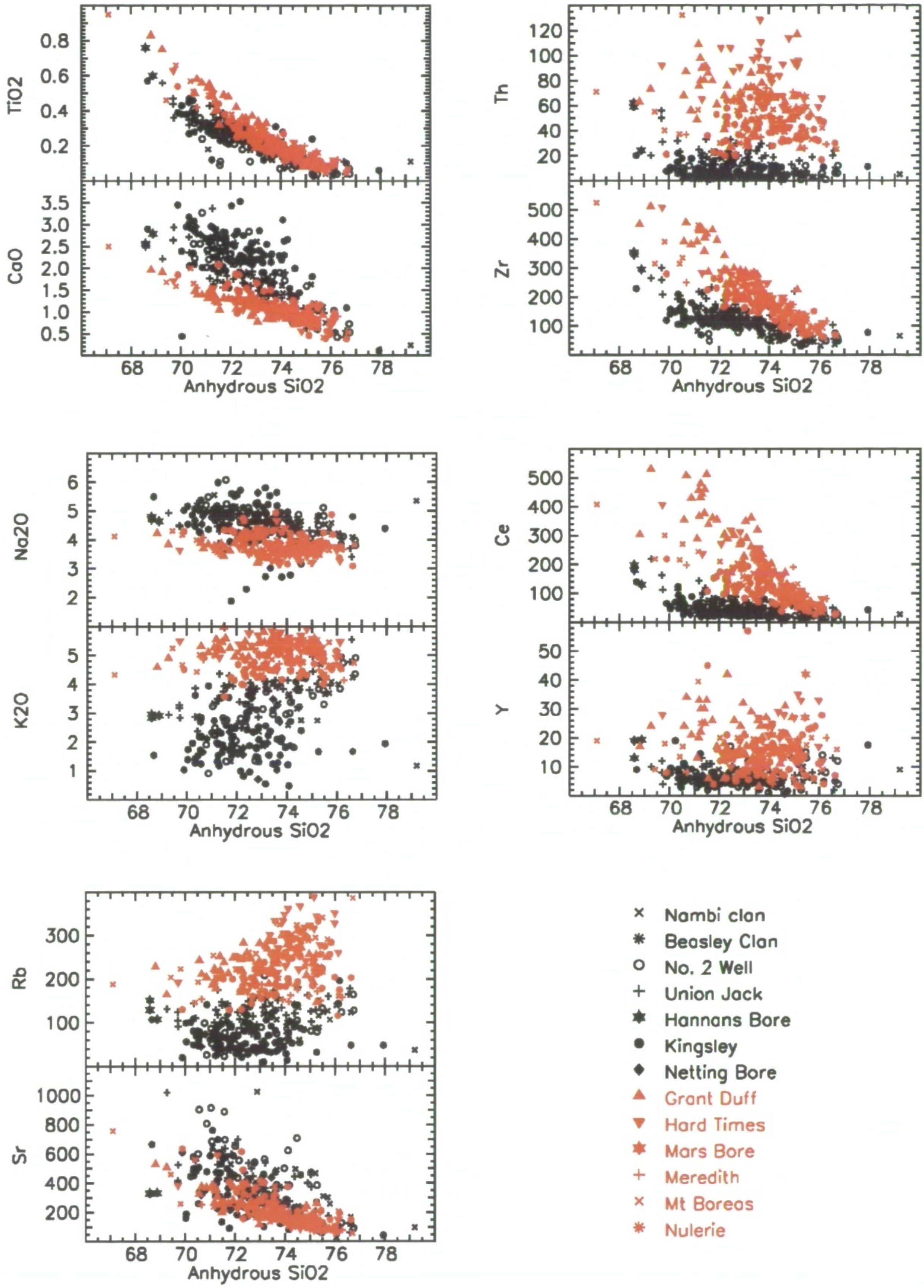

Figure 14. Discrimant plots for the High-Ca and Low-Ca groups of the Eastern Goldfields Province.

Granitoids of the southeastern Yilgarn Craton: Distribution, geochronology, geochemistry, petrogenesis and relationship to mineralisation

Kevin F. Cassidy & David C. Champion

Summary

- Over 360 new analyses have been obtained for the southeastern Yilgarn Craton (MENZIES, EDJUDINA, KALGOORLIE, KURNALPI, BOORABBIN, WIDGIEMOOLTHA, LAKE JOHNSTON and NORSEMAN 1:250 000 sheets) as part of the present project. These, combined with about 700 pre-existing analyses, have been classified into granite suites, supersuites, clans and associations.
- Two groups (High-Ca and Low-Ca) dominant the granitoids in the southeastern Yilgarn Craton. The other main groups are the Mafic, High-HFSE, and Syenitic groups. The majority of the High-Ca group granitoids appear to overlap in age from 2.70 to 2.66 Ga, although older High-Ca gneisses and granitoids and have ages ranging from older than 2720 to about 2700 Ma. The Low-Ca granitoids appear to overlap in age from ca. 2.66 to 2.63 Ga in both provinces (see Summary Table).
- The Diemals (High-Ca) and Beetle (Low-Ca) associations of the Southern Cross Province are chemically equivalent to the Menangina (High-Ca) and Mt Boreas (Low-Ca) associations of the Eastern Goldfield Province, respectively). Although all these groups broadly overlap in age there are some differences between the two regions, with the majority of Diemals Association granitoids (2.70-2.68 Ga) approximately 20 m.y. older than equivalent High-Ca group granitoids (2.68-2.66 Ga) in the Eastern Goldfields Province (see Summary Table).
- High-Ca and Mafic group granitoids can be broadly divided into 'high-LILE' and 'low-LILE' sub-groups. Each province contains several 'high-LILE' and 'low-LILE' clans, with differences in distribution and geochemistry. The 'low-LILE' clans tend to have formed over a longer time interval, and mostly earlier than the 'high-LILE' clans. Other clans have geochemistry that is transitional to both these end-member sub-types.
- A number of granitoid clans and associations appear to be unique to each Province. The Nargalyerin clan (Beetle Association, Low-Ca group) is unique to the Southern Cross Province, although low-silica members of the Nulerie clan (Mt Boreas Association, Low-Ca group) in the Rason-Throssell region have many similarities with the Nargalyerin clan.
- The Erayinia clan (Gilgarna Association, Syenitic group) is unique to the eastern part of the Kurnapli and Widgiemooltha 1:250,000 map sheets. This clan shares many similarities with the Panakin clan in the northern top of the northeastern Yilgarn Craton (see Champion & Cassidy, this report).
- The presence of a number of associations and clans unique to each province, i.e., Gilgarna, Kookynie, Erayinia, Nargalyerin most probably relate not only to differing source rocks but also to changing tectonic environments (e.g., Champion, 1997; Smithies & Champion, 1999).
- A number of Mafic group granitoids, and to a lesser extent High-Ca and Syenitic group granitoids, either host or are spatially associated with gold mineralisation. Both 'low-LILE' and 'high-LILE' clans are represented.
- Some Low-Ca group granitoids contain evidence for late magmatic fluids. Evidence includes pegmatoid fluid-release structures, miarolitic cavities and biotite-rich 'oikocryst' zones. Notably,

quartz crystal in these structures and zones typically contain low-salinity, aqueous-carbonic fluid inclusions, similar to those present in many orogenic gold deposits.

Summary Table. Comparison of granitoid groups in the Southern Cross and Eastern Goldfields Provinces in the southeastern Yilgarn Craton. Age ranges for each association (in bold) reflects the complete range of ages known for the association. Age ranges are also given for clans present in the southeastern Yilgarn Craton. Data compiled from published studies as well as from this study. Eastern Goldfields groups and data expanded from Champion & Sheraton (1997), Champion (1998) and Cassidy (1998).

SOUTHERN CROSS	AGE (Ga)	EASTERN GOLDFIELDS	AGE (Ga)
Mafic Group		*Mafic Group*	
Westonia Association	**2.81-??**	**Granny Smith Association**	**2.695-2.65**
Red Leaf	-	Dinky Boys	-
		Granny Smith	2670-2650
		Kambalda	~2660
		Kanowna-Belle	2695-?2615
		Mafic unassigned	2675-2670
		New Celebration	~2685
		Victory	~2665
High-Ca Group		*High-Ca Group*	
Diemals Association	**2.85-2.8; 2.74-2.72; 2.71-2.655**	**Menangina Association**	**~2.76; 2.72-2.65**
		Ajax	-
Karalee	~2675	Beasley	2695-2655
Spear	~2695	Burra	2690-2655
Stennet Rock	~2690	Goongarrie	2690-2650
Woolgangie	2710-2655	Menangina	2675-2660
		Niagara	-
		Parker Hills	2660-2650
		Yindi	~2660
Low-Ca Group		*Low-Ca Group*	
Beetle Association	**~2.68; 2.66-2.62**	**Mt Boreas Association**	**2.655-2.62**
Beetle	2660-2625	Mt Boreas	~2650
Boorabbin	2635-2630	Mungari	2630-2620
Nargalyerin	2645-2625	Nulerie	2655-2645
Oberwyl	-		
Yeelirrie	2680-2640		
Corriding	-		
		High-HFSE Group	
		Kookynie Association	**?2.74-2.66**
		Outcamp Bore	2720-2700
		Kookynie	2685-2660
		Cashmans	-
Syenitic Group		*Syenitic Group*	
Fitzgerald Peaks Association	**??**	**Gilgarna Association**	**2.665-2.64**
Fitzgerald Peaks		Gilgarna	~2660
		Erayinia	2665-2645

Introduction

This section systematically documents the granitoid groups of the southeastern Yilgarn Craton, principally granitoids of eight 1:250,000 map sheets: MENZIES, EDJUDINA, KALGOORLIE, KURNALPI, BOORABBIN, WIDGIEMOOLTHA, LAKE JOHNSTON and NORSEMAN. These eight map sheets comprise the eastern part of the southern Southern Cross Province, and the majority of the southern Eastern Goldfields Province. The boundary between the Eastern Goldfields Province and the Southern Cross Province is taken as the approximate position of the Ida Lineament and its inferred southern extension through dominantly granitoid terrain on the BOORABBIN and NORSEMAN map sheets.

In this section, the characteristics of the major and minor granitoid groups are discussed with reference to the province and then compared with the granite groups previously recognised in the Eastern Goldfields and Southern Cross Provinces. Two main granite groups, High-Ca, Low-Ca, form the bulk of the granitoids in both provinces, with three minor groups (Mafic, Syenitic, High-HFSE) present in one or both provinces. A standard format is used to detail the distribution, age, geochemistry, petrogenesis and relationship to mineralisation and uses and extends the classification of Champion & Sheraton (1997) to the southeastern Yilgarn Craton.

Granitoids are subdivided into Group, Association, Clan, Supersuite and Suite. Table 1 outlines the subdivision of granitoids. The basic unit of subdivision is the suite; whereas group is used to recognise major granitoid types. Granitoids belonging to the same Group are assigned to different Associations depending on the Province in which they are located. For example, High-Ca group granitoids in the Eastern Goldfields Province belong to the Menangina Association, whereas High-Ca group granitoids in the Southern Cross Province are assigned to the Diemals Association. Associations are divided into Clans that are groups of Supersuites with similar petrographic and geochemical characteristics and are the level of grouping documented in this report. Some Clans of High-Ca and Low-Ca granitoids in the southeastern Yilgarn Craton are similar to Clans documented in the northeastern Yilgarn Craton (Champion & Cassidy, this report). For detailed distribiution of Associations and Clans, the reader is referred to the accompanying 1:500,000 and smaller scale maps provided on CD.

Table 1. Granitoid subdivision used in this project. The subdivision is incorporated into all digital datasets and GIS produced for the project.

Grouping	Broadest granite grouping; Yilgarn-wide
Association	Similar to grouping but Province-specific
Clan	Groups of supersuites with similar petrographic and geochemical characteristics
Supersuite	Groups of suites with similar petrographic and geochemical characteristics
Suite	Groups of plutons of the same magmatic event
Informal	Informal name of the unit

Approach

The major approach to the whole study has been to build on and expand the pre-existing classification from the northern Eastern Goldfields (Champion & Sheraton, 1997) by progressively moving west and south across the Yilgarn Craton. During the project, the following objectives were met:

- undertake an east-west transect from the eastern edge of the Western Gneiss Terrain across to the Eastern Goldfields in the southern part of the Yilgarn Craton;
- undertake an east-west transect from the western edge of the Murchison Province across the Southern Cross Province to join up with detailed pre-existing data from the northern Eastern Goldfields Province;
- infill gaps in the Eastern Goldfields coverage, including detailed sampling on tenements held by sponsors, largely through access to drillcore, both from mine and prospect areas.

Through the AMIRA project, over 360 samples have been collected in the southeastern Yilgarn Craton, principally from regional samples on the MENZIES, KALGOORLIE, BOORABBIN, LAKE JOHNSTON, EDJUDINA, WIDGIEMOOLTHA, and NORSEMAN 1:250,000 map sheets and a number of porphyries in the New Celebration, Bardoc and Kalgoorlie districts. Champion (1998) provided a preliminary classification of granitoids of the BOORABBIN and KALGOORLIE 1:250,000 map sheets, and Cassidy & Champion (1998) provided a preliminary classification of granitoids in the southeastern Yilgarn Craton; this report builds on these classifications.

In the southeastern Yilgarn, this study is built upon a considerable amount of published geochemistry, principally from the work of the GSWA, notably Witt & Davy (1997) and Smithies & Witt (1997). Other major contributions include Bettenay (1977) for the southwestern Southern Cross Province and Johnson (1991) for syenites in both the Eastern Goldfields Province and the Fitzgerald Peaks in the southern Southern Cross Province. Despite these and other studies (e.g., Cassidy, 1992; Perring, 1989) of the granitoids, a number of gaps still exist in the granitoid coverage of the southeastern Yilgarn craton. In particular, within the external granitoids in the south-east (ZANTHUS & CUNDEELEE 1:250 000 sheets) and south-west (LAKE JOHNSTON, NORSEMAN 1:250,000 sheets) of the region. Samples with geochemical analyses currently available from these eight map sheets are listed in Table 2.

Table 2. Available geochemistry for the regions described within this report. AMIRA samples are those collected specifically as part of this project. AGSO samples are those collected by AGSO personnel prior to commencement of the AMIRA project.

	southern Eastern Goldfields (eastern side of Menzies, Kalgoorlie, Boorabbin; all of Edjudina, Kurnalpi, Widgiemooltha; most of Norseman)	**southeastern Southern Cross** (western side of Menzies, Kalgoorlie, Boorabbin; all of Lake Johnston)
AMIRA	260	81
AGSO	68	30
GSWA	251	8
Others	255[1]	76[2]

[1] – includes 23 from Bettenay (1977), 45 from Cassidy (1992), 1 from CSIRO, 104 from Johnson (1991), 4 from Knight (1994) and 78 from Perring (1989).
[2] – includes 47 from Bettenay (1977), and 29 from Johnson (1991).

Previous Work

The Eastern Goldfields Province is the most comprehensively studied area of the Yilgarn Craton with respect to both granite geochemistry (e.g., Champion & Sheraton, 1997; Witt & Davy, 1997) and also geochronology (e.g., Nelson, 1997). Detailed summaries of the granitoids of the north Eastern

Goldfields region are provided by Champion & Sheraton (1997), and the southern Eastern Goldfields region by Witt & Davy (1997) and Smithies & Witt (1997). A summary of previous classifications for granites in the Eastern Goldfields Province is given in Table 3. This table includes the Association names for the various granite groups.

Table 3. Granite classification for the southeastern Yilgarn Craton relative to other classifications for the eastern part of the craton. Shown in bold are the granite groups (expanded from Champion & Sheraton, 1997) and the Association names for each granite group in the Southern Cross and Eastern Goldfields Provinces.

This Report	**Champion & Sheraton**	**Witt & Davy**[d]	**Internal/ External**[a]	**Bettenay**[b]	**Wyborn**[c]
southeastern Yilgarn craton	northern Eastern Goldfields	southern Eastern Goldfields	Eastern Goldfields	southern Southern Cross	
High-Ca Diemals (SCP) Merangina (EGP	**High-Ca**	Woolgangie (Post) Morapoi (Pre)	Internal & external	Synkinematic, postkinematic & banded gneiss	Groups 1, 3 & 4
Low-Ca Beetle (SCP) Mt Boreas (EGP)	**Low-Ca**	Woolgangie (Post)	Internal & external	Synkinematic & postkinematic	Groups 3 & 4
High-HFSE Kookynie (EGP)	**High-HFSE**	Dairy (Post) Morapoi (Pre)	Internal		
Mafic Granny Smith (EGP)	**Mafic**	Liberty (Post) Morapoi (Pre)	Internal		Group 2
Syenite Fitzgerald (SCP) Gil garna (EGP)	**Syenite**	Gilgarna (Post)	Internal		

Explanation and sources: a - pre- and post-folding supersuite classification of Witt & Davy (1997); b - External to or Internal within greenstones; c - Bettenay (1977); d - Wyborn (1993): 1 -early banded g neiss and migmatite; 2 - mafic tonalite to granite; 3 - granodiorite to granite; 4 - monzogranite to granite.

High-Ca group, southeastern Yilgarn Craton

Member Associations: Menangina Association (Eastern Goldfields Province)
Diemals Association (Southern Cross Province)

The High-Ca group is the dominant granitoid group in the southeastern Yilgarn Craton, representing about 60 percent of all granitoids. High-Ca group granitoids consist largely of trondhjemite, sodic granodiorite and monzogranite. All the granitoids are biotite-bearing with some comtaining hornblende. Granitoids exhibit a range of deformation and metamorphic fabircs, with the vast majority displaying variable recrystallisation. High-Ca granitoids form large to very large, internal and external, massive plutons, as well as foliated granite and/or granitic gneiss complexes, including the bulk of the external granitic masses in the Eastern Goldfields Province and the largest proportion of the Southern Cross Province. The granitic gneisses range from relatively homogeneous to strongly layered and are locally migmatitic (e.g., Bettenay, 1977). Many of the granitoid masses form linear belts with a general NNW trend parallel to the general structural fabric in the eastern Yilgarn Craton. High-Ca granitoids also form large zoned plutons that are largely internal to the greenstone belts in the central part of the southern Eastern Goldfields Province. They also form a range of small plutons and dykes intrusive into both greenstone and other High-Ca granitoids throughout the rest of the province.

Eight clans have been delineated in the southern Eastern Goldfields Province on the basis of geochemistry and regional distribution, whereas four clans have been delineated in the Southern Cross Province. Some of the clans (e.g., Ajax, Niagara, Parker Hills, Spear, Yindi) are geographically restricted, whereas more arbitrary boundaries are used for some of the larger High-Ca clans (e.g, Burra, Goongarrie, Menangina, Woolgangie); each clan, however, is characterised by particular geochemical characteristics.

Geochronology on High-Ca granitoids in the southern Eastern Goldfields Province indicate a range in ages from ca. 2.72 to 2.65 Ga (Table 4), with the vast majority ranging from ca. 2.685 to 2.66 Ga. Many High-Ca granitoids in the Eastern Goldfields Province contain some inherited zircons, with ages ranging from 2.68 to >2.86 Ga. There appears to be consistent peaks in the ages of zircon inheritance, possibly indicating discrete magmatic events for the development of the source rocks. These ages are in accord with Nd model ages determined for High-Ca granitoids in the Eastern Goldfields Province (Champion & Sheraton, 1997; Fletcher & McNaughton, this report).

High-Ca granitoids in the southern Southern Cross Province range from 2.71 to ca. 2.66 Ga (Table 5), with a peak at about 2.70 to 2.68 Ma, in contrast to the Eastern Goldfields Province. Some High-Ca granitoids in the Southern Cross Province contain inherited zircons with ages ranging from 2.76 to >3.2 Ga, suggesting the presence of very old crust in the source regions for some of these granitoids. This is consistent with Nd model ages that support the presence of pre-existing crust for some High-Ca granitoids in the Southern Cross Province (Fletcher et al., 1994; Fletcher & McNaughton, this report).

The geochemical characteristics for High-Ca granitoids have been documented by Champion & Sheraton (1997) and several reports provided as part of this AMIRA project and will be only briefly summarised. High-Ca granitoids are characterised by a narrow compositional range (68-76 wt% SiO_2), but exhibit heterogeneity with respect to many elements, in particular large-ion lithophile

elements (LILE). High-Ca granitoids generally have high Al_2O_3, moderate to high Na_2O, moderate K_2O, and low to moderate LILE (K_2O, Rb, Pb, Th) and
HFSE (LREE, HREE, Zr, Y) contents. Towards the high silica end of the compositional spectrum, there is overlap in many elements with Low-Ca granitoids (Figure 1, 2, 3). General trends with increasing silica for selected elements and ratios are listed in Table 6. The High-Ca group granitoids plot along the calc-alkaline trend generally to the right of the TTG field on a K-Na-Ca plot (Figure 2). Some High-Ca granitoids at the high silica end of the compositional spectrum display distinctly fractionated patterns for K_2O, Rb, Pb and Th; note the Ajax and Niagara clans plot in the 'fractionated granitoid' field on a Rb-Ba-Sr plot (Figure 2).

Table 4. Age ranges and ages of inherited zircons for granitoid clans in the Eastern Goldfields Province, and represented in the southeastern Yilgarn Craton. Compiled from published and unpublished sources.

Granitoid Association	Granitoid Clan	*n*	Age Range – Low (Ma)	Age Range – High (Ma)	Xenocryst Ages (Ga)
Menangina	Ajax	-	no age data		
(High-Ca)	Beasley	6	2656±7	2697±6	2.70-2.72, 2.74, 2.77-2.78, 2.87
	Burra	12	2655±6	2689±22	2.685-2.69, 2.8, >2.85
	Goongarrie	5	2646±11	2687±6	2.685, 2.74, 2.78, 2.86
	Menangina	4	2658±13	2675±11	2.70-2.80
	Niagara	-	no age data		-
	Parker Hills	3	2648±11	2657±9	2.705-2.725
	Yindi	1	2660±5		2.70
	unassigned	5	2664±4	2711±6	2.725, 2.81, 2.84, 2.94
Mt Boreas	Mt Boreas	1	2651±10		-
(Low-Ca)	Mungari	4	2603±19	~2630	2.685, 2.81
	Nulerie	4	2647±3	2654±9	2.87, 2.95
	unassigned	4	2619±13	2652±3	2.675, 2.715
Granny Smith	Dinky Boys	-	no age data		-
(Mafic)	Granny Smith	11	2648±6	2667±2	2.675, 2.70-2.715, 2.80-2.81
	Kambalda	1	2662±6		-
	Kanowna-Belle	7	2613±11	2694±8	2.72-2.74, 2.92-2.95
	Mafic unassigned	2	2673±3	2674±6	2.72, 2.875
	New Celebration	1	2686±4		2.72
	Victory	1	2664±8		-
	unassigned	7	2656±4	2686±5	2.685, 2.705-2.715, 2.78, 2.86
Xenolith (Mafic)	Cement	1	2663±11		-
Kookynie	Kookynie	3	2658±7	2686±7	2.705-2.71
(High-HFSE)	Outcamp Bore	3	2698±10	2719±5	2.75
	Cashmans	-	no age data		-
Gilgarna	Erayinia	2	~2660	2660±5	-
(Syenitic)	Gilgarna	4	2644±13	2664±2	2.675, 2.74

Individual clans of High-Ca granitoids can be delineated on the basis of LILE and HFSE contents (Figure 4). Overall, High-Ca granitoids in both provinces represented in the southeastern Yilgarn Craton can be subdivided into 'low-LILE' and 'high-LILE' clans. Individual granitoids plotted on a K_2O versus Ce variation diagram (Figure 2) can be generally subdivided into these two High-Ca subgroups. However, this division is somewhat arbitrary and largely for the purpose of classification of individual suites and super-suites. Some suites and super-suites cannot be easily placed into either 'low-LILE' or 'high-LILE' subgroups (e.g., Parker Hills) or show concentrations transitional to these subgroups. Overall, the range of High-Ca granitoid compositions in the southeastern Yilgarn Craton indicate a range of partial melting conditions for their petrogenesis.

Table 5. Age ranges and ages of inherited zircons for granitoid clans of the Southern Cross Province, and represented in the southeastern Yilgarn Craton. Compiled from published and unpublished sources.

Granitoid Association	Granitoid Clan	*n*	Age Range – Low (Ma)	Age Range – High (Ma)	Xenocryst Ages (Ma)
Diemals	Karalee	1	2676±3		-
(High-Ca)	Spear	1	2693±5		2.84, 3.3
	Stennet Rock	1	2691±8		~2.9, ~3.1, ~3.2
	Woolgangie	2	2656±10	2707±6	2.76
Beetle	Beetle	4	2632±4	2660±3	2.705, 2.80
(Low-Ca)	Boorabbin	3	2631±3	2633±2	2.67-2.68, 2.765
	Nargalyerin	7	2623±7	2646±6	-
	Yeelirrie	4	2638±10	2682±8	~2.9, ~3.0, ~3.1, 3.58, 3.67
Westonia (Mafic)	Red Leaf	-	no age data		-
Fitzgerald Peaks (Syenitic)	Fitzgerald Peaks	-	no age data		-

High-Ca group granitoids are generally characterised by moderately to steeply fractionated rare-earth element (REE) patterns, typically without an Eu anomaly. The majority of High-Ca granitoids are also are characterised by moderate to high Sr contents and variable low to moderate Y contents. These characteristics show up as a relatively Sr-undepleted and variably Y-depleted signature on primitive mantle-normalised multi-element diagrams (Spider-plots) (Figure 3). However, there is a range in concentration of these elements to slightly Sr-depleted and Y-undepleted compositions (e.g., Figure 3). The majority of High-Ca granites also exhibit negative Nb, P and Ti anomalies on the Spider-plots (Figure 3).

Constraints can be placed on the petrogenesis of the High-Ca granitoids by their geochemistry, Nd and Pb isotopic compositions and presence and age of inherited zircons. The broadly silica-rich and sodic nature of the High-Ca group granitoids, as well as generally low-LILE contents, is consistent with derivation from an intermediate to mafic LILE-poor source. The major compositional variations in LILE and HFSE between individual various High-Ca clans suggests a range in the composition of the source as the range cannot be due solely to varying degrees of partial melting.

The variations between the dominant Y-depleted, Sr-undepleted and subordinate Y-undepleted, Sr-depleted clans within the High-Ca granitoid group is consistent with partial melting over a range of pressures. The Y-depleted, Sr-undepleted signature of the majority of the High-Ca granitoids is generally interpreted to indicate derivation from a plagioclase-poor source at pressures high enough to stabilise residual garnet and destabilise plagioclase during melting (e.g., Rapp et al., 1991). Petrogenetic models commonly invoke either partial melting deep within thickened crust (>35-50 km) or partial melting of a subducting slab (e.g., Drummond & Defant, 1990; Martin, 1994). The presence of inherited zircons as well as a range of Nd model ages and variable Y- and Sr-depletion, favour partial melting of, or at least interaction with, a thickened crustal source for the High-Ca group granitoids.

Tectonic models for development of the eastern Yilgarn Craton range from pre-existing continental crust upon which greenstone belts were deposited either in a subduction and/or back-arc environment (e.g., Barley et al., 1989), related to mantle plume tectonics (e.g., Hill et al., 1989) to collisional tectonics involving accretion of micro-plates (e.g., Myers, 1995). Radiogenic isotope (Nd, Pb) compositions, granitoid emplacement ages and inherited zircon populations are consistent with some form of convergent tectonics, however, the timing of convergence is not well understood. The change in the peak age of High-Ca granitoid emplacement from ca. 2.70-2.68 Ga in the Southern Cross Province to ca. 2.68-2.66 Ga in the Eastern Goldfields Province is consistent with such a model. However, the models need to be more fully developed to clearly explain the voluminous High-Ca group granitoids in the southeastern Yilgarn Craton.

Table 6. Summary of typical abundances of selected elements, comparing the Diemals and Beetle associations of the Southern Cross Province to the Menangina and Mt Boreas associations of the Eastern Goldfields Province. Decreasing and increasing refer to overall trends of these elements with increasing silica.

SiO_2	Na_2O/K_2O	Rb/Sr	Th	Zr	Ce
Menangina Association (High-Ca)					
68-76	0.75-2.5 Na_2O 3.4-5.6 K_2O 2.0-4.5	0.1->1.0 Rb 50-200 Sr <100->1000	5-25	50-200 decreasing	15-120 broad decrease
Diemals Association (High-Ca)					
69-74	1.0-2.0 Na_2O 3.8-5.0 K_2O 2.8-4.1	0.2-0.75 Rb 75-175 Sr 150-500	10-40	80-250 decreasing	25-200 decreasing
Mt Boreas Association (Low-Ca)					
70-75	<1 Na_2O 3.3-4.1 K_2O 4.5-5.4	<1 to >>1 Rb 200-350 Sr <50->350	20-65 very broad decrease	60-300 decreasing	30-300 decreasing
Beetle Association (Low-Ca)					
68-75	<1 Na_2O 3.3-4.2 K_2O 4.0-5.5	<1 to >>1 Rb 150-350 Sr 75-300	30-70 broad decrease	100-500 decreasing	<100-400 broad decrease

Clans within the Menangina Association, Eastern Goldfields Province

The Menangina Association is the dominant granitoid grouping in the Eastern Goldfields Province in the southeastern Yilgarn Craton. Eight clans have been delineated on the basis of geographical distribution and geochemical characteristics. Some of the clans (e.g., Ajax, Parker Hills) are small and geographically restricted, whereas the larger High-Ca clans (e.g, Burra, Menangina) form over large regions within the southern Eastern Goldfields Province. Individual clans of the Menangina Association are characterised by specific geochemical characteristics; Table 6 summarises the abundances of selected elements for the clans.

The distribution, age constraints, geochemical characteristics and relationship to mineralisation are summarised for each clan; clans are presented in alphabetical order. General petrogenetic models for the High-Ca granitoids have been summarised above; however, specific petrogenetic implications for individual clans are also highlighted below.

Table 6. Summarised abundances of selected elements for the various clans of the Menangina, Mt Boreas, and Kookynie Associations of the Eastern Goldfields Province. Number in brackets refers to number of geochemical analyses used in calculations.

Group	SiO_2	Na_2O/K_2O	Rb/Sr	Th	Zr	Ce
Menangina Association						
Ajax (n = 10)	74.5-77.5	0.7-0.95 Na_2O 3.0-3.8 K_2O 4.0-4.4	4->10 Rb 130-250 Sr 10-35	15-20	75-100	15-25
Beasley (n = 17)	68.0-71.0	1.5-4.0 Na_2O 4.5-5.6 K_2O 1.5-3.0	0.1-0.2 Rb 45-100 Sr 400-750	5-10	90-130+	30-70
Burra (n = 72)	68.0-76.0	0.9-2.5 Na_2O 3.7-5.5 K_2O 2.0-4.5	0.15->1.0 Rb 60-200 Sr <100-500	5-30	50-160	20-50
Goongarrie (n = 55)	70.0-75.0	0.75-2.0 Na_2O 3.5-5.0 K_2O 2.5-4.5	0.1-1.5 Rb 70-200 Sr 100-750	10-35	80-200	40-125
Menangina (n = 52)	68.0-73.5	1.0-2.0 Na_2O 4.5-6.0 K_2O 2.75-4.4	0.1-0.75 Rb 80-175 Sr 200-1200	5-20	80-200	35-110
Niagara (n = 10)	75.5-78.0	0.75-1.4 Na_2O 3.8-4.8 K_2O 3.5-6.0	>1.0 Rb 110-260 Sr 25-100	10-20	50-100	15-50
Parker Hills (n = 22)	70.0-73.0	1.5-2.2 Na_2O 5.0-6.1 K_2O 2.6-3.5	<0.1 Rb 50-85 Sr 750-1500	<5-8	75-125	20-60
Yindi (n = 39)	70.0-75.5	1.0-2.5 Na_2O 4.4-5.5 K_2O 2.0-4.2	0.15-1.0 Rb 60-175 Sr 100-600	<5-15	60-125	10-50
Mt Boreas Association						
Mt Boreas (n = 21)	73.0-76.0	0.65-0.9 Na_2O 3.4-4.1 K_2O 4.5-5.4	2->10 Rb 250-375 Sr 25-110	20-50	60-175	30-125
Mungari (n = 28)	71.5-75.0	0.6-0.8 Na_2O 3.3-4.0 K_2O 4.75-5.4	1.5-5.0 Rb 200-400 Sr 60-170	25-65	100-300	70-250
Nulerie (n = 11)	70.0-72.5	0.75-0.95 Na_2O 3.6-4.0 K_2O 4.9-5.2	0.5->1.0 Rb 175-250 Sr 200-400	25-45	200->300	150-300
Kookynie Association						
Kookynie (n = 16)	74.0-77.5	1.0-2.5 Na_2O 3.6-4.4 K_2O 1.7-4.0	0.3-2.5 Rb 50-150 Sr 50-150	5-20	100-250	55-105
Outcamp Bore (n = 7)	70.0-76.0	1.2-1.8 Na_2O 4.0-4.5 K_2O 2.5-3.5	0.6-1.2 Rb 70-125 Sr 50->200	7-10	75->250	30-80
Cashmans (n = 6)	75.0-76.5	>1.5 Na_2O 4.2-5.5 K_2O 1.25->2.2	1.5-3.0 Rb 50-100 Sr 25-50	65-75	200-250	60-70

Ajax Clan

Member Supersuites: Ajax

Distribution: Minor High-Ca clan in the Eastern Goldfields Province. Forms series of granitic dykes in the Norseman area. Lithologies are syenogranite and monzogranite reflecting the potassic nature of the rocks.

Geochronology: No SHRIMP geochronology available. A Pb-Pb wholerock + K-feldspar isochron suggests an age of ca. 2680 Ma (Perring, 1989).

Geochemistry: Geochemically the Ajax clan is characterised by fractionated High-Ca characteristics with high SiO_2, K_2O, Rb, Rb/Sr, Y, moderate Pb, Th and low Na_2O/K_2O, Sr, Zr, LREE and *mg* (Table 3.). Ajax granitoids contain low total REE contents, and display flatish REE patterns with a large negative Eu anomalies. They are one of the few High-Ca clans with Sr-depleted, Y-undepleted signature as displayed on a Spider-plot. The low Zr, LREE and only moderate Pb and Th contents clearly distinguish this group from Low-Ca group granitoids.

Mineralisation: Spatially associated with Au mineralisation in the Norseman district (e.g., Ajax mine).

Petrogenesis: The high silica contents, high K_2O and Rb contents and overall low total contents of REE are consistent with crystal fractionation processes. The flat REE patterns with pronounced negative Eu anomalies, Sr-depletion, Y-undepletion are consistent with a source where plagioclase was stable indicating mid- to lower-crustal pressures.

Tectonic and other implications: The felsic nature and lower pressures of formation postulated for the Ajax clan implicates partial melting of pre-existing intermediate crust.

Beasley Clan

Member Supersuites: Barret Well, Beasley, Linden, No.2 Well, Olympic-2

Distribution: A moderate-sized High-Ca clan that occurs dominantly in the northeastern half of the southern Eastern Goldfields Province on the central and eastern parts of the EDJUDINA sheet. It also occurs as banded granitic gneiss (Olympic-2) within Goongarrie clan High-Ca granitoids on the eastern part of the MENZIES sheet. Forms a range of granitoids from undeformed plutons to granitic gneiss (e.g., Barret Well, Two Lids Soak, Olympic-2); also occurs as dykes in several localities. Lithologies include dominant biotite monzogranite and minor granodiorite and tonalite.

Geochronology: SHRIMP zircon ages range from 2697 to 2656 Ma with the majority with ages of ca. 2675 Ma. These includes granitic gneisses at Two Lids Soak and Barret Well on the eastern side of EDJUDINA sheet (Nelson, 1997).

Geochemistry: The Beasley clan forms the 'low-LILE' end-member for High-Ca granitoids in the southern Eastern Goldfields Province, with high Na_2O, *mg#* and Na_2O/K_2O, low LILE (e.g., K_2O, Rb, Pb, Sr, Th) and HFSE (Zr, REE) contents and low Rb/Sr ratios (Figures 4). Beasley clan granitoids are characterised by strongly fractionated REE patterns without Eu anomalies (Figure 3) and low to very low HREE contents. They also are Sr-undepleted and Y-depleted with pronounced Nb and Ti and minor P depletion as displayed on Spider-plots (Figure 3).

Mineralisation: None known

Petrogenesis: The more 'primitive' low-LILE geochemistry and Sr-undepleted, Y-depleted signature of the Beasley clan is consistent with partial melting of a basaltic/amphibolitic source at high pressures. The higher *mg#* may indicate a subducted slab component in the source region rather than thickened crust.

Tectonic and other implications: The suggestion of a subducted slab component in the source has important tectonic implications for the Eastern Goldfields Province, although more work is required to substantiate this suggestion.

Burra Clan

Member Supersuites: AMET-Ballard-1, Bali, Big Porphyry, Buldania, Burra, Connolly, Chalice-Dyke-1, Gladstone-dyke-2, Lake Dundas, Lake Kirk, Riverina, Tonkin, Twin Hills

Distribution: The Burra clan is the dominant High-Ca clan in the western half of the Eastern Goldfields Province. It forms a diverse range of granitoids from granitic dykes in the Norseman and Kookynie areas, massive to deformed granitoid plutons (Bali, Battery, Buldania, Calooli) and domes (e.g., Pioneer) and extensive granitic gneiss complexes (e.g., Lake Kirk, Connolly) along the edge of the Kalgoorlie Terrane. Dykes belonging to the Chalice-Dyke-1 supersuite are tentatively included in the Burra clan. Lithologies are mainly biotite monzogranite with subordinate biotite granodiorite.

Geochronology: Burra clan granitoids have a range of SHRIMP zircon ages from 2689 to 2655 Ma, with the majority around 2675 to 2660 Ma. Some of the granitic gneisses (e.g., Lake Kirk, Connolly, Pioneer) contain ?inherited zircon populations older than 2.7 Ga. Dykes in the Chalice deposit that are tentatively assigned to the Burra clan have ages of ca. 2645 Ma (L. Bucci, written communication, 2000). Syntectonic metamorphic titanite from the Lake Kirk granitic gneisses in the Norseman district is dated at ca. 2630 Ma, indicating deformation along major shear zones extended down to ca. 2630 Ma in some areas.

Geochemistry: The Burra clan is characterised by high Na_2O and Na_2O/K_2O, low LILE (e.g., K_2O, Rb, Pb, Sr, Th) and HFSE (Zr, REE) contents and low-moderate Rb/Sr ratios (Table 3; Figures 4), with members at the high-silica end (>74 wt% SiO_2) displaying weak fractionation trends. Burra granitoids display moderately fractionated REE patterns with no or small negative Eu anomalies. They have Sr-undepleted, Y-depleted to variably Sr-depleted, Y-undepleted signatures as displayed on Spider-plots. These characteristics place the clan in the 'low-LILE' subgroup of High-Ca granitoids in the southern Eastern Goldfields Province.

The variable Sr-Y signatures, variable but generally low LILE and HFSE contents, higher Na_2/K_2O and Rb/Sr ratios and lower mg# contrast this 'low-LILE' clan with the Beasley clan. Both clans have lower Sr, K_2O and higher Total FeO contents than the Yindi clan.

Mineralisation: Burra clan dykes are spatially associated with Au mineralisation in the Norseman (e.g., Big Porphyry) and Kookynie districts. Dykes of the Chalice-Dyke-1 supersuite at the Chalice deposit are mineralised.

Petrogenesis: The 'low-LILE' geochemistry but variably Sr-undepleted, Y-depleted signature of the Burra clan is consistent with partial melting of a mafic to intermediate source at variable pressures (i.e., lower thickened crust). The lower *mg#* (than the Beasley clan) may indicate a minimal or no subducted slab component in the source region.

Tectonic and other implications: As for the High-Ca group granitoids in general. The lower LILE and HFSE may indicate a more primitive source, although not as primitive as postulated for the Beasley clan. The youngest Burra clan members overlap with the oldest Low-Ca granitoids and this has implications regarding tectonic models.

Goongarrie Clan

Member Supersuites: Cave Hill, Chalice-Dyke-2, Dynamite, End of Day, Goongarrie, Larkinville, Lone Hand, Mendleyarri, Nine Mile Rocks, Pine Lodge, Queen Victoria

Distribution: A large High-Ca clan that occurs in the western half of the southern Eastern Goldfields Province. It occurs a range of granitoids from undeformed plutons (e.g., Lone Hand, Pine Lodge) to variably deformed granitic complexes (e.g., extensive areas of the Goongarrie -Mt Pleasant batholith). The Goodia and Theatre Rocks domes in the Norseman district also belong to the Goongarrie clan. This clan also occurs as dykes in several localities. Dykes of the Chalice-Dyke-2 supersuite at the Chalice deposit have been tentatively assigned to the Goongarrie clan. Lithologies include dominant biotite monzogranite and minor granodiorite.

Geochronology: Five Goongarrie clan granitoids have been dated by SHRIMP; these have zircon ages that range from 2687 Ma (Queen Victoria Rocks monzogranite, suite and supersuite) to 2646 Ma (Donnas Soak monzogranite, Siberia-2 suite, Goongarrie supersuite). Chalice-Dyke-2 supersuite dykes from the Chalice deposit have been dated at ca. 2630 Ma (L. Bucci, written communication, 2000); if the tentative classification of these dykes to the Goongarrie clan stands further scrutiny, then High-Ca magmatism continued in some areas to ca. 2630 Ma.

Geochemistry: The Goongarrie clan is characterised by moderate Total FeO, K_2O, Rb, Ce, Pb, Th, Zr contents (Figure 1, 2, 4) and is typical of 'high-LILE' clans by having higher LILE and HFSE contents and Rb/Sr ratios, and lower Sr/Sr* and *mg#*, than 'low-LILE' clans (e.g., Beasley, Burra). Strontium contents of Goongarrie clan members are generally lower than 'low-LILE' High-Ca granitoids. Goongarrie clan granitoids are characterised by strongly fractionated REE patterns with no or variable negative Eu anomalies. The negative Eu anomalies are generally in higher silica members that also show weak fractionation. On Spider-plots, Goongarrie granitoids are Sr-undepleted to moderately Sr-depleted and moderately to slightly Y-depleted.

The Goongarrie clan shares many similarities with the Menangina clan, but with notable differences in Sr and Ba contents. Also the Goongarrie clan is dominantly more siliceous than the Menangina clan. The 'high-LILE' clans of the High-Ca group have geochemistry that is intermediate between 'low-LILE' clans and Low-Ca group granitoids. There is also some overlap at the high silica end with both 'low-LILE' clans and Low-Ca group granitoids.

Mineralisation: The Cawse Gold Mine suite is mineralised at the Cawse gold deposit. Dykes of the Chalice-Dyke-2 supersuite at the Chalice gold deposit are mineralised.

Petrogenesis: The higher LILE and HFSE contents of 'high-LILE' clans require a more LILE-enriched component in their source. Although the 'high-LILE' clans overlap at the high silica end with some Low-Ca group granitoids, Nd and Pb isotope compositions point to distinct sources for both granitoid types. The variable Sr-depleted, Y-depleted signature suggests variable but moderate - high pressures of formation.

Tectonic and other implications: Partial melting of thickened crust is the preferred model for these granitoids.

Menangina Clan

Member Supersuites: Birthday, Coglia Road, Galvalley, Goat Dam, Loafers Well, Menangina, Moon Rock, Yallaburra, Yilgangi, various dykes

Distribution: A large High-Ca clan that occurs dominantly internal to greenstones in the central part of the southern Eastern Goldfields Province. It includes the type locality (Menangina Rocks) for High-Ca granitoids in the Eastern Goldfields Province. It occurs a range of granitoids from discrete internal plutons (e.g., Bulyairdie, Cowarna, Galvalley, Goat Dam,) to variably deformed granitic complexes (e.g., Birthday complex), principally on the EDJUDINA and KURNALPI sheets. A small pluton in the central part of the WIDGIEMOOLTHA sheet is also assigned to the Menangina clan. The clan also includes a number of granitic dykes that intrude greenstones and granitoids throughout the central Eastern Goldfields Province. Lithologies include dominant biotite monzogranite and minor granodiorite. Hornblende-bearing granitoids are present in places.

Geochronology: Four Menangina clan granitoids have been dated by SHRIMP; these have zircon ages that range from 2675 Ma (Cement Well-Barber Well monzogranite, Birthday suite and supersuite) to 2658 Ma (Brady Well monzogranite, Menangina suite & supersuite). Based on interpretation of aeromagnetic data, the Menagina suite intrudes the Birthday suite, and the zircon ages are consistent with this interpretation.

Geochemistry: The Menangina clan is characterised by moderate Total FeO, K_2O, Rb, Ce, Pb, Th, Zr contents (Figure 1, 2, 4) and is typical of 'high-LILE' clans by having higher LILE and HFSE contents and Rb/Sr ratios, and lower Sr/Sr* and *mg#*, than 'low-LILE' clans (e.g., Beasley). Strontium and Ba contents of Menangina clan members are variable but generally low, except for the Galvalley and Loafers Well supersuites that contain high Sr and Ba contents. Menangina clan granitoids are characterised by strongly fractionated REE patterns with no Eu anomalies; HREE display moderately fractionated to 'spoon'-shaped patterns. On Spider-plots, Menangina granitoids are dominantly Sr-undepleted and variably Y-depleted.

The Menangina clan shares many similarities with the Goongarrie clan, but with lower Th and Pb and variable but higher Na_2O contents. The Sr and Ba contents of some supersuites overlap with those of the Parker Hills clan; this is best displayed on a CaO versus Sr diagram (Figure 2).

Mineralisation: None known.

Petrogenesis: The higher LILE and HFSE contents of 'high-LILE' clans require a more LILE-enriched component in their source. Although the 'high-LILE' clans overlap at the high silica end with some Low-Ca group granitoids, Nd and Pb isotope compositions point to distinct sources for both granitoid types. The variable Sr-depleted, Y-depleted signature suggests variable but moderate-high pressures of formation.

Tectonic and other implications: Partial melting of thickened crust is the preferred model for these granitoids, although a LILE-enriched component in the source is required.

Niagara Clan

Member Supersuites: Niagara

Distribution: A small High-Ca clan that occurs in the eastern half of the MENZIES sheet as a series of dykes and small plutons. Most granitoids of this clan are biotite monzogranite.

Geochronology: None available.

Geochemistry: The Niagara clan is characterised by high SiO_2, K_2O, Rb and Y, moderate Pb, Th, and low Ce, Sr, and Zr contents (Figure 1, 2, 4). The K_2O, Rb, Y, Pb and Th trends and high Rb/Sr suggest that these granitoids are fractionated, silica-rich granitoids and have affinities to 'low-LILE' clans (e.g., Beasley, Burra); Niagara granitoids plot in the 'fractionated granitoid' field on a Rb-Ba-Sr diagram (Figure 2).. Niagara clan granitoids are characterised by moderately fractionated LREE and flatish HREE patterns with strong negative Eu anomalies. On Spider-plots, Niagara granitoids are Sr-depleted and Y-undepleted. The Niagara clan shares many similarities with the other 'low-LILE' clans, but are more siliceous than the most granitoids belonging to the Burra and Beasley clans. They are most similar to the Ajax clan, but have lower Y contents. Although they overlap with some silica-rich Low-Ca group granitoids, the low Zr, LREE and only moderate Pb and Th contents clearly distinguish this clan from Low-Ca group granitoids.

Mineralisation: Dykes of Niagara clan granitoids are mineralised in the Niagara and Kookynie areas.

Petrogenesis: The high silica contents, high K_2O and Rb contents and overall low total contents of REE are consistent with crystal fractionation processes. The REE patterns with pronounced negative Eu anomalies, Sr-depletion, Y-undepletion are consistent with a source where plagioclase was stable indicating mid- to lower-crustal pressures.

Tectonic and other implications: The felsic nature and lower pressures of formation postulated for the Niagara clan implicates partial melting of pre-existing intermediate crust.

Parker Hills Clan

Member Supersuites: Fitzgerald Lagoon, Jyndabinbin, Parker Hills, Sinclair

Distribution: A moderate sized High-Ca clan that is geographically restricted to a linear belt in the central and eastern WIDGIEMOOLTHA sheet, as well as part of the NORSEMAN sheet. Parker Hills clan granitoids occur as a large discrete plutons internal to and bounding greenstones in the southeastern corner of the Eastern Goldfields Province. Most granitoids of this clan are hornblende-biotite monzogranite and granodiorite.

Geochronology: Three SHRIMP ages are available for the Parker Hills clan and these range from 2657 Ma (Fitzgerald Lagoon pluton, suite and s/suite) to 2648 Ma (Toil and Trouble granite, Sinclair suite and s/suite).

Geochemistry: The Parker Hills clan is characterised by moderate K_2O and Pb, and low Ce, Rb, Th, Y and Zr contents (Figure 1, 2, 4). Parker Hills clan granitoids are characterised by moderately fractionated REE patterns with no Eu anomalies and on Spider-plots have Sr-undepleted to -enriched and Y-depleted signatures. The Parker Hills clan shares many similarities (e.g., Ce, Rb, Th, Y, Zr contents, high *mg#*) with 'low-LILE' clans, but contrasts by containing significantly higher Ba, Sr contents and Sr/Sr*, moderate K_2O and Pb contents that overlap with 'high-LILE' clans and lower Total FeO contents. The high Ba and Sr contents are very similar to those in New Celebration clan dykes and the Depot supersuite of the Granny Smith Association (Mafic group).

Mineralisation: None known; although highly fractured, veined and altered granitoid is present at one locality (Yardina granitoid, suite). Quartz veins contain CH_4-rich, and locally graphite-bearing, fluid inclusions. At the time of vein formation and alteration, the carbonaceous sedimentary rocks of the Mount Belches Formation is interpreted to have been immediately on top of the Yardina granitoid and may have provided the carbon subsequently trapped in the fluid inclusions.

Petrogenesis: The similar characteristics of the Parker Hills clan (low-moderate LILE and HFSE; Sr-undepleted, Y-depleted signature) to the 'low-LILE' clans is consistent with partial melting of a basaltic/amphibolitic source at high pressures. The higher *mg#* may indicate a subducted slab component in the source region rather than thickened crust. However, the high to very high Ba and Sr contents necessitates interaction with a LILE-enriched (at least Ba and Sr) component, either from subducted sediments, a LILE-enriched fluid phase or melt, or continental crust. The last possibility of not likely, as the Ba and Sr contents are well above those in the rest of the High-Ca group granitoids in the Eastern Goldfields Province.

Tectonic and other implications: The suggestion of a subducted slab component in the source has important tectonic implications for the Eastern Goldfields Province. The linear distribution of this clan as well as the proximity to Ba- and Sr-rich porphyry dykes and plutons of the New Celebration clan, Mafic group, further implicates a highly focussed source for these granitoids. The high Ba and Sr contents implicate interaction with a LILE-enriched (at least Ba and Sr) component; this may have been a metasomatized mantle wedge-derived fluid phase. Further evidence is required to substantiate this suggestion.

Yindi Clan

Member Supersuites: Bronco Plain, Forest Well, Jarrah Well, Pindinnus, Roe, Surprise, Redcastle, Yindi, various dykes

Distribution: A moderate-sized High-Ca clan that forms a roughly linear belt in the northeastern half of the southern Eastern Goldfields Province on the central and eastern parts of the EDJUDINA and KURNALPI sheets. The clan occurs as a range of granitoids from discrete plutons (e.g., Yindi, Yowie) to deformed granitic complexes (e.g., Bronco Plains, Mt Celia Gneiss) that are both internal to and external to the greenstones. Some of the plutons (Redcastle) show strong zonation on aeromagnetic images. The clan also occurs as dykes in several localities. Lithologies include dominant biotite monzogranite and minor granodiorite.

Geochronology: Only one SHRIMP zircon age of 2660 Ma (Redcastle granite, suite) is available for the clan.

Geochemistry: The Yindi clan is characterised by typical 'low-LILE' characteristics including high Na_2O and Na_2O/K_2O, moderate *mg#*, Sr/Sr*, low Total FeO, LILE (e.g., K_2O, Rb, Pb, Sr, Th) and HFSE (Zr, Y, REE) contents and low Rb/Sr ratios (Figures 4). Yindi clan granitoids are characterised by moderately fractionated REE patterns without Eu anomalies (Figure 3) and have variable Sr-enriched to slightly-depleted and variably Y-depleted signatures as displayed on Spider-plots (Figure 3).

Mineralisation: None known.

Petrogenesis: The 'primitive' low-LILE geochemistry and dominantly Sr-undepleted, Y-depleted signature of the Yindi clan is consistent with partial melting of a basaltic/amphibolitic source at high pressures. The moderate *mg#* and variable Y-depletion may indicate a larger proportion of thickened crust in the source region rather than a subducted slab component.

Tectonic and other implications: Similar to that proposed for other 'low-LILE' clans of the High-Ca group.

5.2 Clans within the Diemals Association, Southern Cross Province

The Diemals Association is the dominant granitoid grouping in the Southern Cross Province in the southeastern Yilgarn Craton. Four clans have been delineated on the basis of geographical distribution and geochemical characteristics. Three of the clans (Karalee, Spear and Woolgangie) have geochemistry indicating affinity with the 'high-LILE' clans present in the Eastern Goldfields Province. The other clan (Stennet Rocks) is a minor clan that has geochemistry consistent with affinity with the 'low-LILE' clans. Two clans (Karalee, Woolgangie) are form over large regions within the southeastern Southern Cross Province, and have very similar characteristics; separation is based mainly on distribution of the granitoids rather than geochemistry. Individual clans of the Diemals Association are characterised by specific geochemical characteristics; Table 7 summarises the abundances of selected elements for the clans.

Table 7. Summarised abundances of selected elements for the various clans of the Diemals, Beetle, Westonia and Fitzgerald Peaks Associations of the Southern Cross Province.

Group	SiO_2	Na_2O/K_2O	Rb/Sr	Th	Zr	Ce
Diemals Association						
Karalee (n = 18)	69.2-75.5	0.9-1.5 Na_2O 3.75-5.0 K_2O 3.0-4.25	0.3-1.1 Rb 100-175 Sr 150-375	10-30	80-200	40-80
Spear (n = 10)	70.0-72.0	1.0-1.5 Na_2O 4.0-4.75 K_2O 3.0-4.0	0.25-0.6 Rb 100-175 Sr 300-500	20-40	200-250	100-200
Stennet Rock (n = 10)	69.0-73.5	1.5-4.0 Na_2O 4.5-5.5 K_2O 1.5-3.0	0.15-0.5 Rb 50-125 Sr 250-500	7-15	100-165	25-75
Woolgangie (n = 24)	68.5-74.0	1.1-1.8 Na_2O 3.9-5.0 K_2O 2.6-3.8	0.2-0.5 Rb 75-175 Sr 200-450	10-35	100-220	40-110
Beetle Association						
Beetle (n = 59)	72.5-75.0	0.6-0.9 Na_2O 3.3-4.0 K_2O 4.6-5.5	0.7-4.0 (>1) Rb 175-350 Sr 75-250	35-70	110-250	80-200
Boorabbin (n = 21)	69.5-72.5	0.7-1.0 Na_2O 3.4-4.2 K_2O 4.0-5.1	0.7-1.5 Rb 150-250 Sr 140-300	35-55	200-450	100-300
Oberwyl (n = 4)	76.0-77.0	0.8-0.85 Na_2O 3.6-3.8 K_2O 4.45-4.55	>5 Rb 200-275 Sr 20-30	25-35	70-90	25-30
Yeelirrie (n = 3)	73.0-74.8	0.8-0.9 Na_2O 3.8-3.9 K_2O 4.4-4.8	<1->4 Rb 165-350 Sr 80-275	40-50	115-170	85-150
Nargalyerin (n = 13)	65.0-70.0	0.8-1.4 Na_2O 3.6-4.5 K_2O 3.25-4.5	0.4-1.25 Rb 140-250 Sr 200-400	30-50	400-700	270-400
Corriding (n = 1)	~73.5	0.8 Na_2O 3.5 K_2O 4.5	0.75 Rb 170 Sr 225	35	150	110
Westonia Association						
Red Leaf (n = 2)	~58.25	2.3 Na_2O 3.8-3.9 K_2O 1.65-1.7	0.15-0.2 Rb 85-100 Sr 500-550	~10	120-130	~60
Fitzgerald Peaks Association						
Fitzgerald Peaks (n = 29)	64.0-73.0	0.9-1.2 Na_2O 4.7-6.8 K_2O 4.2-6.0	0.2-0.5 (<<1) Rb 90-200 Sr 250-550	<10-35	10->200	60-200

Karalee Clan

Member Supersuites: Curara, Eagle Well, Karalee, Metzke, Mulline, Perrinvale, Red Leaf-2

Distribution: The major High-Ca clan that occurs dominantly marginal and external to greenstones in the central-eastern part of the Southern Cross Province, principally on the MENZIES and KALGOORLIE sheets. It occurs a range of granitoids from discrete plutons (e.g., Mulline) to variably deformed granitic complexes and gneiss (e.g., Metzke). The clan includes a number of granitic dykes that intrude greenstones and granitoids throughout the central Southern Cross Province. Lithologies include dominant biotite monzogranite and minor granodiorite.

Geochronology: One Karalee clan granitoids has been dated by SHRIMP and has an age of 2676 Ma (Day Rock granite; Nelson, 2000).

Geochemistry: The Karalee clan is characterised by moderate Total FeO, K_2O, Rb, Ce, Pb, Th, Zr contents (Figure 1, 2, 4) and is typical of 'high-LILE' clans by having higher LILE and HFSE contents and Rb/Sr ratios, and lower Sr/Sr* and *mg#* than 'low-LILE' clans (e.g., Stennet Rocks). Strontium and Ba contents of Karalee clan granitoids are variable but generally low. Karalee clan granitoids are characterised by moderately fractionated REE patterns with no Eu anomalies; HREE display slightly fractionated to 'spoon'-shaped patterns. On Spider-plots, Karalee granitoids display minor Sr-depletion and minor to moderate Y-depletion.

With the exception of slightly higher Rb contents, Karalee clan granitoids are very similar to granitoids of the Woolgangie clan. It has many similarities with the Barr Smith clan to the north.

Mineralisation: None known.

Petrogenesis: The similar geochemistry of the Karalee clan to the Goongarrie clan in the Eastern Goldfields Province, suggests very similar source rock and conditions of melting. The higher LILE and HFSE contents of 'high-LILE' clans require a more LILE-enriched component in their source. The variable Sr-depleted, Y-depleted signature suggests variable but moderate-high pressures of formation.

Tectonic and other implications: Partial meling of thickened crust is the preferred model for these granitoids, although a LILE-enriched component in the source is required.

Spear Clan

Member Supersuites: Sharman Well, Spear, Perrinvale-xenoliths

Distribution: A minor High-Ca clan that occurs sporadically throughout the south-eastern part of the Southern Cross Province, principally on the MENZIES and LAKE JOHNSTON sheets. It occurs as granitoids that are marginal (e.g., Sharman Well) or external (Spear) to the greenstone belts and form variably deformed plutons and granitic complexes. The clan includes a number of granitic xenoliths that are enclosed within other High-Ca granitoids throughout the central Southern Cross Province. Lithologies include dominant biotite monzogranite and minor granodiorite.

Geochronology: One Spear clan granitoids has been dated by SHRIMP and has an age of 2693 Ma (Perrinvale-xenolith; AGSO, unpublished data, 2000). The xenolith also contains populations of inherited zircons as old as 3.3 Ga.

Geochemistry: The Spear clan is characterised by high Total FeO, Ce, Th, Zr contents, moderate K_2O, Rb, Pb contents and variable Y contents (Figure 1, 2, 4). The clan displays geochemistry typical of 'high-LILE' clans by having higher LILE and HFSE contents and Rb/Sr ratios, and lower Sr/Sr* and *mg#* than 'low-LILE' clans (e.g., Stennet Rocks). Spear clan granitoids are characterised by high total REE contents, moderately fractionated REE patterns with small negative Eu anomalies; HREE display slightly fractionated to flatish patterns. On Spider-plots, Spear granitoids display minor Sr-depletion and minor to moderate Y-depletion. Spear clan granitoids share some similarities to granitoids of the Karalee and Woolgangie clans, but have higher high Total FeO, TiO_2, P_2O_5, Ce, Th and Zr contents. They are very similar to granitoids of the Calamity clan further to the north in the Southern Cross Province.

Mineralisation: None known.

Petrogenesis: The higher LILE and HFSE content of the Spear clan implicate a source with higher LILE and HFSE. The variable Sr-depleted, Y-depleted signature suggests variable but moderate-high pressures of formation.

Tectonic and other implications: As discussed for other 'high-LILE' clans in the Southern Cross and Eastern Goldfields Provinces, although a source region with higher LILE and HFSE is implicated.

Stennet Rocks Clan

Member Supersuites: Aerodrome, Bank East, Pietro Gneiss, Stennet Rock, Woolgangie-xenoliths

Distribution: A small-sized High-Ca clan that occurs in the southeastern part of the southern Southern Cross Province on the eastern parts of the BOORABBIN, LAKE JOHNSTON and far western NORSEMAN sheets. The clan forms a range of granitoids from deformed plutons (Stennet Rock) to granitic gneiss (e.g., Pietro Gneiss). A number of granitic xenoliths also form part of this clan. Lithologies include biotite-hornblende monzogranite, granodiorite and tonalite.

Geochronology: One SHRIMP zircon ages of 2691 Ma has been determined for the Stennet Rocks pluton (Hill et al., 1989) on the north-western part of the NORSEMAN sheet. This granitoid also includes populations of inherited zircons as old as ~3.2 Ga.

Geochemistry: The Stennet Rocks clan forms the 'low-LILE' end-member for High-Ca granitoids in the southern Southern Cross Province, with high Na_2O, *mg#* and Na_2O/K_2O, low LILE (e.g., K_2O, Rb, Pb, Sr, Th) and HFSE (Zr, REE) contents and low Rb/Sr ratios (Figures 4). Stennet Rocks clan granitoids are characterised by moderately fractionated REE patterns without Eu anomalies and low to very low HREE contents. They also are Sr-undepleted and Y-depleted as displayed on Spider-plots.

Mineralisation: None known.

Petrogenesis: The 'primitive' low-LILE geochemistry and Sr-undepleted, Y-depleted signature of the Stennet Rocks clan is very similar to the Beasley clan in the southern Eastern Goldfields Province. The geochemical characteristics are consistent with partial melting of a basaltic/amphibolitic source at high pressures. The higher *mg#* may indicate a subducted slab component in the source region rather than thickened crust.

Tectonic and other implications: The suggestion of a subducted slab component in the source has important tectonic implications for the south-eastern Southern Cross Province.

Woolgangie Clan

Member Supersuites: Gilmore, McPherson, Woolgangie

Distribution: The major High-Ca clan that occurs dominantly marginal and external to greenstones in the southern part of the Southern Cross Province, principally on the BOORABBIN, LAKE JOHNSTON and western edge of NORSEMAN sheets. It occurs a range of granitoids from discrete plutons to variably deformed granitic complexes and gneiss (e.g., Woolgangie). The clan includes a number of granitic dykes that intrude greenstones and granitoids throughout the central Southern Cross Province. Lithologies include dominant biotite monzogranite and minor granodiorite.

Geochronology: Two Woolgangie clan granitoids has been dated by SHRIMP; these have ages of 2707 Ma (Woolgangie monzogranite, suite, s/suite; Nelson, 1997) and 2656 Ma (McPherson monzogranite, suite, s/suite). The Woolgangie monzogranite also contains a population of zircons with ages of ca. 2676 Ma; these may represent distrubed grains (Nelson, 1997) or be the emplacement age of the granitoid.

Geochemistry: The Woolgangie clan is characterised by moderate Total FeO, K_2O, Rb, Ce, Pb, Th, Zr contents and generally low Ba and Sr contents (Figure 1, 2, 4). The geochemistry is typical of 'high-LILE' clans by having higher LILE and HFSE contents and Rb/Sr ratios, and lower Sr/Sr* and *mg#*, than 'low-LILE' clans (e.g., Stennet Rocks). Woolgangie clan granitoids are characterised by moderately to strongly fractionated REE patterns with minor positive to minor negative Eu anomalies. On Spider-plots, Woolgangue granitoids display slight Sr-depletion and minor to strong Y-depletion.

With the exception of slightly lower Rb contents, Woolgangie clan granitoids are very similar to granitoids of the Karalee clan.

Mineralisation: None known.

Petrogenesis: The similar geochemistry of the Woolgangie clan to the Karalee clan, and High-Ca group granitoids in general, suggests very similar source rock and conditions of melting. The higher LILE and HFSE contents of 'high-LILE' clans require a more LILE-enriched component in their source. The variable Sr-depleted, Y-depleted signature suggests variable but moderate-high pressures of formation.

Tectonic and other implications: As for the Karalee clan and other 'high-LILE' clans of the High-Ca group.

Low-Ca group, southeastern Yilgarn Craton

Member Associations: Mt Boreas Association (Eastern Goldfields Province)
Beetle Association (Southern Cross Province)

The Low-Ca group is the second largest granitoid group in the southeastern Yilgarn Craton, representing over 20 percent of all granitoids. Low-Ca granitoids are dominantly undeformed and unrecrystallised monzogranites, although deformed and gneissic Low-Ca granitoids are known from several localities. Low-Ca group granitoids form a large linear belt of granitoids along the eastern edge of the Southern Cross Province; in particular just west of the Ida lineament on the MENZIES and KALGOORLIE sheets in the Yeelirrie geophysical domain. In the Eastern Goldfields Province, Low-Ca group granitoids form small to large plutons throughout the province, including the Mungari pluton between Kalgoorlie and Coolgardie and some of the dykes as well as the Western Granite at the Chalice deposit. Three clans have been characterised in the Eastern Goldfields Province on the basis of geochemistry and regional distribution, whereas five clans have been delineated in the Southern Cross Province. The Corriding clan is represented by only one pluton and has been fitted into the Low-Ca group for convenience. A number of samples with probable Low-Ca affiliation have not been assigned to a particular clan and are not discussed in this report.

Geochronology on Low-Ca granitoids in the southern Eastern Goldfields Province indicate a relatively narrow range in ages from ca. 2.655 to ?2.62 Ga (Table 4). Zircon inheritance is common and varies from slightly older than the emplacement age of the host pluton to older than 2.9 Ga in some Nulerie clan granitoids in the eastern part of the Eastern Goldfields Province. In the Southern Cross Province, Low-Ca group granitoids have ages ranging from 2.68 to 2.625 Ga (Table 5), with most between 2645 and 2630 Ma. Zircon inheritance in Low-Ca granitoids is widespread and varies from slightly older than the emplacement age of the pluton to older than 3.5 Ga in some Low-Ca granitoids from the northern Southern Cross Province.

The geochemical characteristics for Low-Ca granitoids have been documented by Champion & Sheraton (1997) and several reports provided as part of this AMIRA project and will be only briefly summarised. Low-Ca granites are characterised by high LILE (K_2O, Rb, Pb, Th, U) and HFSE (REE, Y, Zr) and low Al_2O_3, Na_2O and CaO contents, as well as high Rb/Sr and very low Sr/Sr* ratios (Figure 1, 2, 3). The majority of Low-Ca granitoids have silica contents over 70 wt% SiO_2, however, work as part of the AMIRA P482 project has extended this compositional range down to about 65 wt SiO_2. Compared to High-Ca granitoids, Rb, Pb, Th and U contents are higher, Ba is similar and Sr generally lower, for a given SiO2 content. Like the High-Ca granitoids, Low-Ca granitoids also exhibit a range in LILE and HFSE contents. The vast majority of Low-Ca granitoids are also characterised by fractionated REE patterns and large negative Eu anomalies. On Spiderplots, Low-Ca granitoids typically display strongly Sr-depleted and Y-undepleted signatures; the range of Y contents, however, does result in minor but variable Y-depletion in some suites. Systematic variations in Rb/Sr and K/Rb suggest that crystal fractionation processes were significantly more important than in High-Ca granitoids.

Constraints can be placed on the petrogenesis of the Low-Ca granitoids by their geochemistry, Nd and Pb isotopic compositions and presence and age of inherited zircons. The Low-Ca granitoids are characterised by a range of Nd model ages. Low-Ca granitoids in the Eastern Goldfields Province have Nd model ages ranging from 2700 Ma to 2900 Ma, whereas Low-Ca granitoids in the

Southern Cross Province range from about 2900 Ma to 3050 Ma (see Champion & Sheraton, 1997; Fletcher & McNaughton, this report). This is generally interpreted to indicate that the Low-Ca granitoids in the Southern Cross Province were sourced from an older protolith than Low-Ca granitoids in the Eastern Goldfields Province.

The Nd and Pb isotope data clearly implicates reworked crust, consistent with the broadly silica-rich, potassic (high K and LILE contents) and Sr-depleted nature of the Low-Ca group granitoids. Champion & Sheraton (1997) indicate that the similar trace element patterns of the Low-Ca granitoids can be accurately modelled by batch melting of a protolith compositionally similar to the mafic end members of the High-Ca group. However, the generally similar SiO_2, TiO_2, Total FeO and P_2O_5 contents suggest a source more mafic that the High-Ca granitoids. Differences in epsilon Nd for High-Ca and Low-Ca granitoids in the same province also suggest isotopically distinct sources. As suggested by Champion & Sheraton (1997), a possible source candidate are Archean TTG-suite rocks (e.g., tonalitic composition) that are found in Archean terranes throughout the world. The strong negative Eu anomalies, and Sr-depleted and mostly Y-undepleted signature indicate that the Low-Ca granites were generated at moderate pressures and, therefore, at mid to lower-crustal levels (mostly <35 km).

The preferred model for the generation of the Low-Ca granitoids is partial melting at high temperatures and moderate pressures of a tonalitic pre-existing crust. The moderate to high HFSE suggests some affinities with A-type granitoids, and may indicate an extensional environment for the Low-Ca granitoids. The Low-Ca granitoids are dominantly emplaced after 2655 Ma and after cessation of the majority of High-Ca and Mafic group magmatism. The other granitoid group emplaced in the southern Eastern Goldfields Province after this period was Syenitic group granitoids. These are generally thought to have been emplaced in an extensional environment and this supports the suggestion of an overall extensional environment across the Yilgarn Craton during Low-Ca group magmatism. The presence of the Low-Ca granites and Syenitic rocks may indicate a change in tectonic environment from an overall compressional regime during High-Ca group magmatism to an extensional regime during Low-Ca group magmatism.

The distribution, age constraints, geochemical characteristics and relationship to mineralisation are summarised for each clan; clans are presented in alphabetical order. General petrogenetic models for the Low-Ca granitoids have been summarised above; however, specific petrogenetic implications for individual clans are also highlighted below.

Clans with the Mt Boreas Association, Eastern Goldfields Province

The Mt Boreas Association is the second-most common granitoid grouping in the Eastern Goldfields Province. In the southern Eastern Goldfields Province, it constitutes about 10 to 15 percent of granitoids. Three clans have been delineated on the basis of geographical distribution and geochemical characteristics. The clans (Mt Boreas, Mungari and Nulerie) are geographically restricted. The Mt Boreas and Nulerie clans are also present in the northern Eastern Goldfields Province and are described by Champion (this report). Individual clans of the Mt Boreas Association are characterised by specific geochemical characteristics; Table 6 summarises the abundances of selected elements for the clans.

Mt Boreas Clan

Member Supersuites: Cock Robin, Donkey Rocks, Galah, Mars Bore

Distribution: A major Low-Ca clan in the central and northern Eastern Goldfields Province. It includes the type-locality (Mt Boreas) for Low-Ca granitoids in the Eastern Goldfields Province. In the southeastern Yilgarn, Mt Boreas clan granitoids are localised mainly on the eastern half of MENZIES and western half of EDJUDINA sheets. Mt Boreas granitoids range from small largely deformed plutons to large granitic complexes (e.g., Donkey Rocks); undeformed varieties predominate. Lithologies include biotite-, muscovite- and garnet-bearing monzogranite and syenogranite; both seriate and porphyritic varieties are known.

Geochronology: Only one SHRIMP age is available for the Mt Boreas clan. An age of 2651 Ma was obtained for the Mount Eureka monzogranite (Nelson, 1998) on the KINGSTON sheet, in the far north of the Eastern Goldfields Provnce. No ages are available for Mt Boreas granitoids in the southern Eastern Goldfields Province.

Geochemistry: The Mt Boreas clan characterised by typical Low-Ca group chemistry, including high LILE (K_2O, Rb, Pb, Th, U) and HFSE (REE, Y, Zr) contents (Figures 1, 2, 3). Mt Boreas clan granitoids are characterised by moderately fractionated LREE and slightly fractionated HREE patterns with large negative Eu anomalies, as well as strong Sr-depletion and Y-undepletion to slight Y-depletion on Spider-plots (Figure 3). The Mt Boreas clan has many similarities to the Mungari clan in the southern Eastern Goldfields Province, and the Beetle clan in the southern Southern Cross Province. These two clans have higher Rb, Pb, Th, Y and Zr (Figure 1, 2) when compared with the Nulerie clan. However, like the Nulerie clan, the Mt Boreas clan falls into the lower-LILE, lower-HFSE end of the Low-Ca compositional range when compared with the Grant Duff clan present in the northern Eastern Goldfields Province.

Mineralisation: None known.

Petrogenesis: The petrogenesis of the Mt Boreas clan is probably as discussed for the Low-Ca granitoids in general. The Mt Boreas and Mungari clans have LILE and HFSE contents higher than for the Nulerie clan but are still at the lower end of the spectrum for Low-Ca group granitoids. This may indicate slightly lower degrees of partial melting or a slightly more LILE-enriched source for the Mt Boreas and Mungari clans. At the high silica-end of the Mt Boreas clan, significant crystal fractionation is evident.

Tectonic implications: As discussed for Low-Ca group granitoids.

Mungari Clan

Member Supersuites: Bullabulling, Chalice, Chalice-2, Comet Hill, Mungari, Scotia, Talbot, Widgiemooltha

Distribution: The Mungari clan is the dominant Low-Ca clan in the south-western part of the southern Eastern Goldfields Province. Mungari clan granitoids occur as plutons internal to greenstones (e.g., Bullabulling, Mungari) as well as a series of granitoids, possibly intruded as sheets, marginal or external to the greenstone belts (e.g., Scotia). Lithologies are dominantly biotite monzogranite with minor syenogranite.

Geochronology: Although several Mungari clan granitoids have been dated by the SHRIMP technique, only imprecise ages of ca. 2630 to 2620 Ma are available for three granitoids. Three unsuccessful attempts have been made to date the Mungari granitoid; the only published age of 2603±19 Ma (Hill et al., 1992) is interpreted to be too young and not date granitoid emplacement.

Geochemistry: The Mungari clan characterised by typical Low-Ca group chemistry, including high LILE (K_2O, Rb, Pb, Th, U) and HFSE (REE, Y, Zr) contents (Figures 1, 2, 3). Mungari clan granitoids are further characterised by moderately fractionated LREE and slightly fractionated HREE patterns with moderate negative Eu anomalies, as well as strong Sr-depletion and Y-undepletion to slight Y-depletion on Spider-plots. The Mungari clan has many similarities to the Mt Boreas clan in the southern Eastern Goldfields Province, and the Beetle clan in the southern Southern Cross Province. These two clans have higher Rb, Pb, Th, Y and Zr (Figure 1, 2) when compared with the Nulerie clan. However, like the Nulerie clan, the Mungari clan falls into the lower-LILE, lower-HFSE end of the Low-Ca compositional range when compared with the Grant Duff clan present in the northern Eastern Goldfields Province.

Mineralisation: Gold mineralisation is spatially associated with the Chalice and Chalice-2 supersuites at the Chalice deposit. The Bullabulling intrus ion is spatially associated with gold mineralisation at Bullabulling.

Petrogenesis: The petrogenesis of the Mungari clan is probably as discussed for the Low-Ca granitoids in general. The Mt Boreas and Mungari clans have LILE and HFSE contents higher than for the Nulerie clan but are still at the lower end of the spectrum for Low-Ca group granitoids. This may indicate slightly lower degrees of partial melting or a slightly more LILE-enriched source for the Mt Boreas and Mungari clans. At the high silica-end of the Mungari clan, significant crystal fractionation is evident.

Tectonic implications: As discussed for Low-Ca group granitoids.

Nulerie Clan

Member Supersuites: Elora, Irwin Hills

Distribution: The Nulerie clan is a small to mdeium-sized clan that occurs as a series of plutons, granitic gneiss complexes and dykes external to the greenstone belts on the eastern side of EDJUDINA and western part of MINIGWAL. It also extends into the northern Eastern Goldfields Province, as described by Champion (this report).

Geochronology: Four ages are available for Nulerie clan granitoids. These are all for granitoids in the northern Eastern Goldfields Province and range from 2654 to 2647 Ma (Nelson, 1997, 1998; L.Black, written communication, 2000); all of the ages are within error of each other.

Geochemistry: The Nulerie clan characterised by high LILE (K_2O, Rb, Pb, Th, U) and HFSE (LREE, HREE, Y, Zr) contents (Figures 1, 2, 3) that are typical for Low-Ca group granitoids. The clan falls into the lower-LILE, lower-HFSE end of the Low-Ca compositional range, with lower Rb, Pb, Th, Y, and Zr variable to lower K_2O, Pb and Nb, and variable to higher Na_2O, CaO and Ba, relative to the Mt Boreas and Mungari clans (Figure 1, 2). Nulerie clan granitoids are further characterised by moderately fractionated LREE and slightly fractionated HREE patterns with moderate negative Eu anomalies, as well as moderate Sr-depletion and moderate Y-depletion on Spider-plots. The Nulerie clan has many similarities to the Meredith clan in the northern Eastern Goldfields. The Nulerie clan clearly contains higher LILE and HFSE contents than 'high-LILE' clans of the High-Ca group.

Mineralisation: None known, although some of the Irwin Hills granitoids contain minor quartz veining and associated wallrock alteration.

Petrogenesis: The petrogenesis of the Nulerie clan is probably as discussed for the Low-Ca granitoids in general. The Nulerie clan has LILE and HFSE contents at the lower end of the spectrum for Low-Ca group granitoids and this may result from either a greater degree of partial melting or a LILE source that was not as enriched.

Tectonic implications: As discussed for Low-Ca group granitoids.

Clans within the Beetle Association, Southern Cross Province

The Beetle Association is the second-most common granitoid grouping in the Southern Cross Province, and constitutes over 30 percent of granitoids in the southeastern Southern Cross Province. In the eastern part of the Southern Cross Province on the MENZIES and KALGOORLIE sheets, Low-Ca granitoids constitute up to 50 percent of the granitoids. Five clans have been delineated on the basis of geographical distribution and geochemical characteristics. The dominant clan in the Southern Cross Province is the Beetle clan; other clans are subordinate in size and generally geographically restricted. Two clans (Boorabbin, Nargalyerin) form moderate-sized clans that are represented over much of the southern Southern Cross Province, whereas the Yeelirrie clan is restricted to the northern half of the MENZIES sheet. The Oberwyl clan is represented by a single unit along the boundary of the Southern Cross Province with the Eastern Goldfields Province, at the top of the MENZIES sheet. Another clan, Corriding, represented by a single unit, is compositionally intermediate between Low-Ca and High-Ca granitoids, and is included in the Beetle Association for the purposes of reporting. Individual clans of the Beetle Association are characterised by specific geochemical characteristics; Table 7 summarises the abundances of selected elements for the clans.

Beetle Clan

Member Supersuites: Beetle, Holland, Perry, Rundle, Banks, Bromus, Maggie Hays, Yerdanie, Yowie

Distribution: The Beetle clan is the dominant Low-Ca clan in the southern Southern Cross Province. Forms large granitoid bodies along the eastern edge of the Southern Cross Province in proximity to the Ida Lineament; constitutes up to 50 percent of granitoids west of the Ida Lineament on the MENZIES and KALGOORLIE sheets. The Ularring and Clark Wel monzogranites, plutons internal to the greenstone belt along the Ida Lineament, are also members of this clan. Most of these granitoid bodies are characterised by high magnetisation as displayed on aeromagnetic images. Most of the granites are largely undeformed, although some are foliated and even gneiss in places. Lithologies are syenogranite and monzogranite reflecting the potassic nature of the rocks; both seriate and porphyritic varieties are common.

Geochronology: Four granitoids belonging to the Beetle clan have been dated by SHRIMP; ages range from 2660 to 2630 Ma. Two plutons (Rundle granite, Tom Rock granite) have ages of ca. 2660 Ma, whereas two plutons (Clark Well monzogranite, Ularring monzogranite) have ages of 2640 Ma and 2632 Ma, respectively. All four granitoids are member of the Rundle supersuite. Some of the plutons contain inherited zircons with ages ranging from ~2700 to older than 2800 Ma.

Geochemistry: Geochemically the group is characterised by typical Low-Ca characteristics with high K_2O, Rb, Rb/Sr, Pb, Th, Zr, LREE, Y and low CaO, Na_2O, Na_2O/K_2O, Sr (Table 3; Figures 1, 2). Beetle clan granitoids are further characterised by moderately fractionated LREE and slightly fractionated HREE patterns with moderate to large negative Eu anomalies, as well as moderate to strong Sr-depletion and Y-undepletion to moderate Y-depletion on Spider-plots. The Beetle clan has many similarities to the Mt Boreas and Mungari clans in the southern Eastern Goldfields Province, although the Beetle clan has slightly higher Th and Zr and lower Rb contents. It is also similar to the Yeelirrie clan, although in the northern Southern Cross Province, this clan has elevated LILE and HFSE contents. However, like the Mt Boreas and Mungari clans, the Beetle clan falls into the lower-LILE, lower-HFSE end of the Low-Ca compositional range when compared with the Grant Duff clan present in the northern Eastern Goldfields Province.

Mineralisation: None known; although pegmatites with tourmaline and minor rare metals known from elsewhere in SCP.

Petrogenesis: The petrogenesis of the Beetle clan is probably as discussed for the Low-Ca granitoids in general. High silica contents, relatively low CaO and Na_2O contents, high Th, U, Pb and K_2O contents, fractionated REE patterns with pronounced negative Eu anomalies, Sr-depletion, Y-undepletion are consistent with a source where plagioclase was stable indicating mid- to lower-crustal pressures. Geochemistry is consistent with partial melting in the mid-lower crust at moderate pressures from source rocks of intermediate composition (e.g., tonalite). Pronounced negative E_{Nd}, the presence of inherited zircons are consistent with melting of pre-existing old crust.

Tectonic implications: As discussed for Low-Ca granitoids in general.

Boorabbin Clan

Member Supersuites: Boorabbin, Hospital, Nearanging, Walling Rock

Distribution: The Boorabbin clan is a moderate sized clan in the southern Southern Cross Province. It forms a variety of granitoid bodies, including plutons and dykes along the eastern edge of the Province in proximity to the Ida Lineament. The clan includes the Hospital and Walling Rock granitoids, as well as the pluton at the Boorabbin quarry. Most of these granitoid bodies are characterised by high magnetisation. Most of the granites are largely undeformed. Lithologies are syenogranite and monzogranite reflecting the potassic nature of the rocks. The Boorabbin granitoid contains unusual biotite-rich 'oikocrysts' that are interpreted to have formed late during the magmatic history of the granitoid.

Geochronology: Three Boorabbin clan granitoids have been dated by SHRIMP and have ages of that are within error; Hospital – 2631 Ma, Scorpion – 2633 Ma and Walling Rock – 2633 Ma. Inherited zircons with ages of ca. 2675 Ma and >2760 Ma are present in the Scorpion and Walling Rocks granitoids. Field relations support the younger ages for the Boorabbin clan granitoids.

Geochemistry: Geochemically the Boorabbin clan is characterised by lower silica and higher Zr, LREE, TiO_2 and variable Y contents relative to Beetle clan (Table 7; Figures 1, 2). High silica end members of this clan overlap with the Beetle and other Low-Ca clans (e.g., Nulerie). Boorabbin clan granitoids are also characterised by a high total REE content, moderately fractionated LREE and slightly fractionated HREE patterns with moderate negative Eu anomalies, as well as moderate Sr-depletion and variable Y (Y-enriched to moderately Y-depleted) on Spider-plots. The Boorabbin clan has some similarities to the Nulerie clan in the southern Eastern Goldfields Province, but has higher Pb, Th, Y and Zr and lower Rb contents. It is also similar to the Nargalyerin clan, although this clan has lower silica contents and even higher LILE and HFSE contents. However, like the Beetle clan, the Boorabbin clan falls into the lower-LILE, lower-HFSE end of the Low-Ca compositional range when compared with the Grant Duff clan present in the northern Eastern Goldfields Province.

Mineralisation: None known; although pegmatites with tourmaline crosscut the Boorabbin type-locality at Boorabbin quarry. The biotite-rich 'oikocrysts' in the Boorabbin pluton contain (sub)hedral quartz and feldspar grains that contain low-salinity, carbonic (H_2O-CO_2-CH_4) fluid inclusions, similar to the mineralising fluids inferred for many Archean orogenic gold deposits.

Petrogenesis: The petrogenesis of the Boorabbin clan is probably as discussed for the Low-Ca granitoids in general. The high LREE, Pb, Th, Y and Zr contents, fractionated REE patterns with pronounced negative Eu anomalies, Sr-depletion, and variable Y-undepletion are consistent with a mixed LILE-enriched source where plagioclase was stable indicating mid- to lower-crustal pressures. The lower silica contents suggest either a larger degree of partial melting or a more mafic source rock. However, to maintain and increase the LILE and HFSE contents in the Boorabbin clan granitoids relative to the Beetle clan, a more mafic source also would need to be more LILE-enriched than inferred for the higher silica clans. The higher Zr contents also implies high temperature melting conditions were attained.

Tectonic implications: The age of the Boorabbin clan granitoids is younger than that established for the Beetle clan. The lower silica content of the Boorabbin clan suggests that the source became more mafic over time. Higher percentage partial melting is also implied.

Nargalyerin Clan

Supersuites: Wargangering; also Tank No. 28 and Lake Hope

Distribution: The Nargalyerin clan forms a number of small plutons and dykes throughout the southern Southern Cross Province; in particular, granitoid bodies along the eastern edge of the Province in proximity to the Ida Lineament. They also occur as xenoliths within other Low-Ca granitoids (e.g., Wargangering-xenolith unit). Most of these granitoid bodies are characterised by very high magnetisation. Most of the granites are largely undeformed. Lithologies are syenogranite and monzogranite reflecting the potassic nature of the rocks; some are amphibole-bearing in places. These granitoids typically contain appreciable allanite and/or titanite as accessory phases.

Geochronology: Seven ages are available for the Nargalyerin clan and these range from 2646 Ma (Wargangering-dyke phase) to 2623 Ma (Tank No.28 granite). However, only two of these ages are for Nargalyerin clan granitoids in the southeastern Southern Cross Province. A monzogranite in the Woolgangie area, inferred to be a member of the Nargalyerin clan on the basis of containing very high LREE and Zr contents, was dated at 2645 Ma by Hill et al. (1992). Qiu & McNaughton (1999) present U-Pb zircon ages of 2632 and 2637 Ma for two samples from the Nargalyerin type-locality on the SOUTHERN CROSS map sheet.

Geochemistry: Geochemically the group is characterised by low silica contents (mostly 65-71% SiO_2) relative to other Low-Ca clans as well as low CaO, Na_2O, Sr, moderate to high K_2O, Rb, Th, and high Zr, LREE and Y contents (Table 7; Figures 1, 2). The high to very high Zr and LREE combined with low SiO_2 is especially diagnostic. Nargalyerin clan granitoids are also characterised by a high total REE content, moderately fractionated LREE and slightly fractionated HREE patterns with moderate negative Eu anomalies, as well as moderate Sr-depletion and variable Y (Y-enriched to moderately Y-depleted) on Spider-plots. It is quite feasible that the Nargalyerin clan granitoids represent mafic variants, perhaps cumulates, of the Beetle Association with which it shares many features.

Mineralisation: None known.

Petrogenesis: The petrogenesis of the Nargalyerin clan is probably as discussed for the Low-Ca granitoids in general. The high LREE, Pb, Th, Y and Zr contents, fractionated REE patterns with pronounced negative Eu anomalies, Sr-depletion, and variable Y-undepletion are consistent with a mixed LILE-enriched source where plagioclase was stable indicating mid- to lower-crustal pressures. The high HFSE contents also imply that high temperature melting conditions were attained. The lower silica contents suggest either a larger degree of partial melting or a more mafic source rock. However, to maintain and increase the LILE and HFSE contents in the Nargalyerin clan granitoids relative to the Beetle or even Boorabbin clans, a source also would need to be more LILE-enriched than inferred for the higher silica clans if a larger degree of melting was attained.

Tectonic implications: The ages of the Nargalyerin clan granitoids overlap or are younger than those established for the Beetle and Boorabbin clans. The low silica content of the Nargalyerin clan requires higher temperatures were attained or a higher percentage partial melt; again the latter suggestion requires a source to be increasingly LILE-enriched over time.

Oberwyl Clan

Supersuites: Oberwyl

Distribution: The Oberwyl clan is a very minor clan comprising one pluton on the eastern edge of the Southern Cross Province. The pluton is a strongly foliated and lineated granitoid that is marginal to the greenstone belt in proximity to the Ida Lineament on the MENZIES sheet. The granitoid body is characterised by moderate magnetisation. The granitoid is very felsic with mafic minerals forming less than 7 modal percent.

Geochronology: None available.

Geochemistry: Geochemically the Oberwyl clan is characterised by very high silica contents as well as high K_2O, Rb, Rb/Sr, Pb, Th, Zr, LREE, Y and low CaO, Na_2O, Na_2O/K_2O, Sr (Table 7). The silica contents clearly distinguish this minor clan from other clans in the Beetle Association. The Oberwyl clan is further characterised by a slightly fractionated to flat LREE and flat HREE pattern with large negative Eu anomalies, and strong Sr-depletion and Y-undepletion on Spider-plots. The Oberwyl clan has some similarities with other Low-Ca clans, but also shares similarities with silica-rich High-Ca group granitoids (e.g., Ajax and Niagara clans). It has been placed in the Low-Ca group on the basis of its overall geochemistry, but may be a fractionated High-Ca group member.

Mineralisation: None known.

Petrogenesis: The petrogenesis of the Oberwyl clan is probably as discussed for the Low-Ca granitoids in general. The high silica contents, relatively low CaO and Na_2O contents, high Th, U, Pb and K_2O contents, REE patterns with pronounced negative Eu anomalies, Sr-depletion, Y-undepletion are consistent with a source where plagioclase was stable indicating mid - to lower-crustal pressures. It probably represents a low percentage partial melt of an intermediate source.

Tectonic implications: As discussed for Low-Ca granitoids in general.

Yeelirrie Clan

Supersuites: Sunday Bore, Yendang

Distribution: A major Low-Ca clan in the northern and central Southern Cross Province. It forms large granitoid bodies that are largely external to the greenstone belt in proximity to the Ida Lineament. In the southern Southern Cross Province, it forms several units on the northern half of the MENZIES sheet.

Geochronology: Four SHRIMP ages are available for granitoids of the Yeelirrie clan; the ages range from 2682 Ma to 2638 Ma. Three ages are for Yeelirrie clan granitoids in the far northern Southern Cross Province around the Gum Creek. The fourth age of 2653 Ma is from the Wallaby Knob granitoid on the LEONORA sheet (L. Black, written communication, 2000).

Geochemistry: Geochemically the group is characterised by typical Low-Ca characteristics with high K_2O, Rb, Rb/Sr, Pb, Th, Zr, LREE, Y and low CaO, Na_2O, Na_2O/K_2O, Sr (Table 3; Figures 1, 2). Yeelirrie clan granitoids are further characterised by moderately fractionated LREE and slightly fractionated HREE patterns with moderate to large negative Eu anomalies, as well as moderate Sr-depletion and variable Y-depletion on Spider-plots. The Yeelirrie clan has many similarities to the Beetle clan, although it has slightly elevated LILE and HFSE contents.

Mineralisation: None known; although calcrete U mineralisation at Yeelirrie may be indirectly related.

Petrogenesis: The petrogenesis of the Yeelirrie clan is probably as discussed for the Low-Ca granitoids in general.

Tectonic implications: As discussed for Low-Ca granitoids in general.

Corriding Clan

Supersuites: Corriding

Distribution: One unit localised within the central part of the Southern Cross Province.

Geochronology: None available..

Geochemistry: Geochemically Corriding is intermediate between Low-Ca and High-Ca granitoids and is difficult to assign to either group. It has been tentatively assigned to the Low-Ca group on the basis of its relative high LREE, Rb, Pb and Th contents and Na_2O/K_2O ratio. It is characterised by moderately fractionated REE with a medium negative Eu anomaly and also slight to moderate Sr-depletion and moderate Y-depletion.

Mineralisation: None known.

Petrogenesis: Geochemistry cannot discriminate between either a Low-Ca or a High-Ca petrogenetic model for the Corriding suite.

Tectonic implications: None.

Mafic group, southeastern Yilgarn Craton

Member Associations: Granny Smith Association (Eastern Goldfields Province)
Westonia Association (Southern Cross Province)

The Mafic group is an important granitic group in the southeastern Yilgarn Craton and represents up to 10 to 15 percent of all granitoids by surface area, but perhaps over 50 percent of the compositional spectrum of Yilgarn granitoids. The majority of Mafic group granitoids form as small plutons or porphyry dykes internal or at the margins of greenstone belts. In many cases, in particular the porphyry dyke swarms, they have been deformed by later deformation. The main occurrences of Mafic group granitoids in the southern Eastern Goldfields Province are:

- a diverse range of porphyries and stocks are localised along most of the major deformation zones (e.g., Zuleika, Bardoc, Boulder-Lefroy),
- a diverse range of plutons (e.g., Liberty, Depot, Golden Cities etc.) internal or marginal to the greenstone belts in the Kambalda-Mt Pleasant region (Kalgoorlie terrane),
- a diverse range of plutons (e.g., Porphyry etc.) internal or marginal to the greenstone belts in the Edjudina-Laverton region (?Laverton Tectonic zone),
- small plutons and porphyries in the Norseman district.

Six clans have been delineated on the basis of geochemistry and geographic distribution in the southern Eastern Goldfields Province. In the southern Eastern Goldfields Province, they comprise two widely distributed clans (Kanowna Belle, Granny Smith) and four small clans that are geographically restricted. The Victory and Kambalda clans are similar and are geographically restricted to these locations; the New Celebration clan is characterised by distinct geochemistry and is also geographically restricted to around the New Celebration area. The last clan, Dinky Boys, is a small clan in the Norseman district. A number of relatively mafic porphyry samples have also been assigned to another clan (Mafic unassigned clan); these are not discussed in this report. There is also a series of granitic xenoliths from a number of granitoids from throughout the Eastern Goldfields Province. This compositionally diverse clan (Cement clan) has been assigned at its own association (Xenolith association) and will not be discussed in this report.

In the Southern Cross Province, only one very small clan of Mafic group granitoids has been identified and this clan (Red Leaf) is localised along the Ida Lineament at the boundary of the Southern Cross and Eastern Goldfields Provinces. This clan has been kept within the Southern Cross Province for reporting purposes, but may be a supersuite within the Kanowna-Belle clan.

A large number of Mafic group granitoids in the Eastern Goldfields Province have been dated by robust techniques. This is because many Mafic group granitoids either host or are spatially associated with gold mineralisation (e.g., Porphyry, Golden Cities, Bonnievale, Kambalda, Kanowna-Belle, etc.) and have attracted the interest of researchers. The majority of recorded ages for the Mafic group cluster around 2665 Ma (especially within the Granny Smith clan; Table 4). The range for Mafic group granitoids varies from ca. 2694 Ma (Kanowna-Belle porphyry, Wang et al., in press; Krapez et al., 2000) to ca. 2648 Ma (Liberty granodiorite, Kent, 1994). An age of 2613 Ma for the Four Mile Hill porphyry dyke in the Kanowna district (Nelson, 1995) is interpreted to date a disturbance event rather than the emplacement age of the dyke.

Cassidy et al. (1991), Champion & Sheraton (1997) and Champion (1997) have discussed the geochemical characteristics of many of the Mafic group granitoids. Champion & Sheraton (1997) defined the group as a variety of granitoid suites and supersuites largely characterised by their lower (and variable) silica contents (55-70 wt%) and variable LILE and LREE content (Figures 5, 6, 7). Despite the variation in LILE and LREE, the majority of Mafic group granitoids are Sr-undepleted. Y contents generally decreases with increasing silica, from Y-undepleted levels becoming Y-depleted. All Mafic group granites show strong negative Nb, Ti and P anomalies on Spider-plots. Sr/Sr* is mainly around 1.0 with little correlation with silica contents. Most display fractionated REE patterns with variable HREE fractionation and no or negligible Eu anomalies. At the high silica end, some Mafic group granitoids trend towards High-Ca group compositions.

Champion & Cassidy (1998) further studied the Mafic group, and subdivided them into two broad subtypes based on LILE and HFSE contents; the 'high-LILE' and 'low-LILE' end-member subtypes are called the Granny Smith and Kanowna-Belle clans, respectively. The approximate dividing line for these two clans is the same as the arbitrary boundary used to divide the 'low-LILE' and 'high-LILE' members of the High-Ca group (Figure 3, 6). The high LILE and LREE character of the Granny Smith clan extends to the most mafic end-members of the clan, clearly indicating the fundamental differences with the Kanowna-Belle clan. Epsilon Nd values are similar for both clans (Champion & Sheraton, 1997; Fletcher & McNaughton, this report). The other clans in the southern Eastern Goldfields Province have compositions transitional to the 'high-LILE' and 'low-LILE' end-member clans or have distinct chemical characteristics (e.g., New Celebration).

The Mafic group granitoids have been the best studied group of granitoids in the Eastern Goldfields Province (e.g., Witt and Swager, 1989; Cassidy et al., 1991; Wyborn, 1993; Champion & Sheraton, 1993, 1997; Champion & Cassidy, 1998). They form a chemically diverse group and may have been derived by a variety of processes and from a variety of sources. Most petrogenetic models involve crustal protoliths with or without a mantle component. The variation in the LILE and LREE contents, evident in even the most mafic end-members, requires at least two separate components to produce the Granny Smith and Kanowna-Belle clans. A direct mantle contribution is probable for at least some of the Mafic group suites (e.g., Lawlers tonalite). Champion (1997) suggests two such sources, namely a mafic 'basaltic' source, similar to that proposed for the High-Ca granites, and a more mafic, perhaps mantle-derived, LILE-rich source component. The similarity of the silica-rich end-members of the Kanowna-Belle clan and the High-Ca group supports a common origin at least for some suites. The Ba and Sr-enriched New Celebration clan is in the same region as the Ba and Sr-enriched Parker Hills (High-Ca) clan; however, with the exception of Ba and Sr, these clans have closer similarities with 'Low-LILE' clans of both the Mafic group and the High-Ca group. An enriched source in Ba and Sr is required for these clans; perhaps interaction with lamprophyric magmas as suggested by Perring (1989) may provide these LILE, without increasing the other LILE. The origin of the High-LILE clans (e.g., Granny Smith) is more equivocal. Champion (this report) suggests that Syenitic group magmatism is a possible source of, at least part of, the LILE and LREE enrichment in the Granny Smith clan; such a model may explain the some of the supersuites (e.g., Porphyry).

Tectonic models for the southern Eastern Goldfields Province granitoids range from rift-related magmatism to arc- and collisional-related magmatism. The diverse range of Mafic group granitoids requires at least two and probably three sources. The majority of low-LILE (Kanowna-Belle clan) Mafic group granitoids were emplaced prior to emplacement of either high-LILE (Granny Smith clan) or New Celebration clan Mafic group granitoids. Granny Smith clan granitoids were dominantly emplaced over a short time period at ca. 2665-2660 Ma. This was also the time of emplacement of the Parker Hills clan High-Ca group granitoids as well as the Erayinia clan Syenitic group granitoids, indicating a range of high-LILE magmatism throughout the southern Eastern Goldfields Province at this time.

Clans within the Granny Smith Association, Eastern Goldfields Province

Granny Smith Association granitoids constitute a metallogenically and petrogenetically important group of granitoids in the southern Eastern Goldfields Province. Six clans have been delineated on the basis of geochemistry and geographic distribution in the southern Eastern Goldfields Province. The main two clans (Kanowna-Belle, Granny Smith) are lithologically and compositionally diverse and form a variety of undeformed and deformed plutons and series of porphyry dykes. They are geographically widespread, however, separate supersuites and suites are geographically restricted. The Victory and Kambalda clans are similar and are geographically restricted to these locations; the New Celebration clan is characterised by distinct geochemistry and is also geographically restricted to around the New Celebration area. The Dinky Boys clan is a small clan in the Norseman district.

There is also a number of mafic porphyry dykes from several localities in the Kambalda-Kalgoorlie-Mt Pleasant region. These have been assigned to a particular clan (Mafic unassigned clan), but their composition is diverse and they are not discussed in this report. There is also a series of granitic xenoliths from a number of granitoids from throughout the Eastern Goldfields Province. This compositionally diverse clan (Cement clan) has been assigned at its own association (Xenolith association) and will not be discussed in this report.

Individual clans of the Granny Smith Association are characterised by specific geochemical characteristics; Table 8 summarises the abundances of selected elements for the clans. The distribution, age constraints, geochemical characteristics and relationship to mineralisation are summarised for each clan; clans are presented in alphabetical order. General petrogenetic models for the High-Ca granitoids have been summarised above; however, specific petrogenetic implications for individual clans are also highlighted below.

Table 8. Summarised abundances of selected elements for the various clans of the Granny Smith and Gilgarna Associations of the Eastern Goldfields Province. Number in brackets refers to number of geochemical analyses used in calculations.

Group	SiO_2	Na_2O/K_2O	Rb/Sr	Th	Zr	Ce
Granny Smith Association						
Dinky Boys (n = 7)	72.0-73.0	2.1-3.1 Na_2O 4.7-5.2 K_2O 1.75-2.2	0.06-0.1 Rb 40-55 Sr 600-750	5-7	110-120	35-40
Granny Smith (n = 76)	62.5-70.5	1.0-2.5 Na_2O 4.0-5.4 K_2O 2.0-4.5	<0.1-0.15 Rb 60-125 Sr 500-1400	8-16	125-250	70-170
Kambalda (n = 15)	68.0-72.0	2.0-4.0 Na_2O 5.0-6.1 K_2O 1.5-3.0	0.05-0.1 Rb 40-70 Sr 600-1000	6-15	100-160	30-100
Kanowna-Belle (n = 104)	60.0-72.5	1.5->4.0 Na_2O 3.5->6.0 K_2O <1.5-3.0	<0.1-0.2 Rb 25-85 Sr 150-900	<10	100-175	20-100
New Celebration (n = 16)	68.0-71.5	1.75->10 Na_2O 5.5->7.0 K_2O <1.0-3.0	0.01-<0.1 Rb 20-75 Sr 700-1300	8-13	100-150	40-120
Mafic unassigned (n = 18)	50.0-57.0	1.0->5.0 Na_2O 2.5-6.5 K_2O 1.0-3.0	0.05-0.4 Rb 40-100 Sr 150-750	5-15	100-180	50-170
Victory (n = 27)	59.5-72.5	2.0->5.0 Na_2O 4.0-6.5 K_2O 0.70-2.25	0.01-0.1 Rb <10-75 Sr 350-1150	5-12	90-160	40-135
Gilgarna Association						
Erayinia (n = 37)	65.5-70.5	0.9-1.4 Na_2O 5.0-6.0 K_2O 4.0-6.0	0.1-0.2 Rb 100-200 Sr 800-1200	10-20	150-300	50-175
Gilgarna (n = 108)	53.0-72.0	0.8->2.5 Na_2O 5.0-8.0 K_2O 2.0-5.5	<0.05-0.25 Rb 50-160 Sr 500-2000	5-25	50-400	25-250

Dinky Boys Clan

Member Supersuites: Dinky Boys

Distribution: A small clan consisting of one suite of granitic dykes in the Norseman area.

Geochronology: None available.

Geochemistry: Dinky Boys has many similarities with 'low-LILE' clans of the Mafic group, including low to moderate K_2O, Ba, Rb, Sr, Zr contents. However, they are also characterised by high silica (~72 wt%), higher Pb and Th contents and lower Y contents and *mg#* than other 'low-LILE' clans. Dinky Boys is characterised by moderately fractionated REE and a Sr-undepleted and strongly Y-depleted signature. The clan may belong to one of the 'low-LILE' High-Ca group clans.

Mineralisation: Spatially associated with gold mineralisation in the Norseman area.

Petrogenesis: As discussed for the Mafic group granitoids in general.

Tectonic implications: As discussed for the Mafic group granitoids in general.

Granny Smith Clan

Member Supersuites: Bonnievale, Brazier, Cement Well, Depot, Granite Dam, Granny Smith, Liberty, Mount Belches, Porphyry

Distribution: A lithologically and compositionally diverse clan comprising small to large plutons (Liberty, Porphyry, Golden Cities) and porphyry dykes that is widely distributed throughout the greenstone belts in the southern Eastern Goldfields Province. The main areas include:

- plutons and porphyry dykes spatially associated with regional deformation zones (e.g., Boulder-Lefroy, Zuleika, Bardoc Deformation Zone, Laverton Tectonic Zone, etc.)
- plutons and porphyry dykes in the Norseman area
- discrete plutons internal to the greenstone belts (Liberty, Porphyry)
- discrete plutons marginal to the greenstone belts (e.g., Golden Cities)

Geochronology: A total of 11 ages are available for the Granny Smith clan. This includes ages for the Liberty, Porphyry, Golden Cities and Lake Brazier plutons in the southern Eastern Goldfields Province. Ages range from 2667 Ma to 2648 Ma, with the majority of plutons having an emplacement age of ca. 2665 Ma. The age of the Liberty granodiorite (2648±6 Ma, Kent, 1994) is unusual for Granny Smith clan granitoids.

Geochemistry: The Granny Smith clan is the 'high-LILE' archetypal end-member of Mafic group granitoids in the Eastern Goldfields Province. Granitoids of this clan are characterised by higher K_2O, Rb, Sr, Pb, LREE relative to the Kanowna-Belle clan (Figure 6). Champion & Cassidy (1998) noted that a simple K_2O-Ce plot can be used to discriminate between the majority of Kanowna Belle and Granny Smith clan members (Figure 6). Granny Smith clan granitoids are characterised by moderately to strongly fractionated REE patterns with no Eu anomalies as well as are generally Sr-undepleted and Y-depleted. Individual supersuites tend to be characterised by enrichment or depletion of specific elements. For instance, the Depot supersuite contains very high Ba and Sr contents relative to other supersuites and is similar to the New Celebration clan. The Porphyry supersuite is characterised by high K_2O, whereas the Golden Cities suite has higher *mg#* than the other suites and supersuites in the Granny Smith clan. This diversity indicates subtle changes in the composition of the source or sources for individual suites and supersuites.

Mineralisation: Many of the Granny Smith clan granitoids host gold mineralisation (e.g., Golden Cities, Porphyry, Liberty, Granny Smith, etc.) or are spatially associated with mineralisation (many of the porphyry dykes). Some of the granitoids may also host early 'magmatic' mineralisation; for instance, low-grade Au-Mo mineralisation at Granny Smith is attributed to late-magmatic fluids (Ojala, 1994). Some researchers have also suggested that some of the porphyry dyke swarms are the source for mineralised fluids and/or Au.

Petrogenesis: As discussed for the Mafic group granitoids in general. Of note, is that the Granny Smith clan granitoids are generally restricted in time. In contrast, Kanowna-Belle clan granitoids tend to have spread in emplacement ages from ca. 2690 Ma to ca. 2660 Ma, with most emplaced prior to ca. 2675 Ma. This temporal progression from 'low-LILE' to 'high-LILE' magmatism follows a similar pattern to that determined for the High-Ca group granitoids.

Specific supersuites and suites require specialised sources; e.g., Porphyry, Depot, etc. A variably LILE-enriched source can produce the majority of the Granny Smith (and Kanowna-Belle) clan granitoids, with the LILE-enrichment possibly increasing with time.

Tectonic implications: As discussed for the Mafic group granitoids in general.

Kambalda Clan

Member Supersuites: Kambalda, Kambalda-2

Distribution: The Victory and Kambalda clans are spatially restricted to the Kambalda-St Ives district. They comprise a series of small plutons (e.g., Kambalda trondhjemite) and porphyry dykes that intrude the greenstone sequence throughout the district, but tend to be spatially associated with major deformation zones such as the Boulder-Lefroy fault and subsidiary structures.

Geochronology: The Kambalda trondhjemite (Kambalda clan) is dated at 2662 Ma and a granitoid dyke at Victory (Victory clan) is dated at ca. 2664 Ma (Hill et al., 1992).

Geochemistry: The Kambalda and Victory clans are transitional to the 'low-LILE' and 'high-LILE' Mafic group clans. They are characterised by similar K_2O, Ce, Pb, Rb, Zr contents and *mg#* and *k* to 'low-LILE' clans but have elevated Sr, Y and Ba contents similar to 'high-LILE' clans. The Ba and Sr contents are not as elevated as for the New Celebration clan. The Kambalda and Victory clans are characterised by moderately fractionated REE patterns with no or slight Eu anomalies and Sr-undepleted, Y-depleted signatures in Spider-plots. The Kambalda and Victory clans have very similar chemistry and perhaps should be joined into a single transitional clan.

Mineralisation: Porphyry dykes and plutons of the Kambalda and Victory clans are mineralised in many deposits throughout the district. Gold mineralisation post-dated intrusion of the porphyry dykes and plutons (Perring, 1989).

Petrogenesis: As discussed for the Mafic group granitoids in general. The Kambalda and Victory clans are transitional to the 'low-LILE' and 'high-LILE' clans suggesting a mixed source or variable LILE-enrichment in the source region.

Tectonic implications: As discussed for the Mafic group granitoids in general.

Kanowna-Belle Clan

Member Supersuites: Braiser Well, Cosmopolitan, Doyle Dam, Freddo, Hawkins Find, Kalgoorlie-1, Kanowna-Belle, Lady Grace Darling, Lanarkshire, Maori Queen, Mt Pleasant, Mt Lucky, Pig Face Flat, Siberia Dam, unassigned porphyries

Distribution: The Kanowna-Belle clan forms a very diverse range of small plutons and porphyry dykes that are widespread throughout the southern Eastern Goldfields Province. Many of the clan members are spatially associated with large deformation zones and have been emplaced along active deformation zones. The ages of emplacement may indicate periods when the deformation zones were open to deep-seated fluids and magmas. In many places (e.g, Kanowna area, New Celebration area), both Kanowna-Belle and Granny Smith clan porphyry dykes have been emplaced in the same areas. Generally, the Kanowna-Belle clan granitoids were emplaced earlier than Granny Smith clan granitoids. In the Kanowna district, Champion & Cassidy (1998) identified over 10 suites of porphyries, with the majority being of Kanowna-Belle clan lineage.

Geochronology: Seven ages are available for Kanowna-Belle clan granitoids, with four of these ages from granitoids in the southern Eastern Goldfields Province. These range from 2694 Ma for the Kanowna-Belle porphyry (Wang et al., in press) to 2669 Ma for a porphyry dyke at Mt Percy (Yeats et al., 1999). An age of 2613 Ma was obtained for the Four Mile Hill porphyry by Nelson (1995), but this age is interpreted to reflect zircon disturbance rather than emplacement.

Geochemistry: The Kanowna-Belle clan is the archetypal 'low-LILE' clan of the Mafic group in the Eastern Goldfields Provionce. Kanowna-Belle clan granitoids are characterised by low to moderate K_2O, Ba, Rb, Sr, Pb, Y, Zr and Ce contents (Figure 6) relative to Granny Smith clan granitoids. They also tend to have higher Ni, *mg#* but lower *k* and FeO. They are characterised by moderately fractionated LREE and flat to fractionated HREE with no to slight negative Eu anomalies, and also Sr-undepleted, Y-depleted signatures. At the high silica end of the Kanowna-Belle compositional spectrum there is considerable overlap with members of low-LILE clans of the High-Ca group (Beasley, Burra, Yindi).

Mineralisation: A number of Kanowna-Belle clan granitoids are mineralised. The best know example, is at Kanowna-Belle itself, where the type locality for the Kanowna-Belle clan is overprinted by orogenic gold mineralisation. Minor earlier mineralisation may be related to the porphyry dykes throughout the district. Other districts (e.g., Yundamindera, Kalgoorlie, Mt Pleasant, Lanarkshire, Mt Lucky, Hawkins Find) have mineralisation spatially associated with Kanowna-Belle clan granitoids.

Petrogenesis: As discussed for the Mafic group granitoids in general. Of note, is that 'low-LILE' Kanowna-Belle clan granitoids tend to have spread in emplacement ages from ca. 2690 Ma to ca. 2660 Ma, with most emplaced prior to ca. 2675 Ma; this contrasts with the 'high-LILE' Granny Smith clan. This temporal progression from 'low-LILE' to 'high-LILE' magmatism follows a similar pattern to that determined for the High-Ca group granitoids.

Tectonic implications: As discussed for the Mafic group granitoids in general. Models for the generation of the 'low-LILE' High-Ca group granitoids may also be applicable to the 'low-LILE' Mafic group granitoids. This may implicate either thickened crust or partial melting of a subducted slab. The higher *mg#* would support the subducted slab model.

New Celebration Clan

Member Supersuites: Mount Shea, New Celebration-1

Distribution: The New Celebration clan consists of a couple of suites from within the same district. The district also contains both Granny Smith and Kanowna-Belle clan granitoids. The New Celebration clan is centred on the porphyry dykes at the Hampton-Boulder gold deposit. Note that this district is an extension to the NNW-trend displayed by the Parker Hills clan (High-Ca group) that shares many similarities with the New Celebration clan.

Geochronology: An age of 2686 Ma is available for a porphyry dyke from the New Celebration area (Hill et al.). This dyke is tentatively assigned to the New Celebration clan, but could belong to the Kanowna-Belle clan.

Geochemistry: The New Celebration clan shares many similarities with granitoids of the 'low-LILE' Kanowna-Belle clan, including low to moderate K_2O, FeO, Ce, Rb, Y, Zr contents, high *mg#* and low *k*. However, it does contain elevated Ba, Sr and Pb contents. The New Celebration clan is also characterised by strongly fractionated REE patterns with no Eu anomalies and by Sr-undepleted and Y-depleted signatures. These characteristics make the New Celebration clan very similar to the Parker Hills clan (High-Ca group) that is located to the southeast of new Celebration. The Depot suite of the Granny Smith clan is also characterised by elevated Ba and Sr and may also be part of a Ba- and Sr-enriched suite of granitoids in the central part of the Kalgoorlie terrane.

Mineralisation: New Celebration clan porphyry dykes are the host to gold mineralisation at Hampton-Boulder and Freddo deposits.

Petrogenesis: As discussed for the Mafic group granitoids in general. The enriched Ba and Sr signature and high *mg#* of the New Celebration and Parker Hills clans may be consistent with interaction between a 'low-LILE' Mafic group source with a lamprophyric or mantle-metasomatised source.

Tectonic implications: As discussed for the Mafic group granitoids in general.

Victory Clan

Member Supersuites: Hunt-2, Victory-1, Victory-2

Distribution: The Victory and Kambalda clans are spatially restricted to the Kambalda-St Ives district. They comprise a series of small plutons (e.g., Kambalda trondhjemite) and porphyry dykes that intrude the greenstone sequence throughout the district, but tend to be spatially associated with major deformation zones such as the Boulder-Lefroy fault and subsidiary structures.

Geochronology: The Kambalda trondhjemite (Kambalda clan) is dated at 2662 Ma and a granitoid dyke at Victory (Victory clan) is dated at ca. 2664 Ma (Hill et al., 1992).

Geochemistry: The Kambalda and Victory clans are transitional to the 'low-LILE' and 'high-LILE' Mafic group clans. They are characterised by similar K_2O, Ce, Pb, Rb, Zr contents and *mg#* and *k* to 'low-LILE' clans but have elevated Sr, Y and Ba contents similar to 'high-LILE' clans. The Ba and Sr contents are not as elevated as for the New Celebration clan. The

Kambalda and Victory clans are characterised by moderately fractionated REE patterns with no or slight Eu anomalies and Sr-undepleted, Y-depleted signatures in Spider-plots. The Kambalda and Victory clans have very similar chemistry and perhaps should be joined into a single transitional clan.

Mineralisation: Porphyry dykes and plutons of the Kambalda and Victory clans are mineralised in many deposits throughout the district. Gold mineralisation post-dated intrusion of the porphyry dykes and plutons (Perring, 1989).

Petrogenesis: As discussed for the Mafic group granitoids in general. The Kambalda and Victory clans are transitional to the 'low-LILE' and 'high-LILE' clans suggesting a mixed source or variable LILE-enrichment in the source region.

Tectonic implications: As discussed for the Mafic group granitoids in general.

Clans within the Westonia Association, Southern Cross Province

In the southeastern part of the Southern Cross Province, only one small Mafic group clan is present. This clan, Red Leaf, occurs as porphyry dykes and small plutons internal to the greenstones that are along the Ida Lineament on the MENZIES sheet. The location of the Red Leaf clan close to the Eastern Goldfields Province boundary also means that it could be placed within the Eastern Goldfields Province. The wholerock chemistry suggests affinity with 'low-LILE' Mafic group granitoids (e.g., Kanowna-Belle clan). The other clans of Mafic group granitoids that occur within the Southern Cross Province (e.g., Westonia; Courlbarloo, Ravensthorpe) have not been found within the southeastern Yilgarn Craton.

Red Leaf Clan

Member Supersuites: Red Leaf-1

Distribution: Red Leaf occurs as a series of small plutons and porphyry dykes intrusive into the greenstones that are along the Ida Lineament on the MENZIES sheet. It is very close to the arbitrary boundary between the Southern Cross and Eastern Goldfields provinces, but has been placed within the Southern Cross Province for reporting purposes.

Geochronology: None available.

Geochemistry: The Red Leaf is very similar to the 'low-LILE' Kanowna-Belle clan in the Eastern Goldfields Province. Red Leaf granitoids are characterised by low to moderate K_2O, Ba, Rb, Sr, Pb, Y, Zr and Ce contents (Figure 6) relative to 'high-LILE' granitoids. They also tend to have high Ni, *mg#* but lower *k* and FeO. They are characterised by slightly fractionated LREE and HREE with no Eu anomalies, and also Sr-undepleted, and weakly Y-depleted signatures.

Mineralisation: The Red Leaf granitoids are spatially associated with gold mineralisation.

Petrogenesis: As discussed for the Mafic group granitoids in general.

Tectonic implications: As discussed for the Mafic group granitoids in general.

High-HFSE group, southeastern Yilgarn Craton

Member Associations: Kookynie Association (Eastern Goldfields Province)

High-HFSE granitoids form a minor component of the Eastern Goldfields Province. The Kookynie clan is the main clan and is largely localised to a belt running from south of Kookynie (southwestern corner of EDJUDINA sheet) to north of Wiluna. A few smaller localities for the clan have also been identified, including a linear belt in the central part of the EDJUDINA sheet. These include phases within granitic gneiss along the western edge of the Eastern Goldfields Province on the MENZIES sheet, and dykes within greenstone on the BARDOC 1:100,000 sheet. Three clans (Cashmans, Kookynie, Outcamp Bore) have been delineated on the basis of geochemistry and geographical distribution in the southern Eastern Goldfields Province.

Eight ages are available for the Kookynie Association; however, four of these are from the northern Eastern Goldfields, with three between 2700 and 2680 Ma (Table 4). These ages overlap with those found for spatially associated, and, at least locally, genetically-related felsic volcanics (Nelson, 1997). Other ages include the Weebo granitoid with a younger age of 2658 Ma, the Outcamp Bore and Yarri granitoids at ca. 2710 Ma and an anomalous older 2738 Ma obtained for the granitic gneiss at Parmelia (Nelson, 1997, 1998).

High-HFSE group granitoids in the southern Yilgarn Craton are characterised by a limited silica range and generally >74 wt% SiO_2. This contrasts with the broader compositional variation for the group present in the northern Eastern Goldfields Province (Champion, this report). Kookynie Association granitoids in the southern Eastern Goldfields Province are characterised by high Total FeO, MgO, TiO_2, HFSE, low to moderate LILE, low Al_2O_3, and Sr-depleted, Y-undepleted character and are readily distinguished from other granite groups (Figure 8). They generally have CaO and Na_2O contents similar to those in the High-Ca group granitoids. Minor differences are evident between the two clans that constitute the Kookynie Association.

As discussed by Champion & Sheraton (1997), High-HFSE group granitoids are crustally-derived melts from an intermediate to more siliceous source. This scenario readily explains the high silica contents and strongly Sr-depleted signature of the granitoids. The combination of low Rb and K_2O and moderate Ba contents argue against small degrees of partial melting. The high TiO_2, MgO, Total FeO, Y, Zr, and Nb contents for a given silica content suggest A-type affinities. High temperatures are inferred to be required to melt the preferred source rocks. The Sr-depleted, Y-undepleted nature of the group, strongly infer generation at only moderate crustal pressures, i.e., <10 kbars (<35 km thick). Similarly, as discussed by Champion & Sheraton (1997), the Sm-Nd isotope data indicate significant involvement of pre-existing crustal rocks in the generation of the High-HFSE granites.

Hallberg (1985) noted felsic volcanic rocks in the Eastern Goldfields Province with very similar geochemistry to the High-HFSE group granitoids. These felsic volcanics also have a similar localised distribution that has been attributed to be due to extension during rifting (e.g., Hallberg & Giles, 1986). The close spatial, temporal, and, at least locally, genetic, relationship between the High-HFSE granitoids (e.g., Kookynie) and felsic volcanics (e.g., Melita volcanics), indicates that these granites were intimately related to greenstone formation. More importantly, the geochemistry of the High-HFSE granites and their A-type affinities indicates emplacement in an, at least locally, extensional environment (Champion & Sheraton, 1997). The ages of these granitoids may then be used to date periods of local extension.

Clans within the Kookynie Association, Eastern Goldfields Province

Three clans (Cashmans, Kookynie, Outcamp Bore) have been delineated on the basis of geochemical characteristics and geographical distribution. The Cashmans clan is a very small clan made up of two supersuites in the Bardoc district. The Kookynie clan is the archetypal clan for High-HFSE group granitoids in the Eastern Goldfields Province. It is spatially associated with felsic volcanic rocks in most localities and is inferred to have been emplaced contemporaneous with the felsic volcanism. The presence of the Outcamp Bore clan in the central Kurnalpi terrane suggests that bimodal volcanism may have been extruded or tectonically emplaced in the Kurnalpi terrane.

Cashmans Clan

Member Supersuites: Cashmans, Paddy's Knob

Distribution: The Cashmans clan is a minor clan that is geographically restricted to dykes and small plutons in the Bardoc and Davyhurst districts.

Geochronology: None available

Geochemistry: The Cashmans clan is characterised by very high silica contents, high Zr, Y, moderate FeO, TiO_2, and low K_2O and Rb, and is only tentatively assigned to the High-HFSE group. Cashmans clan granitoids also characterised by very fractionated LREE and flat HREE patterns with no Eu anomaly, and Sr-depleted, and slightly Y-depleted signatures on Spider-plots. They contrast with Kookynie and other clans of the High-HFSE group by their lower TiO_2 and FeO contents. The Cashmans granitoids are also altered and may have changed the chemical characteristics of the clan.

Mineralisation: Spatially associated with gold mineralisation in the Ora Banda area.

Petrogenesis: Similar to the Kookynie clan; however, the lower TiO_2 and FeO require a less mafic source rock.

Tectonic implications: As for the High-HFSE group in general

Kookynie Clan

Member Supersuites: Hawkes Nest, Kookynie, Minyma, Providence

Distribution: The Kookynie clan is strongly localised along zone extending from south of Kookynie up to north of Wiluna. In the majority of cases, there is strong spatial association with Melita-type felsic volcanics. In the southern Eastern Goldfields Province it comprises four supersuites. Two of the supersuites (Kookynie, Minyma) are localised along the main zone. The Hawkes

Nest supersuite occurs as dykes and small plutons on the EDJUDINA and LAVERTON sheets, whereas the fourth supersuite (Providence) is localised as small units and phases within granitic gneiss on the far western edge of the Eastern Goldfields Province on the northern MENZIES sheet. Lithologies include biotite monzogranite and syenogranite.

Geochronology: Three ages are available for Kookynie clan granitoids; only one age is for a High-HFSE granitoid in the southern Eastern Goldfields Province. This is an age of 2679 Ma for the Kookynie granitoid. The other two ages are for granitoids in the northern Eastern Goldfields Province (2679 Ma for the Kent Complex; L. Black, written communication, 2000; 2658 Ma for the Weebo granodiorite, Nelson, 1997). All three granitoids contain some inheritance ca. 2705 to 2710 Ma.

Geochemistry: The Kookynie clan is the archetypal High-HFSE clan, containing the rocks that earlier published descriptions of the group were based on (e.g., Champion & Sheraton, 1997). Geochemical characteristics include the variably elevated total Fe, MgO, Y, LREE, Zr coupled with low to moderate Al_2O_3, K_2O, Rb, Sr, and only moderate Na_2O (Figure 8). Kookynie clan granitoids are also characterised by moderately fractionated REE patterns and Sr-depleted, Y-undepleted signatures on Spider-plots.

Mineralisation: Granitoids and porphyries of the Kookynie clan are spatially associated with gold mineralisation (e.g., Cosmopolitan deposit) on the EDJUDINA and MENZIES sheets.

Petrogenesis: As for the High-HFSE group in general.

Tectonic implications: As for the High-HFSE group in general. The presence of High-HFSE group granitoids within granitic gneiss on the western edge of the Eastern Goldfields Province, suggests that spatially and temporally felsic volcanism may also have been active in this district.

Outcamp Bore Clan

Member Supersuites: Outcamp Bore, Yarri

Distribution: A small High-HFSE clan that occurs along a linear belt in the eastern half of the EDJUDINA and KURNALPI sheets as a series of foliated granitoids and dykes internal to the greenstone sequences. Granitoids of this clan range from biotite monzogranite to tonalite.

Geochronology: Three ages are available for the Outcamp Bore clan; these range from 2719 Ma (Outcamp Bore tonalite, suite & supersuite) to 2698 Ma (Round Hill tonalite; Outcamp Bore supersuite). No age is available for the Yarri supersuite.

Geochemistry: The Outcamp Bore clan is characterised by unusual geochemistry and shares features with other High-HFSE clans. Outcamp Bore granitoids have high Y, TiO_2, Total FeO contents, moderate Na_2O, Ce, and low Al_2O_3, K_2O, Pb, Rb, Sr and Th contents (Figure 1, 2, 4). Very low mg# and Sr/Sr* are also a characteristic of the clan. Two supersuites can be separated on the basis of Zr and Total FeO contents; Yarri s/suite has low Zr and Total FeO whereas the Outcamp Bore s/suite has high Zr and Total FeO contents. Outcamp Bore clan granitoids are characterised by weakly to moderately fractionated LREE and flat HREE patterns with small to moderate negative Eu anomalies (Figure 3). On Spider-plots, Outcamp Bore granitoids are weakly Sr-depleted and Y-undepleted to slightly Y-depleted (Figure 3). The chemical characteristics of Outcamp Bore granitoids are intermediate between more typical High-Ca granitoids and High-HFSE granitoids (e.g., Bullshead clan, Kookynie Association).

Mineralisation: Very minor gold mineralisation is known from the Yarri monzogranite on the south-central part of the EDJUDINA sheet.

Petrogenesis: The variable silica contents, low LILE contents, overall high but variable Total FeO, TiO_2, Y and Zr contents suggest affinities with A-type granitoids and implicate an intermediate, but reasonably primitive, source for Outcamp Bore clan granitoids. The REE patterns with small negative Eu anomalies, and Sr-depleted, Y-undepleted signature are consistent with a source where plagioclase was stable indicating mid- to lower-crustal pressures. In combination with the high Y and Zr contents, the Outcamp Bore granitoids may result from high temperature melting of an intermediate source at moderate (crustal) pressures.

Tectonic and other implications: The similarities of the Outcamp Bore clan granitoids with the high-HFSE group granitoids and A-type granitoids in general implicates an extensional environment for their genesis. The localised distribution of these granitoids is consistent with this interpretation.

Syenitic group, southeastern Yilgarn Craton

Member Associations: Gilgarna Association (Eastern Goldfields Province)
Fitzgerald Association (Southern Cross Province)

The Syenitic group is a minor but important granitic group in the southeastern Yilgarn Craton and represents up to 5 to 10 percent of all granitoids. The majority of Syenitic group granitoids form as small to large plutons or dykes internal or at the margins of greenstone belts. Others occur as small intrusions within large external granitoids (e.g., Rainbow complex). In the majority of occurrences, the syenites are spatially associated with major deformation zones (e.g., Emu, Claypan faults; Celia lineament). The main occurrences of Syenitic group granitoids in the southern Eastern Goldfields Province are along the Emu, Claypan faults in the Edjudina terrane as well as the southern extension of the Celia lineament and the Laverton tectonic zone to the southern KURNALPI and WIDGIEMOOLTHA sheets. Other syenitic granitoids are localised throughout the Mount Monger district and on the western WIDGIEMOOLTHA sheet.

Two clans have been delineated on the basis of geochemistry and geographic distribution in the southern Eastern Goldfields Province. The Gilgarna clan is lithologically and chemically diverse and geographically restricted to four NNW-trending zones. Smithies & Champion (1999) describe in detail the four supersuites that are restricted to each of the NNW-trending zones. The Erayinia clan forms large plutons throughout a broad linear zone in the southeastern part of the southern Eastern Goldfields Province.

In the Southern Cross Province, only one small clan of Syenitic group granitoids has been identified and this clan (Fitzgerald Peaks) is geographically restricted to the Peak Charles area on the LAKE JOHNSTON sheet.

Granitoids of the Erayinia and Gilgarna clan have a restricted age range from 2665 to 2640 Ma (Nelson, 1997, 1998; L. Black, written communication, 2000; this study). The Gilgarna clan has ages over the full range, although there does appear to be a bimodal distribution at ca. 2660 Ma and ca. 2645 Ma. In contrast, the Erayinia clan has been dated at ca. 2660-2655 Ma; a similar age is inferred for the Panakin clan in the northern Eastern Goldfields Province. The ages of the Erayinia clan and the early Gilgarna clan event overlap with the end of High-Ca and Mafic group magmatism and the start of Low-Ca group magmatism in the Eastern Yilgarn Craton. Partial melting of a variety of sources is required to produce the diverse range of granitoids at this time.

The geochemistry of the Syenitic group granitoids has been described in detail by Johnson (1991), Champion & Sheraton (1997) and Smithies & Champion (1999). The Syenitic group are characterised by high total alkalis (Na_2O+K_2O), high K_2O, variable to high Rb, Ba, Sr, Pb, Th, U, Zr, LREE, Y, combined with mostly lower MgO, CaO, Total FeO and *mg#*, relative to the High-Ca group granites (Figure 9). Even though there is considerable lithological diversity, the Erayinia and Gilgarna clan granitoids have very similar wholerock geochemistry; differences include lower K_2O, Rb, Th, U, Nb and marginally higher Sr in the Erayinia clan. The Gilgarna clan is characterised by large variations in total REE and in the level of fractionation as displayed by REE.

The source rocks for the Syenitic group granitoids is equivocal (Champion & Sheraton, 1997; Smithies & Champion, 1999). The geochemistry of the Gilgarna and Erayinia clans is similar to that of some A-type granitoids. Models for A-type granitoids include high temperature crustal partial melting along localised zones, fractionation coupled with crustal assimilation of mantle-derived melts and complex models involving metasomatism of source rocks or during crystallisation (e.g., Eby, 1990). The large compositional range of the Syenitic group makes it difficult to comment on the origins; in particular, the relative contributions of mantle and crustal components. Smithies & Champion (1999) suggest that the lack of associated mafic rocks, the presence of quartz within all syenites, the variable but mostly high LILE contents, the presence of some ?inherited zircons in some plutons and strong negative Nb, P and Ti anomalies on multi-element diagrams support a dominantly crustal origin.

By analogy with syenitic granitoids elsewhere, and A-type granitoids in general, an extensional regime is inferred for the Syenitic group granitoids. The presence of possibly two separate Syenitic magmatic events at ca. 2660 Ma and ca. 2645 Ma may indicate that there was several, at least local, extensional events in the southern Eastern Goldfields Province. The first event coincides with the peak of 'high-LILE' Mafic group magmatism and the waning phase of 'high-LILE' High-Ca group magmatism. After this time, a significant shift in granitoid genesis to Low-Ca magmatism occurred at approximately 2655-2650 Ma. This shift moved towards extension on the scale of the whole Yilgarn Craton. Smithies & Champion (1999) speculated that may reflect lower crustal delamination, caused by an unstable thickened crust produced in the D_2 compressional event.

Clans within the Gilgarna Association, Eastern Goldfields Province

Erayinia Clan

Member Supersuites: Charnleigh, Erayinia, Yardilla

Distribution: The Erayinia clan is spatially restricted to a broad NNW-trending linear belt on the southeastern edge of the Eastern Goldfields Province on the southern KURNALPI and WIDGIEMOOLTHA sheets. It occurs are as series of large plutons that are strongly magnetic as displayed on aeromagnetic images. Lithologies include clinopyroxene- and amphibole-bearing quartz monzonites and monzonites.

Geochronology: Three Erayinia clan granitoids have been dated by SHRIMP; two zircon ages of 2660 Ma (Erayinia and Yardilla North granitoids) and a titanite age of 2645±12 Ma (Yardilla South; this project). A similar age is inferred for the Panakin clan in the northern Eastern Goldfields Province. The age of the Erayinia clan is therefore probably ca. 2660-2655 Ma and overlaps with the end of High-Ca and Mafic group magmatism and the start of Low-Ca group magmatism.

Geochemistry: The Erayinia clan is characterised high K_2O, total alkalis (Na_2O+K_2O), Ba, Sr and LREE, and is very similar to members of the Gilgarna clan (Figures 9, 10); the main differences is marginally lower K_2O and Rb. The Erayinia is characterised by high total REE contents, strongly fractionated REE patterns with no Eu anomaly and a Sr-undepleted, Y-depleted signature. The clan also exhibits strong negative Nb, P and Ti anomalies on multi-element diagrams. The Erayinia clan is virtually identical to the Panakin clan in the far northern Eastern Goldfields Province.

Mineralisation: None recorded.

Petrogenesis: As discussed for the Syenitic group in general.

Tectonic implications: Smithies & Witt (1997) postulated that the eastern part of the southern Eastern Goldfields Province was part of a different domain with a contrasting basement to that under the Kalgoorlie terrane. The existence of the broadly linear Erayinia clan and its affinity with the Syenitic group suggests that the clan was emplaced during ?local extension at ca. 2660-2655 Ma. It is quite possible for the extension to have taken place within an overall compressive regime.

Gilgarna Clan

Member Supersuites: Claypan, Emu, Mount Monger, Ninnis

Distribution: The syenites exhibit a restricted distribution lying mostly along lineaments (e.g., Libby, 1978). Four supersuites (Claypan, Emu, Mount Monger and Ninnis) have been identified by Smithies & Champion (1999). Each supersuite is spatially restricted to distinct NNW-trending belts that correspond to major NNW-trending deformation zones (e.g., Ninnis Fault). In the southern Eastern Goldfields Province, members of all four supersuites are present. They form small to moderate plutons (e.g., Gilgarna, Binneringie) and/or dykes that are generally undeformed, locally layered and largely comprise amphibole - and pyroxene -bearing quartz syenite and syenite. The McAuliffe Well complex is deformed and mineralised at its margins.

Geochronology: Four Gilgarna clan syenitic intrusions have been dated, although three of these are for granitoids in the northern Eastern Goldfields Province; ages range from 2664 Ma (Hanns Camp Complex; L. Black, written communication, 2000) to 2644 Ma (Woorana syenite; Nelson, 1998). The one Gilgarna clan granitoid in the southern Eastern Goldfields Province, McAuliffe Well syenite, has an age of 2651 Ma (Nelson, 1997).

Geochemistry: The Gilgarna clan is the archetypal Syenitic group clan in the Eastern Goldfields Province. Gilgarna clan syenites are characterised by their high K_2O, Na_2O and total alkalis ($Na_2O+K_2O > 10$ wt%). They are also peralkaline to alkaline, high Agpaitic indicies (Figure 9) and have low mg#. Large variations in Ba, Sr, Y and LREE are apparent for individual supersuites. Gilgarna clan syenites are characterised by extreme variation in REE, ranging from slightly to very strongly fractionated REE patterns with no or very small Eu anomalies. They also display variably Sr-undepleted, Y-depleted signatures on Spider-plots. Many other elements show considerable scatter and probably reflect lithological heterogeneity and local layered or cumulus features. Smithies & Champion (1999) highlight the main geochemical features of each of the supersuites in the southern Eastern Goldfields Province.

Mineralisation: Several plutons of the Gilgarna clan (e.g., McAuliffe Well, Tin Dog) host minor gold mineralisation. Members of the clan are regularly targeted as potential hosts to mineralisation.

Petrogenesis: As for the Syenitic group in general. The small differences between the various supersuites probably reflect minor variations in the composition of the source across the Eastern Goldfields Province (Smithies & Champion, 1999).

Tectonic implications: As for the Syenitic group in general.

Clans within the Fitzgerald Peaks Association, Southern Cross Province

The Fitzgerald Peaks Association comprises one supersuite (Peak Charles) at the Fitzgerald Peaks complex on the LAKE JOHNSTON sheet.

Fitzgerald Peaks Clan

Member Supersuites: Peak Charles

Distribution: The Fitzgerald Peaks clan is localised at Peak Charles on the LAKE JOHNSTON sheet. It forms a very prominent hill at Peak Charles. Lithologically it consists of mainly amphibole-bearing quartz syenite.

Geochronology: An Archean age is inferred for the Fitzgerald Peaks complex.

Geochemistry: The Fitzgerald Peaks clan is characterised by high K_2O, Na_2O and total alkalis ($Na_2O+K_2O > 10$ wt%). They are also peralkaline to alkaline, and have low mg#. Large variations in Ba, Sr, Y and LREE are apparent. The Fitzgerald Peaks clan syenites are characterised by extreme variation in REE, ranging from slightly to very strongly fractionated REE patterns with no or very small Eu anomalies. They also display minor Sr-depleted, and minor Y-depleted signatures on Spider-plots.

Mineralisation: None recorded.

Petrogenesis: As discussed for the Syenitic group in general.

Tectonic implications: As discussed for the Syenitic group in general.

References

Bettenay, L.F. 1977. Regional geology and petrogenesis of Archaean granitoids in the southeastern Yilgarn Block. Ph.D. thesis, University of Western Australia. 328 pp.

Cassidy, K.F., 1992. Archaean granitoid-hosted gold deposits in greenschist to amphibolite facies terrains: A high P-T to low P-T depositional continuum equivalent to greenstone-hosted deposits. Unpublished Ph.D. thesis, University of Western Australia, 296 p.

Cassidy, K.F., 1998. Geochemistry of porphyries from the Kalgoorlie Terrane and Yandal Belt. In: AMIRA P482/MERIWA M281 Sponsors Meeting Notes, August, 1998, unpaginated (Confidential Report)

Champion, D.C., 1997. Granitoids in the Eastern Goldfields. In: Cassidy, K.F., Whitaker, A.J. & Liu, S.F. (Compilers) An International Conference on Crustal Evolution, Metallogeny and Exploration of the Yilgarn Craton - An Update. Australian Geological Survey Organisation, Record 1997/41, 71-76.

Champion, D.C., 1998. Granites of the northern and central Southern Cross region. In: AMIRA P482/MERIWA M281 Annual Report, Year 1, pp. 2.1-2.59 (Confidential Report)

Champion, D.C., 1998. Granites of the Kalgoorlie and Boorabbin sheets. In: AMIRA P482/MERIWA M281 Sponsors Meeting Notes, August, 1998, unpaginated (Confidential Report)

Champion, D. & Cassidy, K., 1998. Metallogenic potential of granitoids: Kanowna Belle and Granny Smith regions. Final Report to Golden Valley Joint Venture and Placer Pacific Ltd. Unpublished AGSO report.

Champion, D.C. & Sheraton. J.W., 1997. Geochemistry and Sm-Nd isotope systematics of Archaean granitoids of the Eastern Goldfields Province, Yilgarn Craton, Australia: constraints on crustal growth. Precambrian Research, 83, 109-132.

Hill, R.I., Chappell, B.W. & Campbell, I.H., 1992. Late Archaean granites of the southeastern Yilgarn Block, Western Australia: age, geochemistry and origin. Transactions Royal Society of Edinburgh, Earth Sciences, 83, 211-226.

Johnson, G.I., 1991. The petrology, geochemistry and geochronology of the felsic alkaline suite of the eastern Yilgarn Block, Western Australia. PhD thesis, University of Adelaide.

Kent, A.J.R., 1994. Chronological constraints on the timing of Archaean gold mineralisation in the Yilgarn Craton, Western Australia. PhD thesis, Australian National University,

Kent, A.J.R., Cassidy, K.F. & Fanning, C.M., 1996. Archaean gold mineralisation synchronous with the final stages of cratonisation, Yilgarn Craton, Western Australia. Geology, 24, 879-882.

Knight, J.T., 1994. The geology and genesis of Archaean amphibolite-facies lode-gold deposits in the Coolgardie Goldfield, Western Australia, with special emphasis on the role of granitoids. Unpublished Ph.D. thesis, University of Western Australia, 239 p.

Krapez, B., Brown, S.J.A., Hand, J., Barley, M.E. & Cas, R.A.F., 2000. Age constraints on recycled crustal and supracrustal sources of Archaean metasedimenatry sequences, Eastern Goldfields Province, Western Australia: evidence from SHRIMP zircon dating. Tectonophysics, 322, 89-133.

Martin, H., 1986. Effect of steeper Archaean geothermal gradient on geochemistry of subduction-zone magmas. Geology, 14, 753-756.

Nelson, D.R., 1995. Compilation of SHRIMP U-Pb zircon geochronology data, 1994. Geological Survey of Western Australia, Record 1995/3.

Nelson, D.R., 1996. Compilation of SHRIMP U-Pb zircon geochronology data, 1995. Geological Survey of Western Australia, Record 1996/5.

Nelson, D.R. 1997a. Evolution of the Archaean granite-greenstone terrane of the Eastern Goldfields, Western Australia : SHRIMP U-Pb zircon constraints. Precambrian Research, 83,

Nelson, D.R., 1997b. Compilation of SHRIMP U-Pb zircon geochronology data, 1996. Geological Survey of Western Australia, Record 1997/2.

Nelson, D.R., 1998. Compilation of SHRIMP U-Pb zircon geochronology data, 1997. Geological Survey of Western Australia, Record 1998/2.

Nelson, D.R., 1999. Compilation of SHRIMP U-Pb zircon geochronology data, 1998. Geological Survey of Western Australia, Record 1999/3.

Ojala, V.J., McNaughton, N.J., Ridley, J.R., Groves, D.I. & Fanning, C.M., 1997. The Archaean Granny Smith gold deposit, Western Australia: Age and Pb-isotope tracer studies. Chronique de la Recherche Miniere.

Perring, C.S., 1989. The significance of 'Porphyry' intrusions to Archaean gold mineralization in the Norseman-Wiluna Belt of Western Australia. Unpublished Ph.D. thesis, University of Western Australia, 229p.

Qui, Y.M., Groves, D.I. & McNaughton, N.J., 1997. Deep-seated granitoids: Implications for Late Archaean subduction-collision-lithospheric delamination and gold mineralisation in the Yilgarn Craton. Australian Geological Survey Organisation, Record 1997/42, 65-70.

Smithies, R.H, & Champion, D.C., 1999. Late Archaean felsic alkaline igneous rocks in the Eastern Goldfields, Yilgarn Craton, Western Australia: a result of lower crustal delamination? Geological Society of London, 156, 561-576.

Smithies, R.H. & Witt, W.K. 1997. Distinct basement terranes identified from granite geochemistry in late Archaean granite-greenstones, Yilgarn Craton, Western Australia. Precambrian Research 83, 185-201.

Witt, W.K. & Davy, R. 1997. Geology and geochemistry of Archaean granitoids in the southwest Eastern Goldfields Province, Western Australia: a syn-collisional tectonic setting? Precambrian Research, 83, 133-183

Wyborn, L.A.I., 1993. Constraints on interpretations of lower crustal structure, tectonic setting and metallogeny of the Eastern Goldfields and Southern Cross Provinces provided by granite geochemistry. Ore Geology Reviews, 8, 125-140.

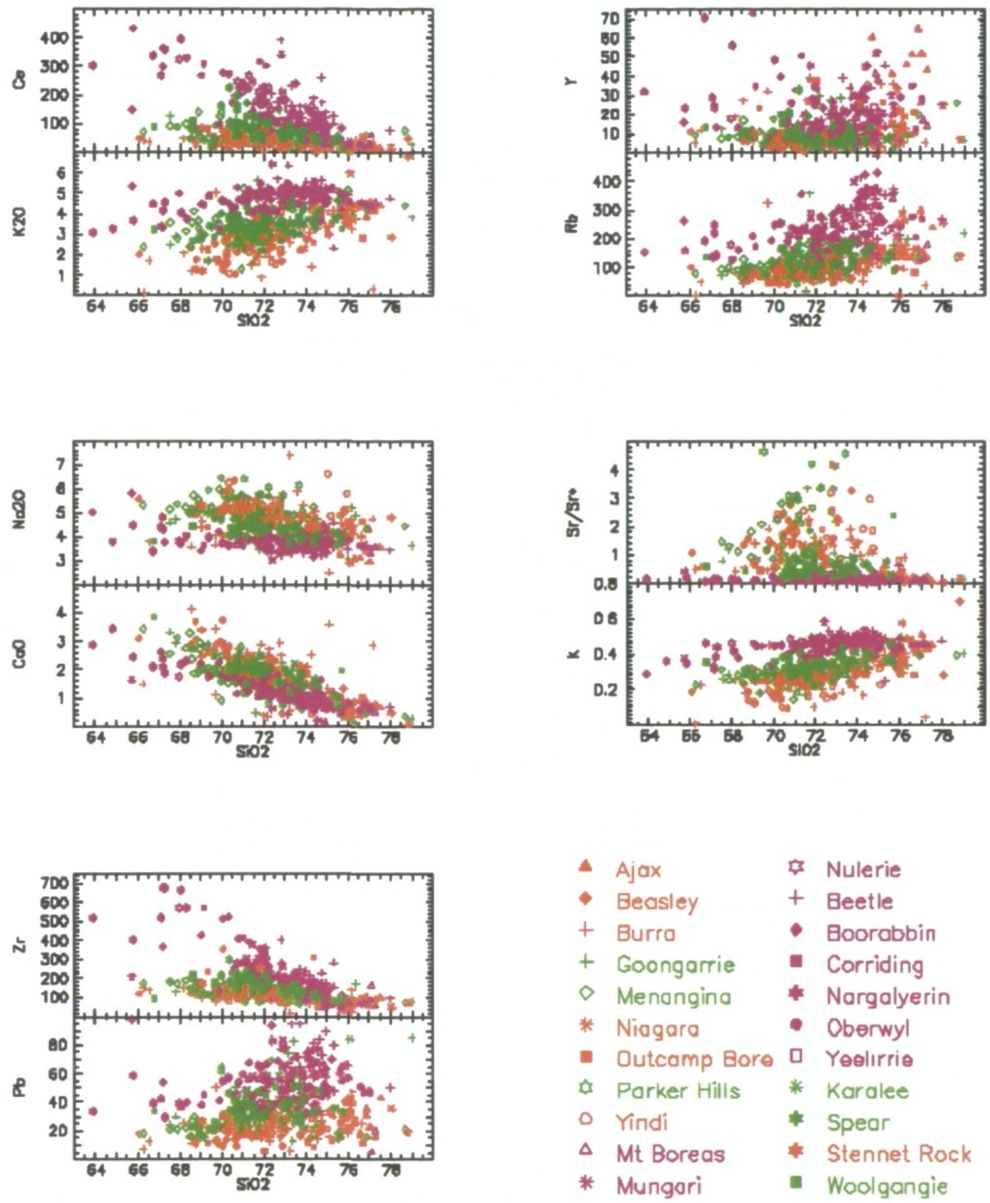

Figure 3.1 Discriminant plots for granitoids of the Low-Ca group (Mt Boreas (EGP) and Beetle (SCP) Associations) and High-Ca group (Menangina (EGP) and Diemals (SCP) Associations), southeastern Yilgarn Craton. High-LILE clans of the High-Ca group are shown in green, low-LILE clans of the High-Ca group in red, and all Low-Ca granitoids in magenta.

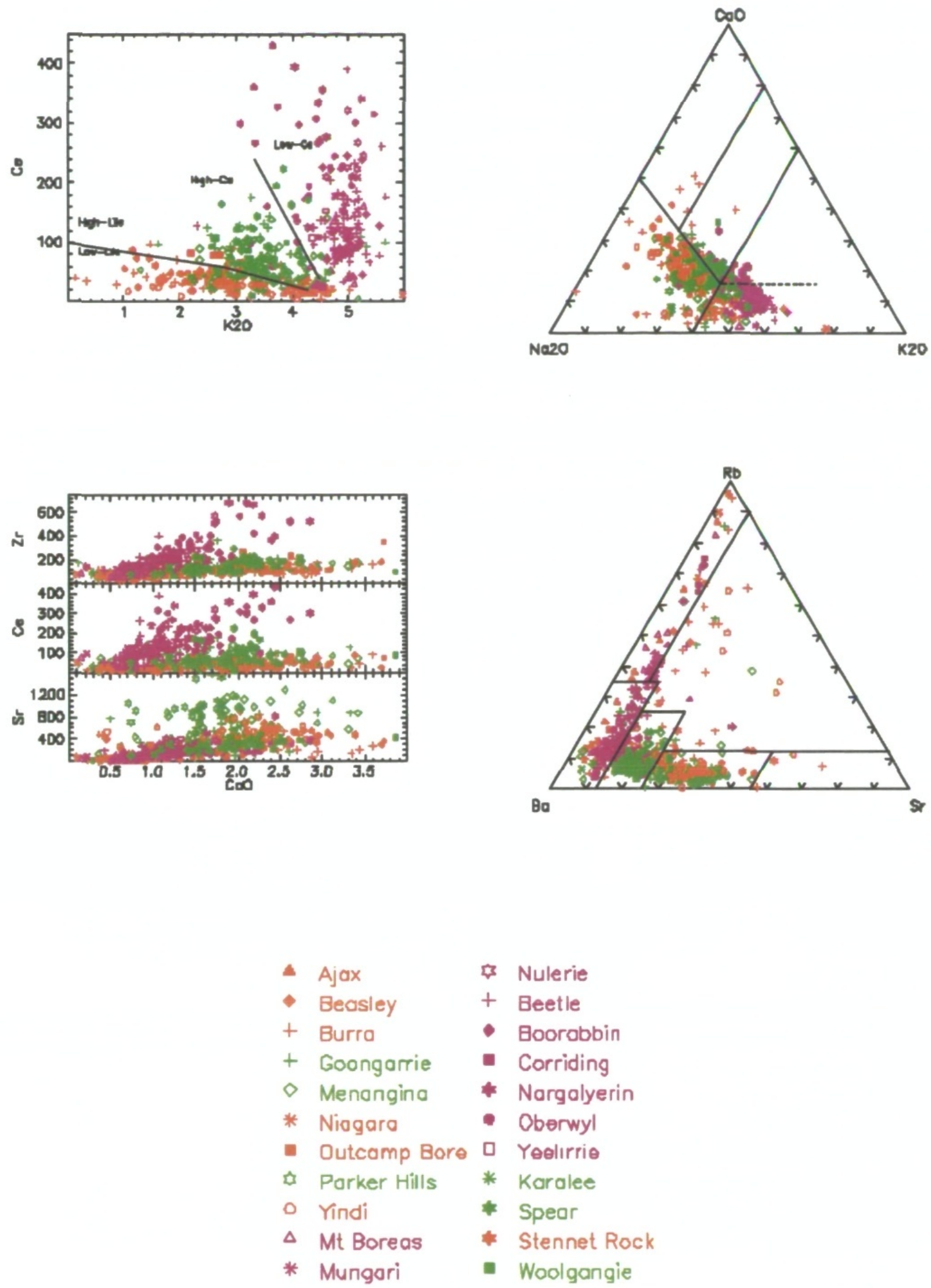

Figure 3.2 Discriminant plots for granitoids of the Low-Ca group (Mt Boreas (EGP) and Beetle (SCP) Associations) and High-Ca group (Menangina (EGP) and Diemals (SCP) Associations), southeastern Yilgarn Craton. High-LILE clans of the High-Ca group are shown in green, low-LILE clans of the High-Ca group in red, and all Low-Ca granitoids in magenta.

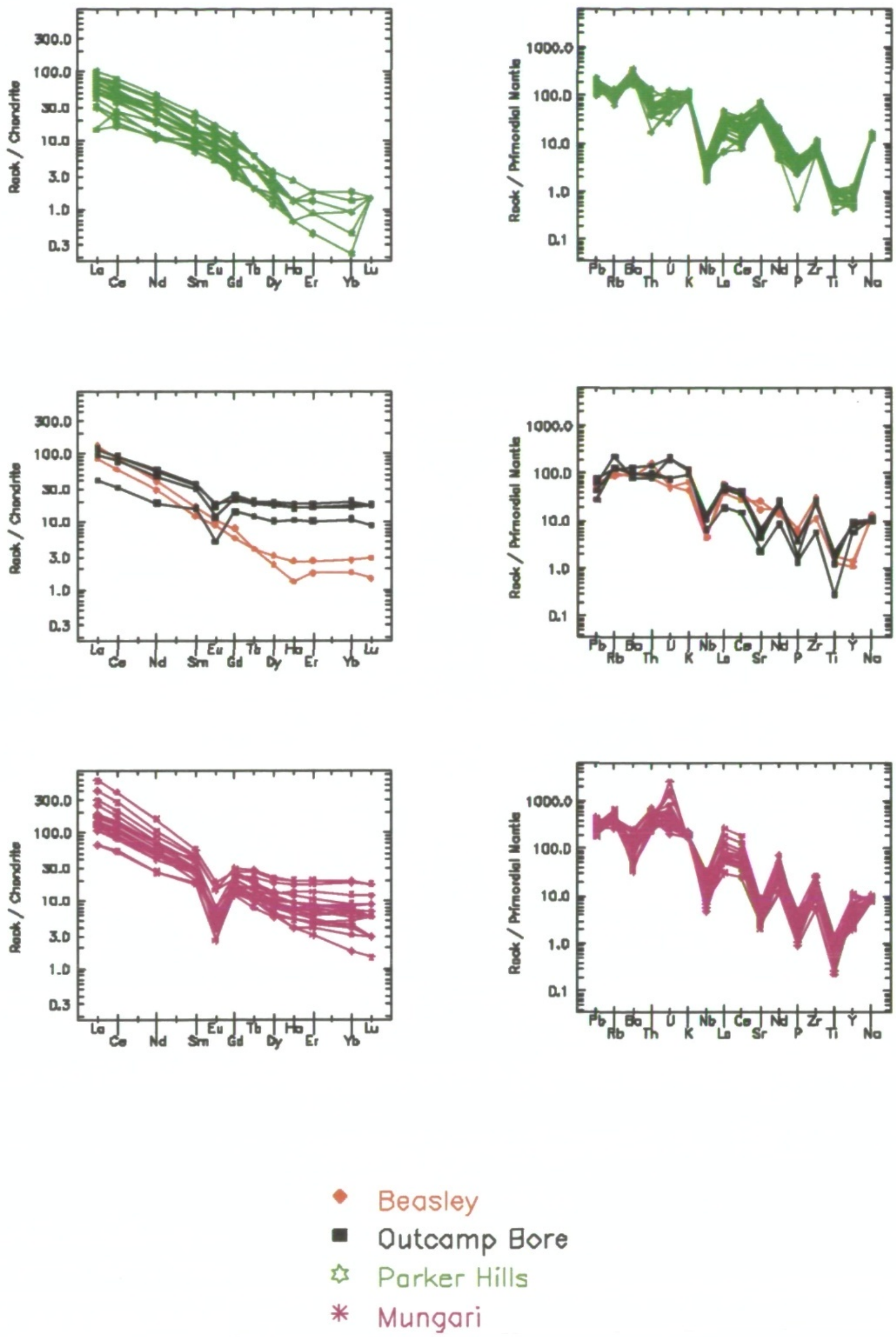

Figure 3.3 Rare-Earth Element (REE) and Primitive-Mantle Normalised multi-element diagrams (Spider-plots) for selected clans (Beasley, Parker Hills) of the Menangina (EGP) Association, High-Ca group, the Mungari clan of the Mt Boreas (EGP) Association, Low-Ca group, and the Outcamp Bore clan of the Kookynie (EGP) Association, High-HFSE group, southeastern Yilgarn Craton.

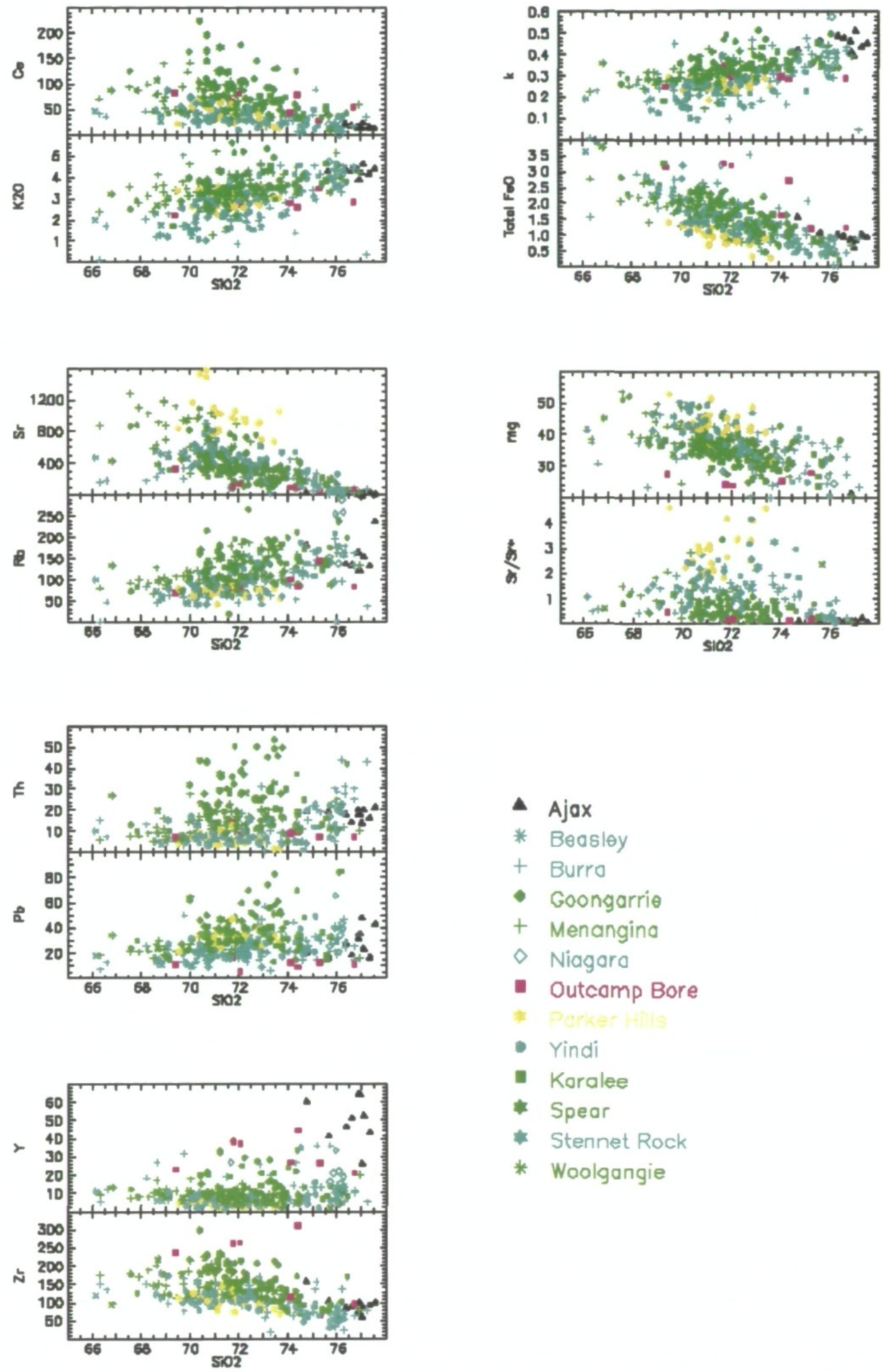

Figure 3.4 Discriminant plots for clans of the Menangina (EGP) and Diemals (SCP) Associations, High-Ca group, southeastern Yilgarn Craton. High-LILE clans are shown in green, low-LILE clans in blue and two unusual small clans in black (Ajax) and yellow (Parker Hills). The unusual Outcamp Bore clan (magenta) of the Kookynie (EGP) Association, High-HFSE group is shown for comparison.

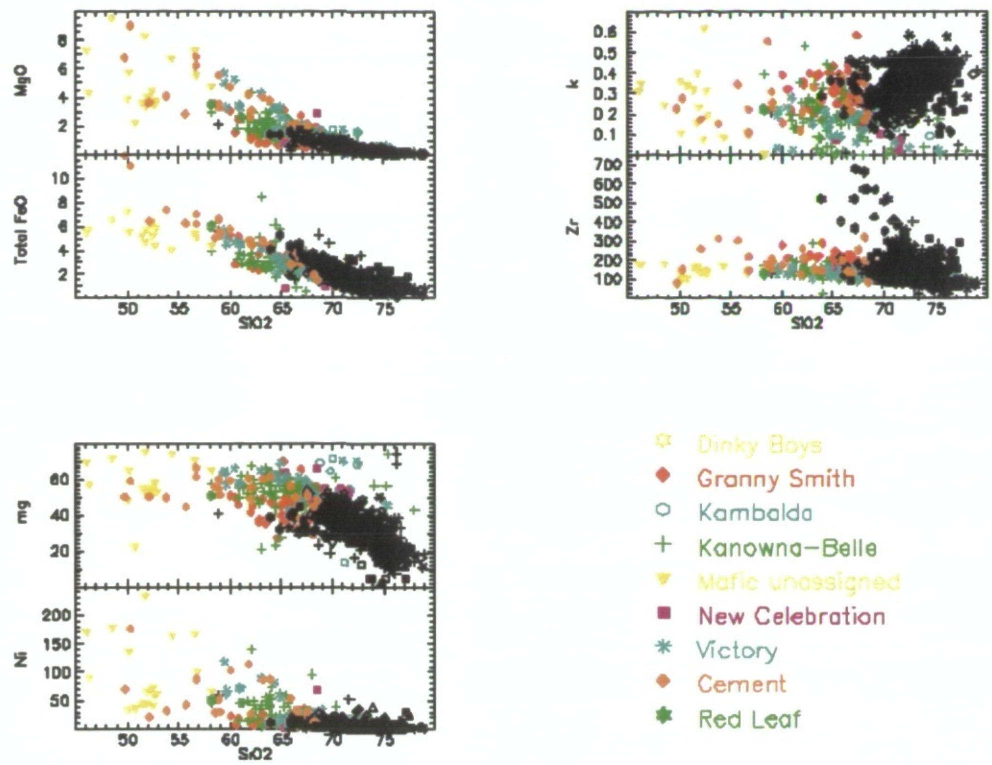

Figure 3.5 Discriminant plots for clans of the Granny Smith (EGP) and Westonia (SCP) Associations, Mafic group, southeastern Yilgarn Craton, with all other granitoids shown in black for comparison. The Cement clan comprises mafic granitoid xenoliths usually within High-Ca and/or Mafic group granitoids. The Mafic unassigned clan comprises mafic dykes in the Kalgoorlie and Kambalda areas. The Red Leaf clan is the only Mafic group clan within the Southern Cross Province in the southeastern Yilgarn Craton.

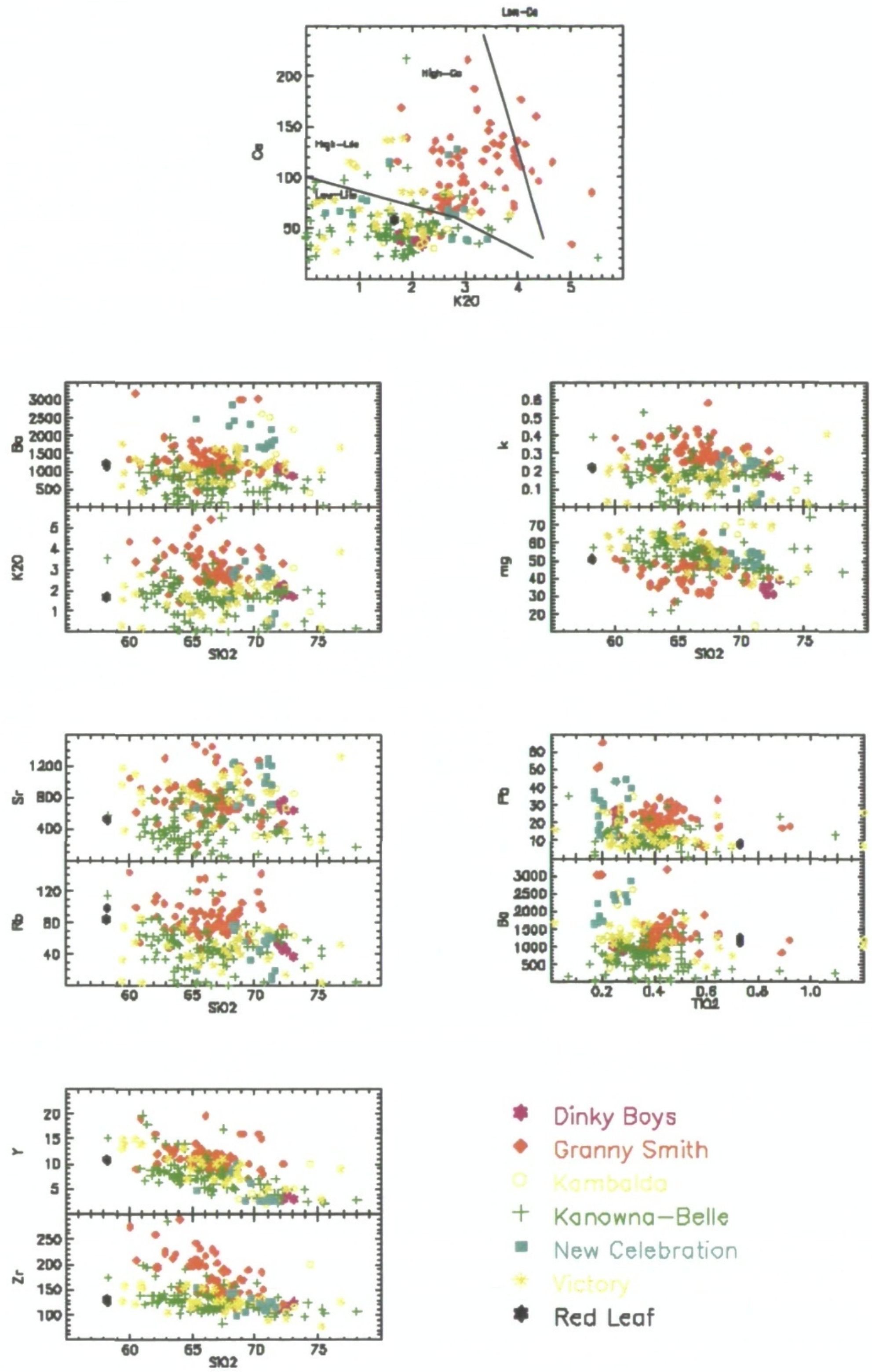

Figure 3.6 Discriminant plots for clans of the Granny Smith (EGP) and Westonia (SCP) Associations, Mafic group, southeastern Yilgarn Craton.

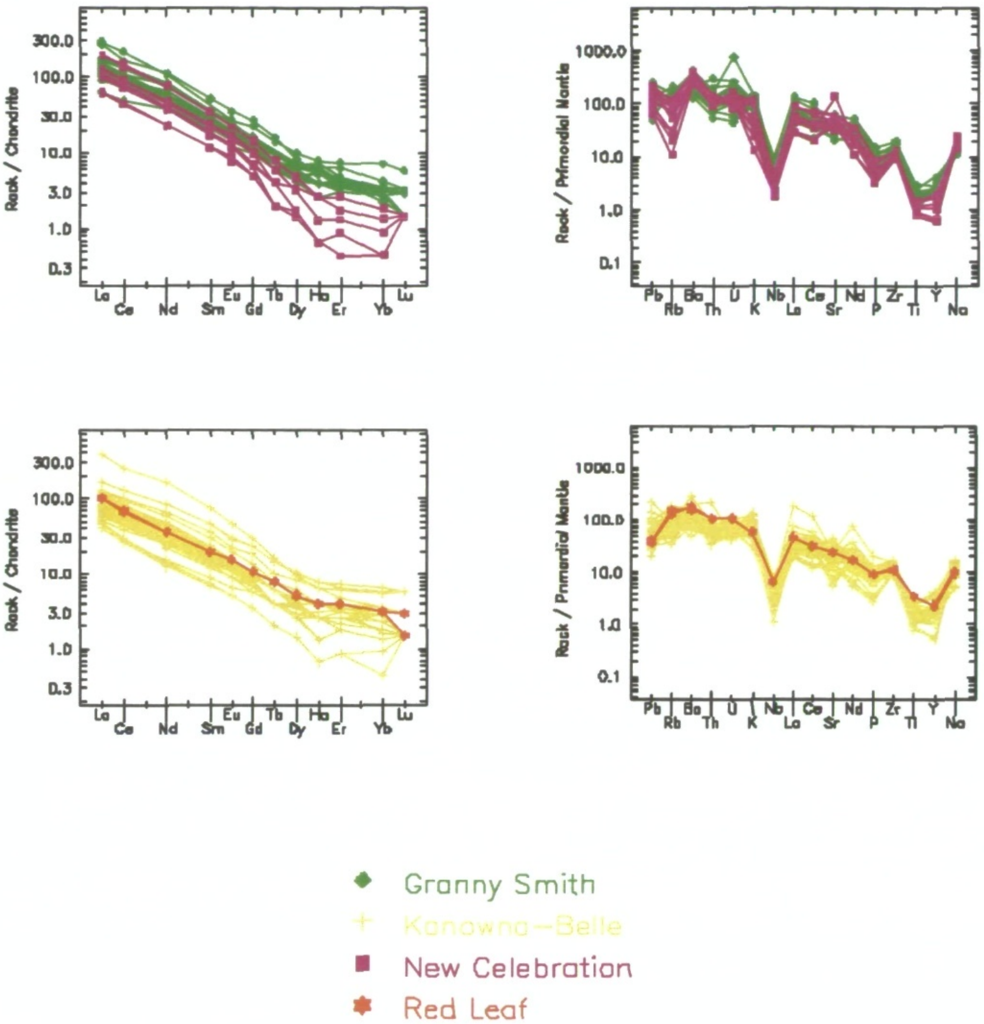

Figure 3.7 Rare-Earth Element (REE) and Primitive-Mantle Normalised multi-element diagrams (Spider-plots) for four clans of the Granny Smith and Westonia Associations, Mafic group, southeastern Yilgarn Craton. Note the consistent fractionated REE patterns without Eu anomalies as well as Sr-undepleted and Y-depleted signature on the Spider-plots.

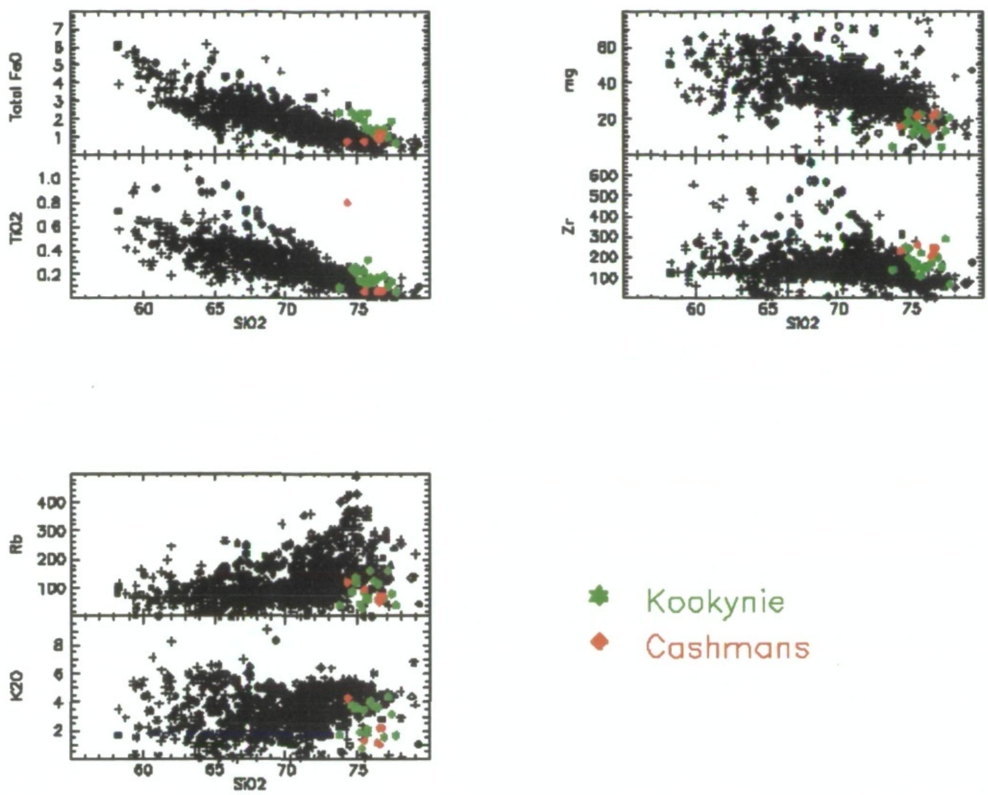

Figure 3.8 Discriminant plots for the Kookynie and Cashmans clans of the Kookynie Associations, High-HFSE group, southeastern Yilgarn Craton, with all other granitoids shown in black for comparison.

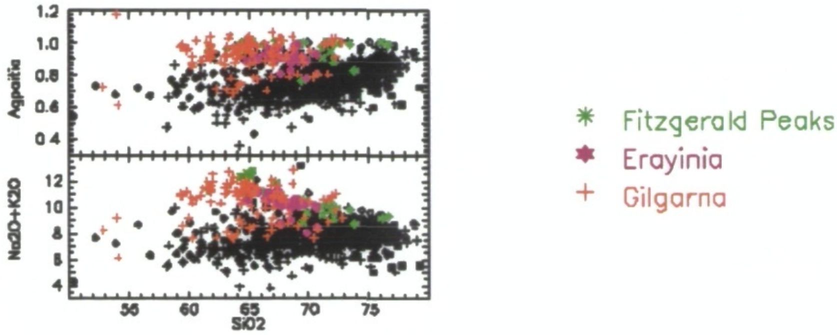

Figure 3.9 Discriminant plots for clans of the Gilgarna (EGP) and Fitzgerald Peaks (SCP) Associations, Syenitic group, southeastern Yilgarn Craton, with all other granitoids shown in black for comparison.

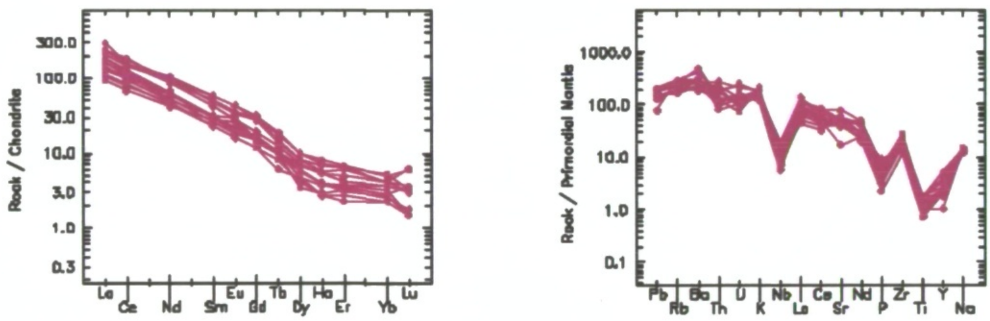

Figure 3.10 Rare-Earth Element (REE) plot and Primitive-Mantle Normalised multi-element diagram (Spider-plot) for the Erayinia clan, Gilgarna Association (EGP), Syenitic group, southeastern Yilgarn Craton.

Chapter 4.
Granites of the northern Southern Cross Province: their distribution, age, geochemistry, petrogenesis, relationship with mineralisation, and implications for tectonic environment.

Anthony R. Budd & David C. Champion

Introduction

This section describes the granites occurring in the northern part of the Southern Cross Province (nSCP) occurring on the Glengarry, Sandstone, Youanmi, Barlee & Jackson 1:250 000 mapsheets. It follows the format and nomenclature of other areas in this volume. The area is dominated by High-Ca and Low-Ca group granites, each occupying about 50% of the outcrop area. Two units are classified as High-HFSE group, although one of these may actually be a fractionated Mafic group granite. One unit is classified as a differentiated Mafic group granite, but may be an unusual High-Ca group granite. No Syenite group granites are recognised. Relatively few granites and volcanics have been dated, and the dating has been restricted mostly to two general areas. These are around the Marda–Diemals area, and the Gum Creek greenstone complex.

This chapter systematically lists and details all groups, associations and clans of the northern Southern Cross Province. A standard format is used for all entries. This covers distribution, geochronology, chemical characteristics, related mineralisation (if any), and includes a brief summary on petrogenesis and tectonic implications by comparison with granites from other areas of the Yilgarn, particularly the Eastern Goldfields Province (EGP).

The following section describes clans under the respective granite group, with individual clan descriptions following a more detailed description of the whole group. All groups are discussed first as a whole – this effectively providing an overall summary of the granites of the nSCP.

Granite groups of the northern Southern Cross Province (nSCP)

Member groups: High-Ca (Diemals association), Low-Ca (Beetle association), High-HFSE (Courlbarloo, Marda clans) & Mafic (Deception Hill clan).

Distribution: The High-Ca and Low-Ca group granites are distributed throughout the report area. Local areas however, are apparently dominated by one group (although this may be a sampling artefact); these include:

- The Yeerlirie Mass (east of the Gum Creek Greenstone belt, see also Champion & Cassidy, northern Eastern Goldfields Province report, this volume) is dominated by the Low-Ca Yeerlirie Clan.
- The area between the Windamurra Mafic Complex and the Barrambie-Youanmi Greenstone belts is dominated by the Low-Ca Skinny Bore and Yarabubba Clans.
- The area surrounded by the Sandstone-Youanmi-Diemals-Illaara-Maynard Hills Greenstone belts is dominated by parts of the High-Ca Yoothapinna, Diemals, Two Mile Hill, Pigeon Rocks and Mondie Clans.

The distribution of the minor granite groups is as follows:

- High-HFSE group granites are very restricted, occurring as two small plutons internal to the Youanmi and Marda Greenstone belts.

- The single Mafic group granite (Deception Hill), occurs internal to the Diemals Greenstone belt.

Geochronology: Relatively few granites and volcanics have been dated, with the dating largely restricted to two general areas. These are around the Marda–Diemals area, and the Gum Creek greenstone belt and surrounds. 27 ages are available (Table 1). The available data show that:

- emplacement of High-Ca group granites (2740–2660 Ma) mostly preceded that of the Low-Ca group granites (2700–~2600 Ma), with some overlap.
- The main period of granite emplacement is around 2700 Ma (Figure 1), which is earlier than in the Eastern Goldfields Province.
- Mafic and ultramafic rocks of the Gum Creek and Diemals–Marda Greenstone belts are also suggested by Wang et al. (1998) to be older than those of the Eastern Goldfields, forming at between 2900 – 3000 Ma. This is the same age as the komatiites in the Lake Johnston greenstone belt, southern SCP (Wang et al. 1996). It is also similar to ages of the older greenstone sequences in the MP (see Champion & Cassidy, this volume).
- The probably syn-volcanic (very high level) Mafic Deception Hill granite is dated at 3023 ± 10 Ma (Nelson 1998), which is older than age estimates for the host Diemals greenstone belt. Either this age is actually an inheritance age and the emplacement age is 2787 ± 26 Ma (one of the age clusters of Nelson 1998), the greenstones were unconformably emplaced above the granite (not likely), or the Diemals greenstone is in part older or synchronous to the granite.

The general sequence of thermal events can be summarised as follows:

3670 Ma	inheritance, Munroes Well granite in Gum Creek greenstone belt (Wang et al. 1998).
3120 – 2900 Ma	inheritance, Buttercup Bore & Munroes Well granites in Gum Creek greenstone belt (Wang et al. 1998), McLeod Rock granite.
3020 Ma	felsic volcanics, Deception Hill porphyry.
2815 Ma	High-HFSE group granite (Courlbarloo plagiogranite). Also approximate age of tholeiite intrusions (eg Windimurra, Youanmi, Atley layered intrusions) – may be a localised rifting event.
2735 – 2730 Ma	felsic volcanics, Marda & Koolyanobbing. High-Ca granites, McLeod Rocks & Pigeon Rocks.
2730 – 2700 Ma	felsic volcanics, Gum Creek. Woodley Bluff & Montague granites.
2700 – 2670 Ma	dominantly High-Ca group, some Low-Ca, specifically Bulga Downs Clan.
2660 - ~2600 Ma	dominantly Low-Ca group, some High-Ca group, and felsic volcanics (Gum Creek).

Chemical characteristics: The geochemistry of the granite groups is summarised by Champion & Cassidy (this volume) in the northern Eastern Goldfields Province (EGP) section of this volume. All groups found in the EGP, except the Syenite group, are also found in the nSCP. However, there are only two occurrences of High-HFSE group granites, one of Mafic group granites, and one suite of lamprophyres. The geochemistry of each granite group in the nSCP is discussed in more detail in the relevant sections below, but a number of generalisations and comparisons can be made here:

- As in the EGP, based on limited dating, clans of the High-Ca associations show an apparent increase in LILE and HFSE with decreasing age (see Fig. 8 and Table 2). This trend mirrors that seen in the change from High-Ca to Low-Ca magmatism.
- There are no significant differences between clans of the High-Ca and Low-Ca groups in the nSCP and EGP, i.e., chemically very similar clans can be found in both provinces. However, the proportions of each granite group are different in the nSCP to the proportions in the EGP. In the nSCP the High-Ca and Low-Ca groups are equally represented, and there are very few High-HFSE or Mafic group granites present, and

no Syenite group granites.

Mineralised members: There are no significant mineral occurrences associated with granitoids in the nSCP.

Petrogenesis: Given the similarities of the granites in the nSCP to those in the EGP, petrogenic models for the nSCP granitoids are as for those of the nMP and the nEGP. A summary of the discussion on petrogenic models for the nEGP granitoids (Champion & Cassidy, this volume) is given below:

- the general characteristics of the High-Ca granites (low LILEs, sodic, Sr-undepleted) indicate derivation, at high pressures (>10 kbar), from a mostly mafic (broadly basaltic/amphibolitic), LILE-poor source. The range in the LILE and HFSE (between clans), however, indicates a more complex model, i.e., the involvement of at least two-components, either as a heterogeneous source (basaltic to quartz dioritic), or by some other process (assimilation of pre-existing crust, magma-mixing etc).
- the potassic, high LILE, high HFSE, Sr-undepleted nature of the Low-Ca group is most consistent with derivation, at moderate pressures (<10 kbar) from a relatively potassic and LILE-rich crustal source, i.e., reworked continental crust with compositions not unlike typical Archaean tonalites. A number of features, though, e.g., low CaO, very minor occurrence of amphibole, indicate partial melting was either via small volume melts or from a source with only minor amphibole. Additionally, the high levels of the HFSEs, in particular Zr, indicate high melting temperatures, suggesting elevated thermal gradients.
- the combination of high HFSE and low to moderate LILE, suggests the High-HFSE group granites were derived by melting of, or fractionation from, LILE-poor mafic to intermediate compositions. The chemistry of the group (elevated Fe, Zr, Y), is also consistent with A-type granitoids in general, indicating high-temperature melts. The Sr-depleted, Y-undepleted nature of all members of the group, strongly imply generation at only moderate pressures, i.e., <10 kbar (<35 km thick), while the Sm-Nd isotope data indicate the significant involvement of pre-existing crustal rocks in the generation of the High-HFSE granites.
- in the EGP, the more felsic clans within the High-HFSE group (Satisfaction, Kookynie) may possibly represent fractionates of rocks similar in composition to the more mafic Bullshead clan of the same group. It was also evident in the EGP that members of the High-HFSE group, especially the less siliceous ones, have some similarities to the members of the Kathleen Valley and Sweet Nell clans (tholeiites of Mafic group), possibly implying some minor involvement of such rocks in the history of the High-HFSE granites. In the nSCP, the Courlbarloo granite has been included in the High-HFSE group, however it is possible that it is a differentiated Mafic group of the tholeiite series, and may be linked to the tholeiitic layered intrusives of the area.
- petrogenetic models for the Mafic group granites are largely equivocal, with evidence for both crustal and mantle-derived contributions. Notably, the variation in the LILE and LREE (between and within clans), requires at least two separate components, e.g., a mafic 'basaltic' source, (like the High-Ca source), and a more mafic, perhaps mantle-derived, LILE-rich source component. The origin of the LILE-rich component is equivocal, although within the EGP the overlap of ages (ca. 2665 Ma), between the high LILE Mafic and some Syenitic group magmatism, indicates a possible source of, at least part of, the LILE and LREE enrichment. In the EGP, the minor Kathleen Valley and Sweet Nell clans of the Mafic group largely represent fractionates from a basaltic, tholeiitic parent. Such rocks may also exist within the nSCP, e.g., related to the mafic complexes. Also it is possible that the Courlbarloo granite belongs to this type, as mentioned earlier.

Tectonic and other implications: The Southern Cross Province and the Murchison Province (MP) share a similar crustal history since about 3020 Ma, as is evidenced by the similarity of magmatic events in both provinces since this time. It is probable that the nSCP and nMP have been one crustal block since that time. The reader is referred to the discussions on tectonics in both the northern Murchison and northern Eastern Goldfields Provinces in this volume. Two points are made:

- The peak of granite activity is earlier in the nSCP and nMP than in the nEGP.
- Rifting along the eastern nMP/western nSCP is marked by tholeiitic magmatism at ~2800 Ma, and this indicates a minimum age that the two provinces must have been joined.

Sampno	1:250 000	Unit	Supersuite	Clan	Age	inherited	Ref	Com
High-Ca								
98969033	Sandstone	Tom Bore	Tom Bore	Diemals	2671 ± 3		1	OK
97969082A	Youanmi	The Spring	Diemals	Diemals	2682 ± 5		1	OK
97969104	Barlee	Native Well	Diemals	Diemals	2682 ± 6		1	OK
168903	Barlee	Johnson Rocks	Johnson Rocks	Diemals	2693 ± 4		4	OK
98969045	Sandstone	Monty Bore	Atley	Yoothapinna	2700 ± 15		1	OK
98969055	Sandstone	Woodley Bluff	Atley	Yoothapinna	2712 ± 6		1	OK
93-992	Sandstone	Old Gidgee	Old Gidgee	Gnabberdocking	2699 ± 7		2	OK
95YQ 87	Jackson	Koolyanobbing	Gnabberdocking	Gnabberdocking	2656 ± 3		6	OK
121380	Jackson	Maries Find	?	?	2688 ± 3		6	Pb-Pb min
97969102B	Barlee	McLeod Rock	Mondie	Mondie	2737 ± 7	~3010	1	OK
142919	Barlee	Pigeon Rocks	Pigeon Rocks	Pigeon Rocks	2729 ± 4		8	OK
93-994	Sandstone	Montague Granite	Montague	unassigned	2722 ± 7		2	OK?
Low-Ca								
98969025	Sandstone	Buttercup Bore	Buttercup Bore	Yeerlirie	2661 ± 7		1	OK
93-1000	Sandstone	Bonza Bore	Buttercup Bore	Yeerlirie	2682 ± 8	3124±41,2908±26	2	OK?
93-993	Sandstone	Munroes Well	Munroes Well	Yeerlirie	2638 ± 10	3671±29, ~3000	2	OK?
93-1006	Sandstone	NE Coomb Bore	NE Coomb Bore	Bulga Downs	2680 ± 5		3	OK?
97969063	Youanmi	Bulga Downs	Bulga Downs	Bulga Downs	2684 ± 8		1	OK
142915	Barlee	Olby Rock	Olby Rocks	Bulga Downs	2697 ± 8	2738 ± 16	8	OK
98969042	Sandstone	Barlangi Well	Yarrabubba	Yarrabubba	no date	2714 ± 18	1	OK
98969044	Sandstone	Yarrabubba	Yarrabubba	Yarrabubba	2650 ± 9		1	OK
93-1007	Youanmi	Mica Well	Mica Well	Skinny Bore	~2600		3	uncertain?
High-HFSE								
168959	Jackson	Butcher Bird	Butcher Bird	Marda	2730 ± 4		7	OK
98968104	Youanmi	Courlbarloo	Courlbarloo	Courlbarloo	2813 ± 5		1	OK
Mafic								
142920	Barlee	Deception Hill	Deception Hill	Deception Hill	3023 ± 10		8	OK
Felsic volcanics								
93-995	Sandstone	Gum Creek metarhyolite			2702 ± 6		2	OK?
93-996	Sandstone	Gum Creek metarhyolite			2652 ± 18	2722 ± 14	2	OK?
W165	Barlee	Marda Complex felsic volcanic			2735 ± 2		5	Con U-Pb
W193	Jackson	Koolyanobbing felsic volcanic			2736 ± 10		5	Con U-Pb

Table 1. Geochronological data for all groups of the northern Southern Cross province; all ages (in Ma) are SHRIMP zircon ages unless indicated otherwise. Data sources: 1 – AMIRA P482; 2 – Wang et al. 1998; 3 – Wang (ANU) unpublished; 4 – Nelson 1999; 5 – Pidgeon & Wilde 1990 conventional U-Pb zircon; 6 – Qiu et al (in press, AJES); 7 – Nelson 2001 (in press); 8 – Nelson 1998.

Com = comments and refers to the interpreted reliability of the age.

High-Ca group, northern Southern Cross

Member Associations: Diemals Association.

Distribution: The High-Ca group makes up about 50% of the granites of the northern Southern Cross Province, and is distributed fairly evenly throughout the area. Three associations with eight clans have been recognised in the area.

Geochronology: The dating available indicates an age range from 2.74 to 2.65 Ga, with the majority falling at about 2.7 Ga (Table 1, Figure 1). This age range is similar to that seen in the EGP, but the peak of intrusive activity is older in the nSCP than the EGP (peak of activity in EGP is between 2.685 to 2.66 Ga, Champion & Cassidy, this volume).

Few ages from inherited zircons are noted in the literature. Seven Sm-Nd analyses are available, see Fletcher & McNaughton (this volume).

Chemical characteristics. Characteristics for this group have been summarised by Champion & Sheraton (1997), and Champion (1997). Basically the High-Ca granites comprise sodic trondhjemite, granodiorite and granite characterised by low to moderate LILE (K_2O, Rb, Pb) and HFSE (LREE, HREE, Y, Zr) contents. In detail individual clans (Table 2), define a quasi-continuous range in LILE and HFSE contents, from low (Yoothapinna clan) to moderate (Diemals clan, see Fig. 3), approaching values seen in the Low-Ca granites (Fig. 5). Given the range in the LILE and HFSE, an arbitrary divide splitting the High-Ca group into low-LILE and high-LILE members has been produced, largely for the basis of classification and descriptive purposes (Fig. 8).

The majority of granitoids from the High-Ca group are further characterised by moderate to high Sr contents (Sr-undepleted) coupled with low to moderate Y (and HREE) contents (Y-depleted; Fig. 4). However, like the LILE, there is a range in concentration of these elements, albeit it less pronounced, to Sr-depleted and Y-undepleted compositions.

Geochemical discrimination between the High-Ca and other groups is mostly relatively straightforward (Figs. 6, 7, 8). Most difficulty occurs with the siliceous Deception Hill clan of the Mafic group, as its composition strongly converges with that of the low-LILE clans of the High-Ca group (Figs. 6, 7, 8). Although differences between the two are apparent, e.g., Ni, Cr, MgO, mg# (Fig. 6), it is possible that the High-Ca group includes some members which more correctly belong to the Mafic group, and vice versa.

Mineralised members? None.

Petrogenesis: The following discussion is modified from the summary of the petrogenesis of the High-Ca group granites in the nEGP (Champion & Cassidy, this volume). The general characteristics (low LILEs, sodic) indicate derivation from a mostly mafic LILE-poor source, probably broadly basaltic in composition. The range in the LILE and HFSE (between clans), however, points to a compositional range in the source also, i.e., the differences can not be solely due to varying degrees of partial melting. Such a compositional variety strongly indicates the involvement of at least two-components, either as a heterogeneous source (basaltic to quartz dioritic), or by some other process (assimilation of pre-existing crust, magma-mixing etc). Notably in this regard, Sm-Nd isotopic evidence indicates no significant component of the Low-Ca source was involved in the generation of the High-Ca granites in either the Murchison or Eastern Goldfields, i.e., the higher LILE and HFSE contents in some members of the High-Ca group (in those provinces) can not have resulted from the involvement of Low-Ca granites or their sources. Although the isotopic data is more equivocal for the SCP, a similar conclusion is to be expected.

The Sr-undepleted, Y-depleted nature of the majority of the High-Ca granites indicate derivation at pressures great enough to stabilise garnet and destabilise plagioclase (10-15 kbar) either deep within a thickened crust (>35-50 km) or, perhaps, from melting of a subducting slab (e.g., Martin, 1986). Either process is feasible, though the presence of inherited zircons, the range in Sr and Y to Sr-depleted and Y-undepleted compositions, and the Sm-Nd isotopic data favour a thickened crust source.

Tectonic & other implications: The following discussion is taken from the section of High-Ca group granites of the northern Murchison Province (Champion & Cassidy, this volume; the reader is referred to that section). As shown earlier in this chapter, it is apparent that the nMP and nSCP have shared a similar crustal history at least since ~3020 Ma.

The bulk of the evidence for the MP, and hence for the SCP, appears to favour a thickened crust (>35-50 km) origin for the High-Ca granites. It is, however, also apparent that derivation from a subducting slab is also a possible viable mechanism for production of at least some of the High-Ca granites. Importantly, both the thickened crust or melting of a subducting slab hypotheses, require the operation of some form of convergent tectonics contemporaneous or just prior to granite generation. This can be interpolated, therefore, to infer that all periods of High-Ca granite formation correspond roughly to times of convergent tectonics in the Murchison (and Southern Cross) Provinces, i.e., 2675-2765 Ma, 2780-2825 Ma, 2920-2960 Ma, and 3000-3025 Ma. As noted before (Champion & Cassidy, this volume), the timing of these tectonic settings, especially post 2.72 Ga, contrasts somewhat with that for the Eastern Goldfields Province, i.e., pre 2.68 Ga High-Ca magmatism was very common in the Murchison and Southern Cross provinces but relatively minor in the Eastern Goldfields Province, 2.68 to 2.66 Ga magmatism was minor in the Murchison and Southern Cross provinces but voluminous in the Eastern Goldfields Province. Clearly there are a number of possible scenarios, not mutually exclusive, that may explain these apparent differences, e.g., the Murchison and Southern Cross provinces were separate from the Eastern Goldfields Province before and/or during this period, the change across the Murchison and Southern Cross provinces to the Eastern Goldfields Province is actually diachronous, as in a migrating arc-environment, or perhaps the thermal regime at 2.68-2.66 Ga was such that granite production was largely confined to the Eastern Goldfields Province, such as in a typical modern-day convergent environment. Clearly further geochronology would be helpful, particularly along the eastern margin of the Southern Cross Province and western margin of the Eastern Goldfields Province.

In addition, the large volume of High-Ca granites in the northern Southern Cross Province, and the other provinces, clearly requires a correspondingly larger source (3 or more times volumetrically larger). This has important implications if the High-Ca granites were crustal-derived, requiring a very significant volume of pre-existing crust of relatively homogenous 'basaltic to andesitic' composition.

High-Ca Clan	Diemals Association Supersuite	northern Southern Cross Province Suite
Diemals	Diemals	Christmas Bore, Diemals, Jan Bore, Lana Bore, North Diemals, Outcamp Bore, The Spring, Wungrun, Moola Bore Complex
	Johnson Rocks	Johnson Rocks
	Porcupine	Baum Well, Patent Well, Porcupine Well, Rafferty Patch Well, Ramona Well, Sommer Well, Two Brothers Well
	Tom Bore	Tom Bore
	Unaly Hill	Unaly Hill
	Waukenjerrie	Waukenjerrie, Hill 490
Gnabberdocking	Gnabberdocking	Gnabberdocking, Kangaroo, Koolyanobbing Gneiss, West Chidarcooping Hill
	Nierguine	Chadwick, Nierguine, Three Mile Rocks, unassigned
	Old Gidgee	Old Gidgee
	Shaws Bore	Shaws Bore
Suggard	Suggard Bore	Suggard Bore
Two Mile Hill	Two Mile Hill	Two Mile Hill
Yoothapinna	Atley	Atley, Babba Wallia, Beaton Bore, Bowman Well, Bradley Well, Bull Oak, Bullock Bore, Bux's Bore, Dooly Well, Monty Bore, Nanadie Well, Number Six Well, Poison Hills, Woodley Bluff
	Ayer Well	Ayer Well
	Bulchina Well	Bulchina Well
	Darrine Rock	Darrine Rock
	Edale Fault Gneiss	Edale Fault Gneiss
	Mallee Hen	Mallee Hen
	Peregrine Bore	Peregrine Bore
	Yoothapinna	Red Tank, Yoothapinna
	Yuinmery	North Johnson Rocks, Number One Bore, Tom Well, Walgarry, Yuinmery
Pigeon Rocks	Little Noondie	Little Noondie, Noondie Well
	Pigeon Rocks	Dooling, East Evanston, Manning-Hunt, West Yarbu, Wolgling, unassigned
	Marda Complex	Butcher Bird

High-Ca Gneissic Clans	Diemals Association Supersuite	northern Southern Cross Province Suite
Mondie	Mondie	Jan Bore, McLeod Rock, Visitors Bore
Lake Seabrook	Lake Seabrook	Lake Seabrook, unassigned

Table 2. Suites, supersuites, clans and associations of the High-Ca group, northern Southern Cross Province.

Clans of the Diemals Association, High-Ca Group, Southern Cross Province

Diemals Clan

Member Supersuites: Diemals, Johnson Rocks, Porcupine, Toms Bore, Unaly Hill, Waukenjerrie.

Distribution: Considerable north-south extent, from south of the Sandstone greenstone belt to the north of the Marda greenstone belt. Western side of the Yeerlirie Mass of the northern Eastern Goldfields.

Geochronology: Four samples have been dated: Toms Bore Granite (Tome Bore Supersuite) at 2671 ± 3 Ma, The Spring Granite (Diemals Supersuite) at 2682 ± 5 Ma, Native Well Granite (Lana Bore Suite, Diemals Supersuite) at 2682 ± 6 Ma, and Johnson Rocks Granite (Johnson Rocks Supersuite) at 2693 ± 4 Ma.

Chemical characteristics: Falls into high LILE and HFSE end-members of the High-Ca group (Figs. 3, 4, 8). Some samples have elevated K_2O, Th, Y and Rb relative to other members of the Diemals Association.

Mineralised members? None.

Petrogenesis: As for the High-Ca group generally.

Tectonic & other implications: As for the High-Ca group generally.

Gnabberdocking Clan

Member Supersuites: Gnabberdocking, Nierguine, Old Gidgee, Shaws Bore.

Distribution: Dominantly on central Jackson Sheet (south of Marda greenstone belt – Nierguine & Gnabberdocking Supersuites). Two outcrops occur on the eastern part of Sandstone (east of Gidgee greenstone belt): the Old Gidgee syenogranite and the Shaws Bore Granite.

Geochronology: Two ages are available for units assigned to the Gnabberdocking Clan, but there is some uncertainty that both units are correctly assigned. The Koolyanobbing monzogranite (Gnabberdocking Supersuite) has an age of 2656 ± 3 Ma, and the Old Gidgee syenogranite (Old Gidegee Supersuite) has an age of 2699 ± 7 Ma.

Chemical characteristics: Mostly this clan is similar to the Diemals Clan in having higher Rb, Th, Y and Ce and lower Sr than other clans of the Diemals Association (particularly Yoothapinna Clan). The Gnabberdocking clan has an unusual flat trend for Ce, whereas most other members of the Diemals Association have decreasing Ce with increasing SiO_2 (Fig. 4). Overall, the clan fits in the High LILE and HFSE end member of the High-Ca group.

Mineralised members? None.

Petrogenesis: As for the High-Ca group in general.

Tectonic & other implications: As for the High-Ca group in general.

Suggard Clan

Member Supersuites: Suggard Bore.

Distribution: Restricted to only two samples in the Yuinmery Gneiss Zone, central southern Youanmi Sheet.

Geochronology: None.

Chemical characteristics: Felsic (~74.5 wt% SiO_2), high LILE and HFSE end of High-Ca group (Fig. 4).

Mineralised members? None.

Petrogenesis: As for the High-Ca group in general.

Tectonic & other implications: As for the High-Ca group in general.

Two Mile Hill Clan

Member Supersuites: Two Mile Hill.

Distribution: One of the few internal granites in the northern Southern Cross Province, intruding the Sandstone Greenstone Belt. Very restricted in extent, only one occurrence.

Geochronology: None.

Chemical characteristics: Three samples, all approximately 69 wt% SiO_2, low LILE member of High-Ca group (Fig. 4).

Mineralised members? None.

Petrogenesis: As for the High-Ca group in general.

Tectonic & other implications: As for the High-Ca group in general.

Yoothapinna Clan

Member Supersuites: Atley, Ayer Well, Bulchina Well, Darrine Rock, Edale Fault Gneiss, Malle Hen, Peregrine Bore, Yoothapinna, Yuinmery.

Distribution: Very extensive, occurring mostly on the Glengarry, Sandstone & Youanmi Sheets, but with limited outcrop on the Barlee & Jackson Sheets.

Geochronology: This is one of the oldest clans of the Diemals Association, with two samples of the Atley Supersuite, dated at 2700 ± 5 Ma and 2712 ± 6 Ma.

Chemical characteristics: Extensive silica range, from 66 to >75 wt%. Low LILE and HFSE member of High-Ca group.

Mineralised members? None.

Petrogenesis: As for the High-Ca group in general.

Tectonic & other implications: As for the High-Ca group in general.

Pigeon Rocks Clan

Member Supersuites: Little Noondie, Pigeon Rocks.

Distribution: The majority of this clan occur in and around the Johnson Range – Blue Hills greenstone belts on the Barlee and Jackson sheets. Also has a limited occurrence in the Yuinmery Gneiss Zone (Younami Sheet). The Pigeon Rocks Supersuite is unusual for the northern Southern Cross Province in that it is one of the few granites that are internal to the greenstone belts.

Geochronology: A sample of foliated biotite monzogranite from the Pigeon Rocks (Nelson 1999) gives an age of 2729 ± 4 Ma. This is one of the oldest High-Ca granites in the northern Southern Cross Province.

Chemical characteristics: Mostly as for the High-Ca group in general, but is notable for lower CaO and Sr than most, and correspondingly high Rb, Pb and Y. Compared to the Diemals Association, the Pigeon Rocks Clan is higher in some of the LILE (K_2O, Pb and Rb) and Y, and lower in Sr and CaO. These characteristics are partly intermediate between the High- and Low-Ca groups.

Mineralised members? None.

Petrogenesis: As for the High-Ca group in general.

Tectonic & other implications: As for the High-Ca group in general.

Gneissic clans of the Diemals Association, High-Ca Group, Southern Cross Province

Mondie Clan

Member Supersuites: Mondie.

Distribution: Occurs in southeastern Youanmi Sheet, around the Mount Elvire and Crook Well greenstone belts. Limited extent.

Geochronology: McLeod Rock is dated at 2737 ± 7 Ma, with inheritance at ~3010 Ma..

Chemical characteristics: Low LILE and HFSE (Fig. 4). Compared to the Diemals Association, the Southern Cross Gneiss Association is low-LILE, including K_2O, Ce, Pb and Rb, and lower in some HFSE including Y and Th. It is similar to the Yoothapinna Clan, which also occurs in the same broad area, but the Yoothapinna clan is younger.

Mineralised members? None.

Petrogenesis: As for the High-Ca group in general.

Tectonic & other implications: As for the High-Ca group in general.

Lake Seabrook Clan

Member Supersuites: Lake Seabrook.

Distribution: Four samples, restricted to the southern Jackson Sheet around Lake Deborah East and Lake Seabrook, between the Marda and Bullfinch greenstone belts.

Geochronology: None.

Chemical characteristics: Falls in the low LILE and HFSE part of the High-Ca group. Some spread in values. See discussion for Mondie Clan.

Mineralised members? None.

Petrogenesis: As for the High-Ca group in general.

Tectonic & other implications: As for the High-Ca group in general.

Low-Ca Group, northern Southern Cross Province

Member Associations: Beetle Association

Distribution: The Low-Ca granites of the Beetle Association (Table 3), northern Southern Cross Province (nSCP), are fairly evenly distributed throughout the five mapsheets, and account for approximately 45% of samples. There are very few internal granites in the nSCP; some of these are of the Beetle Association. The Beetle Association also occurs in the northern Eastern Goldfields (Champion, this volume) and the northern Murchison (Champion & Cassidy, this volume). Eleven clans are recognised in the nSCP, most are moderately localised.

Geochronology: Eight ages are available for this Group (Table 2), but only six appear to be reasonable. The age range (of the six) is from 2684 Ma to 2638 Ma. Half of these ages are within error of 2680 Ma.

Chemical characteristics: Characteristics for this group have been summarised by Champion & Sheraton (1997), and Champion (1997). The Low-Ca group comprise potassic granites characterised by high LILE (K_2O, Rb, Pb, Th, U) and HFSE (LREE, HREE, Y, Zr) contents (Figs. 2, 7, 10), with moderate to strong negative Eu anomalies (Sr-depleted), flat HREE patters, and mostly Y-undepleted, but ranging to Y-depleted, compositions. As in the nMP and nEGP, individual clans exhibit a range in LILE and HFSE contents, and are described in the following sections.

Both the nMP and nEGP Low-Ca group granites exhibit a narrow range in ε_{Nd} (-3.4 to –4.6), that overlap completely with members of the High-HFSE group, but are clearly more evolved (more negative), than High-Ca and Mafic group granites (Fletcher & McNaughton, this volume, and Champion & Sheraton 1997). Sm-Nd isotopic data available for the nSCP shows that the range for ε_{Nd} is wider (-3.46 to 0.28), and is within the range of the High-Ca group (-4.20 to 0.75). The Courlbarloo plagiogranite, which has been classified as an High-HFSE group granite (but may belong to the Mafic group) has a very primitive ε_{Nd} value of 3.88.

Mineralised members? None.

Petrogenesis: The characteristics of the Beetle Association, and the Low-Ca group granite in general, i.e., potassic, high LILEs, elevated HFSEs, indicate derivation from an, at least moderately, potassic and LILE-rich crustal source, i.e., some form of pre-existing continental crust, possibly compositions not unlike typical Archæan tonalites (Champion & Sheraton 1997). The low CaO in the Low-Ca granites and the very minor occurrence of amphibole in the granites themselves, indicate partial melting was largely via dehydration melting driven by biotite breakdown, i.e., either small volume melts or from a source with only minor amphibole. Further the high levels of the HFSEs, in particular Zr, in the Low-Ca granites, strongly indicate high temperature melting (i.e., zircon saturation and, hence, levels of Zr in a granite melt are strongly temperature dependent), a fact which may also be consistent with a generally water-poor (limited amphibole) source. Finally, the mostly Y-undepleted and Sr-depleted nature suggests that the Low-Ca granites were generated at moderate crustal levels (mostly <35 km).

The variation in LILE, in particular, and the HFSE, between the Low-Ca clans, may reflect a variety of processes, including:

- changes in the percentage of partial melting, i.e., the greater percentage of melt, the

lower the concentration of LILEs in the melt,
- variations in source compositions,
- variable mixing of two or more source components, e.g., perhaps a component of a source similar to that envisaged for the High-Ca granites.

Finally, it is evident that the variation in the HFSE, Na_2O and K_2O, and Sr and Ba, between clans, also indicate some differences in LILE and HFSE contents of the source rocks for the Low-Ca clans.

Tectonic & other implications: The following discussion is modified from Champion & Cassidy: northern Murchison Province (this volume).

The simplest model for the Low-Ca granites, would appear to require their generation from moderately dry tonalitic (or more felsic) pre-existing crust, in an extensional environment most probably with an elevated geothermal gradient (needed to get the postulated high melting temperatures). This is clearly contrary to the general scenario for the High-Ca granites, indicating not only distinct source rocks, but distinct sites of granite generation for the two granites. These differences between the High-Ca and Low-Ca sources are also supported by the available Sm-Nd isotopic data which indicate isotopically distinct source reservoirs for the two granite groups (Fletcher & McNaughton, this volume). As for the Eastern Goldfields Province, these differences are even more significant when the age distributions of the two granites groups are taken into consideration, i.e., the temporal change from dominantly High-Ca magmatism to less voluminous, but very widespread, dominantly Low-Ca magmatism, around 2660 to 2650 Ma. This changeover in magmatism presumably must correspond to some fundamental change in tectonic environment, perhaps from a compressional or arc-related environment to one dominated by extension or post-tectonic relaxation, i.e., some mechanism produced a change in the thermal regime, that not only increased the thermal gradient (to allow generation of Low-Ca granites) but effectively turned off production of High-Ca granites.

As discussed for the Eastern Goldfields Province (Champion and Cassidy, this volume), the exact nature of this tectonic transition is largely dependent on the origin of the High-Ca granites. If, as favoured for the northern Murchison, the High-Ca granites were generated by partial melting in thickened crust, then the change to Low-Ca magmatism indicates melting shifted to higher crustal-levels (the site of Low-Ca generation), with the thickened lower crust (High-Ca source) either somehow insulated from further melting or removed. In this regard, Smithies & Champion (1999) suggested that this post 2660 Ma thermal event may have resulted from Yilgarn-wide lower-crustal delamination following crustal thickening during the main D_2 shortening deformation in the Eastern Goldfields Province. These authors further speculated that this event represented an additional tectonothermal event in the Yilgarn Craton, contemporaneous with lower-middle crustal high-grade metamorphism and regional Au mineralisation (e.g., Kent et al. 1996).

If, however, the High-Ca granites were largely generated by slab-melting, a scenario considered less likely, then the change over to Low-Ca (and High-HFSE) magmatism may simply reflect some form of wide-scale extension, perhaps not unlike that presently operating in the Basin and Range province in the western United States, although with some differences, e.g., lack of contemporaneous felsic volcanism.

Finally, the possible component of High-HFSE group source in the Horseshoe clan, suggests an overlap in not only time but also in process and/or crustal level of generation between the Low-Ca and High-HFSE groups. Notably, this is consistent with the Sm-Nd isotopic data, which indicate similar isotopic signatures for both granites groups.

Tectonic & other implications: The reader is referred to discussions in the northern Eastern Goldfields (Champion, this volume) and northern Murchison Province (Champion and Cassidy, this volume) Low-Ca group sections. However, there do appear to be some differences in the northern Southern Cross Province which should be taken into account. From the limited isotopic data available, Low-Ca granites appeared earlier than in either the nEGP or the nMP, and there is more significant overlap in ε_{Nd} values of the Low-Ca group with the High-Ca group than in the other two provinces (but this is only based on three analyses).

Low-Ca (SCP) Clan	Beetle Association Supersuite	Suite
Barcoo	Barcoo Bore	Barcoo Bore
Bulga Downs	Bulga Downs	Bulga Downs, Cabaret Bore, Denham Bore, Edale, Kohler Bore, Moola Moola, Rising Fast, Stock Well
	Olby Rocks	Olby Rocks
	NE Coomb Bore	NE Coomb Bore gneiss
	Salt Bore	Salt Bore
Bacon Hill	Mt Correll	Chidarcooping, Elachbutting, Mt Correll
	Speen Hill	Speen Hill, unassigned
Weowanie	Journalogwin	Journalogwin
Cooliboo Bore	Cooliboo Bore	Cooliboo Bore
Lake Barlee	Lake Barlee	Lake Barlee, Ullamby Soak
Rainy Rocks	Rainy Rocks	Rainy Rocks
Red Knob	Corkscrew Well	Corkscrew Well, Everett Creek
	Red Knob	Elspon Well, Red Knob, Rocky Well, Yingarrie
	West Clampton	West Clampton
Rocky Dump	Rocky Dump Well	Rocky Dump Well
Skinny Bore	Skinny Bore	Dowden Well, Mica Well, Nalganadga Bore, No-Ibla, Skinny Bore
Unassigned	Gum Tree Bore	Gum Tree Bore
Yarrabubba	Yarrabubba	Yarrabubba, Barlangi Rock
Yeerlirie	Black Hill	Black Hill
	Buttercup Bore	Buttercup Bore, Bonza Bore
	Caluyu Bore	Caluyu Bore, O'Connor, Samaria
	Dummy Well	Dummy Well
	Milgoo Well	Milgoo Well
	Munroes Well	Munroes Well
	North Alston	North Alston
	Satan	Hell Gates, Les Bore, Number Two Bore, Satan
	Wallaby Knob	Wallaby Knob
	Yarloo Spring	Yarloo Spring
	Yeerlirie	Bluff Point, Easter Mile, Red Handed, Yeerlirie, unassigned

Table 3. Suites, supersuites, clans and associations of the Low-Ca group, northern Southern Cross Province.

Clans of the Beetle Association, Low-Ca Group, Southern Cross Province

Barcoo Clan

Member Supersuites: Barcoo Bore

Distribution: One granite, located in the northeastern Sandstone sheet, within what is otherwise dominantly Yeerlirie Clan granites. Between Gum Creek and Booylgoo Range greenstone belts.

Geochronology: None.

Chemical characteristics: Two samples. Separated from the Yeerlirie Clan by significantly higher Sr, otherwise geochemistry is as for Yeerlirie Clan (Fig. 5).

Mineralised members? None.

Petrogenesis: As for the Low-Ca granites in general.

Tectonic & other implications: As for the Low-Ca granites in general.

Bulga Downs Clan

Member Supersuites: Bulga Downs, NE Coomb Bore, Salt Bore and Olby Rock.

Distribution: The NE Coomb Bore Gneiss occurs on the northeastern margin of the Sandstone greenstone belt. The Salt Bore granite occurs near the centre of the Youanmi Sheet. Olby Rock occurs just to the northeast of the Marda Greenstone Belt. The majority of the Bulga Downs Supersuite occurs between the Elvirie Greenstone Belt and the White Cloud Gneiss Zone on the Youanmi sheet.

Geochronology: Three samples have been dated. The Bulga Downs granite (Bulga Downs Supersuite) is dated at 2684 ± 8 Ma and the NE Coomb Bore gneiss (NE Coomb Bore Supersuite) at 2680 ± 5 Ma. No inheritance was recorded. A sample of foliated biotite monzogranite from Olby Rock (Olby Rocks Supersuite) was dated at 2697 ± 8 Ma. This is within error of the age of the Bulga Downs granite. Xenocryst zircons from this sample give an age of 2738 ± 16 Ma. Samples from this clan are the oldest recorded unequivocal Low-Ca granites within the Yilgarn.

Chemical characteristics: SiO_2 range of 70.5 – 75.5 wt%. This clan is within the normal ranges for the Beetle Association, but with some samples having slightly higher Rb, Th and Y (Fig. 5).

Mineralised members?: None.

Petrogenesis: As for the Low-Ca granites in general.

Tectonic & other implications: As for the Low-Ca granites in general.

Bacon Hill Clan

Member Supersuites: Mt Correll, and Speen Hill.

Distribution: Speen Hill & Mt Correll Supersuites occur on southwestern Jackson Sheet, west of the Bullfinch greenstone belt.

Geochronology: None.

Chemical characteristics: SiO_2 range of 69.5 – 76 wt%. As noted above, there is some scatter in this group, possibly indicating that the clan should be broken into two. Otherwise, this clan is within the normal ranges for the Beetle Association, but with some samples having slightly higher Rb, Th and Y.

Mineralised members?: None.

Petrogenesis: As for the Low-Ca granites in general.

Tectonic & other implications: As for the Low-Ca granites in general.

Weowanie Clan

Member Supersuites: Journalogwin.

Distribution: Between Bullfinch/South Cross Greenstone Belt & Marda Greenstone Belt, Jackson sheet. Two occurrences.

Geochronology: None.

Chemical characteristics: The two samples are very similar; both are quite felsic (~74 wt% SiO_2). This clan is very similar to the Bulga Downs and Bacon Hill clans. One sample has slightly lower Rb & Pb.

Mineralised members?: None.

Petrogenesis: As for the Low-Ca group in general.

Tectonic & other implications: As for the Low-Ca group in general.

Cooliboo Bore Clan

Member Supersuites: Cooliboo Bore.

Distribution: Four samples taken from southwest of the Youanmi Layered Mafic Intrusion on the southwest of the Youanmi Sheet. The granite is probably about 10x10 km in dimension.

Geochronology: None.

Chemical characteristics: Slightly lower K_2O and higher Y than the rest of the Association, otherwise normal. Low LILE & moderate HFSE endmember of Low-Ca group.

Mineralised members?: None.

Petrogenesis: As for the Low-Ca granites in general.

Tectonic & other implications: As for the Low-Ca granites in general.

Lake Barlee Clan

Member Supersuites: Lake Barlee.

Distribution: The six samples form an interesting north-northwest trending arc extending from Ullumbay Soak (Jackson Sheet) to Midget Bore in the Yuinmery Gneiss Zone (Youanmi).

Geochronology: None.

Chemical characteristics: All samples are between 69 – 70 wt% SiO_2, which is near the mafic end of the Beetle Association. Three of the samples have slightly higher total Fe than other members of the Association, but otherwise the chemical characteristics are as for the rest of the Association. Low LILE and low HFSE endmember of Low-Ca group; very similar to Yeerlirie clan to the north.

Mineralised members?: None.

Petrogenesis: As for the Low-Ca granites in general.

Tectonic & other implications: As for the Low-Ca granites in general.

Rainy Rocks Clan

Member Supersuites: Rainy Rocks.

Distribution: Confined to the Diemals greenstone belt, which is also host to the Marda Complex, on the southern Barlee Sheet. Forms a narrow (<5 km) northeast-trending belt 20 km long. One of few internal Low-Ca group granites in nSCP.

Geochronology: None.

Chemical characteristics: Covers a range of ~71 – 76 wt% SiO_2, and is distinguished by higher Pb, Y, CaO, and for some samples Ce. Otherwise normal for Beetle Association. Probably low LILE high HFSE endmember.

Mineralised members?: None.

Petrogenesis: As for the Low-Ca granites in general.

Tectonic & other implications: As for the Low-Ca granites in general.

Red Knob Clan

Member Supersuites: Corkscrew Well, Red Knob, West Clampton.

Distribution: A distinct NW-linear trend along the White Cloud Gneiss Zone/North Crook Well greenstone belt (Youanmi Sheet) to the Barrambie Belt (Sandstone Sheet). A subtle magnetic feature is visible on this trend.

Geochronology: None.

Chemical characteristics: The Red Knob Clan is fairly distinct – it shows the same trends as the rest of the Beetle Association, but element abundances are slightly different (Fig. 7). The SiO_2 range is wide, from 67 to 75 wt%. K_2O, Ce, Zr, and for some samples Ce, Pb and Th, is higher, whereas Na_2O and CaO are lower than most for the Beetle Association.

Mineralised members?: None.

Petrogenesis: As for the Low-Ca granites in general.

Tectonic & other implications: As for the Low-Ca granites in general.

Rocky Dump Clan

Member Supersuites: Rocky Dump Well.

Distribution: Single occurrence, northeast of the Windamurra Intrusion.

Geochronology: None.

Chemical characteristics: 74.78 wt% SiO_2. Normal for Beetle Association (Fig. 7).

Mineralised members?: None.

Petrogenesis: As for the Low-Ca granites in general.

Tectonic & other implications: As for the Low-Ca granites in general.

Skinny Bore Clan

Member Supersuites: Skinny Bore.

Distribution: Mica Well and Skinny Bore are the most sampled Suites, and occur on the western join of the Sandstone and Youanmi Sheets, east and northeast of the Windimurra Intrusion. The No-Ibla Suite on Glengarry may be up to 25x30 km (on the aeromagnetics), but only two samples have been taken from it. The Nalganadga and Dowden Well Suites occur adjacent to each other, in the northwestern part of the Sandstone Sheet.

Geochronology: One sample has been dated; the Mica Well Granite has an age of ~2600 Ma, but is not considered to be a good result.

Chemical characteristics: The Clan has a SiO_2 range from ~69 wt% to ~76 wt%. Some samples have slightly higher Y than other members of the Beetle Association, but otherwise is within the normal range for the Association. It is a low LILE, possibly high HFSE member of the Low-Ca group.

Mineralised members?: None.

Petrogenesis: As for the Low-Ca granites in general.

Tectonic & other implications: As for the Low-Ca granites in general.

Yarrabubba Clan

Member Supersuites: Yarrabubba, Barlangi Rock.

Distribution: Northwestern corner of Sandstone, a slight but distinguishable magnetic low, oval in shape. The Barlangi Rock granophyre and quartz monzonite is restricted to two small outcrops showing intrusive relationships to the Yarabubba Granite.

Geochronology: A sample of the Yarrabubba Granite is dated at 2650 ± 15 Ma. SHRIMP U-Pb on zircon has produced an age of 2714 ± 18 for the Barlangi Quartz Monzonite, and is regarded as an inheritance age.

Chemical characteristics: The Yarrabubba Clan is very felsic, between 74 – 76 wt% SiO_2 (Fig. 7). Compared to the bulk of the rest of the Beetle Association, the Clan has lower CaO, Sr, Pb, and higher MgO and Na_2O. One sample of the Yarrabubba Granite shows potassic alteration. The Barlangi Suite rocks have even lower Pb and CaO, and higher K_2O, the others of the Clan. It is not understood why Pb is so low for this Clan.

Mineralised members?: None.

Petrogenesis: As for the Low-Ca granites in general.

Tectonic & other implications: As for the Low-Ca granites in general.

Yeerlirie Clan

Member Supersuites: Black Hill, Buttercup Bore, Caluyu Bore, Dummy Well, Milgoo Well, Munroes Well, North Alston, Satan, Wallaby Knob, Yarloo Spring, Yeerlirie.

Distribution: Extensive clan spanning the entire north-south range of the Yeelirrie mass in both the western part of the northern Eastern Goldfields, and the northeastern part of the Southern Cross Province.

Geochronology: Three ages are available on the Sandstone sheet. The Buttercup Bore Granite is dated at 2661 ± 7 Ma; the Bonza Bore Granite is dated at 2682 ± 8 Ma, with inheritance at 3124 ± 41 and 2908 ± 26 Ma; and the Munroes Well Granite at 2638 ± 10 with inheritance at 3671 ± 29 Ma and ~3000 Ma. In the Yeelirrie Mass (north Eastern Goldfields Province), one age is available (L. Black, written communication, 2000) of 2653 Ma on the Wallaby Knob granite, Rowe Range supersuite.

Chemical characteristics: The Yeelirrie clan falls into the high LILE, low HFSE end of the Low-Ca compositional range (Fig. 5), though is clearly not as evolved as the Grant Duff clan of the northern Eastern Goldfields Province. The Yeelirrie clan is compositionally very similar to the spatially close Mars Bore clan of the Eastern Goldfields Province, including having the distinctive higher total Fe contents present in the latter.

Mineralised members? None, though probably indirectly related to the Yeelirrie U in calcrete deposit, being the most likely source of the U (via weathering of the granites).

Petrogenesis: As for the Low-Ca group in general.

Tectonic & other implications: As for the Low-Ca group in general.

High-HFSE	**Marda Association**	
Clan	**Supersuite**	**Suite**
Marda	Marda	Butcher Bird, Marda Volcanics
Courlbarloo	Courlbarloo	Courlbarloo
Mafic	**Westonia Association**	
Clan	**Supersuite**	**Suite**
Deception Hill	Deception Hill	Deception Hill

Table 4: High–HFSE and Mafic Group granites, northern Southern Cross province.

High-HFSE group, Marda Association, northern Southern Cross Province

Member clans: Courlbarloo and Marda.

Distribution: Limited in extent, all are internal to greenstones. The Marda clan is internal to the Marda greenstone belt, and together with the comagmatic felsic volcanics, makes up an area of < 300 km^2. The Courlbarloo clan consists of a single pluton in the Youanmi greenstone belt.

Geochronology: The Courlbarloo pluton is older than most granites in the nSCP, dated at 2813 ± 5 Ma. This age corresponds with the age of the mafic layered intrusions of the area (e.g. Windamurra Intrusion). It has a primitive ε_{Nd} value of 3.88, which is very different from any other values obtained for the nSCP (Fletcher & McNaughton, this volume). The Marda Clan includes granites and comagmatic felsic volcanics, and is dated at ~2730 Ma. This is also the age of the first significant granite intrusive activity in the nSCP, being that of the Pigeon Rocks and Southern Cross Gneiss associations of the High-Ca group.

Chemical characteristics: The members of the High-HFSE group have been described in detail by Champion & Sheraton (1997), and Champion (1997), though additional work, largely as part of this AMIRA/MERIWA project, has resulted in some redefinition of the group. Originally only containing high silica (>74% SiO_2) members, the high-HFSE group now has a silica range greater than both the High-Ca and Low-Ca groups. The group, however, is still characterised by its combination of high total Fe, MgO, TiO_2, HFSE, low to moderate LILE, and Sr-depleted, Y-undepleted character (Fig. 8), features that readily distinguish the group from other granite groups in the nSCP (Figs. 8–10).

Petrogenesis: The following discussion is from the section on High-HFSE group granites in the northern Eastern Goldfields Province (Champion, this volume). Champion & Sheraton (1997), and Champion (1997), suggested that the High-HFSE group granites were crustal-derived melts from an intermediate to more siliceous source, the latter hypothesis based on the combination of high HFSE and only low to moderate LILE. While such a scenario is consistent with both the Satisfaction and Kookynie clans (nEGP), the presence of less siliceous granites, such as those in the Bullshead clan (nEGP), raises the possibility that the more siliceous end-members are actually fractionates of rocks similar in composition to the Bullshead clan granitoids. If the latter scenario is correct, then the ultimate source rocks for the granitoids of this group must have been both more mafic and even more LILE-poor than originally envisaged. Such a hypothesis is also consistent with the, high-temperature A-type characteristics of the High-HFSE group (elevated Fe, Zr, Y).

The Sr-depleted, Y-undepleted nature of the group, strongly infer generation at only moderate crustal pressures, i.e., <10 kbar (<35 km thick). Similarly, as discussed by Champion & Sheraton (1997), the Sm-Nd isotope data indicate significant involvement of pre-existing crustal rocks in the generation of the High-HFSE granites.

In many regards, it is evident that members of the High-HFSE group, especially the less siliceous ones, have a number of similarities (though not as extreme) to the tholeiitic fractionates in the Kathleen Valley and Sweet Nell clans (nEGP, and perhaps the Deception Hill clan, nSCP) of the Mafic group, e.g., elevated Fe, Zr, Y, low LILEs, especially K_2O, Rb, Sr. It is tempting, therefore, to suggest some minor involvement of such rocks in the history of the High-HFSE granites.

Tectonics and other implications: The close spatial, temporal, and, at least locally, genetic, relationship between the High-HFSE granites and volcanics (e.g., at Kookynie–nEGP, and Marda–nSCP), indicates that these granites were intimately related to greenstone formation. More importantly, the geochemistry of the High-HFSE granites and their A-type affinities indicates emplacement in an, at least locally, extensional environment (as pointed out by Champion & Sheraton, 1997). The ages of these granites (in the nEGP), mostly 2700 to 2680 Ma, especially the latter, can be then be used to indicate periods of local extension. In this regard, the veracity of the 2738 Ma age on part of the Satisfaction Complex (Nelson, 1998) becomes important, in that it may signify earlier greenstone development in the northern Eastern Goldfields than currently envisaged. Likewise, the ages of 2730 Ma for the Butcher Bird granite (Marda complex) and 2735 & 2736 Ma for felsic volcanics in the Marda and Koolyanobbing areas, is possibly the age of upper greenstone formation in this area, and is slightly older than the onset of High Ca group granites in the area.

The age of the Courlbarloo granite (2815 Ma) is probably indicative of the age of rifting which resulted in the emplacement of tholeiitic mafic layered intrusions in the area between the nSCP and nMP.

Mafic Group, Westonia Clan, northern Southern Cross Province

Member clan: Deception Hill.

Distribution: Single pluton internal to the southern part of the Diemals greenstone belt.

Geochronology: The Deception Hill Clan is the oldest dated granite in the Southern Cross Province, having an intrusive SHRIMP zircon age of 3023 ± 10 Ma. This would indicate that the Diemals greenstone, and probably other greenstone belts in the Southern Cross Province, are older than 3025 Ma.

Chemical characteristics: The Mafic group as originally defined by Champion & Sheraton (1997) was, as the name suggests, comprised of granitoids with <70 wt% SiO_2. With further work (e.g. this project), the Mafic group has been expanded, and includes more differentiated clans such as Sweet Nell (see northern Eastern Goldfields, Champion & Cassidy, this volume). For a description of the characteristics of the Mafic group, the reader is referred to the appropriate sections in the northern Eastern Goldfields Province (Champion & Cassidy, this volume) and northern Murchison Province (Champion &

Cassidy, this volume).

The Deception Hill granites have been classified as Mafic group granites because of their elevated Ni, mg# and Na_2O, and low Ce, K_2O and Y.

Mineralised members? None.

Petrogenesis: The reader is referred to the appropriate sections in the northern Eastern Goldfields Province (Champion & Cassidy, this volume) and northern Murchison Province (Champion & Cassidy, this volume).

Tectonic & other implications: Assuming the age of this granite is correct (3023 ± 10 Ma, Nelson 1998), it provides a better upper age limit on the formation of the Diemals greenstone. Wang et al. (1996) and Wang et al. (1998) gave age estimates of 2.9–3 Ga for the earlier, mafic sequences of the Lake Johnson and Gum Creek greenstone belts. Other possibilities are that the 3023 Ma age is actually an inheritance age (not favoured by Nelson, 1998), or that the granite is basement remnant to the greenstones. It is noted that there are greenstones of this age within the nMP (See Champion & Cassidy, this volume), and so, given the similarities between the two provinces, such ages should be expected in the SCP.

References:

Champion, D.C., 1997. Granitoids in the Eastern Goldfields. Australian Geological Survey Organisation, Record 1997/41, 71-76.

Champion, D.C. & Sheraton, J.W., 1997. Geochemistry and Sm-Nd isotopic systematics of Archaean granitoids of the Eastern Goldfields Province, Yilgarn Craton, Australia: constraints on crustal growth. Precambrian Research, 83, 109-132.

Griffin, T.J. 1990. Southern Cross Province, Geology and Mineral Resources of Western Australia, Memoir 3, Geological Survey of Western Australia, 60-77.

Kent, A.J.R., Cassidy, K.F. & Fanning, C.M., 1996. Archaean gold mineralisation synchronous with the final stages of cratonisation, Yilgarn Craton, Western Australia. Geology, 24, 879-882.

Martin, H., 1986. Effect of steeper Archaean geothermal gradient on geochemistry of subduction-zone magmas. Geology, 14, 753-756.

Nelson, D.R., 1998. Compilation of SHRIMP U-Pb zircon geochronology data, 1997. Geological Survey of Western Australia, Record 1998/2.

Nelson, D.R., 1999. Compilation of SHRIMP U-Pb zircon geochronology data, 1998. Geological Survey of Western Australia, Record 1999/3.

Pidgeon, R.T. & Wilde, S.A., 1990. The distribution of 3.0 and 2.7 Ga volcanic episodes in the Yilgarn Craton of Western Australia. Precambrian Research, 48, 309-325.

Smithies, R.H. & Champion, D.C., 1999. Láte Archaean felsic alkaline igneous rocks in the Eastern Goldfields, Yilgarn Craton, Western Australia: a result of lower crustal delamination? Journal of the Geological Society of London, 156, 561-576.

Wang, Q., Beeson, J. & Campbell, I.H. 1998. Granite-greenstone zircon U-Pb geochronology of the gum Creek greenstone belt, Southern Cross Province, Yilgarn Craton: tectonic implications, Structure and Evolution of the Australian Continent, Geodynamics 26, American Geophysical Union.

Wang, Q., Schiøtte, L. & Campbell, I.H. 1996. Geochronological constraints on the age of komatiites and nickel mineralisation in the Lake Johnston greenstone belt, Yilgarn Craton, Western Australia, Australian Journal of Earth Sciences, 43, 381-385.

Clans

- Diemals
- Gnabberdocking
- Lake Barlee
- Mondie
- Pigeon Rocks
- Suggard
- Two Mile Hill
- Yoothapinna
- Bacon Hill
- Barcoo
- Beetle
- Bulga Downs
- Bullfrog?
- Cooliboo Bore
- Lake Seabrook
- Rainy Rocks
- Red Knob
- Rocky Dump
- Skinny Bore
- Weowanie
- Yarrabubba
- Yeerlirie
- Courlbarloo
- Deception Hills
- Marda
- Lamprophyre
- Unassigned
- Unnamed
- Greenstone
- Proterozoic

N

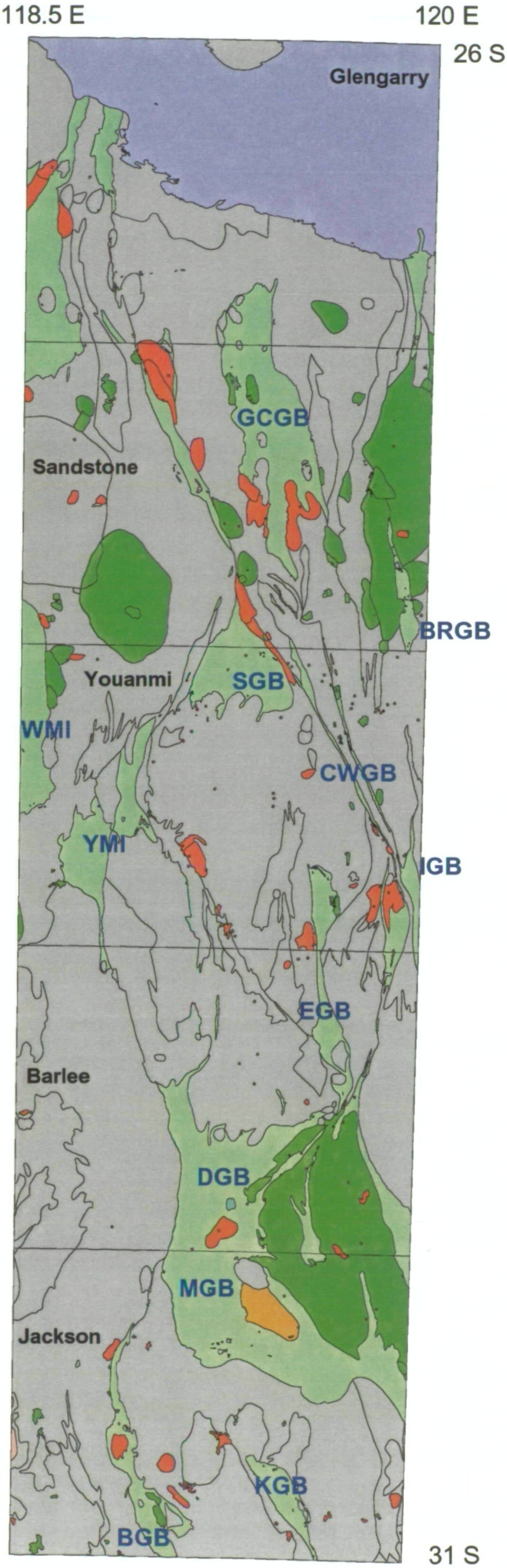

Greenstone Belts (after Griffin 1990)
GCGB = Gum Creek greenstone belt
SGB = Sandstone greenstone belt
BRGB = Booylgoo Range greenstone belt
WMI = Windimurra mafic intrusion
YMI = Youanmi mafic intrusion
CWGB = Cook Well greenstone belt
IGB = Illaara greenstone belt
EGB = Elvire greenstone belt
DGB = Diemals greenstone belt
MGB = Marda greenstone belt
BGB = Bullfinch greenstone belt
KGB = Koolyanobbing greenstone belt

Location Map: Granitoids of the northern Southern Cross Belt

Figure 1: Northern Southern Cross Province ages histogram

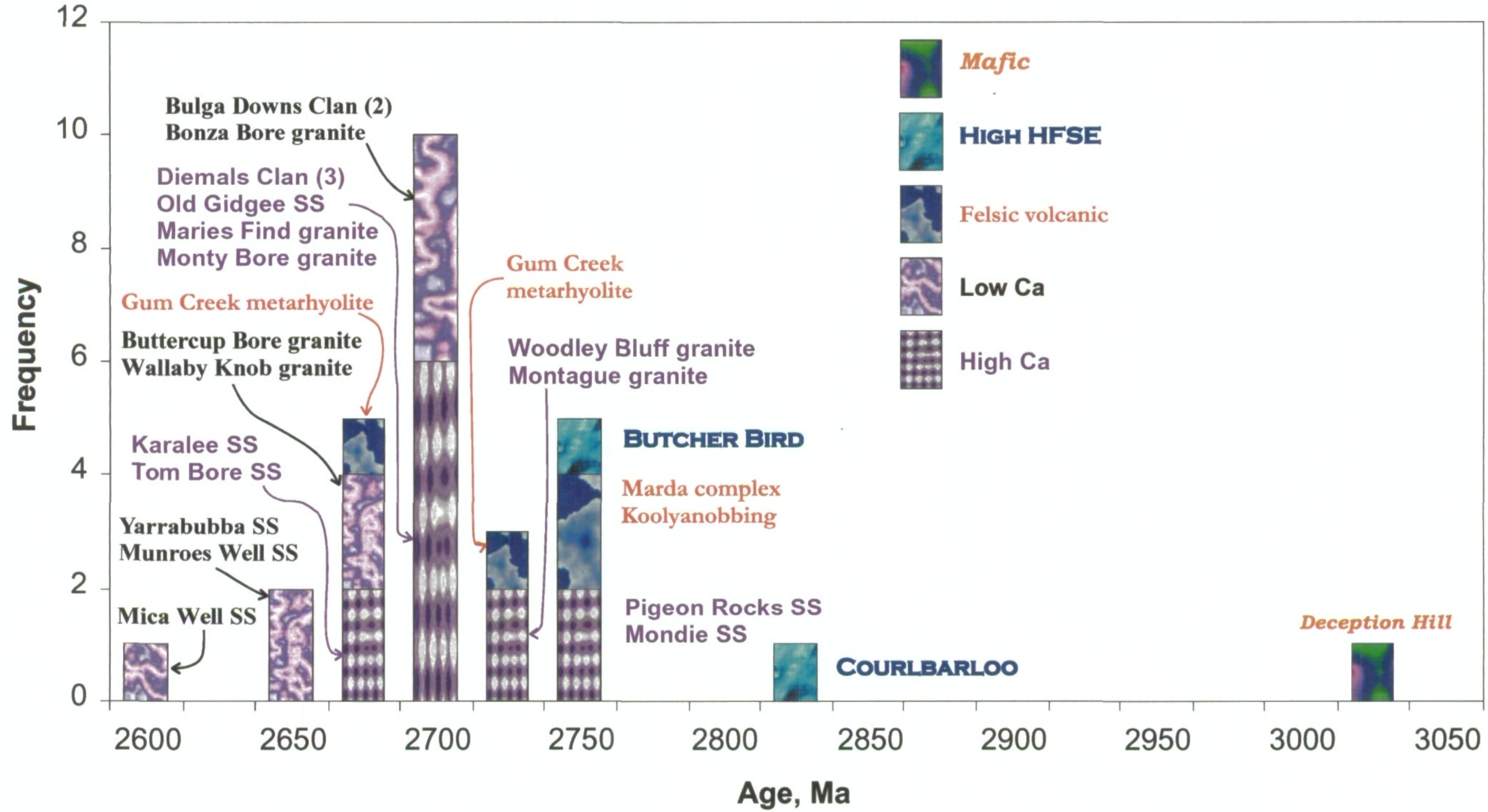

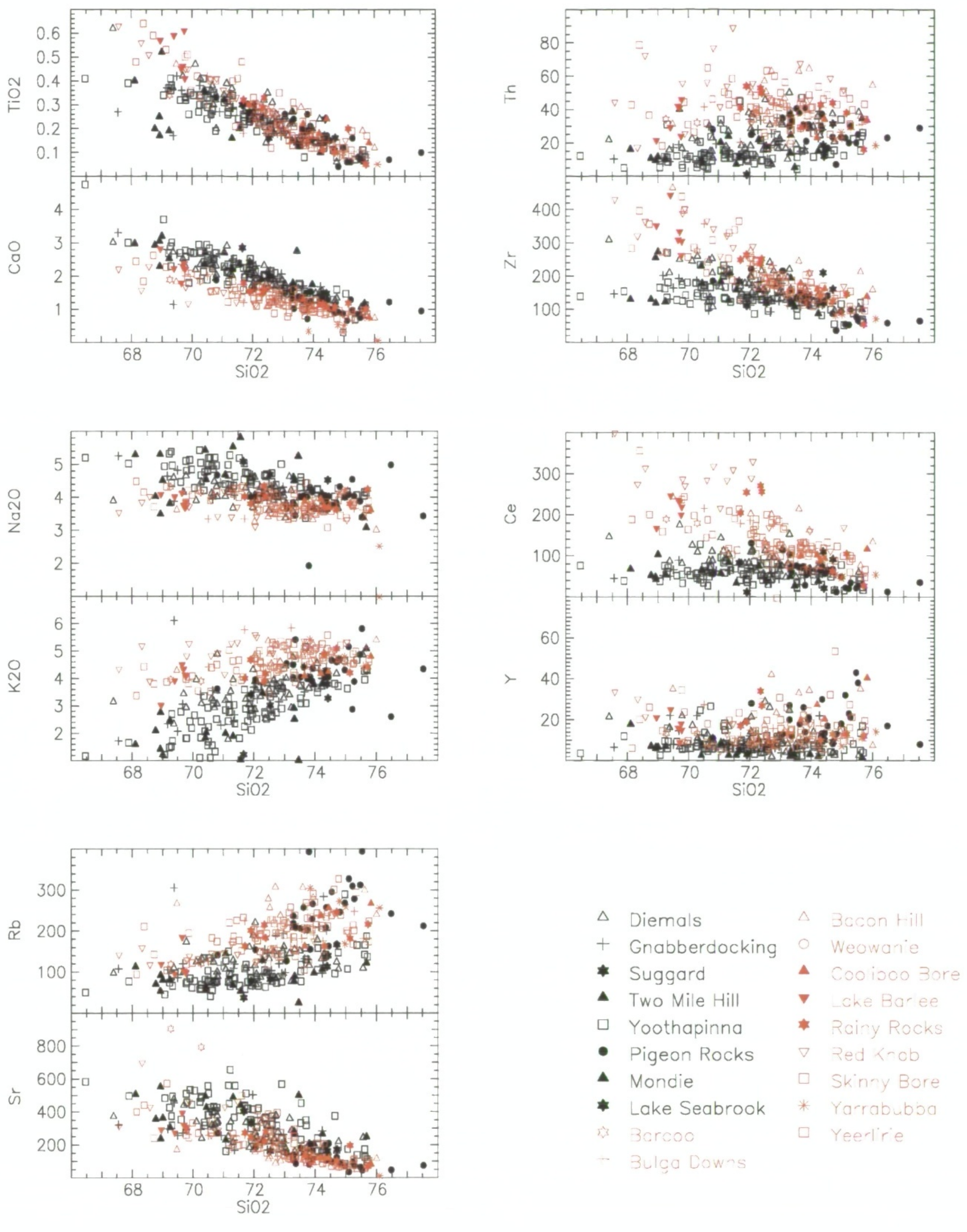

Figure 2. Discriminant plots for the High-Ca and Low-Ca groups of the northern Southern Cross Province.

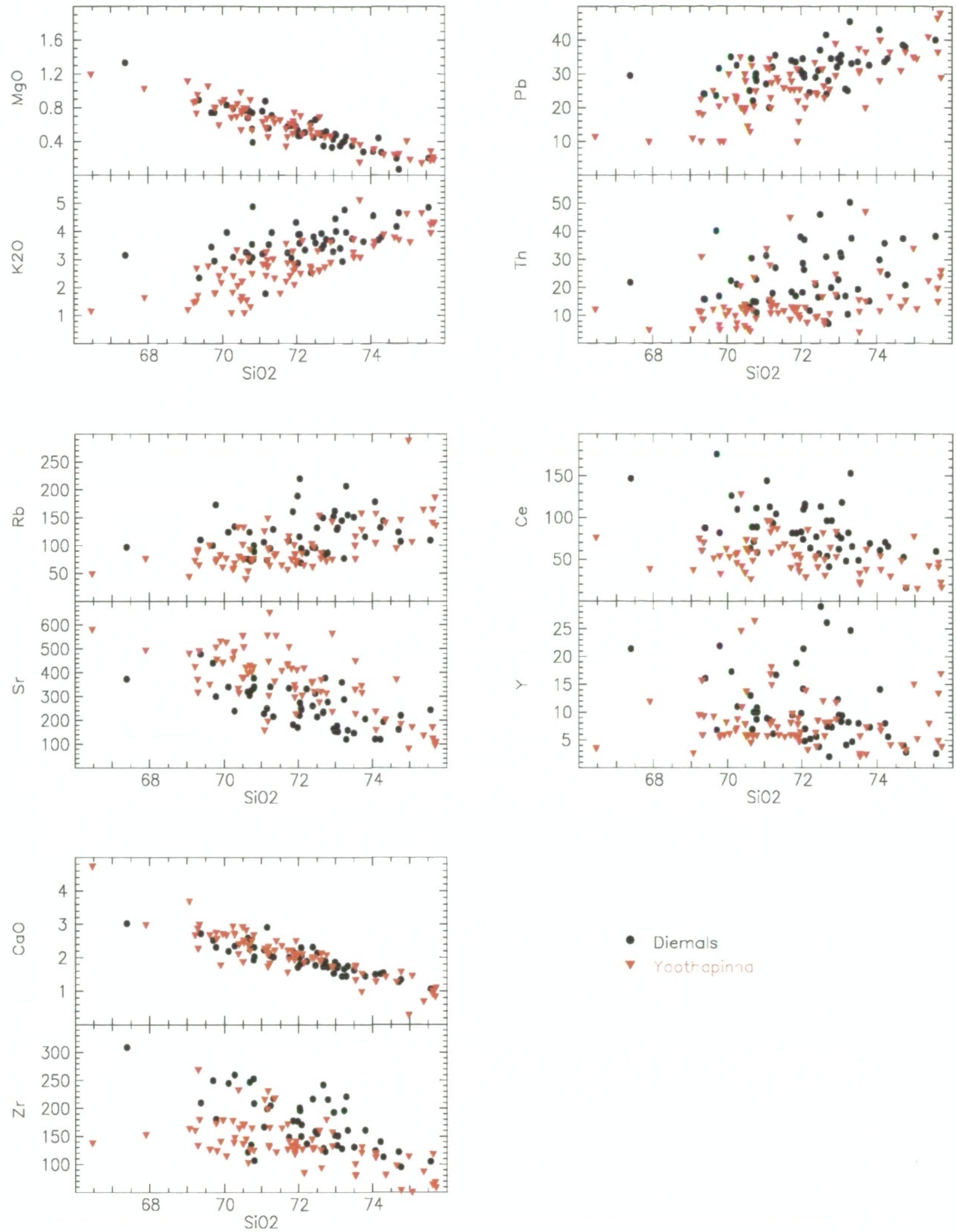

Figure 3. Comparison of the ‘ high-LILE’ Diemals Clan and the ‘ low-LILE’ Yoothapinna Clan, both of the Diemals Association, High-Ca group, northern Southern Cross Province. NB: ‘ High-‘ and ‘ Low-LILE’ terms are relative, not absolute.

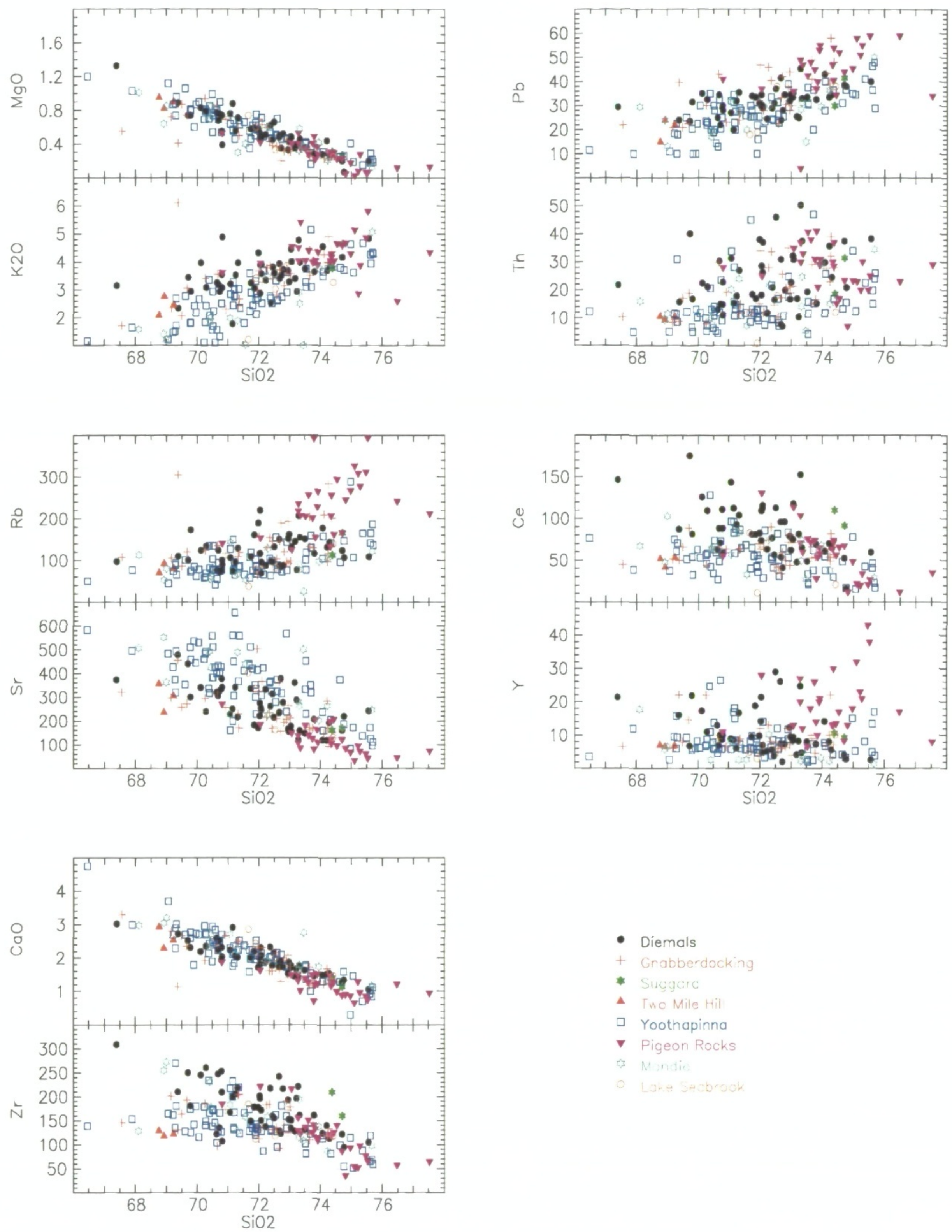

Figure 4. Clans of the Diemals Association, High-Ca group, northern Southern Cross Province.

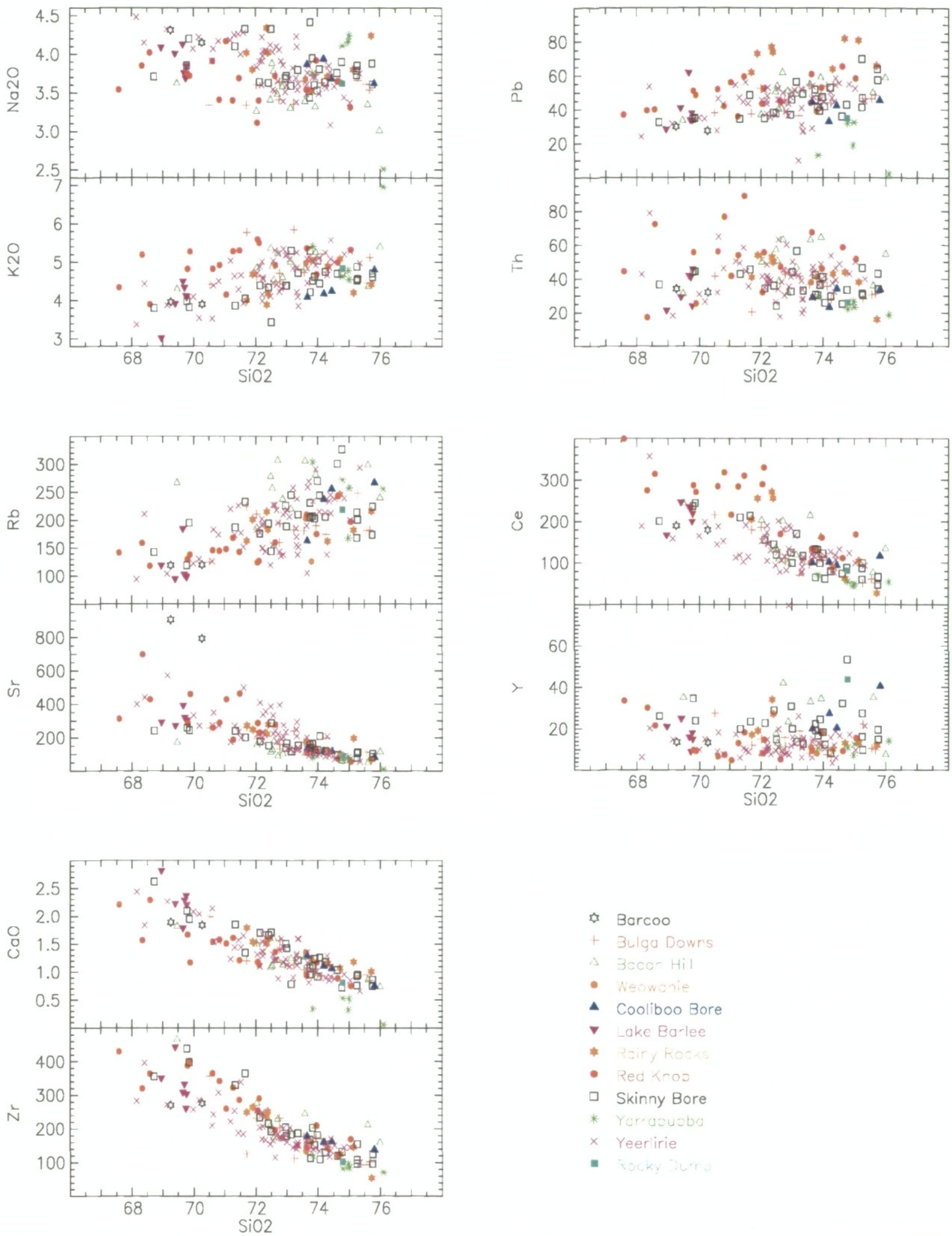

Figure 5. Clans of the Beetle Association, Low-Ca group, northern Southern Cross Province.

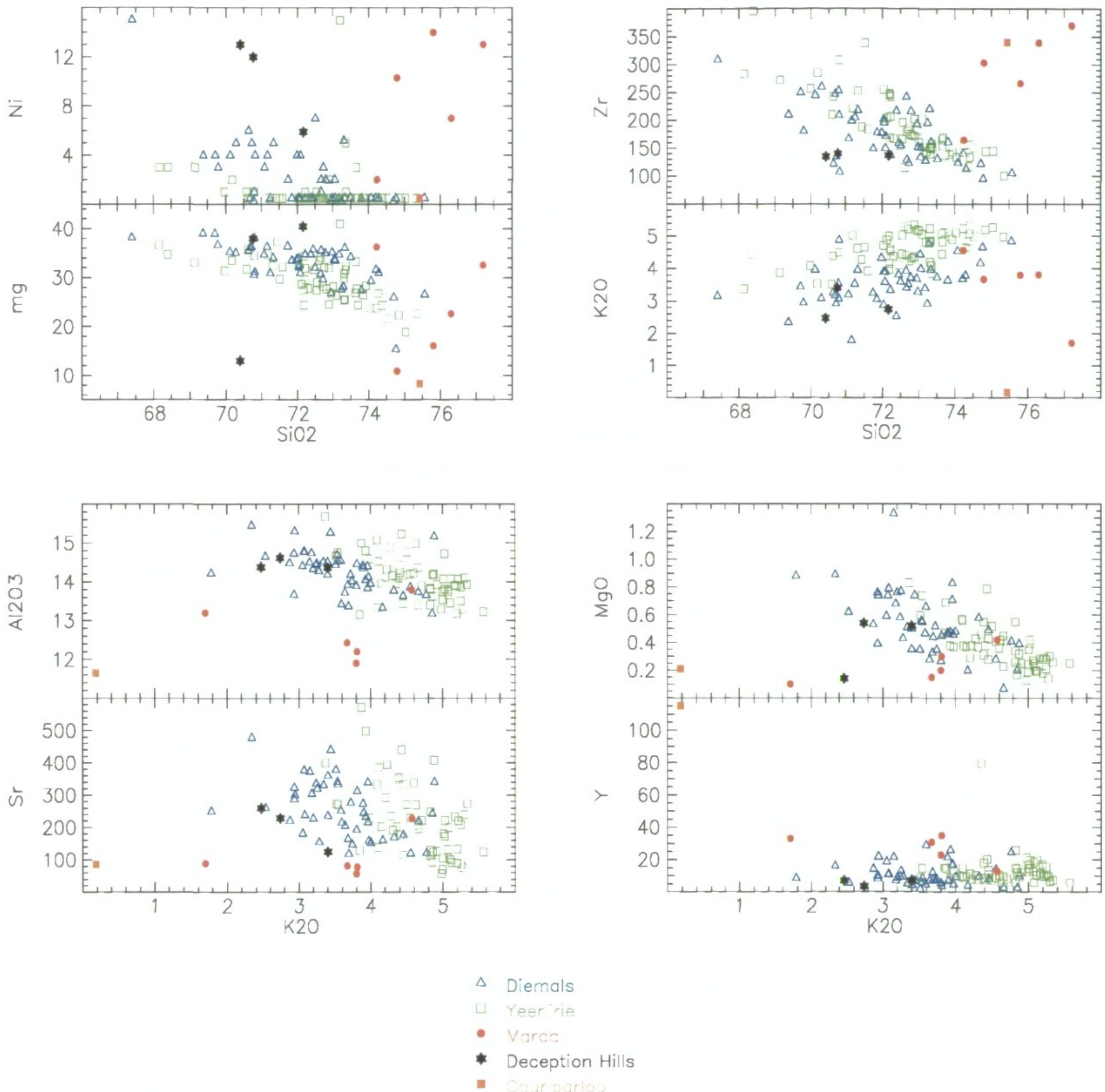

Figure 6. Discriminant plots for the Mafic (MgO, K_2O, Zr, Ni, mg# - ratio of Mg to Mg+Fe), and High-HFSE (Al_2O_3, K_2O, Sr, Zr, Y) groups. Marda & Courlbarloo Associations – High-HFSE group, Deception Hill Association – Mafic group; Diemals Clan (High-Ca) and Yeelirie Clan (Low-Ca group) shown for comparison.

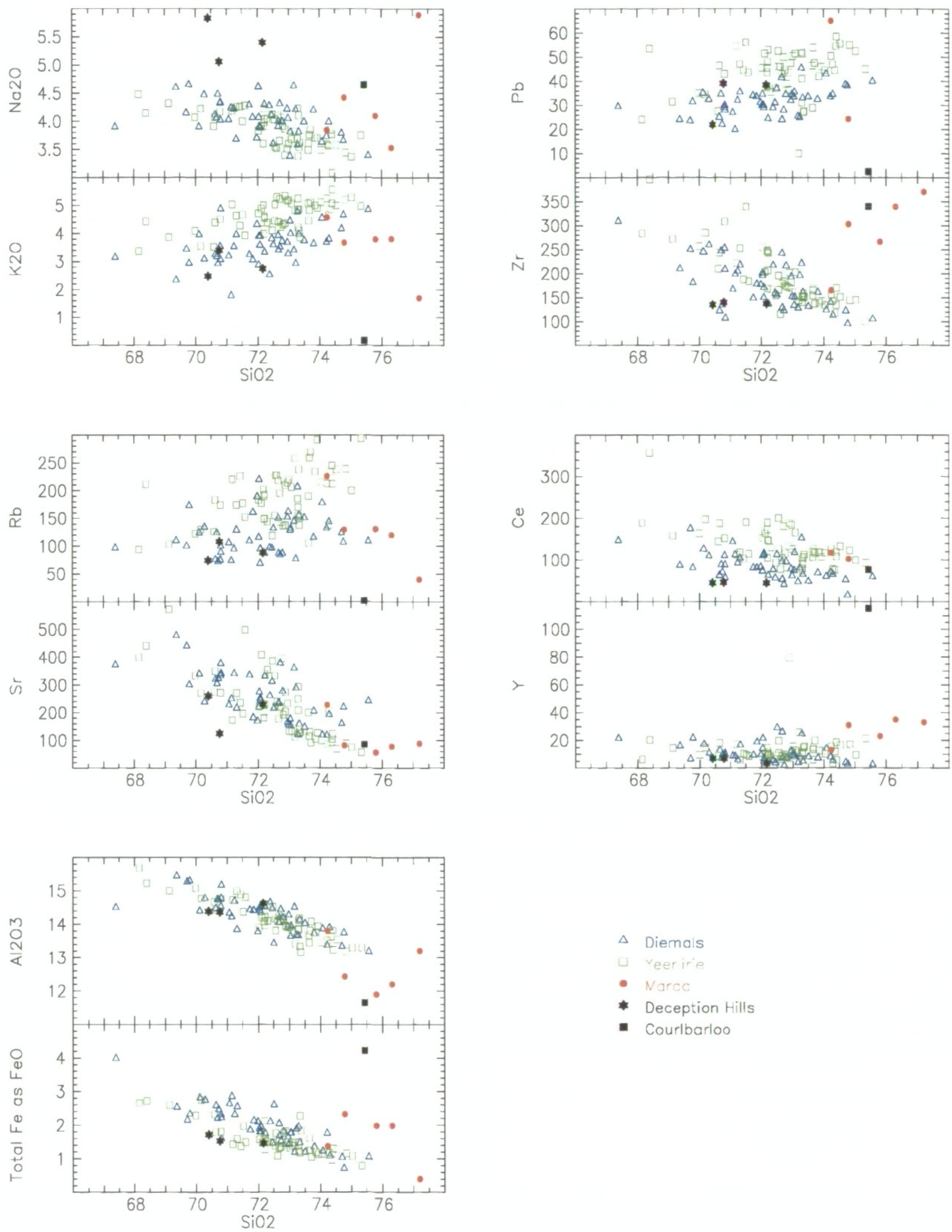

Figure 7. Marda and Courlbarloo Associations, High-HFSE group, and Deception Hill Association, Mafic Group, northern Southern Cross Province. Diemals Clan (Diemals Association, High-Ca group) and Yeerlirie Clan (Beetle Association, Low-Ca group) shown for comparison.

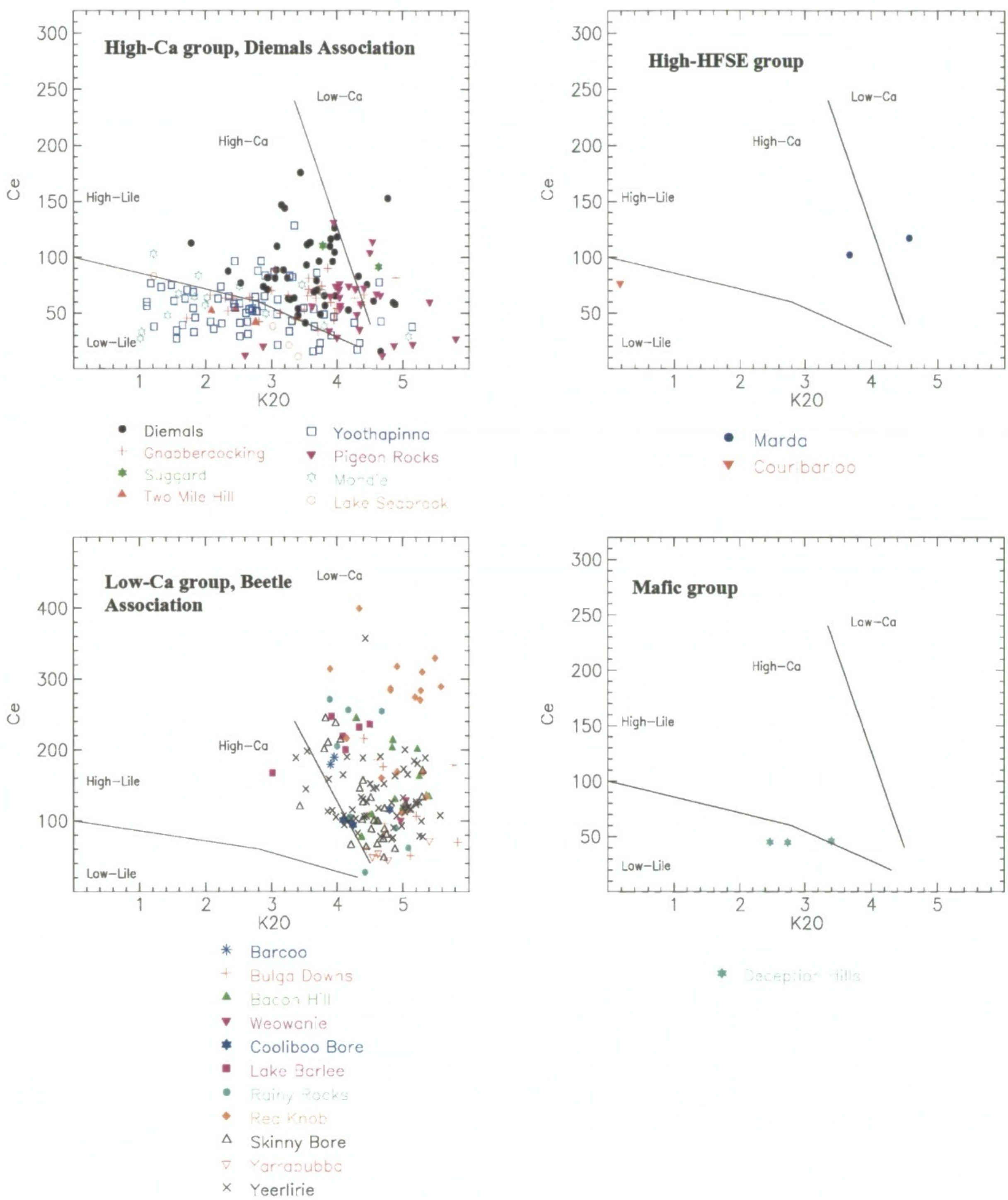

Figure 8. K_2O-Ce plots illustrating the range in LILE and HFSE in the Diemals, Southern Cross Gneisses and Pigeon Rocks Associations of the High-Ca group, the Beetle Association of the Low-Ca group, the Marda and Courlbarloo Associations of the High-HFSE group, and the Deception Hill Association of the Mafic group. The lower line is an arbitary divide between ' low-LILE' and ' high-LILE' end-members of the High-Ca and Mafic groups. NB: the terms ' low-' and ' high-LILE' are used in a relative, not absolute, sense. Note the expanded Ce axis for the Low-Ca group.

Chapter 5.
Granites of the northern Murchison Province: their distribution, age, geochemistry, petrogenesis, relationship with mineralisation, and implications for tectonic environment.

David C. Champion & Kevin F. Cassidy

Introduction

The most comprehensive study of the granites of the Murchison Province, prior to the current study, has been by Watkins and co-workers, e.g., Watkins & Hickman (1990). These workers developed a classification scheme based on both geochemical differences and structural timing (Table 1). This classification had the disadvantage of lack of geochronological control. Accordingly, as was also the case in the Eastern Goldfields Province, later geochronology clearly showed that relative ages deduced from structural history to be flawed, e.g., the Post-folding suites were mostly older than the external recrystallised granites. Later workers either concentrated on small regions or were focussed on geochronology, e.g., L. Wang et al. (1993, 1995), Wiedenbeck & Watkins (1993), Q. Wang (written commun, 1998), Schiotte & Campbell (1996), Mueller et al. (1996), Yeats et al. (1996). These workers largely followed the classification scheme of Watkins and co-workers, though L. Wang et al. (1993, 1995) modified the Watkins & Hickman scheme slightly, largely in name only and ignoring the gneisses (Table 1).

Pegmatite-banded gneiss
- mixtures of granodiorite, monzogranite, pegmatite
- thought to be older than other granites
- most abundant to west, enclaves only in the east
- multiple deformations & generations

Recrystallised Monzogranite (Suite 1 - monzogranite-granodiorite suite of Wang et al.)
- Most voluminous group
- Mostly external
- multiply deformed & recrystallised
- common gneiss inclusions and other xenoliths

Post-Folding Suite 1 (Suite 2 - trondhjemite-tonalite suite)
- Sub-circular to oval, tonalite, granodiorite, trondhjemite, monzogranite & syenogranite
- mostly internal or marginal; none wholly external
- discordant relationships with greenstones
- mostly in northeast part of Murchison Province

Post-Folding Suite 2 (suite 3 - monzogranite-syenogranite suite)
- Sub-circular to oval, quartz-rich monzogranite & syenogranite
- mostly internal or marginal; none wholly external
- discordant relationships with greenstones
- mostly in southwest part of Murchison Province
- higher LILE & HFSE contents, e.g., higher K_2O, Rb, Y, relative to Suite 1

Table 1. Granite classification scheme of Watkins & Hickman (1990). Modified classification of L. Wang et al. (1993, 1995) also shown, in parentheses.

More recent work (the current AMIRA P482 study), covering the whole of the northern Murchison Province, has followed the approach of Champion & Sheraton (1993, 1997) and subdivided the granites on the basis of chemistry and petrology, largely ignoring structural characteristics. Importantly, the granite groups identified by Champion & Sheraton (1993, 1997) were found to be applicable across the Yilgarn and have been used in the northern Murchison Province, along with the detailed subdivision introduced in the current work, e.g., Association, Supersuite.

The new classification has resulted in the identification of 28 clans within the five groups and the two provinces (Tables 2, 6, 7, 8, 9). This current work has been greatly assisted by the growing database of SHRIMP U-Pb geochronology, e.g., L. Wang et al. (1993, 1995), Wiedenbeck & Watkins (1993), Q. Wang (written commun, 1998), Schiotte & Campbell (1996), Mueller et al. (1996), Yeats et al. (1996), AMIRA P482. Some 58 ages have now been determined for granites of the Murchison Province (44 for the northern Murchison; see Tables 3, 4), complemented by another 22 for supracrustal and volcanic rocks from the greenstones (Table 4), and many ages from the gneiss terranes (Table 5). The combination of granite geochemistry and petrogenesis, with the geochronological data, is not only providing an overall framework for the region, but also insights into the finer detail, now emerging from the larger data sets (Table 2).

This chapter systematically lists and details all groups, associations and clans of the northern Murchison Province, and the westernmost part of the Southern Cross Province, i.e., Byro, Belele, Murgoo, Cue, Yalgoo, Kirkalocka and northern halves of Perenjori and Ninghan 1:250 000 sheets (collectively referred to as the northern Murchison). This region also includes a significant part of the Western Gneiss Terrane (WGT) - the latter does not form part of the current study and, apart from geochronology, is not discussed in any detail. The distribution of rocks of the WGT are shown on the accompanying map (on CD & Fig. 1), split into a number of units, based on magnetic signature in the gneiss provinces proper, pendants of gneiss within the MP, but also including later granites intrusive into the WGT. Chemical analyses are available for a small number of the younger (i.e., non-gneissic) intrusives into the WGT; these have been classified into granite group, clan etc., and treated as belonging to the Murchison Province.

A standard format is used for all entries, covering distribution, geochronology, chemical characteristics, related mineralisation (if any), and including a brief summary on petrogenesis and tectonic implications. The latter should be considered speculative, given the difficulties of assigning tectonic environment from granites alone, and the uncertain nature of plate tectonics in the Archaean. Similarly, the petrogenesis of the granites and their interpreted source rocks are treated in a simplified manner, mostly assuming a one- or two-component source, thereby facilitating a more coherent and more easily understood comparison between clans and groups etc.

Descriptions of granite group and clan distributions in the northern Murchison are based on 1:250 000 subdivisions, with the terms northeast (NE), north-central (NC), northwest (NW), southeast (SE), south-central (SC), southwest (SW) basically corresponding to the 1:100 000 sheet areas within the 1:250 000 sheets. The boundary between the Murchison Province and the Southern Cross Province, along the eastern margin of the northern Murchison region is shown in Figure 1, taken from the geophysical interpretation of Whitaker (this volume). For the detailed distribution of associations and clans, the reader is referred to the accompanying 1:500 000 and smaller scale maps (on CD); the distribution of the granite groups is shown on Fig. 1.

The following section describes clans under the respective granite group, with the individual clan descriptions following a more detailed description of the whole group. All five groups are discussed first as a whole – this effectively providing an overall summary of the granites of the northern Murchison.

Granite groups of the northern Murchison

Member groups: High-Ca (Mainland & Diemals associations), Low-Ca (Goolthan & Beetle associations), Mafic (Gem of Cue association), High-HFSE (Damperwah association), Syenitic group (Udagalia association)

Distribution: The distribution of granites groups within the northern Murchison is shown in Figure 1, from which a number of features are evident:

- both the High-Ca and Low-Ca groups make up the bulk of the granites, occurring across the region. This includes representatives in the Southern Cross Province (Fig. 1). Members of both groups are commonly spatially associated, there are no obvious zones where only one group dominates, contrary to the situation for the northern Eastern Goldfields.
- the High-Ca group granites comprise the largest granite group within the northern Murchison, representing up to and greater than 60% of the total granites (Fig. 1), within both the internal and external granites. Eleven clans have been recognised in the northern Murchison Province, and 2 small clans in the western Southern Cross Province (Table 6).
- the Low-Ca group, the second most dominant granite group within the northern Murchison, represents up to 15 to 20% of total granites (Fig. 1). The group has a widespread occurrence across the northern Murchison, ranging from large plutons to numerous small pods and dykes into older granites. Eight clans have been recognised in the northern Murchison Province, and one small clan in the western Southern Cross Province (Table 7).
- the High-HFSE group is sparsely (<10%), but widely distributed. Members of the group are very commonly spatially associated with greenstones, either internal or marginal (Fig. 1). Unlike the Eastern Goldfields Province, there is no indication that the group is spatially localised, although it is evident that many of the High-HFSE units are concentrated within the north-western half of the northern Murchison region (Fig. 1). No High-HFSE group granites occur within the Southern Cross Province in the northern Murchison region.
- the Mafic group, is also sparse (<10%), but distributed across the Murchison Province. Members of the group are almost solely confined to within or marginal to the greenstones, with the exception of one unit that occurs as a pendant or pod within an external Low-Ca granite (NW Kirkalocka). No Mafic group granites occur within the Southern Cross Province in the northern Murchison region.
- the Syenitic group is largely absent from the northern Murchison region, with one recorded unit occurring as a dyke within a High-Ca granite (NC Yalgoo). No Syenitic group granites occur within the Southern Cross Province in the northern Murchison region.

Geochronology: Over 44 ages are now available for the granites of the northern Murchison (Tables 3, 4, 5), with the following observations (summarised in Table 2):

- There is a large spread of ages, spanning 2600 Ma to 3010 Ma, in total, with identifiable groups at 2600-2765 Ma, 2780-2820 Ma, 2920-2960 Ma, and 3000-3015 Ma. Younger ages (<2765 Ma) form a number of broad peaks at 2620-2660 Ma, 2665-2705 Ma, 2710-2720 Ma, 2725-2765 Ma, with largest peaks at ca. 2625, 2680, 2700, 2720, and 2750 Ma. Given the large spread in data and the relatively small sample set the full significance of these latter sub-groups is not clear, i.e., further dating may alter the current interpretation.

- Granite ages within the Southern Cross Province further to the east clearly show similar age groupings to the Murchison Province, with most magmatism at 2630-2740 Ma, and older groups at 2780-2825 Ma, and 2900-3020 Ma. In both the Murchison Province and Southern Cross Province there is no apparent large peak, in granite ages, unlike that seen for the Eastern Goldfields Province. Notably, the period 2670 to 2660 Ma, a time of voluminous magmatism in the Eastern Goldfields Province, appears to be largely unrepresented in the Murchison Province (and Southern Cross Province). This gap is even evident within younger granites intrusive into the Narryer Terrane (Table 5).
- The High-Ca granites span the entire age range, although most are greater than 2670 Ma (Tables 3-4). This contrasts with the situation for the Eastern Goldfields Province, where the majority have ages between 2680 and 2660 Ma, i.e., High-Ca (and other), magmatism was largely absent in the Murchison Province (and Southern Cross Province), during the period of most voluminous High-Ca (and Mafic) magmatism in the Eastern Goldfields Province. The geochronology data indicate that all dated intrusive magmatism within the Murchison Province prior to ca. 2670 Ma was High-Ca in origin. This, however, probably reflects bias in the data set rather than the true picture. For example, felsic volcanic rocks within the Luke Creek group, i.e., >2930 Ma, appear to have chemistry (Watkins & Hickman, 1990), similar to members of the High-HFSE group.
- the Low-Ca granites, in the Murchison Province, lie between 2654 and 2626 Ma, with one outlier at 2676 Ma. This is largely similar to that observed for the Low-Ca granites within the Eastern Goldfields Province (2660 to 2630 Ma). This range is very similar to that observed for the Low-Ca granites within the Southern Cross and Eastern Goldfields provinces (2660 to 2630 Ma), providing good evidence that Low-Ca magmatism, unlike the High-Ca magmatism, was largely synchronous across both provinces (and the Southern Cross Province), though as noted elsewhere (Champion & Cassidy, this volume), the Eastern Goldfields Province appears to lack significant Low-Ca magmatism of 2.64-2.63 Ga and younger. Further geochronology will help clarify whether these differences are indeed real or just artefacts of the limited data to date.
- the Mafic granites in the northern Murchison, have ages indicating two periods of magmatism, at ca. 2715 Ma (Gem of Cue, Britania clans), and 2747-2760 Ma (Gem of Cue, Britania, Norie clans), with a possible outlier at 2788 ± 32 Ma (tentatively identified as Mafic group), but within error of the older sub-group. Even older Mafic group granites (ca. 2800 and 3020 Ma) are known from the Southern Cross Province (Budd & Champion, this volume); it is expected that similarly-old Mafic granites also exist in the Murchison Province.
- the High-HFSE group granites of the northern Murchison, like the Mafic group granites, also fall into two temporal periods, with the older Nannine clan at ca. 2745-2750 Ma, and the Damperwah clan at 2640 Ma or younger. Similar granites within the southern Murchison Province have ages less than 2640 Ma (Tables 3, 4). Like the Mafic group, it is highly likely that older (>2780 Ma) High-HFSE granites exist within the Murchison Province, particularly when it is noted that 2930 Ma and older felsic volcanic rocks, with similar chemistry to the High-HFSE group, are found within the Luke Creek group (Watkins & Hickman, 1990).
- the Syenitic group which forms a very minor component within the Murchison Province, has not been dated.
- like the case for the Eastern Goldfields Province, there is a change from largely High-Ca magmatism to dominantly Low-Ca within the Murchison Province. In the former this occurs at around 2655 Ma; a similar period appears to be evident in the Murchison Province, though High-Ca granites are largely absent after 2670 Ma.

- Greenstone ages are largely similar to the granites, though are confined to 2703 Ma and older (Table 4). As noted by Schiotte & Campbell (1996), the available data indicate good evidence for three periods of greenstone formation, i.e., 2700-2750 Ma (Mt Farmer group), ca. 2780-2820 Ma (upper part of Luke Creek group), and 2930-3010 Ma (Luke Creek Group) (Table 4), not the two periods envisaged by Watkins & Hickman (1990). The data also suggest the possibility that the 2930-3010 Ma period may be actually comprised of 2 discrete periods, 2930-2965 Ma and 3000-3010 Ma.
- Inherited zircon ages also closely follow granite and greenstone ages as may be expected. Most notably, however, there appears to be no evidence for old inherited zircon (>3100 Ma) that may be expected if WGT-type crust was being reactivated (compare Tables 3 & 4 with 5). This result is consistent with the Sm-Nd isotopic data (Fletcher & McNaughton, this volume), and with the suggestion of Nutman et al. (1993) that the Narryer Terrane was thrust over the Murchison Province.
- There is abundant evidence for younger events (<3100 Ma), within the WGT, that match those seen within the Murchison Province, especially less than 2750 Ma (Table 5). There are a couple of 2800 Ma ages (inherited) that may correspond with a similar event within the Murchison Province. The commonality of age data are, perhaps, best interpreted to indicate collision between the Murchison Province and Narryer at sometime between 2750 & 2810 Ma. Notably, Nutman et al. (1993) reached similar conclusions. They further suggested, however, that the pre-3300 Ma rocks of the Narryer complex were confined to the eastern part of the gneiss complex, and that these older gneisses formed an allochthonous terrane overthrust onto pre-existing 3000-2920 Ma gneisses (and also greenstone age), at ca. 2750 Ma.
- Notably there also appears to be a dearth of older ages within the southwest gneiss terrane (SWGT; Table 5), with almost all ages (magmatic and inherited), 2800 Ma or younger. The presence of 2800 Ma inherited zircons may suggest docking had occurred before this time. The lack of ages between 2680 and 2800 Ma, however, may suggest commonality wasn't achieved until around 2680 or before. The SWGT certainly lacks the 2680-2750 Ma ages evident in both the Murchison Province and the Narryer (and also in the Southern Cross and Eastern Goldfields provinces), though this could reflect resetting of zircon core ages as suggested by Nemchin & Pidgeon (1997a).

The general sequence with relationship to greenstones and granite groups is summarised in Table 2, and discussed in more detail by Champion et al. (this volume).

Chemical characteristics: The geochemistry of the granite groups is discussed in detail under the relevant groups in the following sections. A number of broad generalisations can be made concerning possible trends:

- the High-Ca, High-HFSE and Mafic groups exhibit a marked range in the LILE and some of the HFSE. Similar, but smaller ranges in the LILE are evident in the Low-Ca group. The available geochronological data indicates that while there is a trend of increasing LILE contents with decreasing ages for the High-HFSE group (Nannine to Damperwah clan), this does not appear to be the case for the Mafic or High-Ca groups, with high LILE clans as old as 2760 Ma. The data is too limited to make any comments on trends within older magmatism (>2760 Ma).
- the younger magmatism, post 2655 Ma, is markedly more potassic and LILE enriched, reflecting the change to Low-Ca and high LILE High-HFSE group magmatism.
- there are no significant chemical differences between the High-Ca groups in the Murchison Province/Southern Cross Province and Eastern Goldfields Province, with the possible exception of the Eily Eily clan (Murchison Province). The latter differs in two main aspects: first, the clan trends to relatively high LILE and HFSE contents, in

part overlapping with the Low-Ca group; and second, the clan is characterised by its generally Sr-depleted nature (i.e., minor to significant negative Eu anomalies). The Union Jack clan of the High-Ca group, Eastern Goldfields Province, does share some characteristics with the Eily Eily clan, but does not reach the more extreme compositions shown in the latter.

- there are no significant chemical differences between the Low-Ca groups in the Murchison Province/Southern Cross Province and Eastern Goldfields Province. Clearly the process that produced such widespread magmatism must have been very similar across the entire Yilgarn craton.
- the young (high LILE) Damperwah clan of the High-HFSE group appears to have no chemical equivalents within the Eastern Goldfields Province. It is notable that in the latter province the younger magmatism accompanying the Low-Ca group is Syenitic - a group that appears to be largely absent within the Murchison and Southern Cross provinces. Similarly, the high-Mg Norie clan of the Mafic group, appears to have no recorded equivalents within the Eastern Goldfields Province.
- Sm-Nd data suggest a number of competing trends, based largely on geographic position. Most of the Murchison Province High-Ca granites have relatively unevolved Nd signatures, with ε_{Nd} between +1.4 and –1.7. These values are clearly distinct from the Low-Ca group granites (-3.4 to -4.5), notably even for the Eily Eily clan (which chemically overlaps with clans of the Low-Ca group), i.e., the two groups were derived from isotopically distinct sources, (data from Fletcher & McNaughton, this volume; Nutman et al., 1993; Fletcher et al., 1994; Watkins & Hickman, 1990). Uncommon, more evolved values (i.e., more negative), occur in some of the High-Ca granites within the Narryer Gneiss Terrane, and, importantly, also to the east of the gneiss terrane in older gneisses and pendants within the Murchison Province (Nutman et al., 1993; Watkins & Hickman, 1990); such isotopic signatures clearly reflect the involvement of older crust. The available Sm-Nd isotopic data for the High-HFSE group indicate a narrow range in ε_{Nd} (-3.7 to -4.7), that overlaps completely with the Low-Ca granites, but are clearly more evolved (more negative), than High-Ca, and Mafic group granites (Fletcher & McNaughton, this volume). Champion & Sheraton (1997) reported similar relationships between the granite groups in the Eastern Goldfields Province.

Mineralised members: Examples from the Murchison Province of granitoids hosting gold mineralisation or closely spatially associated, are apparently confined to granites of the High-Ca and Mafic groups. Examples of granitoids directly hosting significant gold mineralisation are rare in the Murchison Province, though a number hosting 'minor' gold mineralisation (typically in quartz veins and/or shears) are known, e.g., deposits in the Gem of Cue granite around Cue, in the Lady Lydia granite at Noongal, in the Gold Bay and Britania granites south of Mt Magnet. One of the largest deposits in the region, Big Bell, is closely spatially associated with a High-Ca granite, though the main zone of mineralisation appears to be located within the greenstones (Mueller et al., 1996).

It is apparent from descriptions in Watkins & Hickman (1990), that feldspar porphyry sills and dykes are a common lithology found within Au deposits of the Murchison Province, though most appear to be spatially associated rather than hosting mineralisation e.g., in Hill 50 and other deposits around Mt Magnet (Watkins & Hickman, 1990). These porphyries would also appear to belong to either the Mafic or High-Ca groups. Perhaps the best documented porphyries associated with gold mineralisation are those in the Meekatharra - Paddys flat mining camp region (see Watkins & Hickman, 1990).

3800 - 4100 Ma	inherited zircons – Narryer Gneiss Terrane (e.g., Froude et al., 1983)
3600-3730 Ma	Narryer Gneiss Terrane, e.g., Meeberrie gneiss
3440-3500 Ma	Narryer Gneiss Terrane, e.g., Eurada gneiss
3380-3350 Ma	Narryer Gneiss Terrane, e.g., Dugel gneiss
3290-3315 Ma	Narryer Gneiss Terrane, e.g., unnamed gneisses Pendants of gneiss, e.g., Murgoo gneiss, within the western Murchison Province – related to Narryer Gneiss Terrane?
3119? Ma	Narryer Gneiss Terrane, e.g., unnamed gneisses
ca. 3010-3000 Ma ↑	greenstones (and komatiite?), of Luke Creek group, High-Ca group Mafic and High-HFSE groups?
continuous?	Narryer Gneiss Terrane – magmatism of this age appears to be absent
↓ *2965-2920 Ma*	greenstones (and komatiite?), of Luke Creek group, High-Ca group granites and gneisses, Mafic and High-HFSE groups?
>2810-2750 Ma	Narryer Gneiss Terrane overthrust over Murchison Province?
2815-2780 Ma	greenstones (upper part of Luke Creek group), High-Ca group, rift-related? layered mafic intrusive complexes along Southern Cross Province/Murchison Province boundary, Mafic and High-HFSE groups?
2760-2745 Ma	High-HFSE (Nannine clan), Mafic and High-Ca groups
2750-2700 Ma	greenstones, including komatiite, of the Mount Farmer group
2745-2725 Ma	High-Ca group
2725-2710 Ma	High-Ca and Mafic (Gem of Cue, Britania clans) groups
2700-2665 Ma	common High-Ca magmatism, very minor Low-Ca group magmatism?
2655-2620 Ma	Low Ca and High-HFSE (Damperwah clan) group magmatism.
2650-2640 Ma	Granulite metamorphism - Southwest Gneiss Terrane

Table 2. Tectonothermal history for the northern Murchison Province (and western Southern Cross Province). Narryer Gneiss Terrane data largely from Nutman et al. (1993); sources for other age data given in Tables 3, 4, 5.

Sampno	Unit	Supersuite	Clan	Map	Age	Inheritance	Ref	Com
High-Ca								
74459	Eily Eily	Eily Eily	Eily Eily	Cue	2681 ±6	2831 ±15	7	OK?
91966186	Eily Eily	Eily Eily	Eily Eily	Cue	2678 ±5	2778 ±20	2	OK
91966187	Dixie Well	Eily Eily	Eily Eily	Cue	2670 ±6	2697±25; 2724 ±14	2	OK
91966188	Dorothy	Eily Eily	Eily Eily	Cue	2680 ±5	2797±24; 2913 ±16	2	OK
92966263	dyke in Dorothy	Eily Eily	Eily Eily	Cue		2741 to 2935	2	?
92966261	Bookine	Bookine	Eily Eily	Kirka	2655 ±10	2707±12	2	OK
99969164A	Courin Hill	Courin Hill	Eily Eily?	Yalgoo	2742 ±6		5	OK
9996 4016C	Mt Mulgine	Mt Mulgine	Eily Eily?	Peren	2756 ±20		4	OK
93-978	unnamed porphyry	unnamed	Kyle Kyle?	Belele	2718 ±10		3	OK?
93-979	unnamed porphyry	unnamed	Kyle Kyle?	Belele	2727 ±10		3	OK?
89-438	Big Bell	Mainland?	Mainland	Cue	2737 ±4	~2800-2900	17	OK
91966158	Clarry Bore	Mainland	Mainland	Cue	2700 ±7	2741 ±15	17	OK
93-969	Buttercup	Mainland?	Mainland	Cue	2666 ±4		3	OK?
93-981	Taincrow	Mainland	Mainland	Cue	2612 ±10		3	??
91966190	Wardatharra	Wardatharra	Mainland	Kirka	2694 ±7	2730 ±26	2	OK
93-967	altered Meehan?	unassigned	Mainland	Cue	2684 ±5		3	OK?
83339	Badja gneiss	Badja	Uanna	Yalgoo	2920 ±12		7	?
91966189	Gold Bay	Gold Bay	Uanna?	Kirka	2696 ±5	2730 ±12; 2741 ±28	2	OK
99969192A	Mangatah	Younga?	Wardiacca	Kirka	2686 ±5		5	OK
83481	Darn Hill	Wardiacca	Wardiacca	Kirka	2704 ±50	2811±8	7	?
92966259	Nannowtharra	Wardiacca?	Wardiacca	Kirka	2710 ±10	2958±10	2	OK
92-265	Wheel of Fortune	Wheel Fort.	Wheel Fort.	Cue	2702 ±6	2725; 2789; 2943	2	OK
9996 4100	Basin	Lady Lydia	Wheel Fort.	Yalgoo	2743 ±4		4	OK
RE8	Pearce Well	unassigned	unassigned	Cue	2710 ±10		8	OK?
RE80	Triton	unassigned	unassigned	Cue	2785 ±8		8	OK?
High-HFSE								
83407	Damperwah	Damperwah	Damperwah	Yalgoo	2641 ±5	2863 ±8	7	OK?
83551	Koolanooka	Koolanooka	Damperwah	Yalgoo	2602 ±16		7	?
99967141	Keygo	Keygo	Nannine	Cue	2745		5	OK
93-989	Eelya	Nannine	Nannine	Cue	2752 ±4		3	OK
93-990	Eelya	Nannine	Nannine	Cue	2753 ±4		3	OK
93-991	Eelya	Nannine	Nannine	Cue	2746 ±5		3	OK
Low-Ca								
92966258	unnamed dyke	Edah	Edah	Kirka	2640 ±10	2798-2810	2	OK
99964003	Goolthan Goolthan	Goolthan	Goolthan	Yalgoo	2626 ±6		5	OK
93-982	Jungar	Jungar	Myagar?	Cue	2676 ±7		3	OK?
92966366	altered Coodardy?	Bocadeera?	Nakedah?	Cue	2627 ±8	2670 ±34	17	OK?
Mafic								
99969142	Triangle	Triangle	Britania	Yalgoo	2747 ±3		5	OK
91966153	Britania	Britania	Britania	Kirka	2716 ±4		2	OK
92966278	Milky Way	Milky Way	Gem of Cue	Kirka	2715 ±7	2932 ±21	2	OK
92966283	dyke in Boomer pit	Milky Way	Gem of Cue	Kirka	2752 ±5	2931 ±9	2	OK
W378	Gem of Cue	Gem of Cue	Gem of Cue	Cue	2759 ± 4		19*	OK?
PFG-1	Norie	Norie	Norie	Belele	2760 ±8		7	OK?
SG111	Reedy	Reedy	Norie	Cue	2752 ±10		8	OK?
SG122	Reedy	Reedy	Norie	Cue	2751 ±6		8	OK?
87-322	unnamed dyke				2788 ±32	~3000?	7	?
Unassigned								
91966185	LREE-poor dykes	LREE-poor	unassigned	Cue	2657 ±9		2	?
Unassigned late granites flanking Narryer gneiss complex								
88-179	grt intruding gneiss				2643 ±5		18	OK?
88-189	grt intruding gneiss				2679 ±2		18	??
88-192	grt intruding gneiss				2685 ±6		18	??
88-195	grt intruding gneiss				2620		18	??
89-457	grt intruding gneiss, Pindaring Rock?				2753 ±10	~2920	18	??
105015	No 7 Bore grt dyke				2666 ±6	2730 ±22	11	OK
105017	No 8 Bore grt				2680 ±3	~2965	11	OK

Table 3. Geochronological data for the granite groups of the northern Murchison region; all ages (in Ma) are SHRIMP zircon ages, except those with an asterisk which are conventional U-Pb zircon ages. Data sources: 1 - Q. Wang et al. (1998); 2 - Schiotte & Campbell (1996); 3 - Q. Wang (ANU) – unpublished data; 4 - Oliver (BSc Hons, 1999); 5 - AMIRA P482; 6 - Yeats et al. (1996); 7 - Weidenbeck & Watkins (1993); 8 - L. Wang et al. (1995); 9 - Pidgeon & Wilde (1990); 10 - Pidgeon et al. (1990); 11 - Nelson (1996); 12 - Nelson (1997); 13 - Kinny et al. (1990); 14 - Nemchin et al. (1994); 15 - Nemchin & Pidgeon (1997b); 16 - Pidgeon et al. (1996); 17 - Mueller et al. (1996); 18 - Nutman et al. (1991, 1993); 19 - Pidgeon & Hallberg (2000); 20 - Pidgeon (1992); 21 - Pidgeon & Wilde (1998). Com = comments and refers to the interpreted reliability of the age.

Sampno	Unit	Map	Age	Inheritance	Ref	Com
Supracrustal						
92-272	Galtee Moore Chert		2798 ±8	2949 ±11	2	MAX
92-382	Windaning Fm sandstone	Ninghan	2809 ±5	2945 ±7	1	OK
93-1010	Warramboo Chert		2810 ±19		2	MAX
93-970**	Gabanintha Fm?		2749 ±7		3	MAX
93-971**	Gabanintha Fm?		2731 ±5		3	MAX
93-974**	Windaning Fm?		2785 ±30		3	MAX
HN97	Supracrustal		2934 ±6		6	MAX
OR77	Supracrustal		2929 ±3	2942-2963?	6	MAX
Volcanic						
92-385	Scuddles Unit rhyodacite	Ninghan	2945 ±4		1	OK
92-388	Golden Grove rhyolite	Ninghan	2960 ±6		1	OK
92-386	Gossan Valley unit rhyolite	Ninghan	2953 ±7		1	OK
92-266	Mt Farmer group		2703 ±10	2805 ±10	2	OK
92966269	Morning Star		2739 ±11	2762 ±19?	2	OK
93-976**	Windaning Fm?		2815 ±7		3	OK?
93-977**	Windaning Fm?		2780 ±11		3	OK?
93-986**	Gabanintha Fm?		2747 ±6		3	OK?
94-117	Morning Star		2727 ±6		2	OK
W116	Tallering greenstone belt		2935 ±2		9*	OK
W50	Weld Range greenstone belt		~3010		9*	??
W56	Koolanooka Hills		~3000		9*	??
W78	Twin Peaks greenstone belt		3003 ±10		9*	??
W90	Golden Grove greenstone belt		2938 ±10		9*	OK
W296	Dalgaranga belt felsic tuff		2745 ± 4		19*	OK?
W297	Dalgaranga belt felsic tuff		2746 ±8	3034 ± 8	19	OK?
W308	Dalgaranga belt felsic tuff		2749 ±2		19*	OK?
W310	Dalgaranga belt felsic tuff		2743 ±4		19*	OK?
W369	Cue area felsic tuff		2716 ±4		19*	?
W372/373	Cue area felsic tuff		2761 ± 1		19*	OK
W379	Cue area felsic tuff			~2900	19	OK
W360	Gabbro sill, Dalgaranga area		2719 ± 6		19	OK
Southern Murchison Province						
High-Ca						
99967049A	Goddard Quarry		2790 ±10		5	?
99967082C	Dookaling gneiss		2940 ±5		5	OK
99969093B	Moora – Agg gneiss		3007 ±3		5	OK
99969066	Moora – fol. Mzg			2680-2780, >3100	5	OK
GWE	Western Grt		2935 ±3		6	OK?
W7	Moonagarrin gneiss		2800 ±9	2997 ±47	10	OK?
High-HFSE?						
GNE	Northeast Grt		2623 ±7		6	OK
9996 9049	Bencubbin Hb-Bt grt		2640 ±5		5	OK
Low-Ca						
9996 7055	Bencubbin grt		2637 ±10		5	OK
9996 7066	Namban grt		2646 ±5		5	OK
9996 9063	Moora – Aln-Ttn mzg		2630 ±6		5	OK
9996 9096	Moora – Hb-Bt grd		2639 ±6		5	OK
GIN	Post-tectonic grt		2627 ±3	2682?, 2770?	6	??
W6	Wongan Hills grt		2654 ±4	2833 ±2*	10	OK?

Table 4. Geochronological data for the supracrustal rocks and volcanics of the Murchison region, and the granites of the southern Murchison Province; all ages (in Ma) are SHRIMP zircon ages, except those with an asterisk which are conventional U-Pb zircon ages. Data sources as for Table 3. Com = comments and refers to the interpreted reliability of the age; MAX = maximum age for the sedimentary unit.

Sampno	Unit	Group	Age	Inheritance	Ref	Com
Narryer Gneiss Terrane						
105002	Cargarra Well ?xeno		2994 ±6	3313 ±15, 3502 ±3	11	OK
105005	Bluebush Well gneiss		2735 ±9		11	OK
105007	Churla Well gneiss		2636 ±4	3000-3200; >4000	12	OK?
105009	Duffies Well ?xeno		3495 ±3		11	OK
105010	Duffies Well gneiss		3487 ±3		11	OK
105011	Sharpe Bore grt		3312 ±3	3484 ±6	11	OK
105012	Sharpe Bore grt		3479 ±4		11	OK
105014	Noonie Hill gneiss		3489 ±3	3587 ±2	11	OK
88-168	eastern Narryer gneiss and/or grt		3298 ±6		18	??
88-173	Meeberrie gneiss, eastern Narryer		3731 ±4		18	OK?
88-175	Eurada gneiss, eastern Narryer		3439 ±3	3490	18	OK
88-176	Eurada gneiss, eastern Narryer		3466 ±4	3055-metam?	18	OK??
88-180	eastern Narryer gneiss and/or grt		3302 ±9	3730	18	OK?
88-181	eastern Narryer gneiss		3119 ±21		18	??
88-191	Meeberrie gneiss, eastern Narryer		3597 ±7		18	??
88-197	Eurada gneiss, eastern Narryer		3489 ±6		13	OK
88-198	gneiss		3462 ±6		13	??
88-199	gneiss		3289 ±11	>3670	13	??
88-200	gneiss		2950		13	??
89-456	Meeberrie gneiss, eastern Narryer		3626 ±10	~3740	18	??
84-81	Meeberrie gneiss, eastern Narryer		3662 ±8		18	??
84-82	Meeberrie gneiss, eastern Narryer		3633 ±8		18	??
84-83	Eurada gneiss, eastern Narryer		3483 ±4		18	??
84-96	eastern Narryer gneiss		3302 ±6		18	??
88-26	Meeberrie gneiss, eastern Narryer		3600 ±9		18	??
88-27	Meeberrie gneiss, eastern Narryer		3623 ±7		18	??
77218	Dugel gneiss		3375 ±26		18	OK?
W61	porph granite gneiss, Meeberrie?		3290 ±20		21	OK??
W29	tonalitic gneiss, Meeberrie?		3608 ±22		21	OK??
W35	granodioritic gneiss, Meeberrie?		~3516 ±32		21	OK??
Late granites within the Narryer Gneiss Terrane						
84-97	eastern Narryer late grt		2638 ±11	~2680, ~2920	18	??
88-170	eastern Narryer late grt?		2620 ±12		13	OK
88-178	eastern Narryer late grt?		2679 ±5		13	??
88-182	eastern Narryer late grt		2748 ±12	~3050	18	??
88-186	eastern Narryer late grt		2672 ±2	~3300	18	??
88-187b	eastern Narryer late grt		2656 ±2		18	??
88-188	eastern Narryer late grt		2654 ±2	~3600	18	??
88-193	eastern Narryer late grt?		2673 ±30		13	??
88-196	eastern Narryer late grt		2648 ±2	~3600	18	??
105001	Hungry Well mzg		2683 ±4		11	??
105004	Balla Rock mzg		2638 ±6		11	OK
W34	monzogranite dyke	Low-Ca	2660 ±20		20	OK
W62	monzogranite	Low-Ca	2654 ±7		21	OK
Narryer Gneiss Terrane pendants within Murchison Province						
88-166	migmatite, Murgoo gneiss, flanking Narryer		2727 ±8	3286 ±13	18	??
88-169	Murgoo gneiss, flanking Narryer		3005 ±6		18	??
88-171	Murgoo gneiss, flanking Narryer		2918 ±6		18	OK?
91-615	Murgoo gneiss, flanking Narryer		2994 ±9		18	OK
105016	No 8 Bore gneiss ?xeno		2717 ±45	2995; 3236	11	OK?
105018A	No 8 Bore gneiss,		2689 ±17	2723 ±10; >3800	12	OK??

Table 5. Geochronological data for granites, gneisses and granulites from the gneiss terranes; all ages (in Ma) are SHRIMP zircon ages, except those with an asterisk which are conventional U-Pb zircon ages. Data sources as for Table 3. Com = comments and refers to the interpreted reliability of the age.

Sampno	Unit	Group	Age	Inheritance	Ref	Com
Mafic granulite - Southwest Gneiss Terrane						
W17	Griffins Find		2640 ±1		14*	OK
W22	Jinkas Hill		2641 ±5	2798 ±6	14*	OK
W129	Corrigin		2643 ±4		14*	OK
W178	Mt Dick		2649 ±6		14*	OK
W236	Mt Dick		2643 ±5		14*	OK
W306	Althorpe Peaks		2648 ±4		14*	OK
Gneiss – Southwest Gneiss Terrane						
W323	Canning Dam grt		~2640	2665 ±7	15	??
W330	Stathams Quarry grt		2629 ±8	2662 ±5	15	??
W332	Stathams Quarry-2 grt		2626 ±6	2659 ±5; 2680 ±3;	15	??
W382	York South grt		2638 ±3	2668 ±4	15	??
W390	Williams East aplite		2648 ±4	2665 ±4; 2801 ±12	15	??
W393	Northam West aplite		2633 ±8	2663 ±7	15	??
W395	Katrine syenite gneiss		2654 ±5	~3250	16	OK
W427	Logue Brook grt		2613 ±8	2680 ±8	15	??

Table 5 (continued). Geochronological data for granites, gneisses and granulites from the gneiss terranes; all ages (in Ma) are SHRIMP zircon ages, except those with an asterisk which are conventional U-Pb zircon ages. Data sources as for Table 3. Com = comments and refers to the interpreted reliability of the age.

Other mineralisation asssociated with granites includes Mo and W, best seen at Mt Mulgine where it is associated with the High-Ca Mt Mulgine granite (Oliver, 1999), and Be and/or Sn-Ta mineralisation associated with pegmatites, the latter most probably related to the Low-Ca group. These pegmatites, as described by Watkins & Hickman (1990), occur both within greenstones, e.g., Rothsay, Dalgaranga, Poona or within Low-Ca granites, e.g., Edah. Like the Low-Ca granites in the Eastern Goldfields Province, it is considered highly likely that the Low-Ca granites of the Murchison Province have, contributed, by weathering, to the U in calcrete deposits in the region.

Petrogenesis: Petrogenetic models are discussed in detail for each group in the following section; results can be summarised as follows:

- the general characteristics of the High-Ca granites (low LILEs, sodic) indicate derivation from a mostly mafic (broadly basaltic/amphibolitic), LILE-poor source. The range in the LILE and HFSE (and Na_2O, Sr), between clans, however, indicates a more complex model, i.e., the involvement of a number of components, either as a heterogeneous source (basaltic to quartz dioritic), or by some other process (assimilation of pre-existing crust, magma-mixing, alteration of the source etc). The flat HREE patterns and lack of negative Eu anomalies in the majority of High-Ca granites in the Murchison Province, suggest that there was at best only minor residual feldspar, and that amphibole not garnet, was a dominant residual phase, indicate derivation at pressures great enough to stabilise amphibole ± garnet and destabilise plagioclase (10-15 kbars) either deep within a thickened crust (>35-50 km) or, perhaps, from melting of a subducting slab (e.g., Martin, 1986). Either process is feasible, though the Sm-Nd isotopic data and the chemistry of the Eily Eily clan tend to favour a thickened crust source. The Sr-depleted chemistry of the Eily Eily clan, the most LILE-rich High-Ca clan, indicates derivation at lower pressures than other High-Ca clans, probably much closer to the site of generation for the Low-Ca group. This immediately suggests some involvement of the Low-Ca-type source in the generation of the Eily Eily clan granites, a process that would also explain the high LILE contents in the latter. The available Sm-Nd data, which suggest largely isotopically-distinct sources for the Low-Ca and High-Ca groups, limits the amount of possible Low-Ca-type source-component in the Eily Eily clan to probably less than 20-25%; this is considered enough, however, to impart the high LILE characteristic to the Eily Eily clan. Such a mechanism, if correct, also indicates that at least some (all?) of the High-Ca granites were generated within the crust, not a subducting slab.

- the potassic, high LILE, high HFSE, Sr-undepleted nature of the Low-Ca group is most consistent with derivation, at moderate pressures (<10 kbars) from a relatively potassic and LILE-rich crustal source, i.e., reworked continental crust with compositions not unlike typical Archaean tonalites (e.g., Champion & Sheraton, 1997). A number of features, though, e.g., low CaO, minor occurrence of amphibole, indicate partial melting was either via small volume melts or from a source with only minor amphibole. Also, the high levels of the HFSEs, in particular Zr, indicate high melting temperatures, suggesting elevated thermal gradients. The variation in LILE, in particular, and the HFSE, between the Low-Ca clans, appears to result from a variety of processes, including: changes in the percentage of partial melting, variations in source compositions, and some input of other source components (e.g., High-Ca source, High-HFSE source).
- the chemistry of the Nannine and Damperwah clans of the northern Murchison region (high HFSE, high SiO_2), is consistent with the suggestions of Champion & Sheraton (1997), and Champion (1997), that they are crustal-derived melts from an intermediate to more siliceous source. However, as discussed for High-HFSE granites in the Eastern Goldfields Province (Champion & Cassidy, this volume), it is also possible that the granites are actually fractionates of more mafic rocks, similar in composition to the Bullshead clan of the Eastern Goldfields Province. If the latter scenario is correct, then the ultimate source rocks for the granitoids of this group must have been even more mafic. Such a mafic source, and the temperatures required for partial melting, is also consistent with the, high-temperature A-type characteristics of the High-HFSE group (elevated Fe, Zr, Y; Fig. 6). Unlike the Eastern Goldfields Province, the High-HFSE clans of the northern Murchison region show a large difference in the LILE, from low (Nannine) to high (Damperwah), which given the similarity of SiO_2, mg*, size of the negative Eu anomaly etc., must reflect original source differences, i.e., the source for the Damperwah clan was more LILE-rich. Notably, many of the high LILE characteristics of the Damperwah clan are also shared by the contemporaneous Low-Ca group in general, suggesting the possibility of partly common sources, as has already been suggested for the Horseshoe Clan of the Low-Ca group. In this regard, it is notable that the Low-Ca and High-HFSE groups share similar Sm-Nd signatures, both significantly more evolved than those for the High-Ca and Mafic groups. It is noted, however, that members of the LILE-poor Nannine clan also have similar Sm-Nd signatures, pointing to both long-lived high and low LILE sources for the High-HFSE group granites in the northern Murchison region, i.e., pre-existing crustal rocks. The Sr-depleted, Y-undepleted nature of the group, strongly infer generation at only moderate crustal pressures, i.e., <10 kbars (<35 km thick).
- petrogenetic models for the Mafic group granites are largely equivocal, with evidence for both crustal and mantle-derived contributions. Notably, the variation in the LILE and LREE (between and within clans of the Mafic group), requires at least two separate components, as suggested by Champion (1997) for the Eastern Goldfields Province, e.g., a mafic 'basaltic' source, (similar to that proposed for the High-Ca granites), and a mafic, perhaps mantle-derived, LILE-rich source component. These differing components may reflect entirely separate source regions for the Britania and Gem of Cue clans, or may result from more complex interactions, e.g., a similar overall source, variably LILE-enriched (metasomatised) before partial melting, with the non- or poorly-metasomatised regions producing the Gem of Cue clan, and the more strongly-

enriched regions producing the Britania clan. Another feasible mechanism is post-melting modification by a LILE-enriched fluid or melt, e.g., some form of magma mixing, such as lamprophyres, introducing the high LILE into the Britania clan granites. The granites of the ca. 2755 Ma Norie Clan with their elevated MgO, mg#, Ni, Cr, clearly require a mantle-component in their genesis. Even more important, however, is the combination of high MgO, Ni etc, with moderate LILE contents, which is thought to reflect metasomatism of a depleted mantle source by LILE-enriched melts from a subducting slab, either before or during genesis of the granitoids (see discussion in Smithies & Champion, 2000).

- the petrogenesis of the one recorded syenitic unit in the northern Murchison (Udagalia) is equivocal with regards to the relative contributions of mantle versus crustal components, though, like the syenites in the Eastern Goldfields Province, a significant crustal contribution is implied by features such as the presence of quartz, the high LILE contents, and strong negative Nb and Ti anomalies. The Udagalia syenite has chemistry somewhat similar to, but not as extreme, as that recorded for the Wallaby clan syenites in the Eastern Goldfields Province. Notably syenites at Wallaby appear to have had some interaction with a carbonatite, and, perhaps a similar relationship is also the case for the Udagalia unit.

Tectonic and other implications: The following discussion is a summary of the tectonic implications as indicated by the granite petrogenesis and geochronology, and consideration of the geochronology and inherited zircon data from the Narryer Gneiss Terrane (and Southwest Gneiss Terrane). More detailed discussions of tectonics are given for each granite group in the next section.

The bulk of the evidence appears to favour a thickened crust origin for the High-Ca granites, especially for the Eily Eily clan. As such, the periods of magmatism involving granites of the Eily Eily clan (i.e., 2670-2680 Ma, 2740-2760 Ma), also correspond to those times when the Murchison Province crust was thickened (>35-50 km). It is, however, also apparent that derivation from a subducting slab is also a possible viable mechanism for production of at least some of the High-Ca granites. Importantly, both the thickened crust or melting of a subducting slab hypotheses, require the operation of some form of convergent tectonics contemporaneous or just prior to granite generation. This can be interpolated, therefore, to infer that all periods of High-Ca granite formation correspond roughly to times of convergent tectonics in the Murchison (and Southern Cross) Provinces, i.e., 2675-2765 Ma, 2780-2825 Ma, 2920-2960 Ma, and 3000-3025 Ma. As noted before (Champion & Cassidy, this volume), the timing of these tectonic settings, especially post 2.72 Ga, contrasts somewhat with that for the Eastern Goldfields Province, i.e., pre 2.68 Ga High-Ca magmatism was common in the Murchison and Southern Cross provinces but minor in the Eastern Goldfields Province, 2.68 to 2.66 Ga magmatism was minor to absent in the Murchison and Southern Cross provinces but voluminous in the Eastern Goldfields Province. Clearly there are a number of possible scenarios, not mutually exclusive, that may explain these apparent differences, e.g., the Murchison and Southern Cross provinces were separate from the Eastern Goldfields Province before and/or during this period, the change across the Murchison and Southern Cross provinces to the Eastern Goldfields Province is actually diachronous, as in a migrating arc-environment, or perhaps the thermal regime at 2.68-2.66 Ga was such that granite production was largely confined to the Eastern Goldfields Province, such as in a typical modern-day convergent environment. Clearly further geochronology would be helpful, particularly along the eastern margin of the Southern Cross Province and western margin of the Eastern Goldfields Province.

The simplest model for the Low-Ca granites is that they were generated from moderately dry tonalitic (or more felsic) pre-existing crust, in an extensional environment with an elevated geothermal gradient. This is clearly contrary to the environment proposed for the High-Ca granites, indicating not only distinct source rocks, but distinct sites of granite generation for the two granite types, consistent with available Sm-Nd isotopic data (Fletcher & McNaughton, this volume). These differences are even more significant given the temporal change around 2660 to 2650 Ma, from voluminous dominantly High-Ca magmatism to less voluminous, but very widespread, dominantly Low-Ca (and Syenitic) magmatism. This changeover in magmatism most probably indicates a corresponding change in tectonic environment, presumably from a compressional or arc-related environment to one dominated by extension (and higher geothermal gradients), i.e., some mechanism produced a change in the thermal regime, that not only increased the thermal gradient (to allow generation of Low-Ca granites) but effectively turned off production of High-Ca granites.

The exact nature of this tectonic transition is largely dependent on the origin of the High-Ca granites. If, as favoured for the northern Murchison, the High-Ca granites were generated in thickened crust, then melting shifted to higher crustal-levels (the site of Low-Ca generation), with the thickened lower crust (High-Ca source) either somehow insulated from further melting or removed. The latter is favoured given the apparently higher geotherm required for the Low-Ca granites. In this regard, Smithies & Champion (1999) suggested that this post 2660 Ma thermal event may have resulted from Yilgarn-wide lower-crustal delamination following the D_2 shortening deformation in the Eastern Goldfields Province, perhaps heralding an additional tectonothermal event, contemporaneous with lower-middle crustal high-grade metamorphism and regional Au mineralisation (e.g., Kent et al. 1996). If, however, the High-Ca granites were largely generated by slab-melting, then the change over to Low-Ca (and syenitic) magmatism may simply reflect some form of wide-scale extension, perhaps not unlike that presently operating in the Basin and Range province in the western United States, although with some differences.

The geochemistry of the High-HFSE granites and their A-type affinities indicates emplacement in an, at least locally, extensional environment (as pointed out for the Eastern Goldfields Province by Champion & Sheraton, 1997). The ages of these granites, mostly 2740-2750 Ma, and post-2640 Ma, can be then be used to indicate periods of local extension. In the Eastern Goldfields Province, the close spatial, and genetic, association between High-HFSE granites and volcanics suggested that the granites there were intimately related to greenstone formation. Within the northern Murchison region, such an association would appear to only hold for the Nannine Clan; the granites of the post 2640 Ma Damperwah clan clearly post-date felsic volcanism (Tables 3, 4); their formation being related to the same extensional(?) tectonic environment responsible for the Low-Ca granites. The Nannine clan granites, on the other hand, overlap in age with, and share similar geochemical characteristics to some of the younger felsic volcanics (Mt Farmer group, e.g., Watkins & Hickman, 1990), and so must, at least in part, be related to greenstone formation. Similarly, there is also good reason to expect older (>2930 Ma) members of this clan to be present within the northern Murchison region.

It is notable that the younger granites within the northern Murchison region (Low-Ca and High-HFSE groups) contrast with those in the Eastern Goldfields Province (Low-Ca and Syenitic, and carbonatitic?). The reasons for this are not completely understood but may have something to do with proximity to recently active convergent margins, i.e., immediately prior subduction along the eastern margin of the Eastern Goldfields Province may have been responsible for producing suitably metasomatised mantle and lower crustal

(?) rocks as source rocks for syenites (e.g., Smithies & Champion, 1999). Given the dominance of Low-Ca granites of this age across the craton, however, it is still evident that the bulk of the middle-lower crust across the craton must have been of largely similar composition, or at least, similarly capable of producing voluminous Low-Ca magmatism.

In this regard, it was originally envisaged, that many of the Mafic group granites, especially those generated around 2665 Ma were produced in some form of arc-environment, co-incident with the proposed main period of crustal shortening (D_2) in the Eastern Goldfields Province. The evidence for, at least locally, spatially associated Syenitic and, perhaps High-HFSE group magmatism, of similar age, however, raises the possibility, that all granitoids of this age were produced in a similar (locally?) extensional environment. Note that this could still be in an overall arc-environment.

One notable feature of the Mafic group within the northern Murchison region is the ca. 2755 Ma Norie Clan comprising granites with chemistry similar to Archaean high-Mg diorites elsewhere (e.g., Smithies & Champion, 2000). These granites with their elevated MgO, mg#, Ni, Cr, clearly require a mantle-component in their genesis. Even more important, however, is the combination of high MgO, Ni etc, with moderate LILE contents. This combination of chemical features is thought to reflect metasomatism of the mantle source by LILE-enriched melts from a subducting slab, either before or during genesis of the granitoids (see discussion in Smithies & Champion, 2000); if correct this indicates subduction occurred at or before 2755 Ma, affecting the northern half, at least, of the northern Murchison region.

As indicated by Smithies & Champion (1999), alkaline and sub-alkaline rocks such as those in the Syenitic group are good indicators of regions undergoing, at least local, extension, or an anorogenic (post-tectonic) environment. It is difficult, however, to make any serious conclusions regarding tectonic environments, given that there is only one recognised syenitic unit in the northern Murchison. The lack of age control for this unit is also another problem.

High-Ca group, northern Murchison

Member Associations: Mainland Association (Murchison Province)
Diemals Association (Southern Cross Province)

Distribution: The largest granite group within the northern Murchison, representing up to and greater than 60% of the total granites (Fig. 1), within both the internal and external granites. Well represented across the entire region. Eleven clans have been recognised in the northern Murchison Province, and 2 small clans in the western Southern Cross Province (Table 6).

Geochronology: A large number of dated samples indicate a large age range from >3000 Ma to 2650 Ma, with the majority falling between 2760 to 2670 Ma (Tables 3, 4). One anomalously young age of 2612 ± 12 Ma has been recorded; the veracity of this age is not clear. Four distinct periods of High-Ca magmatism are evident, at 3010-3000 Ma, 2965-2930 Ma, 2815-2780 Ma, and 2760-2665 Ma. The latter age range may itself comprise a discrete sub-periods, with a number of apparent gaps; this may simply reflect the limited data set though. The periods of High-Ca magmatism closely correspond to the ages of greenstone formation within the region. The geochronology data indicate that all dated intrusive magmatism within the Murchison Province prior to ca. 2670 Ma was High-Ca in origin. This, however, probably reflects bias in the data set rather than the true picture. For example, felsic volcanic rocks within the Luke Creek group, i.e., >2930 Ma, appear to have chemistry (Watkins & Hickman, 1990), similar to members of the High-HFSE group. Furthermore, Mafic group granites of 2800 and 3020 Ma age are known from the Southern Cross Province, e.g., Westonia (Budd & Champion, this volume).

Inherited zircons, either from the source region or via assimilation of older crustal rocks, are relatively common within the High-Ca granites. As expected, the inherited zircon ages closely correspond, to the periods of known magmatism and greenstone formation (Tables 3, 4), consistent with at least some crustal input into the High-Ca granites.

No dates have been determined on the High-Ca granites in the Southern Cross Province region of the northern Murchison. Granite ages within the Southern Cross Province further to the east clearly show similar age groupings to the Murchison Province, with most magmatism at 2630-2740 Ma, and older groups at 2780-2825 Ma, and 2900-3020 Ma. Comparisons of the Murchison and Southern Cross provinces, with the Eastern Goldfields Province, suggests a marked difference between the age distributions of the High-Ca granites. In particular, there appears to be an apparent dearth of High-Ca (and other group) granites within the Murchison and Southern Cross provinces, in the 2.67 to 2.66 Ga age range, clearly contrary to the situation in the Eastern Goldfields Province.

Chemical characteristics. Characteristics of this group have been summarised by Champion & Sheraton (1997), and Champion (1997) for the Eastern Goldfields Province. Basically, the High-Ca granites comprise sodic trondhjemite, granodiorite and granite characterised by low to moderate LILE (K_2O, Rb, Pb) and HFSE (LREE, HREE, Y, Zr) contents. In detail, like the Eastern Goldfields Province, individual clans (Table 6), define a quasi-continuous range in LILE and HFSE contents, from low (Mainland clan) to moderate-high (Eily Eily clan, see Fig. 2), approaching and overlapping values seen in the Low-Ca granites (Fig. 4). Given this range in the LILE and HFSE, an arbitrary divide splitting the High-Ca group (and Mafic group) into low-LILE and high-LILE members was produced for the granites of the Eastern Goldfields Province, largely for the basis of classification and descriptive purposes (Fig. 4). It is apparent that this divide is also applicable for the Murchison Province (Fig. 4), and as such has been utilised in the following clan descriptions to subdivide the High-Ca group (and Mafic & High-HFSE groups) into high-LILE and low-LILE members; note that use of this terminology is relative, not absolute.

It is also evident that there is a decoupling between the LILE and HFSE in some clans, especially within the low LILE clans; for example, both the Euro and Mainland clans have low LILE, but the former has much higher contents of the HFSE than the latter. This picture is further complicated by the behaviour of Na_2O and Sr, which also exhibit large inter-clan differences, for clans with similar LILE and HFSE (e.g., Berbo Hill - low Na_2O, Sr, and Wheel of Fortune - high Na_2O, Sr). Notably, however, there is no variation in Eu, i.e., no relationship between the amount of Sr and Eu (both elements typically residing in plagioclase).

The majority of granitoids from the High-Ca group, in the Murchison Province, are characterised by low to moderate Y (and HREE) contents (Y-depleted; Fig. 3). HREE patterns are, however, largely unfractionated to flat, the only exceptions to this are members of the Wardiacca clan, and perhaps some of the Euro clan, which have significantly steeper HREE patterns. Notably, all except the Eily Eily, Yoothapina and

Wardiacca clans, are characterised by positive to very minor negative Eu anomalies.

Geochemical discrimination between the High-Ca and other groups is largely relatively straightforward (Figs 3, 4, 5, 6). Most difficulty occurs with the Eily Eily clan of the High-Ca group, and two clans (Nakedah and Myagar) of the Low-Ca group, which overlap for many elements (Fig. 5). Although differences between these clans are apparent, e.g., Ce, Zr, Sr, it is possible that the Eily Eily clan of the High-Ca group includes some members which more correctly belong to either the Myagar or Nakedah clans of the Low-Ca group, and vice versa. As discussed under individual clans below, it is possible that the Myagar clan, in particular, may actually be more correctly placed within the High-Ca group.

Sm-Nd data indicate a number of competing trends, based largely on geographic position. Most of the Murchison Province High-Ca granites have relatively unevolved Nd signatures, with ε_{Nd} between +1.4 and −1.7 (data from Fletcher & McNaughton, this volume; Nutman et al., 1993; Fletcher et al., 1994; Watkins & Hickman, 1990), notably irrespective of LILE and HFSE contents. More evolved values (i.e., more negative) occur, as expected, within the Narryer Gneiss Terrane, and, importantly, also to the east of the terrane in the older gneisses and pendants within the Murchison Province (Nutman et al., 1993; Watkins & Hickman, 1990), though they are not common. Ignoring the latter, it is clear that there is a pronounced isotopic difference between the High-Ca and Low-Ca groups, indicating isotopically distinct sources, notably even for the Eily Eily clan (which chemically overlaps with clans of the Low-Ca group).

Mineralised members? One of the larger Au mines within the northern Murchison region, Big Bell, is apparently associated with a granite of the High-Ca group, although the ore itself is largely hosted within greenstone (e.g., Mueller et al., 1996). Other units hosting gold mineralisation include Gold Bay, near Mt Magnet, and Lady Lydia near Noongal In addition, many of the deposits and mining camps described by Watkins & Hickman (1990) are characterised by the presence of porphyry dykes and sills, e.g., Hill 50, deposits in the Meekatharra mining camp. Many of these porphyries probably belong to the High-Ca group, though, some, at least, are definitely members of the Mafic group.

Other mineralisation associated with High-Ca granites include Mo-W. Significant Mo-W mineralisation is recorded for the 2756 Ma Mt Mulgine granite (Oliver, 1999). The mineralisation hosted within this granite, and within the greenstones nearby (Watkins & Hickman, 1990), appears to be closely related to the Mt Mulgine granite indicating orthomagmatic Mo-W mineralisation at ca. 2750 Ma (Oliver, 1999). Notably, the gold mineralisation around the Mt Mulgine granite overprints the W-Mo mineralisation and is not related (Oliver, 1999).

Petrogenesis: As for the Eastern Goldfields Province, the general characteristics of the High-Ca group (low LILEs, sodic), indicate derivation from a mostly mafic LILE-poor source, probably broadly basaltic in composition (Champion & Sheraton, 1997). Also like the Eastern Goldfields Province, the range in the LILE and HFSE (and Na_2O, Sr), between clans, however, points to a compositional range in the source also, i.e., the differences can not be solely due to varying degrees of partial melting. Such a compositional variety strongly indicates the involvement of at least two-components, either as a heterogeneous source (basaltic to quartz dioritic), or by some other process (assimilation of pre-existing crust, magma-mixing etc). Importantly, the decoupling between the LILE and HFSE, in some clans, suggests, either some further variation within the source, or the existence of an extra source component, or, perhaps, changes in the melting conditions (e.g., differences in initial water content resulting in differing residual mineral phases, especially accessory phases which largely control the HFSE). This picture is further complicated by the behaviour of Na_2O and Sr, and the lack of a Sr-Eu relationship, which may reflect an additional source component, or perhaps, if slab derived, variations in the degree of sea-floor alteration prior to subduction, and possibly even post-emplacement alteration.

The flat HREE patterns and lack of negative Eu anomalies in the majority of High-Ca granites in the Murchison Province, suggest that there was at best only minor residual feldspar, and that amphibole not garnet, was a dominant residual phase; the only possible exceptions being members of the Wardiacca and Euro clans, which may have had more dominant residual garnet, and the Eily Eily, Yoothapina and Wardiacca clans, which probably have had more significant amounts of residual feldspar.

The Sr-undepleted, Y-depleted nature of the majority of the High-Ca clans indicate derivation at pressures great enough to stabilise amphibole ± garnet and destabilise plagioclase (10-15 kbars) either deep within a thickened crust (>35-50 km) or, perhaps, from melting of a subducting slab (e.g., Martin, 1986). Either process is feasible, though the Sm-Nd isotopic data tend to favour a thickened crust source. This is even more evident when the Eily Eily clan is considered. The latter, with its Y-depleted but also Sr-depleted nature, requires either melting within the plagioclase-garnet stable region (10-15 kbars), or, perhaps, low pressure fractionation of feldspar. The presence of significant negative Eu anomalies in even the most mafic end-members suggests this is a source feature, hence, strongly arguing for partial melting within the crust, given that it is unlikely that slab-melting would occur at such low pressures. Notably if this is correct, i.e., the Eily Eily clan, the most LILE-rich High-Ca clan, was derived at lower pressures (higher crustal levels), than the other High-Ca clans, then it also follows that the Eily Eily clan was possibly generated closer to the site of partial melting for the Low-Ca group, i.e., closer to the source rocks for the Low-Ca granites. Such a hypothesis immediately suggests some involvement of the Low-Ca-type source in the generation of the Eily Eily clan granites, a process that would also explain the high LILE contents in the latter. Although the available Sm-Nd data, which suggest isotopically-distinct sources for the Low-Ca and High-Ca groups, limits the amount of possible Low-Ca-type source-component in the Eily Eily clan to probably less than 20-25%, this is considered sufficient to impart the high LILE characteristic to the Eily Eily clan. Note that this doesn't preclude a slab origin for other High-Ca clans, e.g., Mainland, Wheel of Fortune.

Tectonic & other implications: The bulk of the evidence appears to favour a thickened crust origin for the High-Ca granites, especially for the Eily Eily clan. As such, the periods of magmatism involving granites of the Eily Eily clan (i.e., 2670-2680 Ma, 2740-2760 Ma), also correspond to those times when the Murchison Province crust was thickened (>35-50 km). It is, however, also apparent that derivation from a subducting slab is also a possible viable mechanism for production of at least some of the High-Ca granites. Importantly, both the thickened crust or melting of a subducting slab hypotheses, require the operation of some form of convergent tectonics contemporaneous or just prior to granite generation. This can be interpolated, therefore, to infer that all periods of High-Ca granite formation correspond roughly to times of convergent tectonics in the Murchison (and Southern Cross) Provinces, i.e., 2675-2765 Ma, 2780-2825 Ma, 2920-2960 Ma, and 3000-3025 Ma. As noted before (Champion & Cassidy, this volume), the timing of these tectonic settings, especially post 2.72 Ga, contrasts somewhat with that for the Eastern Goldfields Province, i.e., pre 2.68 Ga High-Ca magmatism was common in the Murchison and Southern Cross provinces but minor in the Eastern Goldfields Province, 2.68 to 2.66 Ga magmatism was minor to absent in the Murchison and Southern Cross provinces but voluminous in the Eastern Goldfields Province. Clearly there are a number of possible scenarios, not mutually exclusive, that may explain these apparent differences, e.g., the Murchison and Southern Cross provinces were separate from the Eastern Goldfields Province before and/or during this period, the change across the Murchison and Southern Cross provinces to the Eastern Goldfields Province is actually diachronous, as in a migrating arc-environment, or perhaps the thermal regime at 2.68-2.66 Ga was such that granite production was largely confined to the Eastern Goldfields Province, such as in a typical modern-day convergent environment. Clearly further geochronology would be helpful, particularly along the eastern margin of the Southern Cross Province and western margin of the Eastern Goldfields Province.

In addition, the large volume of High-Ca granites in the northern Murchison clearly requires a correspondingly larger source (3 or more times volumetrically larger). This has important implications if the High-Ca granites were crustal-derived, requiring a very significant volume of pre-existing crust of relatively homogenous 'basaltic to andesitic' composition.

High-Ca (SCP)	Diemals Association	
Clan	**Supersuite**	**Suite**
Dewar	Dewar	Dewar
Janjather	Janjather	Janjather
unnamed	unnamed	unnamed

High-Ca (MP)	Mainland Association	
Clan	**Supersuite**	**Suite**
Berbo Hill	Berbo Hill	Berbo Hill, Edamurta, unnamed
	North Paradise	Morawa, Petroden, North Paradise, Windinie
Eily Eily	Barnong	Barnong, Coodardoo, Booladoo, Munboocarderbungah, Worarawar
	Bookine	Bookine
	Bundine	Woolbertharra, Bundine, Bolly
	Bundabinna	Killarnie, Bundabinna
	Buongnoo?	Buongnoo?, unnamed
	Coobawarn	Coobawarn, unnamed
	Coombeloona	Coombeloona
	Coompacoomper	Yallabanodka, McCarthy, Coompacoomper, unnamed, Ballan
	Courin Hill	Courin Hill, Wandaminya Vee
	Dinny	Dinny, Mungarra, unnamed
	Eily Eily	Dorothy, Eily Eily, Uloganna?, Dartmoor, Gorge Well, IXL, unnamed
	Fishers Bore	Fishers Bore , unnamed
	Gabbobobby	Gabbobobby?
	Linders Fern	Linders Fern
	Marlomumbo	Marlomumbo, unnamed, Meelo, Pereira?, Chiggarie
	Mt Mulgine	Mt Mulgine
	Murnini	Murnini, Bardenu, unnamed, First Pop
	North Weaner	North Weaner
	Payne Well	Payne Well, unnamed
	Peendubba	Mardooganna, Peendubba, Ero Creek, Boodrah
	Walga	Walga, Poona
	unnamed	Tharandah
	Yarlot	Yarlot
	Yilgiddie	Yilgiddie
Euro	Euro	Euro, Cootamarra, Dicks Well
Gudgeman?	Gudgeman	Gudgeman, Fenton, Balbaroo
Kyle Kyle	Kyle Kyle	unnamed, Kyle Kyle?, Wheelocks
	unnamed	unnamed porphyries in Gabanintha Fm
Mainland	Bunnajarra	Bunnajarra, Franks Well, Warratarra, Curbura
	Mainland	Mungo, Weedah Yalan, Mainland, Pollick, Clarry Bore, Taincrow, Wadu, Koweragabbie, Big Bell, Buttercup
	Mardah?	Mardah, unnamed
	Mt Farmer	Mt Farmer
	Tall Tower	unnamed, Wyagoola, Tall Tower, Yoweragabbie, East Kia, Nungajinny, Congoo, Cockarra, Jordans, Carngo
	Toben	Toben
	Wardatharra	Wardatharra, McNab
	Wattamulga	Wattamulga, unnamed
Uanna	Badja	Badja, Dampacoppy
	Gold Bay	Gold Bay
	Kurrajong Well	Kurrajong Well, Gabyon
	Uanna	Uanna
	Wiregaminda	Wiregaminda, Zadow, Jindooloo, Camel Paddock, unnamed
unassigned	unassigned	unassigned

Table 6. Suites, supersuites, clans and associations of the High-Ca group, northern Murchison.

High-Ca (MP)	Mainland Association	
Clan	**Supersuite**	**Suite**
Wardiacca	Wardiacca	Wardiacca, Darn Hill?, Tobins, Gnudabigbee, Nannowtharra?
	Warragee	Warragee, Murrungnulg
	Younga	Younga, Wagstaff, Mungada, Mangatah
Wheel of Fortune	Lady Lydia	Lady Lydia, Dabyilmurra?
	Wheel of Fortune	Wheel of Fortune
Woolbong	Wolbar	Wolbar
	Wolla Wolla	Wolla Wolla, Mick Well, Minjar, Chulla, Moorgabby, Gnows Nest, unnamed, Boona, Nargunger
	Woolbong	Woolbong, Beardie, Eraballe, Collyakko, Beardie, Marlandy
Yoothapina	Yoothapina	Yoothapina, unnamed

Table 6 (continued). Suites, supersuites, clans and associations of the High-Ca group, northern Murchison.

Clans of the Menangina Association, High-Ca Group, Eastern Goldfields Province.

Eily Eily Clan

Member Supersuites: Barnong, Bookine, Bundine, Bundabinna, Buongnoo?, Coobawarn, Coombeloona, Coompacoomper, Courin Hill, Dinny, Eily Eily, Fishers Bore, Gabbobobby?, Linders Fern, Marlomumbo, Mt Mulgine, Murninip, North Weaner, Payne Well, Peendubba, Walga. unnamed, Yarlot, Yilgiddie

Distribution: The most dominant clan within the Mainland Association (Table 6), the 94 units of the Eily Eily clan include intrusive units, gneiss complexes, dykes and gneiss pendants, both external and internal to greenstone belts. The clan is widespread, but is particularly concentrated within two broad zones:

- a broad belt from NE Belele to NC and NE Perenjori, and
- in a NNE zone from SC Cue to SW Kirkalocka.

Geochronology: Eight recorded ages for 7 units are available for the Eily Eily clan (Table 3). These fall into three distinct age groups, most at 2670-2680 Ma (all Eily Eily supersuite), 2 at ca. 2740-2760 Ma (Courin Hill & Mt Mulgine supersuites), and one younger outlier at 2655 ±10 Ma (Bookine supersuite). Most also show evidence for zircon inheritance, with ages for the latter from 2700 to 2935 Ma.

Chemical characteristics: This clan represents the high LILE and higher HFSE end-member of the Mainland Association (Fig. 2), and as such is distinguished by its elevated to higher K_2O, Rb, Pb, Th, Zr, Ce, relative to most other High-Ca clans (Figs 2, 3, 4). Another feature of the Eily Eily clan is the low Sr (Fig. 3), and correspondingly negative Eu anomalies, relative to most other clans, even though all High-Ca clans are Y- (and HREE-) depleted. The Eily Eily clan shares a number of similarities with the Berbo Hill (similar low Sr but lower LILE, HFSE in the latter), Gudgeman (similar low Sr but lower HFSE), Wardiacca (similar high HFSE but higher Sr & lower LILE), Euro (similar high HFSE but higher Sr & lower LILE), and Yoothapina (similar high HFSE but higher Sr & lower LILE) clans, but with notable differences (Fig. 3). The Southern Cross Province Dewar clan, is the most similar to Eily Eily.

Mineralised members? Significant Mo-W mineralisation is recorded for the older (2756 Ma) Mt Mulgine granite (Oliver, 1999). The mineralisation, hosted within this granite and within the greenstones nearby (Watkins & Hickman, 1990), appears to be closely related to the Mt Mulgine granite indicating orthomagmatic Mo-W mineralisation at ca. 2750 Ma (Oliver, 1999). Notably, the gold mineralisation around the Mt Mulgine granite overprints the W-Mo mineralisation and is not related (Oliver, 1999).

Petrogenesis: As for the High-Ca group in general, though the higher LILE and HFSE require a more LILE-enriched component in their source. In addition the Sr- and Y-depleted natures of the Eily Eily clan granites requires the involvement of both garnet and feldspar in their production, most probably as residual minerals within the source region. The Sr depletion could also be due to low pressure feldspar fractionation, however, the presence of negative Eu anomalies in even the most mafic members of the clan argues strongly against such a mechanism. If the latter is correct this places the generation of the Eily Eily granites within a small pressure range where both garnet and plagioclase are stable (approximately 10-15 Kbar, e.g., Patino Deuce & Beard, 1995). Importantly, these constraints would tend to imply the Eily Eily clan was largely crustal-derived, not slab-derived. Geochemically, many of the features evident in the Eily Eily clan trend towards and actually overlap with the less-evolved members of the Low-Ca group, especially the Nakedah and Myagar clans in the latter (Fig. 5). This geochemical overlap is significant, particularly when the apparent depth (pressure) of generation is taken into account. Unlike the Eastern Goldfields Province, where the sites of generation for the Low- Ca and High-Ca groups were largely separate (low-moderate pressure versus high pressure, respectively), it is evident that in the Murchison Province the respective source regions overlapped; it is no surprise, therefore, that there is also some overlap in chemistry, i.e., a mixing of sources for some members of both groups. The available Sm-Nd isotopic data, which suggest isotopically-distinct sources for the Low-Ca and High-Ca groups (including the Eily Eily clan), limits the amount of possible Low-Ca-type source-component in the Eily Eily clan to probably less than 20-25%, this is considered sufficient, however, to impart the high LILE characteristic to the Eily Eily clan.

Tectonic & other implications: As for the High-Ca group in general. The Sr depleted nature of the Eily Eily clan appears to indicate derivation within continental crust, not the subducting slab. As such, the periods of magmatism involving granites of the Eily Eily clan (i.e., 2670-2680 Ma, 2740-2760 Ma), also correspond to those times when the Murchison Province crust was thickened (>35-50 km).

Berbo Hill Clan

Member Supersuites: Berbo Hill, North Paradise

Distribution: A moderate sized clan, comprising less than 10 units, ranging from large intrusive bodies, to gneiss complexes and including dykes and gneiss pendants, all either external or marginal to the Gullewa, Yalgoo-Singleton and Koolanooka greenstone belts. The clan is confined to a broad north-south zone encompassing the eastern and central parts of the Yalgoo and northern Perenjori sheets. The largest units (intrusive bodies and gneiss complexes) occur within the southern part of this zone, along the Perenjori-Yalgoo sheet boundary.

Geochronology: No ages have been recorded for members of this clan.

Chemical characteristics: The Berbo Hill clan falls into the low LILE end-member of the High-Ca group, and as such has most similarities to the Mainland clan. Differences with the latter include lower Na_2O, Sr, and slightly lower HFSE in the Berbo Hill clan. Both clans are Sr-undepleted with no or slightly negative Eu anomalies, Y-depleted, and have elevated MgO and mg#, relative to other High-Ca clans.

Mineralised members? There is no known mineralisation associated with the Berbo Hill clan.

Petrogenesis: As for the High-Ca group in general. Like the Mainland clan, the Berbo Hill clan granites clearly represent derivation from a low-LILE basaltic source, with little or no input from other components. The lower Sr and Na_2O in the Berbo Hill clan, relative to the Mainland clan, most likely represents a source difference, given the similar levels of LILE between the two, i.e., it can not be due to additional components or variable degrees of partial melting.

Tectonic & other implications:
Mostly as for the Mainland clan and the High-Ca group in general.

Euro Clan

Member Supersuites: Euro

Distribution: A small clan comprised of 5 units, including one pod, all external to greenstones. Two main regions of occurrence:

- 4 units in the in SW Kirkalocka, and
- one unit in NE Kirkalocka

Geochronology: No ages have been recorded for this clan.

Chemical characteristics: The Euro clan straddles the high- LILE/low-LILE boundary and as such shares geochemical features with both the low LILE Mainland and high LILE Eily Eily clans (Figs 3, 5), e.g., elevated HFSE, lower CaO, MgO and moderate Na_2O, like Eily Eily, with low LILE, including K_2O, Rb, Pb, like Mainland. The Euro clan is further characterised by elevated Ba and Sr, strongly depleted Y, and no or slightly negative Eu anomalies.

Mineralised members? None known associated mineralisation.

Petrogenesis: As for the High-Ca group in general. The low LILE contents suggest an essentially low LILE source, e.g., as postulated for Mainland. The elevated HFSE, indicate an additional component, perhaps some metasomatic mantle product, e.g., lamprophyre, given the elevated Sr and Ba of the clan.

Tectonic & other implications: In general, as for the High-Ca group. The chemistry of the Euro clan raises the possibility of a third source component, one with low LILE but elevated HFSE component.

Gudgeman Clan

Member Supersuites: Gudgeman

Distribution: Small clan of 3 units, one a gneiss complex, localised to SE Yalgoo within and marginal to the external granite mass between the Yalgoo-Singleton and Gullewa greenstone belts.

Geochronology: No recorded age determinations. One unit, the Fenton gneiss complex, is spatially associated with the Badja gneiss which has a tentative age of 2920 Ma (Table 3). It is possible that the Fenton gneiss complex is also of this age, though it is noted that the Badja gneiss, which is distinctive on the aeromagnetic data, is more complexly deformed and folded (Watkins & Hickman, 1990), and, hence, probably older.

Chemical characteristics: The Gudgeman clan falls into the high LILE end-member and as such has many similarities with the Eily Eily clan. Differences with the latter include significantly higher Sr, Ba, lack of Eu anomalies, and generally lower HFSE contents. The high Sr and Ba, with moderate to high LILE is distinctive. Like many other High-Ca clans, there is a pronounced flattening of the HREE.

Mineralised members? No known associated mineralisation.

Petrogenesis: Generally as discussed for the High-Ca group, with the high LILE contents indicating the involvement of a moderate-LILE source component, as for the Eily Eily clan, though at greater pressures. The lower HFSE in the Gudgeman clan probably reflects a source feature.

Tectonic & other implications: As for High-Ca group in general.

Kyle Kyle Clan

Member Supersuites: Kyle Kyle and unnamed

Distribution: A small clan, comprising three intrusive units, and a number of external and internal dykes, occurring within three regions:

- NE and NC Kirkalocka,
- external dykes in NW Kirkalocka, and
- internal porphyry dykes(?) near the Norie tonalite, SE Belele, in the Meekatharra-Wydgee greenstone belt. These samples collected by Q. Wang (ANU, unpublished data), are described as porphyry and may actually be felsic volcanics not granites.

Geochronology: None available.

Chemical characteristics: Very similar to the Mainland clan, i.e., a low-LILE member, with actually lower LILE and HFSE relative to the former (Figs 3, 4). Typically, Sr-undepleted, with no or slightly negative Eu anomalies, and Y-depleted, with markedly flat HREE.

Mineralised members? No recorded associated mineralisation.

Petrogenesis: As for the Mainland clan and the High-Ca group in general. The lower

LILE and HFSE, relative to the Mainland clan, indicates an even more LILE-poor source. The flat HREE indicate significant involvement of amphibole, probably within the source (as a residue).

Tectonic & other implications: As for the Mainland clan and the High-Ca group in general.

Mainland Clan

Member Supersuites: Bunnajarra, Mainland, Mardah?, Mt Farmer, Tall Tower, Toben, Wardatharra, Wattamulga

Distribution: Widespread clan, comprising some 47 units (intrusive units, gneiss complexes, dykes, pods, and gneiss pendants), both internal and external to greenstones. Mainly concentrated within the Cue, and Kirkalocka sheets, especially within a north-east trending zone from NE Cue to SC Kirkalocka. Minor units also occur along the eastern parts of the Murgoo and Yalgoo sheets.

Geochronology: Six ages, four from the one supersuite, are available for the Mainland clan (Table 3), that range from 2737 to 2684 Ma (4 ages), with a young 2666 Ma age, and an anomalously-young (for any granite group), 2612 Ma age. Inherited zircon ages are mostly young (<2750 Ma), except for the Big Bell granite which contains inherited zircons with ages ca. 2800-2900 Ma (Table 3).

Chemical characteristics: The archetypal low LILE clan of the High-Ca group, with low LILE and HFSE (Figs 2, 3, 4). No Eu anomaly is present within mafic end-members, but becoming slightly negative with increasing silica. Members of the clan are Y-depleted and mostly Sr-undepleted, with relatively flat HREE patterns. Most similar to the Kyle Kyle, Uanna, and Wheel of Fortune clans, though the latter have higher Sr and even more-depleted Y.

Mineralised members? The Big Bell porphyry is spatially associated with gold mineralisation at the Big Bell deposit. Most gold mineralisation, at the latter, is, however, hosted within the greenstones (e.g., Mueller et al., 1996). Porphyries spatially associated with mineralisation at the Pinnacles, Tuckabiana, Tuckanarra, Cuddingwarra, Lennonville and, perhaps Mt Magnet, mining camps (Watkins & Hickman, 1990), are also likely to belong to this clan, given the close geographic proximity of these mining camps to known granites of this clan.

Petrogenesis: The sodic nature, and low LILE and HFSE indicate derivation from a source even more depleted in these elements, most probably broadly basaltic in composition. Although Y-depleted, the flat HREE patterns suggest more the involvement of hornblende as versus garnet, indicating slightly lower depths, i.e., lower pressures, of generation.

Tectonic & other implications: As for the High-Ca group in general.

Uanna Clan

Member Supersuites: Badja, Gold Bay, Kurrajong Well, Uanna, Wiregaminda

Distribution: A small clan of 16 units comprising gneisses, gneiss pendants, moderate-sized plutons, small pods, and dykes, mostly external or marginal to greenstone belts (e.g., Yalgoo-Singleton, Warda Warra greenstone belts), with one internal body (Gold Bay, near Mt Magnet). Distribution is largely confined to one region, in the eastern half of the Yalgoo sheet (Badja, Kurrajong Well, Wiregaminda supersuites). Three units occur elsewhere, two in SW Cue (both Uanna supersuite), the other in NC Kirkalocka (Gold Bay supersuite).

Geochronology: Two units from the Uanna clan have been dated. The Badja gneiss (Badja supersuite), on the Yalgoo sheet, gives a tentative age of 2920 ± 12 Ma (Weidenbeck & Watkins, 1993), the other Gold Bay (Gold Bay supersuite) with a 2696 ±5 Ma age. The latter falls within the dominant age range of the High-Ca granites, while the former is one of the oldest ages recorded in the northern Murchison Province. Similar old ages, however, are well know within the Narryer Terrane and in the southern Murchison Province (Tables 4, 5). The younger, internal, Gold Bay granite shows evidence for young inherited zircons (<2750 Ma) that may have been sourced from greenstones or granites.

Chemical characteristics: Members of the Uanna clan largely fall within the high-LILE end-members, though only just. As such they have chemistry somewhat intermediate between the Eily Eily clan and the Mainland clan (Figs 3, 4), e.g., not as LILE- or as HFSE-enriched as Eily Eily. Best characterised, like Wheel of Fortune, by their high to very high Sr, higher than both the Mainland clan and Eily Eily clan. All members have positive to no or very slight negative Eu anomalies and are strongly Y-depleted.

Mineralised members? The Gold Bay granite, south of Mt Magnet hosts minor Au mineralisation. Elsewhere units not associated with mineralisation.

Petrogenesis: Largely as for the High-Ca group in general. The intermediate contents of the LILE and HFSE suggest a mixed source, though one not as LILE-rich as for the Eily Eily clan. The high to very high Sr and low Y indicate residual garnet, and no plagioclase, i.e., at high pressures (15 kbar+).

Tectonic & other implications: As for the High-Ca group in general. Clearly derived at high pressures, either within thickened crust or the slab.

Wardiacca Clan

Member Supersuites: Wardiacca, Warragee, Younga

Distribution: A small clan of 11 units comprising small to large granite plutons, mostly external with one marginal unit (marginal to the Gullewa greenstone belt).
Distribution is largely confined to two regions, with the majority of units forming a cluster in the western third of the Kirkalocka sheet (Younga and Wardiacca supersuites), and the two plutons of the Warragee supersuite occurring in NE Perenjori.

Geochronology: Three units of the Wardiacca clan have been dated, giving ages between 2685 and 2710 (Table 3), all falling within the dominant age range of the High-Ca group in the Murchison Province. Inherited zircon data indicate ages of ca. 2800 and 2960 Ma, similar to both greenstone formation ages and periods of granite magmatism. Significantly, the two dated units showing inheritance are external to the greenstones, suggesting sampling of older granites as the source of the inheritance.

Chemical characteristics: Clearly falls within the high LILE end-member of the High-Ca group. As such similar to Eily Eily clan, though with some notable differences, e.g., similar to higher Ba, LREE and Zr, similar to lower Y and Nb, lower Rb, higher Sr, and smaller Eu anomalies; the latter ranging from slightly positive to slightly negative. Notably, negative Eu anomalies occur within the most mafic end-members of the clan, suggesting, like the Eily Eily clan, that this may be a primary feature of the clan. The Wardiacca clan is most similar to the Euro clan, though the latter has higher Sr and lower K_2O, REE and Y (Fig. 3).

Mineralised members? No known associated mineralisation.

Petrogenesis:
Largely as for the Eily Eily clan, and the High-Ca group in general.

Tectonic & other implications:
As for the Eily Eily clan, and the High-Ca group in general.

Wheel of Fortune Clan

Member Supersuites: Lady Lydia, Wheel of Fortune

Distribution: A small clan of 5 units comprising small to moderate-sized plutons, both external and internal (within Yalgoo-Singleton and Meekatharra-Wydgee greenstone belts). Distribution is confined to 2 small regions, in NE Yalgoo (Lady Lydia supersuite), and SC Cue (Wheel of Fortune supersuite).

Geochronology: Two units have been dated from the Wheel of Fortune, 2743 ± 4 (Lady Lydia supersuite), and 2702 ±6 (Wheel of Fortune supersuite). These results indicate a significant time-break between the supersuites, though both are within the broad range shown by the majority of High-Ca granites in this region (Table 3). Inherited zircon data correspond to the three periods of greenstone development and granite magmatism; given the internal setting of the dated plutons, the inherited zircons may reflect either.

Chemical characteristics: A low LILE end-member, the Wheel of Fortune clan is characterised by low LILE, and HFSE, coupled with high Na_2O, Sr, and Ba; the latter three being characteristic. The clan is similar to the Mainland and Kyle Kyle clans but readily distinguished by its higher Na_2O and Sr from the former, and higher K_2O, Sr, Ba relative to the latter. All members are strongly HREE- and Y-depleted with no or very minimal, slightly positive to slightly negative, Eu anomalies.

Mineralised members? The Lady Lydia granite (Lady Lydia supersuite) hosts gold mineralisation and is according to Oliver (1999) hydrothermally altered. Similarly, porphyries related to the Basin granite are spatially associated with mineralisation in the same area (Noongal mining camp). Oliver (1999) reported a titanite age from the Basin granite of 2631 ±7 Ma, which he interpreted to date movement on the Noongal shear zone and an indirect age for gold mineralisation. Although, the Wheel of Fortune granite is spatially close (within 1km), to the deposits of the Lennonville mining camp (north of Mt Magnet), Watkins & Hickman (1990), record no porphyries within these deposits.

Petrogenesis: Largely as for the Mainland and Kyle Kyle clans.

Tectonic & other implications: As for the Mainland and Kyle Kyle clans, and the High-Ca group in general.

Woolbong Clan

Member Supersuites: Wolbar, Wolla Wolla, Woolbong

Distribution: A moderate clan of 20 units comprising gneiss complexes, small to large-sized plutons, and small pods, mostly external, but including a few internal or marginal to greenstone belts (Gullewa greenstone belt). Distribution is strongly localised with all units confined to the eastern half of the Yalgoo sheet.

Geochronology: No units of the Woolbong clan have been dated.

Chemical characteristics: Mostly falls within the high LILE end-member, characterised by moderate (to high) LILE, but shares some features with the low LILE end-members, i.e., low to moderate HFSE, and moderate to high Sr. The latter is reflected by most samples having with no or only slight negative or positive Eu anomalies, though some felsic members have either small negative Eu or moderate to large positive anomalies. The clan is strongly Y-depleted. The coupling of moderate LILE with low HFSE is distinctive. A similar feature is shared by the Gudgeman clan, which shares many similarities with the Woolbong clan, though the latter lacks the elevated Sr and Ba of the former.

Mineralised members? Not associated with known mineralisation.

Petrogenesis: Largely as for the Eily Eily and Gudgeman clans.

Tectonic & other implications: As for the Eily Eily and Gudgeman clans, and the High-Ca group in general.

Yoothapina Clan

Member Supersuites: Yoothapina

Distribution: A very small clan of just 2 units, comprising a moderate-sized internal foliated granite in the Meekatharra-Wydgee greenstone belt, SE Belele, and a small external pod, in SW Belele.

Geochronology: No units of the Yoothapina clan have been dated.

Chemical characteristics: Clearly falls within the high LILE end-members of the High-Ca group, and as such such has many similarities with the Eily Eily clan, including negative Eu anomalies. The Yoothapina clan is, however, characterised by a number of element decouplings, e.g., has moderate Sr and low Rb and Pb, coupled with moderate Na_2O, and K_2O. Also characterised by moderate to high HFSE contents, small negative Eu anomalies, and higher FeO*, MgO than the majority of High-Ca granites in the region. Has many similarities with the Euro clan, in particular the low-moderate LILE and moderate-high HFSE, though the Euro clan has distinctly higher Sr and Ba.

Mineralised members? No known association with mineralisation.

Petrogenesis:
Largely as for the Euro and Eily Eily clans.

Tectonic & other implications: As for the Euro and Eily Eily clans, and the High-Ca group in general.

Clans of the Diemals Association, High-Ca Group, Southern Cross Province

Dewar Clan

Member Supersuites: Dewar

Distribution: A small clan comprising two small to moderate external plutons in SE Cue.

Geochronology: No reported geochronology for this clan.

Chemical characteristics: Belongs to the high LILE end-member of the High-Ca group. Chemically, very similar to the Eily Eily clan of the Murchison Province (Figs 3, 4), including having moderate Sr and small to moderate negative Eu anomalies. Readily distinguished from the more chemically-primitive Janjather clan; the latter having lower LILE and HFSE, and significantly higher Na_2O and Sr. Relative to Southern Cross Province clans to the east (Budd & Champion, this volume), the Dewar clan is very similar to the Diemals clan, and may actually belong in the latter.

Mineralised members? No known associated mineralisation.

Petrogenesis: Essentially similar to that for the Eily Eily clan, Murchison Province, i.e., from a 'source' more chemically evolved than basalt/amphibolite.

Tectonic & other implications: Largely as for the Eily Eily Clan, Murchison Province, and the High-Ca group granites in general.

Janjather Clan

Member Supersuites: Janjather

Distribution: Very small clan comprising one external small pluton in SE Cue.

Geochronology: No reported geochronology for this clan.

Chemical characteristics: Clearly falls into the low LILE end-member with its low to very low K_2O, Rb, Pb, and high Na_2O and Sr. Most similarities with the Wheel of Fortune and Mainland clans in the Murchison Province, though the former has higher LILE contents, and the latter has lower Na_2O, Sr and Ba and higher MgO and FeO*, relative to the Janjather clan. Relative to SCP clans to the east (Budd & Champion, this volume), the Janjather clan is clearly more primitive with lower LILE (especially K_2O and Rb) and much higher Sr. The most similar clan, the Hong Kong clan, occurs within the very easternmost part of the Southern Cross Province in the northern Eastern Goldfields region (Champion & Cassidy, this volume), although the latter lacks the high Sr found in the Janjather clan.

Mineralised members? No known associated mineralisation.

Petrogenesis: As for the Mainland and Wheel of Fortune clans of the Murchison Province, and the High-Ca granites in general. The Low-LILE composition, is most consistent with a basaltic/amphibolitic source composition.

Tectonic & other implications: As for the Mainland and Wheel of Fortune clans of the Murchison Province, and High-Ca group in general.

Low-Ca Group, northern Murchison

Member Associations: Goolthan Association (Murchison Province)
Beetle Association (Southern Cross Province)

Distribution: The second most dominant granite group within the northern Murchison, representing up to 15 to 20% of total granites (Fig. 1). Widespread occurrence across the northern Murchison, ranging from large plutons to numerous small pods and dykes into older granites. Eight clans have been recognised in the northern Murchison Province, and one small clan in the western Southern Cross Province (Table 7).

Geochronology: Only 4 ages are available for the Low-Ca granites, in the Murchison Province, 3 lying between 2654 and 2626 Ma, with one outlier at 2676 Ma (Table 3). The older age should be treated with some caution as it is not entirely unequivocal whether this sample belongs to the High-Ca or Low-Ca group (see Myagar clan section). Except for the outlier, these ages are similar to those for Low-Ca granites in the southern Murchison Province (Table 4), which fall between 2627 and 2654 Ma. This range is very similar to that observed for the Low-Ca granites within the Southern Cross and Eastern Goldfields provinces (2660 to 2630 Ma), providing good evidence that Low-Ca magmatism, unlike the High-Ca magmatism, was largely synchronous across both provinces (and the Southern Cross Province), though as noted elsewhere (Champion & Cassidy, this volume), the Eastern Goldfields Province appears to lack significant Low-Ca magmatism of 2.64-2.63 Ga and younger. Further geochronology will help clarify whether these differences are indeed real or just artefacts of the limited data to date.

Although inherited zircons would not expected within Low-Ca granites (i.e., high Zr levels indicating that the initial melts weren't zircon saturated), there is some evidence for older zircon. Data, available for the whole Murchison Province (Tables 3, 4) give inherited(?) ages of 2670-2680, and ca. 2770-2830 Ma. These 'inherited' ages are much younger than would be expected given the Nd model ages (3000 to 3200 Ma, Fletcher & McNaughton, this volume).

Chemical characteristics.
Characteristics for this group have been summarised by Champion & Sheraton (1997), and Champion (1997), for the Eastern Goldfields Province. Basically, the Low-Ca granites in the Murchison Province are very similar, comprising potassic granite and lesser granodiorite, characterised by high LILE (K_2O, Rb, Pb, Th, U) and HFSE (LREE, HREE, Y, Zr) contents (Figs 4, 5), with moderate to strong negative Eu anomalies (Sr-depleted), flat HREE patterns, and mostly Y-undepleted, but ranging to Y-depleted, compositions. The Deep Mucca Bunna, Midge and Goolthan clans of the northern Murchison, are the archetypal Low-Ca clans, exhibiting most of the features of this granite group (Figs 4, 5). As for the Eastern Goldfields Province, individual clans (Table 7), exhibit a range in LILE and HFSE contents, from moderate (Myagar, Nakedah clan) to high (Deep Mucca Bunna, Midge and Goolthan clans; Fig. 4), though the range isn't as large as for the High-Ca group. Other chemical variations include high to very high Sr and Ba (Nakedah, Deep Mucca Bunna clans), and, in the Horseshoe clan, elevated FeO*, Y. Available Sm-Nd isotopic data, indicate a narrow range in ε_{Nd} (-3.4 to -4.6), that overlap completely with members of the High-HFSE group, but are clearly more evolved (more negative), than High-Ca, and Mafic group granites (Fletcher & McNaughton, this volume). Champion & Sheraton (1997) reported similar relationships between the granite groups in the Eastern Goldfields Province.

The Myagar and Nakedah clans, two of the most chemically primitive clans of the Low-Ca group, are characterised by moderate to high Na_2O, moderate K_2O, with only moderate LILE and HFSE, and as such, their geochemistry overlaps with the more LILE-rich members of the Eily Eily clan of the High-Ca group, with only minor differences, e.g., slightly lower HFSE, and slightly higher CaO, in the Eily Eily clan (Fig. 5). This raises the problem that it is not entirely evident to which group the Myagar and Nakedah clans actually belong, i.e. either Low-Ca or High-Ca, although part of this overlapping chemistry reflects lack of documentation by Watkins & Hickman (1990), for their sample sites where multiple samples were collected, i.e., it is not entirely clear what has been sampled, e.g., dominant phase, dyke, enclaves. Obviously, there is no satisfactory solution to this classification problem; additional work is clearly required, in particular, Sm-Nd data for both the Myagar and Nakedah clans would be helpful.

Mineralised members? Like the Eastern Goldfields Province, there are no recorded examples of Low-Ca granites hosting gold mineralisation, despite them apparently being either older or contemporaneous with the postulated main period of gold mineralisation around 2640 to 2630 Ma (e.g., Yeats et al., 1996). The Low-Ca granites are, however, younger than the gold mineralisation recorded at Big Bell, if the 2662 ± 5 Ma age of Mueller et al. (1996), is correct.

Like the Low-Ca granites in the Eastern Goldfields Province, it is considered highly likely that the Low-Ca granites of the Murchison Province have, contributed, by weathering, to the U in calcrete deposits in the region. It is also considered likely that pegmatites associated with Be (and Li), and/or Sn-Ta mineralisation are also related to the Low-Ca granites. These pegmatites, as described by Watkins & Hickman (1990), occur both within greenstones, e.g., Rothsay, Dalgaranga, Poona or within Low-Ca granites, e.g., Edah.

Petrogenesis: The characteristics of the Goolthan Association, and the Low-Ca group granites in general, i.e., potassic, high LILEs, elevated HFSEs, indicate derivation from an, at least moderately, potassic and LILE-rich crustal source, i.e., some form of pre-existing continental crust, possibly compositions not unlike typical Archaean tonalites (Champion & Sheraton, 1997). The low CaO in the Low-Ca granites and the very minor occurrence of amphibole in the granites themselves, indicate partial melting was largely via dehydration melting driven by biotite breakdown, i.e., either small volume melts or from a source with only minor amphibole. Further the high levels of the HFSEs, in particular Zr, in the Low-Ca granites, strongly indicate high temperature melting (i.e., zircon saturation and, hence, levels of Zr in a granite melt are strongly temperature dependent), a fact which may also be consistent with a generally water-poor (limited amphibole) source. Finally, the mostly Y-undepleted and Sr-depleted nature suggests that the Low-Ca granites were generated at moderate crustal levels (mostly <35 km).

The variation in LILE, in particular, and the HFSE, between the Low-Ca clans, may reflect a variety of processes, including:

- changes in the percentage of partial melting, i.e., the greater percentage of melt, the lower the concentration of LILEs in the melt,
- variations in source compositions,
- variable mixing of two or more source components, e.g., perhaps a component of a source similar to that envisaged for the High-Ca granites.

It is apparent that a number of these processes may have viable. For example, the chemical characteristics of the Goolthan clan, e.g., lower K/Rb, mg#, more negative Eu anomalies and higher Ca/Sr ratios, for given silica content, are consistent with smaller degree partial melts. On the other hand features such as those shown by the Horseshoe clan, e.g., higher FeO*, and lower K_2O, Rb, coupled with low Sr, are also characteristics of the High-HFSE group in the northern Murchison, suggesting that there may be a component of the High-HFSE group source involved in the generation of the Horseshoe clan. Finally, it is evident that the variation in the HFSE, Na_2O and K_2O, and Sr and Ba, between clans, also indicate some differences in LILE and HFSE contents of the source rocks for the Low-Ca clans.

Tectonic & other implications: The simplest model for the Low-Ca granites, would appear to require their generation from moderately dry tonalitic (or more felsic) pre-existing crust, in an extensional environment most probably with an elevated geothermal gradient (needed to get the postulated high melting temperatures). This is clearly contrary to the general scenario for the High-Ca granites, indicating not only distinct source rocks, but distinct sites of granite generation for the two granite types (though there is some evidence that the Eily Eily clan of the High-Ca group may have been derived at similar crustal levels as the Low-Ca granites). These differences between the High-Ca and Low-Ca sources are also supported by the available Sm-Nd isotopic data which indicate isotopically distinct source reservoirs for the two granite groups (Fletcher & McNaughton, this volume). As for the Eastern Goldfields Province, these differences are even more significant when the age distributions of the two granites groups are taken into consideration, i.e., the temporal change from dominantly High-Ca magmatism to less voluminous, but very widespread, dominantly Low-Ca magmatism, around 2660 to 2650 Ma. This changeover in magmatism presumably must correspond to some fundamental change in tectonic environment, perhaps from a compressional or arc-related environment to one dominated by extension or post-tectonic relaxation, i.e., some mechanism produced a change in the thermal regime, that not only increased the thermal gradient (to allow generation of Low-Ca granites) but effectively turned off production of High-Ca granites.

As discussed for the Eastern Goldfields Province (Champion & Cassidy, this volume), the exact nature of this tectonic transition is largely dependent on the origin of the High-Ca granites. If, as favoured for the northern Murchison, the High-Ca granites were generated by partial melting in thickened crust, then the change to Low-Ca magmatism indicates melting shifted to higher crustal-levels (the site of Low-Ca generation), with the thickened lower crust (High-Ca source) either somehow insulated from further melting or removed. In this regard, Smithies & Champion (1999) suggested that this post 2660 Ma thermal event may have resulted from Yilgarn-wide lower-crustal delamination following crustal thickening during the main D_2 shortening deformation in the Eastern Goldfields Province. These authors further speculated that this event represented an additional tectonothermal event in the Yilgarn Craton, contemporaneous with lower-middle crustal high-grade metamorphism and regional Au mineralisation (e.g., Kent et al. 1996).

If, however, the High-Ca granites were largely generated by slab-melting, a scenario considered less likely, then the change over to Low-Ca (and High-HFSE) magmatism may simply reflect some form of wide-scale extension, perhaps not unlike that presently operating in the Basin and Range province in the western United States, although with some differences, e.g., lack of contemporaneous felsic volcanism.

Finally, the possible component of High-HFSE group source in the Horseshoe clan, suggests an overlap in not only time but also in process and/or crustal level of generation between the Low-Ca and High-HFSE groups. Notably, this is consistent with the Sm-Nd isotopic data, which indicate similar isotopic signatures for both granites groups.

Low-Ca (SCP) Clan	Beetle Association Supersuite	Suite
Bullfrog?	Bullfrog	Bullfrog

Low-Ca (MP) Clan	Goolthan Association Supersuite	Suite
Deep Mucca-Bunna	Poordy	Poordy
	Bidjeroo	Bidjeroo
	Bubbamunga?	Bubbamunga , unnamed
	Deep Mucca Bunna	Deep Mucca Bunna, Meru, Yalgoora
	Minjin	Minjin
	Tallering	Tallering
	Candoo	Candoo
Edah	Edah	Edah
	Woolpah	Woolpah
	Yarnga	Yarnga, Wollanoo, Kutmia
Goolthan	Ben Davey	Ben Davey, Cunby Cunby, unnamed
	Bubbowroo	Bubbowroo
	Goolthan?	Goolthan?
	Jingemarra	Jingemarra
	Omega	Omega
	Poothea	Poothea
	Telegootherra	Dalgaranga, Wambury?, Telegootherra, unnamed
Horseshoe	Horseshoe	Horseshoe
	Ubloo	Ubloo
Midge	Midge	Goodoona, Doodawannie, Midge HQ, unnamed
Myagar	Goonamoodey	Mullawagga, Jumbulyer, Rasik, unnamed
	Koolagabby	Koolagabby
	Myagar	Beeringunjer, Myagar, Kerbar, Hegarties well, unnamed
	Jungar	Jungar
Nakedah	Bocadeera	Bocadeera, Borehole Bore
	Fionabell	Fionabell
	Nakedah	Nakedah-2, Nakedah-1, Sherron, Murrawalla, Cricket Well
	Nalbarra	Nalbarra, Nalbarra-2
	Tura	Tura
	unnamed	unnamed
Tardiwarra	Tardiwarra	Warra Warra, Tardiwarra
	Beergoona	Boojall, Beergoona
unassigned	unassigned	unassigned

Table 7. Suites, supersuites, clans and associations of the Low-Ca group, northern Murchison Province.

Clans of the Goolthan Association, Low-Ca Group, northern Murchison Province

Deep Mucca Bunna Clan

Member Supersuites: Poordy, Bidjeroo, Bubbamunga, Deep Mucca Bunna, Minjin, Tallering, Candoo

Distribution: Widely distributed clan of seven supersuites and 26 units, comprising mainly external, dykes, small pods and small plutons, occurring within two regions:
- dykes, and small bodies in the eastern two-thirds of Yalgoo (Bidjeroo, Deep Mucca Bunna, Tallering, Candoo supersuites)
- small bodies within NW Cue and SW Belele (Poordy, Bubbamunga, Minjin supersuites)

Geochronology: No recorded ages for the Deep Mucca Bunna clan.

Chemical characteristics: The Deep Mucca Bunna clan, with the Midge and Goolthan clans, are the archetypal Low-Ca clans, exhibiting most of the features of this granite group, namely, high K_2O, Rb, Pb, Th, LREE, Zr, Nb, moderate to high HREE and Y, and low Na_2O, (Figs 4, 5). The Deep Mucca Bunna clan is most similar to the Midge clan, though not as HFSE-enriched as the latter. Differences between the Goolthan and Deep Mucca Bunna clans include lower Rb, Nb, Zr, and higher Sr and Ba, in the latter. Like the Low-Ca group in general, all members of the Deep Mucca Bunna clan are Sr-depleted (moderate negative Eu anomalies), and mostly Y-undepleted.

Mineralised members? No known associated mineralisation, though it is possible that some of the lithophile mineralisation (Sn, Li, Be, U) in the NW Cue area, may be related to this clan; note that members of the Midge and Goolthan clans also occur within that region also.

Petrogenesis: As for the Low-Ca group in general, particularly given the moderate-high LILE, and high HFSE nature of this clan. The lower Rb, Y, Nb and higher Sr, Ba, relative to the Goolthan clan, appears to reflect both differences in the crustal level of generation (deeper levels and higher pressures for the Deep Mucca Bunna clan), and geochemical differences between the respective sources.

Tectonic & other implications: As for the Low-Ca group in general.

Edah Clan

Member Supersuites: Edah, Woolpah, Yarnga,

Distribution:
The 6 units of this clan comprise moderate to large plutons and granite dykes; all are external to greenstone belts. The clan is confined to three regions, that probably really constitute one broad distribution:
- NW Kirkalocka - NE Yalgoo (Edah, Yarnga supersuites),
- SC-SE Yalgoo and NE-Perenjori (Yarnga supersuite),
- and dykes within NC Yalgoo (Woolpah supersuite).

Geochronology: One age has been reported for the Edah clan, on an unnamed dyke in NW Kirkalocka (Edah supersuite), which gives an age of 2640 ± 10 Ma (Schiotte & Campbell, 1996, Table 3). This dyke also contained inherited zircons of ca. 2800 Ma age.

Chemical characteristics: Geochemically, falls into the high LILE, high HFSE end of the range shown by the Low-Ca group, and as such is chemically very similar to the Goolthan Clan (Figs 4, 5). Minor differences include slightly lower Pb, Th, U in the Edah clan; other apparent differences include lower K_2O and higher Na_2O, though given the high silica, these differences may simply reflect advanced fractionation in the Edah clan. As expected from such silicic fractionated compositions, members of the Edah clan have strong to very strong negative Eu anomalies, with high Rb (to 400 ppm and over), and high Rb/Sr ratios (to 8).

Mineralised members? Spatially associated with Be mineralisation, north of Edah homestead. No other apparent related mineralisation.

Petrogenesis: As for the Goolthan clan, and the Low-Ca group in general.

Tectonic & other implications: As for the Goolthan clan, and the Low-Ca group in general. The minor differences between the Goolthan and Edah clans most probably reflect minor compositional differences in the source. It is possible that further work may see this clan amalgamated with the Goolthan clan.

Goolthan Clan

Member Supersuites: Ben Davey, Bubbowroo, Goolthan, Jingemarra, Omega, Poothea, Telegootherra

Distribution: This clan, the most areally extensive in the northern Murchison, includes 24 units, comprising small to large plutons, small pods and numerous dykes. The clan is apparently confined to one large band trending NE, from NC-NE Murgoo to NW-NC Cue. Units occur either external or marginal to greenstone belts.

Geochronology: One unit from this clan has been dated, the Goolthan Goolthan granite, giving an age of 2626 ± 6 Ma (Table 3).

Chemical characteristics: The archetypal Low-Ca group, characterised by high LILE, high HFSE, potassic compositions, depleted-Sr, large negative Eu anomalies and mostly undepleted Y (and HREE). With the Edah clan, has the lowest Sr and Ba, and highest Rb of the Low-Ca clans in the northern Murchison region (Fig 5).

Mineralised members? No known associated mineralisation, though it is probable that some of the lithophile mineralisation (Sn, Li, Be, U) in the regions where this granite clan occurs, e.g., NW Cue area, and around the Dalgaranga and Wardawarra greenstone belts, is related to the clan, particularly given the clan's fractionated and lithophile-rich nature.

Petrogenesis: As discussed for the Low-Ca group in general, the characteristics of the Goolthan clan, i.e., potassic, high LILEs, elevated HFSEs, indicate derivation from an, at least moderately, potassic and LILE-rich crustal source at moderate crustal levels (mostly <35 km). Given that the Goolthan clan represents the most LILE- and HFSE-enriched compositions of the Low-Ca granites in the northern Murchison region, suggests either it was derived from a more enriched source and/or by smaller degrees of partial melting. The chemical evidence, features such as lower K/Rb, mg#, more negative Eu anomalies and higher Ca/Sr ratios, for given silica content, are consistent with smaller degree partial melts, though the variation in the HFSE, Na_2O and K_2O, also indicate some differences in LILE and HFSE contents of the source rocks for the Low-Ca clans.

Tectonic & other implications: As for the Low-ca group in general.

Horseshoe Clan

Member Supersuites: Horseshoe, Ubloo

Distribution:
A small clan, comprising two units, one per supersuite, one on SC Kirkalocka - NC Ninghan (Ubloo supersuite), the other near Mt Mulgine, on NE Pernjori (Horseshoe supersuite).

Geochronology: None recorded geochronology for this clan.

Chemical characteristics: The Horseshoe clan is largely intermediate in chemistry, between the Goolthan and Deep Mucca Bunna clans, e.g., low Sr, Ba, moderate to high LREE, Zr, Y, with some notable differences, including higher FeO*, and only moderate K_2O and Rb, coupled with low Na_2O and Sr (Fig. 5). Like all Low-Ca clans in this region, members of the Horseshoe clan are strongly Sr-depleted with large negative Eu anomalies, and undepleted Y (and HREE).

Mineralised members? No known associated mineralisation.

Petrogenesis: Largely as for the Goolthan and Deep Mucca Bunna clans, and the Low-Ca group in general. The higher FeO*, and lower K_2O, Rb, coupled with low Sr, are features also shared by the High-HFSE group in this region, though much more extreme in the latter. It is possible that there may be a component of the High-HFSE group source involved in the generation of the Horseshoe clan.

Tectonic & other implications: As for the Low-Ca group in general. The possible component of High-HFSE group source in the Horseshoe clan, suggests an overlap in not only time but also in process and/or crustal level of generation between the Low-Ca and High-HFSE groups.

Midge Clan

Member Supersuites: Midge

Distribution: This small clan of 7 units comprises dykes, pods and small to moderate sized plutons, all confined to the a localised cluster in the NW Cue to SW Belele area. All appear to be external to greenstone belts.

Geochronology: No recorded geochronology for this clan.

Chemical characteristics: Belongs to the high LILE end-member of the Low-Ca clan, with many similarities to both Goolthan and Deep Mucca Bunna clans (Figs 4, 5). Like the latter, characterised by high Sr and Ba, coupled with low to moderate Rb, that clearly distinguish it from the Goolthan clan. Higher HFSE than the Deep Mucca Bunna clan, especially Y, which is high to very high in the Midge clan (Fig. 5).

Mineralised members?
No known associated mineralisation, though it is possible that some of the lithophile mineralisation (Sn, Li, Be, U) in the NW Cue area, may be related to this clan; note that members of the Deep Mucca Bunna and Goolthan clans also occur within that region also.

Petrogenesis: As for the Deep Mucca Bunna and Goolthan clans and the Low-Ca group in general.

Tectonic & other implications: As for the Deep Mucca Bunna and Goolthan clans and the Low-Ca group in general.

Myagar Clan

Member Supersuites: Goonamoodey, Koolagabby, Myagar, Nalbarra, Jungar, unnamed

Distribution: A small to moderate sized clan of 17 units, comprising, dykes, pods, and small to moderate plutons, occurring as both internal (to the Meekatharra-Wydgee greenstone belt), and external units. Largely confined to one region, and as isolated bodies elsewhere, namely:

- the eastern two-thirds of the Kirkalocka sheet, both sides of, and internal to, the Meekatharra-Wydgee greenstone belt (Goonamoodey, Myagar, Nalbarra supersuites), and
- isolated units on Murgoo (unnamed supersuite), NC Cue (Jungar supersuite), and Perenjori (Koolagabby supersuite).

Geochronology: One age determination is available for the Myagar clan. The Jungar granite (Jungar supersuite), tentatively included within the Myagar clan, gives an age of 2676 ± 7 Ma (Q. Wang, written communication, 1995; Table 3). This age is somewhat anomalous for the Low-Ca group, and may suggest, either, that this unit does not belong to this group, or as discussed below, the possibility that this clan does not fit within the Low-Ca group. However, it is noted that several, more-unequivocal, Low-Ca granites of the age are known from the Southern Cross Province to the east (see Budd & Champion, this volume).

Chemical characteristics: The Myagar clan, along with the Nakedah clan, are characterised by moderate to high Na_2O, moderate K_2O, with only moderate LILE and HFSE. As such they are two of the most chemically primitive clans of the Low-Ca group, clearly falling into the low LILE (and low HFSE) end-member of that group (Figs 4, 5). The members of the Myagar clan are further characterised by mostly moderate negative Eu anomalies (Sr-depleted), and range from Y-undepleted to Y-depleted, with flat HREE patterns. Importantly, the Myagar clan overlaps strongly with the more LILE-rich members of the Eily Eily clan of the High-Ca group, with only minor differences, e.g., slightly lower HFSE, and slightly higher CaO, in the Eily Eily clan (Fig. 5). This raises the obvious problem that it is not entirely evident to which group the Myagar clan actually belong, i.e. either Low-Ca or High-Ca. Part of this overlapping chemistry problem is caused by lack of documentation, for those sample sites where multiple samples were collected, by Watkins & Hickman (1990), i.e., it is not entirely clear what has been sampled, e.g., dominant phase, dyke, enclaves. Obviously, there is no satisfactory solution to this classification problem; additional work is clearly required, in particular, Sm-Nd data for both the Myagar and Nakedah clans would be helpful. For the moment, on the basis of the dominant characteristics of each individual supersuite, the clan is placed within the Low-Ca group.

Mineralised members? No known associated mineralisation.

Petrogenesis: Largely as for the Eily Eily clan of the High-Ca group, and the High-Ca and Low-Ca groups in general. The convergence in compositions between the most LILE- and HFSE-poor Low-Ca clans, and the most LILE- and HFSE-rich member of the High-Ca group (Eily Eily clan; Fig. 5), strongly suggests a convergence in source compositions for the two clans. As discussed earlier, though, the differences in Sm-Nd isotopic signatures for the High- Ca and Low-Ca groups would appear to effectively rule out any commonality of sources.

Tectonic & other implications: Any implications from this clan are largely speculative given the difficulty in assigning it to a group. However, if the clan is indeed in the Low-ca group, then the reported age (2676 Ma) is the oldest recorded for this group within the northern Murchison region; as mentioned earlier, it is noted that Low-Ca granites of this age are recorded within the Southern Cross Province.

Nakedah Clan

Member Supersuites: Bocadeera, Fionabell, Nakedah, Tura, unnamed

Distribution: The Nakedah clan comprises 15 units ranging from dykes and small pods to small to medium-sized plutons. Units occur both externally and internal to greenstone belts (e.g., Meekatharra-Wydgee greenstone belt), outcropping within 2 regions:

- mostly in a north-south band from SC Kirkalocka to SC Belele (Bocadeera, Fionabell, Nakedah supersuites), and
- as isolated units on Murgoo (Tura, unnamed supersuites)

Geochronology: One recorded age determination for this clan, on the altered Coodardy? granite near the Big Bell deposit, with an age of 2627 ± 8 (Mueller et al., 1996). Although the unit is altered, the geochemistry fits best with the Low-Ca group, and the surrounding granites within the region.

Chemical characteristics: Like the Myagar clan (see above), the Nakedah clan is one of the more chemically primitive clans of the Low-Ca group, i.e., lower LILE and lower HFSE (see Figs 4, 5). Members of the Nakedah clan range from Y-depleted to Y-undepleted, and are mostly Sr-depleted with minor to moderate negative Eu anomalies. It is evident from Figure 5, that the Nakedah clan also overlaps in chemistry with the Eily Eily clan of the High-Ca group, though the former can be distinguished from the latter by its higher Sr and Ba. Such high Sr and Ba is also a characteristic of a few other Low-Ca clans, e.g., Midge clan (Fig. 5). As for the Myagar clan, it is not entirely evident to which group the Nakedah clan actually belongs, i.e. either Low-Ca or High-Ca, though, on the basis of the dominant characteristics of each individual supersuite, the clan is placed within the Low-Ca group.

Mineralised members? No known associated mineralisation.

Petrogenesis: As for the Myagar clan.

Tectonic & other implications: As for the Myagar clan.

Tardiwarra Clan

Member Supersuites: Tardiwarra, Beergoona

Distribution: A small clan of 11 units in two supersuites, occurring as dykes and small to medium sized plutons, all external to greenstone belts. Units are confined to two regions, namely:

- in a north-south band, along the eastern third of the Murgoo sheet and the very top part of the Yalgoo sheet (Tardiwarra supersuite), and
- NE Perenjori (Beergoona supersuite).

Geochronology: No reccorded ages for this clan.

Chemical characteristics: The Tardiwarra clan largely has chemistry somewhat intermediate between the Goolthan and Deep Mucca Bunna clans, e.g., moderate-high Pb, Th, U, LREE, Zr, low Sr and Ba, strongly negative Eu anomalies, but with some significant differences, largely in the alkalis, e.g., only moderate levels of K_2O, and elevated Na_2O (Figs 4, 5).

Mineralised members? No known associated mineralisation.

Petrogenesis: As for the Goolthan and Deep Mucca Bunna clans, and the Low-Ca group in general.

Tectonic & other implications: As for the Goolthan and Deep Mucca Bunna clans, and the Low-Ca group in general.

Clans of the Beetle Association, Low-Ca Group, Southern Cross Province

Bullfrog Clan

Member Supersuites: Bullfrog

Distribution: One unit occurring in SE Kirkalocka.

Geochronology: None recorded.

Chemical characteristics: Only one available analysis, which shows a chemistry very similar to the Myagar clan, Goolthan Association, i.e., moderate K_2O, Na_2O, LILE, HFSE, though, more unequivocally belongs to the Low-Ca group.

Mineralised members? No associated mineralisation.

Petrogenesis: Largely as for the Myagar clan, Goolthan Association, and the Low-Ca granites in general.

Tectonic & other implications: Suggests, like for the High-Ca granites, that there is similar chemistry across the Murchison Province - Southern Cross Province boundary, though based on very limited data.

Damperwah Association, High-HFSE group, Murchison Province

Member clans: Damperwah, Nannine

Distribution: The High-HFSE group is sparsely (<10%), but widely distributed. Members of both clans within the group (Table 8), are very commonly spatially associated with greenstones, either internal or marginal (Fig. 1). Unlike the Eastern Goldfields Province, there is no obvious indication that the group is sgeographically localised, although it is apparent that many of the defined units are concentrated within the north-western half of the northern Murchison region, a trend transverse to the dominant structural grain within the region. No High-HFSE group granites occur within the Southern Cross Province in the northern Murchison region.

Geochronology: Six ages determinations on 4 units are available for the High-HFSE group granites of the northern Murchison region. This small data set, shows that the granites of the group fall into two temporal periods, based on clan; the older Nannine clan with ages of ca. 2745-2750 Ma, and the Damperwah clan with ages of 2640 Ma or younger (Table 3). Similar granites within the southern Murchison Province have ages less than 2640 Ma (Tables 4). It is considered highly likely that older (>2780 Ma) High-HFSE granites do exist within the Murchison Province, given that 2930 Ma and older felsic volcanic rocks, which have similar geochemistry to the High-HFSE group, are relatively common within the Luke Creek group (Watkins & Hickman, 1990).

Chemical characteristics: Members of the High-HFSE group within the Eastern Goldfields Province have been described in detail by Champion & Sheraton (1997), Champion (1997), and Champion & Cassidy (this volume); as expected these granites share many characteristics with those High-HFSE granites in the northern Murchison region. The latter are characterised, and easily recognisable from other granites within the region, by their high total Fe (FeO*), moderate to high TiO_2, and high LREE, Zr and Y, i.e., high HFSE as their name suggests. Other characteristics include moderate silica range (69-78% SiO_2), moderate to large negative Eu anomalies (which increase with increasing silica), depleted Sr and mostly undepleted Y (and HREE). Two clans are recognised, largely on the basis of LILE contents, with the younger Damperwah clan having significantly higher K_2O, Rb, Th, Pb, Nb and lower Na_2O and Sr (Fig. 6).

Petrogenesis: Champion & Sheraton (1997), and Champion (1997), suggested that the High-HFSE group granites were crustal-derived melts from an intermediate to more siliceous source, the latter hypothesis based on the combination of high HFSE, high silica, and the Sr-depleted and Y-undepleted nature. Such a scenario is also consistent with both the Nannine and Damperwah clans of the northern Murchison region. However, as discussed for High-HFSE granites in the Eastern Goldfields Province (Champion & Cassidy, this volume), it is also possible that the granites are actually fractionates of more mafic rocks, similar in composition to the Bullshead clan of the Eastern Goldfields Province. If the latter scenario is correct, then the ultimate source rocks for the granitoids of this group must have been even more mafic. Such a mafic source, and the temperatures required for partial melting, is also consistent with the, high-temperature A-type characteristics of the High-HFSE group (elevated Fe, Zr, Y; Fig. 6). Unlike the Eastern Goldfields Province, the High-HFSE clans of the northern Murchison region show a large difference in the LILE, from low (Nannine) to high (Damperwah). Given the similarity of such factors as SiO_2, mg*, size of the negative Eu anomaly, it is clear that these differences in LILE must reflect original source differences, i.e., the source for the Damperwah clan was more LILE-rich. Notably, many of the high LILE characteristics of the Damperwah clan are also shared by the contemporaneous Low-Ca group in general, suggesting the possibility of partly common sources, as has already been suggested for the Horseshoe Clan of the Low-Ca group. In this regard, it is notable that the Low-Ca and High-HFSE groups share similar Sm-Nd signatures, both significantly more evolved than those for the High-Ca and Mafic groups. It is noted, however, that members of the LILE-poor Nannine clan also have similar Sm-Nd signatures, pointing to both long-lived high and low LILE sources for the High-HFSE group granites in the northern Murchison region, i.e., pre-existing crustal rocks. The Sr-depleted, Y-undepleted nature of the group, strongly infer generation at only moderate crustal pressures, i.e., <10 kbars (<35 km thick).

Tectonics and other implications: The close spatial, and genetic, relationship between the High-HFSE granites and volcanics in the Eastern Goldfields Province suggested that in that province those granites were intimately related to greenstone formation. Within the northern Murchison region, however, although there is an undoubted spatial relationship, it is evident that many of the associated volcanics are apparently much older (e.g., Watkins & Hickman, 1990). Given the ages of the Nannine clan granites, which overlap with ages for the younger felsic volcanics (Mt Farmer group), and the similarity in chemistry of some of the Luke Creek and Mt Farmer group felsic volcanics, to the High-HFSE granites, it is reasonable to suggest that the latter are, at least in part, related to greenstone formation. Similarly, there is also good reason to expect older (>2930 Ma) members of this clan to be present within the northern Murchison region. More importantly, the geochemistry of the High-HFSE granites and their A-type affinities indicates emplacement in an, at least locally, extensional environment (as pointed out by Champion & Sheraton, 1997). The ages of these granites, mostly 2740-2750 Ma, and 2640 Ma and younger, can be then be used to indicate periods of local extension.

It is notable that the younger granites within the northern Murchison region (Low-Ca and High-HFSE groups) contrast with those in the Eastern Goldfields Province (Low-Ca and Syenitic, and carbonatitic?). The reasons for this are not completely understood but may have something to do with proximity to recently active convergent margins, i.e., immediately prior subduction along the eastern margin of the Eastern Goldfields Province may have been responsible for producing suitably metasomatised mantle and lower crustal (?) rocks as source rocks for syenites (e.g., Smithies & Champion, 1999). Given the dominance of Low-Ca granites of this age across the craton, however, it is still evident that the bulk of the middle-lower crust across the craton must have been of largely similar composition, or at least, similarly capable of producing voluminous Low-Ca magmatism.

High-HFSE (MP) Damperwah Association

Clan	**Supersuite**	**Suite**
Damperwah	Bootra	Bootra
	Cootinge	Cootinge
	Damperwah	Damperwah, Kadji Kadji, Mingewanah?, Goodingnow
	Koolanooka	Koolanooka
	Tinderlong	Tinderlong
	Toola	Toola
	Urawa	Urawa
Nannine	Keygo	Keygo
	Nannine	Nannine, Eelya?

Table 8. Suites, supersuites, clans and associations of the High-HFSE group, northern Murchison Province.

Clans of the Damperwah Association, High-HFSE Group, northern Murchison region

Damperwah clan

Member Supersuites: Bootra, Cootinge, Damperwah, Koolanooka, Tinderlong, Toola, Urawa

Distribution: A small to moderate clan of 7 supersuites (Table 8), comprising small to moderate sized plutons occurring across the north-west half of the northern Murchison region, either external or marginal to the greenstone belts.

Geochronology: Two units have been dated (Weidenbeck & Watkins, 1993), both from the northern half of the Perenjori sheet, with ages of 2641 ± 5 (Damperwah supersuite), and 2602 ± 16 Ma (Koolanooka supersuite). Zircon inheritance ages of ca. 2863 Ma were reported for the Damperwah unit (Table 3).

Chemical characteristics: The Damperwah clan clearly falls within the high LILE end-member of the High-HFSE group (Fig. 4), with its elevated K_2O, Rb, Pb, Th and low Na_2O and Sr (Fig. 6). Like all High-HFSE granites, the Damperwah clan is clearly distinguished from other granite groups by the elevated FeO*, Zr, Y, etc. (Fig. 6).

Mineralised members? No recorded associated mineralisation.

Petrogenesis: As for the High-HFSE group in general. The high LILE contents of the Damperwah clan, relative to the Nannine clan, indicate a more LILE rich source for the former.

Tectonic & other implications: As for the High-HFSE group in general.

Nannine clan

Member Supersuites: Keygo, Nannine

Distribution: A small clan of three units (Table 8), within and marginal to the Meekatharra-Wydgee greenstone belt (Nannine supersuite), and marginal to the Dalgaranga greenstone belt (Keygo supersuite). Given the apparent association with felsic volcanics, and the similar chemistry of the latter to the former (e.g., Watkins & Hickman, 1990), it is to be expected that more units of this clan exist.

Geochronology: Four ages are recorded from two units for this clan, all falling between 2745 and 2753 Ma (Table 3). These ages indicate that the Nannine clan is significantly older than the Damperwah clan.

Chemical characteristics: Clearly falls into the low LILE end-member of the High-HFSE group (Fig. 4), with low to moderate K_2O, Rb, Pb, Th, and moderate to high Na_2O and Sr (Fig. 6). Like the Damperwah clan, is characterised by high total Fe, LREE, Zr, Y, and is Sr-depleted with moderate to strong negative Eu anomalies. Clearly distinguished from the Damperwah clan by its lower LILE contents (Fig. 6).

Mineralised members? No known associated mineralisation.

Petrogenesis: As for the High-HFSE group in general. Source rocks for the Nannine clan were clearly low in LILE.

Tectonic & other implications: As for the High-HFSE group in general.

Gem of Cue Association, Mafic group, northern Murchison Province

Member clans: Britania, Gem of Cue, Norie

Distribution: This group, comprising 3 clans (Table 9), is widely distributed across the northern Murchison Province, but overall, like the High-HFSE group, forms only a minor component of the total granites (Fig. 1). With the exception of one pendant within a Low-Ca granite (NW Kirkalocka), all units of the group are either internal or marginal to greenstone belts. Most units appear to occur within the Meekatharra-Wydgee greenstone belt.

Geochronology: Geochronology has been undertaken on 9 units from the Mafic group (Table 3), from which it is evident that there are at least two periods of magmatism, at ca. 2715 Ma (Gem of Cue, Britania clans), and 2747-2760 Ma (Gem of Cue, Britania, Norie clans), with a possible outlier at 2788 ± 32 Ma (unit tentatively identified as Mafic group), but within error of the older sub-group. Notably, older Mafic group granites (ca. 2800 and 3020 Ma) have been recorded within the Southern Cross Province (Budd & Champion, this volume), and, accordingly it is expected that similarly-old Mafic granites probably also exist in the Murchison Province.

Chemical characteristics: As for the Mafic group granites within the Eastern Goldfields Province (Champion & Sheraton, 1997; Champion, 1997; Champion & Cassidy, this volume), the chief characteristic of the Mafic group granites in the northern Murchison region is the expanded silica range, in particular, compositions between 58-68% SiO_2, and the presence, in hand specimen of common hornblende. Other characteristics include variable LILE and LREE content, with mostly Y-undepleted (Y decreasing with increasing silica), and mostly Sr-undepleted (with no or mildly negative Eu anomalies) signatures (Fig. 6). In the Eastern Goldfields Province, Champion & Cassidy (1998) subdivided the Mafic group into two broad subtypes on the basis of their LILE contents. A similar approach has been adopted for the northern Murchison region, with the Gem of Cue (low LILE) and Britania (high LILE) clans (Table 9, Figs 4, 6), though it is apparent that no strongly LILE-enriched Mafic group granites are yet known from the region. In addition to these clans, it is evident that there exists an additional clan (Norie), largely characterised by high MgO, mg*, Ni and Cr - chemical features that strongly indicate a subduction-type environment was present before or during their generation (see below). Available Sm-Nd isotopic data for the Mafic group (ε_{Nd} of 0.7 and -1.7; Fletcher & McNaughton, this volume), indicates a strong overlap with values recorded for the High-Ca group, similar to the situation in the Eastern Goldfields Province (Champion & Sheraton, 1997).

Mineralised members? Examples of Mafic group granitoids directly hosting significant gold mineralisation are rare in the Murchison Province, though a number hosting 'minor' gold mineralisation (typically in quartz veins and/or shears) are known, e.g., deposits in the Gem of Cue granite around Cue, in the Britania granite south of Mt Magnet, and small deposits in the Annean granite near Nannine. It is also evident from descriptions in Watkins & Hickman (1990), that feldspar porphyry sills and dykes are a common lithology found at Au deposits of the Murchison Province, though most appear to be spatially associated rather than hosting mineralisation e.g., mafic group dykes in Hill 50 and other deposits around Mt Magnet (Watkins & Hickman, 1990). These porphyries appear to belong to either the Mafic or High-Ca groups. Perhaps the best documented porphyries associated with gold mineralisation are those in the Meekatharra - Paddys flat mining camp region (see Watkins & Hickman, 1990).

It is clear that the strong common association of members of the Mafic group with gold mineralisation seen in the Eastern Goldfields Province, e.g., Granny Smith, Lawlers, Liberty, Kanowna Belle, Golden Cities, is not evident within the northern Murchison region. This may be a true and correct feature of the northern Murchison region or, alternatively, may simply reflect lack of exploration within such Mafic group granites in the region. If the latter is correct, then given the overall structural control of Yilgarn gold deposits, any interplay of structural features and Mafic group granites is worthy of exploration.

Petrogenesis: As indicated by Champion (1997), the source for most of the Mafic group granites is largely equivocal, with evidence for both crustal and mantle-derived contributions. Clearly, the variation in the LILE and LREE, evident in even the most mafic end-members, requires at least two separate components, just to produce the Britania and Gem of Cue clans. Champion (1997) suggested two such sources for the Eastern Goldfields Province, namely a mafic 'basaltic' source, similar to that proposed for the High-Ca granites, and a more mafic, perhaps mantle-derived, LILE-rich source component. Such sources would also appear to be apt for the northern Murchison region, though it is clear that there is no requirement that the LILE-enriched source be mantle-derived or even as mafic as the low LILE 'basaltic' source component. Other possible mechanisms for producing the LILE differences between the Britania and Gem of Cue clans, include:

- a similar overall source, variably LILE-enriched (metasomatised) before partial melting, with the non- or poorly-metasomatised regions producing the Gem of Cue clan, and the more strongly-enriched regions producing the Britania clan,
- a heterogeneous (mixed) source region, or
- post-melting modification by a LILE-enriched fluid or melt, e.g., some form of magma mixing introducing the high LILE into the Britania clan granites.

At present it is difficult to choose between one or more of these models. although the magma-mixing model would appear to be least likely, given the lack of evidence for LILE-enriched melts, such as Low-Ca or Syenitic magmatism, prior to 2700 Ma.

One notable feature of the Mafic group within the northern Murchison region is the ca. 2755 Ma Norie Clan comprising granites with chemistry similar to high-Mg diorites elsewhere (e.g., Smithies & Champion, 2000). These granites with their elevated MgO, mg#, Ni, Cr, clearly require a mantle-component in their genesis. Even more important, however, is the combination of high MgO, Ni etc, with moderate LILE contents. This combination of chemical features is thought to reflect metasomatism of the mantle source by LILE-enriched melts from a subducting slab, either before or during genesis of the granitoids (see discussion in Smithies & Champion, 2000); if correct this indicates subduction occurred at or before 2755 Ma, affecting the northern half, at least, of the northern Murchison region.

Tectonic & other implications: As discussed above, the major tectonic implication from the Mafic group is provided by the Norie Clan, whose high-Mg diorite affinities, suggest subduction and slab melting occurred at or before ca. 2755 Ma, at least in the northern half, of the northern Murchison region. The presence of such an arc raises a number of questions, not least of which what was the possible orientation of such an arc. Assuming the Murchison Province and Southern Cross Province were one before 2800 Ma (see Champion et al., this volume), suggests either an arc somewhere to the north or the west of the current Murchison province boundaries. The position of such an arc also has implications for the timing of collision between the Narryer Gneiss Terrane and the Murchison Province. As suggested earlier, and also by Nutman et al. (1991), the best timing on docking of the Narryer would be sometime between 2810 and 2750 Ma. This appears to fit well with the postulated presence of a subduction zone environment at this time, and may suggest that such a subduction zone was to the north-west, probably close to or north-west of the Narryer terrane's present position. Such a theory would suggest that the members of the Mafic group at ca. 2755 Ma, including the Norie clan, were derived within a back-arc environment. This is consistent with the presence of High-HFSE granites, and felsic (and bi-modal volcanism, Watkins & Hickman, 1990), all indicative of at least local extension. How such an environment fits with the High-Ca granites is unclear. The environment of formation for the younger (ca. 2715 Ma) Mafic group granites is not unequivocal but may largely be as for the older Mafic granites.

Mafic group (MP) Gem of Cue Association

Clan	**Supersuite**	**Suite**
Britania	Britania	Britania
	Carbar	Carbar
	Nookagoo	Nookagoo
	Triangle	Triangle
Gem of Cue	Deatys	Deatys
	Divine Well	Divine Well
	Gem of Cue	Gem of Cue, Annean
	Milky Way	Milky Way, Eclipse Hill?
	Moyagee	Moyagee
	unnamed	unnamed
Norie	Norie	Norie
	Reedy	Reedy

Table 9. Suites, supersuites, clans and associations of the Mafic group, northern Murchison Province.

Clans of the Gem of Cue Association, Mafic Group, Murchison Province

Britania clan

Member Supersuites: Britania, Carbar, Nookagoo, Triangle

Distribution: A small clan of 4 units (Table 9), comprising small to moderate sized plutons, within the Meekatharra-Wydgee (Britania, Carbar supersuites), Gullewa (Triangle supersuite), and the Twin Peaks (Nookagoo supersuite) greenstone belts.

Geochronology: Two units have been dated, with results of 2747 ± 3 Ma (Triangle supersuite), and 2716 ± 4 Ma (Britania supersuite), indicating that members of this clan were emplaced during both known periods of Mafic group magmatism.

Chemical characteristics: As discussed earlier, the members of the Britania clan, comprise the high LILE end-member compositional range of the Mafic group in the northern Murchison region (Fig. 4). Geochemical characteristics include higher K_2O, Rb, Sr, Ba, Th, U, LREE, Nb, and lower CaO, relative to the Gem of Cue and Norie clans (Fig. 6). It is noted, that the LILE-enrichment within the Britania clan is not as great as that within some supersuites of the Granny Smith clan, in the Eastern Goldfields Province.

Mineralised members? Examples of Britania clan granitoids directly hosting or associated with gold mineralisation are confined to the Britania granite south of Mt Magnet. It is also possible that some feldspar porphyry sills and dykes found at Au deposits of the Murchison Province, may belong to the Britania clan; it is noted, however, that no dykes of this clan have yet been identified.

Petrogenesis: Largely as for the Mafic group in general.

Tectonic & other implications: Largely as for the Mafic group in general.

<u>Gem of Cue clan</u>

Member Supersuites: Deatys, Divine Well, Gem of Cue, Milky Way, Moyagee, unnamed

Distribution: A small clan of 8 suites and 10 units (Table 9), comprising dykes, sub-surface granites (detected by aeromagnetics and intersected in drill hole), one small pod or pendant, and as small to moderate sized plutons. All units are either marginal or internal to the Meekatharra-Wydgee (Deatys, Gem of Cue, Milky Way, unnamed supersuites), or Tallering (Divine Well supersuite) greenstone belts; the one exception being the Moyagee supersuite, which occurs as a pod or pendant within a Low-Ca granite in NW Kirkalocka. The distribution of units of the Gem of Cue clan strongly overlap with those of the Britania and Norie clans, within the Meekatharra-Wydgee greenstone belt.

Geochronology: Two SHRIMP ages are recorded for granites of this clan, both by Schiotte & Campbell (1996), both from the same Milky Way supersuite, both within the region around Mt Magnet. One, on a small pluton gives an age of 2715 ± 7 Ma, the other on a dyke returns a significantly older age of 2752 ± 5 Ma. Pidgeon & Hallberg (2000), record a conventional U-Pb zircon age of 2759 ± 4 for the Gem of Cue tonalite (Gem of Cue supersuite). Notably, these 3 ages overlap with those of the Britania clan, adding support for the existence of at least two periods of Mafic group magmatism. Both dated samples contained inherited zircons of ca. 2930 Ma (Table 3). Given the internal nature of the dated units these inherited zircons may either reflect source ages or, more likely, some contamination from greenstone sequences.

Chemical characteristics: The Gem of Cue clan encompasses the low LILE and LREE part of the Mafic group compositional range, evident in the low to moderate levels of K_2O, Rb, Sr, Pb, Ce (Figs 4, 5), and also extends to less siliceous compositions than the Britania clan (Fig. 6). Many of the chemical characteristics of the Gem of Cue clan are similar to those observed in the low-LILE clans of the High-Ca group (e.g., Mainland, Wheel of Fortune), making it somewhat difficult to separate members of the two groups in the region of overlap (around 69-72% SiO_2); it is notable, however, that the Gem of Cue clan has lower TiO_2, Sr, Ba, LREE, and Zr with similar to higher MgO, than nearly all High-Ca granites.

Mineralised members? Examples of Gem of Cue clan granitoids associated with gold mineralisation include deposits in the Gem of Cue granite around Cue, and in the Annean granite near Nannine. It is also evident that feldspar porphyry sills and dykes found at Au deposits of the Murchison Province, are at least locally, part of this clan, e.g., dykes in Hill 50 and other deposits around Mt Magnet (Watkins & Hickman, 1990). Other porphyries within the northern Murchison region probably also belong to this clan, but may also include members of the High-Ca group.

Petrogenesis: Largely as for the Mafic group in general. The apparent chemical distinctions between members of the Gem of Cue clan and the High-Ca group, suggests that the sources for these two granite types were at least partly different.

Tectonic & other implications: Largely as for the Mafic group in general.

Norie clan

Member Supersuites: Norie, Reedy

Distribution: A small clan comprising two units, one per supersuite, of small to moderate sized plutons, closely spatially associated within the northern part of the Meekatharra-Wydgee greenstone belt, on the NE Cue and SE Belele sheets.

Geochronology: Both units have been dated, the Norie granite twice (Table 3), all giving ages between 2750-2760 Ma. No inherited zircons have been reported.

Chemical characteristics: The two members of the Norie clan, with their elevated MgO, mg#, Ni, Cr, are clearly chemically distinct from other Mafic group granites (Figs 6). Notably, despite high concentrations of such elements, which strongly imply a mantle origin, the Norie clan granites also have LILE and HFSE contents similar to those of the Gem of Cue clan.

Mineralised members? No recorded associated mineralisation.

Petrogenesis: As discussed for the Mafic group in general, the coupling of high MgO, mg# etc., with moderate LILE contents, and comparisons with similar Archaean granites elsewhere, strongly implicate mantle derivation with a subducted slab melt component (e.g., Smithies & Champion, 2000).

Tectonic & other implications: As discussed for the Mafic group in general, the proposed mechanism of genesis for granites of the Norie clan, indicate the existence of a subduction environment either before or at the time of generation of these granites, i.e., before or during ca. 2760-2750 Ma.

Udagalia Association, Syenitic group, Murchison Province

Member clans: Udagalia

Distribution: Only one unit recorded in the northern Murchison region (Table 10), occurring as a dyke within High-Ca granite on NC Yalgoo. Williams et al. (1983) record two small gneissic quartz syenites (Dallah and Yungan quartz syenites), within the Narryer terrane on the NE part of the Byro sheet.

Syenitic (MP)	Udagalia Association	
Clan	**Supersuite**	**Suite**
Udagalia	Udagalia	Udagalia

Table 10. Suites, supersuites, clans and associations of the Syenitic group, northern Murchison Province.

Geochronology: No recorded geochronology.

Geochemical characteristics: The one unit is characterised by a very convincing syenitic chemistry, e.g., low MgO, FeO*, CaO, Ni, Cr, high K_2O, Rb, Nb, total alkalis, very high Sr, Pb, Th, U, Zr, LREE, and extreme Ba. In addition, the unit is Sr-undepleted with a minimal negative Eu anomaly, is Y-undepleted, and shows strong negative Ti and Nb anomalies on primitive-mantle normalised plots. Notably, the chemistry of the unit is somewhat similar to, but not as extreme, as that recorded for the Wallaby clan syenites in the Eastern Goldfields Province. The latter syenites appear to have had some interaction with a carbonatite, and, perhaps a similar relationship is also the case for the Udagalia unit.

Mineralised members? No recorded associated mineralisation.

Petrogenesis: The petrogenesis of the syenites of the Yilgarn craton, especially of the Eastern Goldfields Province, have been described in some detail by Johnson (1991) and Smithies & Champion (1999), with most emphasis on deciphering the relative contributions of mantle versus crustal components in their origin – a common problem in petrogenetic models for syenites. Smithies & Champion (1999), pointed out that features such as the lack of associated mafic rocks, the presence of quartz, the high LILE contents, the presence of strong negative Nb and Ti anomalies, when combined indicated a significant crustal component. Smithies & Champion (1999), and Champion & Cassidy (this volume), however, also indicated that there was, at least in some units within the Eastern Goldfields Province, good evidence, e.g., the high Sr and Ba contents, the presence of a carbonatite at Wallaby, for the existence of some metasomatised mantle/lower crustal component. The similarity of the Udagalia clan chemistry to the Wallaby clan, invites the suggestion that the source for the former also contained some metasomatised component.

Tectonic and other implications: As indicated by Champion (1997), and Smithies & Champion (1999), alkaline and sub-alkaline rocks such as those in the Syenitic group are good indicators of regions undergoing, at least local, extension, or an anorogenic (post-tectonic) environment. It is difficult, however, to make any serious conclusions regarding tectonic environments, given that there is only one recognised syenitic unit in the northern Murchison. The lack of age control is also another serious problem.

It is noted, however, that the interpreted possible involvement of carbonatitic magmatism, may indicate the existence of a major deep-crustal fault zone within the NE Yalgoo area.

References:

Champion, D.C., 1997. Granitoids in the Eastern Goldfields. Australian Geological Survey Organisation, Record 1997/41, 71-76.

Champion, D. & Cassidy, K., 1998. Metallogenic potential of granitoids: Kanowna Belle and Granny Smith regions. Final Report to Golden Valley Joint Venture and Placer Pacific Ltd. Unpublished AGSO report.

Champion, D. C. and Sheraton, J. W., 1993, Geochemistry of granitoids of the Leonora-Laverton region, Eastern Goldfields Province.: Australian Geological Survey Organisation. Record, v. 1993/54, p. 39-46. Notes: Issue title: Kalgoorlie 93. An International Conference on Crustal Evolution, Metallogeny and Exploration of the Eastern Goldfields. Extended abstracts, compiled by P.R. Williams and J.A. Haldane

Champion, D.C. & Sheraton, J.W., 1997. Geochemistry and Sm-Nd isotopic systematics of Archaean granitoids of the Eastern Goldfields Province, Yilgarn Craton, Australia: constraints on crustal growth. Precambrian Research, 83, 109-132.

Fletcher, I.R., Libby, W.G. & Rosman, K.J.R., 1994. Sm-Nd model ages of granitoid rocks in the Yilgarn Craton. Geological Survey of Western Australia, Professional Papers Report 37, pp. 61-74.

Froude, D. O., Ireland, T. R., Kinny, P. D., Williams, I. S., Compston, W., Williams, I. R., and Myers, J. S., 1983, Ion microprobe identification of 4,100-4,200 Myr-old terrestrial zircons.: Nature, 304, 616-618

Johnson, G.I., 1991. The petrology, geochemistry and geochronology of the felsic alkaline suite of the eastern Yilgarn Block, Western Australia. PhD thesis, University of Adelaide.

Kent, A.J.R., Cassidy, K.F. & Fanning, C.M., 1996. Archaean gold mineralisation synchronous with the final stages of cratonisation, Yilgarn Craton, Western Australia. Geology, 24, 879-882.

Kinny, P. D., Wijbrans, J. R., Froude, D. O., Williams, I. S., and Compston, W., 1990, Age constraints on the geological evolution of the Narryer Gneiss Complex, Western Australia.: Australian Journal of Earth Sciences, v. 37(1) March. p51-69.

Martin, H., 1986. Effect of steeper Archaean geothermal gradient on geochemistry of subduction-zone magmas. Geology, 14, 753-756.

Mueller, A. G., Campbell, I. H., Schiøtte, L., Sevigny, J. H., and Layer, P. W., 1996, Constraints on the age of granitoid emplacement, metamorphism, gold mineralisation, and subsequent cooling of the Archaean greenstone belt terrane at Big Bell, Western Australia: Economic Geology, v. 91, p. 896-915.

Nelson, D.R., 1996. Compilation of SHRIMP U-Pb zircon geochronology data, 1995. Geological Survey of Western Australia, Record 1996/5.

Nelson, D.R., 1997. Compilation of SHRIMP U-Pb zircon geochronology data, 1996. Geological Survey of Western Australia, Record 1997/2.

Nemchin, A.A. & Pidgeon, R.T., 1997a. Geochronology of granitoids in the western Yilgarn Craton. Australian Geological Survey Organisation, Record 1997/41, 59-64.

Nemchin, A.A. and Pidgeon, R.T., 1997b. Evolution of the Darling Range Batholith, Yilgarn Craton, Western Australia: a SHRIMP zircon study.: Journal of Petrology, 38, 625-649.

Nemchin, A.A., Pidgeon, R.T. & Wilde, S.A., 1994. Timing of late Archaean granulite facies metamorphism in the southwest Yilgarn Craton of Western Australia: evidence from U-Pb ages of zircons from mafic granulites. Precambrian Research, 68, 307-321.

Nutman, A.P., Kinny, P.D., Compston, W. & Williams, I.S., 1991. SHRIMP U-Pb zircon geochronology of the Narryer Gneiss Complex, Western Australia. Precambrian Research, 52, 275-300.

Nutman, A.P., Kinny, P.D. & Price, R., 1993. Large-scale crustal structure of the northwestern Yilgarn Craton, Western Australia: evidence from Nd isotopic data and zircon geochronology. Tectonics, 12, 971-981.

Oliver, B., 1999. Granitoids of the Mount Mulgine and Noongal areas. Unpublished B.Sc (honours) thesis, University of Western Australia.

Patino Deuce, A.E. & Beard, J.S., 1995. Dehydration melting of biotite gneiss and quartz amphibolite from 3 to 15 kbar. Journal of Petrology, 36, 707-738.

Pidgeon, R.T., 1992. Recrystallisation of oscillatory zoned zircon: some geochronological and petrological implications. Contributions to Mineralogical and Petrology. 110, 463-472.

Pidgeon, R.T & Hallberg, J.A.,2000. Age relationships in supracrustal sequences of the northern part of the Murchison Terrane, Archaean Yilgarn Craton, Western Australia: a combined field and zircon U-Pb study. Australian Journal of Earth Sciences, 47, 153-165.

Pidgeon, R.T. & Wilde, S.A., 1990. The distribution of 3.0 and 2.7 Ga volcanic episodes in the Yilgarn Craton of Western Australia. Precambrian Research, 48, 309-325.

Pidgeon, R.T. & Wilde, S.A., 1998. The interpretation of complex zircon U-Pb systems in Archaean granitoids and gneisses from the Jack Hills, Narryer Gneiss terrane, Western Australia. Precambrian Research, 91, 309-332.

Pidgeon, R.T., Wilde, S.A., Compston, W. & Shield, M.W., 1990. Archaean evolution of the Wongan hills Greenstone belt, Yilgarn Craton, Western Australia. Australian Journal of Earth Sciences, 37, 279-292.

Schiøtte, L. and Campbell, I. H., 1996, Chronology of the Mount magnet granite-greenstone terrain, Yilgarn Craton, Western Australia: implications for field based predictions of the relative timing of granitoid emplacement.: Precambrian Research, v. 78, p. 237-260.

Smithies, R.H. & Champion, D.C., 1999. Late Archaean felsic alkaline igneous rocks in the Eastern Goldfields, Yilgarn Craton, Western Australia: a result of lower crustal delamination? Journal of the Geological Society of London, 156, 561-576.

Smithies, R.H. & Champion, D.C., 2000. The Archaean High-Mg diorite suite: Links to tonalite-trondhjemite-granodiorite magmatism and implications for early Archaean crustal growth. Journal of Petrology, 41, 1653-1671.

Wang, L. G., McNaughton, N. J., and Groves, D. I., 1993, An overview of the relationship between granitoid intrusions and gold mineralisation in the Archaean Murchison Province, Western Australia: Mineralium Deposita, v. 28, p. 482-494.

Wang, L., McNaughton, N.J. & Groves, D.I., 1995. New geochronological data for granitoid intrusions in the Reedy's area, Murchison Province, Western Australia: constraints on genesis of gold mineralisation. Third Australian Conference in Geochronology and Isotope Geoscience, Perth, Workshop Program and Abstracts, p. 37.

Wang, Q., Schiøtte, L. & Campbell, I.H., 1998. Geochronology of the supracrustal rocks from the golden Grove area, Murchison Province, Yilgarn block, Western Australia. Australian Journal of Earth Sciences, 45, 571-577.

Watkins, K.P & Hickman, A.H., 1990. Geological evolution and mineralisation of the Murchison Province, Western Australia. Geological Survey of Western Australia, Bulletin 137.

Wiedenbeck, M. and Watkins, K. P., 1993, A time scale for granitoid emplacement in the Archaean Murchison Province, Western Australia, by single zircon geochronology: Precambrian Research, v. 61, p. 1-26.

Williams, I.R., Walker, I.M., Hocking, R.M. & Williams, S.J., 1983. Byro, Western Australia sheet SG50-10. 1:250 000 Geological Series - explanatory notes, Geological Survey of Western Australia.

Yeats, C. J., McNaughton, N. J., and Groves, D. I., 1996, SHRIMP U-Pb geochronological constraints on Archaean volcanic-hosted massive sulphide and lode gold mineralisation at Mount Gibson, Yilgarn craton, Western Australia.: Economic Geology, v. 91, p. 1354-1371.

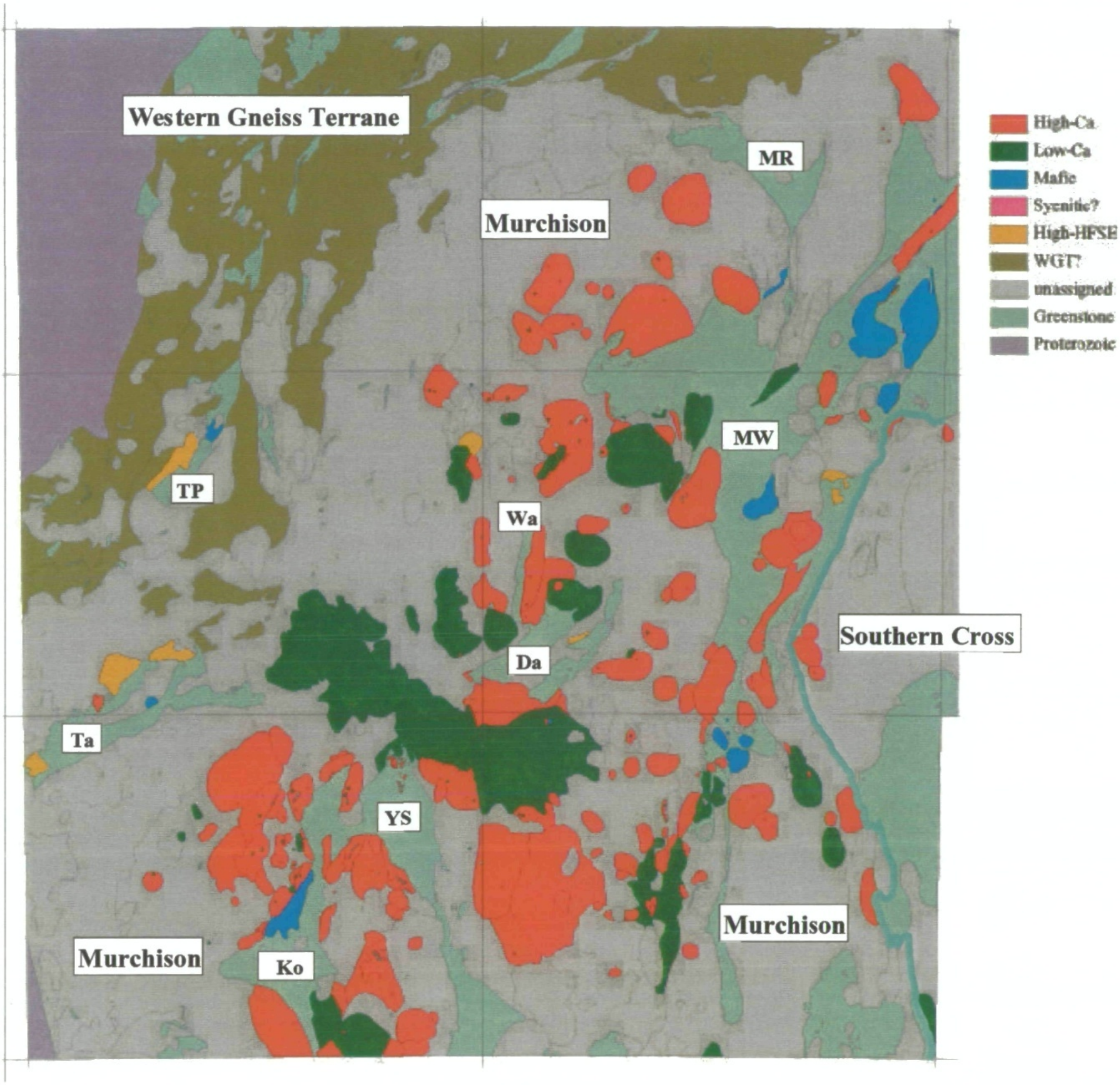

Figure 1. Granite groups in the northern Murchison and northwestern Southern Cross provinces. Greenstone belts (after Watkins & Hickman, 1990), as follows: MR - Mingah Range; MW - Meekatharra-Wydgee; Ta - Tallering; TP - Twin peaks; YS - Yalgoo-Singleton; Ko - Koolanooka; Da - Dalgaranga; Wa - Wardatharra.

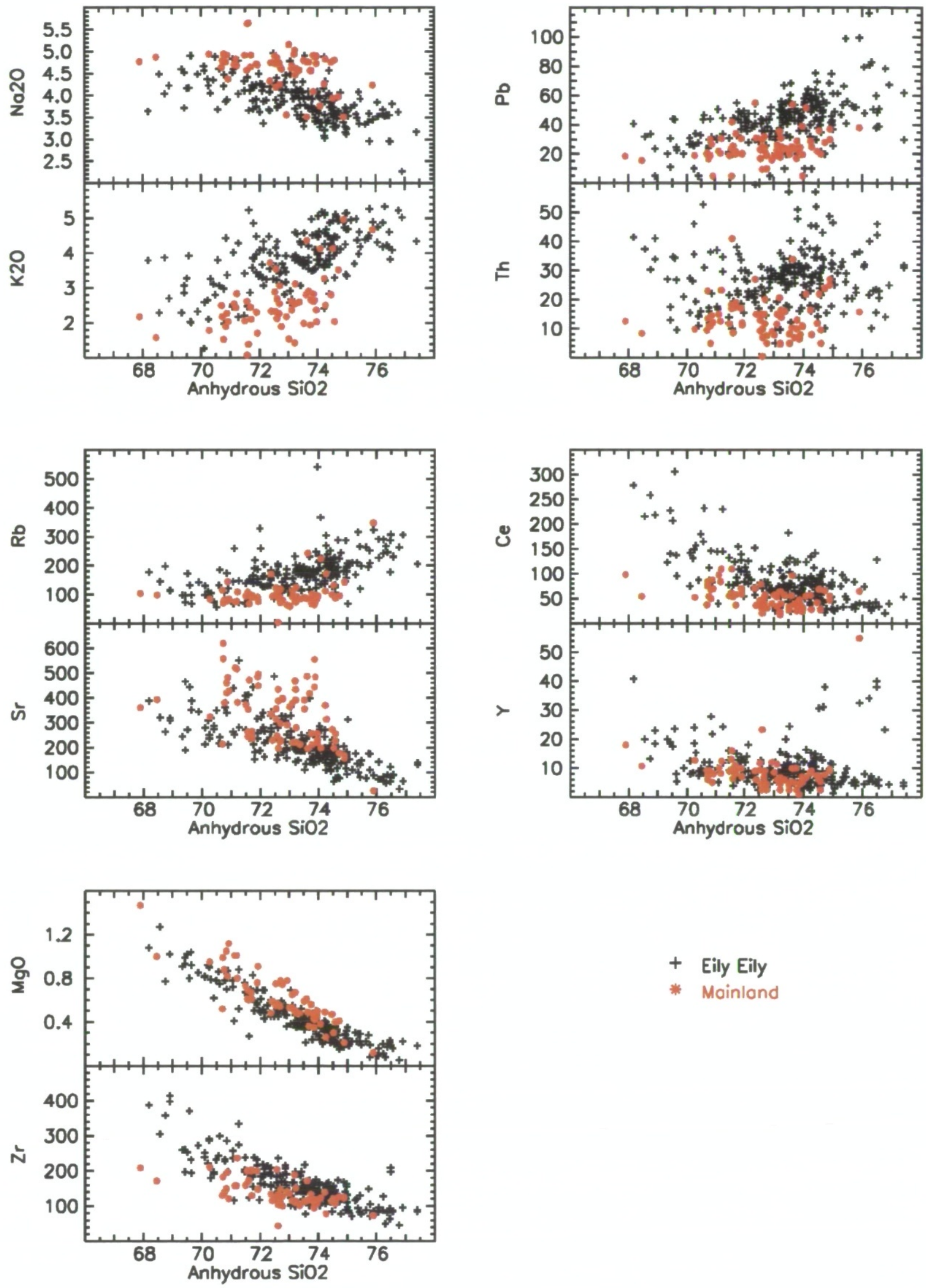

Figure 2. Comparison of the 'high-LILE' Eily Eily clan, and the 'low-LILE' Mainland clan, both of the Mainland Association, High-Ca group, northern Murchison Province. Nb. 'High-' and 'low-LILE' terms are relative, not absolute.

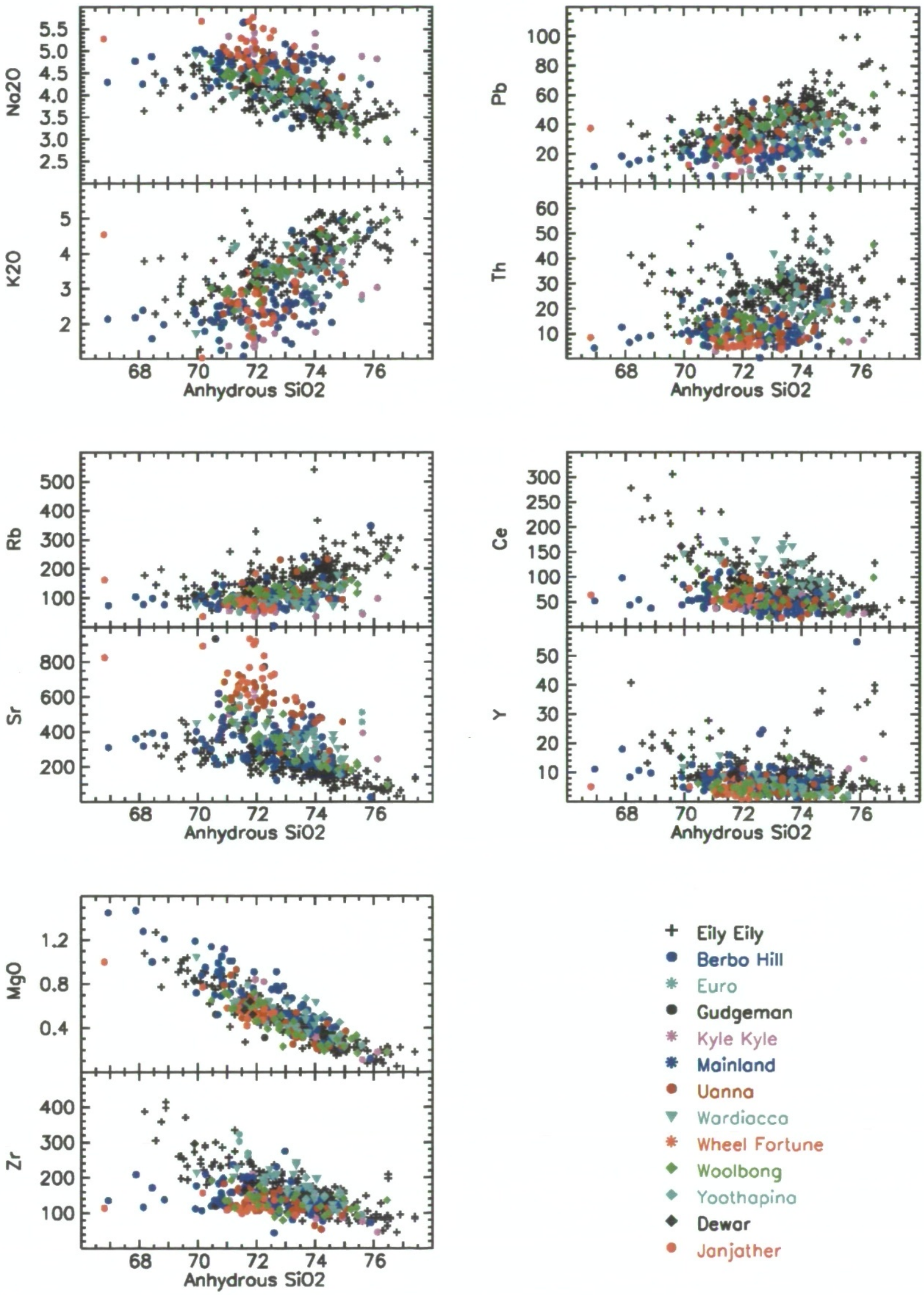

Figure 3. Clans of the Mainland and Diemals (Janjather, Dewar clans) associations, High-Ca Group, northern Murchison region.

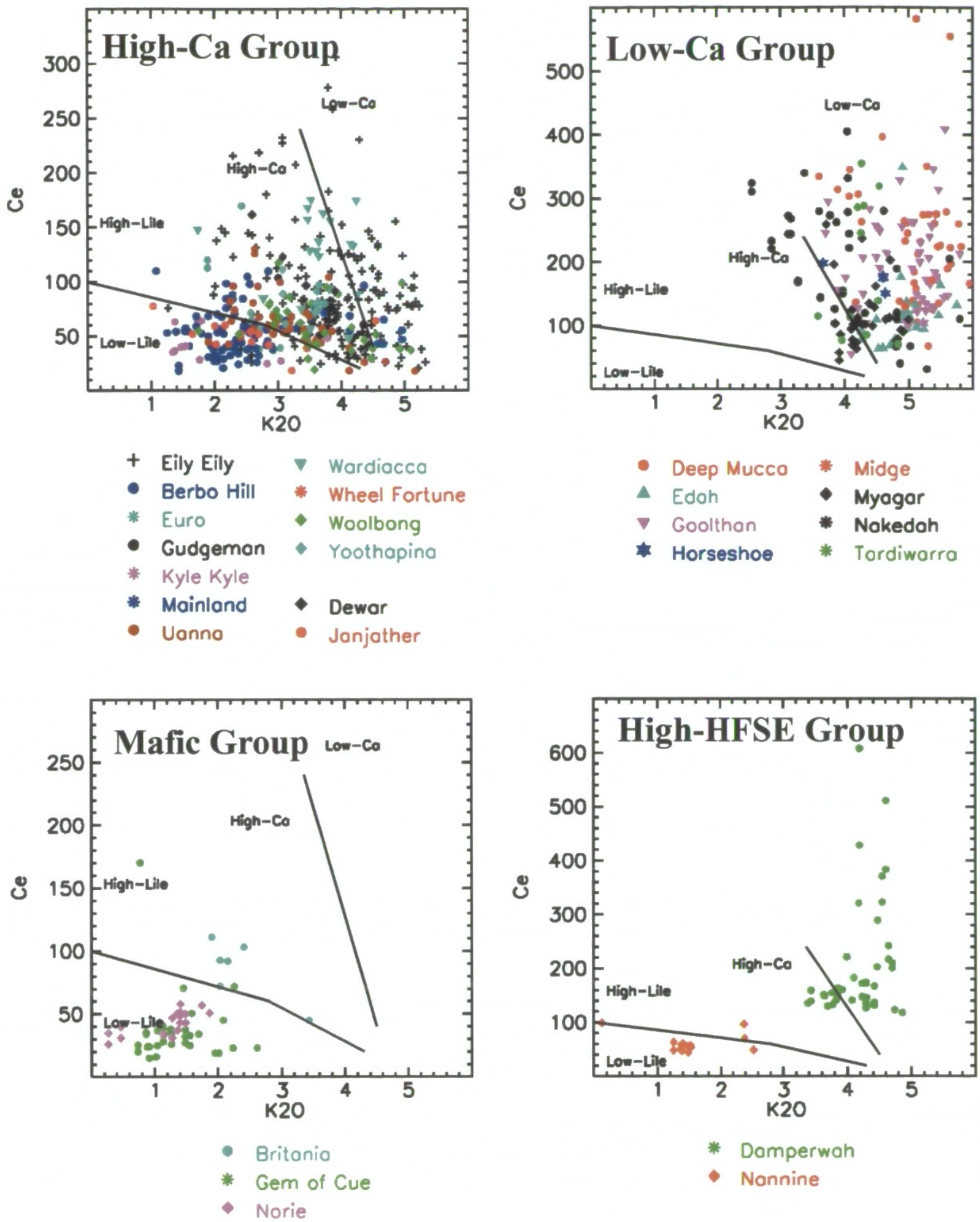

Figure 4. K2O-Ce plots illustrating the range in LILE and HFSE in the Mainland and Diemals (Dewar, Janjather clans)Associations of the High-Ca group, in the Goolthan Association, Low-Ca group, in the Gem of Cue Association, Mafic Group, and in the DamperwahAssociation, High-HFSE group. The central line is an arbitrary divide between 'low-LILE' and 'high-LILE' end-members of the High-Ca and Mafic groups. Nb. The terms 'low-' and 'high-LILE' are used in a relative, not absolute, sense. Note expanded Ce axis for the Low-Ca and High-HFSE groups.

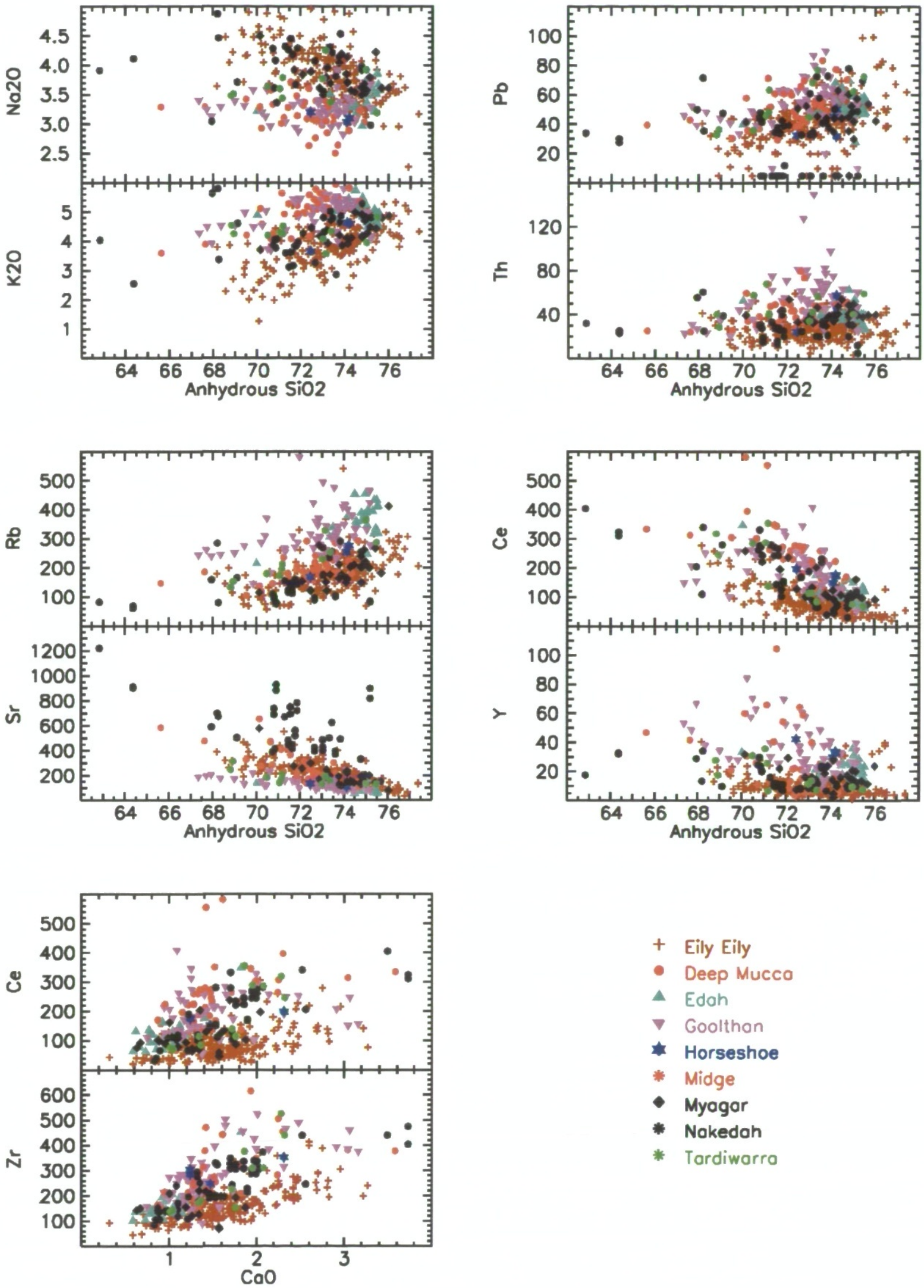

Figure 5. Clans of the Goolthan Association, Low-Ca group,Murchison Province. The high-LILE Eily Eily Clan of the Mainland Association, High-Ca group is shown for comparison.

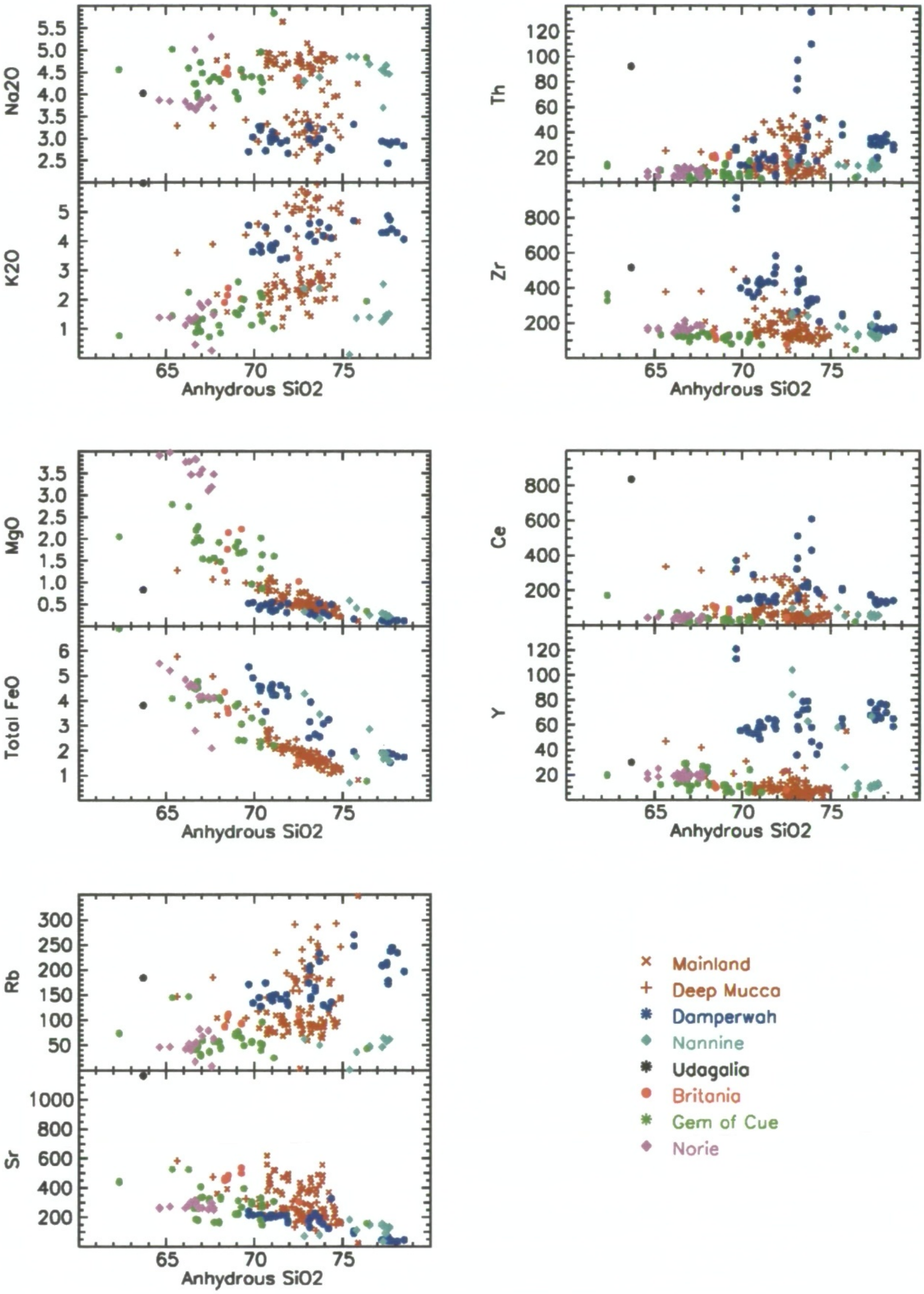

Figure 6. Udagalia clan of the Syenitic group, Gem of Cue, Britania and Norie clans of the Mafic group, and Damperwah and Nannine clans of the High-HFSE group, northern Murchison Province. Also shown, in brown, are the low-LILE Mainland clan, High-Ca group, and the Deep Mucca Bunna clan, Low-Ca group.

Granitoid geochronology: SHRIMP zircon and titanite data

Ian R. Fletcher and Neal J. McNaughton

Summary

A total of 60 granitoid samples, most of them collected during the 1997–1999 field seasons for this project, were selected for SHRIMP geochronological studies, as well as Sm–Nd and Pb/Pb isotopic analysis. The samples are fairly evenly distributed between the three Provinces of the Yilgarn Craton. Zircons were recovered from almost all samples, but in a significant proportion of cases the zircons were not sufficiently well preserved to provide useful geochronological data. This problem was partially overcome by analysing titanite separated from some of these samples. In some cases the use of both zircon and titanite revealed aspects of the geochronology which would not have emerged from either mineral in isolation. However, there were several cases where titanites were not found, or were too low in U to be used for dating. Approximately 75% of the samples are considered to be well dated, with a further 5–10% having approximate dates that are interpreted to be valid ages.

Data summary

Table 1 summarises the results of SHRIMP dating, and subsequent pages provide brief descriptions of each of the samples, data tables and figures, and comments on the results. In most cases, the zircon and titanite dates listed in Table 1 are interpreted to be magmatic ages, but they should not be used as such without reference to the discussion which follows.

Figures 1 and 2 display the distribution of ages from Table 1. There are several events which appear to be strongly represented in two Provinces but none which is a major component of the distribution in all Provinces, and some events are represented in only one of the three Provinces. Note, however, that some 'peaks' include only one or two analyses, and that some of this sampling programme was intended to will gaps in the previous data record. The long-recognised west–east younging of the Yilgarn Craton is clearly reflected.

Table 1: Summary of SHRIMP zircon and titanite geochronological data.

AGSO Number	Pluton Number	Unit Name	Rock Type	Chemical Grouping	Ages ± 2σ (Ma) Zircon	Titanite	Xenocryst zircon
Murchison Province							
9796 9138	243614	Waddouring	monzogranite	Low-Ca	2628 ± 3	2626 ± 4	
9996 4003	224112	Goolthan Goolthan	bt monzogranite	Low-Ca	2626 ± 6	2630 ± 5	
9996 4016C	223916	Mount Mulgine	bt syenogranite	High-Ca	2756 ± 20		
9996 4100	224107	Basin	bt monzogranite	High-Ca	2743 ± 4	2632 ± 8	
9996 7049A	233501	Goddard nebulitic gneiss	granitic gneiss	High-Ca	2787 ± 4		~2840; ~2890
9996 7055	233623	Fox Lair	bt monzogranite	Low-Ca	2641 ± 5		
9996 7066	213701	Namban	Kfs-phyric bt granite	Low-Ca	2646 ± 5	2638 ± 7	
9996 7082C	213722	Dookaling-xenolith	augen gneiss	High-Ca	?2940	2619 ± 8	
9996 7114	244301	Telegootherra	bt granodiorite	Low-Ca	no date		
9996 7141	234208	Keygo	granophyric granodiorite	High-HFSE	~2745		
9996 9049	253621	Coolamen-dyke	hb-bt granite	High-HFSE?	2640 ± 5		
9996 9063	223622	Barrambie-dyke	aln-ttn-bt granite	Low-Ca	2630 ± 6		~2670
9996 9066	213601	Donga Well	foliated bt-granite	High-Ca	no date		~2780; ~3100; ~3200; ~3300
9996 9093B	223703	Coolangatta	granodiorite gneiss	High-Ca	3007 ± 3	2632 ± 6	
9996 9096	223701	Wubin	hb-bt granodiorite	Low-Ca	2639 ± 6		
9996 9142	214006	Triangle	bt-hb qtz-monzonite	Mafic	2747 ± 3		~2790
9996 9164A	214114	Courin Hill	foliated bt-granite	High-Ca	2742 ± 7		
Southern Cross Province							
9796 9023	293713	Turturdine	bt monzogranite	Low-Ca	no date	no date	
9796 9034	303505	Yerdanie	bt monzogranite	Low-Ca	no date	no date	~2705
9796 9063	284001	Bulga Downs	bt monzogranite	Low-Ca	2684 ± 8		
9796 9082A	284006	The Spring	bt granodiorite	High-Ca	2682 ± 5		
9796 9102B	283905	McLeod Rock	granitic gneiss	High-Ca	~2740		~2790; ~3010
9796 9104	283908	Native Well	monzogranite	High-Ca	2682 ± 6		
9796 9125	263504	Warren-2	monzogranite	Low-Ca	2617 ± 3		~2650
9796 9126	0	Proterozoic dyke	diorite	Prot dyke	1201 ± 7		2629 ± 4; ~2650
9796 9201	323203	Tank No. 28	monzogranite	Low-Ca	2623 ± 7		
9796 9202	323304	McPherson	bt monzogranite	High-Ca	2656 ± 10		
9896 7100A	293504	Boorabbin	bt monzogranite	Low-Ca	no date		
9896 7102E	0	Koolyanobbing xenolith	bt granodiorite	Mafic?	2699 ± 10		

AGSO Number	Pluton Number	Unit Name	Rock Type	Chemical Grouping	Ages ± 2σ (Ma) Zircon	Titanite	Xenocryst zircon
Southern Cross Province (cont.)							
9896 8104	264001	Courlbarloo	tonalite	Mafic	2813 ± 5		
9896 9019	284301	Bluff Point	monzogranite	Low-Ca	no date		~3105; ~3585
9896 9025	274302	Buttercup Bore	granodiorite	Low-Ca	2661 ± 7		
9896 9033	274304	Tom Bore	granitic gneiss	High-Ca	2671 ± 3		
9896 9042	264305	Barlanga Well	quartz monzonite	Low-Ca	no date		~2715; ~2820
9896 9044	264304	Yarrabubba	granite	Low-Ca	2650 ± 10		~2750
9896 9045	264314	Monty Bore	monzogranite	High-Ca	~2700		
9896 9055	274205	Woodley Bluff	monzogranite	High-Ca	2712 ± 6		~3025
Eastern Goldfields Province							
9796 7038G	313726	Golden Cities	bt-hb granodiorite	Mafic	2656 ± 3		~2675
9796 7069A	314308	Sundowner-dyke	feldspar porphryry	Mafic		2644 ± 6	
9796 7069B	304301	Gemchapps	bt monzogranite	High-HFSE		2608 ± 10	
9796 7150	343401	Yardilla	bt-hb granite	Syenite		2645 ± 12	
9796 7152	343401	Yardilla	bt-hb granite	Syenite	?2660		
9796 7153	333419	Talbot	bt monzogranite	Low-Ca	?2625		~2685
9796 9044	313605	Mungari	monzogranite	Low-Ca	no date		~2810
9796 9209	323308	Dundas	bt monzogranite	Low-Ca	?2620		
9796 9212	323303	Lake Kirk	granitic gneiss	High-Ca	?2685	2631 ± 6	
9796 9223	333301	Buldania	bt granodiorite	High-Ca		2660 ± 9	
9796 9237	323310	Boojerbeenyer	monzogranite	Low-Ca	?2625		>2800
9796 9243	323311	Buldania-2	bt-hb granodiorite	High-Ca		2655 ± 6	
9796 9245	333414	Tramways South	monzogranite	Low-Ca	no date		
9796 9248	333415	Toil and Trouble	bt monzogranite	High-Ca	2648 ± 11	2652 ± 14	
9796 9249	333409	Sinclair	monzogranite	High-Ca	no date	2655 ± 20	?2725
9796 9256B	333413	End of Day xenolith	granodiorite	Mafic	2663 ± 11	2658 ± 20	
9896 7008	343613	Erayinia Complex	bt-hb qtz-monzonite	Syenite	2660 ± 5		
9896 9003	343501	Fitzgerald Lagoon	bt granodiorite	High-Ca	2657 ± 9		~2710
9996 7170A	314126	Bullshead	bt diorite	High-HFSE	no date		
9996 7174A	334022	Wallaby	K-spar-phyric syenite	Syenite	no zircon or titanite recovered		
9996 7176	334023	Wallaby	carbonatite	Carbonatite	no zircon or titanite recovered		
9996 7177B	334022	Wallaby	carbonatitic syenite	Syenite		2657 ± 15	

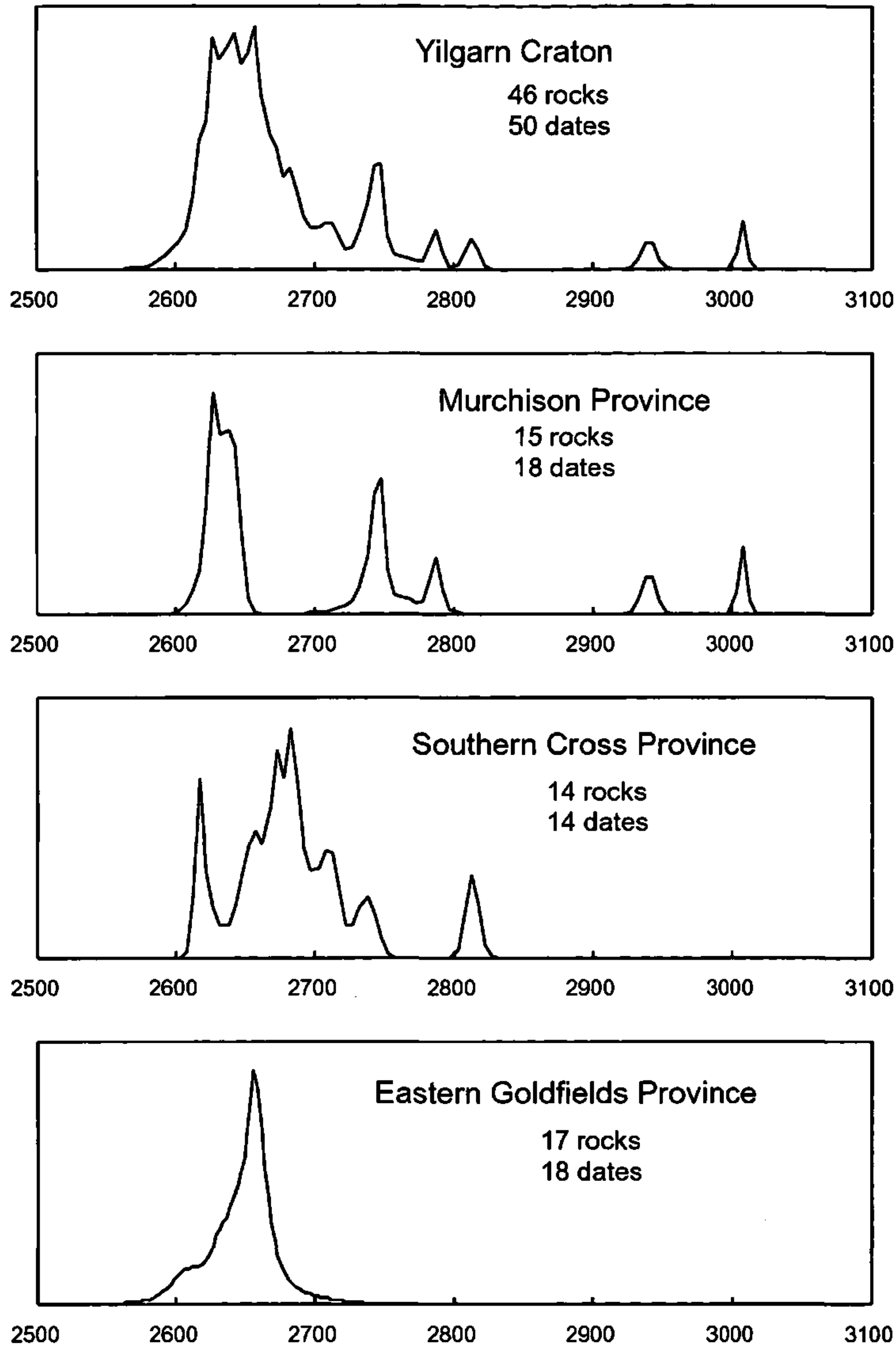

Figure 1: Cumulative frequency plots for the data in Table 1. In cases where titanite and zircon register different dates, both are used; when the two minerals record the same date it is used as a single entry. Dates which are only approximately determined have been assigned an uncertainty of 25 Ma.

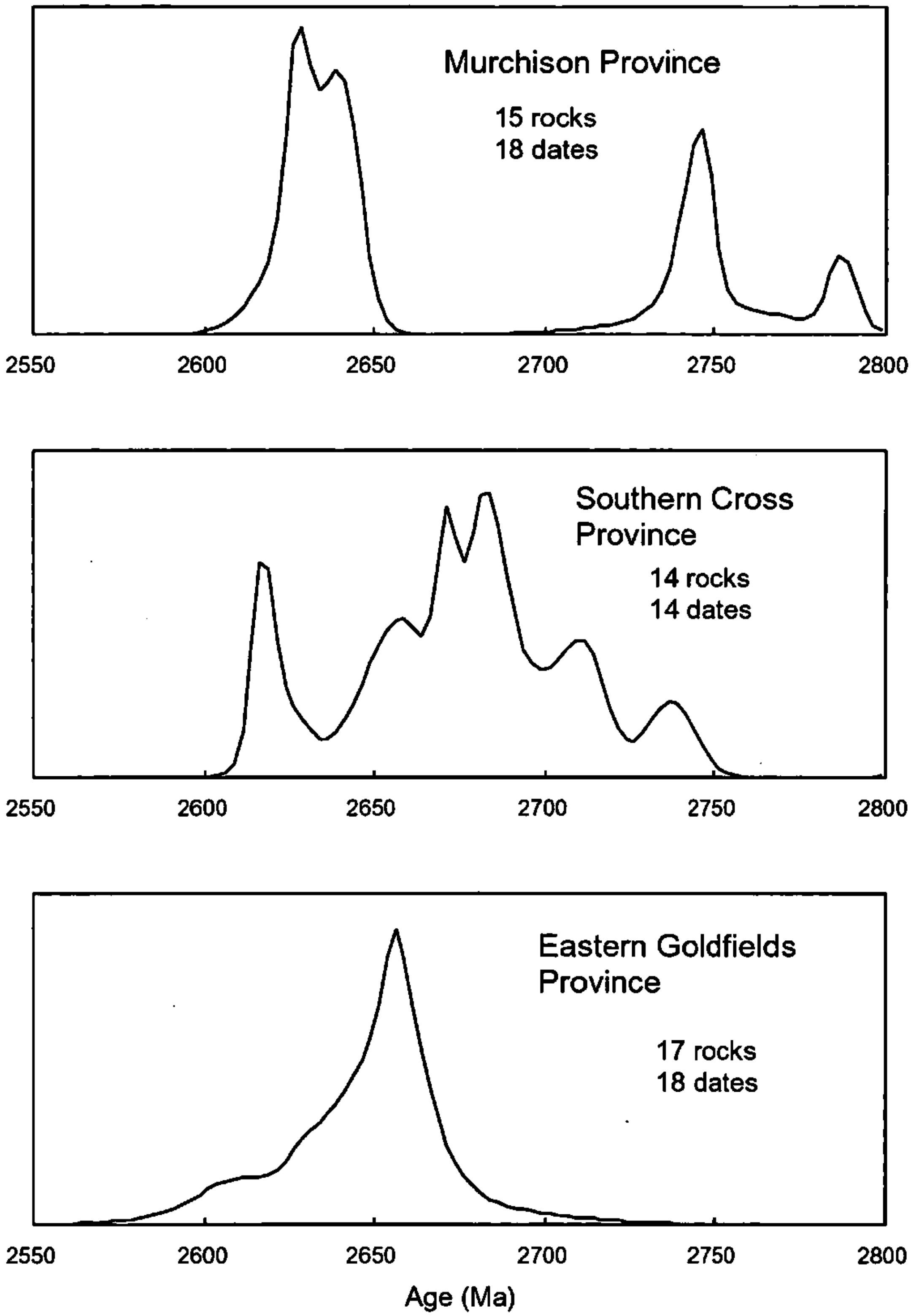

Figure 2: Expanded detail of the main sections of Figure 1.

Sample processing

All samples were inspected in the laboratory and weathered material discarded. The samples were then washed and scrubbed with a nylon brush in town water, rinsed in distilled water and dried. Each sample was then crushed in a precleaned jaw crusher and about 100 g of material was unbiassedly split off using a perspex splitter. This was milled in agate to give a representative wholerock aliquot for geochemical and/or isotopic analysis. The remaining rock was milled in a tungsten carbide ring mill to pass through a 60# disposable nylon sieve, and then washed and decanted in town water to remove fine particles (i.e. nominally <10 μm). The samples were then dried, and minerals separated as follows:

- LST heavy liquid separation to separate material lighter than about 2.9 gms/cc;
- Frantz Isodynamic Separator: magnetic separation to remove strongly to moderately magnetic minerals;
- Di-iodomethane heavy liquid separation to remove material lighter than about 3.3 gms/cc;
- Dissolution of sulphides in weak nitric acid (if applicable); and
- Handpicking of zircons and/or titanite from the remaining heavy mineral concentrate.
- Separation of K-feldspar from the light fraction for Pb isotopic analysis.

All residues from the processing have been retained at UWA.

Mount preparation and imaging

Sample grains were mounted in epoxy with chips of the CZ3 zircon standard (564 Ma; $^{206}Pb/^{238}U = 0.0914$) or the Khan titanite standard (518 Ma; $^{206}Pb/^{238}U = 0.08367$). The mounts were ground and polished to remove about half of each grain, and photographed at low and high magnification in preparation for SHRIMP analysis.

Representative zircons from each sample were imaged using Scanning Electron Microscope (SEM) techniques at the Centre for Microscopy and Microanalysis (CMM), UWA. Images from backscattered electrons (BSE) and charge contrast (CCI) were obtained using an environmental SEM. The BSE images show variations in the average atomic number of the grains and usually show the internal morphology of the grain due to variations in the trace element contents. The CCI technique, developed by Dr Brendan Griffin from the CMM, gives images similar to those obtained from cathodoluminescence (CL). Variations in CCI image intensity correspond to variations in specific trace elements and to radiation damage caused by U-Th-decay over time. The CCI method was used in preference to CL because it is quicker and gave a higher resolution of the digital image, it did not require carbon coating prior to imaging and subsequent removal prior to gold coating for SHRIMP analysis, and caused less damage to the epoxy surface of the mount than a CL image.

Titanite samples were also examined by SEM but growth structures were recognised in very few cases.

SHRIMP method and operating conditions for zircon

The SHRIMP procedure for zircons has been described by Compston et al. (1984), Williams and Claesson (1987) and Smith et al. (1997). The overall advantage of using SHRIMP compared to other isotope geochronology methods makes use of the fact that zircons are refractory and can preserve a complex geological history within zircon populations found in one rock, and even within one zircon grain. Small areas of grains (20–30 μm diameter) can be analysed to give age information on progressive growth zones of single crystals (ie. rims and cores). If this growth history is common to a number of grains, a temporal history of the rock can be determined and related to overall geological history of the area.

The normal monitor of machine performance for SHRIMP is the reproducibility of the U/Pb ratio of the CZ3 standard during the analytical session. This value is given with each sample described below. For comparison, at the Australian National University, SHRIMP data for their SL3 zircon standard typically has U/Pb ± 2.0% (1σ), whereas data from this project is normally better than this. This is considered to be partly due to the CZ3 standard being more isotopically homogeneous than the SL3 standard.

The SHRIMP operating parameters used for zircon were as follows:

Mass	**Species**	**Counting time (secs)**	**Magnet delay time (secs)**
196	Zr_2O	2	8
204	^{204}Pb	10	3
204.1	Background	10	1
206	^{206}Pb	10	2
207	^{207}Pb	30	1
208	^{208}Pb	10	1
238	^{238}U	5	3
248	$^{232}Th^{16}O$	5	2
254	$^{238}U^{16}O$	2	2

Six (sometimes seven) cycles of data constitute each of the 'spot' analyses reported.

A correction was made for common Pb by using the measured ^{204}Pb and the Broken Hill Pb isotopic composition to remove the common Pb from the measured isotopic ratios. This is an approximation, in that samples with significant ^{204}Pb are generally metamict or cracked, and the isotopic composition of the common Pb component cannot be determined independently. Surface Pb contamination of the sample, which would be dominantly of Broken Hill composition, was monitored in data for CZ3 and was always insignificantly small. Data were excluded from age determinations if the potential error introduced by the common Pb correction could be significant.

Data were processed using the program Krill (version 007), written by Dr Peter Kinny (Curtin University). In determining whether the spread in a data set is that expected from a homogeneous sample population, we accept χ^2 (equivalent to MSWD) less than ~1.6, preferably less than ~1.2. Other research groups may be less conservative and accept data populations with a larger χ^2, whereas others may be more conservative. In the interpretations presented below, a discussion of the influence of this aspect on the age estimates is given, where appropriate.

SHRIMP method and operating conditions for titanite

The SHRIMP procedure for titanites is similar to that for zircons, and has been described by Kinny (1994; 1997). The micro-analytical advantages are also similar to those for zircon, although in this project they have served to demonstrate the extreme rarity of growth zonation in the samples analysed, rather than to date different growth phases.

The monitor of machine performance for SHRIMP of titanite is the reproducibility of the U/Pb ratio of the Khan standard during the analytical session. This value is given with each sample described below, and is generally <2.0% (i.e. comparable to data for CZ3).

The operating parameters used for SHRIMP during the period of analysis were as follows:

Mass	Species	Counting time (secs)	Magnet delay time (secs)
200	$CaTi_2O_4$	2	8
204	^{204}Pb	10	2
204.1	Background	10	1
206	^{206}Pb	10	2
207	^{207}Pb	30	1
208	^{208}Pb	10	1
248	$^{232}Th^{16}O$	3	3
254	$^{238}U^{16}O$	2	2
270	$^{238}U^{16}O_2$	2	2

Six (sometimes seven) cycles of data constitute each of the 'spot' analyses reported.

Unlike zircons, titanites commonly incorporate a small amount of common Pb when they form. For the data reported below, common-Pb corrections were made using the measured ^{204}Pb for each analysis and the Pb isotopic composition determined by the Cumming and Richards (1975) Model 3 average-Earth evolution model at an age estimated from the raw data for all analyses of that sample. Surface Pb contamination of the samples, which would be dominantly of Broken Hill composition, was assumed to be insignificantly small, as observed for zircons. Data were generally excluded from age determinations if the potential error introduced by the common Pb correction could be significant, but in some cases the U abundances (and hence radiogenic Pb) were sufficiently low that all data had significant corrections. In these cases, the effect of choosing possible common Pb compositions is discussed.

For some of the titanite analyses, a combination of low U (and hence low radiogenic Pb) contents and limited available O_2^- primary ion beam current led to unacceptably low secondary ion count rates. To compensate, analyses were sometimes performed using NO_2^- primary ions. The NO_2^- current is normally stronger than O_2^-, and the resulting increase in secondary Pb^+ counts sometimes allowed data acquisition with adequate precision. The Pb/U calibration is not well determined in these cases, due mainly to uncalibrated matrix effects which appear to cause greater variation in recorded Pb^+/UO^+ when using NO_2^-. Therefore, for these analyses, the consistency in processed Pb/U data was considered to be a stronger indicator of concordance than the absolute relationship between the two decay schemes. In no case is it considered likely that the measured ages, which are calculated from $^{207}Pb/^{206}Pb$, are perturbed by this assumption. The Pb/Th calibration is not known for these operating conditions, and Pb/Th data are not reported for these analyses.

Data reduction for titanites was carried out using Krill, and similar data criteria were applied to the identification of coherent data groups as described above for zircons.

Data presentation

Data are presented below in sample number order, with data tables and figures identified by sample number and prefixes 'z' and 't' for zircon and titanite data, respectively. In all tables:

4f206% is the percent of ^{206}Pb calculated to be common Pb;

all Pb data are corrected for common Pb (denoted *);
conc. is concordance, stated as the ratio of the ages calculated from $^{206}Pb/^{238}U$ and $^{207}Pb/^{206}Pb$.

Uncertainties listed in the tables and shown in concordia plots are 1 σ, based on counting statistics and propagated through data processing. In tables, the uncertainties refer to the last digits quoted. Ages determined from pooled analyses are calculated from $^{207}Pb/^{206}Pb$ and are quoted with 95% confidence limits, determined by the larger of [1] the population scatter (when $\chi^2 > 1$), or [2] the theoretical precision calculated from the internal precision of the individual data points (when $\chi^2 < 1$).

Acknowledgements

Mrs Marion Marshall performed the zircon and titanite separations, prepared the SHRIMP mounts and supervised the microphotography and SEM imaging. SHRIMP analyses were undertaken by the authors with assistance from graduate students in CGM. Zircon analyses were carried out on a Sensitive High Resolution Ion Micro Probe mass spectrometer (SHRIMP II) operated by a consortium consisting of Curtin University of Technology, the Geological Survey of Western Australia and the University of Western Australia with the support of the Australian Research Council. This study was funded by AMIRA and ARC Collaborative grants.

References

Compston, W., Williams, I.S. & Meyer, C., 1984, U-Pb geochronology of zircons from lunar basalt 73217 using a sensitive high mass-resolution ion microprobe. Journal of Geophysical Research 89: B525-B534.

Smith, J.B., Barley, M.E., Groves, D.I., Krapez, B., McNaughton, N.J., Bickle, M.J. & Chapman, H.J., 1997, The Scholl shear zone, West Pilbara: evidence for a terrane boundary structure from integrated tectonic analyses, SHRIMP U-Pb dating and isotopic and geochemical data of granitoids. Precambrian Research.

Williams, I.S. & Claesson, S., 1987. Isotopic evidence for the Precambrian provenance and Caledonian metamorphism of high grade paragneisses from the Seve Nappes, Scandanavian Caledonides. II. Ion microprobe U-Th-Pb. Contributions to Mineralogy and Petrology 97: 205-217.

9796 7038G: hornblende-biotite granodiorite, Golden Cities Granodiorite

1:250,000 sheet:	Kalgoorlie (SH 51-9)
AMG:	347377.6 mE, 6634826.1 mN
Location:	Woodcutters prospect drillhole WCVCD-73, depth interval 310.75–312.70 m
Province:	Eastern Goldfields
Description:	This sample is a least-altered hornblende-biotite granodiorite from the Golden Cities granodiorite, a pluton within the Scotia-Kanowna batholith. The hornblende-biotite granodiorite contains abundant small mafic dioritic enclaves and some small greenstone xenoliths and is, in places, cross-cut by thin aplites
Chemical group:	Mafic group, Granny Smith association, Granny Smith clan
Pluton No:	313726
UWA mounts:	97-22D

Description of zircons

The zircon population in this sample consists of one morphologic type with uniform grain size, mostly with grains of the order of 100 x 50 μm. Grains are typically euhedral to subhedral in external morphology with continuous euhedral internal zoning from core to rim. Inclusions are not common and consist of opaque or rod-like to equant minerals. All inclusions occur throughout the grains and show no preference for core or rim regions. The grains range from clear to pale brown, to dark brown in colour. Strong euhedral zoning is observed in both optical and SEM images: no obvious xenocrystic cores were observed. Discordant alteration patches, which characterised zircons from the previous two samples, are not present in this sample.

Results and interpretation

Twenty nine analyses were obtained from 24 grains. The corrections for common Pb are low and the U-contents of all analyses are <250 ppm. The age data show a relatively tight group, with grains being either concordant or slightly discordant. When all data are treated as one population, the population exhibits more scatter than would be expected from the analytical uncertainties. Three analyses which are significantly discordant, and one which has similar 4f206 to the discordant points and is statistically younger than the main population, are omitted (pale-shaded analyses in Figure z9796 7038G). Also omitted is one analysis from the core of a grain (grain #22) which gives an age of 2676±8 Ma, slightly older than the main population. The remaining 24 analyses have a $\chi^2 < 1.0$ and are considered to be a single age population at 2656±3 Ma.

Given the magmatic morphology of the grains which form the main group, the emplacement age of the granitoid is inferred to be 2656±3 Ma.

Table z9796 7038G: SHRIMP zircon data for the hornblende-biotite granodiorite, Golden Cities Granodiorite (UWA mount 97-22D).

grain-spot	U (ppm)	Th (ppm)	4f206 (%)	$^{207}Pb^*/^{206}Pb^*$	$^{208}Pb^*/^{206}Pb^*$	$^{206}Pb^*/^{238}U$	$^{207}Pb^*/^{235}U$	$^{208}Pb^*/^{232}Th$	conc. (%)	$^{207}Pb/^{206}Pb$ age (Ma)
2-1	196	137	0.050	0.1797 ± 7	0.1906 ± 12	0.4767	11.810	0.1295	95	2650 ± 7
3-1	135	101	0.042	0.1808 ± 8	0.2089 ± 15	0.4884	12.176	0.1359	96	2661 ± 8
4-1	111	64	0.000	0.1803 ± 8	0.1477 ± 11	0.5041	12.533	0.1289	99	2656 ± 7
5-1	195	122	0.000	0.1806 ± 6	0.1700 ± 9	0.4794	11.939	0.1300	95	2659 ± 6
6-1	183	122	0.025	0.1802 ± 7	0.1764 ± 12	0.4926	12.237	0.1308	97	2655 ± 7
7-1	135	131	0.086	0.1792 ± 9	0.2628 ± 17	0.4949	12.230	0.1339	98	2646 ± 8
8-1	177	105	0.011	0.1799 ± 7	0.1631 ± 11	0.4940	12.256	0.1358	98	2652 ± 7
9-1	209	146	0.000	0.1796 ± 6	0.1913 ± 10	0.5016	12.423	0.1368	99	2649 ± 6
9-2	148	104	0.093	0.1810 ± 9	0.1567 ± 14	0.4983	12.436	0.1107	98	2662 ± 8
10-1	137	77	0.000	0.1810 ± 8	0.1568 ± 11	0.4998	12.474	0.1391	98	2662 ± 7
11-1	242	148	0.001	0.1804 ± 6	0.1698 ± 9	0.5104	12.699	0.1419	100	2657 ± 5
12-1	226	158	0.009	0.1806 ± 6	0.1962 ± 10	0.4997	12.444	0.1399	98	2659 ± 6
14-1	207	128	0.013	0.1808 ± 7	0.1732 ± 11	0.4816	12.003	0.1346	95	2660 ± 6
15-1	239	294	0.039	0.1800 ± 6	0.2369 ± 12	0.4890	12.136	0.0943	97	2653 ± 6
16-1	152	86	0.040	0.1806 ± 9	0.1564 ± 14	0.4896	12.191	0.1347	97	2658 ± 8
16-2	127	75	0.025	0.1813 ± 9	0.1706 ± 15	0.4902	12.255	0.1412	96	2665 ± 9
16-3	132	56	0.018	0.1803 ± 9	0.1182 ± 12	0.4967	12.345	0.1385	98	2655 ± 8
17-1	187	109	0.000	0.1816 ± 7	0.1630 ± 9	0.4955	12.406	0.1386	97	2667 ± 6
19-1	84	61	0.004	0.1792 ± 11	0.2001 ± 19	0.5061	12.504	0.1390	100	2646 ± 10
20-1	114	79	0.000	0.1805 ± 9	0.1930 ± 13	0.5133	12.775	0.1431	100	2658 ± 8
21-1	245	148	0.023	0.1789 ± 6	0.1662 ± 9	0.5090	12.556	0.1403	100	2643 ± 6
23-1	173	87	0.063	0.1811 ± 8	0.1338 ± 12	0.5223	13.041	0.1397	102	2663 ± 7
24-1	90	36	0.066	0.1798 ± 11	0.1087 ± 16	0.5137	12.736	0.1378	101	2651 ± 10
24-2	125	56	0.000	0.1816 ± 8	0.1242 ± 10	0.5105	12.783	0.1414	100	2668 ± 8
Discordant and/or higher common Pb										
1-1	94	64	0.185	0.1813 ± 11	0.1804 ± 20	0.4644	11.609	0.1226	92	2665 ± 10
1-2	164	77	0.178	0.1777 ± 8	0.1302 ± 13	0.4684	11.477	0.1303	94	2632 ± 7
13-1	249	206	0.278	0.1775 ± 7	0.2337 ± 15	0.4407	10.787	0.1249	89	2630 ± 7
18-1	100	68	0.255	0.1774 ± 11	0.1777 ± 20	0.5020	12.279	0.1321	100	2629 ± 11
Inherited core (?)										
22-1	137	78	0.076	0.1825 ± 9	0.1575 ± 14	0.5117	12.878	0.1413	100	2676 ± 8

Data 11/7/97.

U/Pb scatter (1σ) for cz3 standard = 1.77% (n=15).

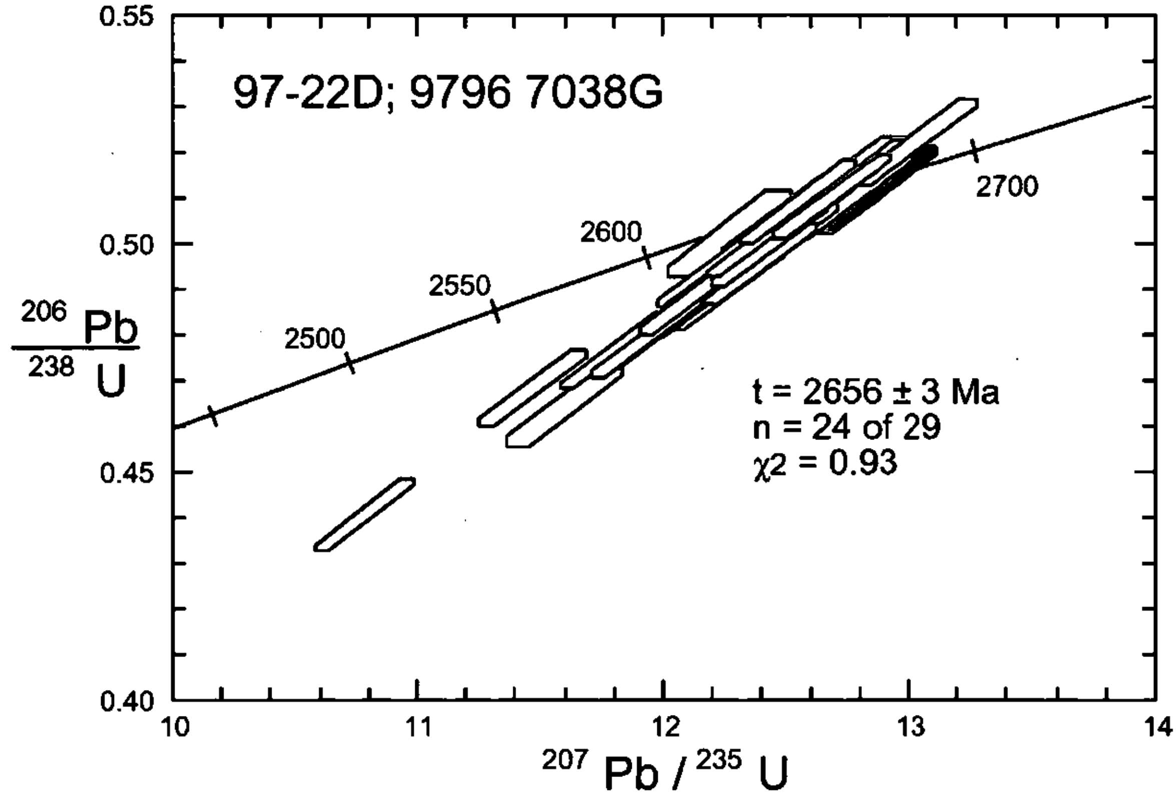

Figure z9796 7038G: Concordia plot of SHRIMP zircon data for the hornblende-biotite granodiorite, Golden Cities Granodiorite (UWA mount 97-22D).

9796 7069A: feldspar porphryry dyke , Sundowner

1:250,000 sheet:	Sir Samuel (SG5113)
AMG:	307195 mE, 6977734 mN
Location:	Sundowner prospect drillhole DDH BWRCD 2996, depth interval 347.80-349.70 m
Province:	Eastern Goldfields
Description:	Thin mafic-feldspar porphyry dyke intrusive into greenstone sequence at the Sundowner prospect north of Bronzewing. Porphyry dykes and mafic-ultramafic greenstone sequence are sheared, veined and hydrothermally altered to chlorite-sericite-bearing assemblages.
Chemical group:	Mafic group, Granny Smith association, Kanowna-Belle clan
Pluton No:	314308
UWA mounts:	A-38D

Description of titanites

The titanites from this sample are all 50-200 μm fragments of larger grains. Only rarely do grains show growth surfaces; most surfaces are fractures. Little internal morphology is detectable from SEM images, with faint sector growth zones and twinning just visible in a minority of grains. The grains are dark brown to brown-red to honey brown in colour. Some grains are almost black and have evenly distributed dense and very fine inclusion populations. Isolated inclusions and small and rare, and tend to be within or in close association with fractures. Areas of SHRIMP analysis were in clean parts of the grains, avoiding inclusions and fractures.

Results and interpretation

Twenty analyses were obtained from 19 fragments. Most of the U abundances are low, resulting in significant common Pb corrections and only modest precision in some analyses. However, the age data show a relatively tight group, with most grains being concordant. Omitting five analyses with the highest 4f206 values, including the one significantly discordant analysis (shaded analyses in Figure t9796 7069A), leaves a population with $\chi^2 = 0.52$. The corresponding age of 2644 ± 6 Ma is interpreted to be the magmatic age of the sample.

Table t9796 7069A: SHRIMP titanite data for the Sundowner porphyry dyke (UWA mount A-38D).

grain-spot	U (ppm)	Th (ppm)	4f206 (%)	$^{207}Pb^*/^{206}Pb^*$	$^{208}Pb^*/^{206}Pb^*$	$^{206}Pb^*/^{238}U$	$^{207}Pb^*/^{235}U$	$^{208}Pb^*/^{232}Th$	conc. (%)	$^{207}Pb/^{206}Pb$ age (Ma)
1-1	47	9	1.678	0.1791 ± 19	0.0514 ± 38	0.5005	12.360	0.1431	99	2645 ± 18
2-1	95	18	1.045	0.1781 ± 12	0.0517 ± 22	0.4906	12.049	0.1365	98	2635 ± 11
3-1	225	38	0.405	0.1800 ± 6	0.0512 ± 10	0.4884	12.117	0.1470	97	2652 ± 6
4-1	41	6	1.958	0.1789 ± 23	0.0417 ± 45	0.5044	12.443	0.1367	100	2643 ± 21
5-1	80	11	0.950	0.1794 ± 12	0.0417 ± 23	0.4992	12.351	0.1504	99	2648 ± 12
6-1	85	21	1.084	0.1788 ± 12	0.0728 ± 23	0.4996	12.315	0.1466	99	2641 ± 11
7-1	97	24	1.015	0.1779 ± 12	0.0697 ± 22	0.4910	12.046	0.1411	98	2634 ± 11
8-1	111	28	0.807	0.1790 ± 11	0.0741 ± 21	0.4941	12.199	0.1436	98	2644 ± 11
11-1	47	8	1.629	0.1782 ± 19	0.0504 ± 37	0.5129	12.600	0.1499	101	2636 ± 17
13-1	48	10	1.714	0.1800 ± 20	0.0570 ± 39	0.4969	12.333	0.1363	98	2653 ± 18
14-1	46	10	1.676	0.1793 ± 19	0.0592 ± 38	0.5090	12.583	0.1436	100	2646 ± 18
14-2	56	11	1.481	0.1779 ± 17	0.0545 ± 34	0.4958	12.162	0.1385	99	2633 ± 16
15-1	188	41	0.568	0.1786 ± 7	0.0621 ± 12	0.4962	12.219	0.1418	98	2640 ± 6
16-1	383	40	0.357	0.1793 ± 4	0.0304 ± 7	0.4952	12.242	0.1433	98	2646 ± 4
17-1	54	11	1.608	0.1780 ± 18	0.0577 ± 35	0.4970	12.195	0.1408	99	2634 ± 16
Discordant or f206>2%.										
9-1	31	12	3.412	0.1811 ± 33	0.1148 ± 69	0.4884	12.193	0.1442	96	2663 ± 30
10-1	31	8	2.836	0.1740 ± 29	0.0667 ± 60	0.4941	11.856	0.1248	100	2597 ± 28
12-1	46	16	2.754	0.1771 ± 31	0.0891 ± 65	0.4626	11.293	0.1210	93	2626 ± 29
18-1	39	8	2.605	0.1764 ± 25	0.0504 ± 51	0.4952	12.044	0.1189	99	2619 ± 24
19-1	40	9	2.260	0.1759 ± 24	0.0606 ± 49	0.5024	12.183	0.1310	100	2614 ± 22

Data 22/7/00.
U/Pb scatter (1σ) for Khan standard = 1.05% (n = 12).
Common-Pb corrected using Cumming & Richards (1975) Model III @ 2630 Ma.

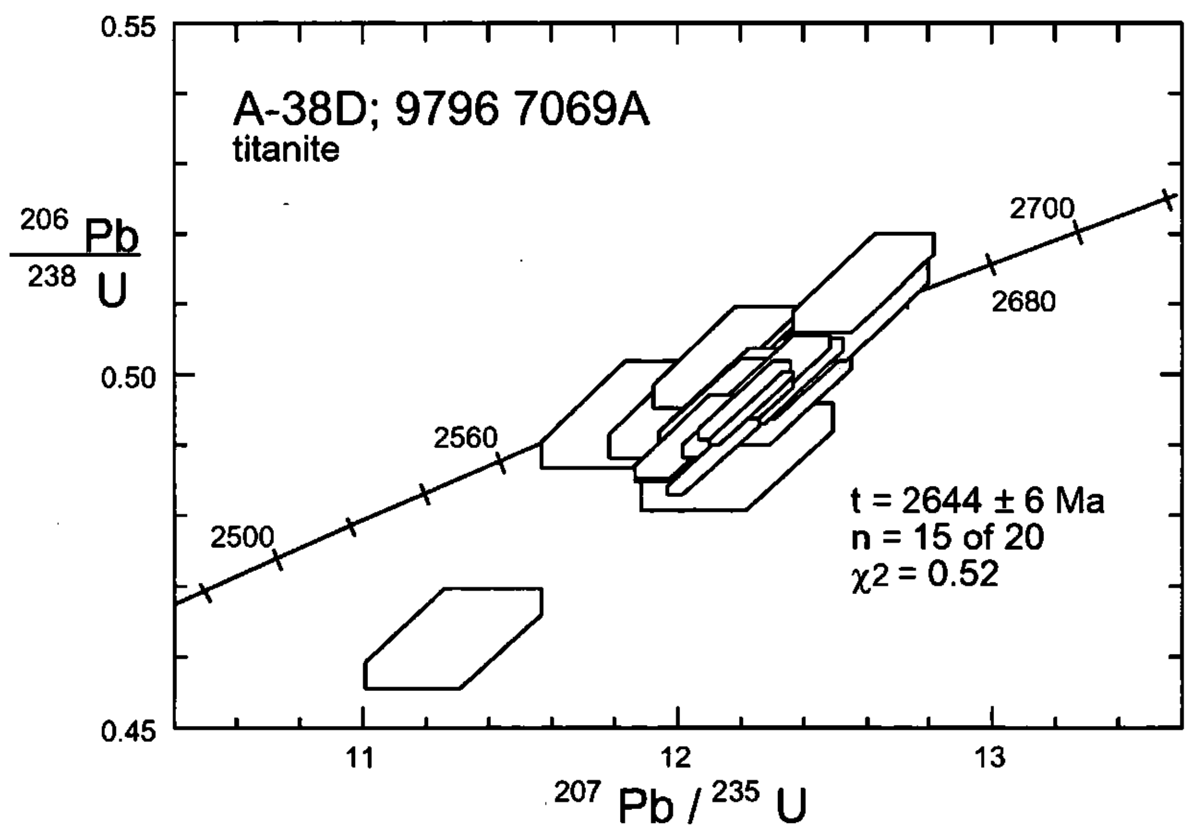

Figure t9796 7069A. Concordia plot showing all SHRIMP titanite data for the Sundowner porphyry dyke (UWA mount A-38D).

9796 7069B: biotite monzogranite, Gemchapps

1:250,000 sheet:	Sir Samuel (SG5113)
AMG:	307195 mE, 6977734 mN
Location:	Sundowner prospect drillhole DDH BWRCD 2996, depth interval 522.00-524.20 m
Province:	Eastern Goldfields
Description:	Variably deformed and altered seriate medium-grained biotite monzogranite that forms the footwall granitoid to the Sundowner Prospect. Footwall granite is sheared and veined (quartz-chlorite-carbonate-sericite) with accompanying wallrock alteration (mainly sericite-carbonate-albite). Minor hematite alteration surrounding some veins and alteration zones.
Chemical group:	High-HFSE group, Kookynie association, Satisfaction clan
Pluton No:	304301
UWA mounts:	A-38B

Description of titanites

The titanites from this sample are 100-250 μm fragments of larger grains. Only rarely do grains show growth surfaces; most surfaces are fractures. Little internal morphology is detectable from SEM images, with faint sector growth zones and twinning just visible in a minority of grains. The grains are dark brown to brown-red to pale brown in colour. Some grains are almost black and have evenly distributed dense inclusion populations. Isolated inclusions and small and rare, and tend to be within or in close association with fractures. Areas of SHRIMP analysis were in clean parts of the grains, avoiding inclusions and fractures.

Results and interpretation

Twenty three analyses were obtained from 23 fragments. Although the U abundances are all <100 ppm, the common Pb corrections are all quite modest. The age data show a relatively tight group, with all grains being concordant. One sample (#21-1, shaded in Fig. t9796 7069B) is a statistical outlier; this has been omitted from the age calculation although there is no apparent reason for the difference. The remaining 22 analyses form a single age population with $\chi^2 = 0.88$. The corresponding age of 2608 ± 10 Ma is interpreted to be the magmatic age of the sample.

Table t9796 7069B SHRIMP titanite data for the Gemchapps monzogranite (UWA mount A-38B).

grain-spot	U (ppm)	Th (ppm)	4f206 (%)	$^{207}Pb^*/^{206}Pb^*$	$^{208}Pb^*/^{206}Pb^*$	$^{206}Pb^*/^{238}U$	$^{207}Pb^*/^{235}U$	$^{208}Pb^*/^{232}Th$	conc. (%)	$^{207}Pb/^{206}Pb$ age (Ma)
1-1	68	15	0.374	0.1761 ± 15	0.0648 ± 24	0.5044	12.245	0.1503	101	2616 ± 14
2-1	41	9	0.534	0.1759 ± 20	0.0647 ± 34	0.4911	11.913	0.1442	98	2615 ± 19
3-1	30	6	0.765	0.1753 ± 29	0.0582 ± 57	0.5048	12.204	0.1444	101	2609 ± 28
4-1	29	10	0.860	0.1769 ± 28	0.0904 ± 56	0.5070	12.371	0.1375	101	2624 ± 27
5-1	30	19	1.433	0.1730 ± 30	0.1573 ± 62	0.5062	12.073	0.1296	102	2587 ± 29
6-1	39	9	0.488	0.1792 ± 23	0.0672 ± 39	0.4920	12.157	0.1448	97	2646 ± 21
7-1	52	19	0.763	0.1739 ± 20	0.1029 ± 38	0.5038	12.077	0.1390	101	2595 ± 19
8-1	30	8	1.224	0.1753 ± 30	0.0635 ± 59	0.5094	12.310	0.1282	102	2609 ± 29
9-1	37	10	0.790	0.1746 ± 24	0.0798 ± 45	0.5068	12.199	0.1446	102	2602 ± 23
10-1	48	13	1.010	0.1719 ± 23	0.0665 ± 44	0.5065	12.008	0.1266	103	2577 ± 22
11-1	28	6	1.321	0.1719 ± 31	0.0460 ± 62	0.4868	11.536	0.1117	99	2576 ± 31
12-1	25	6	1.480	0.1716 ± 35	0.0521 ± 70	0.4986	11.801	0.1197	101	2574 ± 34
13-1	36	11	0.737	0.1759 ± 22	0.0816 ± 40	0.5010	12.152	0.1410	100	2615 ± 21
14-1	29	8	1.675	0.1691 ± 38	0.0696 ± 78	0.5004	11.668	0.1197	103	2549 ± 38
15-1	28	7	1.250	0.1746 ± 30	0.0712 ± 59	0.5004	12.048	0.1456	101	2602 ± 29
16-1	36	7	0.871	0.1755 ± 26	0.0533 ± 48	0.4977	12.042	0.1335	100	2611 ± 24
17-1	69	18	0.536	0.1743 ± 15	0.0750 ± 26	0.4957	11.916	0.1392	100	2600 ± 14
18-1	35	12	0.753	0.1792 ± 23	0.1001 ± 43	0.5040	12.453	0.1505	99	2646 ± 21
19-1	49	11	0.713	0.1763 ± 20	0.0663 ± 37	0.5031	12.232	0.1478	100	2619 ± 19
20-1	29	7	0.893	0.1788 ± 30	0.0756 ± 59	0.4800	11.835	0.1452	96	2642 ± 28
22-1	39	13	1.074	0.1721 ± 25	0.0919 ± 50	0.4983	11.825	0.1390	101	2578 ± 25
23-1	29	10	1.059	0.1773 ± 28	0.1086 ± 54	0.5083	12.425	0.1536	101	2628 ± 26
Possible old outlier.										
21-1	46	5	0.180	0.1810 ± 19	0.0436 ± 31	0.4897	12.218	0.1855	97	2662 ± 18

Data 22/7/00.
U/Pb scatter (1σ) for Khan standard = 1.05% (n = 12).
Common-Pb corrected using Cumming & Richards (1975) Model III @ 2600 Ma.

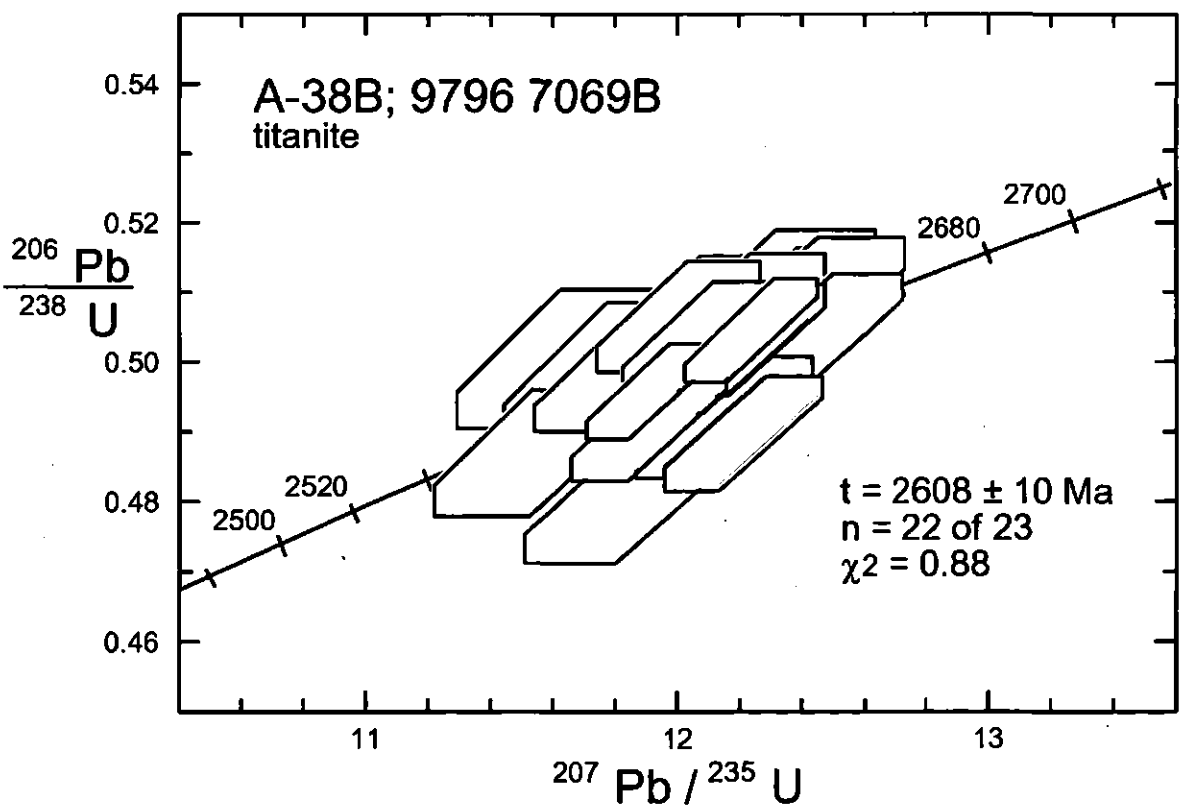

Figure t9796 7069B Concordia plot showing all SHRIMP titanite data for the Gemchapps monzogranite (UWA mount A-38B).

9796 7150: K-feldspar porphyritic biotite-hornblende granite, Yardilla

1:250,000 sheet:	Widgiemooltha (SH5114)
AMG:	457380.9 mE, 6479579.1 mN
Location:	Yardilla granite, part of regional extensive granitoid south of Mt Belches metasedimentary domain; sample drilled from large outcrop
Province:	Eastern Goldfields
Description:	Moderately to locally strongly K-feldspar porphyritic medium-grained hornblende-biotite granite. Minor aplite and pegmatite and thin shear zones (<50 cm). Granitoid contains weak fabric.
Chemical group:	Syenite group, Gilgarna association, Erayinia clan
Pluton No:	343401
UWA mounts:	98-76A

Description of titanites

The titanites from this sample are all 50->200 μm fragments of larger grains. Only rarely do grains show growth surfaces; most surfaces are fractures. Little internal morphology is detectable from SEM images, with faint euhedral growth zoning visible in a few grains. The grains are dark brown to brown-red to honey brown in colour. Some very dark grains have evenly distributed dense and very fine inclusion populations, sometimes highlighting euhedral growth zoning. Isolated inclusions and small and rare. Areas of SHRIMP analysis were in clean parts of the grains, avoiding inclusions and fractures.

Results and interpretation

Thirty analyses were obtained from 30 fragments. The U abundances are all <100 ppm and the common Pb corrections are all significant, most being in the range 1%–4%. The lack of correlation between 4f206 and corrected $^{207}Pb/^{206}Pb$ is taken as evidence that the common Pb composition used in making the corrections is appropriate. One sample (#26-1, shaded in Fig. t9796 7150) has 4f206 ~7%; this has been omitted from the age calculation. The remaining data show a tight grouping in both $^{207}Pb/^{206}Pb$ and Pb/U, which is taken as evidence that these data are concordant. The remaining 29 analyses form a single age population with $\chi^2 = 0.95$. The corresponding age of 2645 ± 12 Ma is interpreted to be the magmatic age of the sample.

Table t9796 7150. SHRIMP titanite data for the Yardilla biotite-hornblende granite (UWA mount 98-76A).

grain-spot	U (ppm)	Th# (ppm)	4f206 (%)	$^{207}Pb^*/^{206}Pb^*$	$^{208}Pb^*/^{206}Pb^*$	$^{206}Pb^*/^{238}U$	$^{207}Pb^*/^{235}U$	#	conc. (%)	$^{207}Pb/^{206}Pb$ age (Ma)
Main group.										
1-1	36	113	2.898	0.1788 ± 36	0.9529 ±111	0.4966	12.242		98	2642 ± 34
2-1	41	118	2.130	0.1807 ± 29	0.9005 ± 92	0.4739	11.805		94	2659 ± 27
3-1	31	91	2.377	0.1854 ± 36	0.8993 ±110	0.5124	13.100		99	2702 ± 32
4-1	32	97	2.593	0.1810 ± 36	0.9601 ±112	0.5355	13.366		104	2662 ± 33
5-1	40	109	3.157	0.1759 ± 34	0.8201 ± 98	0.5126	12.431		102	2615 ± 32
6-1	39	110	3.225	0.1738 ± 35	0.8376 ±101	0.4978	11.926		100	2594 ± 33
7-1	33	112	2.441	0.1842 ± 33	0.9902 ±105	0.5176	13.150		100	2691 ± 29
8-1	32	95	2.909	0.1790 ± 35	0.9056 ±105	0.5168	12.752		102	2643 ± 32
9-1	31	100	4.098	0.1795 ± 41	0.9879 ±122	0.5171	12.801		101	2649 ± 38
10-1	28	87	2.992	0.1795 ± 37	0.9007 ±110	0.5061	12.528		100	2649 ± 34
11-1	31	87	3.380	0.1798 ± 37	0.8749 ±108	0.4999	12.394		99	2651 ± 34
12-1	29	91	3.172	0.1752 ± 39	0.9026 ±116	0.5126	12.385		102	2608 ± 37
13-1	29	89	2.776	0.1816 ± 37	0.9583 ±114	0.5179	12.968		101	2667 ± 34
14-1	30	94	2.791	0.1801 ± 37	0.9456 ±113	0.4964	12.328		98	2654 ± 34
15-1	32	101	3.746	0.1758 ± 42	0.9701 ±124	0.4898	11.870		98	2613 ± 40
16-1	31	86	2.275	0.1832 ± 32	0.8173 ± 97	0.5331	13.465		103	2682 ± 29
17-1	28	87	3.073	0.1781 ± 38	0.9222 ±113	0.5105	12.537		101	2636 ± 35
18-1	29	87	2.964	0.1779 ± 39	0.8798 ±114	0.5166	12.674		102	2634 ± 36
19-1	25	87	3.446	0.1843 ± 45	1.0373 ±137	0.4985	12.665		97	2692 ± 40
20-1	33	105	2.867	0.1787 ± 37	0.9386 ±113	0.5305	13.072		104	2641 ± 35
21-1	40	161	2.344	0.1779 ± 30	1.2559 ±108	0.5070	12.434		100	2633 ± 28
22-1	27	81	2.944	0.1782 ± 38	0.8818 ±112	0.5096	12.519		101	2636 ± 35
23-1	27	81	2.485	0.1834 ± 36	0.9007 ±110	0.5023	12.703		98	2684 ± 33
24-1	27	83	3.042	0.1779 ± 37	0.9025 ±112	0.5078	12.452		101	2633 ± 35
25-1	40	137	2.649	0.1768 ± 30	1.0288 ± 97	0.5033	12.271		100	2623 ± 28
27-1	74	178	1.496	0.1746 ± 18	0.7204 ± 56	0.5017	12.080		101	2603 ± 17
28-1	30	87	2.571	0.1800 ± 38	0.8730 ±115	0.5092	12.638		100	2653 ± 35
29-1	37	91	2.313	0.1860 ± 31	0.7574 ± 91	0.5109	13.099		98	2707 ± 28
30-1	43	175	2.351	0.1791 ± 27	1.2235 ± 97	0.5114	12.627		101	2645 ± 25
4f206>5%.										
26-1	18	13	6.847	0.1647 ± 76	0.1934 ±172	0.5004	11.363		104	2504 ± 77

Data 11/5/99.
U/Pb scatter (1σ) for Khan standard = 2.58% (n = 15).
Common-Pb corrected using Cumming & Richards (1975) Model III @ 2650 Ma.
Analysed using NO_2^- primary ion beam.
Pb/U calibration might be slightly disturbed.
Th/U calibration is not reliable; Th abundances are indicative only, and Pb/Th are not reported.

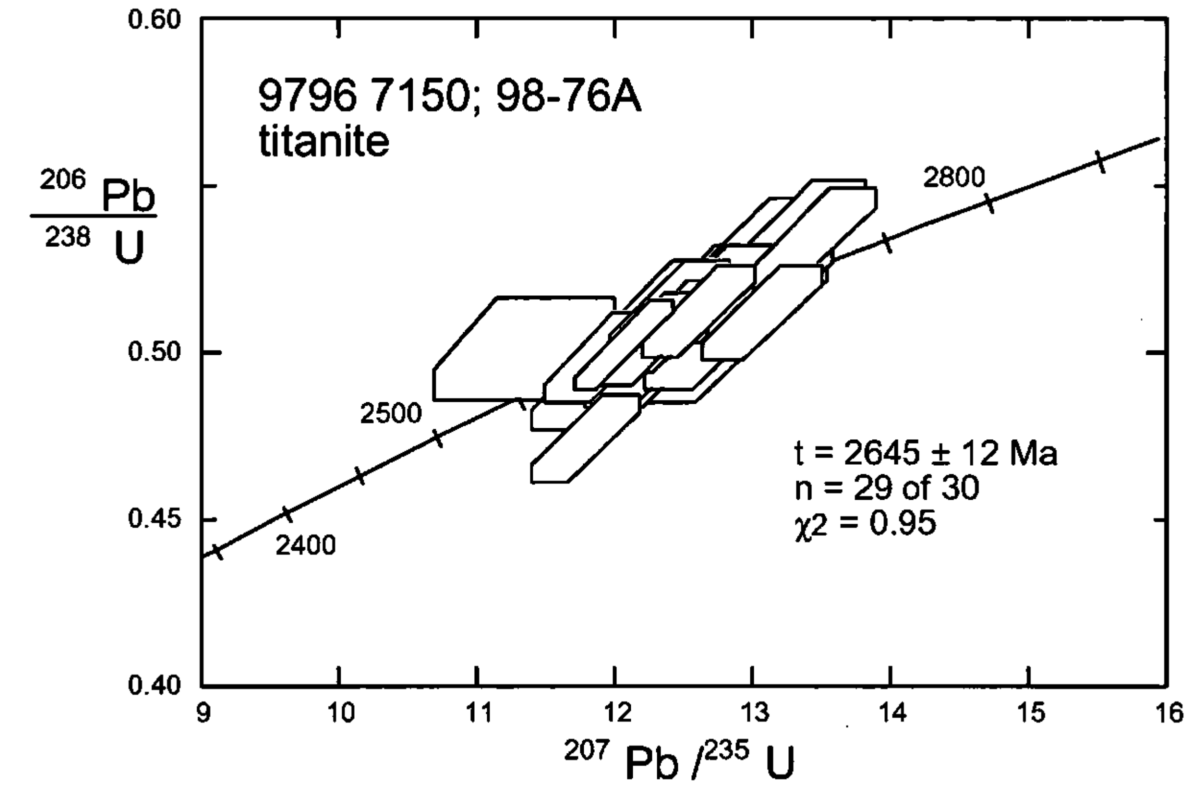

Figure t9796 7150 Concordia plot showing all SHRIMP titanite data for the Yardilla biotite-hornblende granite (UWA mount 98-76A).

9796 7152: K-feldspar porphyritic hornblende-biotite granite, Yardilla

1:250,000 sheet:	Widgiemooltha (SH5114)
AMG:	461195.0 mE, 6498254.1 mN
Location:	Yardilla granite S., part of regional extensive granitoid south of Mt Belches metasedimentary domain; sample drilled from large outcrop
Province:	Eastern Goldfields
Description:	Moderately to locally strongly K-feldspar porphyritic medium-grained hornblende-biotite granite; slight alignment of ferromagnesian minerals forming weak foliation
Chemical group:	Syenite group, Gilgarna association, Erayinia clan
Pluton No:	343401
UWA mounts:	97-43C

Description of zircons

The zircon population in this sample consists of one morphologic type of uniformly fine to medium grains, with most grains being 30-80 μm long and a uniform aspect ration of 2-3:1. Grains are typically subhedral in external morphology with faintly preserved continuous euhedral internal zoning from core to rim. Many grains show patchy annealed areas which overprint the internal euhedral zoning, and pervasive fracture networks which normally indicate high U-contents and metamictisation. Inclusions are not common and consist of opaque or rod-like to equant minerals. All inclusions occur throughout the grains and show no preference for core or rim regions. The grains range from pale brown to dark brown in colour. Strong relict euhedral zoning observed on both optical and SEM images and again suggest high U-Th-contents and radiation damage. The fracture networks and annealling patches were avoided during data collection.

Results and interpretation

Thirteen analyses on 13 grains are presented in Table z9796 7152 and shown on a concordia diagram in Figure z9796 7152. Although the majority of analyses show U contents <300 ppm, there is only a small proportion which are not affected by common Pb contamination or radiogenic Pb loss. The data suggest an age of ~2660 Ma. Further data might improve the age estimate, but a definitive age determination is unlikely.

Table z9796 7152: SHRIMP zircon data for the Yardilla hornblende-biotite granite. (UWA mount 97-43C).

grain-spot	U (ppm)	Th (ppm)	4f206 (%)	$^{207}Pb^*/^{206}Pb^*$	$^{208}Pb^*/^{206}Pb^*$	$^{206}Pb^*/^{238}U$	$^{207}Pb^*/^{235}U$	$^{208}Pb^*/^{232}Th$	conc. (%)	$^{207}Pb/^{206}Pb$ age (Ma)
1-1	145	46	0.061	0.1800 ± 11	0.0855 ± 16	0.4870	12.087	0.1326	96	2653 ± 11
2-1	167	77	0.560	0.1793 ± 13	0.1353 ± 25	0.4890	12.092	0.1428	97	2647 ± 12
3-1	471	400	7.370	0.1663 ± 28	0.1465 ± 62	0.2275	5.216	0.0393	52	2520 ± 28
4-1	55	24	0.220	0.1849 ± 21	0.1167 ± 37	0.5116	13.042	0.1387	99	2697 ± 19
5-1	249	115	0.367	0.1775 ± 10	0.1212 ± 18	0.4697	11.497	0.1238	94	2630 ± 9
7-1	291	96	1.333	0.1721 ± 13	0.0825 ± 26	0.4236	10.051	0.1052	88	2578 ± 13
31-1	123	32	2.767	0.1749 ± 32	0.1023 ± 67	0.4027	9.709	0.1579	84	2605 ± 30
9-1	472	258	9.522	0.1718 ± 35	0.2023 ± 79	0.1989	4.711	0.0736	45	2575 ± 34
10-1	272	132	4.869	0.1703 ± 23	0.1220 ± 51	0.4498	10.562	0.1135	94	2561 ± 23
12-1	193	74	0.239	0.1795 ± 11	0.1044 ± 18	0.4892	12.109	0.1333	97	2648 ± 10
14-1	224	227	3.487	0.1719 ± 25	0.2314 ± 57	0.3344	7.924	0.0764	72	2576 ± 25
15-1	326	246	0.129	0.1807 ± 7	0.2061 ± 14	0.4936	12.297	0.1348	97	2659 ± 7
16-1	222	103	0.852	0.1726 ± 14	0.1437 ± 27	0.4072	9.688	0.1262	85	2583 ± 13

Data from 27/8/98.
U/Pb scatter (1σ) for cz3 standard = 1.78% (n=14).

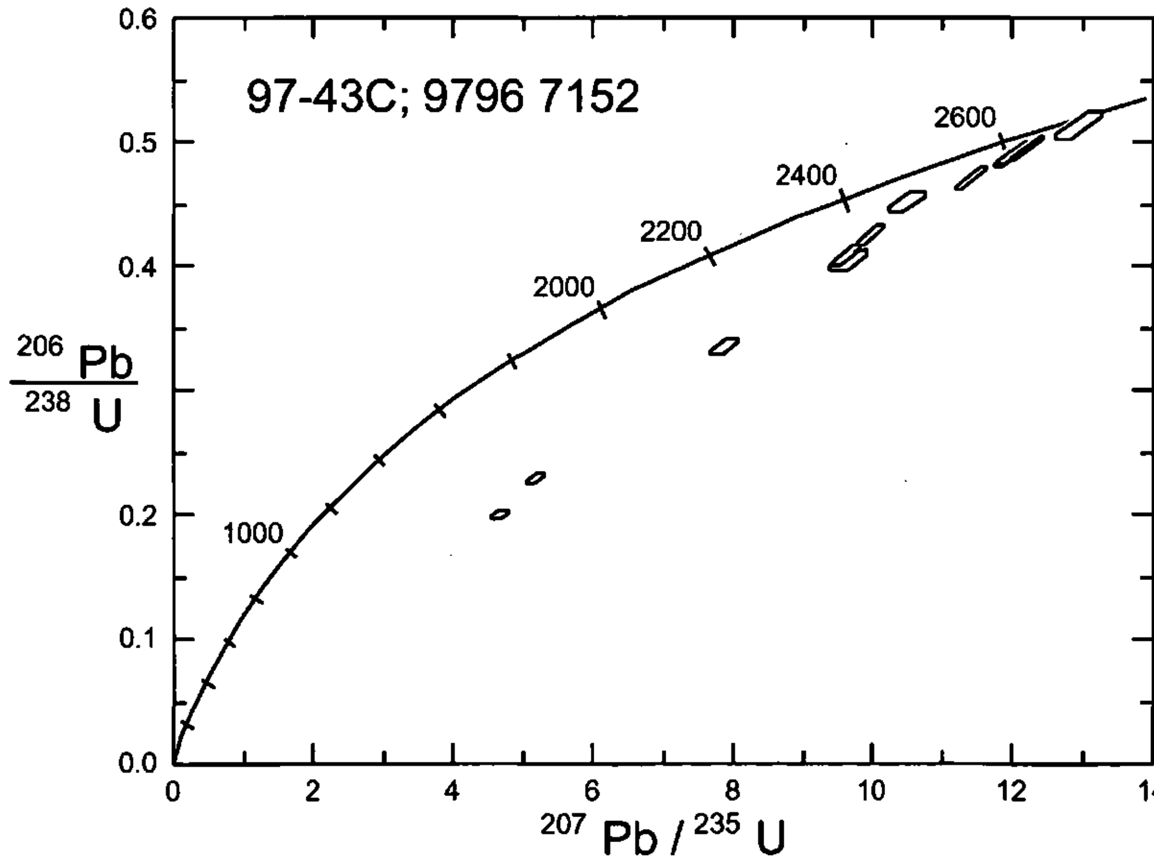

Figure z9796 7152. Concordia plot of SHRIMP zircon data for the Yardilla hornblende-biotite granite (UWA mount 97-43C).

9796 7153: biotite monzogranite, Talbot

1:250,000 sheet:	Widgiemooltha (SH5114)
AMG:	426706.6 mE, 6493675.6 mN
Location:	Talbot Rock, part of regional extensive granitoid south of Lake Cowan; sample drilled from old blast site in large outcrop.
Province:	Eastern Goldfields
Description:	Equigranular to seriate medium-grained biotite monzogranite. This sample is from a complex granite outcrop with at least three granitoid phases. Contains xenoliths/enclaves of foliated feldspar-phyric diorite and dyke-like bodies of fine-medium grained felsic granitoid.
Chemical group:	Low-Ca group, Mt Boreas association, Mungari clan
Pluton No:	333419
UWA mounts:	97-44A

Description of zircons

Sample 9796-9153 contains numerous small grains and fragments (less than 50 µm in size) as well as larger grains (up to 150 µm), present with both euhedral morphologies as well as more rounded external forms. Approximately half of the grains are clear, translucent and light yellow to white in colour, while the others are darker and more opaque. Some inclusions are visible in many grains. The slightly darker grains appear to have internal structures compared to the clearer grains, as seen in the photos, which may account for their more opaque character. The SEM images more clearly documents the internal features of the grains, with systematic zoning visible in some grains while others appear relatively amorphous with thin (1 µm) to thick (10 µm) metamict rims. Some of these grains can be interpreted as having distinct cores although they may not always represent older xenocrystic grains (they may actually represent an early crystallised grain of different chemical composition to the subsequently crystallised rims). Zones and fronts of recrystallisation are apparent in some of the grains.

Results and interpretation

Nineteen analyses on 19 grains are presented in Table z9796 7153 and shown on a concordia diagram in Figure z9796 7153. The data are mostly highly discordant, with both the concordant and discordant analyses giving $^{207}Pb/^{206}Pb$ dates ranging from ~2600 Ma to ~2685 Ma. It seems most likely that the magmatic age of the sample is ~2625 Ma, and that the older grains are xenocryts. However, it is also possible that the ~2685 Ma date is a minimum age for the rock and the data spread is due to a combination of recent and old Pb loss, the latter possibly being due to a resetting event at ~2625 Ma. Additional data and subsequent interpretation may improve the age estimates, but definitive age determinations are unlikely.

Table z9796 7153: SHRIMP zircon data for the biotite monzogranite, Talbot Rock (UWA mount 97-44A).

grain-spot	U (ppm)	Th (ppm)	4f206 (%)	$^{207}Pb^*/^{206}Pb^*$	$^{208}Pb^*/^{206}Pb^*$	$^{206}Pb^*/^{238}U$	$^{207}Pb^*/^{235}U$	$^{208}Pb^*/^{232}Th$	conc. (%)	$^{207}Pb/^{206}Pb$ age (Ma)
1-1	147	90	5.306	0.1741 ± 22	0.1499 ± 48	0.5180	12.437	0.1262	104	2598 ± 21
2-1	67	43	0.040	0.1846 ± 12	0.1743 ± 21	0.5080	12.928	0.1363	98	2694 ± 11
4-1	286	263	7.961	0.1834 ± 27	0.2958 ± 61	0.4026	10.180	0.1293	81	2684 ± 24
7-1	188	112	8.568	0.1855 ± 26	0.2484 ± 58	0.4089	10.457	0.1707	82	2703 ± 23
42-1	624	966	19.079	0.1727 ± 29	0.3066 ± 66	0.2837	6.754	0.0562	62	2584 ± 28
8-1	118	38	5.411	0.1760 ± 28	0.0662 ± 60	0.3960	9.611	0.0814	82	2616 ± 26
9-1	299	298	14.660	0.1767 ± 26	0.3098 ± 60	0.3919	9.551	0.1220	81	2623 ± 25
13-1	751	625	13.300	0.1802 ± 24	0.2739 ± 54	0.2663	6.616	0.0876	57	2655 ± 22
14-1	38	64	15.024	0.1782 ± 56	0.3763 ±128	0.6581	16.166	0.1478	124	2636 ± 52
17-1	547	808	17.961	0.1775 ± 25	0.3609 ± 58	0.3952	9.670	0.0966	82	2629 ± 24
18-1	125	135	0.015	0.1828 ± 8	0.2923 ± 16	0.5145	12.966	0.1388	100	2678 ± 7
20-1	678	592	20.843	0.1694 ± 28	0.4080 ± 65	0.3199	7.472	0.1495	70	2552 ± 28
22-1	142	76	2.623	0.1788 ± 21	0.1699 ± 46	0.4634	11.426	0.1476	93	2642 ± 20
27-1	196	141	8.285	0.1723 ± 25	0.2203 ± 57	0.4936	11.726	0.1513	100	2580 ± 25
30-1	529	662	12.201	0.1783 ± 21	0.2430 ± 47	0.3162	7.772	0.0614	67	2637 ± 19
32-1	718	1423	19.546	0.1773 ± 20	0.3855 ± 45	0.4581	11.200	0.0892	93	2628 ± 18
33-1	727	561	20.093	0.1751 ± 22	0.3748 ± 52	0.3111	7.509	0.1510	67	2607 ± 21
36-1	138	103	5.225	0.1783 ± 24	0.2515 ± 55	0.4469	10.990	0.1515	90	2637 ± 23

Data from 2/3/98.
U/Pb scatter (1σ) for cz3 standard = 1.70% (n=11 of 12).

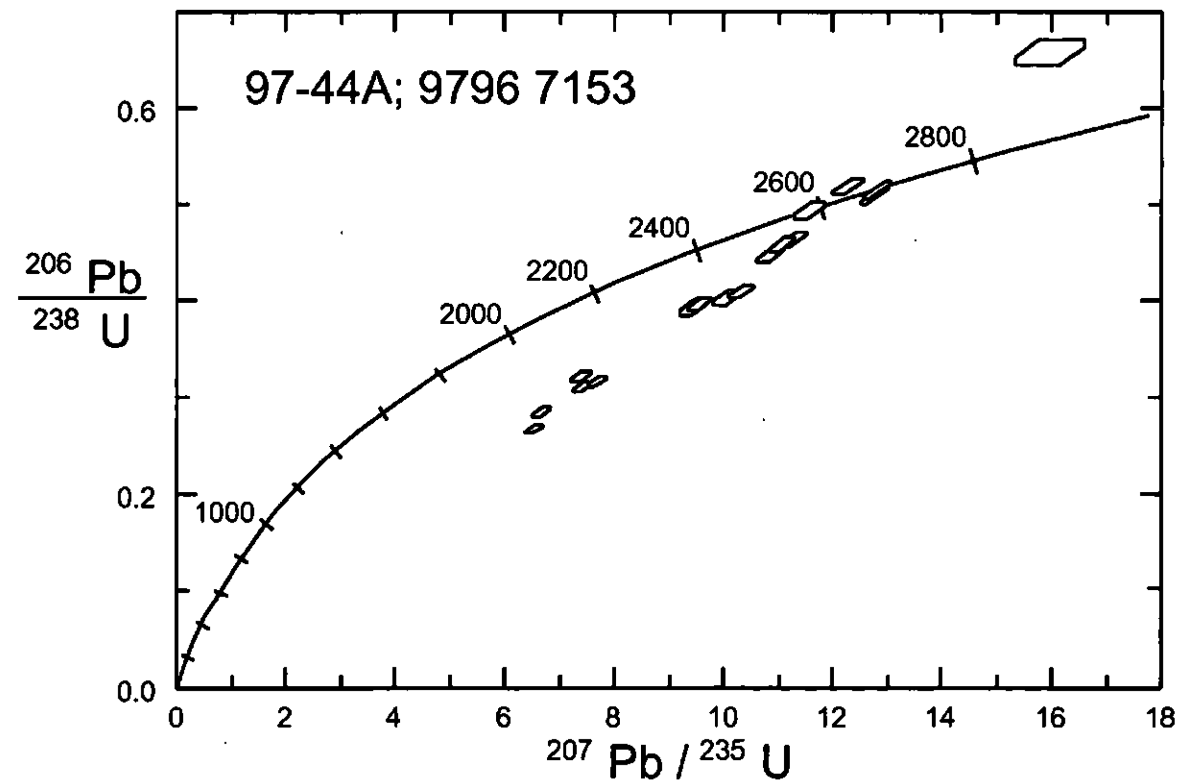

Figure z9796 7153: Concordia plot showing all SHRIMP zircon data for the biotite monzogranite, Talbot Rock (UWA mount 97-44A).

9796 9023: biotite monzogranite, Turturdine

1:250,000 sheet:	Kalgoorlie (SH5109)
AMG:	257561.6 mE, 6632077.4 mN
Location:	This sample was drilled from a 'whaleback' that forms part of Turturdine Rock
Province:	Southern Cross
Description:	Equigranular to sparsely feldspar-phyric biotite monzogranite that forms the major granitic phase at the locality, and contains accessory titanite and allanite. The monzogranite has very minor pegmatite veins.
Chemical group:	Low-Ca group, Beetle association, Beetle clan
Pluton No:	293713
UWA mounts:	97-22C (zircon) and 98-84B and C (titanite)

Description of zircons

The zircon population in this sample consists of two morphologic types of uniformly fine grain size. The first type is the same as for sample 9796 9044, with grains typically euhedral in external morphology, with continuous euhedral internal zoning from core to rim. The second type has a structureless internal morphology (e.g., grains #3, #5, #6, #7) with a euhedral to anhedral external shape. The appearance of both types is somewhat similar to those in sample 9796 9044, with similar discordant alteration patches again suggestive of high U-Th-contents and corresponding radiation damage to the zircon structure.

Description of titanites

The titanites from this sample are typically ~100 µm fragments of larger grains. Only rarely do grains show growth surfaces; most surfaces are fractures. Little internal morphology is detectable from SEM images, with faint euhedral growth zones just visible in a minority of grains. The grains are black to dark brown and rarely to pale brown in colour. Some grains are almost black and have evenly distributed dense inclusion populations. Isolated inclusions and rare, and tend to be within or in close association with fractures. Areas of SHRIMP analysis were in clean parts of the grains, avoiding inclusions and fractures where possible.

Results and interpretation

Zircon

Ten analyses on 10 zircon grains are presented in Table z9796 9023. Further analysis on this sample was terminated after it became apparent that the best grains gave unsatisfactory age data. The zircons have very high U-contents (up to 1.5% U) and gave scattered and discordant age data. The U-contents for all analyses, except one, are >300 and essentially do not allow a reliable age estimate to be made. This can also be seen in the high common Pb contents which also reflects radiation damage of the zircon structure.

Titanite

Thirteen analyses on 10 titanite fragments (Table t9796 9023) were also found to be unsatisfactory for dating, primarily because of low U contents.

Table z9796 9023: SHRIMP zircon data for the biotite monzogranite, Turturdine Rock (UWA mount 97-22C).

grain-spot	U (ppm)	Th (ppm)	4f206 (%)	$^{207}Pb^*/^{206}Pb^*$	$^{208}Pb^*/^{206}Pb^*$	$^{206}Pb^*/^{238}U$	$^{207}Pb^*/^{235}U$	$^{208}Pb^*/^{232}Th$	conc. (%)	$^{207}Pb/^{206}Pb$ age (Ma)
1-1	14059	6165	3.440	0.1523 ± 2	0.1218 ± 4	0.5194	10.907	0.1442	114	2372 ± 2
2-1	6025	2121	2.430	0.1293 ± 5	0.1148 ± 11	0.3515	6.267	0.1146	93	2089 ± 7
3-1	14939	7943	0.611	0.1409 ± 3	0.1415 ± 5	0.4841	9.402	0.1288	114	2238 ± 3
7-1	126	240	4.511	0.1746 ± 31	0.5784 ± 76	0.4089	9.842	0.1236	85	2602 ± 30
9-1	634	331	4.071	0.1770 ± 13	0.1845 ± 28	0.5896	14.387	0.2083	114	2625 ± 12
4f206>5%										
4-1	2297	1859	23.368	0.1682 ± 27	0.4384 ± 63	0.1498	3.473	0.0812	35	2539 ± 27
5-1	354	216	6.578	0.1756 ± 25	0.2327 ± 55	0.3210	7.771	0.1224	69	2612 ± 23
6-1	2606	2993	25.895	0.1764 ± 24	0.5422 ± 56	0.2297	5.587	0.1085	51	2619 ± 23
8-1	627	1224	19.903	0.1729 ± 40	0.5026 ± 94	0.2232	5.321	0.0575	50	2586 ± 39
10-1	385	893	18.684	0.1819 ± 40	0.4270 ± 92	0.3993	10.016	0.0734	81	2670 ± 36

Data 22/8/97.
U/Pb scatter (1σ) for cz3 standard = 2.83% (n=4).

Table t9796 9023: SHRIMP titanite data for the biotite monzogranite, Turturdine Rock (UWA mount 98-84B,C).

grain-spot	U (ppm)	Th# (ppm)	4f206 (%)	$^{207}Pb^*/^{206}Pb^*$	$^{208}Pb^*/^{206}Pb^*$	$^{206}Pb^*/^{238}U$	$^{207}Pb^*/^{235}U$	#	conc. (%)	$^{207}Pb/^{206}Pb$ age (Ma)
98-84B; 9796 9023 non-mag.										
1-1	13	<1	1.274	0.1677 ± 75		0.5358	12.386		109	2534 ± 75
10-1	10	1	2.394	0.1635 ± 74	0.0767 ±156	0.4883	11.007		103	2492 ± 76
3-1	59	17	2.190	0.1689 ± 57	0.0639 ±120	0.5522	12.861		111	2547 ± 57
8-1	16	1	3.330	0.1645 ± 65	0.0128 ±138	0.4776	10.834		101	2503 ± 67
9-1	32	<1	1.172	0.1798 ± 50		0.5721	14.186		110	2651 ± 46
4f206>4%										
1-2	12	4	18.326	0.1645 ±166	0.3304 ±376	1.0512	23.840		185	2502 ±171
19-1	10	1	7.632	0.1846 ±117	0.1091 ±255	0.5672	14.438		107	2695 ±105
5-1	15	0	4.863	0.1866 ± 92	0.0554 ±196	0.5015	12.903		97	2712 ± 81
7-1	25	8	11.703	0.1873 ±123	0.2211 ±272	0.6338	16.368		116	2719 ±108
98-84C; 9796 9023 mag III.										
1-1	42	15	0.982	0.1735 ± 34	0.1012 ± 67	0.5307	12.692		106	2591 ± 32
1-2	79	22	1.275	0.1725 ± 30	0.0783 ± 59	0.5483	13.045		109	2582 ± 29
2-1	45	15	3.064	0.1634 ± 66	0.0650 ±140	0.5348	12.048		111	2491 ± 68
2-2	54	20	1.936	0.1761 ± 63	0.1177 ±134	0.5428	13.181		107	2617 ± 60

Data 5/5/99. Data are not reported for spots with U<10 ppm.
U/Pb scatter (1σ) for Khan standard = 2.53% (n = 14).
Common-Pb corrected using Cumming & Richards (1975) Model III @ 2650 Ma.
Analysed using NO_2^- primary ion beam.
Pb/U calibration might be slightly disturbed.
Th/U calibration is not reliable; Th abundances are indicative only, and Pb/Th are not reported.

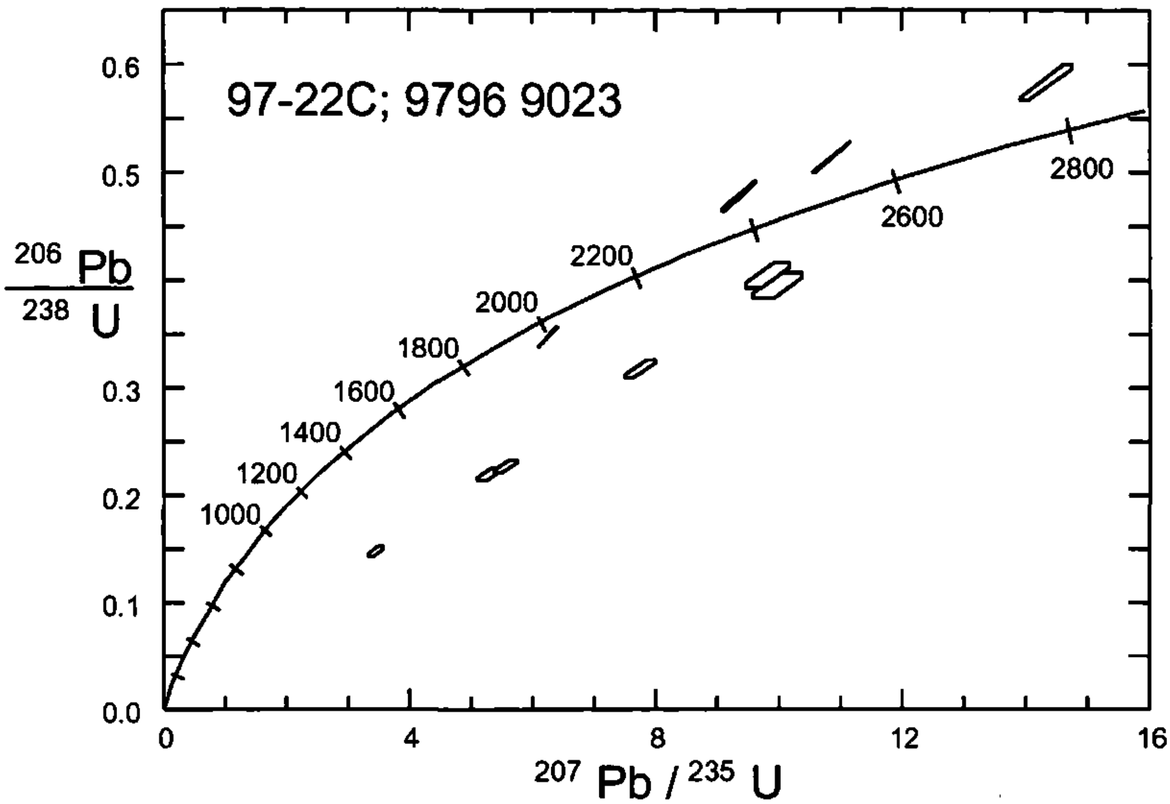

Figure z9796 9023: Concordia plot showing all SHRIMP zircon data for the biotite monzogranite, Turturdine Rock (UWA mount 97-22C).

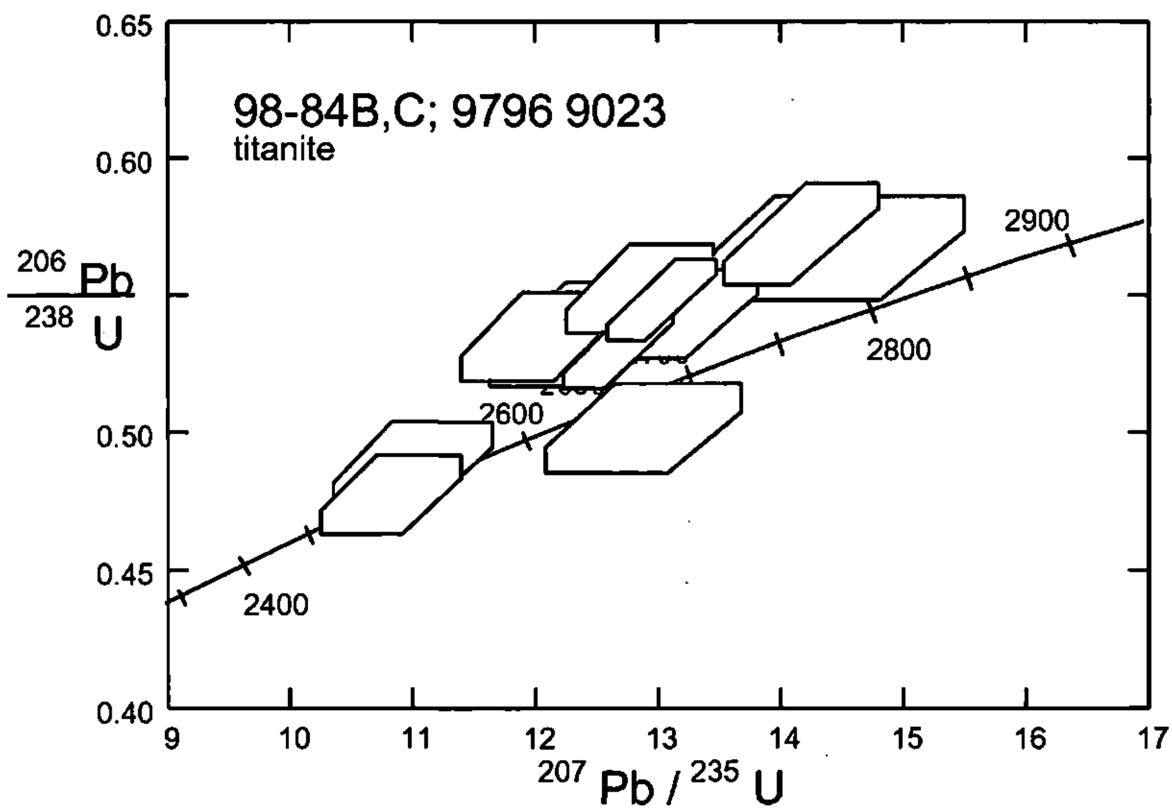

Figure t9796 9023: Concordia plot of SHRIMP titanite data for the biotite monzogranite, Turturdine Rock (UWA mount 98-84B,C). Data with 4f206>10% are not plotted.

9796 9034: porphyritic biotite monzogranite, Yerdanie

1:250,000 sheet:	Boorabbin (SH5113)
AMG:	274137.4 mE, 6547216.2 mN
Location:	The sample was drilled from the east side of Yerdanie Rock
Province:	Southern Cross
Description:	Variably K-feldspar porphyritic medium-coarse grained biotite monzogranite that contains abundant pegmatite veins and dykes, ovoid biotite-rich granitic enclaves and biotite-rich schlieren. This granitoid phase intrudes a medium-grained biotite granodiorite
Chemical group:	Low-Ca group, Beetle association, Beetle clan
Pluton No:	303505
UWA mounts:	97-23C (zircon) and 98-84D (titanite)

Description of zircons

The zircon population in this sample consists of one morphologic type of variable grain size. Many grains have an aspect ratio of about 4-5 and are similar to zircons in sample 9796 9082A. Grains are typically euhedral in external morphology with the majority showing continuous euhedral internal zoning from core to rim. Some grains have structureless cores. Inclusions are not common and consist of opaque or rod-like to equant minerals. All inclusions occur throughout the grains and show no preference for core or rim regions. The grains are generally medium to dark brown in colour. Rare discordant alteration patches are visible on SEM images, particularly as a thin discontinuous outer rim and along some cracks in a minority of grains: these were avoided during analyses.

Description of titanites

Only small quantities of titanite were recovered from this sample. It is all in the form of 30-80 μm fragments of larger grains. Only rarely do grains show growth surfaces; most surfaces are fractures. Little internal morphology is detectable from SEM images, with faint euhedral alteration patches and growth zones visible in a couple of grains. The grains are black to dark brown in colour. Inclusions are rare. Areas of SHRIMP analysis were in clean parts of the grains, avoiding inclusions and fractures where possible.

Results and interpretation

Zircon

Thirty analyses on 30 zircon are presented in Table z9796 9034 and shown in Figures z9796 9034a, b. The common Pb corrections were mostly low, although about two-thirds of the analyses have >400 ppm U and half the analyses have >1000 ppm U. Almost all the data is discordant and show a large range in their $^{207}Pb/^{206}Pb$ ages. The strong reverse discordance of some data probably results from extreme metamictisation of those grains. The most concordant analyses are also variable in age and, given the high U-contents, it is likely that many of the analyses represent minimum ages for the analysed grains due to old Pb-loss. If the grains represent a single genetic population, as suggested by their similar internal and external morphology, their minimum age can be estimated from the oldest concordant group to be ~2700 Ma (Fig. z9796 9034a). Amongst this data cluster, only the two oldest (shaded in Fig. z9796 9034b) have ages within analytical uncertainty of each other, and give a pooled age of 2706±7 Ma. As with sample 9796 8153, this could be taken as the minimum emplacement age of the granitoid, but it seems more likely that all most of these grains are xenocrysts in a rock with a magmatic age ~2630 Ma. Neither the appearance of the grains nor the structure of the data set provides a strong distinction between the two possibilities.

Titanite

Only preliminary analyses were performed, to assess the small quantity of titanite that was obtained from the sample. Results (not tabulated) suggest that dating might be possible, and that the titanite date probably corresponds to the younger of the possible interpretations of the zircon data.

Table z9796 9034: SHRIMP zircon data for the porphyritic biotite monzogranite, Yerdanie Rock (UWA mount 97-23C).

grain-spot	U (ppm)	Th (ppm)	4f206 (%)	$^{207}Pb^*/^{206}Pb^*$	$^{208}Pb^*/^{206}Pb^*$	$^{206}Pb^*/^{238}U$	$^{207}Pb^*/^{235}U$	$^{208}Pb^*/^{232}Th$	conc. (%)	$^{207}Pb/^{206}Pb$ age (Ma)
1-1	1383	642	1.765	0.1620 ± 4	0.5031 ± 9	0.7664	17.115	0.8301	148	2476 ± 4
2-1	1693	361	0.417	0.1765 ± 3	0.0618 ± 5	0.5056	12.304	0.1463	101	2620 ± 3
3-1	1129	2394	6.123	0.1752 ± 8	0.8028 ± 20	0.7326	17.693	0.2774	136	2608 ± 7
4-1	280	413	1.951	0.1786 ± 13	0.4916 ± 31	0.4928	12.131	0.1638	98	2639 ± 12
5-1	947	584	0.369	0.1633 ± 6	0.1332 ± 11	0.2894	6.516	0.0625	66	2490 ± 6
6-1	295	295	3.889	0.1769 ± 16	0.5946 ± 40	0.3548	8.654	0.2107	75	2624 ± 15
7-1	275	127	0.127	0.1816 ± 6	0.1053 ± 9	0.4986	12.483	0.1134	98	2668 ± 5
8-1	192	254	0.010	0.1812 ± 7	0.3606 ± 15	0.5027	12.557	0.1368	99	2663 ± 6
9-1	919	991	0.116	0.1733 ± 3	0.3031 ± 7	0.4654	11.121	0.1308	95	2590 ± 3
10-1	190	325	1.647	0.1805 ± 13	0.6364 ± 35	0.3981	9.907	0.1480	81	2657 ± 12
11-1	124	218	0.072	0.1794 ± 8	0.4932 ± 23	0.4992	12.348	0.1399	99	2647 ± 8
12-1	185	238	0.366	0.1794 ± 9	0.4226 ± 22	0.4599	11.377	0.1510	92	2647 ± 8
13-1	2654	1818	0.698	0.1678 ± 2	0.6015 ± 6	0.7643	17.684	0.6712	144	2536 ± 2
14-1	3468	2451	0.018	0.1444 ± 1	0.1929 ± 3	0.4042	8.046	0.1103	96	2280 ± 2
15-1	3340	471	0.030	0.1859 ± 1	0.0393 ± 1	0.5362	13.742	0.1494	102	2706 ± 1
16-1	1439	648	0.265	0.1773 ± 3	0.1305 ± 5	0.4551	11.127	0.1317	92	2628 ± 3
17-1	1462	1656	0.441	0.1619 ± 3	0.3170 ± 7	0.4131	9.222	0.1156	90	2476 ± 3
18-1	255	150	0.044	0.1838 ± 6	0.1702 ± 10	0.4795	12.153	0.1389	94	2688 ± 6
19-1	1327	57	0.015	0.1794 ± 2	0.0113 ± 1	0.4940	12.222	0.1311	98	2648 ± 2
20-1	1399	1195	0.074	0.1842 ± 2	0.2119 ± 4	0.5310	13.483	0.1318	102	2691 ± 2
21-1	1099	511	0.262	0.1794 ± 3	0.0946 ± 5	0.4752	11.753	0.0966	95	2647 ± 3
22-1	2001	3247	0.032	0.1844 ± 2	0.4142 ± 5	0.5258	13.370	0.1342	101	2693 ± 2
23-1	1908	2488	3.802	0.1673 ± 5	0.7028 ± 12	0.7700	17.766	0.4149	145	2531 ± 5
24-1	6087	1537	0.012	0.1787 ± 1	0.0955 ± 1	0.5970	14.714	0.2259	114	2641 ± 1
25-1	2214	831	0.011	0.1795 ± 2	0.1099 ± 3	0.5340	13.217	0.1563	104	2648 ± 2
26-1	335	342	0.102	0.1861 ± 8	0.2679 ± 15	0.5327	13.667	0.1398	102	2708 ± 7
27-1	321	506	2.054	0.1777 ± 12	0.5318 ± 30	0.5406	13.246	0.1821	106	2632 ± 11
28-1	372	1014	0.088	0.1799 ± 6	0.7471 ± 22	0.4839	12.001	0.1325	96	2652 ± 6
29-1	1208	778	0.171	0.1772 ± 4	0.1837 ± 6	0.4776	11.667	0.1362	96	2627 ± 3
30-1	725	1255	0.153	0.1790 ± 5	0.4934 ± 13	0.4767	11.763	0.1358	95	2643 ± 5

Data 13/8/97 and 19/8/97.
U/Pb scatter (1σ) for cz3 standard = 1.40% (n = 10) and 1.27% (n=11).

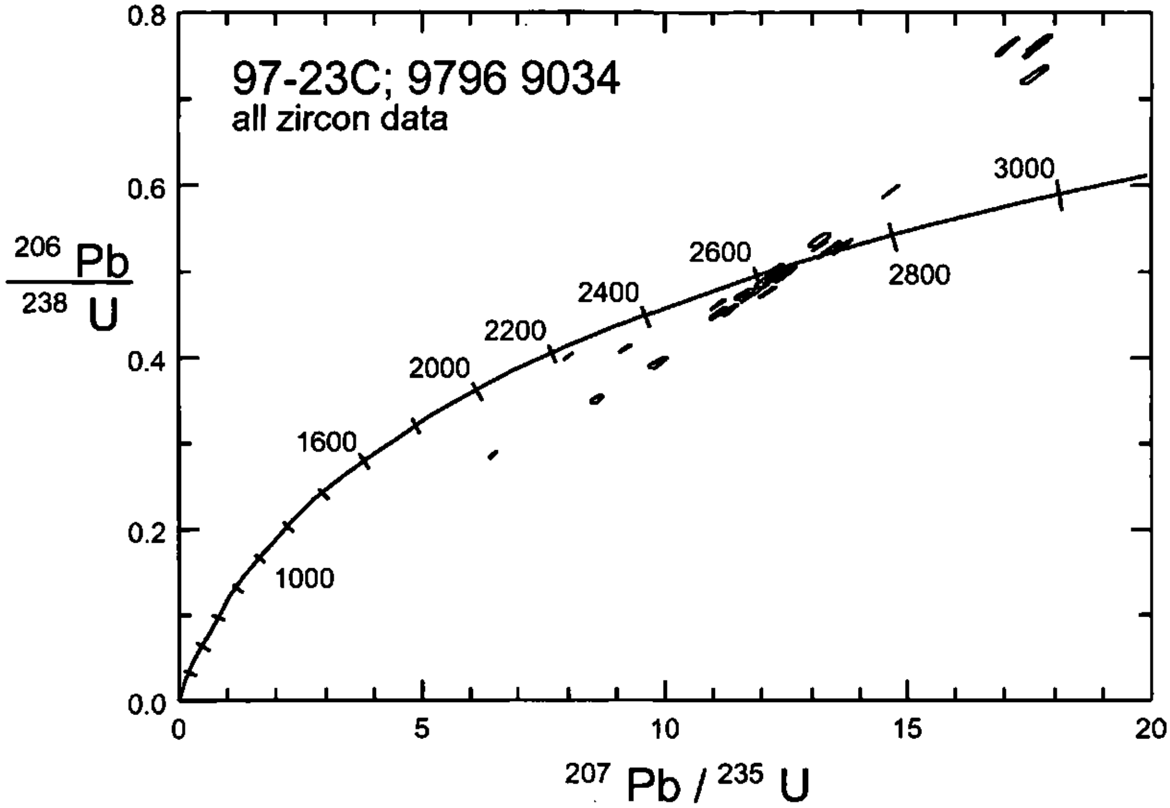

Figure z9796 9034a. Concordia plot of all SHRIMP zircon data for the porphyritic biotite monzogranite, Yerdanie Rock (UWA mount 97-23C).

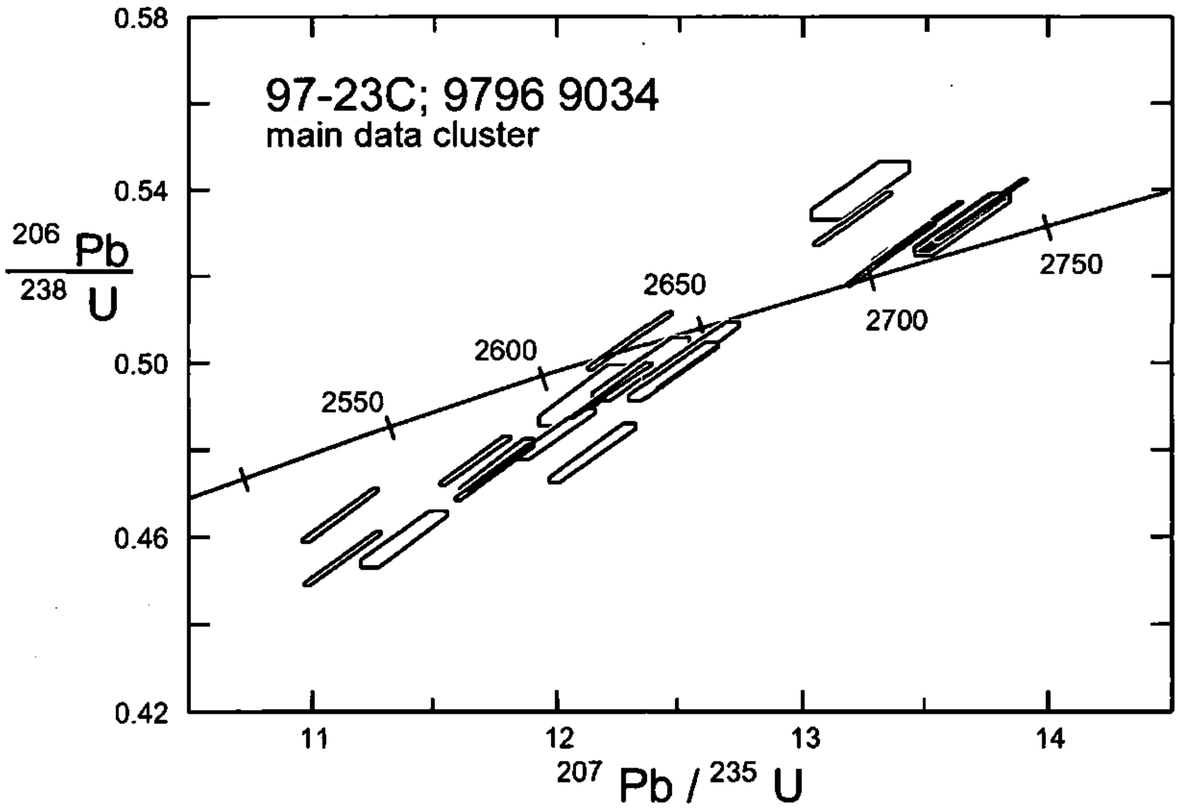

Figure z9796 9034b. Concordia plot showing the main cluster of SHRIMP zircon data for the porphyritic biotite monzogranite, Yerdanie Rock (UWA mount 97-23C).

9796 9044: biotite monzogranite, Mungari Monzogranite

1:250,000 sheet:	Kalgoorlie (SH5109)
AMG:	332406.8 mE, 6585646.4 mN
Location:	Taken from blasted material 50 metres east of the Mungari facing stone quarry
Province:	Eastern Goldfields
Description:	This sample is an equigranular to very sparsely feldspar porphyritic medium-grained biotite monzogranite. It is weakly to moderately altered and contains accessory metamict allanite. The monzogranite contains very minor pegmatite veins and is well jointed
Chemical group:	Low-Ca group, Mt Boreas association, Mungari clan
Pluton No:	313605
UWA mount:	97-22A

Description of zircons

The zircon population is of one morphologic type of uniformly fine grains, with most grains being 20-30 μm wide and 40-60 μm long. Grains are typically euhedral in external morphology with continuous euhedral internal zoning from core to rim. Inclusions are not common and consist of opaque or rod-like to equant minerals. All inclusions occur throughout the grains and show no preference for core or rim regions. The grains range from clear to pale brown, to dark brown in colour. Strong euhedral zoning observed on both optical and SEM images suggest high U-Th-contents and radiation damage. Discordant alteration patches, which are visible on SEM images, overgrow the euhedral zoning in many grains and are preferentially concentrated along the outer zones of grains, although some irregular patches occur within the grains without visible connection to the outer areas. In normal magmatic growth, the outer parts of the grains are typically more U-Th-rich and hence more radiation-damaged. Annealing of radiation damaged areas often occurs as a magmatic or later metamorphic process. These patches were avoided during data collection.

Results and interpretation

Seventeen analyses were made on 17 grains, although one data set could not be processed because of exceptionally high count rates (Table z9796 9044). The data are shown on a concordia diagram in Figure z9796 9044. The age data show considerable scatter, with many of the grains being discordant. Also, the U-contents of most analyses are >300 ppm U, which for Archaean grains is often the upper limit above which discordance and Pb-mobility is observed. The spread in ages is undoubtedly due to Pb-loss which accompanied the radiation damage of the zircon structure caused by the high U-Th-contents. Therefore only the oldest grains are considered acceptable to decipher the history of the rock. There is one grain (#4) which gives an age of 2810 Ma. This grain is not morphologically different to any of the other grains and it could be inferred that it best reflects the original age of the zircon population. If so, the age of 2810±9 (1σ) Ma may be the minimum age of the rock, or alternatively the minimum age of a xenocryst population. Given the post-tectonic timing of the granite, this grain (and possibly others) is undoubtedly a xenocryst.

The SHRIMP zircon data for this sample do not allow its magmatic age to be reliably estimated.

Table z9796 9044: SHRIMP zircon data for the Mungari biotite monzogranite (UWA 97-22A).

grain-spot	U (ppm)	Th (ppm)	4f206 (%)	$^{207}Pb^*/^{206}Pb^*$	$^{208}Pb^*/^{206}Pb^*$	$^{206}Pb^*/^{238}U$	$^{207}Pb^*/^{235}U$	$^{208}Pb^*/^{232}Th$	conc. (%)	$^{207}Pb/^{206}Pb$ age (Ma)
1-1	6698	2289	0.056	0.1327 ± 1	0.0991 ± 2	0.3683	6.737	0.1068	95	2134 ± 2
2-1	5078	1440	0.033	0.1281 ± 1	0.0802 ± 2	0.3543	6.259	0.1002	94	2073 ± 2
3-1	366	184	1.144	0.1767 ± 8	0.1479 ± 17	0.4858	11.832	0.1433	97	2622 ± 8
4-1	83	36	0.032	0.1981 ± 10	0.1183 ± 13	0.5643	15.411	0.1543	103	2810 ± 9
5-1	9195	3807	0.031	0.1352 ± 1	0.1280 ± 2	0.4085	7.616	0.1263	102	2167 ± 1
6-1	14376	7964	0.018	0.1373 ± 1	0.1515 ± 1	0.4365	8.264	0.1194	106	2193 ± 1
8-1	14124	8108	0.092	0.1523 ± 1	0.1560 ± 1	0.4630	9.724	0.1258	103	2372 ± 1
9-1	11461	5723	0.004	0.1704 ± 1	0.1286 ± 1	0.5215	12.250	0.1343	106	2561 ± 1
10-1	12024	6230	0.172	0.1274 ± 1	0.1418 ± 2	0.3923	6.889	0.1073	103	2062 ± 1
11-1	317	845	30.317	0.1716 ± 41	0.4523 ± 94	0.4568	10.807	0.0774	94	2573 ± 40
12-1	11925	6045	0.004	0.1760 ± 1	0.1383 ± 1	0.5694	13.814	0.1554	111	2615 ± 1
13-1	21825	7471	0.269	0.1618 ± 1	0.2371 ± 2	0.5971	13.321	0.4136	122	2475 ± 1
14-1	8309	3055	0.092	0.1320 ± 1	0.1041 ± 2	0.3886	7.073	0.1100	100	2125 ± 2
15-1	18030	12390	0.005	0.1749 ± 1	0.1815 ± 1	0.6151	14.832	0.1625	119	2605 ± 1
16-1	15997	10078	0.142	0.1696 ± 1	0.1608 ± 1	0.5713	13.357	0.1458	114	2553 ± 1
17-1	15981	10408	0.001	0.1739 ± 1	0.1698 ± 1	0.5751	13.789	0.1499	113	2596 ± 1

Data from 11/7/97 and 12/7/97.
U/Pb scatter (1 σ) for cz3 standard = 1.77% (n=15) and 1.75% (n = 5).
Spot 7-1 deleted because of data processing problems due to excessively high count rates.

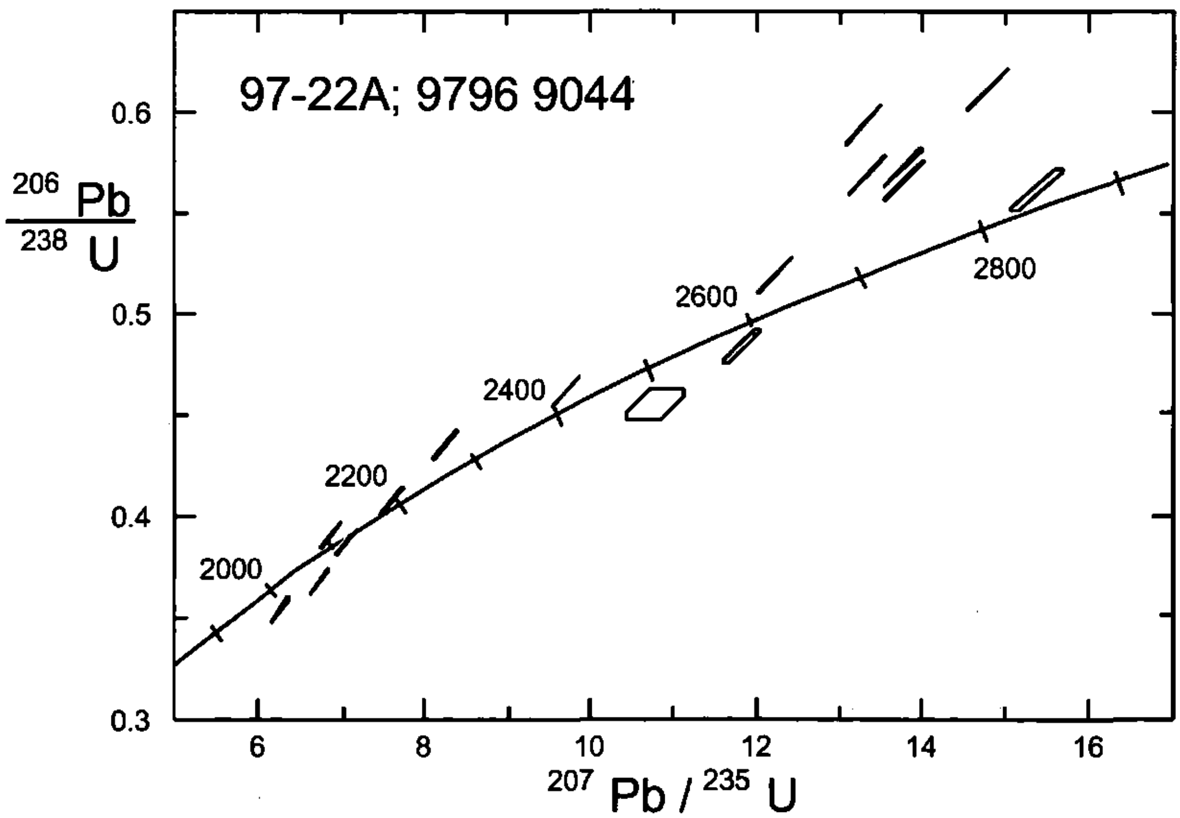

Figure z9796 9044. Concordia plot of SHRIMP zircon data for the Mungari biotite monzogranite (UWA 97-22A).

9796 9063: biotite monzogranite, Bulga Downs Granite

1:250,000 sheet:	Youanmi (SH5004)
AMG:	768036.5 mE, 6843150.1 mN
Location:	This sample was taken from a very large blasted boulder located south of the Bulga Downs homestead.
Province:	Southern Cross
Description:	The sample is representative of the extremely good bouldery outcrop in the area. It is a sparsely feldspar porphyritic medium-grained biotite monzogranite that contains sparse, irregular biotite-rich enclaves and is weakly altered.
Chemical group:	Low-Ca group, Beetle association, Bulga Downs clan
Pluton No:	284001
UWA mount:	97-23B

Description of zircons

The zircon population in this sample consists of one morphologic type of variable grain size. Many grains have an aspect ratio >5 although they grade to more equant varieties. The appearance of the zircons is similar to those in sample 9796 9082A. Grains are typically euhedral in external morphology with the majority showing continuous euhedral internal zoning from core to rim. Some grains have structureless cores. Inclusions are rare and consist of opaque or rod-like to equant minerals. All inclusions occur throughout the grains and show no preference for core or rim regions. The grains are generally dark brown in colour. Some discordant alteration patches are visible on SEM images, particularly as a thin discontinuous outer rim and along some cracks in a minority of grains: these were avoided during analyses.

Results and interpretation

Twenty one analyses on 21 grains are presented in Table z9796 9063 and shown on a concordia diagram in Figure z9796 9063. The common Pb corrections were mostly high, although about a third had 4f206<1.0%. About three-quarters of the data are discordant. However, the eight or the nine oldest and most concordant analyses, including five concordant analyses, comprise a single age population (Fig. z9796 9063) with a pooled age of 2684±8 Ma. The age of the five concordant (±5%) analyses are indistinguishable from this, at 2687±10 Ma. No older ages are apparent and 2684±8 Ma is taken to be the emplacement age of the granitoid. The younger and more discordant analyses are considered to represent old and Recent Pb-loss from partly radiation-damaged zircon structure, due to the relatively high U-Th contents.

Table z9796 9063: SHRIMP zircon data for the biotite monzogranite, Bulga Downs (UWA mount 97-23B).

grain-spot	U (ppm)	Th (ppm)	4f206 (%)	$^{207}Pb^*/^{206}Pb^*$	$^{208}Pb^*/^{206}Pb^*$	$^{206}Pb^*/^{238}U$	$^{207}Pb^*/^{235}U$	$^{208}Pb^*/^{232}Th$	conc. (%)	$^{207}Pb/^{206}Pb$ age (Ma)
5-1	117	133	2.313	0.1839 ± 19	0.3269 ± 42	0.4647	11.783	0.1329	92	2688 ± 17
7-1	322	470	0.086	0.1839 ± 5	0.4007 ± 12	0.5188	13.158	0.1427	100	2689 ± 4
14-1	98	62	0.033	0.1841 ± 12	0.1743 ± 21	0.5151	13.075	0.1405	100	2690 ± 11
15-1	99	195	0.027	0.1830 ± 12	0.5466 ± 34	0.5094	12.856	0.1411	99	2681 ± 11
17-1	109	246	1.450	0.1829 ± 21	0.4724 ± 50	0.4396	11.085	0.0921	88	2679 ± 19
18-1	81	66	0.216	0.1831 ± 14	0.2205 ± 27	0.5182	13.085	0.1398	100	2681 ± 13
20-1	85	97	0.053	0.1834 ± 14	0.3115 ± 29	0.5251	13.280	0.1427	101	2684 ± 12
21-1	341	531	0.666	0.1816 ± 9	0.4114 ± 20	0.4928	12.335	0.1304	97	2667 ± 8
Discordant (>15%).										
1-1	300	443	27.899	0.1828 ± 43	0.4309 ± 99	0.4009	10.104	0.1169	81	2678 ± 39
2-1	1778	4311	51.804	0.1692 ± 52	0.9650 ±130	0.1530	3.569	0.0609	36	2550 ± 52
3-1	176	545	11.862	0.1841 ± 36	0.4470 ± 84	0.3465	8.798	0.0502	71	2690 ± 32
4-1	257	299	6.553	0.1809 ± 21	0.3231 ± 49	0.3515	8.764	0.0974	73	2661 ± 20
6-1	121	72	6.302	0.1858 ± 32	0.2642 ± 73	0.3493	8.947	0.1552	71	2705 ± 29
8-1	312	358	2.007	0.1843 ± 11	0.1176 ± 23	0.3968	10.084	0.0407	80	2692 ± 10
9-1	197	341	2.029	0.1820 ± 14	0.3689 ± 31	0.4180	10.488	0.0892	84	2671 ± 12
10-1	94	357	6.669	0.1800 ± 36	0.5994 ± 86	0.3525	8.749	0.0559	73	2653 ± 33
11-1	955	898	2.187	0.1418 ± 8	0.4145 ± 19	0.2583	5.051	0.1138	66	2249 ± 9
12-1	208	135	4.610	0.1645 ± 29	0.1996 ± 64	0.3699	8.390	0.1140	81	2503 ± 29
13-1	228	351	17.153	0.1772 ± 46	0.5987 ±109	0.4041	9.870	0.1569	83	2626 ± 43
19-1	278	325	12.811	0.1892 ± 81	0.6094 ±193	0.0847	2.210	0.0442	19	2735 ± 70
Statistical outlier.										
16-1	414	194	0.459	0.1783 ± 7	0.1331 ± 12	0.4946	12.162	0.1404	98	2638 ± 6

Data 13/8/97 and 19/8/97.
U/Pb scatter (1σ) for cz3 standard = 1.40% (n = 10) and 1.27% (n=11).

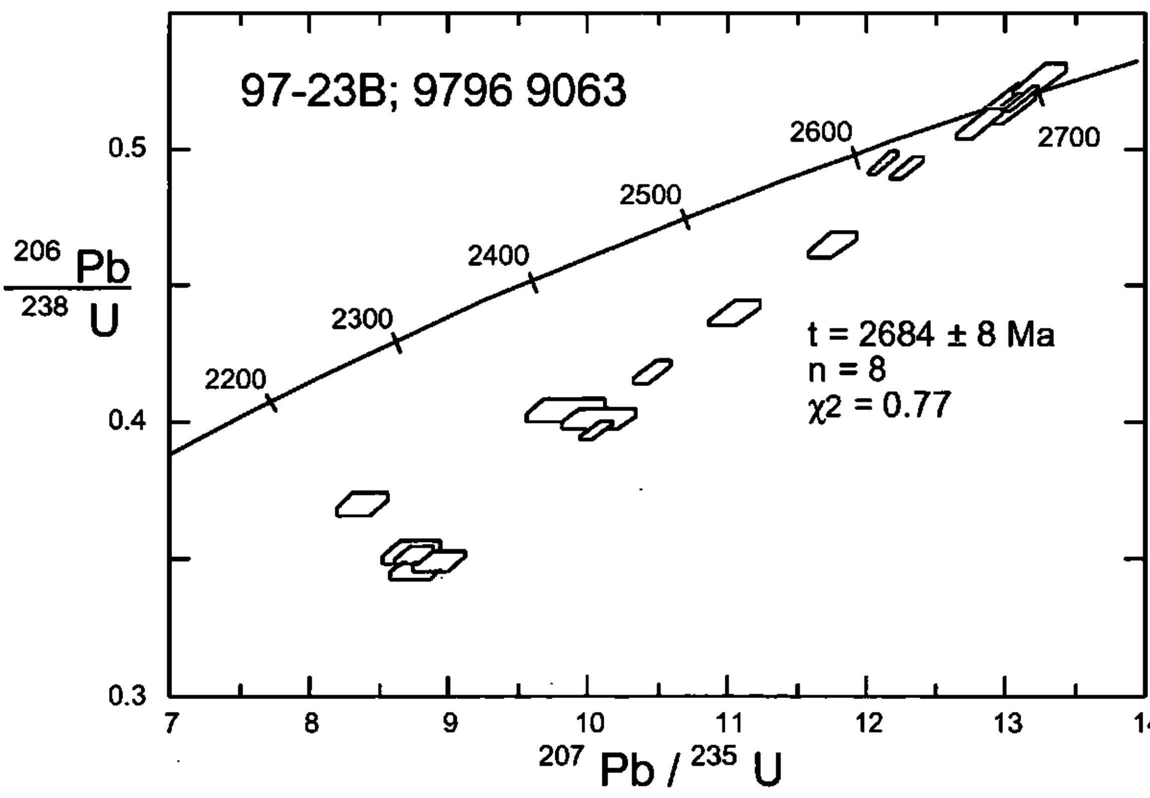

Figure z9796 9063. Concordia plot of SHRIMP zircon data for the biotite monzogranite, Bulga Downs (UWA mount 97-23B). Note that three highly discordant points fall below the range of this figure.

9796 9082A: biotite monzogranite, The Spring Granite

1:250,000 sheet:	Youanmi (SH5004)
AMG:	766945.1 mE, 6821040.4 mN
Location:	The sample was drilled from a large outcrop near Jan Bore
Province:	Southern Cross
Description:	This is a moderately to strongly feldspar-phyric fine-medium-grained biotite monzogranite that contains moderately common thin pegmatite veins and dykes. Titanite and ?hornblende occur as minor mineral phases. The granitoid also contains common amphibole lamprophyre enclaves and/or disrupted dykes
Chemical group:	High-Ca group, Diemals association, Diemals clan
Pluton No:	284006
UWA mount:	97-23A

A feldspar-phyric hornblende-biotite granodiorite outcrops to the east of, and sub-parallel to the biotite monzogranite, and both exhibit similar textures and a sub-parallel, weak mineral alignment. No contact relations were established between the two granitoid phases.

Description of zircons

The zircon population in this sample consists of one morphologic type of variable grain size. Most grains have an aspect ratio of 4-6 and some are up to 500 μm long, although morphologically indistinguishable grains also occur down to the 30 μm size range. Grains are typically euhedral in external morphology with the majority showing continuous euhedral internal zoning from core to rim. Some grains have extremely faint euhedral zoning and are almost structureless. Inclusions are not common and consist of opaque or rod-like to equant minerals. All inclusions occur throughout the grains and show no preference for core or rim regions. The grains are generally dark brown in colour. Some discordant alteration patches are visible on SEM images, particularly as a thin discontinuous outer rim and along some cracks in a minority of grains: these were avoided during analyses.

Results and interpretation

Twenty six analyses on 26 grains are presented in Table z9796 9082A and shown on a concordia diagram in Figure z9796 9082A. The common Pb corrections were generally low, although about half the analyses had >300 ppm U which is reflected in common Pb corrections of 4f206 = 1.0%–2.5% for most of these. Almost all the data are discordant. However, the oldest and most concordant analyses comprise a single age population (Fig. z9796 9082A) with a pooled age of 2682±5 Ma. No older ages are apparent and this is taken to be the emplacement age of the granitoid. The younger and more discordant analyses are considered to represent a combination of Archaean and Recent Pb-loss, the Archaean disturbance possibly being related to the extensive dyke networks in the rock.

Table z9796 9082A: SHRIMP analytical data for the biotite monzogranite, Jan Bore (UWA mount 97-23A).

grain-spot	U (ppm)	Th (ppm)	4f206 (%)	$^{207}Pb^*/^{206}Pb^*$	$^{208}Pb^*/^{206}Pb^*$	$^{206}Pb^*/^{238}U$	$^{207}Pb^*/^{235}U$	$^{208}Pb^*/^{232}Th$	conc. (%)	$^{207}Pb/^{206}Pb$ age (Ma)
1-1	214	224	1.341	0.1821 ± 13	0.2980 ± 29	0.4864	12.215	0.1387	96	2672 ± 12
3-1	236	180	0.834	0.1822 ± 11	0.2088 ± 23	0.4764	11.971	0.1306	94	2673 ± 10
4-1	283	301	0.183	0.1833 ± 7	0.2596 ± 15	0.4841	12.234	0.1184	95	2683 ± 7
5-1	287	359	0.221	0.1827 ± 8	0.3224 ± 17	0.4839	12.190	0.1248	95	2677 ± 7
6-1	286	153	0.013	0.1830 ± 7	0.1477 ± 10	0.4923	12.421	0.1358	96	2680 ± 6
8-1	446	868	1.163	0.1835 ± 9	0.5687 ± 24	0.4521	11.441	0.1320	90	2685 ± 8
9-1	155	153	0.127	0.1833 ± 10	0.2705 ± 21	0.5001	12.640	0.1371	97	2683 ± 9
10-1	217	368	1.613	0.1842 ± 15	0.4665 ± 36	0.4505	11.443	0.1240	89	2691 ± 13
11-1	317	405	0.487	0.1829 ± 8	0.3476 ± 18	0.4921	12.409	0.1339	96	2679 ± 7
12-1	166	314	2.727	0.1825 ± 19	0.5308 ± 47	0.4664	11.737	0.1310	92	2676 ± 18
14-1	211	297	2.502	0.1828 ± 17	0.3941 ± 39	0.4501	11.341	0.1261	89	2678 ± 15
16-1	256	233	0.666	0.1839 ± 11	0.2717 ± 22	0.4453	11.291	0.1327	88	2689 ± 10
17-1	175	255	2.589	0.1825 ± 19	0.4362 ± 45	0.4534	11.410	0.1355	90	2676 ± 17
26-1	367	430	0.163	0.1838 ± 6	0.3144 ± 13	0.4980	12.622	0.1336	97	2688 ± 6
Discordant (>12%)										
7-1	382	561	0.043	0.1825 ± 6	0.3964 ± 15	0.4230	10.641	0.1142	85	2675 ± 6
24-1	1314	3017	0.571	0.1294 ± 5	0.5928 ± 15	0.2837	5.064	0.0733	77	2090 ± 7
25-1	446	259	1.018	0.1630 ± 9	0.2062 ± 19	0.3771	8.472	0.1341	83	2487 ± 9
Statistical outliers (younger than main group).										
2-1	415	396	0.425	0.1788 ± 7	0.2563 ± 15	0.4631	11.414	0.1244	93	2641 ± 7
13-1	652	723	0.324	0.1769 ± 6	0.3046 ± 12	0.4640	11.318	0.1273	94	2624 ± 5
15-1	531	756	1.462	0.1732 ± 9	0.3854 ± 20	0.4550	10.863	0.1232	93	2589 ± 8
18-1	342	246	1.381	0.1770 ± 11	0.2111 ± 22	0.4545	11.093	0.1332	92	2625 ± 10
19-1	194	257	1.969	0.1788 ± 16	0.3708 ± 36	0.5010	12.353	0.1406	99	2642 ± 15
20-1	433	629	0.377	0.1754 ± 7	0.3922 ± 16	0.4392	10.623	0.1187	90	2610 ± 6
21-1	324	259	1.073	0.1775 ± 11	0.2876 ± 23	0.4299	10.523	0.1547	88	2630 ± 10
22-1	449	518	1.792	0.1727 ± 11	0.3283 ± 24	0.4369	10.400	0.1242	90	2584 ± 10
23-1	284	240	0.122	0.1791 ± 7	0.2269 ± 13	0.4924	12.163	0.1318	98	2645 ± 6

Data 19/8/97.
U/Pb scatter (1σ) for cz3 standard = 1.27% (n=11).

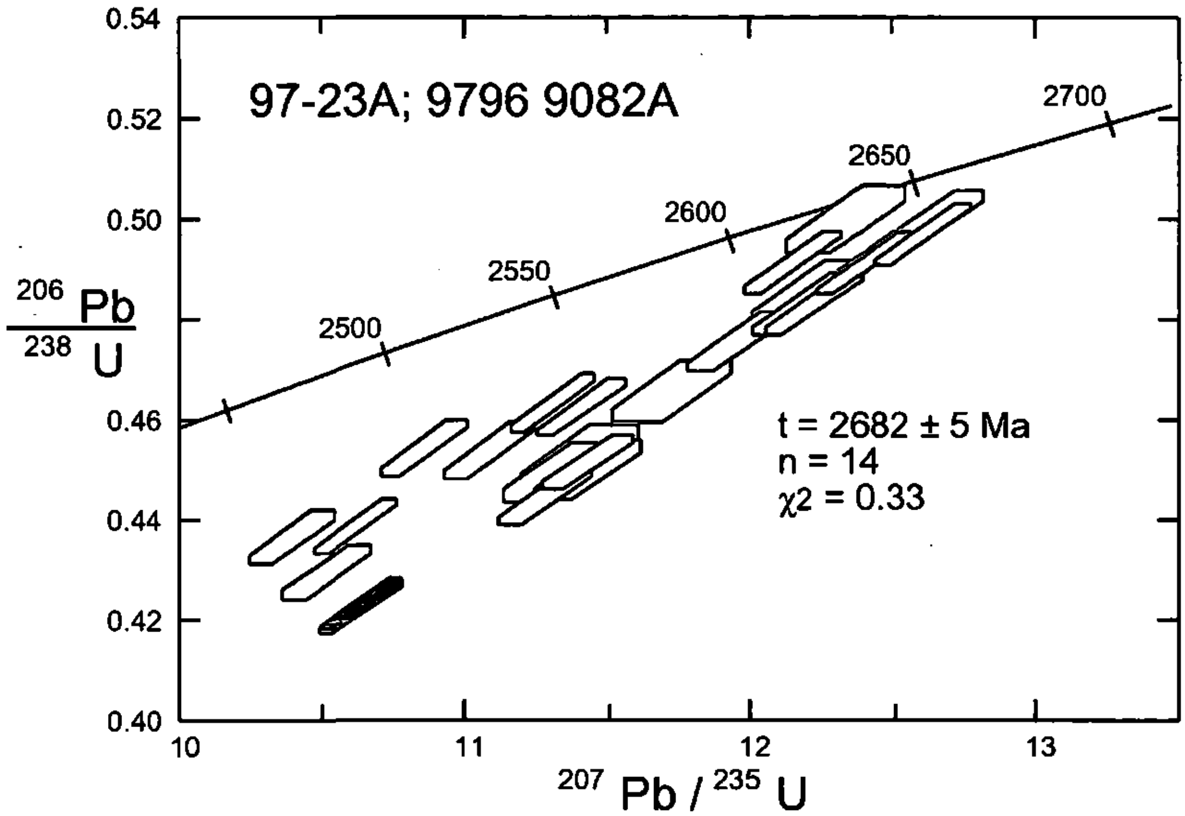

Figure z9796 9082A. Concordia plot of SHRIMP analytical data for the biotite monzogranite, Jan Bore (UWA mount 97-23A). Note that two highly discordant points fall below the range of the figure.

9796 9102B: gneissic porphyritic biotite monzogranite, McLeod Rock Granite

1:250,000 sheet:	Barlee (SH5008)
AMG:	752427.4 mE, 6786529.2 mN
Location:	This sample was drilled from outcrop forming part of McLeod Rock
Province:	Southern Cross
Description:	The bulk of this outcrop comprises strongly banded to gneissic granitic rocks intruded by pegmatite veins and dykes. Sample 9796 9102B is from a band of moderately to strongly feldspar-phyric to megacrystic medium-grained biotite monzogranite. It occurs as irregular bands in the banded/gneissic granitoid together with a seriate medium-grained biotite monzogranite (9796 9102A). The gneissic banding is cross-cut by dyke sample 9796 9104.
Chemical group:	High-Ca group, Diemals association, Mondie clan
Pluton No:	283905
UWA mount:	97-26A

Description of zircons

The zircon population in this sample consists of one morphologic type of grains of variable size. Grains are typically euhedral in external morphology with continuous euhedral internal zoning from core to rim. Some of the larger grains have visible cores, but these are euhedrally zoned and are coherent with the zoned rims of the grains. Inclusions are not common and consist of opaque or rod-like to equant minerals. All inclusions occur throughout the grains and show no preference for core or rim regions. The grains range from pale to dark brown in colour.

Results and interpretation

Thirty analyses on 30 grains are presented in Table z9796 9102B and shown on a concordia diagram in Figures z9796 9102Ba, b. The data show considerable scatter with most grains being significantly discordant. Also, the U-contents of most analyses are >300 ppm U, and many analyses have a high common Pb correction. Of the six analyses with a low common Pb correction (i.e. 4f206<1.5%) and less than about 400 ppm U, one is dated at ca. 3010 Ma whereas the others are in the range 2714 -2724 Ma. The more discordant analyses are considered to represent old and Recent Pb-loss from radiation-damaged zircon structure, due to the relatively high U-Th-contents. When all near concordant analyses with low common Pb are pooled, the eight analyses form a population at 2737±7 Ma, although with a very high χ^2 value (Fig. z9796 9102Bb). These analyses all come from the cores of larger grains; they may represent either older xenocrystic cores, or the earliest growth stage of the zircons before the U-content of the magma had built up due to fractionation. These alternative interpretations would see the 2737 Ma age being either a xenocryst age or the emplacement age of the granitoid. The distinction between these cannot be made unequivocally with the current data, but it is notable that the discordant data conform more closely to a 2700 Ma – ~1200 Ma discordia trend than to a zero-age Pb-loss trend originating from any date <2740 Ma.

It is not possible to unequivocally determine the age of the magmatic episode which formed the rock. However, the best estimate at this stage is that granitoid emplacement occurred at ~2740 Ma, with two of the analysed grains being xenocrysts with ages ~2790 Ma and ~3010 Ma.

Table z9796 9102B: SHRIMP zircon data for the gneissic porphyritic biotite monzogranite, McLeod Rock (UWA mount 97-26A).

grain-spot	U (ppm)	Th (ppm)	4f206 (%)	$^{207}Pb^*/^{206}Pb^*$	$^{208}Pb^*/^{206}Pb^*$	$^{206}Pb^*/^{238}U$	$^{207}Pb^*/^{235}U$	$^{208}Pb^*/^{232}Th$	conc. (%)	$^{207}Pb/^{206}Pb$ age (Ma)
7-1	1808	143	0.678	0.1893 ± 3	0.0531 ± 6	0.5175	13.508	0.3485	98	2736 ± 3
10-1	3496	164	0.000	0.1901 ± 2	0.0132 ± 1	0.5156	13.517	0.1448	98	2743 ± 1
13-1	1895	165	0.628	0.1882 ± 3	0.0210 ± 5	0.4949	12.839	0.1191	95	2726 ± 3
18-1	262	54	0.028	0.1880 ± 6	0.0564 ± 7	0.5063	13.122	0.1383	97	2724 ± 5
22-1	2180	185	0.000	0.1894 ± 2	0.0228 ± 1	0.5197	13.570	0.1393	99	2737 ± 2
24-1	344	65	0.688	0.1867 ± 7	0.0362 ± 13	0.4890	12.590	0.0942	95	2714 ± 7
26-1	2127	1367	0.086	0.1900 ± 2	0.1664 ± 3	0.5025	13.160	0.1300	96	2742 ± 2
28-1	360	57	0.010	0.1870 ± 5	0.0429 ± 4	0.5107	13.166	0.1382	98	2716 ± 4
Older grains										
4-1	46	117	1.029	0.2245 ± 23	0.7466 ± 64	0.5580	17.272	0.1618	95	3013 ± 17
21-1	1049	1494	0.337	0.1954 ± 3	0.3381 ± 7	0.5762	15.523	0.1367	105	2788 ± 3
Discordant (>5%) and/or high common Pb.										
1-1	824	528	1.623	0.1706 ± 6	0.1938 ± 14	0.4070	9.572	0.1231	86	2563 ± 6
2-1	212	68	5.128	0.1932 ± 20	0.1118 ± 44	0.4681	12.471	0.1642	89	2770 ± 17
3-1	713	48	0.735	0.1791 ± 5	0.0202 ± 9	0.4580	11.310	0.1378	92	2644 ± 5
5-1	962	81	0.893	0.1722 ± 5	0.0787 ± 10	0.3975	9.435	0.3720	84	2579 ± 5
6-1	1121	129	0.733	0.1466 ± 5	0.0562 ± 9	0.3105	6.275	0.1510	76	2306 ± 5
8-1	1111	892	0.222	0.1489 ± 4	0.2355 ± 8	0.3273	6.720	0.0959	78	2334 ± 4
9-1	593	85	1.268	0.1690 ± 7	0.0512 ± 14	0.3892	9.068	0.1385	83	2548 ± 7
11-1	580	136	1.360	0.1696 ± 8	0.0923 ± 16	0.3579	8.367	0.1409	77	2554 ± 8
12-1	406	256	0.797	0.1882 ± 7	0.1731 ± 14	0.4833	12.538	0.1328	93	2726 ± 6
14-1	164	87	3.248	0.1894 ± 17	0.1711 ± 36	0.5442	14.210	0.1757	102	2737 ± 15
15-1	892	629	1.445	0.1831 ± 6	0.2196 ± 12	0.4760	12.017	0.1481	94	2681 ± 5
16-1	1103	441	1.935	0.1562 ± 7	0.1313 ± 14	0.3034	6.533	0.0996	71	2415 ± 7
17-1	1258	193	1.539	0.1497 ± 6	0.0470 ± 11	0.3391	7.000	0.1035	80	2343 ± 6
19-1	143	184	1.340	0.1871 ± 14	0.3246 ± 32	0.4921	12.698	0.1243	95	2717 ± 13
20-1	1564	412	1.519	0.1351 ± 5	0.0942 ± 10	0.2926	5.451	0.1046	76	2166 ± 6
23-1	567	89	0.549	0.1789 ± 6	0.0516 ± 9	0.4605	11.359	0.1510	92	2643 ± 5
25-1	445	273	0.952	0.1788 ± 8	0.1481 ± 16	0.4017	9.900	0.0969	82	2641 ± 7
27-1	857	504	0.734	0.1699 ± 5	0.1341 ± 10	0.3503	8.206	0.0799	76	2557 ± 5
29-1	1763	78	0.711	0.1861 ± 3	0.0136 ± 6	0.4758	12.207	0.1460	93	2708 ± 3
30-1	1344	204	1.557	0.1558 ± 6	0.0417 ± 11	0.3380	7.260	0.0928	78	2411 ± 6

Data 11/11/97.
U/Pb scatter (1σ) for cz3 standard = 1.45% (n=10).

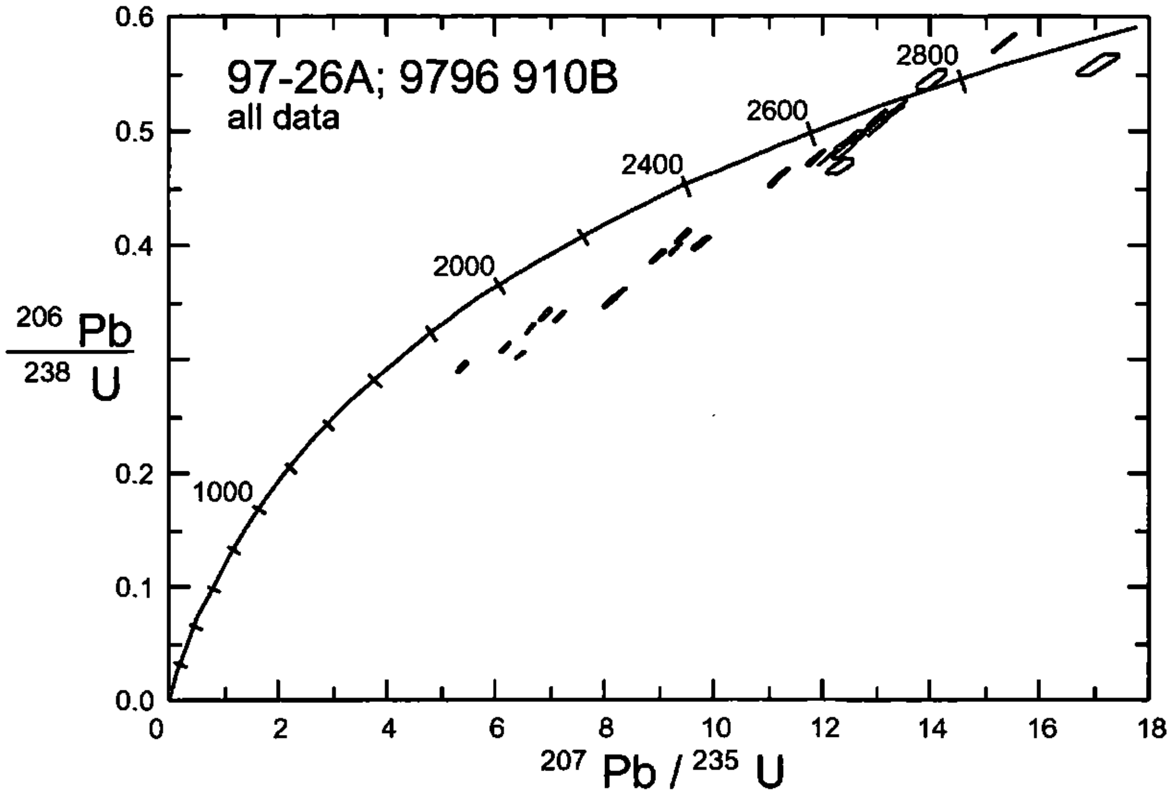

Figure z9796 9102Ba. Concordia plot of all SHRIMP zircon data for the gneissic porphyritic biotite monzogranite, McLeod Rock (UWA mount 97-26A).

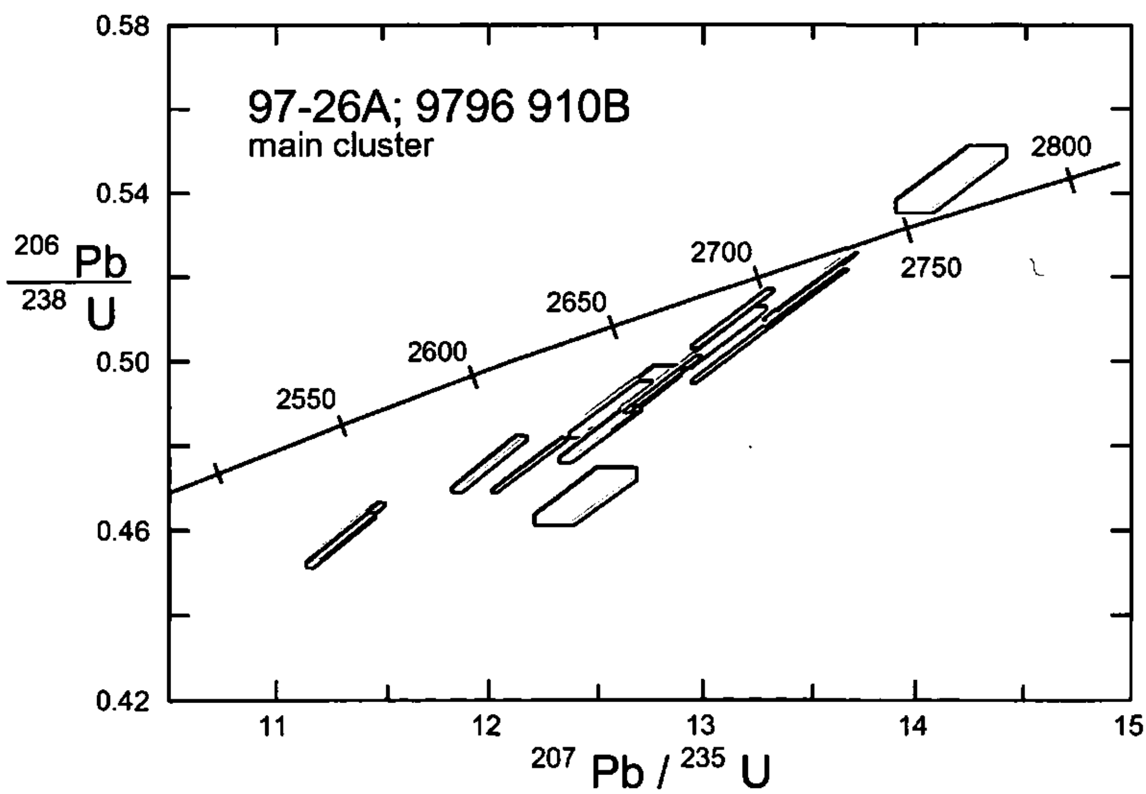

Figure z9796 9102Bb. Concordia plot of the most concordant SHRIMP zircon data for the gneissic porphyritic biotite monzogranite, McLeod Rock (UWA mount 97-26A).

9796 9104: biotite monzogranite dyke, Native Well Monzogranite

1:250,000 sheet:	Barlee (SH5008)
AMG:	745407.3 mE, 6783679.2 mN
Location:	The sample was drilled from outcrop near Native Well
Province:	Southern Cross
Description:	The sample is from a foliated sparsely feldspar-phyric medium-grained biotite monzogranite dyke. This irregular foliated dyke cross-cuts the gneissic banding, but locally is incorporated suggesting a syn- to late-deformation age. The age of the dyke should tie in with 9796 9102B, and give a minimum age for the gneiss
Chemical group:	High-Ca group, Diemals association, Diemals clan
Pluton No:	283908
UWA mount:	97-24A

Description of zircons

The zircon population in this sample consists of one morphologic type of variable grain size. Most grains are of the order of 50 x 100 μm in dimension, although morphologically indistinguishable grains also occur down to 20 x 30 μm. Grains are typically euhedral in external morphology with the majority showing continuous euhedral internal zoning from core to rim. Some grains have extremely faint euhedral zoning and are almost structureless. Inclusions are not common and consist of opaque or rod-like to equant minerals. All inclusions occur throughout the grains and show no preference for core or rim regions. The grains range from clear to dark brown in colour. Some grains have dark brown cores with clearer rims, but the cores are unsuitable for SHRIMP analysis and it is not known whether they are older than the rims. Rare discordant alteration patches are visible on SEM images as a very thin discontinuous rim and along some cracks in a minority of grains: these were avoided during analyses.

Results and interpretation

Twenty two analyses on 22 grains are presented in Table z9796 9104 and shown on a concordia diagram in Figure z9796 9104. With the exception of four analyses, the common Pb corrections were relatively low and all analyses had <330 ppm U. The data falls largely along an array from the origin of the concordia diagram to ca. 2.68 Ga, with one reverse discordant analysis (Fig. z9796 9104). Omitting all the discordant analyses, the population comprising the remaining 16 analyses in the concordant to near-concordant group (Fig. z9796 9104) has a χ^2<1.0, indicating that the analyses come from a single age population at 2682±6 Ma. No older ages are apparent and this is taken to be the emplacement age of the dyke.

Table z9796 9104: SHRIMP zircon data for the biotite monzogranite dyke, Native Well (UWA mount 97-24A).

grain-spot	U (ppm)	Th (ppm)	4f206 (%)	$^{207}Pb^*/^{206}Pb^*$	$^{208}Pb^*/^{206}Pb^*$	$^{206}Pb^*/^{238}U$	$^{207}Pb^*/^{235}U$	$^{208}Pb^*/^{232}Th$	conc. (%)	$^{207}Pb/^{206}Pb$ age (Ma)
1-1	120	123	0.031	0.1827 ± 9	0.2763 ± 18	0.5101	12.847	0.1379	99	2677 ± 8
2-1	36	30	0.024	0.1836 ± 21	0.2270 ± 41	0.4950	12.528	0.1351	97	2685 ± 19
3-1	90	104	0.054	0.1827 ± 12	0.3377 ± 26	0.4815	12.125	0.1419	95	2677 ± 11
4-1	80	80	0.014	0.1845 ± 13	0.2736 ± 25	0.5107	12.993	0.1392	99	2694 ± 11
6-1	76	88	0.034	0.1838 ± 12	0.3225 ± 26	0.5021	12.723	0.1397	98	2687 ± 11
7-1	131	218	0.052	0.1851 ± 10	0.4578 ± 25	0.5009	12.786	0.1379	97	2700 ± 9
8-1	36	38	0.003	0.1814 ± 22	0.2972 ± 46	0.5065	12.669	0.1396	99	2666 ± 20
9-1	69	85	0.111	0.1833 ± 13	0.3349 ± 28	0.5075	12.825	0.1382	99	2683 ± 11
10-1	52	47	0.357	0.1846 ± 17	0.2527 ± 36	0.5082	12.936	0.1446	98	2695 ± 16
12-1	109	168	0.054	0.1840 ± 10	0.4230 ± 24	0.5111	12.963	0.1401	99	2689 ± 9
13-1	51	54	0.232	0.1809 ± 18	0.2933 ± 38	0.5038	12.563	0.1399	99	2661 ± 16
13-2	102	121	0.110	0.1815 ± 11	0.3395 ± 25	0.5046	12.626	0.1437	99	2666 ± 10
14-1	97	74	0.154	0.1836 ± 12	0.2121 ± 22	0.5032	12.737	0.1406	98	2686 ± 10
16-1	47	43	0.169	0.1806 ± 15	0.2474 ± 30	0.5130	12.776	0.1398	100	2659 ± 14
20-1	139	184	0.019	0.1828 ± 8	0.3627 ± 18	0.5322	13.416	0.1451	103	2679 ± 7
22-1	220	263	0.240	0.1830 ± 7	0.3483 ± 17	0.5113	12.904	0.1493	99	2680 ± 7
Discordant (>5%) and/or high common Pb.										
5-1	39	43	0.042	0.1855 ± 24	0.2973 ± 52	0.4700	12.023	0.1283	92	2703 ± 22
11-1	235	117	3.164	0.1820 ± 24	0.3611 ± 56	0.2437	6.116	0.1771	53	2671 ± 22
15-1	105	31	1.295	0.1868 ± 32	0.2556 ± 70	0.1054	2.716	0.0924	24	2714 ± 28
17-1	322	236	3.613	0.1721 ± 18	0.3090 ± 42	0.3809	9.040	0.1605	81	2579 ± 18
18-1	125	78	0.179	0.1838 ± 10	0.1393 ± 17	0.4655	11.796	0.1049	92	2687 ± 9
18-2	195	234	0.920	0.1840 ± 12	0.1775 ± 24	0.3684	9.347	0.0543	75	2689 ± 11
19-1	310	348	1.120	0.1805 ± 10	0.3300 ± 22	0.4727	11.764	0.1389	94	2657 ± 9
21-1	69	68	0.060	0.1826 ± 14	0.2675 ± 27	0.5670	14.278	0.1529	108	2677 ± 12

Data 30/8/97 and 12/9/97.
U/Pb scatter (1σ) for cz3 standard = 1.07% (n = 13) and 2.29% (n=14).

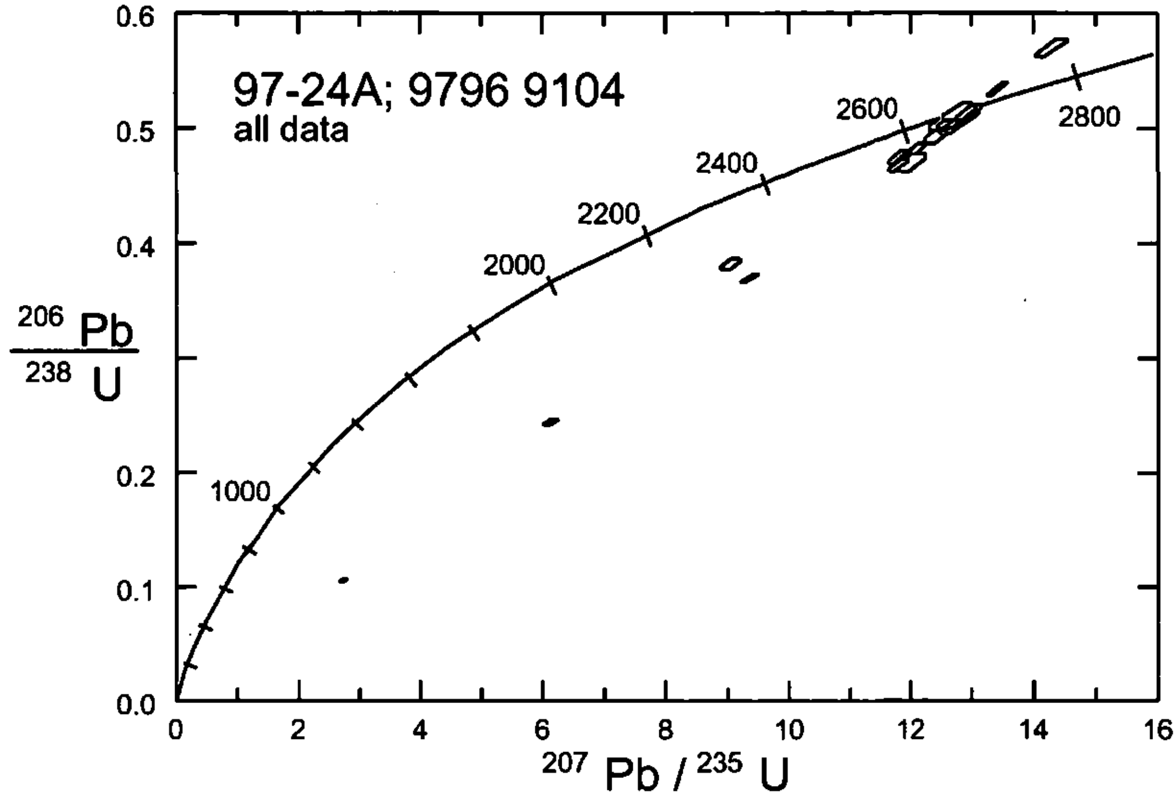

Figure z9796 9104a. Concordia plot of all SHRIMP zircon data for the biotite monzogranite dyke, Native Well (UWA mount 97-24A).

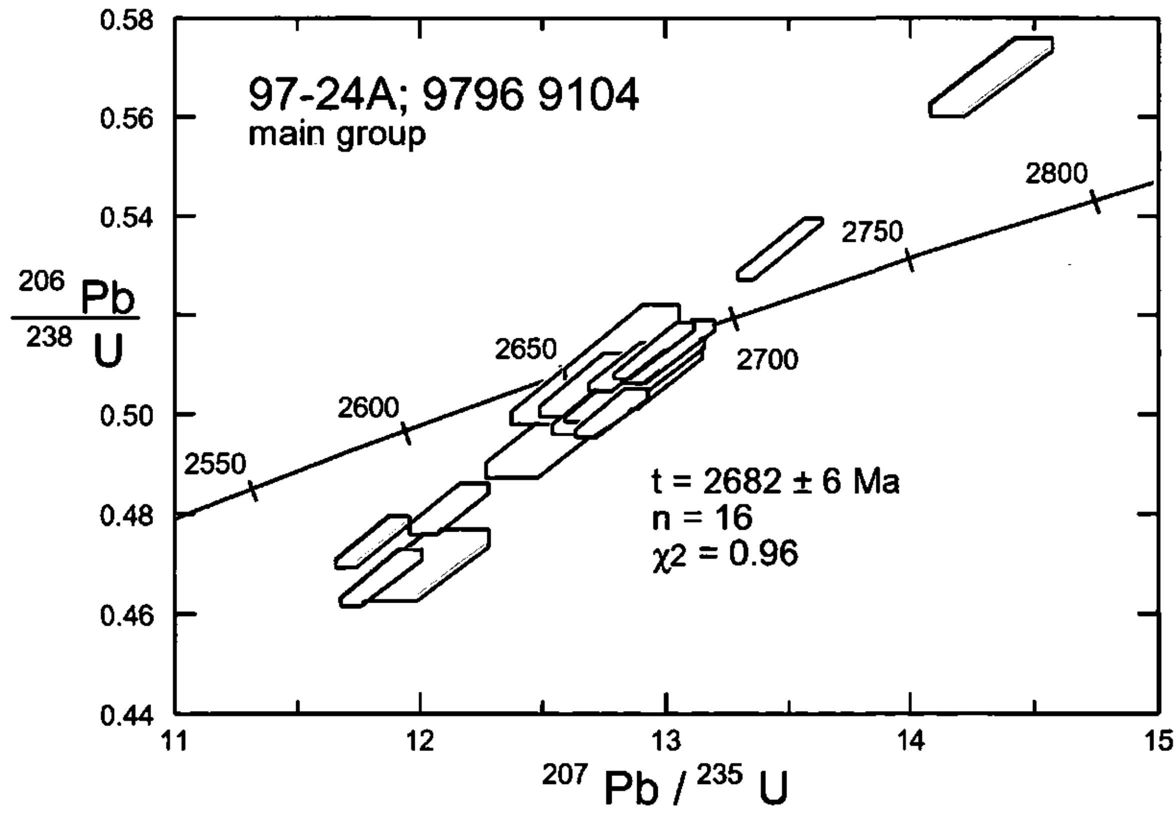

Figure z9796 9104b. Concordia plot of the main cluster of SHRIMP zircon data for the biotite monzogranite dyke, Native Well (UWA mount 97-24A).

9796 9125: porphyritic biotite monzogranite, Warren-2

1:250,000 sheet:	Southern Cross (SH5016)
AMG:	658682.5 mE, 6562693.3 mN
Location:	Warren Double Cunyan Hill; sample drilled from large outcrop.
Province:	Southern Cross
Description:	Moderate quartz-K-feldspar-porphyritic to seriate medium-coarse grained biotite monzogranite. This sample is from the main granite-type spread over Southern Cross, Kellerberrin and Bencubbin sheets. Close to 1200 Ma granitoid (9796 9126), and paler than other Low-Ca granitoids in area, suggesting that it may show a thermal overprint from the intrusion of the Proterozoic granitoid.
Chemical group:	Low-Ca group, Beetle association, Boodarockin clan
Pluton No:	263504
UWA mount:	97-40A

Description of zircons

Apart from one very large grain (>475 μm in length), most zircons from sample 9796-9125 are less than 200 μm in length. Most grains are medium to dark brown in colour, euhedral or with slightly rounded terminations, and display visible internal structures and occasional inclusions. The SEM images reveal some very complex patterns in the internal structure of some grains, with irregular, patchy replacement and recrystallisation found in a large number of grains. Potential older cores were identified in several grains. Cracks and fractures are present in many grains.

Results and interpretation

Forty-four analyses on 44 grains are presented in Table z9796 9125 and shown on concordia diagrams in Figures z9796 9125a, b. Thirty of the analyses constitute a main group that is unusually coherent and concordant for zircons with such high U-contents. The high χ^2 is partly attributable to the high U (and consequently high Pb) contents. For measurements of samples with such abundant Pb, the ion count rates are sufficiently high that sources of systematic variability other than counting statistics become significant, but they have not been quantified and are not included in the estimates of internal precision. After omission of four statistical outliers, the main group gives an age of 2617.2±3.2 Ma, with a χ^2 of 6.0, and this is interpreted to be the age of granitoid emplacement, with the ~2650 Ma grains being considered to be xenocrysts.

Table z9796 9125: SHRIMP zircon data for the porphyritic biotite monzogranite, Warren-2 (UWA mount 97-40A).

grain-spot	U (ppm)	Th (ppm)	4f206 (%)	$^{207}Pb^*/^{206}Pb^*$	$^{208}Pb^*/^{206}Pb^*$	$^{206}Pb^*/^{238}U$	$^{207}Pb^*/^{235}U$	$^{208}Pb^*/^{232}Th$	conc. (%)	$^{207}Pb/^{206}Pb$ age (Ma)
1-1	887	393	0.817	0.1768 ± 5	0.1051 ± 9	0.4874	11.885	0.1157	98	2623 ± 4
3-1	548	218	0.250	0.1767 ± 5	0.0991 ± 8	0.4967	12.098	0.1237	99	2622 ± 5
7-1	743	212	0.290	0.1763 ± 4	0.0794 ± 7	0.5043	12.258	0.1401	101	2618 ± 4
8-1	616	229	0.277	0.1754 ± 4	0.0865 ± 7	0.4847	11.723	0.1125	98	2610 ± 4
42-1	641	328	0.930	0.1761 ± 6	0.1349 ± 11	0.4956	12.034	0.1304	99	2617 ± 5
43-1	1282	485	0.070	0.1757 ± 3	0.1029 ± 3	0.4860	11.775	0.1323	98	2613 ± 2
44-1	819	416	0.019	0.1775 ± 3	0.1368 ± 5	0.4994	12.222	0.1344	99	2630 ± 3
14-1	459	204	0.039	0.1775 ± 4	0.1206 ± 6	0.5051	12.365	0.1373	100	2630 ± 4
15-1	512	168	0.500	0.1755 ± 6	0.0911 ± 10	0.4826	11.678	0.1338	97	2611 ± 5
45-1	465	179	0.043	0.1758 ± 4	0.1037 ± 6	0.4982	12.077	0.1339	100	2614 ± 4
16-1	945	377	0.337	0.1760 ± 4	0.1094 ± 6	0.4973	12.065	0.1365	100	2615 ± 3
46-1	866	346	0.442	0.1755 ± 4	0.1095 ± 7	0.4752	11.499	0.1303	96	2611 ± 4
47-1	223	12	0.120	0.1769 ± 7	0.0118 ± 9	0.4922	12.007	0.1080	98	2624 ± 7
21-1	766	277	0.063	0.1760 ± 3	0.0969 ± 5	0.4952	12.019	0.1327	99	2616 ± 3
22-1	718	358	0.038	0.1763 ± 3	0.1346 ± 5	0.5036	12.241	0.1362	100	2618 ± 3
48-1	806	407	0.042	0.1771 ± 3	0.1365 ± 5	0.5013	12.237	0.1356	100	2625 ± 3
49-1	555	205	0.152	0.1770 ± 4	0.1010 ± 6	0.4943	12.064	0.1351	99	2625 ± 4
25-1	1096	417	0.257	0.1749 ± 3	0.1074 ± 5	0.4882	11.771	0.1377	98	2605 ± 3
50-1	676	308	0.836	0.1772 ± 5	0.1291 ± 11	0.4982	12.170	0.1415	99	2626 ± 5
51-1	472	156	0.221	0.1768 ± 5	0.0867 ± 7	0.4929	12.017	0.1295	98	2623 ± 5
56-1	1014	463	0.196	0.1770 ± 3	0.1183 ± 5	0.4884	11.915	0.1264	98	2625 ± 3
58-1	869	437	0.044	0.1744 ± 3	0.1352 ± 5	0.4835	11.628	0.1300	98	2601 ± 3
60-1	1287	765	0.144	0.1766 ± 3	0.1583 ± 4	0.5173	12.596	0.1378	103	2621 ± 2
61-1	815	326	0.431	0.1750 ± 4	0.1103 ± 7	0.4718	11.385	0.1302	96	2606 ± 4
63-1	991	422	0.081	0.1753 ± 3	0.1164 ± 5	0.4928	11.914	0.1347	99	2609 ± 3
64-1	1024	412	0.027	0.1775 ± 3	0.1097 ± 4	0.4947	12.109	0.1350	99	2630 ± 3
65-1	813	408	0.043	0.1771 ± 3	0.1338 ± 5	0.4926	12.028	0.1315	98	2626 ± 3
66-1	1199	619	0.370	0.1756 ± 3	0.1428 ± 6	0.4907	11.879	0.1358	99	2612 ± 3
32-1	602	241	0.098	0.1765 ± 4	0.1057 ± 6	0.4973	12.103	0.1311	99	2620 ± 4
67-1	1152	516	0.192	0.1750 ± 3	0.1243 ± 5	0.4762	11.491	0.1321	96	2606 ± 3
>5% discordant or 4f206>1%.										
4-1	581	54	0.554	0.1792 ± 5	0.0256 ± 9	0.4580	11.315	0.1255	92	2645 ± 5
5-1	471	139	0.057	0.1750 ± 5	0.0789 ± 6	0.5418	13.071	0.1451	107	2606 ± 5
9-1	1810	103	0.065	0.1647 ± 2	0.0135 ± 2	0.4110	9.330	0.0979	89	2504 ± 2
11-1	1735	543	0.474	0.1362 ± 4	0.0902 ± 7	0.2346	4.404	0.0676	62	2179 ± 5
52-1	1342	467	0.220	0.1720 ± 3	0.0999 ± 5	0.4473	10.609	0.1285	92	2577 ± 3
53-1	1287	459	0.140	0.1648 ± 3	0.0991 ± 5	0.4015	9.124	0.1116	87	2506 ± 3
54-1	1123	426	0.453	0.1707 ± 4	0.0806 ± 7	0.4242	9.985	0.0902	89	2565 ± 4
59-1	855	240	2.483	0.1752 ± 7	0.0892 ± 15	0.4858	11.734	0.1544	98	2608 ± 7
62-1	910	290	0.345	0.1690 ± 4	0.0930 ± 6	0.4422	10.304	0.1293	93	2548 ± 4
68-1	790	401	0.177	0.1742 ± 4	0.1409 ± 6	0.4561	10.951	0.1267	93	2598 ± 4
Age outliers										
41-1	1141	446	0.057	0.1734 ± 3	0.1056 ± 4	0.4941	11.814	0.1337	100	2591 ± 3
55-1	754	790	0.473	0.1792 ± 5	0.2894 ± 10	0.4868	12.028	0.1344	97	2645 ± 4
57-1	215	174	0.422	0.1804 ± 8	0.2211 ± 16	0.4874	12.127	0.1338	96	2657 ± 8
69-1	488	581	0.848	0.1789 ± 6	0.3203 ± 14	0.4909	12.109	0.1321	97	2643 ± 6

Data 27/2/98.
U/Pb scatter (1σ) for cz3 standard = 1.00% (n=14 of 16).

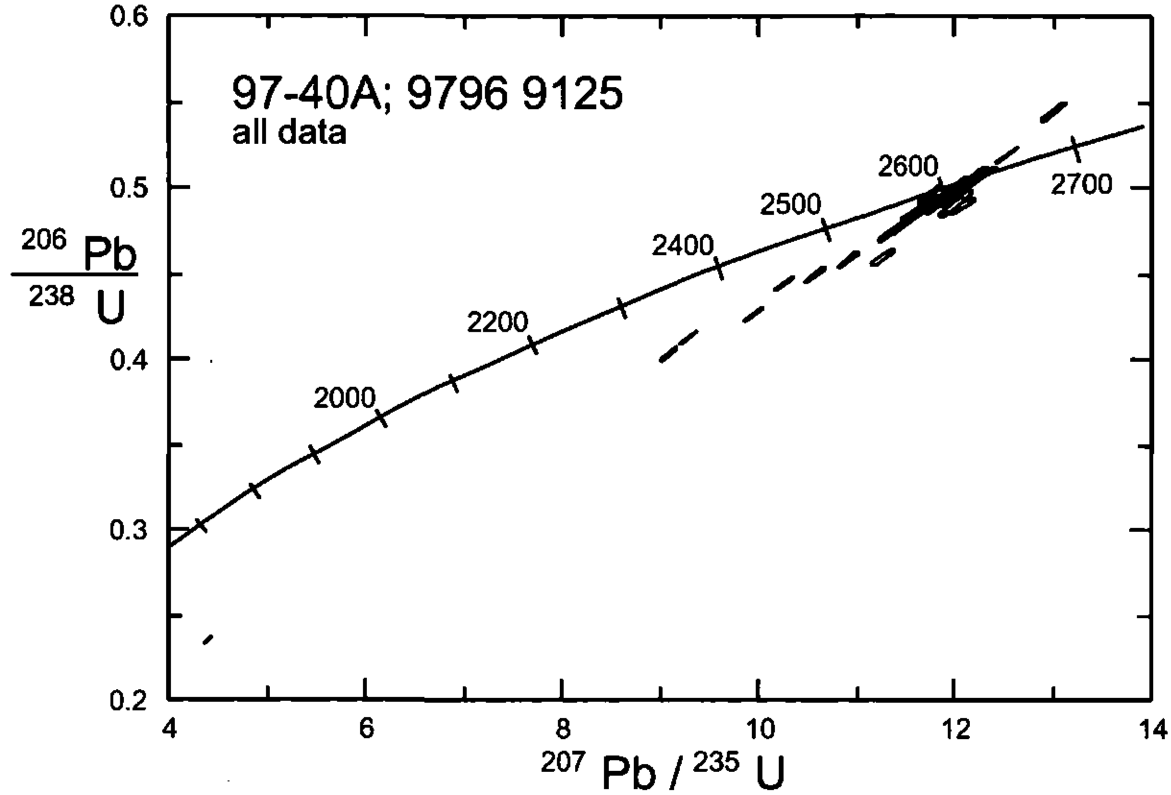

Figure z9796 9125a: Concordia plot showing all SHRIMP zircon data for the biotite monzogranite, Warren-2 (UWA mount 97-40A).

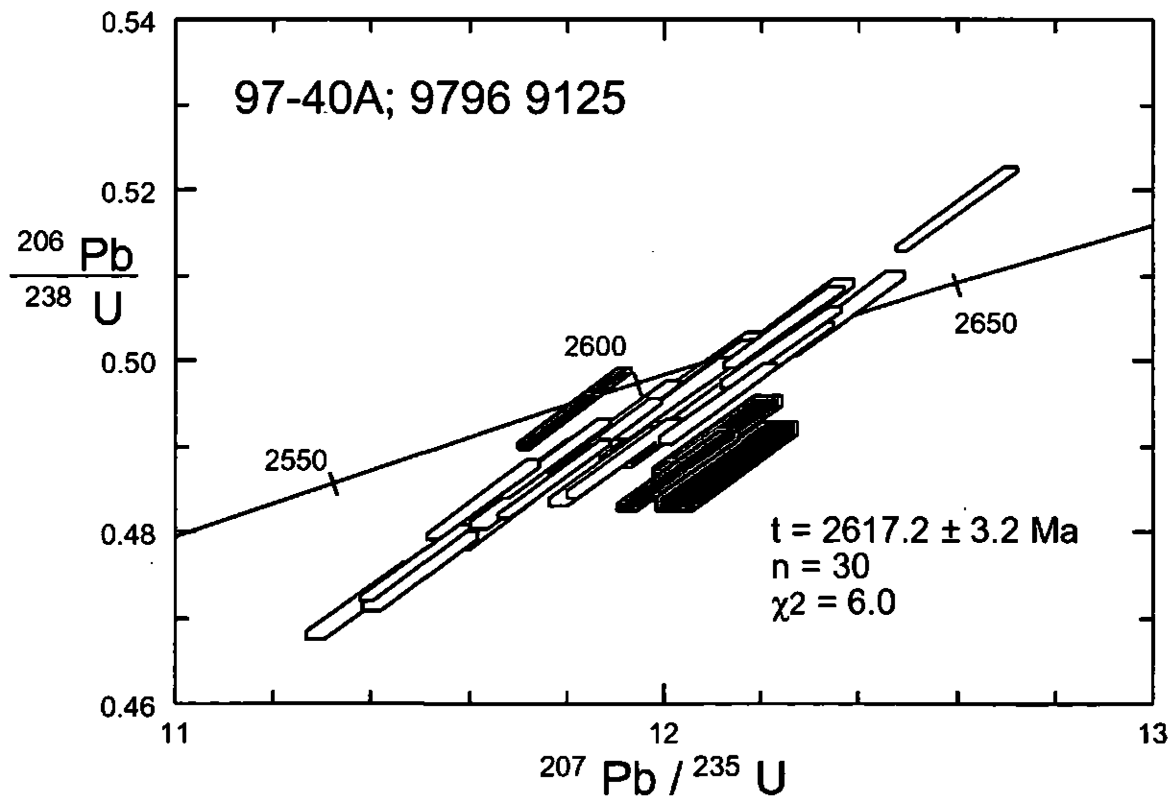

Figure z9796 9125b: Concordia plot of the main group of SHRIMP zircon data for the biotite monzogranite, Warren-2 (UWA mount 97-40A).

9796 9126: diorite, Proterozoic dyke

1:250,000 sheet:	Southern Cross (SH5016)
AMG:	658797.4 mE, 6562718.3 mN
Location:	The sample was hammered from blasted *in situ* boulders
Province:	Southern Cross
Description:	This is a moderately altered biotite-pyroxene-amphibole diorite that occurs as a 60 m wide dyke or small intrusion. It is characterised by sericitic, chloritic and pyritic alteration and contains abundant Fe-oxides. The rock type also occurs as thin fine-grained dykes to the north of this outcrop. The surrounding granitoid (9796 9125) is a moderately quartz-feldpsar porphyritic to seriate medium-coarse-grained biotite monzogranite, which is common throughout the Southern Cross-Kellerberrin-Bencubbin region.
Chemical group:	Proterozoic mafic dyke
Pluton No:	none given
UWA mount:	97-26B

Description of zircons

The zircon population in this sample consists of two distinctively different morphologic types. The first group is fine grained, dark to light brown in colour and is similar to many of the other Archaean zircons described in this report. The other group, however, is distinctive in that they consist of essentially structureless, colourless to pale brown grains which have a euhedral external shape and an aspect ratio of about 3. Inclusions in both types are rare and consist of opaque or rod-like to equant minerals. All inclusions occur throughout the grains and show no preference for core or rim regions.

Results and interpretation

Fifty one analyses on 48 grains are presented in Table z9796 9126 and shown on concordia diagrams in Figures z9796 9126a, b.. The data show considerable scatter with many of the grains being discordant. They fall into two distinct age groups at ~ 2.6 Ga and ~1.2 Ga.

Considering only concordant to near-concordant data, the Archaean grains form a statistically coherent group with an age of 2629±4 Ma (Fig. z9796 9126a). There is one older analysis at ~ 2.65 Ga (the core of grain #8), but this grain has two rim analyses which form part of the 2629 Ma group and it is clearly an older xenocryst with a magmatic overgrowth at 2629 Ma. All of the other grains which yield Archean $^{207}Pb/^{206}Pb$ ages are discordant but are morphologically indistinguishable from the 2629 Ma group and are considered to be grains of this age which have lost Pb mostly in Recent times. The discordant nature of most of these grains is compatible with the high U-contents (Table z9796 9126), radiation damage of the zircon structure with time and modern Pb-loss from the damaged areas of the grains.

The clear euhedral grains form a coherent data group (Fig. z9796 9126b), the most concordant of them giving indistinguishable ages which, when pooled, yield 1201±7 Ma. Many analyses of these grains have high U-contents and are discordant due to Recent Pb-loss. The morphology of these zircons is magmatic and as this is the youngest magmatic population in the rock, the emplacement age of the granitoid is taken to be 1201±7 Ma. The Archaean grains are therefore considered to be xenocrysts.

Table z9796 9126: SHRIMP zircon data for the diorite, Warrachupin Tank (UWA mount 97-26B).

grain-spot	U (ppm)	Th (ppm)	4f206 (%)	$^{207}Pb^*/^{206}Pb^*$	$^{208}Pb^*/^{206}Pb^*$	$^{206}Pb^*/^{238}U$	$^{207}Pb^*/^{235}U$	$^{208}Pb^*/^{232}Th$	conc. (%)	$^{207}Pb/^{206}Pb$ age (Ma)
Archaean, main group										
8-1	345	218	0.070	0.1770 ± 5	0.1755 ± 9	0.4664	11.381	0.1294	94	2625 ± 5
8-3	952	495	0.028	0.1775 ± 3	0.1437 ± 4	0.4904	12.000	0.1355	98	2629 ± 3
18-1	182	306	0.469	0.1776 ± 10	0.4948 ± 27	0.4699	11.506	0.1385	94	2630 ± 10
21-1	454	670	0.053	0.1774 ± 4	0.4313 ± 11	0.4743	11.599	0.1387	95	2629 ± 4
28-1	92	166	0.071	0.1767 ± 11	0.5010 ± 29	0.4973	12.115	0.1380	99	2622 ± 10
45-1	152	235	0.001	0.1787 ± 8	0.4245 ± 20	0.4971	12.252	0.1367	98	2641 ± 7
47-1	166	189	0.048	0.1780 ± 8	0.3180 ± 17	0.4863	11.938	0.1356	97	2635 ± 7
48-1	190	382	0.067	0.1772 ± 7	0.5719 ± 21	0.4876	11.914	0.1386	97	2627 ± 7
Proterozoic, main group										
2-1	517	467	0.050	0.0796 ± 5	0.2672 ± 13	0.2045	2.244	0.0604	101	1186 ± 11
3-1	558	1281	0.064	0.0800 ± 4	0.6745 ± 20	0.1965	2.168	0.0578	97	1197 ± 11
14-1	368	271	0.035	0.0800 ± 6	0.2238 ± 17	0.2013	2.221	0.0612	99	1198 ± 16
17-1	227	142	0.201	0.0793 ± 9	0.1857 ± 22	0.1965	2.150	0.0586	98	1181 ± 23
19-1	242	68	0.010	0.0807 ± 8	0.0836 ± 15	0.2068	2.301	0.0611	100	1214 ± 19
26-1	416	346	0.057	0.0801 ± 5	0.2452 ± 14	0.2040	2.253	0.0601	100	1199 ± 12
30-1	1229	2197	0.022	0.0802 ± 3	0.5305 ± 12	0.2038	2.255	0.0605	99	1203 ± 6
32-1	219	130	0.137	0.0789 ± 8	0.1721 ± 19	0.2046	2.226	0.0596	102	1171 ± 20
32-2	395	373	0.189	0.0800 ± 6	0.2838 ± 17	0.2005	2.211	0.0602	98	1197 ± 15
38-1	387	323	0.151	0.0804 ± 7	0.2358 ± 17	0.1999	2.217	0.0566	97	1207 ± 16
46-1	888	1445	0.023	0.0803 ± 3	0.4747 ± 13	0.2028	2.244	0.0591	99	1204 ± 8
49-1	784	1057	0.009	0.0799 ± 3	0.3913 ± 13	0.1951	2.151	0.0566	96	1195 ± 8
50-1	644	221	0.000	0.0809 ± 3	0.1032 ± 6	0.2017	2.251	0.0607	97	1220 ± 8
Archaean, discordant (>6%)										
1-1	1166	404	0.094	0.1747 ± 3	0.0905 ± 4	0.4005	9.648	0.1046	83	2603 ± 3
4-1	507	106	0.767	0.1715 ± 25	0.2786 ± 55	0.0361	0.852	0.0480	9	2572 ± 24
7-1	463	263	0.087	0.1768 ± 5	0.1665 ± 8	0.3458	8.430	0.1013	73	2623 ± 5
10-1	1398	1041	0.179	0.1599 ± 3	0.3488 ± 7	0.2950	6.502	0.1382	68	2454 ± 3
12-1	495	546	1.331	0.1775 ± 11	0.6828 ± 31	0.1924	4.708	0.1193	43	2629 ± 11
15-1	428	246	0.331	0.1767 ± 6	0.1845 ± 11	0.3534	8.608	0.1135	74	2622 ± 6
16-1	1718	635	0.357	0.1655 ± 3	0.1225 ± 5	0.2909	6.638	0.0964	66	2512 ± 3
23-1	151	144	0.270	0.1783 ± 10	0.3545 ± 24	0.3527	8.673	0.1314	74	2637 ± 10
25-1	369	334	1.366	0.1779 ± 10	0.3320 ± 23	0.3330	8.170	0.1223	70	2634 ± 9
33-1	324	169	0.176	0.1765 ± 7	0.2010 ± 13	0.2838	6.906	0.1092	61	2620 ± 6
39-1	725	465	0.534	0.1770 ± 7	0.3725 ± 16	0.1797	4.387	0.1044	41	2625 ± 6
40-1	487	183	0.594	0.1755 ± 12	0.2577 ± 25	0.1452	3.512	0.0998	33	2610 ± 11
42-1	768	344	0.361	0.1752 ± 6	0.2091 ± 11	0.2795	6.751	0.1306	61	2608 ± 6
51-1	695	277	0.878	0.1777 ± 11	0.4178 ± 27	0.1106	2.710	0.1159	26	2631 ± 11
Proterozoic, discordant and/or Pb-loss										
5-1	249	210	0.202	0.0799 ± 8	0.0968 ± 17	0.1903	2.097	0.0218	94	1195 ± 19
11-1	886	1717	0.025	0.0779 ± 3	0.5504 ± 15	0.1874	2.014	0.0532	97	1145 ± 8
13-1	1414	1276	0.039	0.0787 ± 2	0.2676 ± 8	0.1862	2.020	0.0552	95	1164 ± 6
20-1	832	1271	0.078	0.0794 ± 4	0.4557 ± 14	0.1814	1.986	0.0541	91	1182 ± 9
22-1	2013	4820	0.066	0.0792 ± 2	0.7079 ± 12	0.1769	1.932	0.0523	89	1177 ± 6
24-1	1683	4690	0.122	0.0745 ± 3	0.8201 ± 15	0.1654	1.698	0.0487	94	1054 ± 8
27-1	688	1580	0.084	0.0788 ± 4	0.6733 ± 18	0.1880	2.043	0.0551	95	1168 ± 10
29-1	1113	2289	0.438	0.0780 ± 4	0.6023 ± 16	0.1789	1.924	0.0524	92	1147 ± 11
31-1	269	196	0.172	0.0810 ± 8	0.2188 ± 20	0.1917	2.141	0.0576	93	1222 ± 20
34-1	1970	5913	0.079	0.0770 ± 2	0.9110 ± 15	0.1821	1.934	0.0553	96	1122 ± 6
35-1	635	964	0.083	0.0797 ± 4	0.4128 ± 15	0.1875	2.061	0.0510	93	1190 ± 10
36-1	1248	2672	0.420	0.0777 ± 5	0.6498 ± 19	0.1497	1.603	0.0454	79	1138 ± 13
37-1	1151	2468	0.024	0.0778 ± 3	0.6337 ± 14	0.1772	1.902	0.0524	92	1142 ± 7
44-1	925	1378	0.087	0.0801 ± 4	0.3954 ± 13	0.1851	2.045	0.0491	91	1200 ± 9
Archaean, statistical outliers										
8-2	533	927	0.027	0.1799 ± 4	0.5153 ± 10	0.5245	13.009	0.1553	103	2652 ± 3
9-1	985	1311	0.081	0.1700 ± 3	0.3699 ± 7	0.4625	10.841	0.1285	96	2558 ± 3

Data 20/10/97.
U/Pb scatter (1σ) for cz3 standard = 1.07% (n=17).

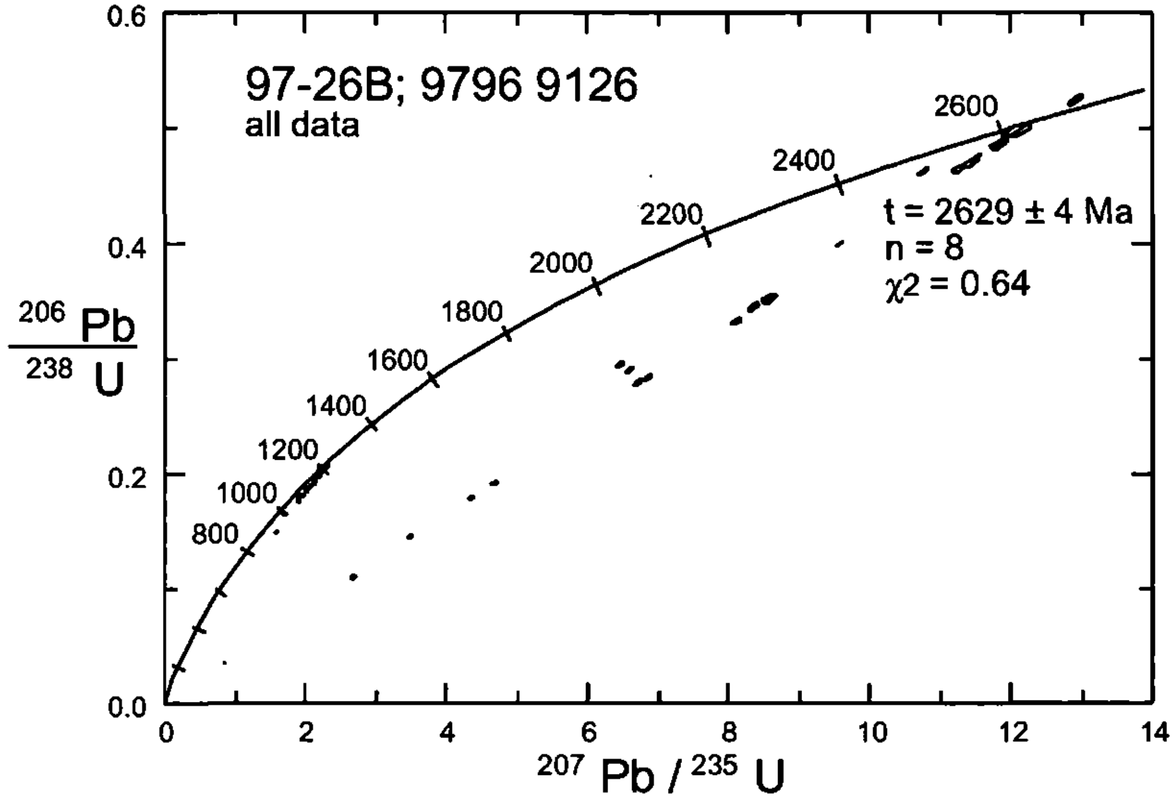

Figure z9796 9125a: Concordia plot of all SHRIMP zircon data for the Proterozoic diorite, Warrachupin Tank (UWA mount 97-26B).

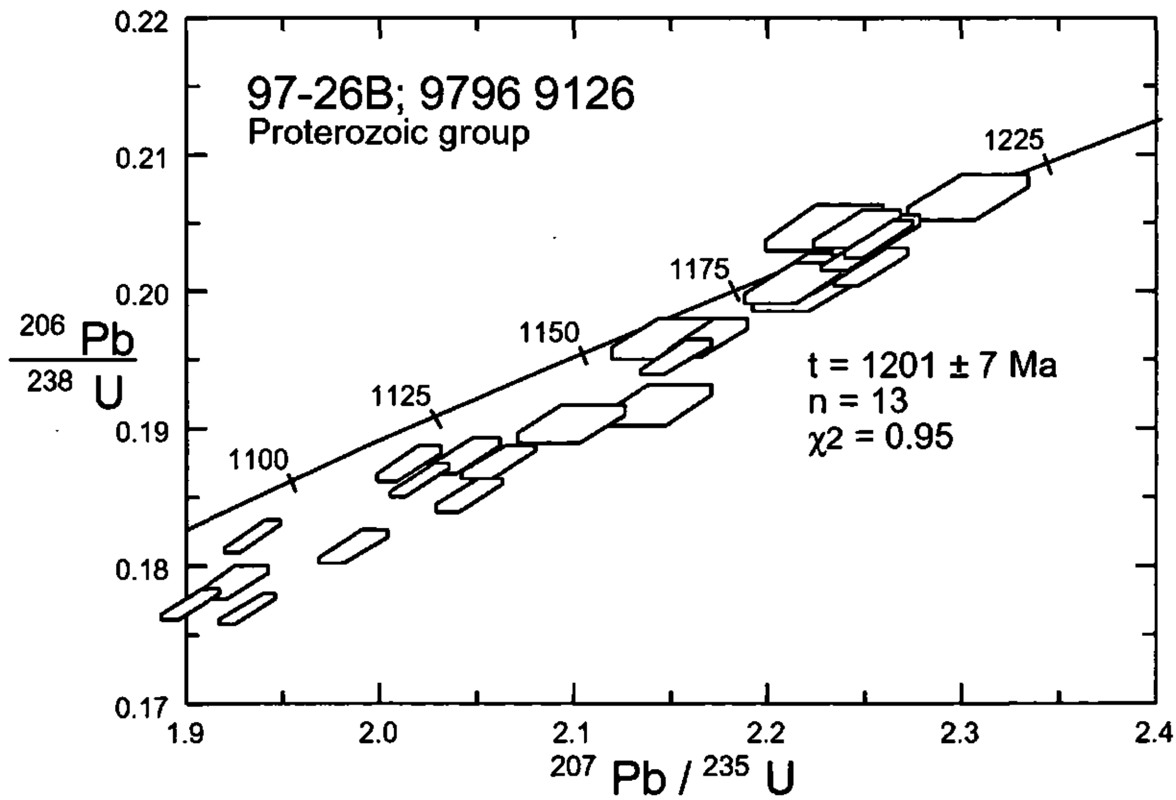

Figure z9796 9125b: Concordia plot of the Proterozoic group of SHRIMP zircon data for the Proterozoic diorite, Warrachupin Tank (UWA mount 97-26B).

9796 9138: biotite monzogranite, Waddouring

1:250,000 sheet:	Bencubbin (SH5011)
AMG:	582119.5 mE, 6575453.5 mN
Location:	Sample was hammered from a blasted boulder on the road near a large quarry.
Province:	Murchison
Description:	Moderately quartz-K-feldspar-porphyritic medium-grained biotite monzogranite. This granitoid type is typical of granitoids in the district, although is not as porphyritic or as coarse as sample 9796 9125. The outcrop contains minor pegmatite veins
Chemical group:	Low-Ca group, Goolthan association, Knungomen clan
Pluton No:	243614
UWA mounts:	97-24B (zircon) and 97-48B(titanite)

Description of zircons

The zircon population in this sample consists of one morphologic type but with a wide range of grain sizes (i.e. 30 - 200 μm long). Grains are typically euhedral to subhedral in external morphology with faint continuous euhedral internal zoning from core to rim. Inclusions are not common and mostly consist of rod-like minerals with minor opaque or equant grains. All inclusions occur throughout the grains and show no preference for core or rim regions. The grains range from clear to pale brown, to dark brown in colour. Discordant alteration patches, which are visible on SEM images, overgrow the euhedral zoning in some grains and are preferentially concentrated along the outer zones of grains, along specific growth zones and as irregular patches within the grains, often in close association with fractures. These patches were avoided during data collection.

Description of titanites

All recovered titanites are fragments of grains, and grain morphologies cannot be determined. In addition, there are generally no internal growth structures visible either optically or by SEM imaging. Occasionally there are faint compositional boundaries visible by SEM (BSE) imaging, but these have no distinct mineralogical form.

Some grains have regions which are spotted or clouded, presumably due to breakdown of crystal structure or the presence of sub-microscopic inclusions. These areas are avoided during analysis.

Results and interpretation

Zircon

Twenty nine analyses on 25 grains are presented in Table z9796 9138 and shown on a concordia diagram in Figure z9796 9138a and b. With the exception of five analyses, the common Pb corrections were low, even though all but one analysis had >300 ppm U and the zircons would be expected to have suffered element mobility subsequent to formation. The data falls largely along an array from the origin of the concordia diagram to ca. 2.63 Ga, with one reverse discordant analysis (Fig. z9796 9138a). Omitting all the discordant analyses, the population comprising the remaining 12 analyses in the concordant to near-concordant group (Fig. z9796 9138b) has a χ^2 of 1.8. This is interpreted as a single age population at 2628±3 Ma, although the larger than expected scatter in the data coupled with high U suggests this may be a minimum age. Nonetheless, if some of the data is affected by non-Recent Pb-loss, the zircon formation ages are probably not significantly older than this. No older ages are apparent and 2628±3 Ma is taken to be the emplacement age of the granitoid.

Titanite

Twenty-seven analyses on 26 grains of titanite are presented in Table t9796 9138 and shown on a concordia diagram in Figure t9796 9138. The analyses are interpreted as a single population of titanite at 2626±4 Ma, with a χ^2 of 1.43. Two analyses (9-1 and 20-1) are slightly younger and older, respectively, than the other analyses but cannot be omitted from the main group. The titanite age of 2626±4 Ma is within error of the SHRIMP zircon age of 2628±3 Ma.

Table t9796 9138: SHRIMP titanite data for the biotite monzogranite, Waddouring (UWA mount 97-48B).

grain-spot	U (ppm)	Th (ppm)	4f206 (%)	$^{207}Pb^*/^{206}Pb^*$	$^{208}Pb^*/^{206}Pb^*$	$^{206}Pb^*/^{238}U$	$^{207}Pb^*/^{235}U$	$^{208}Pb^*/^{232}Th$	conc. (%)	$^{207}Pb/^{206}Pb$ age (Ma)
1-1	256	382	0.499	0.1756 ± 8	0.3950 ± 20	0.5114	12.381	0.1352	102	2612 ± 8
1-2	270	226	0.476	0.1763 ± 9	0.2250 ± 17	0.5177	12.586	0.1394	103	2619 ± 8
1-3	303	241	0.369	0.1774 ± 7	0.2155 ± 14	0.5123	12.528	0.1388	101	2628 ± 7
10-1	288	240	0.276	0.1769 ± 8	0.2229 ± 15	0.5249	12.807	0.1406	104	2624 ± 7
11-1	261	213	0.386	0.1772 ± 9	0.2216 ± 17	0.5149	12.580	0.1398	102	2627 ± 8
12-1	284	236	0.310	0.1775 ± 8	0.2224 ± 16	0.5152	12.605	0.1381	102	2629 ± 8
13-1	351	284	0.354	0.1766 ± 8	0.2150 ± 15	0.5134	12.501	0.1363	102	2621 ± 7
14-1	280	289	0.380	0.1761 ± 9	0.2754 ± 19	0.5172	12.558	0.1380	103	2616 ± 8
15-1	282	230	0.325	0.1762 ± 8	0.2184 ± 16	0.5082	12.349	0.1361	101	2618 ± 8
17-1	295	238	0.384	0.1787 ± 9	0.2178 ± 19	0.5059	12.467	0.1363	100	2641 ± 9
18-1	274	226	0.326	0.1786 ± 8	0.2212 ± 16	0.5202	12.808	0.1397	102	2640 ± 8
19-1	306	237	0.261	0.1772 ± 8	0.2050 ± 15	0.5288	12.918	0.1401	104	2627 ± 7
2-1	304	233	0.444	0.1769 ± 8	0.2075 ± 16	0.5172	12.619	0.1399	102	2624 ± 8
2-2	278	221	0.411	0.1773 ± 9	0.2116 ± 17	0.5226	12.773	0.1393	103	2627 ± 8
20-1	109	157	0.622	0.1810 ± 19	0.3919 ± 43	0.5386	13.444	0.1465	104	2662 ± 17
21-1	349	273	0.263	0.1781 ± 9	0.2083 ± 17	0.5078	12.467	0.1350	100	2635 ± 8
23-1	338	286	0.250	0.1772 ± 7	0.2253 ± 13	0.5412	13.222	0.1439	106	2627 ± 6
24-1	204	398	0.257	0.1782 ± 9	0.5239 ± 25	0.5216	12.815	0.1402	103	2636 ± 9
25-1	298	235	0.354	0.1771 ± 9	0.2116 ± 17	0.5274	12.879	0.1416	104	2626 ± 8
26-1	286	255	0.271	0.1774 ± 8	0.2376 ± 15	0.5511	13.479	0.1474	108	2629 ± 7
28-1	333	260	0.208	0.1781 ± 8	0.2089 ± 15	0.5193	12.749	0.1387	102	2635 ± 7
29-1	300	236	0.274	0.1783 ± 8	0.2086 ± 15	0.5197	12.778	0.1375	102	2637 ± 7
3-1	297	237	0.455	0.1775 ± 8	0.2176 ± 16	0.5208	12.745	0.1420	103	2629 ± 8
31-1	292	236	0.262	0.1774 ± 8	0.2180 ± 17	0.5401	13.214	0.1458	106	2629 ± 8
7-1	267	221	0.829	0.1769 ± 10	0.2217 ± 21	0.5237	12.773	0.1401	103	2624 ± 10
8-1	282	322	0.487	0.1757 ± 9	0.3060 ± 19	0.5283	12.796	0.1418	105	2612 ± 8
9-1	284	229	0.526	0.1742 ± 9	0.2148 ± 18	0.5230	12.563	0.1394	104	2598 ± 8

Data 29/6/98.
U/Pb scatter (1σ) for Khan standard = 2.04% (n=11).
Common-Pb corrected using Cumming & Richards (1975) Model III @ 2630 Ma.

Table z9796 9138: SHRIMP zircon data for the biotite monzogranite, Waddouring (UWA mount 97-48B).

grain-spot	U (ppm)	Th (ppm)	4f206 (%)	$^{207}Pb^*/^{206}Pb^*$	$^{208}Pb^*/^{206}Pb^*$	$^{206}Pb^*/^{238}U$	$^{207}Pb^*/^{235}U$	$^{208}Pb^*/^{232}Th$	conc. (%)	$^{207}Pb/^{206}Pb$ age (Ma)
7-1	120	146	0.000	0.1788 ± 9	0.3445 ± 21	0.5100	12.571	0.1449	101	2642 ± 9
8-1	125	324	0.014	0.1781 ± 10	0.7066 ± 32	0.4843	11.889	0.1322	97	2635 ± 9
10-1	130	108	0.000	0.1778 ± 8	0.2161 ± 14	0.4972	12.189	0.1301	99	2632 ± 8
11-1	1016	227	0.010	0.1773 ± 3	0.0609 ± 3	0.5001	12.228	0.1364	99	2628 ± 3
11-2	1396	191	0.094	0.1770 ± 3	0.0620 ± 3	0.4852	11.843	0.2200	97	2625 ± 3
11-3	1150	406	0.224	0.1784 ± 3	0.1700 ± 6	0.5213	12.819	0.2507	103	2638 ± 3
24-1	247	492	0.000	0.1777 ± 6	0.5385 ± 18	0.4948	12.120	0.1336	98	2631 ± 6
32-1	1454	321	0.024	0.1772 ± 2	0.0603 ± 2	0.4982	12.170	0.1358	99	2627 ± 2
34-1	995	310	0.014	0.1770 ± 3	0.0997 ± 4	0.4910	11.981	0.1571	98	2625 ± 3
37-1	305	808	0.031	0.1768 ± 6	0.7276 ± 21	0.5038	12.282	0.1383	100	2623 ± 5
39-1	363	545	0.141	0.1775 ± 6	0.4188 ± 14	0.5188	12.701	0.1448	102	2630 ± 5
40-1	1141	494	0.014	0.1768 ± 3	0.1136 ± 3	0.5049	12.311	0.1327	100	2623 ± 3
Statistical outlier										
4-1	749	430	0.147	0.1710 ± 4	0.2054 ± 7	0.5116	12.064	0.1833	104	2568 ± 4
Discordant (>3%) and/or high common Pb.										
1-1	669	417	0.249	0.1770 ± 7	0.3071 ± 16	0.1662	4.054	0.0819	38	2625 ± 7
2-1	1048	344	0.835	0.1751 ± 5	0.0878 ± 9	0.4067	9.817	0.1089	84	2607 ± 5
3-1	1319	624	0.507	0.1767 ± 5	0.1995 ± 10	0.3313	8.070	0.1397	70	2622 ± 5
3-2	3342	858	2.777	0.1561 ± 8	0.6173 ± 20	0.1346	2.899	0.3237	34	2414 ± 8
5-1	421	227	0.225	0.1755 ± 8	0.2362 ± 17	0.2446	5.918	0.1070	54	2611 ± 8
6-1	568	301	0.157	0.1738 ± 5	0.1610 ± 9	0.3852	9.230	0.1169	81	2594 ± 5
9-1	1747	504	1.808	0.1754 ± 6	0.1257 ± 12	0.3131	7.574	0.1366	67	2610 ± 6
12-1	494	248	6.943	0.1746 ± 26	0.3657 ± 59	0.1667	4.015	0.1215	38	2602 ± 25
13-1	911	216	0.277	0.1718 ± 4	0.0814 ± 6	0.4559	10.797	0.1565	94	2575 ± 4
14-1	1351	697	0.069	0.1755 ± 3	0.1523 ± 5	0.4605	11.145	0.1359	94	2611 ± 3
15-1	734	1043	0.110	0.1774 ± 4	0.4300 ± 11	0.4331	10.593	0.1310	88	2629 ± 4
16-1	2951	1015	9.524	0.1843 ± 11	0.4180 ± 26	0.1878	4.774	0.2282	41	2692 ± 10
17-1	1284	554	0.867	0.1724 ± 5	0.1412 ± 10	0.3519	8.367	0.1152	75	2581 ± 5
18-1	999	488	0.117	0.1716 ± 3	0.1360 ± 5	0.4323	10.230	0.1203	90	2573 ± 3
18-2	1512	933	0.022	0.1616 ± 3	0.1679 ± 5	0.3921	8.738	0.1066	86	2473 ± 3
19-1	866	229	0.096	0.1775 ± 4	0.1002 ± 6	0.2867	7.019	0.1085	62	2630 ± 4
20-1	631	553	0.809	0.1766 ± 8	0.3781 ± 18	0.2787	6.784	0.1202	60	2621 ± 7
21-1	416	203	0.791	0.1762 ± 11	0.2305 ± 22	0.2160	5.247	0.1020	48	2617 ± 10
22-1	752	580	4.524	0.1772 ± 12	0.2897 ± 26	0.3917	9.568	0.1471	81	2626 ± 11
23-1	876	116	0.042	0.1773 ± 4	0.0408 ± 3	0.3967	9.697	0.1225	82	2628 ± 3
25-1	554	236	0.219	0.1732 ± 6	0.1409 ± 10	0.3876	9.257	0.1280	82	2589 ± 5
26-1	726	252	14.048	0.1792 ± 49	0.4559 ±115	0.0860	2.125	0.1130	20	2646 ± 46
27-1	185	119	0.117	0.1780 ± 9	0.2064 ± 17	0.5881	14.431	0.1891	113	2634 ± 9
28-1	475	396	6.296	0.1770 ± 17	0.3091 ± 38	0.3563	8.695	0.1320	75	2625 ± 16
29-1	896	313	0.057	0.1778 ± 3	0.0917 ± 4	0.4690	11.495	0.1230	94	2632 ± 3
30-1	246	162	2.996	0.1798 ± 26	0.4818 ± 61	0.1385	3.432	0.1014	32	2651 ± 24
31-1	225	296	0.581	0.1786 ± 10	0.4502 ± 25	0.4132	10.176	0.1412	84	2640 ± 9
33-1	156	194	0.497	0.1780 ± 10	0.3495 ± 24	0.4697	11.530	0.1317	94	2635 ± 10
35-1	384	133	1.225	0.1791 ± 9	0.1138 ± 18	0.4195	10.359	0.1378	85	2644 ± 9
36-1	222	129	0.077	0.1771 ± 8	0.1828 ± 14	0.4064	9.924	0.1280	84	2626 ± 7
38-1	405	178	2.545	0.1765 ± 15	0.2307 ± 33	0.2250	5.474	0.1184	50	2620 ± 14

Data 30/8/97.
U/Pb scatter (1σ) for cz3 standard = 1.07% (n = 13).

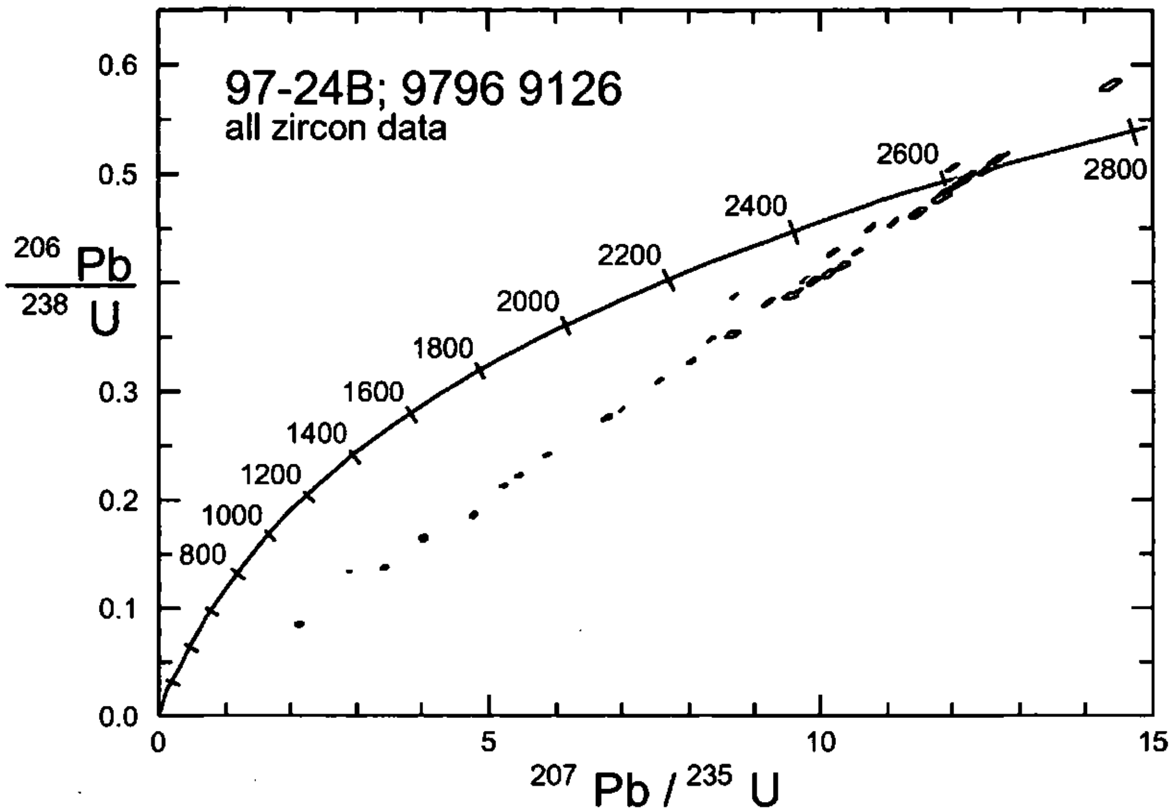

Figure z9796 9138a: Concordia plot of all SHRIMP zircon data from the biotite monzogranite, Waddouring (UWA mount 97-48B).

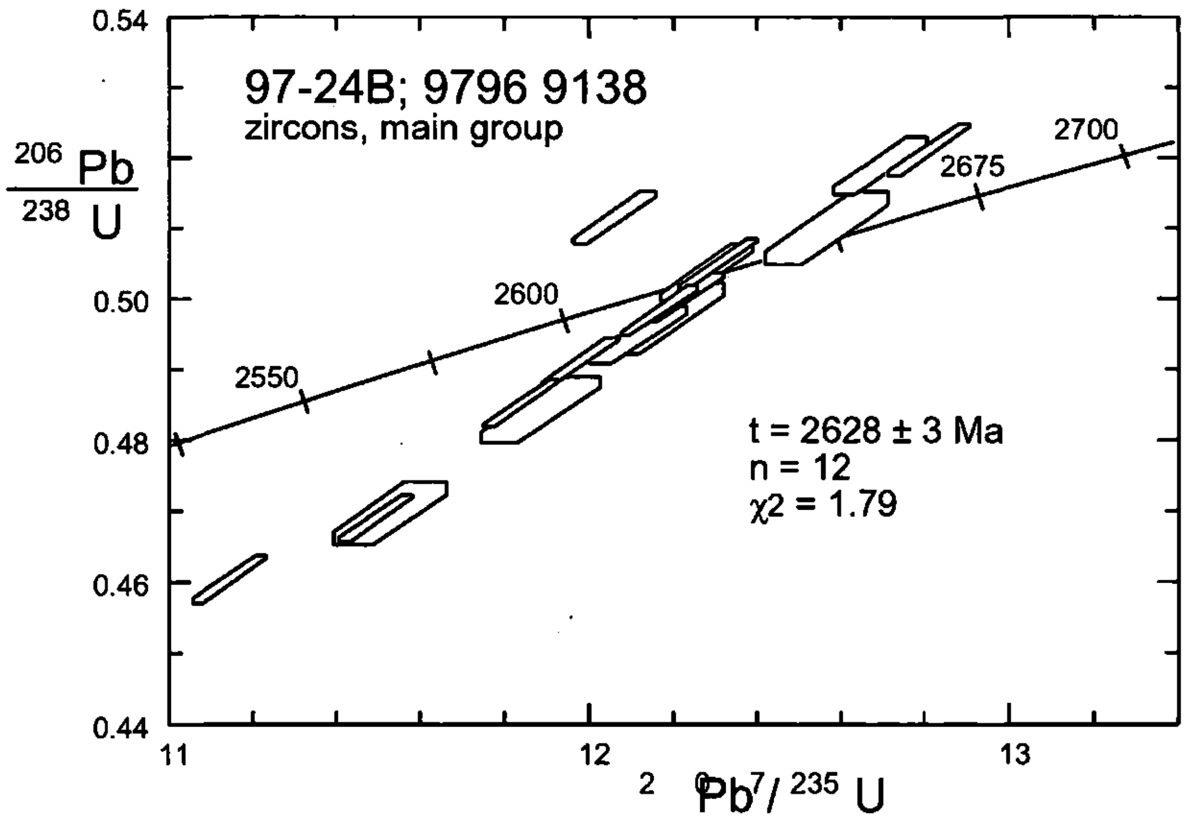

Figure z9796 9138a: Concordia plot of the main group of SHRIMP zircon data from the biotite monzogranite, Waddouring (UWA mount 97-48B).

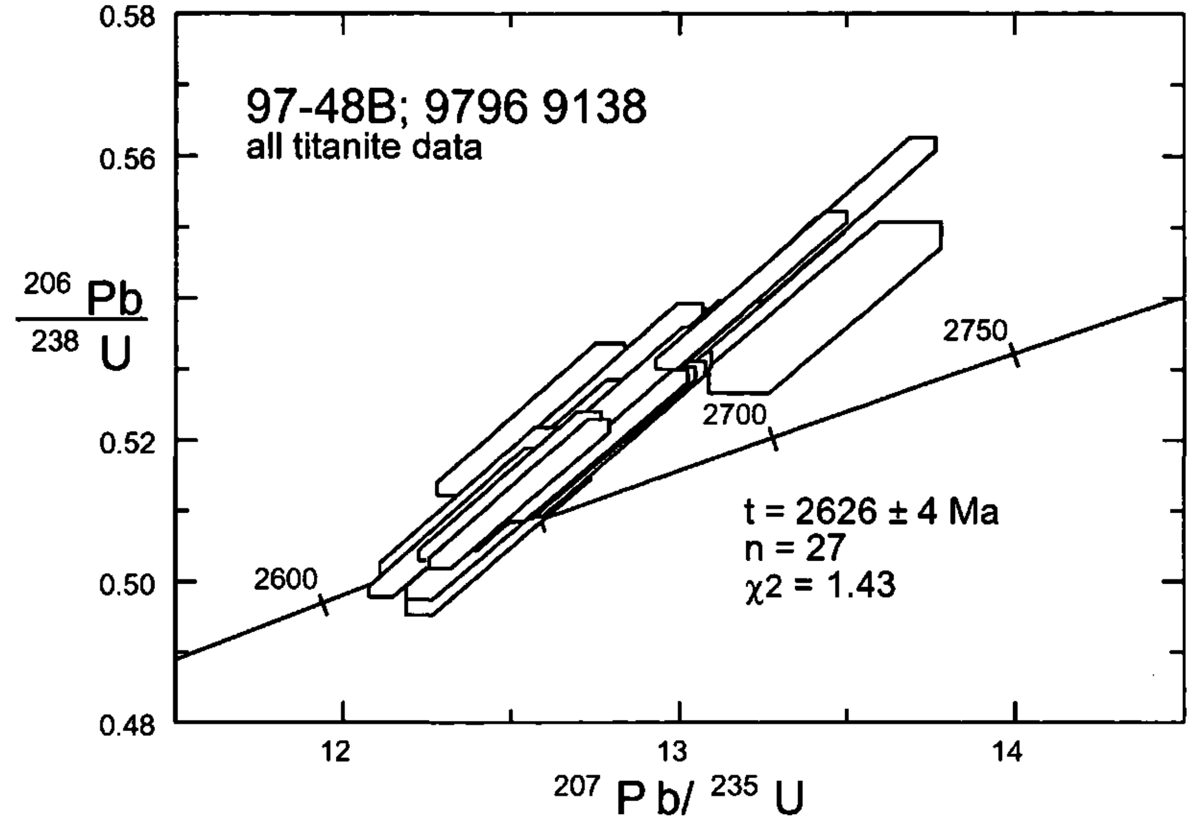

Figure t9796 9138: Concordia plot of all SHRIMP titanite data from the biotite monzogranite, Waddouring (UWA mount 97-48B).

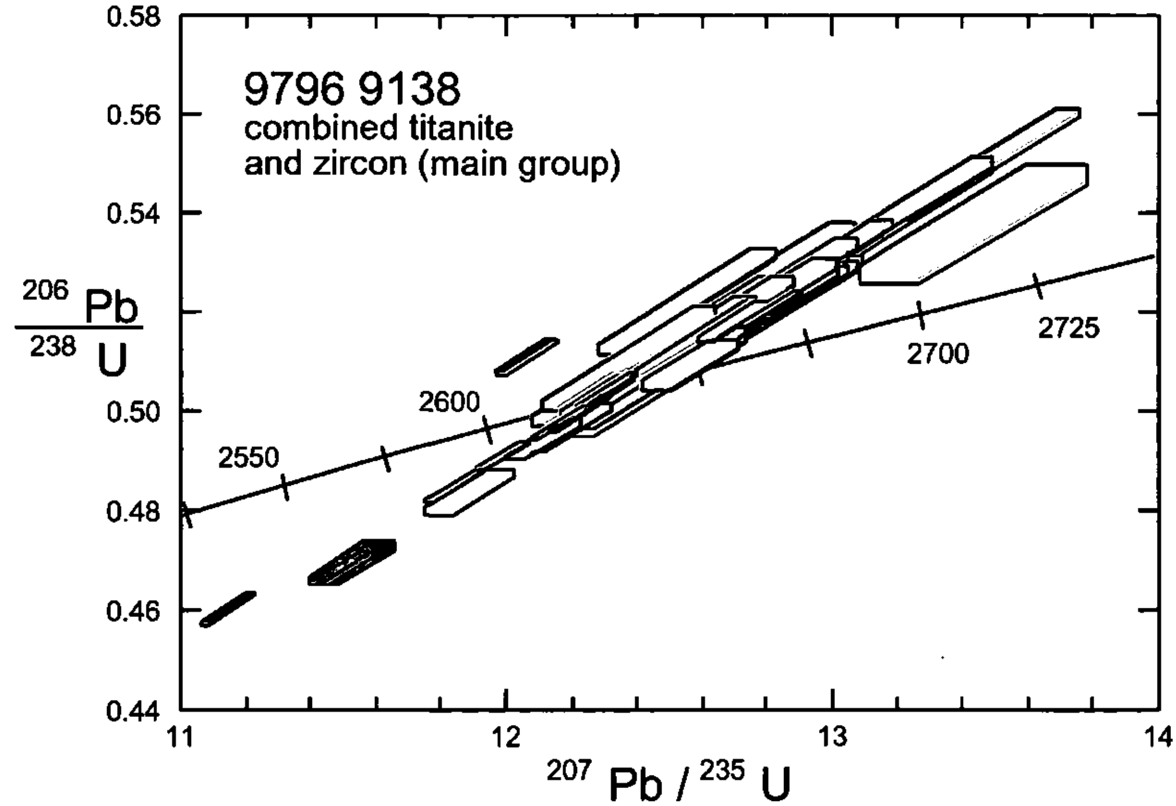

Figure c9796 9138: Combined SHRIMP zircon (main group only; unshaded and dark shaded) and titanite (light shaded) data from the biotite monzogranite, Waddouring (UWA mount 97-48B). Dark shaded zircon data are omitted from the age determination

9796 9201: biotite monzogranite, Tank No. 28

1:250,000 sheet:	Norseman (SI5102)
AMG:	383438.0 mE, 6393056.0 mN
Location:	Tank No. 28 granite, south of Scotia. Sample hammered from outcrop on the western edge of Lake Dundas.
Province:	Southern Cross
Description:	Sparsely feldspar-porphyritic fine-grained biotite monzogranite that contains rare quartz xenocrysts and amphibole xenoliths.
Chemical group:	Low-Ca group, Beetle association, Nargalyerin clan
Pluton No:	323203
UWA mount:	98-12B

Description of zircons

A large number of zircon grains from sample 9796-9201 were recovered, covering a large range in size, from small, equant fragments with rounded edges, as small as approximately 30 µm, up to elongate, euhedral grains over 200 µm long, to grains with characteristics between these two end-members. Colour and clarity also vary, from clear, pale yellow-white grains to pale brown and dark brown opaque grains. Most grains contain numerous inclusions although some grains are completely devoid. Apart from the inclusions, internal structures are generally not visible in the photos, although rare zoning and possible core-rim relationships may be present in some grains.

Results and interpretation

Thirty one analyses on 29 grains are presented in Table z9796 9201 and shown on a concordia diagram in Figure z9796 9201. Omitting all the discordant analyses, the population comprising the remaining 21 analyses in the concordant to near-concordant group has a χ^2 of 1.33. This is interpreted as a single population at 2623±7 Ma, although the larger than expected scatter in the data suggests that this may be a minimum age.

Table z9796 9201: SHRIMP zircon data for the biotite monzogranite, Tank No. 28, Lake Dundas (UWA mount 98-12B).

grain-spot	U (ppm)	Th (ppm)	4f206 (%)	$^{207}Pb^*/^{206}Pb^*$	$^{208}Pb^*/^{206}Pb^*$	$^{206}Pb^*/^{238}U$	$^{207}Pb^*/^{235}U$	$^{208}Pb^*/^{232}Th$	conc. (%)	$^{207}Pb/^{206}Pb$ age (Ma)
3-1	102	111	0.189	0.1783 ± 14	0.3031 ± 29	0.4944	12.154	0.1375	98	2637 ± 13
4-1	148	133	1.379	0.1751 ± 18	0.2456 ± 40	0.4916	11.871	0.1343	99	2607 ± 18
7-1	62	106	0.882	0.1761 ± 25	0.4797 ± 62	0.4960	12.042	0.1382	99	2616 ± 23
8-1	87	68	0.530	0.1736 ± 18	0.2042 ± 36	0.4915	11.766	0.1281	99	2593 ± 17
10-1	140	191	0.229	0.1777 ± 13	0.3655 ± 30	0.4968	12.170	0.1327	99	2631 ± 12
11-1	62	88	0.828	0.1766 ± 19	0.3883 ± 45	0.5121	12.469	0.1407	102	2621 ± 18
12-1	112	98	0.437	0.1741 ± 12	0.2309 ± 24	0.5150	12.359	0.1362	103	2597 ± 11
13-2	113	116	0.321	0.1766 ± 13	0.2865 ± 27	0.4970	12.103	0.1385	99	2621 ± 12
14-1	110	97	0.062	0.1789 ± 10	0.2404 ± 18	0.5049	12.452	0.1370	100	2642 ± 9
15-1	84	101	0.190	0.1747 ± 13	0.3296 ± 28	0.4928	11.869	0.1353	99	2603 ± 12
17-1	76	92	0.176	0.1784 ± 12	0.3355 ± 27	0.4948	12.170	0.1362	98	2638 ± 11
18-1	55	80	0.957	0.1786 ± 21	0.4090 ± 51	0.4982	12.269	0.1405	99	2640 ± 20
19-1	154	226	0.225	0.1774 ± 9	0.4070 ± 22	0.4998	12.223	0.1387	99	2628 ± 9
21-1	92	98	0.268	0.1774 ± 13	0.2961 ± 28	0.4927	12.054	0.1370	98	2629 ± 12
23-1	92	91	0.811	0.1754 ± 17	0.2811 ± 36	0.4809	11.632	0.1367	97	2610 ± 16
24-1	64	64	0.389	0.1736 ± 16	0.2654 ± 33	0.5099	12.209	0.1359	102	2593 ± 15
25-1	78	102	0.044	0.1779 ± 13	0.3627 ± 31	0.5081	12.465	0.1416	101	2634 ± 12
26-1	115	133	0.019	0.1775 ± 10	0.3136 ± 21	0.5091	12.460	0.1388	101	2630 ± 9
27-1	51	76	0.000	0.1760 ± 14	0.4083 ± 36	0.5131	12.450	0.1396	102	2615 ± 14
29-1	80	83	0.253	0.1762 ± 14	0.2814 ± 29	0.5094	12.378	0.1372	101	2618 ± 13
30-1	88	95	0.935	0.1767 ± 17	0.2932 ± 38	0.4848	11.810	0.1317	97	2622 ± 16
Discordant >5%.										
1-1	280	455	7.731	0.1616 ± 30	0.4930 ± 70	0.3852	8.582	0.1171	85	2472 ± 31
5-1	141	176	0.346	0.1762 ± 15	0.3773 ± 35	0.4478	10.876	0.1351	91	2617 ± 14
9-1	200	123	4.754	0.1704 ± 30	0.1921 ± 67	0.4094	9.618	0.1278	86	2561 ± 30
?Discordant 4-5%.										
2-1	101	121	1.126	0.1733 ± 22	0.3255 ± 49	0.4728	11.298	0.1287	96	2590 ± 21
13-1	58	46	0.388	0.1744 ± 20	0.2286 ± 41	0.4749	11.419	0.1355	96	2600 ± 19
16-1	176	83	0.534	0.1732 ± 10	0.1331 ± 20	0.4698	11.222	0.1329	96	2589 ± 10
20-1	152	134	0.033	0.1775 ± 9	0.2453 ± 18	0.4789	11.719	0.1338	96	2629 ± 9
22-1	123	124	0.043	0.1751 ± 11	0.2835 ± 23	0.4667	11.267	0.1316	95	2607 ± 10
28-1	45	65	1.335	0.1748 ± 28	0.4180 ± 66	0.4730	11.403	0.1379	96	2605 ± 26
?Young outlier										
18-2	64	79	0.647	0.1721 ± 19	0.3432 ± 43	0.4774	11.327	0.1344	98	2578 ± 18

Data 18/6/98 and 8/1/99.
U/Pb scatter (1σ) for cz3 standard = 0.96% (n=8) and 1.08% (n=8).

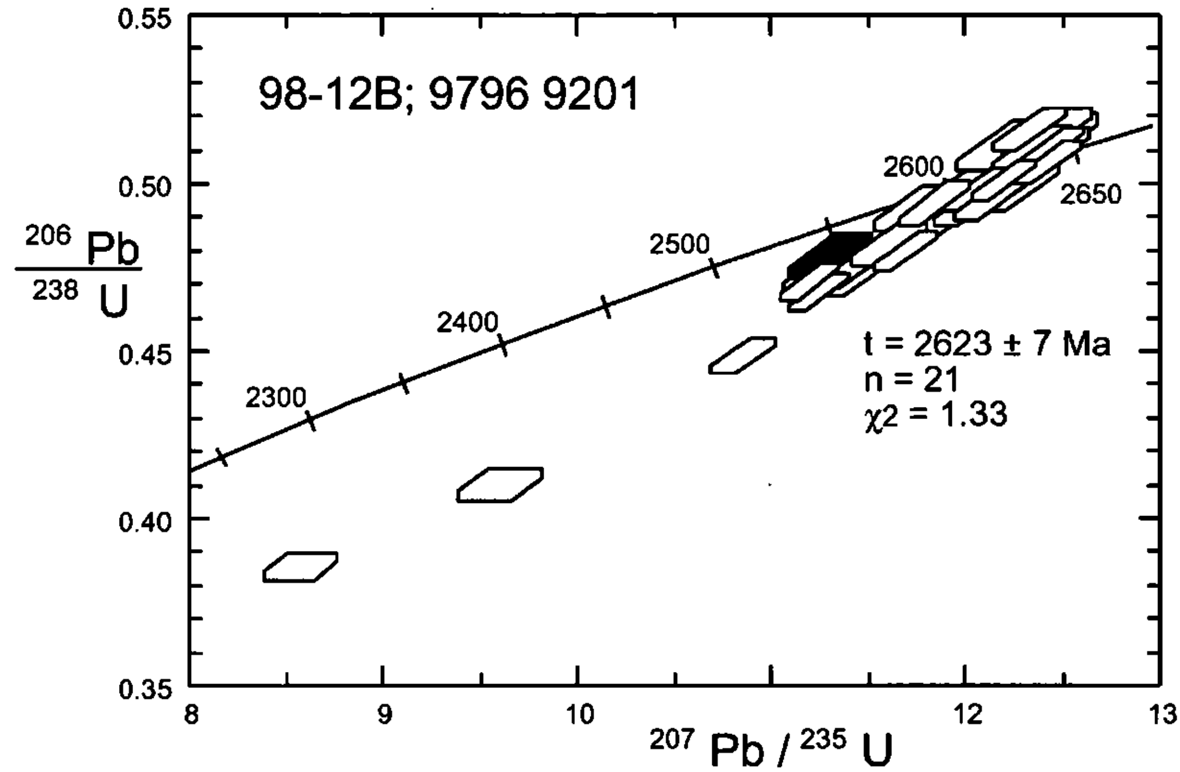

Figure z9796 9201: Concordia plot of all SHRIMP zircon data for the biotite monzogranite, Tank No. 28, Lake Dundas (UWA mount 98-12B). Shaded data are excluded from the age determination.

9796 9202: biotite monzogranite, McPherson

1:250,000 sheet:	Norseman (SI5102)
AMG:	370377.1 mE, 6406909.6 mN
Location:	Three Mile Rock, southwest of Norseman; sample drilled from outcrop.
Province:	Southern Cross
Description:	Foliated equigranular medium-grained biotite leuco-granodiorite. This outcrop is one of several High-Ca granitoids on the boundary between the Southern Cross Province and Eastern Goldfields Province.
Chemical group:	High-Ca group, Diemals association, Woolgangie clan
Pluton No:	323304
UWA mount:	97-40C

Description of zircons

Sample 9796-9202 contains a large number of generally euhedral to slightly rounded zircon grains and fragments, ranging from light to dark brown in colour. Most grains are slightly opaque, containing visible internal structures, but some grains are more translucent and clear. Typical grain size is about 75-100 μm with an aspect ratio of 2:1 (but ranging from 1:1 to more rarely 3:1). Some more irregular, anhedral fragments are also present in the population. Many grains are metamict and have well defined zoning. More complex internal features such as recrystallisation and distinct cores are observed in some SEM images. Occasional inclusions are also noted.

Results and interpretation

Ten analyses on 10 grains are presented in Table z9796 9202 and shown on a concordia diagram in Figure z9796 9202. The five oldest and most concordant analyses comprise a single age population with a pooled age of 2656±10 Ma, and a χ^2 of 0.47. This is interpreted as the emplacement age of the granitoid.

Table z9796 9202: SHRIMP zircon data for the McPherson biotite leuco-granodiorite, Three Mile Rock (UWA mount 97-40C).

grain-spot	U (ppm)	Th (ppm)	4f206 (%)	$^{207}Pb^*/^{206}Pb^*$	$^{208}Pb^*/^{206}Pb^*$	$^{206}Pb^*/^{238}U$	$^{207}Pb^*/^{235}U$	$^{208}Pb^*/^{232}Th$	conc. (%)	$^{207}Pb/^{206}Pb$ age (Ma)
38-1	104	101	0.058	0.1810 ± 11	0.2635 ± 22	0.5034	12.559	0.1367	99	2662 ± 10
39-1	160	62	0.653	0.1803 ± 10	0.1035 ± 19	0.4945	12.291	0.1333	98	2655 ± 9
42-1	314	275	0.315	0.1797 ± 6	0.2425 ± 12	0.5017	12.427	0.1387	99	2650 ± 6
45-1	178	93	0.175	0.1810 ± 9	0.1456 ± 15	0.4890	12.205	0.1371	96	2662 ± 8
46-1	100	106	0.004	0.1808 ± 11	0.2875 ± 23	0.5033	12.549	0.1371	99	2660 ± 10
Discordant or high common Pb										
37-1	154	194	2.097	0.1787 ± 16	0.3562 ± 36	0.4782	11.780	0.1356	95	2640 ± 15
40-1	217	92	0.959	0.1800 ± 11	0.1332 ± 21	0.4225	10.486	0.1324	86	2653 ± 10
41-1	181	151	3.779	0.1791 ± 22	0.3011 ± 49	0.3735	9.225	0.1354	77	2645 ± 20
43-1	202	101	4.160	0.1804 ± 19	0.1436 ± 41	0.4524	11.254	0.1301	91	2657 ± 17
44-1	135	130	3.950	0.1797 ± 22	0.2876 ± 50	0.4818	11.936	0.1439	96	2650 ± 21

Data 27/2/98.
U/Pb scatter (1σ) for cz3 standard = 1.00% (n=14 of 16).

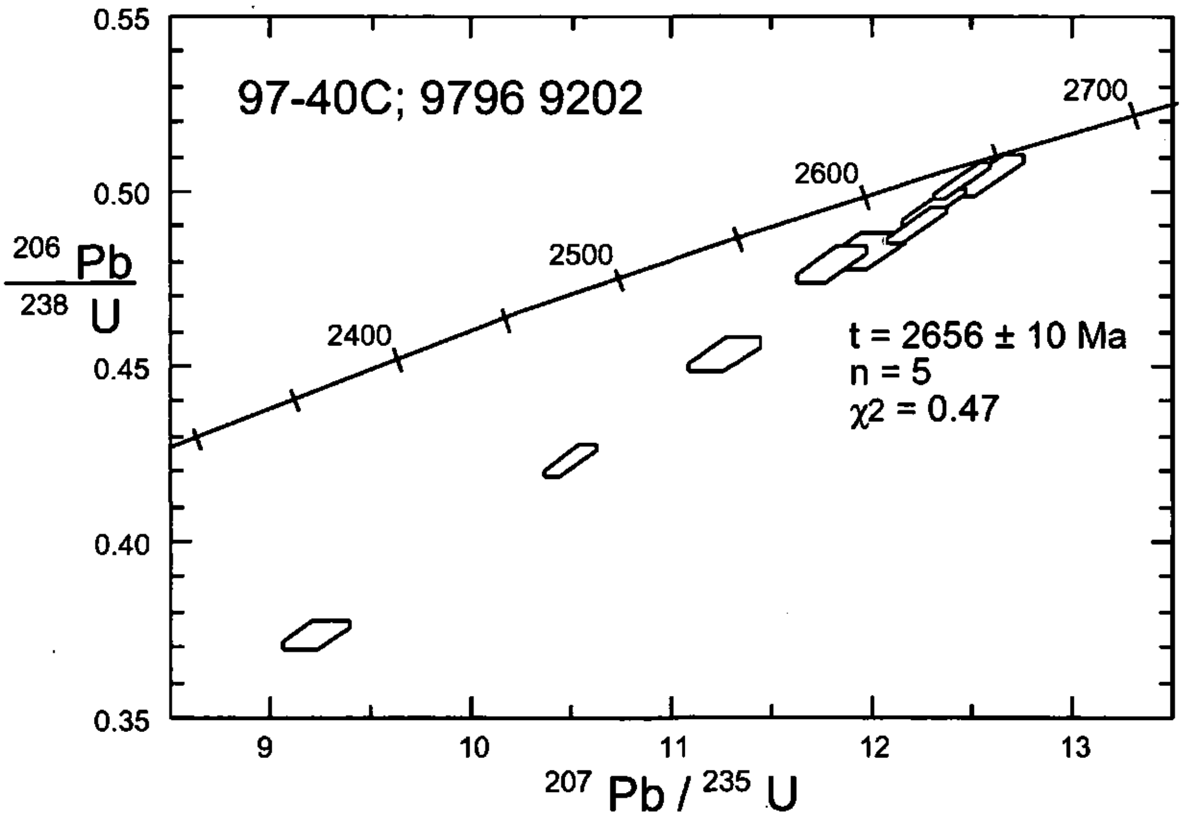

Figure z9796 9202: Concordia plot of SHRIMP zircon data for the McPherson biotite leuco-granodiorite, Three Mile Rock (UWA mount 97-40C). Shaded data are excluded from the age determination shown.

9796 9209: biotite monzogranite, Dundas Monzogranite

1:250,000 sheet:	Norseman (SI5102)
AMG:	383830.4 mE, 6415134.2 mN
Location:	Dundas Rocks; sample drilled from old blast site
Province:	Eastern Goldfields
Description:	Equigranular to sparsely K-feldspar-porphyritic medium-coarse grained biotite monzogranite
Chemical group:	Low-Ca group, Mt Boreas association, Mungari clan
Pluton No:	323308
UWA mount:	97-43A

Description of zircons

Sample 9796-9209 contains relatively large zircons (90-175 μm in length) with rare very large (>300 μm) grains present. Most grains and fragments are euhedral, although some do show slight rounding of external edges, with an aspect ratio of 2:1 to 3:1 (and rarely 4:1). Inclusions are present in some of the zircons. Many grains are pale to medium brown in colour although a lesser number of both lighter and darker coloured grains are also present. Both the transmitted and reflected light photos as well as the SEM images show the well zoned internal morphology of most grains. Some grains contain central regions of intense metamictisation, giving the appearance of a core-rim relationship, although the "core" may not necessarily represent an older xenocryst.

Results and interpretation

Thirteen analyses on 13 grains are presented in Table z9796 9209 and shown on a concordia diagram in Figure z9796 9209. The analyses show a wide scatter with major discordance. An approximate minimum age of ~2620 Ma can be estimated from the data. Further data and interpretation are unlikely to provide a reliable age estimate.

Table z9796 9209: SHRIMP zircon data for the biotite monzogranite, Dundas Rocks (UWA mount 97-43A).

grain-spot	U (ppm)	Th (ppm)	4f206 (%)	$^{207}Pb^*/^{206}Pb^*$	$^{208}Pb^*/^{206}Pb^*$	$^{206}Pb^*/^{238}U$	$^{207}Pb^*/^{235}U$	$^{208}Pb^*/^{232}Th$	conc. (%)	$^{207}Pb/^{206}Pb$ age (Ma)
1-1	1706	863	0.000	0.1680 ± 2	0.1616 ± 4	0.4133	9.574	0.1321	88	2538 ± 2
4-1	624	198	0.018	0.1684 ± 9	0.0957 ± 19	0.4517	10.489	0.1363	95	2542 ± 9
5-1	1260	55	0.004	0.1188 ± 6	0.0168 ± 9	0.1700	2.785	0.0660	52	1939 ± 8
6-1	1000	642	0.007	0.1384 ± 7	0.1929 ± 15	0.2455	4.684	0.0738	64	2207 ± 9
7-1	97	100	0.133	0.1762 ± 46	0.2937 ±104	0.7547	18.333	0.2153	139	2617 ± 43
8-1	861	556	0.009	0.1321 ± 9	0.1921 ± 19	0.2089	3.804	0.0621	58	2126 ± 12
9-1	2512	334	0.019	0.1154 ± 6	0.1040 ± 13	0.2907	4.626	0.2273	87	1886 ± 9
10-1	7268	1775	0.024	0.1234 ± 4	0.0935 ± 8	0.3079	5.239	0.1178	86	2006 ± 6
11-1	480	260	0.000	0.1778 ± 5	0.1504 ± 8	0.4956	12.150	0.1379	99	2632 ± 5
12-1	1092	505	0.056	0.1403 ± 15	0.1619 ± 33	0.2996	5.797	0.1048	76	2231 ± 18
13-1	1369	617	0.026	0.1018 ± 12	0.1545 ± 28	0.1435	2.014	0.0492	52	1657 ± 22
14-1	1106	230	0.022	0.0773 ± 14	0.0851 ± 31	0.1102	1.175	0.0452	60	1130 ± 36
15-1	1104	73	0.002	0.1611 ± 5	0.0227 ± 7	0.3364	7.474	0.1155	76	2468 ± 5

Data 27/8/98.
U/Pb scatter (1σ) for cz3 standard = 1.78% (n=14).

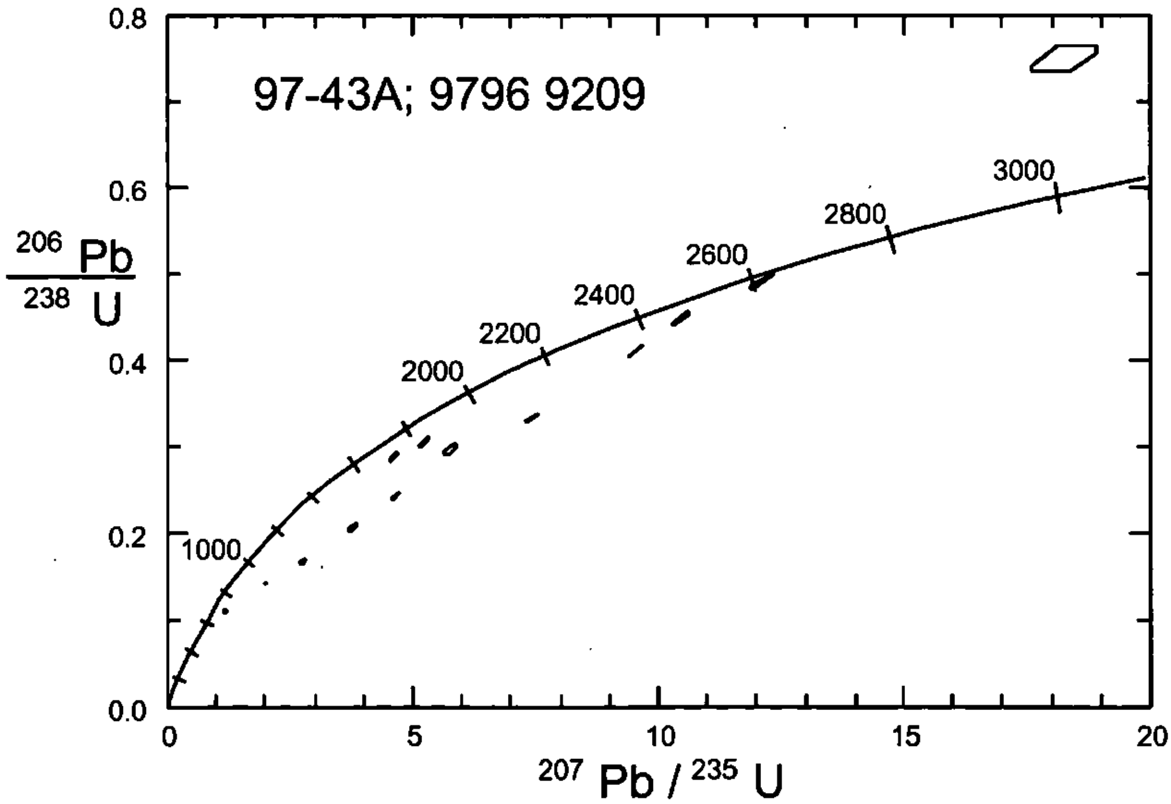

Figure z9796 9209: Concordia plot of all SHRIMP zircon data for the biotite monzogranite, Dundas Rocks (UWA mount 97-43A).

9796 9212: amphibole-bearing granitic gneiss, Lake Kirk

1:250,000 sheet:	Norseman (SI5102)
AMG:	378143.2 mE, 6419277.5 mN
Location:	Goodia Siding; sample drilled from recently blasted boulder.
Province:	Eastern Goldfields
Description:	Foliated recrystallised fine-medium grained amphibole-bearing granitic gneiss. The granitoid displays strongly recrystallised texture and a moderate foliation.
Chemical group:	High-Ca group, Menangina association, Burra clan
Pluton No:	323303
UWA mounts:	97-44B (zircon) and 98-72C (titanite)

Description of zircons

The majority of zircons from sample 9796 9212 are pale yellow in colour and are relatively clear, translucent grains and fragments. They are generally subhedral with a slightly rounded external form – no thin, elongate needles are present and only rare elongate stubby grains. Some darker brownish coloured grains are present but they do not make up a significant population. Inclusions are visible in a number of grains. Grain size varies from as little as 50 μm to over 180 μm. Internal features such as zoning and possible core-rim relationships are visible in the photos and confirmed in the SEM images. A significant amount of metamictisation and recrystallisation has occurred in many grains, as is reflected in the intense bright zones visible in some of the SEM images.

Description of titanites

The titanites from this sample are all 40-120 μm fragments of larger grains. Only rarely do grains show growth surfaces; most surfaces are fractures. The grains are dark brown to pale brown in colour. Some grains are almost black and have evenly distributed dense and very fine inclusion populations. Isolated inclusions are small and rare. Areas of SHRIMP analysis were in clean parts of the grains, avoiding inclusions and fractures.

Results and interpretation

Zircon

Twenty analyses on 20 grains are presented in Table z9796 9212 and shown on a concordia diagram in Figure z9796 9212. The analyses show a wide scatter with major discordance. A minimum age of ~2685 Ma can be estimated from these data. Further data and interpretation may improve the age estimate, but a definitive age probably cannot be determined from these zircons.

Titanite

24 analyses were obtained from 24 grains. The U-contents of average ~100 ppm and corrections for common Pb are generally small. The data form a relatively tight group, with almost all grains being concordant. Three analyses with 4f206>3% are omitted, as is one which is significantly discordant (shaded analyses in Figure t9796 9212). The remaining 24 analyses have a $\chi^2 = 0.94$ and are considered to be a single age population at 2631 ± Ma. The titanite records a significant event which is not seen at all in the zircon data. It is therefore most likely recording a metamorphic event, and is interpreted to be the time of

gneiss formation from a granitic protolith whose minimum magmatic age is ~2685 Ma, as recorded by the zircons.

Table z9796 9212: SHRIMP zircon data for the amphibole-bearing granitic gneiss, Lake Kirk (UWA mount 97-44B).

grain-spot	U (ppm)	Th (ppm)	4f206 (%)	$^{207}Pb^*/^{206}Pb^*$	$^{208}Pb^*/^{206}Pb^*$	$^{206}Pb^*/^{238}U$	$^{207}Pb^*/^{235}U$	$^{208}Pb^*/^{232}Th$	conc. (%)	$^{207}Pb/^{206}Pb$ age (Ma)
2-1	448	235	0.009	0.1831 ± 4	0.1395 ± 6	0.5032	12.704	0.1340	98	2681 ± 4
8-1	348	393	5.687	0.1820 ± 17	0.1318 ± 37	0.3725	9.346	0.0435	76	2671 ± 16
10-1	353	228	1.879	0.1753 ± 10	0.1276 ± 21	0.3388	8.191	0.0667	72	2609 ± 10
16-1	692	1098	11.108	0.1448 ± 31	0.2027 ± 71	0.1456	2.909	0.0186	38	2286 ± 37
18-1	262	316	1.890	0.1798 ± 14	0.1230 ± 29	0.4165	10.326	0.0424	85	2651 ± 13
19-1	408	120	1.306	0.1649 ± 9	0.0613 ± 18	0.3382	7.692	0.0706	75	2507 ± 10
22-1	582	476	13.600	0.1722 ± 30	0.1152 ± 67	0.2055	4.878	0.0289	47	2579 ± 29
23-1	859	1781	6.716	0.1505 ± 20	0.3467 ± 47	0.1473	3.057	0.0246	38	2352 ± 23
26-1	405	1044	3.327	0.1784 ± 14	0.1206 ± 29	0.2983	7.337	0.0139	64	2638 ± 13
27-1	420	638	13.102	0.1810 ± 26	0.1618 ± 59	0.3187	7.953	0.0340	67	2662 ± 24
28-1	379	381	1.244	0.1803 ± 10	0.1110 ± 20	0.3573	8.882	0.0394	74	2655 ± 9
29-1	656	514	2.446	0.1571 ± 11	0.0878 ± 22	0.2925	6.334	0.0328	68	2424 ± 11
30-1	353	312	1.595	0.1843 ± 9	0.1376 ± 19	0.4267	10.844	0.0663	85	2692 ± 8
31-1	310	95	0.023	0.1837 ± 5	0.0794 ± 6	0.5145	13.027	0.1327	100	2686 ± 4
33-1	352	166	1.707	0.1833 ± 10	0.1158 ± 21	0.4563	11.531	0.1121	90	2683 ± 9
34-1	697	2710	11.144	0.1756 ± 27	0.2806 ± 62	0.1731	4.191	0.0125	39	2612 ± 26
37-1	569	963	3.008	0.1652 ± 14	0.1428 ± 29	0.2381	5.422	0.0201	55	2509 ± 14
38-1	439	626	3.053	0.1834 ± 12	0.1880 ± 25	0.3718	9.401	0.0490	76	2684 ± 11
39-1	531	1156	4.399	0.1600 ± 15	0.1489 ± 33	0.2290	5.051	0.0157	54	2455 ± 16
40-1	445	710	7.105	0.1761 ± 24	0.1528 ± 53	0.2548	6.188	0.0244	56	2617 ± 23

Data 2/3/98.
U/Pb scatter (1σ) for cz3 standard = 1.70% (n=11 of 12).

Table t9796 9212: SHRIMP titanite data for the amphibole-bearing granitic gneiss, Lake Kirk (UWA mount 98-72C).

grain-spot	U (ppm)	Th (ppm)	4f206 (%)	$^{207}Pb^*/^{206}Pb^*$	$^{208}Pb^*/^{206}Pb^*$	$^{206}Pb^*/^{238}U$	$^{207}Pb^*/^{235}U$	$^{208}Pb^*/^{232}Th$	conc. (%)	$^{207}Pb/^{206}Pb$ age (Ma)
Main group.										
2-1	46	6	1.743	0.1752 ± 28	0.0256 ± 57	0.5157	12.461		103	2608 ± 27
3-1	67	13	0.678	0.1776 ± 19	0.0573 ± 36	0.5203	12.745	0.1552	103	2631 ± 17
4-1	146	71	0.538	0.1787 ± 11	0.1358 ± 22	0.5061	12.469	0.1410	100	2641 ± 10
5-1	139	96	0.468	0.1784 ± 11	0.1962 ± 24	0.5098	12.544	0.1452	101	2639 ± 10
6-1	162	22	0.386	0.1777 ± 10	0.0396 ± 17	0.5052	12.376	0.1441	100	2631 ± 9
7-1	35	2	2.126	0.1777 ± 37	0.0090 ± 77	0.5231	12.814		103	2631 ± 35
8-1	150	<2	0.467	0.1775 ± 10	0.0022 ± 16	0.5097	12.478		101	2630 ± 10
10-1	128	18	0.358	0.1789 ± 11	0.0403 ± 17	0.5125	12.640	0.1483	101	2643 ± 10
11-1	81	11	0.744	0.1792 ± 16	0.0425 ± 30	0.5098	12.596		100	2645 ± 15
12-1	68	11	2.169	0.1778 ± 27	0.0336 ± 55	0.4884	11.972		97	2632 ± 25
13-1	182	39	0.503	0.1772 ± 10	0.0611 ± 18	0.5056	12.353	0.1441	100	2627 ± 9
14-1	217	99	0.288	0.1760 ± 8	0.1222 ± 15	0.5167	12.537	0.1386	103	2615 ± 7
15-1	50	4	0.721	0.1818 ± 22	0.0238 ± 40	0.5045	12.646		99	2669 ± 20
16-1	14	<2	2.545	0.1828 ± 65	0.0299 ±137	0.5463	13.773		105	2679 ± 59
17-1	121	39	1.829	0.1761 ± 19	0.1069 ± 40	0.5259	12.771	0.1756	104	2617 ± 18
19-1	40	3	0.988	0.1815 ± 26	0.0248 ± 49	0.5158	12.912		101	2667 ± 24
20-1	101	28	0.511	0.1771 ± 13	0.0695 ± 25	0.5116	12.491	0.1269	101	2626 ± 12
21-1	27	5	2.052	0.1717 ± 39	0.0314 ± 80	0.5176	12.250		104	2574 ± 38
23-1	147	23	0.884	0.1775 ± 12	0.0445 ± 23	0.5151	12.607	0.1451	102	2630 ± 11
24-1	93	18	0.586	0.1776 ± 16	0.0546 ± 30	0.5038	12.340	0.1435	100	2631 ± 15
4f206>3% and highly discordant Pb/Th/U.										
1-1	35	32	3.628	0.1777 ± 48	0.0531 ±104	0.4912	12.036	0.0293	98	2632 ± 45
18-1	63	25	4.351	0.1793 ± 35	0.1581 ± 77	0.5492	13.574	0.2199	107	2646 ± 32
22-1	17	7	3.928	0.1712 ± 68	0.0278 ±147	0.5148	12.153		104	2570 ± 67
Young outlier.										
9-1	63	53	1.435	0.1722 ± 23	0.2311 ± 53	0.5136	12.196	0.1412	104	2579 ± 22

Data 05/06/99 and 07/06/99.

U/Pb scatter (1σ) for Khan standard = 0.64% (n = 6) and 1.75% (n = 7).

Common-Pb corrected using Cumming & Richards (1975) Model III @ 2640 Ma.

Th-related data are considered unreliable for Th <~10 ppm.

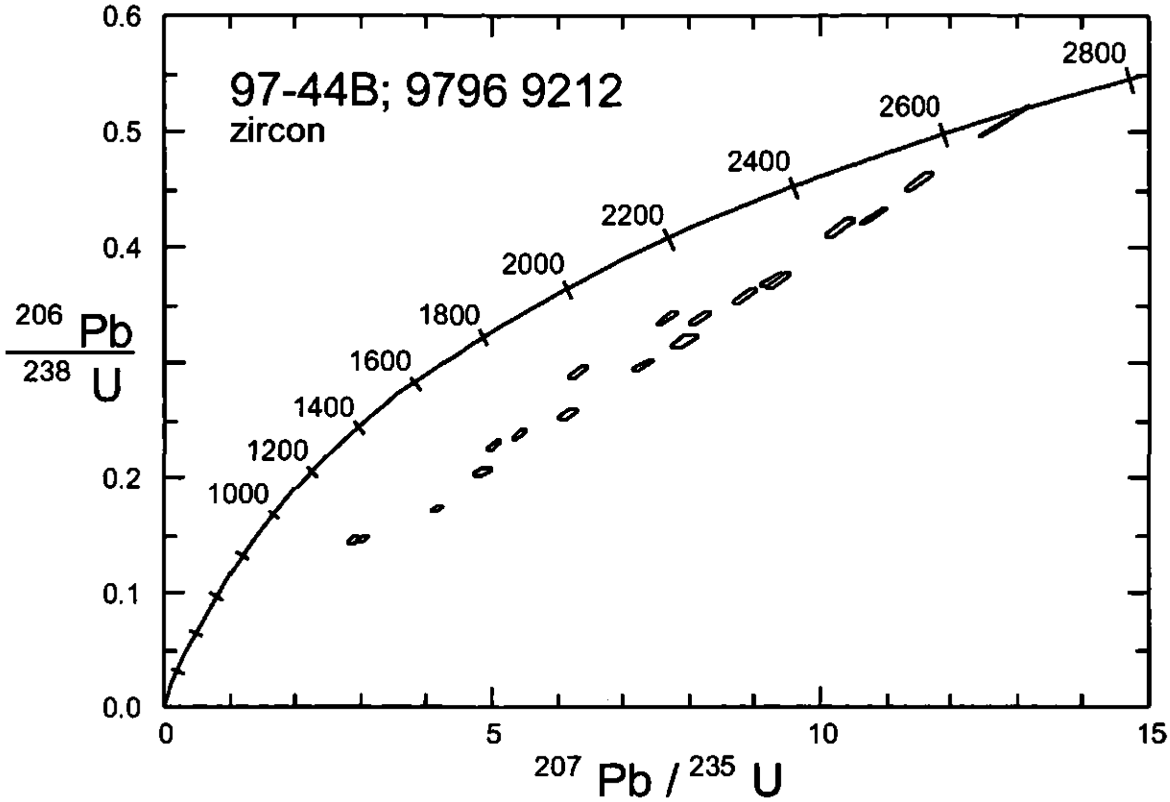

Figure z9796 9212: Concordia plot of all SHRIMP zircon data for the amphibole-bearing granitic gneiss, Lake Kirk (UWA mount 97-44B).

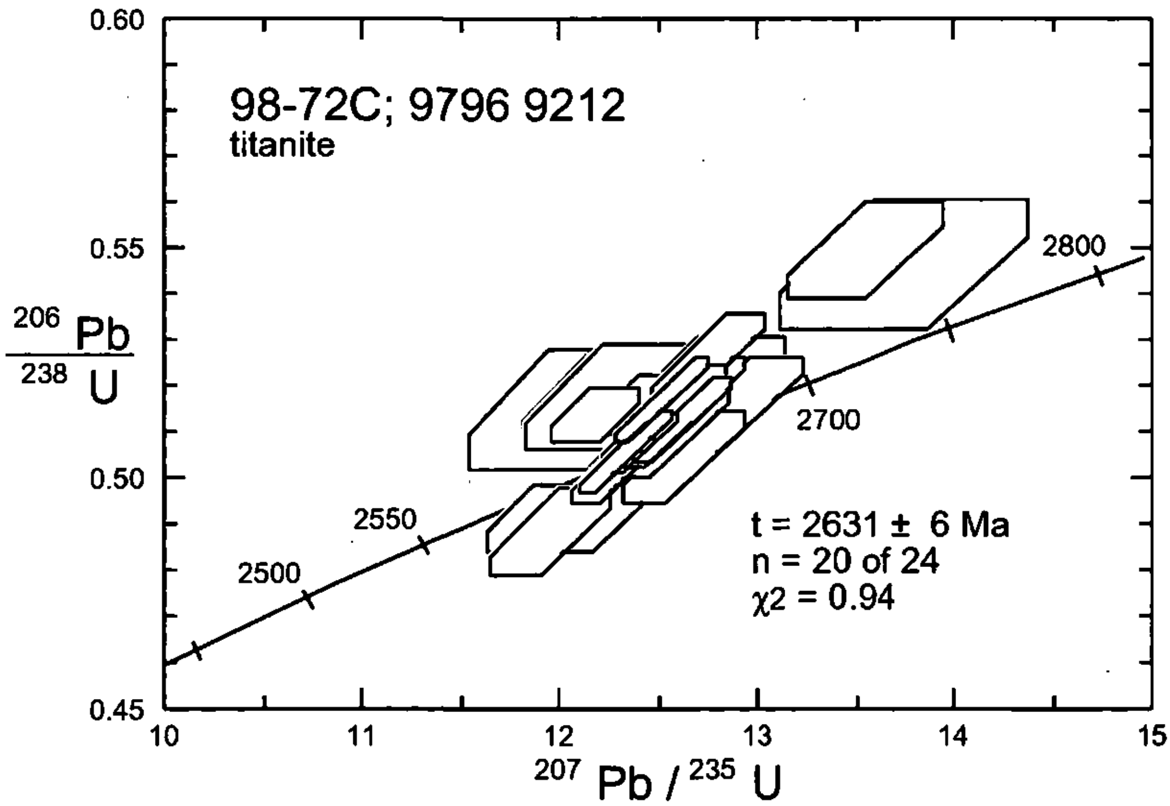

Figure t9796 9212: Concordia plot of SHRIMP titanite data for the amphibole-bearing granitic gneiss, Lake Kirk (UWA mount 98-72C).

9796 9223: biotite-hornblende granodiorite, Buldania

1:250,000 sheet:	Norseman (SI5102)
AMG:	408976.0 mE, 6449993.0 mN
Location:	Buldania Granite; sample drilled from blasted rocks on side of road.
Province:	Eastern Goldfields
Description:	Sparsely to moderately amphibole-K-feldspar porphyritic medium grained biotite-amphibole granodiorite.
Chemical group:	High-Ca group, Menangina association, Burra clan
Pluton No:	333301
UWA mount:	98-72B

Description of titanite

All recovered titanites are fragments of grains, and grain morphologies cannot be determined. In addition, there are generally no internal growth structures visible either optically or by SEM imaging. Occasionally there are faint compositional boundaries visible by SEM (BSE) imaging, but these have no distinct mineralogical form.

Some grains have regions which are spotted or clouded, presumably due to breakdown of crystal structure or the presence of sub-microscopic inclusions. These areas are avoided during analysis.

Results and interpretation

Twenty-three analyses on 23 grains are presented in Table t9796 9223 and shown on a concordia diagram in Figure t9796 9223. Omitting three discordant analyses, the population comprising the remaining 20 analyses in the concordant to near-concordant group has a χ^2 of 0.69. This is interpreted as a single age population at 2660±9 Ma. This age is taken to be the emplacement age of the granitoid.

Table t9796 9223: SHRIMP titanite data for the biotite-hornblende granodiorite, Buldania Rocks (98-72B).

grain-spot	U (ppm)	Th (ppm)	4f206 (%)	$^{207}Pb^*/^{206}Pb^*$	$^{208}Pb^*/^{206}Pb^*$	$^{206}Pb^*/^{238}U$	$^{207}Pb^*/^{235}U$	$^{208}Pb^*/^{232}Th$	conc. (%)	$^{207}Pb/^{206}Pb$ age (Ma)
1-1	44	279	1.585	0.1761 ± 24	1.7226 ±100	0.4939	11.991	0.1346	99	2616 ± 23
2-1	43	239	1.154	0.1809 ± 22	1.4621 ± 86	0.5009	12.498	0.1323	98	2662 ± 20
3-1	41	233	1.394	0.1823 ± 24	1.5244 ± 96	0.4910	12.344	0.1308	96	2674 ± 22
4-1	73	340	1.129	0.1801 ± 19	1.2480 ± 69	0.4986	12.377	0.1342	98	2653 ± 17
5-1	66	379	1.172	0.1814 ± 17	1.5664 ± 73	0.4870	12.180	0.1339	96	2666 ± 16
6-1	48	333	1.583	0.1811 ± 24	1.8792 ±104	0.5030	12.562	0.1355	99	2663 ± 22
7-1	74	274	1.035	0.1796 ± 16	0.9993 ± 53	0.5003	12.393	0.1354	99	2650 ± 15
8-1	39	214	1.395	0.1810 ± 25	1.4781 ± 95	0.4925	12.289	0.1324	97	2662 ± 23
10-1	71	309	0.848	0.1827 ± 16	1.1834 ± 59	0.4925	12.406	0.1342	96	2678 ± 14
11-1	83	296	1.224	0.1780 ± 17	0.9591 ± 53	0.4959	12.169	0.1337	99	2634 ± 16
13-1	52	367	1.041	0.1823 ± 20	1.9004 ± 97	0.4850	12.188	0.1305	95	2673 ± 18
15-1	54	283	1.105	0.1823 ± 21	1.4309 ± 84	0.4983	12.524	0.1362	97	2674 ± 20
16-1	58	287	1.278	0.1786 ± 21	1.3425 ± 78	0.4892	12.044	0.1321	97	2640 ± 20
17-1	60	295	1.105	0.1809 ± 18	1.3376 ± 70	0.4925	12.283	0.1348	97	2661 ± 16
18-1	54	469	1.105	0.1829 ± 21	2.3668 ±117	0.5017	12.652	0.1355	98	2679 ± 19
19-1	58	522	1.291	0.1806 ± 21	2.4693 ±118	0.4884	12.165	0.1343	96	2659 ± 19
20-1	54	280	1.280	0.1814 ± 22	1.3975 ± 83	0.4859	12.154	0.1313	96	2666 ± 20
21-1	75	336	1.051	0.1806 ± 19	1.2053 ± 68	0.4918	12.244	0.1319	97	2658 ± 17
22-1	62	321	0.821	0.1808 ± 20	1.3683 ± 77	0.4957	12.360	0.1308	98	2661 ± 18
23-1	70	385	1.084	0.1829 ± 20	1.4758 ± 80	0.4947	12.476	0.1337	97	2679 ± 18
Discordant; high common .Pb										
9-1	70	310	13.247	0.1845 ± 47	1.2004 ±123	0.6152	15.647	0.1662	115	2694 ± 42
12-1	69	342	2.417	0.1799 ± 25	1.4390 ± 86	0.4640	11.512	0.1342	93	2652 ± 23
14-1	68	307	4.236	0.1768 ± 30	1.2325 ± 91	0.5331	12.992	0.1456	105	2623 ± 29

Data 1/11/98.
U/Pb scatter (1σ) for Khan standard = 1.13% (n=12 of 13).
Common-Pb corrected using Cumming & Richards (1975) Model III @ 2650 Ma.

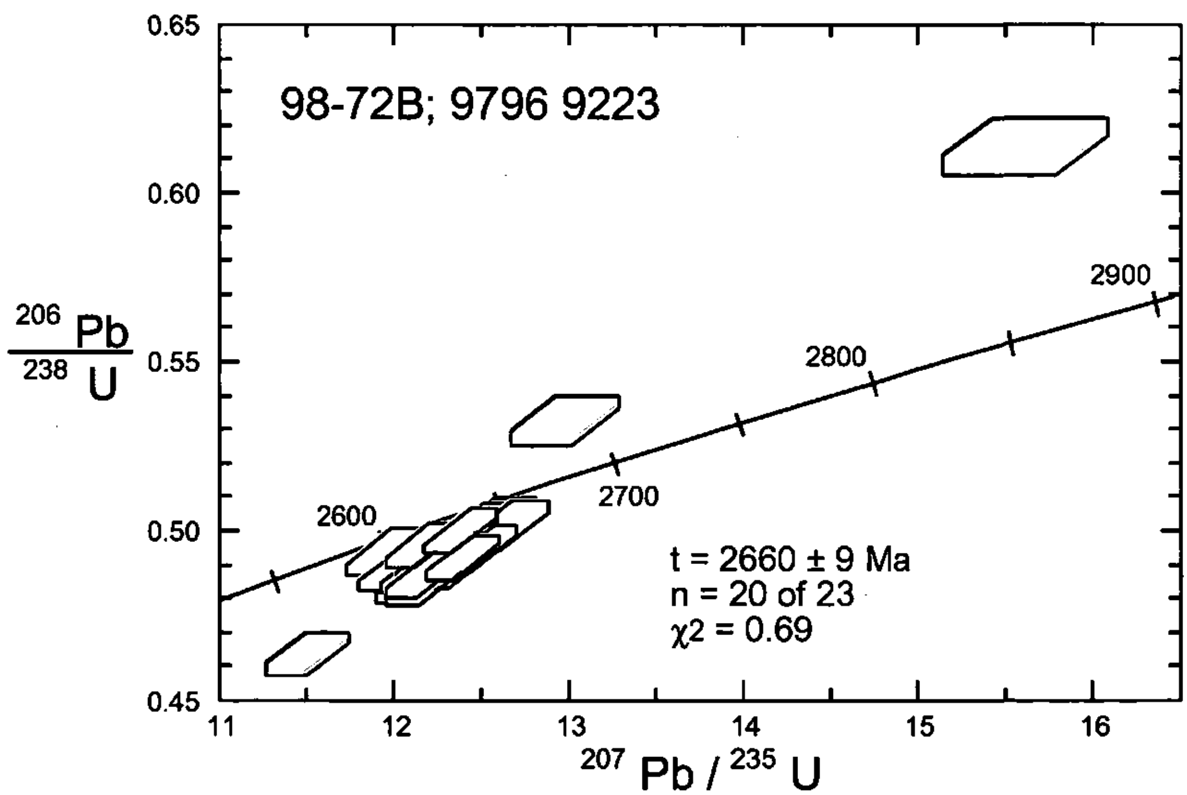

Figure t9796 9223: Concordia plot of SHRIMP titanite data for the biotite-hornblende granodiorite, Buldania Rocks (UWA mount 98-72B).

9796 9237: biotite monzogranite, Boojerbeenyer

1:250,000 sheet:	Norseman (SI5102)
AMG:	391208.0 mE, 6421101.1 mN
Location:	Boojerbeenyer Rock; sample drilled from old blast site.
Province:	Eastern Goldfields
Description:	Equigranular medium grained biotite monzogranite.
Chemical group:	Low-Ca group, Mt Boreas association, Mungari clan
Pluton No:	323310
UWA mount:	97-44C

Description of zircons

Only a relatively small number of zircons were recovered from sample 9796-9237. Two main morphologies are present: small (60-110 µm), euhedral, stubby prisms (aspect ratio ~ 2:1) and similar sized, slightly rounded, grains. Both populations range from translucent and pale yellow in colour to cloudy, darker grains with visible internal structures. Most grains are fractured and many contain zones of intense complex metamictisation and recrystallisation. Inclusions are present in some of the zircons.

Results and interpretation

Eight analyses on z9796 9237 grains are presented in Table 10 and shown on a concordia diagram in Figure z9796 9237. The analyses show a wide scatter with major discordance. The data suggest a minimum age of ~2625 Ma, with one possible inherited grain at >2800 Ma. It is unlikely that additional analyses would generate a reliable age.

Table z9796 9237: SHRIMP analytical data for the biotite monzogranite, Boojerbeenyer Rock (UWA mount 97-44C).

grain-spot	U (ppm)	Th (ppm)	4f206 (%)	$^{207}Pb^*/^{206}Pb^*$	$^{208}Pb^*/^{206}Pb^*$	$^{206}Pb^*/^{238}U$	$^{207}Pb^*/^{235}U$	$^{208}Pb^*/^{232}Th$	conc. (%)	$^{207}Pb/^{206}Pb$ age (Ma)
1-1	965	1597	22.810	0.1771 ± 16	0.3937 ± 38	0.6042	14.751	0.1438	116	2626 ± 15
2-1	9668	11998	0.313	0.1075 ± 1	0.1725 ± 3	0.2732	4.050	0.0380	89	1758 ± 2
3-1	456	399	29.499	0.1570 ± 42	0.2006 ± 95	0.3507	7.591	0.0804	80	2423 ± 45
4-1	248	266	0.070	0.1768 ± 6	0.2897 ± 12	0.5038	12.284	0.1358	100	2623 ± 5
8-1	466	235	5.423	0.1767 ± 12	0.1641 ± 26	0.5520	13.452	0.1798	108	2622 ± 11
12-1	14852	5676	0.011	0.1736 ± 1	0.1101 ± 1	0.5747	13.753	0.1655	113	2592 ± 1
14-1	201	189	2.431	0.2001 ± 20	0.2455 ± 43	0.3273	9.029	0.0856	65	2827 ± 16
17-1	195	207	1.246	0.1784 ± 13	0.3065 ± 28	0.4375	10.763	0.1262	89	2638 ± 12

Data 2/3/98.
U/Pb scatter (1σ) for cz3 standard = 1.70% (n=11 of 12).

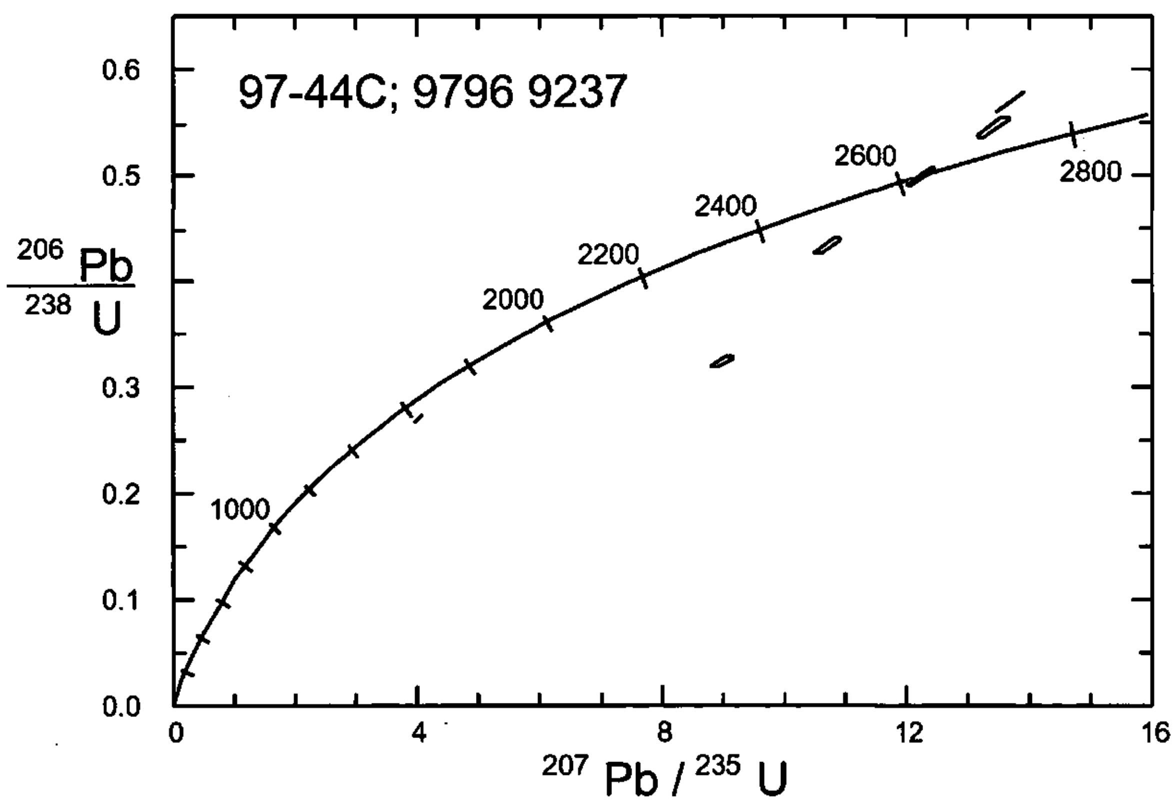

Figure z9796 9237: Concordia plot showing all SHRIMP analytical data for the biotite monzogranite, Boojerbeenyer Rock (UWA mount 97-44C). Data with 4f206>10% are not plotted.

9796 9243: hornblende granodiorite, Buldania-2

1:250,000 sheet:	Norseman (SI5102)
AMG:	399309.0 mE, 6435488.0 mN
Location:	Buldania Rocks; sample drilled from old blast site.
Province:	Eastern Goldfields
Description:	Foliated sparsely hornblende-K-feldspar porphyritic medium grained hornblende granodiorite.
Chemical group:	High-Ca group, Menangina association, Burra clan
Pluton No:	323311
UWA mount:	98-72A

Description of titanites

All recovered titanites are fragments of grains, and grain morphologies cannot be determined. In addition, there are generally no internal growth structures visible either optically or by SEM imaging. Occasionally there are faint compositional boundaries visible by SEM (BSE) imaging, but these have no distinct mineralogical form.

Some grains have regions which are spotted or clouded, presumably due to breakdown of crystal structure or the presence of sub-microscopic inclusions. These areas are avoided during analysis.

Results and interpretation

Twenty-two analyses on 22 fragments are presented in Table t9796 9243 and shown on a concordia diagram in Figure t9796 9243. Omitting two discordant analyses and a statistical outlier, the population comprising the remaining 19 concordant analyses has a χ^2 of 0.97. This is interpreted as a single age population at 2655 ± 6 Ma. This age is taken to be the emplacement age of the granitoid.

This titanite is within error of the SHRIMP titanite age of 2660±9 Ma obtained on another sample of the Buldania granodiorite (9796 9223).

Table t9796 9243: SHRIMP titanite data for the hornblende granodiorite, Buldania Rocks (UWA mount 98-72A).

grain-spot	U (ppm)	Th (ppm)	4f206 (%)	$^{207}Pb^*/^{206}Pb^*$	$^{208}Pb^*/^{206}Pb^*$	$^{206}Pb^*/^{238}U$	$^{207}Pb^*/^{235}U$	$^{208}Pb^*/^{232}Th$	conc. (%)	$^{207}Pb/^{206}Pb$ age (Ma)
1-1	152	393	1.738	0.1805 ± 12	0.7524 ± 34	0.5061	12.599	0.1471	99	2658 ± 11
2-1	170	373	0.674	0.1796 ± 8	0.5997 ± 23	0.5061	12.531	0.1387	100	2649 ± 8
4-1	89	666	1.415	0.1782 ± 16	2.1096 ± 81	0.4877	11.986	0.1370	97	2637 ± 15
5-1	116	565	0.809	0.1816 ± 11	1.3404 ± 46	0.5000	12.519	0.1372	98	2668 ± 10
6-1	90	25	1.137	0.1814 ± 15	0.0805 ± 28	0.5069	12.678	0.1464	99	2666 ± 13
8-1	92	465	1.161	0.1777 ± 14	1.3738 ± 55	0.4909	12.030	0.1332	98	2632 ± 13
9-1	80	435	1.573	0.1804 ± 17	1.5106 ± 66	0.4964	12.350	0.1386	98	2657 ± 16
10-1	70	443	1.571	0.1778 ± 18	1.7045 ± 75	0.4967	12.179	0.1330	99	2633 ± 17
11-1	119	476	0.938	0.1804 ± 12	1.0894 ± 42	0.5003	12.442	0.1365	98	2656 ± 11
12-1	58	415	1.420	0.1829 ± 18	1.9720 ± 87	0.4994	12.591	0.1374	97	2679 ± 17
13-1	69	503	1.402	0.1805 ± 17	2.0001 ± 81	0.5008	12.464	0.1378	98	2658 ± 15
14-1	106	477	0.836	0.1809 ± 12	1.2190 ± 45	0.4999	12.467	0.1360	98	2661 ± 11
15-1	56	397	1.846	0.1807 ± 22	1.8754 ± 93	0.5074	12.646	0.1335	99	2660 ± 20
16-1	172	393	0.680	0.1806 ± 9	0.6309 ± 25	0.5115	12.739	0.1415	100	2659 ± 8
17-1	45	355	1.777	0.1810 ± 25	2.1340 ±114	0.4910	12.251	0.1320	97	2662 ± 23
18-1	144	387	0.726	0.1796 ± 10	0.7340 ± 31	0.5100	12.628	0.1393	100	2649 ± 10
19-1	56	399	2.245	0.1801 ± 24	1.8653 ± 99	0.5125	12.728	0.1353	100	2654 ± 22
20-1	71	447	1.233	0.1832 ± 17	1.7171 ± 76	0.4959	12.528	0.1355	97	2682 ± 16
22-1	72	646	1.887	0.1765 ± 22	2.4004 ±115	0.4979	12.119	0.1335	99	2621 ± 21
Discordant										
3-1	133	567	1.859	0.1840 ± 15	1.2672 ± 52	0.4647	11.792	0.1380	91	2690 ± 14
7-1	146	629	0.954	0.1797 ± 13	1.1563 ± 46	0.4523	11.203	0.1211	91	2650 ± 12
Statistical outlier										
21-1	57	43	1.692	0.1752 ± 22	0.2009 ± 46	0.4922	11.890	0.1320	99	2608 ± 20

Data 1/11/98.
U/Pb scatter (1σ) for Khan standard = 1.13% (n=12 of 13).
Common-Pb corrected using Cumming & Richards (1975) Model III @ 2650 Ma.

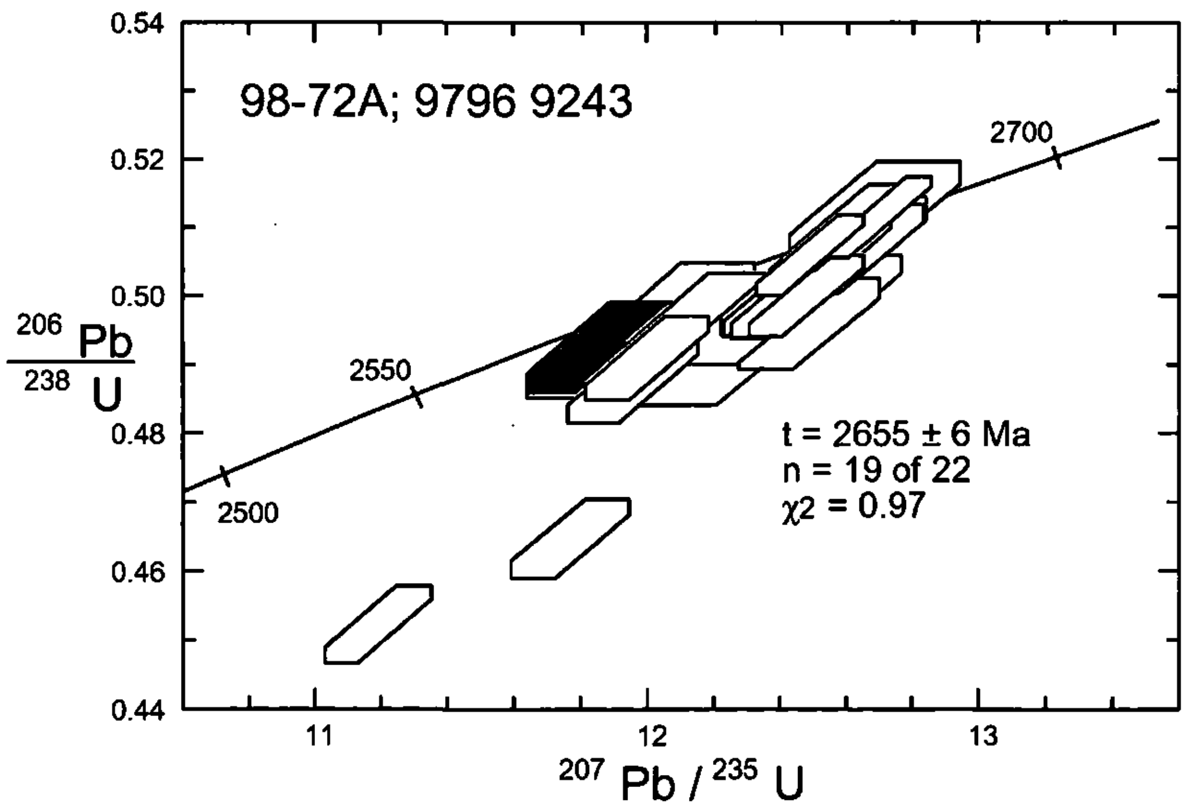

Figure t9796 9243: Concordia plot of SHRIMP titanite data for the hornblende granodiorite, Buldania Rocks (UWA mount 98-72A).

9796 9245: monzogranite, Tramways South

1:250,000 sheet:	Widgiemooltha (SH5114)
AMG:	421724.0 mE, 6465163.0 mN
Location:	Drilled from outcrop
Province:	Eastern Goldfields
Description:	Biotite monzogranite
Chemical group:	Low-Ca group, Mt Boreas association, Mungari clan
Pluton No:	333414
UWA mount:	97-49B

Description of zircons

The zircon population in this sample consists of one morphologic type of finely zoned euhedral grains, with most grains being 40-120 microns long, with a range of aspect ratios from ~2:1 to ~3-4:1. Grains are typically euhedral in external morphology with continuous euhedral internal zoning from core to rim. Inclusions are rare. The grains range from light brown to dark brown to nearly opaque in colour. Strong euhedral zoning observed on both optical and SEM images suggest high U-Th-contents and radiation damage. Discordant alteration patches are visible on SEM images of most grains, and overgrow the euhedral zoning. Some grains have more homogeneous core regions but there is no break in the euhedral growth from core to rim and they are not considered to be xenocrysts. Most grains have fracture networks typical of high-U grains, which have significant metamictisation. The alteration patches and fractures, and dark grains were avoided during data collection, leaving few grains and areas available for analysis.

Results and interpretation

Nine analyses on nine grains are presented in Table z9796 9245 and shown on a concordia diagram in Figure z9796 9245. The analyses show a wide scatter with major discordance, almost certainly reflecting both ancient and Recent Pb-loss. These zircons are considered undatable.

Table z9796 9245: SHRIMP zircon data for the monzogranite, Tramways South (UWA 97-49B).

grain-spot	U (ppm)	Th (ppm)	4f206 (%)	$^{207}Pb^*/^{206}Pb^*$	$^{208}Pb^*/^{206}Pb^*$	$^{206}Pb^*/^{238}U$	$^{207}Pb^*/^{235}U$	$^{208}Pb^*/^{232}Th$	conc. (%)	$^{207}Pb/^{206}Pb$ age (Ma)
1-1	2357	1356	0.024	0.1718 ± 2	0.1416 ± 3	0.4839	11.465	0.1191	99	2576 ± 2
2-1	2732	1413	1.176	0.1394 ± 4	0.1285 ± 9	0.3581	6.883	0.0890	89	2220 ± 5
3-1	1783	818	0.947	0.1247 ± 6	0.1412 ± 12	0.2428	4.176	0.0748	69	2025 ± 8
4-1	199	170	3.764	0.1751 ± 23	0.1305 ± 49	0.4594	11.089	0.0700	93	2607 ± 21
5-1	237	251	6.444	0.1780 ± 29	0.1967 ± 64	0.3792	9.307	0.0706	79	2634 ± 27
6-1	1518	466	0.818	0.1350 ± 5	0.0917 ± 11	0.2881	5.362	0.0862	75	2164 ± 7
7-1	114	103	0.932	0.1872 ± 19	0.2658 ± 40	0.4890	12.620	0.1438	94	2718 ± 16
8-1	2153	1519	2.297	0.1013 ± 9	0.2109 ± 20	0.1829	2.554	0.0546	66	1648 ± 16
9-1	1934	1346	1.115	0.1060 ± 6	0.1740 ± 14	0.2282	3.336	0.0571	76	1733 ± 10

Data 11/2/98.
U/Pb scatter (1σ) for cz3 standard = 1.10% (n=10 of 11).

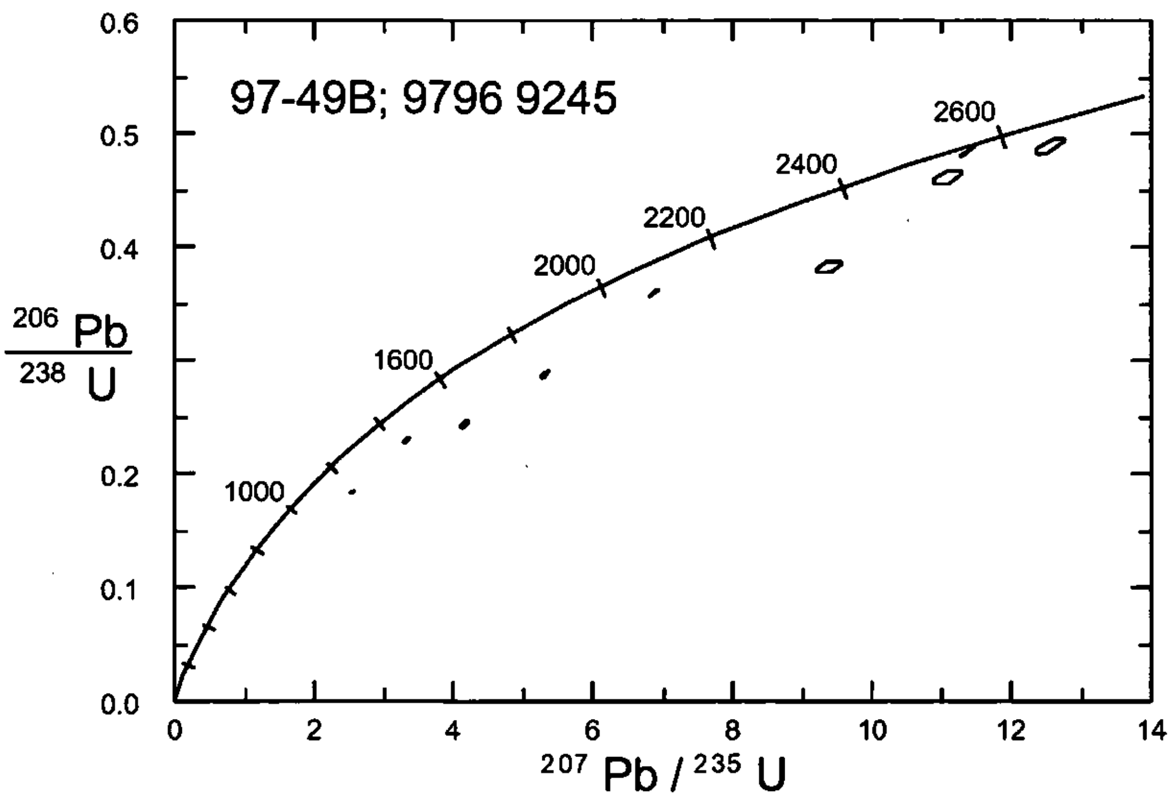

Figure z9796 9245: Concordia plot of SHRIMP analytical zircon for the monzogranite, Tramways South (UWA mount 97-49B).

9796 9248: hornblende-biotite monzogranite, Toil and Trouble

1:250,000 sheet:	Widgiemooltha (SH5114)
AMG:	419738.0 mE, 6472063.1 mN
Location:	Sample drilled from a large outcrop in regionally extensive granitoid south of Lake Cowan.
Province:	Eastern Goldfields
Description:	Sparsely quartz-feldspar porphyritic medium grained hornblende-biotite monzogranite.
Chemical group:	High-Ca group, Menangina association, Parker Hills clan
Pluton No:	33415
UWA mounts:	98-12A (zircon) and 98-72D (titanite)

Description of zircons

Grains and fragments ranging from approximately 70 to 250 μm in length are present in sample 9796 9248, with external morphologies ranging from elongate needles to stubby blocks and somewhat rounded equant fragments. Both very clear, transparent, pale yellow grains and much darker brown opaque grains are present in all morphologies. The transmitted and reflected light photos clearly show that zoning and core-rim relationships are present in a number of grains, as well as occasional inclusions and cracks/fractures.

Description of titanites

All recovered titanites are fragments of grains, and grain morphologies cannot be determined. In addition, there are generally no internal growth structures visible either optically or by SEM imaging. Occasionally there are faint compositional boundaries visible by SEM (BSE) imaging, but these have no distinct mineralogical form. Some grains have regions which are spotted or clouded, presumably due to breakdown of crystal structure or the presence of sub-microscopic inclusions. These areas are avoided during analysis.

Results and interpretation

Zircons
Nineteen analyses on 17 zircon grains are presented in Table z9796 9248 and shown on a concordia diagram in Figure z9796 9248. The data show a wide scatter from concordant and near-concordant analyses to major discordance. Omitting discordant analyses and zircons with high common-Pb, the population comprising the remaining 10 analyses in the concordant group has a χ^2 of 0.90. This is interpreted as a single age population at 2648 ± 11 Ma.

Titanites
Twenty analyses on 20 titanite fragments are presented in Table t9796 9248 and shown on a concordia diagram in Figure t9796 9248. The data are all concordant to near-concordant. Omitting titanites with high common-Pb and one discordant grain (6-1), the remaining 17 analyses in the concordant group has a χ^2 of 0.93. This is interpreted as a single age population at 2652±14 Ma.

The zircon and titanite ages of 2648±11 and 2652±14 Ma are within error and give a weighted mean, interpreted as the emplacement age, of 2649 ± 9 Ma.

Table z9796 9248: SHRIMP analytical data for zircons from the Toil and Trouble hornblende-biotite monzogranite (UWA mount 98-12A).

grain-spot	U (ppm)	Th (ppm)	4f206 (%)	$^{207}Pb^*/^{206}Pb^*$	$^{208}Pb^*/^{206}Pb^*$	$^{206}Pb^*/^{238}U$	$^{207}Pb^*/^{235}U$	$^{208}Pb^*/^{232}Th$	conc. (%)	$^{207}Pb/^{206}Pb$ age (Ma)
1-1	22	n.d.	0.120	0.1813 ± 36	0.0033 ± 64	0.5263	13.156	n.d.	102	2665 ± 32
3-1	123	94	2.562	0.1801 ± 22	0.2130 ± 47	0.5163	12.823	0.1430	101	2654 ± 20
5-1	97	64	3.682	0.1749 ± 28	0.1736 ± 62	0.5113	12.332	0.1342	102	2605 ± 27
8-1	128	187	3.884	0.1826 ± 29	0.4165 ± 66	0.4998	12.583	0.1430	98	2676 ± 26
9-1	72	41	1.763	0.1827 ± 25	0.1454 ± 52	0.5070	12.769	0.1286	99	2677 ± 23
10-1	294	18	0.658	0.1781 ± 10	0.0303 ± 17	0.4992	12.262	0.2406	99	2636 ± 9
12-1	79	83	0.323	0.1808 ± 16	0.2841 ± 33	0.4995	12.447	0.1350	98	2660 ± 14
15-1	113	118	2.322	0.1789 ± 23	0.2803 ± 51	0.5176	12.764	0.1388	102	2642 ± 21
15-2	154	132	0.172	0.1794 ± 10	0.2342 ± 19	0.5235	12.952	0.1433	103	2648 ± 9
16-1	81	79	0.686	0.1810 ± 20	0.2658 ± 42	0.5053	12.608	0.1369	99	2662 ± 18
Discordant										
2-1	636	269	0.582	0.1751 ± 6	0.1138 ± 11	0.4297	10.373	0.1156	88	2607 ± 6
4-1	85	45	1.642	0.1813 ± 40	0.1449 ± 84	0.4072	10.180	0.1109	83	2665 ± 37
6-1	675	157	2.859	0.1608 ± 12	0.0661 ± 26	0.3595	7.971	0.1020	80	2464 ± 13
7-1	8393	3766	0.084	0.1808 ± 1	0.1214 ± 2	0.5705	14.220	0.1543	109	2660 ± 1
7-2	2979	976	0.094	0.1862 ± 2	0.0844 ± 3	0.5967	15.322	0.1538	111	2709 ± 2
11-1	954	264	0.446	0.1334 ± 5	0.1026 ± 10	0.2897	5.328	0.1074	77	2143 ± 7
13-1	1083	196	0.877	0.1711 ± 5	0.0552 ± 10	0.4328	10.208	0.1318	90	2568 ± 5
14-1	203	131	16.963	0.1812 ± 49	0.1984 ±111	0.4386	10.955	0.1348	88	2664 ± 45
High common Pb										
17-1	139	97	8.801	0.1800 ± 40	0.1999 ± 90	0.5052	12.540	0.1446	99	2653 ± 37

Data 18/6/98.
U/Pb scatter (1σ) for cz3 standard = 0.96% (n=8 of 9).

Table t9796 9248: SHRIMP titanite data for zircons from the Toil and Trouble hornblende-biotite monzogranite (UWA mount 98-72D).

grain-spot	U (ppm)	Th (ppm)	4f206 (%)	$^{207}Pb^*/^{206}Pb^*$	$^{208}Pb^*/^{206}Pb^*$	$^{206}Pb^*/^{238}U$	$^{207}Pb^*/^{235}U$	$^{208}Pb^*/^{232}Th$	conc. (%)	$^{207}Pb/^{206}Pb$ age (Ma)
1-1	39	98	3.146	0.1793 ± 29	0.6878 ± 74	0.5151	12.737	0.1404	101	2647 ± 27
2-1	26	32	3.039	0.1802 ± 38	0.3278 ± 84	0.5026	12.488	0.1341	99	2655 ± 35
3-1	37	81	3.339	0.1804 ± 33	0.5990 ± 81	0.5073	12.615	0.1389	100	2656 ± 31
4-1	43	103	2.717	0.1806 ± 26	0.6398 ± 66	0.5114	12.735	0.1381	100	2658 ± 24
5-1	36	10	2.410	0.1807 ± 29	0.0878 ± 59	0.4993	12.442	0.1554	98	2660 ± 26
7-1	35	90	2.792	0.1791 ± 31	0.6793 ± 78	0.5181	12.790	0.1360	102	2644 ± 28
9-1	39	85	2.809	0.1812 ± 29	0.5912 ± 70	0.5301	13.245	0.1432	103	2664 ± 26
10-1	37	84	3.251	0.1749 ± 31	0.6028 ± 75	0.5224	12.594	0.1380	104	2605 ± 29
11-1	55	117	2.371	0.1809 ± 22	0.5793 ± 55	0.5213	12.999	0.1412	102	2661 ± 20
12-1	37	92	2.215	0.1841 ± 26	0.6804 ± 67	0.5283	13.412	0.1435	102	2690 ± 23
13-1	25	81	3.097	0.1779 ± 35	0.8676 ± 96	0.5044	12.369	0.1376	100	2633 ± 33
15-1	38	55	3.001	0.1827 ± 31	0.4029 ± 71	0.5032	12.675	0.1388	98	2678 ± 28
16-1	41	109	2.815	0.1767 ± 28	0.7369 ± 72	0.5133	12.508	0.1412	102	2623 ± 26
17-1	44	129	2.489	0.1803 ± 25	0.7886 ± 67	0.5108	12.697	0.1391	100	2655 ± 23
18-1	41	95	3.095	0.1717 ± 35	0.5497 ± 85	0.5531	13.093	0.1314	110	2574 ± 34
19-1	37	31	2.426	0.1834 ± 29	0.2336 ± 63	0.4954	12.527	0.1399	97	2684 ± 26
20-1	37	92	2.966	0.1787 ± 29	0.6490 ± 73	0.5212	12.840	0.1379	102	2640 ± 27
High Common Pb										
6-1	35	89	13.302	0.1686 ± 63	0.6346 ±149	0.5215	12.120	0.1312	106	2543 ± 63
8-1	46	35	6.824	0.1800 ± 50	0.2262 ±110	0.5057	12.550	0.1537	99	2653 ± 46
14-1	145	436	33.793	0.3556 ±104	1.1329 ±250	0.5255	25.769	0.1975	73	3731 ± 45

Data 20/11/98.
U/Pb scatter (1σ) for Khan standard = 1.90% (n=8).
Common-Pb corrected using Cumming & Richards (1975) Model III @ 2650 Ma.

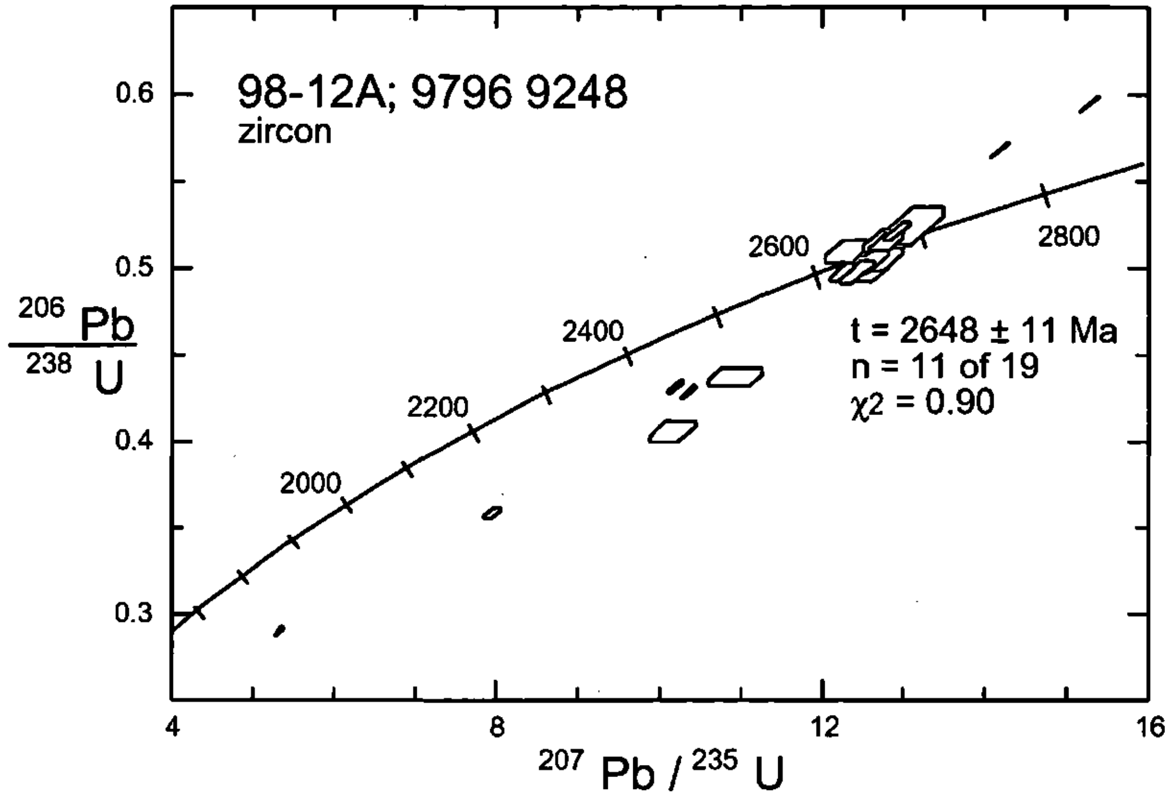

Figure z9796 9248: Concordia plot of all SHRIMP zircon data for zircons from the Toil and Trouble hornblende-biotite monzogranite (UWA mount 98-12A).

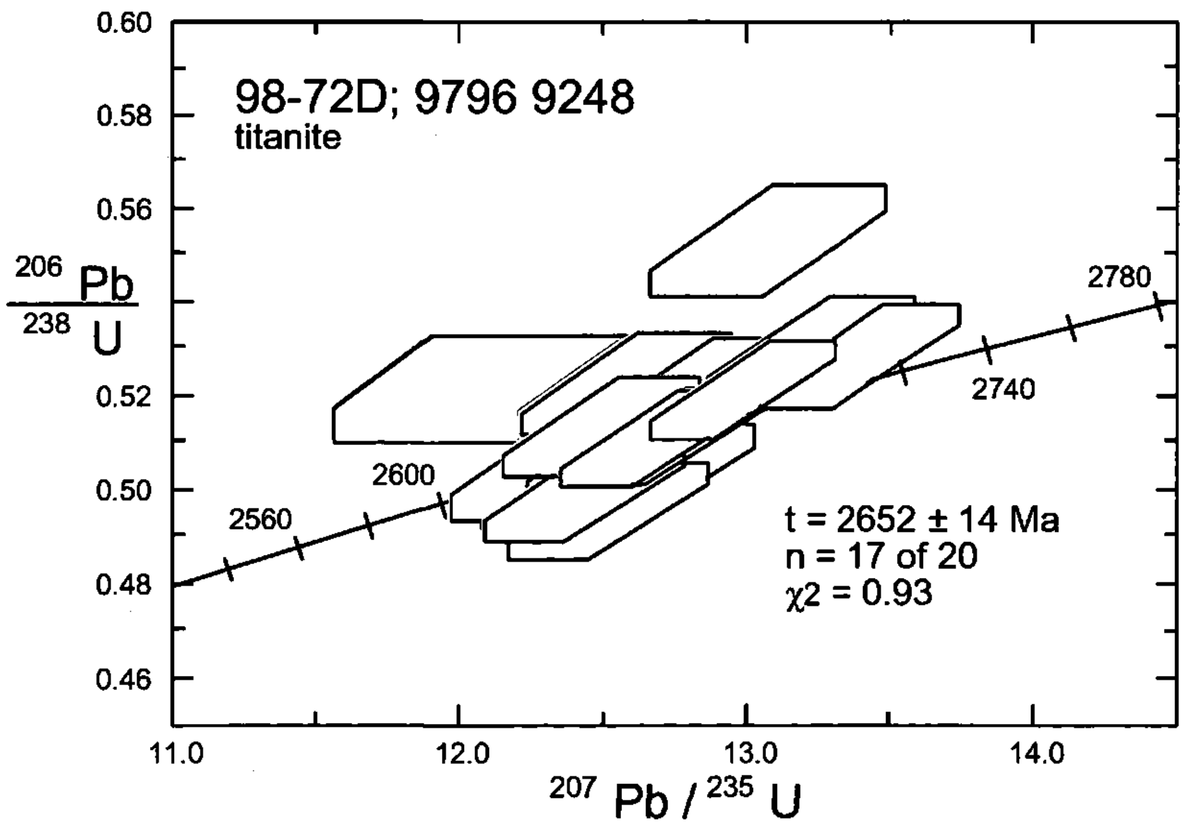

Figure z9796 9248: Concordia plot of SHRIMP titanite data for zircons from the Toil and Trouble hornblende-biotite monzogranite (UWA mount 98-12A). Note that one high-common-Pb analysis falls far to the right of the figure.

9796 9249: biotite monzogranite, Sinclair

1:250,000 sheet:	Widgiemooltha (SH5114)
AMG:	422751.0 mE, 6478254.0 mN
Location:	Tramway Track granites; sample drilled from outcrop in regionally extensive granitoid south of Lake Cowan
Province:	Eastern Goldfields
Description:	Xenolithic equigranular to very sparsely porphyritic feldspar fine-medium grained biotite monzogranite
Chemical group:	High-Ca group, Menangina association, Parker Hills clan
Pluton No:	333409
UWA mounts:	97-43B (zircon) and 98-76D (titanite)

Description of zircons

The majority of zircons from sample 9796-9249 are euhedral grains and fragments up to 200 μm in length (most are smaller than this), having an aspect ratio of 2:1 and are medium to dark brown in colour. Some anhedral fragments are also present, as well as grains that are paler brown in colour. Internal zoning is visible in most grains, both in the photos and on the SEM images. Complex metamictisation and recrystallisation has affected a number of grains. Some zircons contain inclusions.

Description of titanites

The titanites from this sample are all 40-120 micron fragments of larger grains. Only rarely do grains show growth surfaces; most surfaces are fractures. Internal morphology is detectable from SEM images in some grains, with faint growth zones visible. The grains are dark brown to pale brown in colour. Some grains are almost black and have evenly distributed dense and very fine inclusion populations. Areas of SHRIMP analysis were in clean parts of the grains, avoiding inclusions and fractures.

Results and interpretation

Zircon

Twelve analyses on 12 grains are presented in z9796 9249 and shown on a concordia diagram in Figure z9796 9249. The analyses show a wide scatter with major discordance, but there is no evidence for multiple Archaean ages. A minimum age of ~2675 Ma can be estimated on the basis of these data, and there is one concordant date of ~2725 Ma. It is unlikely that a reliable age can be obtained for these zircons.

Titanite

Twenty six analyses on 20 titanite fragments are presented in Table t9796 9249 and shown on a concordia diagram in Figure t9796 9249. Most data are concordant to near-concordant, though Pb/U is unreliable for three of them. The 4f206 values for concordant analyses are in the range 3%–6%, which corresponds to substantial correction in $^{207}Pb/^{206}Pb$. The good clustering of $^{207}Pb/^{206}Pb$ amongst the corrected data is taken as confirmation that the common-Pb composition used for corrections is appropriate, Omitting four analyses with 4f206>6% or >6% discordant, the remaining 22 analyses have a χ^2 of 0.80. This is interpreted as a single age population at 2655 ± 20 Ma.

It is not clear from these data whether the zircons and titanites are dating the same event, though one of the zircons clearly pre-dates the titanite. The simplest, but not definitive, interpretation is that the zircons are predominantly xenocrysts, and the titanite records a magmatic age.

Table z9796 9249: SHRIMP zircon data for the biotite monzogranite, Tramway Track granite (UWA mount 97-43B).

grain-spot	U (ppm)	Th (ppm)	4f206 (%)	$\frac{^{207}Pb^*}{^{206}Pb^*}$	$\frac{^{208}Pb^*}{^{206}Pb^*}$	$\frac{^{206}Pb^*}{^{238}U}$	$\frac{^{207}Pb^*}{^{235}U}$	$\frac{^{208}Pb^*}{^{232}Th}$	conc. (%)	$^{207}Pb/^{206}Pb$ age (Ma)
1-1	452	223	16.153	0.1822 ± 51	0.2225 ±115	0.1852	4.652	0.0837	41	2673 ± 46
2-1	392	67	4.974	0.1756 ± 24	0.0398 ± 51	0.2872	6.954	0.0669	62	2612 ± 22
3-1	147	98	1.035	0.1828 ± 16	0.1242 ± 32	0.4877	12.292	0.0914	96	2678 ± 15
4-1	643	194	10.281	0.1710 ± 31	0.0772 ± 68	0.2110	4.974	0.0539	48	2567 ± 30
5-1	133	241	7.666	0.1662 ± 59	0.0455 ±130	0.1613	3.695	0.0040	38	2519 ± 60
7-1	993	276	10.261	0.1788 ± 23	0.1430 ± 52	0.2333	5.751	0.1202	51	2641 ± 22
8-1	516	96	9.819	0.1782 ± 33	0.0673 ± 72	0.2390	5.872	0.0868	52	2636 ± 30
10-1	192	87	6.577	0.1755 ± 35	0.1463 ± 77	0.3461	8.375	0.1113	73	2611 ± 33
12-1	227	142	6.371	0.1809 ± 35	0.1126 ± 76	0.2812	7.012	0.0506	60	2661 ± 32
13-1	693	187	12.051	0.1745 ± 33	0.0823 ± 74	0.2146	5.164	0.0654	48	2601 ± 32
14-1	228	122	6.107	0.1800 ± 30	0.1533 ± 65	0.3942	9.786	0.1129	81	2653 ± 27
18-1	183	91	0.037	0.1881 ± 9	0.1382 ± 13	0.5307	13.760	0.1468	101	2725 ± 8

Data 27/8/98.
U/Pb scatter (1σ) for cz3 standard = 1.78% (n=14).

Table t9796 9249: SHRIMP titanite data for the biotite monzogranite, Tramway Track granite (UWA mount 98-76D).

grain-spot	U (ppm)	Th# (ppm)	4f206 (%)	$\frac{^{207}Pb^*}{^{206}Pb^*}$	$\frac{^{208}Pb^*}{^{206}Pb^*}$	$\frac{^{206}Pb^*}{^{238}U}$	$\frac{^{207}Pb^*}{^{235}U}$	$\frac{^{208}Pb^*}{^{232}Th\#}$	conc. (%)	$^{207}Pb/^{206}Pb$ age (Ma)
Main group.										
1-1	25	46	4.064	0.1790 ± 48	0.5453 ±121	0.5050	12.460		100	2643 ± 44
4-1	26	45	4.696	0.1762 ± 48	0.4838 ±119	0.5138	12.481		102	2617 ± 45
5-1	33	10	2.579	0.1858 ± 32	0.0948 ± 68	0.5195	13.308		100	2705 ± 28
3-1	41	96	3.900	0.1775 ± 48	0.7423 ±133	0.5251	12.851	0.1644	103	2630 ± 45
27-1	33	108	3.151	0.1755 ± 50	1.0243 ±157	0.5180	12.532	0.1605	103	2611 ± 48
10-1	26	66	5.169	0.1755 ± 64	0.6879 ±165	0.5274	12.765	0.1413	105	2611 ± 60
12-1	39	14	3.147	0.1791 ± 44	0.0923 ± 95	0.4939	12.199	0.1312	98	2645 ± 41
13-1	26	69	5.020	0.1807 ± 64	0.7200 ±169	0.4820	12.009	0.1286	95	2659 ± 58
14-1	31	56	3.467	0.1810 ± 50	0.4779 ±125	0.5112	12.760	0.1367	100	2662 ± 46
15-1	32	74	3.015	0.1849 ± 43	0.6021 ±115	0.4972	12.677	0.1309	96	2698 ± 39
16-1	29	63	4.627	0.1835 ± 60	0.6037 ±152	0.4776	12.087	0.1312	94	2685 ± 54
17-1	29	62	3.911	0.1857 ± 55	0.5672 ±141	0.4986	12.764	0.1336	96	2704 ± 49
18-1	20	21	4.309	0.1835 ± 73	0.2842 ±168	0.4832	12.226	0.1293	95	2685 ± 66
20-1	31	67	4.508	0.1806 ± 57	0.6078 ±146	0.5088	12.667	0.1407	100	2658 ± 52
22-1	27	47	3.523	0.1828 ± 51	0.4779 ±126	0.5119	12.903	0.1435	99	2679 ± 46
23-1	27	52	4.609	0.1683 ± 60	0.5037 ±150	0.4934	11.452	0.1284	102	2541 ± 60
28-1	27	51	5.935	0.1716 ± 66	0.4735 ±162	0.5160	12.207	0.1305	104	2573 ± 65
29-1	32	4	4.102	0.1821 ± 55	0.0388 ±118	0.5071	12.730	0.1652	99	2672 ± 50
30-1	42	84	3.192	0.1743 ± 40	0.5485 ±103	0.5278	12.687	0.1438	105	2600 ± 38
7-1	33	50	2.956	0.1841 ± 43	0.3851 ±106	0.5116	12.989	0.1296	99	2690 ± 39
8-1	29	60	3.813	0.1829 ± 56	0.5783 ±143	0.5383	13.575	0.1506	104	2679 ± 50
9-1	31	11	2.899	0.1791 ± 49	0.0907 ±106	0.5135	12.682	0.1340	101	2645 ± 46
>6% discordant or 4f206 >6%.										
2-1	46	58	3.252	0.1822 ± 50	0.4923 ±127	0.4330	10.881	0.1685	87	2673 ± 46
11-1	16	3	11.804	0.1807 ±127	0.0616 ±282	0.4956	12.345	0.1459	98	2659 ±117
19-1	51	90	4.927	0.1812 ± 54	0.6634 ±141	0.3948	9.863	0.1485	81	2664 ± 49
31-1	21	6	8.265	0.1754 ±112	0.0604 ±247	0.4006	9.690	0.0852	83	2610 ±106

Data 11/05/99 (n = 3), 14/05/99 (n = 3) and 07/06/99 (n = 20).

U/Pb scatter (1σ) for Khan standard = 2.58% (n = 15), ~1% (n = 2) and 3.86% (n = 7).

Common-Pb corrected using Cumming & Richards (1975) Model III @ 2640 Ma.

Analyses on 11/05/99 used NO_2^- primary ion beam.

Pb/U calibration might be slightly disturbed.

Th/U calibration is not reliable; Th abundances are indicative only, and Pb/Th are not reported.

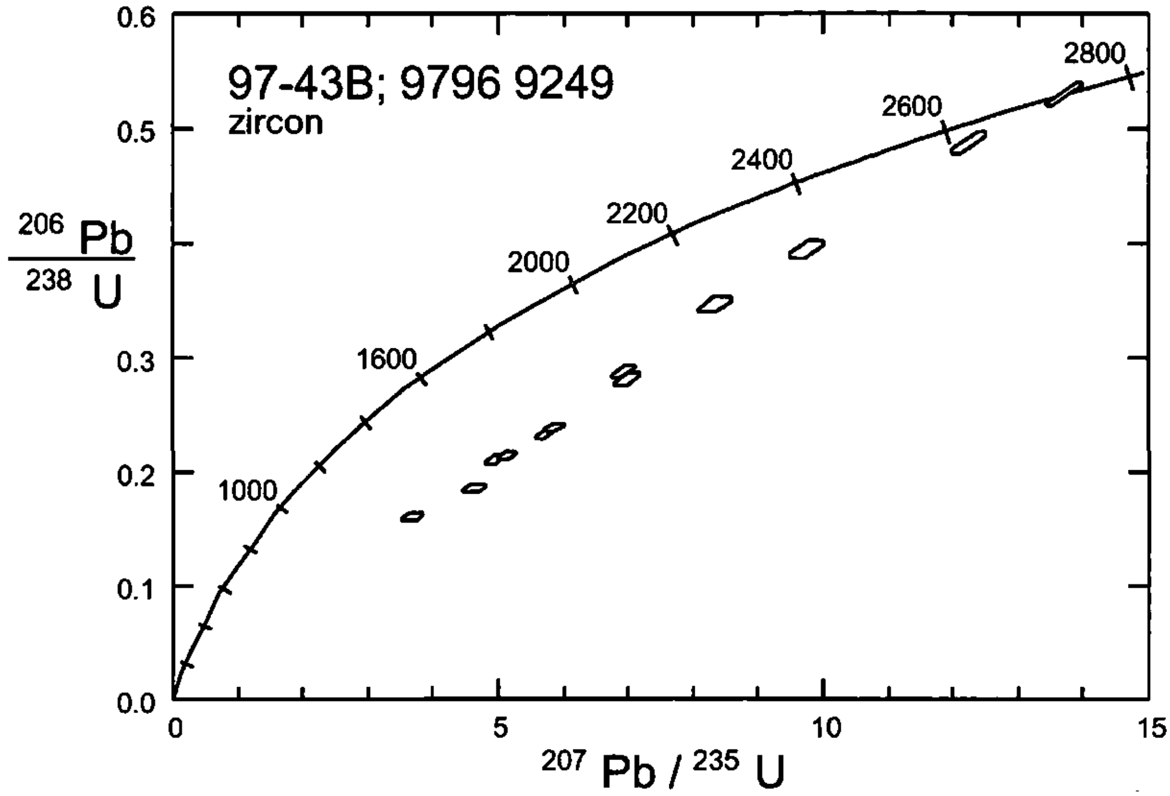

Figure z9796 9249: Concordia plot of all SHRIMP zircon data for the biotite monzogranite, Tramway Track granite (UWA mount 97-43B).

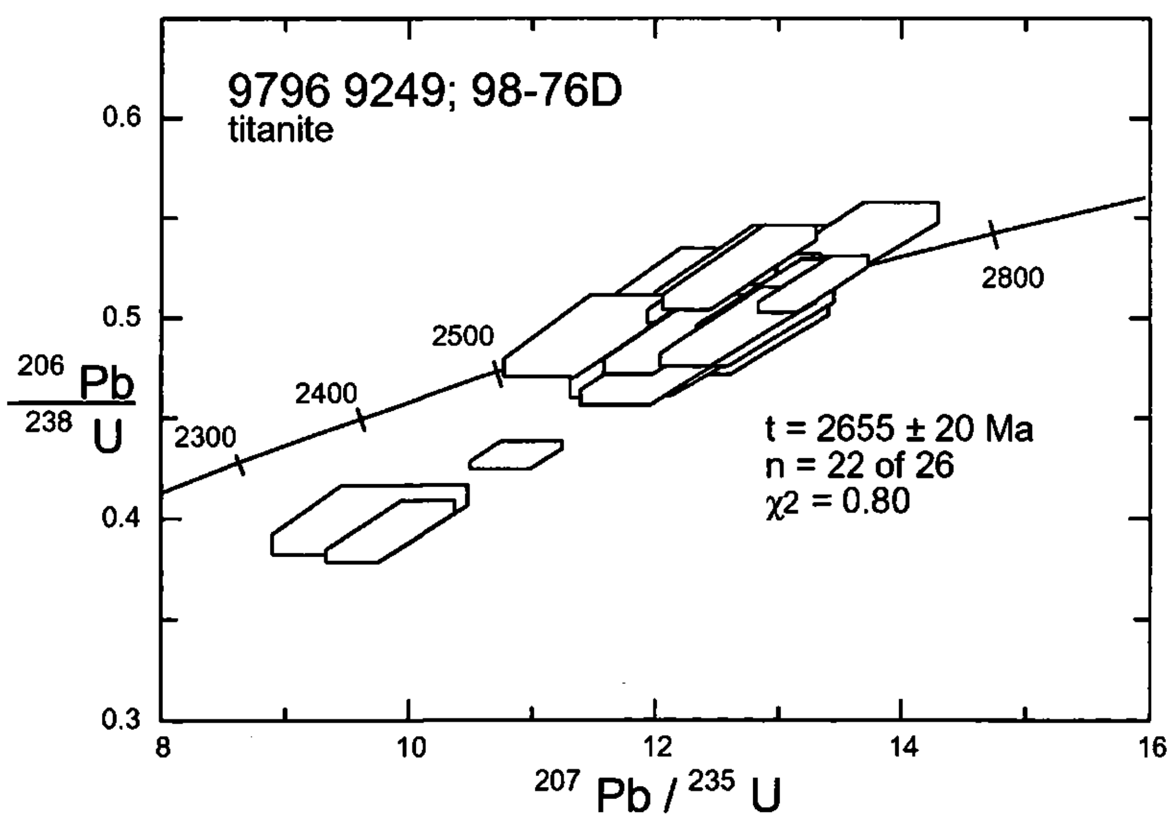

Figure t9796 9249: Concordia plot of SHRIMP titanite data for the biotite monzogranite, Tramway Track granite (UWA mount 97-43B).

9796 9256B: granodiorite, End of Day xenolith

1:250,000 sheet:	Widgiemooltha (SH5114)
AMG:	444041.0 mE, 6460881.0 mN
Location:	Drilled from large outcrop
Province:	Eastern Goldfields
Description:	Foliated K-feldspar-porphyritic biotite granodiorite
Chemical group:	Mafic group, Xenolith association, Cement clan
Pluton No:	333413
UWA mounts:	98-05A (zircon) and 98-84A (titanite)

Description of zircons

The zircon population in this sample consists of one morphologic type of finely zoned euhedral grains, with most grains being 60-120 μm long, with a range of aspect ratios from ~2:1 for the majority to ~3-4:1, particularly for smaller grains. Grains are typically euhedral to subhedral in external morphology with continuous euhedral internal zoning from core to rim. Inclusions are rare. The grains range from pale brown to dark brown to nearly opaque in colour. Strong euhedral zoning observed on both optical and SEM images suggest high U-Th-contents and radiation damage. Discordant alteration patches are visible on SEM images of some grains, and overgrow the euhedral zoning. Many grains have more homogeneous core regions but there is no break in the euhedral growth from core to rim and they are not considered to be xenocrysts. Many grains have fracture networks typical of high-U grains, which have significant metamictisation. The alteration patches and fractures, and dark grains were avoided during data collection.

Description of titanites

The titanites from this sample are all 60-200 μm fragments of larger grains. Only rarely do grains show growth surfaces; most surfaces are fractures. Little internal morphology is detectable from SEM images, with faint growth zones just visible in a minority of grains. The grains are dark brown to honey brown in colour. Some grains are almost black and have evenly distributed dense and very fine inclusion populations. Isolated inclusions are small and rare, and tend to be within or in close association with fractures. Areas of SHRIMP analysis were in clean parts of the grains, avoiding inclusions and fractures.

Results and interpretation

Zircon

Thirty one analyses on 30 zircon are presented in Table z9796 9256B and shown in Figure z9796 9256B, b. Although U contents are not particularly high, most of the data are discordant and show a large range in their $^{207}Pb/^{206}Pb$ ages. There is a broad cluster of data close to concordia, which has considerable spread in $^{207}Pb/^{206}Pb$ as well as $^{206}Pb/^{238}U$. It is likely that many of the analyses represent minimum ages for the analysed grains due to old Pb-loss. By selecting analyses with U<200 ppm, 4f206<2.5% and <5% discordant, a fairly coherent group of nine can be identified. One of these (13-1) is a statistical outlier and is omitted from the pooled age, though this omission is questionable. The remaining eight analyses give a pooled age of 2663 ± 11 Ma. The statistical value of ± 11 Ma almost certainly underestimates the true uncertainty.

Titanite

Twenty one analyses were obtained from 20 fragments. The U abundances average ~50 ppm and the common Pb corrections are all significant, being >2.5%. The lack of correlation between 4f206 and corrected $^{207}Pb/^{206}Pb$ is taken as evidence that the common Pb composition used in making the corrections is appropriate. The grouping data in both 206/207 and $^{206}Pb/^{238}U$ is taken as confirmation that all samples are concordant. Omitting analyses with 4f206 >5% 12 that form a single age population with $\chi^2 = 0.28$. The corresponding age of is 2658 ± 20 Ma.

Neither the zircon nor titanite date could be used without substantial reservations. However the close correspondence of the two results implies that both are probably reliable; combining the two gives 2660 ± 15 Ma.

Table t9796 9256B SHRIMP titanite data for the granodiorite xenolith, End of Day (UWA mount 98-84A).

grain-spot	U (ppm)	Th (ppm)	4f206 (%)	$^{207}Pb^*/^{206}Pb^*$	$^{208}Pb^*/^{206}Pb^*$	$^{206}Pb^*/^{238}U$	$^{207}Pb^*/^{235}U$	#	conc. (%)	$^{207}Pb/^{206}Pb$ age (Ma)
10-1	120	90	2.555	0.1812 ± 17	0.2327 ± 37	0.4895	12.232		96	2664 ± 16
11-1	27	51	4.513	0.1825 ± 61	0.5905 ±148	0.5029	12.652		98	2675 ± 56
12-1	28	190	4.980	0.1819 ± 55	2.1023 ±204	0.4908	12.310		96	2670 ± 50
13-1	53	351	4.258	0.1778 ± 38	2.0733 ±147	0.4656	11.416		94	2633 ± 35
14-1	52	333	3.596	0.1798 ± 32	2.0341 ±126	0.4895	12.132		97	2651 ± 30
17-1	51	250	4.990	0.1844 ± 46	1.5550 ±146	0.4747	12.068		93	2693 ± 41
18-1	48	123	3.971	0.1770 ± 36	0.7834 ± 92	0.4981	12.157		99	2625 ± 34
18-2	37	124	3.680	0.1834 ± 40	1.0298 ±112	0.4918	12.439		96	2684 ± 36
21-1	35	219	4.296	0.1802 ± 42	1.9715 ±157	0.4715	11.714		94	2655 ± 39
5-1	40	217	4.782	0.1789 ± 47	1.6977 ±157	0.4654	11.481		93	2643 ± 43
7-1	34	201	4.721	0.1793 ± 44	1.8651 ±156	0.4860	12.016		96	2646 ± 41
8-1	53	296	4.761	0.1807 ± 40	1.7526 ±137	0.4650	11.585		93	2659 ± 37
4f206>5%										
15-1	48	195	11.507	0.1801 ± 61	1.4633 ±175	0.4840	12.020		96	2654 ± 57
16-1	32	286	6.834	0.1737 ± 58	2.8461 ±250	0.4745	11.363		97	2593 ± 56
19-1	41	232	11.548	0.1864 ± 63	1.8164 ±196	0.4705	12.095		92	2711 ± 56
2-1	44	208	8.057	0.1720 ± 50	1.5054 ±150	0.4748	11.259		97	2577 ± 49
20-1	59	262	15.661	0.1867 ± 75	1.5262 ±212	0.4856	12.499		94	2713 ± 66
22-1	43	278	9.694	0.1832 ± 64	2.0922 ±215	0.4641	11.723		92	2682 ± 57
23-1	49	274	5.722	0.1806 ± 42	1.8271 ±144	0.4937	12.291		97	2658 ± 39
4-1	39	274	9.650	0.1895 ± 71	2.1948 ±248	0.4710	12.302		91	2737 ± 62
9-1	36	170	19.569	0.1807 ± 94	1.6539 ±269	0.4510	11.233		90	2659 ± 86

Data 05/05/99.
U/Pb scatter (1σ) for Khan standard = 2.53% (n = 14).
Common-Pb corrected using Cumming & Richards (1975) Model III @ 2650 Ma.
Analysed using NO2- primary ion beam.
Pb/U calibration might be slightly disturbed.
Th/U calibration is not reliable; Th abundances are indicative only, and Pb/Th are not reported.

Table z9796 9256B SHRIMP zircon data for the granodiorite xenolith, End of Day (UWA mount 98-05A).

grain-spot	U (ppm)	Th (ppm)	4f206 (%)	$^{207}Pb^*/^{206}Pb^*$	$^{208}Pb^*/^{206}Pb^*$	$^{206}Pb^*/^{238}U$	$^{207}Pb^*/^{235}U$	$^{208}Pb^*/^{232}Th$	conc. (%)	$^{207}Pb/^{206}Pb$ age (Ma)
Possible magmatic group.										
6-1	90	40	0.426	0.1817 ± 13	0.1120 ± 23	0.4883	12.232	0.1245	96	2668 ± 12
7-1	102	35	0.238	0.1818 ± 11	0.0867 ± 18	0.5006	12.547	0.1283	98	2669 ± 10
8-1	120	<2	0.253	0.1805 ± 10		0.5071	12.616		100	2657 ± 9
9-1	26	<2	0.674	0.1800 ± 25		0.5057	12.549		99	2653 ± 23
11-1	148	111	2.405	0.1800 ± 17	0.2022 ± 37	0.4919	12.210	0.1330	97	2653 ± 16
13-1	22	<2	0.252	0.1868 ± 39		0.4989	12.847		96	2714 ± 34
16-1	115	8	0.061	0.1815 ± 10	0.0162 ± 12	0.5160	12.910	0.1189	101	2666 ± 9
30-1	45	3	0.720	0.1781 ± 23	0.0062 ± 43	0.4938	12.130	0.0464	98	2636 ± 22
Young outlier.										
25-1	180	59	0.200	0.1780 ± 8	0.0890 ± 13	0.4992	12.253	0.1365	99	2634 ± 8
>5% discordant or 4f206>3%.										
1-1	384	477	57.422	0.1550 ± 87	0.2663 ±199	0.2788	5.957	0.0598	66	2402 ± 95
2-1	87	38	1.556	0.1795 ± 20	0.1245 ± 41	0.4606	11.398	0.1306	92	2648 ± 18
5-1	208	112	6.037	0.1874 ± 21	0.1539 ± 46	0.5099	13.174	0.1453	98	2719 ± 18
10-1	185	10	0.882	0.1799 ± 11	0.0070 ± 20	0.4581	11.361	0.0603	92	2652 ± 10
12-1	419	439	53.454	0.1521 ± 79	0.2353 ±181	0.2639	5.535	0.0593	64	2370 ± 89
14-1	234	276	20.080	0.1784 ± 41	0.1470 ± 93	0.4173	10.265	0.0520	85	2638 ± 39
15-1	68	32	1.555	0.1877 ± 23	0.1310 ± 47	0.4820	12.474	0.1337	93	2722 ± 20
16-2	279	229	8.815	0.1773 ± 25	0.1428 ± 56	0.4665	11.402	0.0811	94	2627 ± 24
17-1	248	127	7.831	0.1812 ± 28	0.1541 ± 61	0.4842	12.101	0.1455	96	2664 ± 25
18-1	204	154	9.506	0.1837 ± 33	0.1982 ± 73	0.4226	10.701	0.1109	85	2686 ± 30
19-1	138	41	2.309	0.1799 ± 20	0.0763 ± 42	0.4213	10.452	0.1069	85	2652 ± 19
20-1	60	27	2.985	0.1860 ± 31	0.1068 ± 66	0.4792	12.291	0.1152	93	2707 ± 27
21-1	77	42	7.964	0.1770 ± 46	0.1110 ±101	0.3538	8.637	0.0725	74	2625 ± 43
22-1	132	3	3.987	0.1793 ± 23	0.0055 ± 48	0.4670	11.548	0.1050	93	2647 ± 21
23-1	220	267	26.852	0.1694 ± 59	0.1500 ±132	0.3502	8.181	0.0432	76	2552 ± 58
24-1	213	111	9.041	0.1814 ± 27	0.1549 ± 59	0.4742	11.863	0.1413	94	2666 ± 24
26-1	63	39	26.764	0.1965 ±143	0.1794 ±320	0.2688	7.281	0.0788	55	2797 ±119
28-1	140	66	4.876	0.1771 ± 26	0.1209 ± 58	0.4595	11.220	0.1182	93	2626 ± 25
29-1	130	73	1.829	0.1864 ± 18	0.1390 ± 37	0.4833	12.419	0.1193	94	2710 ± 16
Others with >200 ppm U.										
3-1	250	105	2.347	0.1761 ± 13	0.1137 ± 28	0.4571	11.097	0.1240	93	2616 ± 13
4-1	355	182	1.316	0.1764 ± 11	0.1401 ± 22	0.4845	11.784	0.1323	97	2619 ± 10
27-1	216	258	0.702	0.1765 ± 9	0.3187 ± 21	0.4980	12.118	0.1330	99	2620 ± 9

Data 15/06/98.
U/Pb scatter (1σ) for cz3 standard = 1.24% (n = 10).
Th-related data not reported for Th <2ppm.

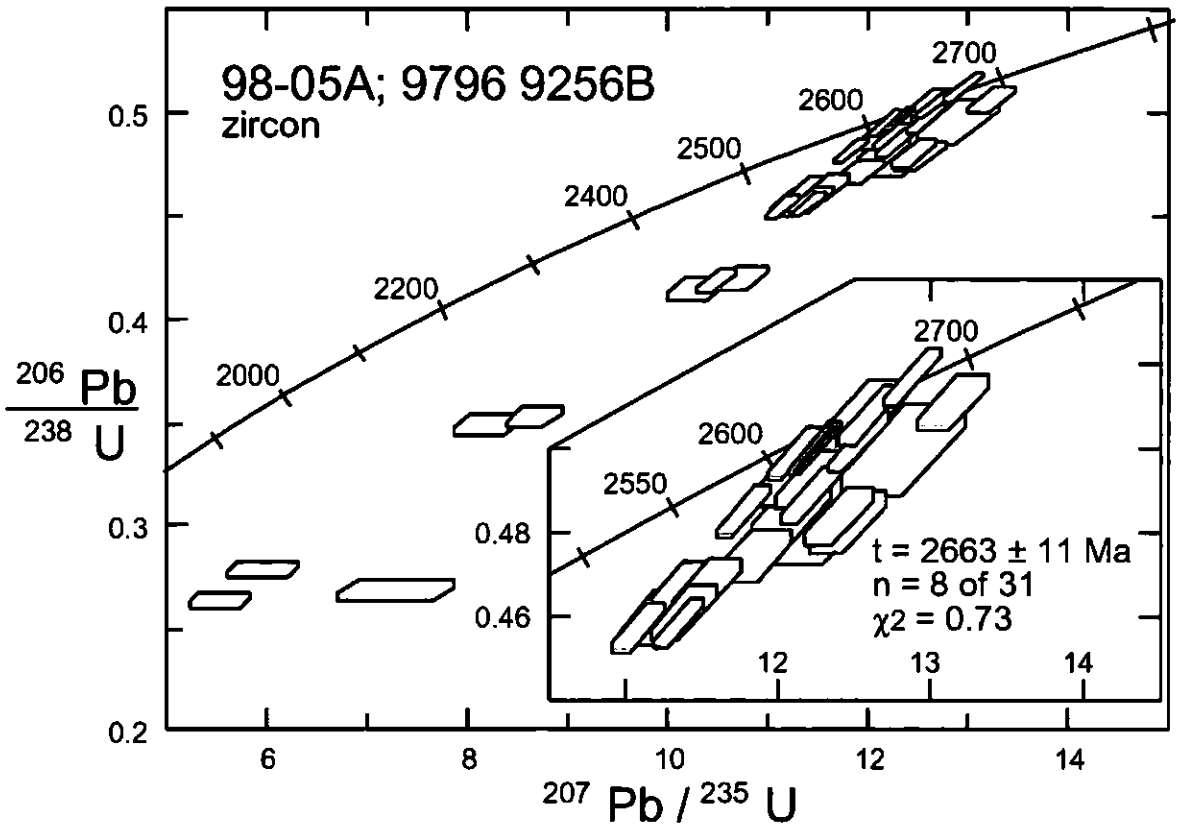

Figure z9796 9256B Concordia plot of SHRIMP zircon data for the granodiorite xenolith, End of Day (UWA mount 98-05A).

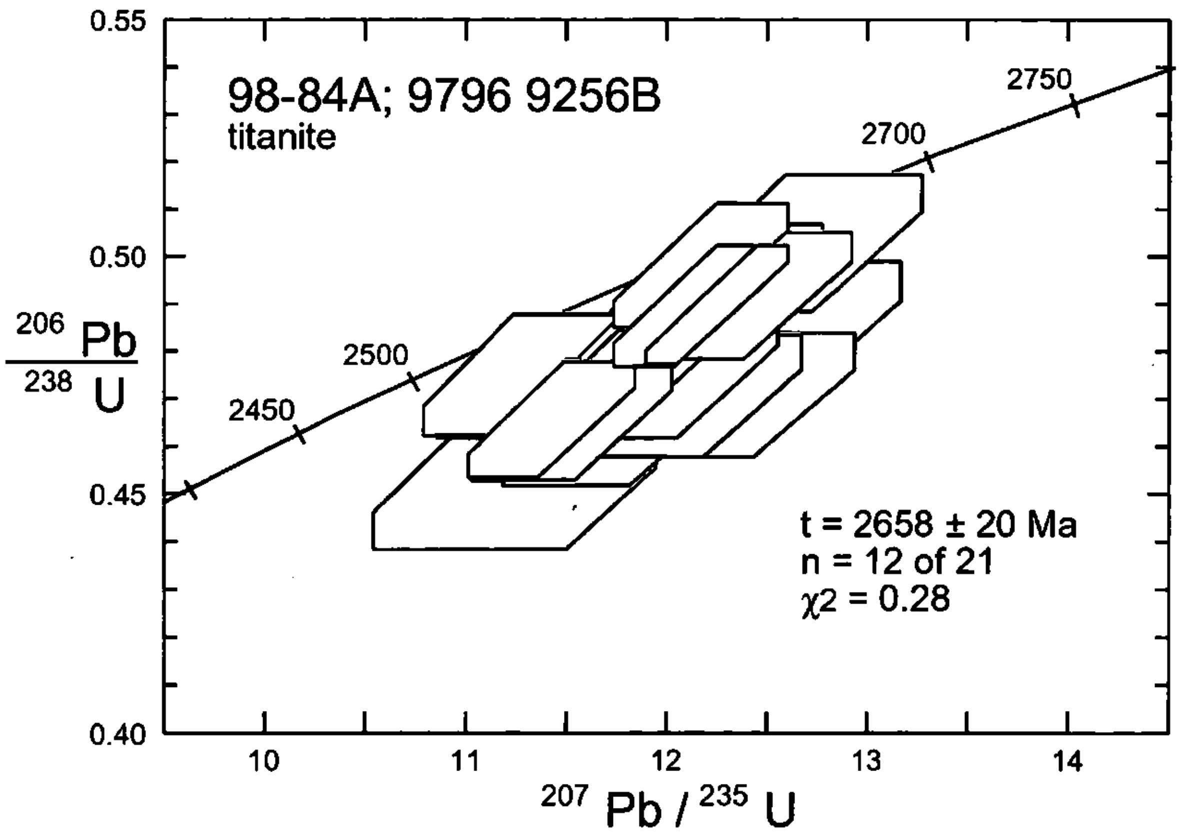

Figure t9796 9256B Concordia plot of SHRIMP titanite data for the granodiorite xenolith, End of Day (UWA mount 98-84A). High-4f206 data are not all plotted.

9896 7008: biotite-clinopyroxene-amphibole granodiorite, Erayinia Complex

1:250,000 sheet:	Kurnalpi (SH5110)
AMG:	461788.0 mE, 6571833.0 mN
Location:	Sample drilled from old blast site north of Erayinia Hill
Province:	Eastern Goldfields
Description:	Seriate to moderately porphyritic medium-grained biotite-clinopyroxene-amphibole quartz-monzonite
Chemical group:	Syenite group, Gilgarna association, Erayinia clan
Pluton No:	343613
UWA mount:	98-51C

Description of zircons

Most zircons recovered from sample 9896-7008 are euhedral crystals and a lesser number of fragments, with only rare irregular shaped fragments. Both elongate needles and more squat, equant grains are present. Grain size varies significantly from less than 40 μm to over 300 μm. Most grains are slightly opaque and dark brown or medium brown in colour, although a number of lighter coloured (pale brown-yellow to white) transparent grains are also present. Minor inclusions are observed in some grains. Cracks and fractures are absent in some zircons, however most contain minor to pervasive fractures. A large number of grains appear to have internal features such as zoning and possible cores as seen in the photos. Some grains also show clearly metamict core regions with radial fractures propagating from core to rim. SEM images confirm this observation for a number of grains and highlight the extent of metamictisation and recrystallisation in a number of grains.

Results and interpretation

Thirteen analyses on 12 grains are presented in Table z9896 7008 and shown on a concordia diagram in Figure z9896 7008. Omitting discordant analyses, the population comprising the remaining 9 analyses in the concordant to near-concordant group (Figure 18) has a χ^2 of 0.40. This is interpreted as a single age population at 2660±5 Ma, and is interpreted as the emplacement age of the granitoid.

Table z9896 7008: SHRIMP zircon data for the biotite-clinopyroxene-amphibole quartz monzonite, Erayinia Hill (UWA mount 98-51C).

grain-spot	U (ppm)	Th (ppm)	4f206 (%)	$^{207}Pb^*/^{206}Pb^*$	$^{208}Pb^*/^{206}Pb^*$	$^{206}Pb^*/^{238}U$	$^{207}Pb^*/^{235}U$	$^{208}Pb^*/^{232}Th$	conc. (%)	$^{207}Pb/^{206}Pb$ age (Ma)
1-1	229	226	0.163	0.1809 ± 7	0.2688 ± 14	0.4968	12.388	0.1355	98	2661 ± 6
2-1	86	95	0.137	0.1797 ± 11	0.2972 ± 23	0.4995	12.378	0.1345	99	2650 ± 10
4-1	399	512	0.012	0.1812 ± 5	0.3475 ± 11	0.4999	12.486	0.1352	98	2664 ± 4
6-1	198	143	0.714	0.1804 ± 10	0.1943 ± 20	0.4737	11.784	0.1276	94	2657 ± 9
7-1	153	226	0.042	0.1804 ± 8	0.4044 ± 20	0.5019	12.487	0.1372	99	2657 ± 8
8-1	185	116	0.047	0.1813 ± 7	0.1689 ± 12	0.5069	12.673	0.1369	99	2665 ± 7
9-1	121	103	0.015	0.1801 ± 9	0.2360 ± 16	0.5040	12.514	0.1395	99	2653 ± 8
10-1	100	111	0.000	0.1809 ± 9	0.2987 ± 19	0.5036	12.560	0.1363	99	2661 ± 8
12-1	130	119	0.622	0.1800 ± 12	0.2580 ± 26	0.4762	11.820	0.1341	95	2653 ± 11
Discordant										
1-2	832	422	37.499	0.1631 ± 63	0.2818 ±143	0.1322	2.973	0.0734	32	2488 ± 65
5-1	748	1515	41.345	0.1458 ± 68	0.4585 ±159	0.1598	3.213	0.0362	42	2298 ± 80
11-1	171	195	1.416	0.1793 ± 14	0.3777 ± 33	0.3925	9.702	0.1298	81	2646 ± 13
15-1	239	221	1.250	0.1794 ± 12	0.2848 ± 26	0.4390	10.860	0.1350	89	2648 ± 11

Data 5/10/98.
U/Pb scatter (1σ) for cz3 standard = 1.99% (n=5).

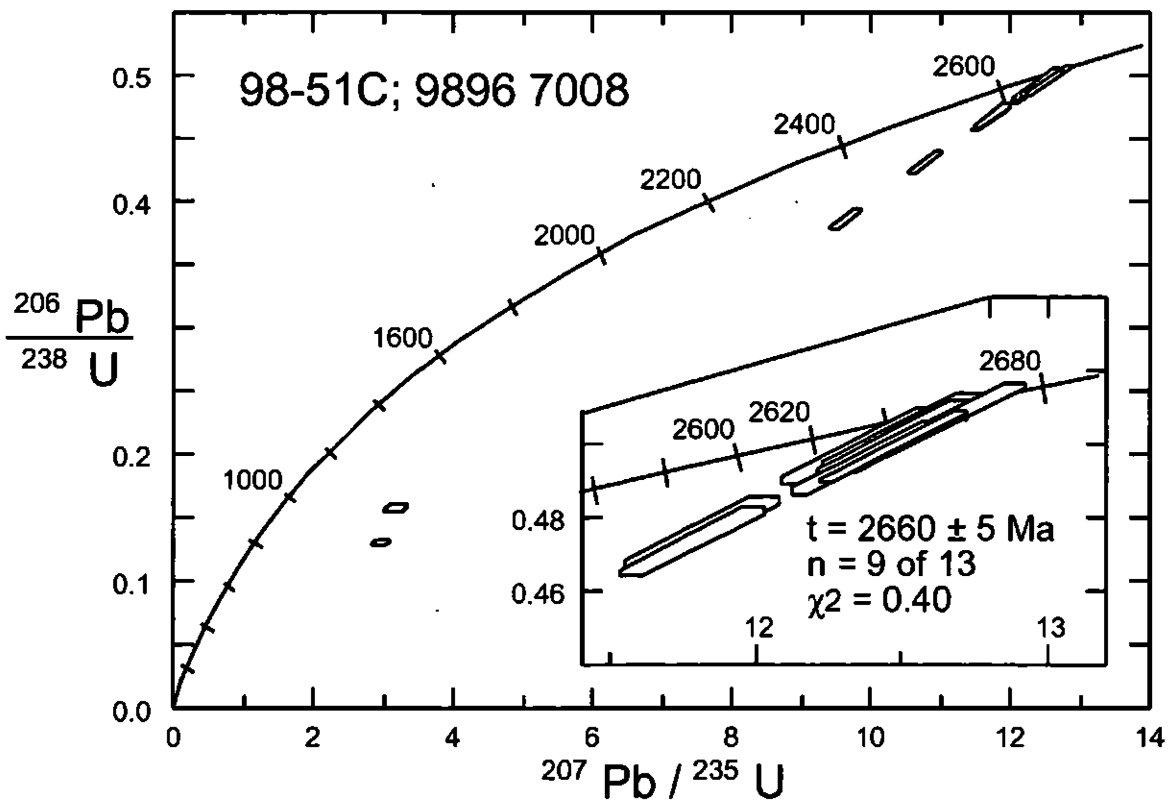

Figure z9896 7008: Concordia plot of SHRIMP zircon data for the biotite-clinopyroxene-amphibole quartz monzonite, Erayinia Hill (UWA mount 98-51C).

9896 7100A: biotite monzogranite, Boorabbin

1:250,000 sheet:	Boorabbin (SH5113)
AMG:	241851.0 mE, 6544566.0 mN
Location:	Boorabbin rock quarry north of main highway. Drilled and hammered from blasted rock face.
Province:	Southern Cross
Description:	Seriate to moderately K-feldspar porphyritic medium-grained biotite monzogranite. Granitoid contains sub-parallel, sub-horizontal zones of biotite-rich oikocrysts; zones possibly sub-parallel to igneous layering. Contains minor biotite-rich clots and schlieren and it cut by rare thin pegmatite veins and dykes.
Chemical group:	Low-Ca group, Beetle association, Boorabbin clan
Pluton No:	293504
UWA mount:	99-08B

Description of zircons

The zircon population in this sample consists of one morphologic type of finely zoned subhedral to euhedral grains, with most grains being 80-200 µm long, with the longer grains tending to higher aspect ratios of 4-5:1 compared to ~2: 1 for the smaller grains. Grains are typically euhedral to subhedral in external morphology with continuous euhedral internal zoning from core to rim. Inclusions are relatively common and consist of opaque or rod-like to equant minerals. All inclusions occur throughout the grains and show no preference for core or rim regions. The grains range from pale brown to dark brown in colour. Strong euhedral zoning observed on both optical and SEM images suggest high U-Th-contents and radiation damage. Discordant alteration patches are visible on SEM images of some grains, and overgrow the euhedral zoning. Most grains have fracture networks typical of high-U grains, which have significant metamictisation. The alteration patches and fractures were avoided during data collection.

Results and interpretation

Twenty analyses on 20 grains are presented in Table z9896 7100A and shown on a concordia diagram in Figure z9896 7100A. The analyses show a wide scatter with major discordance. U contents and common-Pb contamination are highly variable, but there is no apparent coherence amongst the "better" data. No sample age can be estimated from these data; additional data and interpretation are unlikely to provide a reliable age estimate.

Table z9896 7100A: SHRIMP zircon data for the Boorabbin monzogranite (UWA mount 99-08B).

grain-spot	U (ppm)	Th (ppm)	4f206 (%)	$^{207}Pb^*/^{206}Pb^*$	$^{208}Pb^*/^{206}Pb^*$	$^{206}Pb^*/^{238}U$	$^{207}Pb^*/^{235}U$	$^{208}Pb^*/^{232}Th$	conc. (%)	$^{207}Pb/^{206}Pb$ age (Ma)
28-1	101	56	1.208	0.1773 ± 28	0.2187 ± 60	0.4387	10.721	0.1725	89	2627 ± 26
29-1	764	530	0.001	0.1803 ± 5	0.1817 ± 8	0.5086	12.642	0.1332	100	2655 ± 5
23-1	1176	96	0.035	0.1836 ± 5	0.0219 ± 4	0.5104	12.922	0.1370	99	2686 ± 4
24-1	309	1046	4.954	0.1793 ± 30	0.4925 ± 72	0.4453	11.007	0.0648	90	2646 ± 28
30-1	918	211	0.033	0.1818 ± 5	0.0311 ± 6	0.4483	11.239	0.0606	89	2670 ± 5
25-1	1132	106	0.016	0.1807 ± 5	0.0247 ± 4	0.5102	12.715	0.1343	100	2660 ± 4
27-1	985	90	0.028	0.1828 ± 5	0.0248 ± 4	0.5057	12.746	0.1372	98	2678 ± 4
22-1	1034	89	0.087	0.1904 ± 5	0.2041 ± 8	0.5746	15.087	1.3583	107	2746 ± 4
19-1	1043	655	0.089	0.1762 ± 5	0.1661 ± 7	0.5072	12.325	0.1341	101	2618 ± 4
21-1	68	92	0.136	0.1857 ± 23	0.3675 ± 54	0.5143	13.169	0.1402	99	2705 ± 21
16-1	318	287	0.038	0.1792 ± 9	0.2455 ± 18	0.4900	12.107	0.1330	97	2645 ± 9
17-1	1253	158	0.030	0.1812 ± 4	0.0452 ± 4	0.5192	12.971	0.1860	101	2664 ± 4
18-1	97	138	0.138	0.1844 ± 17	0.3482 ± 37	0.5246	13.341	0.1280	101	2693 ± 15
6-1	487	315	0.009	0.1820 ± 8	0.1769 ± 12	0.4815	12.083	0.1319	95	2671 ± 7
5-1	450	376	0.306	0.1719 ± 9	0.1824 ± 17	0.4433	10.508	0.0966	92	2576 ± 9
8-1	1741	657	0.250	0.1703 ± 4	0.1050 ± 7	0.5532	12.991	0.1540	111	2561 ± 4
9-1	530	442	0.139	0.1784 ± 8	0.2419 ± 16	0.4975	12.240	0.1442	99	2638 ± 8
1-1	958	782	0.576	0.1815 ± 7	0.2622 ± 14	0.5033	12.597	0.1617	99	2667 ± 6
2-1	227	148	0.563	0.1578 ± 15	0.2098 ± 30	0.4404	9.581	0.1421	97	2432 ± 16
4-1	708	83	0.001	0.1817 ± 6	0.0326 ± 5	0.4943	12.384	0.1377	97	2669 ± 5

Data 08/08/99.
U/Pb scatter (1σ) for cz3 standard = 0.76% (n = 9).

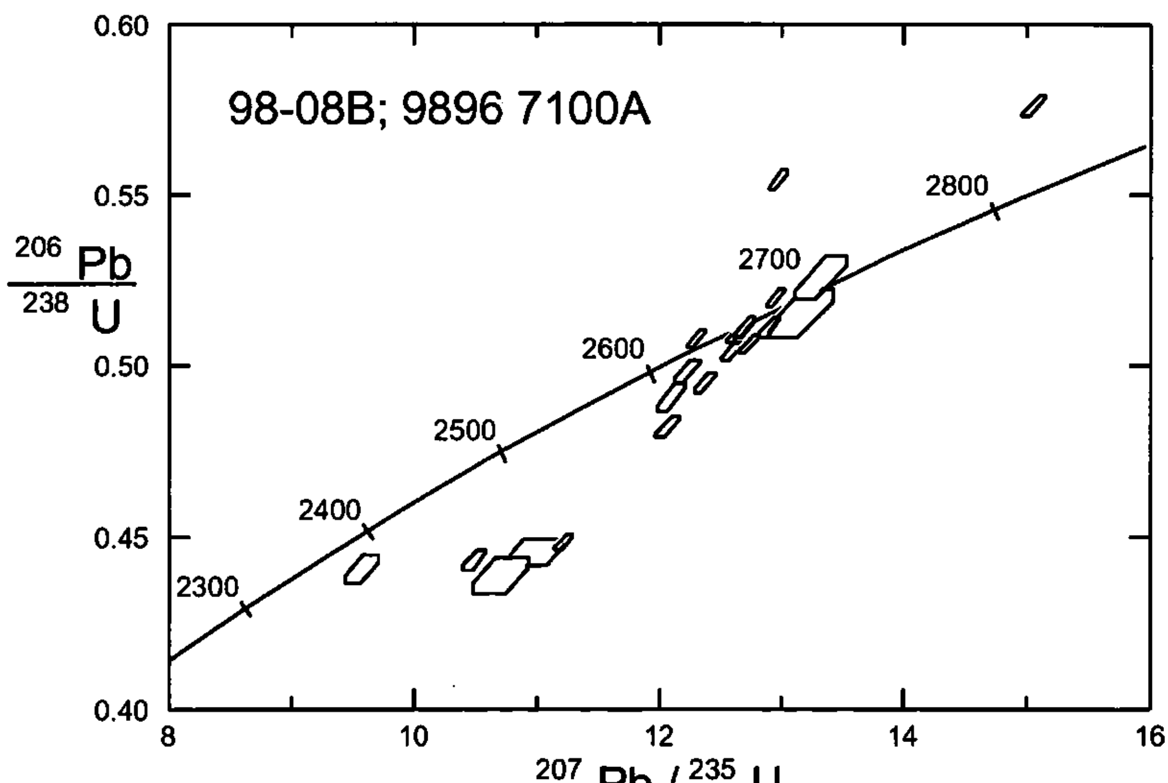

Figure z9896 7100A: Concordia plot of all SHRIMP zircon data for the Boorabbin monzogranite (UWA mount 99-08B).

9896 7102E: biotite granodiorite xenolith, Koolyanobbing

1:250,000 sheet:	Jackson (SH5012)
AMG:	721331.0 mE, 6608767.0 mN
Location:	Koolyanobbing Shear Zone; Drill and hammer on outcrop along small inlet on north side of Lake Deborah East
Province:	Southern Cross
Description:	Sample is an intensely sheared and recrystallised fine- to medium-grained biotite granodiorite/tonalite lens that is intensely deformed and strung out over >25 m, and is probably a xenolith. It forms part of a complex series of deformed to gneissic granitoids and cross-cutting dykes and pegmatites that constitute the Koolyanobbing Shear Zone over several kilometres. All granitoids strongly deformed with foliation trending 330-340°; proto- to ultra-mylonites common.
Chemical group:	Mafic group?
Pluton No:	None given
UWA mount:	99-14C

Description of zircons

The zircon population in this sample consists of one morphologic type of anhedral grains, with most grains being ~100 µm long, with a consistent aspect ratio of 2-3:1. Grains typically have no visible internal zoning in optical or SEM images. Inclusions are not common and consist of opaque or rod-like to equant minerals. All inclusions occur throughout the grains and show no preference for core or rim regions. The grains range from pale brown to dark brown in colour. Discordant alteration patches are visible on SEM images of some grains. Most grains have fracture networks typical of high-U grains, which have significant metamictisation. However, the fractures are not radial as is typical of metamictisation, but more anastomose and tending to parallel in some cases. The corroded anhedral nature and lack of igneous zoning suggests these zircons may be recrystallised. The alteration patches and fractures were avoided during data collection.

Results and interpretation

Twenty one analyses were obtained from 21 grains. The corrections for common Pb are low and the U-contents of all analyses are <300 ppm but many show ancient and/or Recent strong Pb-loss. Omitting discordant analyses and three (young) statistical outliers leaves a coherent group of 12 with $\chi^2 = 1.22$. The corresponding age of 2699 ± 10 Ma is considered to be the emplacement age of the granitoid from which the xenolith was removed. Younger concordant dates for several grains might record ?partial resetting of their U–Pb when the xenolith was entrained in a younger magma, but this age is not well defined.

Table z9896 7102E: SHRIMP zircon data for the granodiorite xenolith, Koolyanobbing (UWA mount 99-14C).

grain-spot	U (ppm)	Th (ppm)	4f206 (%)	$^{207}Pb^*/^{206}Pb^*$	$^{208}Pb^*/^{206}Pb^*$	$^{206}Pb^*/^{238}U$	$^{207}Pb^*/^{235}U$	$^{208}Pb^*/^{232}Th$	conc. (%)	$^{207}Pb/^{206}Pb$ age (Ma)
Main group.										
17-1	118	22	0.045	0.1855 ± 15	0.0521 ± 19	0.5109	13.066	0.1398	98	2703 ± 13
18-1	67	21	0.175	0.1844 ± 22	0.0801 ± 35	0.5184	13.180	0.1324	100	2693 ± 20
27-1	31	18	0.423	0.1864 ± 41	0.1606 ± 82	0.5117	13.153	0.1393	98	2711 ± 37
28-1	81	22	0.000	0.1870 ± 16	0.0752 ± 15	0.5167	13.321	0.1404	99	2716 ± 14
29-1	145	156	0.000	0.1847 ± 11	0.2927 ± 23	0.5121	13.043	0.1388	99	2696 ± 10
30-1	255	222	0.061	0.1859 ± 10	0.2335 ± 18	0.4971	12.738	0.1329	96	2706 ± 9
31-1	159	182	0.000	0.1826 ± 12	0.3047 ± 25	0.5232	13.172	0.1386	101	2676 ± 11
32-1	115	24	0.151	0.1837 ± 19	0.0547 ± 25	0.4909	12.435	0.1299	96	2687 ± 17
33-1	99	24	0.081	0.1869 ± 17	0.0546 ± 24	0.5116	13.186	0.1156	98	2715 ± 15
34-1	112	29	0.000	0.1844 ± 15	0.0595 ± 12	0.5050	12.842	0.1174	98	2693 ± 13
35-1	135	40	0.000	0.1877 ± 13	0.0827 ± 13	0.5100	13.200	0.1426	98	2722 ± 11
36-1	92	20	0.051	0.1827 ± 17	0.0546 ± 24	0.5254	13.235	0.1349	102	2678 ± 15
>5% discordant or Pb/Th discordant.										
16-1	259	242	0.098	0.1829 ± 12	0.2705 ± 25	0.4342	10.950	0.1254	87	2679 ± 11
19-1	131	183	1.289	0.1750 ± 29	0.3121 ± 65	0.2613	6.308	0.0585	57	2607 ± 28
21-1	49	38	0.734	0.1805 ± 35	0.1206 ± 66	0.4001	9.957	0.0618	82	2657 ± 32
22-1	279	61	0.144	0.1850 ± 11	0.0633 ± 15	0.4641	11.836	0.1354	91	2698 ± 10
25-1	130	38	0.011	0.1860 ± 16	0.0768 ± 24	0.4625	11.864	0.1222	91	2707 ± 14
26-1	66	32	0.405	0.1820 ± 27	0.0792 ± 49	0.4966	12.460	0.0799	97	2671 ± 24
Age outliers.										
20-1	89	23	0.316	0.1804 ± 21	0.0660 ± 35	0.5016	12.473	0.1253	99	2656 ± 19
23-1	78	20	0.487	0.1742 ± 32	0.0424 ± 55	0.4840	11.627	0.0813	98	2599 ± 30
24-1	200	44	0.100	0.1811 ± 12	0.0571 ± 15	0.5105	12.750	0.1324	100	2663 ± 11

Data 08/08/99.
U/Pb scatter (1σ) for cz3 standard = 1.48% (n = 9).

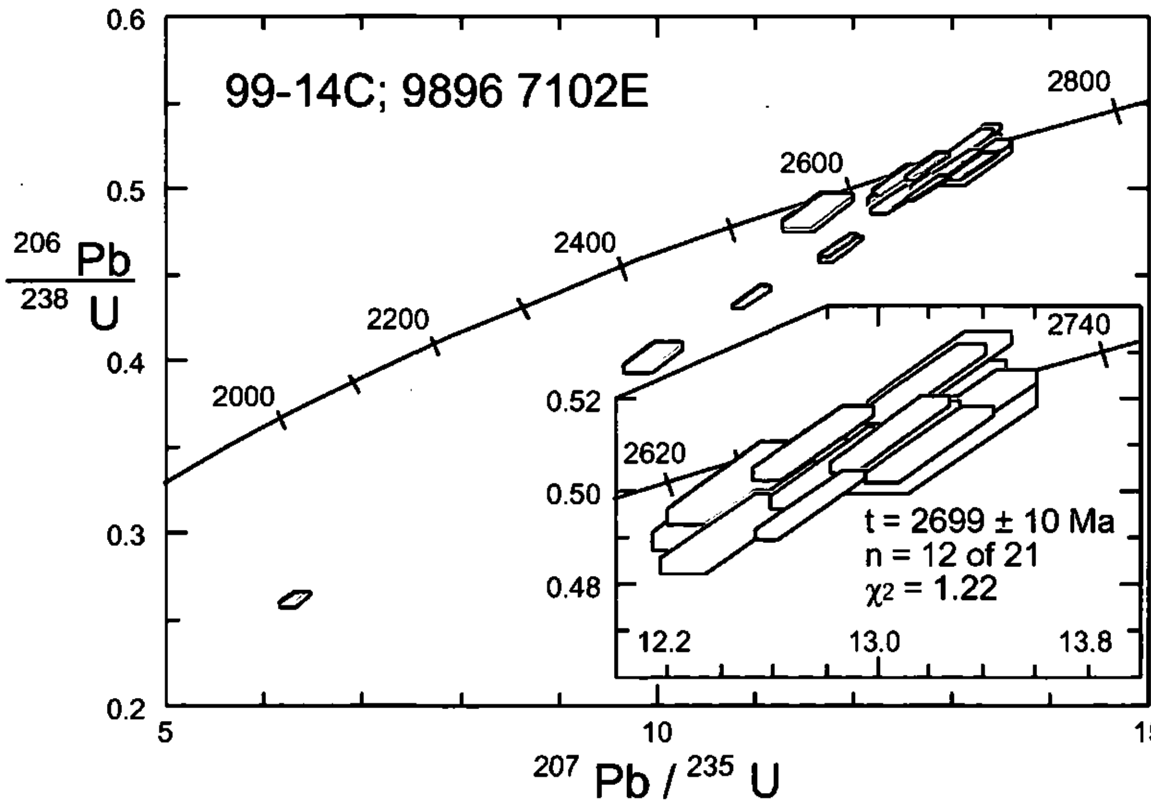

Figure z9896 7102E: Concordia plot of SHRIMP zircon data for the granodiorite xenolith, Koolyanobbing (UWA mount 99-14C).

9896 8104: tonalite, Courlbarloo

1:250,000 sheet:	Youanmi (SH5004)
AMG:	685008 mE, 6837743 mN
Location:	Drilled from outcrop
Province:	Southern Cross
Description:	Equigranular, medium-grained hornblende tonalite containing amphibole-rich xenoliths up to 4 cm.
Chemical group:	Mafic group, Courlbarloo association, Courlbarloo clan
Pluton No:	264001
UWA mount:	A-15A

Description of zircons

The zircon population in this sample consists of one morphologic type of finely zoned euhedral to subhedral grains, with most grains being 30-100 µm long, with a range of aspect ratios from ~2:1 for the majority to ~4:1. Grains are typically euhedral to subhedral in external morphology with continuous euhedral internal zoning from core to rim. Inclusions are not common and consist of opaque or rod-like to equant minerals. All inclusions occur throughout the grains and show no preference for core or rim regions. The grains range from very pale brown to darker brown in colour. Strong euhedral zoning observed on both optical and SEM images suggest high U-Th-contents and radiation damage. Discordant alteration patches are visible on SEM images of some grains, and overgrow the euhedral zoning. Some grains have more homogeneous core regions but there is no break in the euhedral growth from core to rim and they are not considered to be xenocrysts. Many grains have fracture networks typical of high-U grains, which have significant metamictisation. The alteration patches and fractures, and dark grains were avoided during data collection.

Results and interpretation

Twenty six analyses on 26 grains are presented in Table z9896 8104 and shown on a concordia diagram in Figure z9896 8104. The U contents are all <250 ppm and the common-Pb corrections small. Only four analyses show significant discordance. Omitting these and one statistical outlier leaves a highly coherent group of 21 analyses with a pooled age of 2813 ± 5 Ma, and a χ^2 of 0.94. This is interpreted as the emplacement age of the granitoid.

Table z9896 8104: SHRIMP zircon data for the Courlbarloo tonalite (UWA mount A-15A).

grain-spot	U (ppm)	Th (ppm)	4f206 (%)	$^{207}Pb^*/^{206}Pb^*$	$^{208}Pb^*/^{206}Pb^*$	$^{206}Pb^*/^{238}U$	$^{207}Pb^*/^{235}U$	$^{208}Pb^*/^{232}Th$	conc. (%)	$^{207}Pb/^{206}Pb$ age (Ma)
2-1	135	100	0.087	0.1988 ± 14	0.1963 ± 23	0.5367	14.713	0.1417	98	2817 ± 11
15-1	140	107	0.038	0.1957 ± 14	0.2016 ± 23	0.5432	14.655	0.1430	100	2791 ± 11
16-1	209	181	0.097	0.1989 ± 11	0.2260 ± 20	0.5341	14.647	0.1395	98	2817 ± 9
17-1	103	70	0.105	0.1979 ± 16	0.1769 ± 27	0.5407	14.758	0.1419	99	2809 ± 13
8-1	53	28	0.000	0.1987 ± 19	0.1431 ± 24	0.5412	14.829	0.1457	99	2816 ± 16
18-1	201	128	0.036	0.1974 ± 11	0.1804 ± 18	0.5065	13.787	0.1432	94	2805 ± 9
7-1	234	239	0.064	0.1985 ± 10	0.2651 ± 19	0.5320	14.559	0.1383	98	2814 ± 8
14-1	209	167	0.051	0.1982 ± 11	0.2094 ± 18	0.5362	14.653	0.1405	98	2811 ± 9
19-1	84	51	0.245	0.1963 ± 19	0.1560 ± 31	0.5589	15.129	0.1437	102	2796 ± 16
20-1	145	146	0.036	0.1968 ± 13	0.2732 ± 26	0.5432	14.741	0.1473	100	2800 ± 11
21-1	184	186	0.080	0.1993 ± 11	0.2702 ± 21	0.5461	15.002	0.1457	100	2820 ± 9
6-1	120	91	0.000	0.1991 ± 14	0.2003 ± 21	0.5319	14.602	0.1405	98	2819 ± 11
9-1	175	211	0.071	0.1966 ± 11	0.3105 ± 22	0.5415	14.681	0.1392	100	2798 ± 9
23-1	135	103	0.076	0.1999 ± 13	0.2027 ± 23	0.5439	14.991	0.1446	99	2825 ± 11
13-1	111	82	0.000	0.2002 ± 13	0.2011 ± 20	0.5394	14.887	0.1464	98	2828 ± 11
24-1	64	32	0.165	0.1978 ± 22	0.1300 ± 37	0.5552	15.141	0.1442	101	2808 ± 18
25-1	81	52	0.000	0.2007 ± 17	0.1739 ± 23	0.5245	14.514	0.1411	96	2832 ± 13
26-1	238	306	0.004	0.1999 ± 10	0.3409 ± 22	0.5404	14.891	0.1433	99	2825 ± 8
10-1	109	79	0.004	0.1968 ± 17	0.1907 ± 30	0.5471	14.844	0.1442	100	2800 ± 14
29-1	158	188	0.083	0.1988 ± 14	0.2125 ± 25	0.5260	14.415	0.0939	97	2816 ± 11
30-1	165	133	0.000	0.1974 ± 11	0.1937 ± 16	0.5324	14.490	0.1283	98	2805 ± 9
5-1	76	48	0.236	0.1976 ± 21	0.1644 ± 38	0.5301	14.445	0.1376	98	2807 ± 18
Discordant										
22-1	276	323	0.024	0.1968 ± 10	0.3303 ± 20	0.4970	13.484	0.1404	93	2800 ± 8
27-1	133	102	0.051	0.1991 ± 15	0.1706 ± 24	0.4897	13.443	0.1087	91	2819 ± 12
31-1	156	176	0.185	0.1955 ± 14	0.2191 ± 25	0.4977	13.415	0.0966	93	2789 ± 11
Young outlier										
28-1	116	60	0.183	0.1945 ± 15	0.1281 ± 24	0.5244	14.065	0.1306	98	2781 ± 13

Data 12/06/00.
U/Pb scatter (1σ) for cz3 standard = 0.78% (n = 7).

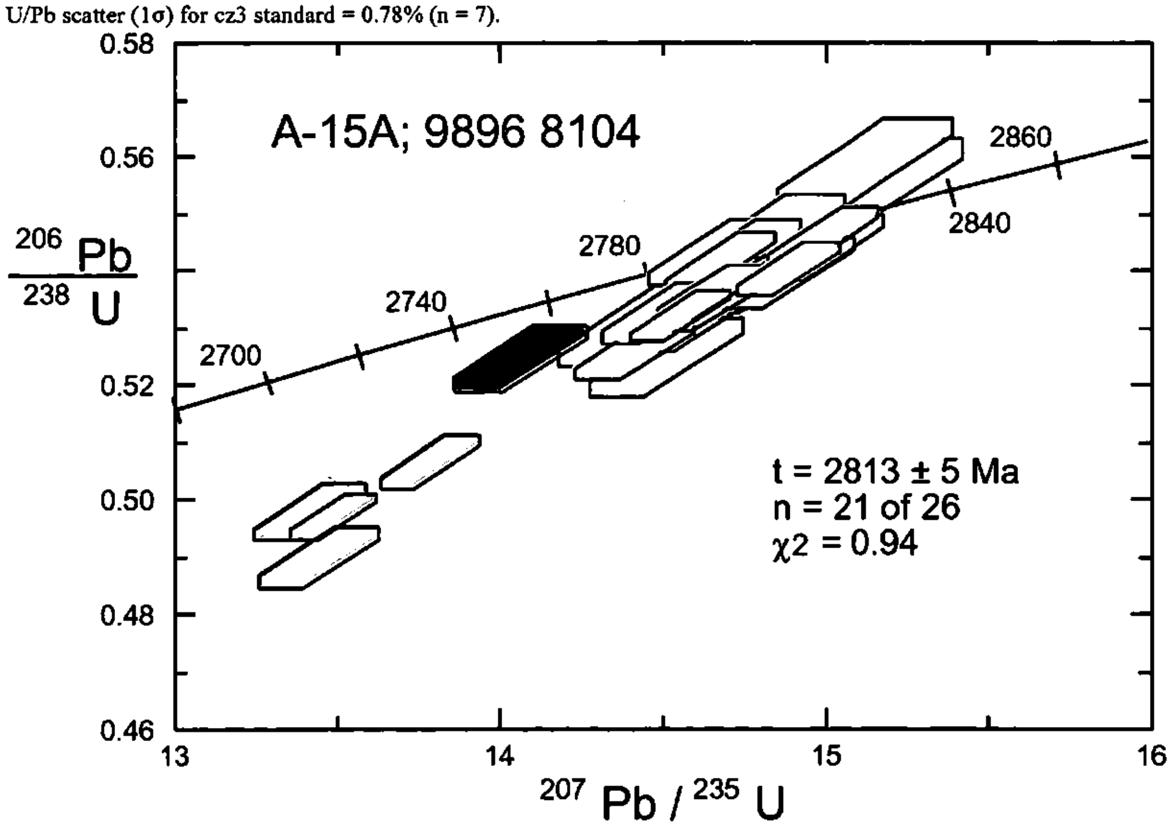

Figure z9896 8104: Concordia plot showing all SHRIMP analytical data for the Courlbarloo tonalite (UWA mount A-15A).

9896 9003: K-feldspar porphyritic biotite granodiorite, Fitzgerald Lagoon

1:250,000 sheet:	Widgiemooltha (SH5114)
AMG:	485973.0 mE, 6526778.0 mN
Location:	Fitzgerald Lagoon area; sample drilled from outcrop.
Province:	Eastern Goldfields
Description:	Moderately to strongly quartz-feldspar porphyritic medium grained biotite monzogranite.
Chemical group:	High-Ca group, Menangina association, Parker Hills clan
Pluton No:	343501
UWA mount:	98-46C

Description of zircons

Sample 9896-9003 contains a variety of zircon grain morphologies. Grains and fragments are generally euhedral and range from elongate (aspect ratio of 4:1) to stubby (3:1 to 2:1) to equant (1:1) in shape. Maximum grain length is approximately 250 µm. The grains also range in colour from completely clear, pale yellow-white to dark brown. The colour and morphology do not show any consistent correlation. Inclusions are present in some grains, but the majority are inclusion-free. Most grains contain visible zoning (both in photos and SEM images) with the zonation in some grains appearing as very pronounced darker zones as seen in the reflected light photos and as bright metamict zones as seen on the charge contrast SEM images. Cracks and fractures are present in most grains. Distinct truncated cores with overgrowing rims are rare, but present. The clearest, light coloured grains do not have any visible internal structures.

Results and interpretation

Thirty one analyses on 29 grains are presented in Table z9896 9003 and shown on a concordia diagram in Figure z9896 9003. Omitting discordant analyses, young outliers and an ?inherited grain, the population comprising the remaining 14 analyses in the concordant to near-concordant group has a χ^2 of 1.01. This is interpreted as a single age population at 2657±9 Ma, and is interpreted as the emplacement age of the granitoid.

Table z9896 9003: SHRIMP analytical data for the K-feldspar porphyritic biotite monzogranite, Fitzgerald Lagoon (UWA mount 98-46C).

grain-spot	U (ppm)	Th (ppm)	4f206 (%)	$^{207}Pb^*/^{206}Pb^*$	$^{208}Pb^*/^{206}Pb^*$	$^{206}Pb^*/^{238}U$	$^{207}Pb^*/^{235}U$	$^{208}Pb^*/^{232}Th$	conc. (%)	$^{207}Pb/^{206}Pb$ age (Ma)
Main group.										
1-1	185	48	0.728	0.1822 ± 16	0.0735 ± 30	0.4823	12.117	0.1356	95	2673 ± 15
3-1	207	63	0.108	0.1817 ± 11	0.0840 ± 15	0.5037	12.616	0.1382	99	2668 ± 10
8-1	179	91	0.150	0.1810 ± 12	0.1349 ± 20	0.5025	12.539	0.1338	99	2662 ± 11
9-1	164	71	0.972	0.1796 ± 19	0.1239 ± 37	0.4977	12.326	0.1426	98	2649 ± 17
11-1	131	35	0.128	0.1797 ± 13	0.0708 ± 18	0.5084	12.598	0.1362	100	2650 ± 12
15-1	138	79	0.584	0.1791 ± 19	0.1573 ± 39	0.5033	12.429	0.1384	99	2644 ± 18
17-1	174	78	0.111	0.1803 ± 11	0.1229 ± 17	0.5125	12.739	0.1400	100	2655 ± 10
22-1	121	45	1.743	0.1784 ± 29	0.0982 ± 60	0.4765	11.719	0.1255	95	2638 ± 27
32-1	127	32	0.599	0.1766 ± 18	0.0557 ± 31	0.4900	11.933	0.1092	98	2622 ± 17
11-2	133	33	0.897	0.1784 ± 19	0.0545 ± 36	0.4945	12.162	0.1096	98	2638 ± 18
36-1	183	96	0.664	0.1833 ± 16	0.1481 ± 31	0.4840	12.234	0.1369	95	2683 ± 15
37-1	89	57	0.345	0.1789 ± 20	0.1660 ± 39	0.4968	12.253	0.1287	98	2643 ± 19
20-1	114	88	0.347	0.1810 ± 19	0.2046 ± 37	0.4972	12.411	0.1313	98	2662 ± 17
39-1	90	93	0.191	0.1801 ± 18	0.2678 ± 37	0.5231	12.992	0.1365	102	2654 ± 16
>5% discordant or 4f206>2%.										
10-1	179	58	2.508	0.1774 ± 26	0.0909 ± 56	0.4674	11.434	0.1314	94	2629 ± 25
31-1	22	12	9.889	0.1461 ±153	0.0951 ±344	0.3905	7.868	0.0678	92	2301 ±181
12-1	486	301	0.062	0.1616 ± 7	0.1458 ± 12	0.4107	9.151	0.0966	90	2473 ± 7
16-1	414	147	2.316	0.1508 ± 19	0.1120 ± 41	0.3459	7.190	0.1089	81	2355 ± 21
14-1	125	41	11.663	0.1846 ± 74	0.2067 ±167	0.3618	9.210	0.2298	74	2695 ± 66
18-1	267	222	1.294	0.1711 ± 17	0.2266 ± 37	0.4286	10.113	0.1169	90	2569 ± 17
21-1	229	105	3.784	0.1747 ± 29	0.1109 ± 63	0.4479	10.787	0.1082	92	2603 ± 28
33-1	375	348	0.798	0.1707 ± 11	0.2306 ± 23	0.4462	10.501	0.1109	93	2564 ± 11
34-1	116	61	1.007	0.1777 ± 22	0.1351 ± 43	0.4658	11.411	0.1189	94	2631 ± 20
35-1	233	166	2.336	0.1725 ± 21	0.1954 ± 46	0.4490	10.682	0.1230	93	2583 ± 21
40-1	135	105	2.076	0.1795 ± 25	0.2106 ± 54	0.4876	12.065	0.1320	97	2648 ± 23
Young outliers.										
6-1	182	149	1.003	0.1688 ± 18	0.2007 ± 38	0.4610	10.729	0.1132	96	2546 ± 18
3-2	208	67	0.189	0.1756 ± 11	0.0844 ± 18	0.4688	11.352	0.1237	95	2612 ± 11
19-1	148	60	0.126	0.1382 ± 14	0.1118 ± 25	0.4039	7.698	0.1104	99	2205 ± 17
19-2	204	131	0.090	0.1395 ± 12	0.1797 ± 24	0.4033	7.755	0.1134	98	2220 ± 14
38-1	250	195	0.728	0.1715 ± 15	0.2080 ± 31	0.4656	11.011	0.1241	96	2573 ± 15
Old outlier.										
4-1	195	130	0.290	0.1860 ± 12	0.1756 ± 23	0.5075	13.013	0.1333	98	2707 ± 11

Data 25/01/99 and 15/01/00.
U/Pb scatter (1σ) for cz3 standard = 1.86% (n = 8) and 1.10% (n = 9).

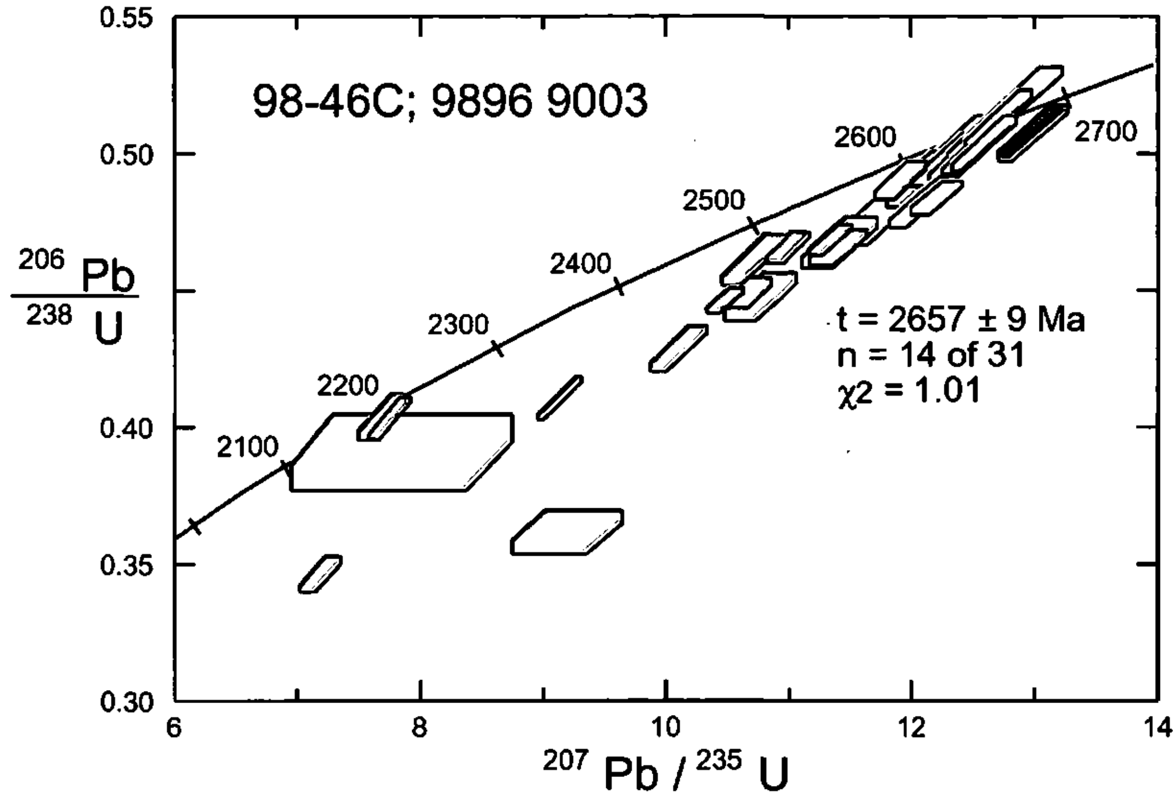

Figure z9896 9003: Concordia plot of SHRIMP analytical data for the K-feldspar porphyritic biotite monzogranite, Fitzgerald Lagoon (UWA mount 98-46C).

9896 9019: monzogranite, Bluff Point Granite

1:250,000 sheet:	Sandstone (SG5016)
AMG:	769888.0 mE, 6993390.0 mN
Location:	Drilled from outcrop
Province:	Southern Cross
Description:	Sparsely to moderately quartz-feldspar porphyritic, medium-grained biotite monzogranite.
Chemical group:	Low-Ca group, Beetle association, Yeelirrie clan
Pluton No:	284301
UWA mount:	98-46A

Description of zircons

The zircon population in this sample consists of one morphologic type with highly variable grain size and shape. Grains range from 20-200 μm long with aspect ratios of 2:1 to 5:1. Grains are typically euhedral in external morphology with continuous euhedral internal zoning from core to rim. Most grains show patchy annealed areas, which overprint the internal euhedral zoning, and pervasive fracture networks, which tend to indicate high U-contents and metamictisation. Many grains have more homogeneous core regions but there is no break in the euhedral growth from core to rim and they are not considered to be xenocrysts. Inclusions are rare. The grains range from pale brown to dark brown to black in colour. Strong relict euhedral zoning observed on both optical and SEM images again suggest high U-Th-contents and radiation damage. The fracture networks and annealed patches were avoided during data collection.

Results and interpretation

Thirteen analyses on 13 grains are presented in Table z9896 9019 and shown on a concordia diagram in Figure z9896 9019. The analyses show high and variable U contents and common-Pb contamination, and the data scatter widely, with major discordance. There are inherited grains with minimum ages of 3106 ± 17 Ma and 3585 ± 7 Ma. It is not possible to determine an age for this sample from these zircons.

Table z9896 9019: SHRIMP zircon data for the monzogranite, Bluff Point (UWA mount 98-46A).

grain-spot	U (ppm)	Th (ppm)	4f206 (%)	$^{207}Pb^*/^{206}Pb^*$	$^{208}Pb^*/^{206}Pb^*$	$^{206}Pb^*/^{238}U$	$^{207}Pb^*/^{235}U$	$^{208}Pb^*/^{232}Th$	conc. (%)	$^{207}Pb/^{206}Pb$ age (Ma)
2-1	1425	2479	56.340	0.1430 ± 71	1.4256 ±194	0.2519	4.968	0.2064	64	2264 ± 86
1-1	653	1307	23.387	0.1627 ± 49	0.3816 ±113	0.3100	6.953	0.0591	70	2483 ± 51
31-1	1265	691	6.094	0.1227 ± 16	0.2565 ± 36	0.2772	4.689	0.1302	79	1996 ± 23
32-1	2757	2847	1.385	0.1481 ± 5	0.2801 ± 11	0.4296	8.774	0.1165	99	2324 ± 5
33-1	137	252	1.128	0.1769 ± 20	0.4331 ± 49	0.4929	12.022	0.1163	98	2624 ± 19
7-1	138	292	0.919	0.1814 ± 17	0.5756 ± 46	0.5202	13.009	0.1420	101	2666 ± 16
10-1	433	850	2.224	0.1688 ± 14	0.5550 ± 34	0.4779	11.124	0.1350	99	2546 ± 14
19-1	274	260	5.426	0.2379 ± 26	0.2954 ± 57	0.5040	16.532	0.1569	85	3106 ± 17
24-1	209	138	0.968	0.3232 ± 15	0.1729 ± 25	0.7155	31.884	0.1877	97	3585 ± 7
34-1	322	483	6.213	0.1765 ± 27	0.3294 ± 61	0.4392	10.690	0.0964	90	2621 ± 25
29-1	346	317	1.832	0.1751 ± 16	0.2589 ± 34	0.4667	11.269	0.1322	95	2607 ± 15
28-1	420	678	4.313	0.1716 ± 20	0.4610 ± 48	0.4591	10.861	0.1313	95	2573 ± 20
30-1	337	585	2.947	0.1775 ± 18	0.4941 ± 43	0.4713	11.532	0.1343	95	2629 ± 17

Data 15/01/00.
U/Pb scatter (1σ) for cz3 standard = 1.10% (n = 9).

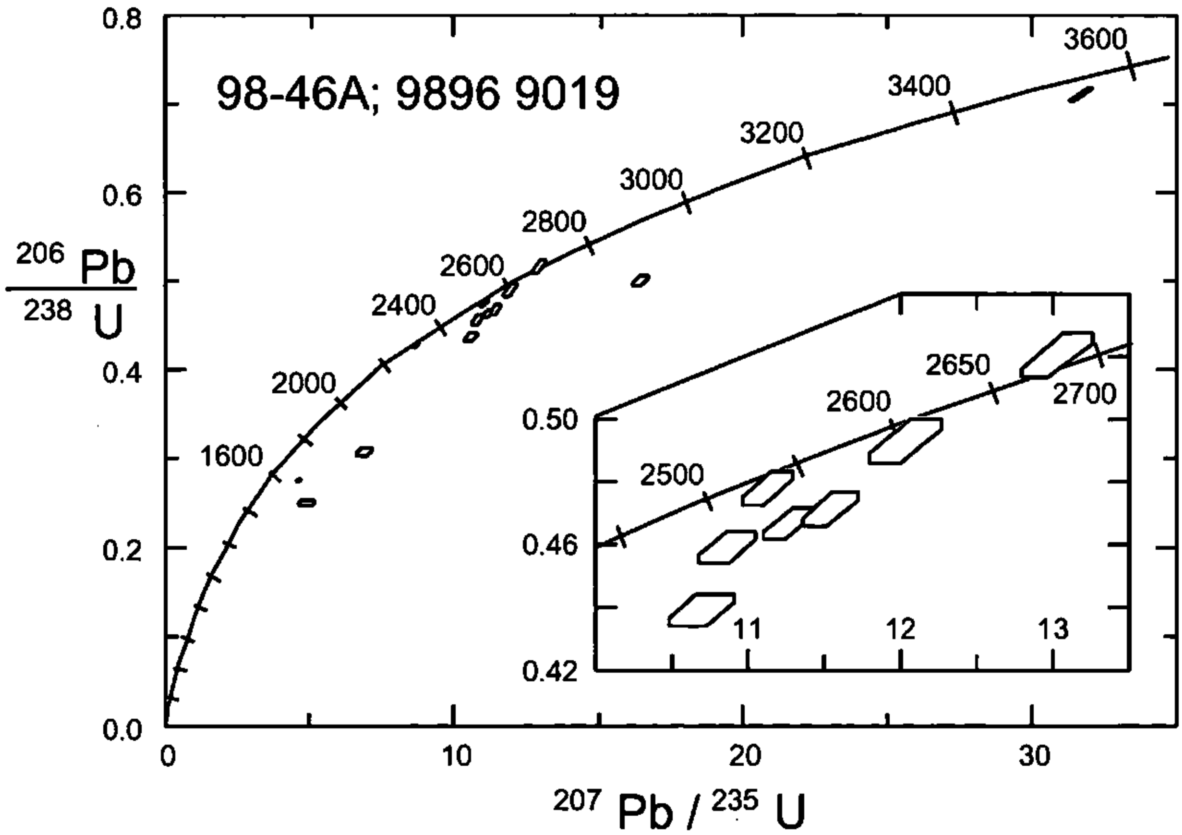

Figure z9896 9019: Concordia plot showing all SHRIMP zircon data for the monzogranite, Bluff Point (UWA mount 98-46A).

9896 9025: granodiorite, Buttercup Bore Granite

1:250,000 sheet:	Sandstone (SG5016)
AMG:	730512.1 mE, 6998495.1 mN
Location:	Drilled from outcrop
Province:	Southern Cross
Description:	Sparsely feldspar-porphyritic to equigranular medium to coarse-grained biotite granodiorite. Contains rare biotite-rich xenoliths and minor pegmatites.
Chemical group:	Low-Ca group, Beetle association, Yeelirrie clan
Pluton No:	274302
UWA mount:	98-46B

Description of zircons

The zircon population in this sample consists of one morphologic type. Grains range from 30-150 μm long with aspect ratios of 2:1 to 4:1. Grains are typically euhedral in external morphology with continuous euhedral internal zoning from core to rim. Most grains have more homogeneous core regions but there is no break in the euhedral growth from core to rim and they are not considered to be xenocrysts. Some grains show patchy annealed areas, particularly in the euhedrally zoned rim regions, which overprint the internal euhedral zoning. Pervasive fracture networks, which tend to indicate high U-contents and metamictisation, are rare and restricted to rim regions. Inclusions are rare. The grains are mostly pale brown in colour, with some grading to dark brown. The rare fracture networks and annealed patches were avoided during data collection.

Results and interpretation

Twenty one analyses on 21 grains are presented in Table z9896 9025 and shown on a concordia diagram in Figure z9896 9025. All analyses have U<250 ppm and most are less than 100 ppm. Omitting analyses that are >5% discordant leaves a population comprising 14 analyses which has a χ^2 of 0.86. The corresponding age is 2661 ± 7 Ma; this is interpreted as the emplacement age of the granitoid.

Table z9896 9025: SHRIMP zircon data for the granodiorite, Buttercup Bore (UWA mount 98-46B).

grain-spot	U (ppm)	Th (ppm)	4f206 (%)	$^{207}Pb^*/^{206}Pb^*$	$^{208}Pb^*/^{206}Pb^*$	$^{206}Pb^*/^{238}U$	$^{207}Pb^*/^{235}U$	$^{208}Pb^*/^{232}Th$	conc. (%)	$^{207}Pb/^{206}Pb$ age (Ma)
Main group.										
31-1	134	137	0.036	0.1827 ± 9	0.2788 ± 18	0.5023	12.654	0.1366	98	2678 ± 8
4-1	99	141	0.592	0.1805 ± 15	0.4065 ± 35	0.4824	12.005	0.1375	96	2657 ± 13
5-1	106	96	0.071	0.1803 ± 11	0.2403 ± 21	0.4994	12.416	0.1335	98	2656 ± 10
33-1	122	93	0.027	0.1814 ± 10	0.2049 ± 18	0.4789	11.975	0.1297	95	2665 ± 9
7-1	53	49	0.055	0.1819 ± 18	0.2490 ± 36	0.5124	12.851	0.1385	100	2670 ± 16
34-1	67	56	0.496	0.1783 ± 18	0.2220 ± 37	0.4939	12.140	0.1312	98	2637 ± 17
35-1	106	88	0.013	0.1809 ± 11	0.2232 ± 21	0.4924	12.282	0.1325	97	2661 ± 10
36-1	46	41	0.277	0.1792 ± 21	0.2437 ± 42	0.4904	12.116	0.1349	97	2645 ± 19
37-1	130	164	0.168	0.1811 ± 10	0.3416 ± 23	0.5029	12.558	0.1358	99	2663 ± 9
38-1	96	87	0.633	0.1792 ± 15	0.2577 ± 33	0.4782	11.816	0.1361	95	2646 ± 14
14-1	63	81	0.000	0.1817 ± 15	0.3529 ± 34	0.4869	12.199	0.1337	96	2669 ± 14
39-1	92	76	0.082	0.1803 ± 12	0.2290 ± 23	0.5048	12.547	0.1409	99	2655 ± 11
41-1	184	137	0.637	0.1795 ± 11	0.2053 ± 22	0.4872	12.059	0.1345	97	2648 ± 10
43-1	139	148	0.449	0.1820 ± 12	0.2869 ± 25	0.4879	12.245	0.1309	96	2671 ± 11
>5% discordant.										
2-1	198	231	2.881	0.1795 ± 19	0.1883 ± 41	0.3876	9.594	0.0626	80	2649 ± 17
3-1	131	148	0.308	0.1807 ± 11	0.2259 ± 22	0.4683	11.668	0.0938	93	2659 ± 10
32-1	69	67	1.434	0.1763 ± 23	0.2880 ± 52	0.4215	10.244	0.1259	87	2618 ± 22
40-1	106	54	11.244	0.1746 ± 54	0.2395 ±123	0.3524	8.485	0.1665	75	2602 ± 52
19-1	99	74	0.367	0.1833 ± 18	0.3346 ± 39	0.3395	8.579	0.1527	70	2683 ± 16
42-1	84	71	1.903	0.1816 ± 24	0.2594 ± 53	0.4559	11.416	0.1391	91	2668 ± 22
22-1	39	51	1.656	0.1820 ± 41	0.2861 ± 91	0.3885	9.752	0.0857	79	2672 ± 37

Data 14/4/99.
U/Pb scatter (1σ) for cz3 standard = 1.57% (n = 9).

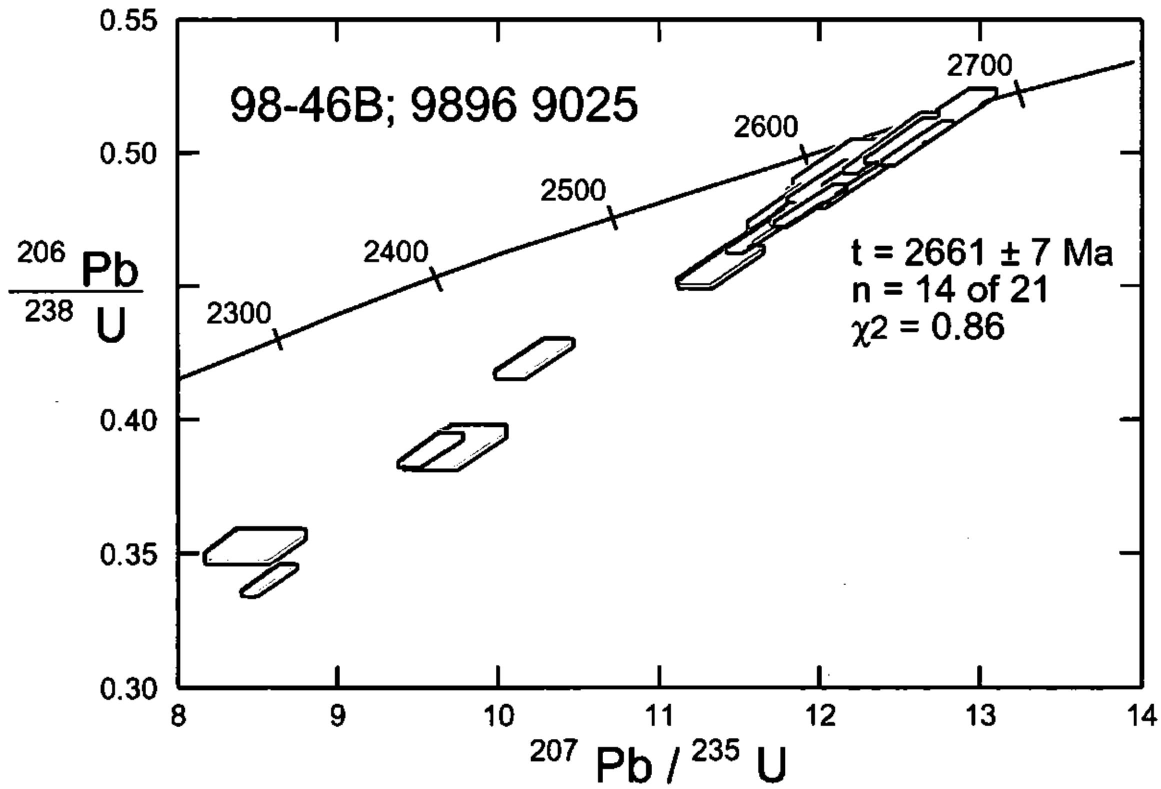

Figure z9896 9025: Concordia plot of all SHRIMP zircon data for the granodiorite, Buttercup Bore (UWA mount 98-46B).

9896 9033: granitic gneiss, Tom Bore Granite

1:250,000 sheet:	Sandstone (SG5016)
AMG:	710560.0 mE, 6974220.0 mN
Location:	Drilled from outcrop
Province:	Southern Cross
Description:	Banded to gneissic moderately to locally strongly feldspar porphyritic mdeium-grained biotite granite, with incipient biotite-rich banding. Cut by moderately abundant thin discordant pegmatites.
Chemical group:	High-Ca group, Diemals association, Diemals clan
Pluton No:	274304
UWA mount:	98-61C

Description of zircons

The zircon population in this sample consists of one morphologic type of euhedral to subhedral grains, with most grains being 80-300 µm long, with a relatively consistent aspect ratio of ~3-4:1. Grains are typically euhedral to subhedral in external morphology with evidence of continuous euhedral internal zoning from core to rim. A distinctive feature from SEM images of many grains is a thick homogeneous rim zone which appears to have recrystallised, preserving only occasional relicts of the former euhedral zoning. In some grains, this recrystallisation has engulfed the whole grain. In other grains, the outermost rim zone has failed to recrystallise. Where this occurs, the outermost rim zone is <10 µm wide and distinctly euhedral. Inclusions are rare. The grains are generally pale brown to light brown in colour, grading to darker brown, particularly in the cores of some grains which correspond to the unrecrystallised areas. Strong euhedral zoning observed on both optical and SEM images suggest high U-Th-contents and radiation damage in the unrecrystallised areas of some grains. Many grains have fracture networks typical of high-U grains, which have significant metamictisation. However, this is far more obvious in the unrecrystallised areas. Fractures often terminate where they enter the recrystallised areas. The fractures and dark areas were avoided during data collection such that all data collected was for the recrystallised areas.

Results and interpretation

Twenty three analyses on 19 grains are presented in Table z9896 9033 and shown on a concordia diagram in Figure z9896 9033. The data all have U<250 ppm and very low common-Pb contamination. Omitting one analysis that is >5% discordant and one statistical outlier leaves a population comprising 21 analyses which has a χ^2 of 0.91. The corresponding age is 2671 ± 3 Ma; this is interpreted as the emplacement age of the granitoid.

Table z9896 9033: SHRIMP zircon data for the granitic gneiss, Tom Bore. (UWA mount 98-61C).

grain-spot	U (ppm)	Th (ppm)	4f206 (%)	$\frac{^{207}Pb^*}{^{206}Pb^*}$	$\frac{^{208}Pb^*}{^{206}Pb^*}$	$\frac{^{206}Pb^*}{^{238}U}$	$\frac{^{207}Pb^*}{^{235}U}$	$\frac{^{208}Pb^*}{^{232}Th}$	conc. (%)	$^{207}Pb/^{206}Pb$ age (Ma)
Main group.										
1-1	167	177	0.121	0.1819 ± 7	0.3016 ± 16	0.4957	12.432	0.1411	97	2670 ± 7
1-2	193	155	0.003	0.1833 ± 6	0.2209 ± 12	0.5133	12.971	0.1414	100	2683 ± 6
2-1	209	183	0.038	0.1818 ± 6	0.2388 ± 10	0.5214	13.070	0.1421	101	2669 ± 5
3-1	176	180	0.000	0.1814 ± 6	0.2755 ± 12	0.5170	12.932	0.1397	101	2666 ± 5
4-1	178	136	0.055	0.1816 ± 7	0.1998 ± 12	0.5058	12.664	0.1329	99	2667 ± 6
5-1	206	227	0.080	0.1814 ± 6	0.3078 ± 14	0.5089	12.730	0.1418	99	2666 ± 6
6-1	212	183	0.148	0.1817 ± 6	0.2384 ± 11	0.5196	13.018	0.1440	101	2668 ± 6
6-2	233	161	0.068	0.1820 ± 6	0.1935 ± 9	0.5193	13.029	0.1449	101	2671 ± 5
7-1	206	120	0.033	0.1822 ± 6	0.1590 ± 9	0.5172	12.997	0.1413	101	2673 ± 5
8-1	242	196	0.009	0.1831 ± 6	0.2234 ± 10	0.5139	12.976	0.1416	100	2682 ± 5
9-1	201	162	0.061	0.1824 ± 6	0.2236 ± 12	0.5113	12.860	0.1414	100	2675 ± 6
11-1	196	246	0.025	0.1815 ± 6	0.3408 ± 14	0.5147	12.883	0.1402	100	2667 ± 6
11-2	195	154	0.034	0.1819 ± 6	0.2145 ± 11	0.5058	12.682	0.1371	99	2670 ± 6
12-1	209	181	0.000	0.1817 ± 6	0.2377 ± 10	0.5128	12.843	0.1405	100	2668 ± 5
13-1	205	198	0.000	0.1831 ± 6	0.2700 ± 12	0.4902	12.379	0.1372	96	2682 ± 6
14-1	196	191	0.000	0.1822 ± 6	0.2652 ± 11	0.5172	12.994	0.1407	101	2673 ± 5
18-1	186	233	0.000	0.1821 ± 6	0.3411 ± 13	0.5259	13.206	0.1430	102	2672 ± 5
19-1	195	240	0.027	0.1821 ± 6	0.3365 ± 14	0.5068	12.725	0.1390	99	2672 ± 6
22-1	145	133	0.014	0.1807 ± 7	0.2531 ± 14	0.5100	12.706	0.1401	100	2659 ± 7
23-1	139	150	0.000	0.1818 ± 7	0.2950 ± 14	0.5228	13.105	0.1423	102	2669 ± 6
26-1	204	223	0.007	0.1820 ± 6	0.2975 ± 13	0.5182	13.002	0.1409	101	2671 ± 6
>5% discordant.										
21-1	221	195	0.285	0.1827 ± 8	0.2468 ± 15	0.4748	11.961	0.1328	94	2678 ± 7
Possible young outlier.										
2-2	279	178	0.113	0.1803 ± 6	0.1737 ± 9	0.5085	12.643	0.1383	100	2656 ± 5

Data 13/02/00.
U/Pb scatter (1σ) for cz3 standard = 1.87% (n = 12).

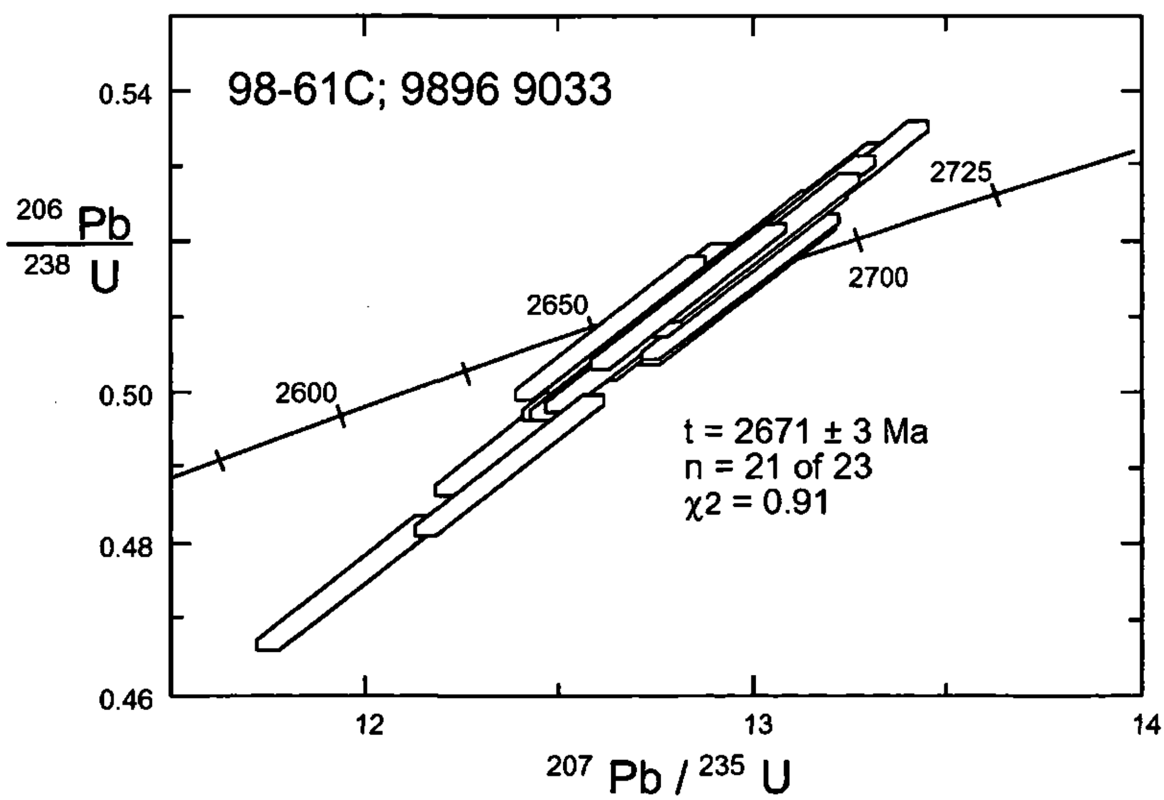

Figure z9896 9033: Concordia plot showing all SHRIMP zircon data for the granitic gneiss, Tom Bore (UWA mount 98-61C).

9896 9042: quartz monzonite granophyre, Barlanga Well Granite

1:250,000 sheet:	Sandstone (SG5016)
AMG:	682020.0 mE, 6992125.0 mN
Location:	Drilled from outcrop
Province:	Southern Cross
Description:	Fine to medium-grained, quartz monzonite granophyre. Granophyric textures, including intergrowths of quartz and feldspar, suggests granitoid emplaced at a high level. Granitoid intrudes Yarrabubba granite (9896 9043/9044).
Chemical group:	Low-Ca group, Beetle association, Barlangi Rock clan
Pluton No:	264305
UWA mount:	98-61A

Description of zircons

The zircon population in this sample consists of one morphologic type of subhedral to anhedral grains, with most grains being 40-80 μm long, with a few grains up to ~120 μm long. The aspect ratios of the smaller grains are ~1-2:1, and grade to ~3:1 for larger grains. On the basis of internal morphology, the grains may be divided into two groups. The first has no internal structure to very faint euhedral zoning and few fractures, whereas the other has strongly developed continuous euhedral zoning from core to rim, discordant alteration patches and generally pervasive fracturing. Some of the latter type have structureless areas which suggests the two are related. Inclusions are relatively rare. The grains range from pale brown to dark brown to nearly opaque in colour. Strong euhedral zoning observed on both optical and SEM images suggest high U-Th-contents and radiation damage. The grains have fracture networks also suggest high-U contents and significant metamictisation. The alteration patches and fractures, and dark grains were avoided during data collection, which limited data collection to the largely structureless grains.

Results and interpretation

Twenty analyses on 20 zircons are presented in Table z9896 9042 and shown in Figure z9896 9042. The U abundances are mostly <250 ppm and the common Pb corrections were low, but about half the data are strongly discordant and there is a large range in $^{207}Pb/^{206}Pb$ ages, even amongst the more concordant data. Omitting data which have 4f206>5%, and four statistical outliers from the remainder, leaves a reasonably coherent group of seven analyses at ~2715 Ma. Although this could be taken as the minimum emplacement age of the granitoid, it is considered more likely that it represents the age of a dominant source of xenocrysts. This interpretation is consistent with the intrusive relationship of this rock with 9896 9044. There are two other grains that are almost certainly xenocrysts, with $^{207}Pb/^{206}Pb$ ages ~ 2820 Ma. The existence of concordant dates <2600 Ma makes interpretation of the 2600–2700 Ma dates particularly difficult.

Table z9896 9042: SHRIMP zircon data for the quartz monzonite granophyre, Barlanga Well. (UWA mount 98-61A).

grain-spot	U (ppm)	Th (ppm)	4f206 (%)	$^{207}Pb^*/^{206}Pb^*$	$^{208}Pb^*/^{206}Pb^*$	$^{206}Pb^*/^{238}U$	$^{207}Pb^*/^{235}U$	$^{208}Pb^*/^{232}Th$	conc. (%)	$^{207}Pb/^{206}Pb$ age (Ma)
Main group.										
24-1	64	20	0.000	0.1883 ± 18	0.0802 ± 17	0.5370	13.945	0.1405	102	2728 ± 15
19-1	197	158	0.108	0.1890 ± 11	0.1987 ± 19	0.5144	13.408	0.1280	98	2734 ± 10
23-1	115	89	0.139	0.1857 ± 16	0.2055 ± 29	0.5204	13.325	0.1373	100	2704 ± 14
29-1	65	35	0.557	0.1906 ± 27	0.1323 ± 51	0.5328	14.000	0.1290	100	2747 ± 23
30-1	132	113	0.145	0.1845 ± 16	0.2249 ± 31	0.4966	12.630	0.1312	96	2694 ± 15
31-1	78	79	0.210	0.1888 ± 20	0.2653 ± 39	0.5199	13.531	0.1365	99	2731 ± 17
10-1	257	164	0.017	0.1849 ± 10	0.1727 ± 16	0.5095	12.988	0.1378	98	2697 ± 9
>5% discordant or 4f206>1%.										
3-1	30	22	1.287	0.1696 ± 46	0.1668 ± 96	0.4841	11.321	0.1117	100	2554 ± 46
25-1	226	401	0.268	0.1910 ± 13	0.1663 ± 23	0.4291	11.302	0.0402	84	2751 ± 11
26-1	232	437	0.359	0.1898 ± 13	0.1632 ± 24	0.4148	10.853	0.0359	82	2740 ± 12
17-1	15	21	0.000	0.1819 ± 43	0.3917 ±104	0.4558	11.434	0.1259	91	2671 ± 39
27-1	147	96	0.092	0.1991 ± 15	0.0794 ± 21	0.4978	13.667	0.0602	92	2819 ± 12
28-1	459	781	0.693	0.1723 ± 13	0.0788 ± 25	0.3079	7.314	0.0142	67	2580 ± 13
15-1	173	215	2.495	0.1828 ± 27	0.3395 ± 60	0.4721	11.897	0.1288	93	2678 ± 24
32-1	47	39	1.135	0.1783 ± 40	0.1183 ± 80	0.4333	10.653	0.0614	88	2637 ± 37
11-1	167	248	0.232	0.1811 ± 16	0.1805 ± 28	0.4241	10.588	0.0513	86	2663 ± 14
Age outliers.										
1-1	136	106	0.000	0.1405 ± 11	0.2041 ± 21	0.4161	8.062	0.1090	100	2234 ± 14
5-1	105	104	0.062	0.1821 ± 15	0.2648 ± 28	0.5022	12.609	0.1339	98	2672 ± 13
6-1	58	23	0.000	0.1997 ± 19	0.1063 ± 20	0.5559	15.307	0.1479	101	2824 ± 16
7-1	151	97	0.000	0.1769 ± 13	0.1796 ± 19	0.4905	11.962	0.1363	98	2624 ± 12

Data 15/01/00.
U/Pb scatter (1σ) for cz3 standard = 1.72% (n = 9).

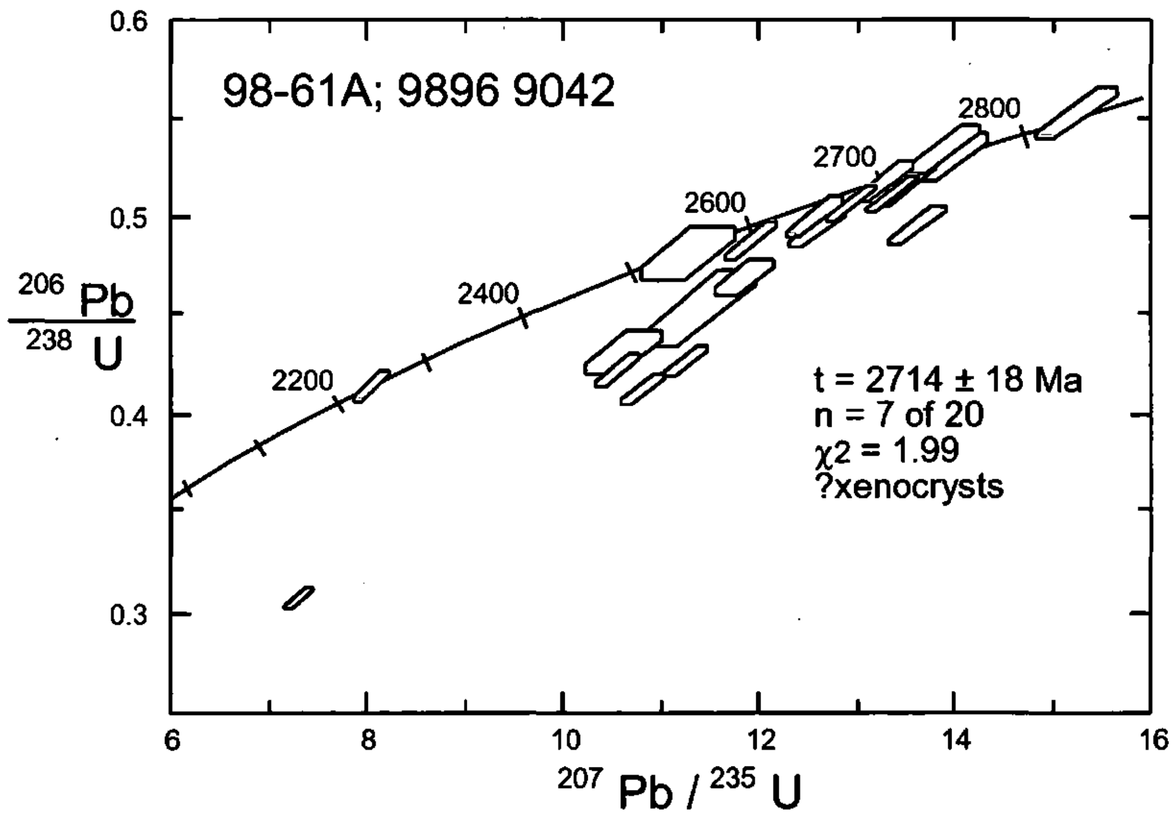

Figure z9896 9042: Concordia plot showing all SHRIMP zircon data for the quartz monzonite granophyre, Barlanga Well (UWA mount 98-61A).

9896 9044: granite, Yarrabubba Granite

1:250,000 sheet:	Sandstone (SG5016)
AMG:	679987 mE, 6995316 mN
Location:	Drilled from outcrop
Province:	Southern Cross
Description:	Weakly altered, seriate medium- to coarse-grained biotite granite containing hematised 'red-spots' throughout rock and local 'brick-red' alteration; minor pegmatite.
Chemical group:	Low-Ca group, Beetle association, Yarrabubba clan
Pluton No:	264304
UWA mount:	A-15B

Description of zircons

The zircon population in this sample consists of one morphologic type of finely zoned euhedral to subhedral grains, with most grains being 30-100 µm long, with a range of aspect ratios from ~2-3:1 for the majority, to ~4:1. Grains are typically euhedral to subhedral in external morphology with continuous euhedral internal zoning from core to rim. Inclusions are rare. The grains range from pale brown to dark brown to nearly opaque in colour. Strong euhedral zoning observed on both optical and SEM images suggest high U-Th-contents and radiation damage. Discordant alteration patches are visible on SEM images of some grains, and overgrow the euhedral zoning. Some grains have more homogeneous core regions but there is no break in the euhedral growth from core to rim and they are not considered to be xenocrysts. Most grains have pervasive fracture networks typical of high-U grains, which have significant metamictisation. The alteration patches and fractures, and dark grains were avoided during data collection.

Results and interpretation

Seventeen analyses on 17 grains are presented in Table z9896 9044 and shown on a concordia diagram in Figure z9896 9044. The analyses show a wide scatter with major discordance, as expected for U abundance ranging ~200 ppm – ~750 ppm, but common-Pb corrections are generally not severe. Omitting all data that are >5% discordant and one statistical outlier (younger; >600 ppm U), leaves a reasonably coherent group of six point which gives an age of ~2650 Ma, with $\chi^2 = 1.41$. The Pb-loss trend is predominantly towards the origin, suggesting there was no Archaean resetting of these zircons, and the 2650 ± 10 Ma age is interpreted to be the emplacement age of the granitoid. There is one apparent xenocryst with an age ~2750 Ma.

Table z9896 9044: SHRIMP zircon data for the granite, Yarrabubba. (UWA mount A-15B).

grain-spot	U (ppm)	Th (ppm)	4f206 (%)	$^{207}Pb^*/^{206}Pb^*$	$^{208}Pb^*/^{206}Pb^*$	$^{206}Pb^*/^{238}U$	$^{207}Pb^*/^{235}U$	$^{208}Pb^*/^{232}Th$	conc. (%)	$^{207}Pb/^{206}Pb$ age (Ma)
12-1	288	66	0.019	0.1800 ± 6	0.0606 ± 7	0.5038	12.505	0.1334	99	2653 ± 6
13-1	460	256	0.374	0.1802 ± 7	0.1501 ± 12	0.4766	11.846	0.1287	95	2655 ± 6
24-1	209	91	0.112	0.1779 ± 8	0.0925 ± 12	0.4724	11.588	0.1001	95	2634 ± 8
26-1	293	249	0.012	0.1801 ± 7	0.2383 ± 12	0.4911	12.196	0.1376	97	2654 ± 6
28-1	394	97	0.010	0.1801 ± 6	0.0655 ± 6	0.4932	12.245	0.1317	97	2654 ± 5
30-1	176	289	0.057	0.1786 ± 9	0.4223 ± 22	0.4959	12.210	0.1277	98	2640 ± 8
>5% discordant										
19-1	307	509	0.216	0.1787 ± 10	0.3036 ± 21	0.3257	8.024	0.0596	69	2641 ± 9
18-1	179	313	0.357	0.1772 ± 11	0.3776 ± 25	0.4429	10.819	0.0955	90	2627 ± 10
21-1	517	552	0.288	0.1746 ± 6	0.2283 ± 12	0.4310	10.376	0.0922	89	2602 ± 6
22-1	152	193	0.326	0.1797 ± 13	0.2980 ± 28	0.4015	9.948	0.0939	82	2650 ± 12
23-1	166	279	0.892	0.1730 ± 16	0.4511 ± 40	0.3707	8.840	0.0998	79	2586 ± 16
25-1	284	281	0.706	0.1774 ± 10	0.3756 ± 23	0.4112	10.058	0.1563	84	2629 ± 9
27-1	574	1616	0.191	0.1705 ± 6	0.3633 ± 14	0.4454	10.468	0.0575	93	2562 ± 6
3-1	735	583	0.255	0.1679 ± 5	0.1890 ± 9	0.4423	10.239	0.1054	93	2537 ± 5
29-1	286	164	0.265	0.1915 ± 9	0.1432 ± 14	0.4041	10.667	0.1011	79	2755 ± 7
31-1	318	135	0.212	0.1787 ± 7	0.0867 ± 11	0.4655	11.467	0.0947	93	2641 ± 7
Young outlier										
20-1	611	114	0.203	0.1755 ± 5	0.0510 ± 7	0.4759	11.519	0.1300	96	2611 ± 5

Data 10/6/00.
U/Pb scatter (1σ) for cz3 standard = 0.86% (n = 7).

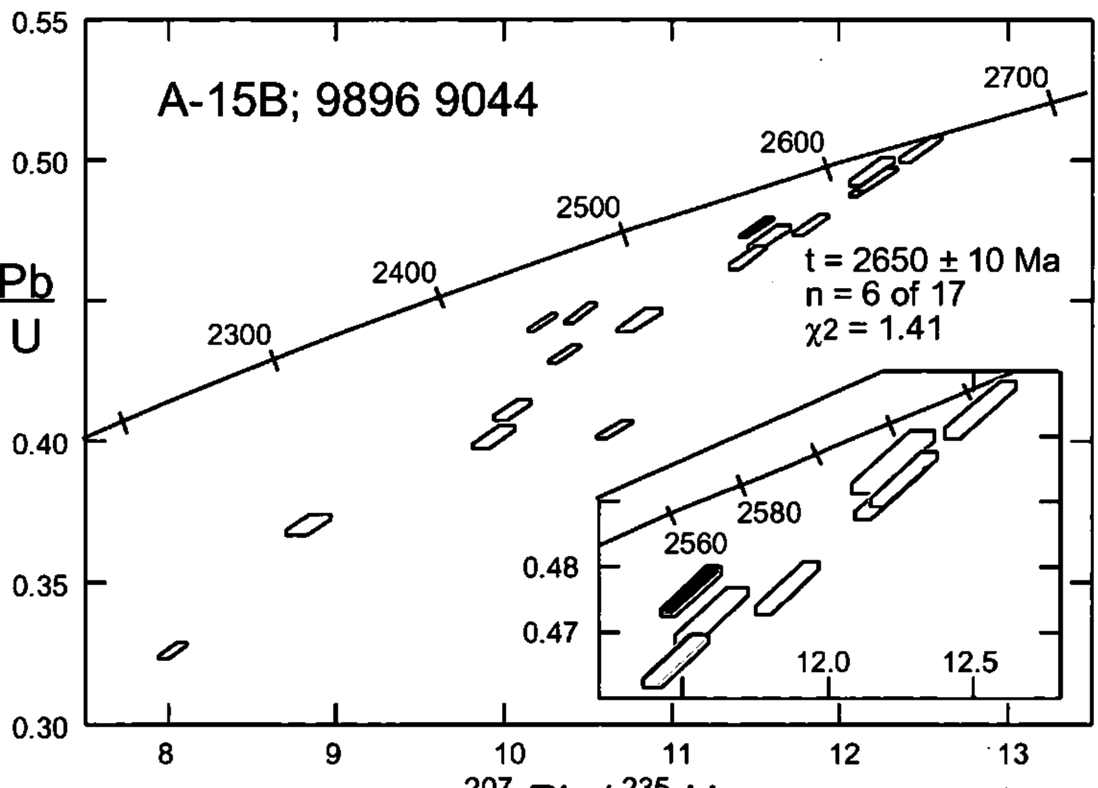

Figure z9896 9044: Concordia plot of SHRIMP zircon data for the granite, Yarrabubba (UWA mount A-15B).

9896 9045: monzogranite, Monty Bore Granite

1:250,000 sheet:	Sandstone (SG5016)
AMG:	696805.0 mE, 6993109.9 mN
Location:	Drilled from outcrop
Province:	Southern Cross
Description:	Foliated seriate medium-grained biotite monzogranite. Granite contains a moderate foliation with strong alignment of biotite, recrystallised quartz and pegmatite dykes to 20 cm.
Chemical group:	High-Ca group, Diemals association, Yoothapinna clan
Pluton No:	264314
UWA mount:	98-61D

Description of zircons

The zircon population in this sample consists of one morphologic type of strongly zoned euhedral grains, with most grains being 60-120 μm long, with a range of aspect ratios from ~2-3:1 for the majority, to ~4:1. Grains are typically euhedral in external morphology with continuous euhedral internal zoning from core to rim. Inclusions are rare. In a few grains, 10-20 μm inclusions of apatite(?) occur in both core and rim areas. The grains range from pale brown to dark brown in colour. Strong euhedral zoning observed on both optical and SEM images suggest high U-Th-contents and radiation damage. Discordant alteration patches are common on SEM images, and overgrow the euhedral zoning. Some grains have more homogeneous core regions but there is no break in the euhedral growth from core to rim and they are not considered to be xenocrysts. Two grains are essentially homogeneous and structureless in their internal morphology, although one has a thin rim of euhedrally zoned growth. Most of the euhedrally zoned grains have fracture networks typical of high-U grains, which have significant metamictisation. The alteration patches and fractures could not be avoided during data collection. However, the only consistent age data has come from the two largely structureless grains (#25, 26).

Results and interpretation

Nine analyses on nine grains are presented in Table z9896 9045 and shown on a concordia diagram in Figure z9896 9045. Analyses of many other grains were aborted when high ^{204}Pb signals were observed. Analyses with >200 ppm U tend to discordance and younger dates. Omitting all data with >5% discordance or >1% 4f206, and one anomalously young discordant point, leaves a concordant group of four analyses which comprise a single age population with a pooled age of 2700 ± 15 Ma, and a χ^2 of 0.38. This could be interpreted as the emplacement age of the granitoid, but since the data are all from only two grains, this could well be a xenocryst age. Additional data would improve this age determination, but finding grains with well-preserved U–Pb systems is very difficult and slow.

Table z9896 9045: SHRIMP zircon data for the monzogranite, Monty Bore (UWA mount 98-61D).

grain-spot	U (ppm)	Th (ppm)	4f206 (%)	$^{207}Pb^*/^{206}Pb^*$	$^{208}Pb^*/^{206}Pb^*$	$^{206}Pb^*/^{238}U$	$^{207}Pb^*/^{235}U$	$^{208}Pb^*/^{232}Th$	conc. (%)	$^{207}Pb/^{206}Pb$ age (Ma)
Possible magmatic group										
25-1	84	106	0.277	0.1837 ± 13	0.3593 ± 29	0.5039	12.762	0.1435	98	2686 ± 11
25-2	67	73	0.016	0.1853 ± 12	0.2972 ± 25	0.5372	13.722	0.1464	103	2701 ± 11
26-1	112	41	0.000	0.1849 ± 8	0.0993 ± 8	0.5340	13.616	0.1442	102	2698 ± 7
26-2	132	71	0.000	0.1853 ± 7	0.1462 ± 9	0.5321	13.592	0.1440	102	2700 ± 6
>5% discordant or 4f206>1%										
2-1	397	179	0.458	0.1766 ± 6	0.1218 ± 11	0.4597	11.193	0.1239	93	2621 ± 6
29-1	236	275	7.862	0.1798 ± 24	0.1285 ± 52	0.4066	10.081	0.0449	83	2651 ± 22
30-1	185	132	5.408	0.1783 ± 21	0.1067 ± 45	0.4729	11.625	0.0710	95	2637 ± 19
31-1	203	51	1.207	0.1802 ± 10	0.0638 ± 20	0.4792	11.903	0.1225	95	2654 ± 9
Young outlier										
28-1	233	230	0.004	0.1083 ± 5	0.2821 ± 13	0.3146	4.698	0.0900	100	1771 ± 8

Data 13/02/00.
U/Pb scatter (1s) for cz3 standard = 1.87% (n = 12).

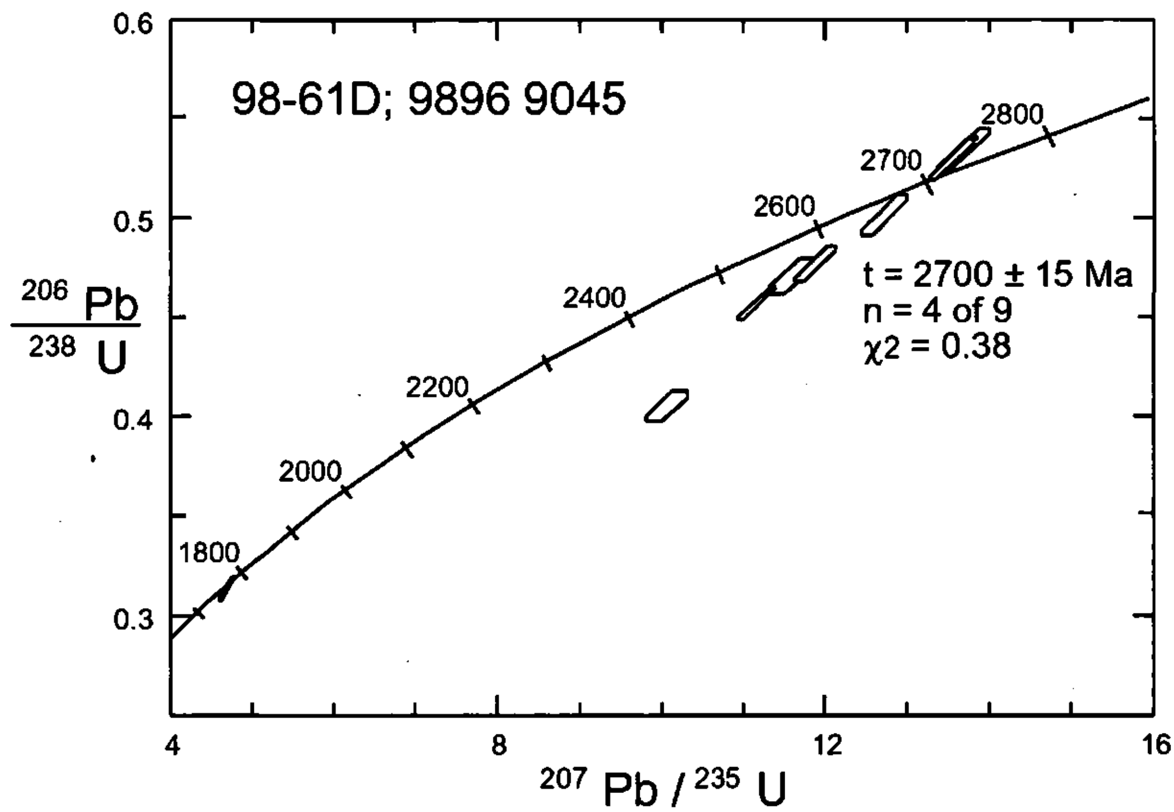

Figure z9896 9045: Concordia plot of SHRIMP zircon data for the monzogranite, Monty Bore (UWA mount 98-61D).

9896 9055: monzogranite, Woodley Bluff Granite

1:250,000 sheet:	Sandstone (SG5016)
AMG:	736455.0 mE, 6946410.0 mN
Location:	Cork Screw Well granitic gneiss complex; sample drilled from outcrop
Province:	Southern Cross
Description:	Foliated medium-grained biotite monzogranite gneiss. Moderate to strongly foliated with large elongated enclaves/pendants to 1-10 m of medium-coarse-grained amphibolite. Discordant pegmatite dykes. Fine- to medium-grained granite dykes are foliated but locally discordant.
Chemical group:	High-Ca group, Diemals association, Yoothapinna clan
Pluton No:	274205
UWA mount:	98-51B

Description of zircons

A large amount (compared to other samples) of the zircon in sample 9896-9055 was recovered as irregular shaped fragments, although most of the grains are more typical euhedral crystals and fragments. Grain size varies from approximately 50 to up to 200 μm long. Clear, transparent, colourless grains, as well as darker (pale brown to dark brown) grains are present. Most grains contain some cracks and fractures. Some grains are totally devoid of internal structures or only contain weak zoning, whereas other grains are more pervasively zoned or contain zones of intense metamictisation. Inclusions are evident in some grains. These features are seen both in the SEM images and on the photos.

Results and interpretation

Twenty-three analyses on 22 grains are presented in Table z9896 9055 and shown on a concordia diagram in Figure z9896 9055. Omitting discordant analyses, zircons with high common-Pb and one ?inherited grain, the population comprising the remaining 13 analyses has a χ^2 of 0.87. The corresponding age is 2712 ± 6 Ma, and this is interpreted as the emplacement age of the granite.

Table z9896 9055: SHRIMP analytical data for the biotite granitic gneiss, Cork Screw Well complex, Woodley Bluff (UWA mount 98-51B).

grain-spot	U (ppm)	Th (ppm)	4f206 (%)	$^{207}Pb^*/^{206}Pb^*$	$^{208}Pb^*/^{206}Pb^*$	$^{206}Pb^*/^{238}U$	$^{207}Pb^*/^{235}U$	$^{208}Pb^*/^{232}Th$	conc. (%)	$^{207}Pb/^{206}Pb$ age (Ma)
1-1	56	32	0.032	0.1866 ± 15	0.1537 ± 26	0.5278	13.577	0.1428	101	2712 ± 13
2-1	113	114	0.085	0.1862 ± 10	0.2749 ± 19	0.5099	13.092	0.1388	98	2709 ± 8
3-1	146	111	0.096	0.1863 ± 8	0.2067 ± 15	0.5155	13.240	0.1401	99	2710 ± 7
8-1	143	156	0.740	0.1877 ± 11	0.3013 ± 25	0.5147	13.321	0.1421	98	2722 ± 10
26-1	159	84	1.655	0.1868 ± 14	0.1556 ± 29	0.5180	13.340	0.1532	99	2714 ± 12
22-1	177	168	0.399	0.1873 ± 9	0.2554 ± 18	0.5201	13.433	0.1399	99	2719 ± 8
20-1	214	126	0.105	0.1848 ± 7	0.1645 ± 12	0.5130	13.072	0.1431	99	2697 ± 6
20-2	171	108	0.201	0.1868 ± 8	0.1751 ± 14	0.5168	13.313	0.1438	99	2714 ± 7
18-1	68	54	0.741	0.1896 ± 17	0.1873 ± 34	0.5097	13.324	0.1216	97	2739 ± 15
17-1	44	21	0.148	0.1869 ± 18	0.1393 ± 31	0.4904	12.639	0.1395	95	2715 ± 16
12-1	97	107	0.142	0.1864 ± 11	0.3006 ± 22	0.5178	13.305	0.1415	99	2710 ± 10
29-1	84	85	0.056	0.1870 ± 11	0.2783 ± 22	0.5244	13.519	0.1446	100	2716 ± 10
30-1	53	55	0.141	0.1868 ± 14	0.2857 ± 27	0.5224	13.454	0.1429	100	2714 ± 12
Discordant										
6-1	900	1130	0.557	0.1074 ± 5	0.3373 ± 14	0.2114	3.130	0.0568	70	1755 ± 9
21-1	1089	118	4.911	0.1301 ± 11	0.0479 ± 24	0.2878	5.164	0.1269	78	2100 ± 14
16-1	218	103	8.976	0.1601 ± 30	0.1782 ± 68	0.3647	8.051	0.1373	82	2457 ± 32
High common Pb										
4-1	77	89	5.863	0.1884 ± 34	0.3383 ± 78	0.5191	13.482	0.1525	99	2728 ± 30
9-1	132	69	5.846	0.1878 ± 26	0.1241 ± 57	0.5215	13.505	0.1241	99	2723 ± 23
25-1	48	32	18.741	0.1701 ± 81	0.2076 ±184	0.5171	12.128	0.1640	105	2559 ± 80
27-1	88	135	10.555	0.1827 ± 42	0.2496 ± 94	0.5436	13.692	0.0890	105	2677 ± 38
24-1	234	249	32.386	0.1873 ± 51	0.4578 ±119	0.5165	13.340	0.2222	99	2719 ± 45
28-1	41	30	5.045	0.1853 ± 46	0.1623 ±101	0.5206	13.303	0.1150	100	2701 ± 41
?Inherited										
10-1	260	220	1.854	0.2262 ± 11	0.2038 ± 22	0.5850	18.245	0.1410	98	3025 ± 8

Data 3/10/98.
U/Pb scatter (1σ) for cz3 standard = 0.96% (n=15).

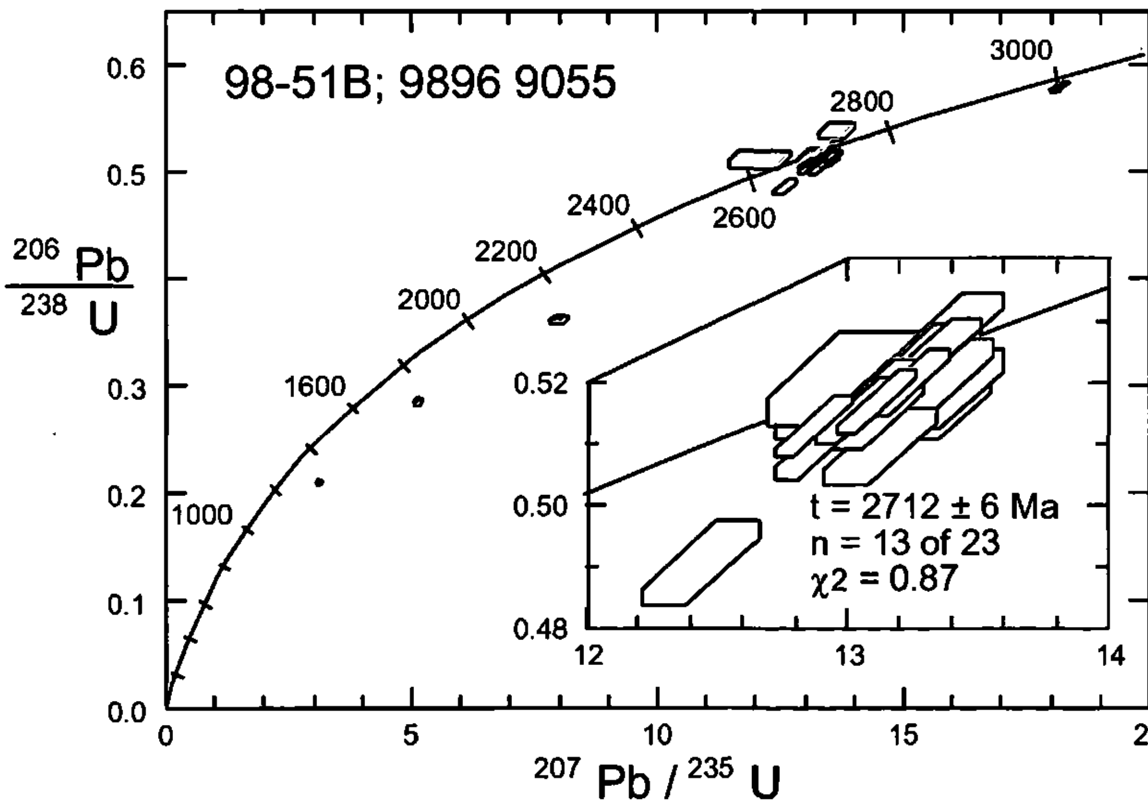

Figure z9896 9055: Concordia plot SHRIMP zircon data for the biotite granitic gneiss, Cork Screw Well complex, Woodley Bluff (UWA mount 98-51B).

9996 4003: biotite monzogranite, Goolthan Goolthan

Acknowledgement: These data were obtained as part of the 1999 BSc Honours (UWA) project of Bill Oliver, and were made available to AMIRA P482 at no cost.

1:250,000 sheet:	Yalgoo (SH5002)
AMG:	474539.6 mE, 6890074.4 mN
Location:	Hammered from boulders from Goolthan Goolthan Rock, that forms the major outcrop of the Goolthan Goolthan regional monzogranite.
Province:	Murchison
Description:	Sparsely feldspar porphyritic medium-grained biotite monzogranite
Chemical group:	Low-Ca group, Goolthan association, Goolthan clan
Pluton No:	224112
UWA mounts:	99-73E (zircon) and 99-71B (titanite)

Description of zircons

The zircon population in this sample consists of one morphologic type of zoned euhedral to subhedral grains, with most grains being 40-120 μm long, with a range of aspect ratios from ~2:1 to ~4:1. Grains are typically euhedral to subhedral in external morphology with continuous euhedral internal zoning from core to rim. Inclusions are rare. The grains range from pale brown to mauve to dark brown in colour. Strong euhedral zoning observed in the darker grains suggest high U-Th-contents and radiation damage. Some grains have fracture networks typical of high-U grains, which have significant metamictisation. The dark grains and fractures were avoided during data collection.

Description of titanites

The titanites from this sample are all 50-200 μm fragments of larger grains. Only rarely do grains show growth surfaces; most surfaces are fractures. The grains are dark brown to pale brown in colour. Some grains are almost black and have evenly distributed dense and very fine inclusion populations. Areas of SHRIMP analysis were in clean parts of the grains, avoiding inclusions and fractures.

Results and interpretation

Zircon

Twenty analyses on 20 grains are presented in Table z9996 4003 and shown on a concordia diagram in Figure z9996 4003. Despite having U contents up to ~500 ppm the data are almost all concordant and have very low common-Pb contamination. Omitting one analysis that is >5% discordant and one (marginal) statistical outlier leaves a population comprising 18 analyses which has a χ^2 of 0.70. The corresponding age is 2626 ± 6 Ma; this is interpreted as the emplacement age of the granitoid.

Titanite

Fifteen analyses on 15 fragments are presented in Table t9996 4003 and shown on a concordia diagram in Figure t9996 4003. The data all fall in a single cluster, with χ^2 of 1.22 for $^{207}Pb/^{206}Pb$. Although this indicates scatter beyond systematic limits, there are no compelling grounds for omitting any particular data points. The data set is interpreted as a single age population at 2630 ± 5 Ma, taken to be the emplacement age of the granitoid.

Combining the zircon and titanite results give an age of 2628 ± 4 Ma for the monzogranite.

Table z9996 4003: SHRIMP zircon data for the monzogranite, Goolthan Goolthan (UWA mount 99-73E).

grain-spot	U (ppm)	Th (ppm)	4f206 (%)	$^{207}Pb^*/^{206}Pb^*$	$^{208}Pb^*/^{206}Pb^*$	$^{206}Pb^*/^{238}U$	$^{207}Pb^*/^{235}U$	$^{208}Pb^*/^{232}Th$	conc. (%)	$^{207}Pb/^{206}Pb$ age (Ma)
1-1	259	72	0.063	0.1764 ± 8	0.0750 ± 7	0.5007	12.179	0.1342	100	2620 ± 8
4-1	109	76	0.141	0.1787 ± 11	0.1947 ± 19	0.5105	12.576	0.1415	101	2640 ± 10
5-1	138	95	0.057	0.1783 ± 10	0.1930 ± 18	0.4868	11.968	0.1355	97	2637 ± 9
6-1	73	64	0.117	0.1745 ± 15	0.2342 ± 29	0.5025	12.091	0.1329	101	2601 ± 14
7-1	125	142	0.068	0.1761 ± 9	0.3056 ± 20	0.4991	12.115	0.1343	100	2616 ± 9
8-1	219	188	0.029	0.1770 ± 12	0.2306 ± 22	0.4834	11.796	0.1302	97	2625 ± 11
9-1	140	133	0.038	0.1779 ± 10	0.2585 ± 19	0.5071	12.436	0.1375	100	2633 ± 9
10-1	93	69	0.179	0.1767 ± 13	0.2005 ± 26	0.4865	11.855	0.1315	97	2623 ± 13
11-1	100	63	0.196	0.1761 ± 20	0.1741 ± 25	0.4856	11.790	0.1351	98	2617 ± 19
12-1	43	33	0.246	0.1765 ± 23	0.2031 ± 47	0.5068	12.337	0.1360	101	2621 ± 21
13-1	581	310	0.074	0.1779 ± 8	0.1465 ± 9	0.5015	12.300	0.1375	100	2633 ± 8
14-1	99	80	0.215	0.1768 ± 18	0.2143 ± 27	0.4884	11.902	0.1307	98	2623 ± 17
15-1	134	119	0.185	0.1759 ± 13	0.2501 ± 22	0.4782	11.597	0.1348	96	2614 ± 12
16-1	58	48	0.120	0.1782 ± 15	0.2202 ± 28	0.4950	12.163	0.1332	98	2636 ± 14
17-1	156	143	0.085	0.1771 ± 11	0.2517 ± 21	0.5223	12.754	0.1436	103	2626 ± 11
18-1	88	78	0.284	0.1770 ± 15	0.2343 ± 31	0.5132	12.527	0.1365	102	2625 ± 14
19-1	108	109	0.136	0.1763 ± 11	0.2743 ± 22	0.5045	12.261	0.1367	101	2618 ± 10
20-1	299	178	0.050	0.1775 ± 9	0.1629 ± 11	0.5181	12.680	0.1413	102	2630 ± 9
>5% discordant.										
3-1	234	155	0.087	0.1730 ± 18	0.1920 ± 23	0.4336	10.343	0.1258	90	2587 ± 17
Possible young outlier.										
2-1	141	116	0.016	0.1742 ± 12	0.2275 ± 20	0.4957	11.910	0.1374	100	2599 ± 12

Data 15/5/00.
U/Pb scatter (1σ) for cz3 standard = 1.18% (n=7).

Table t9996 4003: SHRIMP analytical data for the monzogranite, Goolthan Goolthan (UWA mount 99-71B).

grain-spot	U (ppm)	Th (ppm)	4f206 (%)	$^{207}Pb^*/^{206}Pb^*$	$^{208}Pb^*/^{206}Pb^*$	$^{206}Pb^*/^{238}U$	$^{207}Pb^*/^{235}U$	$^{208}Pb^*/^{232}Th$	conc. (%)	$^{207}Pb/^{206}Pb$ age (Ma)
1-2	292	201	0.660	0.1778 ± 7	0.1887 ± 15	0.5218	12.792	0.1427	103	2633 ± 6
2-2	205	140	0.911	0.1769 ± 9	0.1822 ± 20	0.5112	12.469	0.1365	101	2624 ± 8
3-2	297	216	0.482	0.1774 ± 6	0.1955 ± 13	0.5190	12.695	0.1398	103	2629 ± 6
4-2	210	150	0.625	0.1763 ± 8	0.1945 ± 17	0.5148	12.516	0.1402	102	2619 ± 7
5-1	104	47	0.875	0.1752 ± 12	0.1249 ± 26	0.5139	12.410	0.1413	103	2608 ± 12
6-1	285	204	0.411	0.1782 ± 6	0.1918 ± 13	0.5237	12.868	0.1404	103	2636 ± 5
7-1	248	193	0.427	0.1788 ± 6	0.2044 ± 14	0.5229	12.888	0.1373	103	2641 ± 6
8-1	104	24	2.486	0.1760 ± 18	0.0597 ± 37	0.5227	12.684	0.1360	104	2616 ± 17
9-1	227	117	0.629	0.1767 ± 8	0.1379 ± 16	0.5108	12.449	0.1368	101	2623 ± 7
10-1	295	204	0.815	0.1770 ± 7	0.1851 ± 16	0.5310	12.956	0.1418	105	2625 ± 7
11-1	235	194	0.560	0.1765 ± 7	0.2240 ± 17	0.5163	12.566	0.1401	102	2621 ± 7
12-1	236	165	1.950	0.1779 ± 11	0.1889 ± 24	0.5324	13.056	0.1440	104	2633 ± 10
13-1	245	166	0.468	0.1778 ± 7	0.1815 ± 15	0.5201	12.749	0.1394	103	2632 ± 6
14-1	300	239	0.574	0.1784 ± 6	0.2161 ± 15	0.5232	12.867	0.1417	103	2638 ± 6
15-1	215	158	0.543	0.1774 ± 8	0.1974 ± 17	0.5170	12.642	0.1392	102	2628 ± 7

Data 25/02/00.
U/Pb scatter (1σ) for Khan standard = 1.14% (n = 7).
Common-Pb corrected using Cumming & Richards (1975) Model III @ 2620 Ma.

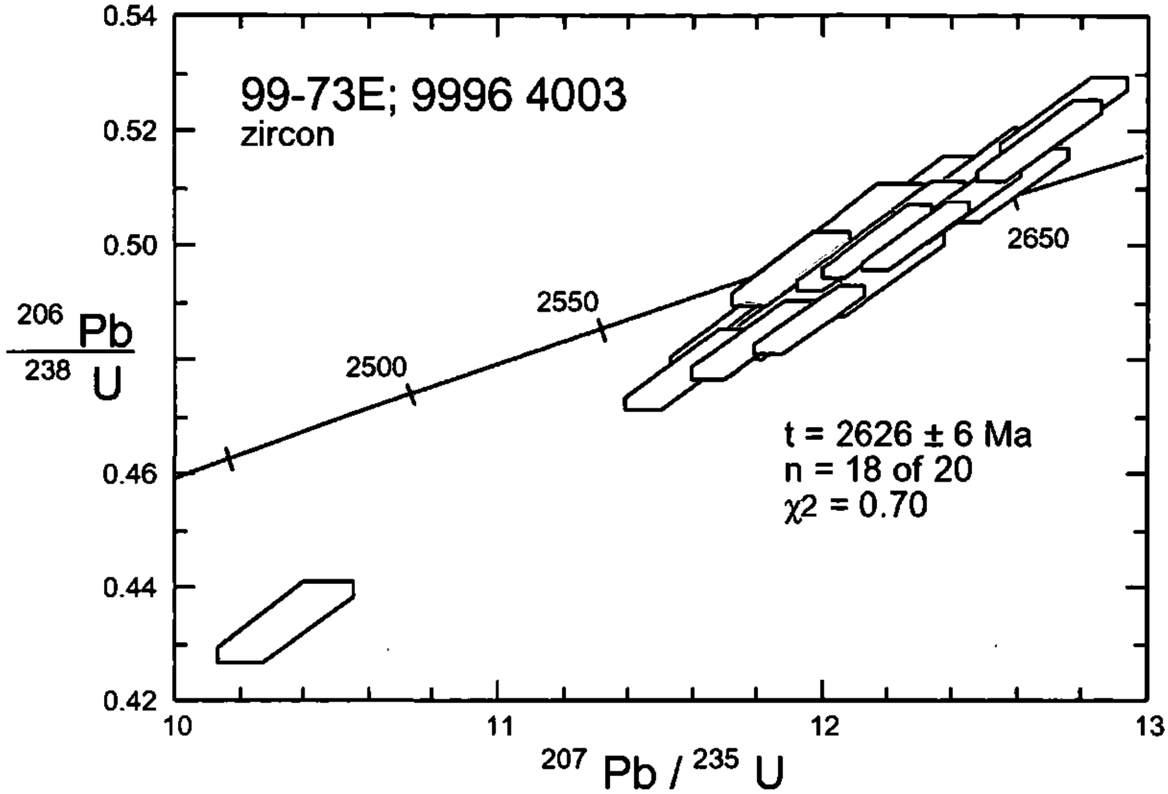

Figure z9996 4003 Concordia plot of all SHRIMP zircon data for the monzogranite, Goolthan Goolthan (UWA mount 99-73E).

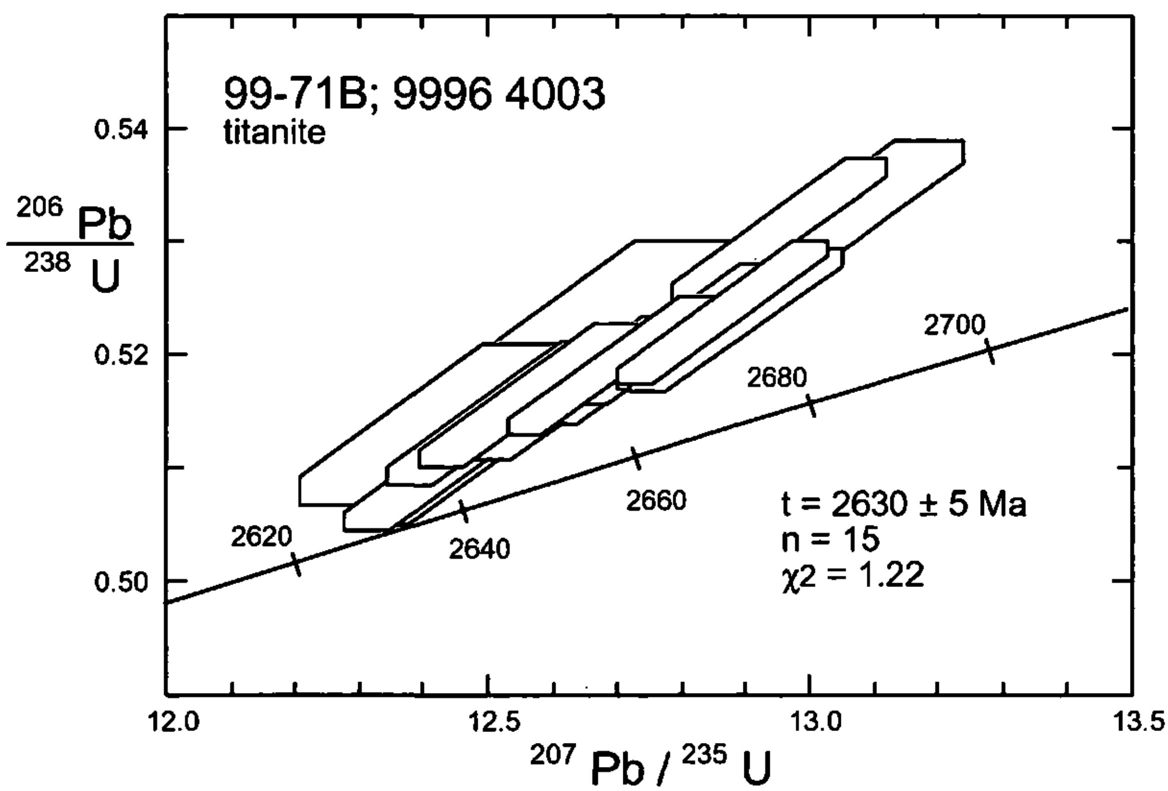

Figure t9996 4003 Concordia plot of SHRIMP titanite data for the monzogranite, Goolthan Goolthan (UWA mount 99-71B).

9996 4016C: biotite syenogranite, Mount Mulgine

1:250,000 sheet:	Perenjori (SH5006)
AMG:	497944.0 mE, 6771112.1 mN
Location:	Mt Mulgine syenogranite, internal to Yalgoo-Singleton greenstone belt; sample from Mt Mulgine deposit drillhole DDM-2, depth interval 108.00-109.00 m
Province:	Murchison
Description:	Weakly foliated sparsely K-feldspar porphyritic medium-grained biotite syenogranite. The Mt Mulgine granitoid is extensively altered and contains both quartz and pegmatite veins. Alteration consists of retrogression and fluid-related alteration dominated by muscovite. The sample is of the 'least-altered' main phase of Mt Mulgine granitoid with alteration restricted to minor sericite and chlorite.
Chemical group:	High-Ca group, Mainland association, Eily Eily clan
Pluton No:	223916
UWA mount:	99-43B

Description of zircons

The zircon population in this sample consists of one morphologic type of finely zoned euhedral to subhedral grains, with most grains being 40-120 μm long and a few up to 400 μm long. The grains show a range of aspect ratios from ~2-3:1 for the majority to ~3-4:1. Grains are typically euhedral to subhedral in external morphology with continuous euhedral internal zoning from core to rim. Inclusions are rare. The grains range from pale brown to dark brown to nearly opaque in colour. Strong euhedral zoning observed on both optical and SEM images suggest high U-Th-contents and radiation damage, particularly in the more strongly zoned rim regions. Discordant alteration patches are visible on SEM images of some grains, and overgrow the euhedral zoning. Many grains have more homogeneous core regions but there is no break in the euhedral growth from core to rim and they are not considered to be xenocrysts. Most grains have fracture networks typical of high-U grains, which have significant metamictisation. The alteration patches and fractures, and dark grains were avoided during data collection. Many grains were too fractured to obtain useful age data.

Results and interpretation

Fifteen analyses on 15 grains are presented in Table z9996 4016C and shown on a concordia diagram in Figure z9996 4016C. The analyses show considerable scatter, reflecting both ancient and Recent radiogenic Pb loss. Many analyses are discordant, as expected for U abundance ranging up to ~1300 ppm, but common-Pb corrections are generally not severe. Omitting all data that are >5% discordant and one statistical outlier (younger; >1300 ppm U), leaves a reasonably coherent group of five points which gives an age of ~2756 ± 20 Ma, with $\chi^2 = 4.4$. This is interpreted to be the emplacement age of the granitoid. Additional data could improve the age determination, by low-U grains are a minority and acquiring sufficient data would be quite slow.

Table z9996 4016C: SHRIMP zircon data for the granite, Mount Mulgine (UWA mount 99-43B).

grain-spot	U (ppm)	Th (ppm)	4f206 (%)	$^{207}Pb^*/^{206}Pb^*$	$^{208}Pb^*/^{206}Pb^*$	$^{206}Pb^*/^{238}U$	$^{207}Pb^*/^{235}U$	$^{208}Pb^*/^{232}Th$	conc. (%)	$^{207}Pb/^{206}Pb$ age (Ma)
34-1	268	203	0.269	0.1893 ± 7	0.1999 ± 13	0.5248	13.700	0.1385	99	2736 ± 6
35-1	377	303	0.068	0.1926 ± 7	0.2204 ± 12	0.5264	13.980	0.1446	99	2765 ± 6
38-1	293	240	0.501	0.1939 ± 8	0.2456 ± 16	0.5154	13.779	0.1545	97	2775 ± 7
6-1	159	82	0.316	0.1915 ± 11	0.1368 ± 19	0.5156	13.613	0.1370	97	2755 ± 10
43-1	257	165	0.782	0.1901 ± 11	0.1869 ± 21	0.5490	14.392	0.1595	103	2743 ± 9
>5% discordant										
20b-1	381	216	0.432	0.1889 ± 7	0.1718 ± 14	0.4029	10.495	0.1220	80	2733 ± 7
36-1	342	300	0.380	0.1873 ± 7	0.1724 ± 13	0.4843	12.504	0.0952	94	2718 ± 6
37-1	563	456	0.399	0.1800 ± 7	0.2204 ± 13	0.4545	11.280	0.1238	91	2653 ± 6
39-1	952	1068	0.332	0.1692 ± 4	0.3110 ± 10	0.3931	9.170	0.1090	84	2550 ± 4
40-1	373	194	0.356	0.1800 ± 7	0.1440 ± 12	0.4323	10.727	0.1199	87	2652 ± 6
41-1	1018	429	0.433	0.1717 ± 4	0.1150 ± 8	0.4161	9.854	0.1137	87	2575 ± 4
42-1	874	532	0.201	0.1752 ± 5	0.2220 ± 10	0.3090	7.464	0.1126	67	2608 ± 5
44-1	1243	690	0.185	0.1871 ± 3	0.1497 ± 6	0.4777	12.322	0.1288	93	2717 ± 3
28-1	390	326	0.552	0.1888 ± 22	0.2090 ± 43	0.4782	12.446	0.1195	92	2732 ± 19
Young outlier										
20a-1	1335	686	0.154	0.1845 ± 3	0.1373 ± 5	0.4881	12.418	0.1305	95	2694 ± 3

Data 1/9/99
U/Pb scatter (1σ) for cz3 standard = 3.32% (n = 12)

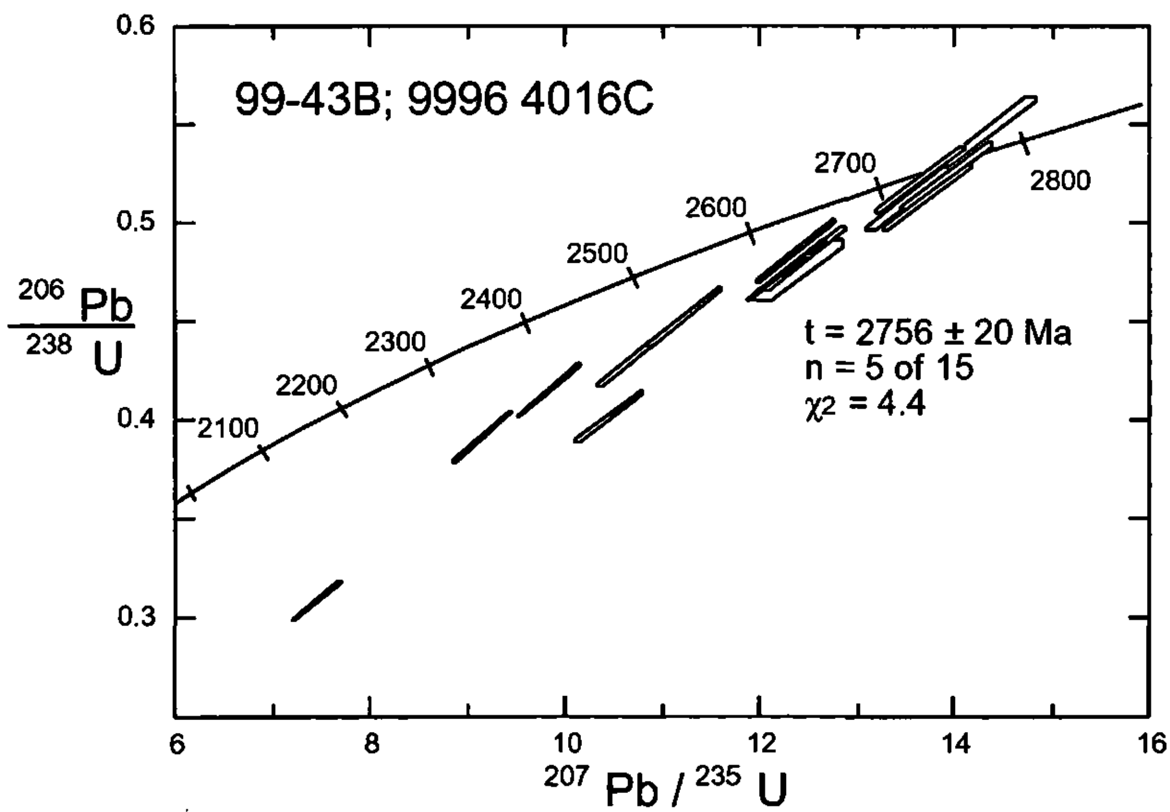

Figure z9996 4016C: Concordia plot of SHRIMP zircon data for the granite, Mount Mulgine (UWA mount 99-43B).

9996 4100: biotite monzogranite, Basin

1:250,000 sheet:	Yalgoo (SH5002)
AMG:	474807.0 mE, 6886266.0 mN
Location:	Blasted from bouldery outcrop near the edge of the Basin monzogranite, an internal granitoid at the north end of the Yalgoo-Singleton greenstone belt.
Province:	Murchison
Description:	Weakly to moderately foliated recrystallised sparsely quartz-feldspar porphyritic fine-grained biotite monzogranite. Foliation is defined by biotite and titanite and dips to the west at 30-40°. Titanite is probably of metamorphic origin. Cut by minor quartz and biotite-chlorite-epidote veins.
Chemical group:	High-Ca group, Mainland association, Wheel of Fortune clan
Pluton No:	224107
UWA mount:	99-43A (zircon) and 99-36C (titanite)

Description of zircons

The zircon population in this sample consists of one morphologic type of euhedral to subhedral grains, with most grains being 30-120 μm long, with a range of aspect ratios from ~2-3:1 for the majority, to ~5:1. In their internal morphology, grains range from continuous euhedral internal zoning from core to rim, to partially recrystallised. Recrystallisation is often minor. There is a gradation between these two end members with progressive recrystallisation overprinting the euhedral zoning, particularly in the more strongly zoned rims areas. Inclusions are rare. The grains range from pale brown to dark brown in colour. Strong euhedral zoning observed towards the rims of some grains in both optical and SEM images suggest high U-Th-contents and radiation damage. Fracture networks indicative of high U-Th and radiation damage are common. Recrystallisation areas have less fractures. Due the small grain size and fracturing, there were limited areas for analysis. Both euhedrally zoned and recrystallised areas yielded indistinguishable ages.

Description of titanites

The titanites from this sample are all 60-200 micron fragments of larger grains. Only rarely do grains show growth surfaces; most surfaces are fractures. The grains are dark brown to light brown in colour. Some grains are almost black and have evenly distributed dense and very fine inclusion populations. Isolated inclusions are small and rare. Areas of SHRIMP analysis were in clean parts of the grains, avoiding inclusions and fractures.

Results and interpretation

Zircon

Nineteen analyses on 19 grains are presented in Table z9996 4100 and shown on a concordia diagram in Figure z9996 4100. The analyses show a significant discordance, though not as much as generally as expected for U abundance ranging up to ~750 ppm. Omitting four data points that are >5% discordant and leaves a coherent group of 15 which gives an age of ~2743 ± 4 Ma, with χ^2 = 1.69. This is interpreted to be the emplacement age of the granitoid.

Titanite

Nineteen analyses on 19 fragments are presented in Table t9996 4100 and shown on a concordia diagram in Figure t9996 4100. The data form a single age population, with $\chi^2 = 0.88$. The age of 2632 ± 8 Ma is interpreted to be a metamorphic age for the granitoid.

Table z9996 4100: SHRIMP zircon data for the Basin granite (UWA mount 99-43A).

grain-spot	U (ppm)	Th (ppm)	4f206 (%)	$^{207}Pb^*/^{206}Pb^*$	$^{208}Pb^*/^{206}Pb^*$	$^{206}Pb^*/^{238}U$	$^{207}Pb^*/^{235}U$	$^{208}Pb^*/^{232}Th$	conc. (%)	$^{207}Pb/^{206}Pb$ age (Ma)
2-1	342	72	0.228	0.1906 ± 6	0.0581 ± 9	0.5385	14.151	0.1479	101	2747 ± 6
6-1	409	72	0.137	0.1899 ± 6	0.0477 ± 7	0.5369	14.061	0.1460	101	2742 ± 5
14-1	483	234	0.339	0.1897 ± 6	0.0920 ± 9	0.4978	13.023	0.0945	95	2740 ± 5
40-1	370	92	0.498	0.1913 ± 7	0.0568 ± 12	0.5295	13.963	0.1204	100	2753 ± 6
26-1	64	64	0.063	0.1921 ± 15	0.2729 ± 29	0.5290	14.015	0.1453	99	2761 ± 12
41-1	462	99	0.182	0.1904 ± 5	0.0567 ± 7	0.5252	13.786	0.1388	99	2745 ± 5
42-1	407	88	0.119	0.1916 ± 5	0.0585 ± 7	0.5321	14.059	0.1442	100	2756 ± 5
32-1	408	154	0.622	0.1890 ± 9	0.1087 ± 16	0.4988	12.995	0.1436	95	2733 ± 8
31-1	136	142	0.102	0.1899 ± 10	0.2855 ± 20	0.5222	13.671	0.1429	99	2741 ± 9
33-1	882	255	0.154	0.1892 ± 4	0.0750 ± 5	0.5111	13.334	0.1324	97	2735 ± 3
35-1	443	147	0.279	0.1906 ± 6	0.0719 ± 9	0.5261	13.829	0.1144	99	2748 ± 5
44-1	67	59	0.201	0.1908 ± 15	0.2491 ± 30	0.5330	14.021	0.1491	100	2749 ± 13
45-1	101	69	0.321	0.1898 ± 13	0.1749 ± 23	0.5144	13.462	0.1321	98	2740 ± 11
46-1	515	146	0.290	0.1902 ± 5	0.0659 ± 8	0.5205	13.649	0.1212	98	2744 ± 5
1-1	692	195	0.370	0.1896 ± 5	0.0756 ± 9	0.5436	14.214	0.1454	102	2739 ± 5
>5% discordant										
7-1	368	92	0.433	0.1830 ± 8	0.0603 ± 13	0.4758	12.006	0.1154	94	2680 ± 7
3-1	749	486	0.155	0.1854 ± 5	0.1787 ± 9	0.4370	11.172	0.1204	86	2702 ± 5
39-1	151	143	4.518	0.1829 ± 34	0.2457 ± 76	0.4313	10.876	0.1113	86	2679 ± 31
47-1	338	83	1.573	0.1891 ± 12	0.0529 ± 23	0.4696	12.246	0.1006	91	2735 ± 10

Data 1/9/99
U/Pb scatter (1σ) for cz3 standard = 3.32% (n = 12)

Table t9996 4100: SHRIMP titanite data for the Basin granite (UWA mount 99-36C).

grain-spot	U (ppm)	Th (ppm)	4f206 (%)	$^{207}Pb^*/^{206}Pb^*$	$^{208}Pb^*/^{206}Pb^*$	$^{206}Pb^*/^{238}U$	$^{207}Pb^*/^{235}U$	$^{208}Pb^*/^{232}Th$	conc. (%)	$^{207}Pb/^{206}Pb$ age (Ma)
1-1	94	57	0.558	0.1792 ± 16	0.1734 ± 34	0.5160	12.753	0.1469	101	2646 ± 15
2-1	98	38	0.611	0.1797 ± 15	0.1056 ± 30	0.5047	12.503	0.1379	99	2650 ± 14
3-1	85	31	0.745	0.1778 ± 17	0.0992 ± 35	0.5081	12.455	0.1392	101	2632 ± 16
4-1	105	29	0.537	0.1776 ± 15	0.0771 ± 28	0.5132	12.567	0.1412	101	2631 ± 14
5-1	91	29	0.627	0.1777 ± 16	0.0871 ± 31	0.5257	12.880	0.1460	103	2631 ± 15
6-1	120	52	0.507	0.1792 ± 13	0.1222 ± 27	0.5061	12.502	0.1426	100	2645 ± 12
7-1	114	55	0.578	0.1764 ± 14	0.1368 ± 29	0.5236	12.738	0.1469	104	2620 ± 13
8-1	89	53	0.745	0.1771 ± 17	0.1638 ± 37	0.5201	12.702	0.1432	103	2626 ± 16
9-1	76	23	1.238	0.1755 ± 29	0.0764 ± 58	0.4856	11.748	0.1214	98	2610 ± 27
10-1	131	58	0.828	0.1753 ± 15	0.1223 ± 31	0.5249	12.685	0.1446	104	2609 ± 14
11-1	189	7	0.243	0.1788 ± 9	0.0124 ± 12	0.5174	12.758	0.1670	102	2642 ± 9
12-1	96	30	0.771	0.1781 ± 16	0.0889 ± 32	0.5209	12.793	0.1469	103	2635 ± 15
13-1	114	74	0.697	0.1754 ± 17	0.1831 ± 37	0.4900	11.851	0.1378	98	2610 ± 16
14-1	100	26	0.622	0.1790 ± 16	0.0730 ± 30	0.5248	12.952	0.1455	103	2644 ± 15
15-1	67	27	0.901	0.1748 ± 21	0.1058 ± 44	0.5219	12.580	0.1356	104	2604 ± 20
16-1	72	26	1.540	0.1775 ± 25	0.1060 ± 52	0.5108	12.500	0.1514	101	2630 ± 23
17-1	65	24	0.722	0.1791 ± 20	0.1082 ± 40	0.5237	12.930	0.1534	103	2644 ± 18
18-1	149	133	0.532	0.1759 ± 13	0.2419 ± 30	0.4975	12.063	0.1350	100	2614 ± 12
19-1	53	9	0.880	0.1790 ± 23	0.0515 ± 43	0.5210	12.856	0.1522	102	2643 ± 21

Data 29/8/99.
U/Pb scatter (1σ) for Khan standard = 1.73% (n = 14 of 15).
Common-Pb corrected using Cumming & Richards (1975) Model III @ 2630 Ma.

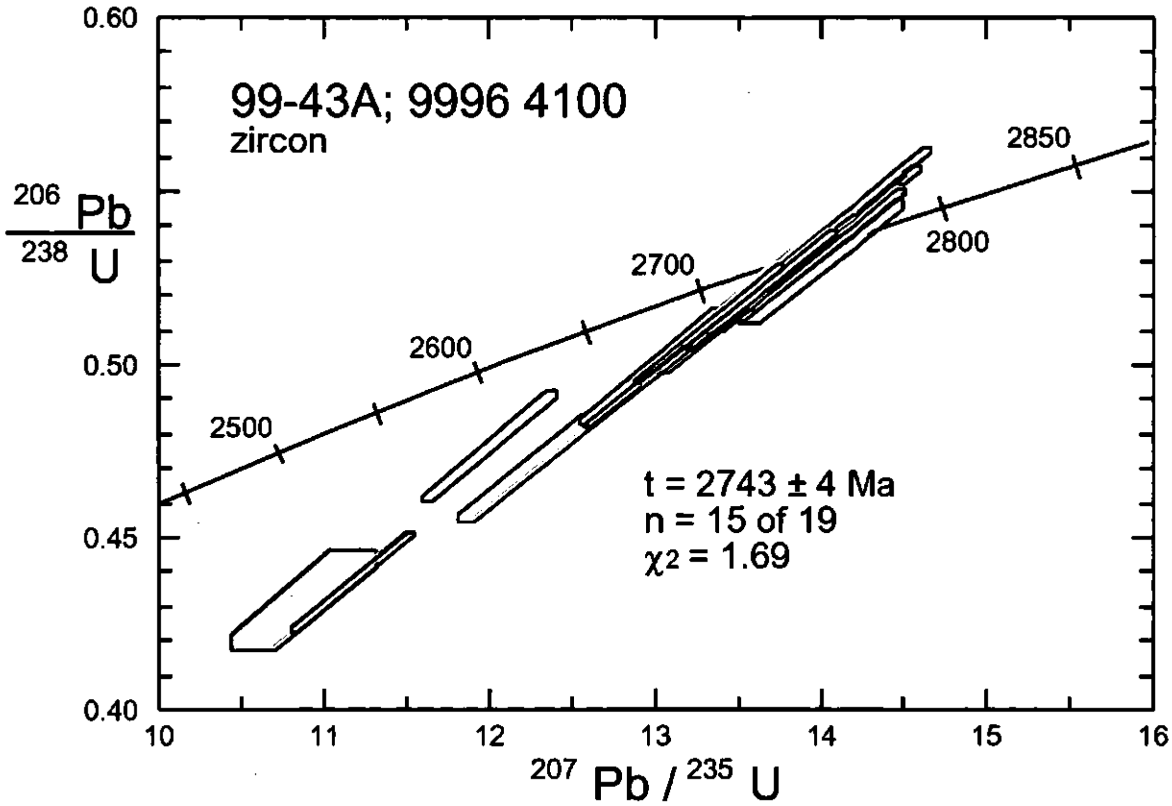

Figure z9996 4100 : Concordia plot of SHRIMP zircon data for the Basin granite (UWA mount 99-43A).

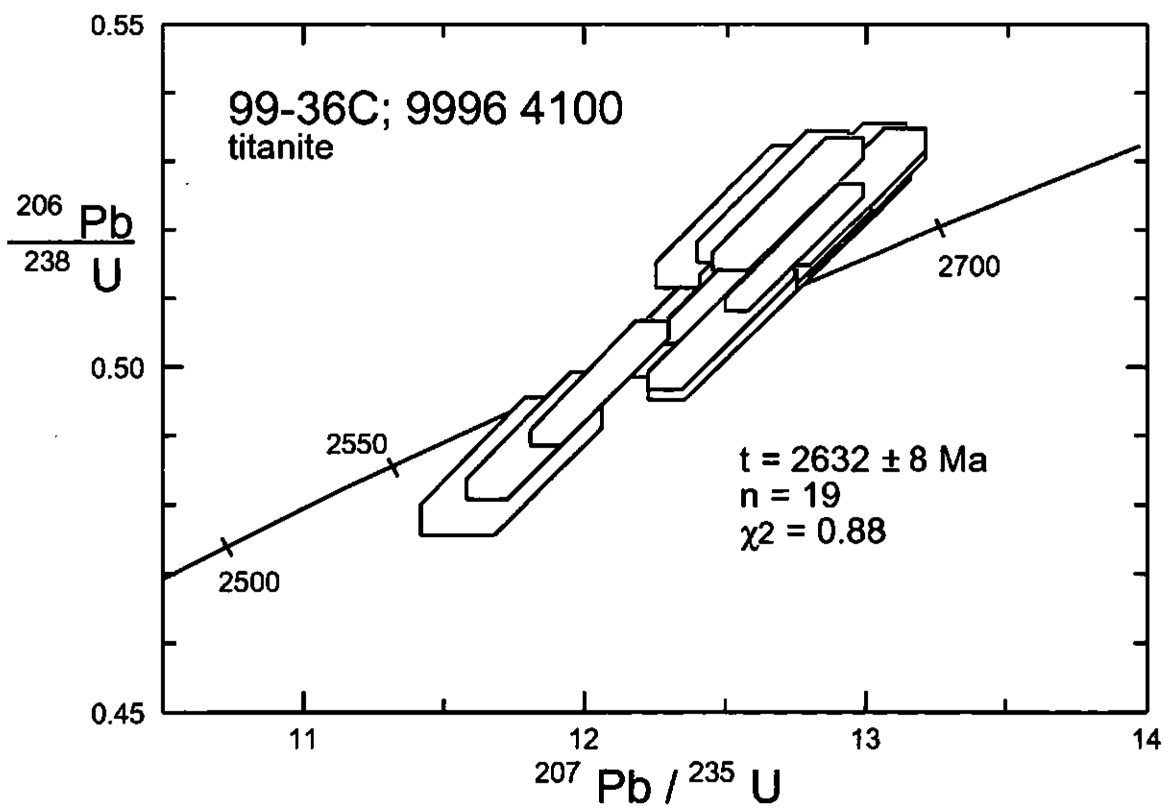

Figure t9996 4100 : Concordia plot of SHRIMP titanite data for the Basin granite (UWA mount 99-36C).

9996 7049A: Foliated K-feldspar-porphyritic biotite granite, Goddard Quarry

1:250,000 sheet:	Kellerberrin (SH5015)
AMG:	509600.0 mE, 6559250.0 mN
Location:	Drilled and hammered from blasted rock in a rock quarry, near Goddard railway siding.
Province:	Murchison
Description:	Seven phases present in quarry. 9996 7049A is a foliated seriate to sparsely feldspar porphyritic medium-grained biotite monzogranite that forms the main nebulitic/banded granite gneiss phase in the quarry. It contains some amphibolite enclaves and is intruded by 4 granitoid phases (pegmatitic granite, schlieren-rich feldspar porphyry, mafic granite dykes and microgranite) and late dolerite dykes.
Chemical group:	High-Ca group, Mainland association, Goddard nebulitic gniess clan
Pluton No:	233501
UWA mount:	99-33C

Description of zircons

The zircon population in this sample consists of one morphologic type of finely zoned subhedral grains, with most grains being 60-250 μm long, with distinctively high aspect ratios of >3:1 for the majority of grains, up to ~10:1. Grains are typically euhedral to subhedral in external morphology with continuous euhedral internal zoning from core to rim. Inclusions are relatively rare. The grains range from pale brown to dark brown in colour. Strong euhedral zoning observed in the grains in both optical and SEM images suggest high U-Th-contents and radiation damage. Discordant alteration patches are visible on SEM images of many grains, and overgrow the euhedral zoning. Some grains have more homogeneous core regions but there is no break in the euhedral growth from core to rim and they are not considered to be xenocrysts. Fracture networks indicative of high U-Th and radiation damage are common. The fractures and darker grains were avoided during data collection.

Results and interpretation

Twenty three analyses on 21 grains are presented in Table z9996 7049A and shown on a concordia diagram in Figure z9996 7049A. The overall pattern of discordance is not as extensive as expected for U abundance ranging up to ~1000 ppm, and common-Pb corrections are generally not severe. Omitting all data that are >5% discordant, two apparent xenocrysts (~2840 Ma and ~2890 Ma) and one (younger) statistical outlier leaves a coherent group of 15 points which gives an age of ~2787 ± 4 Ma, with $\chi^2 = 1.27$. This age is interpreted to be the emplacement age of the granitoid.

Table z9996 7049A: SHRIMP zircon data for the biotite monzogranite, Goddard Quarry (UWA mount 99-33C).

grain-spot	U (ppm)	Th (ppm)	4f206 (%)	$^{207}Pb^*/^{206}Pb^*$	$^{208}Pb^*/^{206}Pb^*$	$^{206}Pb^*/^{238}U$	$^{207}Pb^*/^{235}U$	$^{208}Pb^*/^{232}Th$	conc. (%)	$^{207}Pb/^{206}Pb$ age (Ma)
Main group.										
65-2	91	36	0.019	0.1962 ± 19	0.1025 ± 20	0.5233	14.157	0.1371	97	2795 ± 16
67-1	721	297	0.294	0.1959 ± 7	0.1125 ± 8	0.5386	14.544	0.1471	99	2792 ± 6
72-1	713	418	0.150	0.1970 ± 7	0.1515 ± 8	0.5492	14.922	0.1418	101	2802 ± 6
76-1	221	104	0.212	0.1950 ± 12	0.1280 ± 14	0.5537	14.884	0.1506	102	2784 ± 10
87-1	811	189	1.220	0.1937 ± 9	0.0601 ± 14	0.5460	14.580	0.1408	101	2774 ± 7
82-1	511	336	1.452	0.1959 ± 11	0.1913 ± 20	0.5340	14.424	0.1554	99	2792 ± 9
83-1	726	397	0.559	0.1945 ± 6	0.1408 ± 11	0.5327	14.284	0.1372	99	2780 ± 5
89-1	183	103	0.000	0.1956 ± 9	0.1516 ± 11	0.5286	14.254	0.1424	98	2790 ± 7
90-1	218	129	0.298	0.1944 ± 10	0.1539 ± 19	0.5144	13.787	0.1340	96	2780 ± 9
77-1	902	508	0.166	0.1944 ± 4	0.1491 ± 7	0.5410	14.503	0.1432	100	2780 ± 4
91-1	337	204	0.515	0.1955 ± 9	0.1678 ± 17	0.5156	13.901	0.1430	96	2789 ± 8
69-1	248	94	0.152	0.1959 ± 8	0.1019 ± 12	0.5475	14.788	0.1474	101	2792 ± 7
69-2	478	310	0.016	0.1955 ± 5	0.1749 ± 8	0.5266	14.197	0.1418	98	2789 ± 5
92-1	620	92	0.054	0.1954 ± 5	0.0391 ± 5	0.5374	14.479	0.1421	99	2788 ± 4
70-1	186	68	0.151	0.1953 ± 10	0.1013 ± 14	0.5381	14.491	0.1487	100	2788 ± 8
>5% discordant.										
64-1	450	211	5.558	0.1881 ± 20	0.1961 ± 40	0.4854	12.589	0.2033	94	2726 ± 17
88-1	861	276	0.111	0.1915 ± 6	0.0748 ± 5	0.4975	13.136	0.1160	94	2755 ± 5
75-1	457	237	1.648	0.1947 ± 12	0.1330 ± 22	0.5028	13.501	0.1286	94	2783 ± 10
84-1	608	367	1.228	0.1919 ± 9	0.1697 ± 19	0.4838	12.800	0.1360	92	2758 ± 8
87-2	1061	415	0.143	0.1828 ± 5	0.1127 ± 8	0.4531	11.418	0.1306	90	2678 ± 5
Young outlier.										
74-1	563	333	0.482	0.1924 ± 7	0.1721 ± 12	0.5024	13.329	0.1464	95	2763 ± 6
Old outliers.										
63-1	420	284	9.793	0.2074 ± 30	0.2919 ± 65	0.5294	15.142	0.2284	95	2886 ± 24
65-1	212	108	0.154	0.2017 ± 13	0.1333 ± 14	0.5281	14.683	0.1374	96	2840 ± 10

Data 25/08/99 and 28/10/99.
U/Pb scatter (1σ) for cz3 standard = 2.10% (n = 11) and 1.77% (n = 5).

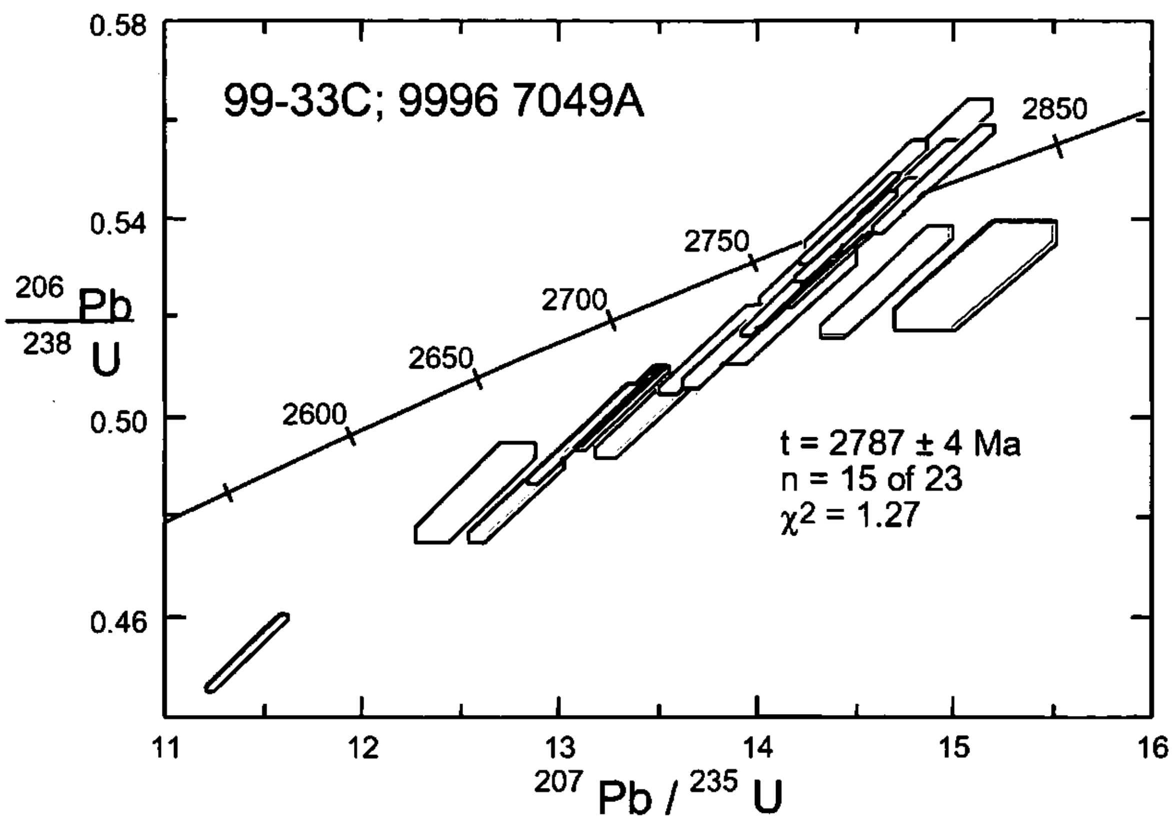

Figure z9996 7049A: Concordia plot showing all SHRIMP analytical data for the biotite monzogranite, Goddard Quarry (UWA mount 99-33C).

9996 7055: biotite monzogranite, Fox Lair

1:250,000 sheet:	Bencubbin (SH5011)
AMG:	538400.0 mE, 6611000.0 mN
Location:	Hammered from large pile of blasted rock on west side of road.
Province:	Murchison
Description:	Massive, homogeneous equigranular medium-grained fluorite-rich biotite monzogranite intrusive into porphyritic biotite monzogranite (sample 9996 7054A). Cut by rare thin pegmatite dykes.
Chemical group:	Low-Ca group, Goolthan association, Knungomen clan
Pluton No:	2336023
UWA mount:	99-34A

Description of zircons

The zircon population in this sample consists of one morphologic type of finely zoned euhedral grains, with most grains being 80-200 μm long, with a range of aspect ratios from ~2:1 for the majority to ~5:1, particularly for longer grains. Grains are typically euhedral to subhedral in external morphology with continuous euhedral internal zoning from core to rim. Inclusions are rare. The grains range from pale brown to dark brown to nearly opaque in colour, with the majority being dark. Strong euhedral zoning observed on both optical and SEM images suggest high U-Th-contents and radiation damage. Discordant alteration patches are visible on SEM images of most grains, and overgrow the euhedral zoning. Some grains have more homogeneous core regions but there is no break in the euhedral growth from core to rim and they are not considered to be xenocrysts. Some grains have fracture networks typical of high-U grains, which have significant metamictisation. The fractures and dark grains were avoided during data collection. Analyses were taken from both euhedrally zoned regions and alteration patches, and yielded indistinguishable ages.

Results and interpretation

Twenty analyses on 16 grains are presented in Table z9996 7055 and shown on a concordia diagram in Figure z9996 7055. Despite having U contents up to ~700 ppm the data are almost all concordant and have very low common-Pb contamination. The data all fall in a single concordant cluster, but three are omitted from the age determination on the grounds of marginal discordance and common-Pb corrections. The remaining group of 17 analyses has a χ^2 of 0.98. The corresponding age is 2641 ± 5 Ma; this is interpreted as the emplacement age of the granitoid.

Table z9996 7055: SHRIMP zircon data for the biotite monzogranite, Fox Lair (UWA mount 99-34A).

grain-spot	U (ppm)	Th (ppm)	4f206 (%)	$^{207}Pb^*/^{206}Pb^*$	$^{208}Pb^*/^{206}Pb^*$	$^{206}Pb^*/^{238}U$	$^{207}Pb^*/^{235}U$	$^{208}Pb^*/^{232}Th$	conc. (%)	$^{207}Pb/^{206}Pb$ age (Ma)
Main group.										
35-1	505	410	0.095	0.1787 ± 6	0.2185 ± 11	0.5093	12.549	0.1369	100	2641 ± 6
56-1	34	45	1.087	0.1756 ± 43	0.3410 ± 98	0.5156	12.484	0.1357	103	2612 ± 41
58-1	697	278	0.171	0.1785 ± 5	0.1056 ± 8	0.5289	13.020	0.1399	104	2639 ± 5
57-1	181	237	0.470	0.1774 ± 14	0.3536 ± 32	0.4983	12.190	0.1348	99	2629 ± 13
60-1	179	232	0.381	0.1773 ± 13	0.3573 ± 29	0.5270	12.881	0.1454	104	2628 ± 12
43-1	103	134	0.176	0.1772 ± 17	0.3446 ± 39	0.4959	12.118	0.1322	99	2627 ± 16
46-1	131	146	0.120	0.1790 ± 12	0.3084 ± 25	0.5015	12.381	0.1382	99	2644 ± 11
46-2	95	95	0.000	0.1799 ± 11	0.2811 ± 22	0.5068	12.567	0.1424	100	2652 ± 10
44-1	170	201	0.084	0.1801 ± 10	0.3393 ± 23	0.4852	12.052	0.1395	96	2654 ± 9
43-2	96	121	0.047	0.1790 ± 14	0.3481 ± 32	0.5064	12.501	0.1394	100	2644 ± 13
42-1	114	242	0.000	0.1789 ± 10	0.5709 ± 31	0.5048	12.453	0.1362	100	2643 ± 9
40-1	78	92	0.121	0.1789 ± 16	0.3242 ± 35	0.5080	12.532	0.1399	100	2643 ± 15
36-2	76	98	0.168	0.1779 ± 16	0.3557 ± 37	0.5014	12.296	0.1384	99	2633 ± 15
50-1	297	313	0.060	0.1778 ± 7	0.2916 ± 15	0.5029	12.327	0.1394	100	2632 ± 7
60-2	452	343	0.072	0.1798 ± 6	0.2119 ± 10	0.5013	12.424	0.1398	99	2651 ± 5
61-1	102	161	0.247	0.1764 ± 14	0.4282 ± 34	0.5115	12.438	0.1392	102	2619 ± 13
62-1	135	222	0.070	0.1802 ± 12	0.4652 ± 31	0.4989	12.396	0.1410	98	2655 ± 11
>5% discordant, Pb/Th discordant or 4f206>2%.										
40-1	479	254	0.254	0.1779 ± 7	0.1249 ± 12	0.4987	12.234	0.1175	99	2634 ± 7
39-1	92	98	0.242	0.1809 ± 20	0.2896 ± 43	0.4764	11.884	0.1300	94	2661 ± 18
49-1	204	353	2.581	0.1791 ± 22	0.4030 ± 50	0.4936	12.193	0.1149	98	2645 ± 20

Data 27/09/99 and 25/10/99.
U/Pb scatter (1σ) for cz3 standard = 2.51% (n = 5) and 2.36% (n = 9).

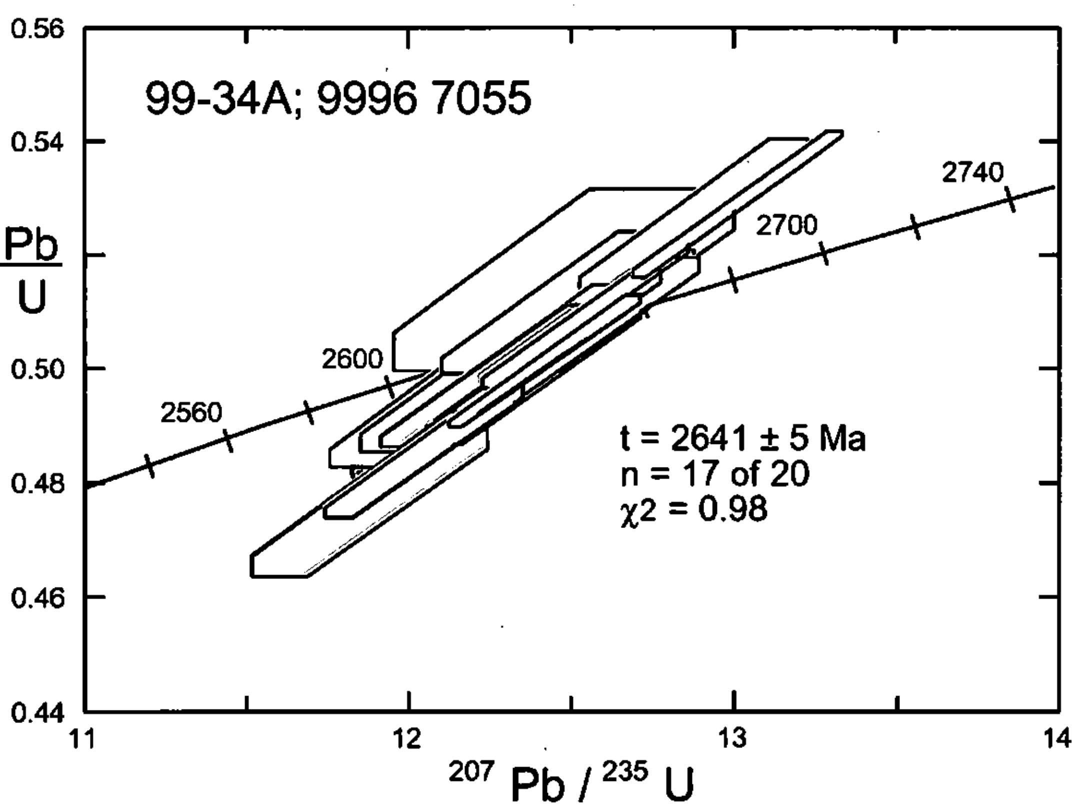

Figure z9996 7055: Concordia plot of all SHRIMP zircon data for the biotite monzogranite, Fox Lair (UWA mount 99-34A).

9996 7066: K-feldspar-porphyritic biotite monzogranite, Namban

1:250,000 sheet:	Moora (SH5010)
AMG:	411940.0 mE, 6644575.0 mN
Location:	A small quarry, south of road, in the Namban Granite; hammered from blasted rock.
Province:	Murchison
Description:	Least-altered, strongly K-feldspar porphyritic coarse-grained biotite monzogranite. Contains minor granitoid xenoliths and cut by brittle faults and fractures with associated minor wallrock alteration. Cut by late dolerite dykes.
Chemical group:	Low-Ca group, Goolthan association, Namban clan
Pluton No:	213701
UWA mounts:	99-28C (zircon) and 99-24E (titanite)

Description of zircons

The zircon population in this sample consists of one morphologic type of euhedral to subhedral grains, with most grains being 60-200 μm long, with a range of aspect ratios from ~2:1 for the majority to ~5:1. In their internal morphology, grains typically have faint continuous euhedral internal zoning from core to rim, with the rims showing stronger zoning. Inclusions are relatively rare. The majority of grains are pale brown to mauve in colour with a minority grading to darker brown. The lack of strong euhedral zoning in both optical and SEM images and pale colour of the majority of grains suggest low U-Th-contents and little radiation damage.

Description of titanites

The titanites from this sample are all 50-200 μm fragments of larger grains. Only rarely do grains show growth surfaces; most surfaces are fractures. The grains are pale brown to honey brown to dark brown in colour. Some grains or parts of grains are almost black and have evenly distributed dense and very fine inclusion populations. Areas of SHRIMP analysis were in clean parts of the grains, avoiding inclusions and fractures.

Results and interpretation

Zircon

Twenty two analyses on 12 grains are presented in Table z9996 7066 and shown on a concordia diagram in Figure z9996 7066. Omitting two statistical outliers, the population comprising the remaining 20 concordant analyses has a χ^2 of 1.14. This is interpreted as a single age population at 2646 ± 5 Ma.

Titanite

Thirty two analyses were obtained from 16 fragments. The U abundances are all ~100 ppm and the common Pb corrections are all small. The data show a tight grouping in both $^{207}Pb/^{206}Pb$ and Pb/U, which is taken as evidence that these data are concordant. All 32 analyses form a single age population with $\chi^2 = 0.68$. The corresponding age of 2638 ±7 Ma.

The zircon and titanite ages agree, within analytical uncertainty, and the 2643 ± 4 Ma age from the combined $^{207}Pb/^{206}Pb$ data is interpreted to be the emplacement age of the granite.

Table z9996 7066: SHRIMP zircon data for the K-feldspar-phyric biotite granite, Namban (UWA mount 99-28C).

grain-spot	U (ppm)	Th (ppm)	4f206 (%)	$^{207}Pb^*/^{206}Pb^*$	$^{208}Pb^*/^{206}Pb^*$	$^{206}Pb^*/^{238}U$	$^{207}Pb^*/^{235}U$	$^{208}Pb^*/^{232}Th$	conc. (%)	$^{207}Pb/^{206}Pb$ age (Ma)
Main group.										
25-1	196	149	0.059	0.1789 ± 9	0.2026 ± 16	0.4940	12.186	0.1316	98	2643 ± 8
25-2	127	119	0.000	0.1816 ± 10	0.2500 ± 19	0.5042	12.623	0.1341	99	2667 ± 10
19-1	209	223	0.068	0.1785 ± 8	0.2860 ± 17	0.4941	12.162	0.1325	98	2639 ± 8
19-2	105	165	0.105	0.1792 ± 15	0.4110 ± 36	0.4926	12.174	0.1291	98	2646 ± 14
20-1	104	135	0.023	0.1798 ± 12	0.3439 ± 26	0.5023	12.454	0.1330	99	2651 ± 11
21-1	85	93	0.000	0.1800 ± 12	0.2895 ± 25	0.4859	12.059	0.1294	96	2653 ± 11
17-1	41	62	0.126	0.1831 ± 26	0.3919 ± 61	0.4862	12.271	0.1258	95	2681 ± 24
17-2	70	127	0.053	0.1802 ± 18	0.4934 ± 48	0.4916	12.215	0.1334	97	2655 ± 17
18-1	76	141	0.119	0.1799 ± 16	0.4985 ± 43	0.4893	12.133	0.1317	97	2652 ± 15
13-1	67	85	0.000	0.1786 ± 14	0.3396 ± 32	0.4745	11.689	0.1275	95	2640 ± 13
13-2	111	153	0.000	0.1781 ± 11	0.3643 ± 25	0.4938	12.127	0.1303	98	2636 ± 10
14-1	253	79	0.044	0.1787 ± 8	0.0819 ± 10	0.4917	12.114	0.1284	98	2641 ± 7
14-2	229	203	0.014	0.1788 ± 9	0.2388 ± 17	0.4936	12.172	0.1330	98	2642 ± 8
11-1	59	49	0.079	0.1789 ± 16	0.2228 ± 31	0.4940	12.188	0.1331	98	2643 ± 15
11-2	43	75	0.000	0.1812 ± 15	0.4671 ± 41	0.5013	12.522	0.1358	98	2663 ± 14
12-1	130	130	0.091	0.1804 ± 10	0.2610 ± 19	0.4943	12.294	0.1292	97	2656 ± 9
12-2	202	299	0.030	0.1783 ± 7	0.3985 ± 18	0.5021	12.345	0.1354	99	2637 ± 7
27-1	296	248	0.000	0.1801 ± 6	0.2294 ± 10	0.4995	12.404	0.1367	98	2654 ± 5
27-2	97	135	0.088	0.1783 ± 12	0.3709 ± 28	0.5151	12.661	0.1381	102	2637 ± 11
28-2	104	146	0.058	0.1770 ± 11	0.3847 ± 26	0.4790	11.689	0.1309	96	2625 ± 10
Young outliers.										
21-2	109	114	0.053	0.1758 ± 12	0.2749 ± 25	0.4888	11.850	0.1284	98	2614 ± 12
28-1	212	192	0.073	0.1764 ± 8	0.2373 ± 15	0.4957	12.059	0.1296	99	2620 ± 7

Data 15/08/99 and 17/08/99.
U/Pb scatter (1σ) for cz3 standard = 1.47% (n = 6) and 1.41% (n = 15).

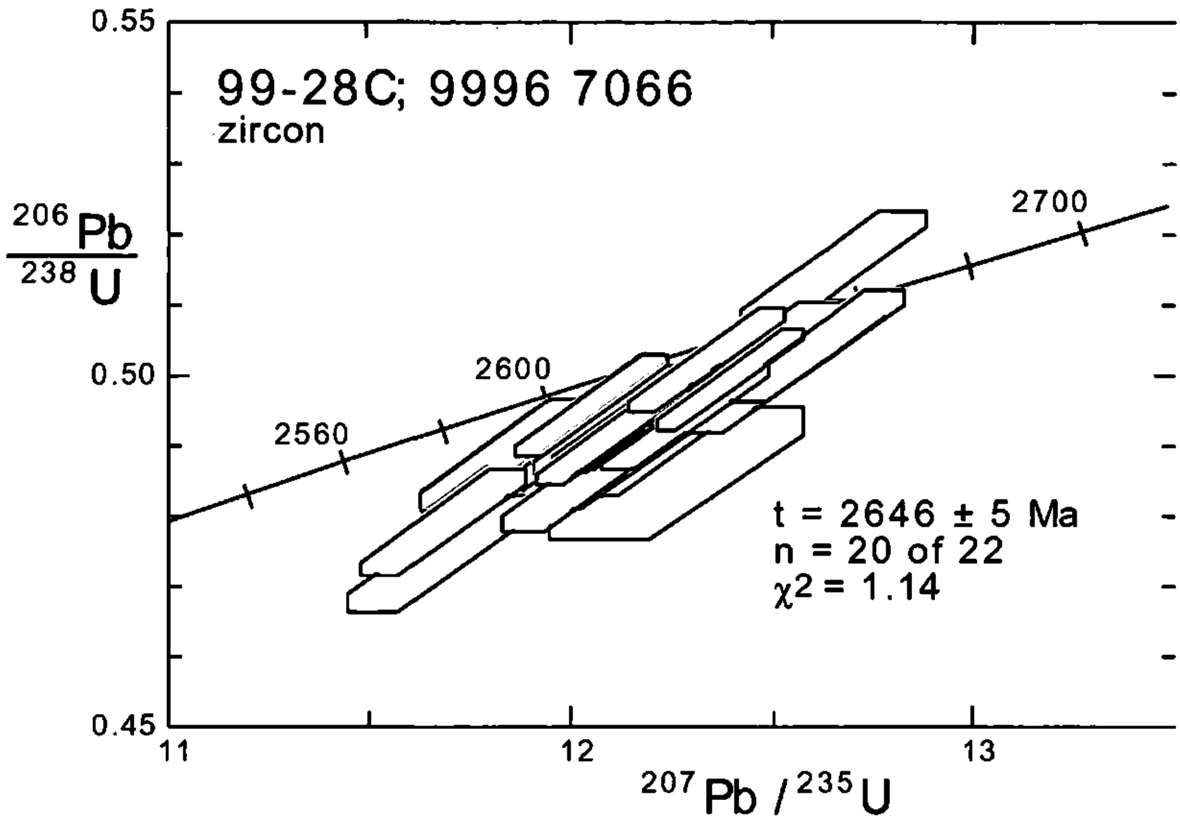

Figure z9996 7066: Concordia plot of all SHRIMP zircon data for the K-feldspar-phyric biotite granite, Namban (UWA mount 99-28C).

Table t9996 7066: SHRIMP titanite data for the K-feldspar-phyric biotite granite, Namban (UWA mount 99-24E).

grain-spot	U (ppm)	Th# (ppm)	4f206 (%)	$^{207}Pb^*/^{206}Pb^*$	$^{208}Pb^*/^{206}Pb^*$	$^{206}Pb^*/^{238}U$	$^{207}Pb^*/^{235}U$ #	conc. (%)	$^{207}Pb/^{206}Pb$ age (Ma)
1-4	214	162	0.480	0.1803 ± 11	0.2330 ± 22	0.5092	12.656	100	2655 ± 10
2-4	101	63	0.751	0.1790 ± 18	0.1985 ± 37	0.4979	12.287	99	2643 ± 17
3-2	87	863	1.907	0.1738 ± 29	3.0160 ±174	0.5146	12.333	103	2595 ± 28
4-2	114	554	0.950	0.1799 ± 18	1.5052 ± 76	0.5128	12.716	101	2652 ± 16
5-1	83	97	0.789	0.1779 ± 23	0.3652 ± 52	0.5277	12.941	104	2633 ± 21
5-2	104	440	0.828	0.1764 ± 20	1.2980 ± 76	0.5130	12.480	102	2620 ± 19
5-3	106	63	0.805	0.1785 ± 19	0.1799 ± 37	0.5493	13.520	107	2639 ± 17
5-4	111	446	0.639	0.1800 ± 20	1.2448 ± 75	0.5324	13.211	104	2652 ± 18
6-1	78	693	1.229	0.1770 ± 27	2.7033 ±160	0.5290	12.913	104	2625 ± 26
6-2	80	748	1.455	0.1793 ± 28	2.8489 ±169	0.5209	12.873	102	2646 ± 26
7-1	103	469	0.869	0.1777 ± 20	1.3836 ± 82	0.5286	12.953	104	2632 ± 19
7-2	103	394	1.269	0.1766 ± 22	1.1609 ± 75	0.5188	12.632	103	2621 ± 20
8-1	171	266	0.539	0.1770 ± 14	0.4691 ± 36	0.5166	12.605	102	2625 ± 13
8-2	118	350	0.741	0.1774 ± 18	0.9415 ± 60	0.5069	12.402	101	2629 ± 17
9-1	113	419	1.254	0.1761 ± 21	1.1383 ± 71	0.5341	12.971	105	2617 ± 19
9-2	82	778	1.300	0.1806 ± 31	2.8567 ±179	0.5098	12.692	100	2658 ± 28
10-1	146	226	0.411	0.1794 ± 13	0.4717 ± 33	0.5251	12.988	103	2647 ± 12
10-2	118	363	0.837	0.1790 ± 18	0.9469 ± 61	0.4993	12.320	99	2643 ± 17
10-3	117	408	0.756	0.1806 ± 20	1.0761 ± 70	0.5117	12.740	100	2658 ± 18
11-1	93	554	1.097	0.1772 ± 23	1.7996 ±105	0.5353	13.079	105	2627 ± 21
11-2	80	694	1.090	0.1816 ± 27	2.7034 ±161	0.5217	13.067	101	2668 ± 25
12-1	150	317	2.054	0.1789 ± 23	0.6672 ± 59	0.5368	13.243	105	2643 ± 21
12-2	99	553	1.151	0.1801 ± 24	1.7999 ±108	0.5284	13.125	103	2654 ± 22
12-3	113	435	1.404	0.1758 ± 24	1.1978 ± 84	0.5038	12.210	101	2613 ± 23
13-1	125	177	0.777	0.1772 ± 19	0.4311 ± 45	0.5012	12.245	100	2627 ± 17
13-2	132	136	0.776	0.1778 ± 17	0.3145 ± 37	0.5121	12.555	101	2633 ± 16
13-3	130	190	0.685	0.1785 ± 17	0.4508 ± 41	0.5274	12.982	103	2639 ± 16
14-1	117	568	1.262	0.1747 ± 26	1.4585 ±102	0.4945	11.913	99	2603 ± 24
15-1	224	233	0.317	0.1784 ± 12	0.3169 ± 26	0.5294	13.024	104	2638 ± 11
15-2	113	353	2.069	0.1812 ± 27	0.9589 ± 79	0.5109	12.765	100	2664 ± 25
15-3	83	563	1.462	0.1764 ± 27	2.0577 ±129	0.5208	12.669	103	2620 ± 26
16-1	90	587	0.952	0.1796 ± 24	2.0057 ±120	0.5126	12.691	101	2649 ± 23

Data 11/12/99 (4 spots), and 18/01/00.

U/Pb scatter (1σ) for Khan standard = 1.36% (n = 13) and 2.50% (n = 15).

Common-Pb corrected using Cumming & Richards (1975) Model III @ 2640 Ma.

Analysed using NO_2^- primary ion beam.

Pb/U calibration might be slightly disturbed.

Th/U calibration is not reliable; Th abundances are indicative only, and Pb/Th are not reported.

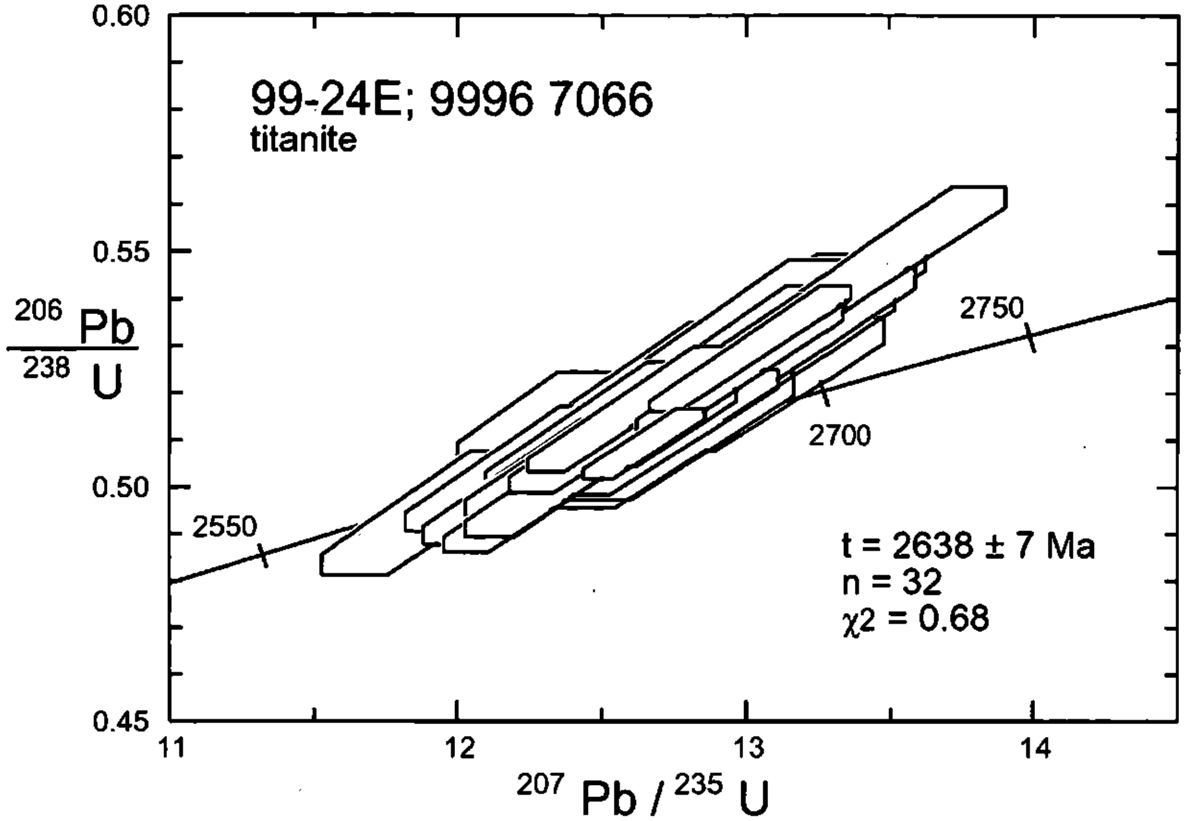

Figure t9996 7066: Concordia plot of SHRIMP titanite data for the K-feldspar-phyric biotite granite, Namban (UWA mount 99-24E).

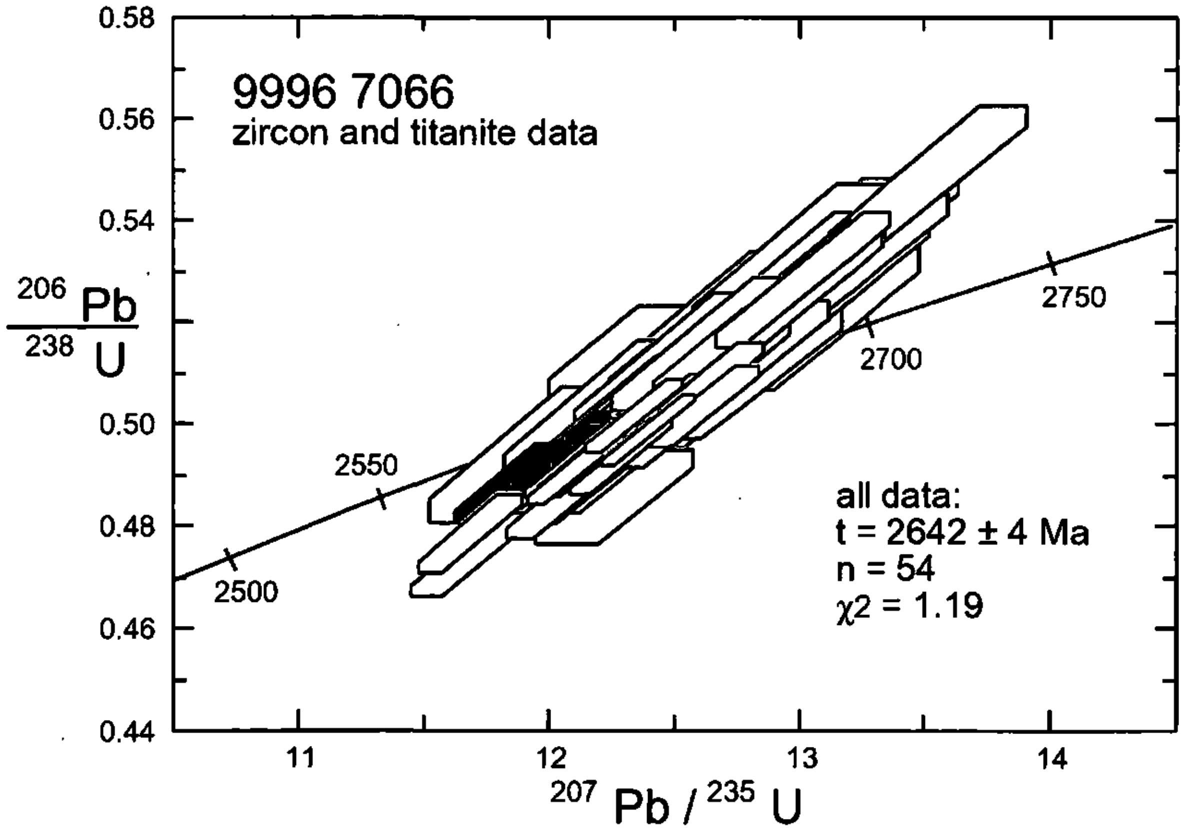

Figure c9996 7066: Concordia plot of titanite (light shaded) and zircon SHRIMP data for the K-feldspar-phyric biotite granite, Namban.

9996 7082C: augen gneiss xenolith, Dookaling

1:250,000 sheet:	Moora (SH5010)
AMG:	448285.0 mE, 6629400.0 mN
Location:	Drilled and hammered from blasted rock south of road.
Province:	Murchison
Description:	Sample is from a large xenolith of strongly feldspar porphyroblastic medium-grained biotite augen gneiss within a relatively homogeneous fine-grained biotite granite. Other xenoliths of banded granitic gneiss. Biotite granite also contains biotite-rich clots and schlieren. All rocks cut by minor pegmatites and rare quartz veins
Chemical group:	High-Ca group, Mainland association, Cootaning clan
Pluton No:	213722
UWA mounts:	99-28B (zircon) and 99-24D (titanite)

Description of zircons

The zircon population in this sample consists of one morphologic type. However, the grains are distinctive by ranging from euhedral to subhedral to anhedral and are considered unlikely to be of one generation. Most grains are 60-120 μm long, with a range of aspect ratios from ~1-2:1 for the majority to ~5:1. Some grains are distinctly corroded. In their internal morphology, grains range from faint continuous euhedral internal zoning from core to rim to partially recrystallised. The former dominate. There is a gradation between these two end members with progressive recrystallisation overprinting the euhedral zoning, particularly in the more strongly zoned rims areas. Inclusions are rare. The grains range from pale brown to dark brown in colour. Strong euhedral zoning observed towards the rims of some grains in both optical and SEM images suggest high U-Th-contents and radiation damage. Fracture networks indicative of radiation damage from high U-Th contents are common. Some grains have more homogeneous core regions but there is no break in the euhedral growth from core to rim and they are not considered to be xenocrysts. The different age populations in the sample could not be identified on morphological grounds.

Description of titanites

The titanites from this sample are all 50-200 μm fragments of larger grains. Only rarely do grains show growth surfaces; most surfaces are fractures. The grains are pale brown to dark brown in colour. Some grains or parts of grains are almost black and have evenly distributed dense and very fine inclusion populations. Areas of SHRIMP analysis were in clean parts of the grains, avoiding inclusions and fractures.

Results and interpretation

Zircon

Twenty three analyses were obtained from 22 grains. The data are all concordant and have very low common-Pb contamination. The data fall into three distinct groups: a cluster of 16 at ~2940 Ma, several at ~2900 Ma and a group of four at ~2750 Ma. All of these groups show scatter in excess of experimental uncertainties.

Titanite

Twenty one analyses were obtained from 21 fragments. The U abundances are ~100 ppm and the common Pb corrections are all small. The data show a tight grouping in both $^{207}Pb/^{206}Pb$ and Pb/U, which is taken as evidence that these data are concordant. Omitting four statistical (old) outliers leaves a single age population of 17 analyses with $\chi^2 = 0.45$. The corresponding age of 2619 ±8 Ma.

The titanite date is distinct from all the zircon data groups. The 2940 ± 5 Ma zircon age is probably the magmatic age if the granitoid from which the xenolith was derived and the titanite age of 2619 ± 8 Ma is considered to be the age of the granitoid in which it now sits. It is not clear whether the intermediate zircon dates represent discrete events experienced by the xenolith; they could represent partial resetting of 2940 Ma zircons at 2619 Ma, although the clustering suggests discrete events.

Table z9996 7082C: SHRIMP zircon data for the augen gneiss xenolith, Dookaling (UWA mount 99-28B).

grain-spot	U (ppm)	Th (ppm)	4f206 (%)	$^{207}Pb^*/^{206}Pb^*$	$^{208}Pb^*/^{206}Pb^*$	$^{206}Pb^*/^{238}U$	$^{207}Pb^*/^{235}U$	$^{208}Pb^*/^{232}Th$	conc. (%)	$^{207}Pb/^{206}Pb$ age (Ma)
Old group.										
53-1	214	140	0.097	0.2141 ± 8	0.1716 ± 12	0.5836	17.229	0.1536	101	2937 ± 6
64-1	127	111	0.020	0.2122 ± 10	0.2270 ± 16	0.5827	17.048	0.1512	101	2922 ± 7
63-1	173	113	0.000	0.2125 ± 8	0.1744 ± 11	0.5687	16.664	0.1516	99	2925 ± 6
67-1	804	339	0.021	0.2145 ± 4	0.1105 ± 4	0.5726	16.933	0.1501	99	2940 ± 3
68-1	662	141	0.006	0.2165 ± 4	0.0554 ± 3	0.5802	17.319	0.1511	100	2955 ± 3
62-1	255	92	0.015	0.2133 ± 7	0.0937 ± 8	0.5607	16.490	0.1455	98	2931 ± 5
61-1	149	111	0.097	0.2141 ± 11	0.1914 ± 18	0.5668	16.733	0.1448	99	2937 ± 8
69-1	357	163	0.004	0.2164 ± 6	0.1203 ± 7	0.5736	17.117	0.1515	99	2954 ± 4
70-1	651	104	0.026	0.2135 ± 4	0.0414 ± 3	0.5806	17.090	0.1503	101	2932 ± 3
60-1	262	184	0.139	0.2137 ± 7	0.1837 ± 11	0.5551	16.356	0.1448	97	2934 ± 6
71-1	598	142	0.095	0.2149 ± 5	0.0633 ± 5	0.5663	16.779	0.1505	98	2943 ± 4
72-1	270	101	0.105	0.2132 ± 7	0.0971 ± 9	0.5663	16.648	0.1462	99	2930 ± 5
73-1	342	115	0.069	0.2143 ± 6	0.0883 ± 7	0.5733	16.944	0.1498	99	2939 ± 5
74-1	190	93	0.089	0.2161 ± 8	0.1304 ± 11	0.5714	17.028	0.1523	99	2952 ± 6
79-1	186	123	0.179	0.2130 ± 9	0.1769 ± 15	0.5701	16.745	0.1519	99	2929 ± 7
63-2	308	199	0.051	0.2136 ± 6	0.1687 ± 9	0.5784	17.038	0.1514	100	2933 ± 5
Young group.										
65-1	607	105	0.064	0.1913 ± 4	0.0464 ± 4	0.5193	13.700	0.1393	98	2754 ± 4
56-1	444	63	0.018	0.1892 ± 5	0.0395 ± 4	0.5330	13.906	0.1477	101	2735 ± 4
77-1	934	95	0.032	0.1908 ± 3	0.0243 ± 3	0.5127	13.489	0.1228	97	2749 ± 3
78-1	867	63	0.026	0.1906 ± 3	0.0194 ± 2	0.5241	13.769	0.1407	99	2747 ± 3
?mixed ages.										
66-1	379	180	0.099	0.2095 ± 6	0.1236 ± 8	0.5592	16.156	0.1455	99	2902 ± 5
75-1	629	87	0.013	0.2094 ± 4	0.0365 ± 3	0.5626	16.241	0.1485	99	2901 ± 3
76-1	234	82	0.080	0.2109 ± 8	0.0908 ± 9	0.5465	15.887	0.1413	97	2912 ± 6

Data 17/08/99.
U/Pb scatter (1σ) for cz3 standard = 1.41% (n = 15).

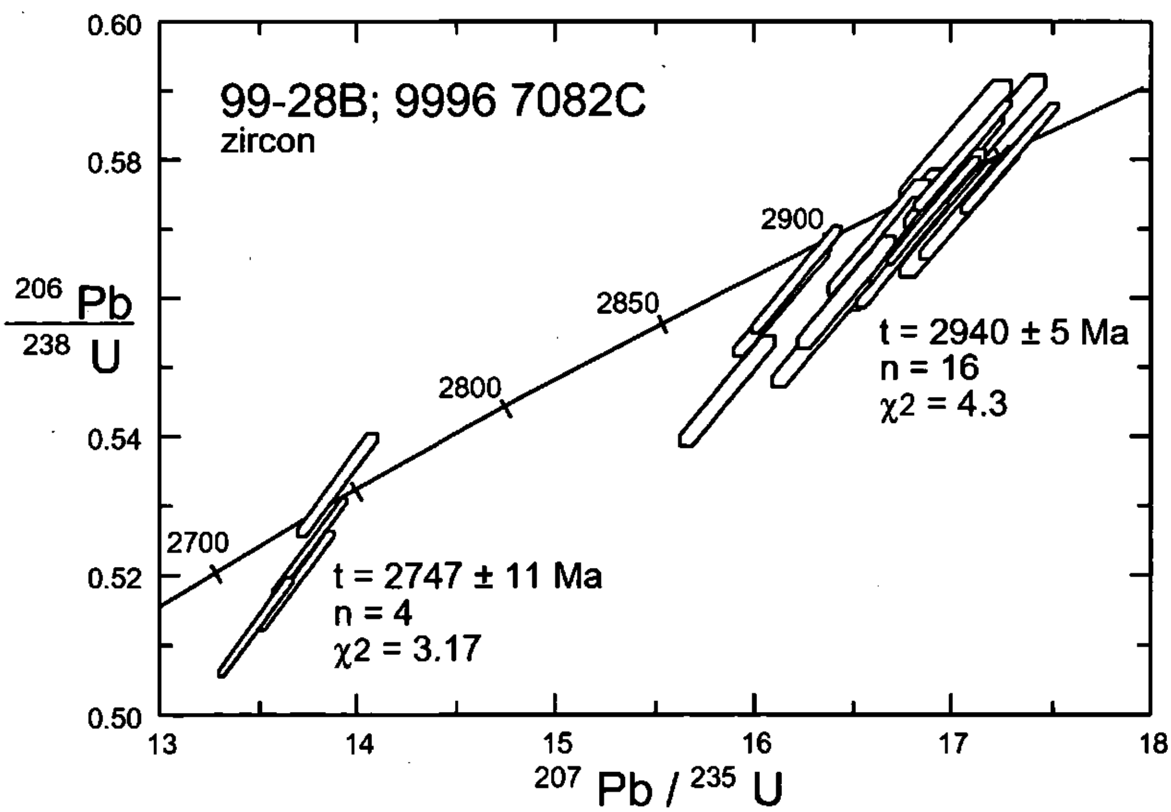

Figure z9996 7082C: Concordia plot of all SHRIMP zircon data for the augen gneiss xenolith, Dookaling (UWA mount 99-28B).

Table t9996 7082C: SHRIMP titanite data for the augen gneiss xenolith, Dookaling (UWA mount 99-24D).

grain-spot	U (ppm)	Th# (ppm)	4f206 (%)	$^{207}Pb^*/^{206}Pb^*$	$^{208}Pb^*/^{206}Pb^*$	$^{206}Pb^*/^{238}U$ #	$^{207}Pb^*/^{235}U$ #	conc. (%)	$^{207}Pb/^{206}Pb$ age (Ma)
Main group.									
1-1	110	49	0.602	0.1757 ± 17	0.1333 ± 31	0.4833	11.710	97	2613 ± 16
2-1	102	37	0.458	0.1770 ± 15	0.1024 ± 27	0.4799	11.710	96	2625 ± 14
3-1	45	20	0.870	0.1752 ± 27	0.1377 ± 54	0.4629	11.184	94	2608 ± 26
5-1	143	35	0.474	0.1752 ± 13	0.0707 ± 23	0.4990	12.053	100	2608 ± 12
6-1	140	97	0.498	0.1767 ± 12	0.2064 ± 24	0.4706	11.464	95	2622 ± 12
8-1	94	82	0.543	0.1746 ± 18	0.2738 ± 38	0.4671	11.245	95	2602 ± 17
9-1	147	71	0.652	0.1763 ± 14	0.1442 ± 26	0.4975	12.093	99	2618 ± 13
10-1	107	34	0.409	0.1767 ± 14	0.0947 ± 24	0.4938	12.031	99	2622 ± 13
12-1	104	25	0.337	0.1770 ± 16	0.0758 ± 26	0.4757	11.611	96	2625 ± 15
13-1	102	11	0.470	0.1783 ± 18	0.0352 ± 30	0.4641	11.411	93	2637 ± 16
14-1	115	54	0.414	0.1773 ± 14	0.1442 ± 26	0.4755	11.622	95	2627 ± 13
15-1	139	13	0.524	0.1745 ± 14	0.0246 ± 23	0.4797	11.539	97	2601 ± 13
16-1	96	57	0.474	0.1776 ± 15	0.1821 ± 30	0.4923	12.057	98	2631 ± 14
17-1	94	24	0.481	0.1753 ± 16	0.0753 ± 29	0.4950	11.964	99	2609 ± 15
18-1	138	52	0.490	0.1760 ± 15	0.1131 ± 27	0.4936	11.976	99	2615 ± 14
19-1	137	43	0.688	0.1765 ± 14	0.0931 ± 25	0.4852	11.809	97	2620 ± 13
20-1	135	44	0.382	0.1771 ± 15	0.0981 ± 26	0.5002	12.212	100	2626 ± 14
Old outliers.									
4-1	89	9	0.198	0.1815 ± 16	0.0366 ± 25	0.4733	11.847	94	2667 ± 14
7-1	180	76	0.150	0.1798 ± 10	0.1332 ± 17	0.5157	12.787	101	2651 ± 10
11-1	122	24	0.217	0.1798 ± 14	0.0641 ± 23	0.4865	12.061	96	2651 ± 13
21-1	86	39	0.219	0.1790 ± 19	0.1459 ± 34	0.5251	12.961	103	2644 ± 17

Data 11/12/99.
U/Pb scatter (1σ) for Khan standard = 1.36% (n = 13).
Common-Pb corrected using Cumming & Richards (1975) Model III @ 2620 Ma.
Analysed using NO_2^- primary ion beam.
Pb/U calibration might be slightly disturbed.
Th/U calibration is not reliable; Th abundances are indicative only, and Pb/Th are not reported.

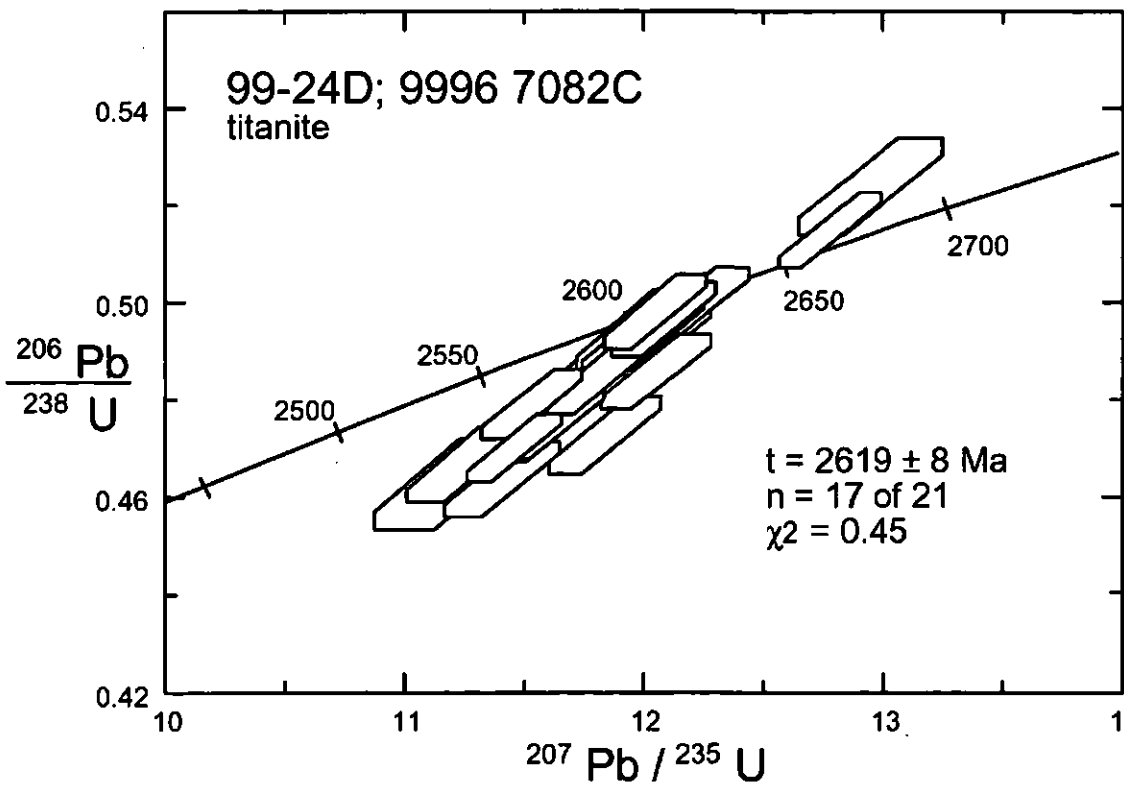

Figure t9996 7082C: Concordia plot of SHRIMP titanite data for the augen gneiss xenolith, Dookaling (UWA mount 99-24D).

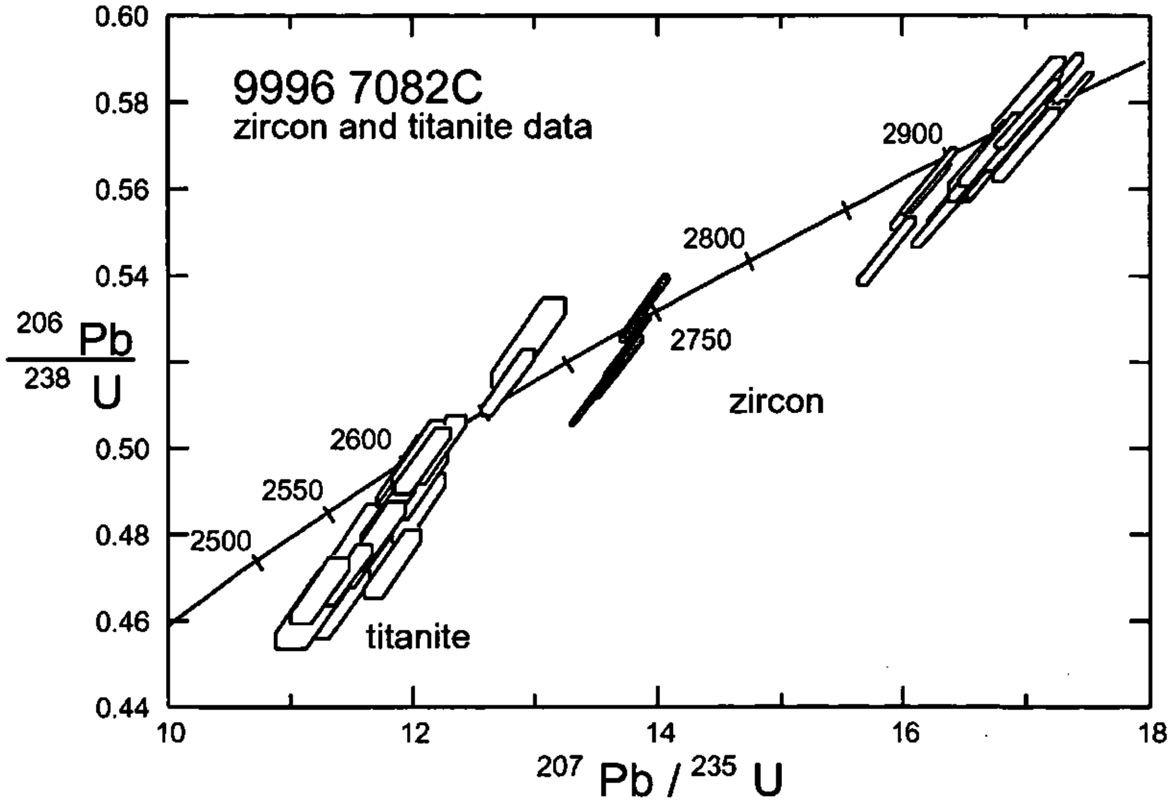

Figure c9996 7082C: Concordia plot of titanite and zircon SHRIMP data for the augen gneiss xenolith, Dookaling.

9996 7114: biotite granodiorite, Telegootherra

1:250,000 sheet:	Cue (SG5015)
AMG:	544607.6 mE, 6998801.7 mN
Location:	Drilled and hammered from outcrop of Telegootherra granite, south of Solomon open pit emerald mine, Poona greenstone belt. Also close to greisen-related tin mineralisation.
Province:	Murchison
Description:	Small pluton of sparsely feldspar-porphyritic fine-grained biotite granodiorite. Rare to minor thin quartz veins and pegmatites cut the granitoid.
Chemical group:	Low-Ca group, Goolthan association, Goolthan clan
Pluton No:	244301
UWA mount:	99-84B

Description of zircons

The zircon population in this sample consists of one morphologic type of zoned euhedral to subhedral grains, with most grains being 60-100 μm long, with a restricted range of aspect ratios from ~1-3:1. Grains are typically euhedral to subhedral in external morphology with continuous euhedral internal zoning from core to rim. Inclusions are relatively common and occur throughout grains. The grains range from pale brown to dark brown to nearly opaque in colour with most being dark. Strong euhedral zoning observed on both optical and SEM images suggest high U-Th-contents and radiation damage. Discordant alteration patches are visible on SEM images of most grains, and overgrow the euhedral zoning. A minority of grains, which tend to be subhedral or fragments, are lighter coloured and have faint zoning. Most grains have fracture networks typical of high-U grains, which have significant metamictisation. The alteration patches and fractures, and dark grains were avoided during data collection.

Results and interpretation

This sample gives zircon SHRIMP data similar to that from other highly radiogenic samples analyses in this project. In this case analyses were discontinued after only six completed analyses when it became apparent that there were few, if any, zircons that had tolerable U contents and preserved U–Pb systems.

Titanite was sought in this sample, but none was found.

Table z9996 7114: SHRIMP zircon data for the biotite granodiorite, Telegootherra (UWA mount 99-84B).

grain-spot	U (ppm)	Th (ppm)	4f206 (%)	$^{207}Pb^*/^{206}Pb^*$	$^{208}Pb^*/^{206}Pb^*$	$^{206}Pb^*/^{238}U$	$^{207}Pb^*/^{235}U$	$^{208}Pb^*/^{232}Th$	conc. (%)	$^{207}Pb/^{206}Pb$ age (Ma)
1-1	1267	1874	3.077	0.1578 ± 7	0.3917 ± 18	0.3694	8.035	0.0979	83	2432 ± 8
2-1	1105	980	7.104	0.1585 ± 12	0.2994 ± 27	0.3568	7.799	0.1204	81	2440 ± 13
3-1	70	154	0.084	0.1775 ± 13	0.6029 ± 38	0.4936	12.080	0.1350	98	2630 ± 12
4-1	1549	2248	71.001	0.1388 ± 75	1.8638 ±223	0.2658	5.088	0.3413	69	2213 ± 94
5-1	1158	1602	4.416	0.1558 ± 10	0.4055 ± 23	0.3413	7.331	0.1000	79	2411 ± 11
6-1	73	72	0.023	0.1836 ± 14	0.2641 ± 29	0.5125	12.971	0.1370	99	2685 ± 13

Data 14/3/00
U/Pb scatter (1σ) for cz3 standard = 0.84% (n = 7).

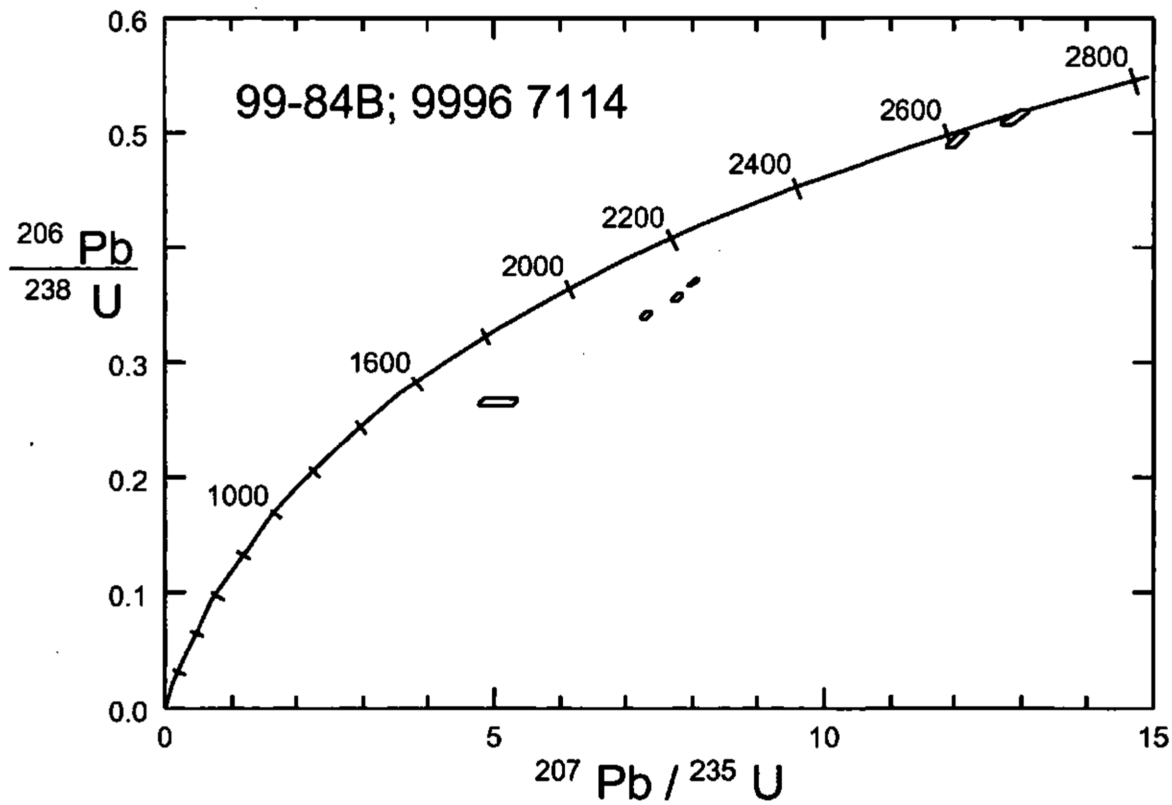

Figure z9996 7114: Concordia plot of SHRIMP zircon data for the biotite granodiorite, Telegootherra (UWA mount 99-84B).

9996 7141: granophyric biotite-amphibole granodiorite, Keygo

1:250,000 sheet:	Cue (SG5015)
AMG:	533337.6 mE, 6928726.7 mN
Location:	Blasted from outcrop of Keygo granodiorite on south side of road
Province:	Murchison
Description:	Granophyric-textured fine-medium-grained biotite-amphibole granodiorite. Quartz occurs as partly resorbed bipyramidal and/or fractured phenocrysts, and as granophyric intergrowths with plagioclase. Small lath-shaped phenocrysts of plagioclase. 'Skeletal' aggregates of amphibole and secondary biotite. Textures are interpreted to indicate high-level emplacement that has been affected by later alteration/metamorphism.
Chemical group:	High-HFSE group, Damperwah association, Nannine clan
Pluton No:	234208
UWA mount:	A-15C

Description of zircons

The zircon population in this sample consists of one morphologic type of finely zoned euhedral to subhedral grains, with most grains being ~30-40 μm long, with a restricted range of aspect ratios from ~1-2:1. Grains are typically euhedral to subhedral in external morphology with continuous euhedral internal zoning from core to rim. Inclusions are rare. The grains range from pale brown to darker brown in colour. Strong euhedral zoning observed on both optical and SEM images suggest high U-Th-contents and radiation damage. Discordant alteration patches are visible on SEM images of all grains, and overgrow the euhedral zoning. A few grains have more homogeneous core regions but there is no break in the euhedral growth from core to rim and they are not considered to be xenocrysts. Many grains have pervasive fracture networks typical of high-U grains, which have significant metamictisation. Due to the small grain size relative to the size of the SHRIMP spot, the alteration patches and fractures could not be avoided during data collection, which limited data quality.

Results and interpretation

Although the U contents of these zircons are not high, they give SHRIMP data similar to that from some of the more highly radiogenic samples analyses in this project. Most grains have high common Pb and give highly discordant data; many analyses were aborted. Analyses were discontinued after only six completed analyses when it became apparent that few of these zircons had well-preserved U–Pb systems. There is no evidence for multiple age groups or Archaean resetting of these samples. The data suggest an age ~2745 Ma.

Table z9996 7141 SHRIMP zircon data for the granodiorite, Keygo (UWA mount A-15C).

grain-spot	U (ppm)	Th (ppm)	4f206 (%)	$\frac{^{207}Pb^*}{^{206}Pb^*}$	$\frac{^{208}Pb^*}{^{206}Pb^*}$	$\frac{^{206}Pb^*}{^{238}U}$	$\frac{^{207}Pb^*}{^{235}U}$	$\frac{^{208}Pb^*}{^{232}Th}$	conc. (%)	$^{207}Pb/^{206}Pb$ age (Ma)
10-1	389	182	0.121	0.1902 ± 6	0.1498 ± 10	0.4656	12.211	0.1493	90	2744 ± 5
11-1	330	164	0.066	0.1902 ± 6	0.1385 ± 9	0.5136	13.473	0.1436	97	2744 ± 5
12-1	676	293	0.877	0.1904 ± 8	0.2310 ± 16	0.3712	9.746	0.1977	74	2746 ± 7
13-1	393	209	0.041	0.1902 ± 6	0.1419 ± 8	0.5207	13.652	0.1386	98	2743 ± 5
14-1	407	187	0.262	0.1898 ± 7	0.1624 ± 12	0.4533	11.864	0.1606	88	2741 ± 6
15-1	343	413	0.324	0.1909 ± 7	0.3084 ± 15	0.5191	13.667	0.1333	98	2750 ± 6

Data 10/6/00.
U/Pb scatter (1σ) for cz3 standard = 0.86% (n = 7).

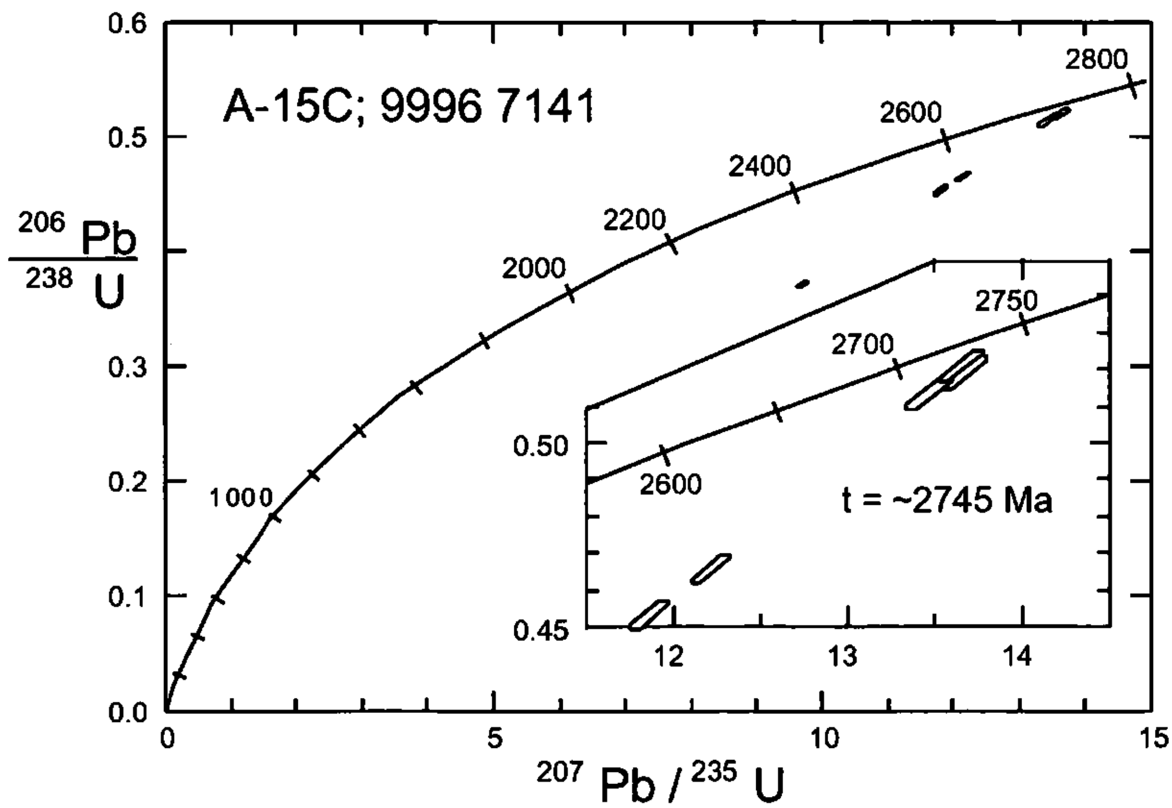

Figure z9996 7141: Concordia plot of SHRIMP zircon data for the granodiorite, Keygo (UWA mount A-15C).

9996 7170A: biotite diorite, Bullshead

1:250,000 sheet:	Leonora (SH5101)
AMG:	319920.8 mE, 6862804 mN
Location:	Celtic Prospect drillhole CRDD2, depth interval 174.10-175.60 m; Prospect is in the Teutonic Bore district
Province:	Eastern Goldfields
Description:	'Least-altered' seriate fine- to medium-grained biotite diorite dyke or pluton. Diorite dykes and small plutons are complexly interfingered with deformed supracrustal sequence and/or supracrustal xenoliths. Hydrothermal alteration comprises hematite staining with chlorite and carbonate.
Chemical group:	High-HFSE group, Kookynie association, Bullshead clan
Pluton No:	314126
UWA mount:	99-84C

Description of zircons

The small zircon population in this sample consists of one morphologic type of zoned subhedral grains, with most grains being 60-120 µm long, with a range of aspect ratios from ~1:1 to ~3-4:1. Grains are typically subhedral or fragments in external morphology with continuous euhedral internal zoning from core to rim. Inclusions are rare. The grains range from pale brown to dark brown to nearly opaque in colour, with the latter dominant. Strong euhedral zoning observed on both optical and SEM images suggest high U-Th-contents and radiation damage. Discordant alteration patches are visible on SEM images of most grains, and overgrow the euhedral zoning. In many grains, the euhedral zoning has been completely overprinted. Some grains have more homogeneous core regions but there is no break in the euhedral growth from core to rim and they are not considered to be xenocrysts. Almost all grains have fracture networks typical of high-U grains, which have significant metamictisation. Almost all the grains are unsuitable for analysis.

Results and interpretation

Preliminary SHRIMP examination of this sample showed data characteristics similar to 9996 7114 and 9996 7141, and analyses were discontinued.

9996 7174A: Flow-aligned strongly K-feldspar-phyric syenite, Wallaby

1:250,000 sheet:	Laverton (SH5102)
AMG:	432489.9 mE, 6808160 mN
Location:	Wallaby prospect drillhole WBAD 081, depth interval 227.55-229.20 m
Province:	Eastern Goldfields
Description:	'Least-altered',. Hydrothermal alteration minerals include biotite, hematite and minor sericite and pyrite.
Chemical group:	Syenite group, Gilgarna association, Wallaby clan
Pluton No:	334022

No zircons or titanites were recovered from this sample

9996 7176: Carbonatite, Wallaby

1:250,000 sheet:	Laverton (SH5102)
AMG:	432489.9 mE, 6808160 mN
Location:	Wallaby prospect drillhole WBAD 066, depth interval 173.45-175.80 m
Province:	Eastern Goldfields
Description:	Pyroxene-bearing carbonatite. Pyroxene altered to purple alkali-amphibole.
Chemical group:	Carbonatite group
Pluton No:	334023

No zircons or titanites were recovered from this sample

9996 7177B: K-feldspar-phyric carbonatitic syenite, Wallaby

1:250,000 sheet:	Laverton (SH5102)
AMG:	432489.9 mE, 6808160 mN
Location:	Wallaby prospect drillhole WBAD 101, depth interval 219.00-220.25 m
Province:	Eastern Goldfields
Description:	Weakly altered, K-feldspar-phyric carbonatitic syenite. Syenite contains large euhedral titanite grains. Alteration minerals include carbonate, hematite, sericite and pyrite.
Chemical group:	Syenite group, Gilgarna association, Wallaby clan
Pluton No:	334022
UWA mount:	99-90B

Description of titanites

The titanites from this sample are all 50-200 μm fragments of larger grains. Only rarely do grains show growth surfaces; most surfaces are fractures. The grains are pale brown to dark brown in colour. Some grains or parts of grains are almost black and have evenly distributed dense and very fine inclusion populations. Areas of SHRIMP analysis were in clean parts of the grains, avoiding inclusions and fractures.

Results and interpretation

Twenty four analyses on 14 fragments are presented in Table t9996 7177B and shown on a concordia diagram in Figure t9996 7177B. The U contents are low, ranging from ~10 ppm to ~50 ppm, and consequently the common-Pb corrections range up to ~4.3%. The lack of any correlation between 4f206 and corrected $^{207}Pb/^{206}Pb$ is taken as confirmation that the common-Pb composition used for corrections was appropriate. The data fall in a single concordant cluster, with $\chi^2 = 0.89$. Omitting the analyses with higher 4f206 values has no significant effect on χ^2 or on the group age. The age of 2657 ± 15 Ma, determined from the entire data set, is taken to be the emplacement age of the granitoid.

Table t9996 7177B: SHRIMP titanite data for the carbonatitic syenite dyke, Wallaby syenite (UWA mount 99-90B).

grain-spot	U (ppm)	Th (ppm)	4f206 (%)	$^{207}Pb^*/^{206}Pb^*$	$^{208}Pb^*/^{206}Pb^*$	$^{206}Pb^*/^{238}U$	$^{207}Pb^*/^{235}U$	$^{208}Pb^*/^{232}Th$	conc. (%)	$^{207}Pb/^{206}Pb$ age (Ma)
1-1	9	54	3.560	0.1789 ± 77	1.7409 ±289	0.5059	12.483	0.1394	100	2643 ± 72
2-1	14	54	3.626	0.1720 ± 56	0.9966 ±170	0.5133	12.178	0.1359	104	2578 ± 55
3-1	18	51	2.022	0.1795 ± 43	0.7762 ±125	0.5298	13.113	0.1447	103	2648 ± 39
4-1	13	63	2.961	0.1817 ± 54	1.3126 ±189	0.5137	12.871	0.1333	100	2668 ± 49
5-1	26	89	2.186	0.1793 ± 33	0.9118 ±104	0.5171	12.784	0.1394	102	2646 ± 30
5-2	16	52	3.525	0.1836 ± 54	0.8552 ±156	0.4990	12.630	0.1342	97	2685 ± 49
6-1	21	62	4.042	0.1758 ± 48	0.8060 ±135	0.5192	12.584	0.1407	103	2614 ± 45
7-1	16	61	2.419	0.1798 ± 45	1.0680 ±149	0.5191	12.871	0.1436	102	2651 ± 42
8-1.	15	65	3.273	0.1795 ± 53	1.1865 ±172	0.5380	13.318	0.1493	105	2648 ± 49
8-2	12	55	2.874	0.1913 ± 61	1.2956 ±204	0.5148	13.575	0.1421	97	2753 ± 52
8-3	10	61	3.819	0.1855 ± 66	1.5942 ±240	0.5183	13.257	0.1402	100	2703 ± 59
9-1	11	69	4.005	0.1845 ± 70	1.8241 ±265	0.5134	13.060	0.1468	99	2694 ± 62
10-1	56	122	1.295	0.1795 ± 19	0.5788 ± 56	0.5150	12.744	0.1353	101	2648 ± 18
10-2	9	47	4.149	0.1843 ± 76	1.4651 ±259	0.5024	12.769	0.1424	97	2692 ± 68
11-1	14	37	2.318	0.1854 ± 49	0.7481 ±139	0.5136	13.126	0.1473	99	2701 ± 43
12-1	22	88	1.480	0.1847 ± 34	1.0782 ±120	0.5211	13.274	0.1407	100	2696 ± 30
12-2	26	57	2.051	0.1832 ± 35	0.5850 ± 96	0.5166	13.051	0.1376	100	2682 ± 32
12-3	11	60	4.297	0.1716 ± 68	1.4581 ±236	0.5132	12.141	0.1388	104	2573 ± 66
13-1	31	90	1.228	0.1848 ± 25	0.7661 ± 80	0.5259	13.403	0.1388	101	2697 ± 22
13-2	31	94	1.937	0.1776 ± 32	0.8017 ± 96	0.5119	12.535	0.1362	101	2631 ± 29
13-3	42	104	1.780	0.1782 ± 27	0.6733 ± 78	0.4987	12.250	0.1348	99	2636 ± 25
13-4	29	92	2.390	0.1742 ± 34	0.8461 ±104	0.5006	12.024	0.1341	101	2599 ± 32
13-5	23	81	3.172	0.1810 ± 45	0.9742 ±136	0.5227	13.047	0.1451	102	2662 ± 41
14-1	21	79	2.302	0.1811 ± 39	0.9917 ±128	0.5070	12.661	0.1344	99	2663 ± 36

Data 21/03/00
U/Pb scatter (1σ) for Khan standard = 2.02% (n = 9).
Common-Pb corrected using Cumming & Richards (1975) Model III @ 2640 Ma.

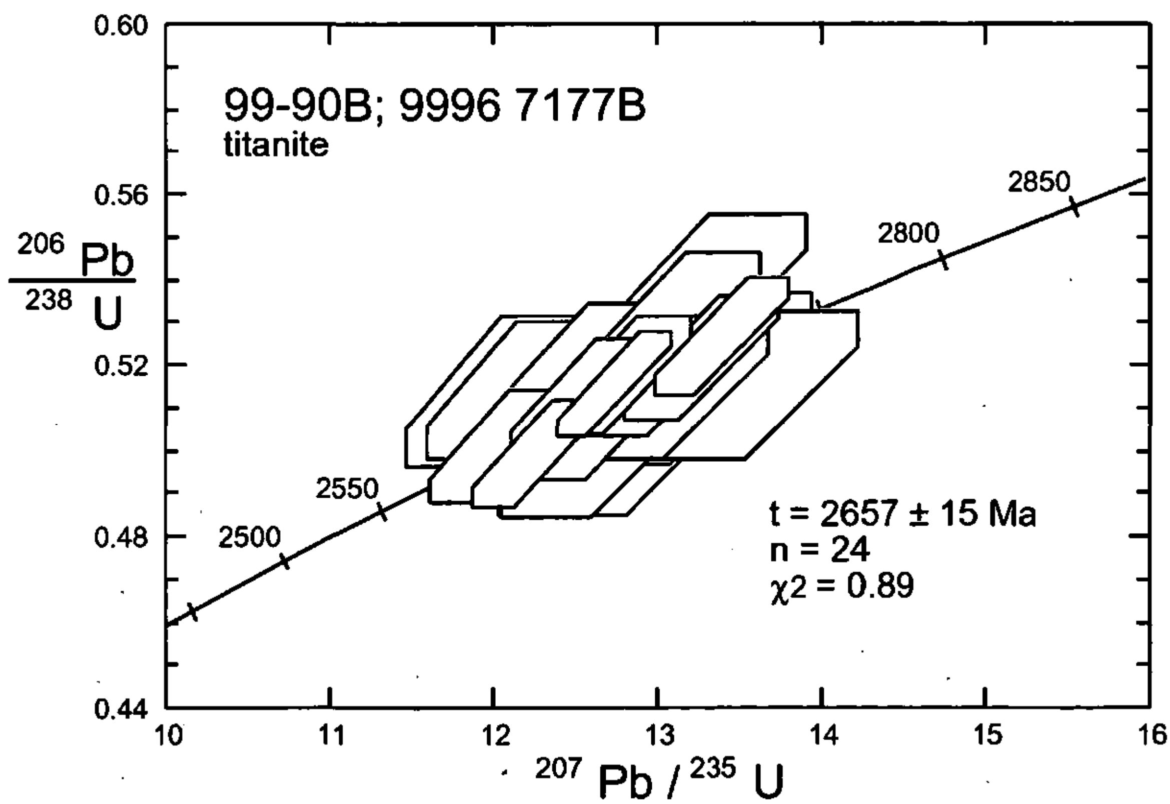

Figure t9996 7177B: Concordia plot of SHRIMP titanite data for the carbonatitic syenite dyke, Wallaby syenite (UWA mount 99-90B).

9996 9049: feldspar porphyritic hornblende-biotite granite dyke, Coolamen

1:250,000 sheet:	Bencubbin (SH5011)
AMG:	606301.0 mE, 6580040.0 mN
Location:	Drilled and hammered from outcrop just west of road.
Province:	Murchison
Description:	Strongly feldspar porphyritic fine-grained biotite-hornblende granite. Probably a dyke; similar to other dykes and pods in area. Very minor pegmatite veins.
Chemical group:	Low-HFSE group, Damperwah Association, Coolamen clan
Pluton No:	253621
UWA mount:	99-33A

Description of zircons

The zircon population in this sample consists of one morphologic type of finely zoned euhedral to subhedral grains, with most grains being 60-200 μm long, with a range of aspect ratios from ~2-3:1 for the majority, to ~5:1. Grains are typically euhedral to subhedral in external morphology with continuous euhedral internal zoning from core to rim. Inclusions are rare. The grains range from very pale brown to darker brown in colour. Strong euhedral zoning observed in some of the darker grains in both optical and SEM images suggest high U-Th-contents and radiation damage. Discordant alteration patches are visible on SEM images of a few grains, and overgrow the euhedral zoning. Some grains have more homogeneous core regions but there is no break in the euhedral growth from core to rim and they are not considered to be xenocrysts. The fractures and darker grains were avoided during data collection.

Results and interpretation

Twenty seven analyses on 27 grains are presented in Table z9996 9049 and shown on a concordia diagram in Figure z9996 9049. The data all have U<220 ppm and low common-Pb contamination. Omitting two analyses, one that is >5% discordant and one with high 4f206, leaves a population comprising 25 analyses which has a χ^2 of 0.81. The corresponding age of 2640 ± 5 Ma is interpreted as the emplacement age of the granitoid.

Table z9996 9049: SHRIMP zircon data for the hornblende-biotite monzogranite, Coolamen-dyke (UWA mount 99-33A).

grain-spot	U (ppm)	Th (ppm)	4f206 (%)	$^{207}Pb^*/^{206}Pb^*$	$^{208}Pb^*/^{206}Pb^*$	$^{206}Pb^*/^{238}U$	$^{207}Pb^*/^{235}U$	$^{208}Pb^*/^{232}Th$	conc. (%)	$^{207}Pb/^{206}Pb$ age (Ma)
Main group.										
3-1	48	69	0.000	0.1781 ± 16	0.3910 ± 39	0.4844	11.895	0.1316	97	2635 ± 15
4-1	109	113	0.074	0.1787 ± 13	0.2783 ± 26	0.4974	12.252	0.1337	99	2641 ± 12
2-1	86	79	0.208	0.1784 ± 17	0.2459 ± 34	0.5001	12.301	0.1340	99	2638 ± 16
33-1	185	133	0.026	0.1783 ± 9	0.1936 ± 15	0.5005	12.305	0.1346	99	2637 ± 8
12-1	60	72	0.065	0.1808 ± 19	0.3174 ± 42	0.5016	12.503	0.1319	99	2660 ± 18
13-1	70	60	0.156	0.1789 ± 19	0.2233 ± 37	0.4942	12.188	0.1285	98	2642 ± 17
11-1	214	191	0.134	0.1772 ± 9	0.2380 ± 17	0.5024	12.278	0.1342	100	2627 ± 8
20-1	110	73	0.160	0.1775 ± 14	0.1765 ± 25	0.5030	12.314	0.1337	100	2630 ± 13
23-1	109	93	0.000	0.1796 ± 11	0.2316 ± 19	0.5051	12.510	0.1368	99	2649 ± 10
16-1	94	71	0.095	0.1782 ± 13	0.2013 ± 24	0.4869	11.961	0.1287	97	2636 ± 13
17-1	164	165	0.000	0.1789 ± 9	0.2768 ± 17	0.5072	12.512	0.1391	100	2643 ± 8
28-1	167	133	0.006	0.1800 ± 11	0.2194 ± 20	0.4887	12.133	0.1347	97	2653 ± 10
30-1	192	142	0.020	0.1789 ± 10	0.1965 ± 18	0.5089	12.552	0.1355	100	2643 ± 9
31-1	99	77	0.161	0.1768 ± 14	0.2092 ± 28	0.4985	12.150	0.1344	99	2623 ± 14
35-1	72	84	0.000	0.1775 ± 13	0.3143 ± 28	0.5170	12.651	0.1399	102	2629 ± 12
27-1	71	49	0.048	0.1793 ± 18	0.1846 ± 32	0.5109	12.635	0.1373	101	2647 ± 16
25-1	131	164	0.082	0.1810 ± 12	0.3371 ± 27	0.5117	12.766	0.1378	100	2662 ± 11
26-1	156	176	0.152	0.1784 ± 11	0.3042 ± 23	0.4818	11.850	0.1300	96	2638 ± 10
36-1	52	49	0.094	0.1770 ± 22	0.2487 ± 44	0.5345	13.042	0.1413	105	2625 ± 20
37-1	96	58	0.015	0.1772 ± 17	0.1652 ± 32	0.4884	11.934	0.1329	98	2627 ± 16
5-1	150	119	0.118	0.1792 ± 11	0.2127 ± 21	0.5059	12.497	0.1361	100	2645 ± 10
6-1	109	89	0.000	0.1776 ± 11	0.2217 ± 18	0.5146	12.604	0.1402	102	2631 ± 10
9-1	104	134	0.074	0.1774 ± 15	0.3515 ± 33	0.4963	12.141	0.1347	99	2629 ± 14
39-1	86	85	0.000	0.1808 ± 12	0.2685 ± 24	0.5024	12.527	0.1358	99	2661 ± 11
40-1	147	145	0.029	0.1786 ± 12	0.2684 ± 24	0.4976	12.252	0.1354	99	2640 ± 11
>5% discordant or high 4f206.										
34-1	53	32	0.186	0.1790 ± 23	0.1587 ± 43	0.4727	11.670	0.1262	94	2644 ± 21
38-1	74	71	3.197	0.1843 ± 43	0.2902 ± 96	0.5024	12.766	0.1528	97	2692 ± 38

Data 26/11/99.

U/Pb scatter (1σ) for cz3 standard = 1.34% (n = 12).

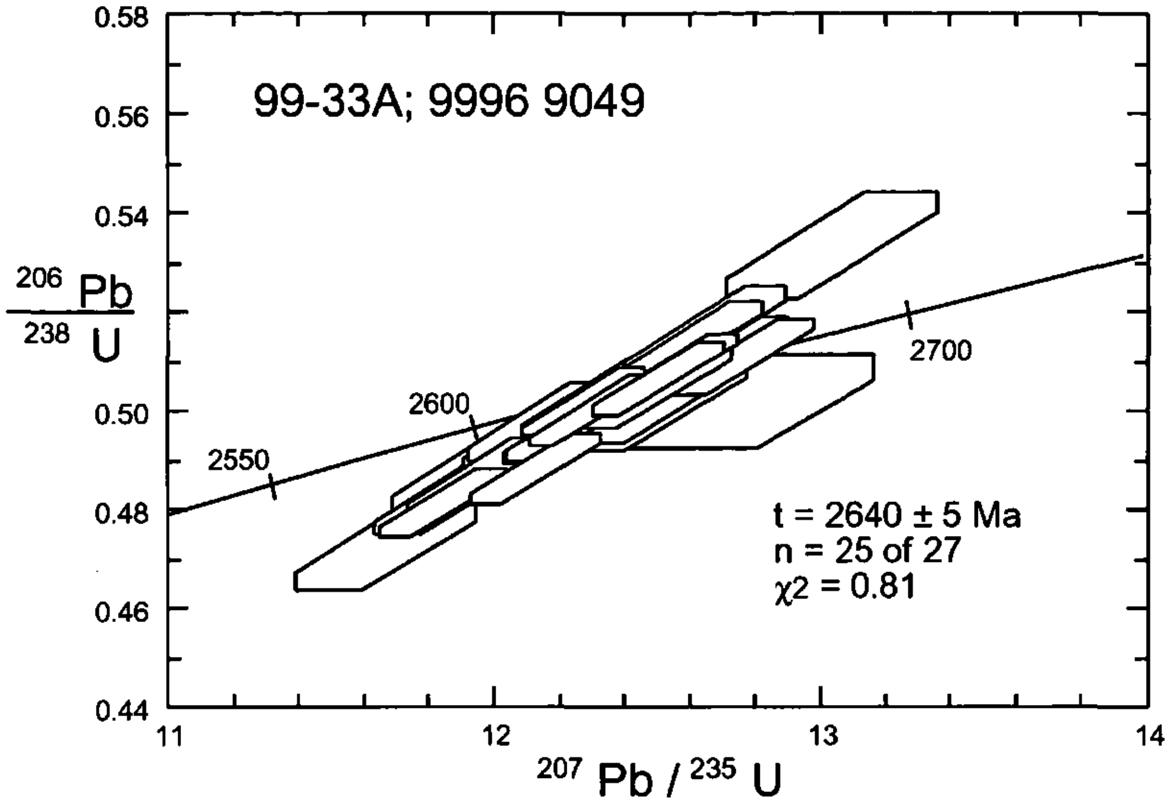

Figure z9996 9049: Concordia plot showing all SHRIMP zircon data for the hornblende-biotite monzogranite, Coolamen-dyke (UWA mount 99-33A).

9996 9063: allanite-titanite-biotite granite dyke, Barrambie

1:250,000 sheet:	Moora (SH5010)
AMG:	477928.0 mE, 6610048.0 mN
Location:	Drilled and hammered from bouldery and pavement outcrop ~50 m west of fence.
Province:	Murchison
Description:	Equigranular fine- to medium-grained allanite-titanite-biotite granite. Probably a dyke, as it forms a ~60m wide ridge. Thin veins of aplite.
Chemical group:	Low-Ca group, Goolthan association, Wubin clan
Pluton No:	223622
UWA mount:	99-33B

Description of zircons

The zircon population in this sample consists of one morphologic type of euhedral to subhedral grains, with most grains being 60-200 µm long, with a range of aspect ratios from ~2-4:1 for the majority, to >5:1 for several grains. Grains are typically euhedral to subhedral in external morphology with faint continuous euhedral internal zoning from core to rim in some grains. However, most grains show a homogeneous internal structure grading to euhedral zoning towards the rim. Inclusions are relatively rare. The grains range from pale brown to dark brown in colour. The lack of strong euhedral zoning observed on both optical and SEM images suggest low U-Th-contents and radiation damage. However, many grains have fracture networks typical of high-U grains, which have significant metamictisation. Therefore, the homogeneous internal structure of most of the grains may represent recrystallisation within largely high-U grains. Fractures and darker grains were avoided during data collection.

Results and interpretation

Twenty analyses on 19 grains are presented in Table z9996 9063 and shown on a concordia diagram in Figure z9996 9063. Despite having U contents up to ~700 ppm the data are almost all concordant and have low common-Pb contamination. Omitting one statistical (old) outlier leaves a population with a χ^2 of 1.47. The corresponding age is 2630 ± 6 Ma; this is interpreted as the emplacement age of the granitoid.

Table z9996 9063: SHRIMP zircon data for the allanite-titanite-biotite granite dyke, Barrambie (UWA mount 99-33B).

grain-spot	U (ppm)	Th (ppm)	4f206 (%)	$^{207}Pb^*/^{206}Pb^*$	$^{208}Pb^*/^{206}Pb^*$	$^{206}Pb^*/^{238}U$	$^{207}Pb^*/^{235}U$	$^{208}Pb^*/^{232}Th$	conc. (%)	$^{207}Pb/^{206}Pb$ age (Ma)
Main group.										
46-1	349	376	0.079	0.1760 ± 11	0.2899 ± 15	0.5164	12.529	0.1390	103	2615 ± 10
33-1	681	288	0.012	0.1784 ± 8	0.1119 ± 7	0.4947	12.172	0.1311	98	2638 ± 7
34-1	460	122	0.059	0.1777 ± 10	0.0686 ± 8	0.5052	12.374	0.1302	100	2631 ± 9
36-1	663	420	0.037	0.1786 ± 8	0.1717 ± 9	0.4937	12.160	0.1340	98	2640 ± 8
37-1	534	145	0.059	0.1773 ± 9	0.0737 ± 9	0.5003	12.232	0.1361	100	2628 ± 9
38-1	124	127	0.116	0.1777 ± 21	0.2845 ± 33	0.4904	12.013	0.1360	98	2631 ± 20
39-1	689	413	0.041	0.1778 ± 8	0.1611 ± 9	0.5122	12.553	0.1377	101	2632 ± 8
40-1	710	367	0.049	0.1762 ± 8	0.1382 ± 8	0.5012	12.177	0.1342	100	2618 ± 8
41-1	633	256	0.058	0.1805 ± 9	0.1074 ± 9	0.5062	12.596	0.1343	99	2657 ± 8
42-1	626	299	0.186	0.1777 ± 10	0.1323 ± 12	0.4923	12.064	0.1365	98	2632 ± 9
43-1	593	321	0.060	0.1775 ± 9	0.1391 ± 10	0.5121	12.535	0.1317	101	2630 ± 9
43-2	190	178	0.072	0.1773 ± 17	0.2514 ± 23	0.4936	12.066	0.1324	98	2628 ± 16
44-1	331	251	0.197	0.1771 ± 13	0.2056 ± 17	0.4917	12.003	0.1330	98	2625 ± 12
61-1	622	309	0.086	0.1775 ± 9	0.1317 ± 10	0.5144	12.592	0.1363	102	2630 ± 9
47-1	519	285	0.102	0.1752 ± 11	0.1416 ± 12	0.4955	11.972	0.1279	99	2608 ± 10
59-1	353	499	0.111	0.1749 ± 13	0.3763 ± 21	0.4839	11.669	0.1289	98	2605 ± 12
58-1	426	237	0.156	0.1783 ± 13	0.1482 ± 15	0.4855	11.933	0.1293	97	2637 ± 12
57-1	155	184	0.176	0.1770 ± 22	0.3095 ± 36	0.5110	12.475	0.1333	101	2625 ± 21
54-1	374	272	0.254	0.1768 ± 14	0.1914 ± 19	0.4933	12.024	0.1295	99	2623 ± 13
Old outlier.										
35-1	628	332	0.032	0.1817 ± 8	0.1424 ± 8	0.5289	13.254	0.1424	103	2669 ± 7

Data 25/08/99.
U/Pb scatter (1σ) for cz3 standard = 2.10% (n = 11).

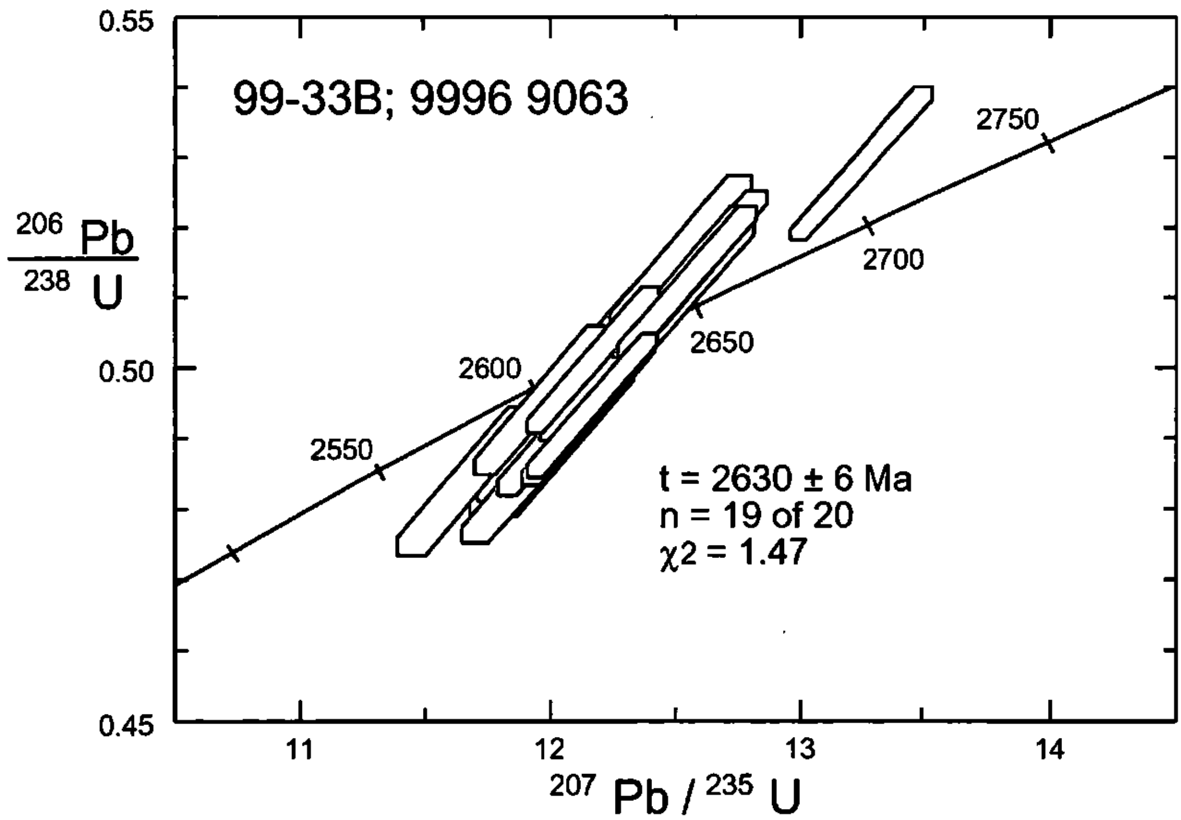

Figure z9996 9063: Concordia plot showing all SHRIMP zircon data for the allanite-titanite-biotite granite dyke, Barrambie (UWA mount 99-33B).

9996 9066: foliated feldspar porphyritic biotite granite, Donga Well

1:250,000 sheet:	Moora (SH5010)
AMG:	451118.0 mE, 6609103.1 mN
Location:	Hammered from outcrop just south of road.
Province:	Murchison
Description:	Foliated moderately feldspar porphyritic medium-grained biotite granite. Contains minor biotite-rich bands or schlieren. Mapped as gneiss 1:250k geological maps.
Chemical group:	High-Ca group, Mainland association, Bonnie Rock clan
Pluton No:	213601
UWA mount:	99-34B

Description of zircons

The zircon population in this sample consists of a number of morphologic types that vary in internal morphology and grain size. Most grains are euhedral to subhedral with fine euhedral internal zoning typical of magmatic growth. A significant proportion of the grains are perfectly euhedral in external form. This type may have either continuous zoning from core to rim, or homogeneous core regions but with no obvious break in the euhedral growth from core to rim. These grains have variable size, 60-300 μm long, and aspect ratios from ~2-3:1 for the majority to ~5:1. They are of variable colour from pale brown to mauve grading to black.

Another group of zircons appear to be completely altered with discordant patches completely overprinting fine euhedral zoning. These may be altered versions of the first group. Many of these grains have fracture networks typical of high-U grains, which have significant metamictisation. Grains from this group are otherwise similar to the first. Another group of zircons are anhedral to subhedral with no internal structure and appear to be completely recrystallised or xenocrysts. These grains are ~100-200 μm long with an aspect ratio of ~2:1.

There is no correlation between the age data and the morphological type and it is probable that all grains are xenocrysts that were trapped in other minerals such that they did not have contact with the zircon undersaturated magma.

Results and interpretation

Fourteen analyses were obtained from 14 grains. The U contents of these zircons are reasonably high, and the samples <2800 Ma fall on a discordance array similar to that some of the more highly radiogenic samples analysed in this project.. Analyses were discontinued when it became apparent that few of these zircons had well-preserved U–Pb systems. There are inherited grains with ages ~2780 Ma, ~3100Ma and ~3200 Ma and 3300 Ma. The younger grains might include a magmatic population, but their age cannot be determined.

Table z9996 9066: SHRIMP analytical data for the foliated feldspar porphyritic biotite granite, Donga Well (UWA mount 99-34B).

grain-spot	U (ppm)	Th (ppm)	4f206 (%)	$\frac{^{207}Pb^*}{^{206}Pb^*}$	$\frac{^{208}Pb^*}{^{206}Pb^*}$	$\frac{^{206}Pb^*}{^{238}U}$	$\frac{^{207}Pb^*}{^{235}U}$	$\frac{^{208}Pb^*}{^{232}Th}$	conc. (%)	$^{207}Pb/^{206}Pb$ age (Ma)
10-1	288	151	0.057	0.2479 ± 8	0.1405 ± 9	0.6165	21.072	0.1651	98	3171 ± 5
31-1	708	360	0.011	0.1828 ± 5	0.1359 ± 7	0.5017	12.646	0.1342	98	2678 ± 5
32-1	100	23	0.194	0.1955 ± 14	0.0623 ± 19	0.5221	14.073	0.1434	97	2789 ± 12
8-1	361	123	0.039	0.1936 ± 6	0.0905 ± 7	0.5322	14.204	0.1416	99	2773 ± 5
33-1	100	67	0.000	0.2688 ± 13	0.1780 ± 15	0.6617	24.520	0.1768	99	3299 ± 8
34-1	524	139	0.032	0.1826 ± 6	0.0727 ± 6	0.4892	12.316	0.1342	96	2677 ± 5
19-1	348	153	0.021	0.2516 ± 7	0.1215 ± 8	0.6294	21.835	0.1737	99	3195 ± 4
35-1	223	66	0.033	0.1955 ± 8	0.0804 ± 9	0.5346	14.408	0.1448	99	2789 ± 7
12-1	277	137	0.040	0.1872 ± 7	0.1347 ± 10	0.5070	13.087	0.1381	97	2718 ± 6
36-1	72	118	0.197	0.2378 ± 16	0.4280 ± 34	0.6176	20.253	0.1624	100	3106 ± 11
13-1	878	241	0.295	0.1766 ± 6	0.0735 ± 9	0.4600	11.198	0.1230	93	2621 ± 5
14-1	664	324	0.000	0.1829 ± 5	0.1352 ± 7	0.5035	12.699	0.1394	98	2680 ± 5
15-1	788	402	0.041	0.1810 ± 5	0.1372 ± 7	0.4697	11.723	0.1261	93	2662 ± 5
37-1	178	31	0.143	0.1870 ± 10	0.0396 ± 11	0.4896	12.622	0.1120	95	2716 ± 8

Data 06/09/99.
U/Pb scatter (1σ) for cz3 standard = 0.34% (n = 6).

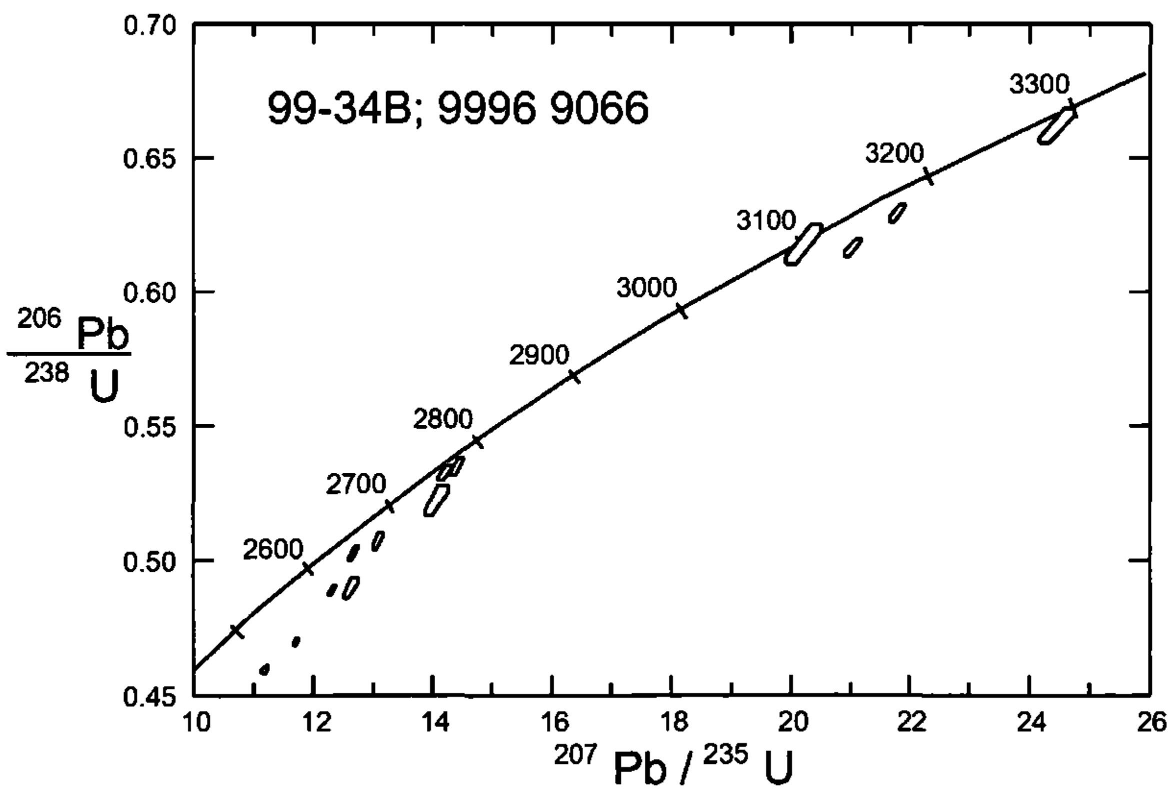

Figure z9996 9066: Concordia plot of SHRIMP zircon data for the foliated feldspar porphyritic biotite granite, Donga Well (UWA mount 99-34B).

9996 9093B: granodiorite gneiss, Coolangatta

1:250,000 sheet:	Moora (SH5010)
AMG:	475938.0 mE, 6663138.0 mN
Location:	Drilled and hammered from small facing stone quarry in middle of wheat paddock
Province:	Murchison
Description:	Nebulitic to banded medium-grained biotite granodiorite gneiss. Bands of biotite-rich and more felsic granitic gneiss as well as other bands of more mafic (ex-amphibolite?) material (originally dykes?). Several generations of pegmatites, including some that are folded, as well as minor aplites.
Chemical group:	High-Ca group, Mainland association, Coolangatta clan
Pluton No:	223703
UWA mounts:	99-28A (zircon) and 99-24C (titanite)

Description of zircons

The zircon population in this sample consists of one morphologic type of subhedral to anhedral grains, with most grains being 60-120 μm long, with a range of aspect ratios from ~2-3:1 for the majority to ~5:1. Some grains are distinctly corroded. In their internal morphology, grains range from continuous euhedral internal zoning from core to rim to partially recrystallised. There is a gradation between these two end members with progressive recrystallisation overprinting the euhedral zoning, particularly in the more strongly zoned rims areas. Inclusions are rare. The grains range from pale brown to dark brown in colour. Strong euhedral zoning observed towards the rims of some grains in both optical and SEM images suggest high U-Th-contents and radiation damage. Some grains have more homogeneous core regions but there is no break in the euhedral growth from core to rim and they are not considered to be xenocrysts. There appears to be no difference in the age of euhedrally zoned and recrystallised areas of grains, suggesting that recrystallisation was due to magmatism. The corroded nature of the grains suggest they may be xenocrysts in their host rock.

Description of titanites

The titanites from this sample are all 40-200 μm fragments of larger grains. Only rarely do grains show growth surfaces; most surfaces are fractures. The grains are pale brown to darker brown in colour. Rare parts of grains are almost black and have evenly distributed dense and very fine inclusion populations. Areas of SHRIMP analysis were in clean parts of the grains, avoiding inclusions and fractures.

Results and interpretation

Zircon

Nineteen analyses on 19 grains are presented in Table z9996 9093B and shown on a concordia diagram in Figure z9996 9093B. The analyses show some scatter and discordance, but less than expected for U abundance ranging ~300 ppm – ~1400 ppm; the common-Pb corrections are generally quite minor. Omitting four data that are >5% discordant and six statistical (younger) outliers leaves a coherent group of nine points which gives an age of ~3007 ± 3 Ma, with $\chi^2 = 0.96$. The scattered Pb-loss trend suggests both Archaean and Recent radiogenic Pb loss.

Titanite

Twenty three analyses were obtained from 23 fragments. The U abundances are mostly in the range 100 ppm–100 ppm and the common Pb corrections are all small (4f206 <1.0%). The apparent discordance of all data is attributed to the use of a NO_2^- primary ion beam, and the tight data clustering is taken as confirmation that the samples are concordant. Two data points which are significantly more discordant have been omitted from the age calculation. The remaining 21 analyses form a single age population with $\chi^2 = 0.85$. The corresponding age is 2632 ± 6 Ma.

Considered together, the zircon and titanite data (Figure c9996 9093B) imply a magmatic age of 3007 ± 3 Ma for the protolith of the gneiss, and a major metamorphic event, probably the gneiss-forming event, at 2632 ± 6 Ma.

Table z9996 9093B: SHRIMP zircon data for the granodiorite gneiss, Coolangatta (UWA mount 99-28A).

grain-spot	U (ppm)	Th (ppm)	4f206 (%)	$^{207}Pb^*/^{206}Pb^*$	$^{208}Pb^*/^{206}Pb^*$	$^{206}Pb^*/^{238}U$	$^{207}Pb^*/^{235}U$	$^{208}Pb^*/^{232}Th$	conc. (%)	$^{207}Pb/^{206}Pb$ age (Ma)
Main group.										
39-1	450	182	0.036	0.2238 ± 5	0.1078 ± 6	0.5867	18.103	0.1562	99	3008 ± 4
47-1	447	180	0.085	0.2239 ± 5	0.1112 ± 6	0.5958	18.390	0.1645	100	3009 ± 4
55-1	425	164	0.000	0.2234 ± 5	0.1025 ± 5	0.5902	18.181	0.1566	99	3006 ± 4
38-1	272	84	0.041	0.2239 ± 7	0.0795 ± 8	0.5869	18.117	0.1511	99	3009 ± 5
57-1	363	169	0.001	0.2230 ± 5	0.1216 ± 6	0.5948	18.288	0.1558	100	3002 ± 4
58-1	424	196	0.091	0.2232 ± 7	0.1201 ± 8	0.5807	17.868	0.1507	98	3004 ± 5
51-1	527	161	0.018	0.2236 ± 5	0.0812 ± 5	0.5771	17.793	0.1539	98	3007 ± 3
49-1	654	155	0.054	0.2232 ± 4	0.0640 ± 4	0.5973	18.379	0.1610	100	3004 ± 3
41-1	669	286	0.026	0.2233 ± 4	0.1095 ± 4	0.5857	18.032	0.1497	99	3005 ± 3
>5% discordant or Pb/Th discordant.										
48-1	1419	642	0.026	0.2028 ± 3	0.1210 ± 4	0.4826	13.495	0.1292	89	2849 ± 2
52-1	454	204	0.018	0.2248 ± 5	0.0797 ± 5	0.5874	18.208	0.1043	99	3016 ± 4
53-1	370	291	0.070	0.2209 ± 6	0.1278 ± 8	0.5851	17.819	0.0950	99	2987 ± 5
Young outliers.										
33-1	1391	737	0.011	0.2172 ± 3	0.1401 ± 4	0.5577	16.702	0.1474	97	2960 ± 2
54-1	287	85	0.175	0.2191 ± 7	0.0771 ± 9	0.5497	16.607	0.1424	95	2974 ± 5
46-1	1100	344	0.010	0.2140 ± 3	0.0827 ± 3	0.5386	15.892	0.1426	95	2936 ± 2
56-1	491	220	0.112	0.2211 ± 5	0.1257 ± 7	0.5860	17.863	0.1646	99	2989 ± 4
59-1	581	162	0.278	0.2210 ± 5	0.0964 ± 7	0.5616	17.115	0.1939	96	2988 ± 4
60-1	639	114	0.105	0.2209 ± 5	0.0416 ± 5	0.5760	17.545	0.1338	98	2987 ± 3
61-1	936	327	0.021	0.2218 ± 4	0.0900 ± 4	0.5849	17.888	0.1508	99	2994 ± 3

Data 17/08/99.
U/Pb scatter (1σ) for cz3 standard = 1.41% (n = 15).

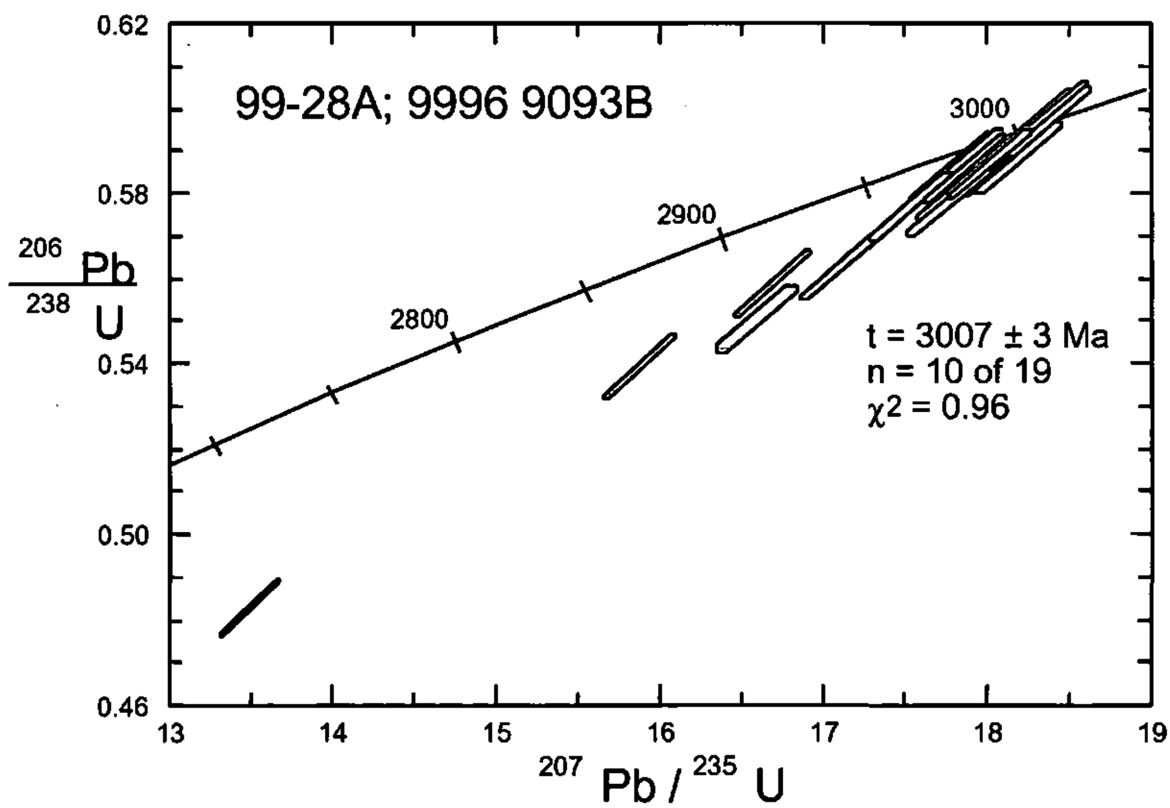

Figure z9996 9093B: Concordia plot of SHRIMP zircon data for the granodiorite gneiss, Coolangatta (UWA mount 99-28A).

Table t9996 9093B: SHRIMP titanite data for the granodiorite gneiss, Coolangatta (UWA mount 99-24C).

grain-spot	U (ppm)	Th# (ppm)	4f206 (%)	$^{207}Pb^*/^{206}Pb^*$	$^{208}Pb^*/^{206}Pb^*$	$^{206}Pb^*/^{238}U$	$^{207}Pb^*/^{235}U$	#	conc. (%)	$^{207}Pb/^{206}Pb$ age (Ma)
Main group.										
1-1	212	98	0.442	0.1770 ± 11	0.1641 ± 20	0.4703	11.474		95	2625 ± 10
10-1	128	36	0.391	0.1775 ± 14	0.0936 ± 25	0.4274	10.460		87	2630 ± 13
11-1	104	107	0.556	0.1780 ± 16	0.3192 ± 34	0.4597	11.283		93	2634 ± 15
12-1	129	53	0.345	0.1790 ± 12	0.1291 ± 22	0.4568	11.272		92	2643 ± 12
13-1	138	18	0.470	0.1752 ± 13	0.0365 ± 21	0.4668	11.276		95	2608 ± 12
14-1	168	86	0.239	0.1792 ± 10	0.1555 ± 18	0.4588	11.335		92	2645 ± 9
15-1	149	79	0.251	0.1776 ± 12	0.1592 ± 22	0.4365	10.691		89	2631 ± 11
16-1	125	50	0.333	0.1791 ± 13	0.1207 ± 23	0.4250	10.496		86	2645 ± 12
17-1	160	74	0.344	0.1787 ± 11	0.1390 ± 20	0.4698	11.576		94	2641 ± 10
18-1	151	75	0.940	0.1769 ± 17	0.1539 ± 33	0.4541	11.077		92	2624 ± 16
2-1	88	17	0.666	0.1799 ± 21	0.0598 ± 37	0.4451	11.044		89	2652 ± 19
20-1	199	54	0.376	0.1755 ± 11	0.0824 ± 18	0.4655	11.263		94	2611 ± 10
21-1	140	52	0.217	0.1774 ± 13	0.1110 ± 22	0.4385	10.725		89	2629 ± 12
23-1	117	37	0.507	0.1778 ± 15	0.0987 ± 27	0.4437	10.875		90	2632 ± 14
3-1	82	40	0.514	0.1778 ± 19	0.1480 ± 36	0.4616	11.316		93	2633 ± 17
4-1	107	72	0.598	0.1792 ± 17	0.2039 ± 33	0.4598	11.361		92	2645 ± 15
5-1	163	30	0.274	0.1777 ± 11	0.0572 ± 16	0.4451	10.905		90	2631 ± 10
6-1	123	29	0.413	0.1789 ± 13	0.0689 ± 22	0.4661	11.499		93	2643 ± 12
7-1	156	47	0.321	0.1777 ± 11	0.0889 ± 18	0.4590	11.248		93	2632 ± 10
8-1	174	37	0.306	0.1771 ± 11	0.0654 ± 17	0.4494	10.974		91	2626 ± 10
9-1	102	21	0.411	0.1789 ± 15	0.0625 ± 26	0.4576	11.289		92	2643 ± 14
Most discordant#.										
19-1	94	51	0.612	0.1763 ± 18	0.1645 ± 34	0.3958	9.619		82	2618 ± 17
22-1	87	111	0.489	0.1771 ± 18	0.3987 ± 42	0.3976	9.707		82	2625 ± 17

Data 11/12/99.
U/Pb scatter (1σ) for Khan standard = 1.36% (n = 13).
Common-Pb corrected using Cumming & Richards (1975) Model III @ 2620 Ma.
\# Analysed using NO_2^- primary ion beam.
Pb/U calibration might be slightly disturbed.
Th/U calibration is not reliable; Th abundances are indicative only, and Pb/Th are not reported.

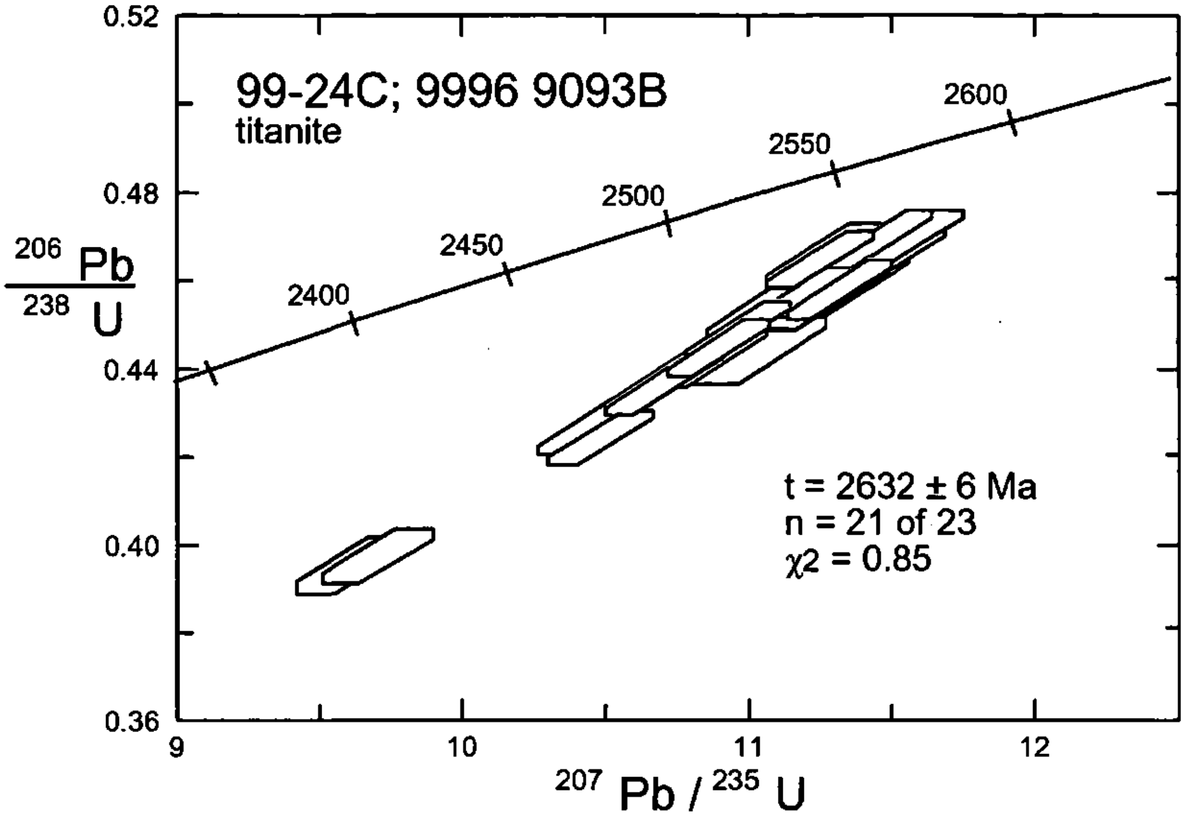

Figure t9996 9093B: Concordia plot of SHRIMP titanite data for the granodiorite gneiss, Coolangatta (UWA mount 99-24C).

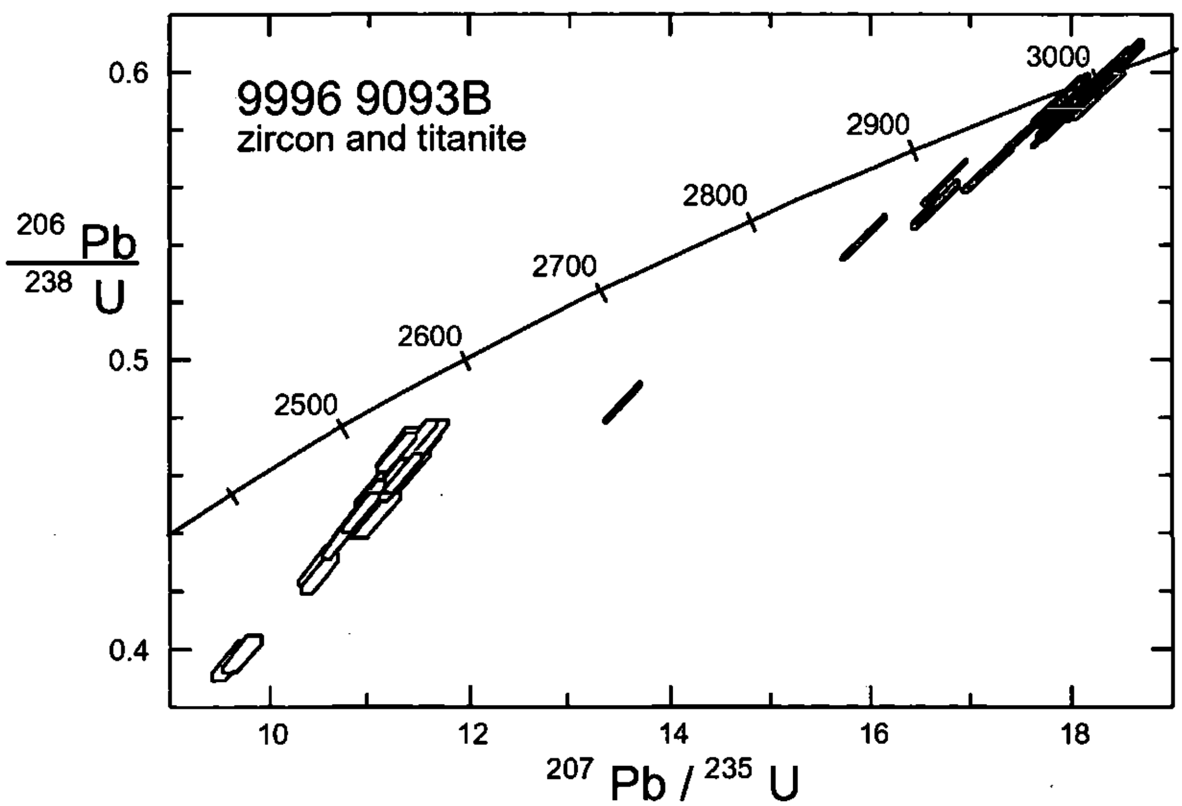

Figure c9996 9093B: Concordia plot of zircon (dark shaded) and titanite SHRIMP data for the granodiorite gneiss, Coolangatta. Note that the discordance of the titanite data is considered to be an artefact of the SHRIMP operating condition on the day of analysis)

9996 9096: hornblende-biotite granodiorite, Wubin

1:250,000 sheet:	Moora (SH5010)
AMG:	468868.0 mE, 6674858.0 mN
Location:	Hammered from a large pushed-up slab on north side of road
Province:	Murchison
Description:	Moderately quartz-feldspar porphyritic medium-grained hornblende-biotite granodiorite.
Chemical group:	Low-Ca group, Goolthan association, Wubin clan
Pluton No:	223701
UWA mount:	99-34C

Description of zircons

The zircon population in this sample consists of one morphologic type of subhedral to anhedral grains, with most grains being 60-120 µm long, with a range of aspect ratios from ~2-3:1 for the majority to ~5:1. Some grains are distinctly corroded. In their internal morphology, grains range from continuous euhedral internal zoning from core to rim to structureless. There is a gradation between these two end members with progressive recrystallisation overprinting the euhedral zoning. Inclusions are relatively common and consist of opaque or rod-like to equant minerals. All inclusions occur throughout the grains and show no preference for core or rim regions. The grains range from very pale brown to dark brown in colour. Strong euhedral zoning observed towards the rims of some grains in both optical and SEM images suggest high U-Th-contents and radiation damage. Some grains have more homogeneous core regions but there is no break in the euhedral growth from core to rim and they are not considered to be xenocrysts. There appears to be no difference in the age of euhedrally zoned and recrystallised areas of grains, suggesting that recrystallisation was due to magmatism.

Results and interpretation

Nineteen analyses on 19 grains are presented in Table z9996 9096 and shown on a concordia diagram in Figure z9996 9096. Omitting two (reversely) discordant analyses, the population comprising the remaining 17 concordant analyses has a χ^2 of 0.90. This is interpreted as a single age population at 2639 ± 6 Ma. This age is taken to be the emplacement age of the granitoid.

Table z9996 9096: SHRIMP zircon data for the hornblende-biotite granodiorite, Wubin (UWA mount 99-34C).

grain-spot	U (ppm)	Th (ppm)	4f206 (%)	$^{207}Pb^*/^{206}Pb^*$	$^{208}Pb^*/^{206}Pb^*$	$^{206}Pb^*/^{238}U$	$^{207}Pb^*/^{235}U$	$^{208}Pb^*/^{232}Th$	conc. (%)	$^{207}Pb/^{206}Pb$ age (Ma)
Main group.										
61-1	121	160	0.271	0.1796 ± 13	0.3635 ± 31	0.5062	12.536	0.1393	100	2649 ± 12
62-1	92	87	0.171	0.1774 ± 16	0.2533 ± 33	0.5107	12.488	0.1376	101	2628 ± 15
64-1	69	121	0.374	0.1786 ± 20	0.4857 ± 50	0.4914	12.101	0.1358	98	2640 ± 18
63-1	113	201	0.335	0.1766 ± 13	0.4983 ± 36	0.4986	12.141	0.1394	99	2621 ± 13
60-1	84	106	0.272	0.1763 ± 17	0.3279 ± 38	0.5044	12.264	0.1320	101	2619 ± 16
67-1	209	238	0.213	0.1801 ± 10	0.2974 ± 20	0.5128	12.732	0.1339	101	2654 ± 9
80a-1	79	133	0.485	0.1776 ± 19	0.4553 ± 46	0.5108	12.505	0.1384	101	2630 ± 17
80b-1	49	86	0.506	0.1785 ± 26	0.4794 ± 65	0.4858	11.957	0.1330	97	2639 ± 24
79-1	228	128	0.206	0.1775 ± 9	0.1527 ± 16	0.5013	12.269	0.1359	100	2630 ± 8
59-1	88	193	0.124	0.1781 ± 15	0.5834 ± 43	0.5095	12.509	0.1350	101	2635 ± 14
78-1	76	110	0.459	0.1797 ± 21	0.3988 ± 49	0.4955	12.278	0.1360	98	2650 ± 19
77-1	250	97	0.053	0.1787 ± 8	0.1037 ± 12	0.5073	12.502	0.1351	100	2641 ± 7
83-1	60	65	0.358	0.1802 ± 21	0.2896 ± 45	0.5161	12.824	0.1378	101	2655 ± 19
85-1	61	53	0.004	0.1790 ± 19	0.2430 ± 38	0.5219	12.880	0.1450	102	2644 ± 17
87-1	389	115	0.100	0.1789 ± 6	0.0809 ± 8	0.5106	12.596	0.1401	101	2643 ± 6
90-1	66	110	0.922	0.1734 ± 24	0.4591 ± 59	0.5132	12.271	0.1398	103	2591 ± 23
58-1	49	57	0.436	0.1777 ± 30	0.3138 ± 66	0.4919	12.052	0.1329	98	2631 ± 28
>5% discordant.										
81-1	37	58	0.656	0.1769 ± 36	0.4320 ± 86	0.5435	13.257	0.1483	107	2624 ± 34
84-1	51	82	0.331	0.1782 ± 26	0.4183 ± 63	0.5418	13.316	0.1409	106	2637 ± 25

Data 27/09/99.
U/Pb scatter (1σ) for cz3 standard = 2.36% (n = 9).

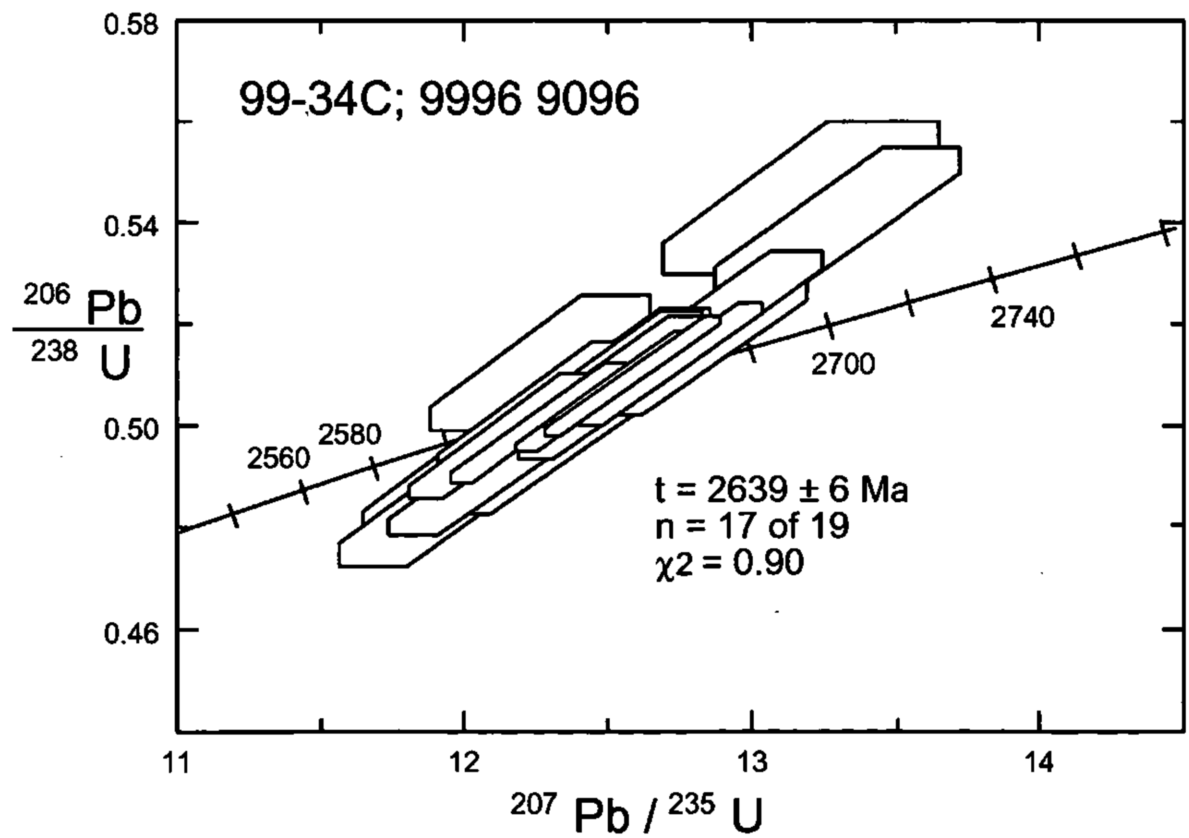

Figure z9996 9096: Concordia plot showing all SHRIMP zircon data for the hornblende-biotite granodiorite, Wubin (UWA mount 99-34C).

9996 9142: biotite-hornblende quartz monzonite, Triangle

1:250,000 sheet:	Yalgoo (SH5002)
AMG:	436576.6 mE, 6830651.4 mN
Location:	Triangle quartz-monzonite on the north-west margin of the Gullewa greenstone belt; hammered from good bouldery outcrop south of Barnong homestead.
Province:	Murchison
Description:	Moderately to strongly feldspar porphyritic medium-grained titanite-biotite-hornblende quartz monzonite. Granitoid contains relatively common mafic enclaves both of cognate and accidental (greenstone) origin, mafic clots from <1 cm and epidote-quartz-filled fractures.
Chemical group:	Mafic group, Gem of Cue association, Britania clan
Pluton No:	214006
UWA mount:	A-14D

Description of zircons

The zircon population in this sample consists of one morphologic type of zoned euhedral grains, with most grains being 60-120 μm long, with restricted aspect ratios from ~1-2:1. Grains are typically euhedral in external morphology with continuous euhedral internal zoning from core to rim. Inclusions are rare. The grains range from pale brown to mauve to dark brown in colour. Many grains have more homogeneous core regions but there is no break in the euhedral growth from core to rim and they are not considered to be xenocrysts. Few grains have fracture networks typical of high-U grains, which have significant metamictisation. Data collection avoided fractures, and included both core and rim regions.

Results and interpretation

Twenty three analyses on 23 grains are presented in Table z9996 9142 and shown on a concordia diagram in Figure z9996 9142. The data are almost all concordant and have low common-Pb contamination. Omitting two analysis that are >5% discordant and one statistical outlier leaves a population comprising 20 analyses which has a χ^2 of 0.65. The corresponding age is 2747 ± 3 Ma; this is interpreted as the emplacement age of the granitoid.

Table z9996 9142: SHRIMP zircon data for the biotite-hornblende quartz monzonite, Triangle (UWA mount A-14D).

grain-spot	U (ppm)	Th (ppm)	4f206 (%)	$^{207}Pb^*/^{206}Pb^*$	$^{208}Pb^*/^{206}Pb^*$	$^{206}Pb^*/^{238}U$	$^{207}Pb^*/^{235}U$	$^{208}Pb^*/^{232}Th$	conc. (%)	$^{207}Pb/^{206}Pb$ age (Ma)
1-1	164	181	0.325	0.1906 ± 9	0.2533 ± 18	0.5397	14.181	0.1238	101	2747 ± 8
2-1	259	294	0.322	0.1907 ± 7	0.2968 ± 15	0.5323	13.998	0.1392	100	2748 ± 6
3-1	293	396	0.277	0.1904 ± 6	0.3092 ± 14	0.5299	13.915	0.1213	100	2746 ± 6
5-1	258	292	0.048	0.1900 ± 6	0.2966 ± 12	0.5491	14.381	0.1436	103	2742 ± 5
6-1	289	351	0.144	0.1902 ± 6	0.3140 ± 13	0.5445	14.277	0.1409	102	2744 ± 5
7-1	283	358	0.901	0.1903 ± 9	0.2954 ± 19	0.5167	13.559	0.1205	98	2745 ± 8
8-1	240	272	0.030	0.1909 ± 6	0.3027 ± 12	0.5350	14.082	0.1426	100	2750 ± 5
9-1	217	215	0.028	0.1915 ± 6	0.2599 ± 12	0.5460	14.418	0.1434	102	2755 ± 6
10-1	135	125	0.106	0.1906 ± 8	0.2442 ± 16	0.5421	14.242	0.1427	102	2747 ± 7
11-1	126	105	0.000	0.1911 ± 8	0.2190 ± 13	0.5375	14.164	0.1421	101	2752 ± 7
12-1	287	341	0.075	0.1911 ± 6	0.3001 ± 12	0.5283	13.921	0.1332	99	2752 ± 5
14-1	280	272	0.041	0.1902 ± 6	0.2560 ± 10	0.5460	14.323	0.1437	102	2744 ± 5
15-1	348	401	0.070	0.1907 ± 5	0.3029 ± 11	0.5455	14.341	0.1432	102	2748 ± 5
16-1	154	164	0.022	0.1902 ± 9	0.2804 ± 17	0.5079	13.322	0.1336	96	2744 ± 8
17-1	376	447	0.025	0.1908 ± 5	0.3159 ± 10	0.5412	14.242	0.1438	101	2749 ± 4
18-1	216	259	0.029	0.1917 ± 7	0.3164 ± 14	0.5473	14.464	0.1445	102	2757 ± 6
19-1	326	378	0.043	0.1909 ± 5	0.3086 ± 11	0.5509	14.504	0.1464	103	2750 ± 4
22-1	276	438	0.120	0.1900 ± 6	0.3896 ± 14	0.5438	14.248	0.1335	102	2742 ± 5
23-1	270	295	0.343	0.1897 ± 7	0.2783 ± 14	0.5362	14.024	0.1365	101	2739 ± 6
24-1	203	270	0.381	0.1898 ± 8	0.2777 ± 17	0.5276	13.805	0.1103	100	2740 ± 7
>5% discordant										
13-1	307	591	3.920	0.1834 ± 28	0.2690 ± 63	0.4485	11.341	0.0626	89	2684 ± 25
20-1	157	215	0.000	0.1879 ± 10	0.3578 ± 22	0.4884	12.651	0.1276	94	2724 ± 9
Old outlier										
21-1	164	164	0.031	0.1956 ± 9	0.2654 ± 17	0.5130	13.835	0.1359	96	2790 ± 7

Data 10/04/00.
U/Pb scatter (1σ) for cz3 standard = 2.28% (n = 6 of 7).

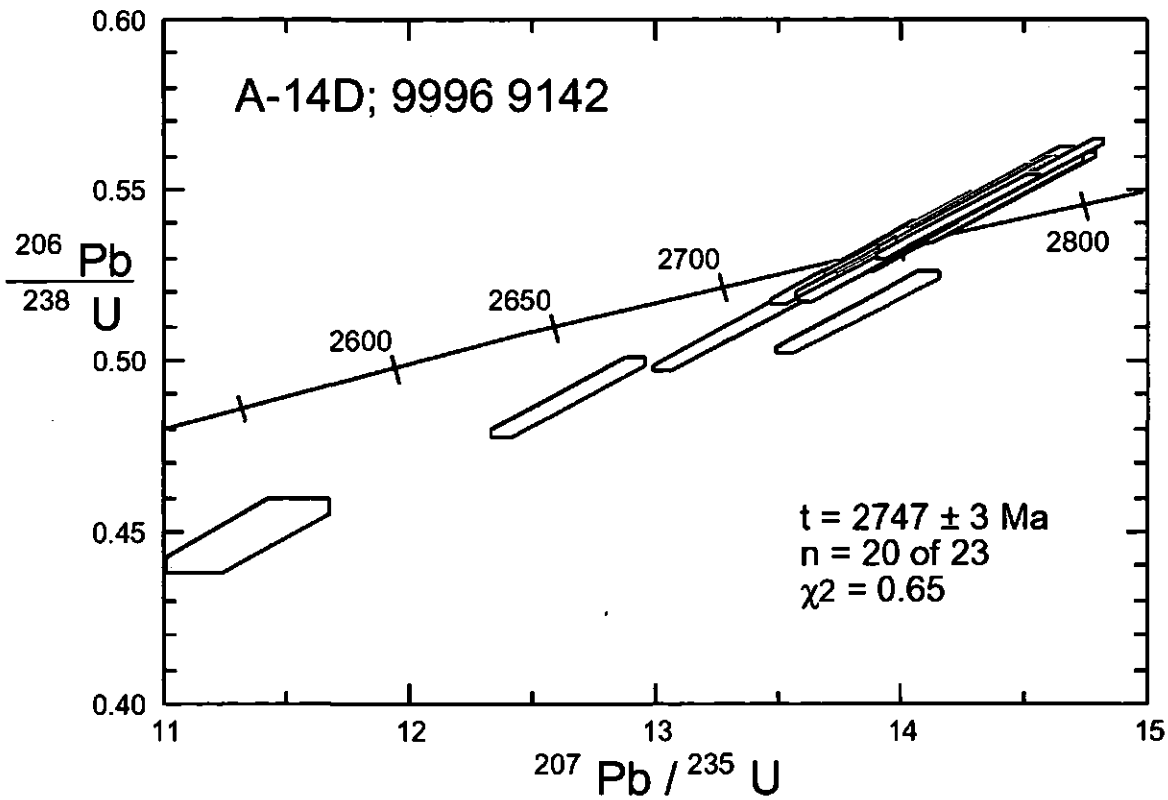

Figure z9996 9142: Concordia plot of SHRIMP zircon data for the biotite-hornblende quartz monzonite, Triangle (UWA mount A-14D).

9996 9164A: foliated biotite granite, Courin Hill Complex

1:250,000 sheet:	Yalgoo (SH5002)
AMG:	443691.6 mE, 6878981.4 mN
Location:	Courin Hill complex, north of fenceline on Gabyon station; blasted and hammered from granitoid pavement.
Province:	Murchison
Description:	The Courin Hill complex forms a 5 by 10 km outcrop along the western margin of the northern arm of the Gullewa greenstone belt. The complex consists of a dominant unit of foliated, variably-feldspar porphyritic biotite monzogranite (9996 9164A). This unit contains common bands of lithologically variable granite, granite dykes and pegmatitic veins. This banding has been folded and cross-cut by later? Pegmatitic dykes, granite dykes and thin shear zones.
Chemical group:	High-Ca group, Mainland association, Eily Eily clan?
Pluton No:	214114
UWA mount:	A-14C

Description of zircons

The zircon population in this sample consists of one morphologic type of zoned euhedral to subhedral grains, with most grains being 40-200 µm long, with a range of aspect ratios from ~2:1 to >5:1. Grains are typically euhedral to subhedral in external morphology with continuous euhedral internal zoning from core to rim. Inclusions are rare. The grains range from pale brown to dark brown to nearly opaque in colour. Strong euhedral zoning observed on both optical and SEM images suggest high U-Th-contents and radiation damage. Discordant alteration patches are common on SEM images, and overgrow the euhedral zoning. Many grains have more homogeneous core regions but there is no break in the euhedral growth from core to rim and they are not considered to be xenocrysts. Many grains have fracture networks typical of high-U grains, which have significant metamictisation. The alteration patches and fractures, and dark grains were avoided during data collection.

Results and interpretation

Eighteen analyses on 18 grains are presented in Table z9996 9164A and shown on a concordia diagram in Figure z9996 9164A. Two analyses are highly discordant, as expected for these high U abundances, but several grains with U>1000 ppm are concordant, and common-Pb corrections are generally low. Omitting four data points that are >5% discordant and four statistical outliers leaves a reasonably coherent group of 10 points which gives an age of 2742 ± 7 Ma, with $\chi^2 = 1.87$. This is interpreted to be the emplacement age of the granitoid.

Table z9996 9164A: SHRIMP zircon data for the foliated biotite granite, Courin Hill (UWA mount A-14C).

grain-spot	U (ppm)	Th (ppm)	4f206 (%)	$^{207}Pb^*/^{206}Pb^*$	$^{208}Pb^*/^{206}Pb^*$	$^{206}Pb^*/^{238}U$	$^{207}Pb^*/^{235}U$	$^{208}Pb^*/^{232}Th$	conc. (%)	$^{207}Pb/^{206}Pb$ age (Ma)
5-1	339	740	0.087	0.1899 ± 10	0.5852 ± 28	0.5293	13.862	0.1418	100	2742 ± 8
6-1	1034	68	0.597	0.1891 ± 7	0.0172 ± 12	0.5204	13.567	0.1359	99	2734 ± 6
7-1	855	120	0.057	0.1909 ± 6	0.0369 ± 5	0.5563	14.646	0.1467	104	2750 ± 5
8-1	1459	1482	0.498	0.1891 ± 6	0.2693 ± 12	0.5075	13.235	0.1346	97	2735 ± 5
11-1	1097	203	0.528	0.1916 ± 7	0.0543 ± 11	0.5094	13.459	0.1494	96	2756 ± 6
12-1	789	811	0.413	0.1910 ± 8	0.2719 ± 15	0.5187	13.661	0.1372	98	2751 ± 7
14-1	756	97	0.115	0.1897 ± 7	0.0339 ± 7	0.5142	13.450	0.1355	98	2740 ± 6
15-1	1103	840	0.216	0.1889 ± 6	0.2038 ± 10	0.5117	13.325	0.1369	97	2732 ± 5
17-1	261	495	0.223	0.1894 ± 12	0.4979 ± 31	0.5367	14.014	0.1412	101	2737 ± 10
18-1	289	324	0.493	0.1889 ± 13	0.3045 ± 29	0.5202	13.547	0.1411	99	2732 ± 12
Discordant										
9-1	771	399	1.113	0.1908 ± 10	0.1482 ± 20	0.4944	13.005	0.1416	94	2749 ± 9
13-1	2222	116	0.014	0.1940 ± 3	0.0136 ± 2	0.5899	15.775	0.1537	108	2776 ± 3
19-1	343	441	2.507	0.1893 ± 21	0.3542 ± 47	0.4916	12.830	0.1357	94	2736 ± 18
22-1	3131	2181	0.398	0.1506 ± 4	0.2059 ± 9	0.3246	6.741	0.0960	77	2353 ± 5
Young outliers										
10-1	267	176	2.495	0.1852 ± 23	0.1733 ± 50	0.4860	12.411	0.1278	95	2700 ± 21
16-1	588	431	0.231	0.1857 ± 8	0.2120 ± 15	0.4987	12.767	0.1444	96	2704 ± 7
20-1	741	372	1.775	0.1865 ± 12	0.0553 ± 25	0.4988	12.828	0.0549	96	2712 ± 11
21-1	2115	851	0.400	0.1748 ± 4	0.1087 ± 7	0.4973	11.987	0.1344	100	2604 ± 4

Data 12/04/00.
U/Pb scatter (1σ) for cz3 standard = 1.62% (n = 10).

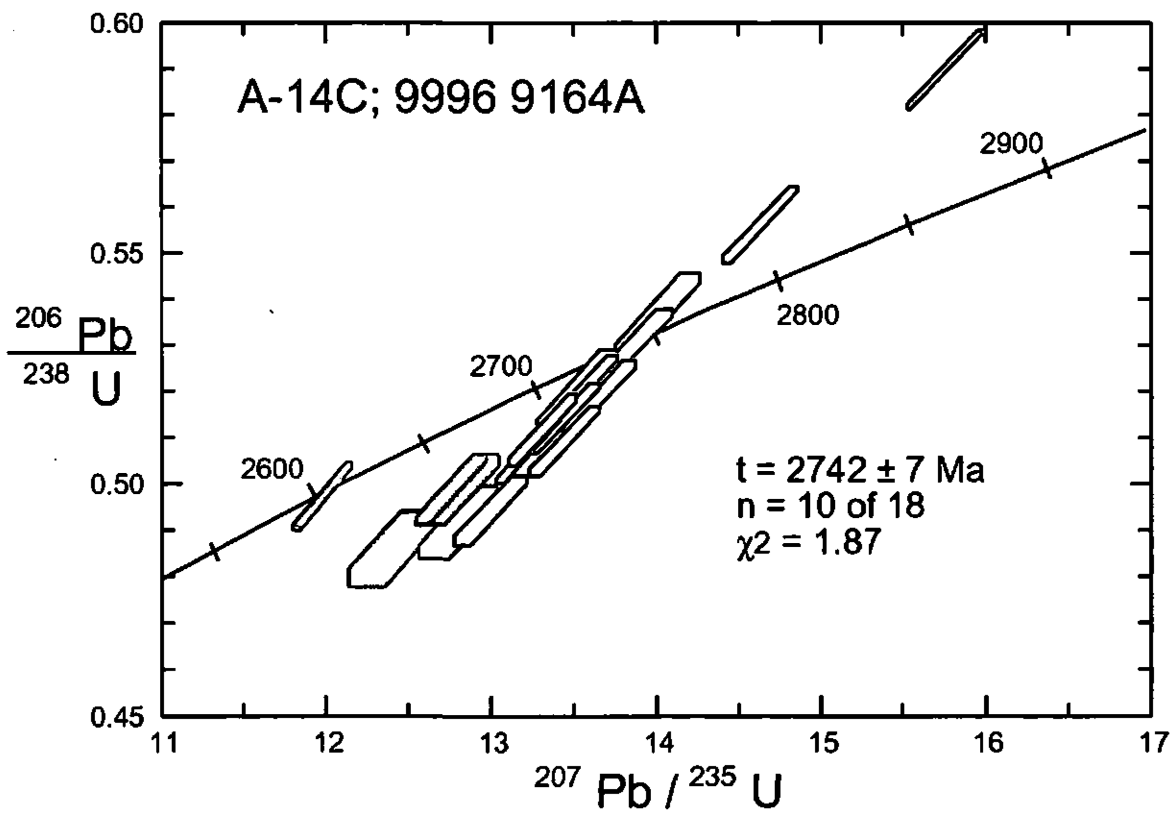

Figure z9996 9164A: Concordia plot showing all SHRIMP zircon data for the foliated biotite granite, Courin Hill (UWA mount A-14C). Note that analysis 22-1 falls below the range of this figure.

Sm-Nd and Pb/Pb isotope geochemistry of Yilgarn granitoids

Ian R. Fletcher and Neal J. McNaughton

Summary

All samples selected for SHRIMP geochronological studies, most of them collected during the 1997ñ1999 field seasons as part of this project, were subjected to Sm-Nd and Pb/Pb isotopic analysis. Several additional samples of known age, or with previously determined Sm-Nd (Champion and Sheraton, 1997) were also analysed.

The Sm-Nd model ages (T_{DM}) of all moderately- to highly fractionated samples ($^{147}Sm/^{144}Nd$ <0.14) have been determined, and SHRIMP ages have been used with the Sm-Nd data to determine initial (magmatic) Nd isotopic compositions for all dated samples. The initial compositions are reported as ε_{Nd}, the deviation in $^{143}Nd/^{144}Nd$ from a chondritic reference value, in parts/10^4. The Pb/Pb data for K-feldspars provide a direct measure of initial Pb isotopic composition for the rocks. Although this may be slightly offset due to minor ingrowth of radiogenic Pb from trace U in the feldspars, a time-integrated U/Pb (traditionally denoted by μ=$^{238}U/^{204}Pb$) for the sources of each sample can still be reliably determined. Together, ε_{Nd} and μ give more powerful 2-dimensional isotopic fingerprints for the petrogenesis of the samples. For completeness, whole-rock Pb/Pb data were also obtained for all samples.

It is important to note that both T_{DM} and μ are model dependent; numerical values have no absolute significance. What can be significant are patterns, coincidences or differences amongst groups of data. Additional details of the models used are given below.

Data

Tables 1 and 2 summarise the SmñNd and Pb/Pb isotopic data, respectively.

Figure 1 shows the T_{DM} differences between the Provinces of the Yilgarn Craton. In general, these data confirm the broad regional differences previously recognised (e.g. Fletcher et al., 1994).

A plot of ε_{Nd} vs μ for all the data from Tables 1 and 2 (Figure 2a), or the Nd data alone, clearly shows there is a fundamental difference in the isotopic nature of the source regions for granitoids in the Murchison and Southern Cross Provinces compared to the Eastern Goldfields Province. Many of the Murchison and Southern Cross granitoids have strongly negative ε_{Nd}, indicative of a long crustal prehistory, whereas the Eastern Goldfields granitoids have more primitive and younger sources, with ε_{Nd} dispersed around zero. The two-element plot enhances some of the distinctions seen in the Nd data.

When the data are coded by chemical grouping (Figure 2b), no strong distinctions are apparent for the entire craton, though there is a partial separation between the high-Ca and low-Ca groups. When the data are considered on a province-by-province basis (Fig. 3a, c, e) this distinction becomes quite clear. It is defined predominantly by differences in ε_{Nd}. This regional comparison can be continued to smaller scales where sufficient data are available: strong distinctions between the sources of granitoids in different parts of the Eastern Goldfields Province have been demonstrated in previous reports. Additional distinctions have also been shown when the sample classification is extended down to 'clan' level.

With points distinguished by granitoid age, the plot for the craton (Fig. 2c) shows that the youngest granitoids (<2645 Ma) have the lowest ε_{Nd}, reflecting the highest degree of incorporation of older crust. However, it is the next age grouping (2645 – 2675 Ma) that has the most primitive overall Nd isotopic signature, not the oldest samples. These distinctions are also seen, to differing extents and with varying confidence due to the numbers of samples, in the province-by-province plots (Figs. 3b, d, f).

Wallaby Pb/Pb isochron

The four Pb/Pb analyses from the Wallaby syenite-carbonatite complex form a highly linear array (MSWD = 1.6) on a Pb/Pb isochron plot (Figure 4), the slope corresponding to an age of 2658 ± 16 Ma. This data array supports the contention that the three rocks have a common source, and the interpretation of the SHRIMP titanite date for 9996 7177B (2657 ± 15 Ma) as their magmatic age.

Table 1: Sm-Nd data.

AGSO Number	Pluton Number	Unit Name	Rock Type	Chemical Grouping	Sm (ppm)	Nd (ppm)	$^{147}Sm/^{144}Nd$	$^{143}Nd/^{144}Nd$	t_{DM} (Ma)	Magmatic age (Ma)	Initial ε_{Nd}
Murchison Province											
97969138	243614	Waddouring	monzogranite	Low-Ca	7.48	44.9	0.1008	0.510816 ± 11	3034	2627 ± 3	-3.40 ± 0.22
99964003#	224112	Goolthan Goolthan	monzogranite	Low-Ca	11.90	79.2	0.0908	0.510507 ± 10	3180	2745 ± 10	-4.55 ± 0.24
99964016C	223916	Mount Mulgine	granite	High-Ca	2.07	13.4	0.0932	0.510700 ± 11	2986	2756 ± 20	-1.34 ± 0.34
99964100	224107	Basin	granite	High-Ca	2.78	19.8	0.0850	0.510578 ± 12	2945	2743 ± 4	-1.12 ± 0.24
99967049A	233501	Goddard nebulitic gneiss	bt granitic gneiss	High-Ca	6.43	33.2	0.1168	0.511122 ± 22	3058	2787 ± 4	-1.17 ± 0.45
99967055	233623	Fox Lair	bt monzogranite	Low-Ca	11.46	76.3	0.0908	0.510626 ± 10	3020	2641 ± 5	-3.54 ± 0.22
99967066	213701	Namban	Kfs-phyric btt granite	Low-Ca	8.46	60.2	0.0849	0.510499 ± 17	3031	2645 ± 5	-3.94 ± 0.34
99967082C	213722	Dookaling xenolith	augen gneiss	High-Ca	5.28	35.8	0.0891	0.510487 ± 13	3154	2940 ± 25	-1.50 ± 0.40
99967114	244301	Telegootherra	granodiorite	Low-Ca	9.67	65.6	0.0890	0.510611 ± 18	2994	2630 ± 50	-3.37 ± 0.69
99967141	234208	Keygo	granodiorite	High-HFSE	5.94	25.4	0.1413	0.511458 ± 30		2745 ± 25	-3.71 ± 0.76
99969049	253621	Coolamen-dyke	hb-bt monzogranite	High-HFSE?	3.26	18.8	0.1047	0.510841 ± 10	3112	2640 ± 5	-4.09 ± 0.22
99969063	223622	Barrambie-dyke	monzogranite	Low-Ca	16.66	85.3	0.1180	0.511103 ± 14	3129	2630 ± 6	-3.58 ± 0.30
99969066	213601	Donga Well	foliated monzogranite	High-Ca	2.10	13.1	0.0967	0.510702 ± 11	3077	2730 ± 75	-2.90 ± 0.98
99969093B	223703	Coolangatta	granodiorite gneiss	High-Ca	1.57	14.1	0.0670	0.510082 ± 15	3093	3007 ± 3	0.14 ± 0.31
99969096	223701	Wubin	hb-bt granodiorite	Low-Ca	13.19	81.0	0.0984	0.510713 ± 10	3110	2639 ± 6	-4.46 ± 0.22
99969142	214006	Triangle	granodiorite	Mafic	8.11	48.4	0.1012	0.510836 ± 15	3017	2747 ± 3	-1.65 ± 0.31
99969164A	214114	Courin Hill	granite	High-Ca	2.81	22.6	0.0750	0.510492 ± 16	2816	2742 ± 7	0.86 ± 0.32
Southern Cross Province											
92964658	294101	Wallaby Knob	monzogranite	Low-Ca	from Champion and Sheraton (1997)						-4.5
96969012	293914	Walling Rock	monzogranite	Low-Ca	8.87	58.7	0.0913	0.510605 ± 15	3060	2633 ± 2	-4.23 ± 0.30
97969023	293713	Turturdine	monzogranite	Low-Ca	3.81	20.6	0.1118	0.511048 ± 10	3015	2640 ± 25	-2.44 ± 0.42
97969034#	303505	Yerdanie	monzogranite	Low-Ca	5.12	43.2	0.0717	0.510436 ± 10	2805	2640 ± 25	-0.72 ± 0.30
97969063#	284001	Bulga Downs	monzogranite	Low-Ca	3.06	23.2	0.0796	0.510399 ± 10	3025	2684 ± 8	-3.46 ± 0.20
97969082A	284006	The Spring	granodiorite	High-Ca	4.73	27.6	0.1038	0.510793 ± 10	3153	2682 ± 5	-4.20 ± 0.22
97969090	283608	Koolyanobbing Quarry	monzogranite	High-Ca	2.65	17.4	0.0922	0.510768 ± 10	2874	2656 ± 25	-1.03 ± 0.37
97969102B	283905	McLeod Rock	granitic gneiss	High-Ca	1.83	13.5	0.0818	0.510539 ± 11	2911	2737 ± 25	-0.73 ± 0.35
97969104	283908	Native Well	monzogranite	High-Ca	2.26	14.1	0.0972	0.510690 ± 11	3105	2682 ± 6	-3.92 ± 0.23
97969125	263504	Warren-2	monzogranite	Low-Ca	4.30	25.9	0.1005	0.510850 ± 11	2978	2617 ± 3	-2.75 ± 0.22
97969126	0	Proterozoic dyke	diorite	Prot. dyke	4.25	15.7	0.1634	0.512624 ± 12	1299	1201 ± 7	4.62 ± 0.28

cont.

Table 1 (cont.)

AGSO Number	Pluton Number	Unit Name	Rock Type	Chemical Grouping	Sm (ppm)	Nd (ppm)	$^{147}Sm/^{144}Nd$	$^{143}Nd/^{144}Nd$	t_{DM} (Ma)	Magmatic age (Ma)	Initial ε_{Nd}
Southern Cross Province (cont.)											
97969201	323203	Tank No. 28	monzogranite	Low-Ca	18.51	117.8	0.0950	0.510710 ± 10	3021	2623 ± 7	-3.57 ± 0.22
97969202	323304	McPherson	monzogranite	High-Ca	1.97	14.4	0.0827	0.510629 ± 10	2824	2656 ± 10	-0.48 ± 0.23
98967100A	293504	Boorabbin	monzogranite	Low-Ca	5.86	39.4	0.0900	0.510632 ± 22	2993	2630 ± 25	-3.30 ± 0.52
98967102E	0	Koolyanobbing xenolith	granodiorite	Mafic?	13.70	49.7	0.1666	0.511978 ± 15		2699 ± 10	-2.70 ± 0.39
98968104	264001	Courlbarloo	tonalite	Mafic	11.52	45.7	0.1524	0.512026 ± 16		2813 ± 5	3.88 ± 0.35
98969019	284301	Bluff Point	monzogranite	Low-Ca	5.16	27.8	0.1122	0.511045 ± 15	3032	2640 ± 50	-2.63 ± 0.79
98969025	274302	Buttercup Bore	granodiorite	Low-Ca	3.51	26.8	0.0792	0.510479 ± 15	2922	2661 ± 7	-2.14 ± 0.31
98969033	274304	Tom Bore	granitic gneiss	High-Ca	2.23	19.6	0.0688	0.510197 ± 15	3010	2671 ± 3	-3.93 ± 0.30
98969042	264305	Barlanga Well	quartz monzonite	Low-Ca	2.24	13.7	0.0985	0.510804 ± 11	2987	2630 ± 50	-2.82 ± 0.68
98969044	264304	Yarrabubba	granite	Low-Ca	2.40	14.9	0.0976	0.510933 ± 18	2789	2650 ± 10	0.28 ± 0.37
98969045	264314	Monty Bore	monzogranite	High-Ca	1.36	7.9	0.1043	0.511043 ± 13	2808	2700 ± 25	0.75 ± 0.43
98969055	274205	Woodley Bluff	monzogranite	High-Ca	0.88	4.9	0.1093	0.510942 ± 14	3100	2712 ± 6	-2.84 ± 0.29
Eastern Goldfields Province											
92969015	323906	Dairy	monzogranite	High-HFSE	from Champion and Sheraton (1997)						1.1
93964145	344012	Hanns Camp	foliated syenite	Syenite	?from Champion and Sheraton (1997)						??
94962258A	304315	Anomaly 45	granodiorite	Mafic	3.65	23.9	0.0924	0.510878 ± 15	2736	2667 ± 3	1.22 ± 0.31
96969044	314327	Kujelan Creek	foliated granite	High-Ca	4.19	26.9	0.0942	0.510949 ± 18	2687	2665 ± 3	1.95 ± 0.37
96969046	324319	Red Bore	foliated granite	Low-Ca	4.42	33.6	0.0794	0.510674 ± 16	2700	2647 ± 3	1.41 ± 0.32
96969076	314102	Kent complex	monzogranite	High-HFSE	8.11	36.5	0.1345	0.511646 ± 21	2719	2686 ± 7	1.92 ± 0.44
96969080A	344105	Durang	foliated granite	High-Ca	3.22	19.6	0.0995	0.510924 ± 17	2847	2671 ± 2	-0.25 ± 0.33
96969087	323901	Redcastle	monzogranite	High-Ca	3.34	22.5	0.0899	0.510836 ± 19	2732	2660 ± 5	1.17 ± 0.38
97967038G#	313726	Golden Cities	granodiorite	Mafic	5.65	34.7	0.0983	0.510985 ± 10	2736	2656 ± 3	1.13 ± 0.20
97967069A	314308	Sundowner dyke	porphryry	Mafic	4.31	26.2	0.0994	0.510999 ± 15	2744	2660 ± 25	1.09 ± 0.44
97967069B	304301	Gemchapps	monzogranite	High-HFSE	2.02	12.6	0.0968	0.510866 ± 13	2857	2680 ± 50	-0.34 ± 0.68
97967150	343401	Yardilla	granodiorite	Syenite	6.20	35.3	0.1062	0.511137 ± 10	2720	2660 ± 25	1.48 ± 0.41
97967152	343401	Yardilla	granodiorite	Syenite	4.43	26.5	0.1010	0.511048 ± 10	2715	2660 ± 25	1.51 ± 0.39
97967153#	333419	Talbot	monzogranite	Low-Ca	4.18	23.4	0.1081	0.511131 ± 10	2781	2630 ± 25	0.34 ± 0.30
97969044	313605	Mungari	monzogranite	Low-Ca	4.47	25.1	0.1076	0.511046 ± 10	2894	2640 ± 25	-1.05 ± 0.41

cont.

Table 1 (cont.)

AGSO Number	Pluton Number	Unit Name	Rock Type	Chemical Grouping	Sm (ppm)	Nd (ppm)	$^{147}Sm/^{144}Nd$	$^{143}Nd/^{144}Nd$	t_{DM} (Ma)	Magmatic age (Ma)	Initial ε_{Nd}
Eastern Goldfields Province(cont.)											
97969209	323308	Dundas	monzogranite	Low-Ca	6.91	31.8	0.1314	0.511460 ± 10	2973	2620 ± 25	-1.22 ± 0.48
97969212	323303	Lake Kirk	granitic gneiss	High-Ca	2.74	14.4	0.1153	0.511226 ± 10	2839	2685 ± 25	0.35 ± 0.43
97969223	333301	Buldania	granodiorite	High-Ca	2.71	17.6	0.0930	0.510857 ± 12	2776	2660 ± 9	0.53 ± 0.27
97969237	323310	Boojerbeenyer	monzogranite	Low-Ca	4.85	27.2	0.1079	0.511079 ± 10	2854	2625 ± 25	-0.69 ± 0.41
97969243	323311	Buldania -2	granodiorite	High-Ca	7.55	51.1	0.0893	0.510804 ± 10	2759	2655 ± 6	0.67 ± 0.22
97969245	333414	Tramways South	monzogranite	Low-Ca	4.46	28.2	0.0958	0.510906 ± 10	2781	2640 ± 25	0.23 ± 0.38
97969248	333415	Toil and Trouble	monzogranite	High-Ca	3.89	22.8	0.1031	0.511067 ± 10	2741	2650 ± 9	1.04 ± 0.24
97969249	333409	Sinclair	monzogranite	High-Ca	2.85	18.9	0.0910	0.510984 ± 10	2570	2655 ± 10	3.62 ± 0.24
97969256B	333413	End of Day xenolith	granodiorite	Mafic	12.45	83.2	0.0904	0.510841 ± 10	2738	2650 ± 25	0.95 ± 0.36
98967008	343613	Erayinia Complex	granodiorite	Syenite	7.70	49.2	0.0946	0.510912 ± 18	2743	2660 ± 5	1.05 ± 0.36
98969003	343501	Fitzgerald Lagoon	granodiorite	High-Ca	1.87	11.8	0.0956	0.510884 ± 11	2804	2659 ± 11	0.13 ± 0.27
99967170A	314126	Bullshead	diorite	High-HFSE	8.32	34.8	0.1445	0.511821 ± 18		2680 ± 50	1.83 ± 1.02
99967174A	334023	Wallaby syenite	syenite	syenite	19.86	138.0	0.0870	0.510825 ± 19	2681	2657 ± 25	1.91 ± 0.47
99967176	334023	Wallaby syenite	carbonatite	syenite	85.18	574.3	0.0896	0.510838 ± 19	2724	2657 ± 25	1.24 ± 0.48
99967177B	334023	Wallaby syenite	carbonatitic syenite	syenite	requires reprocessing (chemistry)					2657 ± 15	
La Jolla Nd standard (n = 37)								0.511878 ± 2 ($2\sigma_m$)			
Caltech Ndβ, from spike calibration checks (n = 4)								0.511920 ± 4 ($2\sigma_m$)			

Data from W. Oliver, BSc(Hons) 1999.
Nd data normalised to $^{146}Nd/^{144}Nd = 0.7219$.
Sm and Nd abundances are ±~5%, due to weighing and spike evaporation limitations.
$^{147}Sm/^{144}Nd$ is assigned an overall uncertainty of 0.2%, including spike calibration, data precision and calculation.
Uncertainties in $^{143}Nd/^{144}Nd$ refer to the last digits listed and are the larger of internal precision (95% c.l.) or 0.000010, an approximate 2σ reproducibility from standards.
t_{DM}, an estimate of mantle derivation age, is calculated from the progressively-depleting mantle model of DePaolo (1981). Considered unreliable for $^{147}Sm/^{144}Nd > 0.14$.
Magmatic ages with uncertainties <25†Ma are directly measured (this project or other sources); others are estimated from structural relationships or other associations.
For notes on ε_{Nd} see main text.

Table 2: Pb isotopic data for K-feldspars and whole-rocks.

AGSO Number	Pluton Number	Unit Name	Rock Type	Chemical Grouping	K-feldspar $^{206}Pb/^{204}Pb$	K-feldspar $^{207}Pb/^{204}Pb$	K-feldspar $^{208}Pb/^{204}Pb$	Whole-rock $^{206}Pb/^{204}Pb$	Whole-rock $^{207}Pb/^{204}Pb$	Whole-rock $^{208}Pb/^{204}Pb$
Murchison Province										
97969138	243614	Waddouring	monzogranite	Low-Ca	13.909	14.915	33.725	27.371	17.323	43.807
99964003#	224112	Goolthan Goolthan	monzogranite	Low-Ca	not analysed			21.899	16.302	38.910
99964016C	223916	Mount Mulgine	granite	High-Ca	13.589	14.707	33.188	18.975	15.736	36.981
99964100	224107	Basin	granite	High-Ca	14.693	14.922	34.009	17.051	15.362	36.409
99967049A	233501	Goddard nebulitic gneiss	bt granitic gneiss	High-Ca	13.777	14.878	33.749	15.137	15.141	41.421
99967055	233623	Fox Lair	bt monzogranite	Low-Ca	14.500	15.070	35.115	23.409	16.573	56.682
99967066	213701	Namban	Kfs-phyric btt granite	Low-Ca	13.682	14.802	33.587	16.660	15.348	40.394
99967082C	213722	Dookaling xenolith	augen gneiss	High-Ca	14.218	15.006	34.111	22.033	16.424	42.729
99967114	244301	Telegootherra	granodiorite	Low-Ca	13.397	15.037	34.361	19.246	15.807	43.903
99967141	234208	Keygo	granodiorite	High-HFSE	no K-feldspar			74.124	26.402	88.736
99969049	253621	Coolamen-dyke	hb-bt monzogranite	High-HFSE?	13.910	14.891	33.844	15.751	15.203	35.833
99969063	223622	Barrambie-dyke	monzogranite	Low-Ca	14.529	15.003	35.746	26.085	17.051	67.475
99969066	213601	Donga Well	foliated monzogranite	High-Ca	13.869	14.835	33.933	14.740	15.001	35.471
99969093B	223703	Coolangatta	granodiorite gneiss	High-Ca	no K-feldspar			19.425	16.120	49.340
99969096	223701	Wubin	hb-bt granodiorite	Low-Ca	13.676	14.833	33.589	14.743	15.018	37.020
99969142	214006	Triangle	granodiorite	Mafic	14.344	14.924	34.248	19.460	15.818	39.800
99969164A	214114	Courin Hill	granite	High-Ca	14.771	15.060	34.209	17.369	15.439	39.207
Southern Cross Province										
92964658	294101	Wallaby Knob	monzogranite	Low-Ca	13.954	14.999	34.090	Whole-rock sample unavailable		
96969012	293914	Walling Rock	monzogranite	Low-Ca	14.111	14.991	34.229	20.439	16.108	44.084
97969023	293713	Turturdine	monzogranite	Low-Ca	14.951	15.122	34.343	25.010	16.882	40.574
97969034	303505	Yerdanie	monzogranite	Low-Ca	14.822	15.151	34.858	26.303	17.265	49.160
97969063	284001	Bulga Downs	monzogranite	Low-Ca	14.735	15.083	34.736	18.591	15.793	39.224
97969082A	284006	The Spring	granodiorite	High-Ca	13.796	14.955	33.786	18.279	15.753	40.957
97969090	283608	Koolyanobbing Quarry	monzogranite	High-Ca?	13.792	14.865	33.554	21.116	16.192	38.977
97969102B	283905	McLeod Rock	granitic gneiss	High-Ca	13.612	14.828	33.534	15.642	15.203	38.266
97969104	283908	Native Well	monzogranite	High-Ca	14.220	14.965	34.256	17.939	15.674	38.948
97969125	263504	Warren-2	monzogranite	Low-Ca	16.040	15.381	35.195	21.285	16.174	39.483
97969126	0	Proterozoic dyke	diorite	Prot. dyke	no K-feldspar			22.306	16.145	42.685

cont.

Table 2 (cont.)

AGSO Number	Pluton Number	Unit Name	Rock Type	Chemical Grouping	K-feldspar $^{206}Pb/^{204}Pb$	K-feldspar $^{207}Pb/^{204}Pb$	K-feldspar $^{208}Pb/^{204}Pb$	Whole-rock $^{206}Pb/^{204}Pb$	Whole-rock $^{207}Pb/^{204}Pb$	Whole-rock $^{208}Pb/^{204}Pb$
Southern Cross Province (cont.)										
97969201	323203	Tank No. 28	monzogranite	Low-Ca	13.992	14.982	33.826	18.748	15.808	39.383
97969202	323304	McPherson	monzogranite	High-Ca	14.041	15.060	33.779	15.262	15.254	35.444
98967100A	293504	Boorabbin	monzogranite	Low-Ca	failed mass spectrometry			16.628	15.464	43.360
98967102E	0	Koolyanobbing xenolith	granodiorite	Mafic?	no K-feldspar			21.204	16.210	43.534
98968104	264001	Courlbarloo	tonalite	Mafic?	not enough K-feldspar			54.186	22.585	78.697
98969019	284301	Bluff Point	monzogranite	Low-Ca	14.476	15.047	34.493	18.628	15.823	42.182
98969025	274302	Buttercup Bore	granodiorite	Low-Ca	14.349	15.133	34.696	18.792	15.868	39.131
98969033	274304	Tom Bore	granitic gneiss	High-Ca	13.899	15.017	34.053	14.771	15.174	41.618
98969042	264305	Barlanga Well	quartz monzonite	Low-Ca	K-feldspar heavily altered			125.887	26.330	116.630
98969044	264304	Yarrabubba	granite	Low-Ca	14.285	14.928	33.956	17.526	15.296	37.422
98969045	264314	Monty Bore	monzogranite	High-Ca	14.368	14.954	33.811	20.274	15.972	36.303
98969055	274205	Woodley Bluff	monzogranite	High-Ca	13.829	14.918	33.550	17.472	15.620	36.691
Eastern Goldfields Province										
92969015	323906	Dairy	monzogranite	High-HFSE	14.382	14.883	34.244	Whole-rocksample unavailable		
93964145	344012	Hanns Camp	foliated syenite	Syenite	14.012	14.924	33.750	Whole-rock sample unavailable		
94962258A	304315	Anomaly 45	granodiorite	Mafic	no K-feldspar			21.868	16.247	43.002
96969044	314327	Kujelan Creek	foliated granite	High-Ca	13.677	14.718	33.395	20.840	16.014	39.132
96969046	324319	Red Bore	foliated granite	Low-Ca	13.852	14.764	33.743	21.543	16.149	46.471
96969076	314102	Kent complex	monzogranite	High-HFSE	14.221	14.717	33.956	25.444	16.784	46.796
96969080A	344105	Durang	foliated granite	High-Ca	14.121	14.994	34.249	16.317	15.332	44.601
96969087	323901	Redcastle	monzogranite	High-Ca	13.663	14.716	33.411	17.089	15.331	36.094
97967038G	313726	Golden Cities	granodiorite	Mafic	13.665	14.780	33.450	16.745	15.322	37.044
97967069A	314308	Sundowner dyke	porphryry	Mafic	no K-feldspar			16.689	15.378	36.562
97967069B	304301	Gemchapps	monzogranite	High-HFSE	14.200	14.997	33.758	20.605	16.236	39.542
97967150	343401	Yardilla	granodiorite	Syenite	13.857	14.814	33.869	15.294	15.059	36.331
97967152	343401	Yardilla	granodiorite	Syenite	13.716	14.757	33.462	16.650	15.286	36.250
97967153	333419	Talbot	monzogranite	Low-Ca	13.941	14.852	33.743	21.715	16.225	39.356
97969044	313605	Mungari	monzogranite	Low-Ca	15.292	15.113	34.483	23.885	16.604	40.642

cont.

Table 2 (cont.)

AGSO Number	Pluton Number	Unit Name	Rock Type	Chemical Grouping	K-feldspar $^{206}Pb/^{204}Pb$	K-feldspar $^{207}Pb/^{204}Pb$	K-feldspar $^{208}Pb/^{204}Pb$	Whole-rock $^{206}Pb/^{204}Pb$	Whole-rock $^{207}Pb/^{204}Pb$	Whole-rock $^{208}Pb/^{204}Pb$
Eastern Goldfields Province (cont.)										
97969209	323308	Dundas	monzo granite	Low-Ca	14.447	15.164	33.831	31.462	18.174	39.424
97969212	323303	Lake Kirk	granitic gneiss	High-Ca	14.346	15.113	33.830	21.446	16.368	39.130
97969223	333301	Buldania	granodiorite	High-Ca	13.399	15.000	33.663	failed mass spectrometry		
97969237	323310	Boojerbeenyer	monzogranite	Low-Ca	14.651	15.120	33.897	30.158	17.893	42.302
97969243	323311	Buldania -2	granodiorite	High-Ca	14.008	15.006	33.674	18.363	15.766	38.675
97969245	333414	Tramways South	monzogranite	Low-Ca	13.896	14.847	33.777	18.289	15.591	40.016
97969248	333415	Toil and Trouble	monzogranite	High-Ca	13.774	14.817	33.502	16.264	15.241	35.096
97969249	333409	Sinclair	monzogranite	High-Ca	13.681	14.771	33.430	15.642	15.103	34.528
97969256B	333413	End of Day xenolith	granodiorite	Mafic	15.033	15.147	34.570	16.952	15.380	36.701
98967008	343613	Erayinia Complex	granodiorite	Syenite	13.811	14.782	33.596	17.223	15.395	38.685
98969003	343501	Fitzgerald Lagoon	granodiorite	High-Ca	13.934	14.898	33.560	16.447	15.348	35.520
99967170A	314126	Bullshead	diorite	High-HFSE	no K-feldspar			19.925	15.751	39.338
99967174A	334023	Wallaby syenite	syenite	syenite	14.199	14.926	33.562	24.234	16.729	38.081
99967176	334023	Wallaby syenite	carbonatite	syenite	no K-feldspar			16.926	15.395	49.116
99967177B	334023	Wallaby syenite	carbonatitic syenite	syenite	no K-feldspar			27.132	17.254	79.151

Data from W. Oliver, BSc(Hons) 1999.
All data are normalised on the basis of concurrent analyses of NBS-981, to correct for mass fractionation during evaporation from the filament.
Uncertainties in all cases are dominated by variability in mass fractionation and are assessed to be 0.15% (95% c.l.).

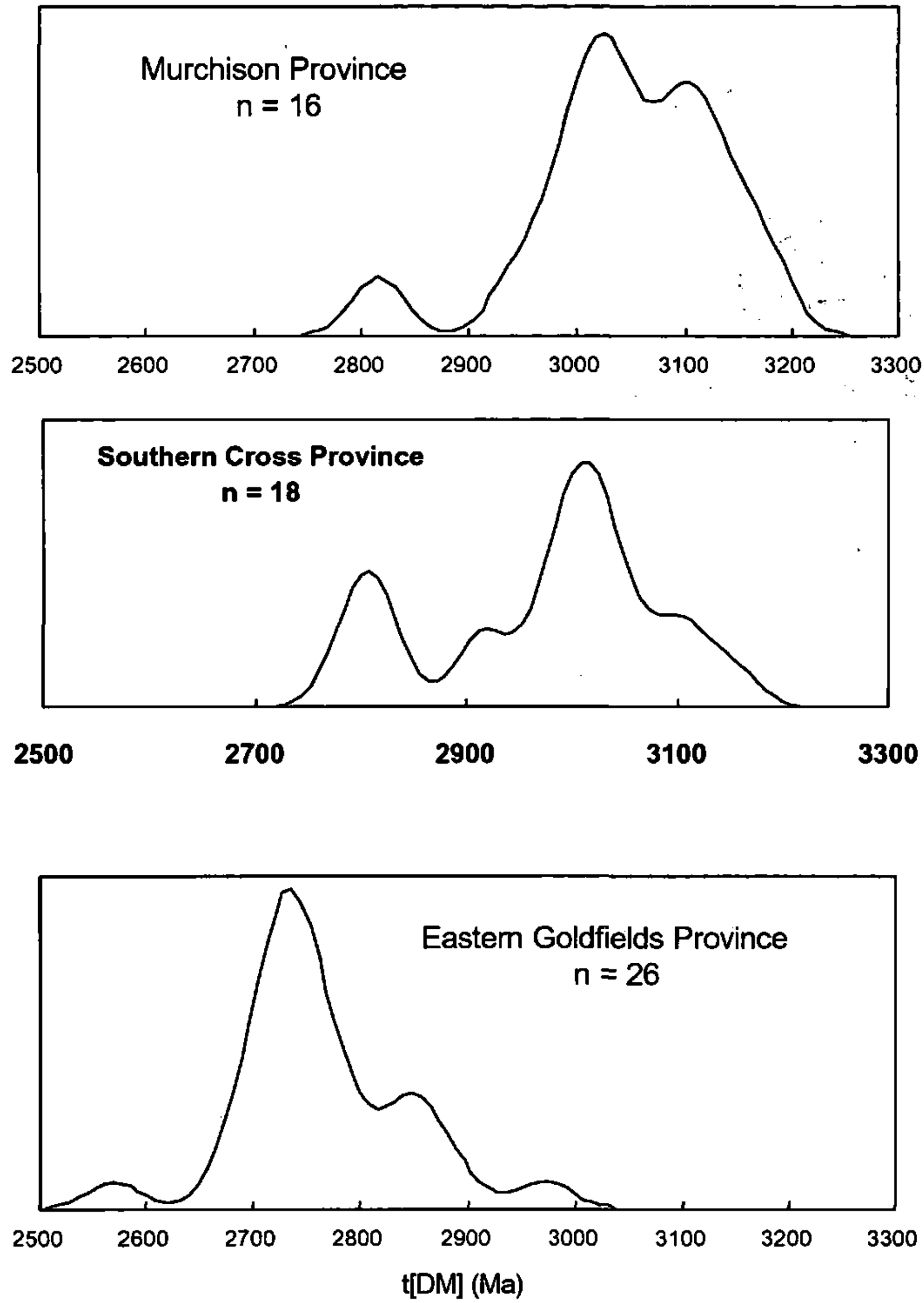

Figure 1: Cumulative frequency plots for the t_{DM} data in Table 1, for the three Provinces of the Yilgarn Craton. For plotting purposes, all ages have been assigned an uncertainty of 25 Ma. (Note that t_{DM} is an estimate of mantle derivation age, not granitoid emplacement age.)

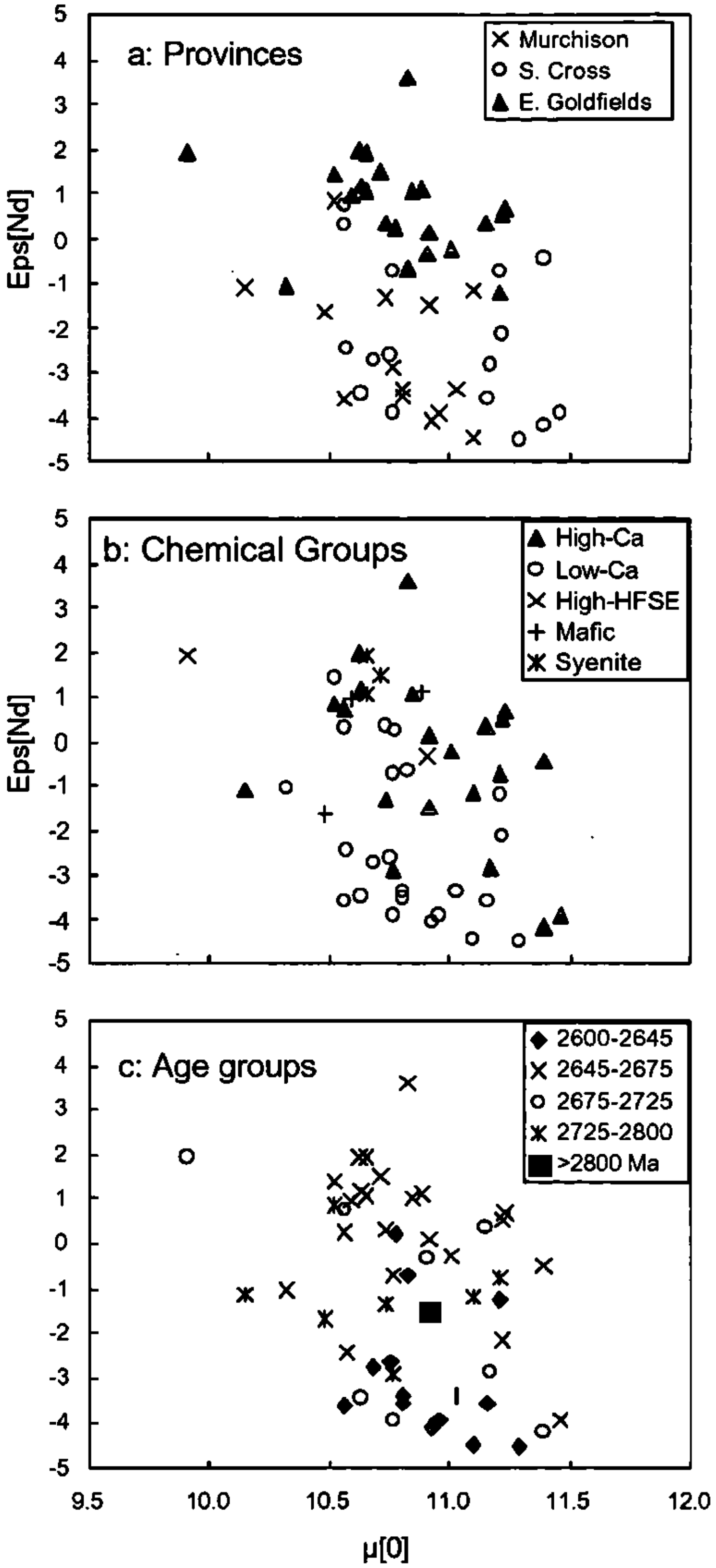

Figure 2: Nd-Pb isotopic correlations for samples from all provinces of the Yilgarn Craton, with points classified by (a) province within the craton, (b) chemical grouping, and (c) emplacement age. Data from Tables 1 and 2.

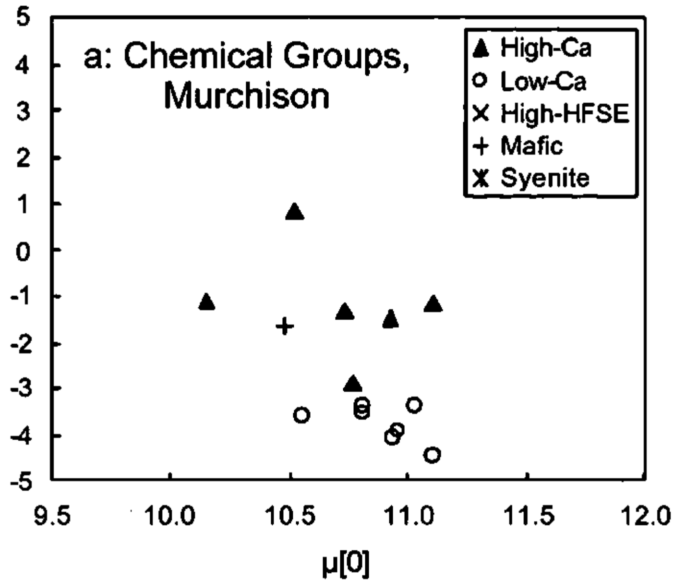

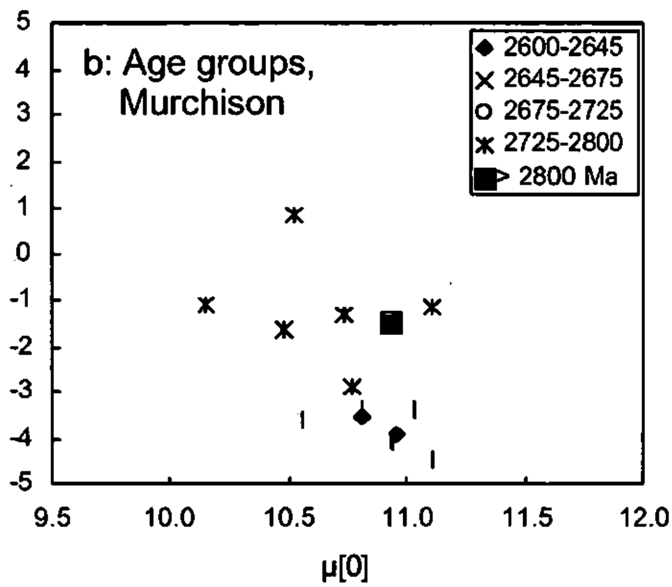

Figure 3: Nd-Pb correlations within each of the structural provinces of the Yilgarn Craton, with points classified by (a, c, e) chemical grouping and (b, d, f) emplacement age. Data fron Tables 1 and 2.

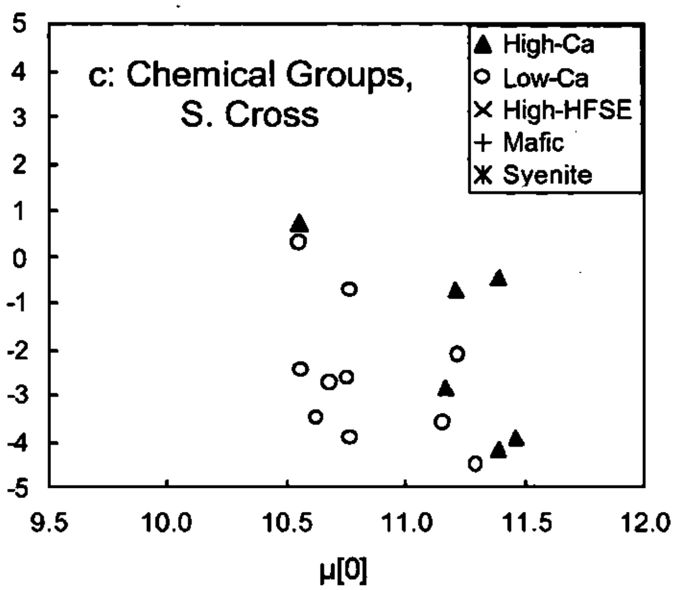

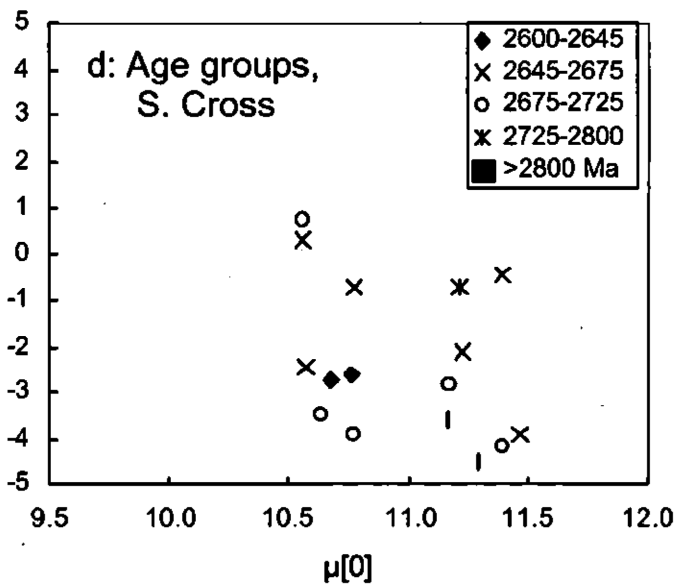

Figure 3 (cont.)

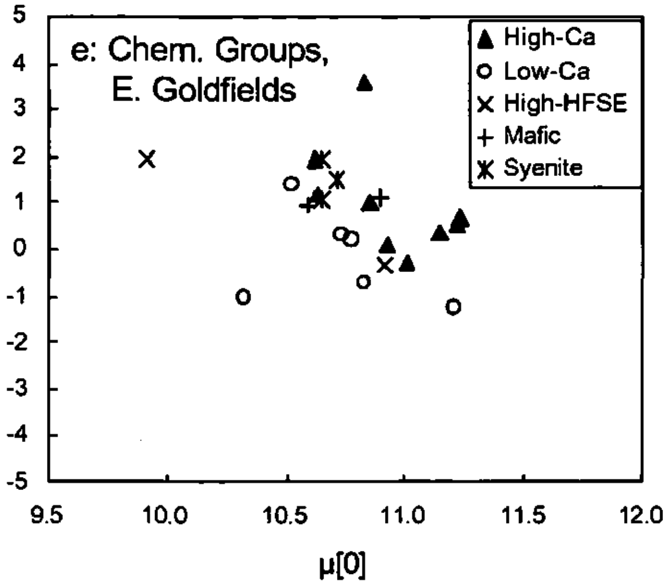

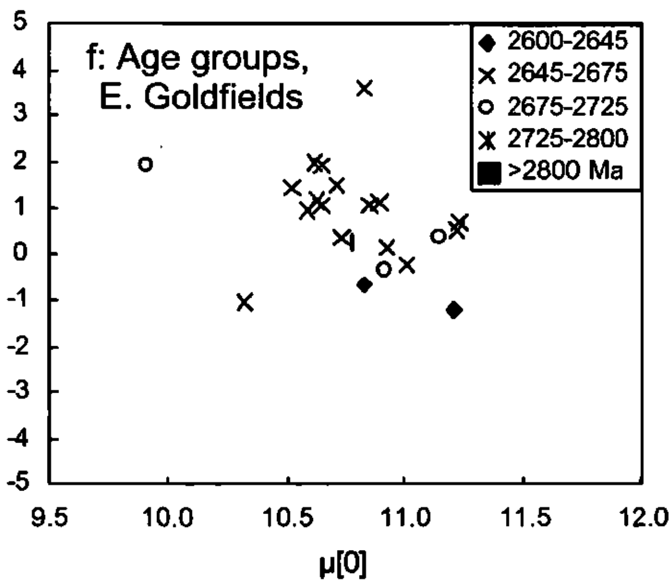

Figure 3 (cont.)

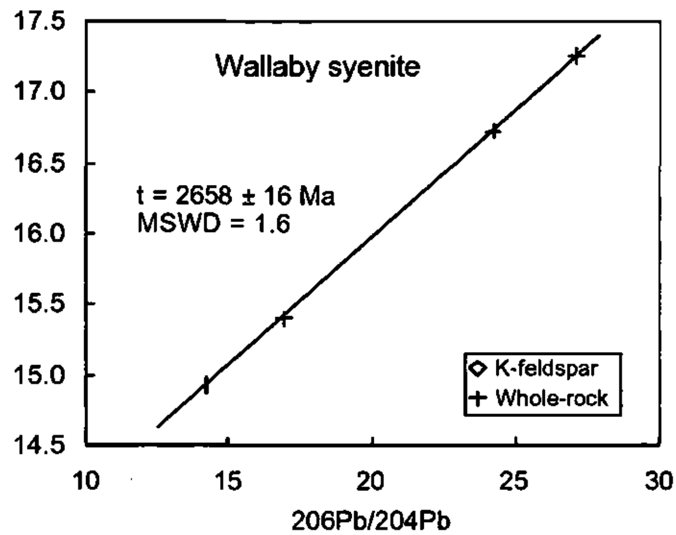

Figure 4: Pb/Pb isochron for the Wallaby syenite. Data from Table 2. Analytical uncertainties are smaller than the plotting symbols, and are highly correlated.

Analytical Procedures

Samples were prepared in an integrated procedure that included separation of zircons for SHRIMP dating; the procedure is described in the SHRIMP section of this report.

About 150 mg of each sample was weighed out, and rock samples were spiked with the ^{147}Sm+^{150}Nd spike prior to digestion. All samples were digested by $HF+HNO_3$ at 190°C in steel-jacketed teflon vessels. After conversion of the dissolved sample to bromide form, Pb was separated on Bio-Rad® AG-1 anion exchange columns. For rock samples, the 'waste' eluate from the Pb columns was converted to nitrate form, and the REEs isolated using Eichrom® TRU© Spec resin (Pin et al., 1994). Samarium and Nd were then separated using Eichrom® Ln© Spec resin in HCl, following procedures modified from Richard et al. (1976).

All isotopic analyses were performed on the Micromass® VG354 mass spectrometer housed at Curtin University. The Sm-Nd analyses followed the replacement of all nine Faraday collectors in the mass spectrometer. Procedures for Nd are based on those previously recorded (e.g. Fletcher et al., 1991) except that the improvement in the collectors justified a modification in the collector spacings, to take ^{150}Nd data in a static-collector configuration during stepped multicollector acquisition of data for the lower-mass isotopes. Sm was also analysed in static multicollector mode. Data for the La Jolla Nd standard are listed above with the sample data, as are data for Caltech ß recovered from spike calibration checks, using the Caltech mixed Sm+Nd standard (Wasserburg et al., 1981). Procedures for Pb were as described by McNaughton and Bickle (1987) and Ho et al. (1994), modified where necessary to utilise the multicollector facility of the VG354.

Concurrent processing blanks for Sm, Nd and Pb were, respectively, <0.2 ng, <1.0 ng and <3 ng. The decay constants used are $\lambda_{238} = 1.55125 \times 10^{-10}$ a^{-1}, $\lambda_{235} = 9.8485 \times 10^{-10}$ a^{-1} and $\lambda_{147} = 6.54 \times 10^{-12} a^{-1}$.

Sm-Nd data normalisation

The fractionation-corrected $^{143}Nd/^{144}Nd$ data recorded for standards during this project are higher than previously reported from this laboratory, and ~0.000020 higher than reference values. This change appears to be entirely due to replacement of the Faraday collectors. To compensate for this offset, ε_{Nd} and T_{DM} are calculated relative to a present CHUR $^{143}Nd/^{144}Nd$ of 0.512655, equivalent to renormalising the $^{143}Nd/^{144}Nd$ data by ~0.1ε.

Model parameters T_{DM} and μ

For this interim report, T_{DM} values have been calculated using the progressively-depleting mantle model of de Paolo (1982). Although the choice of model is irrelevant for any comparisons made within this data set, the final report for this project might present data recalculated to a 2-stage model in order to facilitate comparisons with data from existing AGSO databases. The μ are also based on a continuously-evolving earth model ($\mu(0)$ of Cumming and Richards, 1975). Although using evolving models in bot cases has some philosophical appeal, is is not a necessary condition for the validity of the parameters, given the large degree of decoupling between the Sm-Nd and U-Pb isotopic systems. The main reservation in using the Cumming and Richards model is that is was based on data from major Pb-Zn ore deposits, not granitic crustal rocks. Despite this, it provides a valid means of comparing the time-integrated U/Pb of the sources of the samples analysed.

References

Champion, D.C. and Sheraton, J.W., 1997. Geochemistry and SmñNd isotopic systematics of Archaean granitoids of the Eastern Goldfields Province, Yilgarn Craton, Australia: constraints on crustal growth. Precambrian Res., 83, 109-132.

Cumming, G.L. and Richards, J.R., 1975. Ore lead isotope ratios in a continuously changing Earth. Earth Planet. Sci. Lett., 28, 155-171.

dePaolo, D.J., 1981. Neodymium isotopes in the Colorado Fron Range and crustñmantle evolution in the Proterozoic. Nature, 291, 193-196. (1981)

Fletcher, I.R., Libby, W.G. and Rosman, K.J.R., 1994. SmñNd model ages of granitoid rocks in the Yilgarn Craton. W. Aust. Geol. Survey, Report 37, 61-73.

Fletcher, I.R., Myers, J.S. and Ahmat, A.L., 1991. Isotopic evidence on the age and origin of the Fraser Complex, Western Australia: a sample of mid-Proterozoic lower crust. Chem. Geol., 87, 197-216.

Ho, S.E., McNaughton, N.J. and Groves, D.I., 1994. Criteria for determining initial lead isotopic compositions of pyrite in Archaean lode-gold deposits: a case study at Victory, Kambalda, Western Australia. Chem. Geol., 111, 57-84.

McNaughton, N.J., Cassidy, K.F., Dahl, N., Groves, D.I., Perring, C.S. and Sang, J.H., 1990. Constraints on genesis of primary gold deposits: Lead isotope studies. *In* Ho, S.E., Groves, D.I. & Bennett, J.M. (eds), Gold deposits of the Archaean Yilgarn Block, Western Australia: Nature, genesis and exploration guides. Geol. Dept & Extension, Univ. West. Aust., Publ. 20, 226-236.

McNaughton, N.J. and Bickle, M.J., 1987. K-feldspar Pb-Pb isotope systematics of Archaean post-kinematic granitoid intrusions of the Diemals area, central Yilgarn Block. Chem. Geol., 66, 193-208.

Pin, C., Briot, D., Bassin, C and Poitrasson, F., 1994. Concomitant separation of strontium and samariumñneodymium for isotopic analysis in silicate samples, based on specific extraction chromatography. Anal. Chim., 298, 209-217.

Qiu, Y. and McNaughton, N.J., in press. Source of Pb in orogenic lode-gold mineralization: Pb isotope constraints from deep crustal rocks from the southwestern Archean Yilgarn Craton, Australia. Mineralium Deposita.

Richard, P., Shimizu, N. and AllËgre, C.J., 1976. $^{143}Nd/^{146}Nd$, a natural tracer: an application to oceanic basalts. Earth Planet. Sci. Lett., 3, 269-278.

Wasserburg., G.J., Jacobsen, S.B., DePaolo, D.J., McCulloch, M.T. and Wen, T., 1981. Precise determination of Sm/Nd ratios, Sm and Nd isotopic abundances in standard solutions. Geochim. Cosmochim. Acta, 45, 2311-2323.

Chapter 8.
Overview of the Yilgarn Craton magmatism: Implications for crustal development

D Champion, K Cassidy & A. Budd

Introduction

Previous chapters (2, 3, 4, 5) have described in detail the granite groups, and the clans within these groups, and presented summary chronological histories for the 3 provinces, especially the northern halves (see summaries in Tables 3, 4, 5). Each of these chapters also included a brief discussion on granite petrogenesis and implications for tectonics within that province. This chapter expands on those discussions, to present an integrated tectonothermal model for the Yilgarn Craton, in particular for the three provinces (Murchison, Southern Cross and Eastern Goldfields) that were the subject of the P482 AMIRA project. This approach in undertaken in five parts. The first section summarises the results of the granite classification, in particular comparing and contrasting the granite groups and sub-groups present within each province. The second part looks at the geochronological data, both from this project and public data, to provide a Yilgarn-wide chronology. This chronology is augmented in the third section with a discussion on the implications of the granite isotopic data (chiefly Sm-Nd). The fourth part looks at the implications of the granite types for tectonic environment. The results of the latter are combined with those from the first three sections to provide a preliminary tectonothermal framework for the craton, based on the currently available data. We have suggested a preliminary tectonothermal framework, as it should be noted that constraints on crustal growth and tectonic models for the Yilgarn craton, and cratons in general, are based on a variety of data, that range from mostly fact to mostly model-dependent; such data constraints include the following, in order of decreasing veracity:

1) ages of the granites, granite groups (and greenstones),
2) inherited zircon data in both granites (and greenstones),
3) granite isotopic data, especially Sm-Nd, and Pb-Pb,
4) petrogenetic and tectonic models for mafic and ultramafic igneous rocks,
5) petrogenetic and tectonic models for granites and granite groups,
6) petrogenetic and tectonic models for other felsic igneous rocks, e.g., felsic volcanics,
7) basin formation models, and
8) structural deformation models and relative timing.

Of these data/data models, 1), 2), 3) and 5) were the direct focus of the P482 AMIRA study, involving not only collection of new data but collation of, and combination with, existing public-domain data. Constraints 4), 6), 7), and 8), were not part of this project and, accordingly, are not discussed in any detail, though consideration of 4) is built into the tectonothermal model. It is noted that 8) is still poorly understood for much of the Yilgarn and remains an area needing much more focus and data.

Granite groups and chemical sub-groups within the Murchison, Southern Cross and Eastern Goldfields Provinces: a comparison

Granite Groups

The Granite groups and clans within those groups have been described and discussed in detail for the Murchison, Southern Cross and Eastern Goldfields Provinces within the relevant chapters (see Chaps 2, 3, 4, 5). Groups recognised within each province are listed in Table 1, from which it is obvious that, with perhaps the exception of the Syenitic group, members of all groups are found within each province. Notably, the High-Ca group is most dominant in all provinces, comprising from 50% to >60% of recognised granites. Notably there are no significant chemical differences between the High-Ca groups between the 3 provinces, with the possible exception of the Eily Eily clan (Murchison Province). The latter differs in two main aspects: first, the clan trends to relatively high LILE and HFSE contents, in part overlapping with the Low-Ca group; and second, the clan is characterised by its generally Sr-depleted nature (i.e., minor to significant negative Eu anomalies). The Union Jack clan of the High-Ca group, Eastern Goldfields Province, does share some characteristics with the Eily Eily clan, but does not reach the more extreme compositions shown in the latter.

The second most voluminous magmatism belongs to the Low-Ca group which appears to vary from 10-20%, in the Eastern Goldfields Province, to locally significantly higher in the other two provinces, especially the Southern Cross Province. Within the Eastern Goldfields Province it is further evident that members of the Low-Ca group are more common within the northern half of the province. Like the High-Ca group there is little difference chemically in the Low-Ca group across the 3 provinces. Together the High-Ca and Low-Ca groups comprise 80% or more of the total granites within each province.

Group	MP	SCP	EGP
High-Ca	Mainland	Diemals	Menangina
Low-Ca	Goolthan	Beetle	Mt Boreas
High-HFSE	Damperwah	Marda	Kookynie
Mafic	Gem of Cue	Westonia	Granny Smith
Syenitic	Udagalia	Fitzgerald Peaks?	Gilgarna

Table 1. Comparison of granite groups and their associations found within the Murchison, Southern Cross and Eastern Goldfields Provinces. Granite groups listed in order of abundance, with the High-Ca and Low-Ca groups together comprising 80% or more of the total granites.

The minor groups, Mafic, Syenitic and High-HFSE are best expressed within the Eastern Goldfields Province, where each comprises 5-10% of the total granites. The great majority of these are localised within or marginal to the greenstone belts. The Mafic and High-HFSE groups are also well represented within the Murchison Province, again largely marginal to or within the greenstone belts. Members of these two groups appear to form only a very minor component of the Southern Cross Province. It is not known whether this difference is indeed real or simply an artefact of sampling bias. Members of the Syenitic group are different in that it is strongly evident that they are largely absent from the

Murchison and Southern Cross provinces, forming only a very minor component (1-4 units) in each province. This contrasts greatly with the Eastern Goldfields Province where Syenitic rocks form a significant component. Notably, the late Syenitic rocks within the Eastern Goldfields Province (<2650 Ma) are replaced by similarly young High-HFSE rocks within the Murchison Province (see below).

Geochemical subgroups

Within each province it has become clear that many of the granite groups can be subdivided into a number of subgroups (e.g., clans or groups of clans). The most obvious sub-groups are those based on LILE contents, i.e., high-LILE and low-LILE, with the variation most evident in the High-Ca and Mafic group granites, but also present within the High-HFSE and Low-Ca groups (Table 2). Although in reality the spread in LILE contents between granites supersuites is, in part, continuous, these two subgroups have been established as they can be used as end-members. The relevance of such an approach is well illustrated by a number of results:

- the available evidence indicates that the high-LILE High-Ca subgroup granites are younger or the same age as low-LILE High-Ca granites, within the Eastern Goldfields Province, and probably within the Southern Cross Province also.
- Similarly, the high-LILE Mafic group granites are younger than or the same age as their low-LILE counterpart, within the Eastern Goldfields Province. More importantly, it is evident that the high-LILE Mafic group granites (Granny Smith clan) are almost universally ca 2665 Ma in age.
- Within the Murchison Province it is evident that the high-LILE High-HFSE subgroup is significantly younger than its low-LILE counterpart.

Group	MP	SCP	EGP
High-Ca			
Low LILE	Mainland	Hong Kong	Beasley
High LILE	Eily Eily	Barr Smith	Union Jack
Low-Ca			
Low LILE	Nakedah	Mugs Bore	Meredith
high LILE	Goolthan	Yeelirrie	Grant Duff
High-HFSE			
Low LILE	Nannine	Marda	Satisfaction
high LILE	Damperwah		Kookynie
Mafic			
Low LILE	Gem of Cue	Westonia	Kanowna Belle
high LILE	Britania		Granny Smith
high Mg		Norie	
tholeiite		(Courlbarloo?)	Kathleen Valley

Table 2. Comparison of within-group geochemical variation for granites groups of the Murchison, Southern Cross and Eastern Goldfields Provinces, showing representative clans of each subgroup.

Such trends of younging with increasing LILE contents are consistent with the notion of increasing maturity of the continental crust with time, and mirrors the overall trend from High-Ca to Low-Ca magmatism seen within all 3 provinces. It is notable that there is no apparent differences in age between the high-LILE and low-LILE subgroups within the High-Ca and Mafic groups of the Murchison Province; though this may more be a result of this changeover occurring earlier in this province, i.e., pre 2800 Ma. Unfortunately, the general lack of unequivocally older granites makes this hard to verify or refute.

Other chemical subgroups are recognisable within the granites of the Yilgarn, most notably within the Mafic group. One of the most important is the recognition of the High-Mg clan (Norie clan) in the northern Murchison Province (see Champion & Cassidy, this volume). These rocks are characterised by high MgO, Ni, Cr and mg*, features consistent with a mantle origin, but also have moderate LILE contents. Such rocks are generally interpreted to indicate derivation within a region that is actively undergoing subduction or recently experienced such (see Smithies & Champion, 2000). The presence of such rocks (at ca. 2755 Ma) within the northern Murchison is the strongest evidence yet for subduction within the Yilgarn at or before this time.

The other Mafic subgroup are those with tholeiitic characteristics, notably the Kathleen Valley and Sweet Nell clans in the Eastern Goldfields Province, and, perhaps the Courlbarloo clan in the Southern Cross Province. Such rocks are invariably related to fractionation of a mafic (basaltic) precursor and mostly taken as indicative of a rifted tectonic origin (see below).

Geochronology: Ages of the granites, granite groups and greenstones, and inherited zircon data

The general ages and temporal sequences of the granites, and greenstones, of the Yilgarn craton have previously been summarised for each province (see relevant chapters within this report volume); these are reproduced below (Tables 3, 4, 5) and summarised in Table 6. All available zircon data, including inherited ages, for the 3 provinces, are listed with references in the relevant chapters (this volume). Plots for each province are shown in Figures 1, 2, 3.

Inspection of Figures 1, 2, 3 and the available data, reveal a number of points, detailed below under their relevant headings:

Granites

- The Eastern Goldfields Province shows only a limited granite age range, relative to the other 2 provinces (Fig. 1). The vast majority of granites in the Eastern Goldfields are younger than 2720 Ma (Figs 2, 3), though there is some evidence for older (to 2760 Ma) granites (AGSO, unpublished data). This contrasts with the Murchison and Southern Cross Provinces, where there is good evidence for older granites of the following ages: 2720-2760 Ma, 2780-2820 Ma, 2920-3020 Ma, and older (closer to the Western Gneiss Terrane; Fig. 1).
- Contrary to perceived wisdom, the available data indicate that the peak of granitic magmatism in the Eastern Goldfields Province spanned some 20 Ma from 2680 Ma to younger than 2660. In detail, the High-Ca distribution suggests two overlapping peaks, at ca. 2675 Ma and 2665 Ma (Fig. 2). The Mafic group strongly overlaps with the younger of these peaks, i.e., 2665 Ma; similarly there is increasing evidence for a Syenitic event at this age.

- The major peak in granite magmatism in the Eastern Goldfields Province (2680-2660 Ma) is clearly a more magmatically quiet time in the other two provinces (Fig. 2). In the Southern Cross Province the main peaks of granite magmatism occur at 2700-2680 Ma and 2640-2630 Ma (Fig. 1). The Murchison Province data shows a significant number of peaks, including 3010-3000 Ma, 2960-2920 Ma, 2820-2800 Ma, 2765-2735 Ma, 2710-2670 Ma, and 2650-2630 Ma. The 2800 Ma and older magmatic peaks in the Murchison Province are also present within the Southern Cross Province but are largely poorly recorded in the latter. Further dating may resolve this.
- The 2765-2735 magmatic event, well represented in the Murchison Province, appears to be largely absent within the Southern Cross Province.
- All three provinces show a strong change around ca. 2655-2650 Ma from older dominantly High-Ca magmatism to younger dominantly Low-Ca magmatism. This change is most evident in the Murchison and Southern Cross provinces, largely due to the already mentioned dearth of magmatism in the 2680-2660 Ma period (Figs 2, 3), but also due to the apparently more voluminous Low-Ca magmatism in these regions. The less obvious changeover within the Eastern Goldfields Province data (Fig. 2), reflects the strong 2660-2680 Ma High-Ca peak, the less voluminous Low-Ca magmatism, and the more limited dating of Low-Ca granites in this province. The change in the 3 provinces reflects not just a change in the source of magmatism but a change in the depth of melting from high (High-Ca) to lower pressures (Low-Ca). As discussed by Champion & Cassidy (this volume), this change must reflect some fundamental change in the tectonic regime around this time.
- All parts of the Yilgarn Craton, including the Western and South-West gneiss terranes (Figs 1, 3), experienced the post 2650 Ma Low-Ca magmatism. This relatively voluminous and widespread magmatism also overlaps both with granulite metamorphism in the south-west Yilgarn (Nemchin et al., 1994), and the Yilgarn-wide 2640-2630 Ma gold event.

Greenstones

- Greenstones in the Eastern Goldfields Province mostly fall between 2720 and 2670 Ma (Fig. 2). Krapez et al. (2000) recognised a number of greenstone sequences in the southern Eastern Goldfields Province, with ages from 2715 Ma and earlier, to 2670 Ma, with younger, (2665 Ma or younger) basins (Yilgangi, Kurrawang, Merougil, Penny Dam, Jones Creek). There is increasing evidence for, at least isolated remnants, of older greenstone and granites, between 2730 and 2765 Ma. These may either represent basement to the younger greenstones, or may indicate greenstone development started earlier than thought in the Eastern Goldfields Province. One possibility is that such older greenstones are equivalent to the younger sequences in the Southern Cross and Murchison Provinces.
- Notably, the great majority of granitic magmatism occurs after greenstone development, especially after felsic volcanism. The differences in the ages, is interesting, especially given that there are granites clearly related to spatially associated volcanics, e.g., High-HFSE group. The available data suggests that magmatism appears to have changed around ca. 2675 Ma from both intrusive and extrusive, to almost totally intrusive. This may, in part, reflect either lack of preservation, or lack of recognition. For example, Krapez et al. (2000) report ca. 2665 detrital ages from the upper part of the Black Flag Formation, and numerous ca. 2665 Ma detrital ages from the Kurrawang, Merougil, and Jones Creek sequences, though all these zircon populations, especially for the latter 3 sequences, may have been derived from exposed intrusive felsic magmatism.
- Greenstone ages in the Murchison Province are largely similar to those of the granites, though are confined to 2700 Ma and older (Table 3). As noted by Schiotte & Campbell

(1996), the available data indicate good evidence for three periods of greenstone formation, i.e., 2700-2760 Ma (Mt Farmer group), ca. 2780-2820 Ma (upper part of Luke Creek group), and 2930-3010 Ma (Luke Creek Group) (Table 4), not the two periods envisaged by Watkins & Hickman (1990). The data also suggest the possibility that the 2930-3010 Ma period may be actually comprised of 2 discrete periods, 2930-2965 Ma and 3000-3010 Ma.

- Ages of greenstones in the Southern Cross Province appear to be broadly similar to those in the Murchison Province, with evidence for 3020-2900 Ma, ca 2820 Ma (including the layered mafic complexes) and ca. 2740-2700 Ma (see Table 2, and data in Budd & Champion, this volume).

Inherited and detrital zircons

- Inherited zircons within the granites (and greenstones) of the Murchison and Southern Cross provinces overlap mostly with known ages for older granites and greenstone sequences (Fig. 1). There is little evidence for significant old inherited zircon (i.e., older than 3.05 Ga), though some inheritance of this age is present, most notably within the Southern Cross Province (see Budd & Champion, this volume).
- Inherited zircon data for the granites of the Eastern Goldfields Province fall into a number of discreet periods - 2670-2710, 2720-2760, 2790-2810, 2880-2910, and 2950-2970 Ma. Importantly, the inherited zircon data from the greenstones very closely match the inherited zircons within the granites. More importantly, the identified older inheritance groups (post 2720 Ma), closely mirror identified granite-greenstone ages in the Murchison Province and Southern Cross Province, with the possible exception of the 2880-2910 Ma group. Notably, all inherited zircons >2800 Ma are in those granites close to or internal to greenstones, suggesting the possibility that these older ages may be xenocrystic and perhaps inherited from the greenstones. Importantly, Cassidy et al. (1997 Annual report, AMIRA P482), have shown, however, that the nearly all the older inheritance is confined to granitoids in the western half of the EGP, approximately corresponding to west of the Celia lineament, suggesting that the older crust does exist beneath the western Eastern Goldfields Province, and, further that the Celia Lineament may mark actually approximate an important crustal boundary in this province.
- Inherited zircon ages within the Murchison Province also closely follow granite and greenstone ages as may be expected. Most notably, however, there appears to be no evidence for old inherited zircon (>3100 Ma) that may be expected if Western Gneiss Terrane-type crust was being reactivated (Fig. 1), consistent with the Sm-Nd isotopic data (Fletcher & McNaughton, this volume).

Province comparisons

- There is a pronounced younging of available zircon ages from west from east, from the Western Gneiss Terrane through the Murchison Province, Southern Cross Province and to the Eastern Goldfields Province (Fig. 1). The apparent differences between the Murchison Province and Southern Cross Province may simply reflect the smaller number of ages for the latter, in particular, the lack of greenstone ages. A similar argument may hold for the South-West Gneiss Terrane, which on available evidence appears to lack any rocks older than ca. 2700 Ma.
- The Western Gneiss Terrane clearly contains the oldest dated rocks in the Yilgarn Craton (3300-3650 Ma), with similar old ages evident in inheritance patterns. Notably, however, old inherited zircons are not strongly represented in the Murchison, Southern Cross or Eastern Goldfields provinces, with the strong implication that such rocks are not present within these provinces.

- There is, however, abundant evidence for younger events (<3100 Ma), within the WGT, that match those seen within the Murchison and Southern Cross Provinces, especially less than 2750 Ma (Figs 1, 2). There are a couple of 2800 Ma ages (inherited) that may also correspond with a similar events within the Murchison and Southern Cross Provinces. The commonality of age data are, perhaps, best interpreted to indicate collision between the Murchison Province and Western Gneiss Terrane at sometime between 2750 & 2810 Ma. Notably, Nutman et al. (1993) reached similar conclusions. They further suggested, however, that the pre-3300 Ma rocks of the Narryer complex were confined to the eastern part of the gneiss complex, and that these older gneisses formed an allochthonous terrane overthrust onto pre-existing 3000-2920 Ma gneisses (and also greenstone age), at ca. 2750 Ma.
- Notably there also appears to be a dearth of older ages within the Southwest Gneiss terrane, with almost all ages (magmatic and inherited), 2800 Ma or younger (Fig. 1). The presence of 2800 Ma inherited zircons may suggest docking had occurred before this time. The lack of ages between 2680 and 2800 Ma, however, may suggest commonality wasn't achieved until around 2680 or before. The Southwest Gneiss terrane certainly lacks the 2680-2750 Ma ages evident in both the Murchison Province and the Western Gneiss Terrane (and also in the Southern Cross and Eastern Goldfields provinces), though this could reflect resetting of zircon core ages as suggested by Nemchin & Pidgeon (1997). Qui et al. (1997) suggested collision occurred sometime between 2690 and 2650 Ma; the inherited zircon data would tend to suggest such collision occurred before 2680 though.
- Although, the data for the Southern Cross Province is biased to younger data (especially through lack of ages on older greenstone sequences), it is evident that both the Southern Cross Province and the Murchison Province share very similar histories, i.e., ca. 2920-3030 Ma, 2780-2820 Ma and 2750-2700 Ma greenstone-granite events, with abundant 2740-2620 Ma magmatism. Some differences are apparent, however; these include, the apparently more voluminous magmatism at 2740-2760 Ma in the Murchison Province, such that in the latter the main period of magmatism ranges from 2655 to 2760 Ma, compared with 2650-2740 Ma in the Southern Cross Province.

The chronology of the Yilgarn craton, coupled with the granite group data is presented in Table 6.

Ca. 2760 Ma	Trump granodiorite, Raeside mass; High Ca group
2740-2730 Ma	Kathleen Valley gabbro (Mafic group), and Satisfaction Complex (High-HFSE group), both probably dating greenstone formation ages
2720-2670 Ma	Greenstone, basaltic and felsic volcanism, sedimentation
ca. 2705 Ma	Komatiitic magmatism
2720-2680 Ma	Increasing High-Ca magmatism with decreasing age; also Mafic (low-LILE) and High-HFSE magmatism (& felsic volcanism) throughout this range.
2680-2655 Ma	Voluminous High-Ca magmatism, also Mafic, Syenitic, and minor High-HFSE group magmatism. Peak of magmatism in the Eastern Goldfields Province. Apparently only minor magmatism at this time in the Southern Cross Province.
2665 & younger?	Formation of Yilgangi, Kurrawang, Merougil, Penny Dam, Jones Creek basins
2655-2630 Ma	Widespread Low- Ca magmatism, across the Eastern Goldfields Province, and the Yilgarn. In the Eastern Goldfields Province accompanied by syenitic (and carbonatitic) magmatism. Some High-Ca, and Mafic? magmatism to 2650 Ma and slightly younger.

Table 3. Tectonothermal history for the northern Eastern Goldfields region, including the eastern part of the Southern Cross Province. Data and data sources given in Chapter 2.

ca. 3670 Ma	inheritance, Munroes Well granite in Gum Creek greenstone belt
3120–2900 Ma	inheritance, Buttercup Bore & Munroes Well granites in Gum Creek greenstone belt, McLeod Rock granite
>3020-2920? Ma	greenstone formation, including komatiite
3020 Ma	Deception Hills porphyry
ca. 2820-2800 Ma	Tholeiite intrusions (eg Windimurra, Youanmi, Atley layered intrusions) on the Murchison-Southern Cross provinces boundary; also felsic volcanism.
2815 Ma	Courlbarloo plagiogranite (High-HFSE group?)
>2735-2700 Ma	greenstone formation, including felsic volcanism Marda & Koolyanobbing
2735-2700 Ma	High-Ca magmatism
2700-2670 Ma	dominantly High-Ca group, some Low-Ca (Bulga Downs Clan).
2660-2620 Ma	dominantly Low-Ca group, some High-Ca group

Table 4. Tectonothermal history for the northern Southern Cross Province. Data and data sources detailed in Chapter 4.

3800 - 4100 Ma	inherited zircons – Narryer Gneiss Terrane
3600-3730 Ma	Narryer Gneiss Terrane, e.g., Meeberrie gneiss
3440-3500 Ma	Narryer Gneiss Terrane, e.g., Eurada gneiss
3380-3350 Ma	Narryer Gneiss Terrane, e.g., Dugel gneiss
3290-3315 Ma	Narryer Gneiss Terrane, e.g., unnamed gneisses Pendants of gneiss, e.g., Murgoo gneiss, within the western Murchison Province – related to Narryer Gneiss Terrane?
3119? Ma	Narryer Gneiss Terrane, e.g., unnamed gneisses
ca. 3010-3000 Ma ↑	greenstones (and komatiite?), of Luke Creek group, High-Ca group, Mafic and High-HFSE groups?
continuous? ↓	Western & Narryer Gneiss Terrane – magmatism of this age appears to be absent
2965-2920 Ma	greenstones (and komatiite?), of Luke Creek group, High-Ca group granites and gneisses, Mafic and High-HFSE groups?
>2810-2750 Ma	Narryer Gneiss Terrane overthrust over Murchison Province?
2815-2780 Ma	greenstones (upper part of Luke Creek group), High-Ca group, Mafic and High-HFSE groups?, rift-related? layered mafic intrusive complexes along Southern Cross Province/Murchison Province boundary
2760-2745 Ma	High-HFSE (Nannine clan), Mafic and High-Ca groups
2750-2700 Ma	greenstones, including komatiite, of the Mount Farmer group
2745-2725 Ma	High-Ca group
2725-2710 Ma	High-Ca and Mafic (Gem of Cue, Britania clans) groups
2700-2665 Ma	common High-Ca magmatism, very minor Low-Ca group magmatism?
2655-2620 Ma	Low Ca and High-HFSE (Damperwah clan) group magmatism.
2650-2640 Ma	Granulite metamorphism - Southwest Gneiss Terrane

Table 5. Tectonothermal history for the northern Murchison Province (and western Southern Cross Province), and for the Western Gneiss (including the Narryer), and the Southwest Gneiss terranes. Data and sources detailed in Chap. 5 (this volume).

3800 - 4100 Ma	inherited zircons – Narryer Gneiss Terrane		
3600-3730 Ma	Narryer Gneiss Terrane, e.g., Meeberrie gneiss		
3440-3500 Ma	Narryer Gneiss Terrane, e.g., Eurada gneiss		
3380-3350 Ma	Narryer Gneiss Terrane, e.g., Dugel gneiss		
3290-3315 Ma	Narryer Gneiss Terrane, e.g., unnamed gneisses Pendants of gneiss, e.g., Murgoo gneiss, within the western Murchison Province – related to Narryer Gneiss Terrane?		
3119? Ma	Narryer Gneiss Terrane, e.g., unnamed gneisses		
	Murchison	**Southern Cross**	**Eastern Goldfields**
~3020-3000 Ma	High-Ca Mafic High-HFSE? greenstone komatiite?	High-Ca? Mafic High-HFSE?? greenstone komattiite	
continuous?	Western & Narryer Gneiss Terrane – magmatism of this age appears to be absent		
2965-2920 Ma	High-Ca Mafic High-HFSE? greenstone	High-Ca? Mafic? High-HFSE?? greenstone?	zircon inheritance
>2810-2750 Ma	Narryer Gneiss Terrane thrust over Murchison Province?		
ca. 2820-2800 Ma	Tholeiite intrusions (eg Windimurra, Youanmi, Atley layered intrusions) on the Murchison-Southern Cross provinces boundary; also felsic volcanism.		
2820-2780 Ma	Mafic High-Ca greenstone	Mafic High-Ca greenstone	zircon inheritance
~2760-2745 Ma	Mafic High-HFSE High-Ca? greenstone	?	High-Ca? Mafic
~2745-2720 Ma	High-Ca greenstone	High-Ca greenstone	High-HFSE? Mafic? greenstone?
2720-2700 Ma	High-Ca Mafic greenstone	High-Ca Mafic? greenstone	High-Ca Mafic High-HFSE greenstone komatiite

Table 6a. Temporal and magmatic history for the Murchison, Southern Cross and Eastern Goldfields Provinces, pre-2700 Ma. Events in Southwest and Western gneiss terranes shown in italics.

2700-2670 Ma	High-Ca Low-Ca?	High-Ca Low-Ca?	High-Ca Mafic High-HFSE greenstone
pre-2680 Ma?	Docking of Southwest Gneiss Terrane. Actual age of collision poorly constrained.		
2670-2655 Ma	minor magmatism (High-Ca) (Low-Ca)		High-Ca High-HFSE Mafic Syenitic Low-Ca conglomeratic sediments
2655-2600 Ma	Low-Ca High-HFSE High-Ca?	Low-Ca High-Ca?	Low-Ca Syenite Mafic?
2650-2640 Ma	Granulite metamorphism - Southwest Gneiss Terrane		

Table 6b. Temporal and magmatic history for the Murchison, Southern Cross and Eastern Goldfields Provinces, post-2700 Ma. Events in Southwest and Western gneiss terranes shown in italics.

Isotopic data - evidence from Sm-Nd and Pb-Pb data.

Isotopic data for the Yilgarn Craton has been the subject of a number of studies (e.g., Watkins & Hickman, 1990; Fletcher et al., 1994, Champion & Sheraton, 1997; Nutman et al., 1993), and also has been collected as part of the current AMIRA work (Fletcher & McNaughton, this volume). Fletcher and McNaughton (this volume) drew a number of conclusions from the AMIRA isotopic data (Fig. 4), expanded on below:

- there is a fundamental difference in the isotopic signatures of the Yilgarn provinces, with the granites of the Eastern Goldfields Province being characterised by more primitive ε_{Nd} values (and younger depleted mantle model ages, Fig. 4), relative to the Southern Cross Province and Murchison Province. This can be best interpreted to indicate that the granite source regions for the Eastern Goldfields Province are in general younger than the other provinces. This result is consistent with the earlier interpretations of Fletcher et al. (1994) and Champion & Sheraton (1997). This distinction extends to all granite groups, such that members of the High-Ca, Low-Ca and High-HFSE groups in general have more evolved ε_{Nd} in the Murchison and Southern Cross provinces, than in the Eastern Goldfields Province.
- it is also evident that there is a large number of similarities between the Murchison and Southern Cross provinces, in particular, the main peaks in the Nd depleted mantle model ages (Fig. 4). This result strongly supports the conclusions made from the previous sections, i.e., the Murchison and Southern Cross provinces are quite similar and most probably have been acting as one entity for a long while.
- there is a clear distinction between ε_{Nd} isotopic signatures of the High-Ca and Low-Ca groups on the province scale, with the Low-Ca granites having more evolved isotopic signatures, suggesting they had older source rocks. This distinction is only partly evident on the craton scale, for a variety of reasons, e.g., the Eastern Goldfields Province being isotopically more primitive than the Southern Cross Province and Murchison Province.
- finally, there appears to be broad distinctions between the ε_{Nd} isotopic signature of the granites, on the basis of age, with the youngest (<2645 Ma) granites being the most

evolved, and the 2645-2675 Ma age group being the most primitive (see Figures in Fletcher & McNaughton, this volume). Given the age distribution of granites within the three provinces, these age group observations largely relate to 2 factors: the majority of 2675-2645 granites belong to the Eastern Goldfields Province (the most isotopically primitive province), and the majority of post-2645 Ma granites belong to the Low-Ca and High-HFSE groups, 2 of the most isotopically evolved granite groups.

Other conclusions can be drawn from the combination of the AMIRA data and the publicly-available data (Watkins & Hickman, 1990; Fletcher et al., 1994, Champion & Sheraton, 1997; Nutman et al., 1993), as follows:

- Champion & Sheraton (1997) showed that the ε_{Nd} values for the Low-Ca group granites in the Eastern Goldfields Province became progressively more primitive toward the north-east, and that this trend continues across the Ida Lineament into the Southern Cross Province. This data is best interpreted to show that the average age of the Low-Ca crustal source rocks youngs to the north-east, suggesting this has been the direction of crustal growth in the Eastern Goldfields. The large jump in ε_{Nd} across the Ida lineament seen in these rocks indicates some fundamental difference between the provinces - a difference also seen in the Yilgarn-wide data which indicates the Eastern Goldfields Province is isotopically more primitive.
- it is clear within the Eastern Goldfields Province that members of both the Low-Ca and High-HFSE groups are mostly more isotopically evolved than members of the Mafic, High-Ca and Syenitic groups (Champion & Sheraton, 1997). This can be best interpreted to indicate that the source rocks for the Low-Ca and High-HFSE groups are, on average, significantly older, than those for the Mafic, High-Ca and Syenitic groups. This isotopic difference between groups would also appear to hold for the Murchison Province. The data is more equivocal for the Southern Cross Province, where although the majority of the High-Ca granites have more primitive ε_{Nd} than the majority of the Low-Ca granites, the total range in ε_{Nd} for the two groups completely overlap.
- Nutman et al. (1993) showed that the ε_{Nd} values for the younger granites within the Narryer Gneiss Terrane were too primitive to have been derived from the old (3300 Ma and older) gneisses of that terrane, and more consistent with derivation from crust of similar age to the Murchison Province. Nutman et al. (1993) interpreted this to indicate that the Narryer Gneiss Terrane was actually thrust over the Murchison Province.

Petrogenetic and tectonic models for granites and granite groups

An understanding of petrogenetic and possible tectonic models for the generation of granites from each of the granite groups can be used, in conjunction with the geochronological and isotopic data, to provide a tectonothermal history for the Yilgarn.

Tectonics of granites.

Given the complexities of granite petrogenesis, in particular the relative roles of crustal versus mantle input into any granite it is difficult at best to make any unequivocal statements regarding a granite and the tectonic environment it may have formed in. Despite these problems many workers have attempted to classify granite-types and their respective tectonic environments on the basis of empirical observations with regards to both certain chemical parameters (such as Y, Nb, Rb contents, e.g., Pearce et al., 1984), and to actual dominant granite type (on the basis of M-, I-tonalite, I-granodiorite, A-type, e.g., Pitcher, 1993).

Chemical parameters

A number of workers, most notably Pearce and co-workers (e.g., Pearce et al., 1984) have used certain chemical parameters (trace elements), to empirically constrain tectonic environment. Although such diagrams have not been widely accepted, they are still used, in particular for Palaeozoic and younger granites. Whether such diagrams are applicable for Archaean granites is debateable, and depends largely on the role of modern tectonics in the Archaean. Another feature of the diagrams developed by Pearce et al. (1984), is their inability to discriminate post-orogenic granites, from volcanic-arc and syn-collisional granites. Such a result is not unexpected given that many (probably most) granites in these environments have a dominantly crustal component. Despite the problems with such diagrams there use was investigated for this study (Figs 5, 6).

Examination of Figures 5 and 6 shows that on such tectonic discrimination diagrams, the High-Ca granites of the northern Eastern Goldfields and northern Murchison Province clearly fall into the volcanic arc (VAG) and syn-collisional (Syn-COLG) fields. Such an interpretation is consistent with the one used by us, i.e., these granites represent high-pressure derivation consistent with either melting of thickened crust and/or the subducting slab (see below). Similarly, the Mafic rocks, with the exception of the tholeiitic clans (Kathleen valley and Sweet Nell) also occupy the VAG and Syn-COLG fields. A VAG environment is certainly consistent with our interpretation for the Norie clan in the northern Murchison Province (see Chap 5 this volume). The two tholeiitic clans (and probably Courlbarloo in the Southern Cross Province) are examples of fractionated tholeiitic series granites, often known as plagiogranites. Such rocks are typically found in ocean-ridge settings, be they back-arc or oceanic ridges, hence their plotting in the ORG (ocean-ridge granite) field (Fig. 5). Whilst such a setting is possible for these rocks in the Eastern Goldfields Province, it is most likely that they simply represent in-situ fractionation of moderate-sized gabbro bodies, i.e. layered mafic complexes. This well illustrates one of the problems with such tectonic diagrams, in that solutions can be non-unique.

The Low-Ca granites of the northern Murchison and northern Eastern Goldfields straddle the VAG, Syn-COLG and within-plate (WPG) fields (Figs 5, 6), making their interpretation difficult. One possible way around this is to take into account trends in the elements, i.e., whether they increase or decrease with increasing silica, using only the lower silica end-member values to ascertain what field they plot in. Unfortunately this also produces ambiguous results, for example both Y and Nb actually decrease with increasing silica in a number of clans, meaning such clans start in the WPG field and move into the VAG or Syn-COLG fields, while other clans start in the latter fields. One important point to note, is that these tectonic diagrams were developed and based on, and, hence are most applicable, for Palaeozoic and younger granites. In particular, it has been well documented that Archaean granites are much lower in Y than most post-Archaean granites. What effects these differences have on the tectonic diagrams is not clear, though one effect for the Low-Ca group, at least, would be to move the WPG field to the left, i.e., a higher percentage of Low-Ca granites would fall within the WPG field, though notably not all. The other possible interpretation is that the Low-Ca granites belong to the post-orogenic/post-collisional class, a class not discriminated on such diagrams (Pearce et al., 1984). Such a classification is consistent with our own interpretation (see below).

The Syenitic group appears to suffer from similar problems as the Low-Ca group, also straddling most of the fields (Figs 5, 6). Modern examples of such rocks indicate they are not generated within a VAG environment, and rarely in a Syn-COLG setting (e.g., Eby, 1990; see below); clearly the discrimination diagrams are not valid for Archaean alkaline rocks, and, perhaps other WPG magmatism.

The final group, the High-HFSE group also shows a similar spread as the Low-Ca and Syenitic groups (Figs 5, 6). Notably, however, the Damperwah clan (northern Murchison Province, Fig. 6) falls entirely within the WPG field, consistent with our interpretation for this clan.

Granite types and other petrogenetic considerations
The use of broad granite types and groups as an indicator, also based on empirical observations, appear to have some success in delineating tectonic environments, but like all approaches becomes more difficult the older the rocks. Of all the Yilgarn granites, the Syenitic group is the most diagnostic. As discussed earlier, the bulk of the Syenitic group rocks are confined to the Eastern Goldfields Province, with two apparent age groups: ca. 2665 Ma, and 2650-2640 Ma (see discussion in Champion & Cassidy, this volume). Such rocks, and related sub-alkaline to alkaline granites, often grouped under the A-type granite nomenclature (e.g., Eby, 1990; Figs 7, 8), are typically found in modern environments in either extensional/rift or anorogenic settings - the latter more correctly thought of as regions undergoing tension/attenuation, such as post-orogenic, and/or post-collisional relaxation, or regions above mantle 'hot-spots'. Further, such rocks are associated with the presence of thick crust and high-heat flow, consistent with extension (Pitcher, 1993). If such tectonic and genetic models are adopted for the late Archaean, and more specifically the Eastern Goldfields Province, then it suggests that the periods ca. 2665 Ma and 2650-2640 Ma, the age of the syenites, must have experienced one of the above tectonic settings. The 2650-2640 Ma period has already been proposed to have been in some form of extensional or tensional setting by Smithies & Champion (1999), who suggested crustal delamination as the driving force. The widespread Low-Ca granites of this age are also consistent with such an environment (see below).

The newly documented 2665 Ma Syenitic group magmatism is somewhat more problematical, but would best appear to fit with some form of extensional ridge running up the eastern half of the Norseman-Wiluna belt, where the members of this age appear to be confined. There are a number of features that are unique to these older Syenitic rocks, including:

- the presence of moderate to large intrusions of more felsic and calcic monzonitic to quartz monzonitic rocks (identified by greater abundances of plagioclase, amphibole and quartz), e.g., Erayinia and Panakin clans;
- the temporal association with Mafic group granites, in particular the high-LILE subgroup (the Granny Smith Clan) which is common and largely restricted to ca. 2665 Ma;
- the temporal association with much of the High-Ca group, although the greatest peak in the latter magmatism would appear on present data to have been slightly earlier (Fig. 3).

The temporal association with the High-LILE Mafic subgroup (the Granny Smith clan), is considered particularly important as Champion & Cassidy (Chap. 2, this volume) suggested that the high-LILE component required for this clan may have been supplied by the Syenites or related to the process that produced such Syenitic rocks, e.g., some type of metasomatised mantle input. Such 'mixing' of magmas or, perhaps more probably sources, may also explain why the 2665 Ma syenites, in particular the Panakin and Erayinia clans are more calcic. The origin of the syenites and indeed the fluids required to produce the postulated metasomatised mantle is problematic (see discussion by Smithies & Champion, 1999). Regardless, it is evident from the Sm-Nd isotopic signatures that the LILE enrichment required for these rocks, be it in the mantle or at the base of the crust must have occurred not long before generation of the 2665 Ma syenites and high-LILE Mafic group rocks.

If we assume that the 2665 Ma syenites and high-LILE Mafic group rocks were indeed formed in some form of extensional environment, then it raises the question of how do the High-Ca granites, which on the basis of the present evidence also commonly straddle the 2665 Ma age, fit into such an environment? Given that the High-Ca granites were derived at high pressures, from either thickened crust or from a subducting slab, would suggest that the postulated rift environment was localised, partly consistent with the distribution of the 2665 Ma syenites. Notably, however, within the limits of the dating (errors of ± 3-8+ Ma), it is impossible to tell if the 2665 Ma syenites and High-Ca granites were indeed contemporaneous. One thing would appear certain though, and that is the requirement for a relatively extensive (and thick) continental crust at this time (ca. 2665 Ma). It is noted that the Yilgangi conglomerates which occur reasonably close to the postulated 2665 Ma extensional zone have an age (pre-2662 ± 5 Ma; Nelson, 1996), not inconsistent with such a tectonic interpretation.

As suggested in Chapter 2 (this volume), the chemical and petrological features of the Low-Ca granites are consistent with high temperature melting, from relatively dry source rocks. This is confirmed in Figures 7 and 8, which clearly show the A-type affinities of the Low-Ca granite group, particularly when it is noted that granites of this group trend from right to left on the Zr+Nb+Ce+Y plots (with increasing silica). As stated above, granites with such affinities, are typically generated in regions undergoing extension or tension/attenuation, (e.g., post-orogenic), or regions above mantle 'hot-spots' (Eby, 1990; Pitcher, 1993). The widespread nature of the Low-Ca magmatism, across the Yilgarn craton, at 2650-2630 Ma, suggests the whole craton was undergoing extension or post-orogenic attenuation at this time, possibly related to the end of the major D_2 compression within the Eastern Goldfields Province (as suggested by Smithies & Champion, 1999). This overall environment is consistent with the tectonic interpretation for the younger Syenitic group granites (Eastern Goldfields Province), and also the younger High-HFSE granites in the Murchison Province.

The High-HFSE group granites are also shown on the A-type discrimination diagrams (Figs 7, 8), from which it is clear that the Damperwah clan of the Murchison Province has strong A-type affinities. The other High-HFSE clans are, however, less obviously A-type, though their overall characteristics of elevated FeO*, TiO_2, Zr, Y for given silica content (higher than the Low-Ca granites), are consistent with A-type granites elsewhere (see Whalen et al., 1987; Eby, 1990), suggesting some affinity. It was noted in Chapter 2 that members of the High-HFSE group share a number of similarities (elevated FeO, Zr, Y) with the tholeiitic subgroup (e.g., Kathleen Valley clan) of the Mafic group, raising the possibility of some involvement of such tholeiitic rocks in the genesis of the High-HFSE granites. This notion was more strongly supported by the discovery, during the current project, of the more mafic High-HFSE clan (Bullshead) in the Eastern Goldfields Province. The currently available data is best interpreted to indicate that mafic tholeiitic magmas, or fractionates of such, have contributed to at least some of the High-HFSE granites, possibly via mixing and subsequent fractionation. In this regard it is not surprising, therefore, that many of these granites are spatially and temporally associated with chemically-similar felsic volcanics which form part of a bimodal basalt-rhyolite association (e.g., Hallberg et al., 1993). The obvious conclusion is that both the volcanics and the High-HFSE granites formed in a similar manner in a similar extensional or basin-forming environment, commonly at much the same time.

The latter conclusion, however, probably does not hold for the post-greenstone aged Damperwah clan of the Murchison Province. These younger granites (ca. 2640-2600 Ma) have chemistry clearly more akin to both true A-type granites (Fig. 8) and to within-plate granites (Fig. 6), and, accordingly are best interpreted as high temperatures melts emplaced in a tensional or extensional environment. This is entirely consistent with their temporal association with the Yilgarn-wide Low-Ca magmatism, and the younger Syenitic magmatism of the Eastern Goldfields Province, and the reported ca. 2640 Ma granulite metamorphic age from the south-west Yilgarn (Nemchin et al., 1994).

The final granite group, the High-Ca group, comprised of I-type trondhjemites, granodiorites and true granites, is difficult to assign to an unequivocal tectonic environment. As has been discussed in earlier chapters, the general characteristics of the High-Ca granites (low LILEs, sodic, Sr-undepleted), indicate derivation, at high pressures (>10 kbar), from a mostly mafic (broadly basaltic/amphibolitic), LILE-poor source. The high pressure origins for the majority of the High-Ca granites indicate derivation either deep within a thickened crust (>35-50 km) or, perhaps, from melting of a subducting slab (see Champion & Sheraton, 1997). Importantly, the range in the LILE and HFSE (between clans), however, indicates a more complex model, i.e., the involvement of at least two-components, either as a heterogeneous source (basaltic to quartz dioritic), or by some other process (assimilation of pre-existing crust, magma-mixing etc). The available evidence, e.g., presence of inherited zircons (especially good ca 2.8 Ma inherited ages in the Eastern Goldfields Province High-Ca granites), the Sm-Nd isotopic data (old model ages which suggest significant involvement of older crust), tend to favour a thickened crust as the source. This would particularly appear to be the case for the northern Murchison Province where a range of pressures can be deduced from the chemistry, ranging from the Sr-depleted chemistry of the widespread Eily Eily clan (lower pressure with residual plagioclase in the source), to the flat HREE patterns and lack of negative Eu anomalies in many of the High-Ca granites (no residual plagioclase but residual amphibole instead of garnet), to the Sr-undepleted Y-depleted end-members (no residual plagioclase but residual garnet).

Regardless, of whether a thickened crustal or subducting slab origin is invoked (and possibly both were operative at different times), both hypothesis appear to require the operation of some form of convergent tectonics, to either produce the thickened crust or the subduction environment. Given the range in ages of the High-Ca group, especially within the Murchison Province, it is evident that such an environment must have been operative, at least intermittently, from ca 3.0 Ga to ca 2.66 Ga. This conclusion raises a number of important points. Firstly it is apparent that while voluminous High-Ca magmatism was being produced in such a tectonic environment in the Eastern Goldfields Province at 2680-2660 Ma, this voluminous magmatism did not extend to the Murchison and Southern Cross provinces (Fig 3) where the majority of High-Ca magmatism appears to have occurred earlier (>2700 to 2680 Ma). These differences may reflect a number of possible scenarios: 1) the Murchison and Southern Cross provinces were separate from the Eastern Goldfields Province before and/or during this period; 2) the thermal regime at this time was such that granite production was largely confined to the Eastern Goldfields Province, such as in a typical modern-day convergent environment; or, 3) the change across the two provinces is actually diachronous, as in a migrating arc-environment.

Clearly further geochronology is needed, particularly along the eastern margin of the Southern Cross Province.

Secondly, the change over at ca 2655 Ma from dominantly High-Ca to craton-wide dominantly Low-Ca magmatism must reflect a fundamental change from convergent tectonics, at least in the Eastern Goldfields Province, to craton-wide extension or tension/relaxation (see earlier). The exact nature of this tectonic transition is largely dependent on the origin of the High-Ca granites. If the High-Ca granites were generated in thickened crust, then melting shifted to higher crustal-levels (the site of Low-Ca generation), with the thickened lower crust (High-Ca source) either somehow insulated from further melting or removed. The latter is favoured given the apparently higher thermal gradient required for the Low-Ca granites. In this regard, Smithies & Champion (1999) suggested that this post 2655 Ma thermal event may have resulted from lower-crustal delamination following the D_2 shortening deformation in the Eastern Goldfields Province, heralding an additional tectonothermal event in the Yilgarn Craton, contemporaneous with lower-middle crustal high-grade metamorphism and regional Au mineralisation. If, however, the High-Ca granites were largely generated by slab-melting, then the change over to Low-Ca (and syenitic) magmatism may simply reflect some form of wide-scale extension, perhaps not unlike that presently operating in the Basin and Range province in the western United States, although with some differences.

Finally, the large volume of High-Ca granites across the Yilgarn craton require a correspondingly larger source (3 or more times volumetrically larger), implying, if indeed the High-Ca granites were largely crustal in origin, a very significant volume of pre-existing crust of basaltic to andesitic composition. More importantly, the Sm-Nd isotopic data shows that the High-Ca source rocks are, on average, younger than the sources of the Low-Ca magmatism. This coupled with the modelled depths of formation which indicate the High-Ca source was at a deeper crustal level (pressure) than the Low-Ca source, indicates that not only was the High-Ca source younger, but it was also underlying the older Low-Ca source rocks. If the High-Ca granites were indeed derived within thickened crust then the geometry of sources requires that the High-Ca source must have been underplated onto, or perhaps underthrust beneath, the existing older crust (comprising the Low-Ca and High-HFSE source rocks); further the isotopic data indicates that this process must have happened at different times in the Murchison Province versus the Eastern Goldfields Province. Both of these hypothesised scenarios (underplating/underthrusting) are broadly consistent with the preferred source composition for the High-Ca granites, i.e., largely basaltic. For example, Smithies & Champion (2000), amongst others, have suggested that much of the Archaean was characterised by flat subduction or tectonic underplating rather than modern-day subduction. Such a scenario would produce a younger, deep, mafic layer beneath older crust. This model also has the advantage of making the 2 options for genesis of the High-Ca granites (thickened crust or subducting slab) essentially the same mechanism.

	3800 - 4100 Ma Inherited zircons – Narryer Gneiss Terrane
3730-3300 Ma	Narryer Gneiss Terrane, e.g., Meeberrie gneiss Pendants of gneiss, e.g., Murgoo gneiss, within the western Murchison Province – related to Narryer Gneiss Terrane?
~3020-2920 Ma	Greenstone formation in the Murchison and Southern Cross provinces, including plume-related? komatiitic magmatism. Possibly two periods of greenstone formation with a break ca. 2980-2960 Ma.
~3020-2920 Ma	High-Ca and Mafic? group magmatism in the Murchison and Southern Cross provinces indicate convergent tectonics, while possible High-HFSE group magmatism is related to felsic volcanism within the greenstone belts. Magmatism of this age appears to be absent in the Western Gneiss Terrane.
>2810-2750 Ma	Isotopic and inherited zircon evidence suggest Narryer Gneiss Terrane thrust over Murchison Province some time during this period.
ca. 2820-2800 Ma	Tholeiitic intrusions (eg Windimurra, Youanmi, Atley layered intrusions) emplaced along a broad zone approximating the Murchison-Southern Cross provinces boundary; also felsic volcanism. The presence of these mafic complexes suggest that the Murchison and Southern Cross provinces were already one entity at this time.
2820-2780 Ma	Minor? greenstone formation in the Murchison and Southern Cross provinces during this period. High-Ca and Mafic? group magmatism in the Murchison and Southern Cross provinces indicate convergent tectonics.
~2760-2745 Ma	Greenstone formation in the Murchison province during this period, consistent with High-HFSE magmatism. High-Mg Mafic magmatism (Norie clan) indicates subduction environment at or preceding this period in the north-west Murchison. Also consistent with High-Ca magmatism.
~2760-2750? Ma	Greenstone formation, of unknown extent, of this age or older, in the Duketon region of the Eastern Goldfields Province. High-Ca group magmatism indicate convergent tectonics, at least in west-central Eastern Goldfields Province, while tholeiitic Mafic magmatism (Duketon greenstone belt) indicate some extension.
~2745-2720 Ma	Significant greenstone formation in the Murchison and Southern Cross provinces High-Ca group magmatism indicate convergent tectonics
2740-2730 Ma	Tholeiitic Mafic group and apparent High-HFSE magmatism of this age in the Eastern Goldfields Province, suggests some greenstone formation at this time in the region.
2720-2700 Ma	Greenstone formation in all 3 provinces, though end of greenstone in Murchison and Southern Cross provinces, first phase of major greenstone formation in Eastern Goldfields Province (especially Kalgoorlie terrane). Widespread 2.705 Ma komatiitic (plume-related) magmatism in the Eastern Goldfields Province. High-Ca and Mafic group magmatism in all 3 provinces indicate convergent tectonics, in at least parts of those provinces.

Table 7A. Interpreted tectonothermal history for the Murchison, Southern Cross and Eastern Goldfields Provinces, pre-2700 Ma.

2700-2670 Ma	High-Ca magmatism in the Murchison and Southern Cross provinces suggest some convergent tectonics. Presence of some Low-Ca granites of this age, though, appears to indicate extension in parts of the provinces. Significant greenstone formation in the Eastern Goldfields Province, accompanied by High-HFSE group magmatism. High-Ca and Mafic group magmatism indicate convergent tectonics.
pre-2680 Ma?	Docking of Southwest Gneiss Terrane. Actual age of collision poorly constrained.
2670-2655 Ma	Voluminous High-Ca group magmatism, accompanied by significant Mafic group magmatism, indicate convergent tectonics within the Eastern Goldfields Province. Syenitic (and High-HFSE?) group magmatism at ca. 2665 Ma, indicate the presence of a broad? zone of NNE-SSW extension in the eastern half of the Eastern Goldfields Province, roughly corresponding to the Celia lineament. Conglomeratic sediments (e.g., Yilgangi, Kurrawang, Merougil, Penny Dam), probably deposited within this period. Minor High-Ca and Low-Ca group magmatism in the Murchison and Southern Cross provinces. Compared to the Eastern Goldfields Province, this is a period of relative (but not total) magmatic quiescence.
2655-2600 Ma	Widespread Low-Ca magmatism (especially 2655-2630 Ma) across the craton, including the gneiss terranes. Tectonic environment either extensional or tensional (post-collision or post-orogenic). This interpretation supported by the widely distributed, but minor, Syenitic group magmatism in the Eastern Goldfields Province, and the high-LILE High-HFSE magmatism in the Murchison Province.
2650-2640 Ma	Granulite metamorphism - Southwest Yilgarn region
2640-2630 Ma	Widespread gold mineralisation.

Table 7b. Interpreted tectonothermal history for the Murchison, Southern Cross and Eastern Goldfields Provinces, post-2700 Ma.

Conclusions

A summary tectonothermal history for the Murchison, Southern Cross and Eastern Goldfields provinces is given in Table 7, with speculative tectonic environments listed. A number of overall conclusions can be drawn, as follows:

- The Murchison and Southern Cross provinces have shared a generally common long history from around 3000 Ma. Certainly, the two provinces were largely one entity by ca. 2820 Ma when the large layered mafic complexes were emplaced, presumably in some type of extensional environment. Post-2800 Ma magmatism in the two provinces has largely reworked pre-existing crust. The one apparent difference between the 2 provinces, the presence of 2760-2740 Ma magmatism in the northern Murchison, appears to be related to a subduction environment in that north-west Murchison region at the time. It can be speculated that the docking of the Western Gneiss terrane (including the Narryer) may be related to such an environment.
- The Eastern Goldfields Province, on the other hand appears to be generally younger than the other 2 provinces, with good evidence for some fundamental change approximately corresponding to the position of the Ida Lineament. The isotopic and inherited zircon evidence suggests that while there may be older crust (pre-2800 Ma)

beneath the western half of the Eastern Goldfields Province, it certainly doesn't appear to be underlying the eastern half. The evidence also appears to suggest that the Eastern Goldfields Province grew by lateral accretion from west to east.

- The peak of granite magmatism in the Eastern Goldfields Province corresponds to a period of relative magmatic quiescence in the Murchison and Southern Cross provinces. It may be speculated that this may indicate that collision of the former with the 2 latter provinces occurred around this time (possibly D_2 in the former), but the evidence is equivocal.
- Some fundamental change appears to have occurred across the craton around 2660-2655 Ma, where magmatism changed from dominantly High-Ca to dominantly Low-Ca, the latter generated in some form of extensional or tensional environment, possibly post-collisional, as suggested in the previous point, but almost certainly post-D_2 (in the Eastern Goldfields Province). This widespread post-orogenic? Low-Ca group magmatism extended to 2630 Ma (and younger?), a period that overlaps with the accepted age of major gold mineralisation (2640-2630 Ma) and with granulite-facies metamorphism in the southwest Yilgarn (Nemchin et al., 1994).

Finally, it is noted that a number of conclusions can be made about the general study and approach used:

- this study has demonstrated the validity of the granite group approach (Champion & Sheraton, 1997), but also clearly shown that there are many important sub-groups present within the granites,
- the study has introduced the 'Clan' nomenclature. In a perfect world such an extra layer of classification would not be needed, but the approach was deemed necessary given the lack of outcrop and age control on many of the granites (i.e., correct suite and supersuite classification requires identification of individual plutons - this is not possible for many of the external granites in the Yilgarn),
- the current amount of available geochronology has identified the general magmatic patterns in the granites. Further work is needed to confirm or refute these patterns, and to provide greater within province detail,
- finally, it is becoming very obvious that a temporally-constrained structural history is urgently required.

References

Champion, D.C. & Sheraton, J.W., 1997. Geochemistry and Sm-Nd isotopic systematics of Archaean granitoids of the Eastern Goldfields Province, Yilgarn Craton, Australia: constraints on crustal growth. Precambrian Research, 83, 109-132.

Eby, G.N, 1990. The A-type granitoids: A review of their occurrence and chemical characteristics and speculation on their petrogenesis. Lithos, 26, 115-134.

Fletcher, I.R., Libby, W.G. & Rosman, K.J.R., 1994. Sm-Nd model ages of granitoid rocks in the Yilgarn Craton. Geological Survey of Western Australia, Professional Papers Report 37, pp. 61-74.

Hallberg, J.A., Ahmat, A.L., Morris, P.A., & Witt, W.K., 1993. An overview of felsic volcanism within the Eastern Goldfields Province, Western Australia. Australian Geological Survey organisation, Record 1993/54, p. 29-32.

Nelson, D.R., 1996. Compilation of SHRIMP U-Pb zircon geochronology data, 1995. Geological Survey of Western Australia, Record 1996/5.

Nelson, D.R., 1997. Compilation of SHRIMP U-Pb zircon geochronology data, 1996. Geological Survey of Western Australia, Record 1997/2.

Nemchin, A.A. & Pidgeon, R.T., 1997. Geochronology of granitoids in the western Yilgarn Craton. Australian Geological Survey Organisation, Record 1997/41, 59-64.

Nemchin, A.A., Pidgeon, R.T. & Wilde, S.A., 1994. Timing of late Archaean granulite facies metamorphism in the southwest Yilgarn Craton of Western Australia: evidence from U-Pb ages of zircons from mafic granulites. Precambrian Research, 68, 307-321.

Nutman, A.P., Kinny, P.D. & Price, R., 1993. Large-scale crustal structure of the northwestern Yilgarn Craton, Western Australia: evidence from Nd isotopic data and zircon geochronology. Tectonics, 12, 971-981.

Pearce, J.A., Harris, N.B.W., & Tindle, A.G., 1984. Trace element discrimination diagrams for the tectonic interpretation of granitic rocks. Journal of Petrology, 25, 956-983.

Pitcher, W.S., 1993: The Nature and Origin of Granite. Blackie Academic & Professional, Chapman and Hall, London.

Qiu, Y., groves, D.I., & McNaughton, N.J., 1997. Deep-seated granitoids: implications for late Archaean subduction-collision-lithospheric delamination and gold mineralisation in the Yilgarn Craton. Australian Geological Survey Organisation, Record 1997/41, p. 65-70.

Schiøtte, L. and Campbell, I. H., 1996, Chronology of the Mount magnet granite-greenstone terrain, Yilgarn Craton, Western Australia: implications for field based predictions of the relative timing of granitoid emplacement.: Precambrian Research, v. 78, p. 237-260.

Smithies, R.H. & Champion, D.C., 1999. Late Archaean felsic alkaline igneous rocks in the Eastern Goldfields, Yilgarn Craton, Western Australia: a result of lower crustal delamination? Journal of the Geological Society of London, 156, 561-576.

Smithies, R.H., & Champion, D.C., 2000. The Archaean High-Mg diorite suite: Links to Tonalite-Trondhjemite-Granodiorite magmatism and implications for Early Archaean crustal growth. Journal of Petrology, 41, 1653-1671.

Watkins, K.P & Hickman, A.H., 1990. Geological evolution and mineralisation of the Murchison Province, Western Australia. Geological Survey of Western Australia, Bulletin 137.

Whalen, J.B., Currie, K.L., & Chappell, B.W., 1987. A-type granites: geochemical characteristics, discrimination and petrogenesis. Contributions to Mineralogy and Petrology, 95, 407-419.

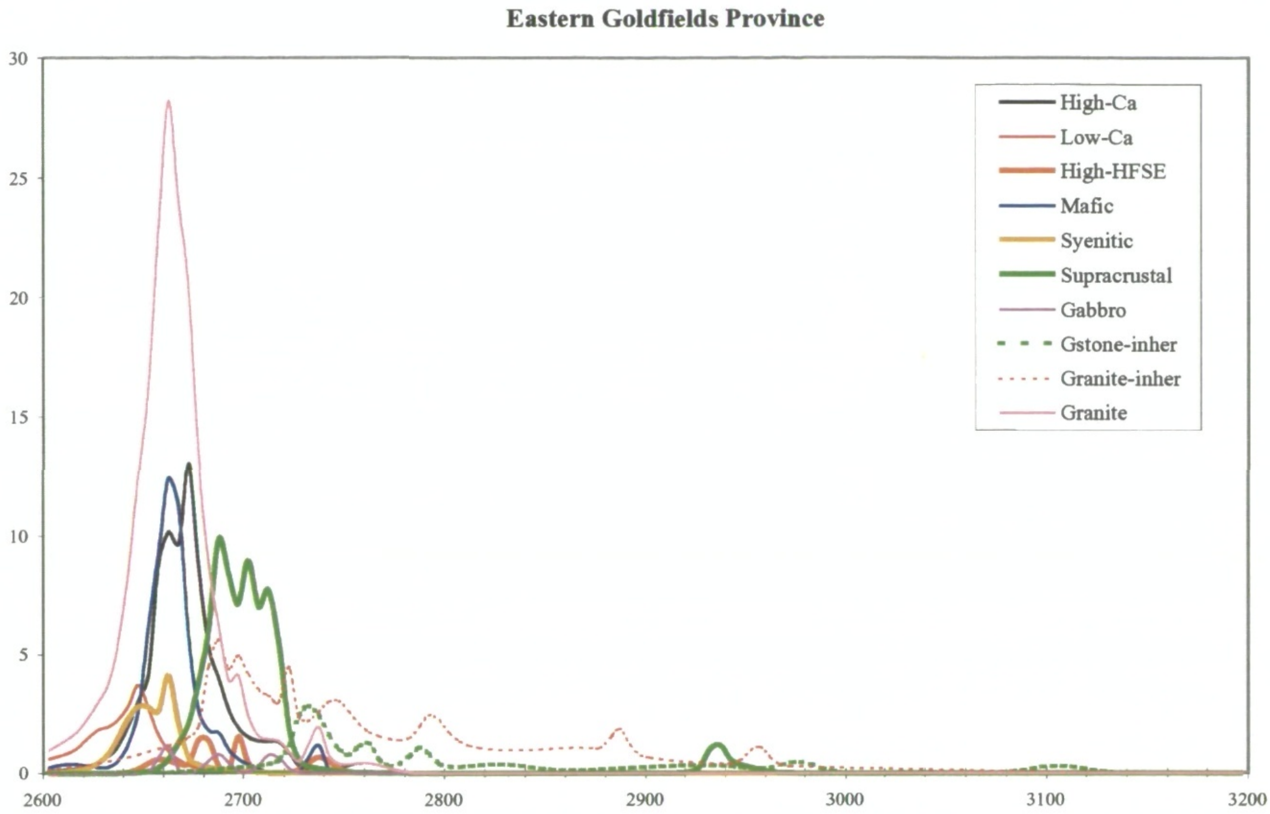

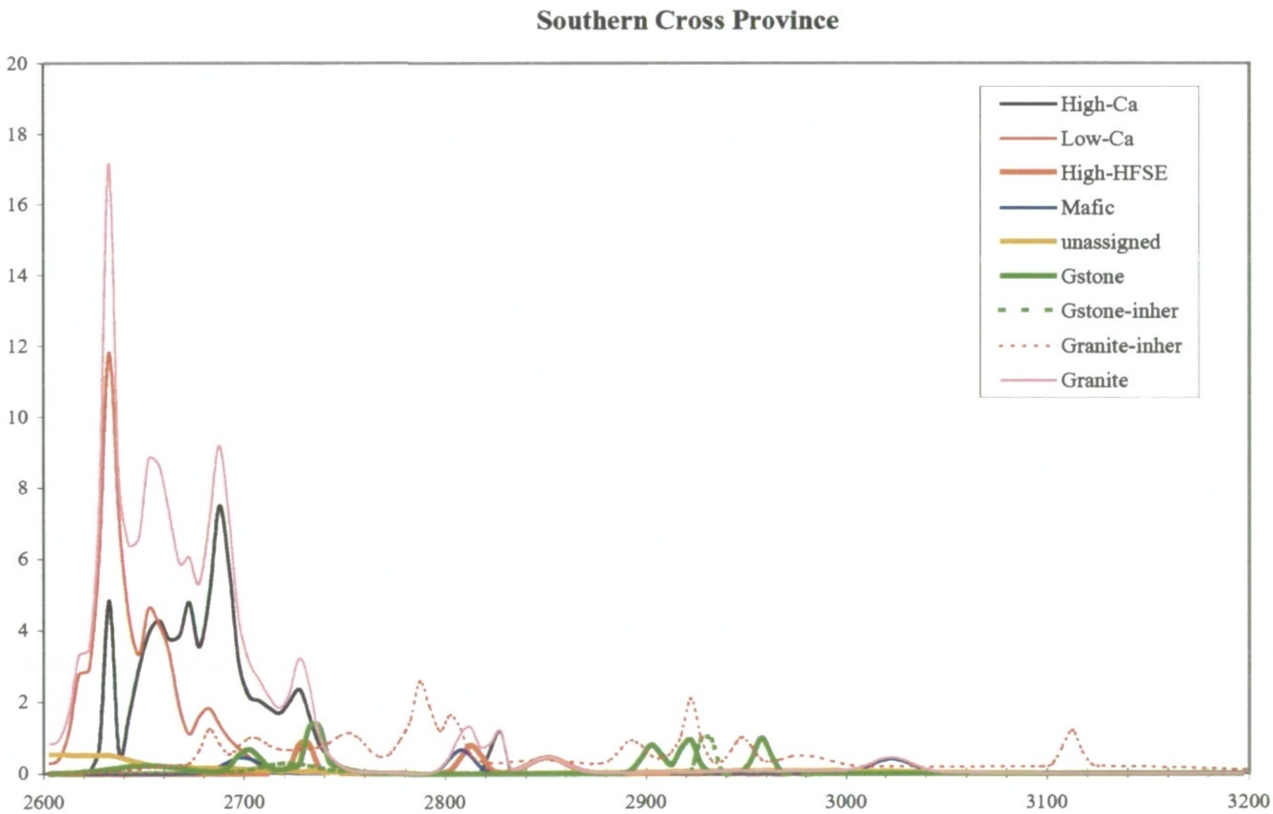

Figure 1A. Frequency plots showing ages of granite magmatism, inherited zircons and greenstone ages (magmatic, xenocrystic or detrital), in the period 2600-3200 Ma, for the Southern Cross and Eastern Goldfields Provinces.

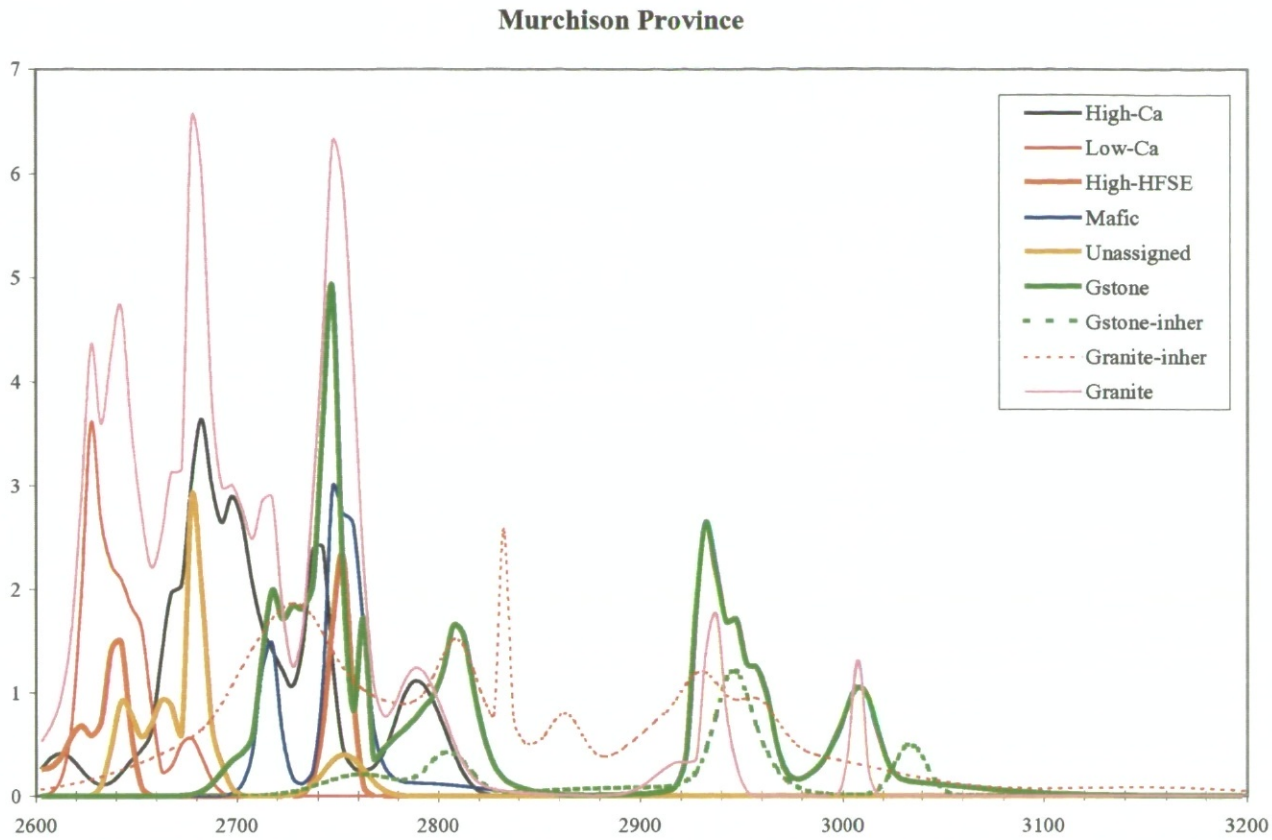

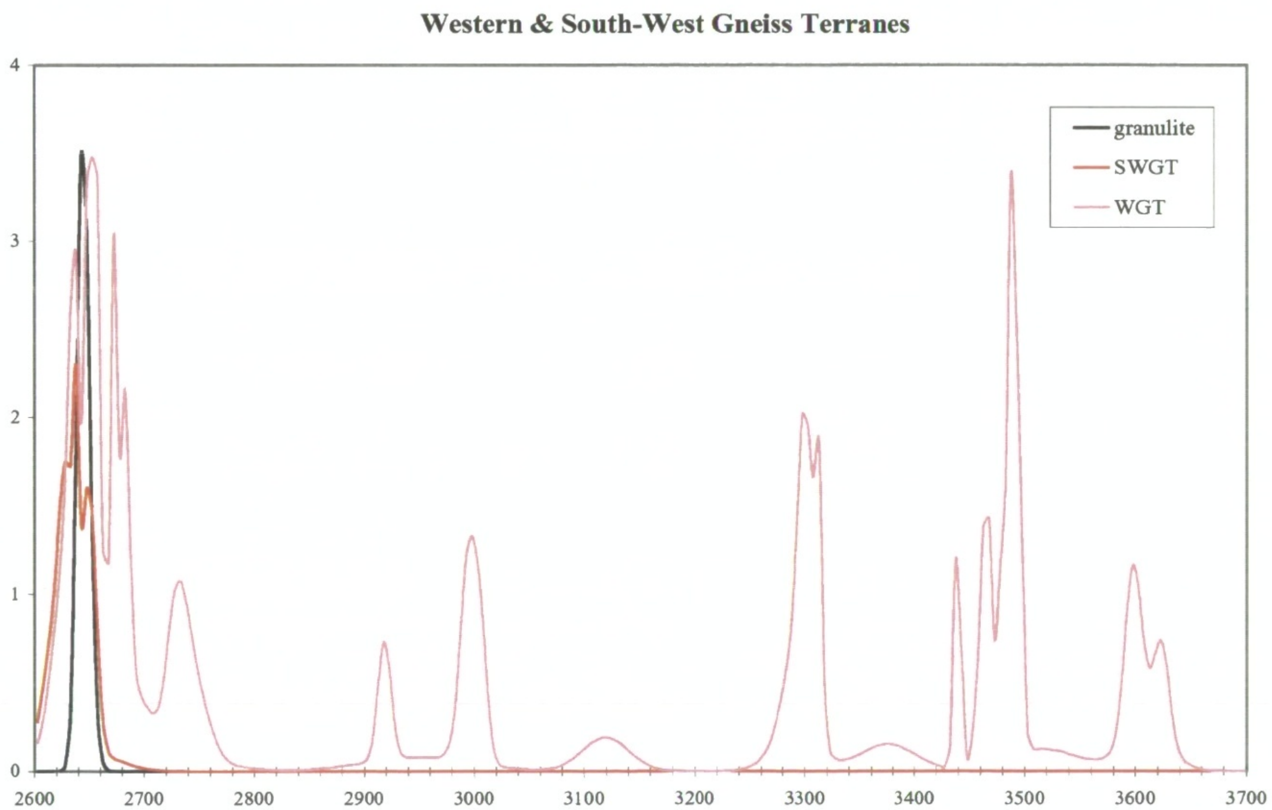

Figure 1B. Frequency plots showing ages of granite magmatism, inherited zircons and greenstone ages (magmatic, xenocrystic or detrital), in the period 2600-3200 Ma for the Murchison Province, and 2600-3700 Ma for the gneiss terranes.

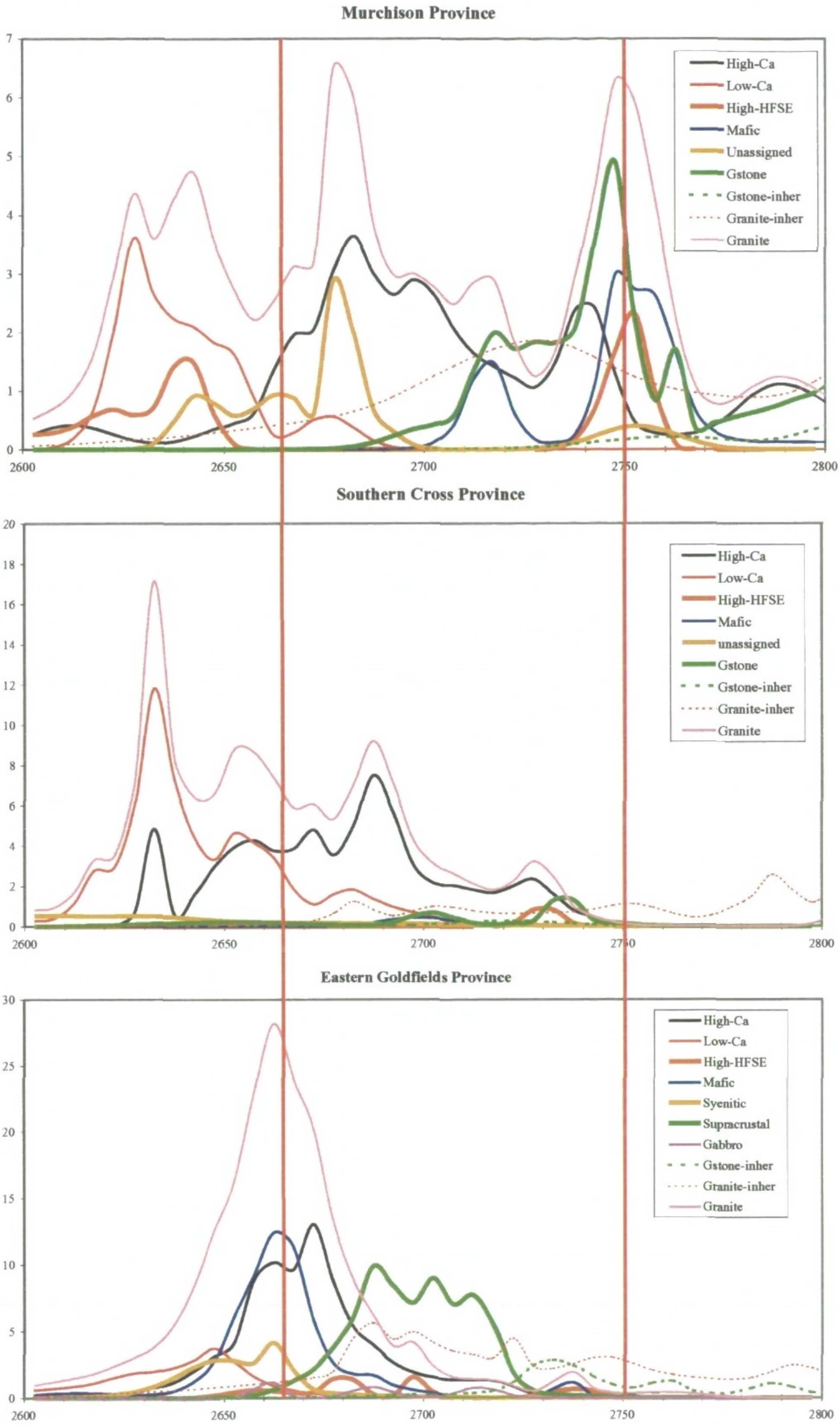

Figure 2. Frequency plots showing ages of granite magmatism, inherited zircons and greenstone ages (magmatic, xenocrystic or detrital), in the period 2600-2800 Ma, for the Murchison, Southern Cross and Eastern Goldfields Provinces. The red tie-lines denote 2665 and 2750 Ma respectively.

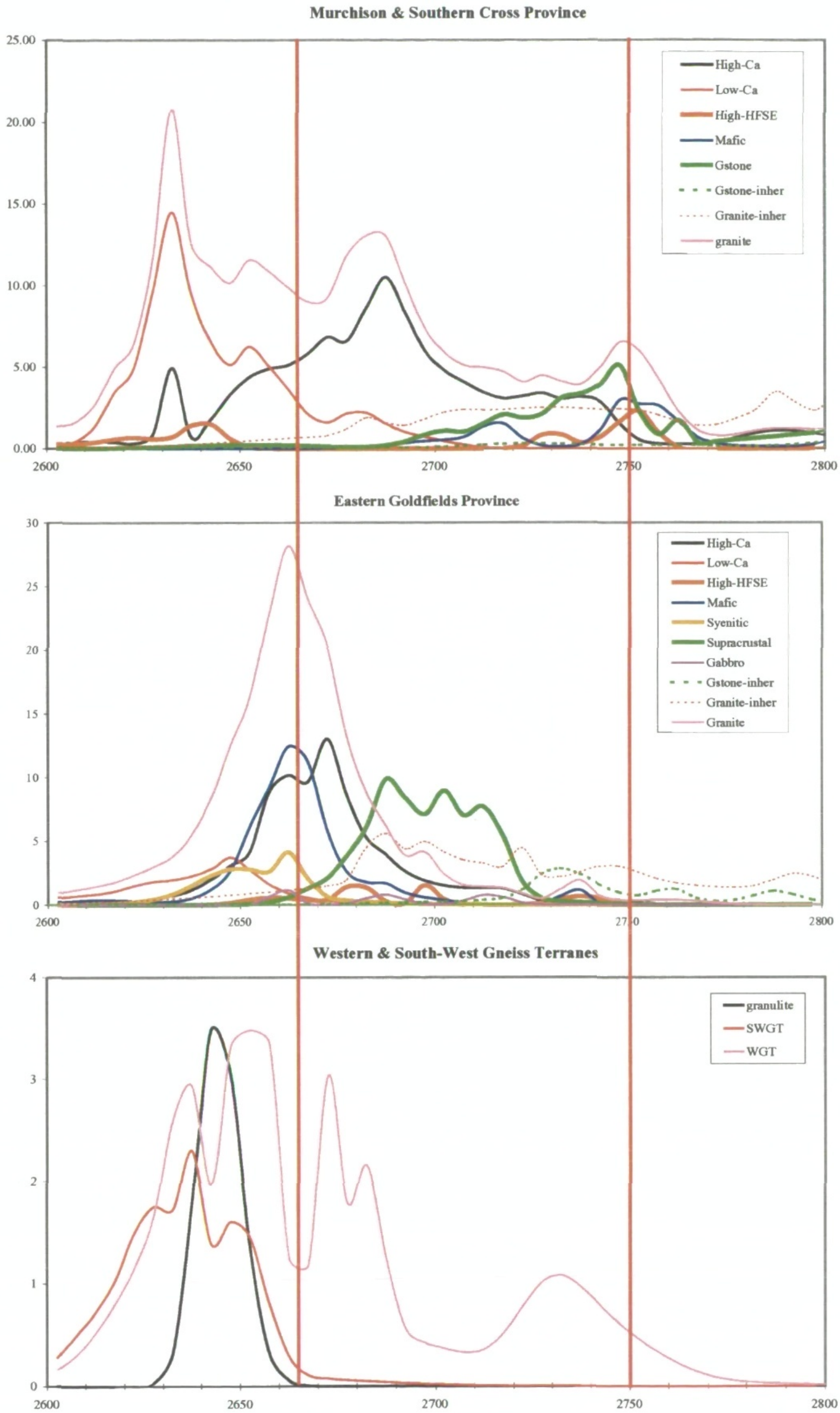

Figure 3. Frequency plots showing ages of granite magmatism, inherited zircons and greenstone ages (magmatic, xenocrystic or detrital), in the period 2600-2800 Ma, for the Murchison-Southern Cross provinces, for the Eastern Goldfields Province, and for the respective gneiss terranes. The red tie-lines denote 2665 and 2750 Ma respectively.

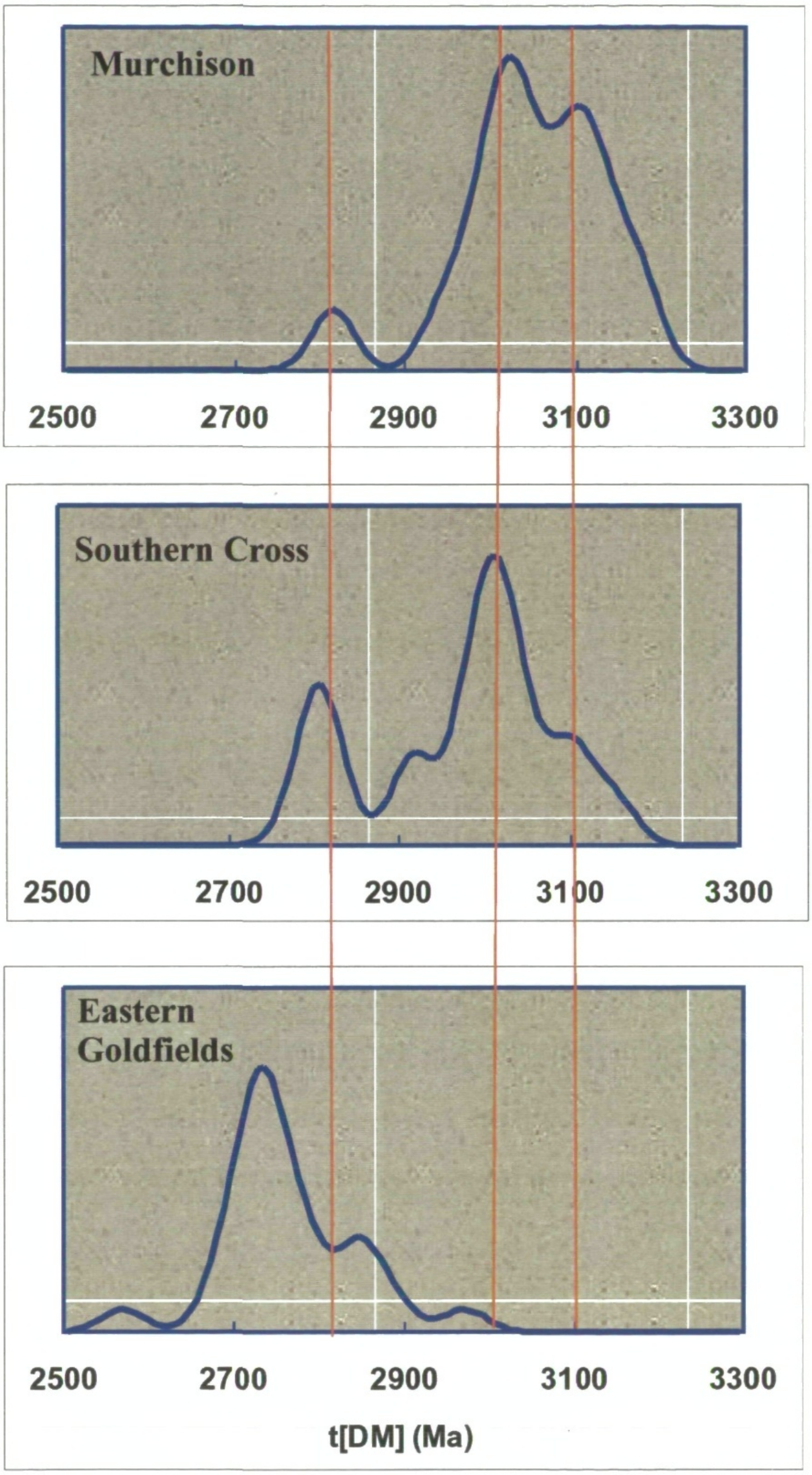

Figure 4. Frequency plots showing Nd depleted mantle model ages for granites of the Murchison, Southern Cross and the Eastern Goldfields Province. The red tie-lines are used to show the similarity of peaks within the Murchison and Southern Cross provinces. Refer to Fletcher & McNaughton (Chap 7, this volume) for isotopic details.

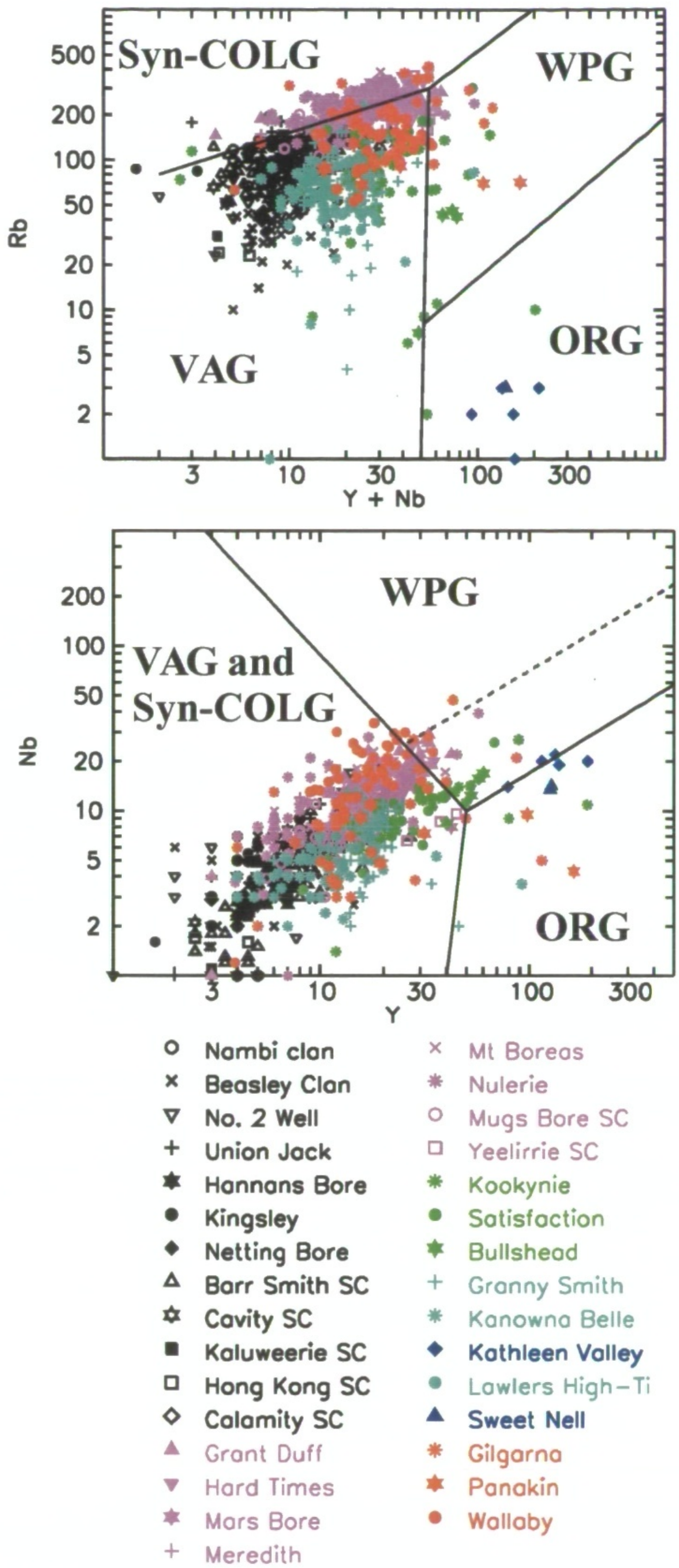

Figure 5. Tectonic discrimination diagrams for the clans of the High-Ca (black), Low-Ca (magenta), High-HFSE (green), Mafic (light & dark blue), and Syenitic (red) groups of the northern Eastern Goldfields and north-eastern Sothern Cross Provinces. Tectonic discrimination fields from Pearce et al. (1984). WPG = within-plate granite; Syn-COLG = syn-collisional granite; VAG = volcanic arc granite, and ORG = ocean ridge granite.

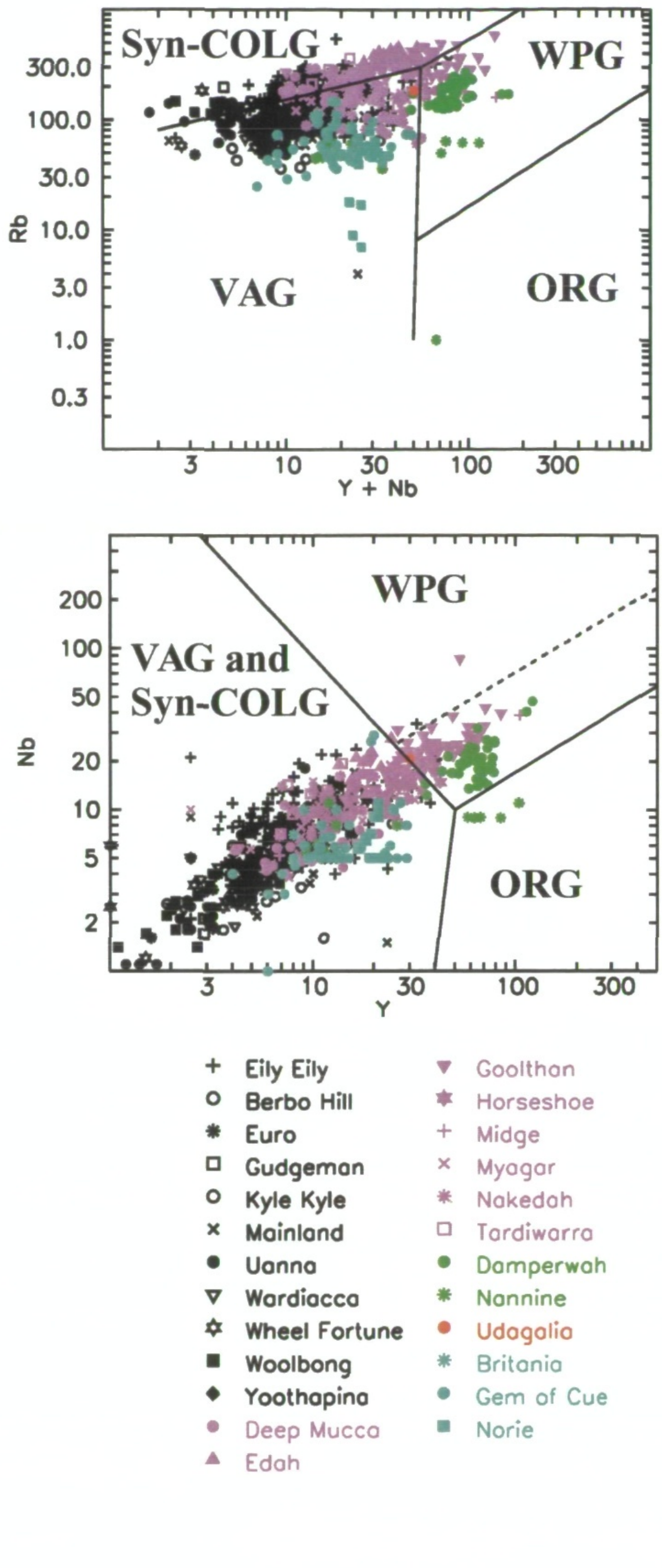

Figure 6. Tectonic discrimination diagrams for the clans of the High-Ca (black), Low-Ca (magenta), High-HFSE (green), Mafic (blue), and Syenitic (red) groups of the northern Murchison Province. Tectonic discrimination fields from Pearce et al. (1984). WPG = within-plate granite; Syn-COLG = syn-collisional granite; VAG = volcanic arc granite, and ORG = ocean ridge granite.

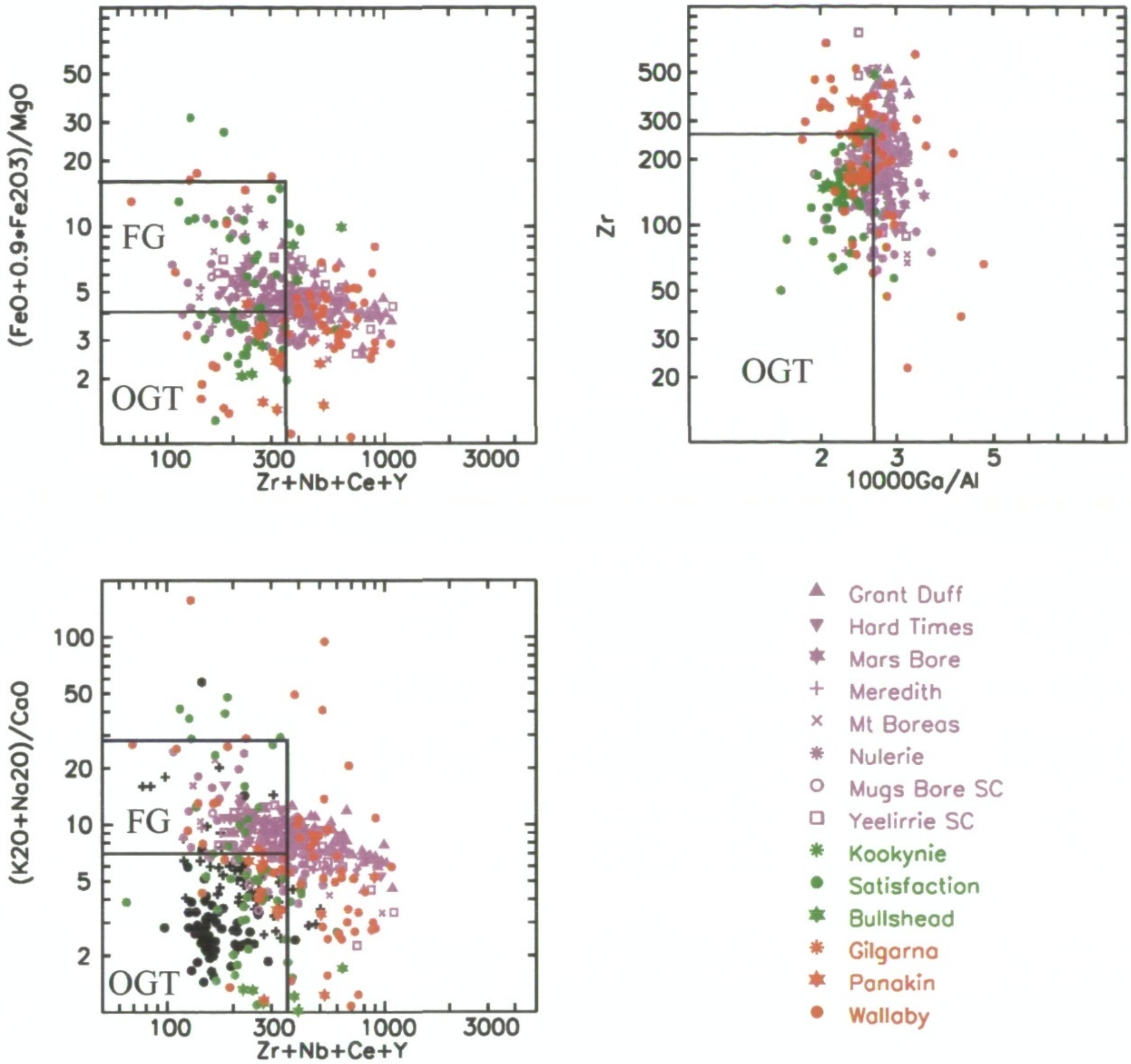

Figure 7. A-type discrimination diagrams for the clans of the Low-Ca (magenta), High-HFSE (green), and Syenitic (red), groups of the Eastern Goldfields Province. Discrimination diagrams from Whalen et al. (1987). FG = fractionated granite, OGT = unfractionated I-, S- and M-types. Union Jack clan (black +) and Beasley clan (black *) of the High-Ca group, also shown on the (K2O+Na2O)/CaO plot for comparison.

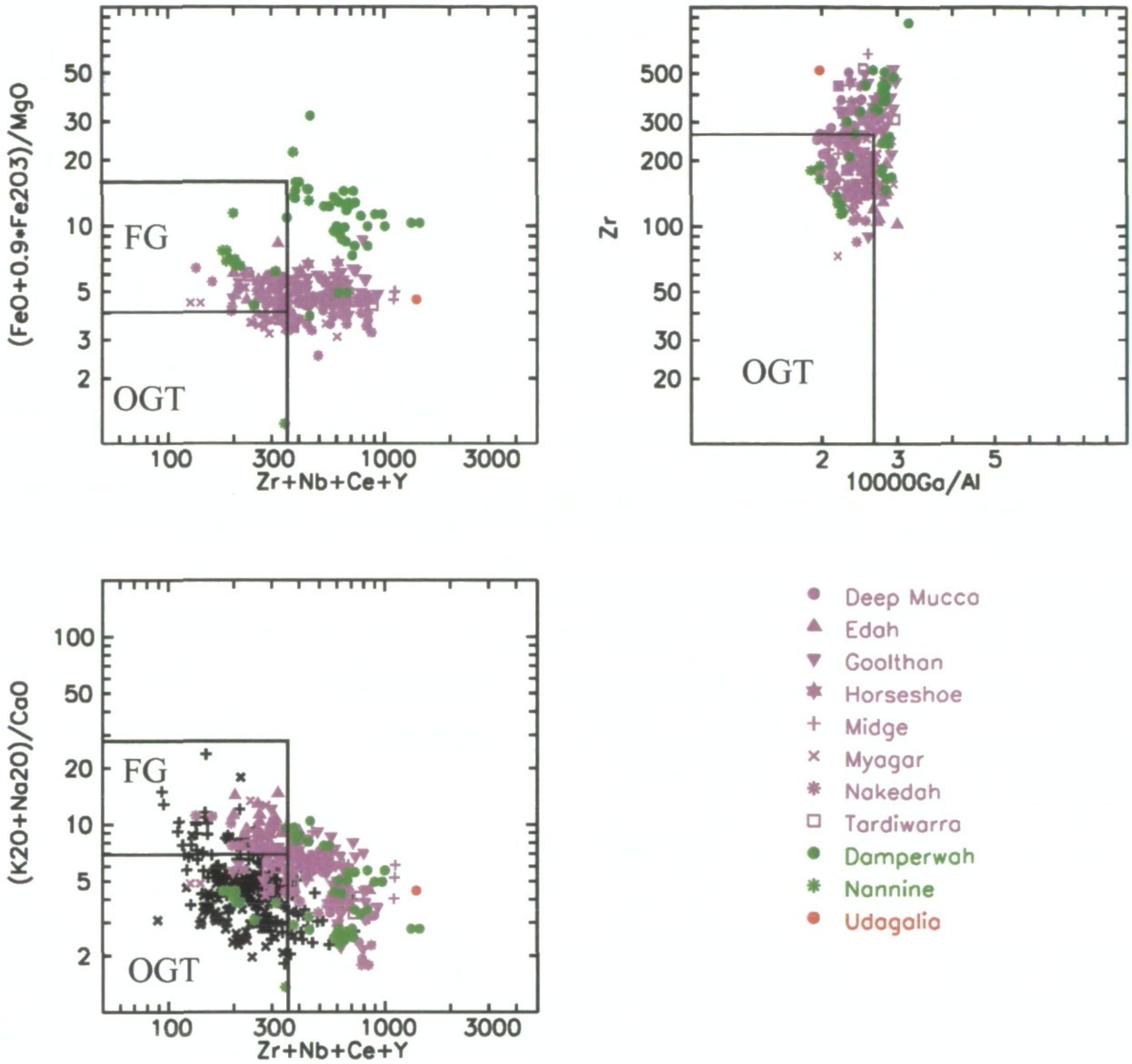

Figure 8. A-tpe discrimination diagrams for the clans of the Low-Ca (magenta), High-HFSE (green), and Syenitic (red), groups of the Murchison Province. Discrimination diagrams from Whalen et al. (1987). FG = fractionated granite, OGT = unfractionated I-, S- and M-types. Eily Eily clan (black +) and Mainland clan (black x) of the High-Ca group, also shown on the (K2O+Na2O)/CaO plot for comparison.

Chapter 9
Granitoids of the Yilgarn Craton: Links to mineralisation

Kevin F. Cassidy & David C. Champion

Summary

The metallogenic significance of granitoids of the Yilgarn Craton, with specific reference to orogenic gold mineralising systems, can be summarised by the following observations.

1. Given the major orogenic gold mineralising event in the Yilgarn Craton was at 2.64-2.63 Ga, then only two granite groups are contemporaneous with this event, namely the Low-Ca and Syenitic groups. The Low-Ca group is the second most dominant group (>20 percent by area) within the Yilgarn Craton. Low-Ca granitoids are more common within the 'external' granitoid regions of all Provinces, and the abundance of these granitoids with greenstones at high metamorphic grades within the Southern Cross Province, strongly suggests that this granite type underlies a significant part of the greenstones within the Eastern Goldfields Province.

2. Low-Ca granitoids are examples of the felsic, moderately to strongly oxidised, fractionated class of granites - a group that includes granitoids elsewhere associated with Au mineralisation, e.g. Telfer. Notably, however, there appear to be no examples of gold mineralisation within these granites in the Yilgarn, although this is also the case at Telfer, Pine Creek, etc., where Au mineralisation is not in the granitoids but is adjacent/distal to granitoids. A possibly similar scenario may exist for the Yilgarn; however, this does not imply that the granitoids are the actual source of Au (i.e., fluids may be magmatic but gold is scavenged from greenstones).

3. Selected Low-Ca group granitoids within the Southern Cross (e.g., Boorabbin suite, Beetle Association) and Murchison (Dutakajin suite, Goolthan Association) provinces contain a variety of fluid release structures and miarolitic-like cavities (this study; also J. Ridley, written communication, 2000). The fluid release structures have the appearance of rootless pegmatoid zones infilled by euhedral feldspar and quartz. Sub-parallel biotite-rich 'oikocrystic' zones are present in the Boorabbin granitoid (plutno 293504) in the Southern Cross Province. The 'oikocrysts' enclose euhedral quartz and feldspar crystals. Quartz from some of the rootless pegmatoid zones and the 'oikocrysts' contain a range of low salinity, aqueous-carbonic (H_2O-CO_2) fluid inclusions. The compositions of the fluid inclusions are very similar to fluids present in the majority of orogenic gold deposits. The late timing of the Beetle Association granitoids (and Low-Ca group granitoids in general) and the presence of abundant fluid inclusions of ?late-magmatic origin suggests that the Low-Ca granitoids may have provided some fluid into the greenstone belts as they crystallised at mid-crustal depths (>5-15 km).

4. Orogenic gold mineralisation appears to be spatially associated with members of all the granitoid groups, i.e., High-Ca, Low-Ca, Mafic, High-HFSE and Syenitic groups; although members of the 'high-LILE' clans of the Mafic host the most significant mineralisation present in granitoids. Significant mineralisation is also present in isolated units of the

Syenitic group and some mafic members of the High-Ca group. The mafic compositions appear to be an important factor given that the Mafic group, in particular, appears to be a strongly favoured host. With the exception of granitoids belonging to the Syenitic and Low-Ca group, granitoids hosting orogenic gold mineralisation in the Yilgarn Craton were emplaced prior to 2.65 Ga. The structural control on the localisation of the gold deposits and the diversity in regard to the degree to which granitoids are mineralised or not within deposits, (e.g., Granny Smith, Wallaby, Sunrise in the Laverton tectonic zone), suggests a largely structural and/or competency contrast role by the granitoids. This does not, however, explain the preferential favouring as hosts for orogenic gold mineralisation of 'high-LILE' and subordinate 'low-LILE' Mafic group granitoids. One possible explanation is that the distribution of the members of the Mafic (as well as the Syenitic) granitoid groups is largely controlled by the same crustal structures that were utilised by the mineralising fluids. It should be noted that other suggestions are possible, e.g., favourable rheologies, favourable reactive chemistry, earlier gold events? One important factor is the presence within a number of orogenic gold deposits (e.g., Granny Smith, Porphyry, ?Wallaby) of early magnetite ± biotite ± hematite (oxidising) alteration (and anomalous mineralisation?) that is overprinted by later (age difference unknown), typical carbonate-sericite alteration and economic mineralisation. This may indicate some degree of host granitoid magmatic input, at least for some granitoid-hosted orogenic gold mineralisation.

5. Finally, given that exploration is now largely concentrating on areas under cover, it is worth noting that it is not easy to discern granitoid groups (or even their ages) undercover (or under greenstones) from either geological or geophysical data alone. The syenites, however, do tend towards stronger magnetic responses, although in some cases this strong magnetic response may be due to early magnetite-rich alteration rather than syenite signature (possibly case at Wallaby, also Tin Dog and Jupiter). In this regard the identification of individual granitoids areas under cover as well as within or under the supracrustal package would appear to be the first priority, followed by the determination of the granitoids role and relationship to the structural evolution within the region. A recommendation for future research includes determining ways of 'seeing' granitoids at depth as well as improving the understanding of the topology of the granite-greenstone interface.

Introduction

Recent advances in the understanding of orogenic lode-gold deposits are summarised by Groves et al. (2000), Hagemann & Cassidy (2000), Kerrich et al. (2000) and Ridley & Diamond (2000). A shortened version of Hagemann & Cassidy with emphasis on the key features of orogenic gold mineralising systems is included as Appendix 1. This includes discussion on the source of hydrothermal fluids in such systems. The general consensus is that the ore fluid in orogenic lode-gold mineralising systems is a low-salinity mixed aqueous-carbonic fluid that have broad similarities in terms of major molecular components, isotope ratios and ore geochemistry. Ridley & Diamond (2000) succinctly demonstrate that, given the present geological and geochemical understanding of the mineralising systems, either a granitic magmatic or a metamorphic devolatilisation model for the fluid source is allowable. The data, however, indicate that whatever the ultimate source of the ore fluids, long travel paths are required for the hydrothermal fluids. The importance of this latter finding implies that the potential relationships between the various granitoids groups of the Yilgarn Craton and orogenic gold mineralising systems cannot be restricted to those suites that are spatially associated with orogenic gold mineralisation.

Metallogenic indicators

A number of researchers have suggested that specific chemical parameters, i.e., oxygen fugacity, degree of fractionation, may be more important with regard to mineralisation potential than simply using geochemistry (e.g., Blevin & Chappell, 1992; Candela, 1992; Champion & Heinemann, 1994). In this regard it is important to investigate such parameters, specifically between members of the various granitoid groups present in the Yilgarn Craton. We have followed the approach of Champion & Heinemann (1994) who utilised the following:

- Igneous rock type, i.e. I-, S-, or A-type
- Potassium content and alkalinity
- Oxidation state
- Degree of fractionation
- Heat production.

Igneous type

Igneous rocks, in general, can be classified, based largely on source-rock characteristics, into one of a number of classes which include I-, S-, and A-types (e.g., Chappell & White, 1984, 1992; Collins et al., 1982). The great majority of granitoids in the Yilgarn Craton are I-type (i.e., derived by melting of an igneous precursor), including those in the Mafic and High-Ca groups. Only the Syenitic group appears to be different, being A-type (Smithies & Champion, 1999). Recent work has suggested that the Aluminium Saturation Index which measures the ratio of Al to total Ca, Na and K, i.e., the degree of deficient or excess Al, is more important than igneous type for interpreting mineralisation potential. For example, changing the ASI can have a dramatic effect on mineral solubilities and also oxidation state (Dickenson & Hess, 1986), most significantly when the ASI changes from metaluminous (<1.0) to peraluminous (>1.0) or vice versa. Figure 9.1D shows the various Yilgarn Craton granitoid groups. Two features are evident: firstly, most High-Ca and Low-Ca group suites are metaluminous to peraluminous (reflecting their I-type nature); and secondly, most Mafic group suites are metaluminous (Table 9.1).

Potassium content

Champion & Heinemann (1994) used K_2O levels (low-, medium- or high-K; see Fig. 9.1C) to discriminate between potential mineralisation-associated granites, based largely on the notion that some Au deposits are associated with K-rich or shoshonitic granitoids, (Muller & Groves, 1993; also in the Lachlan Fold Belt, e.g., Wyborn, 1997). As discussed earlier, however, all granitoid groups, with the exception of the Syenitic group, vary from suites with low LILE contents, to those with high LILE. This is evident on Fig. 9.1C that shows a range from low- to high-K (see Table 9.1). Notably, very few granitoid group suites are truly low-K, with the great majority of High-Ca and Mafic group suites intermediate- to high-K and the majority of Low-Ca group suites high-K in potassium content.

Province	Association	Redox	Fract	Silica range	K level	ASI
Eastern Goldfields	Menangina	(R)O(S)	U(F)	>10	MH	(M)P

	Mt Boreas	O	F	<10	H(U)	P
	Granny Smith	(R)O(S)	U	<7	(L)M(H)	M
	Kookynie	RO	U(F)	>10	LH	MP
	Gilgarna	O(S)	U	15+	HU	M
Southern Cross	Diemals	(R)O(S)	U(F)	<10	MH	(M)P
	Beetle	O	F	>10	H(U)	P
	Westonia	R	U	<7	(L)M	M
	Marda	RO	U	<5	MH	MP
Murchison	Mainland	(R)O(S)	U(F)	<10	MH	(M)P
	Goolthan	O	F	>10	H(U)	P
	Gem of Cue	O	U	15+	M	M
	Damperwah	RO	U(F)	>10	MH	MP
	Udaglia	O	U	<5	H	M

Table 9.1. Metallogenic indicators for granitoid associations in the Yilgarn Craton. Abbreviations: O - oxidised; R - reduced; S – strongly oxidised; U - unfractionated; F – fractionated; L - low-K; M - medium-K; H - high-K; U – ultra-high-K; ASI - Aluminium Saturation Index; M - metaluminous: ASI<1.0; P - mildly peraluminous: 1.0<ASI<1.1; S - strongly peraluminous: ASI>1.1. Also refer to Figure 9.1.

Oxidation state

The oxidation state of a magma is clearly important with respect to mineralisation potential, e.g., behaviour of multivalent metals (Blevin & Chappell, 1992; Candela, 1992; Barton, 1996). Within unaltered granitoids the chief indicators of oxidation state are the opaque minerals, e.g., ilmenite and/or magnetite, although other minerals can also be diagnostic, e.g., titanite in strongly oxidised granitoids. The presence (oxidised) or absence (reduced) of magnetite is easly measured, e.g., magnetic susceptibility. Such measurements, however, are not available for all samples. Further, the affects of weathering and alteration are not well quantified. To overcome these obstacles, Champion & Heinemann (1994) developed an elementary, but surprisingly robust, chemical classification of oxidation state based on the work of Ishihara et al. (1979) who first suggested that whole-rock chemistry could be used to identify magnetite- or ilmenite-bearing granites. Individual granitoid units of the various Associations in the Yilgarn Craton are shown on a modified redox plot (Fig. 9.1E) and listed in Table 9.1. It is readily apparent that the great majority of Yilgarn Craton granitoids are/were magnetite-bearing, i.e., oxidised. The scatter into both the reduced- and strongly-oxidised fields may reflect metamorphism or alteration effects.

Degree of fractionation

Like oxidation state, the degree of fractionation can be critical in controlling the metal budget of the residual magmas (and related exsolved fluids). For example, Blevin & Chappell (1992) and Blevin et al. (1996) have shown that granitoids associated with Cu and Au in eastern Australia have generally undergone little or no fractionation, presumably due to the propensity for these elements to partition into early crystallising phases. It is also evident that the effects of fractionation typically operate in tandem with the oxidation state (Candela, 1992; Blevin et al., 1996), e.g., Sn will only concentrate in reduced, fractionated magmas (see Champion & Mackenzie, 1994). As shown by Champion & Heinemann (1994) the degree of fractionation in intermediate to felsic igneous rocks is best determined using the Rb-Ba-Sr ternary plot of El Bouseily & El Sokkary (1975). This is shown in Figure 9.2 from which it is readily apparent that all the Mafic group suites plot within the unfractionated fields, whereas all the Low-Ca group suites are fractionated. High-Ca group suites range from unfractionated to fractionated. As would be expected the Mafic group overlaps with the unfractionated half of the High-Ca group.

Another potential indicator of degree of fractionation is the observed silica range within suites (Table 9.1). Most of the Mafic group granitoid suites have small ranges (<5%, partly reflecting small sample populations), but there are a number of suites that exhibit moderate ranges of 10 to 15%. Although this range reflects alteration to some extent, e.g., Cassidy (1988) documents changes in silica content up to 10% due to alteration in the Lawlers tonalite, it is also due, in some cases, to in-situ fractionation. The latter is readily demonstrated in the Granny Smith granodiorite which is zoned from diorite to granodiorite (Ojala & Hunt, 1993).

Heat production

The capacity for a granitoid to produce heat, principally from the decay of radiogenic isotopes, can also be critical in the ability of a pluton or granitoid suite to develop and drive a hydrothermal system. The heat producing capacity of individual plutons of the various granitoid groups in the Yilgarn Craton is shown in Figure 9.1g. It is evident that the low-Ca granitoids as well as fractionated members of the High-Ca group have the largest capacity for heat production and may potentially develop and drive hydrothermal as well as late-magmatic fluid circulation during emplacement of these granitoid groups. The temporal association of the Low-Ca group granitoids with orogenic gold mineralising system development may indicate that this granitoid group provided, at least, heat to the mineralising systems.

Summary of spatial and temporal relationships between granitoids and orogenic gold mineralisation

Potential relationships between granitoids groups of the Yilgarn Craton and orogenic gold mineralising systems can be summarised:

- Temporal association:
  - Genetic relationship between specific granitoid suites or groups and hydrothermal fluids and/or components
  - Thermal relationship between specific granitoid suites or groups and development of hydrothermal mineralising system
  - Mineralisation related to independent processes but at the same time
- Spatial association:
  - Specific granitoid group/clan and ore fluids exploit the same structures (indicators of favourable pathways)
  - Preferred sites of mineralisation in specific granitoid group/clan (physical and/or chemical trap)
  - Predictable spatial relationship to specific granitoid group/clan

Once either a spatial and/or temporal association has been determined between a particular granitoid group and orogenic gold mineralisation, the potential genetic relationship can be discussed. These include:

- Specific granitoid group/clan to provide fluids and/or components (either proximal or distal to ore deposit location)
- Specific granitoid group/clan to provide heat engine to drive hydrothermal circulation during granitoid emplacement (granitoids are either proximal or distal to ore deposit location)
- Specific granitoid group/clan to provide heat engine through radiogenic heat build-up and driving hydrothermal systems long after granitoid emplacement (granitoids are either proximal or distal to ore deposit location).

Alternatively, there may be no relationship between any granitoid group and orogenic gold mineralising systems and any spatial and/or temporal association is fortuitous.

Temporal association

Constraining the timing of gold mineralization improves our ability to discriminate between magmatic, thermal or structural events with which mineralization may be genetically related. The temporal relationship between orogenic gold mineralising systems and specific granitoid groups and sub-groups hinges totally on the absolute timing of orogenic gold mineralisation. A summary of the timing of orogenic gold mineralisation and deformation is presented in Appendix 1 and not discussed further here. It is noteworthy, however, that the majority of orogenic gold mineralisation across the Yilgarn Craton took place at 2650-2630 Ma. This is based on a series of robust (i.e., U-Pb, Re-Os) geochronological ages of alteration and ore minerals from several deposits that are geographically widespread across the granitoid-greenstone terranes of the craton, as well as minimum ages of mineralisation derived from the emplacement ages of cross-cutting igneous rocks.

The best-documented age constraints are for the Chalice gold deposit in the southern Kalgoorlie Terrane. Main stage gold mineralization (95% of resource) comprises foliation-parallel quartz-albite-diopside-titanite-garnet-gold veins and wallrock replacement of mafic amphibolite host rocks. Secnd stage mineralization is temporally associated with a second-generation granitoid dyke that cross-cuts the main stage. Uranium-Pb zircon and titanite studies and Re-Os dating of molybdenum identified two discrete gold events at 2644±8 Ma and 2621±10 Ma (Bucci et al., 2000).

In several deposits (Golden Mile, Chalice, Lawlers, Mt Gibson, Granny Smith) there is geological and geochronological evidence for more than one stage of mineralisation. Some of these deposits (Mt Gibson, Boddington, ?Golden Mile) show features of more than one mineralization style (e.g., overprinting of one deposit type by another), or have some features that can be interpreted as being of more than one mineralization type. In some of these deposits, primary mineralization has been remobilized during extensive deformation and metamorphism and/or overprinted by later orogenic lode-gold mineralization. However, careful documentation of the relative timing, ore fluid character and metal association of these deposits clearly necessitates assigning these deposits to other deposit classes.

At Kalgoorlie, early Fimiston-style gold-telluride mineralization is crosscut by Mt Charlotte-style gold-pyrite±pyrrhotite mineralization (Clout et al., 1990). At Wiluna, strike-slip faults that control gold-pyrite-arsenopyrite mineralization offset gold-pyrite-chalcopyrite-galena-bearing quartz reefs by up to 800m (Hagemann et al., 1992). However, in the majority of these cases, the multiple gold mineralizing events are either different types of mineral system (e.g., early VHMS followed by later orogenic lode-gold: Mt Gibson) or reflect different stages of mineralization within a progressive orogenic lode-gold mineralizing system (e.g., Wiluna). Even in these latter cases, the relative timing of the orogenic lode-gold mineralizing events is structurally late.

The giant Boddington gold deposit has been recently debated as a 'porphyry-style' Cu-Mo-Au deposit with distinct orogenic lode-gold overprint (± gold remobilization). Boddington mineralization has some features (metal association, fluid inclusion populations) more typical of 'porphyry-style' mineralising systems as well as some features (structural timing) more aligned with 'orogenic lode-gold' mineralizing systems. Further work is required for the Boddington deposit.

At the terrane-scale, Archean orogenic lode-gold mineralization is late relative to the overall tectonomagmatic evolution of a host terrane (Groves et al., 1989, 1995; Kerrich and Cassidy, 1994; Ridley et al., 1995; Knight et al., 2000). The timing of orogenic gold mineralisation is also constrained by relative timing techniques to syn- to post-D3 (e.g., deposits in the St Ives gold camp: Clark et al., 1989; Nyugen et al., 1998). The absolute timing of deformation has been poorly constrained in many parts of the Yilgarn Craton and should be the focus of future research.

At the camp- and deposit-scale, deposits in subgreenschist- to greenschist-facies metamorphic environments typically postdate and are retrograde with respect to the peak regional metamorphic conditions (e.g., Clark et al., 1989; Hodgson, 1993; McCuaig and Kerrich, 1998), whereas deposits in amphibolite-facies metamorphic environments are essentially synchronous with regional metamorphism (e.g., Knight et al., 1993, 2000; Ridley et al., 1995, 2000; Cassidy and Hagemann, 1999). Mineral fabrics in deposits formed at high temperature and pressures generally show large degrees of dynamic recovery and, in some cases, it becomes difficult to distinguish between deposits that formed at these P-T temperatures (e.g., Mueller and Groves, 1991; Knight et al., 1993; McCuaig et al., 1993; Ridley et al., 2000) and those formed at lower temperatures and were subsequently metamorphosed (e.g., Big Bell: Phillips and de Nooy, 1988). Several gold camps (e.g., Coolgardie and Norseman regions, Yilgarn Craton: Witt, 1993; Knight et al., 1993; 2000; McCuaig et al., 1993) show transitions in the metamorphic grade of deposits and corresponding transitions in the metamorphic-grade of alteration assemblages. In the Coolgardie district, temperature zonation is spatially related to distance from a regional granitoid intrusion (Knight et al., 2000). There is also evidence in high-temperature deposits that the mineralizing event occurred under pressure-temperature conditions close to those of peak regional metamorphism.

There are several localities where deformed granitoids or cross-cutting igneous rocks have been dated and can constrain the absolute timing of the late stages of deformation. These include where deformation has been dated by the age of titanite growth in deformed and metamorphosed granitic gneisses:

- Lake Kirk gneiss (Plutno - 323303), near Norseman, at the boundary between the Eastern Goldfields and Southern Cross Provinces: metamorphic titanite defining foliation dated at ~2631 Ma
- Basin granitoid (Plutno - 224107), near Noongal, in the Yalgoo greenstone belt, Murchison Province: alteration titanite defining foliation dated at ~2632 Ma
- Sundowner granitoid (Plutno - 314308), north of Bronzewing, Yandal greenstone belt, Eastern Goldfields Province: alteration titanite defining foliation dated at ~2644 Ma.

The age of late deformation is also constrained by the age of late granitoids that are deformed by late structural fabrics (D3, D4). These include:

- Deformed granitoids:
    - McAuliffe Well (Syenitic grouping; Plutno 323907) – 2651±5 Ma
    - Woorana Soak (Syenitic grouping; Plutno 314301) – 2644±13 Ma
    - Liberty (Mafic grouping; Plutno 313713) – 2648±6 Ma
    - Sundowner (Mafic grouping; Plutno 314308) – 2644±6 Ma
    - Wildara gneiss (High-Ca grouping; Plutno 304117) – 2648±5 Ma
- Undeformed granitoids cutting structural fabrics:
    - Clark Well (Low-Ca grouping; Plutno 303803) – 2640±8 Ma
    - Nevoria, Westonia, Scotia and other places (Low-Ca grouping pegmatites) – ca. 2640 Ma (see Kent et al., 1996).

The timing of late deformation and orogenic gold mineralisation in the Yilgarn Craton, therefore, is constrained to ca. 2650-2630 Ma. If these ages record the primary orogenic gold mineralisation events, rather than some other event, then they strongly suggest that there are no temporal, genetic and most likely no thermal relationships between the majority of granitoids in the Yilgarn Craton and orogenic gold mineralisation. The temporal relationship between the various granitoid groups and orogenic gold mineralising systems is summarised as follows:

- High-Ca group: mineralisation post-dates emplacement in all cases
- Low-Ca group: strong temporal association with emplacement of the majority of Low-Ca clans in all provinces
- Mafic group: mineralisation post-dates emplacement in all cases
- Syenitic group: temporal association with ca. 2.645 Ga Syenitic clans (e.g., Gilgarna in EGP)

This is clearly indicated by compilations of the emplacement age of granitoids in the Yilgarn Craton and illustrated by Fig 9.3. This is consistent with timing relationships between metamorphism and alteration, particularly in the majority of granitoid-hosted deposits where alteration also affects greenstones and overprints metamorphism (e.g., Cassidy et al., 1998). Similar conclusions have been reached for other Archaean granite-hosted orogenic gold deposits provinces elsewhere (e.g., Abitibi, Colvine et al., 1988; Burrows & Spooner, 1989; Hodgson, 1990), i.e., the granite-hosted Au deposits are not orthomagmatic.

Spatial association

The spatial relationships between orogenic gold deposits and specific granitoid groups/clans is summarised as follows:

- Mafic granitoids host numerous deposits throughout the Eastern Goldfields Province, as well as in the Murchison and Southern Cross Province.
- Most Mafic granitoids hosting orogenic gold mineralisation belong to 'High-LILE' clans (e.g., Granny Smith in the EGP; Gem of Cue in the MP). An important exception is the Kanowna-Belle deposit that is hosted in 'Low-LILE' clan porphyry dykes.
- There is a minor association with some granitoids of the High-Ca group (e.g., Tarmoola in EGP; Lady Lydia in MP).
- There is a minor association with some granitoids of the Syenitic group (e.g., Wallaby, Jupiter, Tin Dog in EGP). There is a spatial relationship of major deposits with major deformation zones (e.g., Boulder-Lefroy, Laverton Tectonic Zone: Perring et al., 1989) and the syenitic granitoids are also spatially related to the major deformation zones (see Smithies & Champion, 1999).
- There is a rare to null association with High-HFSE group granitoids. An exception is the Cosmopolitan deposit near Kookynie that is spatially restricted to a Mafic granitoid pod within the High-HFSE group granitoid.
- Low-Ca granitoids and pegmatites cross-cut orogenic gold mineralisation at a number of localities in the Eastern Goldfields, Southern Cross and Murchison Provinces, including Marvel Loch, Nevoria, Westonia and others in the Southern Cross Province.
- Low-Ca granitoids are co-eval with Stage 2 mineralisation at Chalice (Bucci et al., 2000).

On the basis of the above features, it is clear that the Mafic granitoids show the strongest spatial association with orogenic gold mineralisation. The Mafic granitoids, however, do not show any temporal association with orogenic gold mineralisation and, therefore, other factors must be considered to determine if there is any genetic relationship between Mafic granitoids and orogenic gold mineralisation. The other granitoids groups show, at best, a moderate spatial association with orogenic gold mineralisation.

Potential genetic relationships

On the basis of the contrasting temporal and/or spatial relationships of the various granitoids groups in the Yilgarn Craton to orogenic gold mineralisation, it is important to discuss the potential genetic relationships of orogenic gold to two of the granitoids groups, i.e., Mafic and Low-Ca granitoid groups. The other three granitoid groups, i.e., High-Ca, High-HFSE and Syenitic show neither a specific spatial nor strong temporal relationship to orogenic gold mineralisation in the Yilgarn Craton.

Mafic granitoids

As noted earlier many of the granitoids associated with orogenic gold mineralisation belong to the Mafic group. Those associated with orogenic gold deposits encompass the full range of geochemistry present within the Mafic group, e.g., Granny Smith (high-LILE) and KB (low-LILE). Importantly, it is also evident that there appears little to geochemically differentiate those Mafic group members associated with orogenic gold deposits from those not, i.e., there is no apparent geochemical reason why any specific intrusion is mineralised.

The available evidence suggests that Yilgarn granitoid-hosted deposits (Cassidy et al., 1998), are not ortho-magmatic. Why then do the granitoids of the Mafic group appear to be favoured hosts for granitoid-associated gold mineralisation in the Yilgarn Craton? As summarised by Hagemann & Cassidy (2000), gold deposits typically form due to a combination of a number of critical chemical and physical processes, which at their simplest are: channelling of ore fluids, focussing of ore fluids, and deposition of gold. Studies of Archaean orogenic gold deposits from around the world have illustrated a number of common features, including proximity to large-scale fault zones (Colvine et al., 1988; Eisenlohr et al., 1989), strong structural control at the deposit-scale, in particular, enhanced structural permeability (Colvine et al., 1988; Hodgson, 1989; Hronsky et al., 1990; Groves et al., 1997), and the importance of wall-rock interaction, sulphidation and Fe-rich hosts for gold deposition (Phillips, 1986; Colvine et al., 1988; Mikucki & Groves, 1990; Ridley et al., 1996). Given these features of orogenic gold deposits, a number of possible reasons may be advanced to explain why the Mafic granitoids are favourable host rocks. These include:

1) physical characteristics for structural relationship
- favourable competency, for ground preparation or competency contrast
- favourable size and/or shape
- depth of emplacement

2) chemical trap;
3) indicators of favourable pathways;
4) fortuitous.

It should be noted that the discussion here is concerned with why the Mafic granites are more favourable hosts to economic mineralisation, rather than mineralisation *per se*. This is an important distinction because the processes discussed only need to be able to account for more efficient localisation of mineralisation (and alteration), regarding size and grade, in a mineralising system.

Physical characteristics: Given the obvious structural control on gold mineralisation in the Yilgarn Craton it is possible that the Mafic granitoids possess some favourable physical attribute, such as size, shape, competency (mineral composition), that makes them a favoured host. With regard to size and shape it is readily apparent that Mafic granitoids associated with mineral deposits include a range of sizes and shapes, e.g., compare Granny Smith, Porphyry or Golden Cities plutons with porphyry dyke swarms at Kanowna-Belle, New Celebration or Victory-Defiance. Further, many of the non-Mafic granitoids are of similar sizes and shapes to the Mafic granitoids, e.g., Syenitic bodies are generally of similar to smaller sizes while the High-Ca granites are generally similar to larger in size.

A number of workers have documented contrasting deformation in granitoids, in particular Vernon & Flood (1988) show that foliation versus fracture development in granitoids is largely dependant on the ratio of ductile minerals (mica and quartz) to stronger, more brittle minerals such as feldspars and amphibole. Given this, it is difficult to envisage any significant competency differences between the Mafic granitoids and other Yilgarn Craton granitoid groups, in particular mafic end-members of the High-Ca group and some of the Syenitic granitoids, all of which are dominated by feldspar and amphibole. It is noted, however, that such a mechanism may partly explain the lack of mineralisation in more siliceous granitoids, although it is evident that a significant silica range (>10%) exists in Mafic granitoids that are mineralised. Finally, it is noted that the more important aspects with regards to structural permeability are lithological heterogeneity and competency contrasts between differing rock types (e.g., Colvine et al., 1988; Hronsky et al., 1990; Groves et al., 1995, 2000); in this regard it is considered that there would be little difference between the different granite groups of the Eastern Goldfields. A similar result would also appear to be the case if fluid flow, and hence mineralisation, are controlled by zones of lower mean rock stress (Ridley, 1993; Groves et al., 1995, 2000).

Chemical trap: A number of workers (e.g., Phillips, 1986; Mikucki & Groves, 1990; Ridley et al., 1996) have emphasised the importance of relatively Fe-rich host rocks (both high Fe and high Fe/Mg) with regards to gold deposition, i.e., wall-rock interaction and sulphidation (although other processes are also invoked, e.g., phase separation, see Appendix 1). In this regard, the Mafic granitoids with their high total FeO contents are partly distinct from other granitoids in the Yilgarn Craton. Total FeO contents in the Mafic granites range from high (>5% total FeO, such as at Granny Smith and Lawlers) to low (<2% total FeO, e.g., Tarmoola). However, as with other parameters, there is a significant overlap between the Mafic group and mafic end-members of the Syenitic and High-Ca groups. Additionally, the Syenitic granitoids typically have lower MgO and hence higher Fe/Mg ratios than the Mafic granites at similar levels of total FeO, perhaps making them a better chemical trap.

Favourable pathways: Many workers (e.g., Colvine et al., 1988; Eisenlohr et al., 1989; Hodgson, 1993; Groves et al., 1995) have indicated the importance of large craton- or greenstone belt-scale fault zones and pointed out that there is an apparent relationship between the occurrence of these faults and the more gold-productive greenstone belts. Regardless of whether these large scale faults have acted as fluid conduits or are merely a controlling feature in producing greenstone belts with the right geometry relative to the far-field stress regime (e.g., Groves et al., 1995), it is pertinent to ascertain whether or not Mafic granitoids are favourably disposed along these structures. Perring et al. (1989) demonstrated that for the Eastern Goldfields there is a good spatial association between minor intrusions such as calc-alkaline porphyries, lamprophyres, syenites, and some mineralisation/alteration and the larger faults. Wyman & Kerrich (1988) have indicated a similar relationship for lamprophyres in the Superior Province. Clearly, some granitoids are utilising these structural zones as favourable pathways, not just those with deep-seated or mantle origins, e.g. Mafic, High-Ca and Syenitic group granitoids, but also, as pointed out by Perring et al. (1989), porphyry dyke swarms related to nearby granitoids. Based on present knowledge it is difficult to quantify the relative proportions of granitoid types that may be associated with these structures. It is readily apparent that Mafic granitoids are not the sole granitoid type, for example, syenites have long been recognised to be associated with these large fault zones (e.g. Smithies & Champion, 1999). Additionally, given the geochemical similarity of most porphyry dykes to spatially-associated granitoids, and the distribution of granitoid groups, it is unlikely that the porphyries along these fault zones are predominantly from the Mafic group. For example, the porphyries documented by Witt (1993) in the Bardoc-Kalgoorlie area and pre-mineralisation porphyries in the Norseman region (Perring et al., 1989) clearly include members of both the Mafic and High-Ca groups. Therefore, like the other parameters discussed above, there appears to be no particularly compelling reason why the Mafic group granitoids are favoured hosts for granitoid-hosted orogenic gold deposits.

Low-Ca granitoids

Low-Ca granitoids show the best temporal association with orogenic gold mineralisation in the Yilgarn Craton. However, where they show a spatial association, it is where Low-Ca pegmatite and granitoid dykes cross-cut gold mineralisation. There are few, if any, examples of Low-Ca granitoids hosting orogenic gold mineralisation. The strong temporal association does suggest that there is some relationship between their emplacement and the development of hydrothermal mineralising systems. This relationship can be in the form of the following:

- Specific granitoid group/clan to provide fluids and/or components (either proximal or distal to ore deposit location)
- Specific granitoid group/clan to provide heat engine to drive hydrothermal circulation during granitoid emplacement (granitoids are either proximal or distal to ore deposit location)
- Specific granitoid group/clan to provide heat engine through radiogenic heat build-up and driving hydrothermal systems long after granitoid emplacement (granitoids are either proximal or distal to ore deposit location).

One line of evidence that may be important in determining any genetic relationship is the discovery of 'fluid-escape' structures in the some Low-Ca granitoids. These include biotite-rich 'oikocryst' zones (e.g., Boorabbin granitoid, plutno 293504, Southern Cross Province), miarolitic cavities and pipes (e.g, Dutakajin granitoid, plutno 233719, Murchison Province: this study; De-eranning Hill in the central Southern Cross Province: J. Ridley pers. comm. 2000) and pegmatites (Figure 9.4). Many of the Low-Ca granitoids in the southern Murchison and southern to central Southern Cross Provinces contain these structures that indicate late ?magmatic fluid movement, possibly during crystallisation of the granitoid body.

Many of these structures contain quartz that contains primary and pseudosecondary fluid inclusions. Laboratory studies (fluid inclusion and Raman spectroscopic) on selected material indicate that the fluids are mixed low-salinity aqueous-carbonic fluids (Table 9.2; Figure 9.4). No other gaseous phases were detected using the Raman. In the biotite-rich 'oikocrysts', the inclusions are pseudo-secondary, and the exact timing of trapping is ambiguous; it is possible that the fluids were trapped after quartz growth had ceased but prior to cessation of growth of the biotite oikocrysts. Low-salinity aqueous-carbonic fluids are similar to those found in orogenic gold deposits from all crustal levels and may indicate a genetic association.

On the basis of the temporal association of Low-Ca granitoids and orogenic gold mineralising systems, as well as the presence of similar fluids, the following are worth noting:

- Emplacement of the Low-Ca granitoids may have provided heat to help drive the hydrothermal systems responsible for orogenic gold

- Late ?magmatic fluids trapped in the miarolitic cavities may suggest that either the Low-Ca granitoids were a source of the fluids or 'saw' the same fluids responsible for orogenic gold
- Low-Ca granitoids provided both heat and fluids to the orogenic gold mineralising systems.

The lack of a close spatial association between Low-Ca granitoids and orogenic gold mineralisation can be alleviated by the assertion that the orogenic gold fluids must be distal from their source and were sourced from, or at least interacted with, granitoids along fluid conduits (see Ridley & Diamond, 2000).

Summary and Discussion

The previous sections can be summarised as follows:

- most, but not all, granitoid-hosted orogenic gold mineralisation is related to Mafic group granitoids, other hosts include High-Ca and Syenitic granitoids (e.g., Cassidy, 1997);
- there is no evidence that the granitoid-hosted orogenic gold deposits are orthomagmatic, gold mineralisation appears to post-date granitoid intrusion in all cases;
- the host granitoids do not appear to possess any unique physical characteristics such as size, shape or degree of competency;
- there are no obvious petrogenetic reasons why the Mafic granitoids, as against the High-Ca or Syenitic granitoids, should be favoured hosts for orogenic gold mineralisation;
- the Mafic group granitoids span a considerable range in chemistry, i.e., the High- to Low-LILE subgroups, this geochemistry (Low-LILE subgroup) overlaps with the High-Ca group, and also to some extent (High-LILE) with the Syenitic group;
- the mineralised Mafic granitoids include units covering the range of compositions seen within the Mafic group;
- there appears to be no geochemical distinction between unmineralised and mineralised Mafic granitoids;
- metallogenic indicators for the Mafic group indicate mafic, oxidised, not-strongly fractionated granites consistent with characteristics found in eastern Australian granitoids associated with gold mineralisation, many of these metallogenic indicators are also shared by other Yilgarn Craton granitoid groups (e.g., High-Ca);
- although some Mafic granitoids do have high Fe contents (and hence better possible chemical traps) there is a broad overlap with mafic members of the High-Ca and Syenitic groups;
- there is a possibility that Mafic granitoids, and lamprophyres, may be more favourably located along major fault zones. It is evident, however, that other granitoid types, e.g. syenites, are also similarly distributed.

The above points can be further summarised to indicate that:

- the granitoid-hosted orogenic gold deposits are not orthomagmatic;
- there appears to be no one obvious temporal, physical or chemical reason for the Mafic granitoids being favoured hosts;
- similarly, there appears to be no reasons why some of the mafic High-Ca granitoids and Syenites, based on their similarities to Low- and High-LILE mafic granitoids, should also not be favourably mineralised;
- Low-Ca and Syenitic granitoids are temporally associated with orogenic gold mineralising systems but rarely are spatially associated with them;
- Only Low-Ca granitoids are present in all Provinces at the same time as orogenic gold mineralisation

- Low-Ca granitoids contain ?late-magmatic fluids similar to those present in orogenic gold mineralising systems;
- Low-Ca and Syenitic granitoids are probably the result of extensional tectonics late in the development of the Yilgarn Craton;
- The relationship between Low-Ca granitoids and orogenic gold mineralising systems reflects either:
  - That they are both the product of the same tectono-magmatic event
  - That Low-Ca granitoids provide heat and possibly some fluids to the orogenic gold mineralising systems.

A tectonomagmatic model invoking orogenic collapse and slab detachment has been proposed to explain the late Cenozoic mineralization in the European Alpine belt (de Boorder et al., 1998) and may provide a possible model for orogenic gold mineralisation in the Yilgarn Craton.

Some exploration parameters

Some salient points for exploration models can be summarised from this and previous chapters, these include:

- most, but not all, granitoid-hosted gold mineralisation is related to Mafic group granitoids, other hosts include High-Ca and Syenitic granitoids;
- there appears to be no geochemical distinction between unmineralised and mineralised Mafic granitoids;
- there is no evidence that the granitoid-hosted orogenic gold deposits are orthomagmatic, gold mineralisation appears to post-date granitoid intrusion;
- the Mafic granitoids do not appear to possess any unique physical characteristics such as size, shape or degree of competency;
- although some Mafic granitoids do have high Fe contents (and hence better possible chemical traps) there is a broad overlap with mafic members of the High-Ca and Syenitic groups;
- there is a possibility that Mafic granitoids, and lamprophyres, may be more favourably located along major fault zones. It is evident, however, that other granitoid types, e.g. syenites, are also similarly distributed;
- there are no obvious petrogenetic reasons why the Mafic granitoids, as against the High-Ca or Syenitic granitoids, should be favoured hosts for orogenic gold mineralisation, i.e., there appears to be no reasons why some of the mafic High-Ca granitoids and Syenites, based on their similarities to Low- and High-LILE mafic granitoids, should not also be favourably mineralised;

Regardless of the ultimate Au source it is clear that the Mafic granitoids are a favoured host, relative to other granitoids. The Mafic granitoids are generally petrographically and geochemically distinctive; the presence of common amphibole and abundant ferromagesian minerals (biotite, amphibole and pyroxene) are distinctive characteristics. There is, as noted above, however, some geochemical and petrographic similarities between the Mafic granitoids and members of the Syenitic and High-Ca groups. Accordingly, there is no reason why some members of these groups could not also be favourable hosts for mineralisation, and indeed some examples are known (e.g., Syenitic group – Wallaby; High-Ca – Tarmoola). Probably the most distinctive characteristic of those granitoids hosting deposits is the presence of amphibole and this must, accordingly, be considered an important indicator of favourable hosts. Their appears to be no unique geophysical characteristics to identify Mafic granitoids from other Yilgarn Craton granites.

Many authors have noted the importance of structural controls for Archaean Au deposits, including:

- proximity to large-scale fault zones (Colvine et al., 1988; Eisenlohr et al., 1989);
- strong structural control at the deposit-scale, in particular, enhanced structural permeability, e.g., lithological heterogeneity and competency contrasts (Colvine et al., 1988; Hronsky et al., 1990;Groves et al., 1995);
- the importance of wall-rock interaction, sulphidation and Fe-rich hosts for Au deposition (Phillips, 1986; Colvine et al., 1988; Mikucki & Groves, 1990; Ridley et al., 1996).

With consideration to the above points, in particular the first two, in combination with the recognition of Mafic granitoids, then the following extra points can be raised:

- regions or zones with greater numbers (not simply volume) of Mafic and to a lesser extent Syenitic group granitoids would be more favourable, providing more opportunities for enhanced structural permeability;
- structures are important, especially interaction between larger-scale structures and both granitoids and smaller-scale structures, e.g., Mafic granitoids in areas of disrupted geology proximal to larger-scale structures such as at Victory-Defiance or New Celebration, or within structural corridors such as the Laverton tectonic zone.

Bibliography

Blevin, P.L. & Chappell, B.W., 1992, The role of magma sources, oxidation states and fractionation in determining the granite metallogeny of eastern Australia. Transactions of the Royal Society of Edinburgh, Earth Sciences, 83: 1305-1316.

Blevin, P.L., Chappell, B.W. & Allen, C.M., 1996, Intrusive metallogenic provinces in eastern Australia based on granite source and composition. . Transactions of the Royal Society of Edinburgh, Earth Sciences, 87, 281-290.

Bloem, E.J.M., McNaughton, N.J., Groves, D.I., and Ridley, J.R., 1995, An indirect lead isotope age determination of gold mineralisation at the Corinthia Mine, Yilgarn Block, Western Australia: Australian Journal of Earth Sciences, v.42, p.447-451.

Bucci, L et al., 2000, Two mineralisation events at the Chalice gold deposit, Geological Society of Australia, Abstracts, p.34.

Burrows, D.R., and Spooner, E.T.C., 1989, Relationships between Archean gold quartz vein-shear zone mineralization and igneous intrusions in the Val d'Or and Timmins areas, Abitibi Subprovince, Canada, *in* Keays, R.R., Ramsay, W.R.H., and Groves, D.I., eds., The Geology of Gold Deposits: The Perspective in 1988: Economic Geology, monograph 6, p.424-444.

Candela, P.A., 1992, Controls on ore metal ratios in granite-related ore systems: an experimental and conceptual approach: Transactions of the Royal Society of Edinburgh, Earth Sciences, 83: 317-326.

Cassidy, K.F., Groves, D.I., and McNaughton, N.J., 1998, Late-Archean granitoid-hosted lode-gold deposits, Yilgarn Craton, Western Australia: Deposit characteristics, crustal architecture and implications for ore genesis: Ore Geology Reviews, v.13, p.65-102

Champion D.C., & Heinemann, M.A., 1994, Igneous rocks of nothern Queensland: 1:500 000 map and explanatory notes. AGSO Record 1994/11.

Champion D.C. & Sheraton J.W., 1997, Geochemistry and Sm-Nd systematics of Archean granitoids in the Eastern Goldfields Province, Yilgarn Craton: Constraints on crustal growth. Precambrian Research, 83, 109-132..

Colvine, A.C., 1989, An empirical model for the formation of Archean gold deposits: products of final cratonization of the Superior Province, Canada, *in* Keays, R.R., Ramsay, W.R.H., and Groves, D.I., eds., The Geology of Gold Deposits: The Perspective in 1988: Economic Geology, Monograph 6, p.37-53.

Colvine, A.C., Fyon, J.A., Heather, K.B., Marmont, S., Smith, P.M., and Troop, D.G., 1988, Archean lode gold deposits in Ontario: Ontario Geological Survey, Miscellaneous Paper 139, 136p.

de Boorder, H., Spakman, W., White, S.H., and Wortel, M.J.R., 1998, Late Cenozoic mineralization, orogenic collapse and slab detachment in the European Alpine belt: Earth and Planetary Science Letters, v.164, p.569-575.

Eisenlohr, B.N., Groves, D.I., and Partington, G.A., 1989, Crustal-scale shear zones and their significance to Archaean gold mineralization in Western Australia: Mineralium Deposita, v.24, p.1-8.

Groves, D.I., Barley, M.E., and Ho, S.E., 1989, Nature, genesis, and tectonic setting of mesothermal gold mineralization in the Yilgarn Block, Western Australia, *in* Keays, R.R., Ramsay, W.R.H., and Groves, D.I., eds., The Geology of Gold Deposits: The Perspective in 1988: Economic Geology, Monograph 6, p.71-85.

Groves, D.I., Barnicoat, A.C., Cassidy, K.F., Fare, R.J., Hagemann, S.G., Ho, S.E., Hronsky, J.M.A., McNaughton, N.J., Perring, C.S., Ridley, J.R., and Vearncombe, J.R., 1992, Sub-greenschist to granulite-hosted Archaean lode-gold deposits of the Yilgarn Craton: a depositional continuum from deep-sourced hydrothermal fluids in crustal-scale plumbing systems, *in* Glover, J.E., and Ho, S.E., eds., The Archaean: Terranes, Processes and Metallogeny: Geology Department (Key Centre) & University Extension, The University of Western Australia, Publication 22, p.325-337.

Groves, D.I., Ridley, J.R., Bloem, E.M.J., Gebre-Mariam, M., Hagemann, S.G., Hronsky, J.M.A., Knight, J.T., McNaughton, N.J., Ojala, J., Vielreicher, R.M., McCuaig, T.C., and Holyland, P.W., 1995, Lode-gold deposits of the Yilgarn block: products of Late Archaean crustal-scale overpressured hydrothermal systems, *in* Coward, M.P., and Ries, A.C., eds., Early Precambrian Processes: Geological Society Special Publication, No. 95, p.155-172.

Groves, D.I., Goldfarb, R.J., Gebre-Mariam, M., Hagemann, S.G., and Robert, F., 1998, Orogenic gold deposits: a proposed classification in the context of their crustal distribution and relationship to other gold deposit types: Ore Geology Reviews, v.13, p.7-27.

Groves, D.I., Goldfarb, R.J., Knox-Robinson, C.M, Ojala, J., Gardoll, S., Yun, G., and Holyland, P., 2000, Late-kinematic timing of orogenic gold deposits and significance for computer-based exploration techniques with emphasis on the Yilgarn Block, Western Australia, 53p.

Hodgson, C.J., 1989, The structure of shear-related, vein-type gold deposits: A review: Ore Geology Reviews, v.4, p.231-273.

Hodgson, C.J., 1993, Mesothermal lode-gold deposits, *in* Kirkham, R.V., Sinclair, W.D., Thorpe, R.I., and Duke, J.M., eds., Mineral Deposit Modelling: Geological Association of Canada, Special Paper 40, p.635-678.

Hodgson, C.J., and Hamilton, J.V., 1989, Gold mineralization in the Abitibi greenstone belt: end-stage results of Archean collisional tectonics? *in* Keays, R.R., Ramsay, W.R.H., and Groves, D.I., eds., The Geology of Gold Deposits: The Perspective in 1988: Economic Geology, Monograph 6, p.86-100.

Hronsky, J.M.A., Cassidy, K.F., Grigson, M.W., Groves, D.I., Hagemann, S.G., Mueller, A.G., Ridley, J.R., Skwarnecki, M.S., and Vearncombe, J.R., 1990, Deposit and mine-scale structure, *in* Ho, S.E., Groves, D.I., and Bennett, J.M., ed., Gold Deposits of the Archaean Yilgarn Block, Western Australia: Nature, Genesis and Exploration Guides: Geology Department and University Extension, University of Western Australia, Publication 20, p.38-54.

Kent, A.J.R., 1994, Geochronological constraints on the timing of Archean gold mineralisation in the Yilgarn Craton. Unpublished Ph.D. thesis, Canberra, Australian National University, 268p.

Kent, A.J.R., and Hagemann, S.G., 1996, Constraints on the timing of gold mineralisation in the Wiluna Greenstone Belt, Yilgarn Craton, Western Australia: Australian Journal of Earth Sciences, v.43, p.573-588.

Kent, A.J.R., and McCuaig, T.C., 1997, Disturbed ^{40}Ar-^{39}Ar systematics in hydrothermal biotite and hornblende at the Scotia gold mine, Western Australia: Evidence for argon loss associated with post-mineralization fluid movement: Geochimica et Cosmochimica Acta, v.61, p.4655-4669.

Kent, A.J.R., and McDougall, I., 1995, ^{40}Ar -^{39}Ar and U-Pb age constraints on the timing of gold mineralization in the Kalgoorlie gold field, Western Australia: Economic Geology, v.90, p.845-859.

Kent, A.J.R., Cassidy, K.F., and Fanning, C.M., 1996, Archean gold mineralization synchronous with the final stages of cratonization, Yilgarn Craton: Geology, v.24, p.879-882.

Kerrich, R., and Cassidy, K.F., 1994, Temporal relationships of lode gold mineralization to accretion, magmatism, metamorphism and deformation – Archean to present: A review: Ore Geology Reviews, v.9, p.263-310.

Kerrich, R., and Wyman, D., 1990, The geodynamic setting of mesothermal gold deposits: an association with accretionary tectonic regimes: Geology, v.18, p.882-885.

Kerrich, R., Goldfarb, R., Groves, D.I. and Garwin, S., 2000, The geodynamics of world-class gold deposits: Characteristics, space-time distribution, and origins: Reviews in Economic Geology, vol. 13, p. 501-551.

Knight, J.T., Ridley, J.R., and Groves, D.I., 2000, The Archean amphibolite facies Coolgardie goldfield, Yilgarn Craton, Western Australia: Nature, controls, and gold field-scale patterns of hydrothermal wall-rock alteration: Economic Geology, v.95, p.49-84.

McCuaig, T.C., and Kerrich, R., 1998, P-T-t-deformation-fluid characteristics of lode gold deposits?: evidence from alteration systematics: Ore Geology Reviews, v.12, p.381-453.

McCuaig, T.C., Kerrich, R., Groves, D.I., and Archer, N., 1993, The nature and dimension of regional and local gold-related hydrothermal alteration in tholeiitic metabasalts in the Norseman Goldfields: the missing link in crustal continuum of gold deposits: Mineralium Deposita, v.28, p.420-435.

Mikucki, E.J., 1998, Hydrothermal transport and depositional processes in Archean lode-gold systems: A review: Ore Geology Reviews, v.13, p.307-321.

Mikucki, E.J., and Groves, D.I., 1990, Constraints on genesis of primary gold deposits: Mineralogical constraints, *in* Ho, S.E., Groves, D.I., and Bennett, J.M., eds., Gold Deposits of the Archaean Yilgarn Block, Western Australia: Nature, Genesis and Exploration Guides: Geology Department and University Extension, University of Western Australia, Publication 20, p.212-220.

Mickucki, E.J., and Ridley, J.R., 1993, The hydrothermal fluid of Archaean lode-gold deposits at different metamorphic grades: compositional constraints from ore and wallrock alteration assemblages: Mineralium Deposita, v.28, p.469-481.

Napier, R.W., 1993, ^{40}Ar-^{39}Ar geochronology of gold mineralization and Archaean tectonics in the Yilgarn block, Western Australia: *in* Fenoll Hach-Ali, P., Torres-Ruiz, J., and Gervilla, F., eds, Current Research in Geology Applied to Ore Deposits: University of Granada, Spain, p. 187-190.

Napier, R.W., Guise, P.G., and Rex, D.C., 1998, ^{40}Ar-^{39}Ar constraints on the timing and history of amphibolite facies gold mineralisation in the Southern Cross area, Western Australia: Australian Journal of Earth Sciences, v.45, p.285-296.

Nelson, D.R., 1997, Evolution of the Archaean granite-greenstone terranes of the Eastern Goldfields, Western Australia: SHRIMP U-Pb zircon constraints: Precambrian Research, v.83, p.57-81.

Ojala, V.J., Ridley, J.R., Groves, D.I., and Hall, G.C., 1993, The Granny Smith gold deposit: the role of heterogeneous stress distribution at an irregular granitoid contact in a greenschist facies terrane: Mineralium Deposita, v.28, p.409-419.

Perring, C.S., Barley,M.E., Cassidy, K.F., Groves, D.I., McNaughton, N.J., Rock, N.M.S., Bettenay, L.F., Golding, S.D., and Hallberg, J.A., 1989, The association of linear orogenic belts, mantle-crustal magmatism, and Archean gold mineralization in the eastern Yilgarn Block of Western Australia, *in* Keays, R.R., Ramsay, W.R.H., and Groves, D.I., eds., The Geology of Gold Deposits: The Perspective in 1988: Economic Geology, Monograph 6, p.571-584.

Phillips, G.N., 1986, Geology and alteration in the Golden Mile, Kalgoorlie: Economic Geology, v81, p.779-808.

Phillips, G.N., Groves, D.I., and Kerrich, R., 1996, Factors in the formation of the giant Kalgoorlie gold deposit: Ore Geology Reviews, v.10, p.295-317.

Qiu, Y., and Groves, D.I., 1999, Late Archean collision and delamination in the southwest Yilgarn Craton: The driving force for Archean orogenic lode gold mineralization?: Economic Geology, v.94, p.115-122.

Qiu, Y., and McNaughton, N.J., 1999, Source of Pb in orogenic lode-gold mineralisation: Pb isotopic constraints from deep crustal rocks from the southwestern Archaean Yilgarn Craton, Australia: Mineralium Deposita, v.34, p.366-381.

Ridley, J.R., 1990, Constraints from alteration assemblages on gold-bearing hydrothermal fluid composition and source, *in* Ho, S.E, Groves, D.I., Bennett, J.M., eds., Gold Deposits of the Archaean Yilgarn Block, Western Australia: Nature, Genesis and Exploration Guides: Geological Department and University Extension, University of Western Australia, Publication 20, p.268-272.

Ridley, J.R., and Diamond, L.W., 2000, Fluid chemistry of lode-gold deposits, and implications for genetic models. Reviews in Economic Geology, No.13, p.141-162.

Ridley, J.R., Mikucki, E.J., and Groves, D.I., 1996, Archean lode-gold deposits: fluid flow and chemical evolution in vertically extensive hydrothermal systems: Ore Geology Reviews, v.10, p.279-293.

Ridley, J.R., Groves, D.I., and Knight, J.T., 2000, Gold deposits in amphibolite and granulite facies terranes of the Archean Yilgarn Craton, Western Australia: Evidence and implications of synmetamorphic mineralization: Reviews in Economic Geology, No. 11, p.265-290.

Wang, L.G., McNaughton, N.J., and Groves, D.I., 1993, An overview of the relationship between granitoid intrusions and gold mineralization in the Archaean Murchison Province, Western Australia: Mineralium Deposita, v.28, p.482-494.

Witt, W.K., 1993, Gold mineralization in the Menzies-Kambalda region, Eastern Goldfields, Western Australia: Western Australian Geological Survey, Report 39, 65p.

Witt, W.K., Knight, J.T., and Mikucki, E.J., 1997, A synmetamorphic lateral fluid flow model for gold mineralization in the Archean southern Kalgoorlie and Norseman Terranes, Western Australia: Economic Geology, v.92, p.407-437.

Wyborn, L.A.I., Heinrich, C.A., and Jaques, A.L., 1994, Australian Proterozoic mineral systems: essential ingredients and mappable criteria: *in* AusIMM Annual Conference, Proceedings Volume. Melbourne, Australasian Institute of Mining and Metallurgy, p.109-115.

Wyman, D.A., and Kerrich, R., 1988, Alkaline magmatism, major structures, and gold deposits: Implications for greenstone belt gold metallogeny: Economic Geology, v.83, p.451-458.

Yeats, C.J., McNaughton, N.J., and Groves, D.I., 1996, SHRIMP U-Pb geochronological constraints on Archean volcanic-hosted massive sulfide and lode gold mineralization at Mount Gibson, Yilgarn Craton, Western Australia: Economic Geology, v.91, p.1354-1371.

Yeats, C.J., McNaughton, N.J., Ruettger, D., Bateman, R., Groves, D.I., Harris, J.L., and Kohler, E., 1999, Evidence for diachronous Archean lode gold mineralization in the Yilgarn Craton, Western Australia: A SHRIMP U-Pb study of intrusive rocks: Economic Geology, v.94, p.1259-1276.

Table 9.1 Fluid inclusion data for samples of the Boorabbin Low-Ca granitoid, Southern Cross Province (plutno 293504).

CO2-CH4 fluid inclusions

Sample	FI	Length	Tm	VolFrac	Th to	Th (L-V)	CO2 Density	CO2 MV	XCH4	Equiv CO2 Den	Equiv CO2 MV
98967100D	1_1	12	-56.6	0.5	L	30.9	0.52	85.12			
98967100D	1_2	8	-56.6	0.5	L	30.9	0.52	85.12			
98967100D	1_3	10	-56.6	0.5	L	30.97	0.49	90.17			
98967100D	1_4	12	-56.6	0.5	L	30.9	0.52	85.12			
98967100D	1_5	10	-56.6	0.5	L	30.9	0.52	85.12			
98967100D	1_6	6	-56.6	0.5	L	30.9	0.52	85.12			
98967100D	2_1	10			L	-72.4			0.799	0.562	38.53
98967100D	2_2	7			L	-72.3			0.799	0.562	38.53
98967100D	2_3	6			L	-72.4			0.799	0.562	38.53
98967100D	4_1		-56.6	0.6	V	30.8	0.40	109.75			
98967100D	4_2	10	-56.6	0.5	V	30.97	0.45	98.86			
98967100D	5_2	4	-56.6	0.9	V	29.7	0.34	131.25			
98967100E	4_1	12	-56.7	0.05	L	28.8	0.63	69.39	0.004	0.44	99.71
98967100E	4_2	10	-56.6	0.5	L	28.8	0.63	69.39			
98967100E	4_3	6	-56.6	0.5	L	30.7	0.55	80.57	0.002	0.44	99.9
98967100E	4_4	6	-56.7	0.5	L	28.6	0.64	68.79	0.004	0.442	99.34

H2O-CO2-CH4-NaCl fluid inclusions

Sample	FI	Length	Tm CO2	VolFrac Vap	Tm Clath	Th to	Th CO2 L-V	VolFrac CO2	T of Estim	Th Total	L-V	Aq Density	Molal NaCl
98967100D	3_1	6	-56.6	0	10	L	30.8	1	30.8	30.8	L	0.99	0.003526
98967100D	3_2	4	-56.6	0	10	L	30.9	0.3	30.9	324.8	L	0.99	0.003526
98967100D	5_4	5	-56.6	0.9	10	L	29.8	1	29.8	336.2	V	0.99	0.003526
98967100D	3_1	6	-56.6	0	10	L	30.8	1	30.8	30.8	L	0.99	0.003526
98967100D	3_2	4	-56.6	0	10	L	30.9	0.3	30.9	324.8	L	0.99	0.003526
98967100D	5_4	5	-56.6	0.9	10	L	29.8	1	29.8	336.2	V	0.99	0.003526

H2O-CO2-CH4-NaCl (cont)

Sample	FI	Wt% NaCl	X(NaCl)	Carb Den	Carb MV	Carb XCO2	Carb XCH4	Bulk XH2O	Bulk XCO2	Bulk XNaCl	Bulk XCH4	Bulk Den	Bulk MV
98967100D	3_1	0.0206	0.000064	0.544	80.837	1	0	0	1	0	0	0.544	80.837
98967100D	3_2	0.0206	0.000064	0.532	82.719	1	0	0.914	0.086	0	0	0.852	23.77
98967100D	5_4	0.0206	0.000064	0.604	72.873	1	0	0	1	0	0	0.604	72.873
98967100D	3_1	0.0206	0.000064	0.544	80.837	1	0	0	1	0	0	0.544	80.837
98967100D	3_2	0.0206	0.000064	0.532	82.719	1	0	0.914	0.086	0	0	0.852	23.77
98967100D	5_4	0.0206	0.000064	0.604	72.873	1	0	0	1	0	0	0.604	72.873

H2O-NaCl-[KCl] inclusions

Sample	FI	Length	Tm ice	VolFrac Vap	Th L-V	Th to	Te	Molal NaCl	Wt% NaCl	X(NaCl)	Crit.Temp.	Crit.Press.	Bulk Den	Bulk MV
98967100D	5_1	5	-2.3	0.15	327.1	L		0.67	3.76	0.012	409	308	0.69	26.84
98967100D	5_3	4	-2.4	0.5	333.1	L		0.70	3.92	0.012	410	312	0.68	27.27
98967100E	1_2	20	-1.9	0.5	356.1	L		0.55	3.12	0.010	403	292	0.61	30.35
98967100E	1_3	10	-1.3	0.15	231.5	L		0.38	2.14	0.007	394	267	0.84	21.73
98967100E	1_4	5	-1.6	0.15	227.2	L		0.46	2.63	0.008	398	280	0.85	21.50
98967100E	1_5	25	-1.3	0.15	233.9	L		0.38	2.14	0.007	394	267	0.84	21.82
98967100E	1_6	25	-1.3	0.4	347.9	L		0.38	2.14	0.007	394	267	0.61	30.06
98967100E	1_7	8	-1.4	0.5	220	L		0.40	2.31	0.007	395	271	0.86	21.28
98967100E	1_8	8	-1.3	0.3	246.7	L		0.38	2.14	0.007	394	267	0.82	22.34
98967100E	2_1	15	-1.4	0.6	441.5	C	-13.5	0.40	2.31	0.007			0.31	58.35
98967100E	2_2	3	-10.6	0.05	129.4	L	-13.4	2.92	14.57	0.050	508	579	1.03	19.53
98967100E	2_3	3	-10.8	0.05	169.4	L	-13.8	2.97	14.78	0.051	510	585	1.00	20.09
98967100E	2_4	4	-11	0.05	235.1	L	-13.5	3.01	14.98	0.052	512	590	0.95	21.21
98967100E	2_5	2	-10.7	0.1	232.8	L	-13.5	2.94	14.67	0.050	509	582	0.95	21.13
98967100E	3_1	4	-1.7	0.05	242.7	L		0.49	2.79	0.009	400	284	0.83	22.08
98967100E	3_2	5	-1.6	0.05	251.9	L		0.46	2.63	0.008	398	280	0.82	22.47
98967100E	3_3	5	-10.3	0.3	366.4	L		2.85	14.26	0.049	505	572	0.79	25.47
98967100E	3_4	5	-1.6	0.9	422.1	V		0.46	2.63	0.008			0.39	46.52
98967100E	3_5	5	-1.7	0.05	169.4	L		0.49	2.79	0.009	400	284	0.92	19.94
98967100E	3_6	15	-1.5	0.9	424.7	V		0.43	2.47	0.008			0.38	48.21
98967100E	3_7	20	-1.4	0.9	303.6	L		0.40	2.31	0.007	395	271	0.72	25.54
98967100E	3_8	5	-0.6	0.05	346.8	L		0.17	0.99	0.003	383	240	0.59	30.83

Figure 9.1 Binary plots for the various granitoid groups in the Yilgarn Craton. Each point represents the average values for each pluton in the Craton.

A. TAS plot of total Na_2O+K_2O (wt%) versus SiO_2 (wt%) of Le Maitre et al. (1989) illustrating the felsic nature of the majority of granitoids in the Yilgarn Craton.
B. Alkalinity plot of total Na_2O+K_2O (wt%) versus SiO_2 (wt%) using the alkaline and subalkaline fields of Irvine & Baragar (1971). The plot illustrates the subalkaline nature of granitoids in the Yilgarn Craton, with the exception of granitoids belonging to the Syenitic group.
C. Subdivision of subalkaline rocks using the K_2O (wt%) versus SiO_2 (wt%) plot of Peccerillo & Taylor (1976). Note that the majority of Mafic group granitoids plot in the low- and intermediate-K calc-alkaline fields, whereas the Low-Ca group granitods plot in the high-K field.
D. Degree of Aluminium Saturation (ASI, molecular Al/[Ca+Na+K]) versus SiO_2 (wt%) plot illustrating the largely metaluminous (M) and peraluminous (P) character of vast majority of Yilgarn granitoids.
E. Redox ($[Fe_2O_3/FeO]/[0.5-0.03*FeO]$) versus SiO_2 (wt%) plot illustrating the oxidised (>1.0) to strongly oxidised (>5.0) character of the majority of Yilgarn Craton granitoids.
F. mg* ([100*MgO/40.32]/[FeO/71.85+Fe2O3/79.85+MgO/40.32]) versus SiO2 (wt%) plot illustrating the higher mg* character of the Mafic group granitoids.
G. HGU (Average Heat Production for Unit/density $=0.317*[0.718*U\{ppm\}+0.193*Th\{ppm\}+0.262*0.8301*K_2O\{wt\%\}]$) versus SiO_2 (wt%) plot illustrating the high heat producing character of all Low-Ca group granitoids in the Yilgarn Craton.
H. Rb (ppm) versus SiO_2 (wt%) plot illustrating the fractionated nature of the Low-Ca group granitoids in the Yilgarn Craton.

Granitoid associations of the Yilgarn Craton. High-Ca– black; Low-Ca – magenta; Mafic – blue; High-HFSE – green; Syenitic – red.

+ Menangina
× Mt Boreas
✳ Granny Smith
□ Xenolith
◇ Kookynie
○ Gilgarna
△ Diemals
▽ Beetle
✡ Westonia
■ Marda
◆ Mainland
● Goolthan
▲ Gem of Cue
▼ Damperwah

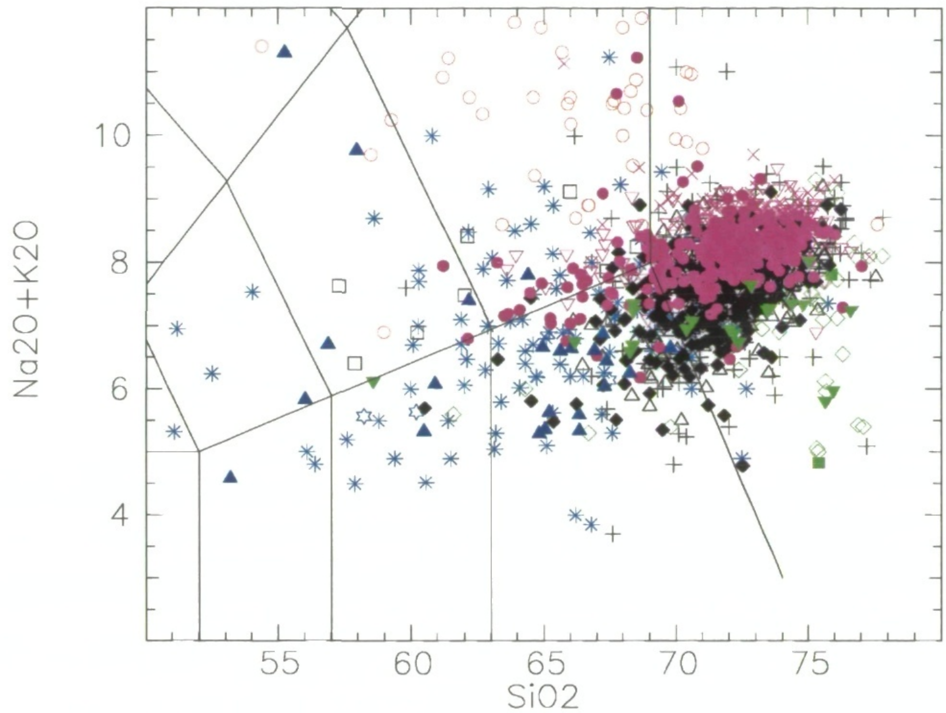

10
8
6
4
Na2O+K2O
55
60
65
70
75
SiO2

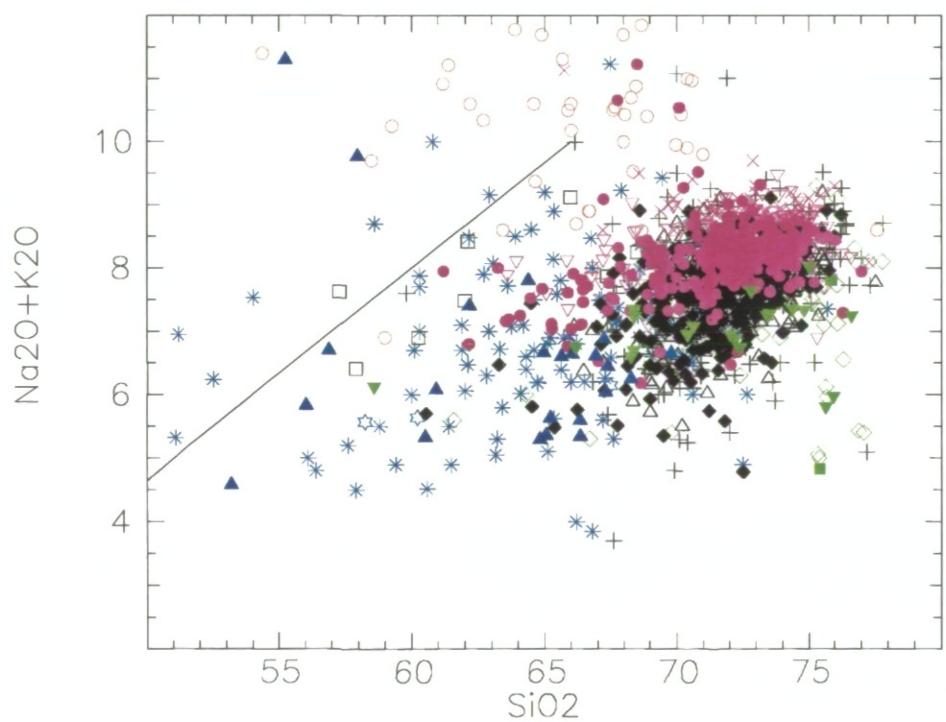

10
8
6
4
Na2O+K2O
55
60
65
70
75
SiO2

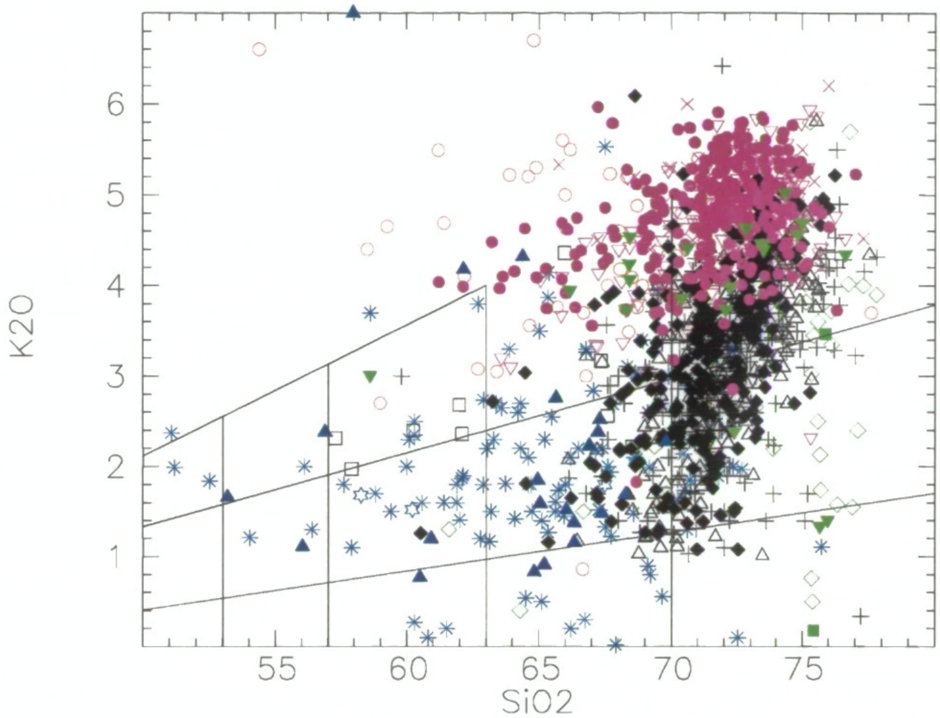
K2O
SiO2
1
2
3
4
5
6
55
60
65
70
75

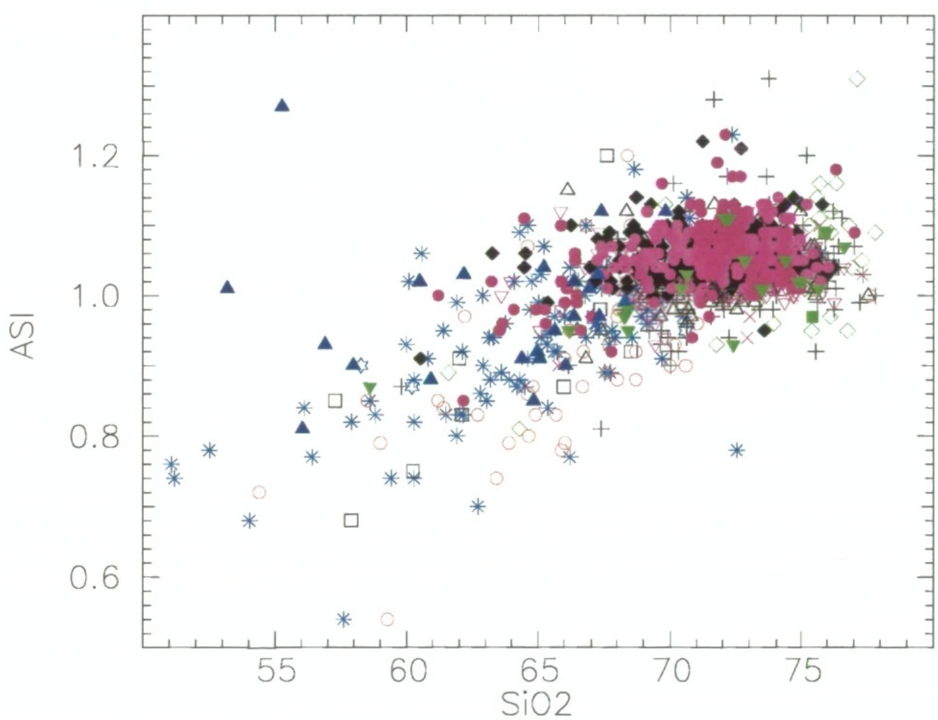
ASI
SiO2
0.6
0.8
1.0
1.2
55
60
65
70
75

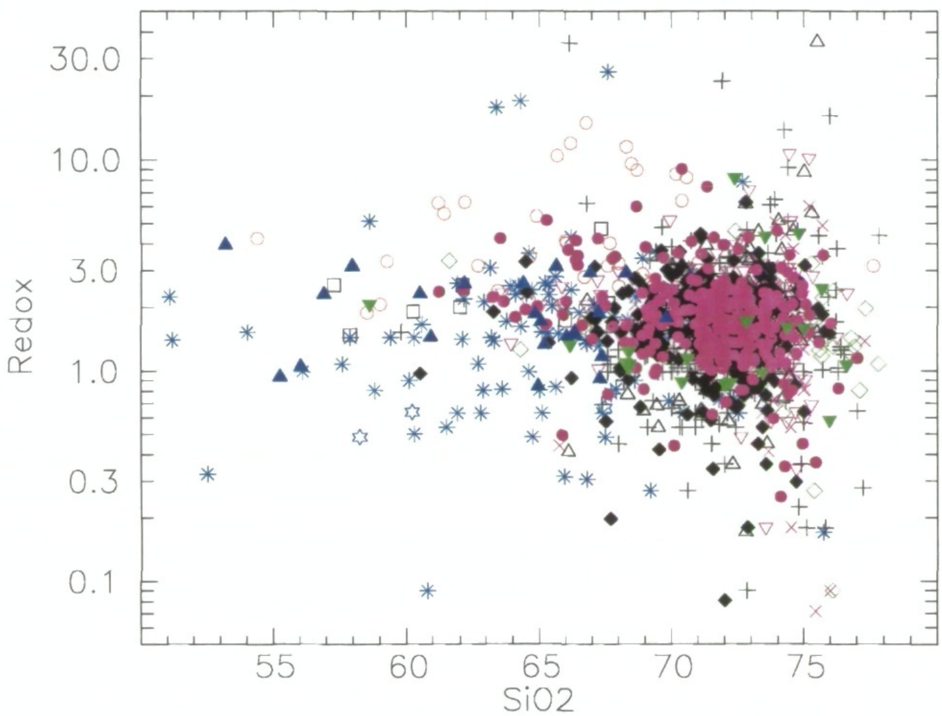
30.0
10.0
3.0
1.0
0.3
0.1
Redox
55
60
65
70
75
SiO2

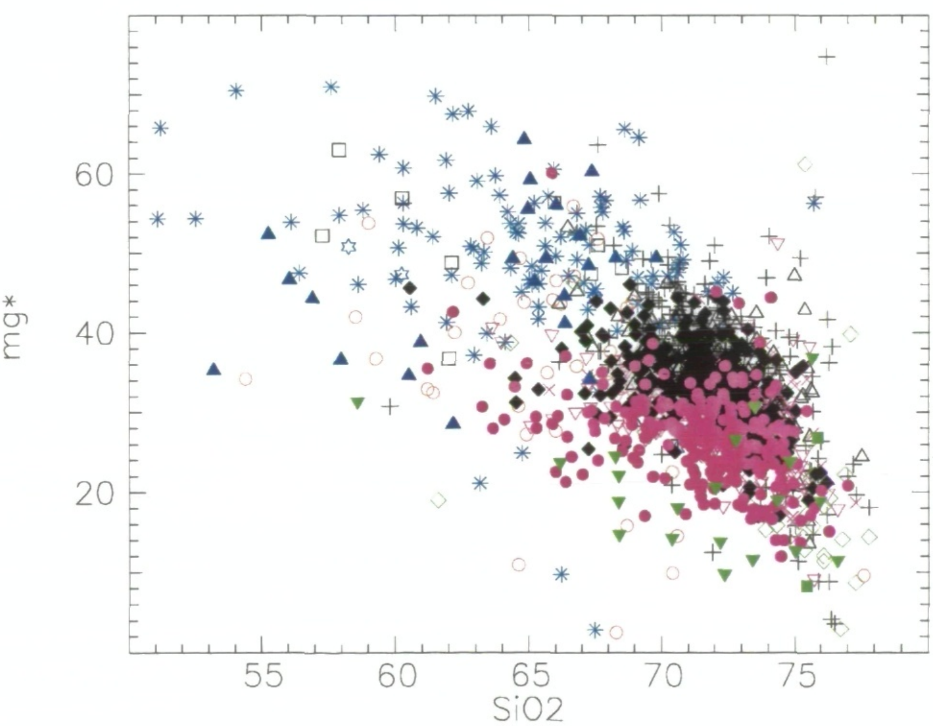
60
40
20
mg*
55
60
65
70
75
SiO2

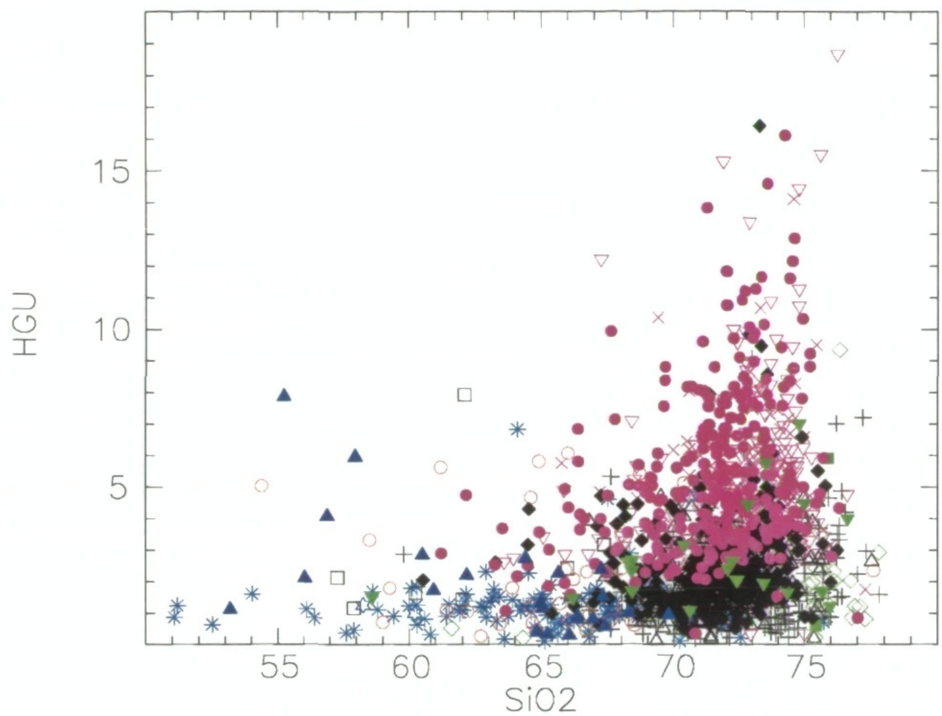

HGU
15
10
5
55
60
65
70
75
SiO2

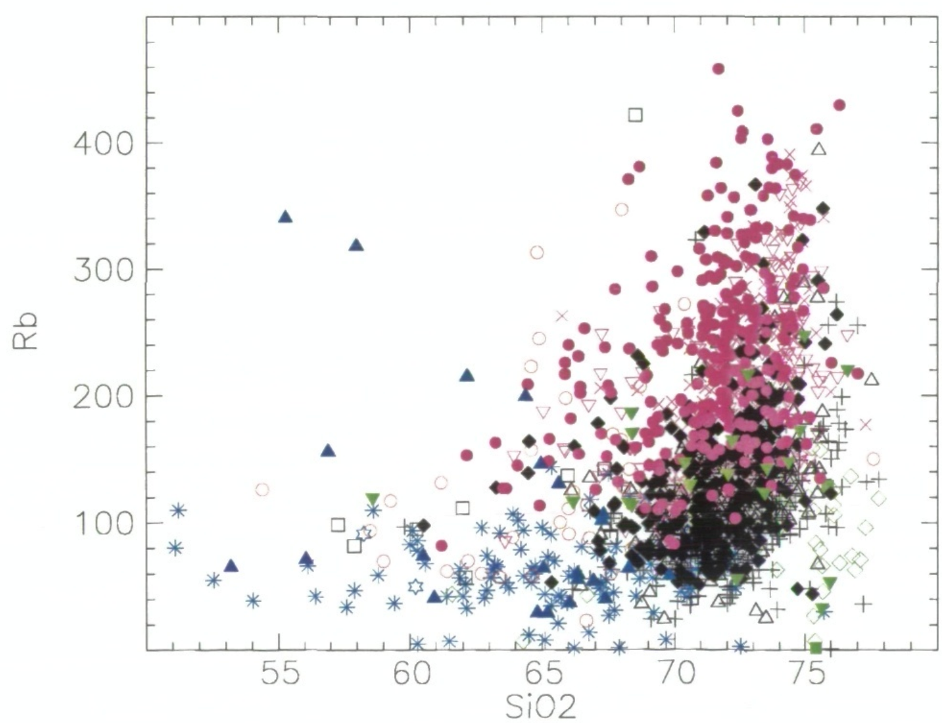

Rb
400
300
200
100
55
60
65
70
75
SiO2

Figure 9.2 Ternary Rb (ppm) – Ba (ppm) – Sr (ppm) plot of El Bouseily & El Sokkary (1975) for granitoid groups in the south-eastern Yilgarn Craton.

A. High-Ca and Low-Ca granitoid clans of the southern Eastern Goldfields Province and south-eastern Southern Cross Province, Yilgarn Craton. 'High-LILE' High-Ca clans – green; 'low-LILE' High-Ca clans – red; Low-Ca – magenta.

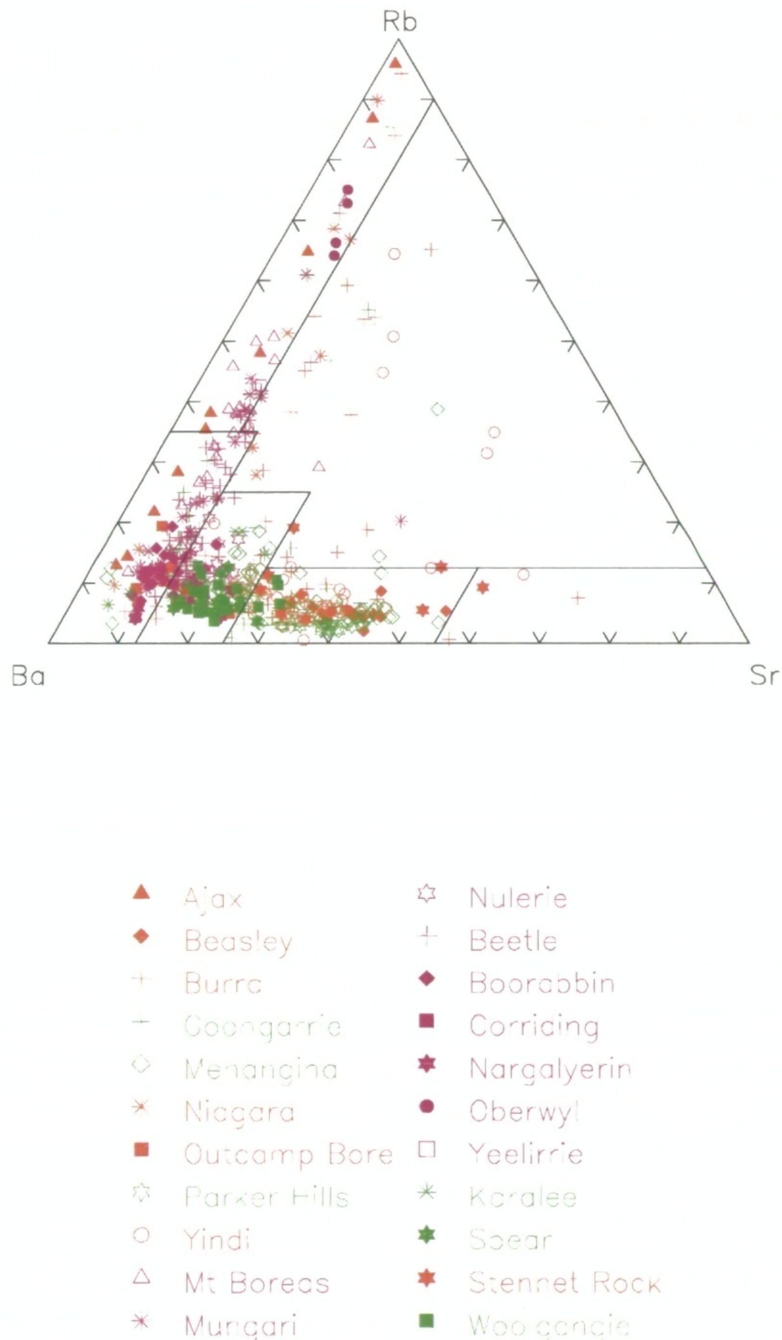

B. Mafic, Syenitic and High-HFSE granitoid clans of the southern Eastern Goldfields Province, Yilgarn Craton. 'High-LILE' Mafic clans – blue; 'low-LILE' Mafic clans – red, Syenitic – black; High-HFSE – green.

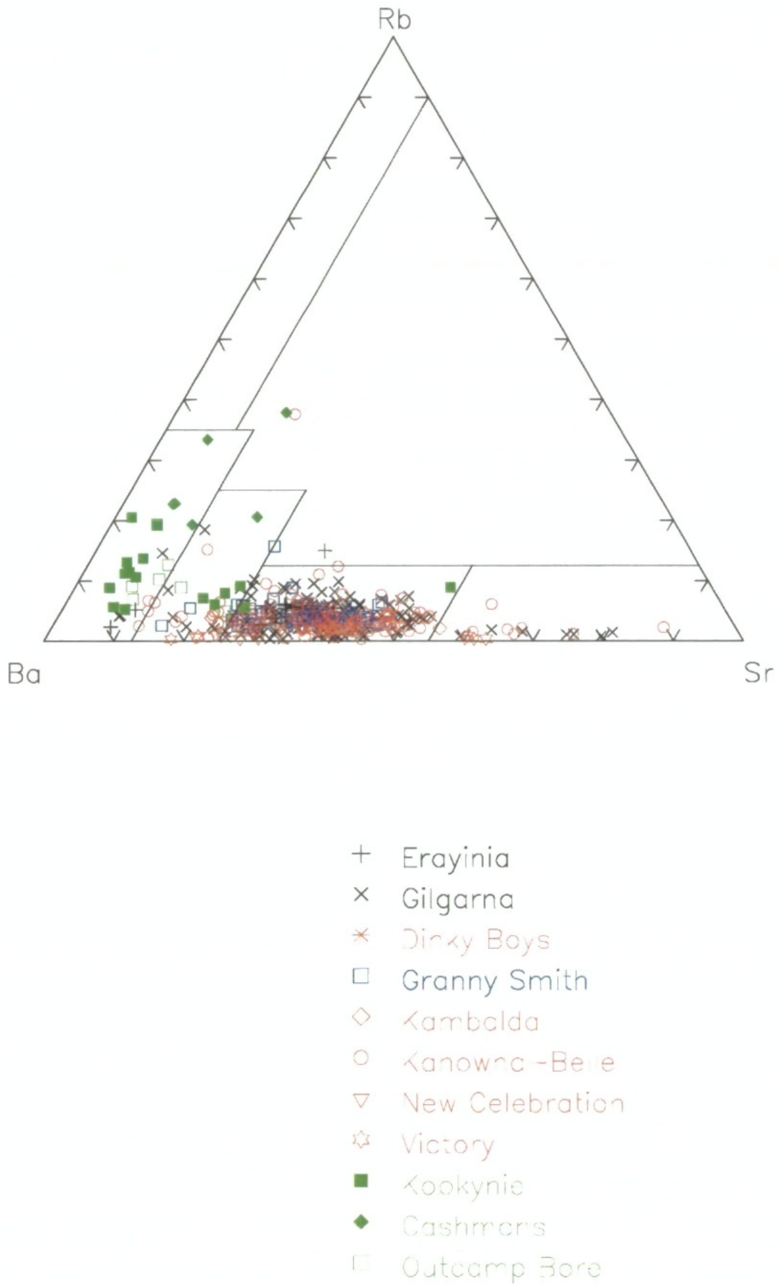

A.

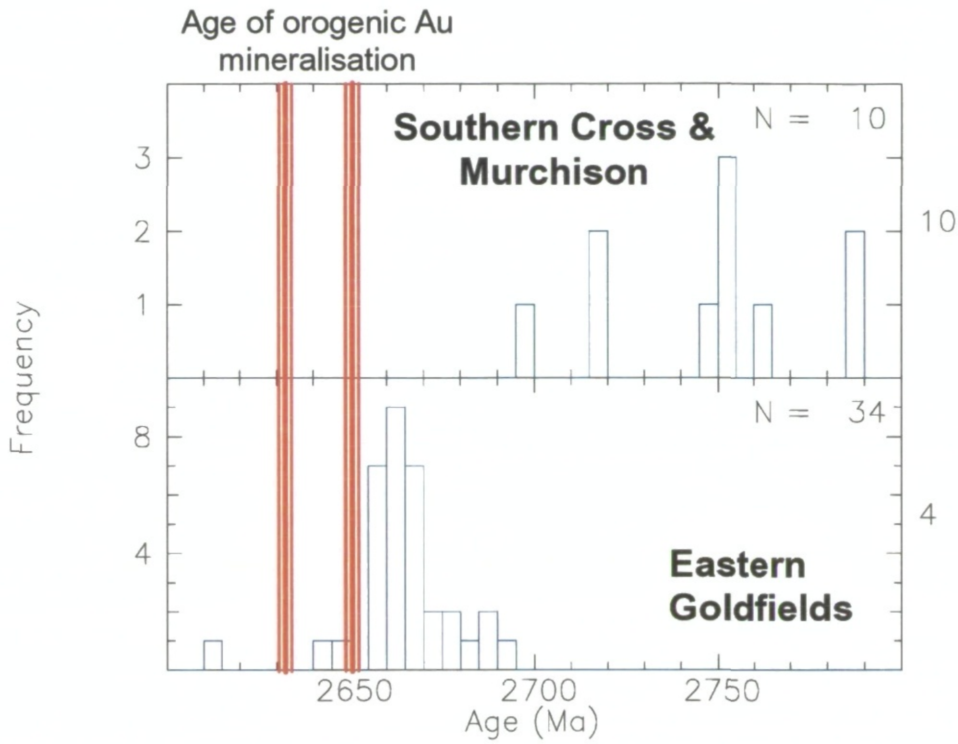

B.

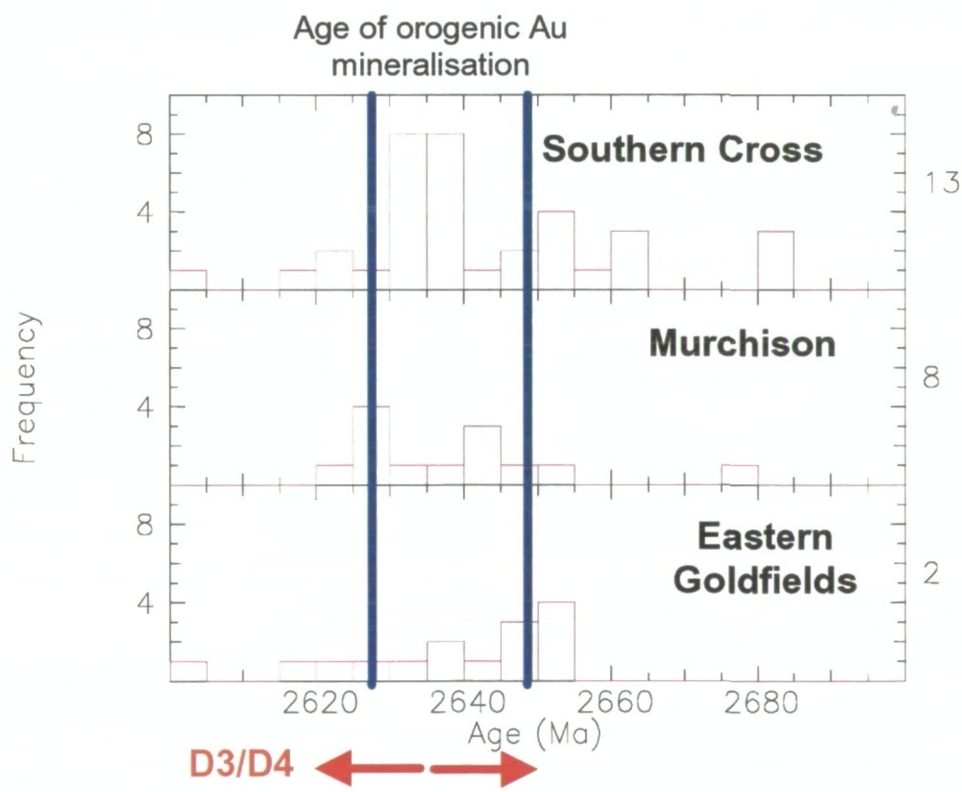

Figure 9.3 A. Summary histogram of ages of Mafic granitoids in the Eastern Goldfields and Southern Cross/Murchison Provinces.
B. Summary histogram of ages of Low-Ca granitoids in the Eastern Goldfields and Southern Cross/Murchison Provinces.

Figure 9.4 Photo(micro)graphs illustrating 'fluid-escape' structures and enclosed fluid inclusions in some Low-Ca granitoid suites, Yilgarn Craton.

A. Biotite-rich 'oikocryst' zones in Boorabbin Low-Ca granitoid (plutno 293504), southeastern Southern Cross Province. 'Oikocrysts' occupy discrete zones sub-parallel to inferred plutong margin and may indicate zones of late magmatic fluid build-up during crystallisation. The biotite-rich 'oikocrysts' enclose euhedral to subhedral quartz and feldspar grains that enclose primary and pseudo-secondary mixed low-salinity aqueous-carbonic fluid inclusions.
B. Miarolitic pipe in Dutakajin Low-Ca granitoid (plutno 233719), southern Murchison Province. The miarolitic cavities and pipes contain euhedral to subhedral quartz-feldspar intergrowths that enclose primary and pseudo-secondary mixed low-salinity aqueous-carbonic fluid inclusions.
C. Trial of pseudosecondary mixed vapour-poor low-salinity H_2O-CO_2-CH_4-NaCl fluid inclusions in quartz within biotite-rich 'oikocrysts' in the Boorabbin Low-Ca granitoid, southeastern Southern Cross Province.
D. Trial of pseudosecondary mixed vapour-rich and vapour-poor low-salinity H_2O-CO_2-CH_4-NaCl fluid inclusions in quartz within biotite-rich 'oikocrysts' in the Boorabbin Low-Ca granitoid, southeastern Southern Cross Province.

A.

B.

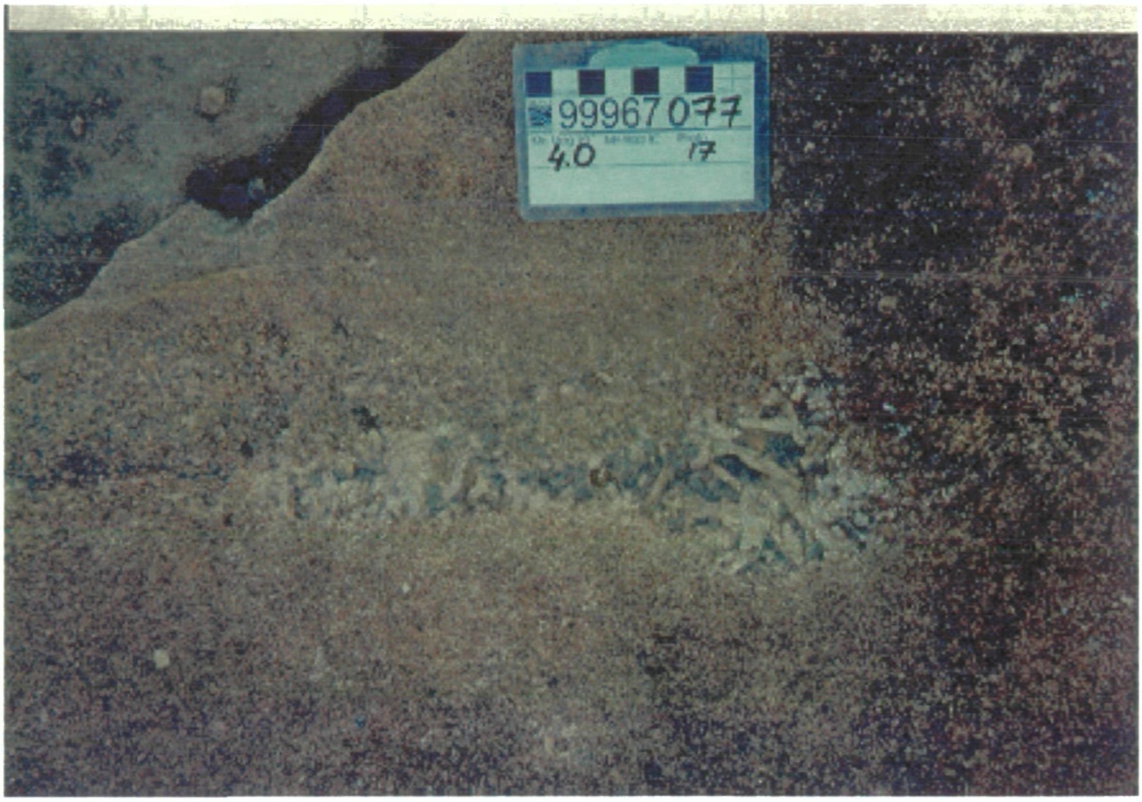

C.

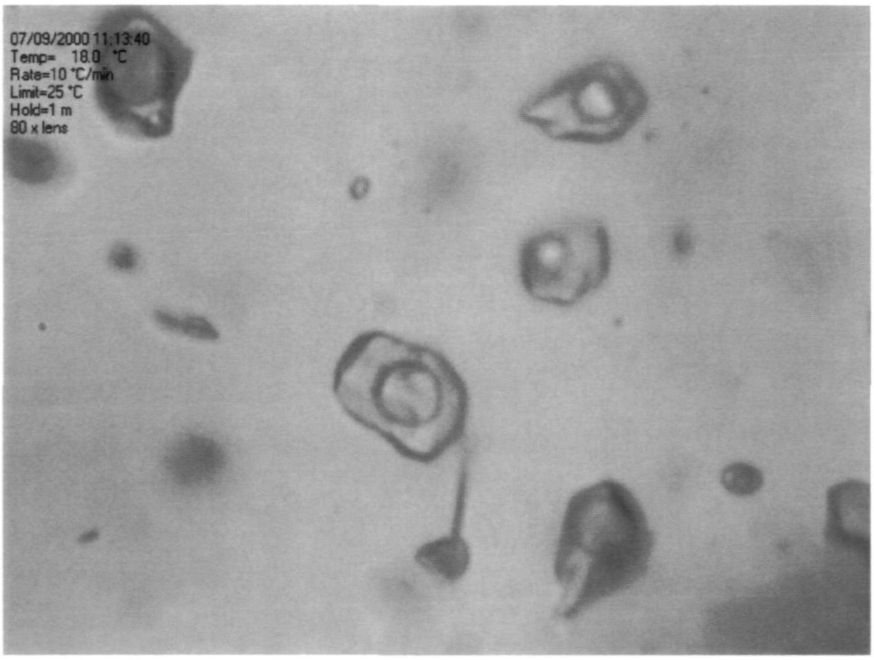
07/09/2000 11:13:40
Temp= 18.0 °C
Rate=10 °C/min
Limit=25 °C
Hold=1 m
80 x lens

D.

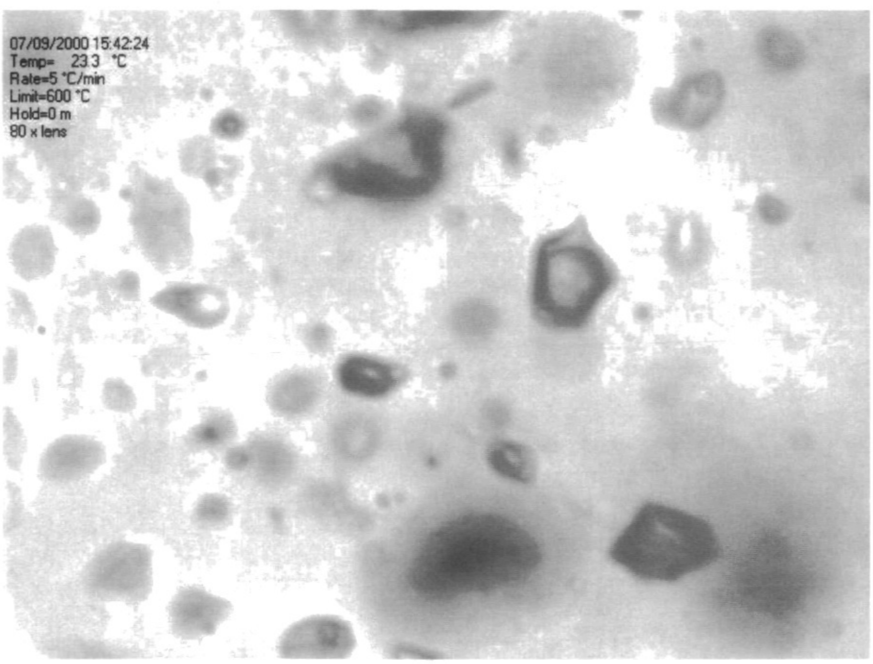
07/09/2000 15:42:24
Temp= 23.3 °C
Rate=5 °C/min
Limit=600 °C
Hold=0 m
80 x lens

Archean orogenic lode-gold mineralising systems: A synthesis of features

Kevin F. Cassidy & Steffen G. Hagemann

Note: This is a modified version of a paper by S.G. Hagemann & K.F. Cassidy, 2000, Archean orogenic lode-gold deposits, Reviews in Economic Geology, vol. 13, p.9-68.

Summary

Archean orogenic lode-gold deposits are the end-result of large, complex mineralizing systems developed within many Archean terrains. Mineralizing systems are defined to include all geological factors that control the generation and preservation of mineral deposits and emphasize the processes responsible for deposit formation at a variety of scales. Deposits belonging to Archean orogenic lode-gold mineralizing systems comprise epigenetic mineralization that formed as a result of focussed fluid flow late during active deformation and metamorphism of volcano-plutonic terranes. They can occur in any lithology and formed at a range of paleo-crustal levels through site-specific and local physical and chemical processes. All Archean orogenic lode-gold deposits formed through broadly similar geological processes, with the unique character of individual deposits resulting mainly from variations at the depositional site. The key feature of Archean orogenic lode-gold systems is a broadly uniform low-moderate salinity, mixed aqueous-carbonic fluid capable of carrying Au, but having limited capacity to transport base metals.

Models for development of orogenic lode-gold mineralizing systems are generally poorly constrained, although geological and geochemical characteristics are consistent with terrane- or larger-scale processes. Archean terranes containing orogenic lode-gold systems include accretionary and collisional settings. Mineralization is generally late in the tectonic evolution of the host terranes, is typically syn- to post-peak metamorphism, becoming increasingly post-peak at higher paleo-crustal levels, is indicative of clockwise metamorphic PT paths and implicating processes involving 'deeper later'-type metamorphism. There are few robust absolute ages on mineralization although, in most terranes, available ages indicate mineralization follows major volcanic, sedimentary and plutonic episodes. In many terranes, mineralization is coincident with mid-crustal felsic magmatism. Young absolute ages recorded in some deposits probably reflect resetting and/or new mineral growth during post-gold mineralization hydrothermal activity and/or slow cooling of host terranes. The source(s) of fluids and metals in orogenic lode-gold systems is poorly understood; however, mineral equilibria and isotope tracers implicate sources deeper than presently exposed greenstones. Isotope tracers and mineral equilibria are also consistent with derivation from and/or equilibration of the ore fluid with felsic rocks during transport of hydrothermal fluids to depositional sites. Stable and radiogenic isotope tracers alone do not distinguish between fluid derivation through metamorphic devolatilization and magmatic fluid evolution. Some deposits formed at high paleo-crustal levels, however, and record the influx of surface waters.

Transport of large volumes of broadly uniform hydrothermal fluids over relatively long distances is implicated and requires channelized fluid flow with minor modification of major molecular components *en route* from source to depositional sites. Selected major deformation zones that are truly 'crustal-scale', as demonstrated by deep seismic profiling, provide ideal fluid pathways for deeply-sourced hydrothermal fluids. The largest gold provinces show spatial proximity of world-class lode-gold deposits to 'crustal-scale' deformation zones (e.g.,

Boulder-Lefroy, Destor-Porcupine). Linking of active faults is important for fluid focussing and effective transport of hydrothermal fluids. The hydrothermal fluids transport gold along the pathways as one or more neutral and reduced sulfide species. Chemical modelling demonstrates that the inferred hydrothermal fluids can effectively transport gold over long distances and over a significant crustal-depth range. Provided the fluids remain effectively channelized during transport to higher crustal levels, camp- and deposit-scale structural focussing and associated local gold precipitation mechanisms are required to ensure development of economic gold mineralization at the trap site.

Archean orogenic lode-gold mineralizing systems have distinctive depositional site characteristics at both the camp- and deposit-scale. Camp-scale features include geochemical signatures related to regional alteration surrounding major deformation zones, large-scale structural inhomogeneities (e.g., bends in major deformation zones, district-scale granitoid-greenstone contacts), and the presence or absence of overlying rock successions that can act as barriers (e.g., seals, aquicludes) to fluid movement. Deposit-scale variables include the local host rocks, structural traps (fault intersections, contacts between contrasting lithologies) typically in zones of low mean stress, and the pressure-temperature conditions in the host sequence. Resulting alteration assemblages primarily reflect interaction of host lithologies with the hydrothermal fluid at a particular pressure and temperature. Alteration assemblages generally show enrichment in K, CO_2 and S in deposits irrespective of paleo-crustal level. A metal association of Au, Ag +/- As, B, Bi, Sb, Te and W is displayed by most deposits. Fluid inclusion-derived data at individual deposits show a range in compositions, although salinity is generally low to moderate, with mixed aqueous-carbonic compositions. Variations in CO_2, CH_4, N_2, salinity and redox-state may reflect district- to local-scale processes and/or specific host rocks rather than differences in fluid source. Deposition at the trap site is likely to reflect catastrophic effects in response to physical changes (e.g., large pressure fluctuations, seismic events), with resultant chemical changes due to local fluid-wallrock interaction, phase separation and/or fluid mixing.

The extreme diversity of Archean orogenic lode-gold deposits reflects the complex interplay of physical and chemical processes at a trap (depositional) site localized at various crustal levels ranging from sub-greenschist to upper-amphibolite facies metamorphic environments, with gold precipitation occurring over a correspondingly wide range of pressures and temperatures. The variability in deposit characteristics largely reflects the pressure-temperature conditions, variability in host rock and local changes in ore fluid composition.

Introduction

Archean orogenic lode-gold deposits are widespread in most Archean granitoid-greenstone terrains (Fig. A1), and account for almost 20 percent of cumulative world gold production (Roberts, 1988). Excluding the 'supergiant' (>2500 tonne Au) Witwatersrand deposits of South Africa, Archean cratons contain some of the world's largest gold deposits, including the giant Golden Mile (>2000 t) deposit near Kalgoorlie, eastern Yilgarn Craton (Fig. A2) and the Hollinger-McIntyre (>1000 t) deposit near Timmins, Superior Province (Fig.A3). The Yilgarn Craton in Western Australia hosts over 160 gold deposits containing more than 1 t Au, with more than 15 world-class single deposit and deposit clusters ('mining camps'; Fig. A4). The Archean Superior and Slave Cratons in Canada host in excess of 220 known gold deposits containing more than 1 t Au (Robert and Poulsen, 1997). Fourteen deposits contain more than 100 t of gold and are regarded as 'world-class', whereas the majority of deposits contain between 0.4 and 10 Mt of ore at grades between 4 and 12 g/t Au, corresponding to 3-100 t of contained gold (Fig. A4). Other Archean cratons, such as the Dharwar Craton of southern

India, the Sao Francisco Craton of South America and the Kaapvaal, Zimbabwe and Tanzania Cratons of southern Africa also contain significant orogenic lode-gold deposits, including the 'giant' Kolar deposit in southern India. Archean cratons in Finland and Russia (Karelian Craton), Greenland and China also contain gold deposits, although exploration in these terrains has not yet revealed the existence of world-class Archean gold deposits.

Archean orogenic lode-gold deposits tend to occur in clusters within mining camps, defined as areas of about 100 km^2. Camps show a characteristic variation in size (Hodgson, 1993) with most of the production coming from world-class (>100 t Au) and a few giant (>500 t Au) deposits. Based on available resource data, Hodgson (1993) estimated that the 28 deposits containing >60 t Au in the Archean provinces of Canada, Zimbabwe and Australia constituted 10 percent of the population of 271 deposits containing >3 t Au, and accounted for two thirds of total production plus reserves in these provinces.

The Archean orogenic lode-gold deposit class is generally defined as structurally-controlled wallrock and/or vein-hosted mineralization that occurs in all rock types of Archean granite-greenstone terrains and is considered to be epigenetic with respect to host rock formation (Groves et al., 1998). These deposits are formed from broadly uniform hydrothermal fluids transporting Au and several other metals. Based on a range of structural, hydrothermal alteration and ore fluid characteristics, these deposits are interpreted to have formed over a range of paleo-crustal levels from shallow (<5 km) to deep (20 km) as a result of focussed fluid flow late during active deformation and metamorphism in volcano-plutonic terranes. Hydrothermal fluids are potentially derived from a variety of fluid sources including metamorphic devolatilization, fluid release from felsic intrusive rocks and mantle sources.

It is recognised that there are several other gold deposit classes in the Archean. These include the Witwatersrand deposits in South Africa that historically have been described as modified 'paleoplacers' (although Phillips and Law (2000) suggest that they have affinities with orogenic lode-gold systems), and the Horne and Bousquet deposits in Canada that are world-class Au-rich VHMS deposits (e.g., Huston, 2000). Some of these deposits (Bousquet, Hemlo, Boddington) show features of more than one mineralization style (e.g., overprinting of one deposit type by another), or have some features that can be interpreted as being of more than one mineralization type. In some of these deposits, primary mineralization has been remobilized during extensive deformation and metamorphism and/or overprinted by later orogenic lode-gold mineralization. However, careful documentation of the relative timing, ore fluid character and metal association of these deposits clearly necessitates assigning these deposits to other deposit classes.

The giant Hemlo deposit in Canada has been interpreted as potentially belonging to various deposit classes, including the orogenic lode-gold class. Detailed structural and textural studies suggest an early introduction of gold and subsequent remobilization during later deformation (e.g., Michibayashi, 1995; Powell and Pattison, 1997), indicating that the deposit cannot be classified as 'orogenic lode-gold'.

The giant Boddington gold deposit has been recently debated as a 'porphyry-style' Cu-Mo-Au deposit with distinct orogenic lode-gold overprint (± gold remobilization). Boddington mineralization has some features (metal association, fluid inclusion populations) more typical of 'porphyry-style' mineralising systems as well as some features (structural timing) more aligned with 'orogenic lode-gold' mineralizing systems. Further work is required for the Boddington deposit.

The *Mineral Systems* concept

The *mineral systems* concept is based largely on the *petroleum systems* concept (e.g., Magoon and Dow, 1991), that has been employed with great success by the petroleum industry. The success of the petroleum systems concept lies in the predictive ability to assess the petroleum potential of individual basins. The strength of the petroleum systems approach is attributed to its strong genetic character that permits the model to adapt to a wide variety of geologic settings. Petroleum system models combine geological characteristics at a variety of scales (basin to local trap) with analysis of the characteristics of sedimentary basins to generate a methodology for selection of individual targets. Petroleum systems generally are applicable to scales, intermediate between regional- (i.e., basin) and local- (i.e., trap site) scale. This approach can provide very useful targeting criteria for exploration and a statistical basis for assessment that identifies favorable areas even before on-site examinations (Barton, 1993).

This concept can also be applied to mineral deposits, although mineral systems are both more diverse and more complex. Wyborn et al. (1994) defined the *mineral system* to be 'all geological factors that control the generation and preservation of mineral deposits, and stress the processes that are involved in mobilizing ore components from a source, transporting and accumulating them in more concentrated form'. Important geological factors defining the characteristics of any mineralizing system (as depicted in Fig. A5) include:

- Source(s) of energy (e.g., far-field geodynamic setting, sources of heat and thermal gradients, etc.) driving the system at the terrane- or regional-scale.
- Source(s) of mineralizing fluids, transporting ligands and metals and other ore components.
- Pathways whereby mineralizing fluids migrate to the 'trap' site, including information on the architecture of the pathways and timing of fluid flow.
- Mechanical and structural focussing mechanisms at the 'trap', or depositional, site (camp- and deposit-scale including structural traps, favorable host lithologies, impermeable 'seals' to fluid flow, etc.).
- Chemical and/or physical processes leading to mineral precipitation at the 'trap' site (camp- to micro-scale).

These geological factors provide a framework for integrating observations at the regional- to deposit-scale which can be used to classify mineral deposits, as well as key criteria for developing predictive exploration models relevant to area selection. In this way, the variability of mineral deposit features in any one mineral system can be incorporated into a larger-scale genetic model. In fact, within a single mineral system, there is the possibility of multiple mineral deposit types. This is best exemplified by the high-level intrusion-related 'porphyry' system that can generate porphyry-Cu-Mo, epithermal and other mineral deposit types within a single system (cf., Barton, 1993; Poulsen et al., 2000). However, the lack of one or more essential ingredients within a particular mineral system may preclude the formation of mineral deposits. The mineral systems approach has been used with increasing success to describe the ore forming systems responsible for VHMS deposits (Huston, 1997), as well as Proterozoic granite-related Au and/or base metal deposits (Wyborn et al., 1994).

The scale of a mineralizing system can vary widely and depends primarily on its type. For instance, the size of a complete intrusion-related 'porphyry' and/or VHMS mineral system may be the size of an individual district, whereas MVT and other sedimentary-hosted mineral systems are potentially the size of the whole basin. The emerging models for some syngenetic sedimentary deposits are increasingly mature and robust because the deposit can be viewed as merely a special facies of the host, and the geology of a geographically extensive host package can provide a dependable targeting tool. However the biggest problem in developing such models, particularly for epigenetic deposits, is to distinguish essential ingredients from incidental geological factors (e.g., Barton, 1993). Nevertheless, the combination of recent advances in understanding lode-gold deposits at the 'trap' site as well as the regional geological framework of host terranes allow the first attempt to be made to define the orogenic lode-gold mineralizing system in Archean terranes.

Archean orogenic lode-gold mineral systems

The key to characterizing a mineral system, by analogy with the petroleum system, is the transport of a fluid of a particular composition from its source(s) to potential trap sites. There is a general consensus that the vast majority of Archean lode-gold deposits record a broadly uniform fluid (e.g., Groves et al., 1992; Ridley et al., 1996; McCuaig and Kerrich, 1998; Ridley and Diamond, 2000). This fluid is a low-moderate salinity, mixed aqueous-carbonic fluid capable of carrying Au, Ag and several other metals in solution. Although fluid-rock interaction is interpreted to have modified certain molecular components and isotopic compositions *en route* from the source(s) to potential trap sites, the fluid remained broadly uniform as it migrated over relatively long distances to the trap site (Ridley et al., 1996; Ridley and Diamond, 2000). The uniform ore fluid is a key feature of Archean orogenic lode-gold mineral systems.

The other components of the Archean orogenic lode-gold mineral system (source of energy, source of fluids, trap sites, etc.) can be identified in part based on the observations that there is a common fluid. On this basis, deposits belonging to an Archean orogenic lode-gold system comprise primary epigenetic mineralization that formed as a result of focussed fluid flow late during active deformation and metamorphism of a volcano-plutonic terrane, in any lithology and at a range of paleocrustal levels, through site-specific and local physical and chemical processes. In all Archean orogenic lode-gold deposits these similar broad geological processes are responsible for deposit formation, but the final character of each deposit results ultimately from variations at the depositional site.

The extreme diversity of Archean orogenic lode-gold deposits reflects the complex interplay of various physical (e.g., fluid pathway architecture, host rock rheology, pressure and temperature) and chemical (e.g., fluid and rock compositions, metal carrying potential of hydrothermal fluids, redox state, acidity, etc.) processes at the trap-site (camp- to micro-scale). The trap-site may be localized at various crustal levels ranging from sub-greenschist to upper-amphibolite facies metamorphic environments, and gold precipitation may occur over a corresponding wide range of pressure and temperature conditions through fluid-wallrock interaction, fluid mixing and/or phase separation (e.g., Groves et al., 1992, 1998; Ridley et al., 2000). The variability in the deposit mineralogical and chemical characteristics largely reflects the pressure-temperature conditions, the variability in host rock and local changes in ore fluid composition (e.g., Colvine et al., 1988; Groves et al., 1992, 1998; Ridley et al., 1995, 2000; Cassidy et al., 1998; McCuaig and Kerrich, 1998).

Use of the mineral system concept clearly demonstrates that the broad deposit-scale variation evident in many Archean orogenic lode-gold deposits is a reflection of local, trap-site variations and not the result of different mineral systems operating within a single terrane. Recognition of the essential features of an orogenic lode-gold mineralizing system within a particular terrane is more important than determining the exact conditions of mineralization at any single trap-site within the system and is paramount to the success of a regional exploration program. Ideally, the explorer would like to rank terranes based on the likelihood of the presence of one or more mineral forming systems. Given that it is likely that different mineral systems may operate at different times during the evolution of a terrane, it is important to consider the relative timing of the mineral system and the effects of later deformation and metamorphism. For instance, orogenic lode-gold systems generally occur during collisional or accretionary tectonics and late in the evolution of a specific terrane (e.g., Barley and Groves, 1992; Kerrich and Cassidy, 1994; Groves et al., 1998). In contrast, shallow intrusion-related systems produce a range of deposit types typically during the constructional phase of the terrane (e.g., Sillitoe, 1991), and potentially could be remobilized and/or overprinted during later fluid-flow and mineralization.

Synthesis of Archean orogenic lode-gold system characteristics

Various detailed studies of numerous deposits (e.g., Clark et al., 1989; Witt, 1993, Ridley et al., 1996; Cassidy et al., 1998; Knight et al., 2000) demonstrate the diversity of characteristics at the depositional site in Archean orogenic lode-gold mineral systems. Through the above studies, the main controlling parameters of each part of the Archean orogenic lode-gold mineral system may be constrained. The overwhelming majority of available geological information is related to the trap site and the reader is referred to several excellent review papers for more detailed syntheses (Colvine et al., 1988; Groves et al., 1989, 1992, 1995; Ho et al., 1990b; McCuaig and Kerrich, 1998).

Prior to synthesising the key features of Archean orogenic lode-gold mineralizing systems, it is important to constrain the absolute and relative timing of Archean orogenic lode-gold mineralization in the Yilgarn Craton. This is followed by a synthesis of the key features of the essential ingredients of Archean orogenic lode-gold mineralizing systems (Fig. A6), namely: (i) the source(s) of energy that drive the system, (ii) the source(s) of fluids and metals, (iii) the migration of fluids along pathways, and (iv) the physical and/or chemical processes leading to ore formation at the depositional site (camp- and deposit-scale). Emphasis is on the Yilgarn Craton, but information for other Archean gold provinces is discussed where applicable.

Timing of mineralization in relation to metamorphism, magmatism and deformation – Yilgarn Craton

Constraining the timing of gold mineralization improves our ability to discriminate between magmatic, thermal or structural events with which mineralization may be genetically related. At the terrane-scale, Archean orogenic lode-gold mineralization is late relative to the overall tectonomagmatic evolution of a host terrane (Groves et al., 1989, 1995; Kerrich and Cassidy, 1994; Ridley et al., 1995; Knight et al., 2000). At the camp- and deposit-scale, deposits in subgreenschist- to greenschist-facies metamorphic environments typically postdate and are retrograde with respect to the peak regional metamorphic conditions (e.g., Clark et al., 1989; Hodgson, 1993; McCuaig and Kerrich, 1998), whereas deposits in amphibolite-facies metamorphic environments are essentially synchronous with regional metamorphism (e.g., Knight et al., 1993, 2000; Ridley et al., 1995, 2000; Cassidy and Hagemann, 1999). Mineral fabrics in deposits formed at high temperature and pressures generally show large degrees of dynamic recovery and, in some cases, it becomes difficult to distinguish between deposits that formed at these P-T temperatures (e.g., Mueller and Groves, 1991; Knight et al., 1993; McCuaig et al., 1993; Ridley et al., 2000) and those formed at lower temperatures and were subsequently metamorphosed (e.g., Big Bell: Phillips and de Nooy, 1988). Several gold camps (e.g., Coolgardie and Norseman regions, Yilgarn Craton: Witt, 1993; Knight et al., 1993; 2000; McCuaig et al., 1993) show transitions in the metamorphic grade of deposits and corresponding transitions in the metamorphic-grade of alteration assemblages. In the Coolgardie district, temperature zonation is spatially related to distance from a regional granitoid intrusion (Knight et al., 2000). There is also evidence in high-temperature deposits that the mineralizing event occurred under pressure-temperature conditions close to those of peak regional metamorphism.

Recent detailed structural and metamorphic studies on a number of orogenic lode-gold deposits in amphibolite facies metamorphic environments in Western Australia have shown that mineralization was broadly contemporaneous with peak metamorphism using the following lines of evidence (Fig. A7):

- Equilibrium textural relationships between native gold and high-temperature silicate and sulfide gangue minerals in ore and proximal alteration zones (e.g., Coolgardie camp: Knight et al., 1993, 2000; Norseman deposits: McCuaig et al., 1993; Southern Cross greenstone belt: Ridley et al., 1995, 2000; Westonia: Cassidy and Hagemann, 1999)
- Sub-microscopic gold in the earliest recognizable sulfarsenide phases in the ore paragenesis (Neumayr et al. 1993; McCuaig et al., 1993; Hagemann et al., 1998)
- Mono- and bi-mineralic alteration assemblages indicative of formation within an open hydrothermal system (e.g., Ridley, 1990; Barnicoat et al., 1991)
- Association of gold deposits with peak metamorphic structures coupled with the absence of known gold mineralization in earlier structures (e.g., Coolgardie camp: Knight et al., 2000)
- Preservation of gold-bearing veins in various states of strain (McCuaig et al., 1993; Ridley et al., 1995), and
- Overprinting of peak metamorphic fabrics by gold-bearing quartz veins and/or gold-associated sulfides (e.g, Coolgardie camp: Knight et al., 2000; Westonia: Cassidy and Hagemann, 1999).

A significant retrograde timing for gold deposition at these deposits appears unlikely, given the correspondence between peak-metamorphic temperatures and equilibration temperatures of silicates and sulfide gangue assemblages associated with gold ores. However, some hypozonal deposits (e.g., Big Bell: Wilkins, 1993; Mueller et al., 1996) contain low-temperature retrograde assemblages that indicate re-equilibration at lower temperatures rather than primary mineralizing conditions.

Some mining camps in the Yilgarn Craton show evidence for more than one episode of gold mineralization. At Kalgoorlie, early Fimiston-style gold-telluride mineralization is crosscut by Mt Charlotte-style gold-pyrite±pyrrhotite mineralization (Clout et al., 1990). At Wiluna, strike-slip faults that control gold-pyrite-arsenopyrite mineralization offset gold-pyrite-chalcopyrite-galena-bearing quartz reefs by up to 800m (Hagemann et al., 1992). However, in the majority of these cases, the multiple gold mineralizing events are either different types of mineral system (e.g., early VHMS followed by later orogenic lode-gold: Mt Gibson) or reflect different stages of mineralization within a progressive orogenic lode-gold mineralizing system (e.g., Wiluna). Even in these latter cases, the relative timing of the orogenic lode-gold mineralizing events is structurally late.

Archean terranes hosting orogenic lode-gold mineralization generally reflect a clockwise peak and retrograde PTt path (Bickle et al., 1985; Dalstra et al., 1997; Ridley et al., 1997). Mineralization is inferred to accompany uplift and exhumation of the greenstone packages (e.g., Barley and Groves, 1992). The short time lag of <40 m.y. between peak metamorphism in orogenic gold host terranes and gold mineralization has been accounted for by thermal rebound during and following collisional tectonism (e.g., Powell et al., 1991; Stuwe et al., 1993; Stuwe, 1998). In particular, during certain types of collision, peak temperatures are attained at progressively later times at increasing crustal levels during thermal reequilibration (e.g., Stuwe et al., 1993). Similar models are invoked to explain the contemporaneity of gold mineralization with high-grade metamorphism in deeper crustal levels in the Yilgarn Craton (e.g., Groves et al., 1995). An alternative view emphasizing differential uplift of hot deep crust resulting in horizontal thermal gradients at higher crustal levels, contemporaneous with gold deposit formation, has been proposed for the southern Norseman-Wiluna belt, Yilgarn Craton (Witt et al., 1997). In this model, felsic intrusions serve to delay retrograde cooling in the uplifted blocks. Dalstra et al. (1997) also invoke a mixed 'magmatic heat – deformation' model to explain variations in the relative timing of deformation and the metamorphic peak and observed metamorphic gradients in the higher-grade, marginal zones of individual greenstone belts in higher temperature terranes in the Yilgarn Craton.

Absolute age of gold mineralization – Yilgarn Craton

Sufficient geochronological data is available to provide constraints on the absolute age of gold mineralization in the Yilgarn Craton. Precise age determinations of gold mineralization derived from robust dating techniques (e.g., U-Pb zircon and titanite, Pb-Pb and Sm-Nd mineral isochrons) show that mineralization formed dominantly, but not exclusively, at ~2.64-2.63 Ga across the Yilgarn Craton (Kerrich and Cassidy, 1994; Kent et al., 1996; Yeats et al., 1999; Bucci et al., 2000; Fig. A8).

The best documented age constraints are for the Chalice gold deposit in the southern Kalgoorlie Terrane. Main stage gold mineralization (95% of resource) comprises foliation-parallel quartz-albite-diopside-titanite-garnet-gold veins and wallrock replacement of mafic amphibolite host rocks. Secnd stage mineralization is temporally associated with a second-generation granitoid dyke that cross-cuts the main stage. Uranium-Pb zircon and titanite studies and Re-Os dating of molybdenum identified two discrete gold events at 2644±8 Ma and 2621±10 Ma (Bucci et al., 2000).

Two stages K-feldspar and titanite Pb-Pb mineral isochrons for the South Emu deposit at Reedys and the Griffins Find deposit yield ages of 2637±4 Ma (Wang et al., 1993) and 2636±3 Ma (Barnicoat et al., 1991), respectively. Hydrothermal zircons associated with lode-gold mineralization at the Hornet deposit at Mount Gibson yield an U-Pb SHRIMP age of 2627±13 Ma and, importantly, there is evidence that the gold mineralizing event was superimposed on pre-existing ~2.95 Ga VHMS mineralization (Yeats et al., 1996).

Less robust dating techniques, including ^{40}Ar -^{39}Ar plateau ages, yield a range of ages from ca. 2.64 Ga to younger than 2.0 Ga for alteration minerals from a number of deposits in the Yilgarn Craton (e.g., Napier, 1993; Kent and McDougall, 1995; Kent and Hagemann, 1996; Mueller et al., 1996; Kent and McCuaig, 1997; Napier et al., 1998). The non-robustness of the ^{40}Ar -^{39}Ar dating technique is demonstrated by the Scotia deposit, south of Norseman, with ages of hydrothermal amphibole and biotite up to 1000 m.y. younger than the minimum age of a cross-cutting pegmatite dike (Kent and McCuaig, 1997). These authors invoke resetting during the Proterozoic by mineral-fluid interaction during movement of a retrograde fluid along mineralized lode structures. Kerrich and Cassidy (1994) suggest similar retrograde resetting to explain aberrantly young 'ages' for mineralization for a number of deposits in the Yilgarn Craton as well as for deposits in the Superior Province of Canada. Napier (1993) and Napier et al. (1998), however, suggest that young ^{40}Ar -^{39}Ar ages of hydrothermal amphibole and biotite from gold deposits in the Coolgardie and Southern Cross districts, Yilgarn Craton, reflect complex cooling paths involving long periods at elevated temperatures followed by exhumation of the host terranes.

Evidence for isotopic resetting is detailed in Kerrich and Cassidy (1994) and Kent and McCuaig (1997) and includes: (i) field and structural evidence indicating reactivation of Archean structures during the Proterozoic; (ii) Proterozoic remobilization of gold and other elements in Archean gold deposits (e.g., Perring and McNaughton, 1990); (iii) reversed blocking temperature sequences in deposits, such that typically more robust systems yield younger ages than more sensitive systems such as Rb-Sr or ^{40}Ar -^{39}Ar (Kerrich and Cassidy, 1994), and (iv) concurrent disturbance of radiogenic and stable isotopes of some Archean gold deposits (e.g., Perring and McNaughton, 1990). Models for gold mineralization based on the young ages are also not consistent with the fundamental field relationships whereby the deposits form in broadly rheological and thermal equilibrium with their host terranes, not 50->200 m.y. later (e.g., Groves, 1993; Kerrich and Cassidy, 1994; McCuaig and Kerrich, 1998). An important implication is that if hydrothermal minerals have experienced isotopic disturbance after gold mineralization, isotopic ages must be carefully considered before they can be interpreted to record the actual age of hydrothermal mineralization.

Constraints on the absolute timing of gold mineralization are also obtained from the ages of pre- and post-gold intrusions in host terranes. In the Yilgarn Craton, there are few deposits that contain cross-cutting post-gold intrusions. Cross-cutting pegmatite and microgranite dikes from several high-temperature deposits in the Southern Cross Province and the Norseman district yield U-Pb zircon and Sm-Nd mineral isochron ages of ~2640-2620 Ma and are interpreted to have intruded broadly contemporaneously with gold mineralization (e.g., Bloem et al., 1995; Kent et al., 1996). Ages of felsic intrusions that also host orogenic lode-gold mineralization generally have U-Pb zircon ages of 2.68-2.65 Ga, with the youngest intrusion having an age of 2648±6 Ma (Kent, 1994; Cassidy et al., 1998). However, in the Yandal greenstone belt in the northeastern Yilgarn Craton, recent geochronology of felsic porphyry dykes that cross-cut gold mineralization have U-Pb zircon ages of ca. 2.66 Ga (Yeats et al., 1999). These ages suggest that mineralization was possibly diachronous over a period of 30 m.y. from northeast to southwest in the Yilgarn Craton. The interpretation of the U-Pb zircon ages for some of the felsic porphyry dykes has recently come under scrutiny with some researchers suggesting that the ages represent inheritance (e.g., N. Vielriecher et al., pers. comm., 2000).

Source(s) of Energy – The Driving Force of orogenic lode-gold systems

Analysis of the geodynamic evolution of a host terrane is essential to determine the possible source(s) of energy that drive individual mineral systems. Mineral systems develop in response to 'far-field' forces such as plate interaction, plume tectonics, or combinations of both. At the terrane- and district-scale, these may manifest themselves as discrete tectonomagmatic events that drive hydrothermal fluids derived from metamorphic devolatilization, magmatic fluid evolution, or surficial fluid circulation. It is, therefore, important to determine spatial and/or temporal links with potential heat or thermal sources that may drive individual mineral systems.

Geodynamic setting of host terranes: In this section, we do not attempt to discuss all the geodynamic models that have been invoked for Archean terranes and may result in the formation of orogenic lode-gold mineralizing systems. Instead, the reader is referred Fyon et al. (1989), Kerrich (1989a), Perring et al. (1989), Kerrich and Wyman (1990), Barley and Groves (1992), Kerrich and Cassidy (1994), Barley et al. (1998) and Kerrich et al. (2000). However, it is important to highlight a number of constraints that can be placed on the geodynamic models. The Abitibi subprovince and Norseman-Wiluna Belt contain a major proportion of the resource of orogenic lode-gold deposits of the cratons (~9000 t contained Au: Spooner and Barrie, 1993), as well as major VHMS Cu-Zn and/or komatiite-hosted Ni mineralization. In contrast, the similar age late-Archean Wabigoon subprovince of the Superior Province lacks major gold deposits. Geodynamic models favoring development of orogenic lode-gold mineralizing systems, therefore, must be able to demonstrate why some Archean cratons, and some terranes or subprovinces, are more prospective.

Although different in detail, the tectonic and metallogenic histories of many Archean cratons have broadly similar magmatic, thermal and deformational histories. In the highly mineralized Yilgarn Craton and Superior Province, deformation, emplacement of granitoid batholiths and orogenic lode-gold mineralization followed within 50 m.y. of volcanism and sedimentation during the Late Archean.

Granitoid-greenstone terranes of the Yilgarn Craton largely consist of metavolcanic and metasedimentary rocks and granitoids that formed between ~3.0 and 2.62 Ga (e.g., Swager, 1997; Barley et al., 1998). Data from the western Yilgarn Craton indicate greenstone sequences and granitoids were emplaced during the mid-Archean (~3.0-2.9 Ga), followed by intermediate to felsic volcanism and sedimentation from ~2.78 to 2.74 Ga (e.g., Barley et al., 1998). Compiled ages indicate that the granitoid-greenstone terranes in the eastern Yilgarn developed dominantly between 2.74 and 2.63 Ga, with several lines of evidence indicating that the terranes developed on substantial pre-existing crust (e.g., Nelson, 1997; Barley et al., 1998). Lode-gold mineralization in the southern Abitibi subprovince has been dated at between 2.71 and 2.67 Ga (e.g., Kerrich and Cassidy, 1994), whereas that in the Norseman-Wiluna Belt is younger and largely dated at ~2.64-2.63 Ga (Groves et al., 1995; Kent and McDougall, 1995; Kent et al., 1996).

The Superior Province is interpreted to comprise a collage of allochthonous tectonostratigraphic terranes, including metasedimentary, metaplutonic and metagreenstone-granitoid-dominated terranes. The various terranes formed in different places over distinct time periods and record diverse magmatic, metamorphic and tectonic histories, primarily from >2.9 to ~2.67 Ga (see reviews by Card, 1990; Thurston et al., 1991). In the late Archean, the various subprovinces underwent transpressive accretionary tectonic assembly that was diachronous from ~2.78 Ga in the north to ca. 2.67 Ga in the southern Abitibi subprovince.

In the Slave Craton, northern Canada, early granitoid emplacement (from ~3.9 Ga) and greenstone magmatism was followed by Late Archean greenstone volcanism and plutonism from ~2.8 to 2.67 Ga. Subsequent sedimentation, granitoid plutonism, metamorphism and gold mineralization is constrained to between 2.67 and 2.60 Ga (Isachsen and Bowring, 1994; Abraham and Spooner, 1995). The Zimbabwe Craton has a similar long history of granitoid emplacement and greenstone belt development. Limited geochronology indicates a progression of mafic and felsic volcanism and sedimentation, followed by deformation, granitoid emplacement and lode-gold mineralization (Wilson et al., 1995), with gold mineralization restricted to a period of deformation between 2.66 and 2.60 Ga. A similar progression is also evident in other Archean terranes (e.g., Karelian Craton: Sorjonen-Ward, 1993; Dharwar Craton: Krogstad et al., 1989; Jayananda et al., 2000) with orogenic lode-gold mineralization dominantly developed late during the evolution of the terrane. In the Pilbara and Kaapvaal Cratons, however, there is evidence for gold mineralization that is earlier than the last, craton-wide igneous and deformation event. In the poorly endowed Pilbara Craton, discrete episodes of lode-gold mineralization closely follow periods of mafic and felsic volcanism, sedimentation, granitoid plutonism, metamorphism and deformation (Blewett and Huston, 1999). Many of the gneiss-dominated Archean terranes, including parts of Greenland, the Superior Province (i.e., Card et al., 1989) and Yilgarn Craton (i.e., Narryer Terrane), do not contain economic concentrations of lode gold.

Several models have been suggested to explain the extensive period of mineralization (i.e., 2.75-2.52 Ga) during the late Archean that generated not only large quantities of orogenic lode-gold mineralization, but also world-class metallogenic provinces of VHMS Cu-Zn and/or komatiite-hosted Ni mineralization in many Archean cratons. Archean orogenic lode gold deposits generally occupy a consistent spatial and temporal position having formed late during compressional to transpressional deformation in accretionary and collisional orogens (e.g., Barley et al., 1989; 1998; Kerrich and Wyman, 1990; Barley and Groves, 1992). This association is the primary reason Groves et al. (1998) invoke the term 'orogenic gold deposits' to encapsulate this class of mineral system for deposits of any age from Archean to Recent.

Many researchers invoke settings involving subduction-related accretion for orogenic lode gold deposits irrespective of whether they are hosted in Archean granite-greenstone terranes or Phanerozoic sedimentary rock-dominated sequences (e.g., Kerrich and Wyman, 1990; Barley and Groves, 1992; Goldfarb et al., 1998; Kerrich et al., 2000). Models for Phanerozoic terranes reflect the better understood tectonic histories and invoke specific processes (e.g., ridge subduction, subduction roll-back, changing plate motions, etc.) occurring during accretion/subduction to explain the generation and migration of deeply sourced fluids, vein formation and gold precipitation (e.g., Goldfarb et al., 1991, 1998). Other models for orogenic lode gold mineralization in the Phanerozoic emphasize the role of collisional tectonics involving lithospheric delamination (e.g., Keppie and Dallmeyer, 1995; de Boorder et al., 1998).

Clearly there is strong support for models invoking development of large-scale hydrothermal systems as a result of accretion/collision, at least during the post-Archean, and similar models have been proposed to explain the Archean orogenic lode gold mineralization as well. For instance, Barley et al. (1998) suggest that the interaction of plume-breakout periods with extremely long-lived convergent margin sectors of external oceans may be responsible for the highly mineralized character of many of the late Archean terranes. Hodgson and Hamilton (1989) suggest that gold mineralization in the Abitibi subprovince was the end-stage result of late Archean collisional tectonics with generation of hydrothermal fluids linked to lower-crust/mantle processes. Wyman et al. (1999) suggest that gold mineralization in the Abitibi subprovince may be related to a geodynamic setting that facilitated asthenospheric upwelling through dislocation and/or delamination of a subducted slab after step-back of earlier subduction zones due to accretion of ocean plateaus. Qiu and Groves (1999) invoke a model of late Archean collision and lithospheric delamination in the southwest Yilgarn Craton as the driving force for orogenic lode-gold mineralization throughout the Yilgarn Craton. Similarly, van Reenen et al. (1987) suggested that collisional tectonics was important in the generation of lode-gold mineralization in the Limpopo belt, southern Africa. In contrast, there are researchers who invoke non-uniformitarian geodynamic models to explain the Archean (e.g., Hamilton, 1998). In summary, although there is currently no generally accepted geodynamic model for Archean host terranes, accretionary and/or collisional settings are favored.

Models for generation of orogenic lode-gold mineralizing fluids: Many recent models for the generation of orogenic lode-gold mineralizing fluids invoke mechanisms whereby the development of the mineralizing fluids is an integral component of specific geodynamic settings. These include the accretion/collision models (e.g., Barley et al., 1998, Wyman et al., 1999, Qiu and Groves, 1999) discussed above. The tectonic processes produce major thermal anomalies and involve liberation of fluids over large areas. These models recognise that lode-gold mineralization is a result of similar processes occurring over a range of crustal levels and over a restricted temporal interval contemporaneously with late accretion/collision tectonics (e.g., Groves et al., 1992, 1998; Groves, 1993). All these models generally invoke mechanisms such as magmatic underplating and/or lithospheric delamination coupled with crustal plutonism, lower crustal granulitization and upper mantle partial melting to generate large volumes of hydrothermal fluids with gold mineralization a by-product of, and integral component of, these processes. Some researchers suggest models for the generation of hydrothermal fluids that do not specify the geodynamic setting of host terranes and involve 'granulitization' (e.g., Cameron, 1988; Card et al., 1989; Fyon et al., 1989) and/or 'cratonization' (e.g., Colvine, 1989; Kent et al., 1996). Alternatively, the generation of synmetamorphic hydrothermal systems with up-temperature, lateral fluid flow is inferred to be related to differential uplift, juxtaposition of uplifted blocks and intrusion of granitoids (Witt et al., 1997). Other researchers link fluid generation with smaller-scale processes such as magmatic fluid evolution of specific plutonic associations (e.g., TTG complexes: Burrows and Spooner, 1989; oxidized felsic intrusions: Cameron and Hattori, 1987).

Source(s) of Fluids and Metals

Numerous models have been proposed for the origin of the hydrothermal fluids that transport gold from source to depositional site. Some models invoke terrane-scale processes whereas others invoke district and even smaller-scale processes. These include:

- Metamorphic devolatilization during prograde, regional metamorphism of greenstone belts (Kerrich and Fyfe, 1981; Phillips and Groves, 1983; Powell et al., 1991);
- Devolatilization of the lower and/or middle crust with or without input from the mantle (e.g., Cameron, 1988; Colvine, 1989; Fyon et al., 1989);
- Magmatic fluid originating from extensive regional batholiths and/or specific granitic associations (e.g., Cameron and Hattori, 1987; Burrows and Spooner, 1989; Mueller et al., 1991a; Qiu and McNaughton, 1999);
- Fluid release during crystallization of gold-rich lamprophyric magmas (Rock et al., 1989); and
- Deep circulation of meteoric waters to depths in the crust (Nesbitt, 1988).

Ridley and Diamond (2000) review available data from orogenic lode-gold deposits of all ages and conclude that the metamorphic devolatilization and felsic magma devolatilization models for the fluid source are allowable. The models make predictions regarding the source of gold and other metals and the timing of mineralization and these predictions can be tested with fluid geochemistry, stable and radiogenic isotope tracer and mineral equilibria studies.
A key feature of orogenic lode-gold deposits is that they contain a broadly uniform hydrothermal fluid in terms of major molecular components (e.g., CO_2, K, S: Ridley and Diamond, 2000). This is taken to indicate that the fluid was neither significantly modified via fluid-rock interaction *en route* from the source(s) to potential trap sites nor modified by mixing with fluid from other sources (see Ridley et al., 1996; Ridley and Diamond, 2000). Ridley et al. (1996) suggest that the fluid flow was strongly channelized with travel distances from source to depositional site of the order of kilometers. Note, however, that local fluid mixing is invoked as a potential gold precipitation mechanism at the trap-site. For the orogenic lode-gold mineral system, the broadly uniform fluid is a low-moderate salinity, mixed aqueous-carbonic fluid capable of carrying Au, Ag, As, Sb but with a limited capacity to transport base metals.

Constraints on the source of the fluid are mainly from stable and radiogenic isotope tracer studies as well as the chemical composition of the fluid. Ridley and Diamond (2000) provide an extensive review of the chemical and isotopic composition of the gold transporting fluid and only salient points are summarized here. Information is provided that constrains the source of ore fluid components and/or demonstrates that a particular component is modified during transport to the depositional site and thus does not add to our understanding of fluid source.

Chemical compositional constraints: Constraints on the source of the fluid are mainly from studies at the depositional site and include direct analysis of fluid inclusions and calculated fluid compositions based on chemical and isotopic analysis of gold-related hydrothermal minerals. The major molecular components are broadly uniform for the vast majority of deposits and do not constrain the fluid source. Components, such as CH_4 and N_2, are present in variable amounts in many deposits reflecting source and trap (camp- or deposit-scale) processes. For instance, presence of graphite-bearing metasedimentary lithologies in some deposits is consistent with local processes (e.g., Lancefield: Hronsky, 1993). A wide range of XCO_2 values of the mixed aqueous-carbonic fluid inclusions have been reported, with most ranging from 0.10 to 0.25 XCO_2 (e.g., Mikucki and Ridley, 1993; Mikucki, 1998; Ridley and Diamond, 2000). However, as discussed by Ridley and Diamond (2000), the presence of CO_2 does not discriminate between fluids derived via metamorphic devolatilization or magmatic fluid evolution, with similar fluids able to be derived from both sources. Likewise, the narrow range of salinities and pH recorded from lode-gold deposits reflects equilibrium with a wide range of lithologies and does not further constrain the fluid source. The subtle gradient in sulfide activity in deposits from shallow to deep paleocrustal levels is also interpreted to indicate the fluid composition remained relatively constant along fluid flow paths (Ridley et al., 1996).

Lithophile element ratios, such as K/Rb, K/Ba, have been used by Kerrich (1989b) to constrain the fluid source. However, ratios from all deposits from a range of paleocrustal levels plot within the range determined for normal crustal lithologies and are, therefore, not diagnostic of a particular source. Ridley (1990) suggests that the fluid was oversaturated with respect to potassic phases and inferred that this reflects derivation from or equilibrium with a granitic source. Furthermore, Ridley et al. (1996) suggest that quartz precipitation in veins or as pervasive silicification in the vast majority of deposits indicates that the hydrothermal fluids were also quartz saturated. Overall, there are few constraints on the source of the fluid based on the chemical composition of the fluid and further work should be directed to determine if there are certain element ratios or chemical components that can distinguish between the potential fluid sources.

Stable isotope tracers: Carbon, oxygen, hydrogen and nitrogen isotopic compositions of hydrothermal minerals (e.g., quartz, carbonate, sericite, biotite, amphibole, pyroxene and garnet) have been used to constrain fluid sources in Archean orogenic lode-gold deposits (Kerrich and Fryer, 1979; Kerrich, 1987; Golding et al., 1989, de Ronde et al., 1992; McNaughton et al., 1992; Jia and Kerrich, 1999; Knight et al., 2000). In mesozonal and hypozonal lode-gold deposits, calculated δD-$\delta^{18}O$ compositions of hydrothermal fluids plot in a relatively small field (δD_{fluids} -30 to -80 ‰; $\delta^{18}O_{fluids}$ +6 to +11 ‰) that overlaps the metamorphic and magmatic fields of Taylor (1974), and are not diagnostic of fluid source (cf. McCuiag and Kerrich, 1998). Carbon isotopes of carbonates in orogenic lode-gold deposits, from all paleocrustal levels and from several Archean provinces, range from -11 to +2 per mil (Golding et al., 1989; Kerrich, 1987, 1989b, 1990; McNaughton et al., 1992) and are also not uniquely diagnostic of a specific carbon source (cf. McCuaig and Kerrich, 1998). However, the isotopic shifts associated with wallrock alteration and vein formation in any single deposit clearly imply high water-rock ratios. Note that many stable isotope studies have been conducted with limited field constraints, i.e., the timing of different quartz vein types, their relationship to metamorphism, magmatism and gold mineralization is often not described. In addition, they are conventional isotope analyses that do not account for intragrain heterogeneities.

In epizonal lode-gold deposits of the Yilgarn Craton, however, δD and $\delta^{18}O$ values of quartz, chlorite and sericite reveal δD and $\delta^{18}O$ fluid compositions from +5 to -60 per mil and -2 to +5 per mil, respectively. These are interpreted to reflect incursion of surface waters into a dominantly deep-sourced hydrothermal system, or advection of a deep-sourced hydrothermal fluid into rocks that have partially equilibrated or mixed with surface-derived waters (Hagemann et al., 1994). Note that the surface water influx does not indicate that gold was contained in the surface water or was leached from the host rocks that equilibrated with the surface waters. The influx of surface waters likely suggests fluid mixing with ascending deep fluids, and, as such, potentially represent an efficient mechanism to precipitate gold and other metals.

Sulfur isotope compositions of sulfides and sulfates in Archean orogenic lode-gold deposits are largely restricted from 0 to 9 per mil $\delta^{34}S$ (Kerrich, 1987, 1989; Golding et al., 1990b; de Ronde et al., 1992). This indicates that the sulfur source was isotopically uniform and derived directly from the mantle, from magmas or indirectly by dissolution and/or desulfidation of primary sulfide minerals or average crustal sulfur. Some epizonal and mesozonal deposits are systematically depleted in $\delta^{34}S$ (Canadian Arrow: Cameron and Hattori 1987; Wiluna: Hagemann et al., 1993; Golden Mile: Phillips et al., 1986; Clout, 1989; Kanowna-Belle: Ren and Hethersay, 1998; Victory: Xu and Palin, 1998) a feature that has been attributed to: (i) significant oxidation of the ore fluids via interaction of hydrothermal fluids with magnetite (Phillips et al., 1986), (ii) oxidized magmatic fluids (Cameron and Hattori, 1987), or (iii) phase immiscibility. The Golden Mile contains locally appreciable amounts of anhydrite that Clout (1989) interpreted as evidence for seawater influx into upper portions of the hydrothermal system. However, Hagemann et al. (1999) show that texturally different pyrites from proximal alteration zones of Fimiston- and Oroya-style lodes have a far greater range in $\delta^{34}S$ (-10 to +18‰) than determined in previous studies. The sulfur isotopic zonation of individual pyrites (up to 6 ‰), individual lodes, and different mineralization styles all point to a complex interplay of different sulfur sources, i.e., magmatic, syn-sedimentary and seawater, and depositional processes (i.e., phase immiscibility, fluid mixing, and equilibration).

Recently, Jia and Kerrich (1999) report the first analyses of $\delta^{15}N$ in hydrothermal micas associated with gold mineralization in several lode-gold deposits from the Superior Province and Yilgarn Craton. The results show a range of $\delta^{15}N$ from 10 to 24 per mil that overlaps with metamorphic and some plutonic rocks but extends to more ^{15}N enriched values. The authors suggest that while the data are limited, they are more consistent with the regional metamorphic field. However, the range of ^{15}N extends beyond all known compositions suggesting that this interpretation may be premature.

In summary, in meso- and hypozonal lode-gold deposits oxygen, hydrogen, carbon and nitrogen isotope values are non-diagnostic in terms of fluid sources. In epizonal lode gold deposits, however, the isotopic values indicate locally substantial influx of surface waters. Sulfur isotopes are mostly restricted to 0 to +9 per mil and are, again, non-diagnostic in terms of fluid source. A few, largely epi- mesozonal deposits display either depleted or enriched values when compared to the main population of data which might suggest multiple sulfur sources and/or different depositional processes.

Radiogenic isotope tracers: Isotopes of Nd, Os, Pb and Sr have been used to determine the source(s) of ore fluid components in orogenic lode-gold systems. Osmium isotopes have been applied to three Archean lode gold districts – Kambalda (Lambert et al., 1998), Kolar (Walker et al., 1989) and Zimbabwe (Frei et al., 1998). All three studies indicate variable levels of interaction with host rocks and underlying older crustal material. Lambert et al. (1998) report radiogenic initial Os isotopic compositions for the Revenge gold deposit at Kambalda, Yilgarn Craton, and interpret this to indicate interaction and/or derivation of the ore fluid component from older, lower crustal sources. In contrast, the initial Os isotopic composition of samples of quartz lodes from the Kolar schist belt, Dharwar Craton, is consistent with derivation from fluids or melts with near-chondritic Os isotopic compositions. Clearly further studies are required to determine the veracity of this technique.

Likewise, Nd isotopes have been used to determine the source(s) of ore fluids in several Archean orogenic lode gold deposits. Kent et al. (1995) and Ghaderi et al. (1996) obtained epsilon Nd values for hydrothermal scheelite from deposits in the Kalgoorlie-Norseman region of the Yilgarn Craton, and inferred that the ore fluid composition was controlled by interaction with a specific lithology. Highly enriched epsilon Nd values from the Mount Charlotte deposit are interpreted to indicate that most of the Nd in the scheelite is derived from komatiites (Kent et al., 1995; Ghaderi et al., 1996). However, other studies suggest that the epsilon Nd values are indistinguishable from those of immediate hostrocks and not diagnostic of interaction with a specific lithology (e.g., Siva Siddaiah and Rajamani, 1989; Frei et al., 1998).

Lead and Sr isotope studies indicate that the Pb and Sr in most Archean lode-gold deposits consists of mixtures of radiogenic Pb and Sr derived from older felsic crust and less radiogenic Pb and Sr derived from mafic rocks within greenstone belts (e.g., Kerrich et al., 1987; Kerrich, 1989b; Mueller et al., 1991a; McNaughton et al., 1992, 1993; Knight, 1994; Qiu and McNaughton, 1999). At the deposit-scale, Pb and Sr isotope compositions are generally less radiogenic than the most radiogenic source in the area at the time of mineralization but are also more radiogenic than mantle-derived lithologies. Some deposits in amphibolite facies terranes, however, do have Pb isotope compositions that closely match adjacent granitoids (e.g., Qiu and McNaughton, 1999). In the eastern Yilgarn Craton, McNaughton et al. (1992, 1993) demonstrate a regional variation in Pb isotope composition with more radiogenic Pb compositions correlating with increasing proximity to regional granitoid-gneiss terrain. Mueller et al. (1991) also document a correlation between the Sr isotope composition of gold-related scheelite and the inferred depth of gold mineralization and interpret this to reflect derviation of the mineralizing fluids from within older felsic lower crust and progressive mixing of this Sr with greenstone-derived Sr during ascent to higher crustal levels. Deposits that formed at deeper paleocrustal levels tend to have the most radiogenic Pb and Sr, are typically from narrow greenstone belts, and an alternative interpretation is that the radiogenic Pb and Sr is derived from adjacent granitoids during hydrothermal circulation (cf. Witt et al., 1997). Lead and Sr isotope data cannot distinguish between a mixed signature and a regionally homogenized signature, but effectively rule out models for lode-gold deposit formation that invoke ore-forming hydrothermal systems that are solely confined to individual greenstone belts.

Lead isotope data from several deposits in the Yilgarn Craton and Superior Province plot along secondary isochrons that are the subject of several possible interpretations. In the Norseman area and at the Lady Bountiful deposit near Kalgoorlie, the secondary isochrons are interpreted to reflect later disturbance and new galena growth from radiogenic Pb (e.g., Perring and McNaughton, 1990; Cassidy, 1992; McNaughton et al., 1992).

Overall, the radiogenic isotope tracers do not unequivocally indicate the source of ore fluids. Transport of fluids along pathways such as regional deformation zones would allow exchange with radiogenic crust and non-radiogenic greenstone sequences. The lithological diversity along individual pathways may explain the complexity of the radiogenic isotope systematics, as well as regional and inter-camp variations (e.g., McNaughton et al., 1992; McCuaig and Kerrich, 1998).

In summary, the stable- and radiogenic-isotope tracer studies do not unequivocally distinguish one proposed source over another and may reflect the relative ability of the isotope to be modified through fluid-rock interaction *en route* from the source to the depositional site. Many of the currently used tracers show local- and district-scale modification and cannot be used to constrain the primary fluid source (Ridley and Diamond, 2000). Further studies on deposits from a variety of crustal levels and application of micro-analytical techniques should improve the understanding of these isotopic systems in Archean orogenic gold deposits. Ridley and Diamond (2000) suggest that analysis of halogen elements may potentially provide better constraints on the source of the hydrothermal fluids.

Migration of Fluids and Fluid pathways

An important component of orogenic lode-gold mineralizing systems is the transport over relatively long distances of large volumes of broadly uniform fluid. Information regarding the architecture of the fluid pathways as well as the medium used to transport gold in solution along the pathways is vital to determine the overall characteristics of a mineralizing system.

Fluid conduits: At a greenstone belt-scale, Archean gold camps are generally spatially related to large-scale (>100 km in length), transcrustal deformation zones. They occur within or along the edges of the greenstone belts, and they commonly mark the boundary between volcano-plutonic and metasedimentary subprovinces or terrains. Economically significant, gold-associated fault zones in the Abitibi greenstone belt of the Superior Province include the Destor-Porcupine and Larder Lake-Cadillac fault zones that are spatially close to the world-class Timmins and Val d'Or camps, respectively. In the Yilgarn Craton the most significant large fault zone system is the Boulder-Lefroy that lies close to the Golden Mile and Victory-Defiance gold deposits (Fig. A9). On a camp-scale, however, most gold deposits are hosted in second- and third-order structures which are considered to be more favorable dilational sites for gold deposition (Kerrich, 1989a; Eisenlohr et al. 1989; Groves et al. 1989; Robert 1990).

In most transcrustal fault zones, significant (>100 t) gold mineralization is scarce, or is extremely localized. Based on the above empirical observations, transcrustal fault zones are considered to be the main conduits for gold-bearing, hydrothermal fluids that are subsequently channelled into the second- and third-order faults (Eisenlohr et al., 1989). This interpretation is mostly based on the close spatial relationship between first-, second-, and third-order fault zones, a documented structural link between second- and third-order structures (e.g., Sigma mine), and similar hydrothermal alteration within the camp (e.g., Val d'Or gold camp: Robert, 1990, 1991). Direct evidence of the structural and hydraulic connectivity of first-order structures, such as identical fluid chemistry, is currently being investigated for the Cadillac Tectonic Zone in the Val d'Or camp (Neumayr et al., 2001; Neumayr and Hagemann, 2001). Neumayr and Hagemann (2001) record a progressive evolution of the hydrothermal fluids within the Cadillac Tectonic Zone. Earliest mixed, low to moderate saline H_2O-CO_2-CH_4-NaCl fluid inclusions, which predate gold mineralization, are superseded by gold-associated, dominantly carbonic CO_2-CH_4±H_2O±NaCl fluid inclusions. The latest fluids in the system are aqueous brines that most likely relate to late fracture infills or Canadian Shield brines (e.g., Guha and Kanwar, 1987). The current preliminary qualitative fluid model involves both modification of the hydrothermal fluid by different hydrothermal processes and reactions with different wallrocks along the fluid path. The elevated salinity in the CO_2-H_2O-NaCl fluids and the CO_2 dominance in the younger fluids within the Cadillac Tectonic Zone is best explained by progressive phase separation, with preferential vapour loss (CO_2-CH_4) into the upper parts of the fault system. This devolatilization process requires that the fault was permeable for the vapor phase during an extended period of time.

Vearncombe (1998) recognized a regional network of late-Archean, high angle, mid- to upper crustal cross faults in the Yandal greenstone belt, northeastern Yilgarn Craton, based on interpretation of high-resolution aeromagnetic data. Rather than the craton-scale transcrustal faults being part of a linked system (e.g., Eisenlohr et al., 1989; Robert, 1990; Neumayr et al., in press) and as potential pathways for gold-mineralizing fluids, Vearncombe (1998) proposes that gold mineralizing fluids were focused by the network of conjugate cross faults. Fluid flow and gold mineralization was preferentially sited in zones of low mean stress, determined by the orientation of lithological units and pre-existing shear zones relative to the late-Archean stress direction. However, the exact timing relationships, hydrothermal alteration characteristics and physico-chemical conditions of the hydrothermal fluids in the cross faults are, at present, poorly known. In addition, there are many areas in the Yilgarn Craton with world-class orogenic lode-gold deposits (e.g., Wiluna), where there is an absence of a conjugate cross fault system. This model is, therefore, probably only of local significance.

According to Cox (1999) localization of fluid flow along relatively limited linked networks of active faults and shear zones is a fundamental aspect in the development of the crustal-scale hydrothermal systems that produce mesozonal Archean lode-gold deposits. Networks of shear zones at deeper crustal levels effectively scavenge fluids and metals that are transferred to higher crustal levels along a restricted flow backbone (first-order structures). Shear systems with very high connectivities generate more dispersed flow in which case individual structures may not have high enough fluid fluxes to generate economic gold deposits. According to percolation theory (Sahimi, 1994) the smaller and most intensely mineralized structures are interpreted as "dangling" elements that have drawn fluid from the backbone in the downstream or discharge part of hydrothermal systems. As downstream dangling structures are sites of localized fluid discharge, they are sites that generate the greatest potential for gold deposition as this involves processes such as phase immiscibility, fluid mixing and fluid-rock interaction.

Sibson et al. (1988) and Sibson and Scott (1998) consider the lower portion of the brittle carapace (transition between a hydrostatically pressured near-surface fluid regime and the near lithostatic fluid pressures) that overlays a prograde metamorphic belt as a low permeability barrier which hosts mesozonal gold-quartz veins systems (Fig. A10a). These are controlled by fault-fracture meshes that comprise low-displacement shear zones interlinked with hydraulic extension fractures. These 'self-generated' mesh structures are generated by the infiltration of overpressured fluids at pressures locally exceeding the least principal compressive stress (i.e., $P_f > \sigma_3$), and form high permeability conduits for episodic large-volume fluid discharge (Fig. A10). Fluids are most easily trapped beneath the carapace in compressional-transpressional regimes where the highest levels of overpressuring may be attained. According to Sibson and Scott (1998) the attainment of extreme overpressures and the formation of high permeability meshes in any given stress regime (Fig. A10b), therefore, requires either intact crust, or crust where faults have become severely misoriented. Containment of overpressured fluids is affected by the stress state and fault structures within the carapace which acts as a containing lid impeding fluid loss from the mid-crust.

Hall (1998) proposed a generic fluid flow model ('Y-front' model) for the Kalgoorlie area of Western Australia based on a ~200 km long, east-west seismic reflection profile across the western part of the Norseman-Wiluna Belt, about 50 km north of Kalgoorlie (Drummond and Goleby, 1993), and regional scale numerical modelling of fluid flow by Ord et al. (1998). Fundamental to the 'Y-front' model are transcrustal fault zones that penetrate and link entire crustal sections. Interpretation of the seismic profile indicates that the east-dipping Ida fault zone intersects the west-dipping Bardoc shear zone in the mid-crust in a Y-like fashion. Thermal and fluid flow modelling for the 55 km section between the two faults suggest an early convection system involving the entire crust, possibly mobilizing metals from the lower crust to the mantle. Cooling and gradual cessation of the convection cell resulted in restricted convection limited to the upper crust, particularly the shallow (<10 km depth) greenstone belts which consequently led to concentration of auriferous hydrothermal fluids into the east-dipping Bardoc shear zone. Thermal modelling suggests both downward fluid flow in the upper crustal section and upward flow in the lower crustal section of the Ida fault zone. Upward flow is indicated along the Bardoc shear zone from its intersection with the Ida fault below the greenstone belt (Fig. A11). This convection cell has the potential to mix mantle fluids and a myriad of metamorphic, magmatic (from "blind" stocks) and meteoric fluids, and to direct this "mixed" fluid along the Bardoc shear zone that acts as a focused discharge zone. The temperature distribution leads to greenschist facies metamorphism in the east progressing to granulite facies in the west and extensive alteration within the greenstone belt sequence near the Bardoc shear zone (Fig. A12a). Metamorphic grade distribution is interpreted by Hall (1998) as the most powerful expression of the existence of a regional, hydrothermal cell. Supporting this Y-model is the spatial association of significant gold deposits adjacent to areas of low metamorphic grade, relative to the average metamorphic gradient of the greenstone belt (Fig. A12b). The Kalgoorlie system covers an area typically 100 km x 100km to a crustal depth of +30 km.

Even though the 'Y-front model' is one of the first models that attempts to interpret regional 3D fluid flow it has several shortcomings. Firstly, the proposed fluid flow is only realistic if all fault segments are present and active during the same time period. Secondly, the model fails to reconcile the fact that the dips of the surface structures are not compatible with the seismic interpretation of shallow dipping faults. Thirdly, potentially steep-dipping structures are not shown in the seismic interpretation, as they are notoriously difficult to interpret in seismic reflection data. Despite these problems the Y-front model represents the first attempt of modelling large-scale (100km) hydrothermal cells that explain the extraordinary endowment of gold (3000 tonnes) in the Menzies-Kambalda area.

Ridley (1993) in an innovative analyses of mean rock stress and fluid flow in the crust pointed out that fluid focusing in gold deposits occurs where there are lateral gradients in hydraulic head at any depth, generally fluid flow will be dominated by upward flow (Etheridge et al., 1983). The main cause for lateral gradients in hydraulic head is the variation in mean rock stress as a consequence of tectonic stresses acting on an inhomogeneous rock sequence. Analysis of stress fields shows a wide variety of potential sites of low mean stress, dependent on the geometry of rock units and on patterns of faults, fractures or shear zones (Ridley, 1993). Holyland (1990) used these principles to develop stress mapping, a numerical modelling technique to target sites of dilation or low minimum principal stress ($\sigma 3$). Successful application of stress mapping depends on critical input parameters, including an accurate geological map, rock properties, knowledge of magnitude and orientation of the far-field stress field, rock deformation properties such as strength and moduli, fault deformation properties, including friction angles and stiffness. The most severe limiting assumption of two-dimensional stress mapping is that the plane of a map does not accurately reflect the stress pattern in an area with complex three-dimensional geometry. Furthermore, stress mapping can only be applied if fluid flow in structures was late in the tectonic history and the structural pattern in the area of modelling has not been affected by subsequent structural events.

Holyland et al. (1993), Hall (1998) and Groves et al. (2000) successfully applied stress mapping to the Kalgoorlie area and showed that sites of low minimum principal stress (σ 3) define all of the major goldfields in the area (Fig. A13) and are located adjacent to first order faults. Groves et al. (2000) show that low stress anomalies in the Kalgoorlie area constitute less than 10 percent of the map area, and that they relate largely to changes in strike of first-order faults and to intersections of two or more first-order faults or of first- and second-order faults. Hall (1998) proposes that the areas of low mean stress in the Kalgoorlie area, when favorably linked to the outflow zones, become major gold deposits.

Transport of gold in solution: The chemistry of transporting gold in solution over long distances is extremely complex and has been reviewed by various researchers (e.g., Seward, 1973, 1991; Shenberger and Barnes, 1989; Mikucki and Ridley, 1993; Ridley et al., 1996; Mikucki, 1998). Thermodynamic data on gold-complexing ligands are available for an increasing range of pressures and temperatures (e.g., Seward, 1991; Zotov et al., 1991; Benning and Seward, 1996; Gibert et al., 1998; Loucks and Mavrogenes, 1999), broadly corresponding to the P-T conditions of lode-gold forming hydrothermal systems. Three gold bisulfide complexes, $Au(HS)^{\circ}$, $HAu(HS)_2^{\circ}$ and $Au(HS)_2^-$, are potentially important in transporting gold under hydrothermal conditions (e.g., Seward, 1973; Shenberger and Barnes, 1989; Mikucki, 1998), although Loucks and Mavrogenes (1999) suggest that $AuHS(H_2S)_3^{\circ}$ may be important at high temperatures and pressures. In addition, $AuCl_2^-$ may be important at high temperatures (Mikucki, 1998). A range of other complexes, including thioarsenide, carbonyl, carbonyl-chloride, and carbonyl-sulfide complexes, may be significant carriers of gold in some cases (e.g., Kerrich and Fyfe, 1981).

At low water-rock ratios and high temperatures (>400°C), calculated solubility of gold is high enough (e.g., >1000 ppb) to completely scavenge gold from a range of magmatic host rocks. Calculations indicate that high-temperature Archean hydrothermal fluids were probably undersaturated in gold in their source region (e.g., Mikucki, 1998; Bastrakov et al., 2000). Bastrakov et al. (2000) modelled the effects of pervasive fluid-flow in a rock-dominated system to determine the potential effect on gold solubility along fluid pathways. The results of modelling imply different efficiency of gold mobilization and precipitation at different crustal levels and suggest that gold-undersaturation of rock-buffered fluids would permit gold transport over long distances, preventing gold precipitation during pervasive fluid flow in high-temperature deeper crustal levels (Mikucki, 1998; Bastrakov et al., 2000). Inefficient gold and sulfur precipitation mechanisms are also implied over a significant crustal depth range based on S:Au ratios (Ridley et al., 1996). The transportation of large volumes of gold-bearing fluid over a significant crustal depth range may, therefore, account for the relatively low gold production from amphibolite-facies terranes (Groves, 1990; Ridley et al., 1995). Provided fluids remained effectively channelled during their transport to higher crustal levels, camp- and deposit-scale structural focussing and associated local gold precipitation mechanisms are required to ensure development of economic gold mineralization at the trap site.

Depositional Site Characteristics: Camp-scale

Camp-scale traps include first-order fault zones and associated hydrothermal alteration zones, and large-scale structural inhomogeneities such as anticlines, synclines, and bends along strike in major structures (cf. Phillips et al., 1996). In many Archean terrains (e.g., Yilgarn Craton), they are poorly exposed with limited information available from diamond drilling.

Regional alteration: Hydrothermal alteration zones associated with orogenic lode-gold mineralization are manifested on both camp- and deposit-scales. The former is often expressed as regional carbonation or chloritization and can extend up to one kilometer away from the deposit. Well-documented regional alteration zones are the carbonate and chlorite zones of the Golden Mile deposit (Clout, 1989). Other zones of regional alteration with uncertain genetic relationships to gold mineralization are spatially related to first-order transcrustal fault zones that exert a large-scale structural control on gold mineralization (see above). These regional alteration zones are generally restricted to, or centered on, first-order transcrustal fault zones and characterized by intense carbonatization of the host rocks.

Regionally extensive, locally elongate, zones of carbonate alteration in gold camps in the Yilgarn Craton and Superior Province occur around major, first-order fault systems (as defined in the fluid conduits within the transport-migration part of the system) that may or may not be restricted to individual camps. They are well expressed in komatiitic sequences within greenstone belts; magnesite and dolomite are dominant in these rocks, whereas calcite and lesser ankerite or dolomite typify altered mafic and felsic rocks (Barley and Groves, 1989; Hodgson, 1990). The spatial extent of carbonation in gold camps in the Yilgarn Craton is several orders larger than in individual gold lodes (Barley and Groves, 1987).

In the Timmins camp, Smith and Kesler (1985) demonstrated, with chromatographic analyses of gases released by decrepitation of fluid inclusions trapped in quartz veins, a distinct gradient of increasing XCO_2 towards the major gold deposits (Fig. A14). Detailed regional mapping around the Hollinger-McIntyre deposit (Wood et al., 1986a) shows a widespread progressive carbonation alteration in the dominantly basalt-hosted system, thus supporting a regional CO_2 gradient (Fig. A14).

In mafic rocks of the Kalgoorlie area regionally extensive albite-actinolite±epidote greenschist facies metamorphic assemblages are replaced by chlorite+magnetite+muscovite+calcite± pyrite±siderite alteration assemblage (Bartram and McCall, 1971; Phillips, 1986; Clout, 1989). This 'regional' alteration is present as an irregular 0.2 to 1.0 km wide zone around the Golden Mile fault system, spatially encompassing the distinct lode-gold alteration zonation (described above). Gold values are typically 20-100 ppb (Clout, 1989). This zone is then gradationally replaced by ankerite-siderite±quartz±sericite± leucoxene±rutile±hematite, irregularly along fault zones and/or preferentially in Paringa Basalt.

Golding et al. (1987) conducted a systematic carbon isotope analysis of the Kambalda camp and concluded that carbon isotope values in talc-carbonate altered komatiites form a discrete population, with $\delta^{13}C$ values between -5.0 and -6.0 per mil. The $\delta^{13}C$ values close to -5 per mil are consistent with either a mantle or magmatic source for this carbon. In the Norseman-Wiluna belt, Barley and Groves (1987) interpret the association of regional talc-carbonate alteration with major fault zones, and the general absence of an obvious widespread magmatic source that is spatially associated with the fault zones, as indication for a mantle origin of the carbon. The exact timing of this alteration is not precisely known, but it appears to be largely post-volcanism and could have continued until or during peak metamorphism and gold related hydrothermal alteration; alternatively it may represent more than one alteration event.

Large-scale structural inhomogeneities: Phillips et al. (1996) compare the Kalgoorlie and Timmins camps and conclude that both contain a high density of first-order craton- to regional-scale deformation zones that were oriented at a high angle to the far-field stress at the time of gold mineralization. These camp-scale structural heterogeneities include changes in the orientation and mismatches of lithostratigraphic successions across them. As pointed out by Phillips et al. (1996), the geometry of both the Kalgoorlie and Timmins camps is controlled by refolded thrusted sequences in which units of competent rocks (Golden Mile Dolerite and tholeiitic basalt at Kalgoorlie and Timmins, respectively) are almost totally enclosed by less-competent successions, dominated by sedimentary rocks. These larger-scale structural inhomogeneities thus appear to be a camp-scale trap for, in this case, the world's two largest Archean orogenic lode-gold systems (>1000 Au).

Allen (1998) applied stress mapping to the regional Three Mile Hill gabbro unit in the Coolgardie camp, Yilgarn Craton, and showed a good correlation between stress anomalies and known ore deposits in this unit. In addition, stress anomalies are closely related to 'weak' contacts and stronger rheologies develop a greater differential stress within them as their low tensile strength restricts their ability to accommodate strain. Some lithological units can accommodate greater amounts of strain than others and can act as a buffer to the regional stress, if the unit is thick enough.

Depositional Site Characteristics: Deposit-scale

Host rocks: As summarized by Hodgson (1993), gold mineralization may occur in any rock type, however, not all rocks within a greenstone belt with gold mineralization are equally mineralized, and some rocks are more common in proximity to gold deposits than they are in the host sequence as a whole. The importance of specific host rocks as traps for gold mineralization lies in their strong influence on the structural form and geometry and, through fluid-rock interaction, on the hydrothermal alteration mineralogy, zoning and geochemistry of gold deposits (cf. Hodgson, 1993). It is not unusual, for example, for a single deposit with several different ore bodies to be hosted by vastly different lithologies. At Kalgoorlie, ore is hosted predominantly in Unit 8 of the Golden Mile Dolerite, but the Paringa Basalt and associated sedimentary rocks also host significant, high-grade ore bodies. In the Dome mine within the Timmins camp, ore is hosted in a variety of rock types including intrusion breccia, felsic porphyry, Timmiskaming sedimentary rocks, fault zone rocks on the Timmiskaming sedimentary rock-volcanic contact, and volcanic rocks (Hodgson, 1993).

In the Abitibi subprovince, Hodgson and Troop (1988) show that felsic intrusions and highly carbonated rocks are more common in gold deposits than in equivalent-sized unmineralized areas. Forty percent of deposits contain one or more of the rock types syenite, syenite porphyry and feldspar porphyry; an additional 14 percent of deposits contain quartz or quartz-feldspar porphyry. Groves (1990) and Watkins and Hickman (1990) show that the distribution of deposits among the variety of rock types present varies greatly in the four major provinces within the Yilgarn Craton (Fig. A15a). For example, in the Murchison Province, BIF and chert, ultramafic and felsic porphyry rocks are much more common as mine-scale host rocks than they are in the greenstone belt succession as a whole. In contrast, in the Norseman-Wiluna Belt almost all production is from deposits hosted in mafic volcanic rocks and intrusions, despite the fact that a significant part of the belt consists of ultramafic, felsic volcanic and sedimentary rocks. However, these statistics may need revising as newly discovered world-class deposits (e.g., Kanowna Belle and Wallaby; Fig. A2) are located in conglomerates and other non-mafic rocks, thus demonstrating that gold mineralization can occur in any rock type in the Yilgarn Craton (cf. Hodgson, 1993). Ridley et al. (1995) show that one quarter of greenstone belt outcrop in the Yilgarn Craton has been metamorphosed to the amphibolite facies or higher grades (Fig. A15b). Furthermore, about 13 percent of gold in the Yilgarn Craton is from amphibolite facies terrains (Fig. A15c).

Structural traps: Archean lode-gold deposits are characterized by a wide variety of structural traps at scales ranging from mining camp to individual deposit and oreshoot. Structures and structural control on the deposit-scale include fault-, shear-, thrust- and/or vein-systems, and orebody-scale structures such as fault intersections and bends, stockworks, and linear bodies parallel to local stretching lineations. Deposit-scale structures are controlled by a combinations of: (i) crustal depth, (ii) regional strain state, (iii) lithology of hosting successions, (iv) contrasts in rock competency, (v) shape of granite-greenstone contacts, and (vi) lateral fluid pressure gradients and variations in mean rock stress as a consequence of regional deviatoric stress. Furthermore, at all depths fluid flow can either be dominantly in fault or shear zones or within a subvertical zone of fractured rock within a single lithological unit (cf. Groves et al., 1995). Hodgson (1989) provides an excellent summary of structures of shear related, vein-type gold deposits. Hronsky et al. (1990) describe ore-controlling structures and analyze deposit- and mine-scale structural controls of Archean lode-gold deposits in the Yilgarn Craton.

Deposit-scale structures assert a major influence on the mineralization style, which is defined as a characteristic association of the shape and form of a mineralized zone (Hronsky et al., 1990). Most Archean lode-gold deposits are spatially associated with brittle-ductile shear zones that range from well-defined individual shear zones to large shear zone systems. They range in shape from tabular to linear, and in form including disseminated, breccia, stockwork, sheeted quartz vein sets and single shear veins. They can be brittle, brittle-ductile to ductile in nature. Typically, they record a complex history of mineral deposition that overlaps, and is genetically related to, the deformation that generated the host structural zones.

Many Archean lode gold deposits display a geometrical pattern of mineralization that is to a large part controlled by veins or vein arrays from cm- to m-scale. They are an integral part of the mineralization architecture and display a variety of characteristic textures (Dowling and Morrison, 1989). Many mesozonal gold deposits contain complex networks of veins that are localized along high-angle reverse or reverse-oblique brittle-ductile shear zones. Many of these vein systems are of considerable vertical extent (>2 km; Kolar deposit is over 3 km) and include steeply dipping, lenticular fault veins subparallel to the shear zone schistosity, and locally associated, and apparently cross-cutting, subhorizontally extensional veins (the so-called 'flats'). Sibson et al. (1988) used field relationships and textures of both steep and flat vein sets at the Sigma mine (Robert and Brown, 1986a, b), and friction theory (Sibson, 1981; 1983) to suggest that the high-angle reverse faults at Sigma acted as valves, promoting cyclic fluctuations in fluid pressure from supralithostatic to hydrostatic values. Due to their misorientation in the prevailing stress field, reactivation of the steep faults can only occur when fluid pressure exceeds the lithostatic pressure. Seismogenic fault failure then creates fracture permeability within the fault zone and allows sudden draining of the overpressured fluid reservoir at depth. Boullier and Robert (1992) and Robert et al. (1995) in detailed textural and fluid inclusion studies on the steep and flat veins of the Sigma mine refined a multistage model for vein formation (Fig. A16). Incremental opening of flats is attributed to the preseismic stage of supralithostatic fluid pressures followed by seismic rupture whereas the deposition within fault veins is attributed to the immediate postrupture discharge phase. Hydrothermal fault-sealing leads to reaccumulation of fluid pressure and a repetition of the cycle. This model adequately explains the apparent cross-cutting relationships between steep and flat veins as a natural consequence of the cyclicity of the process.

Holyland and Ojala (1997) used 3-dimensional stress modelling to model stress fields around the eastern margin of the Granny Smith Granodiorite under east-west compression at the Granny Smith mine near Laverton in Western Australia. At a deposit scale, the patterns of the simulated minimum principal-stress indicate maximum dilatancy and fluid flow and correlate well with known areas of gold mineralization (Fig. A17) near the contact between the Granny Smith Granodiorite and sedimentary rocks.

Table A1 summarizes the mineralization and structural styles of Archean lode-gold deposits at epi- meso- and hypozonal crustal levels. Groves et al. (1995) show for the Yilgarn Craton that lode-gold deposits follow a broad correlation between structural style and depth level of emplacement. Epizonal deposits, hosted in subgreenschist facies rocks, are controlled by dominantly brittle styles of deformation such as cataclasites, tensional quartz veins and breccias (e.g., Wiluna, Ross; Table 2). In contrast, in hypozonal deposits, hosted in amphibolite facies rocks, the style of deformation changes largely to ductile shear zones with laminated veins, diffuse quartz veins and veinlets (e.g., Norseman deposits, Transvaal, Renco; Table A1). Locally, however, massive quartz reefs are present in some hypozonal deposits, such as Westonia (Cassidy and Hagemann, 1999). Note also that mineralization styles may be transitional and that multiple deformation styles may exist within single deposits. Colvine et al. (1988) report that mineralization in the Campbell-Red Lake and Dickenson mines, Red Lake, exhibit vertical and lateral transitions from brittle-ductile to more brittle deformation with decreasing metamorphic grade, and decreasing paleo-crustal depth. In addition, in the Duport deposit at Lake of the Woods, a change from brittle-ductile to brittle vein systems reflects a decrease in ambient temperature (Colvine et al., 1988).

As with deposit-scale structures the geometry of oreshoots is influenced by a variety of factors including geological complexity, rock rheology and paleo-crustal depth of formation (Table A1). Lithologically complex environments are generally favorable horizons for gold mineralization. The interaction of mechanical heterogeneities imposed during the mineralizing event with those of the protolith, generally results in mineralized zones that are wider and geometrically more complex and variable, but not necessarily with a higher gold tenor. For example, weak anisotropic interflow sedimentary rocks may be the loci of ductile shear zones that have dilated (e.g., parts of the Oroya shoot in the Golden Mile: Scantlebury, 1983; many of the large veins in the Hollinger Mine: Mason and Melnik, 1986). In contrast, rheologically strong flow units of differentiated dolerites may be preferentially fractured (e.g., Three Mile Hill gabbro unit, Coolgardie: Knight et al., 1996; 2000; Allen, 1998). Ore shoots may be localized where a mineralized shear zone is in a chemically and/or mechanically favorable horizon. For example, the BIF-formation at Mt Morgans (Vielreicher et al., 1994) or the iron-rich sill and BIF in the Camflo Mine (Sauve and Malika, 1990). Granitoid hosted ore bodies generally have narrow and straight, locally conjugate, quartz vein sets, as there is little initial mechanical anisotropy in the host rock. Exceptions occur where there are anisotropic complexities such as mafic dikes and granite-greenstone contacts. Examples include conjugate quartz vein sets at Tarmoola (Duuring and Hagemann, in press) and Granny Smith (Ojala et al., 1993), quartz vein sets at Lady Bountiful (Cassidy and Bennett, 1993) and massive quartz reefs at Westonia (Cassidy and Hagemann, 1999) in the Yilgarn Craton and at Renabie (Callan and Spooner, 1998) in the Superior Province. Strong mechanical anisotropy of previously weakly anisotropic rocks is locally also caused by (early) hydrothermal and/or magmatic processes which result in a marked change in the rheology of the host rock.

Individual oreshoots or orebodies may also be controlled by complexities in deposit-scale structures. The main controlling factors on the geometry of oreshoots are: (i) the line of intersections (plunge or pitch) of different structures such as shear zones or faults, (ii) the line of intersections (plunge or pitch) of structures and dip of rock units, (iii) bends and jogs in planar structures such as faults and shear zones (iv) folds and associated hinge lines and vein types.

In summary, structural control of Archean lode-gold deposits occurs on scales from deposits to individual oreshoots. Deposit scale mineralization styles are strongly influenced by the deformation inventory and can be summarized in eight major different styles (see Table A1) with the geometry of single oreshoots being controlled by a combination of inhomogeneities of the structures, rheology and anisotropies in surrounding rocks.

Hydrothermal alteration: Factors that control the extent and mineralogy of hydrothermal alteration associated with Archean lode gold mineralization include: (1) the structural regime and far-field stress field in which the deposit is formed, (2) chemical composition of the lithostratigraphic units that interact with hydrothermal fluids, (3) chemical composition of the hydrothermal fluids, including gases, cations, anions and metals, and (4) physical conditions including pressure, temperature, and oxygen and sulfur fugacity. The interplay of these factors influence properties such as rock rheology and permeability, fluid pressure, deformation mechanism, fluid to rock ratios and metasomatic reaction paths and flux rates.

Zonation of hydrothermal alteration is present: (i) with increasing distance orthogonally to the fluid conduit, (ii) increasing depth within the same fluid conduit, (iii) between host lithologies of differing bulk compositions, and (iv) with increases of temperature and pressure, i.e., the crustal level of emplacement. Pronounced changes in alteration mineralogy occur dominantly perpendicular to the fluid conduit and are generally defined by distinct diagnostic mineral assemblages. Proximal alteration zones are in areas of greatest fluid flux within shear zones, adjacent to veins or breccias and hence are fluid dominated metasomatic zones. Distal alteration zones are marked by progressive infiltration of hydrothermal fluid into the wallrock and simultaneous decrease in fluid:rock ratios as well as chemical gradients. Boundaries between individual alteration zones can be both knife-sharp and diffuse; commonly distal alteration zones display gradational boundaries, this is especially true where distal alteration zones grade into least metasomatized regional metamorphic rocks.

At the deposit-scale, the main controlling factors of diagnostic alteration minerals and mineral assemblages include the type of host rocks and the crustal level of emplacement, i.e., epi-, meso-, or hypozonal depth. The most typical silicate, oxide and sulfide assemblages within the four dominant host lithologies of late orogenic Archean lode-gold deposits, mafic, ultramafic, granitoid and BIF rocks, are shown in Table A2. For example, proximal wallrock assemblages in mafic/ultramafic rocks show progressive variations from ankerite/dolomite-white mica-chlorite at epizonal crustal levels, through ankerite/dolomite-white mica-biotite (phlogopite)-chlorite±albite at mesozonal levels to amphibole-biotite-plagioclase and diopside-biotite-garnet±K-feldspar assemblages at hypozonal crustal levels. The sulfide mineral assemblages show also a sympathetic relationship from S-rich pyrite-arsenopyrite, to pyrite-arsenopyrite-pyrrhotite and pyrrhotite-arsenopyrite, to pyrrhotite-arsenopyrite-loellingite with increasing paleocrustal depth. Low temperature tellurides, sulfosalts, tetrahedrite are more common at shallow crustal levels, whereas molybdenite and chalcopyrite are locally more abundant at deeper paleo-crustal levels.

Despite the systematic variations in alteration mineralogy at different crustal levels there appears to be generally little evidence for systematic vertical zoning on the scale of a single deposit (Kerrich, 1987; Groves et al., 1988; Hodgson, 1993). Exceptions are the antithetic relationship between tourmaline and chlorite-biotite in vein and alteration haloes at Sigma (Robert and Brown, 1986b) where chlorite-muscovite-tourmaline alteration gives way to biotite-chlorite-muscovite at depths greater than 1300 m. Other changes with increasing depth include the presence of amphibole in the unaltered rock and outer alteration zones, and pyrrhotite and chalcopyrite abundance in all veins. These changes in alteration mineralogy apparently parallel changes in regional metamorphic grade with depth. Hodgson (1993) reports that at depth in the Hollinger-McIntyre mine: (1) the quartz-carbonate veins are more widely spaced, (2) the zones of ankerite alteration along the margins of veins are narrower, (3) ratios of gold and of sulfides to gold in veins and to sulfides in vein envelopes increases, (4) pyrrhotite appears as a vein mineral, and (5) albite and tourmaline are more abundant than they are at the surface. Vertical metal zonation has also been reported from Mt Charlotte (Clark, 1980) where over a vertical interval of 800 m a progressive change from pyrite to pyrite-pyrrhotite assemblages is observed. At Wiluna stibnite is only observed in the preserved top 200 m of some of the deposits (Hagemann, et al., 1993).

Major oxides and trace element signatures: Most gold deposits record a major- and trace-element dispersion halo that surrounds orebodies. These patterns are highly dependent on the original protolith and mineral stability relationships within alteration zones. In epi- and mesozonal deposits, besides Au, massive additions of CO_2, H_2O, K and S are recorded. In some deposits Ag, As, Sb, W, Mo, B, Li, Ba and Rb are also enriched. In distal alteration zones chemical additions are restricted to CO_2 and H_2O. In proximal alteration zones, however, metasomatic effects on element distribution become more pronounced and volume additions of up to 70 percent, due to vein formation, have been recorded in some of the lodes in the Golden Mile (Ramos et al., 1987). In the wallrocks, chemical changes are strongly influenced by the host rocks with ultramafic rocks commonly showing chemical changes that include the addition of Ca, Mg, K and CO_2 to the wallrocks whereas H_2O is lost. In mafic host rocks, K, S, CO_2, Rb and Ba are generally added. Silica is only added in zones of very intense alteration. Epi- and mesozonal deposits may show Na enrichment in addition to, or instead of, K. Several hypozonal deposits are characterized by substantial additions of Ca to inner alteration zones and depletion of Na (e.g., Westonia: Cassidy, 1992; Scotia: McCuaig et al., 1993; Coolgardie district: Knight, 1994; Knight et al., 2000). Generally orogenic lode-gold deposits are characterized by a metal inventory that consists of Au, Ag, As, Sb, Te ±Se, ±W,

±Mo and ±Bi, Au/Ag ratios averaging 5 and low Cu, Zn and Pb contents. Several hypozonal deposits have greater Ag, W, Cu and Pb abundances than epi- and mesozonal deposits.

Alteration indices, such as CO_2/(Fe+Mg+Ca) or (3K+Na)/Al, reflect the CO_2 and alkali enrichment or depletion of hydrothermal alteration zones. Detailed studies at the Kerr Addison (Kishida and Kerrich, 1987) and Wiluna (Fig. A18; Hagemann et al., in revision) deposits, hosted in predominantly ultramafic and mafic rocks, respectively, show that distal alteration zones are characterized by moderate CO_2/(Fe+Mg+Ca) and low (3K+Na)/Al ratios due to the moderate carbonatization and abundant chlorite. In contrast, proximal alteration zones are characterized by abundant carbonate and white mica and low chlorite contents reflected in elevated CO_2/(Fe+Mg+Ca) and (3K+Na)/Al ratios. The correlation of 3K/Al and Na/Al indices with gold in the Wiluna deposits show that in the core of the highly mineralized zone Na/Al increases dramatically and exceeds 3K/Al, this crossover in 3K/Al and Na/Al indices marks the contact between the carbonate-quartz-muscovite and albite-quartz-carbonate subzones and correlates with peak Au content (Fig. A18).

Physico-chemical conditions: The physico-chemical conditions of mineralization can be constrained by fluid and mineral equilibria from fluid inclusion and ore and alteration mineralogy studies, respectively. Parameters such as Pressure-Temperature-Density-Composition (including salinity, XCO_2, XCH_4) are determined by fluid inclusion investigations, whereas fO_2, fS_2, XCO_2, mineral stabilities and pH are generally constrained by mineral equilibria studies. Excellent comprehensive summaries of ore fluid conditions and particularly phase equilibria results for epi- to hypozonal gold deposits are provided in Colvine et al. (1988), Ho et al. (1992), Mikucki and Ridley (1993), and Mikucki (1998). The most important requirement in applying fluid and mineral equilibria is that the fluid inclusion and mineral phases used are representative of the ore-fluid conditions at the time of mineralization, i.e., that the observed fluid inclusion, alteration and vein assemblages largely reflect equilibrium with the ore-forming fluids at the conditions at which mineralization took place.

Fluid equilibria: There are numerous comprehensive fluid inclusion studies on Archean orogenic epi- and mesozonal gold deposits including deposits hosted in the Barberton greenstone belt in southern Africa (de Ronde et al., 1992); Hollinger-McIntyre (Smith et al. 1984; Wood et al., 1986a, b), Pamour (Walsh et al., 1988), Henderson II (Guha et al., 1983) and Sigma (Robert and Kelly, 1987) in Canada; and Mt. Charlotte (Ho et al., 1990a), Hunt (Ho et al., 1990a), Lady Bountiful (Cassidy and Bennett, 1993), Wiluna and Racetrack (Hagemann et al., 1994), Golden Kilometre (Gebre-Mariam et al., 1997) and Bronzewing (Dugdale and Hagemann, 2001) in Australia.

Numerous fluid inclusion studies (see above), and constraints based on proximal alteration assemblages, are consistent with neutral to weakly alkaline ore fluids of low to moderate salinity (typically <6 wt percent NaCl equiv) and H_2O-CO_2±CH_4 inclusions with a typically high CO_2 (±CH_4) content of 5 to 25 mole percent CO_2. The CO_2/CH_4 molar ratios are variable from 0.25 to >2 with the CH_4 content likely reflecting the fO_2 of the ore fluid. The saline phase consists of Na>Ca>K>Mg, and daughter minerals are rare. The P-T conditions typically range from 200° to 350°C and 1-3 kbar, and fluid trapping generally occurred at or near the solvus, i.e., trapped during fluid immiscibility (e.g. Pamour: Walsh et al., 1988; Sigma: Robert and Kelly, 1987; Au quartz vein deposits in the Barberton greenstone belt: de Ronde et al., 1992), or from unmixed fluids (parts of McIntyre-Hollinger: Smith et al., 1984). In shallow deposits fluid mixing of two different fluid sources (surface waters and deep magmatic and/or metamorphic fluids) has also been proposed (e.g., Golden Kilometre: Gebre-Mariam et al., 1997).

A innovative approach by Channer and Spooner (1994) and Channer et al. (1999) used combined gas and ion chromatographic analysis of well characterized samples from the Hollinger-McIntyre and Kerr Addison deposits to constrain bulk fluid compositions of 80-90 mole percent H_2O, 2-15 mole percent CO_2, 1-3 mole percent Cl^-, 2-4 mole percent Na^+, and trace species (< 1 mole percent) of hydrocarbons. Characteristic trace gas depletion (as shown in a $CO_2/100$-CH_4-N_2 ternary diagram, Channer and Spooner, 1994), suggests that wallrock sulfidation reactions have been more important than phase separation for gold deposition at Hollinger-McIntyre, whereas volatiles in green carbonate ore from Kerr Addison show evidence for significant phase separation which was likely the main gold depositional process. De Ronde et al. (1992) used gas-chromatographic analysis to show that shear zone related gold quartz vein deposits in the Barberton greenstone belt in South Africa show dominant H_2O (~90 mole percent) and CO_2 (~10 mole percent) with minor CH_4 (~0.06 mole percent) and N_2 (~0.04 mole percent) and traces of COS, C_2H_6, C_3H_8, and other hydrocarbons. A combined H_2O-CO_2-NaCl "average" fluid for the Barberton gold deposits has ~88.5 mole percent H_2O, ~9.8 mole percent CO_2, and ~1.7 mole percent NaCl equiv (de Ronde et al., 1992). Hagemann et al. (1996) in a preliminary study on the Wiluna lode-gold deposits showed that there are locally differences in volatile contents (e.g., CO_2, CH_4) between fluid inclusions trapped in equilibrium quartz and sulfides (e.g., stibnite) which might indicate that fluid inclusions in quartz and sulfides are not trapped simultaneously and/or were preferentially effected by post-entrapment processes.

Guha et al. (1991) used solid probe mass spectrometry to show that during hydrothermal alteration associated with gold mineralization in the Tadd prospect in Chibougamau all generations of inclusions at all sites contained CO_2 and H_2O, but that a decrease in XCO_2 could be mapped outward from the mineralized zone. In the case of the vein-hosted Sigma mine a nearly complete segregation into CO_2 and H_2O end members was observed which was interpreted as the result of extreme fluid pressure fluctuations causing free gold deposition in veins.

Many fluid inclusion studies (e.g. Sigma, Wiluna, Bronzewing) report relatively low homogenization temperatures for the co-genetically trapped aqueous inclusions compared to temperatures for the mixed aqueous-carbonic inclusions (by about 100°C). This phenomena has been interpreted to be the result of CO_2 effervescence from a CO_2-saturated aqueous fluid due to pressure fluctuations (cf. Robert and Kelly, 1987). Entrapment of different fluids generated by multiple unmixing events over large vertical extents within a fault system may also lead to discrepancies between homogenization temperatures of aqueous and mixed aqueous-carbonic inclusions (cf., Ho et al., 1992).

Saline aqueous fluids (>10 to 35 wt percent NaCl equiv) are observed in many Archean lode-gold deposits but their origin remains at most equivocal. In many cases they are clearly related to post-mineralization circulation of basinal brines (Guha and Kanwar, 1987; Boullier et al., 1998; Ho et al., 1990c, 1992). In epi- and mesozonal lode-gold deposits, however, aqueous inclusions with salinities of up to 21 wt percent NaCl equiv can be explained by fractionation of salt into the aqueous, liquid-rich phase during phase immiscibility (Robert and Kelly, 1987; Dugdale and Hagemann, in press). In the hypozonal Zakanaka lode gold deposit, located in the Pilbara Craton, Neumayr (1993) showed that phase immiscibility at 550°C resulted in cogenetic aqueous-carbonic inclusions with 0.25 XCO_2 and aqueous inclusions that contain up to 45 wt percent NaCl equiv. High salinity inclusions (>21 wt percent NaCl equiv) can also form as a result of mixing of descending evolved saline brines with an ascending aqueous-carbonic phase as indicated for the Golden Kilometre deposits north of Kalgoorlie (Gebre-Mariam et al., 1997).

Pure methane inclusions have been reported from several Archean lode gold deposits including Lancefield (Hronsky, 1993), Wiluna (Hagemann et al., 1996), Golden Kilometre (Gebre-Mariam et al., 1997). In many cases these inclusions were explained by reaction of the hydrothermal fluids with graphite-bearing rocks or devolatilization of the latter (Ho, 1987; Naden and Shepherd, 1989; Gebre-Mariam et al., 1997). Alternative processes that potentially can explain methane-rich inclusions include post-entrapment hydrogen diffusion (Hall and Bodnar, 1990; and see below) or fluid unmixing (Naden and Shepherd, 1989).

Despite petrographical evidence of cogenetically trapped aqueous and aqueous-carbonic inclusion assemblages, significant ranges of pressure and temperature are recorded (Robert and Kelly, 1987; Ho et al., 1992; Hronsky, 1993; Gebre-Mariam et al., 1997; Dugdale and Hagemann, in press). In combination with structural and vein textural constraints these P-T ranges are interpreted as transient fluid pressures fluctuations during seismic fault activity, i.e., catastrophic pressure drops from sublithostatic to supralithostatic fluid pressures, and mineral deposition. Detailed analyses on the structural control of fluid inclusion planes and fluid inclusions in the Sigma mine by Boullier and Robert (1992) indicated that successive cycles of opening and collapse in subhorizontal extension veins correlated with opening and slip on high-angle shear veins. They interpret the observations as recording fluid pressure fluctuations in successive coseismic-interseismic cycles.

Fluid inclusion studies on hypozonal lode-gold deposits are rare with Santosh (1986) and Mishra and Panigrahi (1999) reporting apparently contradicting fluid inclusion results from the Champion reefs in Kolar, South India. Mernagh and Witt (1995) report fluid inclusion data from the Missouri and Sand King deposits in the Eastern Goldfields Province whereas Ridley and Hagemann (1999) report results from the Three Mile Hill, Marvel Loch and Griffins Find deposits, and Hagemann and Cassidy (1999) for the Westonia deposit in Western Australia.

Ridley and Hagemann (1999) demonstrate that inclusion densities for the Three Mile Hill, Marvel Loch and Griffins Find deposits are consistent with a range of P-T conditions of entrapment, and are in general not consistent with the conditions of vein formation indicated by vein assemblages (Fig. A19). Diffusional addition of H_2 into inclusions, diffusional loss of H_2O, and reduction of inclusion volume are possible during cooling and uplift along the inferred P-T path. The mixed carbonic-aqueous and carbonic inclusion populations could have been derived from an originally uniform population of low-salinity, aqueous dominated H_2O-CO_2 inclusions by a combination of these processes. Inclusion modification as the cause of the complex inclusion populations is supported by relations of molar volume to composition, and, to an extent, by variations in fluid salinity. If inclusion re-equilibration is the cause of inclusion variability, it was of variable intensity within a single vein system, and within individual clusters of inclusions in some samples, and is suggested to have been a function of the local petrological and textural environment. The Westonia deposit, however, contains primary, mixed (H_2O-CO_2-CH_4-NaCl) inclusions that are likely unaffected by post-entrapment modification, despite the estimated temperatures of mineralization around 600°C (Hagemann and Cassidy, 1999). As shown in Fig. A19 mean oxygen fugacities obtained from fluid and mineral equilibria overlap, and in combination with similar mean fluid inclusion and mineral equilibria pressures of 4±2 kbar, suggest that these inclusions have not been affected by post-entrapment modification, thus representing pristine ore fluids. Fluid inclusion data from the Champion reef (Santosh, 1986; Mishra and Panigrahi, 1999) also show significant discrepancies between fluid and mineral equilibria, indicating that they may also be affected by post-entrapment modification, or alternatively represent fluids unrelated to hydrothermal alteration and associated gold mineralization (cf Santosh, 1986).

Hagemann and Brown (1996) show that calculated fluid pressures of epi- to hypozonal deposits display a continuum of formation pressures from <0.5 to 7.0 kbar thereby confirming a continuum of depths for the formation of the late-orogenic, epigenetic lode-gold deposits proposed by Groves et al. (1989). Three major depth levels were identified: (1) epizonal levels (at <1.5 kbar corresponding to <6 km e.g., Wiluna and Racetrack), mesozonal levels (at >1.5 to 3.0 kbar corresponding to >6 to <12 km, e.g., Hollinger-McIntyre, Pamour, Mt Charlotte) and hypozonal deposits (at > 3.0 kbar corresponding to >12 km; e.g., Westonia, Sand King/Missouri).

Straub et al. (1996) describe a wide compositional range of fluid inclusions (aqueous to carbonic and mixtures thereof) from the base-metal-rich Mt Gibson gold-silver deposits, Murchison Province. Textural evidence suggest that early, synvolcanic polymetallic volcanic hosted massive sulfide (VHMS) related fluid inclusions were likely modified or destroyed by the later orogenic lode-gold style mineralization. However, in contrast to epi- and mesozonal, and partly also to hypozonal orogenic lode-gold deposits, the aqueous inclusions display very high salinities (ave. 47 wt percent NaCl equiv) with up to five solid (salt) inclusions and dissolution temperatures of many daughter crystals >600°C. These inclusions were interpreted as evidence for the involvement of at least a major component of magmatic fluids in the ore forming process.

Mineral equilibria: Phase equilibria studies have been recently used to decipher the nature and composition of auriferous ore fluids (e.g., Neall and Phillips, 1987; Dube et al., 1987; Mikucki and Groves, 1990; Mikucki and Ridley, 1993; Mikucki, 1998). The following is a summary of the results of mineral equilibria studies on epi-, meso- and hypozonal deposits. Vein and vein selvedge assemblages in gold deposits hosted at different paleo-crustal levels are consistent with formation in equilibrium with a fluid of similar XCO_2 but at contrasting pressures and temperatures (Fig. A20). The pH of the ore fluid is approximately near neutral (5.2) to slightly alkaline (between 5.2 and 6.8) and buffered by albite-sericite±paragonite, biotite-ankerite and plagioclase-amphibole±diopside mineral assemblages at epi-, meso-, and hypozonal levels, respectively (Table A2). Therefore, calculated pH values are about constant for lode-gold fluids, irrespective of the P-T range of ore formation. Oxygen fugacity (fO_2) and total sulfur content (mS), i.e., redox conditions, are fundamental in controlling the capacity and mechanism of the hydrothermal fluid to transport and precipitate gold. Most deposits in the epi-, meso-, and hypozonal environment are characterized by assemblages of pyrite± arsenopyrite±stibnite, pyrite±arsenopyrite± pyrrhotite and loellingite+arsenopyrite± magnetite± ilmenite±pyrrhotite, respectively. These sulfide-oxide assemblages are consistent with oxidation states of the ore fluids remaining relatively constant with respect to major aqueous redox buffers (fO_2 about 0 to 3 log units above the CO_2-CH_4 buffer; Fig. A21), although hypozonal deposits generally formed under higher fO_2 conditions then epi- and mesozonal deposits.

There is, however, a group of deposits that formed from relatively oxidized fluids and are characterized by magnetite-pyrite±V-muscovite±sulfate (anhydrite and/or barite)±hematite in epizonal deposits (e.g., Fimiston-style mineralization in the Golden Mile deposit) and pyrrhotite-pyrite±chalcopyrite±ilmenite ±spinel (e.g., Westonia) in hypozonal deposits. These epi- to mesozonal deposits show fO_2 conditions close to the pyrite-hematite-magnetite triple point near the total SO_4-H_2S buffer, consistent with depleted $\delta^{34}S$ values (e.g., some of the Fimiston-style gold lodes: Phillips et al., 1986). The total sulfur content of the ore fluid (aH_2S) varied from 10^{o} to 10^{-4} with a correlation between lower aH_2S and decreasing temperatures of the ore fluids (Mikucki 1998). Ore fluid conditions at all paleo-crustal levels broadly parallel the aqueous sulfide-sulfate and CO_2-CH_4 redox buffers. The fO_2 values of the ore fluids, therefore, are consistent with oxidized and reduced equilibria of aqueous carbon and sulfur species controlling the oxidation state at different crustal levels. As Mikucki and Ridley

(1993) pointed out the oxidation state of the ore fluid (i.e., sulfide-sulfate versus carbonate-methane buffer) will depend on: (1) initial oxidation state of the fluid, (2) relative abundances of sulfur and carbon species, and, at low temperatures (3) kinetic factors. Ore fluids in hypozonal deposits and redox conditions near the CO_2-CH_4 buffer and low initial aH_2S display fO_2 values buffered by CO_2-CH_4, and contain relatively reduced ore assemblages. Ore fluids with slightly higher fO_2 and aH_2S values are buffered by the SO_2-H_2S equilibria and contain oxidized assemblages. The range of oxidation states in hypozonal deposits suggests that the fluid oxidation state is not a critical parameter in deciphering potential fluid sources for hypozonal lode gold deposits. However, at shallow crustal levels under low lithostatic or hydrostatic pressures oxidized ore fluids are compatible with the influx of oxidized meteoric and/or seawater. At deeper crustal levels the occurrence of oxidized assemblages, such as those observed at Westonia (Cassidy and Hagemann, 1999), remain unexplained.

Deposition of gold from solution: At the depositional site, gold is precipitated from the hydrothermal fluids in response to changes in the physico-chemical conditions of the fluid (e.g., Mikucki and Ridley, 1993). Based on available data, changes in ore-fluid chemistry can result from a number of processes, including: (i) large-scale temperature and pressure gradients along the fluid pathways, (ii) phase separation in response to pressure fluctuations at the camp- or deposit-scale, (iii) reaction of the fluid with wallrocks surrounding the fluid conduit generally at the deposit- or lode-scale, and (iv) mixing of two or more fluids at camp- to ore shoot-scale. All of the above processes have been invoked as important gold precipitation mechanisms of Archean orogenic lode-gold deposits. Mikucki and Ridley (1993), Ridley et al. (1996) and Mikucki (1998) provide detailed discussions of these main depositional mechanisms and only salient points are presented here.

Broad pressure and temperature gradients are unlikely to cause major gold precipitation in lode-gold mineralizing systems. This is mainly due to the relative inefficiency of gold precipitation as the fluid migrates from source to depositional trap site (e.g., Ridley et al., 1996; Bastrakov et al., 2000). However, such pressure-temperature gradients may be important at the terrane-scale through providing a depositional pressure-temperature 'window' (e.g., Phillips and Powell, 1993; Mikucki, 1998). It has been inferred that such gradients may explain the localization of the majority of world-class lode-gold deposits in greenschist facies environments (Ridley et al., 1996; Mikucki, 1998; Bastrakov et al., 2000). At this crustal level, local geological environments are within the brittle-ductile transition, thereby enhancing structural focussing mechanisms at the camp- and deposit-scale (cf., McCuaig and Kerrich, 1998).

Fluid-rock interaction is invoked as a depositional mechanism for a substantial proportion of orogenic lode-gold deposits in sub-amphibolite and amphibolite-facies environments. In particular, it is favored when gold is sited in wallrock alteration haloes surrounding fluid conduits or in replacement bodies (e.g., Groves and Phillips, 1987; Ridley et al., 1995). Sulfidation of Fe-rich wallrocks has been demonstrated as an efficient depositional mechanism for large orebodies in a variety of mafic lithologies and BIF (e.g., Mt Charlotte, Kambalda: Phillips and Groves, 1983; Clark et al., 1986; Neall and Phillips, 1987). It has also been used to account for the close association between wallrock Fe-sulfides and gold and the importance of mafic host rocks with high Fe/Mg (e.g., Groves and Phillips, 1987; Groves et al., 1989). Other metasomatic processes during fluid-rock interaction are also effective gold depositional mechanisms. For instance, intense Ca and CO_2 metasomatism, whereby H_2 is released into the hydrothermal fluid resulting in a decrease in pH and potential gold precipitation, is invoked for ultramafic-hosted gold mineralization at Kerr-Addison deposit, Superior Province (Kishida and Kerrich, 1987). However, significant decreases in ore fluid pH during fluid-rock interaction are unlikely to be an effective depositional mechanism in other lithologies (Mikucki, 1998). Reduction of the hydrothermal fluid due to reaction with graphitic metasedimentary lithologies is also invoked as a potential depositional mechanism (McCuaig and Kerrich, 1998).

Phase separation has been suggested as an important mechanism for deposition of free gold in quartz veins and breccias, and the formation of high-grade ore-shoots within individual deposits. Several studies have proposed phase separation for a variety of lode-gold deposits that are predominantly localized in sub-greenschist to greenschist-facies environments (e.g., Robert and Kelly, 1987; Guha et al., 1991; Cassidy and Bennett, 1993). Phase separation in ore fluids may arise from transient pressure fluctuations during fault-valve mechanisms or expansion of the ore fluid solvus through incorporation of CH_4- or N_2-rich fluids, and results in an increase in ore fluid pH and oxygen fugacity in the aqueous phase and a decrease in total sulfur content (e.g., Mikucki and Ridley, 1993; Mikucki, 1998). These have competing effects on gold solubility, and precipitation will depend on the initial redox and pH conditions of the fluid and relative magnitude of the oxygen fugacity and pH changes. This may explain why in some deposits gold is hosted primarily in wallrock alteration envelopes even though evidence for phase separation is reported from fluid inclusion studies (e.g., Victory-Defiance: Clark et al., 1989).

Fluid mixing is also invoked as a gold depositional mechanism for several Archean lode-gold deposits. For example, mixing of deeply sourced fluids with surface waters is invoked for some sub-greenschist facies deposits (e.g., Wiluna: Hagemann et al., 1994; Golden Kilometre: Gebre-Mariam et al., 1997). Fluid mixing has also been proposed for the Golden Mile deposit (Walshe et al., 1998) on the basis of variations in the composition of sulfur isotopes suggesting the presence of oxidized and reduced fluids. However, the variation in sulfur isotope compositions is alternatively interpreted to reflect complex local processes (Hagemann et al., 1999). Fluid mixing can also occur through the mixing of internally derived end-member fluids and may explain the location of large gold concentrations within quartz veins where there is little gold in the surrounding wallrock alteration haloes (McCuaig and Kerrich, 1998).

A variety of gold depositional mechanisms have been discussed and indicate the importance of the interplay of structural focussing of ore fluids into favorable trap-sites in conjunction with the various physical and chemical processes that can enhance precipitation. Without the structural focussing or without a suitable precipitation mechanism, the hydrothermal fluids may pass through the potential trap site without gold accumulation.

Zones of Outflow and Discharge

In many instances, orogenic lode-gold mineralizing fluids do not encounter the necessary structural focussing and trap-site processes that produce a gold deposit and the fluid continues to flow up-temperature through discharge or outflow zones. Even when fluids have combined with suitable physical and chemical processes to allow formation of a large deposit there is discharge of the 'spent' fluids through outflow zones. Evidence for outflow zones may indicate presence of a mineralized system within a terrane and potentially may be mapped on the surface. Outflow zones have yet to be documented in Archean orogenic lode-gold systems, largely due to the fact that they occur naturally on top of the mineralizing system and, therefore, are the first to be eroded during the dynamic evolution of the Earth. In the Kalgoorlie Terrane of the Yilgarn Craton, Hall (1998) suggests that primary outflow zones may include major crustal fault systems such as the Bardoc shear zone (Fig. A12). A spatial link is postulated between primary outflow zones and occurrence of significant gold deposits.

In the Kalgoorlie camp area, stratigraphic seals to the Golden Mile deposit may include the Black Flag sedimentary rocks. Clout (1989) interpreted these as the cap of the Golden Mile mineralizing system. Hall (1998) also suggests that regressive sedimentary sequences that overlie the greenstone packages in the Kalgoorlie Terrane potentially acted as regional seals. Systematic analyses of all structural-hydrothermal events at the Wiluna lode-gold deposits show that widespread hydrothermal alteration associated with Stage I gold-arsenopyrite-pyrite and Stage II gold-stibnite mineralization is actually followed by silica-only fluid flow along the major principal displacement faults. This fluid is characterized by low temperature (180°C) aqueous inclusions of medium salinity (5 to 15 wt percent NaCl equiv) and light $\delta^{18}O_{fluid}$ values (-4 to +2 ‰), thus indicating influx of substantial amount of surface waters.

The influx of surface waters might have promoted the precipitation of quartz, and thus indirectly sealed the fault system. Late-stage hydrothermal activity along fault systems has also been reported by Gebre-Mariam et al. (1997) at the Racetrack and Golden Kilometre deposits. Further studies on outflow zones and regional or local seals may allow recognition of mappable criteria to determine if such zones are present in other terranes.

Acknowledgments

Many of the concepts developed here arose from extensive interaction and discussions over the past 10 years with the research staff and students at the Centre for Global Metallogeny (formerly Key Centre for Strategic Mineral Deposits) at the University of Western Australia (in particular David Groves, Steffen Hagemann, John Ridley, Neal McNaughton, Mark Barley, Edward Mikucki), as well as Rob Kerrich (Univ. Saskatchewan), Rich Goldfarb (USGS), Cam McCuaig (SRK International), David Huston (AGSO), Roger Bateman (KCGM), John Hronsky (WMC Resources), Wally Witt (Sons of Gwalia) and Joe Knight (BHP Exploration).

References

Abraham, A.P.G., and Spooner E.T.C., 1995, Late Archaean regional deformation and structural controls on gold-quartz vein mineralization in the northwestern Slave Province, NWT: Canadian Journal of Earth Sciences, v.32, p.1132-1154.

Allen, N., 1998, Factors controlling the distribution of gold mineralisation in the Three Mile Hill gabbro, Coolgardie, Western Australia: Unpublished B.Sc.Hons. thesis, University of Western Australia, 121p.

Barley, M.E., and Groves, D.I., 1987, Hydrothermal alteration of Archaean supracrustal sequences in the central Norseman-Wiluna Belt, Western Australia: a brief review, *in* Ho, S.E., and Groves, D.I., eds., Recent Advances in Understanding Precambrian Gold Deposits: Geology Department and University Extension, The University of Western Australia, Publication 11, p.51-66.

Barley, M.E., and Groves, D.I., 1989, Exploration significance of regional and local scale hydrothermal alteration patterns in greenstone belts: Minerals and Energy Research Institute of Western Australia, Report 65, 83p.

Barley, M.E., and Groves, D.I., 1992, Supercontinent cycles and the distribution of metal deposits through time: Geology, v.20, p.291-294.

Barley, M.E., Eisenlohr, B., Groves, D.I., Perring, C.S., and Vearncombe, J.R., 1989, Late Archaean convergent margin tectonics and gold mineralization: a new look at the Norseman-Wiluna Belt: Geology, v.17, p.826-829.

Barley, M.E., Krapez, B., Groves, D.I., and Kerrich, R., 1998, The Late Archean bonanza: metallogenic and environmental consequences of the interaction between mantle plumes, lithospheric tectonics and global cyclicity: Precambrian Research, v.91, p.65-90.

Barnicoat, A.C., Fare, R.J., Groves, D.I., and McNaughton, N.J., 1991, Synmetamorphic lode-gold deposits in high-grade Archean settings: Geology, v.19, p.921-924.

Barton, P.B., Jr., 1993, Problems and opportunities for mineral deposit models, *in* Kirkham, R.V., Sinclair, W.D., Thorpe, R.I., and Duke, J.M., eds., Mineral Deposit Modelling: Geological Association of Canada, Special Paper 40, p.7-13.

Bartram, G.D., and McCall, G.J.H., 1971, Wall-rock alteration associated with auriferous lodes in the Golden Mile, Kalgoorlie, *in* Glover, J.E., ed., Symposium on Archaean Rocks: Geological Society of Australia, Special Publication 3, p.191-199.

Bastrakov, E.N., Cassidy, K.F., Shvarov, Y.V., 2000, Gold transport at Archaean lode gold deposits: gold solubility along the rock-buffered pathways: Geological Society of Australia, Abstracts, v.XX, p.XXX.

Benning, L.G., and Seward, T.M., 1996, Hydrosulphide complexing of gold(I) in hydrothermal solutions from 150 to 500°C and 500 to 1500 bars: Geochimica et Cosmochimica Acta, v.60, p.1849-1871.

Bickle, M.J., Morant, P., Bettenay, L.F., Boulter, C.A., Blake, T.S., and Groves, D.I., 1985, Archean tectonics of the Shaw Batholith, Pilbara Block Western Australia: Structural and metamorphic tests of the batholith concept: Geological Association of Canada Special Paper, 28, p.325-341.

Blewett, R., and Huston, D.L., 1999, Deformation and gold mineralisation of the Archaean Pilbara Craton, Western Australia: AGSO Research Newsletter No. 30, p.12-15.

Bloem, E.J.M., McNaughton, N.J., Groves, D.I., and Ridley, J.R., 1995, An indirect lead isotope age determination of gold mineralisation at the Corinthia Mine, Yilgarn Block, Western Australia: Australian Journal of Earth Sciences, v.42, p.447-451.

Boullier, A-.M., and Robert, F., 1992, Palaeoseismic events recorded in Archaean gold-quartz vein networks, Val d'Or, Abitibi, Quebec, Canada: Journal of Structural Geology, v.14, p.161-179.

Boullier, A-.M., Firdaous, K., and Robert, F., 1998, On the Significance of aqueous fluid inclusions in gold-bearing quartz vein deposits from the southeastern Abitibi Subprovince (Quebec, Canada): Economic Geology, v.93, p.216-223.

Bucci, L et al., 2000

Burrows, D.R., and Spooner, E.T.C., 1986, The McIntyre Cu-Au deposit, Timmins, Ontario, Canada, *in* Macdonald, A.J., Proceedings of Gold '86, an International Symposium on the Geology of Gold Deposits: Toronto, p.23-39.

Burrows, D.R., and Spooner, E.T.C., 1989, Relationships between Archean gold quartz vein-shear zone mineralization and igneous intrusions in the Val d'Or and Timmins areas, Abitibi Subprovince, Canada, *in* Keays, R.R., Ramsay, W.R.H., and Groves, D.I., eds., The Geology of Gold Deposits: The Perspective in 1988: Economic Geology, monograph 6, p.424-444.

Callan, N.J., and Spooner, E.T.C., 1998, Repetitive hydraulic fracturing and shear zone inflation in an Archean granitoid-hosted, ribbon banded, Au-quartz vein system, Renabie area, Ontario, Canada: Ore Geology Reviews, v.12, p.237-266.

Cameron, E.M., 1988, Archean gold: relation to granulite formation and redox zoning in the crust: Geology, v.16, p.109-112.

Cameron, E.M., and Hattori, K., 1987, Archean gold mineralization and oxidized hydrothermal fluids: Economic Geology, v.82, p.1177-1191.

Card, K.D., 1990, A review of the superior Province of the Canadian Shield: a product of Archean accretion: Precambrian Research: v.48, p.99-156.

Card, K.D., Poulsen, K.H., and Robert, F., 1989, The Archean Superior Province and its lode gold deposits, *in* Keays, R.R., Ramsay, W.R.H., and Groves, D.I., eds., The Geology of Gold Deposits: The Perspective in 1988: Economic Geology, Monograph 6, p.19-36.

Cassidy, K.F., 1992, Archaean granitoid-hosted gold deposits in greenschist to amphibolite facies terrains: A high P-T to low P-T depositional continuum equivalent to greenstone-hosted deposits. Unpublished Ph.D. thesis, University of Western Australia, 296p.

Cassidy, K.F., and Bennett, J.M., 1993, Gold mineralisation at the Lady Bountiful Mine, Western Australia: An example of a granitoid-hosted Archaean lode gold deposit: Mineralium Deposita, v.28, p.388-408.

Cassidy, K.F., and Hagemann, S.G., 1999, Archean high-P-T, granitoid-hosted gold mineralisation at Westonia, Western Australia: I. Evidence for syn-peak metamorphic mineralisation in a high-grade terrain, *in* Stanley, C.J., et al., eds, Mineral Deposits: Processes to Processing: Rotterdam, A.A. Balkema, p.1013-1016.

Cassidy, K.F., Groves, D.I., and McNaughton, N.J., 1998, Late-Archean granitoid-hosted lode-gold deposits, Yilgarn Craton, Western Australia: Deposit characteristics, crustal architecture and implications for ore genesis: Ore Geology Reviews, v.13, p.65-102.

Channer, D.M.DeR., and Spooner, E.T.C., 1994, Geochemistry of late (1.1Ga) fluid inclusions in rocks of the Kapuskasing Archean granite pegmatite and gold-quartz vein fluids: Geochimica et Cosmochimica Acta, 58, p.1101-1118.

Channer, D.M.DeR., Bray, C.J., and Spooner, E.T.C., 1999, Integrated cation-anion/volatile fluid inclusion analysis by gas and ion chromatography; methodology and examples: Chemical Geology, v.154, p.59-82.

Clark, M.E., 1980, Localisation of gold, Mt Charlotte, Kalgoorlie, Western Australia. Unpublished B.Sc. Hons thesis, University of Western Australia.

Clark, M.E., Archibald, N.J., and Hodgson, C.J., 1986, The structural and metamorphic setting of the Victory Gold Mine, Kambalda, Western Australia, *in* Macdonald, A.J., eds, Proceedings of Gold '86, An International Symposium on the Geology of Gold: Toronto, p.243-254.

Clark, M.E., Carmichael, D.M., Hodgson, C.J., and Fu, M., 1989, Wall-rock alteration, Victory gold mine, Kambalda, Western Australia: Processes and P-T-XCO2 conditions of metasomatism, *in* Keays, R.R., Ramsay, W.R.H., and Groves, D.I., eds., The Geology of Gold Deposits: The Perspective in 1988: Economic Geology, Monograph 6, p.445-459.

Clout, J.M.F., 1989, Structural and isotopic studies of the golden mile gold-telluride deposit, Kalgoorlie, Western Australia. Unpublished PhD thesis, Monash University, Clayton, Victoria, 352p.

Clout, J.M.F., Cleghorn, J.H., and Eaton, P.C., 1990. Geology of the Kalgoorlie gold field, *in* Hughes, F.E., ed., Geology of the Mineral Deposits of Australia and Papua New Guinea: Melbourne, Australasian Institute of Mining and Metallurgy, Monograph 14, p.411-431.

Colvine, A.C., 1989, An empirical model for the formation of Archean gold deposits: products of final cratonization of the Superior Province, Canada, *in* Keays, R.R., Ramsay, W.R.H., and Groves, D.I., eds., The Geology of Gold Deposits: The Perspective in 1988: Economic Geology, Monograph 6, p.37-53.

Colvine, A.C., Fyon, J.A., Heather, K.B., Marmont, S., Smith, P.M., and Troop, D.G., 1988, Archean lode gold deposits in Ontario: Ontario Geological Survey, Miscellaneous Paper 139, 136p.

Cox, S.F., 1999, Deformational controls on the dynamics of fluid flow in mesothermal gold systems, *in* McCaffrey, K.J.W., Lonergan, L., and Wilkinson, J.J., eds., Fractures, Fluid Flow and Mineralization: Geological Society, London, Special Publication 155, p.123-140.

Dalstra, H.J., Bloem, E.J.M., and Ridley, J.R., 1997, Gold in amphibolite facies terrains and its relationship to metamorphism, exemplified by syn-peak metamorphic gold in the Transvaal deposit, Yilgarn Block, Western Australia: Chronique de la Recherche Miniere, No.529, p.3-24.

de Boorder, H., Spakman, W., White, S.H., and Wortel, M.J.R., 1998, Late Cenozoic mineralization, orogenic collapse and slab detachment in the European Alpine belt: Earth and Planetary Science Letters, v.164, p.569-575.

de Ronde, C.E.J., Spooner, E.T.C., de Wit, M.J., Bray, C.J., 1992, Shear zone-related, Au quartz veins deposits in the Barberton greenstone belt, South Africa: field and petrographic characteristics, fluid properties, and light stable isotope geochemistry: Economic Geology, v.87, p.366-402.

Dowling, K, and Morrison, G., 1989, Application of quartz textures to the classification of gold deposits using North Queensland examples, *in* Keays, R.R., Ramsay, W.R.H., and Groves, D.I., eds., The Geology of Gold Deposits: The Perspective in 1988: Economic Geology, Monograph 6, p.342-355.

Drummond, B.J., and Goleby, B.R., 1993, Seismic reflection images of the major ore-controlling structures in the Eastern Goldfields Province, Western Australia: Exploration Geophysics, v.24, p.473-478.

Dube, B., Guha, J., and Rocheleau, M., 1987, Alteration patterns related to gold mineralization and their relation to CO_2/H_2O ratios: Mineralogy and Petrology, v.37, p.267-291.

Dugdale, A.L., and Hagemann, S.G., in press, The Bronzewing lode-gold deposit, Western Australia: P-T-X evidence for fluid immiscibility caused by cyclic decompression in gold-bearing quartz-veins: Chemical Geology.

Duuring, P., and Hagemann, S.G., in press, A thrust-ramp model for gold mineralisation at the Archaean trondhjemite-hosted Tarmoola Deposit, Leonora Camp, Western Australia: Geological Society of Australia, Abstracts.

Eisenlohr, B.N., Groves, D.I., and Partington, G.A., 1989, Crustal-scale shear zones and their significance to Archaean gold mineralization in Western Australia: Mineralium Deposita, v.24, p.1-8.

Etheridge, M.A., Wall, V.J., and Vernon, R.H., 1983, The role of the fluid phase during regional metamorphism and deformation: Journal of Metamorphic Geology, v.1, p.205-226.

Frei, R., Naegler, T.F., Schoenberg, R., and Kramers, J.D., 1998, Re-Os, Sm-Nd, U-Pb, and stepwise lead leaching isotope systematics in shear-zone hosted gold mineralization: genetic tracing and age constraints of hydrothermal activity: Geochimica et Cosmochimica Acta, v.62, p.1925-1936.

Fyon, J.A., Troop, D.G., Marmont, S., and Macdonald, A.J., 1989, Introduction of gold into Archean crust, Superior Province, Ontario - coupling between mantle-initiated magmatism and lower crustal thermal maturation, *in* Keays, R.R., Ramsay, W.R.H., and Groves, D.I., eds., The Geology of Gold Deposits: The Perspective in 1988: Economic Geology, Monograph 6, p479-490.

Gebre-Mariam, M., Groves, D.I., and McNaughton, N.J., 1997, Aqueous and CO_2- and CH_4- rich inclusions at the Archean Golden Kilometre gold deposit: multiple fluid sources and depositional mechanisms: Chronicle of Mineral Research and Exploration, v.529, p.59-73.

Ghaderi, M., Campbell, I.H., McCulloch, M.T., Bennett, V.C., and Mortimer, G.E., 1996, The use of Nd-Sr isotopic tracing in the study of Archaean gold deposits in the Norseman-Kambalda area, Western Australia: Geological Society of Australia, Abstracts, v.41, p.156.

Gibert, F., Pacsal, M.L., and Pichavant, M., 1998, Gold solubility and speciation in hydrothermal solutions: Experimental study of the stability of hydrosulphide complex of gold ($AuHS^{\circ}$) at 350 to 450°C and 500 bars: Geochimica et Cosmochimica Acta, v.62, p.2931-2947.

Goldfarb, R.J., Snee, L.W., Miller, M.L., and Newberry, R.J., 1991, Rapid dewatering of the crust deduced from ages of mesothermal gold deposits: Nature, v.354, p.296-298.

Goldfarb, R.J., Phillips, G.N., and Nokleberg, W.J., 1998, Tectonic setting of synorogenic gold deposits of the Pacific Rim: Ore Geology Reviews, v.13, p.185-218.

Golding, S.D, Groves, D.I., McNaughton, N.J., Barley, M.E., and Rock, N.M.S., 1987, Carbon isotopic composition of carbonates from contrasting alteration styles in supracrustal rocks of the Norseman-Wiluna Belt, Yilgarn Block, Western Australia: their significance to the source of Archaean auriferous fluids, *in* Ho, S.E., and Groves, D.I., eds., Recent Advances in Understanding Precambrian Gold Deposits: Geology Department and University Extension, The University of Western Australia, Publication 11, p.215-238.

Golding, S.D., McNaughton, N.J., Barley, M.E., Groves, D.I., Ho, S.E., Rock, N.M.S., and Turner, J.V., 1989, Archean carbon and oxygen reservoirs: their significance for fluid sources and circulation paths for

Archean mesothermal gold deposits of the Norseman-Wiluna belt, Western Australia, *in* Keays, R.R., Ramsay, W.R.H., Groves, D.I., eds., The Geology of Gold Deposits: The Perspective in 1988: Economic Geology, Monograph 6, p.376-388.

Golding, S.D., Barley, M.E., Cassidy, K.F., Groves, D.I., Ho, S.E., Hronsky, J.M.A., McNaughton, N.J., Sang, J.H., and Turner, J.V., 1990a, Constraints on genesis of primary gold deposits, *in* Ho, S.E., Groves, D.I., and Bennett, J.M., eds., Gold deposits of the Archaean Yilgarn Block, Western Australia: nature, genesis and exploration guides: Geology Department (Key Centre) and University Extension, The University of Western Australia, Publication No. 20, p.252-258.

Golding, S.D., Groves, D.I., McNaughton, N.J., Mikucki, E.J., and Sang, J.H., 1990b, Constraints on genesis of primary gold deposits, *in* Ho, S.E., Groves, D.I., and Bennett, J.M., eds., Gold deposits of the Archaean Yilgarn Block, Western Australia: nature, genesis and exploration guides: Geology Department (Key Centre) and University Extension, The University of Western Australia, Publication No. 20, p.259-262.

Goleby, B.R., Drummond, B.J., Owen, A., Yeates, A.N., Jackson, J., Swager, C., and Upton, P., 1997, Structurally controlled mineralization in Australia – How seismic profiling helps find minerals: Recent case histories, *in* Gubins, A.G., ed., Proceedings of Exploration '97: Fourth Decennial International Conference on Mineral Exploration: GEO F/X, Toronto, p.409-420.

Groves, D.I., 1990, Excursion No. 3: Eastern Goldfields mineral deposits. 1: Overview of gold mineralization in the Norseman-Wiluna Belt, *in* Ho, S.E., Glover, J.E., Myers, J.S., and Muhling, J.R., eds., Third International Archaean Symposium Excursion Guidebook: Geology Department and University Extension, University of Western Australia, Perth, Publication 21, p.307-317.

Groves, D.I., 1993, The crustal continuum model for late-Archaean lode-gold deposits of the Yilgarn Block, Western Australia: Mineralium Deposita, v.28, p.366-374.

Groves, D.I., Barley, M.E., and Ho, S.E., 1989, Nature, genesis, and tectonic setting of mesothermal gold mineralization in the Yilgarn Block, Western Australia, *in* Keays, R.R., Ramsay, W.R.H., and Groves, D.I., eds., The Geology of Gold Deposits: The Perspective in 1988: Economic Geology, Monograph 6, p.71-85.

Groves, D.I., Barnicoat, A.C., Cassidy, K.F., Fare, R.J., Hagemann, S.G., Ho, S.E., Hronsky, J.M.A., McNaughton, N.J., Perring, C.S., Ridley, J.R., and Vearncombe, J.R., 1992, Sub-greenschist to granulite-hosted Archaean lode-gold deposits of the Yilgarn Craton: a depositional continuum from deep-sourced hydrothermal fluids in crustal-scale plumbing systems, *in* Glover, J.E., and Ho, S.E., eds., The Archaean: Terranes, Processes and Metallogeny: Geology Department (Key Centre) & University Extension, The University of Western Australia, Publication 22, p.325-337.

Groves, D.I., Ridley, J.R., Bloem, E.M.J., Gebre-Mariam, M., Hagemann, S.G., Hronsky, J.M.A., Knight, J.T., McNaughton, N.J., Ojala, J., Vielreicher, R.M., McCuaig, T.C., and Holyland, P.W., 1995, Lode-gold deposits of the Yilgarn block: products of Late Archaean crustal-scale overpressured hydrothermal systems, *in* Coward, M.P., and Ries, A.C., eds., Early Precambrian Processes: Geological Society Special Publication, No. 95, p.155-172.

Groves, D.I., Goldfarb, R.J., Gebre-Mariam, M., Hagemann, S.G., and Robert, F., 1998, Orogenic gold deposits: a proposed classification in the context of their crustal distribution and relationship to other gold deposit types: Ore Geology Reviews, v.13, p.7-27.

Groves, D.I., Goldfarb, R.J., Knox-Robinson, C.M, Ojala, J., Gardoll, S., Yun, G., and Holyland, P., 2000, Late-kinematic timing of orogenic gold deposits and significance for computer-based exploration techniques with emphasis on the Yilgarn Block, Western Australia, 53p.

Guha, J., and Kanwar, R., 1987, Vug brines-fluid inclusions: A key to understanding of secondary gold enrichment processes and the evolution of deep brines in the Canadian Shield, *in* Fritz, P., and Frape, S.K., eds., Saline Water and Gases in the Crystalline Rocks: Geological Association of Canada Special Paper, 33, p.95-101.

Guha, J., Archambault, G., and Leroy, J., 1983, A correlation between the evolution of mineralizing fluids and the geomechanical development of a shear zone as illustrated by the Henderson 2 mine, Quebec: Economic Geology, v.78, p.1605-1618.

Guha, J., Lu, H.-Z., Dube, B., Robert, F., and Gagnon, M., 1991, Fluid characteristics of vein and altered wallrock in Archean mesothermal gold deposits: Economic Geology, v.86, p.667-684.

Hagemann, S.G., and Brown, P.E., 1996, Geobarometry in Archean lode-gold deposits: European Journal of Mineralogy., v.8, p.937-960.

Hagemann, S.G., and Cassidy, K.F., 1999, Archean high-P-T, granitoid-hosted gold mineralisation at Westonia, Western Australia: II. P-T-X constraints on a gold-bearing paleohydrothermal system in a high-grade terrain, *in* Stanley, C.J., et al., eds, Mineral Deposits: Processes to Processing: Rotterdam, A.A. Balkema, p.1021-1024.

Hagemann, S.G., Groves, D.I., Ridley, J.R., and Vearncombe, J.R., 1992, The Archaean lode gold deposits at Wiluna, Western Australia: high-level brittle-style mineralization in a strike-slip regime: Economic Geology, v.87, p.1022-1053.

Hagemann, S.G., Groves, D.I., Ridley, J.R., 1993, The Wiluna lode-gold deposits, Western Australia: an example of a high crustal-level Archaean lode-gold system, *in* Fenoll Hach-Ali, P., Torres-Ruiz, J., and

Gervilla, F., eds., Current Research in Geology Applied to Ore Deposits: University of Granada, Spain, p.469-472.

Hagemann, S.G., Gebre-Mariam, M., and Groves, D.I., 1994, Surface-water influx in shallow-level Archaean lode-gold deposits in Western Australia: Geology, v.22, p.1067-1070.

Hagemann, S.G., Bray, C., Brown, P.E., and Spooner, E.T.C., 1996, Combined gas and ion chromatography of fluid inclusions and sulfides from the Archean epizonal Wiluna lode-gold deposits, Western Australia, *in* Brown, P.E., and Hagemann, S.G., eds., Pan-American Conference on Research on Fluid Inclusions 6: Program and Abstracts: Department of Geology and Geophysics, University of Wisconsin-Madison, Wisconsin, U.S.A., p.56-58.

Hagemann, S.G., Brown, P.E., Ridley, J., Stern, P., and Fournelle, J., 1998, Ore petrology, chemistry and timing of electrum in the Archean hypozonal Transvaal lode gold deposit, Western Australia: Economic Geology, v.93, p.271-291.

Hagemann, S.G., Bateman, R., and Vielreicher, R., 1999, In situ sulfur isotope composition of pyrites from the Fimiston- and Oroya- style gold lodes in the Golden Mile Camp, Kalgoorlie: implications for sulfur source(s) and depositional processes: Geological Society of America, Abstracts with Programs, v.31, no.7, p.A-32.

Hagemann, S.G., Ridley, J.R., Mikucki, E.J., and Groves, D.I., in revision, The Wiluna lode-gold deposits, Western Australia: hydrothermal alteration and mineralization in an Archean epizonal Au-As-Sb deposit. Economic Geology.

Hall, D.L., and Bodnar, R.J., 1990, Methane in fluid inclusions from granulites: a product from hydrogen diffusion?: Geochimica Cosmochimica Acta, v.54, p.641-651.

Hall, G., 1998, Autochthonous model for gold metallogenesis and exploration in the Yilgarn, *in* Wood, S.E., ed., Geodynamics & Gold Exploration in the Yilgarn, Workshop Abstracts. Australian Geodynamics Cooperative Research Centre, Western Australia, p.32-35.

Hamilton, W.B., 1998, Archean magmatism and deformation were not products of plate tectonics: Precambrian Research, v.91, p.143-179.

Ho, S.E., 1987, Fluid inclusions: their potential as an exploration tool for Archaean gold deposits, *in* Ho, S.E., and Groves, D.I., eds., Recent Advances in Understanding Precambrian Gold Deposits: Geology Department and University Extension, University of Western Australia, Publication 11, p.239-263.

Ho, S.E., Bennett, J.M., Cassidy, K.F., Hronsky, J.M.A., Mikucki, E.J., and Sang, J.H., 1990a, Nature of ore fluid, and transportational and depositional conditions in sub-amphibolite facies deposits, *in* Ho, S.E., Groves, D.I., and Bennett, J.M., eds., Gold Deposits of the Archaean Yilgarn Block, Western Australia: Nature, Genesis and Exploration Guides: Geology Department (Key Centre) and University Extension, The University of Western Australia, Publication No. 20, p.198-211.

Ho, S.E., Groves, D.I., and Bennett, J.M., eds., 1990b, Gold deposits of the Archaean Yilgarn Block, Western Australia: nature, genesis and exploration guides: Geology Department (Key Centre) and University Extension, The University of Western Australia, Publication No. 20, 407p.

Ho, S.E., Bennett, J.M., Cassidy, K.F., and Hronsky, J.M.A., 1990c, Assessment of mineralized zones and exploration guides: Fluid inclusion surveys, *in* Ho, S.E., Groves, D.I., and Bennett, J.M., eds., Gold Deposits of the Archaean Yilgarn Block, Western Australia: Nature, Genesis and Exploration Guides: Geology Department (Key Centre) and University Extension, The University of Western Australia, Publication No. 20, p.328-330.

Ho, S.E., Groves, D.I., McNaughton, N.J., and Mikucki, E.J., 1992, The source of ore fluids and solutes in Archean lode gold deposits of Western Australia: Journal of Volcanology and Geothermal Research, v.50, p.173-196.

Hodgson, C.J., 1989, The structure of shear-related, vein-type gold deposits: A review: Ore Geology Reviews, v.4, p.231-273.

Hodgson, C.J., 1990, An overview of the geological characteristics of gold deposits in the Abitibi Subprovince, *in* Ho, S.E., Robert, F., and Groves, D.I., eds., Gold and Base Metal Mineralization in the Abitibi Subprovince, Canada, with Emphasis on the Quebec Segment: Geology Department and University Extension, University of Western Australia, Perth, Publication 24, p.63-100.

Hodgson, C.J., 1993, Mesothermal lode-gold deposits, *in* Kirkham, R.V., Sinclair, W.D., Thorpe, R.I., and Duke, J.M., eds., Mineral Deposit Modelling: Geological Association of Canada, Special Paper 40, p.635-678.

Hodgson, C.J., and Hamilton, J.V., 1989, Gold mineralization in the Abitibi greenstone belt: end-stage results of Archean collisional tectonics? *in* Keays, R.R., Ramsay, W.R.H., and Groves, D.I., eds., The Geology of Gold Deposits: The Perspective in 1988: Economic Geology, Monograph 6, p.86-100.

Hodgson, C.J., and Troop, D.G., 1988, A new computer-aided methodology for area selection in gold exploration: A case study from the Abitibi greenstone belt: Economic Geology, v.83, p.952-977.

Holyland, P.W., 1990, Simulation of the dynamics of Archaean deformation in the Yilgarn Block, Western Australia, *in* Glover, J.E., and Ho, S.E., eds., Third International Archaean Symposium, Perth, Abstracts: Geoconferences (W.A.) Inc. Perth, p.347-349.

Holyland, P.W., and Ojala, V.J., 1997, Computer-aided structural targeting in mineral exploration: two- and three-dimensional stress mapping: Australian Journal of Earth Sciences, v.44, p.421-432.

Holyland, P., Ridley, J.R., and Vearncombe, J.R., 1993, Stress mapping technology, *in* Parnell, J., Ruffel, A.H., and Moles, N.R., eds., Geofluids '93: Contributions to an International Conference on Fluid Evolution, Migration and Interaction in Rocks, Torquay, England, Abstracts: Geological Society of London, p.272-275.

Hronsky, J.M.A., 1993, The role of physical and chemical processes in the formation of gold-ore shoots at the Lancefield gold deposit, Western Australia: Unpublished Ph.D. thesis, University of Western Australia, 205p.

Hronsky, J.M.A., Cassidy, K.F., Grigson, M.W., Groves, D.I., Hagemann, S.G., Mueller, A.G., Ridley, J.R., Skwarnecki, M.S., and Vearncombe, J.R., 1990, Deposit and mine-scale structure, *in* Ho, S.E., Groves, D.I., and Bennett, J.M., ed., Gold Deposits of the Archaean Yilgarn Block, Western Australia: Nature, Genesis and Exploration Guides: Geology Department and University Extension, University of Western Australia, Publication 20, p.38-54.

Huston, D.L., 1997, Archaean volcanogenic massive sulphide deposits: review and critical controls: *in* Cassidy, K.F., Whitaker, A.J., and Liu, S.F., eds., An International Conference on Crustal Evolution, Metallogeny and Exploration of the Yilgarn Craton – An Update. Extended Abstracts: Australian Geological Survey Organisation, Record 1997/41, p.77-82.

Huston, D.L., 2000,

Isachsen, C.E., and Bowring, S.A., 1994, Evolution of the Slave Craton: Geology, v.22, p.917-920.

Jayananda, M., Moyen, J.-F., Martin, H., Peucat, J.-J., Auvray, B., and Mahabaleswar, B., 2000, Late Archaean (2550-2520 Ma) juvenile magmatism in the Eastern Dharwar Craton, southern India: constraints from geochronology, Nd-Sr isotopes and whole rock geochemistry: Precambrian Research, v.99, p.225-254.

Jia, Y., and Kerrich, R., 1999, Nitrogen isotope systematics of mesothermal lode gold deposits: Metamorphic, granitic, meteoric water, or mantle origin: Geology, v.27, p.1051-1054.

Kamineni, D.C., Stone,D., and Peterman, Z.E., 1990, Early Proterozoic deformation in the western Superior Province, Canadian Shield: Geological Society of America Bulletin, v.102, p.1623-1634.

Kent, A.J.R., 1994, Geochronological constraints on the timing of Archean gold mineralisation in the Yilgarn Craton. Unpublished Ph.D. thesis, Canberra, Australian National University, 268p.

Kent, A.J.R., and Hagemann, S.G., 1996, Constraints on the timing of gold mineralisation in the Wiluna Greenstone Belt, Yilgarn Craton, Western Australia: Australian Journal of Earth Sciences, v.43, p.573-588.

Kent, A.J.R., and McCuaig, T.C., 1997, Disturbed ^{40}Ar-^{39}Ar systematics in hydrothermal biotite and hornblende at the Scotia gold mine, Western Australia: Evidence for argon loss associated with post-mineralization fluid movement: Geochimica et Cosmochimica Acta, v.61, p.4655-4669.

Kent, A.J.R., and McDougall, I., 1995, ^{40}Ar -^{39}Ar and U-Pb age constraints on the timing of gold mineralization in the Kalgoorlie gold field, Western Australia: Economic Geology, v.90, p.845-859.

Kent, A.J.R., Campbell, I.H., and McCulloch, M.T., 1995, Sm-Nd systematics of hydrothermal scheelite from the Mount Charlotte mine, Kalgoorlie, Western Australia. An isotopic link between gold mineralization and komatiites: Economic Geology, v.60, p.2329-2335.

Kent, A.J.R., Cassidy, K.F., and Fanning, C.M., 1996, Archean gold mineralization synchronous with the final stages of cratonization, Yilgarn Craton: Geology, v.24, p.879-882.

Keppie, J.D., and Dallmeyer, R.D., 1995, Late Paleozoic collision, delamination, short-lived magmatism and rapid denudation in the Meguma Terrane (Nova Scotia, Canada): constraints from ^{40}Ar -^{39}Ar isotopic data: Canadian Journal of Earth Sciences, v.32, p.644-659.

Kerrich, R., 1987, The stable isotope geochemistry of Au-Ag vein deposits in metamorphic rocks, *in* Kyser, T.K., ed., Mineralogical Association of Canada, Short Course 13, p.287-336.

Kerrich, R., 1989a, Geodynamic setting and hydraulic regimes: shear zone hosted mesothermal gold deposits, *in* Bursnall, J.T., ed., Mineralization and Shear Zones: Geological Association of Canada, Short Course Notes 6, p.89-128.

Kerrich, R., 1989b, Geochemical evidence on the sources of fluids and solutes for shear zone hosted mesothermal Au deposits, *in* Bursnall, J.T., ed., Mineralization and Shear Zones: Geological Association of Canada, Short Course Notes, 6, p.129-197.

Kerrich, R., 1990, Carbon-isotope systematics of Archean Au-Ag vein deposits in the Superior Province: Canadian Journal of Earth Sciences, v.27, p.40-56.

Kerrich, R., and Cassidy, K.F., 1994, Temporal relationships of lode gold mineralization to accretion, magmatism, metamorphism and deformation – Archean to present: A review: Ore Geology Reviews, v.9, p.263-310.

Kerrich, R., and Fryer, B.J., 1979, Archaean precious metal hydrothermal systems, Dome mine, Abitibi greenstone belt. II. REE and oxygen isotope relations: Canadian Journal of Earth Sciences, v.16, p.440-458.

Kerrich, R., and Fyfe, W.S., 1981, The gold-carbonate association: source of CO2 and CO2 fixation reactions in Archean lode gold deposits: Chemical Geology, v.33, p.265-294.

Kerrich, R., and Wyman, D., 1990, The geodynamic setting of mesothermal gold deposits: an association with accretionary tectonic regimes: Geology, v.18, p.882-885.

Kerrich, R., Fryer, B.J., King, R.W., Willmore, L.M., and van Hees, E., 1987, Crustal outgassing and LILE enrichment in major lithosphere structures, Archean Abitibi greenstone belt: Evidence on the source reservoir from strontium and carbon isotope tracers: Contributions to Mineralogy and Petrology, v.97, p.156-168.

Kerrich, R., Goldfarb, R., Groves, D.I. and Garwin, S., 2000, The geodynamics of world-class gold deposits: Characteristics, space-time distribution, and origins: Reviews in Economic Geology, vol. 13, p. 501-551.

Kishida, A., and Kerrich, R., 1987, Hydrothermal alteration zoning and gold concentration tat the Kerr-Addison Archean lode gold deposit, Kirkland Lake, Ontario: Economic Geology, v.82, p.649-660.

Knight, J.T., 1994, The geology and genesis of Archaean amphibolite-facies lode-gold deposits in the Coolgardie Goldfield, Western Australia, with special emphasis on the role of granitoids: Unpublished Ph.D. thesis, University of Western Australia, 205p.

Knight, J.T., Groves, D.I., and Ridley, J.R., 1993, The Coolgardie goldfield, Western Australia: District-scale controls on an Archaean gold camp in an amphibolite facies terrane: Mineralium Deposita, v.28, 436-456.

Knight, J.T., Ridley, J.R., Groves, D.I., and McCall, C., 1996, Syn-peak metamorphic gold mineralization in the amphibolite-facies, gabbro-hosted Three Mile Hill deposit, Coolgardie Goldfield, Western Australia: a high temperature analogue of mesothermal gabbro-hosted gold deposits: Transactions of the Institution of Mining and Metallurgy (London), v.105, p.B175-B199.

Knight, J.T., Ridley, J.R., and Groves, D.I., 2000, The Archean amphibolite facies Coolgardie goldfield, Yilgarn Craton, Western Australia: Nature, controls, and gold field-scale patterns of hydrothermal wall-rock alteration: Economic Geology, v.95, p.49-84.

Krogstad, E.J., Balakrishnan, S., Mukhopadhyay, D.K., Rajamani, V., and Hanson, G.N., 1989, Plate tectonics at 2.5 billion years ago: Evidence at Kolar, south India: Science, v.243, p.1337-1340.

Lambert, D., Frick, L., Bateman, R., and Stone, W., 1998, Geochemistry and rock-fluid interactions in Archaean lode-gold systems: New insights from the Re-Os isotopic system, *in* Wood, S.E., ed., Geodynamics & Gold Exploration in the Yilgarn, Workshop Abstracts. Australian Geodynamics Cooperative Research Centre, Western Australia, p.40-44.

Loucks, R.R., and Mavrogenes, J.A., 1999, Gold solubility in supercritical hydrothermal brines measured in synthetic fluid inclusions: Science, v.284, p.2159-2163.

Magoon, L.B., and Dow, W.G., 1991, The petroleum system – from source to trap: American Association of Petroleum Geologists, v.75(3), p.627.

Mason, R. and Melnik, N., 1986, The anatomy of an Archean gold system – the McIntyre-Hollinger complex at Timmins, Ontario, Canada, *in* Macdonald, A.J., ed., Proceedings of Gold '86, an International Symposium on the Geology of Gold Deposits: Toronto, p.40-55.

McCuaig, T.C., and Kerrich, R., 1998, P-T-t-deformation-fluid characteristics of lode gold deposits?: evidence from alteration systematics: Ore Geology Reviews, v.12, p.381-453.

McCuaig, T.C., Kerrich, R., Groves, D.I., and Archer, N., 1993, The nature and dimension of regional and local gold-related hydrothermal alteration in tholeiitic metabasalts in the Norseman Goldfields: the missing link in crustal continuum of gold deposits: Mineralium Deposita, v.28, p.420-435.

McNaughton, N.J., Cassidy, K.F., Dahl, N., de Laeter, J.R., Golding, S.D., Groves, D.I., Ho, S.E., Mueller, A.G., Perring, C.S., Sang, J.H., and Turner, J.V., 1992, The source of ore components in lode-gold deposits of the Yilgarn Block, Western Australia, *in* Glover, J.E., and Ho, S.E., eds., The Archaean: Terrains, Processes and Metallogeny: Geological Department (Key Centre) and University Extension, University of Western Australia, Publication 22, p.351-363.

McNaughton, N.J., Groves, D.I., and Witt, W.K., 1993, The source of lead in Archaean lode-gold deposits of the Menzies-Kalgoorlie-Kambalda region, Yilgarn Block, Western Australia: Mineralium Deposita, v.28, p.495-502.

Mernagh, T.P., and Witt, W.K., 1995, Early, methane-rich fluids and their role in Archaean gold mineralisation at the Sand King and Missouri deposits, Eastern Goldfield Province, Western Australia: AGSO Journal of Australian Geology and Geophysics, v.15, p.297-312.

Michibayashi, K., 1995, Two phase syntectonic gold mineralization and barite remobilization within the main ore body of the Golden Giant mine, Hemlo, Ontario, Canada: Ore Geology Reviews, v.10, p31-50.

Mikucki, E.J., 1998, Hydrothermal transport and depositional processes in Archean lode-gold systems: A review: Ore Geology Reviews, v.13, p.307-321.

Mikucki, E.J., and Groves, D.I., 1990, Constraints on genesis of primary gold deposits: Mineralogical constraints, *in* Ho, S.E., Groves, D.I., and Bennett, J.M., eds., Gold Deposits of the Archaean Yilgarn Block, Western Australia: Nature, Genesis and Exploration Guides: Geology Department and University Extension, University of Western Australia, Publication 20, p.212-220.

Mickucki, E.J., and Ridley, J.R., 1993, The hydrothermal fluid of Archaean lode-gold deposits at different metamorphic grades: compositional constraints from ore and wallrock alteration assemblages: Mineralium Deposita, v.28, p.469-481.

Mishra, B., and Panigrahi, M.K., 1999, Fluid evolution in the Kolar Gold Field: evidence from fluid inclusion studies: Mineralium Deposita, v.34, p.173-181.

Mueller, A.G., and Groves, D.I., 1991, The classification of Western Australian greenstone-hosted gold deposits according to wallrock alteration mineral assemblages: Ore Geology Reviews, v.6, p.291-331.

Mueller, A.G., de Laeter, J.R., and Groves, D.I., 1991, Strontium isotope systematics of hydrothermal minerals from epigenetic Archaean gold deposits in the Yilgarn Block, Western Australia: Economic Geology, v.86, p.780-809.

Mueller, A.G., Campbell, I.H., Schiotte, L., Sevigny, J.H., and Layer, P.W., 1996, Constraints on the age of granitoid emplacement, metamorphism, gold mineralisation, and subsequent cooling of the Archean greenstone terrane at Big Bell, Western Australia: Economic Geology, v.91, p.896-915.

Naden, J., and Shepherd, T.J., 1989, Role of methane and carbon dioxide in gold deposition: Nature, v.342, p.793-795.

Napier, R.W., 1993, ^{40}Ar -^{39}Ar geochronology of gold mineralization and Archaean tectonics in the Yilgarn block, Western Australia: *in* Fenoll Hach-Ali, P., Torres-Ruiz, J., and Gervilla, F., eds, Current Research in Geology Applied to Ore Deposits: University of Granada, Spain, p. 187-190.

Napier, R.W., Guise, P.G., and Rex, D.C., 1998, ^{40}Ar -^{39}Ar constraints on the timing and history of amphibolite facies gold mineralisation in the Southern Cross area, Western Australia: Australian Journal of Earth Sciences, v.45, p.285-296.

Neall, F.B., and Phillips, G.N., 1987, Fluid-wall rock interaction in an Archean hydrothermal gold deposit: A thermodynamic model for the Hunt mine, Kambalda: Economic Geology, v.82, p.1679-1694.

Nelson, D.R., 1997, Evolution of the Archaean granite-greenstone terranes of the Eastern Goldfields, Western Australia: SHRIMP U-Pb zircon constraints: Precambrian Research, v.83, p.57-81.

Nesbitt, B.E., 1988, The gold deposit continuum: A genetic model for lode Au mineralization in the continental crust: Geology, v.15, p.1044-1048.

Neumayr, P., 1993, The nature and genesis of Archaean, syn-amphibolite-facies gold mineralization in the Mt. York district, Pilbara Craton, Western Australia: Unpublished Ph.D thesis, University of Western Australia, 172p.

Neumayr, P., and Hagemann, S.G., submitted, Hydrothermal fluid evolution within the transcrustal Cadillac Tectonic Zone, Abitibi greenstone belt, Canada: Relationship and significance to auriferous fluids in adjacent second- and third-order shear zones. Economic Geology.

Neumayr, P., Cabri, L.J., Groves,D.I., Mikucki, E.J., and Jackman, J., 1993, the mineralogical distribution of gold and relative timing of gold mineralization in two Archean settings of high metamorphic grades in Australia: Canadian Mineralogist, v.31, p.711-725.

Neumayr, P., Hagemann, S.G., and Couture, J.-F., in press, Structural setting, textures, and timing of hydrothermal vein systems in the Val d'Or camp, Abitibi, Canada: implications for the evolution of transcrustal, second- and third-order fault zones and gold mineralization. Canadian Journal of Earth Science.

Ojala, V.J., Ridley, J.R., Groves, D.I., and Hall, G.C., 1993, The Granny Smith gold deposit: the role of heterogeneous stress distribution at an irregular granitoid contact in a greenschist facies terrane: Mineralium Deposita, v.28, p.409-419.

Ord, A., Hobbs, B.E., Walshe, J.L., and Zhao, C., 1998, Developments in the simulation of geodynamic processes with direct application to Yilgarn gold mineralization, *in* Wood, S.E., ed., Geodynamics & Gold Exploration in the Yilgarn, Workshop Abstracts. Australian Geodynamics Cooperative Research Centre, Nedlands, Western Australia, p.45-51.

Perring, C.S., and McNaughton, N.J., 1990, Proterozoic remobilization of ore metals within Archaean gold deposits: lead-isotope evidence from Norseman, Western Australia: Australian Journal of Earth Sciences, v.37, p.369-372.

Perring, C.S., Barley,M.E., Cassidy, K.F., Groves, D.I., McNaughton, N.J., Rock, N.M.S., Bettenay, L.F., Golding, S.D., and Hallberg, J.A., 1989, The association of linear orogenic belts, mantle-crustal magmatism, and Archean gold mineralization in the eastern Yilgarn Block of Western Australia, *in* Keays, R.R., Ramsay, W.R.H., and Groves, D.I., eds., The Geology of Gold Deposits: The Perspective in 1988: Economic Geology, Monograph 6, p.571-584.

Phillips, G.N., 1986, Geology and alteration in the Golden Mile, Kalgoorlie: Economic Geology, v81, p.779-808.

Phillips, G.N., and de Nooy, D., 1988, High-grade metamorphic processes which influence Archaean gold deposits, with particular reference to Big Bell, Australia: Journal of Metamorphic Petrology, v.6., p.95-114.

Phillips, G.N., and Groves, D.I., 1983, The nature of Archaean gold-bearing fluids as deduced from gold deposits of Western Australia: Journal of the Geological Society of Australia, v.30, p.25-39,

Phillips & Law, 2000,

Phillips, G.N., and Powell, R., 1993, Link between gold provinces: Economic Geology, v.88, p.1084-1098.

Phillips, G.N., Groves, D.I., Neall, F.B., Donnelly, T.H., and Lambert, I.B., 1986, Anomalous sulfur isotope compositions in the Golden Mile, Kalgoorlie: Economic Geology, v.81, p.2008-2015.

Phillips, G.N., Groves, D.I., and Brown, I.J., 1987, Source requirements for the Golden Mile, Kalgoorlie: significance to the metamorphic replacement model for Archean gold deposits: Canadian Journal of Earth Sciences, v.24, p.1643-1651.

Phillips, G.N., Groves, D.I., and Kerrich, R., 1996, Factors in the formation of the giant Kalgoorlie gold deposit: Ore Geology Reviews, v.10, p.295-317.

Poulsen, K.H., Robert, F., and Dube, B., 2000, Geological classification of Canadian gold deposits: Geological Survey of Canada, Bulletin 540, 106p.

Powell, R., Will, T.M., and Phillips, G.N., 1991, Metamorphism in Archaean greenstone belts: Calculated fluid compositions and implications for gold mineralization: Journal of Metamorphic Geology, v.9, p.141-150.

Powell, W.G., and Pattison, D.R.M., 1997, An exsolution origin for low-temperature sulfides at the Hemlo gold deposit, Ontario, Canada: Economic Geology, v.92, p.569-577.

Qiu, Y., and Groves, D.I., 1999, Late Archean collision and delamination in the southwest Yilgarn Craton: The driving force for Archean orogenic lode gold mineralization?: Economic Geology, v.94, p.115-122.

Qiu, Y., and McNaughton, N.J., 1999, Source of Pb in orogenic lode-gold mineralisation: Pb isotopic constraints from deep crustal rocks from the southwestern Archaean Yilgarn Craton, Australia: Mineralium Deposita, v.34, p.366-381.

Ramos, Z.N.C., Phillips, G.N., and Groves, D.I., 1987, Alteration processes related to gold mineralization in the Golden Mile, Kalgoorlie: a preliminary quantitative study, *in* Ho, S.E., and Groves, D.I., eds., Recent Advances in Understanding Precambrian Gold Deposits: Geology Department and University Extension, The University of Western Australia, Perth, Publication 11, p.161-165.

Ren, S.K., and Heithersay, P.S., 1998, The Kanowna Belle gold deposit and its implications to Archaean gold metallogeny of the Yilgarn Craton, Western Australia, *in* Proceedings of the Ninth Quadrennial IAGOD Symposium, 1994, Beijing: Stuttgart, E Schweizerbart'sche Verlagsbuchhandlung, p.303-318.

Ridley, J.R., 1990, Constraints from alteration assemblages on gold-bearing hydrothermal fluid composition and source, *in* Ho, S.E, Groves, D.I., Bennett, J.M., eds., Gold Deposits of the Archaean Yilgarn Block, Western Australia: Nature, Genesis and Exploration Guides: Geological Department and University Extension, University of Western Australia, Publication 20, p.268-272.

Ridley, J.R., 1993, The relations between mean rock stress fluid flow in the crust: with reference to vein- and lode-style gold deposits: Ore Geology Reviews, v.8, p.23-37.

Ridley, J.R., and Diamond, L.W., 2000, Fluid chemistry of lode-gold deposits, and implications for genetic models. Reviews in Economic Geology, No.13, p.141-162.

Ridley, J.R., and Hagemann, S.G., 1999, Interpretation of post-entrapment fluid-inclusion re-equilibration at the Three Mile Hill, Marvel Lock and Griffins Find high-temperature lode-gold deposits, Yilgarn Craton, Western Australia: Chemical Geology, v.154, p.257-278.

Ridley, J.R., Groves, D.I., and Hagemann, S.G., 1995, Exploration and deposit models for gold deposits in amphibolite/granulite facies terrains: Minerals and Energy Research Institute of Western Australia, Report No.142, 151p.

Ridley, J.R., Mikucki, E.J., and Groves, D.I., 1996, Archean lode-gold deposits: fluid flow and chemical evolution in vertically extensive hydrothermal systems: Ore Geology Reviews, v.10, p.279-293.

Ridley, J.R., Dalstra, H.J., and Bloem, E.J.M., 1997, Metamorphic and structural evolution of amphibolite-facies and lower grade terrains of the Yilgarn Craton, *in* Cassidy, K.F., Whitaker, A.J., and Liu, S.F., eds., An International Conference on Crustal Evolution, Metallogeny and Exploration of the Yilgarn Craton – An Update. Extended Abstracts: Australian Geological Survey Organisation, Record 1997/41, p.77-82.

Ridley, J.R., Groves, D.I., and Knight, J.T., 2000, Gold deposits in amphibolite and granulite facies terranes of the Archean Yilgarn Craton, Western Australia: Evidence and implications of synmetamorphic mineralization: Reviews in Economic Geology, No. 11, p.265-290.

Robert, F., 1990, Structural setting and control of gold-quartz veins of the Val d'Or area, southeastern Abitibi subprovince, *in* Ho, S.E., Robert, F., and Groves, D.I., eds., Gold and Base-Metal Mineralization in the Abitibi Subprovince, Canada, with Emphasis on the Quebec Segment – Short Course Notes: Geology Department (Key Centre) & University Extension, The University of Western Australia, Publication 24, p.167-210.

Robert, F., 1991, Gold metallogeny of greenstone belts: considerations from the eastern Abitibi subprovince, Canada, *in* Ladeira, E.A., ed., Brazil Gold '91: The Economics, Geology, Geochemistry and Genesis of Gold Deposits: Belo Horizonte, Balkema, Rotterdam, p.31-47.

Robert, F., and Brown, A.C., 1986a, Archaean gold-bearing quartz veins at the Sigma mine, Abitibi greenstone belt, Quebec. Part I: geologic relations and formation of the vein system: Economic Geology, v.81, p.578-592.

Robert, F., and Brown, A.C., 1986b, Archaean gold-bearing quartz veins at the Sigma mine, Abitibi greenstone belt, Quebec. Part II: vein paragenesis and hydrothermal alteration: Economic Geology, v.81, p.593-616.

Robert, F., and Kelly, W.C., 1987, Ore-forming fluids in Archean gold-bearing quartz veins at the Sigma Mine, Abitibi greenstone belt, Quebec, Canada: Economic Geology, v.82, p.56-74.

Robert, F., and Poulsen, K.H., 1997, World-class Archaean gold deposits in Canada: an overview: Australian Journal of Earth Sciences, v.44, p.329-351.

Robert, F., Boullier, A.M., and Firdaous, K., 1995, Gold-quartz veins in metamorphic terranes and their bearing on the role of fluids in faulting: Journal of Geophysical Research, v.100, no.B7, p.12861-12879.

Roberts, R.G., 1988, Archean lode-gold deposits, *in* Roberts, R.G., and Sheahan, P.A., eds., Ore Deposit Models: Geoscience Canada, Reprint Series 3, p.1-19.

Rock, N.M.S., Groves, D.I., Perring, C.S., and Golding, S.D., 1989, Gold, lamprophyres, and porphyries: What does their association mean? *in* Keays, R.R., Ramsay, W.R.H., and Groves, D.I., eds., The Geology of Gold Deposits: The Perspective in 1988: Economic Geology, Monograph 6, p.609-625.

Sahimi, M., 1994, Apllications of percolation theory: Taylor and Francis, London.

Santosh, M., 1986, Ore fluids in the auriferous Champion Reef of Kolar, south India: Economic Geology, v.81, p.1546-1552.

Sauve, P., and Makila, A., 1990, Geology of the Camflo Mine, Malartic, Quebec, *in* Rive, M., Verpaelst, P., Gagnon, Y., Lulin, J., Riverin, G., and Simard, A., eds., The North-western Quebec polymetallic belt: a summary of 60 years of mining exploration: Canadian Institute of Mining and Metallurgy, Special Volume 43, p.245-254.

Scantlebury, G.M., 1983, The characteristics and origin of gold lodes in and around the Brownhill syncline, Golden Mile, Kalgoorlie, Western Australia: Unpublished B.Sc.Hons. thesis, University of Western Australia, 103p.

Seward, T.M., 1973, Thio complexes of gold and the transport of gold in hydrothermal ore solutions: Geochimica et Cosmochimica Acta, v.37, p.379-399.

Seward, T.M., 1991, The hydrothermal geochemistry of gold, *in* Foster, R.P., ed., Gold Metallogeny and Exploration. London, Chapman and Hall, p.37-62.

Shenberger, D.M., and Barnes, H.L., 1989, Solubility of gold in aqueous sulfide solutions from 150 to 350°C: Geochimica et Cosmochimica Acta, v.53, p.269-278.

Sibson, R.H., 1981, Fluid flow accompanying faulting: field evidence and models, *in* Simpson, D.W., and Richards, P.G., eds., Earthquake Prediction: An International Review: American Geophysical Union, Maurice Ewing Series, v.4, p.593-603.

Sibson, R.H., 1983, Continental fault structure and the shallow earthquake source: Geological Society of London Journal, v.140, p.741-767.

Sibson, R.H., and Scott, J., 1998, Stress/fault controls on the containment and release of overpressured fluids: examples from gold-quartz vein systems in Juneau, Alaska; Victoria, Australia and Otago, New Zealand: Ore Geology Reviews, v.13, p.293-306.

Sibson, R.H., Robert, F., Poulsen, K.H., 1988, High-angle reverse faults, fluid-pressure cycling, and mesothermal gold-quartz deposits: Geology, v.16, p.551-555.

Sillitoe, R.H., 1991, Intrusion-related gold deposits, *in* Foster, R.P., ed., Gold Metallogeny and Exploration: Blackie and Son, Glasgow, p.165-209.

Siva Siddaiah, N., and Rajamani, V., 1989, The geologic setting, mineralogy, geochemistry, and genesis of gold deposits of the Archean Kolar Schist Belt, India: Economic Geology, v.84, p.2155-2172.

Smith, T.J., and Kesler, S.E., 1985, Relation of fluid inclusion geochemistry to wallrock alteration and lithogeochemical zonation at the Hollinger-McIntyre gold deposit, Timmins, Ontario, Canada: CIM Bulletin v.78, No.876, p.35-46.

Smith, T.J., Cloke, P.L., and Kesler, S.E., 1984, Geochemistry of fluid inclusions from the McIntyre-Hollinger gold deposit, Timmins, Ontario, Canada: Economic Geology, v.79, p.1265-1285.

Sorjonen-Ward, P., 1993, An overview of structural evolution and lithic units within and intruding the late Archean Hattu schist belt, Ilomantsi, eastern Finland, *in* Nurmi, P.A., and Sorjonen-Ward, P., eds., Geological development, gold mineralization and exploration methods in the late Archean Hattu schist belt, Ilomantsi, eastern Finland. Geological Survey of Finland, Special Paper 17, p.9-102.

Spooner, E.T.C., and Barrie, C.T., 1993, A special issue devoted to Abitibi ore deposits in a modern context - preface: Economic Geology, v.88, p.1307-1322.

Straub, K.T., Hagemann, S.G., Brown, P.E., and Yeats, C.J., 1996, Fluid inclusion constraints on the mineralizing fluid from the composite VHMS and lode-gold deposits at Mt Gibson, Western Australia, *in* Brown, P.E., and Hagemann, S.G., eds., Pan-American Conference on Research on Fluid Inclusions 6: Program and Abstracts: Department of Geology and Geophysics, University of Wisconsin-Madison, Wisconsin, U.S.A., p.126-130.

Stuwe, K., 1998, Tectonic constraints on the timing relationships of metamorphism, fluid production and gold - bearing quartz vein emplacement: Ore Geology Reviews, v.13, p.219-228.

Stuwe, K., Will, T.M., and Zhou, S., 1993, On the timing relationship between fluid production and metamorphism in metamorphic piles: some implications for the origin of post-metamorphic gold mineralization: Earth and Planetary Science Letters, v.114, p.417-430.

Swager, C.P., 1997, Tectono-stratigraphy of late Archaean greenstone terranes in the southern Eastern Goldfields, Western Australia: Precambrian Research, v.83, p.11-41.

Taylor, H.P., Jr., 1974, The application of oxygen and hydrogen isotope studies to problems of hydrothermal alteration and ore deposition: Economic Geology, v.69, p.843-883.

Thurston, P.C., Williams, H.R., Sutcliffe, R.H., and Stott, G.M., eds, 1991, Geology of Ontario: Ontario Geological Survey, Special Volume 4, 1525p.

Van Reenen, D.D., Barton, J.M., Roering, C., Smit, C.A., and Van Schalkwyk, J.F., 1987, Deep-crustal response to continental collision: the Limpopo Belt of southern Africa: Geology, v.15, p.11-14.

Vearncombe, J.R., 1998, Shear zones, fault networks, and Archean gold: Geology, v. 26, p. 855-858.

Vielreicher, R.M., Groves, D.I., Ridley, J.R., and McNaughton, N.J., 1994, A replacement origin for the BIF-hosted gold deposit at Mt. Morgans, Yilgarn Block, W.A.: Ore Geology Reviews, v.9m p.325-347.

Walker, R.J., Shirey, S.B., Hanson, G.N., Rajamani, V., and Horan, M.F., 1989, Re-Os, Rb-Sr, and O isotopic systematics of the Archean Kolar schist belt, Karnataka, India: Geochimica et Cosmochimica Acta, v.53, p.3005-3013.

Walsh, J.F., Kesler, S.E., Duff, D., and Cloke, P.L., 1988, Fluid inclusion geochemistry of high-grade, vein-hosted gold ore at the Pamour Mine, Porcupine Camp, Ontario: Economic Geology, v.83, p.1347-1367.

Wang, L.G., McNaughton, N.J., and Groves, D.I., 1993, An overview of the relationship between granitoid intrusions and gold mineralization in the Archaean Murchison Province, Western Australia: Mineralium Deposita, v.28, p.482-494.

Watkins, K.P., and Hickman, A.H., 1990, Excursion No. 2: Murchison granite-greenstone terrain. 1: Geology of the Murchison granite-greenstone terrain, *in* Ho, S.E., Glover, J.E., Myers, J.S., and Muhling, J.R., eds., Third International Archaean Symposium, Excursion Guidebook: Geology Department and University Extension, University of Western Australia, Perth, Publication 21, p.147-171.

Wilkins, C., 1993, A post-deformational, post-peak metamorphic timing for mineralization at the Archean Big Bell gold deposit, Western Australia: Ore Geology Reviews, v.7, p.439-483.

Wilson, J.F., Nesbitt, R.W., and Fanning, C.M., 1995, Zircon geochronology of Archaean felsic sequences in the Zimbabwe Craton: a revision of greenstone stratigraphy and a model for crustal growth, *in* Coward, M.P., and Ries, A.C., eds., Early Precambrian Processes: Geological Society of London, Special Publication 95, p.109-126.

Witt, W.K., 1993, Gold mineralization in the Menzies-Kambalda region, Eastern Goldfields, Western Australia: Western Australian Geological Survey, Report 39, 65p.

Witt, W.K., Knight, J.T., and Mikucki, E.J., 1997, A synmetamorphic lateral fluid flow model for gold mineralization in the Archean southern Kalgoorlie and Norseman Terranes, Western Australia: Economic Geology, v.92, p.407-437.

Wood, P.C., Burrows, D.R., Thomas, A.V., and Spooner, E.T.C., 1986a, The Hollinger-McIntyre Au-quartz vein system: geologic characteristics, gold occurrence, fluid properties and light stable isotope geochemistry, *in* Macdonald A.J., of Gold '86, an International Symposium on the Geology of Gold Deposits: Toronto, p.56-80.

Wood, P.C., Burrows, D.R., and Spooner, E.T.C., 1986b, Grant 236. Au-quartz vein and intrusion-hosted Cu-Au-Ag-Mo mineralization, Hollinger-McIntyre mines, Timmins, Ontario: geological characteristics, structural examination, igneous and hydrothermal alteration geochemistry, and light stable isotope (hydrogen and oxygen) geochemistry: Ontario Geological Survey, Miscellaneous Paper 130, p.115-137.

Wyborn, L.A.I., Heinrich, C.A., and Jaques, A.L., 1994, Australian Proterozoic mineral systems: essential ingredients and mappable criteria: *in* AusIMM Annual Conference, Proceedings Volume. Melbourne, Australasian Institute of Mining and Metallurgy, p.109-115.

Wyman, D.A., and Kerrich, R., 1988, Alkaline magmatism, major structures, and gold deposits: Implications for greenstone belt gold metallogeny: Economic Geology, v.83, p.451-458.

Wyman, D.A., Kerrich, R., and Groves, D.I., 1999, Lode gold deposits and Archean mantle plume-island arc interaction, Abitibi Subprovince, Canada: The Journal of Geology, v.107, p.715-725.

Xu, Y., and Palin, J.M., 1998, Sulfur isotopes in the Victory Gold deposit: Australian National University, Research School of Earth Sciences, Annual Report 1998, p.16-17.

Yeats, C.J., McNaughton, N.J., and Groves, D.I., 1996, SHRIMP U-Pb geochronological constraints on Archean volcanic-hosted massive sulfide and lode gold mineralization at Mount Gibson, Yilgarn Craton, Western Australia: Economic Geology, v.91, p.1354-1371.

Yeats, C.J., McNaughton, N.J., Ruettger, D., Bateman, R., Groves, D.I., Harris, J.L., and Kohler, E., 1999, Evidence for diachronous Archean lode gold mineralization in the Yilgarn Craton, Western Australia: A SHRIMP U-Pb study of intrusive rocks: Economic Geology, v.94, p.1259-1276.

Zotov, A., Baranova, N., Dar'yina, T., and Bannykh, L., 1991, The solubility of gold in aqueous chloride fluids at 350-500°C and 500-1500 atm. Thermodynamic parameters of $AuCl_2$-(sol) up to 750°C and 5000 atm: Geochemistry International, v.28, p.63-71.

Figure and Table Captions

Fig. A1: Distribution of world-class (>100 t) Archean gold deposits.

Fig. A2: Simplified geological map of the eastern Yilgarn Craton showing the distribution of major fault zones and world-class (>100 t; solid circles) and selected other deposits (<100 t; open circles).

Fig. A3: Simplified geological map of the southern Abitibi subprovince (modified after Poulsen et al. (2000) showing the distribution of major fault zones and world-class (>100 t; solid circles) and selected other deposits (<100 t; open circles).

Fig. A4: Grade-tonnage diagram representing gold deposits in the (A) Superior and Slave Province (redrawn after Poulsen et al., 2000), and (B) the Yilgarn Craton. Open circles denote gold deposits containing <100 t of gold, solid circles denote world class deposits (>100 t). Note that the tonnage and grade diagram for the Yilgarn Craton is based on resource estimates compiled from the Australian Geological Survey Organization OZMIN database of Australian mineral deposits with additional data from unpublished company reports. The Agnew deposits include the Reedemer and Crusader deposits and several small satellite deposits.

Fig. A5: The mineral system concept of hydrothermal ore body formation.

Fig. A6: The mineral system concept as applied to Archean orogenic lode-gold deposits.

Fig. A9: The Boulder-Lefroy fault zone system, Yilgarn Craton, Western Australia. Modified after Hodgson (1993).

Fig. A10: A. Fluid pressure regimes and associated strength profile for the carapace to a region undergoing prograde regional metamorphism; B. Fluid pressure profile across an impermeable sealing horizon of tensile strength, Ts, illustrating the control on the vertical extent of hydrofracture development and mesh activation. After Sibson and Scott (1998).

Fig. A11: Fluid flow modeling of the interpreted profile for the Eastern Goldfields deep seismic transect, Yilgarn Craton. The arrows represent fluid flow direction, their length representing the volume of fluid flow. The 'Y-front' model predicts increased fluid flow within the greenstone package along several major structures. Modified after Goleby et al. (1997).

Fig. A12: A. Simplified metamorphic map of the Kalgoorlie area, Yilgarn Craton, showing the inferred hydrothermal cell footprint and large gold deposits; B. Approximate gold accumulation of the Kalgoorlie area inferred hydrothermal cell footprint and large gold deposits. Redrawn after Hall (1998), Hall (unpublished company report) and http://www.agcrc.csiro.au/projects/3067CO/index.html.

Fig. A13: A. Simplified geological map of the Kalgoorlie area, Yilgarn Craton, showing major gold deposits and gold occurrences. B. Numerical low mean stress model of the Kalgoorlie area using stress Mapping Technology (Terra Sancta) and showing areas of high minimum principal stress. Redrawn after Hall (unpublished company report) and http://www.agcrc.csiro.au/projects/3067CO/index.html.

Fig. A14: A. Distribution of alteration assemblages on the surface area surrounding the Hollinger and McIntyre mines, Superior Province. Each dot represents a sample location. The stippled areas are the porphyries, the black lines represent quartz veins. The alteration assemblages are as follows: Assemblage 1. Quartz-albite-chlorite-epidote-actinolite-(calcite); Assemblage 2: quartz-albite-chlorite-calcite-epidote; Assemblage 3: Quartz-ankerite-sericite-(chlorite-calcite); Assemblage 4. Quartz-albite-ankerite-sericite. B. Contours of CO_2 content in mole percent for fluid inclusions in surface vein samples. Each dot represents a sample location. The stippled areas are the porphyries, the black lines represent quartz veins. Redrawn after Smith and Kesler (1985).

Fig. A15: A. Relative gold resource (production plus reserves) and nature of host rocks to gold mineralization in the Archean greenstone belts of the Yilgarn Craton (Groves, 1990). B. Estimated proportions of greenstone belt outcrop in the Yilgarn Craton by metamorphic grade. C. Proportions of total gold production and known resources from terranes of different metamorphic grade. D. Proportions of current gold production (year 1988-90) by host-rock metamorphic grade. Redrawn from Ridley et al., 1995).

Fig. A16: Diagram illustrating the main stages of vein development and selected microstructures in relation to the earthquake stress cycle. After Robert et al. (1995).

Fig. A17: A. Contours of ó 3 (shaded) and gold grade thickness illustrating the good correlation of the simulated low-stress areas and gold mineralization, Granny Smith deposit. Pit outlines show the broad extent of economic mineralization. B. Section through the northern part of the Windich open pit, Granny Smith deposit, showing the gold mineralization and low ó 3. Note the widening of the gold mineralization and the low ó 3 area within the granitoid where the dip of the contact steepens. The low ó3 anomalies deeper in the section are the result of a curve on the modeled surface caused by interpolation beyond drillhole intersections. Redrawn after Holyland and Ojala (1997).

Fig. A18: Variations of CO_2 and alkali metal saturation indices across the northern part of the East Lode orebody, Wiluna camp, relative to the major host rocks. Also shown are the concentrations of gold and arsenic and the down-depth lithostratigraphic rock units in the diamond hole. Modified after Hagemann et al. (in revision).

Fig. A19: Temperature-oxygen fugacity constraints on mineralization (shaded fields) and aqueous-carbonic inclusions (unshaded boxes) at four orogenic lode-gold deposits, Yilgarn Craton. Thick solid lines are sulfide and oxide equilibria. Thick dashed lines are CO_2-CH_4 ratios of mixed aqueous-carbonic fluids with X_{CAR}=0.2. These lines will not significantly shift for 0.1shift for 0.1 < X_{CAR}<0.9. Redrawn after Ridley and Hagemann (1999).

Fig. A20: T-X CO_2 phase diagram showing isobaric equilibrium curves for mineral assemblages at specific deposits in the Yilgarn Craton, Western Australia. La – Lancefield, NR, CM and SC – North Royal, Crown-Mararoa and Scotia, respectively, ML – Marvel Loch, Vi – Victory, We – Westonia, Wi – Wiluna. Reactions for the Victory mine are: (1) Ms+Dol = Bt+Chl+Cal; (2) Bt+Chl+Dol = Tr+Ms; (3) Bt+Chl+Dol = Act+Ms. Abbreviations: Act – actinolite, An – anorthite, Bt – biotite, Cal – calcite, Di – diopside, Fo – forsterite, Ilm – ilmenite, Kfs – K-feldspar, Phl – phlogopite, Rt – rutile, Sid – siderite, Spl – spinel, Tr – tremolite, Wo – wollastonite. Modified after Mikucki and Ridley (1993) and McCuaig and Kerrich (1998).

Fig. A21: A. Estimated compositions of gold bearing hydrothermal fluids with respect to fluid oxidation state (a_{H2}) and sulfide content (a_{H2S}), based on the common vein and proximal alteration assemblages of pyrite±arsenopyrite, pyrite-pyrrhotite or pyrite-chalcopyrite-anhydrite at mesozonal conditions (vertical and diagonal lined fields). Note that at these conditions reduced (near CO_2-CH_4 buffer) and oxidized (near sulfide-sulfate buffer) types of gold deposits are observed. Pyrite-pyrrhotite, pyrrhotite or pyrrhotite-loellingite±ilmenite are the common vein and proximal alteration assemblages at hypozonal conditions (darker stippled field). For further discussion of the assemblages and data source see Mikucki and Ridley (1993), and Ridley et al. (1996). Redrawn from Ridley et al. (1996).

B. Oxidation states for Archean lode-gold deposits relative to that of the CO_2-CH_4 redox buffer as a function of temperature. log f_{O2} measures the displacement in log f_{O2} from the CO_2-CH_4 buffer. Heavy black bars represent estimated ore-fluid conditions for the deposits considered based on combined fluid inclusion and mineral assemblages and mineral chemistry data for proximal alteration zones. Arrows represent deposits for which only maximum f_{O2} constraints are available. Important redox buffers at P = 2 kbar (solid curves) are shown for reference. (a) Racetrack, (b) North Kalgurli, (c) Lady Bountiful (stages I and II), (d) Wiluna (stage I), (e) Mt Charlotte, (f) Hunt, (g) Norseman, (h) Main Hill, (i) Zakanaka, (j) Nevoria, (m) Griffins Find. Abbreviations: As – arsenic metal, Aspy – arsenopyrite, Fay – fayalite, Hem – hematite, Lo – loellingite, Mt – magnetite, Po – pyrrhotite, Py – pyrite, Qtz – quartz, $(S, As)_{liq}$ – S- and As-rich melt. Redrawn from Mikucki (1998) where complete data sources are listed.

Table 2: Mineralization and structural styles of Australian and Canadian Archean orogenic lode-gold deposits.

Table 3: Summary table of silicate, sulfide and oxide hydrothermal alteration assemblages from proximal alteration zones from the four dominant host lithologies of Archean orogenic lode-gold deposits in the Yilgarn Craton.

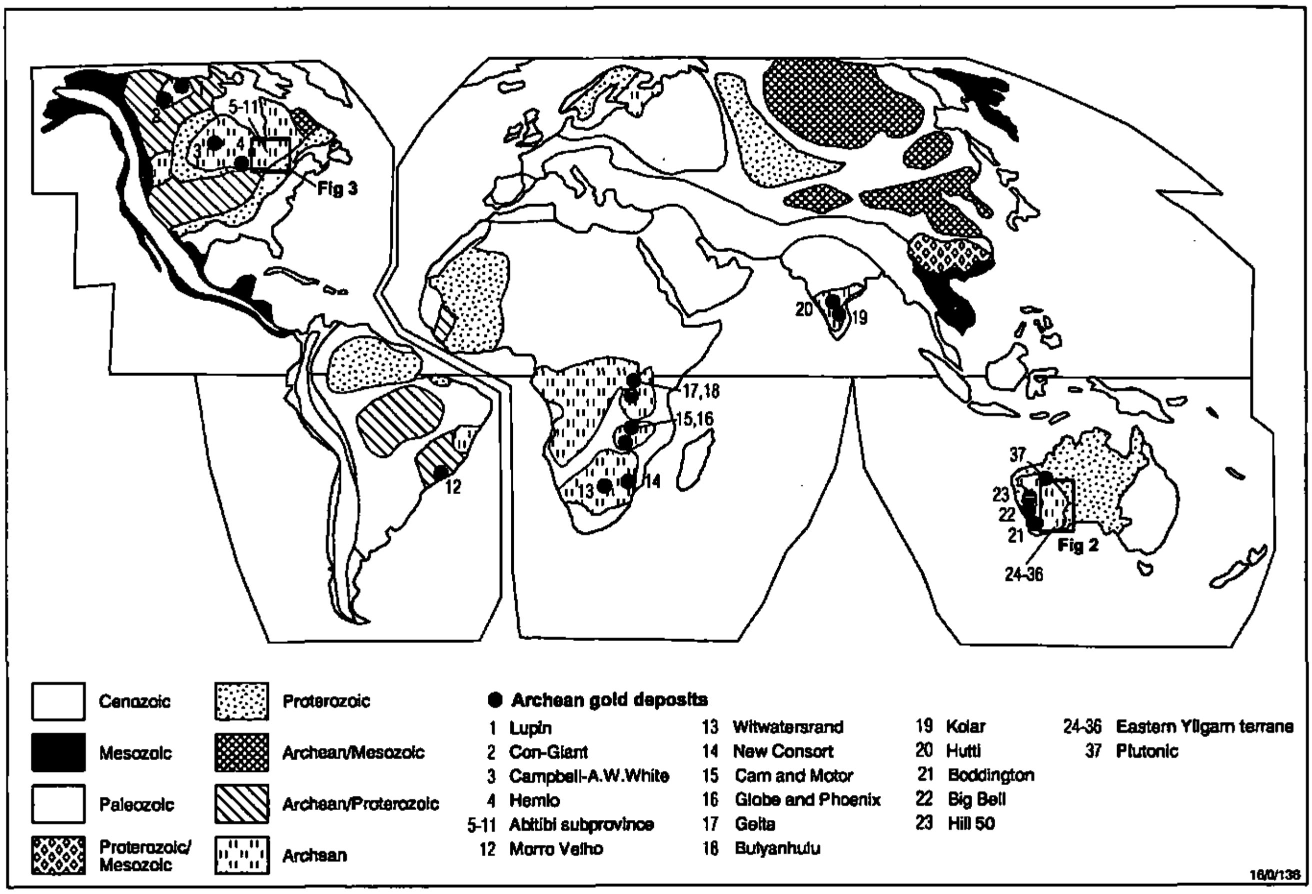

Fig 3
Fig 2
Cenozoic
Mesozoic
Paleozoic
Proterozoic/ Mesozoic
Proterozoic
Archean/Mesozoic
Archean/Proterozoic
Archean
● Archean gold deposits
1 Lupin
2 Con-Giant
3 Campbell-A.W.White
4 Hemlo
5-11 Abitibi subprovince
12 Morro Velho
13 Witwatersrand
14 New Consort
15 Cam and Motor
16 Globe and Phoenix
17 Geita
18 Bulyanhulu
19 Kolar
20 Hutti
21 Boddington
22 Big Bell
23 Hill 50
24-36 Eastern Yilgarn terrane
37 Plutonic
16/0/136

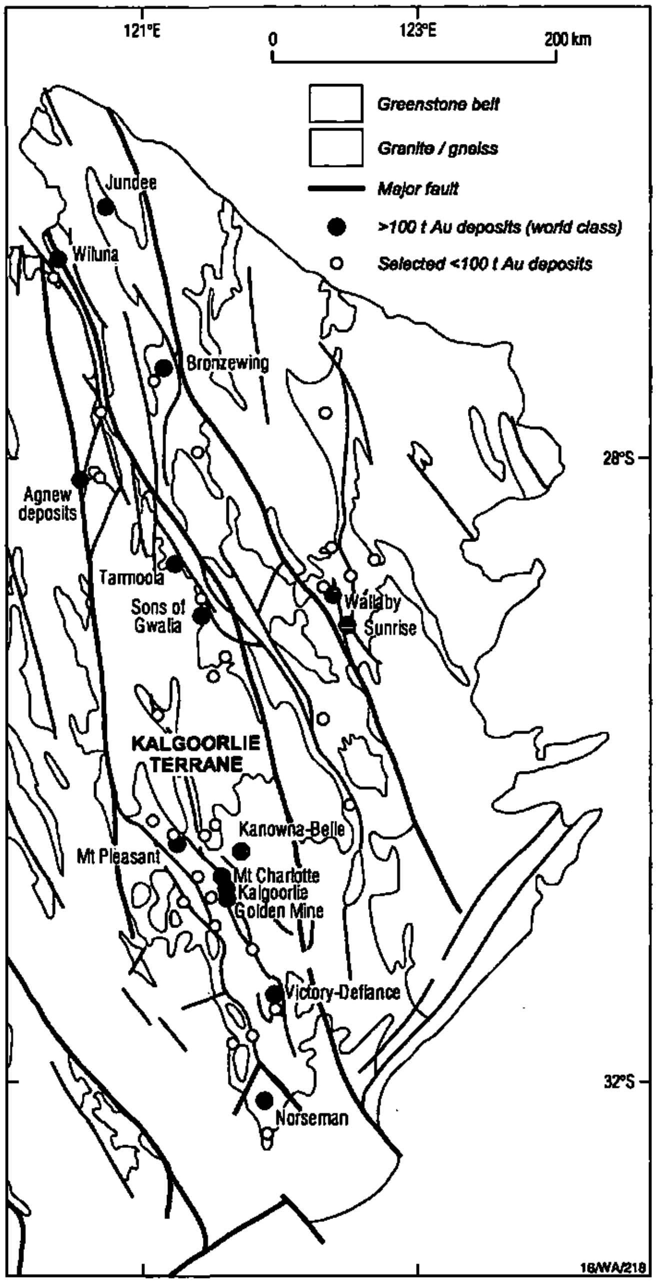

121°E
0
123°E
200 km
Greenstone belt
Granite / gneiss
Major fault
>100 t Au deposits (world class)
Selected <100 t Au deposits
Jundee
Wiluna
Bronzewing
28°S
Agnew deposits
Tarmoola
Sons of Gwalia
Wallaby
Sunrise
KALGOORLIE TERRANE
Kanowna-Belle
Mt Pleasant
Mt Charlotte
Kalgoorlie
Golden Mine
Victory-Defiance
32°S
Norseman
18/WA/218

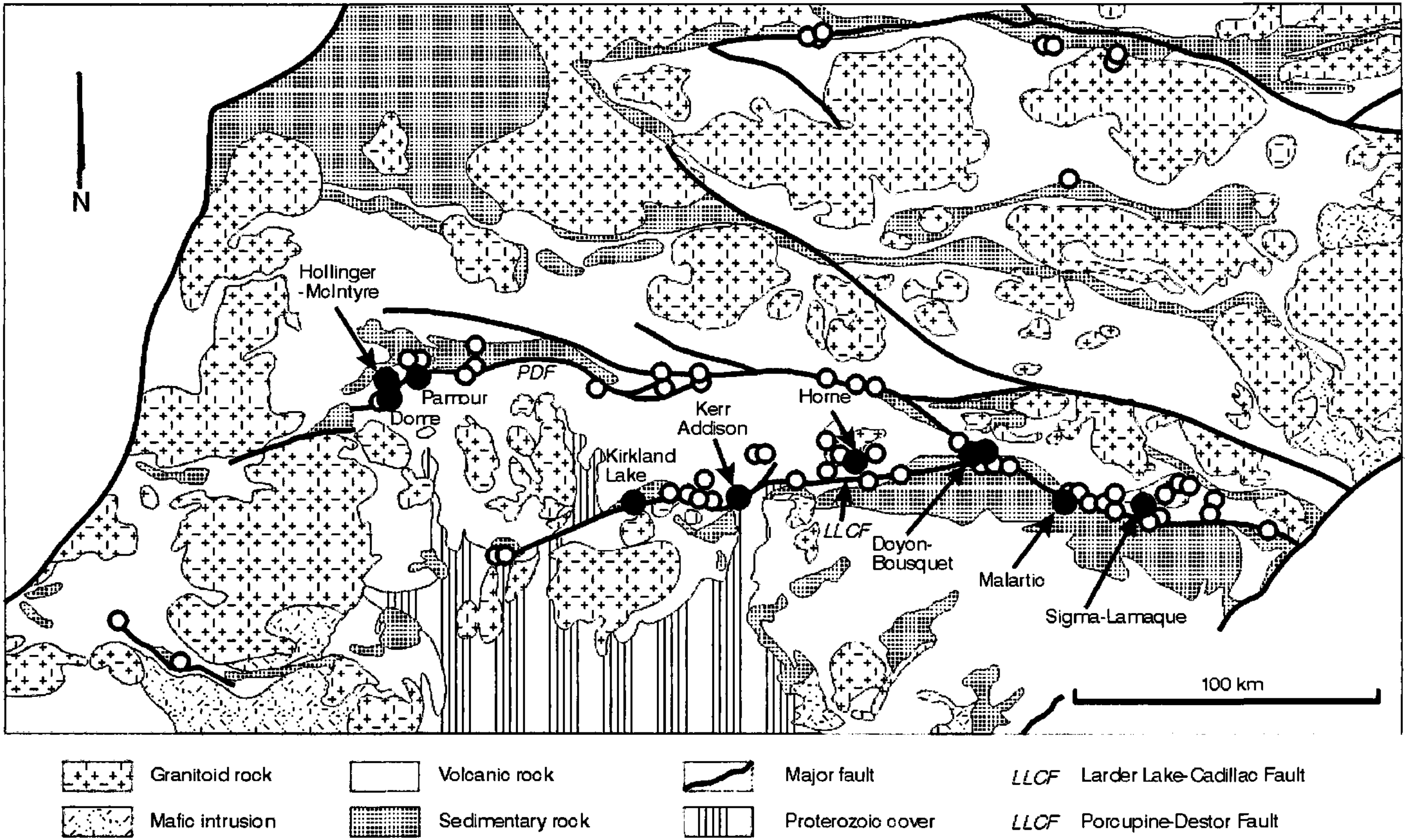
N
Hollinger
-McIntyre
Pamour
Dome
PDF
Kirkland
Lake
Kerr
Addison
Horne
LLCF
Doyon-
Bousquet
Malartic
Sigma-Lamaque
100 km
Granitoid rock
Mafic intrusion
Volcanic rock
Sedimentary rock
Major fault
Proterozoic cover
LLCF Larder Lake-Cadillac Fault
LLCF Porcupine-Destor Fault

SHf007-00

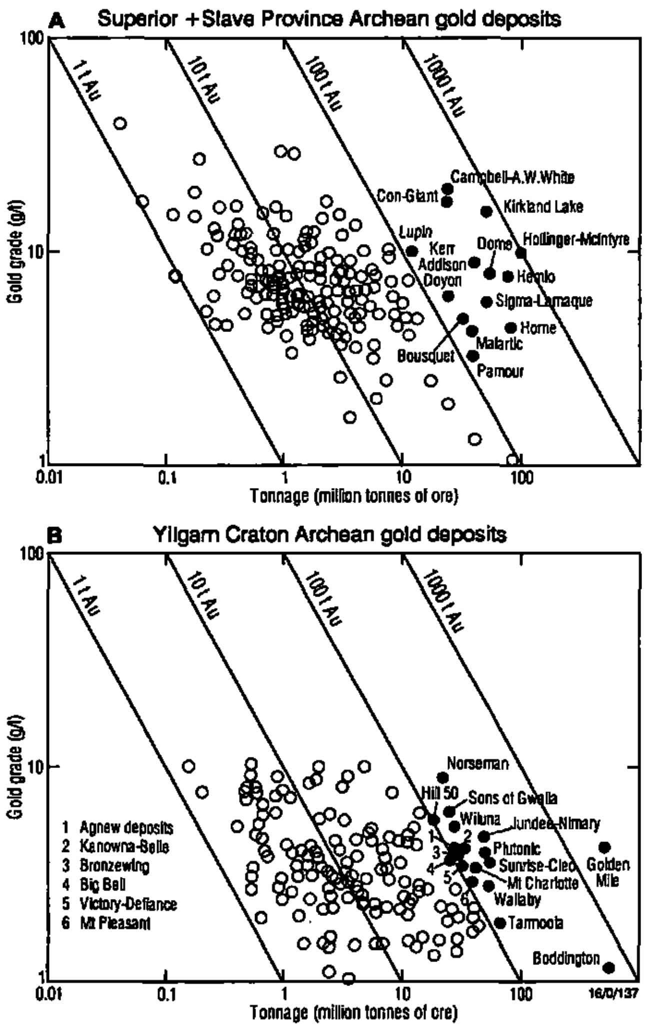

A Superior + Slave Province Archean gold deposits
1 t Au
10 t Au
100 t Au
1000 t Au
Gold grade (g/t)
Tonnage (million tonnes of ore)
Campbell-A.W.White
Con-Giant
Kirkland Lake
Lupin
Kerr Addison
Doyon
Dome
Hollinger-McIntyre
Hemlo
Sigma-Lamaque
Horne
Malartic
Bousquet
Pamour
B Yilgarn Craton Archean gold deposits
Norseman
Hill 50
Sons of Gwalia
Wiluna
Jundee-Nimary
Plutonic
Sunrise-Cleo
Mt Charlotte
Wallaby
Tarmoola
Golden Mile
Boddington
1 Agnew deposits
2 Kanowna-Belle
3 Bronzewing
4 Big Bell
5 Victory-Defiance
6 Mt Pleasant
16/0/137

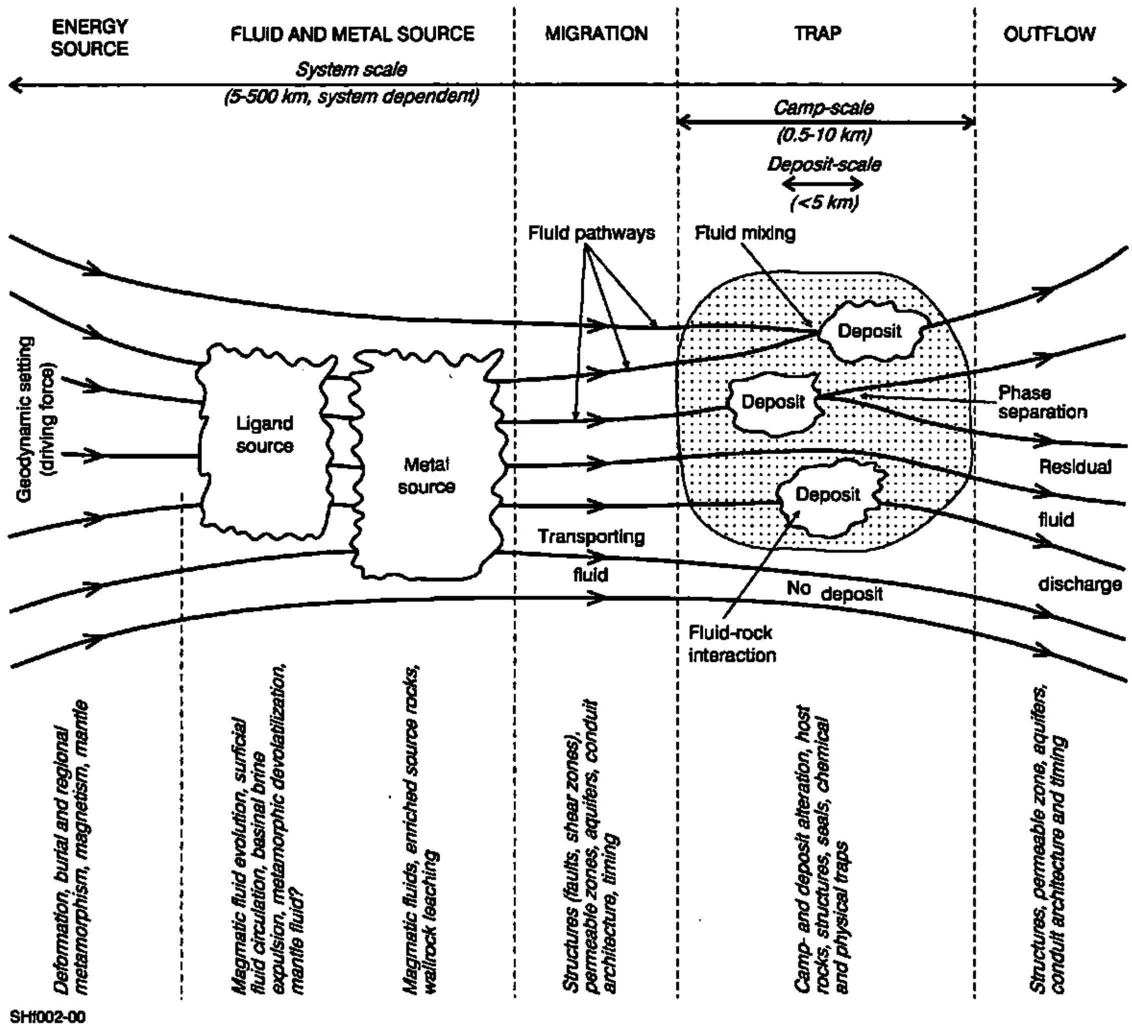
ENERGY SOURCE
FLUID AND METAL SOURCE
MIGRATION
TRAP
OUTFLOW
System scale
(5-500 km, system dependent)
Camp-scale
(0.5-10 km)
Deposit-scale
(<5 km)
Fluid pathways
Fluid mixing
Deposit
Deposit
Deposit
Phase separation
Geodynamic setting (driving force)
Ligand source
Metal source
Residual
fluid
discharge
Transporting
fluid
No deposit
Fluid-rock interaction
Deformation, burial and regional metamorphism, magnetism, mantle
Magmatic fluid evolution, surficial fluid circulation, basinal brine expulsion, metamorphic devolatilization, mantle fluid?
Magmatic fluids, enriched source rocks, wallrock leaching
Structures (faults, shear zones), permeable zones, aquifers, conduit architecture, timing
Camp- and deposit alteration, host rocks, structures, seals, chemical and physical traps
Structures, permeable zone, aquifers, conduit architecture and timing
SHf002-00

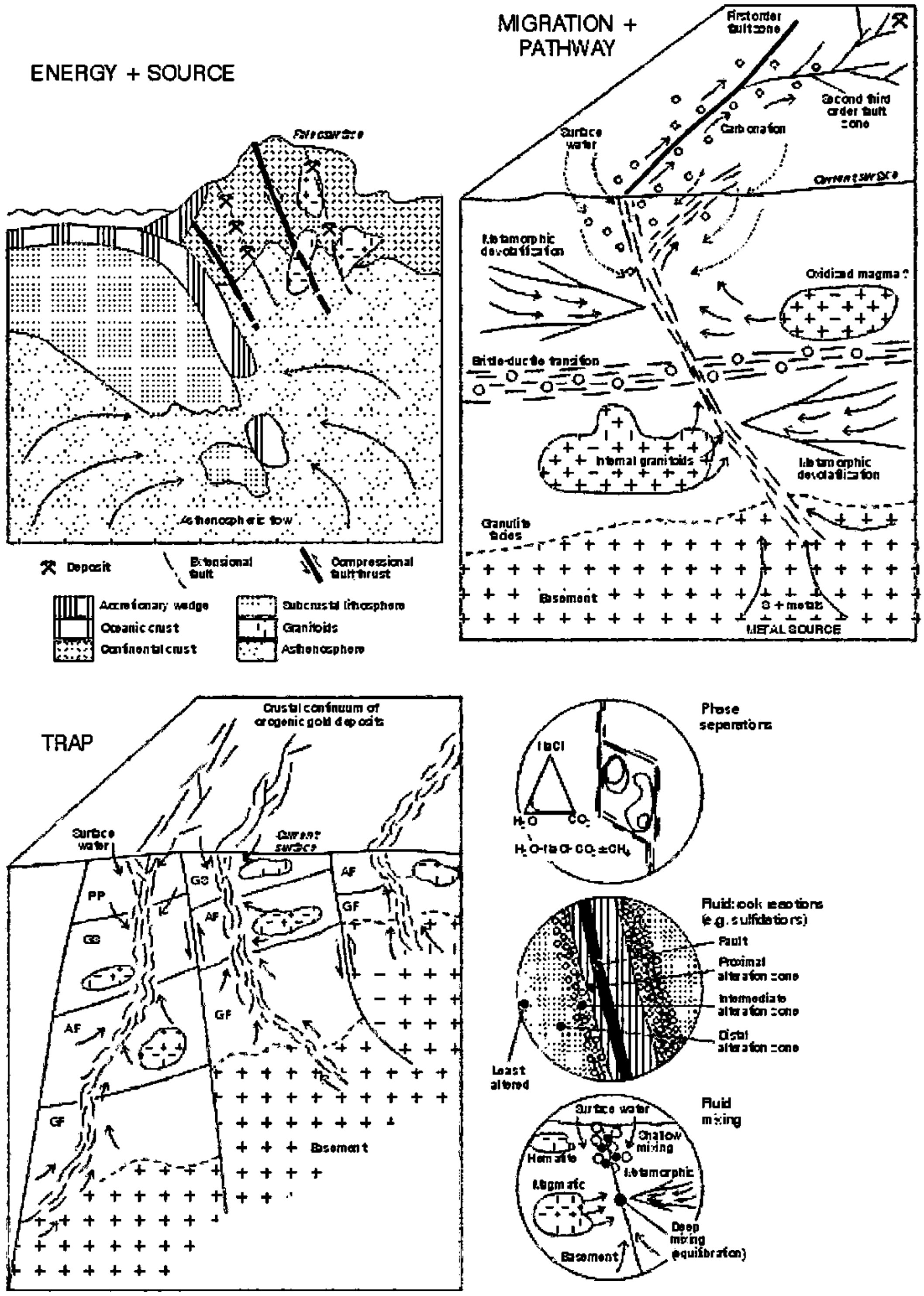

ENERGY + SOURCE
Paleosurface
Asthenospheric flow
Deposit
Extensional fault
Compressional fault/thrust
Accretionary wedge
Oceanic crust
Continental crust
Subcrustal lithosphere
Granitoids
Asthenosphere
MIGRATION + PATHWAY
First order fault zone
Second/third order fault zone
Surface water
Carbonation
Current surface
Metamorphic devolatilization
Oxidized magma?
Brittle-ductile transition
Internal granitoids
Granulite facies
Basement
METAL SOURCE
TRAP
Crustal continuum of orogenic gold deposits
Surface water
Current surface
PP
GS
AF
GF
Basement
Phase separations
Fluid:rock reactions
(e.g. sulfidations)
Fault
Proximal alteration zone
Intermediate alteration zone
Distal alteration zone
Least altered
Fluid mixing
Surface water
Shallow mixing
Hematite
Metamorphic
Magmatic
Deep mixing
(equilibration)
Basement

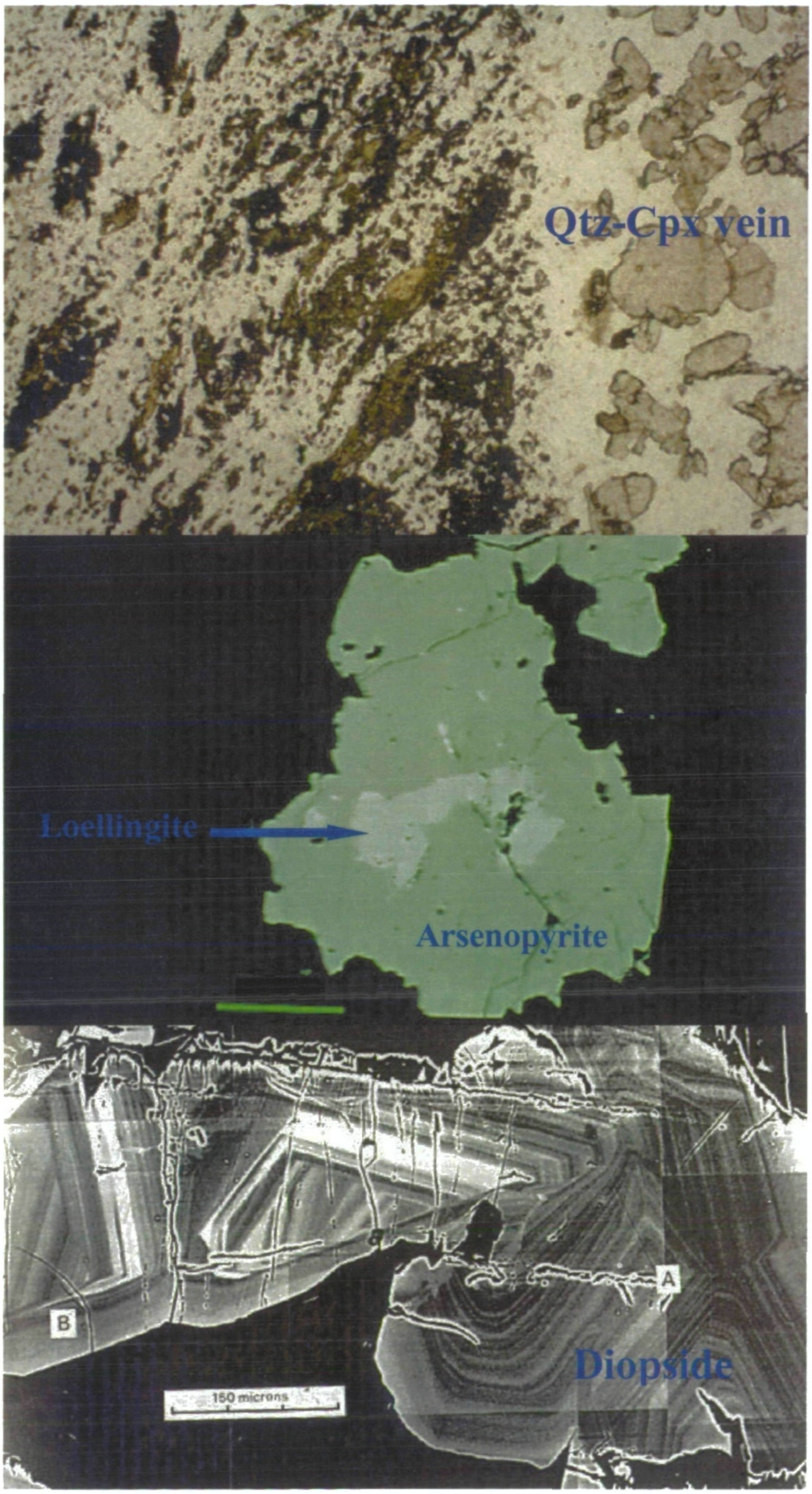

Figure A7 Textural evidence supporting orogenic lode-gold mineralization broadly contemporaneous with peak metamorphism in the Yilgarn Craton, Western Australia.

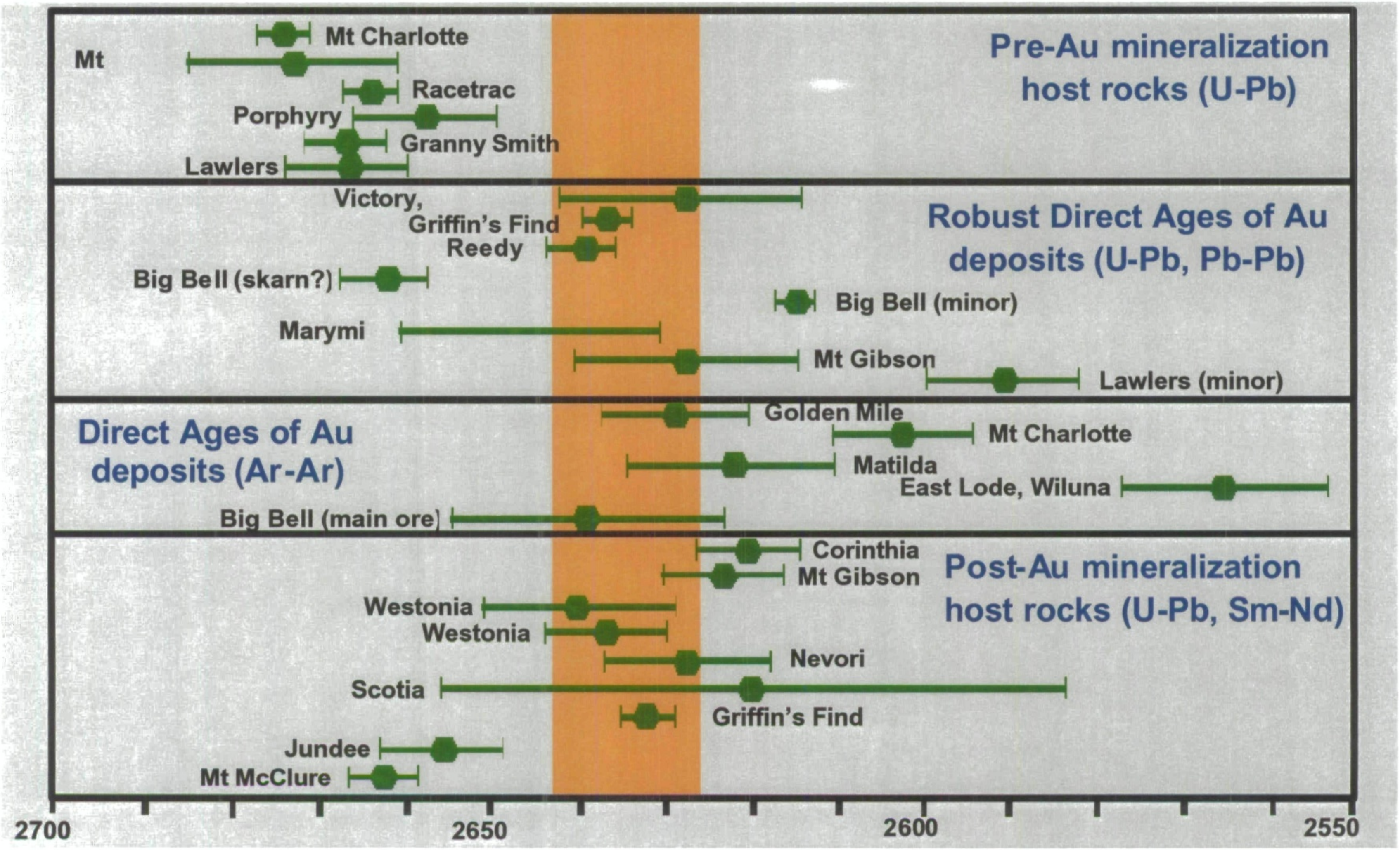

Figure A8 Diagram illustrating the available geochronological constraints on orogenic lode-gold deposits in the Yilgarn Craton, Western Australia. Ages are shown as $\pm 2\sigma$ (modified after Groves *et al*, 2000).

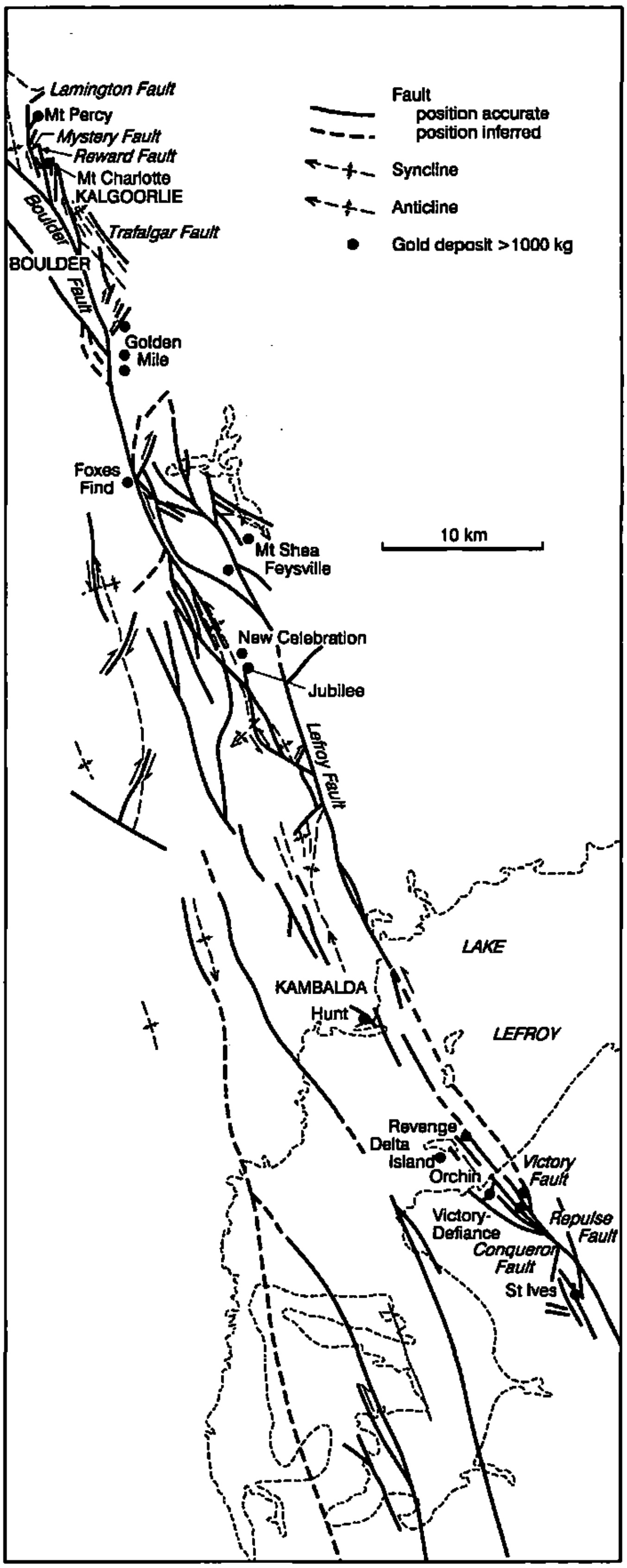

Lamington Fault
Mt Percy
Mystery Fault
Reward Fault
Mt Charlotte
KALGOORLIE
Boulder
Trafalgar Fault
BOULDER
Fault
Golden
Mile
Foxes
Find
Mt Shea
Feysville
New Celebration
Jubilee
Lefroy Fault
KAMBALDA
Hunt
LAKE
LEFROY
Revenge
Delta
Island
Orchin
Victory
Fault
Victory-
Defiance
Repulse
Fault
Conqueror
Fault
St Ives
Fault
position accurate
position inferred
Syncline
Anticline
Gold deposit >1000 kg
10 km

SHf011-00

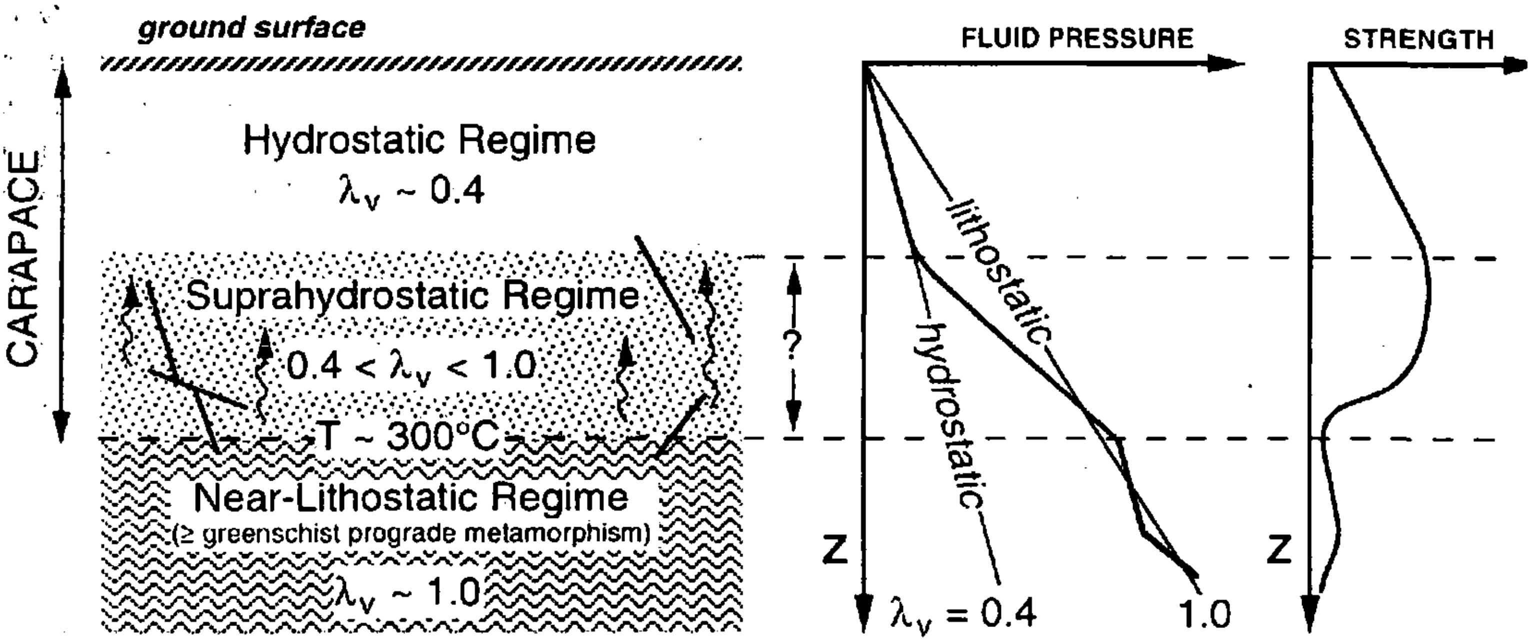
ground surface
CARAPACE
Hydrostatic Regime
λv ~ 0.4
Suprahydrostatic Regime
0.4 < λv < 1.0
T ~ 300°C
Near-Lithostatic Regime
(≥ greenschist prograde metamorphism)
λv ~ 1.0
?
FLUID PRESSURE
lithostatic
hydrostatic
Z
λv = 0.4
1.0
STRENGTH
Z

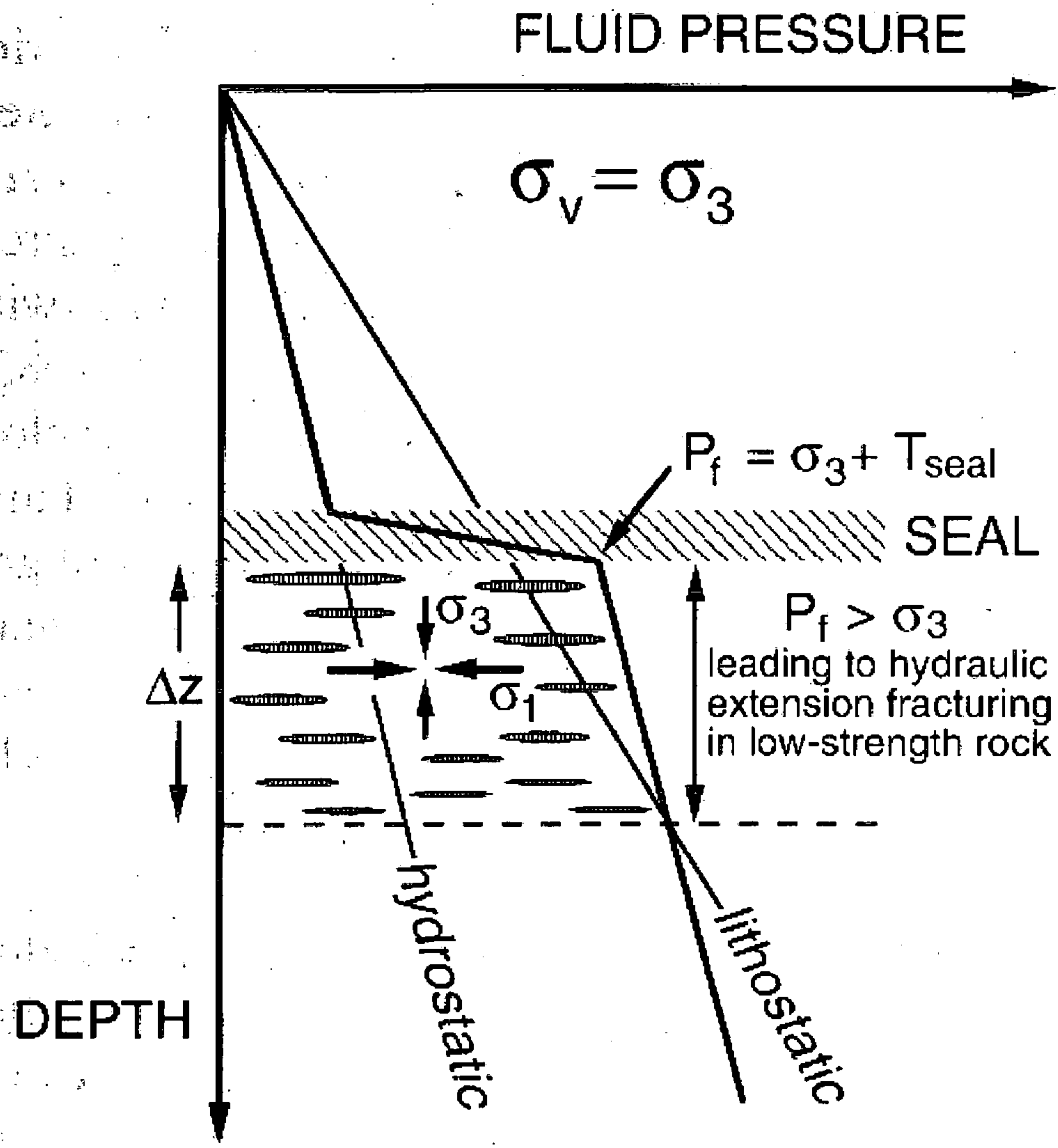
FLUID PRESSURE
σv = σ3
Pf = σ3+ Tseal
SEAL
σ3
σ1
Δz
Pf > σ3
leading to hydraulic
extension fracturing
in low-strength rock
hydrostatic
lithostatic
DEPTH

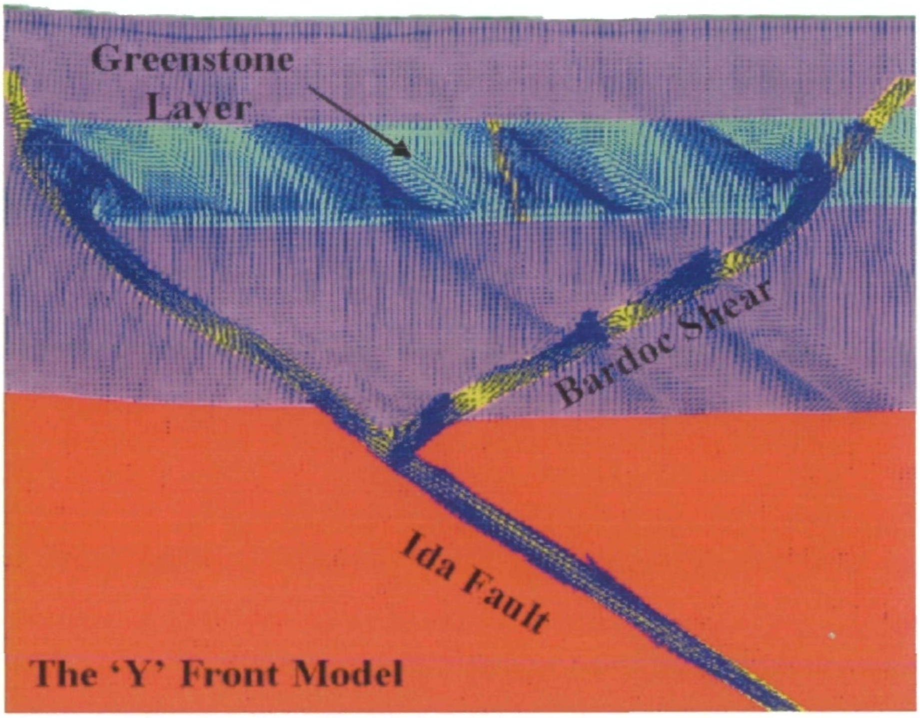
Greenstone
Layer
Bardoc Shear
Ida Fault
The 'Y' Front Model

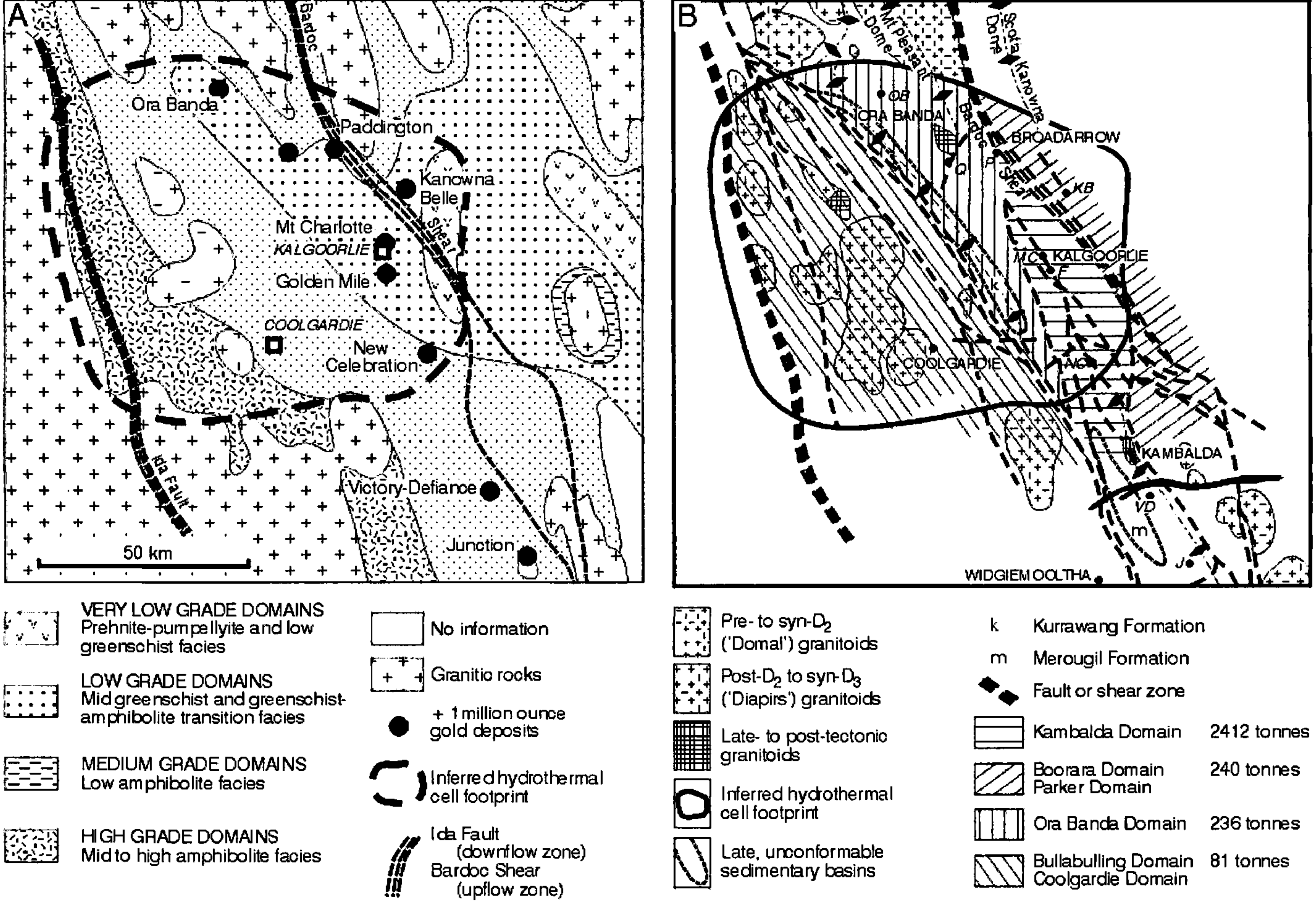

A
Ora Banda
Paddington
Bardoc
Shear
Kanowna Belle
Mt Charlotte
KALGOORLIE
Golden Mile
COOLGARDIE
New Celebration
Victory-Defiance
Junction
Ida Fault
50 km
B
Mt Pleasant Dome
Scotia Kanowna Dome
OB
ORA BANDA
Bardoc Shear
BROADARROW
KB
MC
KALGOORLIE
COOLGARDIE
KAMBALDA
VD
WIDGIEMOOLTHA
VERY LOW GRADE DOMAINS
Prehnite-pumpellyite and low greenschist facies
LOW GRADE DOMAINS
Mid greenschist and greenschist-amphibolite transition facies
MEDIUM GRADE DOMAINS
Low amphibolite facies
HIGH GRADE DOMAINS
Mid to high amphibolite facies
No information
Granitic rocks
+ 1 million ounce gold deposits
Inferred hydrothermal cell footprint
Ida Fault (downflow zone)
Bardoc Shear (upflow zone)
Pre- to syn-D_2 ('Domal') granitoids
Post-D_2 to syn-D_3 ('Diapirs') granitoids
Late- to post-tectonic granitoids
Inferred hydrothermal cell footprint
Late, unconformable sedimentary basins
k Kurrawang Formation
m Merougil Formation
Fault or shear zone
Kambalda Domain 2412 tonnes
Boorara Domain Parker Domain 240 tonnes
Ora Banda Domain 236 tonnes
Bullabulling Domain Coolgardie Domain 81 tonnes

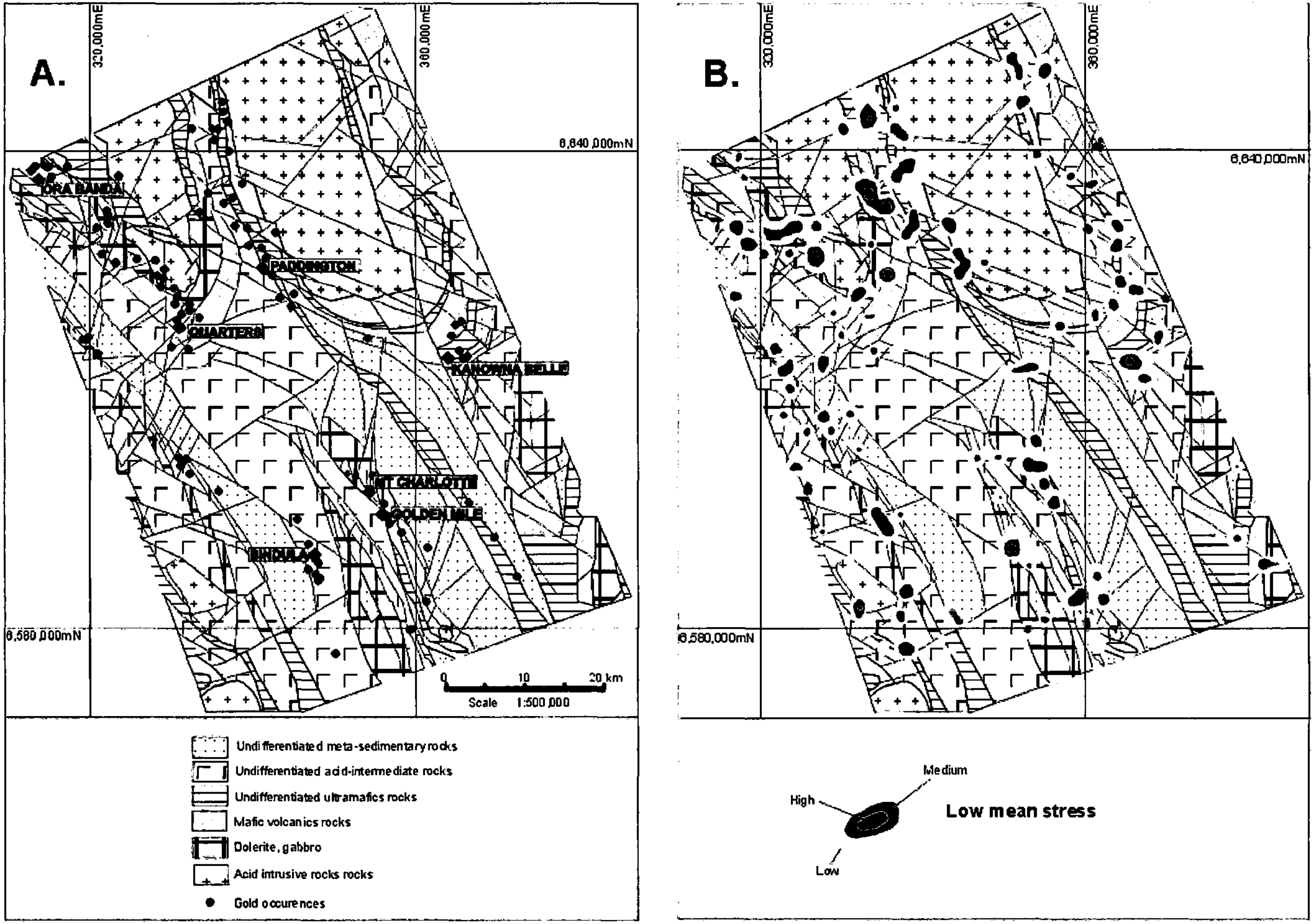
A.
320,000mE
360,000mE
6,640,000mN
6,580,000mN
ORA BANDA
PADDINGTON
QUARTERS
KANOWNA BELLE
MT CHARLOTTE
GOLDEN MILE
BINDULI
0 10 20 km
Scale 1:500,000
Undifferentiated meta-sedimentary rocks
Undifferentiated acid-intermediate rocks
Undifferentiated ultramafics rocks
Mafic volcanics rocks
Dolerite, gabbro
Acid intrusive rocks rocks
Gold occurences
B.
320,000mE
360,000mE
6,640,000mN
6,580,000mN
High
Medium
Low
Low mean stress

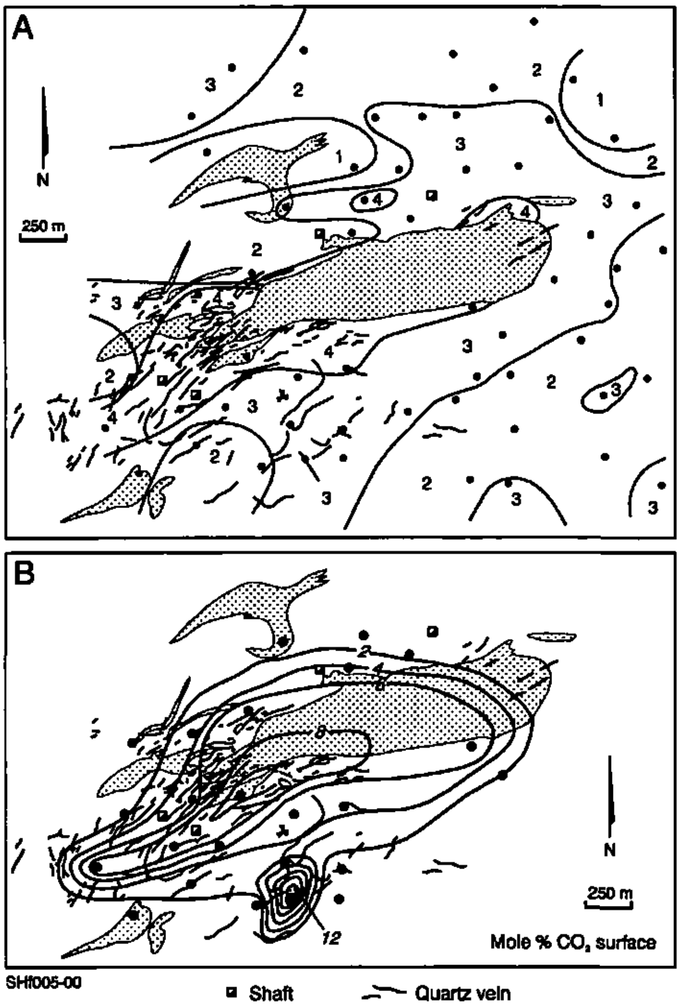
A
N
250 m
B
N
250 m
Mole % CO_2 surface
SHf005-00
Shaft
Quartz vein

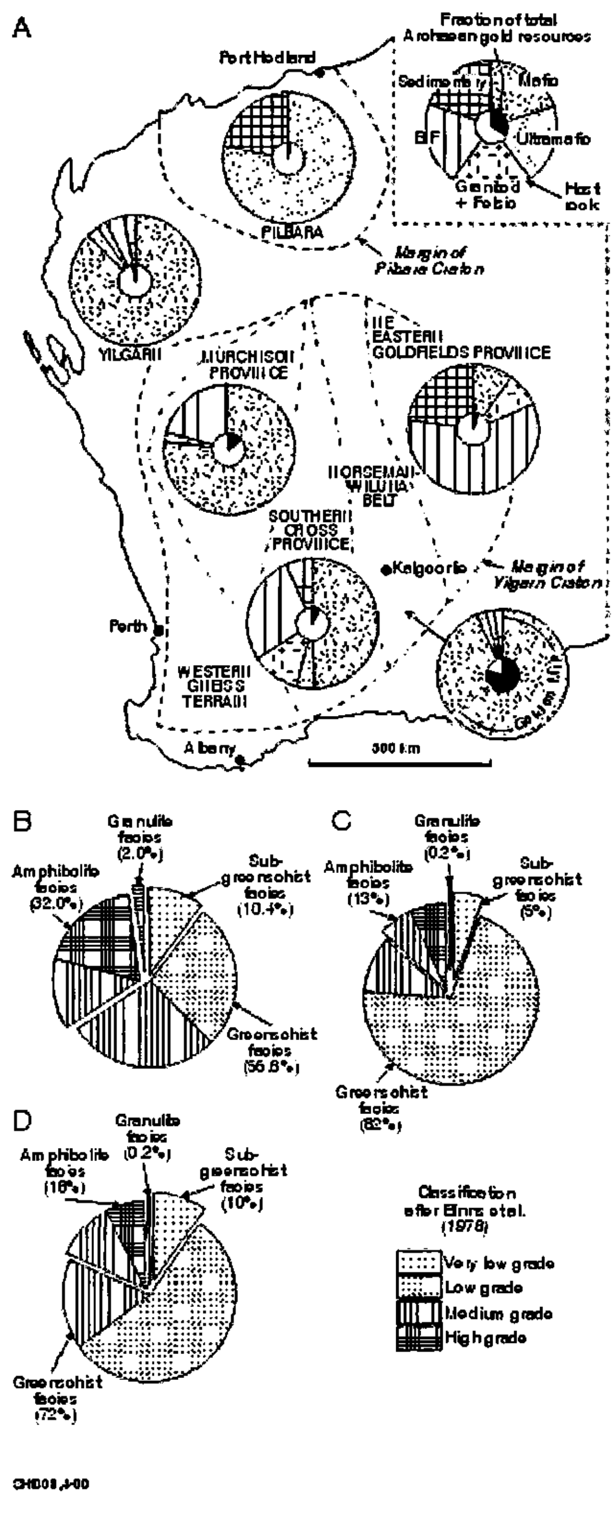

A
Fraction of total Archaean gold resources
Sedimentary
Mafic
BIF
Ultramafic
Granitoid + Felsic
Host rock
Port Hedland
PILBARA
Margin of Pilbara Craton
YILGARN
MURCHISON PROVINCE
EASTERN GOLDFIELDS PROVINCE
NORSEMAN-WILUNA BELT
SOUTHERN CROSS PROVINCE
Kalgoorlie
Margin of Yilgarn Craton
Perth
WESTERN GNEISS TERRAIN
Albany
500 km
B
Granulite facies (2.0%)
Amphibolite facies (32.0%)
Sub-greenschist facies (10.4%)
Greenschist facies (55.6%)
C
Granulite facies (0.2%)
Amphibolite facies (13%)
Sub-greenschist facies (5%)
Greenschist facies (82%)
D
Granulite facies (0.2%)
Amphibolite facies (18%)
Sub-greenschist facies (10%)
Greenschist facies (72%)
Classification after Binns et al. (1976)
Very low grade
Low grade
Medium grade
High grade

GHD08,4-00

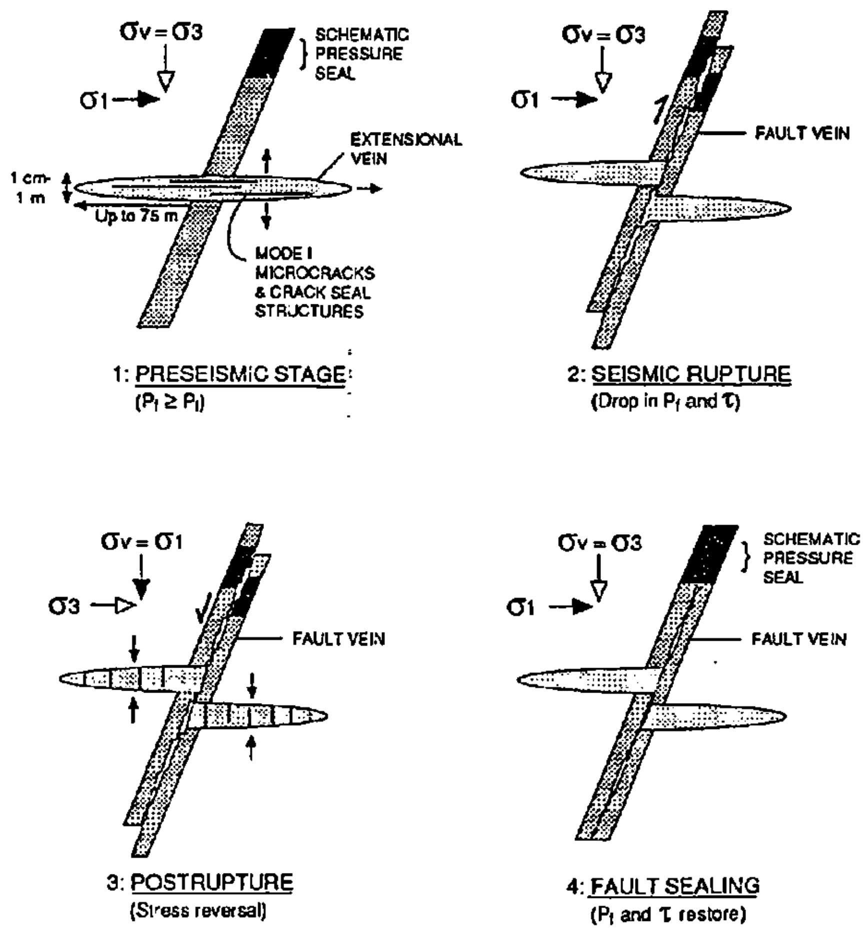
σv = σ3
SCHEMATIC PRESSURE SEAL
σ1
EXTENSIONAL VEIN
1 cm-
1 m
Up to 75 m
MODE I MICROCRACKS & CRACK SEAL STRUCTURES
1: PRESEISMIC STAGE
($P_f \geq P_l$)
σv = σ3
σ1
FAULT VEIN
2: SEISMIC RUPTURE
(Drop in P_f and τ)
σv = σ1
σ3
FAULT VEIN
3: POSTRUPTURE
(Stress reversal)
σv = σ3
SCHEMATIC PRESSURE SEAL
σ1
FAULT VEIN
4: FAULT SEALING
(P_f and τ restore)

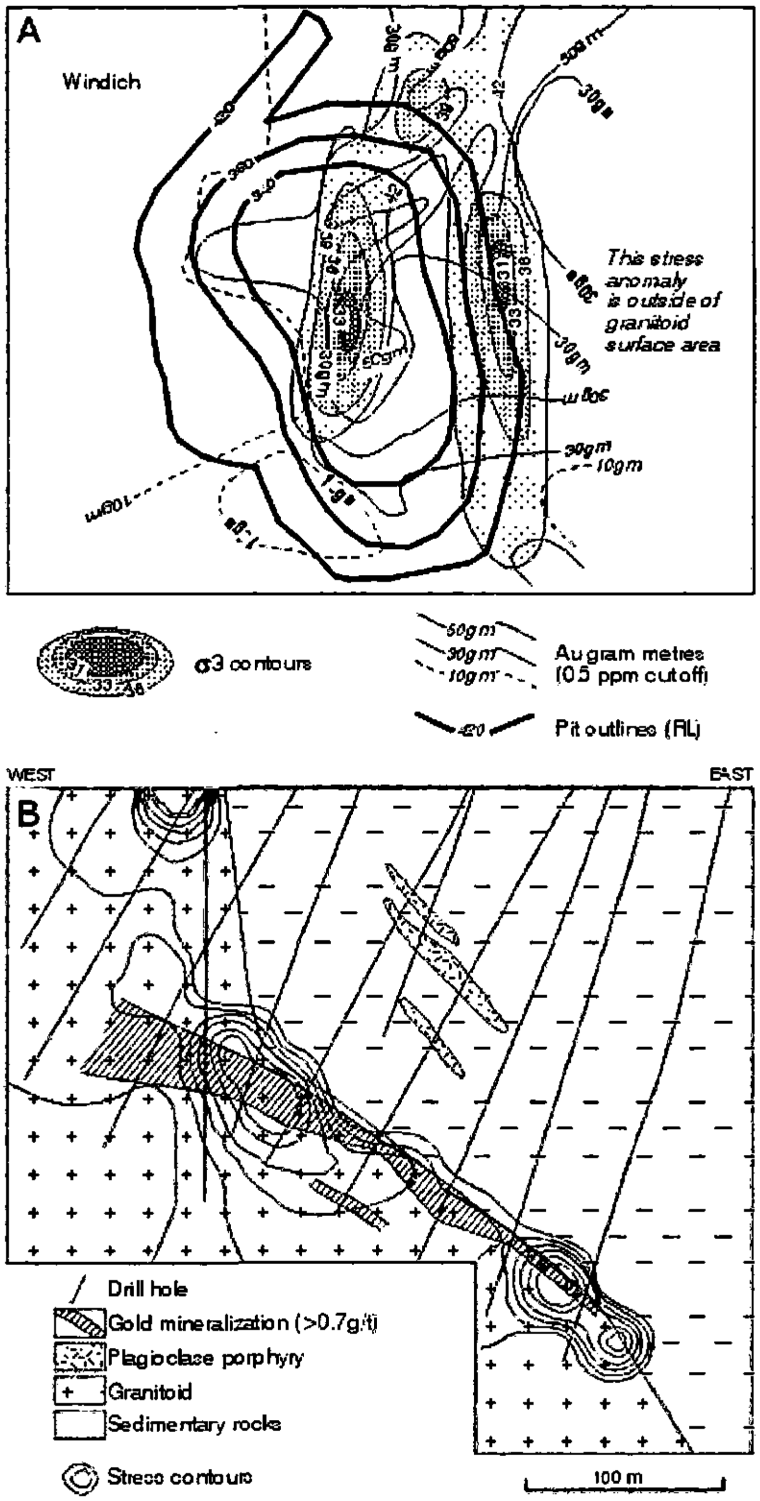
A
Windich
This stress anomaly is outside of granitoid surface area
σ3 contours
50gm
30gm
10gm
Au gram metres (0.5 ppm cutoff)
420
Pit outlines (RL)
WEST
EAST
B
Drill hole
Gold mineralization (>0.7g/t)
Plagioclase porphyry
Granitoid
Sedimentary rocks
Stress contours
100 m

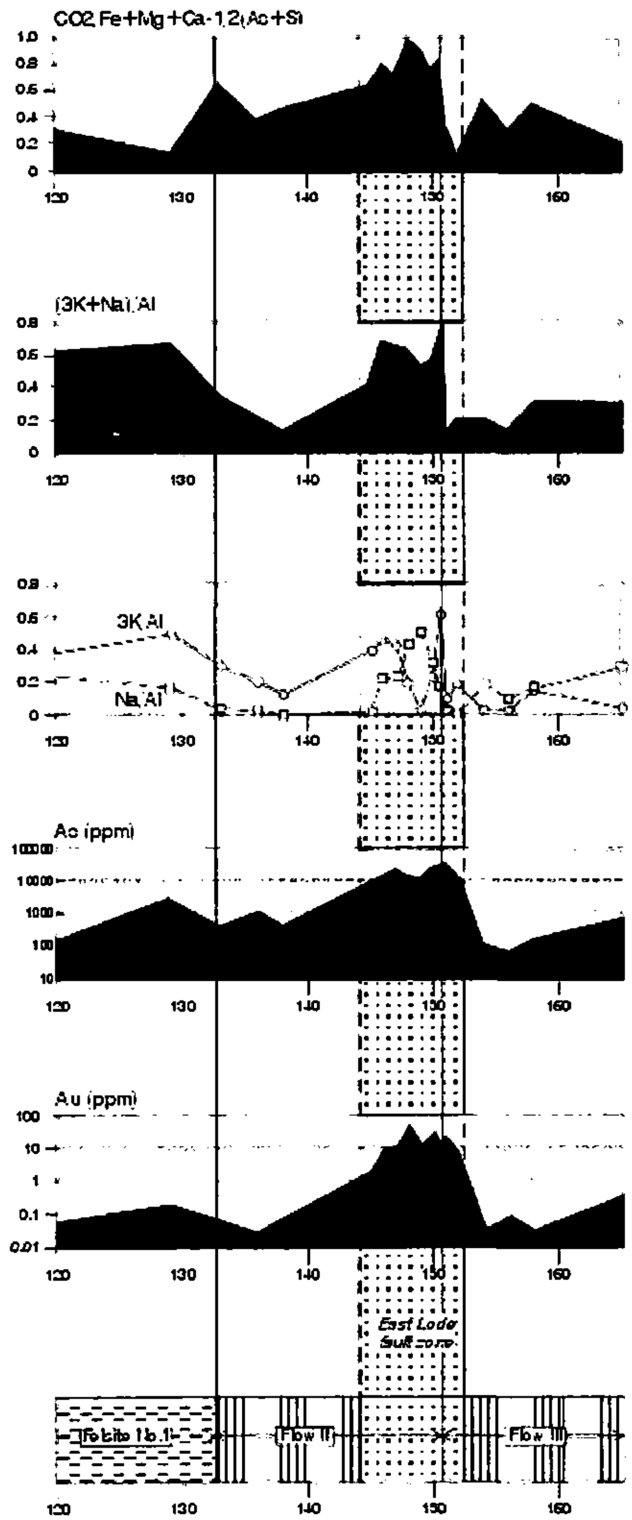

CO2/Fe+Mg+Ca-1.2(As+S)
(3K+Na)/Al
3K/Al
Na/Al
As (ppm)
Au (ppm)
East Lode fault zone
Felsite No.1
Flow II
Flow III
120
130
140
150
160

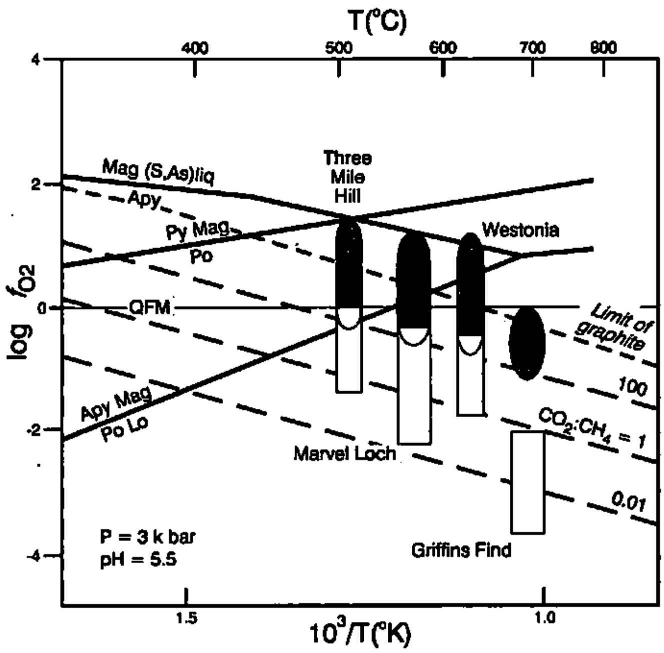

T(°C)
400
500
600
700
800
4
2
0
-2
-4
log f_{O2}
Mag (S,As)liq
Apy
Py Mag
Po
QFM
Apy Mag
Po Lo
Three
Mile
Hill
Westonia
Limit of
graphite
100
CO_2:CH_4 = 1
0.01
Marvel Loch
Griffins Find
P = 3 k bar
pH = 5.5
1.5
1.0
10^3/T(°K)

SHf009-00

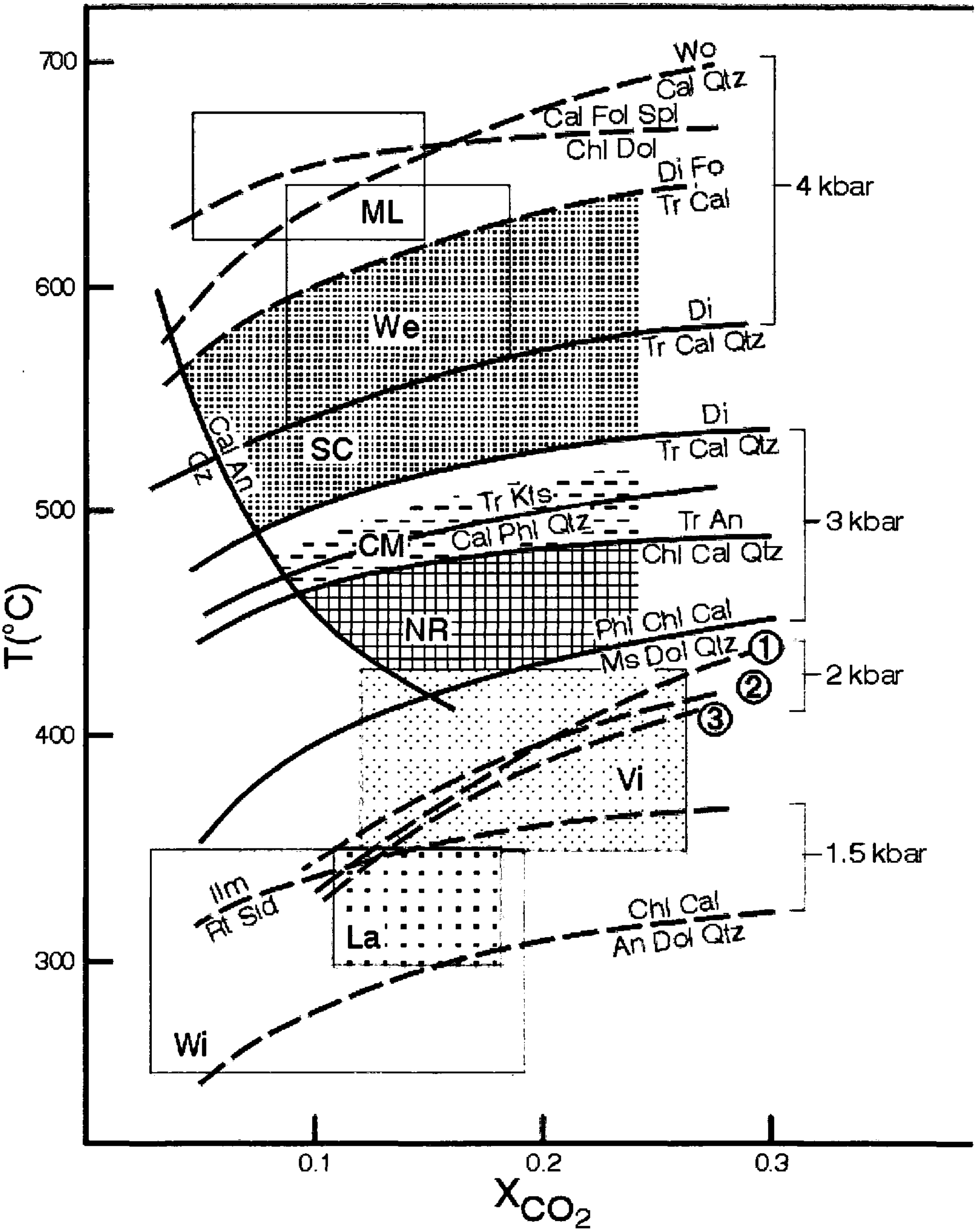

Wo
Cal Qtz
Cal Fol Spl
Chl Dol
Di Fo
Tr Cal
4 kbar
ML
We
Di
Tr Cal Qtz
SC
Cal An
Qz
Di
Tr Cal Qtz
Tr Kls
CM
Cal Phl Qtz
Tr An
Chl Cal Qtz
3 kbar
NR
Phl Chl Cal
Ms Dol Qtz
1
2
3
2 kbar
Vi
1.5 kbar
Ilm
Rt Sid
La
Chl Cal
An Dol Qtz
Wi
700
600
500
400
300
T(°C)
0.1
0.2
0.3
X_{CO_2}

SHf010-00

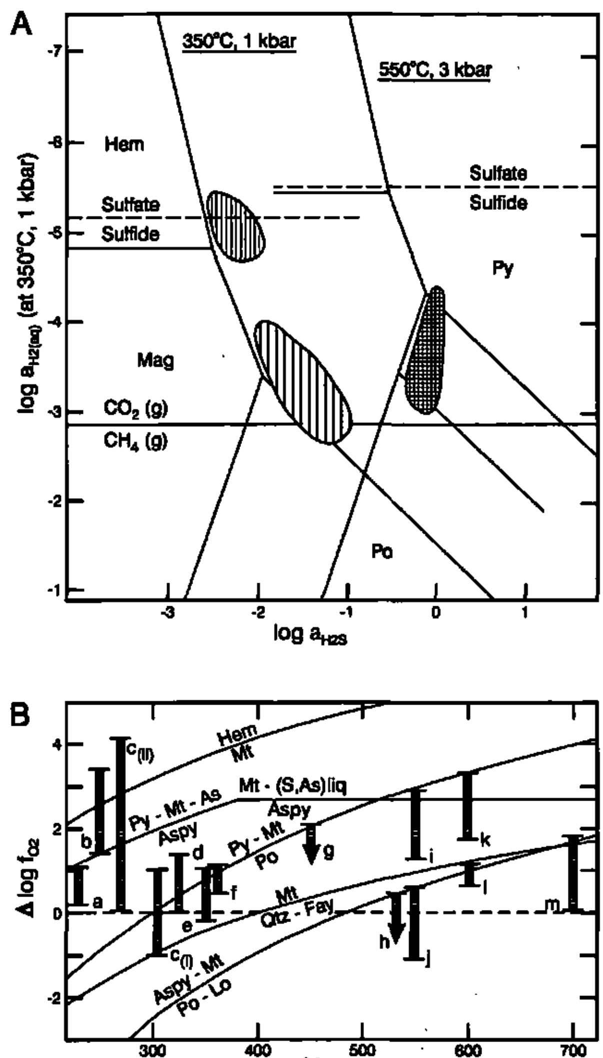
A
350°C, 1 kbar
550°C, 3 kbar
Hem
Sulfate
Sulfide
Mag
CO$_2$ (g)
CH$_4$ (g)
Py
Po
log $a_{H2(aq)}$ (at 350°C, 1 kbar)
log $a_{H2(aq)}$ (at 550°C, 3 kbar)
log a_{H2S}
B
Hem
Mt
Py - Mt - As
Aspy
Mt - (S,As)liq
Aspy
Py - Mt
Po
Mt
Qtz - Fay
Aspy - Mt
Po - Lo
Δ log f_{O2}
T°C

SHf001-00